

104 Biomechanics; Imaging

Sunday, May 05, 2013 8:30 AM-10:15 AM

Exhibit Hall Poster Session

Program #/Board # Range: 50-98/A0037-A0085**Organizing Section:** Glaucoma**Program Number:** 50 **Poster Board Number:** A0037**Presentation Time:** 8:30 AM - 10:15 AM**Circumferential Trabecular Meshwork Stiffness in Glaucomatous Eyes**Lucinda J. Camras¹, W Daniel Stamer², David L. Epstein², Pedro Gonzalez², Fan Yuan¹. ¹Biomedical Engineering, Duke University, Durham, NC; ²Ophthalmology, Duke University, Durham, NC.**Purpose:** Our previous work indicated that a larger bulk Young's modulus (E) of trabecular meshwork (TM) correlated with a higher outflow facility (C) in normal donor eyes (Camras, et al, IOVS. 2012). This study investigated the influence of TM stiffness on C in glaucomatous donor eyes.**Methods:** The left eyes of eight glaucomatous donors were perfused within 48 hrs postmortem time (PMT). With the exception of cataract surgery, there were no previous ocular surgeries. Outflow rate was measured at pressures of 10, 20, 30, and 40 mmHg to determine C and how outflow resistance ($R=1/C$) varied with pressure. The TM was then isolated and cut into 5-10 mm segments. Optical coherence tomography was used to determine cross-sectional area of the segments. Uniaxial tensile stress was applied longitudinally to TM segments at a rate of 0.1 % stretch per second to generate stress-strain curves. E was calculated at 0.0% strain to represent the circumferential stiffness of the TM at a relaxed state. Regression analysis was used to determine statistical significance of correlations.**Results:** Glaucomatous eyes had lower outflow facilities than normal eyes, which reduced (0.17 ± 0.02 to 0.11 ± 0.02 uL/min/mmHg; arithmetic mean \pm SE, n=8) with increasing pressure from 10 to 40 mmHg. The distribution of E was right-hand skewed and logarithmically converted for linear regression analysis. The geometric mean and standard error of E was 121 & 1.4 kPa. The glaucomatous TM was about 5 times softer than normal TM (n=7) observed in our previous study and showed a similar correlation between stiffness and C. A larger E correlated to smaller cross-sectional area ($p < 0.03$). There were no significant correlations between E and PMT, age, C, or variance of R.**Conclusions:** Glaucomatous TM showed a greater variability in stiffness and a lower average stiffness compared with normal TM. Additionally, E was dependent upon its cross-sectional area, indicating the stiffness heterogeneity within layers of glaucomatous TM. Due to its variability, there were no correlations between stiffness and outflow facility in glaucoma. However in combination with our previous data, it appears that softer TM led to impaired outflow, potentially due to an increased risk of Schlemm's canal collapse. Prospective studies are needed to confirm the influence of TM stiffness on outflow regulation.**Commercial Relationships:** Lucinda J. Camras, None; W Daniel Stamer, Allergan (F), Alcon (F), Acucela (C), Aerie (C), Cytokinetics (C); David L. Epstein, None; Pedro Gonzalez, None; Fan Yuan, None**Program Number:** 51 **Poster Board Number:** A0038**Presentation Time:** 8:30 AM - 10:15 AM**Racial variation in deep optic nerve head structures visualized with SD-OCT**Kulawan Rojananuangnit¹, John K. Johnstone², Massimo A. Fazio³, Mark Clark¹, Cynthia Owsley¹, Brandon Smith¹, Christopher A. Girkin¹. ¹Ophthalmology, University of Alabama at Birmingham,Birmingham, AL; ²Computer and Information Sciences, University of Alabama at Birmingham, Birmingham, AL; ³Center of Ocular Biomechanics and Biotransport, University of Alabama at Birmingham, Birmingham, AL.**Purpose:** To determine associations between variations in optic nerve head connective tissue visible with SD-OCT images with both age and race [African descent (AD), European Descent (ED)].**Methods:** SD-OCT images from 171 normal eyes (66 eyes from 34 AD and 105 eyes from 53 ED) were included. 3D optic nerve head reconstructions were obtained. Delineation of the SD-OCT images was done using Devers Eye Institute Multiview software in 24 radial sagittal sections (Burgoyne C). A best fitting ellipse was computed using principal component analysis to define Bruch's Membrane Opening (BMO) and this was taken as a reference for further analysis. A mesh was reconstructed from the point cloud for the anterior surface of lamina cribrosa (LC) and internal limiting membrane (ILM). We then measured the distance from a uniform sampling of the BMO ellipse to the LC mesh and ILM and calculated the mean and maximum depths for the lamina cribrosa depth (LCD; distance from BMO reference to LC mesh) and the cup depth (CD; distance from BMO reference to ILM). We looked at the variation in CD and LCD across racial strata (ED or AD) adjusted for age, central corneal thickness (CCT), axial length, and BMO area using mixed effects models with generalized estimating equations.**Results:** The AD group showed larger disc area (2.1 ± 0.5 , 1.8 ± 0.3 mm², $p < 0.0001$) and deeper cup depth (p value: 0.046) than the ED group after adjusted for all relevant confounds. (Table 1)**Conclusions:** Increased cup depth as defined by the optic nerve surface tissues differed between AD and ED subjects, however, there was no significant difference in lamina cribrosa depth, suggesting these differences are largely due to difference in overlying pre-lamina surface tissues.

Table 1 Age and Race Correlation Coefficient in Ocular Parameters (Significant p value was bolded.)

	β Coefficient	p value
Mean Lamina Cribrosa Depth		
-Race	56.012	0.296
-Age	-0.748	0.476
-Race x Age	-1.207	0.296
Mean Cup Depth		
-Race	174.33	0.035
-Age	2.05	0.153
-BMO area	43.12	0.136
-Race x Age	-3.33	0.046

Commercial Relationships: Kulawan Rojananuangnit, None; John K. Johnstone, None; Massimo A. Fazio, None; Mark Clark, None; Cynthia Owsley, Genentech (F), Patent Licensed to: MacuLogix (P), Allergan (R); Brandon Smith, None; Christopher A. Girkin, SOLX (F), Heidelberg Engineering (F)
Support: NEI: EY019333, EY018926, NIH: R01AG04212, EyeSight Foundation of Alabama, Research to Prevent Blindness**Program Number:** 52 **Poster Board Number:** A0039**Presentation Time:** 8:30 AM - 10:15 AM**The role of glycosaminoglycans in the mechanical behavior of the posterior sclera**Barbara Murielle¹, Harry Quigley², Thao D. Nguyen¹. ¹Department of Mechanical Engineering, Johns Hopkins University, Baltimore, MD; ²Glaucoma Center of Excellence, Johns Hopkins Wilmer Eye Institute, Baltimore, MD.**Purpose:** To investigate the role of glycosaminoglycans (GAGs) in the mechanical behavior of the posterior sclera.**Methods:** The posterior sclera from 6-9 months old pig eyes was dissected within 72 hours of enucleation. Mechanical testing was performed through a series of pressure-controlled load-unload and

ramp-hold tests (Myers et al., Acta Biomater., 2010). 3D digital image correlation was used to calculate the full-field surface displacements and analytical methods were developed to calculate circumferential and longitudinal strains. Each scleral cup was tested before and after overnight treatment at 37°C with Chondroitinase ABC at 2 units/ml in a modified Tris buffer at pH 8.0 (Sigma). Sulphated GAG (sGAG) removal was assessed quantitatively using the Blyscan assay (Biocolor) after sample digestion with Papain (Boubriak et al., Exp Eye Res., 2003). Student's t-test was used for statistical analysis.

Results: Preliminary results suggest that removing GAGs accelerates the creep and recovery rates (Fig. 1), increases tissue extensibility but has no noticeable effect on the stiffness of the loading curve.

Assessment of sGAG removal showed a $57.7 \pm 9.2\%$ mean decrease in sGAG content after treatment with Chondroitinase ABC (n=4, p<0.01, Fig. 2). Experiments using DPBS instead of Tris buffer to rinse the samples showed a much higher decrease in sGAG content ($94.6 \pm 0.83\%$, n=4, p<0.01), suggesting that even if in average 57.7% sGAGs are extracted out of the tissue using Tris buffer, at least 94% are disconnected from their environment.

Conclusions: Changes in GAG levels may contribute to the observed myopia-related (Phillips et al., Invest Ophthalmol Vis Sci., 2000) or glaucoma-related (Coudrillier et al., Biomech Model Mechanobiol., 2012) changes in the viscoelastic behavior of the sclera.

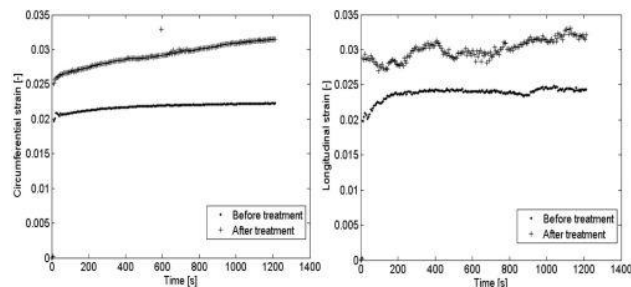


Figure 1. Creep response at 45mmHg in the circumferential and longitudinal directions, before and after enzymatic treatment with Chondroitinase ABC.

57.7% mean ↓ in GAG content

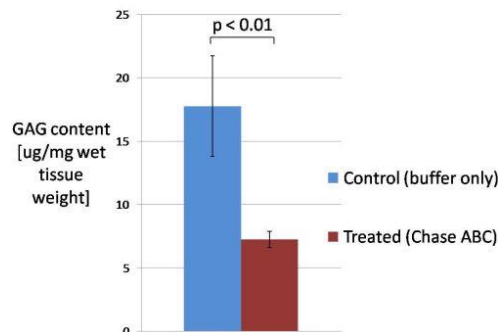


Figure 2. Blyscan assay results for the control and treated groups rinsed with Tris buffer.

Commercial Relationships: Barbara Murienne, None; Harry Quigley, Sensimed (C), Genetech (C), Merck (C), Sucampo (C); Thao D. Nguyen, None

Support: NIH Grant EY021500-01

Program Number: 53 **Poster Board Number:** A0040

Presentation Time: 8:30 AM - 10:15 AM

Spectral Domain Optical Coherence Tomography (SDOCT) Detected Lamina Cribrosa Compliance Change in Non-human Primate (NHP) Early Experimental Glaucoma (EEG)

Lirong Qin¹, Galen Williams¹, Stuart K. Gardiner¹, Brad Fortune¹, J Crawford C. Downs², Claude F. Burgoyne¹, Hongli Yang¹.

¹Discoveries in Sight Research Laboratories, Devers Eye Institute, Legacy Research Institute, Protland, OR; ²Center for Ocular Biomechanics and Biotransport, University of Alabama, Birmingham, AL.

Purpose: To compare optic nerve head (ONH) SDOCT morphology change due to acute IOP elevation from 10 to 30 mmHg (SDOCT compliance) within the contralateral normal (N) and EEG eyes of 13 NHPs at the onset of unilateral EEG.

Methods: Both eyes of each NHP (3-23 y.o.) underwent ONH SDOCT and Confocal Scanning Laser Tomography (CSLT) (both Heidelberg Engineering) ONH imaging 30 minutes after manometric IOP lowering to 10 mmHg and again 30 minutes after elevation to 30 mmHg prior to and every two weeks following the onset of unilateral, laser-induced, chronic IOP elevation. EEG was defined as the onset of CSLT surface change confirmed on two occasions. Within the 40 radial B-scans of the 30 degree SD-OCT volumes from the second EEG confirmation session, masked operators delineated the retinal and ONH landmarks necessary to quantify: anterior lamina cribrosa surface depth (ALCSD) relative to a Bruch's Membrane Opening (BMO) reference plane (ALCSD-BMO), ALCSD and BMO depth relative to a peripheral BM reference plane (ALCSD-BM and BMOdepth), neuroretinal rim width, BMO area, and prelaminar tissue thickness. Mixed effects models were used to assess the effects of IOP (i.e. compliance), disease status, and the interaction between them. A significant interaction was taken as evidence of a change in compliance.

Results: ALCSD-BMO and ALCSD-BM change due to acute IOP elevation was significantly greater in the EEG compared to normal eyes (ALCSD-BMO: $44 \pm 42 \mu\text{m}$ (mean±s.d.) in EEG eyes vs $5 \pm 14 \mu\text{m}$ in N eyes, p=0.0046; ALCSD-BM: 86 ± 63 in EEG eyes vs 37 ± 19 in N eyes, p=0.0141). Significant compliance was observed for all eyes between IOP 10 and 30 for BMO depth, prelaminar tissue thickness and rim width (p<0.0001), but no significant difference in compliance was observed between N and EEG eyes for these parameters. EEG eye compliance (ALCSD-BMO and ALCSD-BM change) was significantly predicted by cumulative IOP difference and peak IOP (maximum IOP of the EEG eye).

Conclusions: In a pooled analysis, NHP EEG eyes cross-sectionally exhibit significantly more SDOCT-measured lamina cribrosa compliance than their contralateral normal eyes as quantified by ALCSD-BMO or ALCSD-BM. This compliance is predicted by the IOP exposure and may be a manifestation of EEG-induced alterations in lamina cribrosa and peripapillary scleral structural stiffness.

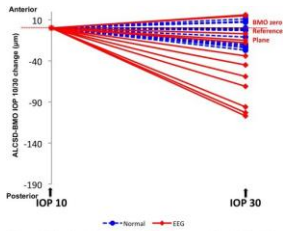


Figure 1a. This chart shows ALCSD-BMO difference at 10 and 30 mmHg. Experimental Glaucoma eyes in red exhibited more posterior deformation and had a larger range than Normal eyes in blue.

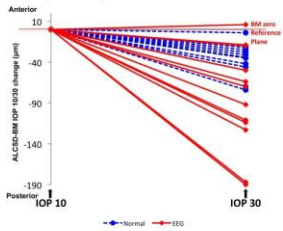


Figure 1b. ALCSD-BM difference at 10 and 30 mmHg. EEG eyes exhibited more deformation as well as a larger range between IOP 10 and 30 mmHg.

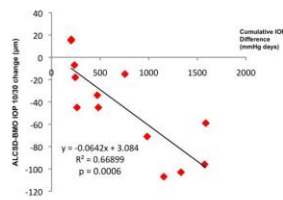


Figure 2a. EEG eye compliance (ALCSD-BMO change from IOP 10 to IOP 30 mmHg) was significantly predicted by cumulative IOP difference (the running difference between the area under its IOP-time curve and that of its contralateral normal eye after the start of lasering).

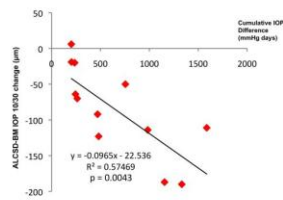


Figure 2b. EEG eye compliance (ALCSD-BMO change from IOP 10 to IOP 30 mmHg) was significantly predicted by cumulative IOP difference.

Commercial Relationships: **Lirong Qin**, None; **Galen Williams**, None; **Stuart K. Gardiner**, Allergan (R); **Brad Fortune**, Heidelberg Engineering, GmbH (F), Carl Zeiss Meditec, Inc (F); **J Crawford C. Downs**, None; **Claude F. Burgoyne**, Heidelberg Engineering (F), Heidelberg Engineering (C); **Hongli Yang**, None
Support: NIH/NEI R01-EY011610

Program Number: 54 **Poster Board Number:** A0041

Presentation Time: 8:30 AM - 10:15 AM

Regional variation of scleral strains measured on human whole globes using ultrasound speckle tracking

Junhua Tang¹, Richard T. Hart¹, Cynthia J. Roberts^{1,2}, Paul A. Weber², Xueliang Pan³, Jun Liu^{1,2}. ¹Department of Biomedical Engineering, Ohio State University, Columbus, OH; ²Department of Ophthalmology, Ohio State University, Columbus, OH; ³Center for Biostatistics, Ohio State University, Columbus, OH.

Purpose: Scleral mechanical properties are important in affecting the optic nerve head response to intraocular pressure (IOP) elevations. The purpose of this study is to examine the regional (anterior to posterior) variance of scleral mechanical responses to IOP elevations on whole human globes using non-invasive ultrasound speckle tracking.

Methods: Five human globes from 4 donors (age: 62 to 75 yo) were tested within 6 days post mortem. The globes were secured by a thin

needle (32G) penetrating through the equator in the superior-inferior direction and another needle (28G) through the central cornea into the anterior chamber. An ultrasound probe (55MHz, Vevo660, Visualsonics) was employed to scan the anterior, equatorial, and posterior sclera in a randomized order. All three regions were on the temporal side of the globe. Two scans (along the meridian direction and the circumferential directions) were taken in each region. Prior to measurements, each globe was subject to preconditioning and allowed for recovery. IOP was then gradually increased from 5 to 15 mmHg at steps of 2.5 mmHg and then 15 to 45 mmHg at steps of 5 mmHg with ultrasound signals being acquired at each step. The displacements and strains were calculated using the algorithm described previously (Tang & Liu, J Biomech Eng 2012, 134(9)).

Results: The average tangential strains were 0.27 ± 0.24 %, 0.54 ± 0.36 %, 0.66 ± 0.39 %, and 0.78 ± 0.43 % in the posterior sclera, 0.18 ± 0.12 %, 0.30 ± 0.19 %, 0.42 ± 0.24 %, and 0.55 ± 0.41 % in the equatorial sclera, and 0.12 ± 0.07 %, 0.24 ± 0.09 %, 0.34 ± 0.14 %, and 0.43 ± 0.17 % in the anterior sclera at pressures of 15, 25, 35 and 45 mmHg, respectively. The tangential strains in the posterior sclera were significantly larger than in the anterior sclera at pressures of 20, 25, 30, and 40 mmHg (P 's < 0.05, paired t-tests). No significant difference was found between the tangential strains along the meridian direction and those along the circumferential direction, likely due to the small sample size for this preliminary study.

Conclusions: Scleral mechanical responses to IOP were characterized in human whole globes. Significant regional variations were found in the mechanical response to IOP in human sclera with the posterior having the largest strains at the same IOP elevations. These results could provide useful information for developing biomechanical models of the whole ocular shell.

Commercial Relationships: **Junhua Tang**, None; **Richard T. Hart**, None; **Cynthia J. Roberts**, Oculus Optikgerate GmbH (C), Ziemer Ophthalmic Systems AG (C), Sooft Italia (R), Carl Zeiss Meditec (F); **Paul A. Weber**, None; **Xueliang Pan**, None; **Jun Liu**, None

Support: NIH RO1EY020929

Program Number: 55 **Poster Board Number:** A0042

Presentation Time: 8:30 AM - 10:15 AM

Scleral anisotropy and its effects on the optic nerve head biomechanics

Thao D. Nguyen¹, Baptiste Coudrillier¹, Harry Quigley², Craig Boote³. ¹Mechanical Engineering, The Johns Hopkins University, Baltimore, MD; ²Wilmer Ophthalmological Institute, The Johns Hopkins University, School of Medicine, Baltimore, MD; ³Structural Biophysics Group, School of Optometry and Vision Sciences, Cardiff University, Cardiff, United Kingdom.

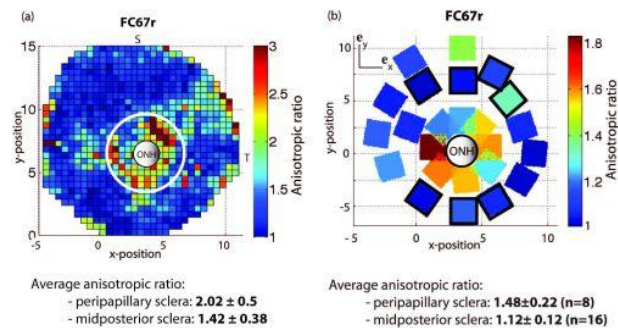
Purpose: To determine the effects of the collagen fiber structure of the sclera on the mechanical response of the sclera and the optic nerve head (ONH)

Methods: Specimen-specific inverse finite element models were developed to calculate the material properties of two normal human sclera (age 67, 71) subjected to inflation testing. A distributed fiber model incorporating wide-angle X-ray scattering (WAXS) measurements of the collagen structure was applied to describe the anisotropic elastic behavior of the sclera. The material parameters were used for micromechanical studies of the mechanical anisotropy at various length scales (0.5, 2, and 4 mm). The effects of the sclera fiber structure on the ONH mechanical response were evaluated by progressively filtering out local anisotropic features (Fig. 2).

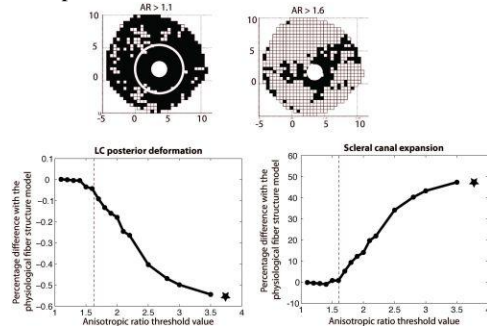
Results: The collagen structure of the midposterior sclera (MPS) showed large variations in the preferred fiber direction and degree of fiber alignment. The mechanical anisotropy of the MPS decreased

with increasing length scale (Fig. 1). At the 4 mm length scale, the MPS was nearly isotropic. The anisotropy of the MPS had little effect on the mechanical response of the ONH. Modeling 71% of the MPS as isotropic caused minimal changes (< 1%) to the scleral canal expansion and posterior lamina bowing (Fig. 2, second row). In the peripapillary sclera (PPS), collagen fibers were circumferentially aligned with spatially heterogeneous degree of alignment. The deformation of the ONH was acutely sensitive to the spatially heterogeneous anisotropy of the PPS.

Conclusions: Alterations in the degree of fiber alignment within the PPS observed in glaucoma eyes (Pijanka et al., IOVS, 2012) may significantly impact the biomechanical environment of the ONH.



Map of the anisotropic ratio at the 0.5 mm (a) and the 2 mm (b) length scale. The anisotropic ratio (AR) was calculated in finite element (FE) simulations of the strain response to an applied 21 kPa equibiaxial tension for a model of square section. AR=1 for an isotropic tissue.



First row: A white square represents a WAXS measurement for which the anisotropic ratio was below the threshold indicated on top of the figure. The corresponding area of the sclera was modeled as isotropic in the FE model of an inflation at 30 mmHg. Second row: Evolution of the posterior deformation of the LC and scleral canal expansion as the sclera becomes more isotropic. The star corresponds to the isotropic model.

Commercial Relationships: Thao D. Nguyen, None; Baptiste Coudrillier, None; Harry Quigley, Sensimed (C), Genetech (C), Merck (C), Sucampo (C); Craig Boote, None

Support: EY021500, EY02120, EY01765, the Fight For Sight grant 1360

Program Number: 56 **Poster Board Number:** A0043

Presentation Time: 8:30 AM - 10:15 AM

Analysis of retinal ganglion cell in lateral geniculate nucleus using ferret ocular hypertension model

Takashi Fujishiro¹, Makoto Aihara², Chihiro Mayama⁴, Makoto Araie³. ¹Ophthalmology, Saitama Red Cross Hospital, Saitama, Japan; ²Ophthalmology, Shirato Eye Clinic, Shinjuku, Japan; ³Ophthalmology, Kanto Chuo Hospital, Setagaya, Japan;

⁴Ophthalmology, University of Tokyo Graduate School of Medicine, Bunkyo, Japan.

Purpose: Ferrets have binocular vision unlike mice and rats, therefore ferrets are more suitable for analyzing the central visual pathway damage caused by glaucoma compared to mice and rats. Recent studies reported that not only optic nerve but also lateral geniculate nucleus (LGN) and visual cortex were damaged by glaucoma.

We reported the ferret ocular hypertension model last year at ARVO 2012 and analyze the damage of the central visual pathway in this model.

Retinal ganglion cells (RGCs) are divided into three cell lines which are known for magno, parvo and konio cells in primates and the corresponding ones in the ferrets are defined as X, Y and W cells. It is reported that magno cells are damaged first, then parvo cells are damaged in early stage glaucoma in primates.

However, there are few reports about the damage of konio cells in early stage glaucoma for now because of difficulty of analysis of konio cells in LGN.

W cells in ferret may be analyzed easily because of being different from structure of LGN in primates. We analyzed X, Y and W cells in LGN using ferret ocular hypertension model.

Methods: We established ferret ocular hypertension model by injecting conjunctival cells into an anterior chamber. Fluorescent labeled cholera toxin B (CTB) was injected to the vitreous space at 3 months after ocular hypertension. Red CTB was injected into the right eye and green CTB was injected into the left eye.

Brain stems were removed from the skull of ferrets in 4 days after CTB injection. Damage of X, Y and W cells in LGN was investigated using fluorescent microscope

Results: Elevation of IOP was occurred and sustained for 3 months after the injection of conjunctival cells. Fluorescence intensity in ocular hypertension model ferret was apparently decreased not only in contralateral LGN projected from eyes of elevated IOP but also in ipsilateral LGN projected from eyes of normal IOP compared to the normal ferret. Histologically, W cells are more damaged than X and Y cells in LGN.

Conclusions: W cells might be more sensitive than W and Y cells in ferret ocular hypertension model. Ferret ocular hypertension model will be a useful tool to investigate glaucomatous optic neuropathy and the secondary damage in the visual pathway.

Commercial Relationships: Takashi Fujishiro, None; Makoto Aihara, Ono pharmaceutical company (F), Pfizer (F); Chihiro Mayama, None; Makoto Araie, Kowa (C), Kowa (R), Zeiss (R), Topcon (R)

Program Number: 57 **Poster Board Number:** A0044

Presentation Time: 8:30 AM - 10:15 AM

Lamina cribrosa pore analysis in glaucomatous human optic nerve heads in vivo

Rachel V. North¹, Katharine E. Mortlock¹, Bethany E. Flynn^{1,2}, James Fergusson^{1,3}, Nick White^{1,3}, Wolfgang Drexler⁴, James E. Morgan^{1,5}, Julie Albon^{1,2}. ¹School of Optometry and Vision Sciences, Cardiff University, Cardiff, United Kingdom; ²CITER, Cardiff University, Cardiff, United Kingdom; ³Vision Science Bioimaging Laboratories, Cardiff University, Cardiff, United Kingdom; ⁴Center for Medical Physics and Biomedical Engineering, Medical University of Vienna, Vienna, Austria; ⁵Ophthalmology, University Hospital of Wales, Cardiff, United Kingdom.

Purpose: The aim of this study was to use a novel semi-automatic segmentation technique to analyse the pore parameters in optical coherence tomography (OCT) datasets of the human glaucomatous lamina cribrosa (LC).

Methods: Optic nerve heads (ONHs) of ten glaucoma and ten age-matched controls were imaged using a laboratory 1050nm spectral domain OCT device, operating at 47,000 a-scans/sec, with 5-7 μ m axial resolution. OCT volumes of 512x512 a-scans over a 18.7 degree field centred on the ONH were acquired. ONH OCT datasets were post-processed using ImageJ. Three different regions of interest (ROIs) were selected within each LC avoiding shadows cast by ONH vasculature. Semi-automatic segmentation was performed in ImageJ on 300x300 μ m ROI within the LC to analyse pore orientation, aspect ratio, area, and count.

Results: Segmentation of individual pores within different regions of interest within the LC was achieved in at least one ROI in all ONHs. However vascular shadowing caused by the temporal arcades or cilioretinal artery prevented the location of the ROI in some subjects, notably in the superior region of control ONHs.

Analysis of the anterior LC to a depth of 10 μ m revealed that pore areas ranged from 436-6853 μ m² in the glaucoma group and 418-4542 μ m² in the controls. Pores were significantly more oval (reflected by an increase in aspect ratio) in the inferior and superior regions of the ONH, when compared to centro-temporal region in the glaucoma group ($p=0.011$, Kruskal Wallis test). Pore count was lower in glaucoma subjects, compared to age-matched controls.

Conclusions: Our preliminary findings indicate that changes in LC pores parameters in the glaucomatous ONHs can be detected using OCT at 1050nm. Further improvements in segmentation methodology and ROI selection will increase the area of ONH available for analysis and improve the accuracy of this technique. Ultimately, this will provide us with an opportunity to analyse the LC *in vivo*, for the detection of changes and monitoring progression in glaucomatous optic neuropathy. In addition, this is likely to be an invaluable tool in assessing the effects of therapeutic interventions on the ONH.

Commercial Relationships: Rachel V. North, None; Katharine E. Mortlock, None; Bethany E. Flynn, None; James Fergusson, None; Nick White, None; Wolfgang Drexler, Zeiss (C); James E. Morgan, None; Julie Albon, None

Support: AHAF

Program Number: 58 **Poster Board Number:** A0045

Presentation Time: 8:30 AM - 10:15 AM

Laminar Beam Orientation and Connective Tissue Volume Fraction in Three-dimensionally (3D) Reconstructed Optic Nerve Heads (ONH) from Human Donor Eyes

Vincent Libertiaux¹, Rafael Grytz¹, Juan Reynaud², Christopher A. Girkin¹, J Crawford C. Downs¹. ¹Ophthalmology, University of Alabama at Birmingham, Birmingham, AL; ²Devers Eye Institute, Portland, OR.

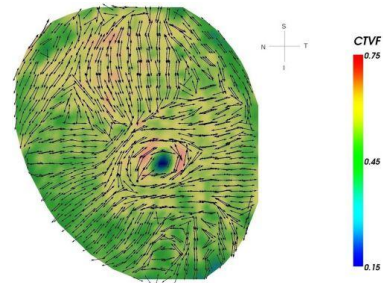
Purpose: To quantify the density and orientation of laminar beams in normal human donor eyes.

Methods: High-resolution, 3D reconstructions of the ONH were generated for three normal human donor eyes immersion fixed at 10 mmHg using a custom, microtome-based 3D tissue reconstruction system that serially images the embedded tissue block face at 1.5 μ m resolution in the fluorescent domain after each 1.5 μ m section is cut. The images are then aligned and stacked into a digital 3D ONH reconstruction with 1.5x1.5x1.5 μ m voxel resolution. The lamina cribrosa (LC) architecture was delineated and segmented (Grau et al., IEEE TMI 2006; Downs et al, IOVS 2007) and the laminar microarchitecture was sampled on a discrete grid to compute the connective tissue volume fraction (CTVF) and the predominant laminar beam orientation within each sampling volume (Roberts et al, IOVS 2009). The use of overlapping sampling volumes allowed the generation of a smooth, continuous CTVF and beam orientation

maps.

Results: For the eyes processed, the laminar beams are generally oriented radially in the periphery of the LC in the inferior-nasal (IN) sector and tangentially aligned in the superior-temporal (ST) quadrant (Figure). The IN region systematically presented the highest degree of beam orientation anisotropy. In these three volumes, no consistent CTVF pattern seemed to emerge.

Conclusions: Results suggest that CTVF and the fiber orientation at the periphery of the LC vary regionally in human eyes, which likely influence the biomechanical behavior of the LC and ONH.



Connective Tissue Volume Fraction (CTVF; colorbar) and predominant laminar beam orientation (arrows) map of a representative normal human donor eye immersion fixed at 10 mmHg within 6 hours post mortem.

Commercial Relationships: Vincent Libertiaux, None; Rafael Grytz, None; Juan Reynaud, None; Christopher A. Girkin, SOLX (F), Heidelberg Engineering (F); J Crawford C. Downs, None

Support: NIH Grant R01-EY18926; NIH Grant R01-EY19333

Program Number: 59 **Poster Board Number:** A0046

Presentation Time: 8:30 AM - 10:15 AM

Lamina Cribrosa Position and Age

Uma J. Damle¹, Sung Chul Park^{2,3}, Rafael L. Furlanetto², Nora Siegal⁴, Christopher C. Teng^{2,3}, Jeffrey M. Liebmann^{2,5}, Robert Ritch^{2,3}. ¹Robert Wood Johnson Medical School, New Brunswick, NJ; ²Moise and Chella Safta Advanced Ocular Imaging Laboratory, Einhorn Clinical Research Center, New York Eye and Ear Infirmary, New York, NY; ³Department of Ophthalmology, New York Medical College, Valhalla, NY; ⁴SUNY Downstate College of Medicine, Brooklyn, NY; ⁵Department of Ophthalmology, New York University School of Medicine, New York, NY.

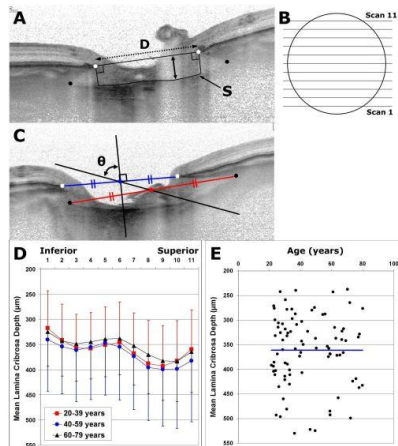
Purpose: To assess age-dependent changes in the lamina cribrosa (LC) position within the optic nerve head in normal eyes.

Methods: Serial horizontal enhanced depth imaging optical coherence tomography (EDI OCT) B-scans of the optic nerve head were obtained from one eye of normal subjects. Interval between EDI OCT B-scans was ~30 μ m. After delineating the anterior LC surface, mean and maximum LC depths (reference plane, Bruch's membrane edges) were measured in 11 equally spaced horizontal B-scans, excluding the LC insertion area under Bruch's membrane and the scleral rim (Fig A and B). Using the horizontal midline EDI OCT B-scan, the lateral LC displacement from the Bruch's membrane opening was measured as an angle (θ ; Fig C). Mean and maximum LC depths were compared between three age groups (20-39, 40-59, and 60-79 years).

Results: The 86 normal subjects (mean age, 44 \pm 18 years) included 44 subjects aged 20-39, 21 aged 40-59, and 21 aged 60-79 years. Both mean and maximum LC depths were similar between the three age groups in all 11 scans, before (all $p>0.51$; Fig D) and after (all $p>0.55$) controlling for the angle of lateral LC displacement (θ) and intraocular pressure. The average value of all 11 mean LC depths was 360 \pm 72 (range, 239 to 530) μ m, 369 \pm 76 (range, 274 to 524) μ m, and

354±72 (range, 237 to 499) μm in the 20-39, 40-59, and 60-79 years, respectively (p=0.78). The mean and maximum LC depths did not correlate with age either before (all p>0.43; **Fig E**) or after (all p>0.54) controlling for the angle of lateral LC displacement (θ) and intraocular pressure.

Conclusions: The central and mid-peripheral LC position within the optic nerve head does not change significantly with age under normal conditions. Changes in the LC position appear to be associated with pathologic processes.



(A) White dots = Bruch's membrane edges; black dots = anterior lamina insertion points; maximum lamina cribrosa (LC) depth = black double arrow; mean LC depth = (area S / length D). (B) The circle indicates the LC. (C) Angle of lateral LC displacement (θ) was measured in the horizontal midline scan of the LC. Blue dot = midpoint between the 2 Bruch's membrane edges. Red dot = midpoint between the 2 anterior lamina insertion points. (D) Mean LC depth profiles in the 3 age groups. (E) Scatter plot of age versus mean LC depth of each eye.

Commercial Relationships: Uma J. Damle, None; Sung Chul Park, None; Rafael L. Furlanetto, None; Nora Siegal, None; Christopher C. Teng, None; Jeffrey M. Liebmann, Alcon Laboratories, Inc. (C), Allergan, Inc. (C), Allergan, Inc. (F), Carl Zeiss Meditech, Inc (F), Heidelberg Engineering, GmbH (F), Topcon Medical Systems, Inc. (F), National Eye Institute (F), New York Glaucoma Research Institute (F), SOLX, Inc. (C), Bausch & Lomb, Inc (C), Diopsys, Inc. (C), Diopsys, Inc. (F), Merz, Inc. (C), Glaukos, Inc. (C), Quark, Inc. (C); **Robert Ritch**, None

Support: Derald H. Ruttenberg Foundation Research Fund of the New York Glaucoma Research Institute, New York, NY; James Cox Chambers Research Fund of the New York Eye and Ear Infirmary, New York, NY; Peter Crowley Research Fund of the New York Eye and Ear Infirmary, New York, NY

Program Number: 60 **Poster Board Number:** A0047

Presentation Time: 8:30 AM - 10:15 AM

The Influence of Substrate Stiffness on the Proliferation and Mechanical Properties of Normal and Glaucoma Trabecular Meshwork (NTM and GTM) Cells

Baiyun Liu¹, Jason I. Kilpatrick¹, Bartłomiej Lukasz¹, Deborah M. Wallace^{2,3}, Abbot F. Clark⁴, Colm J. O'Brien^{2,3}, Suzanne P. Jarvis¹.

¹School of Physics, Conway Inst., University College Dublin, Dublin, Ireland; ²School of Medicine and Medical Science, University College Dublin, Dublin, Ireland; ³Ophthalmology, Mater Misericordiae University Hospital, Dublin, Ireland; ⁴North Texas Eye Inst., University North Texas Health Centre, Forth Worth, TX.

Purpose: Previous work (Last et al, 2011) has shown that the mechanical properties of the Human Trabecular Meshwork (HTM) changes dramatically during the progression of glaucoma. Stiffness of the substratum has been demonstrated to influence a wide range of fundamental cell behaviours including cell morphology, mechanical properties and differentiation. The purpose of this study was to determine the influence of substrate stiffness on the proliferation, morphology, and mechanical properties of normal trabecular meshwork (NTM) and glaucoma trabecular meshwork (GTM) cells.

Methods: NTM and GTM cells were grown on substrates with a stiffness of 5kPa and 100kPa, which mimic the mechanical properties of the normal and glaucomatous human trabecular meshwork, respectively. Atomic force microscopy (AFM) was used to measure the elastic moduli of NTM and GTM cells on both substrates. Cell shape and morphology were also identified using immunohistochemistry.

Results: The morphology of NTM cells which adhered to the glaucomatous (pathomimetic) substrates (100kPa) were predominantly elongated in appearance, compared with NTM on the normal (homeomimetic) substrates (5kPa), which appeared predominately round. GTM cells, however, did not exhibit significant difference in cell morphology when grown on the homeomimetic or pathomimetic substrates. Additionally, the measured elastic moduli of HTM cells grown on pathomimetic and homeomimetic substrates differed dramatically. Differences in cytoskeletal architecture between cells on pathomimetic and homeomimetic surfaces were also observed.

Conclusions: Cellular response to substrate stiffness suggests that alterations in meshwork mechanical properties associated with glaucoma alter NTM but not GTM cell morphology. Additionally, substratum conditions which mimic the changes in environment associated with glaucoma alter the stiffness of both NTM and GTM cells.

Commercial Relationships: Baiyun Liu, None; Jason I. Kilpatrick, None; Bartłomiej Lukasz, None; Deborah M. Wallace, None; Abbot F. Clark, Alcon Research, Ltd. (F); Colm J. O'Brien, None; Suzanne P. Jarvis, None
Support: DGPP/PRTL15 & Health Research Board Ireland

Program Number: 61 **Poster Board Number:** A0048

Presentation Time: 8:30 AM - 10:15 AM

Collagen Microstructure In The Glaucomatous Human Optic Nerve Head: Distribution And Fiber Orientation

Julie Albon^{1,2}, Hannah J. Jones^{1,2}, Nick White^{1,3}, Michael P. Fautsch⁴, James E. Morgan^{1,5}, C.R. Ethier^{6,7}, Michael J. Girard^{8,9}.

¹School of Optometry & Vision Sciences, Cardiff University, Cardiff, United Kingdom; ²Cardiff Institute of Tissue Engineering & Repair, Cardiff University, Cardiff, United Kingdom; ³Vision Science Bioimaging Laboratories, Cardiff University, Cardiff, United Kingdom; ⁴Ophthalmology, Mayo Clinic, Rochester, MN; ⁵Ophthalmology, University Hospital of Wales, Cardiff, United Kingdom; ⁶Wallace H. Coulter Department of Biomedical Engineering, Georgia Institute of Technology & Emory University School of Medicine, Atlanta, GA; ⁷Department of Bioengineering, Imperial College London, London, United Kingdom; ⁸Department of Bioengineering, National University of Singapore, Singapore; ⁹Singapore Eye Research Institute, Singapore National Eye Centre, Singapore.

Purpose: To analyse fibrillar collagen distribution and connective tissue fiber orientation within the glaucomatous human optic nerve head (ONH).

Methods: Human optic nerve heads (ONHs, 3 glaucoma and 3 age-matched controls) were cryosectioned transversely (10-15 100μm-

thick sections from each ONH) from pre- to post-laminar. Using second harmonic generation (SHG) microscopy and small angle light scattering (SALS), the distribution and orientation of fibrillar collagen was visualized and preferred fiber orientation and degree of fiber alignment (DOFA) was calculated in each section. The lamina cribrosa (LC) was subdivided into 12 regions for analysis: 2 regions in the superior (S1, S2), inferior (I1, I2), temporal (T1, T2), nasal (N1, N2), and SN, IN, IT and ST.

Results: In normal human ONHs, SHG scatter identified fibrillar collagen oriented radially in the LC, surrounding central retinal vessels and circumferentially in the peripapillary sclera. In all ONHs, the DOFA was high, average: 0.64 (0 is random and 1 is perfect alignment) in the peripapillary sclera. This can be attributed to highly aligned fibrillar collagen, identified in both SHG and SALS datasets, circumferentially orientated around the ONH. SHG scatter patterns were distinct in areas of glaucomatous LCs; observations that were supported in fiber orientation plots. In glaucomatous LC, quantitative measurements of DOFA showed greater inter-regional variation compared to that determined in a normal LC. In addition, glaucomatous ONH DOFA plots indicated sub-regions of higher alignment within the LC. Interestingly, significant differences in DOFA were observed in all regions when compared between normal and glaucoma ONHs ($p < 0.05$), with the exclusion of the temporal LC region, and in one case the inferonasal region.

Conclusions: Fibrillar collagen distribution and fiber orientation vary with location in the human ONH and appear to be affected in glaucomatous optic neuropathy. Our findings of altered collagen alignment within the glaucomatous LC reflect a change in LC biomechanics, likely a consequence of connective tissue disorganization, remodeling and/or loss. The presence of greater disorganization suggests that homeostatic mechanisms for aligning connective tissue elements in the direction of load may be impaired in the glaucomatous LC.

Commercial Relationships: Julie Albon, None; Hannah J. Jones, None; Nick White, None; Michael P. Fautsch, None; James E. Morgan, None; C R. Ethier, None; Michael J. Girard, None
Support: BBSRC, School of Optometry and Vision Sciences, Research to Prevent Blindness, Mayo Foundation, NIH grant EY21727

Program Number: 62 **Poster Board Number:** A0049

Presentation Time: 8:30 AM - 10:15 AM

Lamina Depth and Pia Insertion are Significant Factors in Optic Nerve Head Biomechanics

Jonathan L. Grimm¹, Richard A. Bilonick^{1,3}, Hiroshi Ishikawa^{1,2}, Gadi Wollstein¹, Larry Kagemann^{1,2}, Joel S. Schuman^{1,2}, Ian A. Sigal^{1,2}. ¹UPMC Eye Center, Eye and Ear Institute, Ophthalmology and Visual Science Research Center, Department of Ophthalmology, University of Pittsburgh School of Medicine, Pittsburgh, PA; ²Department of Bioengineering, Swanson School of Engineering, University of Pittsburgh, Pittsburgh, PA; ³Department of Biostatistics, Graduate School of Public Health, University of Pittsburgh, Pittsburgh, PA.

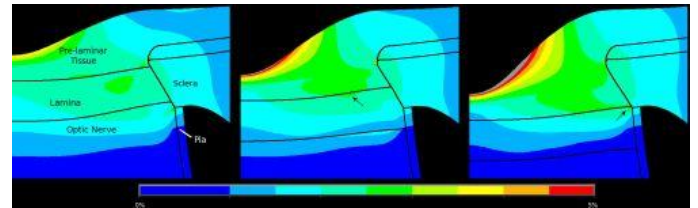
Purpose: Variations in eye anatomy, such as lamina cribrosa depth and the length of its insertion into the pia mater, have been postulated to affect optic nerve head (ONH) sensitivity to elevated IOP. Our goal was to determine how lamina cribrosa depth and lamina insertion into the pia, among other characteristics of the ONH, influence ONH biomechanics.

Methods: We adapted a previously reported finite element model of the eye (IOVS. 2011; 52:5497-506) to incorporate variations in anterior lamina insertion depth (relative to the scleral canal opening), lamina curvature and thickness, scleral canal opening radius, pia

mater thickness and the stiffness of the sclera, lamina and pia mater (through the Young's modulus). The length of the lamina insertion into the pia mater was computed for each ONH. Using a Design of Experiments technique we defined a population of 2603 ONHs. For each one we computed the biomechanical effects on the lamina cribrosa of an increase in IOP of 10 mmHg, and extracted the mean and peak tensile, compressive and shear strains and the von Mises stress. Statistical models allowing up to third order interactions were computed to determine the effects of each parameter on the responses.

Results: Anterior lamina depth accounted for 12% of the variance of mean and peak tensile strain. Increased anterior lamina depth resulted in higher peak (up to 2%) and lower mean (up to 0.5%) tensile strains, and lower mean von Mises stress (up to 10 kPa). Scleral canal opening radius, scleral stiffness and lamina stiffness often had strong and significant interactions with anterior lamina depth. The length of the pia insertion was a significant factor for both the strains and the stresses (all $p < 0.000001$).

Conclusions: Lamina depth and length of lamina insertion into the pia are significant factors in lamina biomechanics. Interestingly, our results suggest that a posterior remodeling of the lamina cribrosa may have both strain-increasing and strain-decreasing effects.



Caption: Tensile strain of three ONH models with increasing anterior lamina depth (left to right 0.05, 0.22 and 0.39 mm), and all other parameters the same. Overall the strain decreased in the lamina, but some lamina regions experienced more strain (arrows). Note that increased lamina depth also increased the strain in the pre-laminar tissue and the peripapillary sclera immediately adjacent to the canal.

Commercial Relationships: Jonathan L. Grimm, None; Richard A. Bilonick, None; Hiroshi Ishikawa, None; Gadi Wollstein, Allergan (C); Larry Kagemann, None; Joel S. Schuman, Carl Zeiss Meditec, Inc. (P); Ian A. Sigal, None
Support: P30 EY008098; Eye and Ear Foundation (Pittsburgh, PA); Research to Prevent Blindness (New York, NY)

Program Number: 63 **Poster Board Number:** A0050

Presentation Time: 8:30 AM - 10:15 AM

Valsalva Maneuver, Intraocular Pressure, Cerebrospinal Fluid Pressure, and Optic Disc Topography: Beijing Intracranial and Intraocular Pressure (iCOP) Study

Ningli Wang¹, Zheng Zhang¹, Jost B. Jonas², Robert Ritch³. ¹Ophthalmology, Beijing Tongren Eye Center, Beijing, China; ²Ophthalmology, Medical Faculty Mannheim of the Ruprecht-Karls-University Heidelberg, Mannheim, Germany; ³Ophthalmology, the New York Medical College, New York, NY.

Purpose: To assess whether a Valsalva maneuver influences intraocular pressure (IOP), cerebrospinal fluid pressure (CSF-P) and, by a change in the trans-lamina cribrosa pressure difference, optic nerve head morphology.

Methods: The study included 20 neurological patients who required lumbar puncture and 20 healthy volunteers. In a first study part, neurological patients underwent measurement of IOP and lumbar CSF-P measurement in a lying position before and during a Valsalva maneuver with a documented continuous expiratory pressure of ≥ 30

mmHg for about 20 seconds. In the second part, 20 healthy subjects underwent ocular tonometry and confocal scanning laser tomography of the optic nerve head before and during a Valsalva maneuver.

Results: During the Valsalva maneuver in the first study part, the increase in CSF-P by 10.5 ± 2.7 mmHg was significantly ($P < 0.001$) higher than the increase in IOP by 1.9 ± 2.4 mmHg. The change in CSF-P was not significantly ($P = 0.61$) correlated with the change in IOP. During the Valsalva maneuver in the second part, IOP increased by 4.5 ± 4.2 mmHg and optic cup volume ($P < 0.001$), cup/disc area ratio ($P = 0.04$), cup/disc diameter ratio ($P = 0.03$) and maximum optic cup depth ($P = 0.02$) significantly decreased, while neuroretinal rim volume ($P = 0.003$) and mean retinal nerve fiber layer thickness ($P = 0.02$) significantly increased.

Conclusions: The Valsalva maneuver-associated increase in CSF-P was significantly larger than, and not correlated with, and a simultaneous increase in IOP. This Valsalva maneuver associated reversal of the trans-lamina cribrosa pressure difference resulted in a change of the three-dimensional optic nerve head morphology with a decrease in optic cup related parameters and an enlargement of neuroretinal rim related parameters. These findings may be relevant to the pathogenesis of glaucomatous optic neuropathy.

Commercial Relationships: Ningli Wang, None; Zheng Zhang, National Natural Science Foundation of China (81271005) (F), Beijing Natural Science Foundation (7122038) (F), Award of Excellent Doctoral Dissertation of Beijing (Beijing YXBSGrant PXM2010_014226_07_000061 and PXM2011_014226_07_000114) (F), China Health and Medical Development Foundation (F); Jost B. Jonas, Allergan (C), MSD (C), Alimera (C), CellMed AG (P); Robert Ritch, None

Support: National Natural Science Foundation of China (81271005), Beijing Natural Science Foundation (7122038), Award of Excellent Doctoral Dissertation of Beijing (Beijing YXBSGrant PXM2010_014226_07_000061 and PXM2011_014226_07_000114), China Health and Medical Development Foundation

Program Number: 64 **Poster Board Number:** A0051

Presentation Time: 8:30 AM - 10:15 AM

Variability in Optic Disc Margin and Rim Assessment by Glaucoma Specialists using Color Stereophotographs

Helen Koenigsman, Ruojin Ren, Hongli Yang, Stuart K. Gardiner, Juan Reynaud, Robert M. Kinast, Steven L. Mansberger, Brad Fortune, Shaban Demirel, Claude F. Burgoyne. Discoveries in Sight Laboratories, Devers Eye Institute, Legacy Research Institute, Portland, OR.

Purpose: To characterize inter-clinician (IC) variability in assigning disc margin and rim margin within 184 color stereophotos of glaucoma and glaucoma suspect eyes.

Methods: Photos of 184 eyes of 184 subjects were independently evaluated by 5 trained glaucoma specialists. Stereophoto pairs were viewed using a handheld stereoscope while the disc margin and rim margin were marked using a separate monitor and customized software. For each photo, the centroid of each clinician's disc margin was calculated, and an average DMcentroid (n=5 clinicians) was determined. Photos were then colocalized to confocal scanning laser ophthalmoscopy (cSLO) infrared fundus reflectance images of the same eye so that the axis between DMcentroid and the fovea could be used to establish anatomic 30-degree sectors in each eye. (Fig 1) Radial distance measurements from DMcentroid to each clinician's disc margin (disc radius) and rim margin (cup radius) were noted and used to calculate the rim width, disc area, cup area and rim area in each sector. IC variability for each parameter (disc radius, cup radius, rim width, disc area, cup area and rim area) within the 184 photos was assessed as the standard deviation of differences from the intra-

eye inter-clinician mean within each sector.

Results: IC variability for each parameter was substantial and regionally variable in these 184 eyes. Among the distance parameters, cup radius was more variable than disc radius in all 12 sectors with each being greatest nasally (see Fig 2 for polar plots of the SD of residuals for all parameters). Cup area was more variable than disc area superotemporally but less variable inferonasally due to the reduced extent of the cup in the inferonasal region. Variability in rim width comprises the effect of variability on both rim margin and disc margin, so is greater than either. Similarly rim area is more variable than either cup area or disc area since it incorporates both sources of variability.

Conclusions: IC variability in rim margin and disc margin assessment was substantial among the glaucoma specialists of this study leading to marked IC variability in rim width and rim area assessment. Reducing variance due to a well known source of anatomical variation is beneficial. A regionalization strategy based on the angle between the disc center and fovea is a useful approach for standardizing optic disc assessment by sectors.

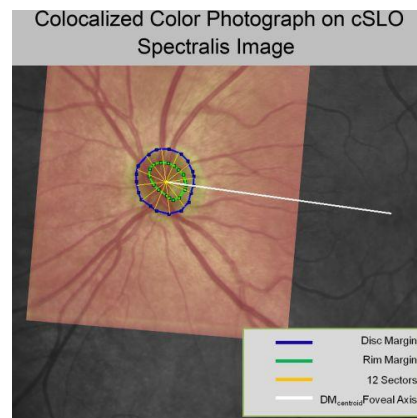


Figure 1

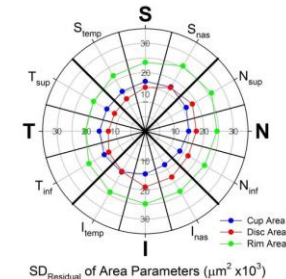
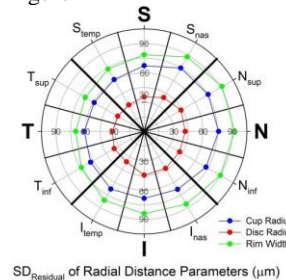


Figure 2

Commercial Relationships: Helen Koenigsman, None; Ruojin Ren, None; Hongli Yang, None; Stuart K. Gardiner, Allergan (R); Juan Reynaud, None; Robert M. Kinast, None; Steven L. Mansberger, Merck (R), Alcon (C), Allergan (C), Allergan (F), Merck (F), Santen (C), Glaukos (C); Brad Fortune, Heidelberg

Engineering, GmbH (F), Carl Zeiss Meditec, Inc (F); **Shaban Demirel**, Carl Zeiss Meditec (F), Heidelberg Engineering (R), Heidelberg Engineering (F); **Claude F. Burgoyne**, Heidelberg Engineering (F), Heidelberg Engineering (C)
Support: NIH/NEI R01-EY021281; NIH/NEI R01-EY-019674; Legacy Good Samaritan Foundation; Sears medical Trust; Alcon Research Institute

Program Number: 65 **Poster Board Number:** A0052

Presentation Time: 8:30 AM - 10:15 AM

Measuring Micron-Scale Collagen Fiber Orientation in the Lamina Cribrosa and Peripapillary Sclera

Ning-Jiun Jan^{1,2}, Jonathan L. Grimm¹, Kira L. Lathrop^{1,2}, Gadi Wollstein¹, Larry Kagemann^{1,2}, Joel S. Schuman^{1,2}, Hiroshi Ishikawa^{1,2}, Ian A. Sigal^{1,2}. ¹Ophthalmology, University of Pittsburgh, Pittsburgh, PA; ²Bioengineering, University of Pittsburgh, Pittsburgh, PA.

Purpose: Collagen fiber orientation is a critical factor in determining the local biomechanical response to loading of the lamina cribrosa (LC) and peripapillary sclera (PPS). Our goal was to evaluate the repeatability of our novel technique for measuring micron-scale collagen fiber orientation in LC and PPS.

Methods: A sheep eye (<2 yo) was obtained from a local slaughterhouse and fixed overnight in formalin (10%) within 24 hours of death. Following fixation the LC and PPS were cryosectioned coronally into 30 µm sections. One section through the LC was selected and imaged using light microscopy (Olympus BX60, 12-bit grayscale 1600x1200 pixels) three times at high resolution (0.73 µm/pixel, 10x objective, NA 0.30) and three times at low resolution (1.48 µm/pixel, 4x objective, NA 0.13). Repeatability was measured by overlying stitched image sets and calculating the angle differences between fiber orientations in each image and the mean angle over all image sets of that resolution.

Results: In both LC and PPS angle differences within resolutions were small, with 95% of the fiber orientations differing by less than 5°, independent of the resolution (Figure 1). Angle differences in the PPS were smaller than in the LC. Overlaid orientations obtained from the three high resolution image sets illustrate the small magnitude of the differences (Figure 2).

Conclusions: Our method was highly reproducible, with multiple measurements differing by only a few degrees. When the measurements are overlaid they are essentially indistinguishable. Micron-scale collagen fiber orientation data of the LC and PPS will enable better understanding of the effects of intraocular pressure on the optic nerve head.

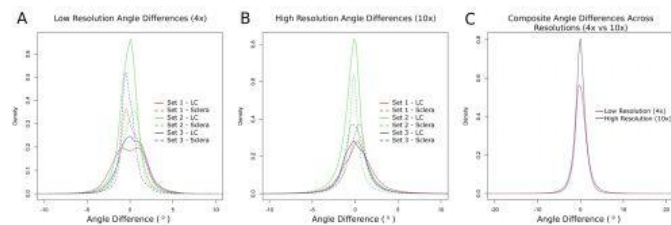


FIGURE 1: Distributions of the differences in fiber orientation. A) Low resolution. B) High resolution. C) Composite (both tissues) low vs. high resolution.

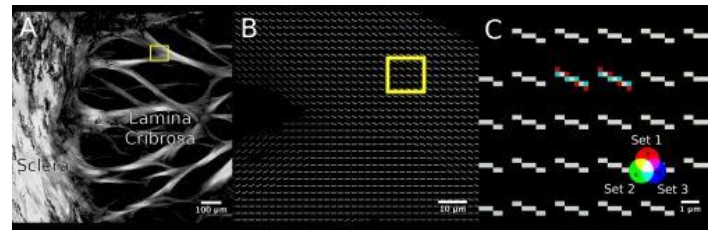


FIGURE 2: A) The LC and PPS; B) Close up of a LC trabeculae (box in A) with lines illustrating collagen fiber orientation in 9x9 superpixels. Shown is an overlay of the three measurements in blue, red and green. Most pixels are white, meaning that the three measurements overlap; C) Close up of box in B.

Commercial Relationships: Ning-Jiun Jan, None; **Jonathan L. Grimm**, None; **Kira L. Lathrop**, PCT/US2012/027268 (P); **Gadi Wollstein**, Allergan (C); **Larry Kagemann**, None; **Joel S. Schuman**, Carl Zeiss Meditec, Inc. (P); **Hiroshi Ishikawa**, None; **Ian A. Sigal**, None
Support: P30 EY008098; Eye and Ear Foundation (Pittsburgh, PA); Research to Prevent Blindness.

Program Number: 66 **Poster Board Number:** A0053

Presentation Time: 8:30 AM - 10:15 AM

A Sequential Digital Image Correlation Technique for Improved Strain Mapping in Pressure Inflation Tests of Posterior Sclera

Jonathan P. Vande Geest^{1,2}, Jeff D. Pyne¹, Katia Genovese³, Luciana Casaletto³. ¹Aerospace and Mechanical Engineering, University of Arizona, Tucson, AZ; ²Biomedical Engineering, University of Arizona, Tucson, AZ; ³School of Engineering, Universita Della Basilicata, Potenza, Italy.

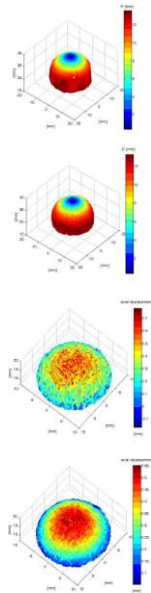
Purpose: Recent research has demonstrated the importance of understanding and quantifying the deformational behavior of human posterior scleral tissues. The peripapillary sclera and surrounding scleral tissue in large part control scleral canal expansion and as such may play an important role in nerve fiber damage in glaucoma. The purpose of this abstract was to demonstrate a new technique for pressure inflation of posterior scleral tissues using a sequential digital image correlation (DIC). The results are reported and compared to those generated using standard stereo DIC. In particular, we seek to address the current challenges of standard DIC by improving both shape reconstruction and axial displacement resolution.

Methods: Differences between the standard stereo technique and the sequential procedure were quantified by analyzing a phantom object with vertical edges (a cylinder extended hemisphere). For investigating differences in displacement calculation, a DIC test was also performed on a flexible polymeric membrane at pressures of 30 and 40 mmHg. All samples were prepared for DIC by applying a speckle pattern using black and white ink. For each configuration of interest (e.g., at a given pressure), a manually controlled bi-rotational gimbal system was utilized to sequentially rotate the object through +/-15 degrees in two orthogonal directions. During rotation, images were acquired at 10 frames per second using a Falcon2 monochrome camera equipped with a 28-105 mm NIKKOR lens approximately 40 cm directly above the pressure inflation device. For each object tested at each configuration, standard 3D-DIC reconstruction was performed using a stereo angle of 10° degrees. Serial reconstruction was then performed using 10 images approximately 30° angles apart. Marker location was compared between the standard and serial approach, with results being reported in the mean percent difference between the two techniques.

Results: The qualitative differences between the two techniques in shape reconstruction and axial displacement are observed in the

attached figure. The mean percent difference in the axial displacement between the standard and stereo DIC techniques was 27% for the polymeric membrane.

Conclusions: These results suggest that our sequential DIC approach may provide better shape reconstruction and axial displacement accuracy than a standard stereo DIC technique.



Top: Shape reconstruction Standard DIC, middle top: Shape reconstruction Sequential DIC, middle bottom: axial displacement Standard DIC, bottom: axial displacement Sequential DIC.

Commercial Relationships: Jonathan P. Vande Geest, None; Jeff D. Pyne, None; Katia Genovese, None; Luciana Casaletto, None
Support: NIH Grant 5R01EY020890-02

Program Number: 67 **Poster Board Number:** A0054

Presentation Time: 8:30 AM - 10:15 AM

Quantitative Measurement of Sleep Body Position Using a Mobile Device and its Application to the Study of Glaucoma Asymmetry

Syril Dorairaj, Jonathan D. Tung, Mona Moshtaghi, John H. Liu, Robert N. Weinreb. Hamilton Glaucoma Center, University of California San Diego, San Diego, CA.

Purpose: To investigate the relationship between right-left sleep body position, as measured with a mobile device, and the progression of glaucoma asymmetry. We hypothesize that a patient's preferred side of sleep position is associated with worsening of glaucomatous progression in the eye of the same side.

Methods: This was a single-masked, cross-sectional study. Primary open-angle glaucoma (POAG) patients with asymmetric glaucoma progression, as determined by perimetry, nerve fiber layer optical coherence tomography (OCT), and/or optic disc appearance, were enrolled. Home recordings of sleep body position were made over seven consecutive nights. A mobile device with the application Sleep Monitor was worn by the patient each night at bedtime. The right-left side sleep position in degrees was recorded, with positive angles indicating orientation on one side, negative angles on the other side, and zero degrees in the supine position. The overall sleep time in each position was also measured, as readings were logged every minute during sleep. The data were collected electronically, and the characteristic parameters of sleep body position were examined for a correlation with asymmetric glaucoma progression.

Results: Ten patients with diagnosed primary open-angle glaucoma (ages, 42 - 73 years) were included in the study. The average right-left sleep body position, as measured by the mean degree from

supine, corresponded with glaucoma asymmetry progression in five patients, while the sleep body position did not correspond with glaucoma asymmetry progression in five patients. Fisher's exact test showed no correlation between the side of sleep and the side of glaucoma ($P=1.00$)

Conclusions: In this pilot study, right-left sleep body position, as measured with a mobile device, demonstrated no significant correlation with the progression of glaucoma asymmetry in treated patients. The measurement of sleep body position with a mobile device offers a promising quantitative evaluation in the correlation between sleep body position and glaucoma asymmetry.

Commercial Relationships: Syril Dorairaj, None; Jonathan D. Tung, None; Mona Moshtaghi, None; John H. Liu, Allergan (F), Alcon (F), Aerie (F), Sensimed (F), Bausch + Lomb (F); Robert N. Weinreb, Aerie (F), Alcon (C), Allergan (C), Altheos (C), Amakem (C), Bausch&Lomb (C), Carl Zeiss-Meditec (C), Genentech (F), Haag-Streit (F), Heidelberg Engineering (F), Konan (F), Lumenis (F), National Eye Institute (F), Nidek (F), Optovue (C), Quark (C), Solx (C), Topcon (C)

Program Number: 68 **Poster Board Number:** A0055

Presentation Time: 8:30 AM - 10:15 AM

Through-thickness Measurement of Porcine Sclera Deformation under Biaxial Loading Using High Resolution Ultrasound

Benjamin Cruz Perez¹, Junhua Tang¹, Hugh J. Morris¹, Richard T. Hart¹, Xueliang Pan^{1,2}, Jun Liu^{1,3}. ¹Department of Biomedical Engineering, Ohio State University, Columbus, OH; ²Center for Biostatistics, Ohio State University, Columbus, OH; ³Department of Ophthalmology, Ohio State University, Columbus, OH.

Purpose: Mechanical properties of the posterior sclera influence the stresses and strains experienced by the optic nerve head. This study aims to characterize the through-thickness deformation of sclera under biaxial loading using high-resolution ultrasound speckle tracking.

Methods: Nine porcine globes were obtained within 24 hrs post-mortem. A 7 mm square sample from the supero-temporal region of the posterior sclera was prepared and mounted biaxially along the circumferential and meridian directions using hooks and suture. The samples were immersed in a saline solution during all tests. Preconditioning was achieved using the built-in sine frequency sweep in the Bose biaxial testing system (ElectroForce Planar Biaxial TestBench, Bose Corporation, Eden Prairie, MN, USA) with a load range from 1 to 18 grams. Specimens were then equilibrated for 15 min at 1 gram preload and ramped biaxially to 25 increasing force levels from 2 to 18 grams simulating the physiological intraocular pressure range of 5 to 45 mmHg. Two ramps were performed to image the deformations within a cross-section of the sclera along both axes with a 55 MHz ultrasound imaging system. Each sample was allowed to equilibrate at a preload of 1 gram for 15 minutes between ramps. A speckle tracking algorithm (Tang & Liu, J Biomech Eng 2012, 134(9)) was used to compute the internal strains of the scanned cross-sections. The average strain in a pre-defined region of interest was calculated for each specimen.

Results: Sclera demonstrated a heterogeneous pattern of strains through thickness and a typical hyperelastic behavior during biaxial loading. The circumferential strains were $2.69 \pm 0.72\%$, $2.97 \pm 0.81\%$, and $3.24 \pm 0.86\%$, and the meridian strains were $3.34 \pm 0.61\%$, $3.62 \pm 0.64\%$, and $3.38 \pm 0.63\%$ at stress levels of 20, 25, and 30 kPa, respectively. The circumferential strains were significantly lower than the meridian strains at these stress levels ($P < 0.05$).

Conclusions: Ultrasound speckle tracking was used to characterize the mechanical responses of sclera during biaxial loading. Porcine posterior sclera displayed heterogeneous and anisotropic responses

ARVO 2013 Annual Meeting Abstracts by Scientific Section/Group – Glaucoma

with a significantly stiffer response along the circumferential direction than the meridian direction. Future studies combining finite element modeling are needed to derive mechanical properties of the sclera.

Commercial Relationships: Benjamin Cruz Perez, None; Junhua Tang, None; Hugh J. Morris, None; Richard T. Hart, None; Xueliang Pan, None; Jun Liu, None
Support: RO1EY020929 & RO1EY020929-S1

Program Number: 69 **Poster Board Number:** A0056

Presentation Time: 8:30 AM - 10:15 AM

Correlation between preferred sleeping side and optic disc cupping in healthy and glaucomatous patients

Igor Rodrigo Lins da Silva, Natália Y. Valdrighi, Luis G. Biteli, Augusto Paranhos, Tiago S. Prata. Ophthalmology, Federal University of Sao Paulo, Sao Paulo, Brazil.

Purpose: To evaluate the preferred nocturnal sleep position and correlate with optic disc cupping in healthy and glaucomatous patients

Methods: We prospectively enrolled healthy individuals and treated glaucomatous patients (glaucomatous optic neuropathy and reproducible visual field defect) from August 2012 to October 2012. Key exclusion criteria were previous intraocular surgery or any ocular disease other than glaucoma. All participants underwent a standard questionnaire regarding age, sex and preferred sleep position. Data collected also included intraocular pressure (IOP), optic disc assessment by color stereo photographs, central corneal thickness (CCT) and standard automated achromatic perimetry results (24-2 SITA-Standard, Humphrey Field Analyzer II) from both eyes. The questionnaire and optic disc assessment were performed by two independent investigators in a masked fashion

Results: A total of 58 patients were included in the study. The mean office measured IOP for eyes of preferred sleeping side was similar to those of non-preferred sleeping side in both glaucomatous (16 ± 3.8 vs 16.1 ± 4.5 mmHg, $p=0.79$) and non-glaucomatous patients (14.7 ± 2.2 vs 14.6 ± 2.1 mmHg, $p=0.81$). There was no significant CCT difference between eyes in both groups as well ($p \geq 0.41$). Although there was a significant mean cup-to-disc ratio difference between eyes of the preferred sleeping side (0.49 ± 0.23) and fellow eyes (0.42 ± 0.20 , $p=0.01$) in healthy individuals, no significant difference was observed in glaucomatous patients (0.68 ± 0.17 vs 0.73 ± 0.15 ; $p=0.31$). Finally, the agreement between the eye of the preferred sleeping side and the eye with larger cup-to-disc ratio (asymmetry defined as a difference ≥ 0.2) was 74% in healthy individuals, but only 45% in glaucomatous patients.

Conclusions: In healthy individuals, eyes of preferred sleeping side tend to have larger cups (as determined by cup-to-disc ratio) than the fellow eyes, independently of office measured IOP and CCT values. We believe that the lack of association found in glaucomatous patients could be due to the fact that the disease itself, including its duration, IOP fluctuation and susceptibility of each eye, would play a more important role than the preferred sleeping side in these cases.

Commercial Relationships: Igor Rodrigo Lins da Silva, None; Natália Y. Valdrighi, None; Luis G. Biteli, None; Augusto Paranhos, Allergan (F), MSD (F); Tiago S. Prata, Allergan (F), Merck (F), Alcon (F), Germed (C)

Program Number: 70 **Poster Board Number:** A0057

Presentation Time: 8:30 AM - 10:15 AM

Age and glaucoma-related changes in the anisotropic mechanical response of the sclera

Baptiste Coudrillier¹, Jacek K. Pijanka³, Craig Boote³, Joan L. Jefferys², Harry Quigley², Thao D. Nguyen¹. ¹Mechanical

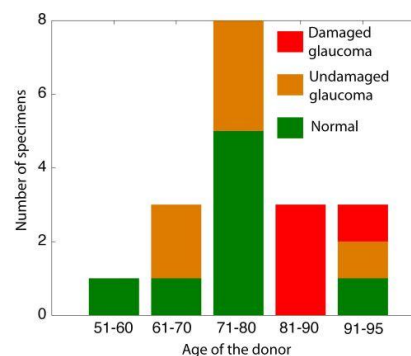
Engineering, The Johns Hopkins University, Baltimore, MD; ²Glaucoma Center of Excellence, Wilmer Ophthalmological Institute, Johns Hopkins University School of Medicine, Baltimore, MD; ³Structural Biophysics Group, School of Optometry and Vision Sciences, Cardiff University, Cardiff, United Kingdom.

Purpose: To determine the effects of glaucoma and age on the mechanical anisotropy of the sclera and the biomechanical environment of the optic nerve head (ONH)

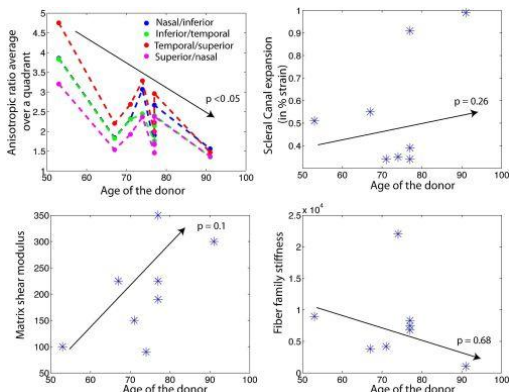
Methods: The biomechanical response to controlled-inflation was measured for 8 normal sclera from 7 donors and 10 glaucoma sclera from 6 donors (Coudrillier et al., Invest. Ophthalmol. Vis. Sci., 2012). Optic nerve cross-sections were graded in masked fashion to determine the presence of axon loss (Fig. 1). Wide-angle x-ray scattering (WAXS) was used to quantify collagen fiber orientation of the prior-inflated specimens (Pijanka et al., IOVS, 2012). Specimen-specific inverse finite element models were developed to calculate the material properties. The mechanical response of the sclera was described using a distributed fiber model incorporating WAXS measurement of the collagen structure. For each specimen, the map of the mechanical anisotropy and measures of the deformation of the ONH were computed (Coudrillier et al., Biomechan. Model. Mechanobiol., 2012). Outcome measures were compared using multivariate analyses accounting for the effects of age and glaucoma damage.

Results: Preliminary results including the 8 normal sclera suggested that the mechanical anisotropy of the peripapillary sclera (PPS) follows a specific pattern with the temporal/superior (TS) quadrant being the most anisotropic and the superior/nasal (SN) quadrant being the least anisotropic ($p < 0.0001$ for the comparison of SN and TN). Older age was predictive of a lower mechanical anisotropy in all quadrants ($p=0.04$, 0.01 , 0.04 and 0.01 for SN, IT, NI, and TS, Fig. 2a), a non-significant increase in matrix stiffness ($p=0.1$, Fig. 2c), and a non-significant increase in fiber family stiffness ($p=0.61$, Fig. 2d).

Conclusions: This study will elucidate how alterations in the degree of fiber alignment within the PPS observed in glaucoma eyes (Pijanka et al., IOVS, 2012) impact the biomechanical environment of the ONH.



Inflated specimens, for which we obtained the WAXS measurements of the fiber structure. Undamaged glaucoma specimens were diagnosed glaucoma by the eye bank but had no axon loss. Damaged glaucoma had mild (10-25%) or severe (50-75%) loss of axons.



(a) Mechanical anisotropy per quadrant of the PPS, (b) scleral canal expansion versus age, (c) matrix shear modulus versus age, and (d) fiber family stiffness versus age.

Commercial Relationships: Baptiste Coudrillier, None; Jacek K. Pijanka, None; Craig Boote, None; Joan L. Jefferys, None; Harry Quigley, Sensimed (C), Genetech (C), Merck (C), Sucampo (C); Thao D. Nguyen, None
Support: EY021500, EY02120, EY01765, the Fight For Sight grant 1360

Program Number: 71 **Poster Board Number:** A0058

Presentation Time: 8:30 AM - 10:15 AM

Correlation of Posterior Scleral Strains with IOP Increase by Volume Controlled Infusion

Hugh J. Morris¹, Benjamin Cruz Perez¹, Junhua Tang¹, Xueliang Pan², Richard T. Hart¹, Paul A. Weber³, Jun Liu^{1,3}. ¹Biomedical Engineering Dept, Ohio State University, Columbus, OH; ²Center for Biostatistics, Ohio State University, Columbus, OH; ³Department of Ophthalmology, Ohio State University, Columbus, OH.

Purpose: Corneoscleral biomechanics may be important modulators of dynamic intraocular pressure (IOP). This study tested the hypothesis that IOP increase, induced by controlled increase in intraocular volume, is correlated with the biomechanical responses of the posterior sclera.

Methods: Eight porcine globes were tested with 24hrs postmortem. The globes were first perfused with PBS at a constant pressure of 15mmHg and then infused at a rate of 15µL/s for one second using a syringe pump (UltraPhD, Havard Apparatus) to induce an IOP increase. IOP was monitored at a sampling rate of 20Hz using a pressure sensor (TAM-A, Havard Apparatus) and the maximal increase in IOP (ΔIOP) during the infusion was recorded. The sclera shells were then prepared and clamped on a custom-built chamber for inflation testing. The strains along the circumferential and meridian directions on the temporal superior region of the posterior sclera, induced by inflation of the sclera shell from 5 to 45 mmHg, were measured by ultrasound speckle tracking (Tang & Liu, J. Biomech Eng 2012, 134(9)). The relationships between the sclera strains and ΔIOP were evaluated using Pearson correlation coefficients.

Results: ΔIOP was 10.9 ± 2.4 mmHg at a 15 µl volume infusion. Along the circumferential direction, the axial strains in the posterior sclera were -1.0 ± -0.3%, -2.1 ± -0.6%, -2.7 ± -0.8%, and -3.4 ± -1.0%, and the lateral strains were 0.7 ± 0.3%, 1.2 ± 0.5%, 1.4 ± 0.5%, and 1.6 ± 0.6%, at pressures of 10, 20, 30, and 45 mmHg. Correlation coefficients between ΔIOP and circumferential axial strains ranged from 0.73 and 0.79 for inflation pressures from 10 to 45 mmHg (all p<0.05). Correlation coefficients between ΔIOP and circumferential lateral strains were -0.57 to -0.73 at different inflation pressures (p-values ranged from 0.039 to 0.139). Similar correlations were observed in the meridian strains, but the p-values were generally

larger.

Conclusions: This study showed lower axial compression and smaller lateral extension in the posterior sclera was associated with a higher IOP increase during a given volume infusion. This result provided preliminary experimental evidences to the link between corneoscleral biomechanics to IOP dynamics, which may play an important role in understanding IOP-associated glaucomatous damage. Future studies with a larger sample size are needed to verify these results..

Commercial Relationships: Hugh J. Morris, None; Benjamin Cruz Perez, None; Junhua Tang, None; Xueliang Pan, None; Richard T. Hart, None; Paul A. Weber, None; Jun Liu, None
Support: NIH Grant RO1EY020929

Program Number: 72 **Poster Board Number:** A0059

Presentation Time: 8:30 AM - 10:15 AM

The Biomechanical Response of Optic Nerve Head Astrocytes to Compressive Insult

Kenneth W. Olsen², John G. Flanagan^{1,2}. ¹Optometry and Vision Science, University of Waterloo, Waterloo, ON, Canada; ²Ophthalmology and Vision Sciences, University of Toronto, Toronto, ON, Canada.

Purpose: To investigate the biomechanical response of human optic nerve head astrocytes to compressive insult.

Methods: Primary human optic nerve head astrocytes were grown to confluence on pre-stretched, syalastic membranes (Flexcell® Bioflex® plates), using a custom built device. Media was changed twice weekly with DMEM/F12 media containing 10% FBS and 1% pen/strep. Upon reaching confluence the cells were serum deprived for 24 hours and subjected to 12% cyclic compression at 1 Hz using the FlexerCell® Strain System FX-4000 for 2 hours (n=3). Control cells were also serum deprived for 24 hours followed by another 2 hours (n=3). Cell lysates were collected and proteomic analysis was carried out to determine protein regulation using the LTQ Orbitrap Velos®. Proteins of interest were selected based on statistical significance (p<0.05) and fold change (>±1.5) and analyzed using the Ingenuity Systems' IPA® biomolecular analysis software.

Results: Of the 875 unique proteins discovered 60 were determined to play an important role in the response of astrocytes to compressive strain. Several networks were identified to be involved in the response including cell morphology, cellular assembly and organization, cellular function and maintenance, cell cycle, and cell-to-cell signaling and interaction. Proteins of particular interest for further mechanistic investigation included FLNB (+4.3 fold), TGFBI (+4.1 fold), and RHOA (+1.6). Proteins previously identified to be regulated by biomechanical stretch were also seen here including ANXA4 (-2.1 fold), S100 (A16, -10.0 fold), and ROA (+1.7 fold).

Conclusions: We have identified several proteins and protein networks of interest following the response of human ONH astrocytes to compressive insult. In particular several proteins involved in pathways known to be regulated in activated astrocytes were identified including TGFBI which is associated with extra cellular matrix remodelling, and RHOA and FLNB which are involved with reorganization of the cytoskeleton and cell morphology.

Commercial Relationships: Kenneth W. Olsen, None; John G. Flanagan, Heidelberg Engineering (C), Heidelberg Engineering (R), Heidelberg Engineering (F), Carl Zeiss Meditec (C), Carl Zeiss Meditec (R), Carl Zeiss Meditec (R), Alcon Pharmaceuticals (R), Alcon Pharmaceuticals (R), Optovue Inc (F), Optovue Inc (F), Photon etc (F), Photon etc (F)

Support: Glaucoma Research Society of Canada, Canadian Institutes of Health Research, Vision Science Research Program Scholarship, U of T.

Program Number: 73 **Poster Board Number:** A0060

Presentation Time: 8:30 AM - 10:15 AM

Correlations between Lamina Cribrosa Microarchitecture and Thickness in Normal Non-Human Primate (NHP) Eyes

Howard Lockwood¹, Juan Reynaud¹, Hongli Yang¹, Stuart K. Gardiner¹, J Crawford C. Downs², Claude F. Burgoyne¹.

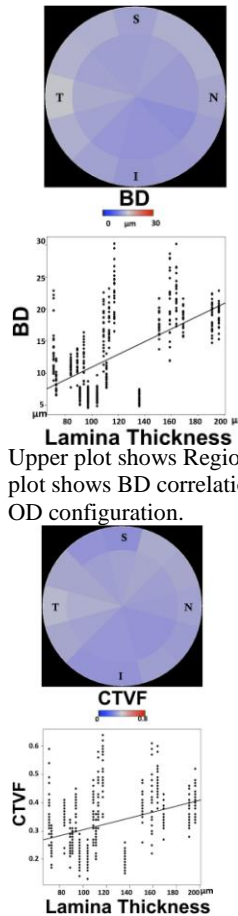
¹Discoveries in Sight Research Laboratories, Devers Eye Institute, Legacy Research Institute, Portland, OR; ²Ophthalmology, University of Alabama at Birmingham, Birmingham, AL.

Purpose: To calculate and characterize the regional distributions of lamina cribrosa (LC) beam diameter (BD), pore diameter (PD), connective tissue volume (CTV) and connective tissue volume fraction (CTVF) from high-resolution, digital 3D optic nerve head (ONH) reconstructions of 23 normal NHP eyes so as to identify their correlations to LC thickness.

Methods: ONH reconstructions of 23 eyes (age 1.4 - 32.2 yrs) were aligned to a clinical photograph or confocal scanning laser tomographic (CSLT) image and the lamina cribrosa was 3D segmented [IEEE Trans Med Imag, 2006; 25:245-255]. Each voxel was assigned a “diameter” value based upon the largest sphere that fit inside the “beam” or “pore” in which it was contained. CTV was defined to be the total volume of beam voxels. CTVF was defined to be the ratio of CTV to total volume (pore + beam voxels). ONH, BD, PD, CTV and CTVF data were transformed into right eye orientation and mapped to a cylinder of radius 1.5 mm and 120 μm thickness. Data were regionalized into 12 sectors using the BMO centroid to foveal (FoBMO) axis as the horizontal midline allowing direct comparisons between eyes with varying laminar and scleral geometries. Mean BD and PD within each sector were normalized by dividing them by the standard deviation to ensure homogeneity of the residuals and hence validity of the subsequent analysis. Mixed effects models were constructed to detect effects of LC thickness accounting for spatially correlated data within each eye.

Results: BD (Mean / SD), CTV and CTVF were all significantly predicted by LC thickness; $p=0.005$ for BD, $p<0.001$ for CTV, and $p=0.043$ for CTVF. No relation was found between LC thickness and PD, $p=0.149$.

Conclusions: These data expand our previous characterizations of normal NHP LMA [H. Lockwood et al, ARVO, 2012; Roberts, et al IOVS. 2009;50:681-690] to include laminar BD, PD, CTV and CTVF to a total of 23 normal eyes. The regional distributions of normal NHP laminar BD, PD, CTV and CTVF are eye-specific, however pooled overall data for all 23 eyes (see plots below) suggest that BD and CTVF are correlated to LC thickness.



Lamina Thickness
Upper plot shows Regional BD averages within 12 sectors. Lower plot shows BD correlation to lamina thickness. All regional data in OD configuration.

Lamina Thickness
Upper plot shows Regional CTVF averages within 12 sectors. Lower plot shows CTVF correlation to lamina thickness. All regional data in OD configuration.

Commercial Relationships: Howard Lockwood, None; Juan Reynaud, None; Hongli Yang, None; Stuart K. Gardiner, Allergan (R); J Crawford C. Downs, None; Claude F. Burgoyne, Heidelberg Engineering (F), Heidelberg Engineering (C)

Support: NIH/NEI R01-EY011610, Legacy Good Samaritan Foundation; Sears Medical Trust; Alcon Research Institute, Heidelberg Engineering, GmbH, Heidelberg, Germany (equipment and unrestricted research support), Reichert Instruments (equipment).

Program Number: 74 **Poster Board Number:** A0061

Presentation Time: 8:30 AM - 10:15 AM

Optic nerve head and peripapillary morphometrics in myopic glaucoma

Sieun Lee¹, Sherry X. Han², Mei Young², Paul Mackenzie², Mirza Faisal Beg¹, Marinko V. Sarunic¹. ¹School of Engineering Science, Simon Fraser University, Burnaby, BC, Canada; ²Ophthalmology and Visual Science, University of British Columbia, Vancouver, BC, Canada.

Purpose: To investigate the shape features in the myopic optic nerve in glaucoma.

Methods: Volumetric images of ONH were acquired using a custom 1060nm Swept Source OCT system at a rate of 100 kHz. The images were semi-automatically segmented for inner limiting membrane (ILM), nerve fiber layer (NFL), Bruch’s membrane (BM), and choroid-sclera boundary. 14 age-matched glaucomatous and normal subjects (9 glaucomatous, 5 normal, mean age = 58.9 ± 6.8) and 5

younger normal subjects (mean age = 29.8 ± 3.4) were imaged. All subjects had axial length > 24 mm. The morphometric parameters were: the BM opening (BMO) shape, the posterior bowing of BM, and the thickness of NFL and choroid. Bowing and thickness were plotted in 2D color maps. Multiple regression was performed with age, axial length (AL), and visual field mean deviation (MD).

Results: The BMO area ($r = .78, p < .001$) and eccentricity ($r = .62, p = .005$) were correlated with AL. Several BMOs displayed “saddling” with the longer ends protruding anteriorly. BM bowing was correlated with AL among the older subjects. Inter-eye BM bowing difference was correlated with inter-eye MD difference ($r = -.684, p = .002$). Choroidal thickness was inversely correlated with age ($r = -.474, p = .003$) and AL ($r = -.484, p = .002$). Superior-nasal and nasal region showed the least amount of BM bowing and the thickest choroid.

Conclusions: We demonstrated a comprehensive shape analysis pipeline in a study of the ONH in normal and glaucomatous subjects with myopia. The results suggest larger axial length is associated with larger and more elliptical BMO, greater BM bowing, and thinner choroid. Severity of glaucoma was associated with increased BM bowing in inter-eye comparison.

Commercial Relationships: Sieun Lee, None; Sherry X. Han, None; Mei Young, None; Paul Mackenzie, None; Mirza Faisal Beg, None; Marinko V. Sarunic, None

Program Number: 75 **Poster Board Number:** A0062

Presentation Time: 8:30 AM - 10:15 AM

Local Stiffness of Rat Trabecular Meshwork

Fan Yuan^{1,2}, Lucinda J. Camras¹. ¹Biomedical Engineering, Duke University, Durham, NC; ²Ophthalmology, Duke University, Durham, NC.

Purpose: Stiffness of trabecular meshwork (TM) may play an important role in regulating outflow resistance in healthy and glaucomatous eyes (Last et al., 2011; Camras, et al., 2012). To investigate its effects on pathogenesis of glaucoma in rodent models, we developed a technique to determine TM stiffness in rat eyes using atomic force microscopy (AFM).

Methods: Rat eyes were enucleated immediately after death and perfused with Evans Blue dye (0.5 mg/mL) for 15 min. The dye perfusion allowed us to better visualize TM location in subsequent tissue dissection and tissue assignment with the AFM probe. Incisions were made in the posterior sclera to remove the iris, lens, choroid, and retina leaving only the ocular shell (cornea, sclera, and TM) intact. The shell, with the TM facing upwards, was flat mounted to a petri dish using glass coverslips. Histological examination was performed to check any damages of TM caused by tissue dissection. A probe with gold-coated colloid (5 μm in diameter) was used to indent the cornea, sclera, and TM at a velocity of 5 $\mu\text{m}/\text{sec}$. The Hertz equation was used to calculate the Young’s modulus (E) of tissues.

Results: The average Young’s modulus of TM was 91.4 ± 0.6 Pa, which was lower than the stiffness of cornea and sclera measured in the same eye. Histological examination confirmed that TM structures were still intact post-dissection. Additional studies are being conducted to determine the accuracy of measurements and regional variation of E in the ocular shell.

Conclusions: A rat model was developed for investigation of TM stiffness and its effects on outflow resistance. The enabling technique developed in this study will allow investigators to use the rat model to evaluate mechanisms of TM stiffness changes related to aging or pathogenesis of glaucoma. It can also be used to study efficacies of interventions and drug treatments that are designed to modulate TM stiffness.

©2013, Copyright by the Association for Research in Vision and Ophthalmology, Inc., all rights reserved. Go to iovs.org to access the version of record. For permission to reproduce any abstract, contact the ARVO Office at arvo@arvo.org.

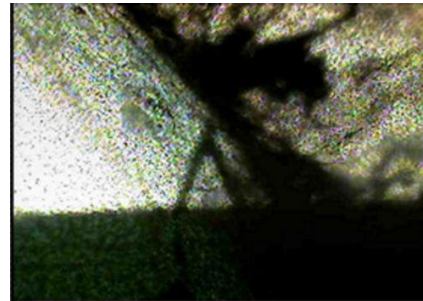


Figure 1. Location of AFM probe. The triangle probe was placed on top of the TM that is indicated by the blue color from Evans blue dye.

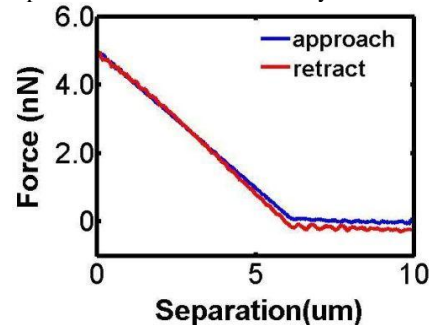


Figure 2. Typical curves of force versus separation distance. Two curves are shown here. One was measured when the AFM probe approached to TM; another was done during probe retraction from the TM sample.

Commercial Relationships: Fan Yuan, None; Lucinda J. Camras, None

Program Number: 76 **Poster Board Number:** A0063

Presentation Time: 8:30 AM - 10:15 AM

Relationship of Optic Disc Cup with Lamina Cribrosa and Prelaminar Tissue in Healthy and Glaucomatous Eyes: In Vivo Quantification with Spectral-Domain Optical Coherence Tomography

Roberto M. Vessani, Vitor G. Prado, Paula D. Borba, Paula D. Silva, Igor Matsubara, Augusto Paranhos, Tiago S. Prata. Glaucoma, Federal University of Sao Paulo, Sao Paulo, Brazil.

Purpose: To investigate the relationship of optic disc cup with lamina cribrosa (LC) thickness and prelaminar tissue thickness in optic nerve head (ONH) using spectral-domain optical coherence tomography (SD-OCT) in healthy and glaucomatous eyes.

Methods: Healthy individuals and glaucomatous patients with a wide range of disease stage (glaucomatous optic neuropathy with reproducible visual field defect) were prospectively enrolled. A complete ophthalmological examination was performed and patients with significant media opacity or any other ocular disease were excluded. All participants underwent SD-OCT imaging (Spectralis; Heidelberg Engineering GmbH, Heidelberg, Germany). Subjects were imaged using the EDI technique. The following ONH parameters were measured by an experienced examiner masked to patients clinical data: central LC thickness, prelaminar tissue thickness, Bruch’s membrane opening and central cup depth. Possible associations between these parameters were evaluated.

Results: Twenty-one eyes of 21 patients were included. Multiple regression analysis (controlled by optic disc size) revealed a significant negative association between cup depth and prelaminar tissue thickness ($r = -0.63, p = 0.01$). Cup depth was also significantly correlated with LC thickness ($r = -0.48, p = 0.02$). Eyes with deeper optic disc cup presented thinner LC.

Conclusions: In this study, in vivo assessment of ONH structures in healthy subjects and glaucomatous patients revealed that eyes with deeper ONH cup presented less prelaminar tissue and thinner lamina cribrosa, independent of optic disc size.

Commercial Relationships: Roberto M. Vessani, ALLERGAN (R); Vitor G. Prado, None; Paula D. Borba, None; Paula D. Silva, None; Igor Matsubara, None; Augusto Paranhos, Allergan (F), MSD (F); Tiago S. Prata, Allergan (F), Merck (F), Alcon (F), Germed (C)

Program Number: 77 **Poster Board Number:** A0064

Presentation Time: 8:30 AM - 10:15 AM

Through-thickness variation of human scleral strains in response to IOP elevation measured by ultrasound speckle tracking

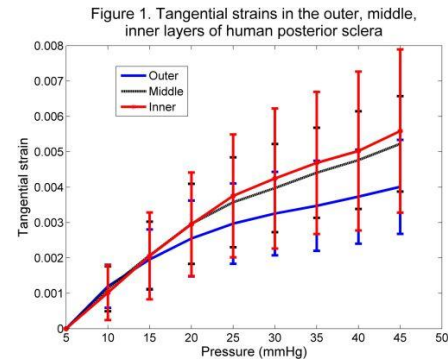
Jun Liu^{1,2}, Junhua Tang¹, Richard T. Hart¹, Cynthia J. Roberts^{2,1}, Paul A. Weber², Xueliang Pan³. ¹Department of Biomedical Engineering, Ohio State University, Columbus, OH; ²Department of Ophthalmology, Ohio State University, Columbus, OH; ³Center for Biostatistics, Ohio State University, Columbus, OH.

Purpose: Scleral mechanical properties are important factors influencing the mechanical states of the optic nerve head (ONH). This study aimed to examine the through-thickness variations of strains experienced by human posterior sclera during intraocular pressure (IOP) elevations.

Methods: Eleven human globes from 7 donors (age from 57 to 73 yo) were tested. Scleral shells were prepared and mounted onto a custom-built inflation chamber. An ultrasound probe (55MHz, Vevo660, Visualsonics) was employed to acquire 2 cross-sectional scans of the posterior sclera near the ONH along the meridian and circumferential directions. Prior to measurements, each globe was preconditioned with 5 cycles of inflation from 5 to 45 mmHg in 60 seconds. Six minutes were allowed for recovery. IOP was then gradually increased from 5 to 45 mmHg at steps of 2.5 or 5 mmHg and the ultrasound radiofrequency signals were acquired at each step. The tangential strains were calculated using a speckle tracking algorithm described previously (Tang & Liu, J Biomech Eng 2012, 134(9)). Each scleral cross-section was divided into three layers (outer, middle and inner) with equal thickness, and the average strains within each layer was calculated and compared.

Results: The average tangential strains in the outer layer were 0.20±0.08%, 0.30±0.11%, 0.35±0.13%, and 0.40±0.13% in the outer layer, 0.21±0.10%, 0.36±0.13%, 0.44±0.13%, and 0.52±0.13% in the middle layer, and 0.21±0.12%, 0.38±0.17%, 0.47±0.20%, and 0.56±0.23% in the inner layer, at pressures of 15, 25, 35 and 45 mmHg, respectively. Consistently lower tangential strains were found in the outer layer than either the inner or middle layer at pressure levels of 30, 35, 40, and 45 mmHg (all P's <0.05, paired t-tests, Fig. 1).

Conclusions: Although tangential strains were small (<0.6%) in average within the physiological range of IOP (< 45 mmHg), significant through-thickness variations were found in the human posterior sclera. This result suggests the need to examine the strains throughout the thickness in order to fully characterize the sclera's response to IOP elevations. The implications and underlying mechanisms of larger strains observed in the inner layers of the sclera need further investigations.



Commercial Relationships: Jun Liu, None; Junhua Tang, None; Richard T. Hart, None; Cynthia J. Roberts, Oculus Optikgerate GmbH (C), Ziemer Ophthalmic Systems AG (C), Sooft Italia (R), Carl Zeiss Meditec (F); Paul A. Weber, None; Xueliang Pan, None **Support:** NIH RO1EY020929

Program Number: 78 **Poster Board Number:** A0065

Presentation Time: 8:30 AM - 10:15 AM

Ultrasound Biomicroscopy in Congenital and Aphakic Glaucoma

Janet Leath, Carmelina Trimboli-Heidler, Mohamad S. Jaafar. Ophthalmology, Children's National Medical Center, Washington, DC.

Purpose: Our purpose was to test the hypothesis that anterior segment anatomy is 1) predictive of disease course and 2) instrumental in prospective surgical planning for children with congenital and aphakic glaucoma. Dynamic ultrasound biomicroscopy affords ophthalmologists the opportunity to assess the anterior segment in 3 dimensions and to assess structures not visible by direct observation such as iris thickness, anterior chamber depth, and ciliary body dimensions. An understanding and characterization of the anatomic abnormalities in eyes with uncontrolled intraocular pressure may help plan an anatomic approach to surgical intervention.

Methods: We evaluated 8 patients with congenital glaucoma, 8 patients with aphakic glaucoma, and 10 age-matched controls without glaucoma nor any history of intraocular surgery. Patient ages ranged from 2 months to 12 years old. Each patient underwent ultrasound biomicroscopy with 4 quadrant analysis of corneal thickness centrally and peripherally, angle of corneal approach, anterior chamber depth, thickness of iris at the pupil, thickness of iris midway from insertion to pupil, and thickness of iris at insertion, ciliary body thickness, ciliary body rotation, presence or absence of a Soemmering ring, the maximal thickness of Soemmering ring. Each patient was categorized into clinical categories based upon intraocular pressure ranges, age at onset of glaucoma, and response to both medical and surgical therapy.

Results: We found that several anterior segment parameters had significant differences among the three groups. Patients with congenital glaucoma all had thicker corneas, larger anterior chamber depth, thicker iris at insertion, and thinner iris near the pupil. The aphakic glaucoma patients had statistically smaller anterior chamber depth, and higher pressures correlated directly with presence and size of Soemmering rings.

Conclusions: An understanding and characterization of the anatomic abnormalities in eyes with uncontrolled intraocular pressure may help predict prognosis. This information may also guide treatment in selecting location for glaucoma surgery in terms of clock hour location and also whether to intervene at the angle, to utilize filtering or tube surgery, or to opt for ciliary body laser intervention. Future

studies will be needed to correlate pre-operative anatomy with results after surgical intervention.

Commercial Relationships: Janet Leath, None; Carmelina Trimboli-Heidler, None; Mohamad S. Jaafar, None

Program Number: 79 **Poster Board Number:** A0066

Presentation Time: 8:30 AM - 10:15 AM

Racial Differences in Human Scleral Material Properties

Rafael Grytz^{1,2}, Massimo A. Fazio¹, Vincent Libertaux¹, Luigi Bruno³, Stuart K. Gardiner⁴, Christopher A. Girkin¹, J Crawford C. Downs^{1,2}. ¹Department of Ophthalmology, University of Alabama at Birmingham, Birmingham, AL; ²Department of Biomedical Engineering, University of Alabama at Birmingham, Birmingham, AL; ³Department of Mechanical Engineering, University of Calabria, Calabria, Italy; ⁴Devers Eye Institute, Portland, OR.

Purpose: To determine the racial differences in the material properties of posterior scleral shells from human donors of European (n=20 eyes) and African (n=11 eyes) descent.

Methods: Posterior scleral shells were subjected to IOP elevations from 5 to 45 mmHg and the resulting full-field displacements were recorded using laser speckle interferometry. Eye-specific finite element models were generated based on experimentally measured scleral shell surface geometry and thickness. Inverse numerical analyses were performed to identify material parameters for each eye by matching experimental deformation measurements to model predictions using a microstructure-based constitutive formulation that incorporates the crimp response and anisotropic architecture of scleral collagen fibrils. Generalized Estimating Equation models were constructed to determine whether there was a significant effect of race on the fitted material parameters while accounting for age and intra-donor correlations.

Results: The age-dependent scleral shear modulus is significantly higher (p=0.019) and the collagen fibril crimp angle is lower in donors from African descent, although this did not reach conventional statistical significance (p=0.057, Fig. 1). The IOP-dependent in-plane strains in the peripapillary sclera are significantly lower in donors from African descent (p<0.015 for all IOP levels, Fig. 2).

Conclusions: Results show that posterior sclera of donors of African descent are stiffer compared to donors of European descent due to both a higher shear stiffness of the nonfibrillar matrix and a lower level of stretch at which the collagen fibrils uncrimp and stiffen. These differences may be due to a higher collagen cross-linking density in donors of African descent and relate to a higher susceptibility to glaucoma.

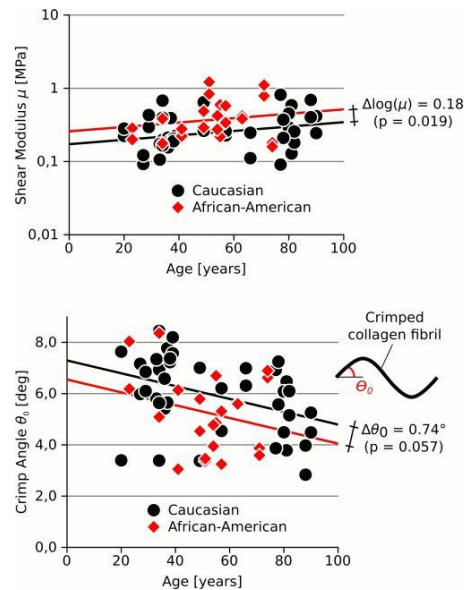


Fig. 1. Top: Fitted shear moduli versus age showing a significantly higher shear modulus in donors of African descent (p=0.019). Bottom: Fitted crimp angle of collagen fibrils versus age showing evidence for a lower crimp angle in donors of African descent (p=0.057).

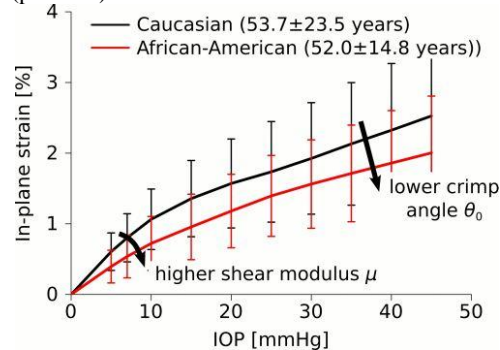


Fig. 2. In-plane strain in the peripapillary sclera versus IOP (mean, standard deviation) showing significantly smaller strains in donors from African descent (p<0.015). The lower compliance of the peripapillary sclera in donors of African descent is mainly due to a higher shear modulus and a lower crimp angle of collagen fibrils.

Commercial Relationships: Rafael Grytz, None; Massimo A. Fazio, None; Vincent Libertaux, None; Luigi Bruno, None; Stuart K. Gardiner, Allergan (R); Christopher A. Girkin, SOLX (F), Heidelberg Engineering (F); J Crawford C. Downs, None **Support:** NIH Grants R01-EY18926, R01-EY19333; Legacy Good Samaritan Foundation Portland, Oregon, USA; Eye Sight Foundation of Alabama; Research to Prevent Blindness Physician-Scientist Award

Program Number: 80 **Poster Board Number:** A0067

Presentation Time: 8:30 AM - 10:15 AM

An Estimate of Intracranial Force on the Optic Nerve Head in Healthy Individuals

John H. Liu¹, Robert N. Weinreb¹, Alan R. Hargens². ¹Dept of Ophthalmology, Univ of California, San Diego, La Jolla, CA; ²Dept of Orthopaedic Surgery, Univ of California, San Diego, San Diego, CA.

Purpose: Recent reports suggest that the physiological imbalance of transmural pressure difference (intraocular pressure minus

intracranial pressure) within the optic nerve head is involved in glaucoma pathogenesis and in visual abnormalities associated with long-duration spaceflight. We explored the usage of pulse amplitude of anterior-posterior transcranial ultrasound waveform as a surrogate measure of intracranial force on the optic nerve head.

Methods: The experimental model of whole body tilt that alters intracranial pressure by shifting body fluids head-ward was employed. Transcranial ultrasound waveforms were examined in 15 healthy volunteers (aged 18-65 years) positioned at randomly ordered tilt angles between +30° and -90° from the horizontal body position. A pulse-echo transducer was placed on the middle forehead and ultrasound waveforms were recorded in an alignment close to the retrolaminar subarachnoid space toward the optic nerve head. Variations in the ultrasonic time-of-flight were monitored using the pulsed phase locked loop technique for the output voltage of ultrasound transducer. We analyzed if the head-down tilt increased the pulse amplitudes in the output voltage synchronized with the heart beats. Simultaneous effects of body tilt on mean blood pressure and heart rate were also evaluated.

Results: Pulse amplitudes of ultrasonic time-of-flight waveforms varied with body tilt. Repeated-measures ANOVA and regression analyses showed a negative correlation between the body tilt angle and the pulse amplitude ($P < 0.01$, $R^2 = 0.191$). The regression line has the equation: Pulse amplitude = $(-0.01023 \times \text{tilt angle} + 1.158) \times 10^{-4}$ voltage. The calculated change of intracranial diameter in the anterior-posterior skull direction is approximately $0.53 \mu\text{m}$ between the +30° to -90° tilt angles (1.227×10^{-4} voltage). There was no significant correlation between head-down body tilt and altered mean blood pressure or heart rate.

Conclusions: Pulse amplitude of anterior-posterior transcranial ultrasonic time-of-flight waveform has potential as a noninvasive surrogate measure of intracranial force on the optic nerve head.
Commercial Relationships: John H. Liu, Allergan (F), Alcon (F), Aerie (F), Sensimed (F), Bausch + Lomb (F); Robert N. Weinreb, Aerie (F), Alcon (C), Allergan (C), Altheos (C), Amakem (C), Bausch&Lomb (C), Carl Zeiss-Meditec (C), Genentech (F), Haag-Streit (F), Heidelberg Engineering (F), Konan (F), Lumenis (F), National Eye Institute (F), Nidek (F), Optovue (C), Quark (C), Solx (C), Topcon (C); Alan R. Hargens, None
Support: NASA Grant NNX12AL66G

Program Number: 81 **Poster Board Number:** A0068

Presentation Time: 8:30 AM - 10:15 AM

Short-term prospective investigation of filtering bleb by three dimensional anterior-segment optical coherence tomography

Sachi Kojima, Toshihiro Inoue, Nakashima Kei-Ichi, Ayako Fukushima, Hidenobu Tanihara. Ophthalmology, Faculty of Life Sciences, Kumamoto University, Kumamoto, Japan.

Purpose: To quantify filtering bleb parameters using three dimensional anterior-segment optical coherence tomography (3D AS-OCT).

Methods: Prospective observational study. Patients who underwent trabeculectomy with mitomycin C were assessed 2 weeks and 3 months after trabeculectomy. At each visit, intraocular pressure (IOP) was measured and 3D AS-OCT images of the bleb were obtained. Total bleb height, fluid-filled cavity height, bleb wall thickness and bleb wall intensity were measured using custom software. Filtration openings in the 3D AS-OCT image were defined by pits and/or troughs in fluid-filled cavities in both horizontal and vertical rasters and corresponding C-scan images of scleral flap margin in the blebs, and the number and site of filtration opening were analyzed. The localizations of filtration openings were recorded as the distance between the top of the scleral flap and the filtration opening (TFD).

Results: Forty-three eyes of 43 subjects were examined. IOP were 10.1 ± 5.0 and 15.7 ± 8.9 mm Hg, total bleb heights were 0.84 ± 0.29 and 0.89 ± 0.42 mm, fluid-filled cavity heights were 0.35 ± 0.28 and 0.36 ± 0.30 mm, bleb wall thicknesses were 0.47 ± 0.25 and 0.51 ± 0.26 mm, bleb wall intensities were 166.6 ± 33.5 and 158.4 ± 39.0 optical density, numbers of filtration openings were 1.4 ± 0.6 and 1.1 ± 0.7 , and TFDs were 1.9 ± 0.6 and 1.9 ± 0.6 mm in the right side and 1.9 ± 0.6 and 1.9 ± 0.5 mm in the left side at the visits 2 week and 3 months after trabeculectomy, respectively. IOP value was significantly increased ($P < 0.001$), and number of filtration opening was significantly reduced ($P = 0.025$). Every bleb parameter at 2 weeks was positively correlated with that at 3 months after trabeculectomy. TFD at 2 weeks was also positively correlated with that at 3 months in both right and left sides ($P = 0.032$ and 0.005 , respectively). Among all measured bleb parameters at 2 weeks, only bleb wall density and number of filtration openings were correlated with IOP at 3 months after trabeculectomy ($P = 0.017$ and 0.042 , respectively).

Conclusions: 3D AS-OCT was useful to quantify time-dependent changes in bleb morphology after trabeculectomy. Bleb wall density and number of filtration openings at 2 weeks after trabeculectomy may be a prognostic factor of IOP at 3 months.

Commercial Relationships: Sachi Kojima, None; Toshihiro Inoue, None; Nakashima Kei-Ichi, None; Ayako Fukushima, None; Hidenobu Tanihara, None
Support: JSPS KAKENHI Grant Number 22390403,23791994

Program Number: 82 **Poster Board Number:** A0069

Presentation Time: 8:30 AM - 10:15 AM

Geometric Morphometric Analysis of the Peripapillary RPE / Bruch's Membrane complex in Glaucomatous and Normal Eyes

Robert A. Honkanen¹, Patrick A. Sibony¹, Crystal R. Kania³, Yuchen Liu³, Pranav H. Patel¹, Kevin Kaplowitz¹, F. James Rohlf².

¹Ophthalmology, Stony Brook Medicine, Stony Brook, NY; ²Ecology and Evolution, SUNY at Stony Brook, Stony Brook, NY; ³School of Medicine, SUNY Stony Brook, Stony Brook, NY.

Purpose: Geometric Morphometrics (GM) was used to evaluate shape variation (SV) of the peripapillary RPE and Bruch's membrane (ppRPE/BM) complex in a well defined glaucoma (Glc) group and normals (NI).

Methods: We compared SD-OCT images of 96 glaucoma (Glc) Glc and 29 normal (NI) eyes. Glc diagnosis required both a glaucomatous visual field (VF) defect and a corresponding optic nerve abnormality. (IOP not used as a criteria) Data was analyzed using standard GM techniques including a generalized least squares Procrustes superimposition, thin-plate spline, permutation statistical analysis, principal component analysis (PCA), and partial least squares analysis (PLS). Glc status, age, central corneal thickness (CCT), refractive error (RE), peak IOP (IOPmax), IOP at time of OCT scan (IOPscan), visual field mean defect (MD) and pattern standard deviation (PSD) were analyzed as covariables.

Results: NI and Glc eyes have a slight V shape that steepens as the neural canal opening (NCO) is approached. Glc status and RE (increasing myopia) show a statistically significant posterior displacement of the ppRPE/BM complex and a widening of the NCO ($p = 0.1\%$, 1000 permutations). Glc and RE account for 6.3%, and 5.9% of the observed SV. PCA showed 2 main effects. PC 1 (anterior/posterior movement of the ppRPE/BM) and PC 2 (variation in NCO width) account for 44.1% and 36.1% of the SV respectively. There is large overlap in SV between NI and Glc eyes. Regression and PLS analysis showed no statistically significant dependence of SV on age, CCT, IOPmax, or IOPscan. In the Glc eyes, SV was not correlated with type of Glc, MD or PSD.

Conclusions: Evaluation of ppRPE/BM SV using GM can detect abnormal eyes in papilledema and optic nerve sheath meningioma. Glc and NI eyes also show a small, statistically significant difference in ppRPE/BM complex shape. However, this technique is of limited value for determining Glc status because of large overlap in SV between NI and Glc eyes. The lack of correlation between SV and cofactors associated with Glc (IOP/CCT/MD/PSD) also suggests this technique is of limited value for this condition. Optimization of the the technique, perhaps with use of a vertical scan line through the ON may improve the ability to differentiate normal from glaucomatous eyes.

Commercial Relationships: Robert A. Honkanen, None; Patrick A. Sibony, None; Crystal R. Kania, None; Yuchen Liu, None; Pranav H. Patel, None; Kevin Kaplowitz, None; F. James Rohlf, None

Program Number: 83 **Poster Board Number:** A0070

Presentation Time: 8:30 AM - 10:15 AM

Reproducibility of Schwalbe's Line identification using time-domain and spectral-domain OCT

Jyotsna Maram, Xiaojing Pan, Zhou Yuan Zhang, Muneeswar Nittala, Peggy W. Romano, Vikas Chopra, Srinivas Sadda.
Ophthalmology, Doheny eye institute, Los Angeles, CA.

Purpose: The purpose of this study was to evaluate the intra and inter grader reproducibility for identifying the location of Schwalbe's line (SL) using time domain (TD) and spectral domain (SD) anterior segment optical coherence tomography (AS-OCT) imaging.

Methods: AS-OCT imaging of the anterior chamber angle was performed on 20 eyes of 10 healthy normal subjects. All subjects underwent imaging with both a TD-OCT (Visante AS OCT) and a SD-OCT (Cirrus HD-OCT) in a darkened room (1 foot candles at eye) without mydriatic drops using a standardized imaging protocol. For the Visante AS-OCT, both vertical and horizontally-oriented B-scans were obtained to image the nasal and inferior angles. For the Cirrus HD-OCT, a 5-line raster scan was obtained of the nasal angle. For intra-grader reproducibility assessments, images were re-graded by the same grader at a later date after random sorting of images to maintain masking. For inter-grader assessments, a second masked grader reviewed the images. For each case, the grader identified and marked the location of Schwalbe's line and determined its coordinate location relative to the borders of the image.

Results: The mean age of the normal subjects was 30±6 years, and all had open angles by biomicroscopy and by OCT. The mean anterior chamber angle (SS angle) was 46.6±6.8 degrees with the Visante OCT. For intra-grader reproducibility in SL identification, excellent agreement was observed for both the TD-OCT and SD-OCT. The Intraclass correlation coefficients (ICC) were 0.99, 0.96, and 0.99 for nasal TD-OCT, inferior TD-OCT, and SD-OCT respectively (p<0.001 for all). For inter-grader reproducibility, excellent agreement was observed for the SD-OCT (ICC=0.95) but was not quite as consistent overall for TD-OCT (nasal ICC=0.99, but inferior ICC=0.89).

Conclusions: The position of Schwalbe's line can be reproducibly determined using both SD and TD anterior segment OCT. The visualization of the termination of the endothelial cell layer made possible by the high-resolution and sensitivity of SD-OCT likely contributed to the excellent precision and reproducibility of this methods. Though Schwalbe's line is often not as well-seen with TD-OCT, this requiring estimation of its position, application of standardized reading center approaches still allow Schwalbe's to be localized reproducibly.

Commercial Relationships: Jyotsna Maram, None; Xiaojing Pan, None; Zhou Yuan Zhang, None; Muneeswar Nittala, None; Peggy

W. Romano, None; Vikas Chopra, Allergan, Inc. (C); Srinivas Sadda, Allergan (C), Genentech (C), Regeneron (C), Optos (C), Carl Zeiss Meditec (C), Optos (F), Carl Zeiss Meditec (F), Optovue (F)

Program Number: 84 **Poster Board Number:** A0071

Presentation Time: 8:30 AM - 10:15 AM

Effect of axial length on false positive rate of sectoral peripapillary retinal nerve fiber layer thickness

Wakako Yoshinaga, Takehiro Yamashita, Yuya Kii, Minoru Tanaka, Kumiko Nakao, Taiji Sakamoto. Ophthalmology, Kagoshima University, Kagoshima-shi, Japan.

Purpose: To investigate the effect of axial length on false positive rate of the sectoral peripapillary retinal nerve fiber layer (RNFL) thickness in young Japanese healthy eyes when using the built-in normative database.

Methods: Prospective observational cross-sectional study comprised 126 right eyes. All participants (mean age 26.0 ± 4.1) underwent comprehensive ophthalmologic examination, including axial length and peripapillary RNFL thickness imaging. Axial length was measured with the AL-2000 ultrasound device (TOMEY, Japan). RNFL thickness was assessed using the TOPCON 3D OCT-1000 MARK II RNFL 3.4 mm circle scan and divided into twelve 30-degree sectors (clock hours) around the optic disc. The twelve sectorial RNFL thicknesses were evaluated at the 5% probability level for significant disparities in comparison with built in RNFL normative database (false positive sector). The relationship between the number of false positive sector and the axial length was investigated using linear regression analysis.

Results: The mean axial length was 25.43 ± 1.45 mm. Thirty six eyes (28.6%) had one or more false positive clock-hour sectors. The false positive sector was seen with a high frequency in sector 6 (25.4 %). The axial length of the eyes with false positive sectors (26.50 mm) was significantly longer than that of the eyes without false positive sectors (25.00 mm) (p<0.001). The number of false positive sectors was significantly positively associated with the axial length (r=0.50, p<0.001).

Conclusions: In clock hour sectoral RNFL thickness, the number of false positive sectors increased as the axial length increased. The relationship should be considered when using the built-in normative database.

Commercial Relationships: Wakako Yoshinaga, None; Takehiro Yamashita, None; Yuya Kii, None; Minoru Tanaka, None; Kumiko Nakao, None; Taiji Sakamoto, None

Clinical Trial: UMIN000006040

Program Number: 85 **Poster Board Number:** A0072

Presentation Time: 8:30 AM - 10:15 AM

Global and Regional Discordance between Colocalized Heidelberg Retinal Tomograph (HRT) Rim Area and Spectral Domain Optical Coherence Tomography (SDOCT) Minimum Rim Measurements

Ruojin Ren, Hongli Yang, Stuart K. Gardiner, Lin He, Juan Reynaud, Brad Fortune, Shaban Demirel, Claude F. Burgoyne. Optic Nerve Head Lab, Devers Eye Institute, Portland, OR.

Purpose: To quantify global and regional neuroretinal rim area discordance between colocalized HRT Rim Area (RAHRT) and SDOCT minimum rim area (MRASDOCT) measurements in 190 glaucoma or high-risk ocular hypertension subjects.

Methods: Same day SDOCT (48 high-resolution, ONH centered, radial B-scans, Spectralis, 870nm, Heidelberg Engineering) and HRT (Heidelberg Engineering) images from one eye of each patient were colocalized using the HRT and SDOCT fundus reflectance images. For each SDOCT data set, Bruch's membrane opening (BMO) and

the internal limiting membrane (ILM) were hand delineated within every other SDOCT radial B-scan (n=24) allowing MRASDOCT, BMO centroid and the Fovea - BMO centroid (FoBMO) axis to be determined. RAHRT was based on a glaucoma specialist's determination of the clinical disc margin and a 320 µm reference plane. Colocalized HRT and SDOCT data were divided into 12 common FoBMO-based segments (Figure 1) and the magnitude of global and sectoral RAHRT vs MRASDOCT discordance among all 190 eyes was assessed.

Results: While global RAHRT was significantly larger than MRASDOCT (P < 0.001, Wilcoxon signed-rank test) there was wide discordance (Figure 2). Regionally, while RAHRT was significantly larger than MRASDOCT in the temporal inferior, temporal superior, superior temporal, superior, superior nasal and nasal superior sectors (all P < 0.001, Wilcoxon signed-rank test), there was no significant difference in the inferonasal quadrant (Figure 2). Sectoral RAHRT vs MRASDOCT discordance was substantial and similarly variable among all sectors.

Conclusions: SDOCT/HRT colocalization and a common, FoBMO regionalization strategy has allowed a precise comparison between HRT rim and SDOCT minimum rim assessments. HRT overestimates neuroretinal rim area compared to SDOCT especially in the superior and temporal quadrants. This discordance is substantial and varies across individual eyes, but its average magnitude is similar for all sectors. The clinical importance of this discordance is under study.

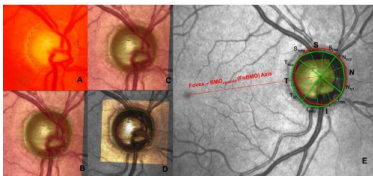


Figure 1. An example of optic disc photograph/SDOCT/HRT fundus reflectance images: colocalization (A-D) and ONH regionalization (E). (A) Optic disc photograph with disc margin (DM) delineation in green. (B) Co-localized disc photograph to the SDOCT IR image to assign HRT contour line in green, using delineated DM points. (C) SDOCT Bruch's membrane opening (BMO) points in red on (B). (D) Co-localized HRT reflective image to SDOCT IR image with HRT contour line in green and BMO line in red. (E) Assignment of fovea to BMOcentroid (FoBMO) axis to SDOCT and HRT data regionalization. 12 ONH sectors (30°/sector) relative to the FoBMO axis in red. The red circle delineating SDOCT BMO line, the green circle representing HRT contour line and yellow area representing HRT cup using the 320µm reference plane.

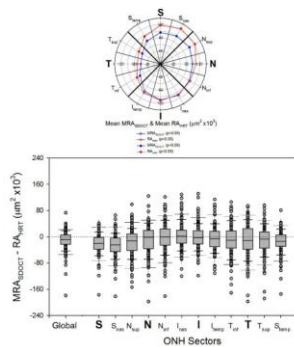


Figure 2. Comparison of colocalized SDOCT minimal rim area (MRA_{SDOCT}) and HRT rim area (RA_{HRT}) values using FoBMO axis regionalization. The upper polar plot shows the mean MRA_{SDOCT} and RA_{HRT} data from 190 patients are regionalized into 12 sectors by using FoBMO axis. The blue circles and lines represent MRA_{SDOCT} while the red circles and lines represent RA_{HRT}. The dashed symbols show sectors that MRA_{SDOCT} are significantly different from RA_{HRT}. The lower bar plot shows individual difference between MRA_{SDOCT} and RA_{HRT} globally and over the 12 regionalized sectors. The circles are the MRA_{SDOCT} - RA_{HRT} difference for each patient. The lower and upper limits of the box indicate +1SD. The horizontal lines inside the box is the median value while the horizontal short lines outside the box represent 5%, 25%, 75%, and 95% quantiles respectively.

Commercial Relationships: Ruojin Ren, None; Hongli Yang, None; Stuart K. Gardiner, Allergan (R); Lin He, None; Juan Reynaud, None; Brad Fortune, Heidelberg Engineering, GmbH (F), Carl Zeiss Meditec, Inc (F); Shaban Demirel, Carl Zeiss Meditec (F), Heidelberg Engineering (R), Heidelberg Engineering (F); Claude F. Burgoyne, Heidelberg Engineering (F), Heidelberg Engineering (C)

Support: NIH R01-EY19674 (SD); NIH R01-EY021281 (CFB); Legacy Good Samaritan Foundation; Sears Medical Trust; Alcon Research Institute, Heidelberg Engineering, GmbH, Heidelberg, Germany (equipment and unrestricted research support), Reichert Instruments (equipment).

Program Number: 86 **Poster Board Number:** A0073

Presentation Time: 8:30 AM - 10:15 AM

Comparisons of optic disc morphology parameters among different optic disc appearances in primary open angle glaucoma - The Glaucoma Stereo Analysis Study (GSAS)

Masaki Tanito¹, Koji Nitta², Maki Katai³, Yasushi Kitaoka⁴, Yu Yokoyama⁵, Kazuko Omodaka⁵, Satoru Tsuda⁵, Toshiaki Nakagawa⁶, Toru Nakazawa⁵. ¹Ophthalmology, Shimane Univ Faculty of Medicine, Izumo, Japan; ²Ophthalmology, Fukui-ken Saiseikai Hospital, Fukui, Japan; ³Ophthalmology, Sapporo Teishin Hospital, Sapporo, Japan; ⁴Ophthalmology, St. Marianna University School of Medicine, Kawasaki, Japan; ⁵Ophthalmology, Tohoku University Graduate School of Medicine, Sendai, Japan; ⁶Research & Development Section, Kowa Company, Ltd., Hamamatsu, Japan.

Purpose: The Glaucoma Stereo Analysis Study (GSAS) is a multicenter, collaborative study to explore characteristics of glaucomatous optic disc morphology by using a stereo fundus camera. Optic disc parameters obtained from GSAS were compared between eyes with different optic disc appearances.

Methods: This five-center, retrospective study enrolled study criteria-eligible 187 primary open angle glaucoma eyes from 187 subjects (100 males, and 87 females, mean ± SD age of 62 ± 9 years). Optic disc recorded by stereo fundus camera (Nonmyd WX3D, Kowa Company Ltd., Japan) were three-dimensionally analyzed by newly developed software to calculate various optic disc parameters. Based on the proposal by Nicoleta and Drance (Ophthalmology 103(4), 640-9, 1996), three independent graders classified subjects' optic disc appearance into 4 subclasses [focal ischemic, FI (n=34); myopic glaucomatous, MY (n=96); senile sclerotic, SS (n=19); and generalized enlargement, GE (n=38)]. Baseline characteristics and optic disc parameters were compared among 4 subclasses by unpaired t-tests. To correct multi-group comparisons, based on Bonferroni's approach, p value of 0.0083 was considered to be statistically significant.

Results: Compared to other subclasses, younger age, lower refractive errors, smaller disc area, larger height variation contour, larger rim volume, and larger horizontal disc tilt angle in MY, lower refractive errors in SS, deeper cup depth and larger cup volume in GE were found. By all 39 optic disc parameters-substituted partition analyses, 3 parameters including horizontal disc tilt angle, mean cup depth, and rim volume were found to be significant; by using these 3 parameters, area under the receiver operating characteristic curves for discrimination of 4 subclasses were calculated to be 0.74, 0.86, 0.81, and 0.87 for FI, MY, SS, and GE, respectively.

Conclusions: The results suggest the possible discrimination of different optic disc appearances by using parameters obtained by stereo fundus camera analyses.

Commercial Relationships: Masaki Tanito, Kowa Company, Ltd. (F), Kowa Company, Ltd. (C); Koji Nitta, Kowa (C); Maki Katai, Kowa Company, Ltd. (F); Yasushi Kitaoka, Kowa Company, Ltd. (F), Kowa Company, Ltd. (C); Yu Yokoyama, Kowa Company (C); Kazuko Omodaka, None; Satoru Tsuda, Kowa (C); Toshiaki Nakagawa, Kowa Company, Ltd. (E); Toru Nakazawa, Kowa Company Ltd. (F), Kowa Company Ltd. (C)

Program Number: 87 **Poster Board Number:** A0074

Presentation Time: 8:30 AM - 10:15 AM

Association between optic disc deformation and lamina cribrosa defects detected on swept-source optical coherence tomography in highly myopic eyes with glaucoma

Yugo Kimura, Masanori Hangai, Kohei Takayama, Hiroshi Yamada, Kenji Suda, Tomoko Hasegawa, Noriyuki Unoki, Tadamichi Akagi, Hanako O. Ikeda, Nagahisa Yoshimura. Ophthalmology, Grad Sch of Med, Kyoto Univ, Kyoto, Japan.

Purpose: Focal lamina cribrosa (LC) defects are reportedly associated with local glaucomatous optic disc changes such as neuroretinal rim thinning/notching and acquired pit of the optic nerve. In this study, we investigated LC defects in highly myopic glaucomatous eyes using 3-dimensional swept-source optical coherence tomography (SS-OCT) and evaluated the association between LC defect location and optic disc parameters indicative of its deformation.

Methods: The eyes (n = 111) of 65 primary open angle glaucoma patients with a spherical equivalent (SE) <-6 diopters were examined with SS-OCT. Mean age of the patients was 51.4 years, mean SE was -9.5 diopters, and mean MD value of the Humphrey visual field analyzer 24-2 program was -11.3 dB. A reference line between the center of the disc and the foveal pit was determined in each eye using SS-OCT fundus photography. The number of LC defects was counted in each eye, and the location was determined by the reference line. The area of peripapillary atrophy (PPA) was measured with a color fundus photograph using image J software, and the PPA area was divided into superior and inferior areas by the reference line. Ovality index and torsion angle of the optic disc (angle of cyclotorsion) were also measured with originally developed software.

Results: LC defects were detected in 46 of 111 eyes (41.4%). Sixteen eyes had a larger number of LC defects in the superior hemisphere (SH group), and 30 eyes had a larger number of defects in the inferior hemisphere (IH group). The area of PPA was larger in the superior hemisphere in 7 eyes of the SH group and 3 eyes of the IH group, whereas it was larger in the inferior hemisphere in 9 eyes of the SH group and 27 eyes of the IH group; this difference was statistically significant (P = 0.02, Fisher exact probability test). The mean cyclotorsion angle was 1.6° in the SH group and 10.3° in the IH group. Mean ovality index was 0.69 in the SH group and 0.72 in the IH group. The optic disc in the IH group was significantly more inferotemporally distorted than in the SH group, whereas no significant differences were found for tilt (cyclotorsion, P = 0.02; ovality index, P = 0.46; unpaired t test).

Conclusions: LC defects were frequently detected in highly myopic eyes with glaucoma. LC defects may be associated with deformation of the optic disc.

Commercial Relationships: Yugo Kimura, None; Masanori Hangai, Topcon (F), Canon (F), Nidek (C), Topcon (C); Kohei Takayama, None; Hiroshi Yamada, None; Kenji Suda, None; Tomoko Hasegawa, None; Noriyuki Unoki, None; Tadamichi Akagi, None; Hanako O. Ikeda, Research grants from the Astellas Foundation for Research on Metabolic Disorders (F), Research grants from the Japan Foundation for Applied Enzymology (F); Nagahisa Yoshimura, Canon (C), Canon (F), Nidek (C), Topcon (F), PCT/JP2011/073160 (P)

Program Number: 88 **Poster Board Number:** A0075

Presentation Time: 8:30 AM - 10:15 AM

Reproducibility of SD-OCT-Based Ganglion-Cell-Complex-Layer Thickness in Early Glaucoma using Commercial and Custom Segmentation Algorithms

Mona K. Garvin^{1,2}, Kyungmoo Lee², Trudy L. Burns⁴, Michael D. Abramoff^{3,1}, Andreas Wahle^{2,1}, Milan Sonka^{2,3}, Young H. Kwon³.

¹Center for the Prevention and Treatment of Visual Loss, Iowa City

VA Health Care System, Iowa City, IA; ²Electrical and Computer Engineering, The University of Iowa, Iowa City, IA; ³Ophthalmology and Visual Sciences, The University of Iowa, Iowa City, IA; ⁴Epidemiology, The University of Iowa, Iowa City, IA.

Purpose: To compute the reproducibility of SD-OCT-based ganglion-cell-layer plus inner-plexiform-layer (GCL+IPL) thickness measurements from both a commercially available algorithm (Cirrus, Carl Zeiss Meditec, Inc.) and a custom-developed algorithm (from the suite of Iowa Reference Algorithms) in early glaucoma patients. **Methods:** Macula SD-OCT volumes (Cirrus, Carl Zeiss Meditec, Inc., Dublin, CA, 200 x 200 x 1024 voxels, 6 x 6 x 2 mm³) were obtained prospectively in both eyes of 58 patients with open-angle glaucoma or glaucoma suspicion on two separate visits. The visits were at most four months apart. The combined GCL+IPL thickness was computed for each SD-OCT volume within an elliptical annulus centered at the fovea (with a vertical inner and outer radius of 0.5 mm and 2.0 mm, respectively; and horizontal inner and outer radius of 0.6 mm and 2.4 mm, respectively) based on two algorithms: (1) a previously published graph-theoretic layer segmentation approach developed at The University of Iowa and (2) the Ganglion Cell Analysis module of version 6 of the Zeiss Cirrus software. The mean overall thickness in the elliptical annulus was computed as well as the thickness within six sectors (Figure 1). For statistical analysis, the SD-OCT volumes of twelve eyes were excluded because of a low signal strength (≤ 5), image acquisition errors, or errors in performing the commercial GCL+IPL analysis in at least one of the repeat acquisitions.

Results: From the 104 analyzed eyes with repeated measurements, the intraclass correlation coefficient (ICC) for the overall elliptical annular GCL+IPL thickness was 0.98 (95% CI 0.97, 0.99) using the Iowa algorithm and 0.95 (0.93, 0.97) using the Cirrus algorithm; the intervisit standard deviation (SD) was 1.63 μ m (Iowa) and 2.52 μ m (Cirrus); and the coefficient of variation (CV) was 2.3% (Iowa) and 3.6% (Cirrus). The sector-based ICCs, intervisit SDs, and CVs are reported in Table 1. The ICCs were significantly higher using the Iowa approach except for Region S where there was no difference in the reproducibility.

Conclusions: SD-OCT-based ganglion cell thickness measurements in early glaucoma patients are highly reproducible.

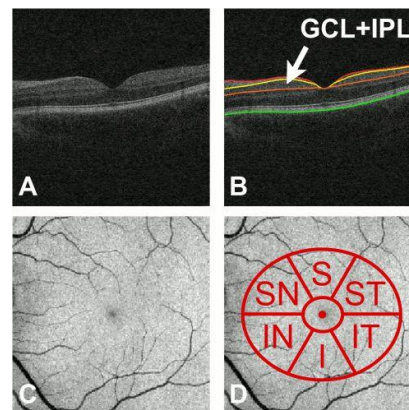


Figure 1. (A) Central B-scan from example volume and (B) corresponding Iowa layer segmentation. (C) Example SD-OCT projection image and (D) six sectors for regional GCL+IPL analysis.

Region	Method	ICC	ICC 95% CI	Intervisit SD	CV (%)
SN	Cirrus	0.86	0.80, 0.90	4.52	6.3
	Iowa	0.94	0.91, 0.96	2.80	3.8
S	Cirrus	0.95	0.93, 0.97	3.04	4.3
	Iowa	0.93	0.90, 0.95	2.85	3.9
ST	Cirrus	0.83	0.76, 0.88	5.12	7.4
	Iowa	0.95	0.93, 0.97	2.74	4.1
IT	Cirrus	0.88	0.83, 0.92	4.61	6.9
	Iowa	0.99	0.99, 0.99	1.60	2.5
I	Cirrus	0.87	0.82, 0.91	4.54	6.7
	Iowa	0.99	0.99, 0.99	1.57	2.3
IN	Cirrus	0.63	0.50, 0.73	7.52	10.8
	Iowa	0.98	0.97, 0.99	1.82	2.5
Overall	Cirrus	0.95	0.93, 0.97	2.52	3.6
	Iowa	0.98	0.97, 0.99	1.63	2.3

* ICCs and CVs estimated for visit 1 and visit 2 data and combined over OD and OS, n=104

Table 1.

Commercial Relationships: Mona K. Garvin, Patent application 12/001,066 (P); Kyungmoo Lee, None; Trudy L. Burns, None; Michael D. Abramoff, IDx LLC (E), IDx LLC (I), University of Iowa (P); Andreas Wahle, None; Milan Sonka, US 7,995,810 (P); Young H. Kwon, None

Support: National Institutes of Health grants R01 EY018853, R01 EY019112, and R01 EB004640; the Department of Veterans Affairs Rehabilitation Research and Development Division (Iowa City Center for the Prevention and Treatment of Visual Loss and Career Development Award 11K2RX000728); Research to Prevent Blindness, New York, NY; an American Glaucoma Society Mid-career Physician Scientist Award; and the Marlene S. and Leonard A. Hadley Glaucoma Research Fund

Program Number: 89 **Poster Board Number:** A0076

Presentation Time: 8:30 AM - 10:15 AM

Observation of human lamina cribrosa in vivo using a novel high sensitive, high resolution optical coherence tomography

Takuhei Shoji, Shin Yoneya, Masayuki Suzuki, Motoyoshi Baba, Hiroto Kuroda. Department of Ophthalmology, Saitama Medical University, Iruma, Japan.

Purpose: To observe the three dimensional structure of human lamina cribrosa (LC) in vivo.

Methods: We have successfully developed a novel optical coherent tomography (OCT) with 200nm band-width spectrometer and femtosecond mode-locked Ti-Sapphire laser as a light source. Twenty healthy volunteers and 20 patients with glaucoma were recruited and examined using this OCT. Raster scan imaging with 10µ step was applied in a 3x3 mm area of the human optic nerve head. Then three dimensional (3D) images was constructed using these image sequences.

Results: Typical, representative tomograms of 10 eyes of healthy volunteers and 10 eyes of glaucoma patients demonstrated the potential of this OCT to detect morphologic change in LC. Lamina pore in the deep layer of LC could be observed in all eyes and seven of 10 eyes in healthy volunteers were confirmed the lamina pore on the surface of LC. The size and configuration of lamina pore were different between the each layer. In the glaucomatous eyes, some of lamina pores on the surface of LC were deformed to linear or oval, but we could observe round pores in deep layer of the LC.

Conclusions: This high sensitive, high resolution prototype OCT and in vivo 3D image could observe lamina pore more deeply and clearly. These findings might lead to better understanding of LC structure and glaucoma pathogenesis.

Commercial Relationships: Takuhei Shoji, None; Shin Yoneya, None; Masayuki Suzuki, None; Motoyoshi Baba, None; Hiroto Kuroda, None

Support: None in the Support field

Program Number: 90 **Poster Board Number:** A0077

Presentation Time: 8:30 AM - 10:15 AM

The Effects of Correcting for Ocular Magnification on Retinal Nerve Fiber Layer and Retinal Ganglion Cell Layer Thicknesses in Macular fdOCT Scans

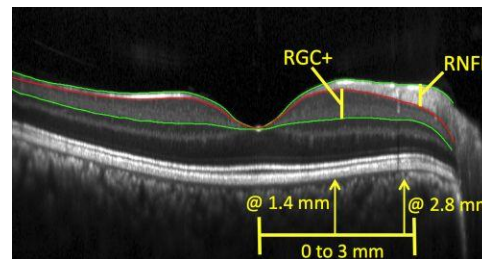
David W. Rhee¹, Alyssa C. Ehrlich¹, Ali S. Raza^{1,2}, Jonathan P. Greenberg³, Tobias Duncker³, Vivienne C. Greenstein³, Donald C. Hood^{1,3}. ¹Psychology, Columbia University, New York, NY; ²Neurobiology and Behavior, Columbia University, New York, NY; ³Ophthalmology, Columbia University, New York, NY.

Purpose: To evaluate the effect of optical corrections on retinal nerve fiber layer (RNFL) and retinal ganglion cell plus inner plexiform layer (RGC+) thicknesses obtained from frequency-domain OCT (fdOCT) macular scans.

Methods: Horizontal line scans across the macula were obtained using fdOCT (Spectralis, Heidelberg, Inc.) from one eye of 253 healthy controls (31.5±29.9 yrs; range 3 to 65 yrs) with biometric data. Eyes were organized into three groups: all 253 eyes (G1), 123 eyes with similar age and refractive errors to those often used in clinical studies (G2; >30 yrs and refractive error ±5 D), and 18 eyes with refractive error <-5 D (G3). RNFL and RGC+ thicknesses were measured over a 3-mm region nasal from the foveal center and at two local regions (see Fig.) using an automated segmentation algorithm with manual corrections.[1] To correct for ocular magnification, the scans were scaled horizontally (corrected) by a factor dependent on corneal curvature and scan focus (in diopters) using the manufacturer's software. This is effectively the same as a correction based on axial length.[2]

Results: The average absolute % differences between uncorrected and corrected scans are shown in the table for the mean and local thicknesses of each group. For all conditions, G3 (high myopes) scans showed the greatest % difference in RNFL and RGC+ thicknesses, while G2 (clinical) scans were affected the least. In addition, RNFL thicknesses were more affected than RGC+ thicknesses in all conditions. For local measurements, the effect of correction depended on the distance from the scan center with both layers more affected at 2.8 than 1.4 mm.

Conclusions: The effect of optical corrections depended on the population characteristics and the nature of the measure; it was relatively small (<5%) for the group with ages and refractive errors similar to those used in clinical studies (G2). While it is thought that optical corrections are necessary for OCT data, in practice, the need for correction will depend on the population, the layer and location of interest, and the purpose of the study. [1] Raza et al. AO, 2011; [2] Bennett et al. Graefe's, 1994.



An fdOCT scan with the RNFL and RGC+ segmented.

Table.		Mean Absolute % Change in Thickness					
		RNFL			RGC+		
		G1	G2	G3	G1	G2	G3
Mean	0 to 3mm	4.0	3.2	11.4	0.9	0.7	2.8
Local	@ 1.4 mm	2.0	1.8	4.4	1.1	1.1	2.5
	@ 2.8 mm	5.2	4.1	13.9	4.2	3.1	13.2

Commercial Relationships: David W. Rhee, None; Alyssa C. Ehrlich, None; Ali S. Raza, None; Jonathan P. Greenberg, None; Tobias Duncker, None; Vivienne C. Greenstein, None; Donald C. Hood, Topcon, In (F)
Support: NIH Grant R01-EY002115

Program Number: 91 **Poster Board Number:** A0078
Presentation Time: 8:30 AM - 10:15 AM

Comparison of Optic Nerve Head Parameters in Myopic and Nonmyopic Glaucoma Eyes

Deana Choi, Martha Kim, Karine D. Bojikian, Mark A. Slabaugh, Philip P. Chen. University of Washington, Seattle, WA.

Purpose: To compare optic nerve head parameters in myopic and nonmyopic glaucoma eyes using enhanced depth imaging spectral-domain optical coherence tomography (EDI SD-OCT) and Heidelberg Retina Tomography (HRT).

Methods: Optic disc images of 103 glaucoma patients were obtained using EDI SD-OCT and HRT. Axial length and central corneal thickness (CCT) were measured. Patients were divided into myopic glaucoma group (axial length more than 24.35 mm; n=52) and nonmyopic glaucoma group (axial length less than 24.35 mm; n=51). Lamina cribrosa thickness and depth, measured with EDI SD-OCT images on Heidelberg Eye Explorer software, were compared between groups. Areas of the optic disc and the cup, cup depth, area and volume of the rims, cup-to-disc area ratio and height variation contour were also compared between groups.

Results: Male gender was more frequent in myopic glaucoma group ($P < 0.001$). Glaucoma type showed no difference between two groups ($P = 0.677$). There was no statistical difference in any parameters related to optic nerve head morphology. The depth and thickness of the lamina cribrosa were not different between myopic and nonmyopic glaucoma groups ($P = 0.536$ and $P = 0.672$, respectively). The CCT of myopic glaucoma group was significantly thinner than that of nonmyopic glaucoma group ($P = 0.011$).

Conclusions: Optic nerve head parameters measured using EDI SD-OCT show no significant difference between myopic and nonmyopic glaucoma patients.

Commercial Relationships: Deana Choi, None; Martha Kim, None; Karine D. Bojikian, None; Mark A. Slabaugh, None; Philip P. Chen, Allergan (C)

Support: D. Franklin Milam MD Fellows Support Fund, Unrestricted grant from Research to Prevent Blindness

Program Number: 92 **Poster Board Number:** A0079
Presentation Time: 8:30 AM - 10:15 AM

The Location of Peripapillary Glaucomatous Defects Seen on Frequency-Domain OCT Scans

Diane L. Wang¹, Ali S. Raza^{1,4}, C. Gustavo De Moraes², Jeffrey M. Liebmann², Robert Ritch³, Donald C. Hood^{1,3}. ¹Psychology, Columbia University, New York, NY; ²Ophthalmology, NYU School of Medicine, New York, NY; ³Ophthalmology, Columbia University, New York, NY; ⁴Neurobiology and Behavior, Columbia University, New York, NY; ⁵Ophthalmology, New York Eye & Ear Infirmary, New York, NY.

Purpose: To examine the locations of glaucomatous damage in the peripapillary retinal nerve fiber layer (RNFL), thickness measurements from frequency domain optical coherence tomography (fdOCT) disc scans were analyzed.

Methods: Optic disc fdOCT volume scans from 54 healthy control eyes and 130 patient eyes, classified as suspect or mild glaucoma, were analyzed. All patient eyes had 24-2 visual fields (VFs) with mean deviations better than -5.5 dB. By hand-correcting automated segmentation [1,2], the RNFL thickness profile was obtained for a

peripapillary circle 1.73mm in radius. RNFL defects were defined as peripapillary regions where the patient's RNFL thickness fell below the 99% confidence limit of control values. The location of a defect in each eye was defined as the point of greatest difference between the patient's and control's RNFL thickness values. The locations of major blood vessels (BVs) were also marked. The BVs were separated into superior-nasal (SN), superior-temporal (ST), inferior-temporal (IT), and inferior-nasal (IN) groups and their locations averaged.

Results: Of the 130 patient eyes, 55 exhibited RNFL defects. The locations of these defects (figure) showed a bimodal distribution in the superior disc, while the locations in the inferior disc showed a single peak. Average BV locations are indicated by the red lines. Defects clustered around the ST, SN, and IT, but not the IN BVs. As expected, the greatest RNFL thickness in controls (green in fig.) was associated with the average locations of the 4 major BV clusters. However, control RNFL thickness was not a perfect predictor for defect location.

Conclusions: The glaucomatous defects in the peripapillary RNFL fall into three regions, two in the superior disc and one in the inferior disc. For the ST, SN and IT region, the locations of the defects are associated both with the major BVs and the regions of thickest RNFL in healthy controls. However, the absence of defects in the IN region indicates that the locations of defects are not simply related to either BV location or RNFL thickness. 1. Raza et al. AO, 2011; 2. Yang et al. Opt Exp, 2011

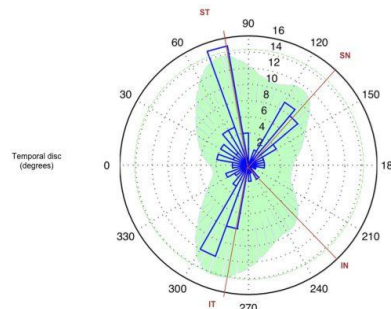


Figure 1. Blue bars: frequency of RNFL defects as a function of location around disc (10° bins). Green region: the mean control thickness scaled to the maximum mean control thickness of 148.9 μm (green circle). Red lines: the locations of the SN, ST, IT, and IN BVs.
Commercial Relationships: Diane L. Wang, None; Ali S. Raza, None; C. Gustavo De Moraes, None; Jeffrey M. Liebmann, Alcon Laboratories, Inc. (C), Allergan, Inc. (C), Allergan, Inc. (F), Carl Zeiss Meditech, Inc (F), Heidelberg Engineering, GmbH (F), Topcon Medical Systems, Inc. (F), National Eye Institute (F), New York Glaucoma Research Institute (F), SOLX, Inc. (C), Bausch & Lomb, Inc (C), Diopsys, Inc. (C), Diopsys, Inc. (F), Merz, Inc. (C), Glaukos, Inc. (C), Quark, Inc. (C); Robert Ritch, None; Donald C. Hood, Topcon, In (F)
Support: NIH Grant EY2115 R01-EY02115

Program Number: 93 **Poster Board Number:** A0080
Presentation Time: 8:30 AM - 10:15 AM

Diagnostic ability of Spectral Domain Optical Coherence Tomography to Detect Diffuse Retinal Nerve Fiber Layer Atrophy: Diffuse Atrophy Imaging Study

Seok Hwan Kim^{1,2}, Ko Eun Kim^{1,3}, Jin Wook Jeoung^{1,3}, Ki Ho Park^{1,3}, Dong Myung Kim^{1,3}. ¹Ophthalmology, Seoul National University College of Medicine, Seoul, Republic of Korea; ²Ophthalmology, Seoul National University Boramae Hospital, Seoul, Republic of

Korea; ³Ophthalmology, Seoul National University Hospital, Seoul, Republic of Korea.

Purpose: To investigate the diagnostic capability of spectral domain (Cirrus) optical coherence tomography (OCT) to detect diffuse retinal nerve fiber layer (RNFL) atrophy.

Methods: This study included 101 eyes from 101 glaucoma patients with diffuse RNFL atrophy and 101 eyes from 101 age-matched healthy individuals. Two experienced glaucoma specialists graded red-free RNFL photographs in eyes with diffuse RNFL atrophy using a 4-level grading system. The area under the receiver operating characteristic curves (AROCs) was compared between normal eyes and eyes with diffuse atrophy. Based on the internal normative database, the sensitivity and specificity of Cirrus OCT were evaluated.

Results: The largest AROC for Cirrus OCT was obtained with the average RNFL thickness, which was 0.94. Comparison of AROC in groups with different RNFL atrophy grades revealed that the Cirrus OCT also has a good discriminating ability. Using an internal normative database with abnormality defined at a <5% level, the overall sensitivity of Cirrus OCT to detect diffuse RNFL atrophy ranged from 75.0% to 87.0%. According to the internal normative database at a <5% level, the highest sensitivity was 87.0% for Cirrus OCT and it was obtained with the TSNIT thickness graph and the deviation map.

Conclusions: The AROC and the sensitivity obtained from Cirrus OCT showed that it has a good diagnostic ability to detect diffuse RNFL atrophy.

Commercial Relationships: Seok Hwan Kim, None; Ko Eun Kim, None; Jin Wook Jeoung, None; Ki Ho Park, None; Dong Myung Kim, None

Program Number: 94 **Poster Board Number:** A0081

Presentation Time: 8:30 AM - 10:15 AM

Peripapillary tilting and central visual field loss in Normal Tension Glaucoma using High-Penetration Optical Coherence Tomography

Shinichi Usui¹, Yasushi Ikuno¹, Yukari Jo¹, Tomoko Asai¹, Tsutomu Kikawa², Masahiro Akiba², Kohji Nishida¹. ¹Ophthalmology, Osaka University Graduate School of Medicine, Suita, Japan; ²Eye Care BU, Topcon Corp, Itabashi-ku, Japan.

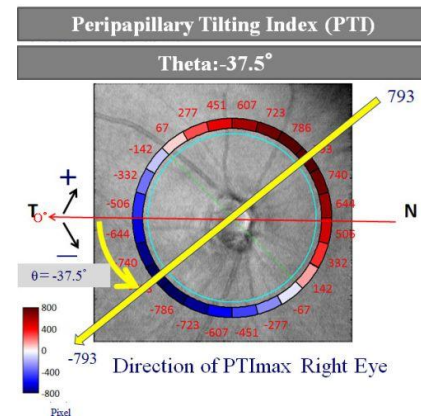
Purpose: To evaluate the relationship between tilting value around the optic disc and visual field loss in normal tension glaucoma (NTG).

Methods: This is a retrospective observational-investigation. Eighty eyes of 47 patients diagnosed as NTG without any other ophthalmic diseases or surgical histories were enrolled. The high penetration OCT (DRI-OCT1, Topcon, Japan) was used for imaging the optic disc. Four-mm diameter circle scan OCT image around the optic disc was extracted from the 3D OCT volume image and then image was divided into the 24 clock hour sectors. To quantify the disc tilting, peripapillary tilting index (PTI; pixel) which was the difference in RPE height between one sector and its counterpart sector was evaluated by using a custom-designed software program. The \pm degree between the tilting line with maximal PTI and the horizontal line of the optic disc was named the tilting degree. Mean deviation (MD,db), mean central threshold value of 4 points within 5 degree (MCTV,db) of visual field were evaluated by Swedish interactive threshold algorithm standard 30-2 test. Axial length (AL,mm) was measured by IOL master. Tukey-Kramer's multiple comparison test was used for statistical comparisons. Differences test for multiple comparisons were judged statically significant at P<0.05.

Results: Eighteen eyes (22.5%) were superiorly tilted disc and 62 eyes (77.5%) were inferiorly. Mean maximal tilting degree was (-

15.1 \pm 14.2 $^\circ$); 31 eyes of -7.5 $^\circ$, 19 eyes of -22.5 $^\circ$, 11 eyes of +7.5 $^\circ$ and 19 eyes of others. Among three group (-7.5 $^\circ$, -22.5 $^\circ$ and +7.5 $^\circ$), age (60.7 \pm 14.7, 55.7 \pm 14.6, 62.6 \pm 12.7)y.o. and AL (25.87 \pm 1.70, 26.21 \pm 1.69, 25.83 \pm 2.37) were no significant differences, whereas maximal PTI was significant differences between -7.5 $^\circ$ and +7.5 $^\circ$ (1155 \pm 545 vs 728 \pm 390, P<0.05) and MD was significant differences between -7.5 $^\circ$ and -22.5 $^\circ$ (-11.5 \pm 7.6 vs -6.5 \pm 5.4, P<0.05). Eighteen eyes of 19 eyes (94.7%) with MCTV under 20db among three group were tilting within \pm 7.5 $^\circ$.

Conclusions: The optic disc of NTG patients with a severe central visual field loss tends to be temporally tilted.



Peripapillary Tilting Index (PTI) and Tilting degree

Commercial Relationships: Shinichi Usui, None; Yasushi Ikuno, Topcon (F), TOMEY (F); Yukari Jo, None; Tomoko Asai, None; Tsutomu Kikawa, TOPCON Corp. (E); Masahiro Akiba, Topcon Corp. (E); Kohji Nishida, Alcon (C), Alcon (F), HOYA (F), Senju (F), Pfizer (F), Santen (F), Osaka University (P)

Program Number: 95 **Poster Board Number:** A0082

Presentation Time: 8:30 AM - 10:15 AM

Imaging the Iris with Swept Source Optical Coherence Tomography - Impact of Iris Volume Measurement on Primary Angle Closure

Heather K. Mak, Guihua Xu, Christopher K. Leung. The Chinese University of Hong Kong, Hong Kong, Hong Kong.

Purpose: To measure iris volume and anterior segment parameters using a swept-source anterior segment optical coherence tomography (OCT) and investigate factors associated with iris volume and iris volume change after pupil dilation in eyes with open-angles and primary angle closure (PAC).

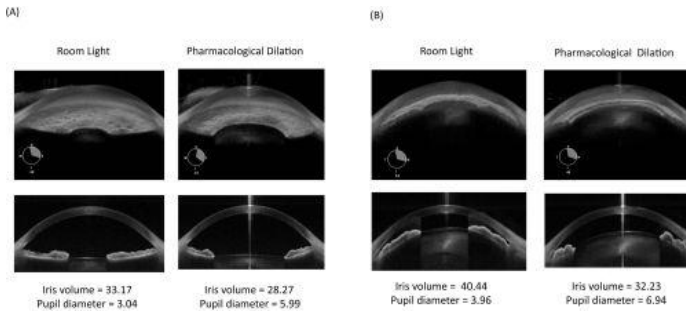
Methods: A total of 73 eyes, including 31 eyes from 21 PAC or PAC-suspect patients, 22 eyes from 14 primary open-angle glaucoma (POAG) patients, and 20 eyes from 13 normal subjects were analyzed as a cross-sectional study. The anterior segment was imaged by the Casia SS-1000 OCT (Tomey, Nogaya, Japan) in room light, dark, and after pharmacological dilation. Iris volume and anterior segment parameters were measured by the instrument software. Linear mixed models were used to examine the association between iris volume and change in iris volume after dilation and each of the following: age, gender, anterior chamber volume (ACV), axial length, pupil diameter, and angle width.

Results: The mean iris volume significantly reduced from light to dark and after pharmacological dilation in angle closure (40.0 \pm 5.2mm³, 38.8 \pm 5.4 mm³ and 32.5 \pm 4.5 mm³, respectively), POAG (39.6 \pm 4.3 mm³, 38.7 \pm 4.4 mm³ and 33.4 \pm 3.4 mm³, respectively) and normal eyes (39.0 \pm 3.9 mm³, 37.0 \pm 3.7 mm³ and 30.4 \pm 3.3 mm³, respectively). Iris volume was negatively associated

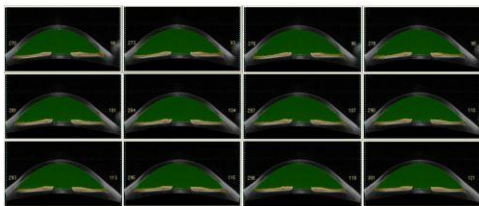
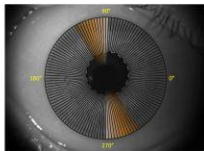
ARVO 2013 Annual Meeting Abstracts by Scientific Section/Group – Glaucoma

with ACV and positively associated with axial length. The change in iris volume/mm change in pupil diameter was 2.11, 2.19 and 2.34 mm³/mm in the angle closure, POAG and normal groups, respectively ($p \geq 0.278$). A smaller ACV and an older age was associated with a smaller change in iris volume/mm change in pupil diameter. A larger iris volume, smaller ACV and larger pupil diameter were significant determinants of smaller angle widths (all with $p \leq 0.001$).

Conclusions: The mean iris volume reduced after pupil dilation in eyes with open-angle as well as in eyes with angle closure, although the degree of reduction was less in eyes with a small ACV. Both iris volume and ACV were important determinants of the anterior chamber angle.



An example illustrating the change in iris volume after pharmacological dilation in an (A) open-angle and (B) angle closure eye.



Shown above are 12 of 64 total B-scans analyzed, illustrating the automated detection by the instrument software of both anterior and posterior boundaries of the iris and posterior boundaries of the cornea.

Commercial Relationships: Heather K. Mak, None; Guihua Xu, None; Christopher K. Leung, Carl Zeiss Meditec (F), Carl Zeiss Meditec (R), Alcon (C), Alcon (R), Alcon (F), Allergan (C), Allergan (R), Tomey (F), Optovue (F)

Program Number: 96 **Poster Board Number:** A0083

Presentation Time: 8:30 AM - 10:15 AM

Diagnostic Efficacy of RNFL Thickness Sectors for Glaucoma Detection

Gary Lee¹, Donald L. Budenz², Robert Chang³, Alan S. Crandall⁴, Christopher A. Girkin⁵, Christopher K. Leung⁶, Arvind Neelakantan⁷, James H. Peace⁸, John S. Werner⁹, Gadi Wollstein¹⁰. ¹Carl Zeiss Meditec, Inc, Dublin, CA; ²Ophthalmology, University of North Carolina School of Medicine, Chapel Hill, NC; ³Stanford Eye Institute, Stanford University, Stanford, CA; ⁴Ophthalmology, Moran Eye Center, University of Utah, Salt Lake City, UT; ⁵Ophthalmology,

University of Alabama at Birmingham, Birmingham, AL; ⁶3/F University Eye Center, Hong Kong Eye Hospital, Hong Kong, China; ⁷Glaucoma Associates of Texas, Dallas, TX; ⁸Ophthalmology and Vision Science, United Medical Research Institute, Inglewood, CA; ⁹Ophthalmology and Vision Science, UC Davis Eye Center, Sacramento, CA; ¹⁰UPMC Eye Center, University of Pittsburgh School of Medicine, Pittsburgh, PA.

Purpose: To compare the diagnostic ability of zones typically used in structure-function mapping against various standard sectors of peripapillary retinal nerve fiber layer (RNFL) measurements in glaucoma.

Methods: SD-OCT data from 140 Glaucoma (MD Mean±SD: -8.4±7.4 dB; 74 mild, 30 moderate, 36 severe by Hodapp-Anderson-Parrish criteria) and 191 age-matched Normal eyes (331 patients total) combined from three prior studies were analyzed post-hoc to generate peripapillary RNFL thickness maps. RNFL TSNIT profiles were extracted and used to generate various sectors, including Average RNFL thickness, quadrants, and clock hours. In addition, sectors proposed by Garway-Heath (GH) for mapping structure to function [1], equivalent sectors used in scanning laser polarimetry (GDx), and mean RNFL thicknesses within all possible combinations of Superior (1-180°) and Inferior (181-360°) sectors were computed. Area under ROC curve (AUC) values and sensitivities at fixed 95% specificity were then calculated from each sector. Pairwise comparisons between AUCs were computed using the standard method of DeLong et al (significance at $P < 0.05$). For comparison purposes, a set of Optimal Superior and Inferior sectors were defined by averaging the endpoints of sectors with AUCs greater than 99.95% of the maximum AUC.

Results: The 99.95% Optimal Superior (41-149°) and Inferior (262-306°) sectors had AUC values of 0.924 and 0.941, respectively, and were significantly better than any other individual sectors in the corresponding hemisphere, except for Average RNFL thickness (0.929), Superior Quadrant (0.922), Inferior Quadrant (0.933), Temporal-Inferior GH sector (0.936), Superior GDx sector (0.919), and Inferior GDx sector (0.929). The sensitivities of those sectors at 95% specificity ranged from 80.0% (Average RNFL thickness) to 75.7% (Temporal-Inferior GH). The AUCs of the four superior/inferior GH sectors (Zones 1-4) were also not significantly worse than any of the 6 standard superior/inferior clock hours (11-1, 5-7 o'clock).

Conclusions: Existing Cirrus sector definitions and Garway-Heath zone-derived RNFL thickness sectors both show good diagnostic ability for glaucoma detection. One GH sector, Temporal-Inferior (Zone 2), is comparable to the best possible RNFL sector (Optimal Inferior).

[1] Garway-Heath, DF et al., 2000. Ophthalmology, 107(10).

Sector	AUC	SE	Sensitivity at 95% Specificity
Average RNFL	0.929	0.016	0.800
SUP-QUAD	0.922	0.017	0.793
CH11	0.875	0.021	0.629
CH12	0.858	0.021	0.457
CH1	0.864	0.021	0.493
TEMPSUP-GH (Zone 4)	0.888	0.020	0.657
NASSUP-GH (Zone 3)	0.865	0.020	0.521
SUP-GDx	0.919	0.017	0.764
SUP-Optimal-99.95%	0.924	0.017	0.786
INF-QUAD	0.933	0.015	0.793
CH5	0.834	0.023	0.564
CH6	0.907	0.017	0.700
CH7	0.909	0.017	0.700
NASINF-GH (Zone 1)	0.865	0.021	0.571
TEMPINF-GH (Zone 2)	0.936	0.014	0.757
INF-GDx	0.929	0.016	0.793
INF-Optimal-99.95	0.941	0.014	0.786

Table 1: AUCs and sensitivities.

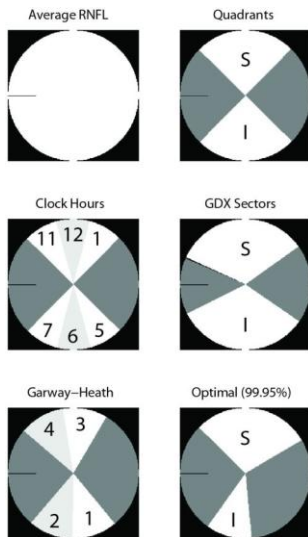


Fig 1: RNFL sectors (right eye orientation).

Commercial Relationships: Gary Lee, Carl Zeiss Meditec, Inc (E); Donald L. Budenz, None; Robert Chang, None; Alan S. Crandall, None; Christopher A. Girkin, SOLX (F), Heidelberg Engineering (F); Christopher K. Leung, Carl Zeiss Meditec (F), Carl Zeiss Meditec (R), Alcon (C), Alcon (R), Alcon (F), Allergan (C), Allergan (R), Tomey (F), Optovue (F); Arvind Neelakantan, None; James H. Peace, B and L (C), merck (C), alcon (C), allergan (C); John S. Werner, None; Gadi Wollstein, Allergan (C)

Program Number: 97 **Poster Board Number:** A0084

Presentation Time: 8:30 AM - 10:15 AM

Comparative evaluation of anterior segment parameters in subgroups of primary angle closure using anterior segment optical coherence tomography

Celeste Guzman¹, Tianxia Gong², Monisha E. Nongpiur¹, Shamira Perera¹, Hwee Kuan Lee², Cheng Li², Baskaran Mani¹, Mingguang He³, Alicia How¹, Tin Aung^{1,4}. ¹Singapore Eye Research Institute, Singapore National Eye Centre, Singapore, Singapore;

²Bioinformatics Institute, A*STAR (Agency for Science, Technology and Research, Singapore, Singapore; ³State Key Laboratory of Ophthalmology, Zhongshan Ophthalmic Center, Sun Yat-sen University, Guangzhou, China; ⁴Yong Loo Lin School of Medicine, National University of Singapore and National University Health System, Singapore, Singapore.

Purpose: Anterior segment optical coherence tomography (ASOCT) allows measurement of anterior segment parameters associated with angle closure. The aim of this study was to compare these parameters in subjects categorized as primary angle closure suspect (PACS), primary angle closure (PAC), primary angle closure glaucoma (PACG), and previous acute primary angle closure (APAC).

Methods: This was a prospective observational study of 425 subjects with angle closure, consisting of 176 PACS, 66 PAC, 125 PACG and 58 APAC subjects. Each subject underwent a standardized eye examination and ASOCT imaging. Customized software (Zhongshan Angle Assessment Program, Guangzhou, China) was used to measure ASOCT parameters, including angle opening distance (AOD), trabecular-iris space area (TISA), angle recess area (ARA), anterior chamber depth (ACD), anterior chamber width (ACW), anterior chamber area (ACA), and anterior chamber volume (ACV), iris thickness (IT), and lens vault (LV). One-way analysis of variance (ANOVA) with Bonferroni adjustments was used to evaluate the mean differences between subgroups. Logistic regression analysis was performed to identify determinants for APAC.

Results: Comparison among the different subgroups showed that ACD, ACA and ACV were significantly smallest, and the iris thickest (IT750) in the APAC group compared to the other subgroups (ANOVA $p < 0.001$ for all). The LV was greatest in the APAC group ($1194 \pm 289 \mu$) followed by PACG ($876 \pm 270 \mu$), PAC ($865 \pm 240 \mu$) and PACS ($789 \pm 253 \mu$), respectively (ANOVA $p < 0.001$). While the APAC group had the narrowest angles, the PACS group had the widest (AOD750: 0.12 ± 0.07 vs. 0.27 ± 0.10 , respectively, $p < 0.001$ and TISA750: 0.07 ± 0.03 vs. 0.15 ± 0.05 , respectively, $p < 0.001$). A multivariate adjusted logistic regression showed that a greater LV ($p < 0.001$), narrower TISA ($p < 0.001$) and a thicker iris ($p = 0.014$) were the major determinants of APAC.

Conclusions: Eyes with APAC had the narrowest angles, smallest anterior segment dimensions, thickest iris and largest LV compared with PACS, PAC and PACG. The LV, TISA750 and IT750 were the major determinants of APAC.

Commercial Relationships: Celeste Guzman, None; Tianxia Gong, None; Monisha E. Nongpiur, None; Shamira Perera, Carl Zeiss Meditec (R), Allergan (R), Pfizer (R); Hwee Kuan Lee, None; Cheng Li, None; Baskaran Mani, None; Mingguang He, None; Alicia How, None; Tin Aung, Alcon (R), Alcon (C), Alcon (F), Allergan (R), Allergan (C), Carl Zeiss Meditec (F), Carl Zeiss Meditec (R), Ellex (F), Ellex (R), Santen (R)

Support: National Medical Research Council, Singapore and Biomedical Research Council, Singapore

Program Number: 98 **Poster Board Number:** A0085

Presentation Time: 8:30 AM - 10:15 AM

Racial Differences in Optic Nerve Head (ONH) and Lamellar Surface Compliance in Normal Human Subjects

Brandon Smith¹, John K. Johnstone², Kulawan Rojananuangnit¹, J Crawford C. Downs¹, Massimo A. Fazio¹, Cynthia Owsley¹, Mark Clark¹, Christopher A. Girkin¹. ¹Department of Ophthalmology, University of Alabama at Birmingham, Birmingham, AL; ²Department of Computer & Information Sciences, University of Alabama at Birmingham, Birmingham, AL.

Purpose: To determine the demographic and ocular factors associated with change in cup depth (CD) and lamina cribrosa depth (LCD) resulting from acute IOP elevations in normal human subjects using Spectral Domain Ocular Coherence Tomography (SDOCT).

Methods: The ONHs of 21 patients were imaged with SDOCT at baseline and after IOP was raised ~15 mm Hg via ophthalmodynamometry for 1 minute. We compared CD and LCD from baseline to increased IOP as follows. Anatomic structures were delineated in 24 radial B-scans of the 48-scan OCT data set using custom software (Strouthidis et al., IOVS 2011). A plane containing the best-fit ellipse was computed using principal component analysis to define Bruch's Membrane Opening (BMO), which was used as the anatomic measurement reference. A mesh was reconstructed from the point cloud for the anterior surface of lamina cribrosa (LC) and Internal Limiting Membrane (ILM). We then measured the distance from the BMO reference plane to the LC mesh and ILM on a uniform sampling grid to calculate the mean position of the LC surface (LCD) and the ILM (cup depth or CD). We analyzed the association of CD and LCD with increased IOP, age, CCT (central corneal thickness), and race (European Descent (ED) or African Descent (AD)).

Results: Significantly greater deepening of the ONH surface upon IOP elevation was independently associated with European heritage, the magnitude of IOP elevation, and thicker CCT. Change in LCD was not significant with any variable.

Conclusions: Individuals of African descent show reduced ONH surface compliance, while greater ONH surface compliance was seen with increasing IOP change and thicker CCT. No significant changes

in laminar compliance were seen within SDOCT volumes with any factor.

	β -coefficient	p-value*
Baseline CD	-631.69	0.00014
Δ CD with Race (ED)	42.6	0.034
Δ CD with Δ IOP	44.1	0.00079
Δ CD with CCT	1.05	0.0002

Models adjusted for race, IOP, CCT, Race*age, Δ IOP*CCT

Commercial Relationships: Brandon Smith, None; John K. Johnstone, None; Kulawan Rojananuangnit, None; J Crawford C. Downs, None; Massimo A. Fazio, None; Cynthia Owsley, Genentech (F), Patent Licensed to: MacuLogix (P), Allergan (R); Mark Clark, None; Christopher A. Girkin, SOLX (F), Heidelberg Engineering (F)

Support: NEI: EY019333, EY018926, NIH: R01AG04212, EyeSight Foundation of Alabama, Research to Prevent Blindness

119 Trabecular Meshwork I

Sunday, May 05, 2013 10:30 AM-12:15 PM

618-620 Paper Session

Program #/Board # Range: 374-380

Organizing Section: Glaucoma

Program Number: 374

Presentation Time: 10:30 AM - 10:45 AM

Expression of ER Stress Markers in the Human Trabecular Meshwork

Markus H. Kuehn, Ophthalmology and Visual Sciences, University of Iowa, Iowa City, IA.

Purpose: Dysfunction and loss of the cells residing within the trabecular meshwork (TM) likely contributes to the development of elevated intraocular pressure (IOP) in glaucoma. Endoplasmic reticulum (ER) stress in TM cells may result from a variety of environmental and genetic factors and can result in cell death. This study was designed to evaluate if ER stress does occur in TM cells of older patients and whether it occurs more frequently in eyes derived from primary open angle glaucoma (POAG) patients than in age-matched controls.

Methods: We conducted an immunohistochemical study using 30 human donor eyes with primary open angle glaucoma and age-matched controls. Human donor eyes were obtained from the local eye bank and preserved in 4% paraformaldehyde within 8 hrs postmortem. Sagittal sections of the anterior segment were incubated with antibodies directed against GADD153/CHOP, GRP78, and caspase 9. Labeling intensities in TM cells were scored independently by two investigators masked to the disease status of the individuals. Levels of these proteins were also determined using Western blots.

Results: Our data demonstrate GADD153 and GRP78 can frequently be detected in the TM of older human eye donors. Moderate or strong immunoreactivity was found in the majority of both POAG eyes and those obtained from control donors. However, samples with the most pronounced immunoreactivity tended to be derived from POAG donors. Caspase-9 immunoreactivity was observed less frequently than that for GADD178 or GRP78 and also occurred in TM cells from both POAG and control donors.

Conclusions: Expression of markers of ER stress is a common feature in TM cell in the aged human eye. These include chaperones (GRP78) as well as pro-apoptotic molecules (Chop, caspase9). The TM of human eyes with POAG contains fewer TM cells suggesting that TM cells in these individuals may be less well equipped to survive sustained ER stress.

Commercial Relationships: Markus H. Kuehn, None

Support: NIH Grants R01EY022044 and RPB Sybil B. Harrington Special Scholar Award

Program Number: 375

Presentation Time: 10:45 AM - 11:00 AM

Functional and Morphological Alterations Associated with Steroid-Induced Ocular Hypertension in Mice

Darryl R. Overby¹, Jacques Bertrand¹, Ozan Tektas², Alexandra Boussommier Calleja¹, W Daniel Stamer³, C R. Ethier^{4,1}, David F. Woodward⁵, Elke Luetjen-Drecoll². ¹Bioengineering, Imperial College London, London, United Kingdom; ²Anatomy II, University of Erlangen-Nürnberg, Erlangen, Germany; ³Ophthalmology, Duke University School of Medicine, Durham, NC; ⁴Biomedical Engineering, Georgia Institute of Technology, Atlanta, GA; ⁵Biological Sciences, Allergan, Inc., Irvine, CA.

Purpose: To determine whether steroid-induced ocular hypertension (OHT) in mice is associated with decreased conventional outflow facility and accumulation of extracellular matrix in the trabecular meshwork (TM) near Schlemm's canal (SC).

Methods: Osmotic mini-pumps (Alzet model 1004; DURECT, Cupertino CA) were implanted subcutaneously in C57BL/6J male mice for systemic delivery of dexamethasone (DEX, 2.7 to 3.8 mg/kg/d, $N = 31$) or PBS control ($N = 28$) over 28 days. IOP was measured weekly by rebound tonometry. After 21-28 days, mice were euthanized and the eyes were enucleated for ex vivo perfusion to measure conventional outflow facility at 35°C with the eye submerged in isotonic saline (21 eyes). Non-perfused eyes were immersion fixed and processed for electron microscopy to visualize the ultrastructure of the TM/SC or immunohistochemistry to stain for alpha-smooth muscle actin (SMA).

Results: In DEX-treated mice, IOP increased from 14.1 ± 1.0 mmHg (mean \pm SD) prior to surgery to 16.7 ± 2.2 mmHg after 21-28 days ($p = 10^{-4}$, $N = 20$ mice). Eleven DEX mice did not survive to 21 days. In PBS-treated mice, IOP was unaffected (13.6 ± 2.3 vs. 12.7 ± 1.6 mmHg, $p = 0.07$, $N = 28$). Conventional outflow facility was 52% lower in DEX-treated mice (0.008 ± 0.003 vs. 0.018 ± 0.005 μ L/min/mmHg, $N = 10$ vs. 11 , $p = 6 \times 10^{-5}$), and there was a significant correlation between facility and final IOP ($p = 2 \times 10^{-3}$, $R^2 = 0.39$, $N = 21$). DEX treatment was associated with increased continuity of the basement membrane underlying the inner wall of SC, which preceded accumulation of plaque-like matrix material within the TM. In DEX-treated mice SMA staining, indicating the presence of myofibroblasts, was observed in the TM and along the outer wall of SC and collector channels but not in the sclera. SMA staining was negligible in the outflow pathway of PBS-treated mice.

Conclusions: Our data show that steroid-induced OHT in mice is associated with a reduction in conventional outflow facility, increased continuity of SC basement membrane, and transformation of outflow pathway cells into myofibroblasts. Because mice have a true SC rather than a discontinuous aqueous plexus as found in most non-human species, the mouse model of steroid-induced OHT may better model steroid-induced glaucoma in humans.

Commercial Relationships: Darryl R. Overby, Allergan, Inc. (F), Allergan, Inc. (C); Jacques Bertrand, None; Ozan Tektas, None; Alexandra Boussommier Calleja, None; W Daniel Stamer, Allergan (F), Alcon (F), Acucela (C), Aerie (C), Cytokinetics (C); C

R. Ethier, None; **David F. Woodward**, Allergan Inc. (E); **Elke Luetjen-Drecoll**, None
Support: Allergan, Inc.

Program Number: 376

Presentation Time: 11:00 AM - 11:15 AM

Effect of transforming growth factor beta-2 signaling and gremlin induction on fibronectin, ocular hypertension, and optic nerve damage in mice

Colleen M. McDowell, Tomi Luan, Iok-Hou Pang, Robert J. Wordinger, Abbot F. Clark. Cell Biology and Anatomy, Univ of North Texas Hlth Sci Ctr, Fort Worth, TX.

Purpose: TGF β 2 induces extracellular matrix (ECM) remodeling and alters the cytoskeleton, which likely contribute to the inefficient function of the TM tissue leading to glaucomatous phenotypes. Bone morphogenetic proteins (BMPs) inhibit these profibrotic effects of TGF β 2. The BMP antagonist gremlin is elevated in glaucomatous TM cells and increases intraocular pressure (IOP) in an ex vivo perfusion culture model. The purpose of this study was to determine whether TGF β 2 and gremlin regulate ECM proteins in the TM, induce ocular hypertension, and cause optic nerve damage in mice.

Methods: Ad5.hTGF $\beta^{226/228}$ or Ad5.Gremlin (2 μ L, 2 X 10⁷ pfu) was injected intravitreally into one eye of A/J mice (n=7-13 mice per group), with the uninjected contralateral eye serving as the control eye. Conscious IOP measurements were taken using a TonoLab rebound tonometer. Optic nerve damage was assessed using the optic nerve damage score of PPD stained optic nerve cross sections. TGF β 2, fibronectin, and gremlin protein expression in the TM was determined by immunofluorescence and immunohistochemistry.

Results: Transduction of the TM with viral vector Ad5.hTGF $\beta^{226/228}$ caused a prolonged, reproducible, and statistically significant IOP elevation. IOPs increased to approximately 25 mm Hg for 8 weeks (p<0.001). IOPs were stable (12-15 mm Hg) in the uninjected control eyes. The TGF β 2 induced ocular hypertension also caused significant optic nerve damage with optic nerve damage scores (ONDS) > 3 (p<0.001) in the injected eye. Intraocular administration of viral vector Ad5.Gremlin also caused significant IOP elevation in A/J mice for 3 weeks (n=9, injected eye 23.2 +/- 5.6 mmHg, uninjected eye 15.5 +/- 2.4; p<0.01). In addition, immunofluorescence and immunohistochemistry demonstrated that intraocular injection of Ad5.hTGF $\beta^{226/228}$ and Ad5.Gremlin increased TGF β 2 and fibronectin expression in the TM.

Conclusions: These results demonstrate that intravitreal injections of Ad5.hTGF $\beta^{226/228}$ and Ad5.Gremlin in A/J mice elevate IOP and upregulate the ECM protein fibronectin. In addition, Ad5.hTGF $\beta^{226/228}$ expression induced significant optic nerve damage. These data demonstrate for the first time gremlin's role in inducing ocular hypertension in an in vivo model system and emphasize the importance of the TGF β 2 signaling pathway in ocular hypertension.

Commercial Relationships: **Colleen M. McDowell**, None; **Tomi Luan**, None; **Iok-Hou Pang**, None; **Robert J. Wordinger**, None; **Abbot F. Clark**, Alcon Research, Ltd. (F)
Support: NIH Grant 5 R21 EY019977-02

Program Number: 377

Presentation Time: 11:15 AM - 11:30 AM

Integrins Modulate Phagocytosis in Human Trabecular Meshwork (TM) Cells

Debjani Gagen¹, Ross W. Clark¹, Paloma B. Liton², Donna M. Peters¹. ¹Pathology, University of Wisconsin, Madison, WI; ²Ophthalmology, Duke University, Durham, NC.

Purpose: To determine if α v β 3 and α v β 5 integrins play a role in phagocytosis in TM cells.

Methods: Phagocytic activity and expression of integrins in immortalized TM-1 cells were analyzed by FACs following a 4h phagocytic challenge with pHrodo-labeled *S. aureus* bioparticles. To determine the role of α v β 5 integrins, TM-1 cells were transfected with siRNA against the β 5 integrin subunit to knockdown α v β 5 integrin expression. Non-targeting siRNA was used as control. To determine if upregulation and/or activation of α v β 3 integrins played a role in phagocytosis in TM cells, TM-1 cells which do not express α v β 3 integrins were transduced with lentiviral vectors expressing wildtype (WT) β 3 integrin or constitutively active (CA) β 3 integrin. The CA- β 3 integrin was created by mutating Thr562 to Asn. In some experiments, HTM cells were treated for 6 days with either Dexamethasone (Dex) to upregulate expression of the β 3 integrin, or EtOH as a control.

Results: Forty-eight hours after transfection, α v β 5 expression was reduced by 70% and phagocytic activity decreased by 74% compared to cells transfected with control siRNA. Dex-treated cells showed a 46% increase in activated α v β 3 integrin expression and exhibited a 50% reduction in phagocytic activity compared to EtOH-treated cells. Expression of the CA- β 3 integrin also decreased phagocytosis by 33% compared to TM-1 cells expressing the WT- β 3 integrin. There was no difference in the phagocytic activity of WT- β 3-expressing cells compared to cells transduced with the empty vector. The decrease in phagocytosis was not due to differences in the level of α v β 3 expression, as α v β 3 integrin levels were similar in WT- and CA- β 3 integrin-expressing TM-1 cells. In contrast, the activated state of α v β 3 integrins was greater by 91% in CA- β 3 integrin-expressing cells compared to WT- β 3 integrin-expressing cells. α v β 5 integrin expression was reduced by 60% in both cell lines compared to cells transduced with an empty vector.

Conclusions: Although α v β 5 integrin is needed for phagocytosis, this study suggests that the Dex-induced decrease in phagocytosis may be due to the activation of α v β 3 integrin. The study also offers some molecular insight into how phagocytosis might be decreased in glaucoma.

Commercial Relationships: **Debjani Gagen**, None; **Ross W. Clark**, None; **Paloma B. Liton**, None; **Donna M. Peters**, None
Support: NIH Grant EY017006 (DMP), NIH Grant EY024090 (DMP)

Program Number: 378

Presentation Time: 11:30 AM - 11:45 AM

Regulation of Cell Plasticity and Fibrogenic Activity in Trabecular Meshwork by Rho/Rho kinase Signaling in the Context of Aqueous Humor Outflow Homeostasis

Padmanabhan P. Pattabiraman¹, Rupalatha Maddala¹, Vasanth Rao^{1,2}. ¹Ophthalmology, Duke University Medical Center, Durham, NC; ²Pharmacology, Duke University, Durham, NC.

Purpose: To test the hypothesis that abnormal activation of Rho/Rho kinase signaling in cells of the aqueous humor outflow pathway may trigger an endothelial to mesenchymal transition (EndMT)-dependent formation of matrix producing myofibroblasts and fibrogenic activity, events which in turn result in impairment of aqueous humor outflow.

Methods: Human primary trabecular meshwork (TM) cell cultures were transfected with plasmids expressing constitutively active RhoA (RhoAV14) or transcription factor MRTF-A, or transduced with adenoviral RhoAV14 and GFP. TM cells were treated separately with lysophosphatidic acid (LPA), TGF- β 2, connective tissue growth factor (CTGF), Rho kinase inhibitor (Y-27632) or anti-fibrotic agent-Pirfenidone. Q-PCR analysis was performed to evaluate fibrogenic activity related changes in gene expression. Quantification of SMA, collagen 1 (Col1), fibroblast-specific protein (FSP1) and secreted total collagen was performed by immunoblotting,

immunofluorescence and the Sircol assay.

Results: Overexpression of RhoAV14 or MRTF-A in serum starved human TM cells resulted in significant increases (>2 fold) in expression of genes involved in fibrosis including Twist1, Slug, FSP1, Col1, miRNA29a and SMA. A significant increase in SMA, FSP1, Col1 and secreted collagen was recorded in TM cells expressing RhoAV14 and cells treated with LPA, TGF β 2 or CTGF (n=4; P<0.05). Inhibition of the transcriptional activity of serum response factor (SRF) using CCG-1423 or knocking down SRF expression, led to a significant decrease in the RhoAV14, LPA and TGF beta-induced increases in the protein levels of SMA, FSP1 and Col1 in TM cells. Finally, Y27632 and Pirfenidone significantly inhibited TGF β 2 induced increases in the protein levels of SMA, FSP1, Col1 and secreted Collagen in TM cells.

Conclusions: Collectively, these observations reveal an important role for the Rho/Rho kinase pathway in induction of TM cell plasticity/ transdifferentiation into matrix and SMA producing myofibroblasts, and identify several significant external cues (TGF-beta, CTGF, LPA) and transcriptional regulators (MRTF, SRF, miRNA-29, Slug, Twist) which control the fibrogenic activity of TM cells via Rho/Rho kinase signaling. These molecular events could be partly responsible for the RhoAV14-induced ocular hypertension in the rat model.

Commercial Relationships: Padmanabhan P. Pattabiraman, None; Rupalatha Maddala, None; Vasanth Rao, None
Support: NEI Grant EY018590

Program Number: 379

Presentation Time: 11:45 AM - 12:00 PM

Elevated stiffness of cultured glaucomatous Schlemm's canal (SC) cells correlates with impaired pore formation

Mark Johnson¹, Ryan M. Pedrigi³, Rocio Vargas-Pinto¹, Ritika Gupta³, Sietse T. Braakman³, C R. Ethier^{4,3}, Kristin M. Perkumas², W Daniel Stamer², Darryl R. Overby³. ¹Biomedical Engineering, Northwestern University, Evanston, IL; ²Ophthalmology, Duke University, Durham, NC; ³Bioengineering, Imperial College London, London, United Kingdom; ⁴Biomedical Engineering, Georgia Tech, Atlanta, GA.

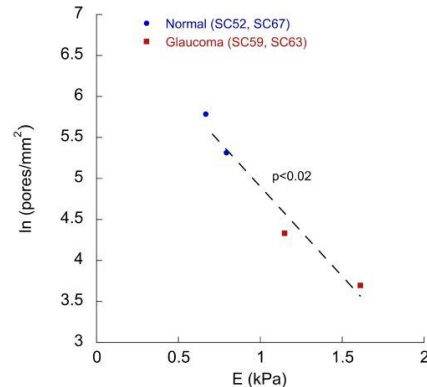
Purpose: SC cells form pores in response to a transcellular pressure drop, likely facilitating aqueous outflow into SC. A characteristic feature of glaucoma is reduced SC cell pore density. We hypothesize that impaired pore formation in glaucoma is due to elevated SC cell stiffness.

Methods: SC cells were isolated from 7 normal and 6 glaucomatous human donor eyes as previously described (Stamer, 1998); 6 strains were used for cell monolayer perfusion to measure pores, and 11 were used for atomic force microscopy (AFM) to measure stiffness. For monolayer perfusion, SC cells were seeded at confluence onto track-etch filter membranes and cultured for 2 days. Monolayers were perfused in the basal-to-apical direction at 6 mmHg for 30 minutes, followed by fixation at the same pressure. Pores were imaged at 12 randomly selected regions (~5500 μm^2 each) per cell layer using scanning electron microscopy, and quantified for total pore area and density. AFM measurements were performed on subconfluent SC cells with pyramidal tips or spherical (4.5 or 10 μm) tips, and Young's modulus (E) was determined using a modified Hertz model. Finite element modeling (FEM) was used to assess the effect of the cell cortex on AFM measurements.

Results: Glaucomatous SC cells were stiffer and formed fewer pores. In comparison to normal SC cell strains, glaucomatous SC cell strains had decreased total pore area (86.9 ± 35.8 vs. 599 ± 128 $\mu\text{m}^2/\text{mm}^2$; mean \pm standard error; p=0.071) and decreased pore density (68.8 ± 14.8 vs 224 ± 53.9 pores/ mm^2 ; p<0.03). Glaucomatous cells were

stiffer (larger E) than normal cells when measured using spherical AFM tips (1.33 ± 0.13 vs 0.90 ± 0.11 kPa; p<0.02), but not pyramidal tips (7.69 ± 1.46 vs. 7.99 ± 0.96 kPa). FEM revealed that stiffness measured by pyramidal tips was more strongly influenced by the cortex, while stiffness measured by spherical tips better reflected the internal cytoskeleton. Comparing cell strains examined by both AFM and perfusions, pore density decreased as SC cell stiffness increased, as measured with spherical tips (see Figure).

Conclusions: Glaucomatous SC cells have impaired pore-forming ability in vitro that correlates with increased cell stiffness. This elevated stiffness appears to reside in the subcortical cytoskeleton as opposed to the cell cortex. Targeting SC cell stiffness may provide a therapeutic approach to lower IOP for glaucoma therapy.



Commercial Relationships: Mark Johnson, None; Ryan M. Pedrigi, None; Rocio Vargas-Pinto, None; Ritika Gupta, None; Sietse T. Braakman, None; C R. Ethier, None; Kristin M. Perkumas, None; W Daniel Stamer, Allergan (F), Alcon (F), Acucela (C), Aerie (C), Cytokinetics (C); Darryl R. Overby, Allergan, Inc. (F), Allergan, Inc. (C)
Support: NIH Grant EY019696, American Health Assistance Foundation (MJ & RV-P), Whitaker International Scholars Program (RMP), Royal Society Wolfson Research Merit Award (CRE)

Program Number: 380

Presentation Time: 12:00 PM - 12:15 PM

Monolayer traction forces of Schlemm's canal endothelial cells

Enhua H. Zhou¹, W Daniel Stamer², Chan Young Park¹, Kristin M. Perkumas², James P. Butler¹, Mark Johnson³, Jeffrey J. Fredberg¹. ¹Environmental Health, Harvard School of Public Health, Boston, MA; ²Duke Eye Center, Duke University School of Medicine, Durham, NC; ³Biomedical Engineering, Ophthalmology, Northwestern University, Evanston, IL.

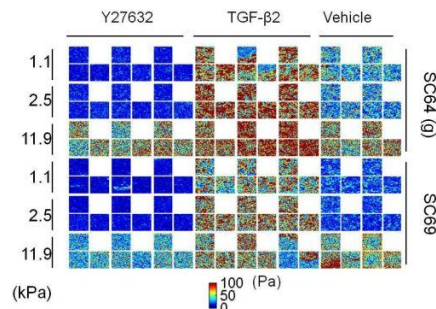
Purpose: The mechanism underlying primary open angle glaucoma is not completely understood, although impaired aqueous humor outflow is implicated. Recent data from our laboratories support the hypothesis that increased outflow resistance in glaucoma is a function of elevated stiffness and contraction of the Schlemm's canal (SC) endothelial cells (Zhou et al. 2011, Journal of the Royal Society, Interface. DOI: 10.1098). However, contractile forces exerted by a confluent SC monolayer have not been studied previously, and the role of substrate stiffness is unknown.

Methods: Human SC cells were isolated from two human donor eyes as previously described (Stamer et al. 1998, IOVS); we cultured human SC endothelial cell monolayers on polyacrylamide gels of 3 stiffnesses, 1.1, 2.5 and 11.9 kPa in shear modulus. Gels were coated with type 1 collagen and labeled with fluorescent beads. Traction forces were obtained using Fourier transform traction microscopy. In a 96-well plate, the effect of TGF- β 2 (1 ng/ml) and Y27632 (10 μM)

on monolayer traction forces was monitored for over 4 days.

Results: We tracked 48 samples simultaneously. TGF- β 2 caused average traction forces to increase gradually over the course of 4 days; the intermediate stiffness gel (2.5 kPa) elicited the greatest increase, by over 3 fold. Y27632 caused average traction forces to decrease abruptly within 2 hours and remained decreased over 4 days; the relative reduction in monolayer traction decreased from about 70% on the softest substrate and to about 20% on the stiffest substrate.

Conclusions: Our data suggest that substrate stiffness significantly affects monolayer contractile responses to TGF- β 2, a potential glaucoma-causing cytokine, and Y27632, a conventional outflow drug candidate. Our high throughput traction platform could be useful for conventional outflow-targeted drug discovery.



High throughput traction microscopy. A snapshot of traction distribution is shown at 3 day treatment.

Commercial Relationships: Enhua H. Zhou, None; W Daniel Stamer, Allergan (F), Alcon (F), Acucela (C), Aerie (C), Cytokinetics (C); Chan Young Park, None; Kristin M. Perkumas, None; James P. Butler, None; Mark Johnson, None; Jeffrey J. Fredberg, None
Support: R01EY019696-01 (MJ, WDS, JJF)

124 Neuroprotection; Clinical Drug Studies

Sunday, May 05, 2013 10:30 AM-12:15 PM

Exhibit Hall Poster Session

Program #/Board # Range: 407-460/A0138-A0191

Organizing Section: Glaucoma

Contributing Section(s): Cornea

Program Number: 407 **Poster Board Number:** A0138

Presentation Time: 10:30 AM - 12:15 PM

Olfactomedin Domain-containing Proteins, Olfm1 and Olfm2, Interact with AMPA Receptors in the Retina

Afia Sultana¹, Naoki Nakaya¹, Lijin Dong², Mones S. Abu-Asab³, Stanislav I. Tomarev¹. ¹Section on Retinal Ganglion Cell Biology, Laboratory of Retinal Cell and Molecular Biology, National Eye Institute, National Institutes of Health, Bethesda, MD; ²Genetic Engineering Facility, National Eye Institute, National Institutes of Health, Bethesda, MD; ³Histopathology Core Facility, National Eye Institute, National Institutes of Health, Bethesda, MD.

Purpose: Olfactomedin 1 (Olfm1) and Olfactomedin 2 (Olfm2) are highly conserved secretory glycoproteins that are preferentially expressed in neuronal tissues of vertebrates during development and in adults. The Arg144Gln mutation in OLFM2 was reported as a possible disease-causing mutation in Japanese patients with open-angle glaucoma (Funayama et al., 2006). The main goal of this study was to elucidate the role of Olfm1 and Olfm2 proteins in the mouse retina and optic nerve.

Methods: Olfm1 knockout (KO) mice were described previously

(Cheng et al., 2007). Olfm2 KO mice were produced by deleting exons 2-5 and replacing them with the beta-galactosidase gene. Optic nerves were assessed by axon quantification of semi-thin cross-sections and by electron microscopy. Retinal ganglion cell (RGC) death was evaluated by whole mount staining with NeuN and Brn3 antibodies. Conductivity of the optic nerve was evaluated by visual evoked potential test. Proteins interacting with Olfm1 were identified using shotgun proteomic analysis.

Results: Olfm1 and Olfm2 proteins are 60% identical. Both Olfm1 and Olfm2 are preferentially expressed in the RGCs. The level of Olfm1 expression is significantly higher than the level of Olfm2 expression in the developing and adult mouse retina. Olfm1 KO demonstrated a significant decrease in the amount of RGCs and a reduction in the amount of axons in the optic nerve with progression of age. Twelve month old Olfm1 KO mice showed a 25% reduction in a total cross-sectional area of the optic nerve. Olfm2 KO mice didn't show a significant decrease in the number of RGCs and axons. Visual evoked potential tests revealed a significantly delayed latency and reduced amplitude in Olfm1 and Olfm2 KO mice, respectively. Proteins interacting with Olfm1 were precipitated from postnatal day one mouse brain using Olfm1-specific polyclonal antibodies. Shotgun sequencing of immunoprecipitates led to the identification of several synaptic proteins including GluR2, an AMPA receptor subunit. GluR2 is expressed and co-localized with Olfm1/2 in RGCs.

Conclusions: Our data suggest that Olfm1 and Olfm2 proteins play an important role in the development and function of RGCs and optic nerve. Interaction of Olfm1/2 with AMPA receptors may lead to the modulation of the receptor activity in the retina.

Commercial Relationships: Afia Sultana, None; Naoki Nakaya, None; Lijin Dong, None; Mones S. Abu-Asab, None; Stanislav I. Tomarev, None

Program Number: 408 **Poster Board Number:** A0139

Presentation Time: 10:30 AM - 12:15 PM

Antioxidant treatment responses on the neuroinflammatory outcomes of ocular hypertension in rats

Gulgun Tezel^{1,2}, Xiangjun Yang¹. ¹Ophthalmology & Visual Sciences, University of Louisville, Louisville, KY; ²Anatomical Sciences & Neurobiology, University of Louisville, Louisville, KY.

Purpose: Findings of our recent in vitro and in vivo studies and studies of human donor eyes indicated that besides primary neurotoxic consequences, oxidative stress may induce glial dysfunction, compromise immune regulation, and shift the immune homeostasis toward neurodegenerative inflammation. To further determine the importance of oxidative stress for neuroinflammatory outcomes of glaucoma, we tested antioxidant treatment responses in an experimental rat model.

Methods: IOP elevation was induced in rats by hypertonic saline injections into episcleral veins in one eye. We gave Tempol (200 mg/kg/day), a superoxide dismutase mimetic and peroxynitrite-derived free radical scavenger that also reduces the formation of hydroxyl radicals, or vehicle (saline), using subcutaneously implanted osmotic mini-pumps for drug delivery by constant infusion. Following a 6-week treatment period, retina samples were analyzed for a number of inflammation markers. We analyzed markers of astroglial and microglial activation (including GFAP, CD-11b, Iba-1) by Western blot analysis and immunohistochemistry, markers of oxidative stress (including antioxidant response, protein carbonyls, and HNE adducts) by specific immunoassays, and cytokine profiles by multiplexed bioassays. In addition, we analyzed the activation of NF- κ B, a redox-sensitive transcription factor that regulates glial inflammatory responses in human glaucoma and experimental models.

Results: Retinal antioxidant capacity exhibited a significant increase, and retinal protein carbonyls and HNE adducts exhibited a significant decrease in ocular hypertensive samples ($p < 0.01$) with Tempol treatment and thereby verified drug delivery and biological function. Among a range of cytokines measured, IL-2, IFN- γ , and TNF- α , exhibited an over two-fold decreased titers in antioxidant-treated samples ($p < 0.05$). Antioxidant treatment also resulted in a prominent decrease in NF- κ B activation, based on Western blot analysis using phosphorylation site-specific antibodies to NF- κ B subunits, including p105/50, and p65 ($p < 0.05$).

Conclusions: These findings support oxidative stress-related neuroinflammatory mechanisms during glaucomatous neurodegeneration, and the potential of antioxidant treatment to restore immune homeostasis. Further work should help better determine the importance of oxidative stress as an immunomodulatory treatment target to provide neuroprotection in glaucoma.

Commercial Relationships: Gulgun Tezel, None; Xiangjun Yang, None

Support: NEI grants (R01 EY013813 and R01 EY017131), and RPB

Program Number: 409 **Poster Board Number:** A0140

Presentation Time: 10:30 AM - 12:15 PM

Up-regulation of autophagy in the glaucomatous human retina
Xiangjun Yang¹, Jian Cai³, David W. Powell³, Markus H. Kuehn⁴, Gulgun Tezel^{1,2}. ¹Ophthalmology and Visual Sciences, University of Louisville, Louisville, KY; ²Anatomical Sciences & Neurobiology, University of Louisville, Louisville, KY; ³Medicine, University of Louisville, Louisville, KY; ⁴Ophthalmology & Visual Sciences, University of Iowa, Iowa City, IA.

Purpose: Recent studies of experimental rat glaucoma have indicated autophagy activation during glaucomatous neurodegeneration. To determine whether autophagy is activated in the glaucomatous human retina, we analyzed the high-throughput proteomics data from human donor eyes in correlation to retinal immunolabeling patterns of selected autophagy-linked proteins.

Methods: Retinal protein samples obtained from human donors with (n:10) or without (n:10) glaucoma were quantitatively analyzed by label-free 2D-LC-MS/MS. To validate proteomics findings, Western blot analysis determined the expression level of two autophagy-enabling proteins, microtubule-associated protein 1A/1B-light chain 3 (LC3) and beclin. In addition, the extent and cellular localization of these proteins were determined by immunohistochemical analysis of retina sections obtained from an additional group of human donor eyes with glaucoma (n:34) and non-glaucomatous controls (n:20).

Results: Quantitative proteomics analysis indicated the up-regulated profile of a number of proteins linked to autophagy in the glaucomatous human retina. These proteins included autophagy proteins required for autophagosome formation, including ATG4, ATG5, ATG7, and LC3-I (ATG8), and negative regulatory proteins, including mammalian target of rapamycin (mTOR) and regulatory-associated protein of mTOR (raptor). Western blot analysis and immunohistochemical analysis validated the proteomics data and indicated an over two-fold up-regulation of the membrane-bound processed form of LC3 (LC3-II) and beclin (ATG6) in the glaucomatous retinas relative to non-glaucomatous controls.

Conclusions: Up-regulation of LC3-II and beclin, established as autophagy-enabling events, supports autophagic activation in the glaucomatous human retina. Although up-regulation of autophagy is a cell-protection mechanism, under specific conditions, it may become an alternative cell-death mechanism or induce autoimmunity. It remains unclear whether autophagic activity reflects a sufficient intrinsic response to meet the increasing demand to maintain cellular

homeostasis during glaucomatous stress/injury, or it is inefficient as a native defense mechanism, or its potential dysregulation compromises the cell survival and/or immune homeostasis. Findings of this study motivate further research to explore the cell-specific regulation of autophagy and implications in neurodegenerative and neuroinflammatory processes of glaucoma.

Commercial Relationships: Xiangjun Yang, None; Jian Cai, None; David W. Powell, None; Markus H. Kuehn, None; Gulgun Tezel, None

Support: NEI grants (R01 EY013813 and R01 EY017131), and RPB

Program Number: 410 **Poster Board Number:** A0141

Presentation Time: 10:30 AM - 12:15 PM

Effect of hypoxia treatment by CoCl₂ on expression of glutamate/aspartate transporters (GLAST) and unfolded protein reaction (UPR) related factors in retinal Müller cells

Dan Hu, Li-Juan Sun. Department of Ophthalmology, Xijing Hospital, The Fourth Military Medical University of Chinese PLA, Xi'an, China.

Purpose: Glaucoma and other optic nerve diseases are some of the major causes of blindness which are characterized by progressive death of the retinal ganglion cells (RGCs) and decreasing number of retinal nerve fiber. Müller cells, the principal glial cells of the retina, play an important role in neuroprotection against glutamate-induced cytotoxicity in RGCs. Recent studies have shown that UPR may be one mainly pathological mechanism of the progressive death of RGCs and the decreasing number of retinal nerve fiber. The present study evaluated the effect of hypoxia on expression of the UPR related factors X-box binding protein 1 (XBP1) and C/EBP homologous protein (CHOP) in Müller cells, thus clarifying the relationship between UPR and GLAST.

Methods: Müller cells were isolated from the retinas of rats on postnatal day 3~7 by using an enzymatic digestion-mechanical trituration technique. Optical microscopy and immunocytochemical method were used to evaluate cells. Cultured retinal Müller cells were exposed to either 0.2mM CoCl₂ or 2mM DTT for 0, 3, 6, 12, 24, 48, and 72 in vitro, respectively. We used Real Time PCR to measure sequential changes of the XBP1, CHOP and GLAST mRNA expression. Levels of XBP1 and GLAST proteins were monitored by immunoblot analysis.

Results: At least 90% cultured cells showed positive reaction for GLAST and glutamine synthetase (GS) with an immunocytochemical assay. The positive rate of GLAST expression was 84.66±3.51% determined by flow cytometry. The expression levels of XBP1, CHOP and GLAST were all ascended at the early stage, reached the summit at 24 hours after hypoxia induced by CoCl₂ and then dropped sharply after 72h, which was consistent with the results of DTT treatment. The protein expression of XBP1, CHOP and GLAST were similar to the transcription level.

Conclusions: These results suggest that UPR exists in the Müller cells after hypoxia, and its related factors XBP1, CHOP expression are equal to GLAST. Our study should facilitate further study of the role of UPR in eye diseases and identification of the potential therapeutic targets.

Commercial Relationships: Dan Hu, None; Li-Juan Sun, None
Support: National Natural Science Foundation of China (NO. 30772368)

Program Number: 411 **Poster Board Number:** A0142

Presentation Time: 10:30 AM - 12:15 PM

The Neuroprotective Effects of Coenzyme Q10 on Retinal Ganglion Cells and Its Reversal of Apoptosis

Miles R. Parnell, Joana M. Galvao, Eduardo M. Normando, Shereen Nizari, Farzana Rahman, M Francesca Cordeiro. Institute of Ophthalmology, UCL, London, United Kingdom.

Purpose: Coenzyme Q10 (CoQ10) is an essential cofactor in the electron transport chain as well as a potent antioxidant and has been shown to exhibit neuroprotective properties. In this study we aim to determine whether CoQ10 can protect retinal ganglion cells (RGCs) from a dimethyl sulfoxide (DMSO) induced apoptotic insult in vitro. In addition we aim to demonstrate a CoQ10 induced reversal of apoptosis in RGCs using live cell imaging.

Methods: Cultured RGC-5s were placed in media containing different concentrations of CoQ10 both as a CoQ10 powder dissolved in sub-toxic concentrations of DMSO (CoQ10 powder) and as a commercially available eyedrop containing α -tocopherol (CoQ10 eyedrop). DMSO was then added at a predetermined toxic dose and the cell viability was assessed at 24 hours using MTT assay. An early stage of apoptosis is phosphatidylserine (PS) exposure which can be visualised using the PS binding protein annexin labelled with the fluorophore fluorescein isothiocyanate (FITC). To assess whether CoQ10 can reverse this, RGCs were pretreated with CoQ10, Hoechst and FITC labelled annexin. The cells were then treated with a DMSO insult and live cell microscopy was used to visualise the morphological changes of the cells.

Results: CoQ10 powder preparation reduced DMSO induced apoptosis in RGCs compared to a non treated control at a concentration of 20 μ m ($p < 0.001$). COQ10 eyedrops were toxic compared to control ($p < 0.05$). Live cell imaging of RGCs labelled with FITC-annexin to stain PS as an early marker of apoptosis, showed morphological changes of apoptosis of PS exposure, apoptotic blebbing and cell death in response to a DMSO insult. In contrast, RGCs pretreated with 5 μ m of CoQ10 developed PS exposure to the DMSO insult which receded with CoQ10 and did not progress to apoptotic blebbing suggesting a CoQ10 reversal of apoptosis.

Conclusions: We have demonstrated a neuroprotective effect of CoQ10 on RGCs in vitro which is able to reverse DMSO-induced apoptosis in RGCs. The ability to protect neurons from a variety of insults using CoQ10 would be of enormous benefit not just in glaucoma but in other neurodegenerative diseases.

Commercial Relationships: Miles R. Parnell, None; Joana M. Galvao, None; Eduardo M. Normando, None; Shereen Nizari, None; Farzana Rahman, None; M Francesca Cordeiro, application (P)

Program Number: 412 **Poster Board Number:** A0143

Presentation Time: 10:30 AM - 12:15 PM

Mechanisms of Neuroprotection by Latanoprost for Retinal Ganglion Cells under Hypoxia

Mari Katsura^{1,2}, Reiko Yamagishi¹, Makoto Aihara^{1,3}.

¹Ophthalmology, The University of Tokyo, Tokyo, Japan;

²Radiosotope Center, The University of Tokyo, Tokyo, Japan;

³Shirato Eye Clinic, Tokyo, Japan.

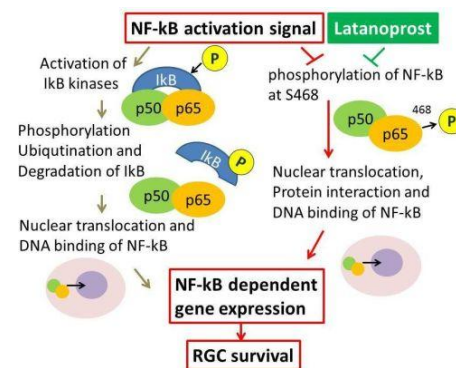
Purpose: Molecular mechanisms of retinal ganglion cell (RGC) survival and death are required to search for neuroprotective strategies. Previous study revealed that one of the prostaglandin analogues, latanoprost, prevents RGC death from hypoxic stresses (Yamagishi et al., 2011 Exp Eye Res.). Here we examined its mechanisms of the neuroprotection, especially of the role in the activity of NF- κ B, a key controller of apoptosis, to understand how we could utilize latanoprost for the treatment of glaucomatous optic neuropathy.

Methods: Using primary cultured rat RGCs, the changes of several proteins concerning apoptosis, including NF- κ B p65 and its post

translational modifications, were examined. Addition of 500 μ M cobalt chloride to the culture medium was used as mimic hypoxic stress. Western blotting was used to analyze whether 100 nM of latanoprost changed the phosphorylation of the protein induced by hypoxic stresses.

Results: Hypoxia significantly down-regulated the phosphorylation of NF- κ B p65 at serine 468, a phosphorylation site for suppression of NF- κ B activity, in cultured rat RGCs 5 min after addition of CoCl₂. With the normalization using actin, we can assure the decrease in phosphorylation in the amount of protein level at serine 468 to 72.2 % ($p = 0.046$). Moreover, addition of 100 nM latanoprost suppressed phosphorylated protein level more (72.2 % to 42.2 %, $p = 0.012$). On the other hands, phosphorylation of NF- κ B at serine 536, a phosphorylation site for activation of NF- κ B, was not significantly changed by addition of CoCl₂.

Conclusions: These findings support that the role for latanoprost in protection of RGCs by activation of NF- κ B through down-regulation of phosphorylation at serine 468 of NF- κ B p65.



Commercial Relationships: Mari Katsura, None; Reiko Yamagishi, None; Makoto Aihara, Ono pharmaceutical company (F), Pfizer (F)

Support: Grants-in-Aid for Scientific Research (C) of Japanese Society for Promoting Science 23592553

Program Number: 413 **Poster Board Number:** A0144

Presentation Time: 10:30 AM - 12:15 PM

Investigating Retinal Toxicity of the Potentially Neuroprotective Substance Tempol

Sebastian Mueller, Rebecca Dollinger, Sebastian Thaler, Johanna Hofmann, Martin S. Spitzer, Karl U. Bartz-Schmidt, Peter Szurman, Kai Januschowski. Department of Ophthalmology I, Eberhard-Karls University of Tuebingen, Tuebingen, Germany.

Purpose: Tempol is a low weight antioxidant that can act as a superoxide dismutase thus preventing the production of radicals via oxidation of Fe(II). Oxidative stress tributes to apoptotic cell death, a main reason for retinal ganglion cell (RGC) degeneration in glaucoma. Tempol already showed neuroprotective effects in models of brain trauma, ischemic stroke and Parkinson's disease. This study evaluated the retinal tolerance to different concentrations of tempol in a model of isolated and perfused bovine retina by measuring an electroretinogramm (ERG) and performing an MTT stationary toxicity assay on retinal ganglion cell cultures.

Methods: For functionality testing bovine retinas were prepared and perfused with an oxygen saturated standard solution and the ERG was recorded until stable b-wave amplitudes were recorded. 0.5 mM, 1 mM, 2 mM or 5 mM tempol concentrations were tested for 45 minutes. To investigate the effects on photoreceptor function 1 mM aspartate was added to obtain a-waves. ERG-recovery was monitored for 110 minutes. For cytotoxicity testing concentrations of 0.1 mM, 1

mM, 2.5 mM, 5mM, 10mM, 25mM, 40mM and 50mM tempol were tested on retinal ganglion cell lines (RGC 5).

Results: While no toxic effects for a concentration of 0.5 mM and 1 mM tempol could be detected, starting from a concentration of 2 mM tempol, statistically significant effects on the b-wave amplitude were noted (48%, $p=0.007$ for 2 mM). The a-wave amplitude remained stable even at higher concentrations of 10 mM. RGC 5 displayed a higher tolerance towards tempol with toxic effects starting at 50 mM (cell viability 86.46%, $p<0.05$).

Conclusions: Although the photoreceptors seem to display a tolerance to higher concentrations of tempol, higher doses than 1mM should be avoided.

Commercial Relationships: Sebastian Mueller, None; Rebecca Dollinger, None; Sebastian Thaler, None; Johanna Hofmann, None; Martin S. Spitzer, None; Karl U. Bartz-Schmidt, None; Peter Szurman, None; Kai Januschowski, TheraMon® (F)

Program Number: 414 **Poster Board Number:** A0145

Presentation Time: 10:30 AM - 12:15 PM

Ganglion cell neuroprotection by angiotensin II blockers identified by drug screening in retinal explants

Andrew J. White^{1,2}, Janosch Heller³, Keith R. Martin^{3,4}. ¹Centre for Vision Research, Westmead Millennium Institute, University of Sydney, Sydney, NSW, Australia; ²Save Sight Institute, University of Sydney, Sydney, NSW, Australia; ³Centre for Brain Repair, University of Cambridge, Cambridge, United Kingdom; ⁴Cambridge NIHR Biomedical Research Centre, Cambridge, United Kingdom.

Purpose: The aim of the current study was to use an ex vivo organotypic retinal explant model to examine retinal survival mechanisms and as a screening tool for potential novel neuroprotective agents relevant to glaucoma

Methods: Intact retina was dissected from adult Sprague Dawley rats immediately post mortem to make 4 retinal explants per eye.

Explants were placed ganglion cell side up on millipore filters with 300 μ L N2/B27 culture media per well in a humidified incubator. Novel therapies were trialled by adding drugs at appropriate concentrations, or vehicle alone. At the conclusion of each experiment, explants were fixed in 4% paraformaldehyde and retinal ganglion cell density was estimated by β III Tubulin immunohistochemistry. Live imaging of superoxide formation over 6 hrs was performed utilising dihydroethidium (DHE) and immunofluorescence microscopy. Analysis of protein expression in these explants was achieved by Western blotting.

Results: Measurement of the retinal ganglion cell (RGC) density at different timepoints suggested that 4 days ex vivo was optimal for assessment of neuroprotection. Viable RGC at an average density of 878 cells/mm² were observed in explanted retinas 4 days post enucleation. The effects of 8 licenced drugs on RGC survival in culture were tested. Angiotensin II blockers conferred > 50 % increase in ganglion cell survival after 4 days. Conversely, administration of Angiotensin II reduced cell survival by 40%. Western blot analysis of protein suppression suggested this effect was mediated by At1R and At2R receptors. Live retinal imaging of the RGC layer showed modulation of intracellular superoxide formation. DHE fluorescence of control explants was approximately 4 times greater than explants treated with irbesartan, an angiotensin II blocker, at 4 hrs post explant imaging, corresponding with an intracellular superoxide burst. The same imaging, undertaken with Angiotensin II treated explants, showed a 4 fold amplification of burst intensity.

Conclusions: Our retinal explant model may be useful in screening for potentially novel neuroprotective agents in a standardised and internally controlled fashion. In addition, this model enables us to

examine the mechanisms underlying neuroprotection. Angiotensin II blockers protect RGC in the explant model and are worth further investigation as a neuroprotective treatment in conditions such as glaucoma.

Commercial Relationships: Andrew J. White, Takeda (R); Janosch Heller, None; Keith R. Martin, None

Support: Financial support was provided by Fight for Sight UK and the Jukes Glaucoma Research Fund

Program Number: 415 **Poster Board Number:** A0146

Presentation Time: 10:30 AM - 12:15 PM

NFkB signaling in retinal glia mediates progressive neural degeneration and vision decline in glaucoma

Caroline Lupien^{1,2}, Philip J. Horner^{1,2}, David J. Calkins³. ¹Institute of stem cell and regenerative medicine, University of Washington, Seattle, WA; ²Neurological surgery, University of Washington, Seattle, WA; ³Vanderbilt Eye Institute, Vanderbilt University, Nashville, TN.

Purpose: Glaucoma is a neurodegenerative disease of the retina, characterized by a loss of vision due to the progressive decline of retinal ganglion cells (RGCs). A number of hypotheses have been proposed to explain the mechanisms underlying RGC death in glaucoma, one of them is glial cells activation. Glial cells are important structural and functional components of the nervous system, including the optic nerve and retina. It has been demonstrated that the retinal glial cells exhibit molecular and morphological signs of reactive gliosis in glaucoma. We have previously shown that pharmacological blockade of the NFkB pathway in a mouse model of glaucoma leads to improved RGCs survival. However, it is postulated that neuronal NFkB is neuroprotective while NFkB activation in glial cells promote neuronal death. The goal of this study is to selectively inhibit the NFkB pathway in retinal glial cells in order to establish the role of gliosis in glaucomatous degeneration.

Methods: To perform this study, we used NFkB transgenic mice expressing a dominant negative form of the inhibitor subunit of I κ B α under the control of the GFAP promoter (GFAP-I κ B α -dn). To induce glaucoma in these animals, we performed an acute ocular hypertension model. Immunohistochemistry, qPCR and Western blot analysis were performed to measure activity of the NFkB pathway and the function of neurons and glia. RGC counts, anterograde and retrograde transport were also assessed. We used an optokinetic testing system (optomotry) to measure visual acuity.

Results: We observed by quantitative PCR analysis a significant decrease in retinal GFAP expression in experimental animals (microbeads injection) compared to control animals (saline injection). We also noted decreased NFkB and I κ B expression in the experimental group. GFAP protein expression was also decreased in experimental animals reflective of decreased gliosis. Retrograde labelling with fluorogold demonstrated a remarkable 95% sparing of RGCs when NFkB was inhibited compared to 66% in control animals. The experimental animals also recovered almost all their visual acuity 15 days after glaucoma was induced.

Conclusions: These results demonstrate that gliosis is detrimental for RGC survival and function during the course of glaucoma. Importantly, selective inhibition of the NFkB pathway in glial may be a potent clinical approach for the treatment of vision loss in glaucoma.

Commercial Relationships: Caroline Lupien, None; Philip J. Horner, None; David J. Calkins, QLT, Inc (F), Allergan (F), QLT, Inc (C), Allergan (C)

Support: NIH grant EY01B203; Glaucoma Research Foundation, Catalyst for a Cure; Fonds de la Recherche en Santé du Québec

Program Number: 416 **Poster Board Number:** A0147

Presentation Time: 10:30 AM - 12:15 PM

RGC Neuroprotection by Manipulating ER Stress Signaling Molecules

Liu Yang, Feisi Liang, Mira Amin, Yaping Qian, Toby Ferguson, Yang Hu. Shriners Center for Neural Repair and Rehabilitation, Temple University School of Medicine, Philadelphia, PA.

Purpose: To explore the therapeutic potential of ER stress modulation in optic nerve (ON) injury mouse model.

Methods: Adeno-associated virus (AAV)-mediated RNA interference was employed to suppress pro-apoptotic ER stress molecule CCAAT/enhancer binding protein homologous protein (CHOP) in RGCs of C57BL/6 mice. The phosphorylation of eukaryotic translation initiation factor 2 α (eIF2 α) induces CHOP expression downstream of ER stress. By overexpression of un-phosphorylated eIF2 α S51A mutant in transgenic mice, we blocked the eIF2 α -CHOP branch of ER stress. Intraorbital ON crush (ONC) was performed in the left eyes of testing animals and the right eyes served as internal naïve controls. The survival RGCs were counted by immunostaining with Tuj1 antibody in whole-mount retinas 14 days post crush (14dpc).

Results: There was about 21.9% RGC survival in wild type (WT) control mice at 14dpc. AAV-CHOP-shRNA efficiently knocked down CHOP expression in RGCs after ONC and RGC survival was increased significantly to 31.9%. Moreover, eIF2 α S51A overexpression increases RGC survival to about 57.2%.

Conclusions: Modulation of the eIF2 α -CHOP branch of ER stress significantly increases RGC survival after ON injury, suggesting targeting ER stress may have considerable therapeutic neuroprotective potential in optic neuropathies including glaucoma.

Commercial Relationships: Liu Yang, None; Feisi Liang, None; Mira Amin, None; Yaping Qian, None; Toby Ferguson, None; Yang Hu, None

Support: Shriners Hospitals For Children Research Fellowship

Program Number: 417 **Poster Board Number:** A0148

Presentation Time: 10:30 AM - 12:15 PM

A peptide derived from Prominin-1 enhances axon regeneration of retinal ganglion cells in an optic nerve injury model

Zai-Long Chi^{1,2}, Amy E. Birsner^{1,2}, Avner Adini^{1,2}, Robert J. D'Amato^{1,2}. ¹Department of Ophthalmology, Harvard Medical School, Boston, MA; ²Vascular Biology Program, Boston Children's Hospital, Boston, MA.

Purpose: Prominin-1 (CD133) is a 5-transmembrane glycoprotein found in both humans and rodents. Prominin-1 was originally identified as a stem cell marker and has been recently identified in neuronal and glial stem cells. It also acts as a key regulator of disk morphogenesis during early retinal development, and mutations in this gene result in retinal degeneration. We recently reported that Prominin-1 interacts with VEGF and enhances its activity. We have developed a short peptide derived from Prominin-1, named PRIP, which also enhances VEGF activity and we investigated its effect on cell death and regeneration of damaged retinal ganglion cells in an optic nerve injury model.

Methods: Primary rat cortical neuron cells and optic nerves obtained from Fischer rats following an optic nerve (ON) crush were utilized in this experiment. Pellets approximately 1 X 1 X 0.6 mm containing either PRIP or vehicle in hydron polymer were cast and implanted into the retrobulbar space at the time of crush. Immunostaining of the retina and optic nerve was performed 2 weeks after surgery and PIP treatment. Total mRNA and proteins were extracted from the retina and optic nerve followed by analysis utilizing PCR arrays, real-time PCR, western blotting and enzyme-linked immunosorbent assay

(ELISA) for searching affected genes and proteins by PRIP.

Results: PRIP increased neuronal sprouting in vitro. In vivo, PRIP significantly increased axonal regeneration and prevented retinal ganglion cell (RGC) death. We also observed that PRIP regulated matrix metalloproteinase-9 (MMP-9) and tissue inhibitor of metalloproteinase-1 (TIMP-1) expression resulting in an increased MMP-9/TIMP-1 ratio in both the retina and ON. Additionally, the expression of chemokines such as CCL2/MCP-1 and CXCL2/MIP2-alpha are notably increased after treatment of PIP compared to the control group.

Conclusions: PRIP has neuroprotective activity in the optic nerve crush model. Further development of PRIP as a neuroprotective therapeutic agent is ongoing.

Commercial Relationships: Zai-Long Chi, None; Amy E. Birsner, None; Avner Adini, None; Robert J. D'Amato, Boston Childrens Hospital (P)

Program Number: 418 **Poster Board Number:** A0149

Presentation Time: 10:30 AM - 12:15 PM

In-vitro Evaluation of the Neuroprotective Effects of Forskolin on Retinal Ganglion Cells

ABUBAKAR HABIB^{1,2}, Gibran F. Butt¹, Ben Davis¹, Joana M. Galvao¹, Shereen Nizari¹, Eduardo M. Normando^{1,3}, Mark Tilley¹, Farzana Rahman¹, Li Guo¹, M Francesca Cordeiro^{1,3}. ¹Glaucoma & Retinal Neurodegeneration Research Group, Institute of Ophthalmology, London, United Kingdom; ²Ophthalmology Department, North Middlesex University Hospital, London, United Kingdom; ³Western Eye Hospital, London, United Kingdom.

Purpose: The diterpene forskolin is the principal active molecule of the *Coleus forskohlii* plant and has been shown to possess neuroprotective properties. The primary mechanism of action of forskolin is to directly increase the activity of the enzyme adenylyl cyclase and subsequently intracellular cyclic adenosine monophosphate (cAMP). The main aim of this study was to determine whether forskolin was neuroprotective to retinal ganglion cells (RGC) using three different apoptotic insults.

Methods: All experiments were performed in the RGC-5 cell line. Cell viability experiments (using the MTT assay) were conducted on RGC-5 using three different insults known to induce cell death through apoptosis: hydrogen peroxide, cobalt chloride and dimethyl sulfoxide. All data was analysed using unpaired two tailed T-test to assess statistical significance. Experiments using both Hoechst staining and propidium iodide staining were used to assess apoptosis pathways and necrosis in the presence of a caspase inhibitor (e.g. caspase-3 inhibitor).

Results: Forskolin (50uM) was associated with greater cell viability compared to the control in the presence of a hypoxia-inducing apoptotic agent (cobalt chloride 200, 250 and 300 μ M) (n=3, p= 0.003, 0.013 and 0.02 respectively). Similar results were noted with forskolin 50 μ M in the presence of dimethyl sulfoxide (DMSO) 4% and 6% concentrations (n=3, p= 0.008 and 0.0001 respectively). There was no significant difference in cell viability between forskolin and the control in the presence of hydrogen peroxide. It was also demonstrated that in the presence of hypoxia, forskolin appeared to exhibit a biphasic dose response with peak effect between 25-50 μ M. Finally, cobalt chloride induced hypoxia was found to be caspase-3 independent.

Conclusions: Forskolin appears to have a neuroprotective role in RGC-5 particularly against hypoxia-induced apoptotic cell death. This may have implications in conditions where loss of retinal ganglion cells (RGC) and their axons is associated with ischaemia.

Commercial Relationships: ABUBAKAR HABIB, None; Gibran F. Butt, None; Ben Davis, None; Joana M. Galvao, None; Shereen

Nizari, None; **Eduardo M. Normando**, None; **Mark Tilley**, None; **Farzana Rahman**, None; **Li Guo**, None; **M Francesca Cordeiro**, application (P)

Program Number: 419 **Poster Board Number:** A0150

Presentation Time: 10:30 AM - 12:15 PM

Neuroprotective effect of VCP inhibitors on mice models of glaucoma

Hanako O. Ikeda¹, Noriko Nakano¹, Yuki Muraoka¹, Masanori Hangai¹, Akira Kakizuka², Nagahisa Yoshimura¹. ¹Graduate school of medicine, Kyoto University, Kyoto, Japan; ²Graduate school of biostudies, Kyoto University, Kyoto, Japan.

Purpose: Valosin-containing protein (VCP) is a ubiquitously expressed ATPase that is reportedly involved in the cell cycle, membrane fusion, endoplasmic reticulum-associated degeneration etc (Nat Cell Biol, 2012. 14: 117). Newly synthesized compounds that inhibit the ATPase activity of VCP have been identified to protect cells under stress conditions. The purpose of this study was to confirm whether the compounds have a neuroprotective effect on mouse models of glaucoma.

Methods: VCP inhibitors (test) or saline (control) were orally administered to DBA/2J (a high intraocular pressure (IOP) model), GLAST knockout (KO) mice (a normal IOP model), or mice intravitreally injected with NMDA (an acute retinal ganglion cell (RGC) injury model). Spectral-domain optical coherence tomography (SD-OCT) examinations (*Multiline* OCT, Heidelberg Engineering) were obtained to assess cupping of the optic nerve head and evaluate the thickness of the ganglion cell complex (GCC: RNFL + GCL + IPL) around the optic nerve head. In GLAST KO and NMDA-injected mice, RGCs were counted by using scSLO images.

Results: The GCC thickness of the control DBA/2J mice gradually decreased from 6 to 10 months. The GCC thickness of the mice treated with VCP inhibitors was greater than the control mice after the age of 7 months ($P < 0.001$). In control DBA/2J mice, enlargement of optic disc cupping was obvious from 8 months on. In contrast, few mice administered with VCP inhibitors showed enlargement of optic disc cupping. In GLAST KO or NMDA-injected mice, the GCC thickness of the mice treated with VCP inhibitors was greater than the control mice during the observation period. The number of remaining RGCs in the treated mice was significantly greater than those in the non-treated mice.

Conclusions: VCP inhibitors have a neuroprotective effect on several mouse models of glaucoma, suggesting that the compounds may provide a new treatment option for glaucoma.

Commercial Relationships: **Hanako O. Ikeda**, Research grants from the Astellas Foundation for Research on Metabolic Disorders (F), Research grants from the Japan Foundation for Applied Enzymology (F); **Noriko Nakano**, PCT/JP2011/073160 (P); **Yuki Muraoka**, None; **Masanori Hangai**, Topcon (F), Canon (F), Nidek (C), Topcon (C); **Akira Kakizuka**, PCT/JP2011/073160 (P); **Nagahisa Yoshimura**, Canon (C), Canon (F), Nidek (C), Topcon (F), PCT/JP2011/073160 (P)

Support: a Grant-in-Aid for Young Scientists (22791656) from the Ministry of Education, Culture, Sports, Science, and Technology of Japan

Program Number: 420 **Poster Board Number:** A0151

Presentation Time: 10:30 AM - 12:15 PM

Activation of Retinal Astrogliosis Compromises Ganglion Cell Survival

Izzy Livne-Bar¹, Adrian Nahirny¹, Jeremy M. Sivak^{1,2}. ¹Vision Science, UHN, Toronto, ON, Canada; ²Ophthalmology and Vision Science, Univ of Toronto, Toronto, ON, Canada.

Purpose: Retinal astrocytes (RA) play an important role in maintaining retinal ganglion cell (RGC) homeostasis. In glaucomatous eyes, astrocyte activation accompanies pathological changes in the RGC layer and optic nerve head. However, roles of RA in glaucoma-associated pathology remain unclear. In order to study the specific roles activation of RA plays in RGC damage, we took advantage of an in vivo model for activation of RA and Muller cells. This model allows us to establish whether activation of retinal glia exerts protective or neurotoxic effect on RGCs exposed to excitotoxic damage.

Methods: Adult C57BL/6 mice were anesthetized and their corneas were mechanically debrided to remove the entire corneal epithelium. Corneal debridement has been reported to induce glial reactivity in the retina, independent of any acute retinal damage. Debridement-induced glial activation was validated by elevated expression of the glial fibrillary acidic protein (GFAP) in retinal astroglia. Excitotoxic damage was induced in control and experimental eyes by ocular injection of Kainic Acid (KA). The KA treated eyes were fixed and processed for TUNEL to detect retinal apoptosis. In addition we evaluated markers of immune infiltration and inflammation.

Results: Quantification of apoptosis revealed that debridement-induced astrogliosis does not cause RGC cell death. However, analysis of KA-induced apoptosis indicates that activation of retinal astroglia generates a five-fold increase in RGC cell death compared to controls. The astroglia activation is not associated with ocular infiltration of immune cells (microglia, macrophages, or neutrophils), indicating the effect is due to local activity.

Conclusions: Our results demonstrate that activation of retinal glia produces neurotoxic activity that increases RGC apoptosis following excitotoxic insult. We are currently working to identify signaling pathways mediating this activity, and whether blocking glial-activation improves RGC survival.

Commercial Relationships: **Izzy Livne-Bar**, None; **Adrian Nahirny**, None; **Jeremy M. Sivak**, None

Support: Canadian National Institute for the Blind, Glaucoma Research Society of Canada, Canadian Institute of Health Research, TGH & TWH Foundation

Program Number: 421 **Poster Board Number:** A0152

Presentation Time: 10:30 AM - 12:15 PM

Complement and Glial Activity in the Retinocollicular Pathway of Mice in a Novel Model of Glaucoma

Sean Silverman, Colleen M. McDowell, Byung-Jin Kim, Robert J. Wordinger, Abbot F. Clark. Cell Biology and Anatomy, UNT Health Science Center, Fort Worth, TX.

Purpose: Glaucoma is a leading cause of irreversible visual impairment and blindness throughout the world. C1q is responsible for axonal pruning in early ocular development and is upregulated in glaucomatous eyes of mice, non-human primates, and humans. We used an inducible mouse model of human primary open angle glaucoma with elevated intraocular pressure (IOP) to examine expression levels of C1q in the retina and superior colliculus (SC), as well as identify changes in cellular homeostasis.

Methods: Anesthetized A/J mice were given a single intravitreal injection of Ad5.MYOC.Y437H (5×10^7 pfu), a mutant glaucoma gene, or Ad5.null control virus. Following injections, conscious IOPs were measured weekly, using a TonoLab tonometer (iCare). Mice were sacrificed at time points between 3 days and 8 weeks. Brains and retinas were harvested for immunofluorescence or immunoblotting studies. Microglia and astrocytes were identified using Iba1 or GFAP, respectively. All quantifications were performed using ImageJ Analysis software (NIH).

Results: IOPs were significantly increased in the

ARVO 2013 Annual Meeting Abstracts by Scientific Section/Group – Glaucoma

Ad5.MYOC.Y437H eyes ($p < 0.01$) compared to the contralateral uninjected eye and eyes receiving Ad5.null. C1q expression was significantly upregulated in retinas receiving Ad5.MYOC.Y437H (2.69-fold \pm 0.38, $p < 0.0001$) compared to contralateral control retinas (0.7-fold \pm 0.29). C1q upregulation was additionally observed in SC hemispheres receiving neural connections from injected eyes. Mice given Ad5.null vector displayed no elevation of C1q in the visual axis. Additionally, colocalization studies demonstrated significant increases of inner retinal microglia density beginning 2 weeks post injection (0.61% \pm 0.07, $p < 0.001$) and continuing at 4 weeks (0.87% \pm 0.09, $p < 0.0001$) compared to untreated retinas (0.41% \pm 0.03 and 0.44% \pm 0.03, respectively). No signs of astrogliosis were detected.

Conclusions: C1q is actively upregulated in the retina and SC, following mutant myocilin induced ocular hypertension, whereas adenovirus alone had no effect. An increased microglial population in the retina accompanied these changes. This suggests that microglia may sense the increased IOP and play a role in upregulating endogenous C1q. Early glaucoma pathogenesis may result from reactivation of the ocular developmental roles of C1q and microglia, suggesting new therapeutic targets for future neuroprotective studies.

Commercial Relationships: Sean Silverman, None; Colleen M. McDowell, None; Byung-Jin Kim, None; Robert J. Wordinger, None; Abbot F. Clark, Alcon Research, Ltd. (F)

Support: DoD grant VISION; NIA grant T32 AG020494

Program Number: 422 **Poster Board Number:** A0153

Presentation Time: 10:30 AM - 12:15 PM

Differential activation of p38 and c-jun N-terminal kinase in the visual pathway following optic nerve crush

Yang Liu^{1,4}, Zhang Zhang^{1,4}, Robert J. Wordinger^{1,4}, Richard T. Libby^{2,5}, Iok-Hou Pang^{3,4}, Abbot F. Clark^{1,4}. ¹Cell Biology and Anatomy, UNT Health Science Center, Fort Worth, TX; ²Ophthalmology and Biomedical Genetics, University of Rochester Medical School, Rochester, NY; ³Department of Pharmaceutical Sciences, University of North Texas Health Science Center, Fort Worth, TX; ⁴North Texas Eye Research Institute, Fort Worth, TX; ⁵Flaum Eye Institute, Rochester, NY.

Purpose: p38 and c-jun N-terminal kinase (JNK) are two major stress-activated signaling pathways. In this study, we compared the activation of p38 and JNK in the retina, optic nerve, and superior colliculus after optic nerve crush (ONC) in adult mice.

Methods: ONC was performed unilaterally in adult mice. The damage to the retinal ganglion cell (RGC) layer and superior colliculus (SC) was determined by Nissl and black gold II staining. The activation of p38 and JNK in the retina, optic nerve, and superior colliculus was examined by immunofluorescence staining.

Results: Starting from 4 weeks after ONC, there were very few RGCs remaining in the RGC layer and fewer neurons ($P < 0.05$) in the contralateral SC compared to the control group. The volume of the contralateral SC was smaller ($P < 0.01$) than that of the control group. Phosphorylated JNK (p-JNK) was observed mainly on the proximal side of the optic nerve crush site as early as 1 hour after ONC. The expression of phosphorylated c-JUN was detected in the RGC layer starting 24 hours after ONC. The activation of p38 started 3 days post-ONC and was observed on both sides of the crush site. An increase of phosphorylated p38 (p-p38) was detected in the inner nuclear layer of the retina from 3 through 28 days following ONC. Two weeks after ONC, both p-JNK and p-p38 increased in the contralateral SC; however, the p38 activation was also observed in the ipsilateral SC.

Conclusions: Optic nerve crush induces damage in both the RGC layer and the superior colliculus. p38 and JNK activation are

differently modulated by optic nerve crush, and might play different roles in neuronal death in the retina and superior colliculus.

Commercial Relationships: Yang Liu, None; Zhang Zhang, None; Robert J. Wordinger, None; Richard T. Libby, None; Iok-Hou Pang, None; Abbot F. Clark, Alcon Research, Ltd. (F)
Support: DoD grant W81XWH-10-2-0003

Program Number: 423 **Poster Board Number:** A0154

Presentation Time: 10:30 AM - 12:15 PM

Coenzyme Q10 ameliorates oxidative stress and preserves mitochondrial transcription factor A in ischemic retinal injury
Dongwook Lee^{1,2}, Keun-Young Kim³, Won-Kyu Ju¹. ¹Hamilton Glaucoma Center and Department of Ophthalmology, University of California San Diego, San Diego, CA; ²Research Institute of Clinical Medicine of Chonbuk National University, Jeonju, Republic of Korea; ³Center for Research on Biological Systems, National Center for Microscopy and Imaging Research and Department of Neuroscience, University of California San Diego, San Diego, CA.

Purpose: Oxidative stress has been linked to mitochondrial dysfunction in retinal ischemia and optic neuropathies including glaucoma. Coenzyme Q10 (CoQ10), an essential cofactor of the electron transport chain, acts by scavenging reactive oxygen species for protecting neuronal cells against oxidative stress in neurodegenerative diseases. Here, we tested whether CoQ10 diet ameliorates oxidative stress and mitochondrial dysfunction, as well as promotes retinal ganglion cell (RGC) survival in ischemic retinal injury.

Methods: Pre-ischemic C57BL/6 mice were fed with 1% CoQ10 daily for 1 week and then transient ischemia was induced by acute intraocular pressure elevation. RGC survival was measured by immunohistochemistry for Brn3a. Apoptotic pathway was assessed by Western blot for Bax and phosphorylated Bad (pBad). The expression levels of glial fibrillary acidic protein (GFAP), Iba1, superoxide dismutase 2 (SOD2), heme oxygenase 1 (HO-1) or mitochondrial transcription factor A (Tfam) were assessed by Western blot or immunohistochemistry.

Results: CoQ10 diet significantly promoted RGC survival at 2 weeks after ischemia. At 12 hours, the upregulation of GFAP and Iba1 protein expression was blocked in ischemic retina treated with CoQ10 diet. Further, we observed that CoQ10 diet significantly prevented the upregulation of Bax protein expression but increased pBad protein expression in ischemic retina at 12 hours. In ischemic retina treated with control diet, the expression level of SOD2 and Tfam protein was peaked at 12 hours and decreased at 24 hours. Importantly, CoQ10 diet blocked the upregulation of SOD2 and HO-1 protein expression, as well as Tfam protein expression in ischemic retina at 12 hours.

Conclusions: Our findings demonstrate that CoQ10 diet ameliorates RGC loss against oxidative stress by blocking Bax/Bad-mediated apoptotic pathway as well as preserves Tfam/OXPHOS complex expression in ischemic retina. Therefore, we suggest that CoQ10 diet may be a useful neuroprotective strategy against oxidative stress-mediated mitochondrial dysfunction in ischemic retinal injury.

Commercial Relationships: Dongwook Lee, None; Keun-Young Kim, None; Won-Kyu Ju, None

Support: NIH/NEI R01 grant EY018658 (WKJ) and unrestricted grant from Research to Prevent Blindness (New York, NY)

Program Number: 424 **Poster Board Number:** A0155

Presentation Time: 10:30 AM - 12:15 PM

Effect of coenzyme Q10 on oxidative stress and mitochondrial DNA alteration in a mouse model of glaucoma

Myoung Sup Sim¹, Dongwook Lee^{1,2}, Keun-Young Kim³, Robert N. Weinreb¹, Won-Kyu Ju¹. ¹Hamilton Glaucoma Center and Department of Ophthalmology, University of California San Diego, La Jolla, CA; ²Research Institute of Clinical Medicine of Chonbuk National University-Biomedical Research Institute, Chonbuk National University Hospital, Jeonju, Republic of Korea; ³Center for Research on Biological Systems, National Center for Microscopy and Imaging Research and Department of Neuroscience, University of California San Diego, La Jolla, CA.

Purpose: Oxidative stress and mitochondrial dysfunction have been implicated as important pathophysiological mechanisms in glaucomatous optic neuropathy. Coenzyme Q10 (CoQ10) acts by scavenging reactive oxygen species for protecting neuronal cells against oxidative stress in neurodegenerative diseases. Here, we tested whether CoQ10 diet ameliorates oxidative stress-mediated retinal ganglion cell loss as well as preserves mitochondrial transcription factor A (Tfam) protein expression and mitochondrial DNA (mtDNA) content in the retina of a mouse model of glaucoma.

Methods: Pre-glaucomatous DBA/2J (D2) mice were fed with 1% CoQ10 and control diet daily for 6 month and intraocular pressure (IOP) in the eyes was measured monthly. RGC survival was measured by immunohistochemistry for Brn3a. Apoptotic pathway was assessed by Western blot for Bax and phosphorylated Bad (pBad). The protein expression levels of glial fibrillary acidic protein (GFAP), superoxide dismutase 2 (SOD2), heme oxygenase-1 (HO-1) or Tfam/oxidative phosphorylation (OXPHOS) complex were assessed by Western blot or immunohistochemistry. mtDNA content was measured by real-time PCR.

Results: There were no significant differences for IOP and body weight between control diet- and 1% CoQ10-treated glaucomatous D2 mice at age of 10 months. In comparison with control diet-treated glaucomatous retina, CoQ10 diet promoted about 30% of RGC survival and prevented the upregulation of GFAP protein expression. CoQ10 diet significantly blocked the upregulation of SOD2 and HO-1 protein expression as well as decreased Bax protein expression, but increased pBad protein expression in glaucomatous D2 mouse retina. Importantly, CoQ10 diet preserved mtDNA content and Tfam/OXPHOS complex protein expression in glaucomatous D2 mouse retina.

Conclusions: Our results demonstrate that CoQ10 diet ameliorates RGC loss against oxidative stress by blocking Bax/Bad-mediated apoptotic pathway as well as preserves mtDNA content and Tfam/OXPHOS complex expression in glaucomatous retina. Based on these observations, CoQ10 diet may provide a promising therapeutic strategy against oxidative stress-mediated mitochondrial dysfunction in glaucomatous optic neuropathy.

Commercial Relationships: Myoung Sup Sim, None; Dongwook Lee, None; Keun-Young Kim, None; Robert N. Weinreb, Aerie (F), Alcon (C), Allergan (C), Altheos (C), Amakem (C), Bausch&Lomb (C), Carl Zeiss-Meditec (C), Genentech (F), Haag-Streit (F), Heidelberg Engineering (F), Konan (F), Lumenis (F), National Eye Institute (F), Nidek (F), Optovue (C), Quark (C), Solx (C), Topcon (C); Won-Kyu Ju, None

Support: NIH/NEI R01 grant EY018658 (WKJ) and unrestricted grant from Research to Prevent Blindness (New York, NY)

Program Number: 425 **Poster Board Number:** A0156

Presentation Time: 10:30 AM - 12:15 PM

Change of the expression of synapses at the retina after ocular hypertension

Hae-Young L. Park, Jie Hyun Kim, Chankee Park. Catholic University of Korea, Seoul St. Mary's Hospital, Seoul, Republic of Korea.

Purpose: The purpose of this study was to examine the changes of the expression of synapses at the retina in a chronic ocular hypertension rat model.

Methods: Chronic ocular hypertension was induced by three episcleral vein cauterization. Expression of synaptophysin was co-localized with ganglion cell marker (NeuN), rod bipolar cell marker (PKC α), and A2-amacrine cell marker (parvalbumin). Electron microscopic examination was done at 1 week, 2 weeks, 4 weeks, and 8 weeks after cauterization.

Results: Expression of synaptophysin was increased throughout the layers of the retina, especially in the inner and outer plexiform layers. Co-localization with NeuN, PCK α , and parvalbumin shows that there are increase in synapses between ganglion cells and rod bipolar cells and between rod bipolar cells and photoreceptors. Immunohistochemical staining shows dendrites of the retinal ganglion cell increases. Electron microscopy shows increase of the dendrites of retinal ganglion cell and increase in the number of ribbon synapses in the inner and outer plexiform layers.

Conclusions: This data suggest that there is increase in synapses between retinal cells after ocular hypertension. The role of this phenomenon needs further investigation.

Commercial Relationships: Hae-Young L. Park, None; Jie Hyun Kim, None; Chankee Park, None

Support: This work was supported by the National Research Foundation of Korea(NRF) grant funded by the Korea government(MEST) (2012003754)

Program Number: 426 **Poster Board Number:** A0157

Presentation Time: 10:30 AM - 12:15 PM

Intraocular pressure and cGMP aqueous humor levels in spontaneous ocular hypertensive rabbits and following transient IOP changes

ennio ongini, Elena Bastia, Francesco Impagnatiello. Nicox Research Institute, Bresso, Milan, Italy.

Purpose: Molecular mechanisms underlying intraocular pressure (IOP) homeostasis are still unclear. There is emerging evidence that nitric oxide (NO) and the cGMP pathway are involved in the regulation of IOP. We studied NO - cGMP signaling and ocular tone in experimental models of glaucoma and following pharmacological modulation of intraocular pressure.

Methods: New Zealand White (NZW) and spontaneously ocular hypertensive Dutch Belted (DB) rabbits were used. Transient IOP raise was induced in NZW rabbits by the injection of 100 μ L hypertonic saline (5%) into the vitreous. cGMP levels were measured in aqueous humor (AH). IOP was monitored using a pneumatonometer prior to drug administration and at different time points thereafter.

Results: Spontaneous ocular hypertensive DB rabbits had constant higher IOP and lower cGMP levels than normotensive NZW rabbits (IOP, 32 \pm 1.2 and 20 \pm 0.9mmHg, respectively p< 0.05; cGMP, 5.6 \pm 0.4 and 21.9 \pm 1.2 pmol/ml, respectively p<0.05). Transient raise in IOP in normotensive NZW rabbits (Tmax=15-60 min Δ max= 35.1 \pm 1.2 mmHg) following hypertonic saline resulted in concomitant decrease in AH cGMP levels (Tmax=60 min; Emax= 37%). Finally, in normotensive NZW rabbits, topical instillation of the IOP-lowering drug, timolol (1%) or the NO donors, S-Nitroso-N-Acetyl-D,L-Penicillamine (SNAP, 0.2%) and isosorbide-5-mononitrate (ISMN, 1%) decreased IOP (Δ max= -3.4 \pm 0.4, -2.4 \pm 0.4 and -2.2 \pm 0.4 mmHg, respectively p< 0.05 vs vehicle treated eyes) and concomitantly raised cGMP content in AH of treated eyes.

Conclusions: Data support the notion that the NO/cGMP signaling pathway is involved in the regulation of IOP.

Commercial Relationships: ennio ongini, Nicox Research Institute (E); Elena Bastia, Nicox Research Institute (E); Francesco Impagnatiello, Nicox Research Institute (C)

Program Number: 427 **Poster Board Number:** A0158

Presentation Time: 10:30 AM - 12:15 PM

Inhibition of Innate Immune Response Alters Detoxification Capacity of ABCB1 Transporters in Trabecular Meshwork Cells

Algis Grybauskas¹, Kevin Skuran¹, Paulius Kuprys¹, Beatrice Yue¹, Paul A. Knepper^{1,2}. ¹Ophthalmology and Visual Sciences, University of Illinois at Chicago, Chicago, IL; ²Ophthalmology, Northwestern Medical School, Chicago, IL.

Purpose: The aqueous humor nourishes the avascular tissues of the anterior segment and the trabecular meshwork (TM) plays a role in removing xenobiotics. The innate immune system within the TM, particularly toll-like receptor 4 (TLR4) and its ligands, low molecular hyaluronic acid (LMW-HA) and lipopolysaccharide (LPS), play a significant role in maintaining a normal environment in the anterior chamber. We hypothesize that the innate immune system affects ATP-binding cassette sub-family member 1 (ABCB1, also known as p-glycoprotein and multidrug resistance protein 1) activity, altering the removal of toxic proteins, such as β -amyloid, heat shock proteins, and CD44.

Methods: Human TM cells and RAW 264.7 macrophages were plated onto 8-well chamber slides at 5000 cells/well overnight in 10% fetal bovine serum (FBS) cell growth medium. Two hours prior to treatment, the medium was changed to 0.1% FBS, and cells were challenged with 100 ng LMW-HA, (20 kDa), 100 ng high molecular weight hyaluronic acid (HMW-HA, 1000 kDa), 100 μ M verapamil, 5 μ M digoxin, 100 ng LPS, and/or 100 μ M naloxone for 0.5, 1, 2, 4 h. Calcein-AM (0.25 μ M, calcein-AM is cleaved by an esterase into a fluorescent product that is normally removed from the cell by ABCB1) was added for the final 15 min treatment. Cells were fixed at 4°C in 3% paraformaldehyde for 15 min, mounted with Vectashield with DAPI mounting medium, and analyzed with Leica confocal microscope and software.

Results: Following a 2h treatment, verapamil, an ABCB1 inhibitor, significantly ($P < 0.001$) increased fluorescent calcein retention in the cytoplasm of both RAW 264.7 and TM cells compared to PBS control. Digoxin, an ABCB1 activator, increased calcein efflux ($P < 0.001$). LPS significantly ($P < 0.001$) reduced ABCB1 activity in TM cells. HMW-HA significantly ($P < 0.001$) reduced ABCB1 activity, as did LMW-HA ($P < 0.02$) and naloxone ($P < 0.001$), a TLR4 inhibitor.

Conclusions: Both TLR4 ligands and inhibitors decrease ABCB1 activity, suggesting modulation of TLR4 is important in ABCB1 function. These results suggest that the innate immune inflammatory response plays a role in the ABCB1 detoxification pathway, and reducing inflammation may aid in the removal of toxic proteins in the TM.

Commercial Relationships: Algis Grybauskas, None; Kevin Skuran, None; Paulius Kuprys, None; Beatrice Yue, None; Paul A. Knepper, None

Support: American Health Assistance Foundation, Research to Prevent Blindness

Program Number: 428 **Poster Board Number:** A0159

Presentation Time: 10:30 AM - 12:15 PM

Essential Role of Brain Derived Neurotrophic Factor in the Preservation of Retinal Ganglion Cell Function

Vivek Kumar Gupta¹, Jonathan C. Li¹, Yuyi You¹, Maarten van den Buuse^{2,3}, Stuart Graham^{1,4}. ¹Australian school of Advanced Medicine, Macquarie university, Sydney, NSW, Australia;

²Behavioural Neuroscience Laboratory, Mental Health Research Institute, University of Melbourne, Melbourne, VIC, Australia;

³Department of Pharmacology, University of Melbourne, Melbourne, VIC, Australia; ⁴Save Sight Institute, Sydney university, Sydney, NSW, Australia.

Purpose: Brain derived neurotrophic factor (BDNF) is a high affinity ligand for the Tropomyosin related kinase B (TrkB) receptor. BDNF stimulation triggers TrkB dimerization and autophosphorylation resulting in activation of pro-survival cell-signalling pathways that can afford neuroprotection to the brain and retina. Our previous studies suggest that BDNF/TrkB signalling plays an important role in the retinal ganglion cell (RGC) protection under normal conditions and in glaucoma. We investigated the role of BDNF in whole retina and ganglion cell layer (GCL) homeostasis in vivo using BDNF heterozygous mice. BDNF interaction with the TrkB receptor in retinal ganglion cells under normal and experimental glaucoma conditions was investigated in a rat ocular hypertensive model.

Methods: Wild type and BDNF heterozygous mice were assessed using the scotopic electroretinogram (ERG) and scotopic threshold response (STR). Retinal structure was evaluated by H & E staining. An ocular hypertension model was established in rats using microbead injections. Rat RGCs were isolated using CD90.1 magnetic separation technique from normal and ocular hypertensive rats. The binding of BDNF with TrkB receptor in RGCs was determined using 1D nanoLC ESI-MS/MS mass spectroscopic analysis. TrkB receptor immunoprecipitations were carried out in the RGC lysates.

Results: The partial genetic ablation of BDNF manifested itself in the form of a retinal phenotype depicting a mild preferential loss of STR in the BDNF^{+/−} compared to the wild type animals ($p < 0.02$). No changes were observed in the scotopic ERGs of these BDNF deficient mice. Interestingly, the functional changes were not accompanied by anatomical changes in the GCL of these mice at 4 months of age. At the molecular level, BDNF was observed to physically interact with TrkB receptor in the isolated rat RGCs and BDNF expression was upregulated in response to chronically increased intraocular pressure (IOP) ($p < 0.05$).

Conclusions: Our studies on BDNF^{+/−} mice reveal that normal levels of BDNF are critical for the preferential preservation of GCL physiology in the retina as determined by STR integrity. Further testing with increasing age will determine if there are longitudinal changes in function or structure. BDNF physically interacts with the TrkB receptor in the RGCs which may facilitate its neuroprotective role.

Commercial Relationships: Vivek Kumar Gupta, None; Jonathan C. Li, None; Yuyi You, None; Maarten van den Buuse, None; Stuart Graham, None

Support: MQNS grant, ORIA Research grant.

Program Number: 429 **Poster Board Number:** A0160

Presentation Time: 10:30 AM - 12:15 PM

Effects of tafluprost on endothelin-1-induced retinal injury in the rat

Atsushi Nagata^{1,2}, Katsumi Oomachi³, Tomomi Higashide², Satoshi Shirai³, Masatsugu Nakamura³, Atsushi Shimazaki³, Naruhiro Ishida³, Kazuhisa Sugiyama². ¹Ophthalmology, Kanazawa Medical Center, Kanazawa-shi, Japan; ²Ophthalmology and Visual Science, Kanazawa University Graduate School of Medical Science, Kanazawa-shi, Japan; ³Research and Development Division, Santen Pharmaceutical Co. Ltd., Ikoma-shi, Japan.

Purpose: To examine neuroprotective effect of tafluprost on endothelin-1 (ET-1)-induced retinal injury in the rat.

Methods: Male Brown-Norway rats, 10 weeks of age and weighing

200 to 250 g, were used in the study. An intravitreal injection of ET-1 (20 pmol/eye) was performed in one eye of each rat, which was followed by topical administration of tafluprost eye drops (n=12) or saline (n=12) once daily for 4 weeks in a double blind fashion. An experimental optical coherence tomography (OCT) system was used which was optimized to acquire retinal images in rat fundus (Nagata A, et al. IOVS 2009). Cross-sectional OCT imaging was performed in a circumpapillary fashion, with a circle diameter of 1000 µm centered on the optic disc 1, 2, 4 weeks after the ET-1 injection under general anesthesia with intraperitoneal pentobarbital. The retinal nerve fiber layer (RNFL) thickness and inner retinal thickness (from RNFL to inner nuclear layer) was measured. Afterwards RGCs were retrogradely labeled with fluorogold which was applied to the superior colliculus. Seven days later, the rats were euthanized, and their retinas were prepared as flatmounts for examination under fluorescence microscopy to estimate RGC survival.

Results: Since two rats treated with saline died during the experimental period, they were excluded. In both groups, RNFL thickness was increased 1 week after the ET-1 injection ($p<0.01$), but then decreased significantly at the fourth week ($p<0.01$).

In both groups, inner retinal thickness progressively decreased after the second week (baseline vs. 2weeks, $p<0.01$; baseline vs. 4 weeks, $p<0.001$). Thickness of RNFL and inner retina in eyes treated with tafluprost was significantly thicker than that in eyes treated with saline (RNFL, $p=0.021$; inner retina, $p=0.046$, two-way repeated ANOVA). The average number of RGCs in the central retina of eyes treated with tafluprost was significantly greater than that of eyes treated with saline (2411 ± 213 vs. 2101 ± 397 cells/mm², $p=0.03$).

Conclusions: Treatment with topical tafluprost reduced the thinning of the inner retinal thickness and RGC loss caused by intravitreal ET-1 injection when compared to saline instillation. Repeated topical administration of tafluprost may be protective against the ET-1-induced retinal injury in the rat.

Commercial Relationships: Atsushi Nagata, None; Katsumi Oomachi, Santen Pharmaceutical co.,Ltd. (E); Tomomi Higashide, None; Satoshi Shirae, SANTEN (E); Masatsugu Nakamura, Santen Pharmaceutical Co. Ltd. (E); Atsushi Shimazaki, Santen Pharmaceutical co., Ltd. (E); Naruhiro Ishida, Santen Pharmaceutical Co. Ltd. (E); Kazuhisa Sugiyama, None

Support: Grant-in-Aid for Scientific Research 23592557 from the Japanese Society for the Promotion of Science.

Program Number: 430 **Poster Board Number:** A0161

Presentation Time: 10:30 AM - 12:15 PM

Celastrol Protects Retinal Ganglion Cells from Optic Nerve Crush but not from Glaucomatous Damage

Haksu Kyung¹, Vlad Bekerman², Jacky Man Kwong Kwong², Joseph Caprioli², Natic Piri². ¹Dept of Ophthalmology, National Medical Center, Seoul, Republic of Korea; ²Ophthalmology, Jules Stein Eye Institute, Los Angeles, CA.

Purpose: Celastrol, a triterpene extracted from *Tripterygium wilfordii* vine, has been used in traditional Chinese medicine as a remedy for inflammation and a variety of autoimmune diseases. It has been demonstrated to have neuroprotective properties in animal models of Parkinson's, Huntington's, Alzheimer's diseases, and amyotrophic lateral sclerosis. Celastrol cell protective effects are associated with activation of heat shock and antioxidant cell stress pathways. This study evaluates celastrol retinal ganglion cell (RGC) protective effect after optic nerve crush (ONC) and intraocular pressure (IOP) elevation.

Methods: ONC and laser trabecular photocoagulation were performed on one eye of adult Brown Norway rats. Daily intraperitoneal(IP) (1mg/kg; for two or five weeks for ONC and

experimental groups, respectively) or a single intravitreal(IVit) (0.2, 1 and 5 mg/kg; for ONC group) injections of Celastrol were administered. The extent of RGC degeneration was evaluated by determining the number of RGCs that were immunolabeled with Rbpms (RNA binding protein with multiple splicing) in a flat-mount retina. The retina was divided into superior, inferior and temporal quadrants and 3 sampling fields (0.32 x 0.24 mm) were collected at each region of 1, 2, and 3 mm from the optic nerve. The RGC number in 27 fields from each retina were counted and averaged.

Results: RGC survival was evaluated two and five weeks after ONC and laser treatment, respectively. An IP injected Celastrol/No-ONC group showed an approximately 15.6% decrease in RGC numbers compared to Vehicle/No-ONC group (n=6, $p=0.006$). In the Vehicle/ONC group, RGCs loss was 90.4%, whereas in the Celastrol/ONC group 59.2% of the cells degenerated (n=6, $p=0.004$). In an IVit injected animals, 22.8% of RGCs survived in Vehicle/ONC group compared to 24.5, 36.8 and 43.9% of RGCs in animals treated with 0.2 (n=4, $p=0.773$), 1 (n=4, $p=0.026$) and 5 (n=4, $p=0.039$) mg/kg of Celastrol, respectively. In Celastrol treated Glaucoma, RGC loss was 56.1% of that of control animals (n=9, $p<0.000$). RGC loss in Vehicle/Glaucoma was 56.6% (n=10, $p<0.000$).

Conclusions: Both IP and IVit treatments with Celastrol support RGC survival in ONC model. In experimental glaucoma, the neuroprotective effect of this drug was not observed. This could be explained by differences in the nature of insults to RGCs that can subsequently activate alternate cell death pathways.

Commercial Relationships: Haksu Kyung, None; Vlad Bekerman, None; Jacky Man Kwong Kwong, MTTI (P); Joseph Caprioli, Allergan Inc. (C), Allergan Inc. (F), Allergan Inc. (R); Natic Piri, None

Support: Research to Prevent Blindness (JC) and NIH/NEI EY018644 (NP)

Program Number: 431 **Poster Board Number:** A0162

Presentation Time: 10:30 AM - 12:15 PM

Role Of Neuritin 1 in Response to Optic Nerve Crush

Tasneem M. Putliwala^{1,2}, Yang Liu^{1,2}, Robert J. Wordinger^{1,2}, Abbot F. Clark^{1,2}. ¹CBAN - Visual Sciences, UNTHSC, Fort Worth, TX; ²NERI, UNTHSC, Fort Worth, TX.

Purpose: Glaucoma is a progressive optic neuropathy characterized by axonal injury, retinal ganglion cell (RGC) loss, and visual field defects. Neuritin1 (*Nrn1*) is an extracellular, GPI-linked protein, which can be secreted as a soluble form. It stimulates axonal plasticity, dendritic arborization, and synapse maturation in the CNS. The purpose of this study was to evaluate the expression of *Nrn1* using an *in vivo* optic nerve crush (ONC) mouse model that mimics features of glaucoma axonopathy.

Methods: Unilateral ONC was performed on 8-10-week-old BALB/cJ eyes using the Nickell's technique. Retinas (N=8) and ONs (N=6) were harvested at six different time points (0, 3, 7, 14, 21, and 28 days) post crush (dpc). Real time PCR and immunohistochemistry (IHC) was performed to evaluate spatial and temporal *Nrn1* expression in the retina and ON.

Results: After ONC, *Nrn1* gene expression in the retina was significantly decreased progressively by 7 dpc from control ($p<0.05$), with a slight recovery by 14 dpc and then a significant reduction by 21 dpc ($p<0.001$). In contrast, we observed basal expression till 21 dpc in the ON, with a significant increase at 28 dpc ($p<0.05$). Corresponding, biphasic NRN1 expression patterns were observed in both retina and ON IHC sections.

Conclusions: Degeneration of neurons and axonopathy are classical hallmarks of glaucoma neuropathy, which is evident in other neurodegenerative diseases such as Parkinson and Alzheimer's.

Nrn1, a vital player in neuronal plasticity, exhibited a biphasic recovery pattern after ONC suggesting that modifications in the regenerative ability of the neurons leads to RGC and ON axonal injury. Future studies will determine whether *Nrn1* gene therapy can prevent the loss of neurons by reviving regeneration of RGCs after optic nerve axonopathy.

Commercial Relationships: Tasneem M. Putliwala, None; Yang Liu, None; Robert J. Wordinger, None; Abbot F. Clark, Alcon Research, Ltd. (F)

Support: W81XWH-10-2-0003

Program Number: 432 **Poster Board Number:** A0163

Presentation Time: 10:30 AM - 12:15 PM

Protective effect of GFAP antibody on RGC5 cells via actin cytoskeleton pathways

Corina Wilding, Katharina Bell, Sebastian Funke, Sabine Beck, Norbert Pfeiffer, Franz H. Grus. Experimental Ophthalmology, Mainz, Germany.

Purpose: The pathogenesis of glaucoma still is unknown. Next to increased reactive oxygen species (ROS) levels, recent studies show the participation of immunological components. Previous studies demonstrate significant changes in the pattern of autoantibodies against ocular antigens in the serum of glaucoma patients in comparison to healthy controls. GFAP antibody (ab) is found in a lower concentration in glaucoma patients. Our aim was to analyse the effect of GFAP ab on neuroretinal cells (RGC5), those cells affected by glaucoma and which pathways are triggered in RGC5, when they are incubated with GFAP ab.

Methods: RGC5 were preincubated with different GFAP ab concentrations (0.05, 0.01, 0.5, 1, 5, 10, 20 µg/ml) for 3h and stressed with 50µM H₂O₂ (1h) to induce ROS. Controls were incubated without ab. Cell viability was measured with crystal violet and ROS with DCFH-DA. We also performed proteomic analysis of cells incubated with GFAP ab. Analysis of peptides was performed using a capillary LC-ESI-MS system. The obtained mass spectra were identified and quantified using MaxQuant and pathway analysis were performed with Ingenuity Pathway Analysis (IPA).

Results: A significant increase of viability and decrease of ROS levels of cells stressed with H₂O₂ and preincubated with different ab levels (0.05, 0.1, 0.5 and 1 µg/ml) was in both detected (9%, p<0.05). Based on IPA we were able to indicate significant changes in actin cytoskeleton pathways, where we could find 6 significant changed proteins in RGC5 after GFAP ab treatment such as Vinculin (2.187), Talin1 (2.157), Profilin1 (-4.399), Cofilin (-3.735), Actin beta (2.036), actin regulated protein 2/3 (-2.285).

Conclusions: We detected significant neuroprotective effects especially of the lower GFAP ab concentrations on the cells stressed with H₂O₂, e.g. raised viability and decreased ROS level. Actin and actin regulated proteins, which we found differently regulated, participated in the mitochondrial apoptosis pathway and could play a key role in the neuroprotective effect of GFAP ab. During the induction of apoptosis e.g. dephosphorylated cofilin gets translocated from the cytosol to mitochondria and is able to induce cytochrome c release. Therefore we hypothesize that the changes of the actin cytoskeleton proteins, found in GFAP Ab treated RGC5, have a pro survival potential against oxidative stress.

Commercial Relationships: Corina Wilding, None; Katharina Bell, None; Sebastian Funke, None; Sabine Beck, None; Norbert Pfeiffer, Sensimed AG (F), Sensimed AG (R), MSD (F), MSD (R), Alcon (F), Allergan (F), Novartis (F), Novartis (R), Bayer (F), Heidelberg Engineering (F), Bausch&Lomb (F), Boehringer-Ingelheim (F), Carl Zeiss Meditech (F), Chibret (F), Nidek (F), Pfizer

(F), Santen (F), Santen (R), Topcon (F), Ivantis Inc (F), Ivantis Inc (R); Franz H. Grus, None

Support: Forschungsschwerpunkt Translationale Neurowissenschaften, Mainz

Program Number: 433 **Poster Board Number:** A0164

Presentation Time: 10:30 AM - 12:15 PM

Adenosine A3 receptor agonist inhibits retinal ganglion cell apoptosis in vivo

Joana M. Galvao^{1,2}, Li Guo¹, Ana Raquel Santiago², Antonio F. Ambrosio², M Francesca Cordeiro^{1,3}. ¹Glaucoma & Retinal Neurodegen, UCL Institute of Ophthalmology, London, United Kingdom; ²Centre of Ophthalmology and Vision Sciences, IBILL, Faculty of Medicine, Coimbra, Portugal; ³Western Eye Hospital, London, United Kingdom.

Purpose: Adenosine receptors (AR) have been considered as potential therapeutic targets in neurodegenerative diseases, such as glaucoma. Adenosine and three of its four receptors have been identified at the level of retinal ganglion cell (RGC) layer. Our previous studies have shown that RGCs express the A3AR, and that the A3AR agonist is protective against an NMDA insult to retinal explants. In this study, we focused on assessing A3AR expression and the potential neuroprotective effects of a selective A3AR agonist, 2-Cl-IB-MECA, in two rat models of RGC degeneration: partial optic nerve transection (pONT) and ocular hypertension model (OHT).

Methods: OHT or pONT was induced in the left eye of Dark Agouti rats, with the opposite eye as control. A pilot study identified 1.2 µM 2-Cl-IB-MECA as the most effective dose at reducing DMSO induced RGC apoptosis in vivo. Both eyes of OHT or pONT were intravitreally injected with either 2-Cl-IB-MECA, PBS (vehicle) or 1.2 µM 2-Cl-IB-MECA + 1.2 µM MRS 1220 (A3AR antagonist) immediately before surgery. IOPs were measured regularly using a Tonolab. Animals were imaged to assess RGC apoptosis in vivo using DARC (Detection of Apoptosis in Retinal Cells) 7 days after pONT or three weeks after IOP elevation, previously described. Immunohistochemical analysis of A3AR expression and TUNEL was performed in 10 µm-thick retinal cryosections.

Results: Treatment with the A3AR agonist resulted in a reduction of IOP in OHT eyes. DARC imaging analysis revealed that the A3AR agonist 2-Cl-IB-MECA significantly reduced RGC apoptosis (p < 0.01) to approximately 50% compared to vehicle treated pONT/OHT (mean 239±93.65 vs 449±84.58, respectively for pONT and mean 215±93.01 vs 409±154.58, respectively for OHT). Rats treated with both A3AR agonist and antagonist did not show significant difference from insult alone. Immunohistochemistry confirmed an increase in the number of apoptotic cells using TUNEL and showed a down regulation in the expression of A3AR in the RGC layer in the eyes with the insult compared to control.

Conclusions: In accordance with our previous findings, these results suggest that A3AR activation is neuroprotective against RGC apoptosis in vivo. Therefore, targeting A3AR and delineation of its relationship with RGC apoptosis could have great potential in the management of retinal neurodegeneration, such as glaucoma.

Commercial Relationships: Joana M. Galvao, None; Li Guo, None; Ana Raquel Santiago, None; Antonio F. Ambrosio, None; M Francesca Cordeiro, application (P)

Support: FCT - Foundation for Science and Technology, Portugal (fellowship SFRH/BD/47947/2008)

Program Number: 434 **Poster Board Number:** A0165

Presentation Time: 10:30 AM - 12:15 PM

Reversal of Apoptosis in Retinal Ganglion Cells

Farzana Rahman, Shereen Nizari, Joana M. Galvao, Miles R. Parnell, ABUBAKAR HABIB, Eduardo M. Normando, M Francesca Cordeiro. UCL Institute of Ophthalmology, London, United Kingdom.

Purpose: Early detection of retinal ganglion cell (RGC) apoptosis and its prevention holds promise as a novel and effective treatment for glaucoma. Reversible apoptosis, during which there is exposure of phosphatidylserine (PS) on to the outer leaflet of the plasma membrane, has recently been described, using Galectin-1(Gal-1). The aim of this study was to determine whether Gal-1 induces apoptosis in RGCs, and to investigate whether this apoptosis is reversible.

Methods: RGCs as part of a mixed cell culture with Muller cells were treated with human Gal-1 at concentrations of 2.5 μ M, 1.25 μ M and 0.63 μ M. Hoechst staining was used to determine cell viability and apoptosis following 30 minutes of treatment with Gal-1. Live cell imaging with Annexin-V was then used to assess PS exposure following Gal-1 treatment. Gal-1 was combined with Annexin-V (2.5 μ l), binding buffer (10 μ l) and Hoechst stain (0.1 μ l) resulting in concentrations of 5.27 μ M, 2.64 μ M, 2.00 μ M and 1.32 μ M. Live cell imaging was performed for 30 minutes on cells in Dulbecco's modified eagle medium (DMEM) alone initially. After 30 minutes, DMEM was replaced with Gal-1 treatments for 30 minutes and then replaced with DMEM again. Live cell imaging continued for 2 hours.

Results: A one-way ANOVA showed significant reduction in the viability of mixed cells following treatment with 1.25 μ M Gal-1 (p<0.05) and 2.50 μ M Gal-1 (p<0.001), compared to the control (DMEM set as 100% viability). A 23.31% decrease in total cells was observed with 1.25 μ M Gal-1 compared to the control (DMEM). A 38.34% decrease in total cells was observed with 2.5 μ M Gal-1 compared to the control. When analysing the dose-response relationship, there was 97.78% certainty that the reduction in cell viability was due to the action of Gal-1 (Pearson r = -0.9777, p = 0.0223).

Live cell imaging demonstrated increased Annexin-V binding following treatment with Gal-1 at concentrations of 1.32 μ M, 2.00 μ M, 2.64 μ M and 5.27 μ M. This suggested that Gal-1 at these concentrations induced PS exposure. Removal of Gal-1 after 30 minutes caused a reduction and redistribution in Annexin-V staining.

Conclusions: These results provide a mechanistic insight into RGC apoptosis and suggest potential for its reversal. This would be of great benefit clinically for the early management of glaucoma and other pathologies such as diabetic retinopathy. A process once considered an irreversible pathway leading to cell death now holds hope as a therapeutic target.

Commercial Relationships: Farzana Rahman, None; Shereen Nizari, None; Joana M. Galvao, None; Miles R. Parnell, None; ABUBAKAR HABIB, None; Eduardo M. Normando, None; M Francesca Cordeiro, application (P)

Program Number: 435 **Poster Board Number:** A0166

Presentation Time: 10:30 AM - 12:15 PM

Expression of CCL5 Signaling Machinery in Healthy and Glaucomatous Retina

D'Anne S. Duncan¹, Sean J. Lee¹, Rebecca M. Sappington^{1,2}.

¹Vanderbilt Eye Institute, Vanderbilt University, Nashville, TN;

²Vanderbilt Vision Research Center, Vanderbilt University Medical Center, Nashville, TN.

Purpose: Retinal inflammation is central to glaucomatous pathogenesis. The inflammatory mechanisms that influence retinal ganglion cell (RGC) function and survival provide insight into glaucomatous pathology and therapeutic strategies. In this study, we sought to examine the potential relevance of CCL5 signaling to

RGCs in healthy and glaucomatous retina.

Methods: We performed immunohistochemistry to assess layer- and cell-specific expression of CCL5, CCR1, CCR3 and CCR5. Label intensity was quantified in retina layers using quantitative digital microscopy and image analysis software. Young (4 month) and aged (8 month) C57 mice were exposed to unilateral ocular hypertension for 4 weeks and RGC-specific expression of CCL5 and its receptors were assessed in whole mount retinas.

Results: CCL5 and its receptors are constitutively expressed in multiple layers of the retina, with highest significant expression of CCL5 and CCR5 in ganglion cell (GCL) and nerve fiber layers (NFLs; p<0.002). In healthy retinal tissue, CCL5 and all 3 receptors co-localize with RGC somas and axons, while retinal glia (Müller glia, microglia and astrocytes) show restricted expression. In response to microbead-induced elevated IOP in vivo, young and aged RGCs exhibit significantly increased expression of CCL5 (p=0.042), but show decreased expression of CCR3 (p>0.01) and CCR5 (p=0.142), compared to saline-treated RGCs. Qualitatively, CCR1 showed increased expression, although this result was not significant.

Conclusions: These data support a functional role for constitutive and inducible CCL5 signaling in RGCs and provide evidence that CCL5 is relevant to RGC maintenance and glaucomatous pathology. Furthermore, expression of CCL5 machinery by RGCs and retinal glia, suggest potential autocrine and paracrine mechanisms of this chemokine in the retina.

Commercial Relationships: D'Anne S. Duncan, None; Sean J. Lee, None; Rebecca M. Sappington, None

Support: NEI Grant 1R01EY020496 (RMS); NEI Supplement 1R01EY020496-02S1 (DSD); Research to Prevent Blindness Career Development Award (RMS); Unrestricted Grant (Vanderbilt Eye Institute); NEI Core Grant P30EY008126 (Vanderbilt Vision Research Center)

Program Number: 436 **Poster Board Number:** A0167

Presentation Time: 10:30 AM - 12:15 PM

Glaucomatous retinopathy and neuropathy following laser-induced ocular hypertension in African green monkeys

Wenzheng Hu¹, Robin J. Goody¹, Michael J. Struharik¹, Steve D. Whittaker^{1,2}, Steve T. Henry^{1,2}, Rohn Brookes^{1,2}, Matthew S. Lawrence¹. ¹RxGen Inc, Hamden, CT; ²St Kitts Biomedical Research Foundation, Lower Bourryeau, Saint Kitts and Nevis.

Purpose: To develop a chronic ocular hypertension model in the African green monkeys, and to investigate the glaucomatous injury to the neuroretina and optic nerve in this model, which shares a lamina cribrosa, macula and other neuroanatomic characteristics unique to humans and nonhuman primates.

Methods: The trabecular meshwork in one eye of each monkey received a single session of laser photocoagulation. Slit-lamp biomicroscopy, tonometry, optical coherence tomography (OCT) and fundus photography were used to monitor changes in intraocular pressure (IOP), anterior chamber inflammation, retinal nerve fiber layer (RNFL) and ganglion cell layer (GCL) thickness, and optic disc morphology. Photomicrographs of histology were obtained and observations qualitatively and quantitatively correlated to OCT findings. All work was conducted in compliance with the ARVO Statement for the Use of Animals in Ophthalmic and Vision Research.

Results: A single session of laser photocoagulation on the trabecular meshwork induced an elevation of IOP \geq 45 mmHg in 67% of eyes starting at one week post-laser and was sustained throughout the 8-week observation period, indicating the chronic ocular hypertension model is reproducible in African Green monkeys. Sustained IOP elevation resulted in glaucomatous changes in the neuroretina and

ONH, including reduction of RNFL, expansion of the ONH cupping, thinning of the neuroretinal rim and displacement of the blood vessels emerging from the disc. Those glaucomatous changes are similar to that observed in human optic discs with glaucoma-induced atrophy, suggesting a high homology of the chronic ocular hypertension model with the human disease.

Conclusions: Sustained IOP elevation achieved by laser ablation and subsequent scarification of the trabecular meshwork can be employed as a chronic ocular hypertension model in African green monkeys and used for testing neuro-protection compounds in translational studies.

Commercial Relationships: Wenzheng Hu, RxGen (E); Robin J. Goody, RxGen, Inc (E); Michael J. Struharik, Rx-Gen (E), St. Kitts Biomedical Research Foundation (E); Steve D. Whittaker, RxGen Inc (E); Steve T. Henry, Rxgen.inc (E); Rohn Brookes, RxGen, Inc (E); Matthew S. Lawrence, RxGen (E)

Program Number: 437 **Poster Board Number:** A0168

Presentation Time: 10:30 AM - 12:15 PM

TRPV1-/- Accelerates Neurodegeneration From Microbead-Induced Ocular Hypertension

Nicholas J. Ward, Karen W. Ho, Wendi S. Lambert, David J. Calkins. Ophthal & Vis Sciences, Vanderbilt Eye Institute, Nashville, TN.

Purpose: Transient receptor potential (TRP) channels transduce information about the extracellular environment via influx of Ca^{2+} . In the central nervous system (CNS), transient receptor potential vanilloid 1 (TRPV1) mediates diverse neuronal responses to stress and is known to modulate synaptic activity. Since TRPV1 activation affects retinal ganglion cell (RGC) survival *in vitro*, we sought to characterize its influence *in vivo* using microbead-induced ocular hypertension (OHT) in TRPV1-/- mice.

Methods: OHT was induced in 4 month C57 and TRPV1-/- mice through microbead occlusion of the anterior chamber. The contralateral eye received an equivalent volume saline injection. Ocular pressure was monitored for 5 weeks using Tono-Pen XL rebound tonometry, and fluorescent cholera toxin subunit β (CTB) was injected intravitreally 2 days prior to sacrifice. CTB transport along the optic projection was quantified in coronal sections through perfusion-fixed midbrains containing superior colliculus. RGC axons were quantified in counter-stained semi-thin sections through optic nerve. C57 paraffin sections were immunolabeled against TRVP1 and RIBEYE, a pre-synaptic marker.

Results: Microbead-injected eyes exhibited a significant increase in IOP over their saline-injected controls in both C57 (19.77 ± 4.23 mmHg vs. 14.75 ± 3.64 mmHg) and TRPV1-/- (19.79 ± 4.47 mmHg vs. 14.96 ± 4.04 mmHg) mice ($p < 0.001$, $n = 13$). OHT resulted in diminished CTB transport to the colliculus compared to saline-injection that was worse for TRPV1-/- mice (63.6% decrease) compared to C57 (43.4%) and ($p < 0.001$). Similarly, axon loss in the optic nerve with OHT was significantly worse in the TRPV1-/- cohort ($p < 0.001$). We found peri-synaptic expression of TRPV1 in normal retina as indicated by its proximity to RIBEYE label. This is consistent with RGC dendritic expression.

Conclusions: Our results indicate that TRPV1-/- accelerates neurodegenerative outcomes resulting from OHT with microbead occlusion. Within the CNS, the Ca^{2+} -mediated activity of TRPV1 has been linked to both protective and degenerative functions depending on the context of its signaling. TRPV1 may constitutively contribute to survival of RGCs in response to stressors like OHT, possibly through a pro-survival response modulating synaptic activity.

Commercial Relationships: Nicholas J. Ward, None; Karen W. Ho, None; Wendi S. Lambert, QLT Inc. (F); David J. Calkins, QLT, Inc (F), Allergan (F), QLT, Inc (C), Allergan (C)

Support: Melza and Theodore Barr and Glaucoma Research Foundations (DJC), AHAF (DJC), NEI Grant (5R01EY017427-03) (DJC), Research to Prevent Blindness Inc., Departmental Unrestricted Grant (DJC), and NEI Core Grant (5P30EY008126-19) (DJC), NEI Training (5T32EY007135-18) (NJW).

Program Number: 438 **Poster Board Number:** A0169

Presentation Time: 10:30 AM - 12:15 PM

Interactions Between Dendritic Cells, Microglia, and Retinal Ganglion Cells Following Injury to the Optic Nerve

Dale S. Gregerson, Neal D. Heuss, Mark J. Pierson, Kim Ramil C. Montaniel, Scott W. McPherson, Thien N. Sam. Dept Ophthalmol & Vis Neurosci, Univ of Minnesota, Minneapolis, MN.

Purpose: Cells of the immune system are known to play roles in the loss of neurons due to injury or disease. While the actions of microglia (MG) are being studied by many labs, there has been less effort devoted to other immune cells, including dendritic cells (DC). We have detected the close, physical contact between dendritic cells and retinal ganglion cell (RGC) axons following an optic nerve crush (ONC), and are working to learn if these DC play a role in promoting survival or death in the RGC.

Methods: A unilateral optic nerve crush was used to provide the RGC injury. RGC were visualized and/or counted by retrograde staining with Fluorogold injected into the superior colliculus, or immunostaining for B3-tubulin. DC were detected by their expression of green fluorescent protein (GFP) from the CD11c promoter, and deleted by treatment with diphtheria toxin (DTx) based on expression of the diphtheria toxin receptor (DTR) on the same CD11c promoter. MG were distinguished by their expression of CD11b, and absence of detectable GFP. Fluorescence microscopy, flow cytometry, funduscopy, and H&E staining were used to detect, count and characterize the cells and their responses to the ONC injury. Multiple strains of transgenic and knockout mice were used to promote the study of the cellular responses.

Results: The earliest detection of close association of GFP+ cells with RGC axons was at 3 days post-injury, with the frequency rising quickly after that. The relative number of GFP+ DC in close contact with RGC axons was much greater than found for the MG. Depletion of DC in CD11c-DTR/GFP mice via DTx treatment promoted RGC survival after an ONC injury. RGC survival after an ONC was enhanced in MyD88/TRIF double knockout mice relative to wt controls. Association of GFP+ DC with axons was associated with the loss of RGC.

Conclusions: These results extend the influence of myeloid cells of the innate immune system to include CD11b+ dendritic cells, previously shown to be substantially recruited from circulating progenitors, in addition to the MG and macrophages investigated by multiple other labs. Depletion of the DC gave a moderate, but significant enhancement of RGC survival at 4 wks post-injury. Since the RGC in mice deficient in MyD88 and TRIF, known to signal from toll-like receptors to NF- κ B, were found to better survive the injury, ligands and specific TLR are being sought.

Commercial Relationships: Dale S. Gregerson, None; Neal D. Heuss, None; Mark J. Pierson, None; Kim Ramil C. Montaniel, None; Scott W. McPherson, None; Thien N. Sam, None
Support: R01 EY021003; P30 EY011374

Program Number: 439 **Poster Board Number:** A0170

Presentation Time: 10:30 AM - 12:15 PM

Caloric Restriction Protects Against Loss of RGC Differentiation Following Optic Nerve Injury

James D. Lindsey¹, Karen Xuandao Duong-Polk¹, Dustin Hammond¹, Christopher K. Leung², Robert N. Weinreb¹. ¹Hamilton Glaucoma

ARVO 2013 Annual Meeting Abstracts by Scientific Section/Group – Glaucoma

Center, University of California San Diego, La Jolla, CA;
²Department of Ophthalmology and Visual Sciences, Chinese University of Hong Kong, Hong Kong, China.

Purpose: Optic nerve injury triggers loss of retinal ganglion cell (RGC) differentiation, including loss of Thy-1 gene expression, followed by RGC death. Caloric restriction can increase lifespan, reduce markers of physiological aging, and delay the onset of certain age-related diseases. This study determined whether caloric restriction inhibits loss of Thy-1 promoter activation in RGCs following optic nerve crush.

Methods: 40 transgenic mice expressing cyan fluorescent protein under control of the Thy-1 promoter were maintained on normal diet until 2 months old. Subsequently, the food was removed every other day for 24 hours from the cages of 20 of the mice until the mice were 16 months old. The control group of mice continued to receive food ad libitum. At 16 weeks of age, baseline images of fluorescent retinal neurons were collected using a blue-light confocal scanning laser ophthalmoscope and then all mice received unilateral optic nerve crush. After this, the retinas of both eyes were imaged weekly for four weeks and fluorescent spots from the same region of each retina were counted manually.

Results: Subject survival at the end of the study was 10/20 mice (50%) in the control group and 14/20 (70%) in the caloric restriction group. The mean proportions of fluorescent retinal neurons remaining in the control group following optic nerve crush were 45±24, 35±19, 21±18, and 18±9 percent, at weeks 1 through 4, respectively. In contrast, the mean proportions of fluorescent retinal neurons remaining in the caloric restriction group were 52±17, 36±12, 27±17, and 42±23 percent at weeks 1-4, respectively (P = 0.0023 at week 4). Within the control group, the change in number of fluorescent retinal neurons between weeks 2 and 4 was > 20% less in 55% of subjects, < 20% different in 33% of subjects, and > 20% increased in 11% of subjects. Within the caloric restriction group, the change in number of fluorescent retinal neurons between weeks 2 and 4 was > 20% less in 31% of subjects, < 20% different in 31% of subjects, and > 20% increased in 38% of subjects.

Conclusions: The greater survival in the caloric restriction group confirms that the experimental treatment induced the lifespan enhancing effect. Because most fluorescent retinal neurons in these mice are RGCs, the imaging results indicate that caloric restriction protects against the loss of RGC differentiation following optic nerve injury.

Commercial Relationships: James D. Lindsey, None; Karen Xuandao Duong-Polk, None; Dustin Hammond, None; Christopher K. Leung, Carl Zeiss Meditec (F), Carl Zeiss Meditec (R), Alcon (C), Alcon (R), Alcon (F), Allergan (C), Allergan (R), Tomey (F), Optovue (F); Robert N. Weinreb, Aerie (F), Alcon (C), Allergan (C), Altheos (C), Amakem (C), Bausch&Lomb (C), Carl Zeiss-Meditec (C), Genentech (F), Haag-Streit (F), Heidelberg Engineering (F), Konan (F), Lumenis (F), National Eye Institute (F), Nidek (F), Optovue (C), Quark (C), Solx (C), Topcon (C)
Support: NIH/NEI EY019692 (RNW) and an unrestricted grant from Research to Prevent Blindness.

Program Number: 440 **Poster Board Number:** A0171

Presentation Time: 10:30 AM - 12:15 PM

Safety and tolerability following single dose of ONO-9054 in healthy volunteers

Cheryl L. Rowe-Rendleman¹, Takafumi Ouchi², Douglas T. Ross², Andrew T. Wood². ¹Pre-Clinical, Ono Pharma/Omar Consulting Grp LLC, Princeton Junction, NJ; ²Drug Development, Ono Pharma USA, Lawrenceville, NJ.

Purpose: ONO-9054 (Ono Pharmaceuticals, Osaka Japan) is a novel ocular hypotensive compound and is the isopropyl ester derivative of the free acid ONO AG-367 a dual FP/EP3 agonist that may be effective in lowering intraocular pressure in humans. The safety and tolerability of the compound was evaluated after instillation of a single drop

Methods: A randomized, double-masked, placebo controlled clinical trial (NCT01508988) was conducted with 48 healthy volunteers who received a single dose of ONO-9054 q.d. ranging in concentration from 0.3-30 ug/mL. Safety parameters were evaluated from predose through 7 days after dosing. Safety evaluations included adverse events, vital signs, spirometry, electrocardiogram, clinical laboratories, ocular tolerability and hyperemia.

Results: All subjects were between the ages of 18-64. Overall, 10 AEs were reported across all doses (0.3-30 ug/mL) from subjects who received ONO-9054. Similarly 7 AEs were reported from subjects who received placebo. There were no dose related trends in incidence or intensity of any ocular AEs including flare. All AEs observed in ONO-9054 group were mild in nature. The majority of responses for eyedrop tolerability were rated as absent or mild. Itching was the most frequently reported symptom with similar frequencies in the placebo group. All hyperemia was transient and resolved to baseline levels by 49 hours postdose.

Conclusions: Ocular safety findings showed that ONO-9054 was well tolerated. Overall, there was no apparent dose-response in any systemic or local tolerability parameters. These early results support the rationale for additional clinical trials to demonstrate the safety and evaluate the efficacy of ONO-9054 ophthalmic solution in randomized, controlled, multiple dose clinical trials.

Commercial Relationships: Cheryl L. Rowe-Rendleman, Ono Pharma USA (C); Takafumi Ouchi, Ono Pharma USA, Inc. (E); Douglas T. Ross, Ono Pharma USA, Inc. (E); Andrew T. Wood, ONO Pharma USA Inc (E)

Clinical Trial: NCT01508988

Program Number: 441 **Poster Board Number:** A0172

Presentation Time: 10:30 AM - 12:15 PM

Single dose pharmacokinetics of ONO-9054 in healthy volunteers

Takafumi Ouchi¹, Cheryl L. Rowe-Rendleman², Douglas T. Ross¹, Fumitaka Suto¹, Andrew T. Wood¹. ¹Ono Pharma USA, Lawrenceville, NJ; ²Pre-clinical, Ono Pharma/Omar Consulting Grp LLC, Princeton Junction, NJ.

Purpose: ONO-9054 (Ono Pharmaceuticals, Osaka Japan) is a novel prodrug compound with ocular hypotensive activity. ONO-9054 is an isopropyl ester derivative of the free acid ONO-AG-367 that has been classified as a dual FP/EP3 agonist that may be effective in lowering intraocular pressure in humans. The serum levels of the parent compound and its active metabolite were measured after instillation of a single dose to the eyes of healthy volunteers.

Methods: A randomized, double-masked, placebo controlled clinical trial (NCT01508988) was conducted with 48 healthy volunteers who received a single dose of ONO-9054 ranging in concentration from 0.3-30 ug/mL q.d. in the morning. Blood samples were collected by venipuncture at predose, 5, 10, 20, 30, and 45 minutes; 1, 1.5, 2, 4, 6, 8, and 12 hours following dose. All samples were centrifuged within 30 minutes of blood collection and the plasma samples were stored at -70°C. The pharmacokinetic parameters of Cmax, Tmax, T1/2, and AUClast were calculated.

Results: The plasma concentration of ONO-9054 was below the limit of quantitation in all but 1 volunteer. The plasma concentration of ONO-AG-367 reached Cmax at a median range Tmax of 10 to 15 minutes for all doses. The mean T1/2 ranged from 0.48 to 0.83h. At 6 h and later time points, the plasma concentration of ONO-AG-367

was below the limit of quantification. Cmax and AUClast of ONO-AG-367 generally increased with dose.

Conclusions: The active compound ONO-AG-367 was almost completely metabolized within the first hour after dosing. Pharmacokinetic modeling based upon these single dose pharmacokinetic results suggests that the systemic concentrations of ONO-AG-367 disappear rapidly but there is a possibility that q.d. dosing may maintain the drug at clinically effective levels which could lower IOP in the eye. Additionally, this pharmacokinetic modeling could be useful to evaluate the relationship between plasma concentration of ONO-AG-367 and the systemic safety. Based upon this rationale, these results support the need for additional clinical trials to demonstrate efficacy, safety and pharmacokinetics of multiple doses of ONO-9054 ophthalmic solution to manage patients with elevated pressures as a result of glaucoma.

Commercial Relationships: Takafumi Ouchi, Ono Pharma USA, Inc. (E); Cheryl L. Rowe-Rendleman, Ono Pharma USA (C); Douglas T. Ross, Ono Pharma USA, Inc. (E); Fumitaka Suto, Ono Pharma USA, INC. (E); Andrew T. Wood, ONO Pharma USA Inc (E)

Clinical Trial: NCT01508988

Program Number: 442 **Poster Board Number:** A0173

Presentation Time: 10:30 AM - 12:15 PM

POSTURAL INTRAOCULAR PRESSURE CHANGES IN TRABECULECTOMIZED AND MEDICALLY-TREATED GLAUCOMA EYES

Akira Sawada, Tetsuya Yamamoto. Ophthalmology, Gifu Univ Grad School of Med, Gifu-shi, Japan.

Purpose: To compare the posture-induced intraocular pressure (IOP) changes in medically-treated and trabeculectomized glaucoma eyes with low IOPs

Methods: Thirty-five post-operated open-angle glaucoma (OAG) eyes with a cystic filtering bleb and 35 medically-treated OAG patients, which of both had IOPs with the Goldmann applanation tonometer (GAT) less than 12 mmHg, were enrolled into the study. The IOP was measured in the sitting and the lateral decubitus position with an ICare rebound tonometer (ICare). The IOP in the lateral decubitus position was measured in the upper-eyes 5 minutes after assuming this posture.

Results: The mean IOP measured with the GAT was 9.9 ± 1.4 mmHg in the trabeculectomized eyes and 10.0 ± 1.2 mmHg in the medically-treated eyes ($P=0.646$). In the surgically-treated group, the IOP with the ICare was 10.7 ± 2.5 mmHg in the sitting position and 11.9 ± 3.1 mmHg in the lateral decubitus position ($P=0.000$). On the other hand, in the medically-treated group, the IOP with the ICare was 11.4 ± 2.3 mmHg in the sitting position and 15.0 ± 2.7 mmHg in the lateral decubitus position ($P=0.000$). There was a significant difference in this postural IOP difference between the two groups, $+1.2$ mmHg in the surgically-treated group and $+3.6$ mmHg in the medically-treated group ($P=0.000$).

Conclusions: Our results indicate that successfully trabeculectomized eyes had less posture-induced IOP changes compared to medically-treated eyes.

Commercial Relationships: Akira Sawada, None; Tetsuya Yamamoto, Alcon Japan (R), Pfizer Japan (R), Senju (R), Santen (R), Kowa (R), Otsuka (R), Pfizer Japan (C), Senju (C), Kowa (C), Otsuka (C)

Program Number: 443 **Poster Board Number:** A0174

Presentation Time: 10:30 AM - 12:15 PM

Association between glaucoma, glaucoma therapies, and erectile dysfunction

©2013, Copyright by the Association for Research in Vision and Ophthalmology, Inc., all rights reserved. Go to iovs.org to access the version of record. For permission to reproduce any abstract, contact the ARVO Office at arvo@arvo.org.

Nawaaz Nathoo¹, Mahyar Etminan^{2,3}, Frederick S. Mikelberg¹.

¹Department of Ophthalmology, University of British Columbia, Vancouver, BC, Canada; ²Child and Family Research Institute, University of British Columbia, Vancouver, BC, Canada; ³Department of Medicine, University of British Columbia, Vancouver, BC, Canada.

Purpose: To examine the association between 1) glaucoma and erectile dysfunction (ED), and 2) topical beta-blocker (BB) use and ED.

Methods: A comprehensive, province-wide database of physician visits and diagnoses, and prescription drug dispensing was used to identify cases of ED (1380) and find corresponding controls (13,800). A conditional logistic regression model was used to estimate rate ratios for two main exposures: 1) diagnosis of glaucoma and 2) use of a prescription of a topical BB prior to the index date. A variety of risk factors were adjusted for.

Results: Cases were more likely to have coronary artery disease, chronic obstructive pulmonary disease, and diabetes. The crude rate ratio of a current diagnosis of ED in a population with at least 2 separate diagnoses of glaucoma was 1.34, and adjusted for a number of variables, this ratio was 1.37 (95% CI 1.06-1.76). Use of topical BB in the 30 days prior to the diagnosis of ED did not have a significant association with a diagnosis of ED, with crude and adjusted rate ratios of 1.05 and 1.10 (95% CI 0.61-1.99). Topical ocular prostaglandin use was also not associated with ED with crude and adjusted rate ratios of 0.96 and 0.93 (95% CI 0.57-1.53).

Conclusions: Our results confirm an association between ED and glaucoma that cannot be attributed to topical BB use. Given that most cardiovascular and metabolic risk factors were adjusted for, further research in this area will be necessary to elucidate the nature of this association and potential causation.

Commercial Relationships: Nawaaz Nathoo, None; Mahyar Etminan, None; Frederick S. Mikelberg, None

Program Number: 444 **Poster Board Number:** A0175

Presentation Time: 10:30 AM - 12:15 PM

Intravitreal Bevacizumab or Ranibizumab for Rubeosis Iridis - 3 years follow up

Joao J. Nassaralla^{1,2}, Joao J. Nassaralla³, Belquiz A. Nassaralla⁴.

¹Retina and Vitreous, Instituto de Olhos de Goiania, Goiania, Brazil; ²Faculdade de Ciências da Saúde, UnB, Brasilia, Brazil; ³Medicine, UNIFENAS, Belo Horizonte, Brazil; ⁴Cornea and Cataract, IOG, Goiania, Brazil.

Purpose: To determine and compare whether intraocular bevacizumab and ranibizumab decreases RI in patients with neovascular glaucoma (NVG).

Methods: The study included 72 eyes of 64 patients with secondary NVG due to proliferative diabetic retinopathy (n=60) or ischemic vessel occlusion (n=12). All patients received an intraocular injection (IOI) of 1.25 mg of bevacizumab (IB) or ranibizumab (IR), from November 2007 to October 2012 at the Goiania Eye Institute. Intraocular injection was performed in topical anaesthesia either in the anterior chamber (n=58) or via pars plana intravitreally (n=14). RI was investigated prospectively by iris biomicroscopy. An expanded informed consent with an off-label use waiver and explanation letter was reviewed with all patients. The IOI was performed under sterile conditions in an operating theatre and was performed with proximetacaine (Anestalcon® - Alcon - Brazil) topical anesthesia and the injection did via pars plana. The follow up

Results: Degree of RI decreased significantly ($p<0.01$) within 1 week after application of both drugs. The improvement was maintained for at least 4 weeks when was did PRP. After 3 years only 5 eyes (3 IB and 2 IR) development recurrent RI, when was did more injection

ARVO 2013 Annual Meeting Abstracts by Scientific Section/Group – Glaucoma

and more PRP. The two drugs are about equal in their effectiveness. An inflammatory response with fibrinous reaction and pseudohypopyon was observed in three cases (2 bevacizumab and 1 with ranibizumab) one day after surgery. The reaction persisted only 2 days. However, that cost differences for those receiving treatment are major at about \$40 per injection for Avastin and \$2,000 per injection for Lucentis.

Conclusions: The preliminary conclusion is that the two drugs are about equal in their effectiveness.

Commercial Relationships: Joao J. Nassaralla, None; Joao J. Nassaralla, None; Belquiza A. Nassaralla, None

Clinical Trial: NCT00557232

Program Number: 445 **Poster Board Number:** A0176

Presentation Time: 10:30 AM - 12:15 PM

The Use of Complementary and Alternative Medicine for Glaucoma in South Korea

Jonghoon Shin¹, Hyun-kyung Cho², Mingui Kong³, Changwon Kee⁴.

¹Ophthalmology, Pusan National University Yangsan Hospital, Busan, Korea, Yangsan, Republic of Korea; ²Ophthalmology, Samsung Medical Center, Seoul, Republic of Korea;

³Ophthalmology, Samsung Medical Center, Seoul, Republic of Korea; ⁴Ophthalmology, Samsung Medical Center, Seoul, Republic of Korea.

Purpose: Since there is no report on the use of complementary and alternative medicines (CAM) in glaucoma patients in Asia where CAM use is relatively common, there is a need for a study on the prevalence of CAM use in glaucoma patients in Asian countries. Hence, we sought to investigate the use of CAM by glaucoma patients.

Methods: A questionnaire-based survey was given to 150 glaucoma patients recruited from a clinic of a glaucoma specialist during the duration of three months between April and August, 2012. After the survey, we reviewed the chart of participants to obtain the glaucomatous information including glaucoma severity and coexisting ocular conditions.

Results: 141 of 150 glaucoma patients (94%) completed the questionnaire-based survey totally. The mean age of the participants was 59.4 ± 14.5 years. 42 patients (29.7%) had used at least one CAM for the specific purpose of glaucoma treatment. Herbal remedies (41.7%) were the most commonly used CAM followed by dietary modification (21.6%). Bilberry (13.7%) was the most popular herbal remedy followed by fish oil (11.5%). The patients using CAM reported that most of them had not consulted with their ophthalmologist about using CAM (83.3%).

Conclusions: The use of CAM in glaucoma patients in South Korea was more prevalent than in Western countries. However, a few patients that use CAM for glaucoma had discussed the information regarding CAM with their ophthalmologists. Therefore, it is required to provide accurate information on CAM for more safe and effective use of CAM.

Commercial Relationships: Jonghoon Shin, None; Hyun-kyung Cho, None; Mingui Kong, None; Changwon Kee, None

Program Number: 446 **Poster Board Number:** A0177

Presentation Time: 10:30 AM - 12:15 PM

Preservative-free tafluprost 0.0015%/timolol 0.5% fixed dose combination: a 6-month double-masked, randomized multicenter P-III comparison to concomitant use of the individual preservative-free components in patients with glaucoma or ocular hypertension

Gabor Hollo¹, Anton B. Hommer², Alfonso Anton³, Auli M. Ropo⁴.

¹Ophthalmology, Drosera BT, Solymar, Hungary; ²Ophthalmology,

Sanatorium Hera, Vienna, Austria; ³Institut Catala de Retina - Inici, Barcelona, Spain; ⁴Clinical Research & Medical Affairs, Santen Oy, Helsinki, Finland.

Purpose: To evaluate the efficacy, tolerability and safety of preservative-free fixed dose combination (FDC) of tafluprost 0.0015% and timolol 0.5% once daily compared to the concomitant use of preservative-free tafluprost 0.0015% once daily and preservative-free timolol 0.5% twice daily (non-fixed combination, NFC).

Methods: This study was a 6-month double-masked randomised, multicenter parallel group investigation (clinicaltrials.gov No: NCT 01306461). After washout patients were randomised to either, preservative-free FDC tafluprost-timolol (once-daily) and placebo (twice daily) (n=201) or NFC of tafluprost (once-daily) and timolol (twice-daily) (n=199). Study visits included screening, baseline, 2, 6 weeks, 3 and 6 months. IOP was measured at 8 a.m., 10 a.m. and 4 p.m. during each visit. Primary efficacy variable was the change from average diurnal baseline IOP at month 6, secondary efficacy variable was the proportion of responders at month 6.

Results: A substantial and comparable IOP reduction from mean baseline IOP of 25.11 mmHg (identical for FDC and NFC) was seen in both groups. Mean IOP decrease from baseline for all IOP measurements was -9.13 to -7.30 mmHg in the FDC and -9.43 to -7.54 mmHg in the NFC group (PP analysis, $p < 0.0001$ for both groups). At 6 months, the estimated overall treatment difference (FDC - NFC) in the PP analysis was 0.308 mmHg with a 95% CI from -0.194 to 0.810 mmHg ($p = 0.228$). The upper limit of the CI was clearly below the pre-specified margin of 1.5 mmHg providing strong evidence on the non-inferiority between FDC and NFC. An IOP lowering effect of >30% from baseline was achieved at month 6 in 58.3% and 66.9% of patients treated with FDC and NFC respectively. Patients with related ocular AEs were evenly distributed between FDC and NFC groups (21.4% and 18.6%). Hyperaemia was reported in 16 patients (8.0%) in the FDC group and in 10 patients (5.0%) in the NFC group, and was generally of mild or moderate severity.

Conclusions: A substantial and comparable IOP reduction was seen both for FDC and NFC throughout the 6-month study period. Both, primary and secondary efficacy variables unanimously evidenced non-inferiority between the two treatment arms in reduction of IOP.

Commercial Relationships: Gabor Hollo, Alcon, Optovue (F), Alcon, MSD, Santen, NiCox, Pfizer, Optovue (C), Alcon, MSD, Santen, Pfizer, Zeiss (R), Alcon, MSD, Santen (S); **Anton B. Hommer**, Allergan (R), Allergan (C), Alcon (R), Santen (R), Merck (R); **Alfonso Anton**, ALCON (F), SANTEN (C), MSD (C), THEA (C), TRANSCEND (C), ALCON (R), ALLERGAN (R), SANTEN (R); **Auli M. Ropo**, Santen Oy (E)

Clinical Trial: NCT 01306461

Program Number: 447 **Poster Board Number:** A0178

Presentation Time: 10:30 AM - 12:15 PM

The investigation of influence of glaucoma surgery for instillation adherence

Tomoko Yoshikawa¹, Itaru Kimura^{1,2}, Satoshi Watanabe¹, Ayumi Usui¹, Akira Murakami³, Nobuyuki Ebihara¹.

¹Department of Ophthalmology, Juntendo Urayasu Hospital, Urayasu City, Japan; ²National Institute of Sensory Organs, Tokyo Medical Center, Tokyo, Japan; ³Department of Ophthalmology, Juntendo University School of Medicine, Tokyo, Japan.

Purpose: To investigate the influence of glaucoma surgery for instillation adherence in the glaucoma patients.

Methods: 128 glaucoma patients who recorded drop diary in instillation therapy were studied. 23 patients had gone through trabeculectomy (TLE group), and 105 patients had no experience of

glaucoma surgery (no-TLE group). The instillation rate, kinds of drops, details of oration (one eye, or both eyes) and instillation eye were studied and compared between two groups.

Results: 5 patients of TLE group were prescribed one drop and the mean instillation rate was 97.7%. 3 patients were prescribed 2 drops, 9 patients were prescribed 3 drops, 6 patients were prescribed 4 drops in TLE group, and the mean instillation rate was 97.8%, 97.6%, 97.5%, respectively. The mean instillation rate of no-TLE group was 97.8%, and no significant difference between them was found ($p > 0.05$). 18 patients had gone through trabeculectomy in one eye, and 17 of 18 patients were using drops in their fellow eyes. 5 patients had gone through trabeculectomy in both eyes in TLE group.

Conclusions: No significant differences of instillation adherence were found between those who had gone through glaucoma surgery and those who had not. It was found that good adherence was kept in both groups in the patients who kept drop diary.

Commercial Relationships: Tomoko Yoshikawa, None; Itaru Kimura, None; Satoshi Watanabe, None; Ayumi Usui, None; Akira Murakami, SEED(Japan) JP4855782 (P), SEED(Japan) JP5132958 (P); Nobuyuki Ebihara, None

Program Number: 448 **Poster Board Number:** A0179

Presentation Time: 10:30 AM - 12:15 PM

Effects of prostaglandin analogues with various preservatives on the ocular surface of the rabbit

Hyun Joo Lee¹, Roo Min Jun², Kyu-Ryong Choi². ¹Department of Ophthalmology, Eulji Medical Center, Eulji University School of Medicine, Seoul, Republic of Korea; ²Department of Ophthalmology, Ewha Womans University Mok-dong Hospital, Institute of Ophthalmology and Optometry, Seoul, Republic of Korea.

Purpose: The aim of this in-vivo study is to compare the effect of the prostaglandin analogues preserved with either 0.015% or 0.001% benzalkonium chloride (BAK) or polyquaternium-1 0.001% (PQ) on the ocular surface of the rabbit eyes.

Methods: Forty white rabbits were randomized to receive once daily instillation of tafluprost 0.0015% preserved with 0.001% BAK (TF-BAK), travoprost 0.004% with 0.015% BAK (TR-BAK) or 0.001% PQ (TR-PQ), or preservative-free artificial tears in one eye for 4-week period. Tear samples collected from the 40 rabbits were analyzed by enzyme-linked immunosorbent assays (ELISA) for the presence of inflammatory cytokines: interleukin (IL)-1 β and IL-6 on day 14. After 4-week instillation, the harvested cornea and bulbar conjunctiva were evaluated by light and transmission electron microscopy (TEM).

Results: In the tear sample ELISA, IL-6 was significantly increased in TF-BAK and TR-BAK groups compared to controls and TR-PQ group; however, IL-1 β level was not significantly different among 4 groups. Rabbits treated with TR-BAK showed decreased goblet cell density of conjunctiva and increased piknotic change and vacuolization of corneal epithelial cells on light microscopy; similar change occurred but was less severe in TF-BAK group. The TR-PQ group showed similar results to the controls. In the TEM, the destruction of the microvillar architecture of conjunctiva and cornea was most prominent in the TR-BAK group.

Conclusions: Preservatives included in the anti-glaucoma eye-drops produced different ocular surface changes according to the concentration and type in the rabbits. Prostaglandin analogues preserved with higher level of BAK may cause more harmful effects on the ocular surface than PQ-preserved medications.

Commercial Relationships: Hyun Joo Lee, None; Roo Min Jun, None; Kyu-Ryong Choi, None

Program Number: 449 **Poster Board Number:** A0180

Presentation Time: 10:30 AM - 12:15 PM

Six-Month Results From a Phase 3 Randomized Trial of Fixed-Combination Brinzolamide 1%/Brimonidine 0.2%

Quang H. Nguyen¹, Jess T. Whitson², Tony Realini³, Stephen M. Goode⁴, Matthew G. McMenemy⁵. ¹Ophthalmology, Scripps Research Institute, La Jolla, CA; ²University of Texas Southwestern Medical Center at Dallas, Dallas, TX; ³West Virginia University Eye Institute, Morgantown, WV; ⁴Alcon Research, Ltd., Fort Worth, TX; ⁵Lone Star Eye Care, Sugar Land, TX.

Purpose: This study compared the intraocular pressure (IOP)-lowering efficacy and safety of fixed-combination brinzolamide 1%/brimonidine 0.2% (BBFC) with that of its component medications in patients with open-angle glaucoma (OAG) or ocular hypertension (OH). This abstract focuses on safety outcomes.

Methods: This was a phase 3, double-masked, multicenter, 3-month safety and efficacy study with a 3-month safety extension. After washout, eligible patients were randomly assigned 1:1:1 to treatment with BBFC, brinzolamide, or brimonidine 3 times daily. IOP was assessed at 8 AM, 10 AM, 3 PM, and 5 PM at 2 weeks, 6 weeks, 3 months, and 6 months. Safety assessments included adverse events (AEs), best-corrected visual acuity (BCVA), slit-lamp biomicroscopy, pachymetry, perimetry, funduscopy, and blood pressure/pulse.

Results: A total of 690 patients were enrolled; 548 completed the 6-month visit. Interim results from the 3-month visit were presented previously. At 6 months, the BBFC group demonstrated the largest IOP reduction from baseline at all time points (20%-31%) compared with the brinzolamide group (16%-22%) and the brimonidine group (12%-25%). Of the 690 patients in the safety population, 175 (25%) experienced at least 1 treatment-related AE (BBFC, 33%; brinzolamide, 19%; brimonidine, 25%). At 6 months, the most common treatment-related AEs for BBFC were eye irritation (6.3%), eye allergy (6.3%), and conjunctivitis (5.0%), for brinzolamide they were dysgeusia (10.3%) and blurred vision (6.8%), and for brimonidine they were conjunctivitis (6.0%) and conjunctivitis allergic (4.3%). No serious AEs were related to treatment. Patients using BBFC or brimonidine experienced a slight decrease in mean blood pressure (3-6 mm Hg) and pulse rate (1 beat/minute). No relevant changes were noted in BCVA, anterior or posterior segment examination, pachymetry or perimetry.

Conclusions: In patients with OAG or OH, no increased topical ocular or systemic risk was identified with BBFC compared with the individual components during 6 months of dosing. Overall, the safety profile of BBFC was similar to its components and did not result in additional risk to patients compared with the known risks of the individual components.

Commercial Relationships: Quang H. Nguyen, Alcon (C), Allergan (C), Merck (C); Jess T. Whitson, Alcon (R), Allergan (R), Merck (R); Tony Realini, Lumenis (F), Alcon (C); Stephen M. Goode, Alcon (C); Matthew G. McMenemy, Alcon (R), Bausch and Lomb (C), Alcon (C), Allergan (R), Alcon (F), Merck (R)

Support: Alcon Research, Ltd.

Clinical Trial: NCT01297920

Program Number: 450 **Poster Board Number:** A0181

Presentation Time: 10:30 AM - 12:15 PM

Short and long-term evaluation of the effects of subconjunctival infiltration of mitomycin C (MMC) in rabbits, comparing dose and time

Luiza R. Vilela^{1,4}, Ana Flávia Oliveira⁴, Fabio N. Kanadani^{2,4}, Maria Luiza Reis⁵, Tereza M. Kanadani³, Rubens Vilela¹, Priscila R. Vilela⁸, Raquel Vilela^{6,7}. ¹Ophthalmology Residency, Centro Oftalmológico de Minas Gerais, Belo Horizonte, Brazil; ²Glaucoma,

ARVO 2013 Annual Meeting Abstracts by Scientific Section/Group – Glaucoma

Clínica de Olhos da Santa Casa de Belo Horizonte, Belo Horizonte, Brazil; ³Retina, Clínica de Olhos da Santa Casa de Belo Horizonte, Belo Horizonte, Brazil; ⁴Faculdade de Ciências Médicas de Minas Gerais, Belo Horizonte, Brazil; ⁵Medical veterinary, Universidade Federal de Minas Gerais, Belo Horizonte, Brazil; ⁶Microbiology, Universidade Federal de Minas Gerais, Belo Horizonte, Brazil; ⁷Biomedical Laboratory Diagnostics Program, Michigan State University, Belo Horizonte, Brazil; ⁸Faculdade de Medicina de Barbacena, UNIPAC, Belo Horizonte, Brazil.

Purpose: To evaluate the effects of subconjunctival infiltration of mitomycin C (MMC) in rabbits, comparing dose and time.

Methods: Mitomycin C was injected subconjunctivally in 248 rabbit eyes. There was a variation in dose [0,5mg/ml, 0,3mg/ml, 0,1mg/ml and 0,01 mg/ml] and time [days 0, 2, 4, 30 and 60]. We analyzed mostly parameters like corneal edema, corneal epithelial disruption, keratitis, Descemet membrane thickening, pannus, angle synechiae, angle granuloma; iris neovascularization, necrosis, vasodilatation, inflammation, hemorrhage and granuloma; ciliary body vasodilatation and edema; perilimbal vasodilatation, granuloma, inflammation, neovascularization, hemorrhage, stromal cell reduction, vessels disruption, stromal necrosis, and characteristics of the epithelium.

Results: Perilimbal hemorrhage, epithelial changes and inflammation are typically dose dependent. Corneal edema, perilimbal stromal cell reduction and perilimbal vascular disruption are mostly time dependent. Other changes, such as iris necrosis, inflammation and hemorrhage seem to be both time and dose dependent. Analyzing the 30 and 60 days groups it is possible to observe a recovery process of conjunctival epithelium and stroma. The first one presents atypical cells with various degrees of pleomorphism. The second one (sub epithelial tissue) repaired by producing a fibrotic and scar tissue. There were intraocular damages when a higher dose of subconjunctival MMC was injected.

Conclusions: The changes after MMC injection in rabbit eyes are both time and dose dependent. There is intraocular damage after subconjunctival injection. It is possible that the areas affected with necrosis and cellular death were replaced by atypical cells that migrated from the non modified periphery tissue. Based on the long term findings the changes caused by MMC may be mostly recovered and probably most of the tissue function is maintained.

Commercial Relationships: **Luiza R. Vilela**, None; **Ana Flávia Oliveira**, None; **Fabio N. Kanadani**, None; **Maria Luiza Reís**, None; **Tereza M. Kanadani**, None; **Rubens Vilela**, None; **Priscila R. Vilela**, None; **Raquel Vilela**, None

Program Number: 451 **Poster Board Number:** A0182

Presentation Time: 10:30 AM - 12:15 PM

Treatment of refractory glaucoma using UC procedure with High Intensity Focused Ultrasound (HIFU) . Prospective series

Jean-Francois J. Rouland¹, Florent Aptel². ¹Ophthalmology, University of Lille, Lille, France; ²Grenoble University Hospital, Grenoble, France.

Purpose: To assess the safety and efficacy of Ultrasound Circular Cyclo-Coagulation (UC Procedure) using HIFU (high intensity focused ultrasound) in patients with refractory glaucoma

Methods: Prospective clinical series performed in two centers, on twenty-seven eyes of twenty-seven patients with refractory glaucoma, treated with the EyeOP1 medical device equipped with six miniaturized cylindrical piezoelectric transducers. All eyes were treated with a 6-second exposure time from each transducer. The main assessment criteria were safety and efficacy as indicated by the incidence of complications and by the IOP reduction. Ophthalmic, ultrasound biomicroscopy and flare examinations were performed

before treatment and during clinical follow-up at D1, D7, M1, M2, M3 and M6.

Results: No major intra- or post-operative complications occurred. Clinical examination showed no lesions of the ocular structures other than the ciliary body and no or few signs of intraocular inflammation after treatment. Visual acuity was not modified after the procedure.

The mean intraocular pressure was reduced from 26.9 ± 8.0 mmHg before treatment to 16.8 ± 7.4 mmHg at last follow-up. Three patients needed to be re-treated. The success rate, as defined by an IOP reduction $>20\%$, was 78%.

The mean IOP reduction achieved was 37.5%. Ocular inflammation evidenced by flare was very limited and non-significant

Conclusions: Coagulation of the ciliary body using high intensity focused ultrasound delivered by miniaturized transducers is a simple, well-tolerated procedure which enables to significantly reduce the intraocular pressure in patients with refractory glaucoma

Commercial Relationships: **Jean-Francois J. Rouland**, Thea (R), Eyetechnicare (R); **Florent Aptel**, EyeTechCare (C)

Program Number: 452 **Poster Board Number:** A0183

Presentation Time: 10:30 AM - 12:15 PM

Analysis of Intraocular Pressure-Lowering Effects of Preservative-Free Tafluprost and Timolol in Patients with Open-Angle Glaucoma and Ocular Hypertension in a Phase-III, Randomized, Double-Masked Study

John W. Grunden¹, Robert J. Lupinacci², Rohit Varma³. ¹Global Medical Affairs, Merck & Co., Whitehouse Station, NJ; ²Merck Research Laboratories, Merck & Co., West Point, PA; ³Ophthalmology and Visual Sciences, University of Illinois at Chicago College of Medicine, Chicago, IL.

Purpose: To evaluate whether baseline intraocular pressure (IOP) and prior therapy significantly influence efficacy of preservative free (PF)-tafluprost and PF-timolol in patients with OAG and OHT.

Methods: The efficacy of PF-tafluprost 0.0015% q.h.s. and PF-timolol 0.5% b.i.d. was analyzed in 610 randomized OAG and OHT subjects in a three-month phase III study. Additional post hoc efficacy analyses were completed after patients were stratified by prior treatment and by baseline diurnal (mean of 8 AM, 10 AM, and 4 PM measures) IOP, ranging from <21 to ≥ 29 mmHg. "Low IOP" groups were defined as subjects having a baseline diurnal IOP <24 mmHg, and "High IOP" groups were defined as subjects having a baseline diurnal ≥ 26 mmHg.

Results: After 12 weeks of treatment, mean diurnal IOP was lowered by 6.9 mmHg (28%) from a baseline of 24.9 mmHg in the PF-tafluprost group (N=298), and by 6.6 mmHg (27%) from a baseline of 24.7 mmHg in the PF-timolol group (N=312); the prespecified non-inferiority margin of 1.5 mmHg was met. Whether or not a patient was treatment naïve did not significantly change overall efficacy results for either treatment group ($p \geq 0.839$). However, in patients specifically naïve to prior prostaglandin treatment, PF-tafluprost (n=122) lowered IOP 7.2 mmHg (28%) compared to 6.5 mmHg (26%) by PF-timolol (n=140), a difference of 0.7 mmHg ($p=0.044$). Analyses of baseline IOP effects showed PF-tafluprost lowered IOP in the Low IOP group (n=125) by 5.6 mmHg (25%) compared to 9.1 mmHg (32%) for PF-tafluprost in the High IOP group, a difference of 3.5 mmHg ($p < 0.001$). In the Low IOP groups, PF-tafluprost (n=125) and PF-timolol (n=132) lowered IOP 5.6 mmHg (25%) and 5.6 mmHg (25%), respectively ($p=0.958$). In the High IOP groups, PF-tafluprost (n=88) and PF-timolol (n=90) lowered IOP 9.1 mmHg (32%) and 7.9 mmHg (29%), respectively (difference between groups = 1.1 mmHg, $p=0.020$).

Conclusions: In patients treated with PF-tafluprost and PF-timolol, the magnitude of reduction in IOP is dependent on the baseline IOP

and may be influenced by prior topical treatments. Understanding the clinical importance of these factors is important when considering various treatment options for patient groups including treatment naïve subjects, individuals with high baseline IOP, and patients switching from other therapies.

Commercial Relationships: John W. Grunden, Merck & Co (E); Robert J. Lupinacci, Merck & Co., Inc. (E); Rohit Varma, Allergan (C), AqueSys (C), Genentech (C), Merck & Co. Inc (C), Replenish (C), Genentech (F), National Eye Institute (F)
Clinical Trial: NCT01026831

Program Number: 453 **Poster Board Number:** A0184

Presentation Time: 10:30 AM - 12:15 PM

Efficacy, safety, and improved tolerability of preservative-free timolol 0.1% gel formulation compared with prior a BAK-preserved therapy

Paolo Frezzotti¹, Michele Figus², Carlo Cagini³, Ilaria Motolese¹, Chiara Posarelli², Anna Bartolini³, Simone Alex Bagaglia¹, Alessandra De Carolis³, Eduardo Motolese¹. ¹Ophthalmology, University of Siena, Siena, Italy; ²University of Pisa, Pisa, Italy; ³University of Perugia, Perugia, Italy.

Purpose: To evaluate the efficacy, safety and tolerability of switching to preservative-free timolol 0.1% gel patients with primary open-angle glaucoma or ocular hypertension previously treated with a BAK-preserved therapy to lower their intraocular pressure

Methods: Patients treated with a BAK-preserved therapy who needed alternative therapy due to tolerability issues were enrolled. Clinical tests (IOP, Schirmer I test, and lacrimal film break-up time BUT) and in vivo conjunctival confocal microscopy (IVCM) were performed in all patients at baseline and after 3 months. IVCM (HRT II Rostock Cornea Module; Heidelberg Engineering GmbH, Heidelberg, Germany) was performed after topical anaesthesia. The main IVCM outcomes were goblet cell density and epithelial regularity. Patients were surveyed using the Ocular Surface Disease Index (OSDI) to evaluate OSD symptoms prior to changing preservative-free timolol 0.1% gel dosed once every morning. Patients were re-evaluated 3 months later.

Results: In 65 patients preservative-free timolol 0.1% gel improved mean OSDI scores compared to either BAK-preserved therapy ($p < 0.0001$). Patients having any baseline OSD symptoms ($n = 65$) demonstrated significant improvement after switching to preservative-free timolol 0.1% gel ($p < 0.0001$). A significant improvement in clinical scores (Schirmer I and BUT) was found between groups on preserved topical hypotensive therapy and the preservative-free timolol 0.1% gel. In 75.3% of these patients, symptoms were reduced in severity. IVCM parameters after 3months: intraepithelial goblet cell density was significantly improved in preservative-free timolol 0.1% gel (86.83 ± 22.17 , $p < 0.001$) than in the BAK-preserved therapy (48.25 ± 7.70 , $p < 0.001$) The epithelial layer was significantly more regular in preservative-free timolol 0.1% gel (0.75 ± 0.6) than in the BAK-preserved therapy (0.87 ± 0.6 , $p < 0.001$)

Conclusions: Patients previously treated with a BAK-preserved therapy who are changed to preservative-free timolol 0.1% gel have clinically and statistically significant improvement in their ICVM parameters, and OSD symptoms

Commercial Relationships: Paolo Frezzotti, None; Michele Figus, None; Carlo Cagini, None; Ilaria Motolese, None; Chiara Posarelli, None; Anna Bartolini, None; Simone Alex Bagaglia, None; Alessandra De Carolis, None; Eduardo Motolese, None

Program Number: 454 **Poster Board Number:** A0185

Presentation Time: 10:30 AM - 12:15 PM

©2013, Copyright by the Association for Research in Vision and Ophthalmology, Inc., all rights reserved. Go to iovs.org to access the version of record. For permission to reproduce any abstract, contact the ARVO Office at arvo@arvo.org.

Preservative-free tafluprost in the treatment of naïve patients with glaucoma and ocular hypertension

Ines M. Lanzl^{1,2}, Thomas Hamacher³, Friedemann Kimmich⁴.

¹Ophthalmology, Technical University of Munich, Munich, Germany; ²Chiemsee Augen Tagesklinik, Prien, Germany; ³Augenzentrum Dr. Hamacher, Starnberg, Germany; ⁴eyecons, Pfinztal, Germany.

Purpose: Efficacy, tolerability and safety of the preservative-free prostaglandin analogue (PGA) tafluprost 0.0015% were investigated in treatment-naïve patients.

Methods: Data were collected in two non-interventional, prospective, multi-center, observational, open label studies of identical design conducted in Germany and Czech Republic. IOP levels were recorded for each eye at untreated baseline and 3 months after initiation of medical treatment. The primary outcome was change in mean IOP from baseline to month 3. In the POAG and OH patient subgroup analyses were stratified by the level of baseline IOP: ≥ 20 to 23 mmHg versus ≥ 24 mmHg. In addition responder rates and the achievement of pre-specified IOP levels at month 3 were evaluated. Local tolerance and overall satisfaction with the medical treatment were evaluated. All adverse events were recorded.

Results: Five-hundred and seventy nine treatment-naïve patients with primary open-angle glaucoma (POAG) (N=349), ocular hypertension (OH) (N=105), normal-tension glaucoma (NTG) (N=71), exfoliative glaucoma (PEX) (N=27) or 'other glaucomas' (N=27) were included in this study. Mean IOP was lowered significantly from 23.6 ± 4.0 mmHg at baseline to 16.8 ± 2.9 mmHg at month 3 in all patients and subgroups of patients by diagnosis ($p < 0.001$). Preservative-free tafluprost lowered mean IOP significantly in the subgroup of POAG and OH patients with lower IOP-levels from 21.9 ± 1.1 mmHg at baseline to 16.5 ± 2.2 mmHg and in the higher IOP-level subgroup of from 26.2 ± 2.4 mmHg to 17.9 ± 2.4 mmHg. In the subgroup of patients with POAG and OH an IOP response of $\geq 20\%$, $\geq 30\%$ and $\geq 40\%$ was achieved by 83.4%, 44.1% and 12.8% respectively. Overall, patients with higher baseline IOP-values (≥ 24 mmHg) showed a better response compared to patients with lower baseline IOP-levels (≥ 20 mmHg to 23 mmHg). Preservative-free tafluprost was well tolerated and safe. After 3 months, 97.9% of all patients remained on therapy.

Conclusions: In this 'real world' observational study, treatment with once daily preservative-free tafluprost was efficacious and safe in treatment naïve patients. Preservative-free tafluprost is a valuable first-choice treatment for POAG and OH patients when long term IOP control and tolerability are desirable.

Commercial Relationships: Ines M. Lanzl, Allergan (C), Alcon (R), Pfizer (R), Santen (R), Novartis (R); Thomas Hamacher, None; Friedemann Kimmich, Santen (C), 1st Q (C), Optovue (C), Oculus (C), AGEPHA (C), Allergan (C), Santen (F)

Program Number: 455 **Poster Board Number:** A0186

Presentation Time: 10:30 AM - 12:15 PM

Topical Glaucoma Therapy Cost

Alejandra Hernández-Oteyza, Gabriel Lazcano-Gomez, María J. Iriarte, Jesus Jimenez-Roman. Glaucoma, Asociacion Para evitar la Ceguera en Mexico, Mexico City, Mexico.

Purpose: To calculate the cost of topical glaucoma medications in Mexico.

Methods: Ten bottles of the common brand name glaucoma medications in Mexico were included in this study. All the bottles were analyzed to obtain the number of drops and volume in milliliters of each drug collecting it in a glass graduated cylinders.

We determined the average wholesale price (AWP) and common doping patterns of each medication, we determined the theoretical

ARVO 2013 Annual Meeting Abstracts by Scientific Section/Group – Glaucoma

cost per year for each drop. Cost per day was calculated by dividing the AWP by the number of drops in each bottle and multiplying by the total average number of drops prescribed daily in both eyes.

Annual cost was calculated by multiplying the cost per day by 365.

Results: Number of drops per milliliter varied among medications. Annual cost of medications had a wide range depending on the volume and common dose of each medication. Yearly cost of PGA's for a single daily drop was, for Lumigan 3 ml (Allergan Inc.) \$208.39, Travatan 2.5 ml (Alcon Lab) \$285.15, and Gaap 3ml (Sophia Lab) \$268.05. For twice daily dose Piobaj 5 ml (Grin lab) and Azopt 5 ml (Alcon Lab) was \$ 313.27 and \$378.78, respectively. Alphagan 5 ml (Allergan Inc) \$578.67, Agglad 5ml (Sophia Lab) \$214.48, Nortenz 5ml (Grin Lab) \$281.92. Anhigot 10 ml (Grin Lab) \$147.87, Cosopt 5ml (Merck & Co Inc) \$317.49, Azarga \$435.16. Combigan 5 ml (Allergan Inc) \$732.00. Krytan tek (Sophia Lab) \$291.67.

Conclusions: The more expensive drugs were the ones with combinations of medications and from these, the combinations containing PGA's were less expensive.

All glaucoma medications increased their prices in a 4 year period, which was not directly related with the yearly cost of each medication.

Therefore, every physician must consider several factors before prescribing a drug for glaucoma treatment not only the price but also adverse effects, systemic diseases, effect of medications and especially, compliance in order to prescribe the best drug for each patient.

Commercial Relationships: Alejandra Hernández-Oteyza, None; Gabriel Lazcano-Gomez, None; María J. Iriarte, None; Jesus Jimenez-Roman, None

Program Number: 456 **Poster Board Number:** A0187

Presentation Time: 10:30 AM - 12:15 PM

Efficacy, safety, and efficiency of self instillation of eye drops by glaucoma patients

Meghan Park¹, Michael B. Choi¹, Marguerite Huff¹, Catherine Clark¹, Clara Choo¹, Mark Maroongroge¹, Jie Peng², Alfred W. Rademaker², Angelo P. Tanna¹. ¹Department of Ophthalmology, Northwestern University Feinberg School of Medicine, Chicago, IL; ²Department of Preventive Medicine, Northwestern University Feinberg School of Medicine, Chicago, IL.

Purpose: To determine the efficacy, safety, and efficiency of eye drop instillation by glaucoma and ocular hypertension (OHT) patients and to identify demographic and behavioral characteristics that impact efficacy of eye drop instillation.

Methods: Subjects (n=117) with open-angle glaucoma or OHT who had at least 6 months of experience with self-instillation of ocular hypotensive eye drops were video recorded while self-instilling artificial tears. All subjects completed the Rapid Estimates of Adult Literacy in Medicine Questionnaire (REALM), the Glaucoma Specific Beliefs about Medicine Questionnaire (BMQ), and a mini mental status examination (MMSE). A single masked observer graded video recordings of eye drop instillation. Efficacy was assessed based on whether the subject successfully instilled at least one eye drop on the ocular surface, and was graded in a binary fashion. Safety was assessed based on whether the bottle tip made contact with the ocular surface or periocular skin, and was graded in a binary fashion. Efficiency was graded as the number of drops expelled. Associations between behavioral and demographic characteristics and the likelihood of successful eye drop instillation were explored using t-tests for continuous variables and chi-square for categorical variables.

Results: 87.8% and 90.4% of subjects successfully instilled at least

one eye drop on the ocular surface of the right and left eyes, respectively. Contact between the bottle tip and the ocular or skin surface during attempted instillation occurred in 32.2% and 37.4% of subjects for the right and left eyes, respectively. The means and standard deviations for the number of eye drops expressed were 1.9 ± 1.6 and 1.8 ± 1.4 for the right and left eyes, respectively.

Male gender (p=0.01), older age (p=0.005), and European ancestry (p=0.016) were associated with a statistically significantly lower likelihood of successful eye drop instillation on the ocular surface. Handedness, baseline diagnosis, number of medications in use, duration of prior eye drop use, visual acuity, and BMQ, REALM, and MMSE scores were not significantly associated with successful instillation.

Conclusions: A large proportion of glaucoma and OHT patients effectively, safely, and efficiently instilled eye drops. Male gender, older age, and European ancestry were associated with lower likelihood of successful instillation.

Commercial Relationships: Meghan Park, None; Michael B. Choi, None; Marguerite Huff, None; Catherine Clark, None; Clara Choo, None; Mark Maroongroge, None; Jie Peng, None; Alfred W. Rademaker, None; Angelo P. Tanna, Merck & Co, Inc. (R), Alcon Laboratories, Inc. (C), Alcon Laboratories, Inc. (R) **Support:** RESEARCH TO PREVENT BLINDNESS, NEW YORK, NY

Clinical Trial: 00051931

Program Number: 457 **Poster Board Number:** A0188

Presentation Time: 10:30 AM - 12:15 PM

Medication persistency of newly medicated Japanese glaucoma patients Short title: Medication persistency of newly glaucoma patients

Toshie Furuya, Kenji Kashiwagi. Ophthalmology, Faculty of Medicine, University of Yamanashi, Chuo, Japan.

Purpose: We investigated medication persistency and its related factors among newly medicated Japanese glaucoma patients using a health insurance database to clarify how many glaucoma patients were dropped out from the glaucoma medication.

Methods: Patients who were covered their medical expense by a social health insurance for same or more than three years during the period between 2005 and 2011 were subject to this study. All analyses were performed based on Japan medical Data Center Claim Data Base. Including criteria were; no history of glaucoma diagnosis, anti-glaucoma medication, and glaucoma surgeries; newly diagnosed glaucoma and started anti-glaucoma medication during the follow up period. Exclusion criteria were; having any type of glaucoma surgeries, change of their health insurance to the others; missing of registered record in the social health insurance during the follow up period. The definition of discontinuation of medication persistency was no health insurance records regarding glaucoma care for same or more than six months, and medication persistency was defined the period between the start of glaucoma medication and the last visit. The medication persistency related factors were also investigated.

Results: A total number of registered subjects was 1,181,102 and 2799 subjects were judged as newly diagnosed and medicated glaucoma patients. Mean (SD) age was 47.3 (13.9) years and there were 1,494 male and 1,305 female patients. Many patients were dropped out during the early period since the start of glaucoma medication. The dropout rates at three months, six months, and twelve months since the start of glaucoma medication were 26.8%, 31.9%, and 39.1%, respectively. Comparison between patients who quit glaucoma medication within six month from the start and those who continued glaucoma medication for more than two years showed younger, less number of anti-glaucoma medications, and cared by

large scale hospitals were risk factors of dropout from the glaucoma medication.

Conclusions: More than one third of newly medicated glaucoma patients were dropped out from glaucoma medication within one year from the start and some risk factors of dropout were revealed. It is important to support glaucoma patients for preventing from dropout especially at early period since start of glaucoma medication.

Commercial Relationships: Toshie Furuya, None; Kenji Kashiwagi, None

Program Number: 458 **Poster Board Number:** A0189

Presentation Time: 10:30 AM - 12:15 PM

A Randomized, Phase I Dose-Escalation Study to Evaluate Tolerability, Safety and Pharmacokinetics (PK) of Trabodenson in Healthy Older-Adult Volunteers

Alan M. Laties¹, Randall Stoltz², Chaim Brickman⁴, Vernon Humbert³, N. Slomowitz⁴, William McVicar⁴, Rudolf Baumgartner⁴.
¹Ophthalmology, Univ of Pennsylvania Sch of Med, Philadelphia, PA; ²Covance, Evansville, IN; ³Evansville Heart Center, IN, Evansville, IN; ⁴Inotek Corp., Lexington, MA.

Purpose: The safety, tolerability and PK of trabodenson eye drops, a highly-selective adenosine-1 agonist, were assessed in healthy adult subjects.

Methods: In a Phase I unit, eligible adults after informed consent entered 1 of 7 sequential 10-subject cohorts (6 trabodenson: 4 placebo). Cohorts 1-6 (Part 1) received monocular treatment with placebo or 200-3200 µg of trabodenson BID for 14 days. Cohort 7 (Part 2) received step-wise escalating binocular doses of trabodenson, from 1800-6400 µg total body dose. A single escalating dose (no punctual occlusion) was applied every 48 hrs to decrease the potential for systemic tolerance.

Results: 70 subjects (35-65 yrs) were randomized to placebo (n=28) or trabodenson (n=42). The highest achievable dose (3200 µg per eye) was reached; no MTD was identified. No severe or study-drug-related serious AEs, or dose-limiting toxicities were reported. Systemic: Cardiovascular evaluations (heart rate, blood pressure, ECG, Holter and telemetry monitoring) showed no effect at any dose or time point. Troponin levels were normal in all subjects except for a transient elevation in one placebo subject. Pulmonary, CNS, and renal measurements showed no treatment-related effects. Ocular: Serial BCVA, IOP, and complete eye examinations elicited no safety signal. Ocular AEs, in Cohorts 1-6, were uncommon, self-limited, and usually mild with similar incidence for placebo (n=4; 14%) and active (n=6; 14%). Ocular hyperemia was reported in Part 1 in one subject (2.8%) (200µg dose, moderate, duration 1 hour and self-limited) and none in Part 2. In Part 2 there was one ocular AE - photophobia, reported in the placebo group. In Part 1, a small dose-dependent reduction in IOP was detected in several Cohorts (baseline IOP ~13 mmHg). PK: exposure to trabodenson was dose-related with a plateau effect at the highest doses (at the 3 highest doses in Part 2, there was no increase in exposure with increasing dose). Median Tmax was 0.08 to 0.27 hrs and the mean t1/2 0.48 to 2.0 hrs across all doses. Drug did not accumulate in plasma following repeated administration.

Conclusions: Trabodenson, up to the highest pragmatic achievable dose, was safe and well-tolerated. No MTD was identified. Trabodenson had a short t1/2, no accumulation after repeated dosing, and limited systemic exposure.

Commercial Relationships: Alan M. Laties, AstraZeneca (C), Forest Research Inst (C), Kendle (C), Lilly (C), Merck (C), Pfizer (C), Sanofi-Aventis (C), TB Alliance for Drug Dev (C); Randall Stoltz, Covance (E); Chaim Brickman, Inotek Pharmaceuticals Corporation (E); Vernon Humbert, Inotek (C); N. Slomowitz,

Inotek Pharmaceutical Corp (E); William McVicar, Inotek Pharmaceuticals (E); Rudolf Baumgartner, Inotek Pharm Corp (E)
Clinical Trial: NCT01123772

Program Number: 459 **Poster Board Number:** A0190

Presentation Time: 10:30 AM - 12:15 PM

Inter-rater reproducibility in the assessment of video recordings of eye drop instillation by glaucoma patients

Marguerite Huff¹, Meghan Park¹, Michael B. Choi¹, Daniel Sarezky¹, Catherine Clark¹, Clara Choo¹, Jie Peng², Alfred W. Rademaker², Angelo P. Tanna¹.
¹Ophthalmology, Northwestern University Feinberg School of Medicine, Chicago, IL; ²Preventative Medicine, Northwestern University Feinberg School of Medicine, Chicago, IL.

Purpose: To determine the level of agreement of eye drop instillation efficacy, safety and efficiency performed by glaucoma patients by three masked graders based on assessment of video recordings.

Methods: Subjects with open-angle glaucoma or ocular hypertension who had at least 6 months of experience with self-instillation of ocular hypotensive eye drops were recruited for a study on eye drop instillation. Subjects were video recorded while self-instilling artificial tears sequentially to both eyes. The video recordings of the first 39 subjects were independently graded by 3 masked observers. Efficacy was assessed based on whether the subject successfully instilled at least one eye drop on the ocular surface (binary). Safety was assessed based on whether the bottle tip made contact with the ocular surface or periocular skin (binary). Efficiency was graded as the number of drops expelled. Cases in which a continuous stream of drops was expressed were graded as 5 drops. Kappa statistics (weighted kappa for efficiency) were used to estimate inter-rater agreement. Analyses were done separately for left and right eye. Kappas and their standard errors were averaged across the three raters and two eyes.

Results: Efficacy: The mean kappa level of agreement for efficacy was 0.69 (95% CI, 0.39-0.98). The range of grader scores of percentages of patients with successful eye drop instillation was 79.5-84.6% and 74.36-84.62% for the right and left eye, respectively. Safety: The mean kappa level of agreement for safety was 0.84 (95% CI, 0.66-1.00). The range of grader scores of percentages of patients making no contact between the bottle tip and ocular or skin surface was 61.5-66.7% and 64.1-74.4% for the right and left eye, respectively.

Efficiency: The mean kappa level of agreement for efficiency was 0.57 (95% CI, 0.31-0.82). The range of grader scores of percentages of patients using 1 drop per instillation was 64.1-74.4% for both the right and left eye separately.

Conclusions: In reviewing digital video recordings of eye drop instillation by patients, there was excellent agreement among the three masked observers in grading safety. Agreement for efficacy was good. Agreement of eye drop instillation efficiency was only fair, indicating that the determination of the number of drops expressed from an eye drop bottle based on digital video recordings may be imprecise.

Commercial Relationships: Marguerite Huff, None; Meghan Park, None; Michael B. Choi, None; Daniel Sarezky, None; Catherine Clark, None; Clara Choo, None; Jie Peng, None; Alfred W. Rademaker, None; Angelo P. Tanna, Merck & Co, Inc. (R), Alcon Laboratories, Inc. (C), Alcon Laboratories, Inc. (R)
Support: Research to Prevent Blindness, New York, NY
Clinical Trial: NCT01416415

Program Number: 460 **Poster Board Number:** A0191

Presentation Time: 10:30 AM - 12:15 PM

Latanoprostene Bunod 0.024% Significantly Reduces and Maintains Mean Diurnal Intra-Ocular Pressure (IOP) Compared to Latanoprost 0.005% in Subjects with Open Angle Glaucoma or Ocular Hypertension

L Jay Katz¹, Paul L. Kaufman², Tuyen Ong³, Baldo Scassellati-Sforzolini³, Jason L. Vittitow³. ¹Glaucoma, Wills Eye Institute and Department of Ophthalmology, Thomas Jefferson University, Philadelphia, PA; ²Department of Ophthalmology and Visual Sciences, University of Wisconsin, Madison, WI; ³Bausch & Lomb, Madison, NJ.

Purpose: To evaluate and compare latanoprostene bunod (INN, USAN) 0.024% vs. latanoprost 0.005% ophthalmic solution in reducing and maintaining mean diurnal intraocular pressure (IOP) for up to 29 days in subjects with open angle glaucoma or ocular hypertension.

Methods: Only the latanoprostene 0.024% data are reported in this analysis; the dose-ranging data have been presented elsewhere. Following randomization, subjects were assigned to either latanoprostene bunod 0.024% (n=83) or latanoprost 0.005% ophthalmic solution (n=82). Enrollment in this dose ranging study consisted of eligible subjects with IOP \geq 26 and \leq 32 mmHg and a diagnosis of open-angle glaucoma or ocular hypertension. Subjects dosed once daily at 8PM for 28 days. Efficacy and safety evaluations occurred on Days 7, 14, 28, and 29. Efficacy assessments included mean diurnal IOPs and the proportion of subjects maintaining a mean diurnal IOP at \leq 18 mmHg. Safety assessments included measurement of adverse events, best-corrected visual acuity, ocular tolerability, ocular signs, and vital sign measurements. An ANCOVA model with fixed-effect terms was performed. For the change from baseline IOP, t-tests were performed for all treatment groups.

Results: Demographic and baseline characteristics were similar across treatment groups. Subjects had a mean age of 61.0 years, were predominantly white (77.6%), and female (66.7%) with 43.0% being naïve to treatment at the time of enrollment. At Days 7, 14, and 28, statistically greater reductions in mean diurnal IOPs were observed for latanoprostene bunod 0.024% compared with latanoprost 0.005% (8.3 vs. 7.3 mmHg, $p = 0.0325$; 8.9 vs. 7.7 mmHg, $p = 0.0145$; and 9.0 vs. 7.8 mmHg, $p = 0.0051$, respectively). Significantly more subjects in the latanoprostene bunod 0.024% group compared with the latanoprost 0.005% group had a study eye mean diurnal IOP \leq 18 mmHg at Days 7 ($p = 0.0057$), 14 ($p = 0.0464$), 28 ($p = 0.0061$), and 29 ($p = 0.026$). All ocular treatment-emergent adverse events were mild or moderate in severity. The percentages of subjects with conjunctival hyperemia were similar across treatment groups.

Conclusions: Latanoprostene bunod 0.024% produced significantly greater reductions (\sim 1 mmHg) in mean diurnal IOP for up to 29 days compared to latanoprost 0.005%.

Commercial Relationships: L Jay Katz, Bausch & Lomb (C), Allergan (R), Allergan (C), Allergan (F), Lumenis (R), Lumenis (F); Paul L. Kaufman, Alcon (C), Allergan (C), Altheos, Inc (C), Bausch & Lomb (C), Amakem Therapeutics (C), Johnson & Johnson (C), Lens AR, Inc (F), Merck (C), Pfizer (C), Santen (C), WARF (F), Z Lens, LLC (F), Alcon (R), Allergan (R), Altheos, Inc (R), Bausch & Lomb (R), Amakem Therapeutics (R), Merck (R), Pfizer (R), Santen (C), Santen (R); Tuyen Ong, Bausch and Lomb (E); Baldo Scassellati-Sforzolini, Bausch & Lomb (E); Jason L. Vittitow, Bausch and Lomb (E)

Clinical Trial: 01223378

134 Pharmacological Interventions; Cellular Mechanisms; Electrophysiology

©2013, Copyright by the Association for Research in Vision and Ophthalmology, Inc., all rights reserved. Go to iovs.org to access the version of record. For permission to reproduce any abstract, contact the ARVO Office at arvo@arvo.org.

Sunday, May 05, 2013 1:00 PM-2:45 PM

Exhibit Hall Poster Session

Program #/Board # Range: 751-802/A0086-A0137

Organizing Section: Glaucoma

Program Number: 751 **Poster Board Number:** A0086

Presentation Time: 1:00 PM - 2:45 PM

Down-regulation of the RNA editing enzyme ADAR2 contributes to RGC death in a mouse model of glaucoma

Ai Ling Wang, Scott A. Nawy. Ophthalmology, Albert Einstein College of Medicine, Bronx, NY.

Purpose: Excitotoxic damage due to elevated intracellular Ca²⁺ levels has been proposed to mediate RGC dysfunction and death in glaucoma. We sought to explore the function and potential role of ADAR2 and Ca²⁺-permeable AMPARs in experimentally induced glaucoma.

Methods: Glaucoma model was set up by intracameral injection of latex microbeads, which elevate intraocular pressure (IOP) by blocking drainage through the trabecular meshwork. Immunohistochemical labeling of ADAR2 was examined in mouse retina using antibodies specific for ADAR2. mRNA expression levels of ADAR2 were measured in glaucoma model. For functional evaluation, primary RGCs were cultured and ADAR2 expression was knocked down using siRNA. TUNEL, Co²⁺ and Ca²⁺ imaging was used to evaluate increased susceptibility of RGCs to excitotoxic cell death.

Results: ADAR2 was specifically expressed in RGCs. We found a 50% decrease in ADAR2 expression in the retina in response to increased IOP in the intracameral injection/TM obstruction glaucoma model at 6 weeks. In primarily cultured RGCs, loss of ADAR2 expression using siRNA increased the susceptibility of RGCs to AMPA induced excitotoxicity. Furthermore, when we knocked down ADAR2, the expression of Ca²⁺ permeable AMPARs was increased.

Conclusions: We initially investigated the function of reduced ADAR2 levels on RGCs function and viability. This work suggests that ADAR2 may play a role in the pathogenesis of glaucoma and identifies a novel target for the therapeutic intervention in glaucoma.

Commercial Relationships: Ai Ling Wang, None; Scott A. Nawy, None

Support: R01EY010254; Unrestricted RPB grant

Program Number: 752 **Poster Board Number:** A0087

Presentation Time: 1:00 PM - 2:45 PM

Ocular hypotensive efficacy and safety of a fixed dose combination of AR-12286 (a Rho Kinase Inhibitor) and travoprost

Brian Levy¹, Richard A. Lewis², Casey Kopczyński³, Thomas J. Van Haarlem¹, Gary D. Novack⁴. ¹Aerie Pharmaceuticals, Bedminster, NJ; ²Private Practice, Sacramento, CA; ³Aerie Pharmaceuticals, Research Triangle Park, CA; ⁴PharmaLogic Development, Inc., San Rafael, CA.

Purpose: Prostaglandin agonists (PGA) facilitate IOP lowering by enhancing uveoscleral outflow. ROCK inhibitors mechanistically lower IOP by enhancing trabecular outflow. For patient convenience, we developed a fixed dose combination (FDC) of a ROCK inhibitor (AR 12286, Williams RD, Novack GD, van Haarlem T, et al. Ocular hypotensive effect of the Rho kinase inhibitor AR-12286 in patients with glaucoma and ocular hypertension. *Am J Ophthalmol* 2011;152:834-41) and a PGA (travoprost).

Methods: Two AR-12286 (0.25% and 0.5%)/ travoprost fixed-dose combination products (PG286) were compared to travoprost (Travatan® Z) in 93 patients with elevated intraocular pressure in a double-masked, randomized, controlled study. All dosing was once-

daily at night.

Results: From a mean baseline IOP of 26.6 to 26.8 mm Hg, 16 hours after first dose, mean IOP was 17.7, 15.8 and 18.1 mmHg in the PG286-0.25%, PG286-0.5% and travoprost groups, respectively. This represented a mean decrease from diurnally adjusted baseline IOP of 8.9 (33%), 11.0 (41%) and 8.5 mmHg (32%), respectively. On day 7 at 08:00 hours, approximately 12 hours after the final dose, mean IOP was 17.5, 14.6 and 17.5 mmHg in the PG286-0.25%, PG286-0.5% and travoprost groups, respectively. This represented a mean decrease from diurnally adjusted baseline IOP of 9.2 (34%), 12.2 (46%), and 9.1 mmHg (34%). Mean IOP remained decreased throughout the day, with mean IOPs of 17.5, 15.0, and 17.1 mmHg, respectively at 16:00 hours. The additional IOP reduction achieved by PG286-0.5% compared to travoprost was statistically significant at each time point on Day 7. The most frequently reported events were mild to moderate conjunctival hyperemia, 32% (10/31), 59% (17/29) and 42% (14/33) in the PG286-0.25%, PG286-0.5% and travoprost groups, respectively. The incidence of conjunctival hyperemia of grade 2 or greater at Day 7 was 0%, 12% and 12%, respectively.

Conclusions: Conclusion: The ocular hypotensive effect of PG286-0.5% was clinically and statistically greater than travoprost alone, with mean IOP less than 16 mm Hg at each time point. Hyperemia with PG286 was similar to travoprost alone. PG286, a ROCK/PGA fixed dose combination, was a highly effective ocular hypotensive treatment.

Commercial Relationships: Brian Levy, Aerie Pharmaceuticals (E); Richard A. Lewis, Allergan (C), Alcon (C), Aerie (C), Aquesys (C), Ivantis (C), Glaukos (C), Otsuka (C), Merck (C); Casey Kopczyński, Aerie Pharmaceuticals, Inc. (E), Aerie Pharmaceuticals, Inc. (P); Thomas J. Van Haarlem, Aerie Pharmaceuticals, Inc (E); Gary D. Novack, Aerie (C), Novabay (C), Nicox (C), Clearside (C), Panoptica (C), Ampio (C), Ocularis (C), Forest (C), Merck (C), Acucela (C)

Support: Aerie Pharmaceuticals, Inc.

Clinical Trial: NCT01474135

Program Number: 753 **Poster Board Number:** A0088

Presentation Time: 1:00 PM - 2:45 PM

Activation of the complement system in an autoimmune model of glaucoma

Sabrina Reinehr, Sebastian Becker, Sandra Kuehn, Christina Casola, Rozina Noristani, Burkhard H. Dick, Stephanie C. Joachim. Experimental Eye Research Institute, Ruhr University Eye Hospital, Bochum, Germany.

Purpose: The complement system, as a part of the innate immune system, plays a crucial role in many neuroinflammatory diseases, such as multiple sclerosis or Alzheimer's disease. In this study, we wanted to investigate the participation of the complement system (CS) in the loss of retinal ganglion cells (RGC) in an immune mediated glaucoma model.

Methods: Rats were immunized with optic nerve homogenate (ONA) or S100. The control group (CO) received sodium chloride. After 14 and 28 days RGC density was quantified with Brn3a-antibody (Santa Cruz) stained flatmounts (n=6). To evaluate the activation of the CS, cross-sections of the retina were stained with C3 (Cedarlane) and membrane attack complex (MAC; Biozol) after 14 or 28 days (n=5 per group). Cell counts of RGC and the complement components were performed using Image J Software. Statistical analysis was performed using [Student] t-test.

Results: No change in the density of the RGCs could be observed in the immunized animals compared to CO after 14 days (ONA: p=0.9; S100: p=0.8), but after 28 days there was a significant RGC loss (ONA: p=0.0005; S100: p=0.005). In the ONA group, MAC was

significantly increased in the ganglion cell layer (GCL) after 14 and 28 days (14 days: CO: 0.5±0.9; ONA: 0.8±0.9; p=0.02; 28 days: CO: 0.4±0.7; ONA: 0.1±0.7; p=0.004). After 28 days the total number of MAC+ cells was also significant higher (Co: 1.1±1.2; ONA: 2.5±1.8; p=0.0001). Regarding C3, no changes could be detected in the GCL at both points in time, whereas after 28 days the total number of C3+ cells was increased (CO: 3.1±1.7; ONA: 4.0±2.0; p=0.0014). In the S100 group, no difference in MAC staining could be seen either 14 or 28 days after immunization. In contrast, the total number of C3+ cells was increased after 14 days (CO: 0.9±1.2; S100:1.5±1.6; p=0.0002), but not in the GCL (CO: 0.8±1.1; S100:0.8±0.9; p=0.696).

Conclusions: No RGC loss could be observed at day 14, but a significant loss can be noted after 28 days. Indeed, the CS seems to be involved in apoptosis of RGC in ONA immunized animals after two weeks. Because after four weeks MAC+ cells increased in total, we assume that secondary effects lead to an additional activation of complement components, like C3, as a consequence of RGC death. The fact that, at both points in time, neither C3 nor MAC could be shown in the GCL of S100 immunized animals could indicate earlier autoimmune mechanisms that lead to the RGC loss.

Commercial Relationships: Sabrina Reinehr, None; Sebastian Becker, None; Sandra Kuehn, None; Christina Casola, None; Rozina Noristani, None; Burkhard H. Dick, None; Stephanie C. Joachim, None

Support: German Research Foundation (DFG) grant JO-886/1-1

Program Number: 754 **Poster Board Number:** A0089

Presentation Time: 1:00 PM - 2:45 PM

Evaluation of AR-13324, a novel dual mechanism agent, in lowering of IOP in glaucoma and ocular hypertension

Mark Weiss¹, Brian Levy², Casey Kopczyński³, Thomas J. Van Haarlem², Gary D. Novack⁴. ¹Private Practice, Tulsa, OK; ²Aerie Pharmaceuticals, Bedminster, NJ; ³Aerie Pharmaceuticals, Research Triangle Park, NC; ⁴PharmaLogic Development, Inc., San Rafael, CA.

Purpose: In this first-in-human study, we sought to evaluate the ocular hypotensive efficacy and safety of AR-13324 ophthalmic solution dosed once-daily in the morning. AR-13324 is both a Rho kinase (ROCK) inhibitor and norepinephrine transporter inhibitor that lowers IOP in animal models through a dual mechanism of action, increasing trabecular outflow and decreasing aqueous production.

Methods: Entry criteria for the study included a diagnosis of open angle glaucoma (OAG) or ocular hypertension (OHT), unmedicated or post-washout IOP \geq 24 mm Hg in one or both eyes at 08:00 hours and \geq 21 mm Hg at 10:00, 12:00 and 16:00 hours. Enrolled were 85 patients with elevated intraocular pressure in this 7-day, double-masked, randomized, vehicle-controlled, monocular study of 3 doses of AR-13324 or its vehicle.

Results: Mean diurnal IOP at baseline in the 85 enrolled patients was 24.3 to 25.6 mm Hg. After a week of dosing, all active groups experienced IOP reductions that were significantly different from vehicle at all time points (p = 0.018 to <0.001). Peak reduction occurred at 8 hours after the final morning dose, ranged from 6.1 to 7.2 mm Hg relative to baseline, and appeared to be continuing downward. IOP reduction at trough (24 hours after dosing) was 5.6 to 6.3 mm Hg relative to baseline. Mild (+1) to moderate (+2) conjunctival hyperemia was the most prevalent biomicroscopic finding.

Conclusions: AR-13324 0.01% to 0.04% q.d. (AM) produced large reductions in IOP that were statistically and clinically significant and lasted at least 24 hours after dosing, with 0.02% AR 13324 appearing to reach the top of the dose response curve. IOP decreased steadily

for 8 hours following dosing, suggesting that peak efficacy may occur beyond 8 hours. The only safety finding of note was dose-related ocular hyperemia that declined in incidence and severity with repeated dosing. AR-13324, with its dual mechanism of action, shows promise as a novel ocular hypotensive agent for the treatment of glaucoma.

Commercial Relationships: Mark Weiss, Aerie (F), Allergan (F), Alcon (F); Brian Levy, Aerie Pharmaceuticals (E); Casey Kopczyński, Aerie Pharmaceuticals, Inc. (E), Aerie Pharmaceuticals, Inc. (P); Thomas J. Van Haarlem, Aerie Pharmaceuticals, Inc (E); Gary D. Novack, Aerie (C), Novabay (C), Nicox (C), Clearside (C), Shantica (C), Ampio (C), Ocularis (C), Forest (C), Merck (C), Acucela (C)

Support: Aerie Pharmaceuticals, Inc.

Clinical Trial: NCT01528787

Program Number: 755 **Poster Board Number:** A0090

Presentation Time: 1:00 PM - 2:45 PM

gp130 Expression and Activation as a Function of Age and IOP in the DBA/2 Mouse Model of Glaucoma

Franklin D. Echevarria^{1,2}, Michelle Won², Caroline Walker², Heather Cathcart², Rebecca M. Sappington². ¹Neuroscience, Vanderbilt University, Nashville, TN; ²Vanderbilt Eye Institute, Vanderbilt University Medical Center, Nashville, TN.

Purpose: To identify potential avenues of interleukin-6 (IL-6) and related cytokine signaling in glaucomatous retina, we examined age- and IOP-related changes in expression and activation of the IL-6-family signal transducer gp130.

Methods: Using immunoassay and qPCR, we measured global expression of gp130 in 4 and 8 month old DBA/2 and C57/Bl6 mice. Ganglion cell- and nerve fiber layer-specific expression in these mice was quantified using immunohistochemistry and quantitative digital microscopy. Co-immunolabeling of gp130 and cell type-specific markers was used to identify potential targets of signaling from members of the IL-6 family of cytokines and correlate gp130 expression with cell loss in retinal ganglion cells (RGCs). Cell types evaluated included: retinal ganglion cells (RGCs; brn3a and β -Tubulin III), astrocytes (GFAP) and Müller cells (glutamine synthetase). To measure gp130 activation, we quantified phosphorylation of STAT3, the downstream target of gp130 signaling, by immunoblotting.

Results: Global expression of gp130 increases by 10 fold in aged C57 mice, compared to young C57 ($p < 0.05$). In contrast, there is no age- or IOP-related change in gp130 expression in DBA/2 mice ($p > 0.05$). However, gp130 expression in DBA/2 mice is ~50% less than age-matched C57 mice ($p < 0.05$). Protein localization studies reveal co-localization of gp130 primarily with RGC and Müller cell markers in the ganglion cell (GCL) and nerve fiber (NFL) layers of the retina. Expression of gp130 in the GCL/NFL increases by ~64% in the peripheral retina of aged C57 mice, compared to young C57 mice. There are no IOP or age-related changes in the peripheral GCL/NFL of DBA/2 mice ($p > 0.05$) or the central GCL/NFL of either strain ($p > 0.05$). Interestingly, the overall number of gp130/brn3a+ RGCs increases by ~20% in DBA/2 retina, as compared to age-matched C57 retina ($p < 0.05$). Despite little to no change in gp130 expression, activation of Stat3 was elevated by as much as 3 fold in DBA/2 mice, compared to C57 mice.

Conclusions: Our data suggests that global changes in gp130 expression are associated with normal aging, while aging in the presence of elevated IOP induces discrete changes in gp130 expression, specifically in RGCs. This increase in gp130 expression by RGCs is accompanied by an increase in STAT3 activation,

suggesting that RGCs are a primary target of gp130-mediated signaling induced by glaucomatous stressors.

Commercial Relationships: Franklin D. Echevarria, None; Michelle Won, None; Caroline Walker, None; Heather Cathcart, None; Rebecca M. Sappington, None

Support: NEI-1R01EY020496-01 (RMS), NEI Core Grant P30 EY08126 (RMS), Research to Prevent Blindness (Career Development Award, RMS) NH Grant R25 GM 62459-9 (FE)

Program Number: 756 **Poster Board Number:** A0091

Presentation Time: 1:00 PM - 2:45 PM

In vivo imaging of mitochondrial axonal transport in the diseased and aged mammalian CNS

Yuji Takihara¹, Masaru Inatani¹, Kei Eto², Toshihiro Inoue³, Keiichiro Iwao⁴, Yoshihiro Takamura¹, Junichi Nabekura^{2,5}, Hidenobu Tanihara³. ¹Ophthalmology, University of Fukui, Yoshida, Japan; ²Division of Homeostatic Development, National Institute for Physiological Sciences, Okazaki, Japan; ³Ophthalmology, Kumamoto University, Kumamoto, Japan; ⁴Ophthalmology, Saga University, Saga, Japan; ⁵Physiological Sciences, The Graduate University for Advanced Studies, Okazaki, Japan.

Purpose: Mitochondrial axonal transport is essential for functions and survival of neurons. The disturbance of the dynamics in neurodegenerative models has been shown using mainly neurons *in vitro* and in *Drosophila*, whereas *in vivo* imaging of mitochondrial axonal transport in the mammalian central nervous system (CNS) has not been achieved. This has limited our knowledge of the dynamics in the diseased and aged mammalian CNS. The purpose of the study is to reveal the disturbance of mitochondrial axonal transport of retinal ganglion cells (RGCs) in a mouse glaucoma model and aged mice.

Methods: Under general anesthesia, *in vivo* imaging of the mice in which fluorescent proteins are expressed specifically in neuronal mitochondria was conducted. As a glaucoma model, ocular hypertension was induced by laser treatment of limbal and episcleral veins in mice 4 months of age.

Results: *In vivo* imaging of mouse RGCs showed active mitochondrial axonal transport. In the glaucoma model, the density of RGCs decreased ($P < 0.0001$) at 14 days after treatment, whereas the density did not significantly decrease at 3 days after treatment. The length of mitochondria transported in RGC axons (measured parallel to the axonal long axis) in the mouse glaucoma model at 3 days after treatment ($1.81 \pm 0.06 \mu\text{m}$; $n = 275$) was shortened ($P < 0.0001$), compared with that in control mice ($2.23 \pm 0.08 \mu\text{m}$; $n = 512$). The number of mitochondria transported in RGC axons in the mouse glaucoma model at 3 days after treatment (65 ± 7 per mm; $n = 67$) decreased ($P = 0.0001$), compared with that in control mice (102 ± 6 per mm; $n = 78$). The length of mitochondria transported in RGC axons in aged mice 12 months of age ($1.57 \pm 0.04 \mu\text{m}$; $n = 579$) was also shortened, compared with that in young mice 4 months of age ($P < 0.0001$). However, the number of mitochondria transported in RGC axons in aged mice (125 ± 8 per mm; $n = 85$) increased, compared with that in young mice ($P = 0.048$).

Conclusions: *In vivo* imaging of RGCs in mice reveals the disturbance of mitochondrial axonal transport in the mouse glaucoma model before RGC death and in aged mice. In both the mouse glaucoma model and aged mice, the length of mitochondria transported in RGC axons is shortened. In contrast with the reduction in the number of mitochondria transported in RGC axons in the mouse glaucoma model, that in aged mice does not decrease.

Commercial Relationships: Yuji Takihara, None; Masaru Inatani, None; Kei Eto, None; Toshihiro Inoue, None; Keiichiro

ARVO 2013 Annual Meeting Abstracts by Scientific Section/Group – Glaucoma

Iwao, None; **Yoshihiro Takamura**, None; **Junichi Nabekura**, None; **Hidenobu Tanihara**, None
Support: Grants-in-Aid for Scientific Research from MEXT and Research Grants from the University of Fukui

Program Number: 757 **Poster Board Number:** A0092

Presentation Time: 1:00 PM - 2:45 PM

Impact of supply problems of preservative-free and low preservative glaucoma medications on patients and hospital staff
Shima Shah, Julia E. Theodosiades. Moorfields Eye Hospital, London, United Kingdom.

Purpose: Since March 2011 there have been recurring problems with the supply of preservative-free (PF) and low preservative (LP) glaucoma medications in the UK. We report a study investigating the impact of these problems from a patient, administrative and clinical perspective.

Methods: The numbers of individuals on PF and LP formulations of glaucoma therapy was determined from the Moorfields Eye Hospital (MEH) pharmaceutical database. Information was sourced from: staff (glaucoma surgeons, secretaries, clerical staff and pharmacists), patients and a notes assessment of the clinical impact on patient management.

Results: A considerable number of patients require LP and PF medication, rising each year, with an 83% increase from April 2009 to April 2013 (extrapolated).

Anecdotal staff evidence - The number and difficulty of enquiries varied across the job spectrum. The largest load fell upon the secretaries who reported receiving up to 30 enquiries a day. Each enquiry involved locating patient notes, consultant review of notes, correspondence with GP and patient, and in some cases expediting the patients' next clinic appointment. All staff had noted a measurable impact on their work load.

Notes assessment - The consequence on patient management included ineffectiveness of alternative drugs, adverse drug reactions and the need for alternative intervention. The most notable impact was increased visits to the medical system, both GP and hospital.

Patient experience - Results showed increased anxiety, communication frustrations and inconvenience of disrupted drug supply.

Conclusions: Glaucoma is a chronic disease that requires long-term medical therapy. Our results show a real impact on patients, disease management and hospital services as a result of erratic drug supply. European legislation states that marketing authorisation holders and distributors have 'an obligation to ensure appropriate and continued supplies of a medicinal product to pharmacies and persons authorised to supply medicinal products'. To the best of our knowledge this represents the first report of the impact of failure to comply with this legislation in the field of glaucoma.

Table 1: MEH, Pharmacy database

Drug	April 2009-March 2010	April 2010-March 2011	April 2011-March 2012	April 2012 - October 2012 (6 months)
Low preservative	317	783	799	340
Preservative free	647	1040	1366	1087
Total	1564	1823	2165	1427

Commercial Relationships: **Shima Shah**, None; **Julia E. Theodosiades**, None

Program Number: 758 **Poster Board Number:** A0093

Presentation Time: 1:00 PM - 2:45 PM

Evaluation of the antioxidant status of human aqueous humor

©2013, Copyright by the Association for Research in Vision and Ophthalmology, Inc., all rights reserved. Go to iovs.org to access the version of record. For permission to reproduce any abstract, contact the ARVO Office at arvo@arvo.org.

Carla J. Siegfried¹, Ying-Bo Shui¹, Fang Bai¹, David C. Beebe^{1,2}.
¹Ophthalmology and Visual Sciences, Washington University, St. Louis, MO; ²Cell Biology/Physiology, Washington University, St. Louis, MO.

Purpose: Previous studies suggest that oxidative stress plays a role in glaucoma development, yet there is a gap in understanding the components of antioxidant protection in the eye. To explore these factors in disease states such as glaucoma and cataract, as well as after vitrectomy surgery, which increases the risk of glaucoma (Koreen, et al. Retina 2012), we measured the contribution of ascorbic acid (AsA) to the Total Reactive Antioxidant Potential (TRAP) of the aqueous humor in patients undergoing intraocular surgery.

Methods: Consenting patients undergoing cataract and/or glaucoma surgery were included. An Oxylab pO₂TM optical oxygen sensor (Oxford Optronix) was used to measure pO₂ in the anterior chamber (AC) angle, mid-AC, and near the corneal endothelium. In pseudophakes and eyes undergoing lens extraction, pO₂ was measured in the posterior chamber and near the anterior lens surface. Aqueous humor samples (n=40) were collected and stored in the gas phase of a liquid nitrogen tank. AsA assay (colorimetric in triplicate) and TRAP assays (chemiluminescence) were performed as previously described. Ascorbate oxidase added to each sample revealed the antioxidant potential not attributable to AsA.

Results: Antioxidant potential contributed by AsA accounted for 40-83% (mean=65%) of TRAP. In post-vitrectomy eyes, the AsA level in aqueous humor was significantly lower (p=0.002) and the contribution of AsA to TRAP was also decreased (p=0.007). The contribution of AsA to TRAP was decreased in females (p=0.017) with a similar trend in African vs. European Americans (p=0.065). Multivariate regression analyses will be performed after pending analysis of an additional 40 samples. Since all patients had cataract and/or glaucoma, TRAP or AsA levels did not correlate with the presence of these diseases, or with oxygen levels at any location in the eye.

Conclusions: AsA accounts for a significant component of TRAP in human aqueous humor. Prior vitrectomy surgery, a risk factor for the development of nuclear cataracts and open angle glaucoma, is associated with significantly lower AsA and TRAP values. Depletion of these antioxidants in at-risk subjects (females and African Americans) provides further support for the importance of antioxidant protection in cataract and glaucoma.

Commercial Relationships: **Carla J. Siegfried**, None; **Ying-Bo Shui**, None; **Fang Bai**, None; **David C. Beebe**, FivePrime (C), Panoptica (C), Vistakon (Johnson and Johnson) (C)

Support: NEI grant R01-EY021515-01, NEI Core grant EY02687, Grace Nelson Lacy Research Endowment Award, Unrestricted grant from Research to Prevent Blindness

Program Number: 759 **Poster Board Number:** A0094

Presentation Time: 1:00 PM - 2:45 PM

Drug therapy of magnesium deficiency in patients with primary open angle glaucoma (POAG)

Iusine arutyunyan, Elena Iomdina. Glaucoma, Moscow Helmholtz Research Institute of Eye Diseases, Moscow, Russian Federation.

Purpose: To assess the effect of a magnesium-containing drug inclusion into the therapy complex of POAG.

Methods: 22 POAG patients aged 42 to 72 (61.1±2.5 yrs) received hypotensive therapy supplemented by Magnerot (Wörwag Pharma, Germany) daily for 6 weeks: 2 tbs. of Magnerot 3 times a day during the first week, then 1-2 tbs. 2-3 times a day. The control group consisted of 16 POAG patients (63.7±2.7 yrs), who received hypotensive therapy but no Magnerot. We assessed the functional

structure of the eye before treatment, as well as 1, 2-3, and 5 months after it. In all patients, we measured corneal-compensated IOPcc, IOP equivalent to Goldmann (IOPG) and corneal hysteresis (CH) using ORA (Reichert), performed computer perimetry and retinal tomography of the optic nerve.

Results: Our previous studies showed a decrease of the magnesium content in aqueous humor, anterior sclera and tear fluid of patients with various stages of POAG. A statistically significant drop in IOPG (by 3.3 ± 0.4 mm Hg) and IOPcc (by 4.1 ± 0.3 mm Hg) was revealed after the treatment with the magnesium-containing drug ($p < 0.05$). Computer perimetry showed a significant increase of the total visual field (from 426.5 ± 7.8 to 452.5 ± 8.8 degrees, $p < 0.05$), mainly in patients with moderate glaucoma. The analysis of MD index showed a tendency to reduction in the total depression of sensitivity from an average of -5.8 dB to -3.9 dB ($p > 0.5$). The main group showed almost twice as many cases with improved visual field as the control group. The results of confocal scanning retina tomography taken after therapy showed that the average thickness of the retinal nerve fiber layer tends to grow in patients with the initial (from 0.25 ± 0.02 mm to 0.27 ± 0.01 mm) and moderate (0.19 ± 0.03 mm to 0.21 ± 0.02 mm) stages of glaucoma.

Conclusions: The first results of Mg-containing drug administration showed its positive effect on IOP and functional condition of eyes with glaucoma. We have thus reasons to suggest that the drug has a stabilizing effect on the course of the glaucomatous process, but future study is needed.

Commercial Relationships: lusine arutyunyan, None; Elena Iomdina, None

Program Number: 760 **Poster Board Number:** A0095

Presentation Time: 1:00 PM - 2:45 PM

Prostaglandin Efficacy in the Hispanic Population

Lindsay T. Davis, Kundandeeep Nagi, Dip S. Jadav. Ophthalmology, UTHSCSA, San Antonio, TX.

Purpose: To compare the intraocular pressure (IOP) reduction with Latanoprost 0.005% in the Hispanic and Caucasian population.

Methods: A retrospective review of 212 subjects was performed. Of these, the prostaglandin (PGA) mediated IOP reduction of 122 Hispanic eyes was compared to 90 Caucasian eyes. In addition, we further examined the medication's effect based on age, gender and phakic status. Main outcome measures included average and percent IOP reduction as a surrogate for efficacy, calculated by comparing the pre-treatment IOP to the IOP taken after six weeks of monotherapy with Latanoprost. Data was summarized and compared using Wilcoxon 2-sample test. A p-value < 0.05 was considered as statistically significant.

Results: Of the 183 eyes that responded to PGA monotherapy, no statistically significant difference was found between ethnic groups ($p = 0.6$). The IOP decreased by 8.02 mm Hg (29.9%, $n = 103$) in Hispanic eyes and by 7.96 (29.6%, $n = 80$) in Caucasian eyes. When comparing Hispanic and Caucasian males and females, no statistically significant difference was found (8.03 vs 8.02 mm Hg in males, $p > 0.05$ and 8.00 vs 7.89 mm Hg in females, $p > 0.05$ respectively). Further analysis comparing specific age groups and lens status between Caucasian and Hispanic eyes yielded no statistically significant difference in IOP lowering.

Conclusions: To our knowledge, no prior study has compared IOP reduction with prostaglandin analogs in the Hispanic and Caucasian population. This study shows equivalent efficacy among Hispanic and Caucasian patients using nightly latanoprost.

Commercial Relationships: Lindsay T. Davis, None; Kundandeeep Nagi, None; Dip S. Jadav, None

Program Number: 761 **Poster Board Number:** A0096

Presentation Time: 1:00 PM - 2:45 PM

Short-term Intraocular Pressure Spike after Combined Phacoemulsification and iStent Implantation: Prednisolone versus Loteprednol

Qianqian Wang¹, Paul Harasymowycz^{1,2}. ¹Ophthalmology, University of Montreal, Montreal, QC, Canada; ²Montreal Glaucoma Institute, Montreal, QC, Canada.

Purpose: Intraocular pressure (IOP) spike may be a short-term complication after combined phacoemulsification and iStent implantation (phaco-iStent). This study aims to compare the impacts of topical prednisolone (P) and of loteprednol (L) on post-operative IOP evolution and to assess their glaucoma medication sparing effects.

Methods: A retrospective chart review was done for patients who underwent phaco-iStent between April 2011 and October 2012. Post-operatively, every patient received a 4-week tapering regimen of either prednisolone or loteprednol. Baseline demographic and clinical data was compared by Student t and chi-square tests. Evolution of IOP and of number of glaucoma medications (NGM) at pre-operative visit, post-operative day 1 (POD 1), 1-2 weeks, 3-4 weeks and 2-3 months was assessed by mixed model for repeated measures.

Results: We identified 124 eyes (L: 79, P: 45) from 96 patients. Pre-operative demographic and clinical parameters are similar ($p > 0.05$) across both groups. The IOP increased from 17.6 [(range) 9-33] mmHg pre-operatively to 21.4 [9 - 41] mmHg at 1-2 weeks in loteprednol group, and from 15.6 [8 - 30] to 19.1 [5 - 50] mmHg in prednisolone group. It then decreased ($p < 0.0001$) by 3-4 weeks in both groups (L: 15.9 [7 - 30] mmHg; P: 14.7 [4 - 28] mmHg) and continued to improve at 2-3 months. NGM showed significant decrease ($p < 0.0001$) from pre-operative visit (L: 2.2 [0-5]; P: 1.8 [0-4]) to POD 1 (L: 0.4 [0-4]; P: 0.6 [0-4]), then remained stable in both groups. No significant difference in IOP or NGM evolution between the 2 groups was detected ($p > 0.05$). The proportion of patients with an IOP spike of 5 mmHg or more ($p = 0.57$) and that of patients needing wound burp ($p = 0.37$) are also similar in both groups.

Conclusions: In our phaco-iStent patients, loteprednol had similar effects to prednisolone in post-operative IOP evolution and glaucoma medication sparing.

Commercial Relationships: Qianqian Wang, None; Paul Harasymowycz, Allergan (C), Alcon (C), Merck (C), SOLX (C), Pfizer (R), Novartis (R), Bausch and Lomb (R), AMO (R)

Program Number: 762 **Poster Board Number:** A0097

Presentation Time: 1:00 PM - 2:45 PM

Association between Genetic Polymorphisms of the Prostaglandin F2 α Receptor Gene and Response to Latanoprost in Glaucoma and Ocular Hypertension Patients

Kazuhisa Sugiyama, Mayumi Sakurai, Tomomi Higashide, Shinji Ohkubo, Hisashi Takeda, Yoshiaki Saito. Ophthalmology and Visual Science, Kanazawa University Graduate School of Medical Science, Kanazawa, Japan.

Purpose: To examine whether intraocular pressure (IOP) reduction by latanoprost correlates with the single nucleotide polymorphism (SNP) of the prostaglandin F2 α (FP) receptor gene in glaucoma and ocular hypertension (OH) patients.

Methods: We retrospectively examined clinical data of glaucoma and OH patients who were treated with latanoprost monotherapy in 1 eye and who had at least two IOP measurements on different days at baseline and also when on the medication. In all patients, IOP reduction was evaluated by the percent IOP reduction (% Δ IOP), estimated by subtracting IOP fluctuations in the untreated fellow eye. Subjects were classified by % Δ IOP into 3 categories: 1) low

responders (% Δ IOP <10%), 2) medium responders (% Δ IOP \geq 10% and <25%), and 3) high responders (% Δ IOP \geq 25%). Nine SNPs in FP receptor gene were examined. The correlation between the % Δ IOP and SNPs in the FP receptor gene was then analyzed.

Results: A total of 82 patients (42 males, 40 females) met the eligibility criteria and were included. The average IOP of the treated eyes was decreased from 16.7 ± 3.2 mmHg (mean \pm SD) to 14.2 ± 2.5 mmHg by latanoprost (mean % Δ IOP: $15.3 \pm 10.5\%$). Three SNPs, rs1073611, rs1073610, and rs12093097 were in strong linkage disequilibrium. The % Δ IOP of the CC homozygote in rs12093097 ($14.1 \pm 1.3\%$ (mean \pm SE)) was significantly lower than that of the T carrier ($20.2 \pm 2.1\%$, $P = 0.039$). The allele or genotype distributions of 3 SNPs, rs1073611, rs1073610, and rs12093097, were found to be significantly associated with the category of IOP response to latanoprost. The results of multivariate logistic regression analysis demonstrated that the genotype of rs12093097 was the only significant factor which has an effect on the IOP response to latanoprost (medium + high responders vs. low responders: $P = 0.032$; odds ratio, 0.103; 95% confidence interval, 0.013-0.824; predictive value, 67.1%).

Conclusions: An association was found between rs12093097, rs1073611, and rs1073610 of the FP receptor gene and the response to latanoprost in patients with glaucoma and OH. These SNPs could affect the degree of IOP reduction by latanoprost.

Commercial Relationships: Kazuhisa Sugiyama, None; Mayumi Sakurai, None; Tomomi Higashide, None; Shinji Ohkubo, Topcon (C), Nidek (C); Hisashi Takeda, None; Yoshiaki Saito, None
Support: Japan Society for the Promotion of Science no. 19592008

Program Number: 763 **Poster Board Number:** A0098

Presentation Time: 1:00 PM - 2:45 PM

Connective Tissue Growth Factor Induction of Lysyl Oxidase (LOX) Enzyme Expression in Human Trabecular Meshwork Cells is reduced by FG-3019

Deborah M. Wallace^{1,2}, Abbot F. Clark³, Noelynn Oliver⁵, John K. Crean⁴, Colm J. O'Brien^{1,2}. ¹School Med & Medical Science, University College Dublin, Dublin, Ireland; ²Ophthalmology, Mater Misericordiae University Hospital, Dublin, Ireland; ³North Texas Eye Inst., University North Texas Health Centre, Fort Worth, TX; ⁴School of Biomolecular and Biomedical Science, University College Dublin, Dublin, Ireland; ⁵Boehringer Ingelheim Pharmaceuticals Inc., Ridgefield, CT.

Purpose: The matricellular protein Connective Tissue Growth Factor (CTGF) has been shown to play an integral role in extracellular matrix (ECM) deposition in trabecular meshwork (TM) cells in glaucoma. Furthermore, we have previously described a role for anti-CTGF immunotherapy (FG-3019, FibroGen Inc. USA) in combating glaucoma-associated fibrosis in *in vitro* models. LOX enzymes are an important class of ECM cross-linking enzymes involved in the pathogenesis of glaucoma with identified single nucleotide polymorphisms (SNP) in LOXL-1 associated with an increased risk of developing pseudoexfoliation glaucoma. The purpose of this study was to firstly investigate if CTGF induced expression of LOX enzymes in human TM cells and whether pre-treatment with anti-CTGF (FG-3019) could decrease LOX expression and therefore be an attractive therapeutic approach for the treatment of glaucoma.

Methods: TM cells from a normal donor (NTM5) were grown to confluence and placed in serum free media for 24 hours prior to treatment with a recombinant fragment of CTGF (25ng/ml for 24hours) (Sigma). Levels of LOX and LOXL genes (1-4) were determined by quantitative PCR using gene specific exon-exon spanning primers and / or specific probes. NTM5 cells were then cultured in the presence or absence of the therapeutic, humanized

monoclonal anti-CTGF antibody FG-3019 (10 μ g/ml) prior to treatment with CTGF as described above. The modulatory effect of FG-3019 (10 μ g/ml) was assessed and IgG (10 μ g/ml) was included as a control. LOX and LOXL genes (1-4) expression were determined by quantitative PCR using gene specific exon-exon spanning primers and / or specific probes. The equation $2^{\Delta\Delta Ct}$ was used to derive a fold difference for gene expression. Results are representative of three independent experiments.

Results: Treatment of NTM cells with CTGF induces a significant ($P < 0.05$) increase in the expression of LOX & LOXL 1-4. Pre-treatment with anti-CTGF (FG-3019) significantly reduces ($P < 0.01$) the CTGF-induced expression of all LOX enzymes.

Conclusions: CTGF can drive the expression of the ECM cross-linking LOX enzymes in NTM cells. The anti-CTGF antibody FG-3019 is effective in reducing LOX production. These observed anti-fibrotic effects support a pathologically significant role for the use of anti-CTGF immunotherapy as a possible approach for treatment of glaucoma.

Commercial Relationships: Deborah M. Wallace, None; Abbot F. Clark, Alcon Research, Ltd. (F); Noelynn Oliver, None; John K. Crean, Fibrogen Inc (F); Colm J. O'Brien, None

Support: The Health Research Board Ireland (HRA_POR/2010/129), The International Glaucoma Association / United Kingdom and Eire Glaucoma Society Award and The Mater College, Ireland

Program Number: 764 **Poster Board Number:** A0099

Presentation Time: 1:00 PM - 2:45 PM

The retinal pigmented epithelial cell and peripapillary atrophy: potential mediators of glaucomatous optic disc cupping?

Emily L. Hughes^{1,2}, Neil G. Docherty³, John K. Crean⁴, Abbot F. Clark⁵, Deborah M. Wallace^{1,2}, Colm J. O'Brien^{1,2}. ¹School of Medicine and Medical Sciences, University College Dublin, Dublin, Ireland; ²Department of Ophthalmology, Mater Misericordiae University Hospital, Dublin, Ireland; ³Department of Physiology, School of Medicine, Trinity College Dublin, Dublin, Ireland; ⁴UCD Conway Institute of Biomolecular and Biomedical Research, School of Biomolecular and Biomedical Science, University College Dublin, Dublin, Ireland; ⁵Department of Cell Biology & Anatomy and the North Texas Eye Research Institute, University North Texas Health Science Center, Fort Worth, TX.

Purpose: There is a well established link between peripapillary atrophy (PPA) and glaucoma. Histologically the zone of PPA adjacent to the optic disc (beta zone), is bare of retinal pigment epithelial cells (RPEC) but the aetiology is unknown. Epithelial cells in other organs have been shown to differentiate to a myofibroblastic phenotype through the process of epithelial to mesenchymal transition (EMT) in response to a variety of stimuli. EMT has been shown to play a role in fibrotic disease. This work examines the possibility that glaucoma-like stimuli such as stretch and growth factor stimulation may induce EMT in the RPEC, causing it to have a migratory ability and myofibroblastic phenotype. This may infer a role for the RPEC, and therefore PPA, in glaucomatous optic disc cupping.

Methods: The human retinal pigment epithelial cell line, ARPE-19, was exposed to cyclical stretch (15% cell elongation, 1Hz cycles). As a positive control, cells were treated with recombinant human transforming growth factor beta-1 (TGF β 1, 10ng/ml) to induce EMT. Post-treatment analysis included real time polymerase chain reaction for gene expression of Zona Occludens 1 (ZO-1), alpha smooth muscle actin (α SMA), collagen type 1A1, and TGF β 1. The migratory capacity of ARPE-19 cells under the influence of growth factors was examined by scratch migration assay. Human optic nerve heads from

normal and glaucomatous donors underwent immunohistochemical analysis for TGF β 1, and RPE65 (visual cycle protein found in RPEC).

Results: Cyclical stretch of ARPE-19 cells resulted in a decrease in epithelial marker ZO-1, and an increase in myofibroblastic marker α SMA, as well as an increase in collagen type 1A1 and TGF β 1 expression (results significant, $p < 0.05$). Growth factor treatment altered the migratory capacity of the cells as measured by scratch assay. Immunohistochemical analysis of human optic nerves demonstrated increased levels of RPE65 and TGF β 1 in the glaucomatous optic nerve compared to normal.

Conclusions: ARPE-19 cells were shown to change from an epithelial to a mesenchymal phenotype after exposure to glaucoma-like stimuli in-vitro. There is also immunohistochemical evidence suggesting the presence of RPEC within the glaucomatous optic nerve head from human eyes. This may indicate a role for the RPEC and PPA in glaucomatous cupping. Future work will examine the use of EMT inhibitors on the process.

Commercial Relationships: Emily L. Hughes, None; Neil G. Docherty, None; John K. Crean, Fibrogen Inc (F); Abbot F. Clark, Alcon Research, Ltd. (F); Deborah M. Wallace, None; Colm J. O'Brien, None

Program Number: 765 **Poster Board Number:** A0100

Presentation Time: 1:00 PM - 2:45 PM

Ocular Pharmacokinetics of ISV-215 (Bimatoprost 0.03%) Formulated in a DuraSite Delivery System Compared to Lumigan in Rabbits

Lyle M. Bowman¹, Afshin Shafiee², Eddie Hou¹, Kamran Hosseini^{2,3}.
¹Development, InSite Vision, Alameda, CA; ²Preclinical, InSite Vision, Alameda, CA; ³Clinical, InSite Vision, Alameda, CA.

Purpose: To compare the ocular pharmacokinetic parameters of ISV-215 (bimatoprost 0.03% formulated in DuraSite) to Lumigan 0.03% in pigmented rabbits.

Methods: The left eye of male and female rabbits (n=32/group) received either a single topical instillation of Lumigan or ISV-215. At predetermined timepoints (0.25, 0.5, 1, 2, 4, 6, 12, and 24 hours), 4 rabbits/group/timepoint were sacrificed and the bimatoprost and bimatoprost acid levels in the aqueous humor (AH) and the iris-ciliary body (ICB) were quantified using LC-MS/MS methodology. PK parameters (C_{max} , T_{max} , $AUC_{0.25-24h}$), was determined.

Results: Both bimatoprost and bimatoprost acid were detected in AH and ICB. ISV-215 had a 2.2-fold higher bimatoprost C_{max} value than Lumigan in the AH (26.57 ± 19.16 ng/mL at 0.5 h postdose vs. 12.11 ± 21.72 ng/mL at 1 h postdose), and a 6.1-fold increase in the ICB (65.06 ± 26.20 ng/g at 0.5h postdose vs. 10.73 ± 9.01 ng/g at 0.5 h postdose). ISV-215 also achieved a 3.5-fold higher bimatoprost acid concentration (C_{max}) in the AH (103.4 ± 42.36 ng/mL at 2 h postdose vs. 29.58 ± 26.37 ng/mL at 1 h postdose) and a 3.7-fold increase in the ICB (68.21 ± 33.00 ng/g at 0.5 h postdose vs. 18.38 ± 4.05 ng/g at 0.25 h postdose). Drug exposure (AUC) was similarly higher for bimatoprost and bimatoprost acid in the AH (2.0- and 3.1-fold, respectively) and in the ICB (6.6- and 3.7-fold, respectively) of ISV-215-treated animals compared to Lumigan.

Conclusions: DuraSite significantly improved delivery of bimatoprost and bimatoprost acid in the AH and ICB of rabbits. This improvement in pharmacokinetic parameters has the potential to enhance intraocular pressure (IOP) lowering properties of bimatoprost in patients with ocular hypertension or reducing bimatoprost levels in the ophthalmic IOP lowering medications while improving the side effect profile.

Commercial Relationships: Lyle M. Bowman, InSite Vision (E); Afshin Shafiee, InSite Vision (E); Eddie Hou, InSite Vision (E); Kamran Hosseini, InSite Vision Inc. (E)

Program Number: 766 **Poster Board Number:** A0101

Presentation Time: 1:00 PM - 2:45 PM

Agonist activity and binding affinity of ONO-9054 to EP3 and FP Receptors

Shinsaku Yamane, Satoshi Nakayama, Tomohiro Karakawa, Shintaro Nakao, Tsutomu Shiroya, Yutaka Shichino. ONO PHARMACEUTICAL CO.,LTD., Osaka, Japan.

Purpose: ONO-9054 (Ono Pharmaceuticals, Osaka Japan) is a novel prodrug compound. ONO-9054 is an isopropyl ester derivative of the free acid ONO-AG-367. The purpose of this study was to investigate the agonist activity and binding affinity of ONO-9054 and ONO-AG-367 to the prostaglandin receptors. To investigate the potential off-target effects of ONO-9054 and ONO-AG-367, the binding affinity for 66 receptors and transporters were studied.

Methods: The binding affinity of ONO-9054 and ONO-AG-367 to prostaglandin receptors (EP1, EP2, EP3, EP4, FP, IP, TP, and DP receptors) was assessed with cells over expressing each prostaglandin receptor. The agonist activities of ONO-9054 and ONO-AG-367 were examined using the intracellular calcium signaling response in EP3 or FP receptor-expressing cells. The binding affinity of ONO-9054 and ONO-AG-367 on 66 additional receptors and transporters were also assessed.

Results: ONO-9054 exhibited high affinity for the FP receptor only and no affinity for any other prostaglandin receptors. ONO-AG-367 exhibited high affinity for both the EP3 and FP receptors. ONO-AG-367 exhibited potent agonist activity with EC50 values of 14.8 nmol/L for the EP3 receptor and 11.1 nmol/L for the FP receptor, respectively. ONO-9054 exhibited a low potency agonist effect on these receptors. ONO-9054 and ONO-AG-367 at 10 μ mol/L did not produce greater than 35% inhibition of binding at any of the 66 other targets examined.

Conclusions: ONO-AG-367, the biologically active free acid of ONO-9054, is a highly selective and potent prostaglandin FP and EP3 receptor agonist. The agonist activity of ONO-AG-367 to FP receptor was similar to previously reported values of FP agonists such as latanoprost acid, bimatoprost acid, and travoprost acid. On the other hand, the agonist activity of ONO-AG-367 to EP3 receptor was more potent than these FP agonists.

Commercial Relationships: Shinsaku Yamane, ONO PHARMACEUTICAL CO., LTD. (E); Satoshi Nakayama, ONO Pharmaceutical Co Ltd (E); Tomohiro Karakawa, ONO PHARMACEUTICAL CO., LTD (E); Shintaro Nakao, ONO Pharmaceutical Co.,LTD (E); Tsutomu Shiroya, ONO Pharmaceutical.Co.Ltd. (E); Yutaka Shichino, ONO Pharmaceutical Co Ltd (E)

Program Number: 767 **Poster Board Number:** A0102

Presentation Time: 1:00 PM - 2:45 PM

Grp94 and Grp78 can triage distinct mutant myocilin species for clearance or for aggregation

Chad A. Dickey¹, Shannon E. Hill², Stanislav I. Tomarev³, Myung Kuk Joe³, Raquel L. Lieberman², Amirthaa Suntharalingam¹.
¹University of South Florida, Tampa, FL; ²Georgia Institute of Technology, Atlanta, GA; ³National Eye Institute, Bethesda, MD.

Purpose: Clearance of misfolded proteins in the endoplasmic reticulum (ER) is traditionally handled by ER-associated degradation, a process that requires retro-translocation and ubiquitination mediated by a luminal chaperone network. Here we investigated whether the secreted, glaucoma-associated protein myocilin was

processed by this pathway. Myocilin is typically transported through the ER/Golgi network, but inherited mutations in myocilin lead to its misfolding and aggregation within trabecular meshwork cells, and ultimately, ER-stress induced cell death. We sought to evaluate whether distinct myocilin mutants were triaged similarly by the ER chaperones Grp94 and Grp78.

Methods: We used a cell culture model of mutant myocilin accumulation to evaluate the effects of chaperones on mutant myocilin triage. We used siRNA, over-expression, Western blot, immunofluorescence, sub-cellular fractionation and drug treatments for these studies.

Results: Using targeted knockdown strategies, we determined that Grp94, the ER equivalent of Hsp90, specifically recognizes mutant myocilin, triaging it through ER-associated protein degradation (ERAD). However, not all mutant myocilin species are handled the same way. The insolubility of mutant myocilin species that cause a more aggressive form of primary open angle glaucoma was enhanced by Grp94 depletion. The addition of mutant myocilin to the short list of Grp94 clients strengthens the hypothesis that beta-strand secondary structure drives client association with Grp94. Interestingly, the ERAD pathway is incapable of efficiently handling the removal of mutant myocilin, but when Grp94 is depleted, degradation of mutant myocilin is shunted away from ERAD towards a more robust clearance pathway or towards further aggregation, suggesting that the kinetics of aggregation and possibly the structure of distinct myocilin mutants are important for successful handling of amyloidogenic proteins in ER.

Conclusions: Grp94 is an essential player in deciding the fates of mutant myocilin species. The balance of Grp94 levels may be an important factor in determining whether distinct mutant myocilin species are cleared from the cell or allowed to aggregate. Regardless, it is possible that both of these outcomes are ultimately protective for the cell. Therefore therapeutic approaches aimed at inhibiting Grp94 could be beneficial for patients suffering from some cases of myocilin glaucoma.

Commercial Relationships: Chad A. Dickey, None; Shannon E. Hill, None; Stanislav I. Tomarev, None; Myung Kuk Joe, None; Raquel L. Lieberman, None; Amirthaa Suntharalingam, None
Support: American Health Assistance Foundation

Program Number: 768 **Poster Board Number:** A0103

Presentation Time: 1:00 PM - 2:45 PM

EFFECT OF LOSARTAN ON FACTORS RELATED TO HEALING PROCESS IN RABBIT TENON'S FIBROBLASTS

Carolina Modulo¹, Marco Andrey C. Frade², Peter Reinach¹, Eduardo M. Rocha¹, Jayter S. Paula¹. ¹Department of Ophthalmology, Otorhinolaryngology and Head & Neck Surgery, School of Medicine of Ribeirão Preto, University of São Paulo, Ribeirão Preto, Brazil; ²Division of Dermatology - Internal Medicine Department, School of Medicine of Ribeirão Preto, University of São Paulo, Ribeirão Preto, Brazil.

Purpose: Glaucoma filtering surgery failure is frequently associated with excessive subconjunctival fibrosis, which may occur as consequence of fibroblast activation. Losartan potassium (LP), an angiotensin-1 receptor inhibitor, has been studied as a new healing modulator. Thus we evaluated the effects of losartan on proliferation of rabbits' Tenon's capsule fibroblasts (RTF).

Methods: Fibroblasts obtained from *New Zealand* rabbits were cultured in Dulbecco's modified Eagle's medium (DMEM). The dose dependent effects of LP (i.e. 0.3, 1.0 and 3.0 μ M) on third passage cell proliferation were determined in triplicate after 24 h or 48 h with the MTT assay. Immunofluorescence of alpha smooth muscle actin (alpha-SMA) assessed myofibroblast differentiation. Real-time

reverse transcription polymerase chain reaction evaluated type I alpha I collagen (COL1A1) gene expression.

Results: LP (3.0 μ M) after 24 h or 48 h inhibited RTF proliferation compared to its controls by 51% and 40%, respectively ($p < 0.001$; $p = 0.0004$). Moreover, decreased myofibroblast transdifferentiation by at least 25% was observed. All LP concentrations also suppressed COL1A1 mRNA expression levels, after 48 h ($p = 0.002$).

Conclusions: Suppression by LP of RTF proliferation, as well as myofibroblast transdifferentiation and COL1A1 gene expression suggests that LP may decrease *in vivo* fibrosis. Such a result indicates LP could be used as adjunctive treatment, improving the outcome of glaucoma filtration surgery.

Commercial Relationships: Carolina Modulo, None; Marco Andrey C. Frade, None; Peter Reinach, None; Eduardo M. Rocha, None; Jayter S. Paula, None
Support: FAPESP 2010/17679-8

Program Number: 769 **Poster Board Number:** A0104

Presentation Time: 1:00 PM - 2:45 PM

Reduction by tissue plasminogen activator (tPA) of steroid-induced intraocular pressure (IOP) elevation in sheep

Oscar A. Candia¹, Rosana Gerometta¹, John Danias².

¹Ophthalmology, Mount Sinai School of Medicine, New York, NY;

²Ophthalmology & Cell Biology, SUNY Downstate, Brooklyn NY 11203, NY.

Purpose: To determine whether human recombinant tPA can reduce steroid-induced IOP elevation.

Methods: Eight sheep of the Corriedale breed were treated with drops of 1% prednisolone acetate 3-times a day in both eyes. After the expected IOP increase, the animals received 100-mL intravitreal injections in one eye of human recombinant tPA containing 100, 200, 500 and 1000 mg concentrations dissolved in BSS (two animals for each concentration). IOP was monitored for 19 more days while the animals continued to receive treatment with prednisolone. Periodic slit lamp examination was also performed.

Results: Treatment with prednisolone for 10 days increased mean (+SD) IOP to 24.1(+1.6) mmHg from a baseline of 10.2(+1.1) mmHg ($p < 0.00001$, t-test). Treatment with tPA decreased IOP within 24h for all doses tested to 14.1(+1.1) mmHg which was significantly lower than that of the contralateral uninjected eye for all animals ($p < 0.00003$, paired t-test). The effect was evident for all tPA doses, independent of the dose ($p > 0.05$, ANOVA) and lasted for 19 days at which time IOP in the two eyes became similar ($p > 0.05$). Transient conjunctival injection and corneal clouding were observed in some eyes, but were unrelated to the dose injected and cleared up in all eyes within 48 hrs.

Conclusions: tPA decreases IOP, probably by affecting extracellular matrix turnover in the TM. This finding may have therapeutic implications in glaucoma.

Commercial Relationships: Oscar A. Candia, None; Rosana Gerometta, None; John Danias, Bausch and Lomb (C), N/A (P)
Support: NIH Grant EY020670 & RPB to Ophthalmology, MSSM and to SUNY Downstate

Program Number: 770 **Poster Board Number:** A0105

Presentation Time: 1:00 PM - 2:45 PM

Upregulation of miR-146a in retina in rodent models of elevated intraocular pressure

Guorong Li¹, Mohammadali Almasieh², Coralina C. Luna¹, Jianming Qiu¹, Pratap Challa¹, Molly M. Walsh¹, Henry Tseng¹, David L. Epstein¹, Adriana Di Polo², Pedro Gonzalez¹. ¹Ophthalmology, Duke Eye Center, Durham, NC; ²Pathology and Cell Biology, Université de Montréal, Montreal, QC, Canada.

Purpose: Glaucoma caused by elevated intraocular pressure (IOP) can lead to retinal ganglion cell (RGC) pathology and a progressive vision loss. RGC degeneration in glaucoma is accompanied by a neuroinflammatory response, but the molecular mechanism that regulates this process is poorly understood. Since miR-146a is a negative regulator of cytokine expression, we hypothesized that miR-146a may be involved in regulating the retinal inflammatory response observed in glaucoma.

Methods: Expression of miR-146a in rodent retina was evaluated by qPCR and in situ hybridization. Elevated IOP was generated in rats by either laser trabecular photocoagulation or episcleral vein injection of hypertonic saline, and in mice by conditional knockout of DICER1 in the cells of the outflow pathway. To evaluate a possible negative feedback effect between inflammatory mediators and miR-146a, mixed rat retina cell cultures were treated with TNF α , and expression of miR-146a was analyzed by qPCR. Additionally, transient overexpression of a miR-146a mimic or scrambled control using NeuroMag transfection was followed by qPCR analysis of inflammatory markers (IL1 α , IL1 β , IL6, and TNF α). Finally, the effect of complete deletion of miR-146a was examined in retinas of 7 week old miR-146a knockout mice.

Results: Baseline miR-146a expression in rat retinas was observed by both in situ hybridization and PCR. In response to elevated IOP, miR-146a upregulation was detected in several animal models (i. laser trabecular photocoagulation in rats: 1wk: 1.5 \pm 0.13 folds, p=0.1266, n=3; 3wks: 2.08 \pm 0.24 folds, p=0.00495, n=3; ii. episcleral vein injection of hypertonic saline: 1wk: 1.99 \pm 0.65 folds, p=0.021, n=4; 3wks: 2.67 \pm 1.48, p=0.021, n=4; iii. Dicer KO in mice: 1.68 \pm 0.57 folds, p=0.0012, n=11 compared to the contralateral non-treated control retinas). Treatment of cultured retinal cells with TNF α for 30h led to a dose responsive increase in miR-146a expression. Conversely, transient overexpression and knockout of miR-146a led to a significant decrease and increase, respectively, of IL1 α , IL1 β , IL6, and TNF α .

Conclusions: Our results suggest that miR-146a forms a negative feedback loop that reduces the levels of expression of inflammatory mediators in the retina. Pressure-induced up-regulation of miR-146a in the retina could play a protective role by limiting potentially deleterious effects of inflammatory mediators in high-pressure glaucoma.

Commercial Relationships: Guorong Li, None; Mohammadali Almasieh, None; Coralía C. Luna, None; Jianming Qiu, None; Pratap Challa, None; Molly M. Walsh, None; Henry Tseng, None; David L. Epstein, None; Adriana Di Polo, None; Pedro Gonzalez, None

Support: NEI EY01894, NEI EY016228, NIH P30 EY-005722, and Research to Prevent Blindness.

Program Number: 771 **Poster Board Number:** A0106

Presentation Time: 1:00 PM - 2:45 PM

Reduction in Long-term Vision Loss with Preoperative Bevacizumab for Neovascular Glaucoma Ramya Swamy, MD, MPH, Vikas Chopra, MD, Srinivas Sadda, MD Doheny Eye Institute, Dept of Ophthalmology, Keck School of Medicine, Los Angeles, CA

Ramya N. Swamy, Vikas Chopra, Srinivas R. Sadda. Ophthalmology, Doheny Eye Institute, Los Angeles, CA.

Purpose: To evaluate the association between intraocular injection of bevacizumab before placement of glaucoma drainage implant (GDI) and objective outcomes in neovascular glaucoma.

Methods: A retrospective nonrandomized review was performed on all eligible patients with neovascular glaucoma (NVG) who presented to the Los Angeles County - University of Southern California (LAC-

USC) Medical Center between 2007 and 2012. All subjects had newly diagnosed NVG with uncontrolled intraocular pressure (IOP) > 30mm Hg on maximally tolerated medical therapy. All subjects were determined to require surgery and underwent a valved GDI (Ahmed Glaucoma Valve, New World Medical, Rancho Cucamonga, CA). The decision to use intraocular bevacizumab (50 μ l, 1.25 mg) was at the discretion of the treating physician. Baseline/preoperative variables collected included age, gender, etiology of neovascularization, IOP, visual acuity, and time to injection. Outcome measures included postoperative IOP and visual acuity at usual postoperative intervals and presence of an immediate postoperative hyphema. Characteristics and outcomes between groups were compared.

Results: A total of 59 eyes were treated with a GDI during the study period. 8 eyes were excluded due to incomplete records. Of the remaining 51 eyes, 29 received intraocular bevacizumab injection before GDI (treatment group) and 22 underwent surgery without bevacizumab (control group). All patients received panretinal photocoagulation. In the treatment group, the mean time to injection was 7.06 days (confidence interval (CI): [0.81-13.27]). No statistically significant difference in IOP control, presence of hyphema, or visual acuity was observed at either postop week 1 or postop month 1 (p > 0.05). With longer term follow-up (> 6months), however, fewer eyes in the treatment group (6.89%) than in the control group (31.81%) progressed to no light perception (p = 0.02).

Conclusions: In our patient population, primarily consisting of complex cases of neovascular glaucoma with approximately three-fourths of the patients with baseline visual acuity at CF or worse, preoperative use of bevacizumab was associated with significantly less long-term progression to NLP vision despite equivalent IOP lowering with GDI placement.

Commercial Relationships: Ramya N. Swamy, None; Vikas Chopra, Allergan, Inc. (C); Srinivas R. Sadda, Regeneron (C), Genentech (C), Allergan (C), Carl Zeiss Meditec (C), Optos (C), Carl Zeiss Meditec (F), Optovue (F), Optos (F)

Program Number: 772 **Poster Board Number:** A0107

Presentation Time: 1:00 PM - 2:45 PM

CHANGES IN RETINAL P2X7 RECEPTORS IN A MURINE MODEL OF GLAUCOMA

Jesus J. Pintor¹, Pedro de la Villa², Maria Jesus Perez de Lara¹.

¹Departamento de Bioquímica, Facultad de Optica y Optometria, Universidad Complutense de Madrid, Madrid, Spain; ²Departamento de Fisiología, Facultad de Medicina, Universidad de Alcalá de Henares, Alcalá de Henares, Spain.

Purpose: To investigate the changes in the P2X7 receptor in a murine model of glaucoma during the development of the disease.

Methods: DBA/2J glaucomatous mice together with C57BL/6J control mice were used along the whole experimentation. Animals were studied from 3 till 15 months of age. For the study of retinal nucleotide release retinas were dissected and prepared as flattened whole-mounts and stimulated in Ringer solution buffer with or without 59 mM KCl. Immunohistochemical, western-blot and PCR analyses were performed with antibodies against the nucleotide vesicular transporter VNUT and the P2X7 nucleotide receptor. ERG recordings were performed on the right eyes of C57BL/6J and DBA/2J mice at different ages (3-15 months) to analyze the changes in the electrophysiological response. Scotopic threshold response determines the onset of functional changes exhibited in the inner retina of the DBA/2J mice.

Results: Glaucomatous mice exhibited changes in retinal ATP release as long as the pathology progressed. Changes occurred when compared to those animals without the pathology which basal retinal

ARVO 2013 Annual Meeting Abstracts by Scientific Section/Group – Glaucoma

ATP level was 6.56 ± 1.81 pmol/retina while the stimulated with KCl was 9.64 ± 1.45 pmol/retina. ATP came mainly from synaptic vesicles since the nucleotide transporter marker VNUT label mainly the inner plexiform layer. Concerning the distribution of P2X7 receptor it was possible to measure a clear increase in the presence of this nucleotide receptor with glaucoma progression in the DBA/2J mice. There was 36 % of increase in the presence of this receptor measured both by immunohistochemical and western-blot techniques. It was also possible to see that at 15 months of age the glaucomatous mice presented 78 % more expression of retinal P2X7 receptors than in control (C57BL/6J) mice. ERG recordings in 15 months glaucomatous mice showed an important/ reduction in the pSTR response correlated with ganglion cell loss.

Conclusions: In the development of the glaucomatous pathology in the DBA/2J mice, the increase in the presence of P2X7 receptors may contribute, together with other factors, to the changes in the functionality of the retina and the concomitant death of retinal ganglion cells.

Commercial Relationships: Jesus J. Pintor, None; Pedro de la Villa, ProRetina Therapeutics, S.L. (I), US2010/0042 A1 (P); Maria Jesus Perez de Lara, None

Support: SAF2010-16024, BES-2011-045936, RETICS RD07/0062/0004, RD07/0062/0012

Program Number: 773 **Poster Board Number:** A0108

Presentation Time: 1:00 PM - 2:45 PM

Global assessment of retinal ganglion cell synapses in a mouse model of ocular hypertension

Yvonne Ou, Ming Lu, David W. Sretavan, Erik M. Ullian. Department of Ophthalmology, University of California San Francisco, San Francisco, CA.

Purpose: Glaucoma is a neurodegenerative disorder characterized by retinal ganglion cell (RGC) loss with optic nerve cupping and visual field defects. Disease mechanisms are not well understood, but evidence suggests that the pathological degeneration of a stressed RGC is compartmentalized at the subcellular level, with changes in the synaptic, dendritic, and axonal compartments. The purpose of this study is to determine the effects of laser-induced ocular hypertension (LIOH) on excitatory synapse number in the inner plexiform layer of the retina.

Methods: Intraocular pressure (IOP) was elevated unilaterally using laser photocoagulation of the limbal and episcleral vessels of adult CD-1 mouse eyes. IOP was measured by rebound tonometry. Retinas were dissected and prepared for whole-mount retina immunohistochemistry using PSD95 to label excitatory postsynaptic sites of RGCs in the inner plexiform layer. Brn3a was used to label RGCs in the ganglion cell layer.

Results: After laser-induced ocular hypertension (LIOH), the IOP of the treated eye was elevated as early as 6 hours and returned to baseline by 1 week. Two months after LIOH, in areas of RGC loss there was concurrent synaptic loss as measured by PSD95 immunostaining. Interestingly, when synaptic puncta were quantified in areas of similar RGC density of the treated eye as compared to the control eye, there was also statistically significant synapse loss.

Conclusions: Excitatory synapse loss occurs concurrently with RGC degeneration in this mouse model of ocular hypertension. However, even in areas of relative preservation of RGCs as measured by RGC soma marker Brn3a, there was significant synaptic loss in the treated eye, suggesting that synapse loss is an early event in glaucomatous RGC degeneration.

Commercial Relationships: Yvonne Ou, None; Ming Lu, None; David W. Sretavan, None; Erik M. Ullian, None

Support: NEI 1K08EY022676-01, American Glaucoma Society Young Clinician Scientist Award

Program Number: 774 **Poster Board Number:** A0109

Presentation Time: 1:00 PM - 2:45 PM

The TRPV1 Cation Channel Contributes to Stress-Induced Retinal Astrocyte Migration

Karen W. Ho, Carl Weitlauf, David J. Calkins. Vanderbilt Eye Institute, Vanderbilt University Medical Center, Nashville, TN.

Purpose: Astrocytes provide both metabolic and structural support to retinal ganglion cells and mediate a variety of stress-related responses in diseases such as glaucoma. Previously we found that retinal astrocytes express the transient receptor potential vanilloid (TRPV1) cation channel. TRPV1 contributes to stress responses in other neural systems via calcium-dependent cascades and is up-regulated in experimental models of glaucoma. Our objective here was to test whether TRPV1 contributes to the migration of retinal astrocytes in response to mechanical injury.

Methods: Primary astrocyte cultures were prepared by immunomagnetic separation of postnatal Sprague-Dawley rat retina using an anti-human α -astrocyte antibody (Leinco). Once confluent, cultures were scratched with a 1mL pipet tip to create a uniform gap of 1mm diameter to induce migration under conditions that minimized cell proliferation. We used DIC imaging to monitor the rate of wound closure in vitro under varying pharmacological conditions. F-actin and proliferation were examined in fixed astrocytes using phalloidin and Ki-67 immunolabeling.

Results: Application of 100pM of the TRPV1-specific agonist capsaicin increased migration by 36% by 36hrs ($p=0.03$, $n=3$) compared to vehicle (ethanol). In contrast, treatment with the TRPV1-specific antagonist 5'-iodoresiniferatoxin (IRTX) reduced astrocyte migration compared to vehicle in a dose-dependent manner, with 3 μ M decreasing migration by 33% by 48 hrs ($p<0.03$, $n=3$). Application of 1 μ M IRTX also reduced phalloidin intensity by 52% compared to control by 12hrs ($p=0.01$, $n=1$). Chelation of extracellular calcium with 1mM EGTA also reduced astrocyte migration by 44% compared to vehicle at 48hrs ($p<0.05$, $n=3$). Wound closure was not due to proliferation, as Ki-67 expression remained low ($5.5 \pm 0.7\%$).

Conclusions: Our results support the hypothesis that in response to injury, TRPV1 contributes to mobilization of retinal astrocytes. This mobilization is at least partially dependent on the influx of extracellular calcium. We are currently using whole-cell voltage clamp recordings to test whether our cultured retinal astrocytes are capable of producing a transient current characteristic of active calcium channels. Our results suggest that TRPV1 may contribute to the known hypertrophy of astrocytes in response to disease-relevant stressors such as ocular pressure.

Commercial Relationships: Karen W. Ho, None; Carl Weitlauf, None; David J. Calkins, QLT, Inc (F), Allergan (F), QLT, Inc (C), Allergan (C)

Support: : Melza and Theodore Barr and Glaucoma Research Foundations (DJC), AHAF (DJC), NEI Grant (5R01EY017427-03) (DJC), Research to Prevent Blindness Inc., Departmental Unrestricted Grant (DJC), and NEI Core Grant (5P30EY008126-19) (DJC)

Program Number: 775 **Poster Board Number:** A0110

Presentation Time: 1:00 PM - 2:45 PM

The Effect of Intravitreal Anti-VEGF Therapy on Intraocular Pressure

Fred B. Chu¹, Claire Kiernan¹, Norbert Becker², Anjali S. Hawkins¹.
¹Ophthalmology, Rush University, Chicago, IL; ²Ophthalmology, Cook County, Chicago, IL.

Purpose: To determine if there is an association between intravitreal injection of anti-VEGF therapies and the etiology of ocular hypertension (Intraocular pressure > 21). To determine what preoperative factors may be associated with ocular hypertension in patients receiving these intravitreal injections

Methods: This is a retrospective chart review of 202 eyes of 148 patients who underwent intravitreal injection of anti-VEGF therapy between January 2007 and December 2011. All injections were performed by the same surgeon (NB). Charts were reviewed for demographic information including age at first injection, diagnosis, pre-treatment IOP, glaucoma status, previous steroid use, and lens status. Post-treatment IOP, glaucoma medications and other glaucoma interventions were recorded. Anti-VEGF therapies included bevacizumab, ranibizumab, and pegaptanib. The primary outcome measure was initiation or escalation of glaucoma therapy (including ocular antihypertensive medications, laser trabeculoplasty and/or filtering or shunting surgeries). Data was analyzed at months 0, 1, and 3 and then in 3-month increments thereafter through December 2011.

Results: Each eye underwent an average of 8.5 injections during the study period. During that time, 18 of 202 (8.9%) eyes required additional ocular anti-hypertensives at some point during follow-up. 16 of these 18 were not previously on antihypertensive treatment. At the end of the follow-up period, 8 of 202 (4.0%) eyes required sustained use of additional ocular anti-hypertensives as compared to their pre-treatment regimens. There was no significant difference between treatment requirements for phakic vs. pseudophakic patients ($p = 0.215$). There was no difference in age between the treated and untreated groups ($p = 0.553$). 1 of the 4 eyes previously diagnosed as “glaucoma suspect” required additional drops. 2 of the 11 eyes previously diagnosed with “glaucoma” required additional drops. 18 of 202 (8.9%) had sustained intraocular pressure (2 or more consecutive visits with IOP > 21 and 30% increase from baseline, or requiring additional ocular anti-hypertensives). 1 patient required laser trabeculoplasty and none required glaucoma filtering surgery.

Conclusions: A small but not insignificant percentage of patients receiving anti-VEGF injections may require transient or sustained anti-hypertensive therapy.

Commercial Relationships: Fred B. Chu, None; Claire Kiernan, None; Norbert Becker, None; Anjali S. Hawkins, None

Program Number: 776 **Poster Board Number:** A0111

Presentation Time: 1:00 PM - 2:45 PM

CX3CR1 signaling modulates retinal ganglion cell degeneration in glaucoma

Kevin Breen¹, Alejandra Bosco¹, David J. Calkins², Monica L. Vetter¹. ¹Neurobiology and Anatomy, University of Utah, Salt lake city, UT; ²Ophthalmology and Visual Sciences, Vanderbilt Eye Institute, Nashville, TN.

Purpose: Microglia become chronically activated in multiple neurodegenerative diseases including glaucoma, but how activation is regulated and impacts disease is unclear. Healthy neurons express signals to limit microglia activation, which are lost in degenerating neurons. Neurons constitutively express fractalkine (CX3CL1, FKN), a chemokine that binds to the CX3CR1 receptor (FKNR) on microglia to balance activation. Because loss of FKNR results in overactivation, here we explore the role of fractalkine signaling in glaucoma. We hypothesize that retinal ganglion cells (RGCs) express FKN, and that loss of FKNR signaling increases microglia activation and neurodegeneration in the DBA/2J (D2) mouse model of

glaucoma.

Methods: We determined whether RGCs express FKN by in-situ hybridization on cryosections from 1 month-old (mo) Thy1+/cfp D2 mice, followed by CFP immunostaining to detect RGCs. We asked if FKNR loss affects RGC degeneration, comparing 10mo D2 (n=9) versus FKNR null retinas (CX3CR1gfp/gfp D2 n=20). We collected confocal images of entire wholemount inner retinas, immunostained for the RGC marker Brn3 or pNF (phospho-neurofilament). We tracked somal pNF accumulation in RGCs as a readout for axonal transport decline, and counted Brn3+ cells in 8 radial sectors at 3 eccentricities, classifying them as “no/mild”, “moderate”, or “severe damage” if average density was >400, 200-400 and <200 RGCs/mm², respectively.

Results: FKN mRNA expression was highest in the RGC layer and in CFP+ RGCs, and lower in other retinal layers. We observed enhanced RGC pathology in null FKNR D2 retinas. 58% of retinal sectors in FKNR null D2 (n=153 sectors) were severely depleted of Brn3+ RGCs vs. 27% (n=59 sectors) in D2. Thus sectors with moderate and mild RGC loss were reduced (43% in FKNR null D2 vs. 73% in D2). The entire retina in 9/20 FKNR null D2 eyes showed severe Brn3+ depletion versus only 1/9 in D2 retinas. FKNR null D2 retinas also had ~4x more RGCs showing abnormal somal pNF build up (average of 1.7 ± 0.5 SEM/mm²) relative to D2 (0.4 ± 0.1 SEM/mm²).

Conclusions: RGCs express FKN, and loss of FKN signaling leads to increased retinal disease severity in RGCs of 10mo D2 mice. Ongoing experiments will assess the effect of FKNR loss and FKN overexpression on microglial activation and severity of optic nerve pathology. Overall, our findings support a contribution of microglia activation to RGC degeneration in glaucoma.

Commercial Relationships: Kevin Breen, None; Alejandra Bosco, University of Utah (P); David J. Calkins, QLT, Inc (F), Allergan (F), QLT, Inc (C), Allergan (C); Monica L. Vetter, University of Utah (P)

Program Number: 777 **Poster Board Number:** A0112

Presentation Time: 1:00 PM - 2:45 PM

Videographic Assessment of Glaucoma Drops Instillation

Antonio Remolina-Villarejo¹, Gabriel Lazcano-Gomez¹, Armando Castillejos-Chevez¹, Jesus Jimenez-Roman¹, Malik Y. Kahook².

¹Glaucoma, Asociacion Para Evitar la Ceguera en Mexico, Mexico, Mexico; ²Ophthalmology, University of Colorado, Denver, CO.

Purpose: To educate medical personal and patients on proper instillation technique for glaucoma drops.

Methods: Patients with glaucoma, ocular hypertension or glaucoma suspects, who were using glaucoma drops for at least 6 months were included. Best corrected visual acuity of 20/100 or better was required for enrollement.

All patients were asked to instill an artificial tear drop, using the same technique they used at home. Data included: number of drops instilled in each eye, number of drops reaching ocular surface, number of times the tip of the bottle touched the eye or surrounding structures. After the first attempt, patients were counseled on proper instillation techniques. After 30 minutes, we asked them to instill a drop of the same tear to ascertain changes in behaviour after the educational session. The second instillation was also videotaped with similar data recording. Pre and post education video were compared.

Results: 45 patients were enrolled with a mean age of 56.8 ± 15.05 years. Seven patients (15.5%) with ocular hypertension, 9 patients (20%) with primary closure angle-glaucoma and 29 patients (64.4%) with POAG were included. At the initial instillation event, the mean number of drops squeezed out from the bottle was 1.51 ± 0.86 , mean number of drops that reached the conjunctival fornix per patient was

0.93±0.71. In 29 patients (64.44%) the tip of the bottle touched the conjunctiva or periocular tissue with a frequency of 1.73±2.15 times. Post-education mean number of drops instilled was 1.22±0.51. The mean number of drops reaching the conjunctival fornix per patient was 1.15±0.42. The tip of the bottle touched the conjunctiva or periocular tissue in 13 patients (28.88%), with a frequency of 0.51±1.03 times per patient.

Conclusions: At baseline, only 66% of patients instilled one drop per application as instructed. The mean number of drops instilled per patient was 1.51 with only a mean of 0.93 drops falling directly on the eye. After the educational session, the number of patients that instilled one drop on the eye increased to 82% with a mean of 1.22 drops per application and a mean of 1.15 drops falling directly on the conjunctival fornix. The educational session appears to have enhanced drop instillation success.

Commercial Relationships: Antonio Remolina-Villarejo, None; Gabriel Lazcano-Gomez, None; Armando Castillejos-Chevez, None; Jesus Jimenez-Roman, None; Malik Y. Kahook, Alcon (C), Allergan (C), Merck (C), B&L (C), Glaukos (C), Ivantis (C), ClarVista Medical (P), Dose Medical (P), AMO (P), Genentech (F), Regeneron (F)

Program Number: 778 **Poster Board Number:** A0113

Presentation Time: 1:00 PM - 2:45 PM

Small-molecule inhibitors of sFRP1

Jie J. Zheng, Structural Biology, St. Jude Children's Research Hospital, Memphis, TN.

Purpose: Wnt signaling pathways play crucial roles during embryonic development and are also very important in adult tissue maintenance. Abnormal activations of Wnt signaling have been implicated in human diseases including eye related diseases such as glaucoma and retinal related diseases. It has been proposed that the Wnt signaling pathway is a target for therapeutic development. In particular, it has been documented that secreted frizzled-related protein-1 (sFRP1), an antagonist of the Wnt signaling pathway, is differentially expressed in glaucomatous human TM cells compared with normal human TM cells. Furthermore, studies in rodent models and perfusion-cultured human anterior segments suggest that Wnt signaling plays a role in regulating IOP, that increased expression of sFRP1 in the TM is associated with elevated IOP and decreased outflow facility. Therefore restoring Wnt signaling in the TM by inhibiting sFRP1 would be an intervention strategy for treating glaucoma.

Methods: Increased computational power has provided us an opportunity to examine proteins and to screen proteins as possible ligands in silico. Structure-based virtual ligand screening is based on known 3D structure of the protein and the small molecules to be screened. Computational models of molecules from small-molecule database are docked to the active site of the target protein. We conducted virtual ligand screen to search for the potential inhibitors of sFRP1. However, despite recent development, the current virtual screening methods still yield a relatively high number of false positive. In our studies, solution NMR spectroscopy was used to filter out those false positive results.

Results: The cysteine-rich domain (CRD) of sFRP1 binds to Wnt molecules and is the functional domain of sFRP1. Through structure-based virtual ligand screening and NMR studies, we initially identified the first inhibitor of the CRD domain of sFRP1 from the ChemDiv small-molecule database. Then, by virtually exploring the existing chemical space and by developing of SAR models, together with additional NMR studies, we have obtained additional small-molecule inhibitors, some of the best drug-like inhibitors bind to the CRD domain of sFRP1 at sub micromolar affinity.

Conclusions: Those small-molecule inhibitors of sFRP1 provide us with a novel approach in glaucoma treatment. Presenting the data at ARVO, we hope that we can establish collaboration with investigators in the glaucoma field to test these compounds.

Commercial Relationships: Jie J. Zheng, None
Support: GM081492

Program Number: 779 **Poster Board Number:** A0114

Presentation Time: 1:00 PM - 2:45 PM

Neurotrophin-4 Promotes Retinal Ganglion Cell Survival Following Neuronal Injury In Thy1-YFP Mice

Chendong Pan, Lihua Guo, Evan Berger, Anna M. Demetriades, Glaucoma Research Laboratory, Weill Cornell Medical College, New York, NY.

Purpose: Neurotrophin-4 is a neurotrophic factor that regulates the survival, differentiation and mature function of neurons. This study aims to determine if an AAV vector expressing NT4 prevents retinal ganglion cell loss following optic nerve crush injury in Thy1-yellow fluorescent protein (Thy1-YFP) mice.

Methods: Thy1-YFP mice, which express yellow fluorescent protein as a marker of viable retinal neurons, were imaged before and after optic nerve crush injury. Two weeks prior to optic nerve crush injury, mice were treated with a 1µl intravitreal injection containing 1x10⁹ vector genomes of either AAV.NT4 or AAV.Null in one eye with no treatment in the contralateral eye. Mice were sacrificed at two weeks following crush injury and retinal flatmounts prepared. Fluorescent spots were counted manually in the same retinal area of each animal. ELISA was performed to quantify NT4 levels in the retina and optic nerve of injected eyes.

Results: ELISA confirmed that NT4 expression was significantly increased in the retina and optic nerve of eyes injected with AAV.NT4 compared to control eyes (n=5). In vivo imaging demonstrated less fluorescent retinal neuron loss in AAV.NT4 treated eyes compared to both AAV.Null treated eyes and uninjected control eyes. At two weeks, the number of fluorescent cells (mean±SEM) in untreated eyes without optic nerve crush injury was 3213±95 cells/mm² (n=8). Eyes that received intravitreal AAV.NT4 (1598±45 cells/mm²) (n=10) showed more remaining fluorescent cells than eyes that received intravitreal AAV.Null (1167±124 cells/mm²) (n=6) or intravitreal PBS (1112±106 cells/mm²) (n=9) or no injection (1017±82 cells/mm²) (n=5). Thus, the number of fluorescent cells remaining in optic nerve crushed eyes that received AAV.NT4 was over 150% greater than optic nerve crushed eyes that received no injection (p<0.01).

Conclusions: Our results indicate that increased NT4 expression in the retina and optic nerve following intravitreal injection of AAV.NT4 results in protection of retinal neurons in Thy1-YFP mice following optic nerve crush injury. In Thy1-YFP mice, fluorescent cells predominantly represent retinal ganglion cells; therefore, these findings suggest that intravitreal AAV.NT4 provides a neuroprotective effect on retinal ganglion cells after optic nerve injury.

Commercial Relationships: Chendong Pan, None; Lihua Guo, None; Evan Berger, None; Anna M. Demetriades, None
Support: Fight for Sight, American Glaucoma Society, Research to Prevent Blindness, Inc.

Program Number: 780 **Poster Board Number:** A0115

Presentation Time: 1:00 PM - 2:45 PM

A twelve-months, randomized, prospective, open-label, parallel-group of in vivo confocal microscopic findings in glaucoma patients treated with bimatoprost 0.01% or bimatoprost 0.03%

Michele Figus, Stefano Lazzeri, Chiara Posarelli, Luca Martini, Marco Nardi. University of Pisa, Pisa, Italy.

Purpose: To evaluate the safety of two commercially available formulations of bimatoprost eye drops: 0.03% and 0.01% ophthalmic solutions.

Methods: Randomized, prospective, open-label, parallel-group cohort study. A total of 60 glaucoma patients (60 eyes) in monotherapy with bimatoprost 0.03% since at least one year. After a baseline visit, qualified subjects were randomized to receive a single drop of bimatoprost 0.01% (n = 30) or bimatoprost 0.03% (n = 30) ophthalmic solutions once per day for 12 months. Statistical analyses were performed using paired t-test and repeated measures ANOVA. Main outcome measures: primary end point was comparison between groups in laser-scanning microscope parameters (corneal epithelium and endothelium cells, goblet cells and conjunctival epithelium). Secondary endpoint was to evaluate and compare changes in functional parameters (meniscus tear, Schirmer test and BUT).

Results: Goblet cells density showed significant increase in bimatoprost 0.01% group from baseline 351.8 ± 192.3 cells/ μm^2 to 425.6 ± 178.5 cells/ μm^2 ($P < 0.001$; mean difference = 73.8 cells/ μm^2 ; 95% CI 42.88 to 104.7) and to 428.5 ± 171 cells/ μm^2 ($P < 0.001$; mean difference = 76.7 cells/ μm^2 , 95% CI 47.17 to 106.1) at 6- and 12-months follow-up, respectively. Significant differences were also found between the two groups ($p < 0.001$). Correspondingly, all functional parameters improved in bimatoprost 0.01% group ($P < 0.05$) with significant differences between groups (meniscus tear $P = 0.043$, Schirmer test $P = 0.010$, and break-up time $P < 0.001$). No differences between groups in lowering IOP ($P > 0.05$).

Conclusions: Bimatoprost 0.01% demonstrated an increase in conjunctival goblet cells density and functional parameters compared to bimatoprost 0.03% eye drop.

Commercial Relationships: Michele Figus, None; Stefano Lazzeri, None; Chiara Posarelli, None; Luca Martini, None; Marco Nardi, Alcon (R), Allergan (R)

Program Number: 781 **Poster Board Number:** A0116

Presentation Time: 1:00 PM - 2:45 PM

Development of a cellular model of human trabecular meshwork to evaluate the role of chemokine ligands in glaucoma

Georges KALOUCHE^{1,2}, Céline Boucher¹, Derock Murielle², Annick Coste², Patrick Avenet², Stéphane Melik-Parsadaniantz¹, Thomas Debeir³, Christophe Baudouin¹, William H. Rostene¹, Xavier Vigé².

¹Institut de la Vision/INSERM/UPMC Univ Paris 06/CNRS/CHNO des Quinze-Vingts, Paris, France; ²Sanofi Research & Development, Chilly-Mazarin, France; ³Sanofi Fovéa, Paris, France.

Purpose: Trabecular meshwork (TM) is the main site of resistance of the aqueous humor (AH) and is implicated in the regulation of the AH outflow. TGF- β 2 and dexamethasone are known to act on TM cells to induce glaucoma. We recently demonstrated that a CXCR3 antagonist can restore the trabecular function in a rat model of ocular hypertension obtained by episcleral veins electro-coagulation. The purpose of this study was firstly to characterize an in vitro model of human TM in order to evaluate the involvement of CXCR3 chemokine receptor and its ligands (CXCL9, CXCL10 and CXCL11) in the biology of TM cells.

Methods: Primary human TM cells obtained from ScienCell were treated with either dexamethasone (100 nM) or TGF- β 2 (10 ng/ml). Myocilin secretion, α -smooth muscle actin (α -SMA) expression and phosphorylation of myosin light chain (MLC) were investigated by western blotting. Collagen I and α -SMA immunolabelling were analyzed by quantitative immunocytochemistry (ICC). CXCR3, CXCL9, CXCL10 and CXCL11 mRNA expressions were measured

using TaqMan assays by quantitative PCR. Immunolabelling of CXCR3 was also quantified by ICC and flow cytometry (FC).

Results: TGF- β 2 treatment induced a myofibroblastic phenotype of TM cells characterized by a dose dependent effect on α -SMA up-regulation (24h), increase phosphorylation of MLC (24h) and collagen I secretion (96h). In addition, we observed that dexamethasone increased significantly myocilin secretion, a specific marker of the TM. In this in vitro model, a low expression of the isoform B of CXCR3 was measured by qPCR and correlated by ICC and FC. Furthermore, CXCL9, CXCL10 and CXCL11 were up-regulated 4h post-treatment with either TGF- β 2 or dexamethasone. This transient increase of CXCL9, CXCL10 and CXCL11 was followed by a subsequent decrease of mRNA below the basal condition after 24h

Conclusions: This study characterizes an in vitro model of TM cells and demonstrates the presence of CXCR3 B isoform on TM cells. Moreover, the regulation of its ligands expression under known inducers of IOP increase (TGF- β 2 and dexamethasone) suggests a role of CXCR3 signaling in the regulation of the AH outflow.

Commercial Relationships: Georges KALOUCHE, Sanofi (E); Céline Boucher, None; Derock Murielle, Sanofi (E); Annick Coste, None; Patrick Avenet, Sanofi (E); Stéphane Melik-Parsadaniantz, None; Thomas Debeir, sanofi fovea (E); Christophe Baudouin, None; William H. Rostene, None; Xavier Vigé, SANOFI (E)

Support: Non

Program Number: 782 **Poster Board Number:** A0117

Presentation Time: 1:00 PM - 2:45 PM

Effect of anecortave acetate (AA) on outflow facility in a mouse model of steroid-induced glaucoma

Sandeep Kumar^{1,2}, Shaily D. Shah^{2,3}, Emily R. Deutsch¹, Hai M. Tang¹, John Danias^{1,2}. ¹Cell Biology, SUNY Downstate Med Center, Brooklyn, NY; ²Ophthalmology, SUNY Downstate Medical Center and the SUNY Eye Institute, Brooklyn, NY; ³Mount Sinai School of Medicine, New York, NY.

Purpose: To determine the effect of AA on the outflow facility in a mouse model of steroid-induced glaucoma.

Methods: Four groups of C57/B6 mice received either i. 20 μ l of Triamcinolone acetonide (TA) (40mg/ml) subconjunctivally bilaterally followed by AA (75mg/ml, Alcon) two weeks later,

ii. TA for 3 weeks,

iii. AA for 1 week

iv. No intervention.

IOP was measured preterminally. Outflow facility was determined using simultaneous pressure and flow measurements. Myocilin expression was investigated in a subset of eyes using quantitative PCR.

Results: Eyes receiving TA had significantly decreased outflow facility compared to naïve control eyes ($p < 0.05$, t-test). Outflow facility was significantly higher ($p < 0.05$) in eyes receiving both TA and AA, and eyes receiving AA alone compared to eyes receiving TA alone but not significantly different from that of naïve control eyes. Eyes receiving AA either alone or together with TA had significantly lower ($p < 0.001$, ANOVA) relative MYOC expression compared to either TA injected or naïve control eyes. IOP was not significantly different among groups of eyes ($p > 0.05$).

Conclusions: Treatment with AA can reverse the decrease in outflow facility caused by steroid treatment in mice. Myocilin expression is not affected by TA treatment in mice but is affected by AA.

Commercial Relationships: Sandeep Kumar, None; Shaily D. Shah, None; Emily R. Deutsch, None; Hai M. Tang, None; John Danias, Bausch and Lomb (C), N/A (P)

Support: NEI Grant EY 20670, RPB unrestricted challenge grant

Program Number: 783 **Poster Board Number:** A0118

Presentation Time: 1:00 PM - 2:45 PM

Live imaging of early microglia activation predicts neurodegeneration in chronic glaucoma

Alejandra Bosco¹, Cesar R. Romero¹, Alexis A. Chagovetz¹, Michael R. Steele¹, Kevin Breen¹, Balamurali K. Ambati^{2,1}, Monica L. Vetter^{1,2}

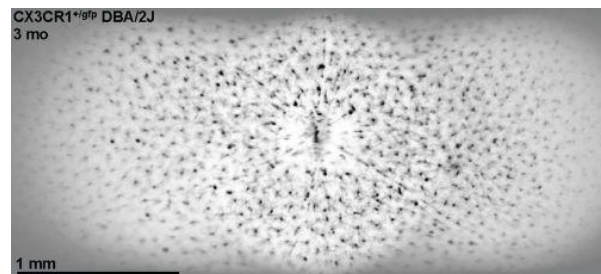
¹Neurobiology and Anatomy, University of Utah, Salt Lake City, UT; ²Moran Eye Center, University of Utah, Salt Lake City, UT.

Purpose: Microglia activation is the earliest reported retinal change preceding detectable retinal ganglion cell (RGC) degeneration in the DBA/2J (D2) model of chronic glaucoma (Bosco et al, 2011). Here, we asked whether early microglia changes are indicators of later RGC pathology. We addressed this question in the D2 model, in which variable and asynchronous RGC degeneration affects discrete retinal sectors and about half of the optic nerves (ONs). We sought to determine whether early microglia activation positively correlates with the severity of optic neuropathy and/or pattern of retinal degeneration at later stages.

Methods: To monitor the progression of microglial changes, we used live laser confocal ophthalmoscopy (Spectralis, Heidelberg Engineering) to image GFP+ microglia in Cx3cr1+/GFP D2 mice (n=30). Each retina was imaged at 2, 3, 4 and 5 months of age (mo) to map sequential changes in the distribution and density of activated microglia in the inner retina, optic disc and nerve head (OD/ONH). At 10 mo, the same eyes were analyzed ex vivo for ON pathology severity and pattern of retinal degeneration. ONs were prepared as semithin plastic cross-sections, stained with PPD, and axonal loss scored in light-microscopy montages. Retinal flatmounts were immunostained for Brn3 or γ -synuclein and p-neurofilament, and the entire inner retina was imaged by confocal microscopy. Last, we compared levels of OD/ONH microgliosis at 2-3mo with severity of ON pathology at 10 mo, and the sectorial distributions of activated microglia at 4-5mo and declining RGCs at 10 mo in the same retinas.

Results: Our live imaging method unambiguously identified activated microglia with large somata and reduced branching, detecting peak OD/ONH microgliosis by 2-3 mo in 81% of the retinas. We found positive correlation between levels of early OD/ONH microgliosis and late ON degeneration, which coincided in 16/18 ONs with severe and moderate pathology, and 5/9 healthy ONs. In the retina, 79% of the areas showing high microglia activation at 4-5 mo, developed RGC somatic and/or axonal degeneration at 10 mo. This colocalization was detected in eyes at all levels of ON pathology (severe, 79±6%, moderate 75±7%, mild/no 83±3%).

Conclusions: These data establish microglia activation as a sensitive and early biomarker of late retinal and ON pathology in D2 glaucoma.



Early microglia activation maps to retinal sectors of future degeneration.

Commercial Relationships: Alejandra Bosco, University of Utah (P); Cesar R. Romero, None; Alexis A. Chagovetz, None; Michael R. Steele, None; Kevin Breen, None; Balamurali K. Ambati, None; Monica L. Vetter, University of Utah (P)
Support: EY020878-01

Program Number: 784 **Poster Board Number:** A0119

Presentation Time: 1:00 PM - 2:45 PM

Elevation of IOP triggers responses from cytokines IL-6 and IL-1 β ; involvement of both optic nerve head astrocytes and retinal ganglion cells

Wenlan Lu¹, Jonathan M. Beckel¹, Jason C. Lim¹, Gulab S. Zode^{4,5}, Val C. Sheffield^{4,5}, Alan M. Laties², Claire H. Mitchell^{1,3}

¹Anatomy & Cell Biology, University of Pennsylvania, Philadelphia, PA; ²Ophthalmology, University of Pennsylvania, Philadelphia, PA; ³Physiology, University of Pennsylvania, Philadelphia, PA; ⁴Howard Hughes Medical Institute, University of Iowa, Iowa, IA; ⁵Pediatrics, University of Iowa, Iowa, IA.

Purpose: Increasing evidence suggests that cytokines contribute to a local inflammatory response in glaucoma. We and others have previously shown that transient elevation of IOP with the “controlled elevation of IOP” (CEI) model increases retinal levels of IL-6 mRNA. In this study, we asked whether an increase in protein levels can accompany this rise, whether IL-1 β is also involved, whether cytokines are elevated during chronic IOP elevation, and probed the cellular source of these cytokines.

Methods: In the CEI model of acute IOP elevation, pressure was increased in rats by canulation of the anterior segment; IOP was raised to 50 mm Hg for 4 hrs and tissue extracted 24 hrs later. The Tg-MYOCY437H mouse was used as a model of chronic glaucoma; IOP in 8 month old Tg-MYOC mice was 15.7 ± 0.5 mmHg compared to 11.8 ± 1 mmHg in littermate controls. Rat optic nerve head astrocytes were cultured onto a silicone substrate and subjected to 5% strain using a custom designed apparatus. Rat retinal ganglion cells (RGCs) were isolated using the immunopanning method and exposed to an analogous stretch. mRNA levels were compared using qPCR and protein was quantified from immunoblots, or for RGCs with an antibody cytokine array.

Results: Elevation of IOP to 50 mm Hg for 4 hrs elevated IL-6 proteins in the retina, consistent with the rise in mRNA. Levels of IL-1 β mRNA were also elevated, and the increase in mature 17 kD IL-1 β protein levels with CEI approached significance. mRNA for IL-1 β was increased in 8 month old Tg-MYOC mice. In isolated rat optic nerve astrocytes, IL-6 was released from astrocytes by stretch. Stretch also increased mRNA for IL-6 and IL-1 β in astrocytes. Stretch of isolated RGCs led to the release of both IL-6 and IL-1 β .

Conclusions: Upregulation and release of the cytokines IL-6 and IL-1 β may be a general response to mechanical strain in the posterior eye. Cytokine levels in the retina were increased in vivo by transient elevation of IOP and by chronic elevation with the Tg-MYOC model, and released from ganglion cells. Cytokines in optic nerve astrocytes also increased in response to stretch. The cellular mechanisms linking mechanical strain to cytokine release are being investigated.

Commercial Relationships: Wenlan Lu, None; Jonathan M. Beckel, None; Jason C. Lim, None; Gulab S. Zode, Alcon Labs (F); Val C. Sheffield, None; Alan M. Laties, AstraZeneca (C), Forest Research Inst (C), Kendle (C), Lilly (C), Merck (C), Pfizer (C), Sanofi-Aventis (C), TB Alliance for Drug Dev (C); Claire H. Mitchell, University of Pennsylvania (P)

Support: EY015537, EY013434

Program Number: 785 **Poster Board Number:** A0120

Presentation Time: 1:00 PM - 2:45 PM

Characterization of Primary Open Angle Glaucomatous Sclera

Alex S. Huang, Karen Xuandao Duong-Polk, Christopher Heichel, Felipe A. Medeiros, James D. Lindsey, Robert N. Weinreb.

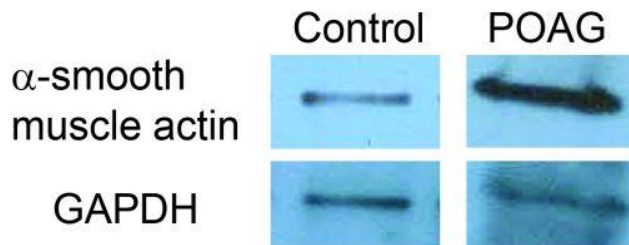
Ophthalmology, Shiley Eye Center, La Jolla, CA.

Purpose: To study biochemical and cellular changes in primary open angle glaucomatous (POAG) sclera. TGF- β is a soluble protein known to be elevated in POAG and implicated in trabecular meshwork (TM) pathologic changes leading to increased aqueous humor outflow resistance and elevated intraocular pressure. As the TM is not entirely occluded in POAG, this soluble factor can still travel beyond the TM into the distal outflow pathway, including the intrascleral venous plexus, where it can mediate pathologic alterations such as myofibroblastic differentiation and elevated α -smooth muscle actin expression.

Methods: Scleral samples have been collected from an age-matched pair of 60 year-old glaucomatous and non-glaucomatous patients. Glaucomatous sclera was collected during canaloplasty surgery from a female with a five-year history of glaucoma with visual field defects and elevated intraocular pressures (20-40 mm Hg) despite multiple aqueous suppressants and a prostaglandin. Control sclera was collected from remnant corneo-scleral rim after corneal transplantation. Scleral samples were homogenized and myofibroblastic activation was evaluated by assessing α -smooth muscle actin expression. GAPDH levels served as protein loading controls.

Results: Expression of α -smooth muscle actin expression was greater in glaucomatous sclera than in age-matched non-glaucomatous sclera.

Conclusions: Elevated α -smooth muscle actin levels in glaucomatous sclera are consistent with TGF- β mediated alterations and scleral myofibroblastic induction. These results support further evaluation of TGF- β mediated scleral changes and the relevance of myofibroblastic activation in glaucoma. Additional scleral samples from glaucomatous and control patients will be collected and evaluated. Primary culture fibroblasts will also be generated from normal and glaucomatous sclera and compared.



Commercial Relationships: Alex S. Huang, None; Karen Xuandao Duong-Polk, None; Christopher Heichel, None; Felipe A. Medeiros, Carl-Zeiss (F), Heidelberg Engineering (F), Topcon (F), Alcon (F), Allergan (F), Sensimed (F), Reichert (F); James D. Lindsey, None; Robert N. Weinreb, Aerie (F), Alcon (C), Allergan (C), Altheos (C), Amakem (C), Bausch&Lomb (C), Carl Zeiss-Meditec (C), Genentech (F), Haag-Streit (F), Heidelberg Engineering (F), Konan (F), Lumenis (F), National Eye Institute (F), Nidek (F), Optovue (C), Quark (C), Solx (C), Topcon (C)
Support: EY019692

Program Number: 786 **Poster Board Number:** A0121

Presentation Time: 1:00 PM - 2:45 PM

Cleavage of IL-6 receptor alpha as a potential mechanism for IL-6 transsignaling in Glaucoma

Payton Russom^{1,2}, Cathryn R. Formichella², Rebecca M. Sappington^{2,3}. ¹Dept. Biological Sciences, Vanderbilt University, Nashville, TN; ²Vanderbilt Eye Institute, Vanderbilt University

School of Medicine, Nashville, TN; ³Dept. Pharmacology, Vanderbilt University School of Medicine, Nashville, TN.

Purpose: Previous work suggests that interleukin-6 (IL-6) signaling via both classical and transsignaling pathways may be important for retinal ganglion cell survival (RGC) in glaucoma. Here we evaluate the possibility that IL-6 transsignaling is mediated by cleavage of membrane-bound IL-6 receptor alpha (IL-6R α) by metalloproteinases ADAM10 and ADAM17.

Methods: Using immunolabeling and immunoblotting, we examined the expression and localization patterns of ADAM10 and ADAM17 in whole eye paraffin sections and protein lysates from glaucomatous DBA/2 and control C57 mice. We then performed co-localization studies to compare expression and localization patterns of ADAM10 and ADAM17 and their potential target, IL-6R α . Cell type-specific markers were used to confirm retinal ganglion cell (β -tubulin), rod bipolar cell (PKC α) and Muller glial cell (glutamine synthetase) identities.

Results: We found that both ADAM10 & ADAM17 are expressed in healthy and glaucomatous retina, where they localize to multiple layers. Co-immunolabeling revealed that ADAM10 and ADAM17 are primarily expressed by RGCs, which also express IL-6R α . Quantification of ADAM10 and ADAM17 expression in the ganglion cell and nerve fiber layers of retina revealed that while ADAM10 expression did not change significantly with age ($p > 0.05$) or IOP ($p > 0.05$), elevated IOP increased ADAM17 expression by up to 55% ($p = 0.03$). There was no age-related increase in ADAM17 expression ($p > 0.05$).

Conclusions: Our data suggests that the necessary machinery (ADAM 10 & ADAM 17) is present in RGCs to cleave existing membrane-bound IL-6R α into soluble IL-6R. Interestingly, elevated IOP only altered the expression ADAM17 by RGCs. This suggests that ADAM17, in particular, may be a mechanism for the induction of IL-6 transsignaling in glaucoma.

Commercial Relationships: Payton Russom, None; Cathryn R. Formichella, None; Rebecca M. Sappington, None

Support: National Eye Institute: RO1EY020496-01 (RMS) and P30 EY08126 (VVRC); Research to Prevent Blindness, Inc.: Career Development Award (RMS) and Unrestricted Institutional Grant (Vanderbilt Eye Institute)

Program Number: 787 **Poster Board Number:** A0122

Presentation Time: 1:00 PM - 2:45 PM

Pharmacological Actions of L-cysteine on Isolated Bovine Ciliary Muscles

Sunny E. Ohia¹, Anita Okpobiri¹, Ya Fatou Njie-Mbye¹, Jenaye Robinson¹, Madhura Chitnis¹, Catherine A. Opere². ¹Pharmaceutical Sciences, Texas Southern University, Houston, TX; ²Department of Pharmacy Sciences, Creighton University, Omaha, NE.

Purpose: We have evidence that hydrogen sulfide (H₂S) donors such as sodium hydrosulfide (NaHS) can produce pharmacological actions on isolated porcine ocular smooth muscles. In this study, we investigated the pharmacological effects of L-cysteine, a substrate for H₂S production, on isolated pre-contracted bovine ciliary muscle.

Methods: Isolated bovine ciliary muscle strips were set up in organ baths containing oxygenated Krebs buffer (pH 7.4) at 37°C. Changes in longitudinal isometric tension were recorded via grass FT03 Force-displacement transducers and analyzed using PolyView software. Effects of L-cysteine on carbachol-induced tone was studied in the presence of enzyme inhibitors for H₂S biosynthetic pathway (AOA; cystathionine β -synthase inhibitor) and prostanoids (flurbiprofen; cyclo-oxygenase (COX) inhibitor).

Results: L-cysteine (0.01 nM-100 μ M) evoked a concentration-dependent relaxation of carbachol-induced tone in bovine ciliary

muscle, reaching a maximum inhibition of 88% at 10 μ M (with an IC_{50} of 2 nM). Relaxations elicited by L-cysteine were unaffected by pre-treatment of tissues with flurbiprofen (3 μ M). The inhibitor of cystathionine β -synthase, AOA (10 μ M) blocked only relaxations caused by high concentrations of L-cysteine (> 500 nM).

Conclusions: L-cysteine can relax pre-contracted bovine ciliary muscle, and this effect is dependent on endogenous production of H_2S . Furthermore, prostanoids are not involved in the inhibitory action of L-cysteine in this smooth muscle.

Commercial Relationships: Sunny E. Ohia, None; Anita Okpobiri, None; Ya Fatou Njie-Mbye, None; Jenaye Robinson, None; Madhura Chitnis, None; Catherine A. Opere, None

Program Number: 788 **Poster Board Number:** A0123

Presentation Time: 1:00 PM - 2:45 PM

Effect of Tissue Plasminogen Activator on Outflow Facility of Steroid Injected Mouse Eyes

Shaily D. Shah^{1,3}, Sandeep Kumar¹, Terete Borrás⁴, Matthew H. Smith⁴, John Danias^{1,2}. ¹Cell Biology, SUNY Downstate Medical Center, Brooklyn, NY; ²Ophthalmology, SUNY Downstate Medical Center and SUNY Eye Institute, Brooklyn, NY; ³Mount Sinai School of Medicine, New York, NY; ⁴Ophthalmology, University of North Carolina School of Medicine, Chapel Hill, NC.

Purpose: To determine whether over-expression of the tissue plasminogen activator (PLAT) gene can increase outflow facility in a mouse model of steroid-induced glaucoma

Methods: Adenoviral vectors carrying cDNA of the sheep PLAT gene and a fluorescent reporter gene (mCherry) (AdPLAT) or with no transgene (AdNull) were created. Transgene expression was driven by the CMV promoter. 3 groups of C57/B6 mice received either:

1. 20 μ l of triamcinolone acetonide (TA) suspension (40mg/ml) subconjunctivally bilaterally followed immediately by unilateral intracameral injection with 2 μ l AdPLAT (3-4x10¹² VG/ml)
2. 20 μ l TA subconjunctivally bilaterally followed one week later by unilateral intracameral injection with 2 μ l AdPLAT
3. 20 μ l TA subconjunctivally bilaterally followed immediately by bilateral injection with 2 μ l AdNull

IOP was measured preterminally. Outflow facility was determined using simultaneous pressure and flow measurements. After outflow facility measurement, all AdPLAT injected eyes were dissected and viewed under a fluorescent microscope to inspect for mCherry expression in the trabecular meshwork (TM). Eyes that showed mCherry expression were analyzed as a separate group from eyes that showed minimal mCherry expression.

Results: IOP was not significantly different between all eye groups ($p > 0.05$) after either one or two weeks of treatment with TA. Eyes subjected to one week of TA treatment that showed mCherry/PLAT expression had 63%, 54%, and 31% higher outflow facility than AdPLAT treated eyes with minimal mCherry/PLAT expression, contralateral control eyes, and AdNull treated eyes respectively (ANOVA, $p < 0.05$). Eyes subjected to two weeks of TA treatment that showed mCherry/PLAT expression had 86% and 58% higher outflow facility than AdPLAT treated eyes with minimal mCherry/PLAT expression and contralateral control eyes respectively (ANOVA, $p < 0.05$).

Conclusions: Treatment with AdPLAT can both prevent and reverse the decrease in outflow facility caused by steroid treatment in mice.

Commercial Relationships: Shaily D. Shah, None; Sandeep Kumar, None; Terete Borrás, None; Matthew H. Smith, None; John Danias, Bausch and Lomb (C), N/A (P)

Support: NEI Grant EY 20670, RPB unrestricted challenge grant

Program Number: 789 **Poster Board Number:** A0124

©2013, Copyright by the Association for Research in Vision and Ophthalmology, Inc., all rights reserved. Go to iovs.org to access the version of record. For permission to reproduce any abstract, contact the ARVO Office at arvo@arvo.org.

Presentation Time: 1:00 PM - 2:45 PM

Latanoprost Lowers Intraocular Pressure in Matrix Metalloproteinase 9-null Mice

Ramez I. Haddadin, Dong-Jin Oh, Douglas J. Rhee. Ophthalmology - Glaucoma Service, Massachusetts Eye & Ear Infirmary, Boston, MA.

Purpose: Prostaglandin F₂ α analogues, such as latanoprost, are effective intraocular pressure (IOP) lowering agents. Our group has previously shown that latanoprost results in upregulation of various matrix metalloproteinases (MMP); however, MMP9 expression is induced from an undetected level in the human ciliary body.

Therefore, we hypothesize that MMP9 is critical to the IOP lowering effect of latanoprost. Transgenic mice are commonly used as models to study molecular mechanisms, and there is significant homology between human and mouse MMP9 mRNA sequences. We studied the role of MMP9 in mice by measuring the IOP reduction with latanoprost treatment in both wild-type (WT) and MMP9-null mice.

Methods: FVB/NJ WT and MMP9-null mice were bred independently, fed ad lib, and housed under identical 12/12-hour light-dark cycles (on 7:00, off 19:00). Two-month-old WT and MMP9-null mice were anesthetized by intraperitoneal (IP) injection of a ketamine/xylazine mixture. A rebound tonometer (TonoLab) was used to take 3 IOP measurements in each eye between 4 and 7 minutes after intraperitoneal injection. WT and MMP9-null mice were also treated with 4 μ l of 0.005% latanoprost in the treated eye and PBS in the contralateral eye. IOPs were measured at 2 hours post-treatment.

Results: Mean daytime IOPs of WT and MMP9-null mice were 13.6 \pm 1.8 mm Hg (n=54) and 14.8 \pm 2.0 mm Hg (n=48), respectively. The difference in IOPs is 8.6% ($p=0.003$). With latanoprost treatment, the IOP-lowering effect was 17.4 \pm 8.0% (n=25) and 16.2 \pm 9.5% (n=23) in WT and MMP9-null mice, respectively. The difference in IOP-lowering effect was not statistically significant ($p=0.64$).

Conclusions: MMP9-null mice have significantly higher IOPs than their WT counterparts; however, the reductions in IOPs with latanoprost administration were not different. These results are contrary to expected given that MMP9 is not expressed at baseline in human ciliary body, and is induced by latanoprost. These are important considerations when studying the role of MMP9 in mice.

Commercial Relationships: Ramez I. Haddadin, None; Dong-Jin Oh, None; Douglas J. Rhee, Alcon (C), Alcon (F), Allergan (C), Aquesys (F), Aquesys (C), Merck (F), Merck (C), Santen (C)
Support: NIH R01 EY 019654-01 (DJR) and NIH EY 014104 (MEEI Vision-Core Grant)

Program Number: 790 **Poster Board Number:** A0125

Presentation Time: 1:00 PM - 2:45 PM

A rat model of glaucoma induced by circumlimbal ligation

Algis J. Vingrys, Hsin-Hua Liu, Christine T. Nguyen, Bang V. Bui, Zheng He. Optometry & Vision Sciences, University of Melbourne, Parkville, VIC, Australia.

Purpose: To develop a reliable and cost-effective model of chronic ocular hypertension which mimics glaucomatous optic neuropathy in rat.

Methods: Long-Evans rats were given unilateral ligation around the limbus via conjunctival suture under anaesthesia (ketamine/xylazine). The fellow eye served as an untreated control (n=8). A sham group (n=8) received the same unilateral treatment except the suture was loosely placed. IOP was monitored pre- and post-ligation for 15 weeks. Electroretinography (ERG) was recorded at baseline (pre-suture), then regularly to 15 weeks. The photoreceptor, bipolar cell and ganglion cell function were extracted and expressed relative to the contralateral untreated control eye (% \pm SEM).

Results: During the first day after ligation, IOP spiked from 16.9 \pm 0.8

ARVO 2013 Annual Meeting Abstracts by Scientific Section/Group – Glaucoma

to 58.2±4.3 mm Hg recovering to 29.9±1.9 mm Hg in treated eyes ($p < 0.05$) and remained elevated for 15 weeks. The sham group gave a small temporary spike (22.8±2.8 mm Hg at 1-hour) before returning to normal. Control eyes remained at normal IOP (baseline 16.4±0.9 mm Hg, week 15 11.7±0.2 mm Hg, $p > 0.05$). In ligated eyes, an early non-selective loss of all ERG components was manifest. From week 8, a selectively larger loss of ganglion cell function compared with bipolar cell and photoreceptor function was found (-36±7% vs -21±7% vs -16±7% respectively; $p < 0.05$). ERG components remained unaltered in the sham group for 15 weeks (4±5%, -3±5%, -2±4% respectively; $p > 0.05$).

Conclusions: Circumlimbal ligation provides a simple and cost-effective way to induce mild chronic ocular hypertension that produces preferential ganglion cell dysfunction. This model may be useful in glaucoma research.

Commercial Relationships: Algis J. Vingrys, None; Hsin-Hua Liu, None; Christine T. Nguyen, None; Bang V. Bui, None; Zheng He, None

Support: NHMRC 566570

Program Number: 791 **Poster Board Number:** A0126

Presentation Time: 1:00 PM - 2:45 PM

The two- global- flash multifocal ERG (mfERG) in the diagnosis of early macular dysfunction in preperimetric glaucoma

Anna A. Ledolter, Margarita G. Todorova, Andreas Schötzau, Anja M. Palmowski-Wolfe. Ophthalmology, University of Basel, Basel, Switzerland.

Purpose: to evaluate the electrophysiological response in patients with preperimetric glaucoma (PPG) compared to control subjects and to patients with perimetric glaucoma (POAG) using a two- global-flash paradigm mfERG.

Methods: A two- global- flash mfERG (VERIS 6.06TM, FMSIII) was recorded in 6 eyes with PPG. The control group consisted of 20 healthy subjects and POAG group - of 25 patients (8- high tension glaucoma (HTG) and 17- normal tension glaucoma (NTG)). Recording parameters: bandpass filter (BPF): 1-300Hz, 103 Hexagons, M-sequence stimulus: LMax 100cd/m², Lmin <1cd/m², global flash: 200cd/m². Responses were filtered at 1-200 Hz. RMS was calculated. Three response epochs were analysed: the response to the focal flash, at 15-45ms (DC) and the response to the global flashes at 45-75ms (IC-1) and at 75-105ms (IC-2). Automated perimetry (Octopus 101, G2) was performed in all glaucoma patients. Measurement of RNFL thickness around the optic disc head was used to determine PPG patients (Cirrus SD-OCT, Carl Zeiss). Statistical analysis was performed using linear mixed effects models in the statistical package R version 12.1.

Results: The mean deviation (MD) of the PPG patients was 0.8±1.2 (dB) and of the POAG was 5.9±3.9 (dB). Visual acuity and IOP did not differ significantly between both patients groups ($p=0.57$ and $p=0.14$ respectively). The mfERG response of the PPG group differed most from control subjects in the central 10° (diameter). When compared to controls, PPG differed more than POAG in IC1&IC2. However for the DC POAG differed more than PPG. (see Table for details).

Conclusions: Multifocal ERG has been shown to be sensitive to detect glaucomatous damages in established glaucoma. In this study we could show, that in preperimetric glaucoma patients, the mfERG response is also reduced in the central 10°. These findings provide additional objective information on early retinal dysfunction in patients with beginning changes in the OCT but without visual field defects on standard automated perimetry.

Group of glaucoma	Epoch of two global flash mfERG	Difference of Means (compared to control), nV/deg ² (95%CI)	p- Value
PPG (n=6)	DC	-3.1 (-5.0 to -1.2)	0.0015
	IC1	-6.6 (-8.5 to -4.7)	<0.0001
	IC2	-6.1 (-8.0 to -4.2)	<0.0001
POAG (n=25)	DC	-2.5 (-3.9 to -1.1)	0.0003
	IC1	-4.3 (-5.7 to -2.9)	<0.0001
	IC2	-3.4 (-4.8 to 2.0)	<0.0001

Commercial Relationships: Anna A. Ledolter, None; Margarita G. Todorova, None; Andreas Schötzau, None; Anja M. Palmowski-Wolfe, None

Support: SNSF Grant 32003B-135219; LHW Stiftung Lichtenstein;

Program Number: 792 **Poster Board Number:** A0127

Presentation Time: 1:00 PM - 2:45 PM

The effect of acute intraocular pressure challenge on retinal oxygen saturation, retinal blood flow and visual function

Rachael A. O'Connell, Bang V. Bui, Andrew J. Anderson, Sarah L. Hosking. Optometry and Vision Sciences, The University of Melbourne, Melbourne, VIC, Australia.

Purpose: To consider the effect of moderate intraocular pressure (IOP) perturbation on retinal oxygen saturation, blood flow and the pattern electroretinogram (PERG) in young, healthy participants.

Methods: 23 young (22-38 years), healthy participants had PERG, retinal oximetry and flowmetry images recorded before, during and after IOP elevation. Using a probe placed on the lower eyelid, IOP was increased to ~30 mmHg to lower ocular perfusion pressure (OPP) by ~30%. Steady-state PERG waveforms (8.3 Hz) were recorded bilaterally (200 sweeps) to return the second harmonic amplitude (16.7 reversals/sec). Peak oxygen saturation for arteries and veins of various diameters on oximetry (Oxymap retinal oximeter) was assessed by fitting Gaussian functions to frequency histograms of all pixels. Blood flow, volume and velocity (Heidelberg retinal flowmeter) were averaged within a 10x10 pixel window at the temporal retina.

Results: OPP reduction remained stable between baseline and perturbation ($F(2,66) = 1.42$, $p = 0.25$). PERG amplitude was significantly reduced ($F(2,44) = 24.24$, $p < 0.01$) and phase significantly delayed ($F(2,44) = 17.00$, $p < 0.01$) during IOP perturbation. Contralateral eyes were unchanged. Arterial oxygen saturation remained the same ($F(1.43,30.08) = 3.69$, $p = 0.05$), whereas venous saturations reduced ($F(1.39,29.15) = 38.64$, $p < 0.01$). Blood flow was shown to change across the 3 conditions ($F(2,36) = 5.37$, $p < 0.01$). Poor correlation was found between OPP reduction and either PERG amplitude, PERG phase or venous oxygen saturation.

Conclusions: PERG amplitude and retinal oxygen saturation are sensitive to an acute, moderate IOP perturbation in young participants.

Commercial Relationships: Rachael A. O'Connell, None; Bang V. Bui, None; Andrew J. Anderson, None; Sarah L. Hosking, None

Program Number: 793 **Poster Board Number:** A0128

Presentation Time: 1:00 PM - 2:45 PM

Motion perception in early glaucoma

Anna Francoz¹, Alessandro Carlini^{2,3}, Catherine Creuzot-Garcher¹, Patrick Quercia¹, Thierry Pozzo², Alain M. Bron¹. ¹Department of Ophthalmology, University Hospital, Dijon, France; ²INSERM

U1093, Cognition, Action et Plasticité Sensorimotrice, Dijon, France; ³CNRS UMR 5022, LEAD, Dijon, France.

Purpose: The aim of our study was to underline the changes in the movement perception for early glaucoma. Our working hypothesis consisted in inquiring if the impairment of the magnocellular pathway may modify the movement perception capabilities in the visual field, more particularly in its peripheral area.

Methods: We included 14 healthy subjects and 14 patients with early primary open angle glaucoma. A moving target was presented on a semicircular screen (1.8 m diameter); participants were asked to localize the Ending Point (EP) of each movement. Each stimulus consisted in a white dot (0.72° of diameter) moving horizontally with the imposed velocity profile. Two different laws of motion were displayed: a “biological” motion corresponding to the recording of an arm pointing movement, consisting in a bell-shaped velocity profile, and a “non-biological” motion corresponding to a constant velocity profile. The study field was divided into 4 quadrants and 2 eccentricities: EP may be displayed in the “peri-central” (10° from the foveal axis) or peripheral (20° from the foveal axis) visual field. Two trajectories length were presented (10° and 20°). Each stimulus with same characteristics was displayed two times. Thus the experiment was constituted by 192 trials, presented in a random order. For every participant we calculated the PCE (Position Constant Error) which was defined as the average difference between the estimation of the EP indicated by the participant versus the true location of the same target. The PVE (Position Variable Error) was defined as the standard deviation of the responses of each participant.

Results: All the participants overestimated the EP (13.23 ± 8.87 mm for healthy subjects and 17.06 ± 13.07 mm for glaucoma patients, $p = 0.2518$). The PVE was 28.14 ± 6.86 mm for healthy subjects and 40.95 ± 9.83 mm for glaucoma patients ($p = 0.0004$). There was a significant difference in the PVE for both groups when stimulus moved accordingly to the “non-biological” velocity profile ($p = 0.0001$). Glaucoma patients had substantial PVE increase when the target image had a “non-biological” speed profile ($p = 0.0388$).

Conclusions: This study described disorders in movement perception and localization in patients with early glaucoma. Particularly, the unexpected lack of difference between normal subjects and patients in localizing a moving stimulus strongly suggested that the visual deficiency could be partly compensated by endogenous informations.

Commercial Relationships: Anna Francoz, None; Alessandro Carlini, None; Catherine Creuzot-Garcher, None; Patrick Quercia, None; Thierry Pozzo, None; Alain M. Bron, Allergan (C), Bausch Lomb (C), Horus (F), Théa (C)

Program Number: 794 **Poster Board Number:** A0129

Presentation Time: 1:00 PM - 2:45 PM

Electrophysiologic Correlates of RNFL Thickness in Experimental Glaucoma

James N. Ver Hoeve^{1,3}, Charlene B. Kim^{1,3}, Carol A. Rasmussen^{1,3}, Christopher J. Murphy^{2,3}, Brian J. Christian⁴, T Michael Nork^{1,3}.

¹Ophthalmology & Visual Science, Univ of Wisconsin-Madison, Madison, WI; ²Veterinary Medicine, University of California-Davis, Davis, CA; ³Ocular Services On Demand, Madison, WI; ⁴Covance, Inc, Madison, WI.

Purpose: To determine the relationship between electrophysiologic measures of retino-cortical function and structural measures of retinal nerve fiber layer thickness (RNFLT) in non-human primates with experimentally-induced glaucoma (EG).

Methods: Six female cynomolgus monkeys underwent laser scarification of the trabecular meshwork in one eye that resulted in chronic ocular hypertension (OH). At the time of assessment, OH had been present > 2 years. Recordings included full-field

electroretinograms (FFERGs) to scotopic and photopic luminance intensity series, 30 Hz flicker, and flash-visual evoked potentials (FVEPs). Transient pattern ERG (PERGs) and pattern VEPs (PRVEPs) were recorded to checker-board stimuli of two check sizes reversing at a rate of 4/s. Animals were anesthetized with ketamine and dexmedetomidine. Pupils were dilated for FFERG. Eyes were refracted for viewing distance for PERG and PVEP recordings. Measures of RNFLT were obtained from each eye using automated and manual segmentation routines from two commercially-available sdOCT instruments (CirrusTM and SpectralisTM).

Results: RNFLT in the EG eye averaged 42-52% of the fellow eye across instruments and segmentation methods. No differences in the amplitudes of the a- and b-wave for the FFERG scotopic and photopic series, oscillatory potentials, nor the P50-like PERG, were noted between EG and fellow eyes. The amplitudes of the FFERG photopic negative response (PhNR), the PERG N95-like wave, and FVEP and PRVEP were significantly reduced in the EG eyes of all six animals. There was a significant linear relationship between RNFLT and the amplitude of the PhNR, FVEP, N95 and PRVEP waves, accounting for 75, 66, 69, and 47 percent of the variance in RNFLT, respectively, using manual segmentation (all p 's < .001). Automatic segmentation by the SpectralisTM or the CirrusTM instruments resulted in only a small reduction in size of the correlation between RNFLT and PhNR, FVEP, N95, and PRVEP.

Conclusions: Non-invasive electrophysiologic responses associated with retinal ganglion cell function (PhNR, FVEP, N95, PRVEP) have a strong linear relationship to RNFLT as assessed by sdOCT. The structural and functional deficits observed in animals with long-standing OH suggest that these associations likely remain stable over time.

Commercial Relationships: James N. Ver Hoeve, OSOD, LLC (C), Covance, Inc (F); Charlene B. Kim, None; Carol A. Rasmussen, None; Christopher J. Murphy, Ocular Services On Demand (I), Ocular Services On Demand (C), Platypus Technologies LLC (I), Imbed LLC (I), EyeKor LLC (I), Allergan (C), Genentech (C), Sarcodex (C), Covance (C); Brian J. Christian, None; T Michael Nork, None

Support: NEI Grant P30EY016665, Research to Prevent Blindness

Program Number: 795 **Poster Board Number:** A0130

Presentation Time: 1:00 PM - 2:45 PM

Functional Degeneration of Retinal Ganglion Cells in a Mouse Model of Chronic Ocular Hypertension

Hui Chen¹, Yan Zhao², Liang Feng¹, Jianhua Cang³, John B. Troy², Xiaorong Liu^{1,3}. ¹Ophthalmology, Northwestern University, Evanston, IL; ²Biomedical Engineering, Northwestern University, Evanston, IL; ³Neurobiology, Northwestern University, Evanston, IL.

Purpose: Glaucoma, characterized by dendritic and axonal degeneration of retinal ganglion cells (RGCs), visual field deficits, and ultimately RGC death, is one of the leading causes of blindness in the US. Although diversity in RGC damage has been reported in glaucomatous retinas, studies in human patients and animal models have so far failed to provide a clear picture of how RGCs degenerate and whether the surviving RGCs are still functional. In this study, we examined the functional degeneration of RGCs in a mouse model of experimental glaucoma.

Methods: We have adopted a laser-induced mouse model of ocular hypertension to mimic human high-tension glaucoma and demonstrated a sustained increase of intraocular pressure (IOP), and a progressive RGC loss. We applied two cutting-edge techniques, the laser-guided focal electro-retinogram (ERG) to measure visual responses from different retinal cell types at various locations, and a large-scale multi-electrode array (MEA) to examine response

properties of different subtype RGCs. We classified RGCs into ON, OFF and ON-OFF subtypes by using the innovative variant of Spike Triggered Covariance (STC) analysis, STC-NC (Cantrell et al., 2010). We compared the response properties of different subtypes of RGCs from hypertensive eyes and age matched controls. We further divided the retina into four quadrants (superior, inferior, temporal and nasal) and examined whether RGCs from different locations of the retina respond differently to the insult of ocular hypertension.

Results: We recorded the visual responses of RGCs from laser-treated right eyes and compared with untreated left eyes. Our preliminary data suggest that at 6 weeks after laser treatment there were more ON cells and fewer OFF cells while the percentage of ON-OFF cells remained unchanged. The receptive field (RF) sizes of mono-laminated ON and OFF RGCs decreased while the bi-laminated ON-OFF RGCs did not change in the glaucomatous eyes.

Conclusions: RGCs degenerate in a subtype- and location-dependent manner in ocular hypertensive mice. This study establishes a valuable model system with which to better understand how RGC degeneration leads to vision loss and a potential time window for early detection of glaucoma.

Commercial Relationships: Hui Chen, None; Yan Zhao, None; Liang Feng, None; Jianhua Cang, None; John B. Troy, None; Xiaorong Liu, None

Support: NIH grants R21EB004200, R01EY018621 and R01EY019034.

Program Number: 796 **Poster Board Number:** A0131

Presentation Time: 1:00 PM - 2:45 PM

Retinal ganglion cell dysfunction precedes death in glaucoma suspects

Gabriel Luna, Eleonore Savatovsky, Brandon Bosse, Michael Banitt, Olga Shif, Lori M. Ventura, Vittorio Porciatti, William J. Feuer. Ophthalmology, Bascom Palmer Eye Institute, Miami, FL.

Purpose: To estimate the timelag between retinal ganglion cell (RGC) dysfunction and death in patients suspected of glaucoma by comparing progressive losses of pattern electroretinogram (PERG) and retinal nerve fiber layer (RNFL) thickness over time.

Methods: Glaucoma suspects (N=107, 201 eyes) were monitored with PERG and optical coherence tomography (OCT) every six months for at least four years. Longitudinal PERG amplitudes and peripapillary retinal nerve fiber layer (RNFL) thicknesses were normalized on their respective dynamic range (difference between the values in normal subjects and advanced stages of the disease) and fitted with linear functions. Individual slopes were pooled. The time lag for PERG and OCT to lose 10% of their baseline value was calculated.

Results: In eyes with abnormal baseline PERG amplitude (50-90% loss from normal average, N=99), pooled PERG amplitude slopes took 1.9 - 2.5 years to lose 10% of their initial amplitude, whereas the RNFL thickness took 9.9 - 10.4 (P<0.05). Thus, the time lag between PERG amplitude and RNFL thickness to lose 10% of their initial values appears to be of the order of 8 years.

Conclusions: In glaucoma suspects, PERG signal anticipates an equivalent loss of OCT signal by several years.

Commercial Relationships: Gabriel Luna, None; Eleonore Savatovsky, None; Brandon Bosse, None; Michael Banitt, None; Olga Shif, None; Lori M. Ventura, None; Vittorio Porciatti, None; William J. Feuer, Abbott Medical optics (F), New World Medical (F)

Support: NIH RO1 EY014957, NIH Grant P30-EYO14801

Program Number: 797 **Poster Board Number:** A0132

Presentation Time: 1:00 PM - 2:45 PM

©2013, Copyright by the Association for Research in Vision and Ophthalmology, Inc., all rights reserved. Go to iovs.org to access the version of record. For permission to reproduce any abstract, contact the ARVO Office at arvo@arvo.org.

Evaluation of Pre-perimetric Glaucoma Patients using Short Duration Transient Visual Evoked Potentials (SD-tVEP)

Peter H. Derr¹, Rafael L. Furlanetto², Gustavo De Moraes^{2,3}, Alberto O. Gonzalez Garcia¹, Celso Tello², Jeffrey M. Liebmann^{1,3}, Robert Ritch^{1,4}. ¹Engineering, Diopsys Inc, Pine Brook, NJ; ²Einhorn Clinical Research Center, New York Eye and Ear Infirmary, New York, NY; ³NYU School of Medicine, New York, NY; ⁴Department of Ophthalmology, New York Medical College, Valhalla, NY.

Purpose: To evaluate the response of the Short Duration Transient Visual Evoked Potentials (SD-tVEP) on patients with pre-perimetric glaucoma (PrG).

Methods: Inclusion criteria were best corrected visual acuity of 20/30 or better normal 24-2 SITA-Standard visual fields (VF) in patients with glaucomatous optic neuropathy. Pre-perimetric glaucoma was defined by the presence of significant retinal nerve fiber layer thinning measured by spectral-domain optical coherence tomography (Spectralis, Heidelberg) whereas normal subjects (control group) had no abnormalities on this test. SD-tVEPs were recorded using the Diopsys NOVA System (Diopsys, Inc. Pine Brook, NJ). Each eye was stimulated with a 15% (Lc) and 85% (Hc) Michelson contrast checkerboard pattern. Test duration was 30 seconds/eye and each test resulted in a low- and high-contrast response. Each response was evaluated for overall waveform quality, P100 latency, and the amplitude difference of the P100 and N75. The two AUC-ROC analysis was performed on the both the Hc and Lc SD-tVEP parameters.

Results: 36 PrG patients and 30 controls with normal eyes were enrolled. There was difference in SD-tVEP Lc latency parameter between cases and controls (P=0.0032). Evaluating the SD-tVEP Lc parameters, the AUCs were 0.72 (0.59-0.86) for P100 latency and 0.58 (0.44-0.72) for P100 amplitude. Evaluating the SD-tVEP Hc parameters, the AUCs were 0.68 (0.55-0.81) for P100 latency and 0.58 (0.44-0.72) for P100 amplitude.

Conclusions: The low contrast SD-tVEP latency parameter produced the greatest AUC. The SD-tVEP low contrast latency parameter was able to differentiate normal and PrG patients and may be useful for the diagnosis of glaucoma with structural abnormalities but normal achromatic perimetry.

Commercial Relationships: Peter H. Derr, Diopsys Inc (E); Rafael L. Furlanetto, None; Gustavo De Moraes, None; Alberto O. Gonzalez Garcia, Diopsys (E); Celso Tello, DIOPSYS (C); Jeffrey M. Liebmann, Alcon Laboratories, Inc. (C), Allergan, Inc. (C), Allergan, Inc. (F), Carl Zeiss Meditech, Inc (F), Heidelberg Engineering, GmbH (F), Topcon Medical Systems, Inc. (F), National Eye Institute (F), New York Glaucoma Research Institute (F), SOLX, Inc. (C), Bausch & Lomb, Inc (C), Diopsys, Inc. (C), Diopsys, Inc. (F), Merz, Inc. (C), Glaukos, Inc. (C), Quark, Inc. (C); Robert Ritch, None

Program Number: 798 **Poster Board Number:** A0133

Presentation Time: 1:00 PM - 2:45 PM

Comparing functional damage by Multifocal ERG and visual fields in all severities of glaucoma

sujoy mukherjee, Abhishek Singh, Mahasweta Chowdhury, Aparna Rao. LV PRasad Eye Institute, Bhubaneswar, India.

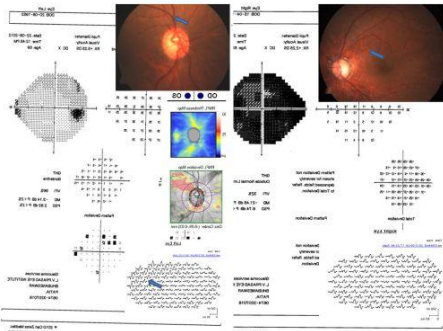
Purpose: To compare the functional changes on Multifocal ERG (MFERG) and visual fields by standard automated perimetry (SAP) with structural changes on Cirrus Spectral domain optical coherence tomography (SD-OCT) in all severities of glaucoma.

Methods: Retrospective review of consecutive patients with different severities of adult glaucoma. Data collected for analysis included age at diagnosis, baseline clinical variables like intraocular pressure, visual field indices including mean deviation and pattern standard

deviation and diagnosis (type of glaucoma). OCT variables including Retinal nerve fibre layer thickness (average and quadrant analysis) and NIP1 amplitudes (average and 4 quadrant analysis). Association between visual field indices with demographic, SD-OCT and NIP1 amplitudes were evaluated by regression statistics and clustered analysis in early (MD>-6dB), moderate (-6 to -12dB) and advanced glaucoma (<-12dB).

Results: Ninety seven eyes of 49 patients were included with a mean age of 54±11.2 years, including 22 early, 32 moderate and 43 with advanced glaucoma. While superior RNFL thickness differed between early (92±22.9 microns), moderate (88±22.4 microns) and severe (52±22.6 microns), p=0.02, NIP1 amplitudes were not statistically significant between early-severe glaucoma subtypes, p=0.2. Visual field index correlated significantly with the superior (r=0.6, p=0.01), inferior (r=0.7, p=0.02) RNFL thickness and superonasal NIP1 amplitude (r=0.6, p=0.02). Multivariate linear regression identified significant relationship between VFI and superior RNFL thickness (β=1.5, p=0.002), inferior RNFL thickness (β=1.6, p=0.004) and superonasal NIP1 (β=1.2, p=0.02) only in severe glaucoma (R²=0.85) while NIP1 amplitudes did not correlate significantly with visual field damage variables in earlier stages of glaucoma.

Conclusions: Functional damage on visual field correlates well with MFERG functional impairment only in advanced glaucoma. This suggests that focal abnormalities seen in moderate and early glaucoma may not be picked up by MFERG whereas diffuse abnormalities as seen in advanced glaucoma may be monitored for functional changes using MFERG.



Commercial Relationships: sujoy mukherjee, None; Abhishek Singh, None; Mahasweta Chowdhury, None; Aparna Rao, None

Program Number: 799 **Poster Board Number:** A0134

Presentation Time: 1:00 PM - 2:45 PM

Transgenic mice expressing mutated Tyr437His human myocilin have progressive loss of retinal ganglion cell electrical responsiveness

Vittorio Porciatti¹, Tsung-Han Chou¹, Xu Yang¹, Stanislav I. Tomarev². ¹Bascom Palmer Eye Inst, Univ of Miami Miller Sch Med, Miami, FL; ²Laboratory of Retinal Cell and Molecular Biology, National Eye Institute, NIH, Bethesda, MD.

Purpose: To characterize retinal ganglion cell (RGC) function in a transgenic mouse model of open-angle glaucoma by expression of mutated human myocilin (Myoc) in the trabecular meshwork (Zhou et al, IOVS, 2008).

Methods: RGC electrical responsiveness was tested with pattern electroretinogram (PERG) in 8 Myoc-mice of different ages (4, 7, 10, and 13 months) under ketamine/xylazine anesthesia. PERGs were recorded from each eye in response to horizontal gratings of 0.05

cycles/deg and 100% contrast. Intraocular pressure (IOP) was measured with a Tonolab tonometer.

Results: In 13 month-old Myoc mice, the PERG amplitude (mean 19.7 μV, SEM 2.1) and latency (mean 109.5 ms, SEM 7.8) were significantly different (P < 0.05) from the PERG amplitude (mean 28.1 μV, SEM 1.7) and latency (mean 81.7 ms, SEM 9.9) of 4 month-old mice. In contrast, PERGs of C57BL/6J mice aged 4 and 13 months had similar amplitudes and latencies. The IOP of older Myoc mice (19.0 mm Hg, SEM 0.7) tended to be higher than that of younger Myoc mice (17.9 mm Hg, SEM 1.05)-difference not significant.

Conclusions: Myoc mice display age-related changes in RGC electrical responsiveness associated with modest IOP elevation. Previous studies (Zhou et al., IOVS 2008) have shown in aged Myoc mice moderate RGC loss in the peripheral retina as well as moderate axonal degeneration in the optic nerve. As IOP, PERG and structural changes are also found in the early stages of human primary open angle glaucoma, Myoc mice may represent a useful genetic model for investigating this disease.

Commercial Relationships: Vittorio Porciatti, None; Tsung-Han Chou, None; Xu Yang, None; Stanislav I. Tomarev, None
Support: NIH-NEI RO1 EY019077, NIH center grant P30-EY014801, unrestricted grant to Bascom Palmer Eye Institute from Research to Prevent Blindness, Inc.

Program Number: 800 **Poster Board Number:** A0135

Presentation Time: 1:00 PM - 2:45 PM

Comparison of Static and Dynamic Contrast Sensitivities with Steady-state Pattern Electroretinography Ratio in Suspected Open Angle Glaucoma Patients

Péter Balázs Kocsis, Imre Zsolt Fejes, Andrea Facskó, Márta Janáky. Department of Ophthalmology, University of Szeged, Szeged, Hungary.

Purpose: Static and dynamic contrast sensitivities were assessed and compared with steady-state 'pattern electroretinography ratio' ('PERG ratio') in open angle glaucoma (OAG) patients. Their efficacy in determination of retinal ganglion cell (RGC) functional damage was compared.

Methods: Overall 36 (24 female, 12 male, mean age: 55.94 ± 16.55) suspected OAG patients were enrolled in the study. Their records were compared to the records of 36 age matched control subjects (22 female 14 male, mean age: 32.19 ± 16.64). Due to the wide age range, subjects were divided in groups of above and below 40 years of age. Inclusion criteria were (i) vertical and horizontal optic disc cupping ratio > 0.4-0.5, (ii) specific visual field defects and (iii) peripapillary alterations. Static and dynamic (frequency: 8.56 rev/sec) contrast sensitivities (CS) were measured at spatial frequencies of 0.48, 1.19, 1.91, 2.87, 3.58, 4.78, 5.73, 7.17, 14.34 cyc/deg by Neuroscientific Venus® 1020. Electrophysiological examinations were performed with Retiport Science 4.9.8.9. Program®. Steady-state PERG (constant frequency: 4.28 Hz) response amplitude to 0.8° checks and the amplitude to 16° checks were recorded and their ratio, the 'PERG ratio' was calculated. ANOVA on Ranks and Spearman correlation were applied (SigmaStat® 3.5).

Results: Above 40 years of age, significant differences were revealed in all dynamic and static spatial frequencies of CSs between suspected OAG and control groups (p<0.05). Below 40 years of age, however, no significant differences were found. There was significant difference in 'PERG ratio' between controls and suspected OAG patients in both age groups (<40 years: 1.1 vs. 0.87, >40 years: 0.98 vs. 0.76; p<0.001; ANOVA on ranks). Both static and dynamic CS correlated with 'PERG ratio' at all spatial frequencies, but correlations were stronger at dynamic CSs (r=0.34-0.46 vs. 0.42-0.68

$p < 0.001$, Spearman correlation).

Conclusions: In our subjects, dynamic CS showed stronger correlation to 'PERG ratio' than static one, which raises the possibility its higher value in determination of glaucomatous-type functional RGC damage. 'PERG ratio' and dynamic CS may help establishing the diagnosis of glaucoma in addition to the widely available perimetry. Further examinations are needed to confirm our findings.

Commercial Relationships: Péter Balázs Kocsis, None; Imre Zsolt Fejes, None; Andrea Facskó, None; Márta Janáky, None
Support: HARVO (Hungarian Association for Research in Vision and Ophthalmology) Travel Grant

Program Number: 801 **Poster Board Number:** A0136

Presentation Time: 1:00 PM - 2:45 PM

Impact of a notch filter on the detection of glaucomatous damage in POAG compared to controls using the 2-global-flash multifocal ERG

Anja M. Palmowski-Wolfe, Margarita G. Todorova, Andreas Schötzau, Anna A. Ledolter. Department of Ophthalmology, University Hospital Basel, Basel, Switzerland.

Purpose: to assess the effect of a 50Hz notch filter on the electrophysiological response in the 2-global-flash mfERG in patients with primary open angle glaucoma (POAG) compared to control subjects and its impact on the detection of glaucomatous damage.

Methods: A 2 global flash mfERG (VERIS 6.06TM, FMSIII) was recorded in 24 healthy control subjects and 34 POAG patients. Recording parameters: bandpass filter (BPF): 1-300Hz, 103 Hexagons, M-sequence stimulus: LMax 100cd/m², Lmin <1cd/m², global flash: 200cd/m². RMS for each subject was calculated with cut-off-frequencies of 1-200Hz with and without a digital 50Hz notch filter (Veris Science, Software 6.2.2 d2). Three response epochs of the central 10° were analysed: the response to the focal flash, at 15-45ms (DC) and the response to the global flashes at 45-75ms (IC-1) and at 75-105ms (IC-2). Statistical analysis: linear mixed effects models in the statistical package R 12.1.

Results: A notch filter of 50Hz had little effect on waveforms uncontaminated by noise. In noisy recordings (4 control, 4POAG), the notch filter changed the waveform dramatically to resemble uncontaminated waveforms. In control subjects' uncontaminated mfERGs the RMS of the DC did not differ with or without a notch filter, while IC1 and IC2 differed significantly. In uncontaminated POAG recordings RMS did not differ with or without the notch filter (DC $p=0.1$, IC1 $p=0.3$, IC2 $p=0.3$). POAG differed significantly from controls whether the notch filter was used or not ($p < 0.001$ for all three epochs). When notch filtered, noisy responses of POAG patients lay within 2 SD of good POAG responses, and noisy responses of healthy subjects within 2 SD of uncontaminated responses of healthy subjects.

Conclusions: Bock M et al. (2000) have shown that in the standard mfERG a 50Hz notch filter primarily affects the second but not the first order kernel. In analogy, in the 2-flash mfERG a 50Hz filter affected primarily the induced components. In good POAG recordings, the notch filter did not alter DC, IC1 or IC2 significantly which may point to a component in this range that is reduced in POAG but not control. Importantly, with a notch filter POAG still differed significantly from normal. Thus a 50 Hz notch filter allows grossly contaminated waveforms to be analysed in a meaningful manner, which can be extremely helpful in a clinical setting.

Commercial Relationships: Anja M. Palmowski-Wolfe, None; Margarita G. Todorova, None; Andreas Schötzau, None; Anna A. Ledolter, None

Support: Swiss Government Scholarship for Foreign Students (FCS) 2009.0251; Swiss National Science Foundation (SNSF) 32003B-135219; LHW Stiftung Lichtenstein

Program Number: 802 **Poster Board Number:** A0137

Presentation Time: 1:00 PM - 2:45 PM

Upregulation of TRPV1 Signaling Boosts RGC Excitation Early in a Mouse Model of Glaucoma

Carl Weitlauf, Nicholas J. Ward, Brian J. Carlson, Wendi S. Lambert, David J. Calkins. Vanderbilt Eye Institute, Vanderbilt University Medical Center, Nashville, TN.

Purpose: Sensitivity to elevated intraocular pressure (IOP) is a major risk factor for degeneration of retinal ganglion cells (RGCs) in glaucoma. Rodent RGCs express the transient receptor potential vanilloid-1 (TRPV1) cation channel, which gates a rapid influx of Ca²⁺ with exposure to stress. Here, we used an inducible mouse model of glaucoma to investigate physiologically whether TRPV1 in RGCs could intrinsically counter loss of excitatory activity in RGCs challenged by elevated IOP.

Methods: IOP of month-old C57 mice was elevated 30-40% for 2-15 days via microbead occlusion of the anterior chamber (15 μ m; 1.5 μ L). Retinas from both microbead- and saline-injected (control) eyes were paraffin-embedded for immunohistochemistry or acutely prepared as whole mounts for electrophysiological patch-clamp recording and morphological analysis. Under whole-cell current clamp, spontaneous and evoked spike-firing were measured in RGCs before and after bath application of the specific TRPV1 agonists capsaicin (2 μ M) and N-oleoyldopamine (N-OLDA; 10 μ M). In a subset of experiments, the TRPV1 competitive antagonist iodoresiniferatoxin (I-RTX; 100 nM) was pre-applied before the agonist. 1% Lucifer Yellow was included in the recording solution to label dendritic arbors.

Results: TRPV1 protein expression was increased in the inner plexiform layer following 1 week of microbead injection. Correspondingly, capsaicin significantly enhanced firing rate in RGCs from microbead-injected eyes compared to saline-injected eyes ($p < 0.001$). Pre-application of I-RTX had no effect on baseline firing rate ($p=0.469$) but did block capsaicin-mediated enhancement ($p=0.062$). N-OLDA elicited the same enhancement of firing rate ($p=0.012$) that was blocked by I-RTX ($p=0.512$). RGCs from microbead-injected eyes exhibited no overt changes in overall dendritic complexity in the period studied.

Conclusions: Our results reveal a putative neuroadaptive response to short-term elevations in IOP through TRPV1-mediated enhancement of neural firing in RGCs. These data further implicate TRPV1 Ca²⁺ channels in the intrinsic stress response to elevated pressure in the eye. Our results suggest these changes precede dendritic pruning. A better understanding of how this cascade could promote RGC activity in the face of glaucomatous stressors could reveal a novel therapeutic avenue to counter degeneration.

Commercial Relationships: Carl Weitlauf, None; Nicholas J. Ward, None; Brian J. Carlson, QLT, Inc. (F); Wendi S. Lambert, QLT Inc. (F); David J. Calkins, QLT, Inc (F), Allergan (F), QLT, Inc (C), Allergan (C)

Support: Melza and Theodore Barr and Glaucoma Research Foundations (DJC), AHAF (DJC), NEI Grant (5R01EY017427-03) (DJC), Research to Prevent Blindness Inc., Departmental Unrestricted Grant (DJC), NEI Core Grant (5P30EY008126-19) (DJC) and NEI Training (5T32EY007135-17) (NJW).

203 Fibrosis in Glaucoma: Mechanisms and Therapy - Minisymposium

ARVO 2013 Annual Meeting Abstracts by Scientific Section/Group – Glaucoma

Monday, May 06, 2013 8:30 AM-10:15 AM
6B Minisymposium

Program #/Board # Range: 1229-1235
Organizing Section: Glaucoma
Contributing Section(s): Glaucoma

Program Number: 1229
Presentation Time: 8:30 AM - 8:50 AM
Mechanisms in Fibrosis: Cast a Cold Eye on the Myofibroblast
Boris Hinz. University of Toronto, Toronto, ON, Canada.
Commercial Relationships: **Boris Hinz,** None

Program Number: 1230
Presentation Time: 8:50 AM - 9:04 AM
Conjunctival Fibrosis Following Glaucoma Surgery
Gunther R. Schlunck. Div Experimental Ophthalmology, Univ Eye Hospital Freiburg, Freiburg, Germany.
Commercial Relationships: **Gunther R. Schlunck,** None

Program Number: 1231
Presentation Time: 9:04 AM - 9:18 AM
Trabecular Meshwork Extracellular Matrix Changes in Glaucoma
Abbot F. Clark. Cell Biology & Anatomy, University of North Texas HSC, Fort Worth, TX.
Commercial Relationships: **Abbot F. Clark,** Alcon Research, Ltd. (F)

Program Number: 1232
Presentation Time: 9:18 AM - 9:32 AM
The Role of the Trabecular Meshwork and Growth Factors in Glaucoma
Ernst R. Tamm. Inst of Anatomy, University of Regensburg, Regensburg, Germany.
Commercial Relationships: **Ernst R. Tamm,** None

Program Number: 1233
Presentation Time: 9:32 AM - 9:46 AM
Connective Tissue Changes in the Optic Nerve Head and Peri-Papillary Sclera in Glaucoma
Harry Quigley. Ophthalmology, Johns Hopkins Wilmer Eye Inst, Baltimore, MD.
Commercial Relationships: **Harry Quigley,** Sensimed (C), Genetech (C), Merck (C), Sucampo (C)

Program Number: 1234
Presentation Time: 9:46 AM - 10:00 AM
Role of Lamina Cribrosa Cells in ONH Fibrosis
Deborah M. Wallace. School Med & Medical Science, University College Dublin, Dublin, Ireland.
Commercial Relationships: **Deborah M. Wallace,** None

Program Number: 1235
Presentation Time: 10:00 AM - 10:14 AM
Role of Optic Nerve Astrocytes
Rudolf Fuchshofer. Institute of Human Anatomy and Embryology, University of Regensburg, Regensburg, Germany.
Commercial Relationships: **Rudolf Fuchshofer,** None

241 Imaging I, GL

Monday, May 06, 2013 11:00 AM-12:45 PM
6B Paper Session

Program #/Board # Range: 1706-1712
Organizing Section: Glaucoma

Program Number: 1706
Presentation Time: 11:00 AM - 11:15 AM
Rates of retinal nerve fiber layer thinning in glaucoma suspect eyes

Atsuya Miki¹, Linda M. Zangwill¹, Sonia Jain², Feng He², Naira Khachatryan¹, Naama Hammel¹, Jeffrey M. Liebmann^{3,4}, Christopher A. Girkin⁵, Felipe A. Medeiros¹, Robert N. Weinreb¹.
¹Hamilton Glaucoma Center, Department of Ophthalmology, University of California, San Diego, La Jolla, CA; ²Department of Family and Preventive Medicine, University of California, San Diego, La Jolla, CA; ³Department of Ophthalmology, New York University School of Medicine, New York, NY; ⁴Department of Ophthalmology, Einhorn Clinical Research Center, New York Eye and Ear Infirmary, New York, NY; ⁵Department of Ophthalmology, University of Alabama at Birmingham, Birmingham, AL.
Purpose: To evaluate the relationship between the rates of change in retinal nerve fiber layer thickness (RNFLT) as measured with Spectralis spectral-domain optical coherence tomography (SD-OCT) and the development of visual field defect (convert) in glaucoma suspect eyes.

Methods: Glaucoma suspects, defined as having glaucomatous optic neuropathy based on stereophotograph review or ocular hypertension (OHT; IOP >21 mm Hg) at baseline without a history of repeatable glaucomatous visual field damage from the Diagnostic Innovations in Glaucoma Study, and the African Descent and Glaucoma Evaluation Study were included. Global and sectoral (temporal, superior-temporal, inferior-temporal, nasal, superior-nasal, inferior-nasal, superior, inferior) RNFLT were measured with the Spectralis SD-OCT. Eyes were classified as converts or nonconverts based on the development of repeatable visual field damage. Linear mixed-effects models were used to evaluate rates of change in RNFLT and their relationship with the development of visual field defect.

Results: Five hundred and fifty two eyes of 361 glaucoma suspects were included. 121 subjects (33.5%) were of African Descent (AD) and 240 subjects (66.5%) were of European Descent (ED). 276 eyes (50%) were categorized as OHT at the baseline examination. Mean age \pm SD at baseline was 64.4 \pm 11.6 years. The average number of OCT examinations per eye was 4.1 (range, 2-11). One hundred and two eyes (18.5%) were classified as converts and 450 eyes were classified as non-converts. Median follow-up time was 2.18 years. Rates of change in RNFLT were significantly faster in converts compared to non-converts in global (-1.16 μ m/year vs. -0.69 μ m/year, P=0.007), superior-temporal (-1.37 μ m/year vs. -0.44 μ m/year, P=0.012), superior (-1.03 μ m/year vs. -0.34 μ m/year, P=0.024), and inferior (-1.84 μ m/year vs. -1.19 μ m/year, P=0.027) sectors. No significant difference in the rate of RNFL loss between converts and non-converts was found in the temporal and nasal sectors.

Conclusions: Even with a relatively short follow-up, the rate of RNFL loss measured with SD-OCT was in some sectors, 3 times faster in visual field converts compared to non-converts. Results of this study suggest that measuring the rate of SD-OCT RNFL loss may be a useful tool to help identify patients that develop visual field damage.

Commercial Relationships: **Atsuya Miki,** NIDEK (C); **Linda M. Zangwill,** Carl Zeiss Meditec Inc (F), Heidelberg Engineering GmbH (F), Optovue Inc (F), Topcon Medical Systems Inc (F), Nidek Inc (F); **Sonia Jain,** None; **Feng He,** None; **Naira Khachatryan,** None; **Naama Hammel,** None; **Jeffrey M. Liebmann,** Alcon Laboratories, Inc. (C), Allergan, Inc. (C), Allergan, Inc. (F), Carl Zeiss Meditec, Inc (F), Heidelberg Engineering, GmbH (F), Topcon Medical

Systems, Inc. (F), National Eye Institute (F), New York Glaucoma Research Institute (F), SOLX, Inc. (C), Bausch & Lomb, Inc (C), Diopsys, Inc. (C), Diopsys, Inc. (F), Merz, Inc. (C), Glaukos, Inc. (C), Quark, Inc. (C); **Christopher A. Girkin**, SOLX (F), Heidelberg Engineering (F); **Felipe A. Medeiros**, Carl-Zeiss (F), Heidelberg Engineering (F), Topcon (F), Alcon (F), Allergan (F), Sensimed (F), Reichert (F); **Robert N. Weinreb**, Aerie (F), Alcon (C), Allergan (C), Altheos (C), Amakem (C), Bausch&Lomb (C), Carl Zeiss-Meditec (C), Genentech (F), Haag-Streit (F), Heidelberg Engineering (F), Konan (F), Lumenis (F), National Eye Institute (F), Nidek (F), Optovue (C), Quark (C), Solx (C), Topcon (C)

Support: National Eye Institute grants U10EY14267, EY019869, EY021818, EY022039 and EY08208, EY11008, and EY13959 and Eyesight Foundation of Alabama; Alcon Laboratories Inc.; Allergan Inc.; Pfizer Inc.; Merck Inc.; Santen Inc.; and the Edith C. Blum Research Fund of the New York Glaucoma Research Institute, New York, NY, Supported by an unrestricted grant from Research to Prevent Blindness, New York, New York
Clinical Trial: NCT00221923

Program Number: 1707

Presentation Time: 11:15 AM - 11:30 AM

Parapapillary Autofluorescence and its Correlation with Neurovascular Fundus Anomalies in Primary Open Angle Glaucoma

Alexandre Plouznikoff¹, Paul Harasymowycz^{2, 3}. ¹Faculty of medicine, Laval University, Quebec, QC, Canada; ²Faculty of medicine, University of Montreal, Montreal, QC, Canada; ³Institute of glaucoma, Montreal, QC, Canada.

Purpose: To study the area, polar distribution and intensity of parapapillary autofluorescence (AF), its progression and its correlation with retinal nerve fiber layer (RNFL) thinning and focal arterial narrowing (FAN) in primary open angle glaucoma (POAG).

Methods: Patients with POAG were randomly selected. Those with a condition interfering with the measurement of AF (ex. cataract, keratopathy, haemorrhage, AMD, 4⁺-dioptr ametropia) were excluded, as were patients with an optic neuropathy. AF images and parapapillary RNFL thickness were acquired using a confocal scanning laser ophthalmoscope. The RNFL polar coordinate system was used to locate the AF areas and the FAN, after registering the RNFL with the AF images via vascular markers. AF areas were segmented using automatic region growing with a floating threshold and manually selected seed points. FAN were manually identified.

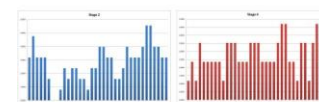
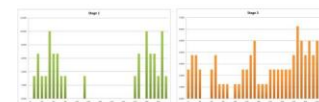
Results: 32 fundi were divided into 4 groups (Jonas' classification). There were no statistically significant differences between the groups in regard to sex, age, ethnicity, maximum IOT, pachymetry and BCVA. The number of AF areas, their size and their polar distribution were strongly correlated with the stage of glaucoma (Spearman, $\rho=0.61$, 0.74 and 0.73 respectively, $p<0.01$). AF areas were almost exclusively located temporally in stage 1; they appeared nasally in later stages and were equally distributed in stage 4 (χ^2 goodness-of-fit test, $p<0.01$). The presence of AF was strongly correlated with borderline RNFL thinning ($p<0.05$) (Spearman, $\rho=0.49$, $p<0.01$). Only 9.7% of AF areas weren't matched to a RNFL anomaly; these areas could precede measurable RNFL thinning. FAN were more often located near AF areas ($\pm 15^\circ$) associated with pathological ($p<0.01$) than with normal RNFL thickness (1 in [4.2;32.3] vs 1 in [21.4; ∞], $p=0.03$). AF minimal intensity was lower when associated with pathological than with normal RNFL thickness (48.9 ± 5.7 vs 58.2 ± 4.3 , 256 shades of gray; Student, $p=0.01$); this could reflect the destruction of the RNFL and its supporting RPE where lipofuscin is stored. AF intensities did not differ statistically significantly between stages.

©2013, Copyright by the Association for Research in Vision and Ophthalmology, Inc., all rights reserved. Go to iovs.org to access the version of record. For permission to reproduce any abstract, contact the ARVO Office at arvo@arvo.org.

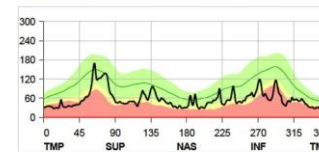
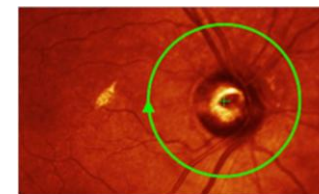
Conclusions: AF correlates with neurovascular fundus anomalies in POAG and could be used to track its progression. A prospective study will determine if AF precedes detectable RNFL destruction; if so, AF could help us act before visual field defects appear.

	Stage 1	Stage 2	Stage 3	Stage 4
Number of fundi	10	13	9	8
Age (years)	[54.83]	[54.89]	[56.84]	[59.89]
Male	20%	38.5%	60.0%	75.0%
Female	80%	61.5%	40.0%	25.0%
Afro-American	10.0%	23.1%	0.0%	25.0%
Caucasian	90.0%	76.9%	100.0%	75.0%
Maximum IOT (mmHg)	[33.28]	[34.61]	[33.29]	[32.52]
Corneal thickness (µm)	[498.573]	[492.585]	[540.574]	[502.584]
Worst BCVA	20/30	20/40	20/40	20/40
Best BCVA	20/20	20/20	20/20	20/20
Phakic	40.0%	23.1%	20.0%	25.0%
Pseudophakic	60.0%	76.9%	80.0%	75.0%
Mean number of AF areas	2.819±0.67	5.69±2.82	9.00±5.55	11.29±10.90
(95% confidence interval)				
Mean AF total area (mm ²)	0.02±0.01	0.12±0.12	0.13±0.10	0.31±0.20
(95% confidence interval)				
Mean AF radial length (°)	17.1±11.2	58.0±29.8	87.6±44.9	143.0±82.2
(95% confidence interval)				
Correl. linear AF presence and RNFL thinning (p)	0.45	0.47	0.45	0.56
(p<0.01)	(p<0.01)	(p<0.01)	(p<0.01)	(p<0.01)
AF areas without matching RNFL thinning (%)	8.3%	10.4%	15.0%	4.2%

Description of the four groups, of the autofluorescence areas and of their correlation with the thinning of the retinal nerve fiber layer



Polar distribution of the autofluorescence areas, for different stages of POAG (stage 1 in green, stage 2 in blue, stage 3 in orange and stage 4 in red; 0 degree is located temporally)



Example of the correlation found between the autofluorescence areas and the thickness of the retinal nerve fiber layer

Commercial Relationships: Alexandre Plouznikoff, None; Paul Harasymowycz, Allergan (C), Alcon (C), Merck (C), SOLX (C), Pfizer (R), Novartis (R), Bausch and Lomb (R), AMO (R)

Support: Fonds de recherche en ophtalmologie de l'Université de Montréal (FROUM)

Program Number: 1708

Presentation Time: 11:30 AM - 11:45 AM

3T Magnetic Resonance Imaging of the Posterior Visual Pathway in Early and Advanced Human Primary Open Angle Glaucoma

Heather R. Connor¹, Sarah L. Hosking^{2, 3}, Jacques-Donald Tournier^{4, 5}, David F. Abbott^{4, 5}. ¹Ophthalmology, University of Melbourne, Melbourne, VIC, Australia; ²Optometry and Vision Sciences, University of Melbourne, Melbourne, VIC, Australia; ³Optometry and Visual Science, City University, London, United Kingdom; ⁴Brain Research Institute, Florey Institute of Neuroscience and

Mental Health, Heidelberg, VIC, Australia; ⁵Medicine, Dentistry and Health Sciences, University of Melbourne, Melbourne, VIC, Australia.

Purpose: To determine the impact of primary open angle glaucoma (POAG) on structures of the posterior visual pathway using 3T Magnetic Resonance Imaging (MRI)

Methods: 57 normal controls (NC: mean age 58 (standard deviation) \pm 12y, range 40 - 82y) and 37 POAG patients (mean age 66 \pm 10y, range 44 - 87y) were included. Patients had repeatable visual field loss (Humphrey 24-2) or optic disc features consistent with the diagnosis of glaucoma. POAG patients were grouped as early (GLE) or advanced (GLA) using the AGIS grading system. MRI (3T Siemens Trio) T1, T2 and diffusion-weighted images were acquired and used to determine retrobulbar optic nerve diameter (ROND), optic radiations volume (ORV), fractional anisotropy (FA) mean diffusion (MD), radial diffusion (RD) (MRTrix software) and grey matter visual cortex volume (VCV: SPM8 software). ANCOVA was used to determine differences between groups using age and gender as covariants (SPSS20).

Results: Mean ROND 15mm behind the globe was significantly thinner in both GLE and GLA groups (NC 2.23mm \pm 0.3; GLE 1.91mm \pm 0.24: p=0.001; GLA 1.68 \pm 0.45: p<0.001). ORV was reduced in GLA (3017.4 mm³ \pm 517.9) compared to both NC (3426.1 mm³ \pm 370.7: p=0.001) and GLE (3306.7 mm³ \pm 301.7: p=0.048). FA was reduced in GLA (0.410 \pm 0.023) compared to NC (0.448 \pm 0.023: p<0.001) and GLE (0.439 \pm 0.021: p<0.01) while RD was increased in GLA (459.34 μ m²/sec \pm 45.72) compared to NC (417.78 μ m²/sec \pm 28.87: p<0.01) and GLE (528.20 μ m²/sec \pm 22.54: p=0.05). There was no difference in VCV between groups.

Conclusions: Advanced glaucoma patients show reduced FA and increased RD in the optic radiations suggesting a loss of axonal integrity associated with glaucoma. ROND was thinner in early and advanced glaucoma patients although ORV was reduced only in the advanced group and there was no difference in VCV between any of the groups suggesting that changes in the posterior visual pathway associated with glaucoma lag anterior change.

Commercial Relationships: Heather R. Connor, None; Sarah L. Hosking, None; Jacques-Donald Tournier, None; David F. Abbott, None

Support: NHMRC Scholarship, VESKI Grant, Brain Imaging Foundation Grant

Program Number: 1709

Presentation Time: 11:45 AM - 12:00 PM

Spectral Domain Optical Coherence Tomography (SDOCT) Optic Nerve Head (ONH) Rim Quantification in Glaucoma and Glaucoma Suspect Eyes Using Anatomic Vs Acquired Image Frame (AIF) Regionalization

Lin He, Ruojin Ren, Christy A. Hardin, Hongli Yang, Stuart K. Gardiner, Brad Fortune, Shaban Demirel, Claude F. Burgoyne. Devers Eye Institute, Legacy Research Institute, Portland, OR.

Purpose: SDOCT can be used to quantify ONH rim parameters. However, the default SDOCT parameterization is based on AIF orientation, which can vary substantially from the axis of a highly influential anatomic relationship: the vertical offset of the fovea relative to the center of the ONH. The latter can be defined reliably as Bruch's membrane opening (BMO) centroid. This study compared neuroretinal rim parameters regionalized according to Fovea-to-BMO axis (FoBMO) versus AIF axis.

Methods: Spectralis SDOCT scans (48, 15° radial B-scans centered on the ONH) were obtained in 190 glaucoma patients and high-risk suspects. Masked technicians delineated the internal limiting membrane (ILM), retinal nerve fiber layer (RNFL) and BMO in half

(24) of the B-scans of each eye. The ONH was regionalized into 12 sectors using the FoBMO axis and the AIF axis (Fig. 1). For each sector, two neuroretinal rim parameters were quantified for both regionalization methods: minimum rim width (MRW) defined as the minimum distance from the BMO to the ILM and minimum rim area (MRA) calculated using MRW and its angle above the BMO plane. For both MRW and MRA, differences between FoBMO and AIF axes were calculated.

Results: Both MRW and MRA were statistically significantly different (Wilcoxon signed-rank test, p<0.05) for 7 of the 12 sectors when FoBMO and AIF regionalizations were compared (Fig. 2). The AIF axis generally tended to result in higher MRW and MRA in Stemp and Tsup sectors and lower MRW and MRA in Tinf and Itemp sectors as compared with FoBMO-based sectors. The largest difference for both MRW and MRA occurred in the Itemp sector where the AIF-based MRW was 12.9 μ m thinner and the MRA was 5397 μ m² smaller than the FoBMO-based rim. For individual eyes, these differences can be as large as 90 μ m for MRW and 40000 μ m² for MRA, corresponding to 36% and 44% of the average values respectively.

Conclusions: Because the angle of declination from the ONH center to the fovea influences axon bundle paths, using a FoBMO axis that is common to nearly all human eyes should reduce between subject variability within normative data bases and improve structure/function relation.

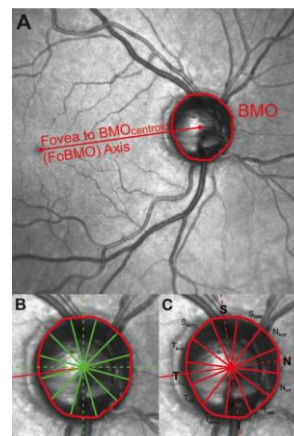


Figure 1. An example of ONH regionalization. (A) A SDOCT IR image of one patient. BMO is marked by the red contour. Another red line connecting BMO centroid with fovea marked the FoBMO axis. (B) 12-sector regionalization of the eye using AIF axis. (C) 12-sector regionalization using the FoBMO axis.

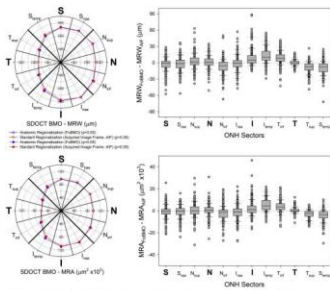


Figure 2. The left polar plots show averaged minimum rim width (MRW) (2A) and minimum rim area (MRA) (2C) from 190 patients which are regionalized into 12 sectors using FoBMO axis vs AIF axis. The blue circles and lines represent anatomical regionalization based on FoBMO axis while the red circles and lines represent acquired image frame regionalization based on AIF axis. The closed symbols show sectors that FoBMO-based MRW and MRA are significantly different from AIF-based MRW and MRA. The box plots on the right show individual eye differences of MRW (2B) and MRA (2D) between FOBMO and AIF regionalization over the 12 sectors. All the differences of MRW and MRA from individual patients are plotted using small filled circles. The lower and upper limits of the box indicate $\pm 1SD$. The horizontal lines inside the box is the median value while the horizontal lines outside the box represent 5%, 25%, 75% and 95% quantiles respectively.

Commercial Relationships: Lin He, None; Ruojin Ren, None; Christy A. Hardin, None; Hongli Yang, None; Stuart K. Gardiner, Allergan (R); Brad Fortune, Heidelberg Engineering, GmbH (F), Carl Zeiss Meditec, Inc (F); Shaban Demirel, Carl Zeiss Meditec (F), Heidelberg Engineering (R), Heidelberg Engineering (F); Claude F. Burgoyne, Heidelberg Engineering (F), Heidelberg Engineering (C)
Support: NIH/NEI R01-EY021281; NIH/NEI R01-EY-019674; The Legacy Good Samaritan Foundation; Sears Medical Trust; Alcon Research Institute

Program Number: 1710

Presentation Time: 12:00 PM - 12:15 PM

Subgrouping of Angle Closure Patients based on Anterior Segment Optical Coherence Tomography Parameters

Tin Aung^{1,2}, Tianxia Gong³, Hwee Kuan Lee³, Shamira Perera¹, Mingguang He⁴, David S. Friedman⁵, Monisha E. Nongpiur^{1,2}

¹Glaucoma, Singapore National Eye Center, Singapore, Singapore;

²Yong Loo Lin School of Medicine, National University of Singapore, Singapore, Singapore; ³Bioinformatics Institute, A*STAR (Agency for Science, Technology and Research), Singapore, Singapore, Singapore; ⁴State Key Laboratory of Ophthalmology, Zhongshan Ophthalmic Center, Sun Yat-sen University, Guangzhou, China; ⁵Wilmer Eye Institute, Dana Center for Preventive Ophthalmology, Johns Hopkins University, Baltimore, MD.

Purpose: To identify subgroups of primary angle closure patients based on anterior segment optical coherence tomography (ASOCT) and biometric parameters.

Methods: We evaluated 315 subjects with primary angle closure, who underwent gonioscopy and ASOCT (Carl Zeiss Meditec, Dublin, CA). Customized software (Zhongshan Angle Assessment Program, Guangzhou, China) was used to measure ASOCT parameters. Agglomerative hierarchical clustering method was first utilized to determine the optimum number of parameters to be included in the determination of subgroups. The best number of subgroups were then determined using the Akaike Information Criterion (AIC) and Gaussian Mixture Model (GMM) method.

Results: The mean age of angle closure subjects was 64.8 years, and 64.4% were female. Using the hierarchical clustering method, the optimal number of parameters was four, namely iris area (IArea),

anterior chamber depth (ACD), anterior chamber width (ACW), and lens vault (LV), each chosen from a different parameter cluster. Using the GMM method, the optimal number of subgroups as given by AIC was three. Subgroup 1 was characterized by a large IArea and a small ACW; subgroup 2 by a large LV and a shallow ACD; while the features in subgroup 3 included elements of both subgroups 1 and 2. The results were replicated in a second independent group of 165 hospital-based subjects with angle closure.

Conclusions: Clustering analysis identified three distinct subgroups of angle closure subjects based on ASOCT and biometric parameters. These findings may be relevant for understanding angle closure pathogenesis and management.

Commercial Relationships: Tin Aung, Alcon (R), Alcon (C), Alcon (F), Allergan (R), Allergan (C), Carl Zeiss Meditec (F), Carl Zeiss Meditec (R), Ellex (F), Ellex (R), Santen (R); Tianxia Gong, None; Hwee Kuan Lee, None; Shamira Perera, Carl Zeiss Meditec (R), Allergan (R), Pfizer (R); Mingguang He, None; David S. Friedman, Alcon (C), Bausch & Lomb (C), Merck (C), QLT, Inc (C), Allergan (C), Nidek (C); Monisha E. Nongpiur, None
Support: BMRC, Singapore

Program Number: 1711

Presentation Time: 12:15 PM - 12:30 PM

In vivo changes to lamina cribrosa pore and optic nerve head geometry in non-human primates with early experimental glaucoma

Kevin M. Ivers¹, Nripun Sredar², Nimesh B. Patel¹, Lakshmi P. Rajagopalan¹, Hope M. Queener¹, Ronald S. Harwerth¹, Jason Porter¹. ¹College of Optometry, University of Houston, Houston, TX; ²Department of Computer Science, University of Houston, Houston, TX.

Purpose: To characterize the time-course of *in vivo* changes in lamina cribrosa pores, optic nerve head (ONH) geometry, and retinal nerve fiber layer thickness (RNFLT) in a monkey model of glaucoma.

Methods: Spectral domain optical coherence tomography (SDOCT) [Spectralis HRA+OCT] radial scans (20° field, 48 B-scans with Enhanced Depth Imaging) and 12° circular scans (to quantify RNFLT) of the ONH were acquired before and every 2 weeks after inducing unilateral experimental glaucoma (EG) in 5 rhesus monkeys. The anterior lamina cribrosa surface (ALCS) and Bruch's membrane opening were manually marked in SDOCT B-scans to determine ALCS depth (ALCSD). High-resolution adaptive optics scanning laser ophthalmoscope (AOSLO) images of the ALCS were acquired. Mean ALCS pore area and elongation were calculated from AOSLO images following 2D to 3D transformation using a thin plate spline surface fit to marked ALCS points.

Results: In EG eyes: (1) mean IOPs were 11.6 ± 2.4 mmHg at baseline, 34.8 ± 10.1 mmHg at Follow-Up 1 (FU1; first change in pore geometry, ALCSD, or RNFLT from baseline), and 39.6 ± 10.1 mmHg at Follow-Up 2 (FU2; most recent time-point), (2) mean ALCSD increased by 133.7 ± 55.3 μ m at FU1 and 222.6 ± 34.5 μ m at FU2, while RNFLT reduced only by an average of 0.4 ± 7.1 μ m at FU1 and 20.8 ± 15.3 μ m at FU2, (3) on average, mean pore area changed by +13.8% from baseline to FU1 and by +0.4% from FU1 to FU2, (4) mean pore elongation changed by -4.6% from baseline to FU1 and by +9.6% from FU1 to FU2. In most EG eyes, pores were larger at FU1 and slightly larger by FU2, whereas pores were more circular by FU1 and more elongated (or elliptical) by FU2. However, there was a reduction in mean area for pores located closer to the ONH center in 3 of 5 EG eyes at FU2. In early EG, increases in ALCSD and mean pore parameters occurred prior to a change in RNFLT in 3 monkeys, an increase in ALCSD occurred before a

change in RNFLT and mean pore parameters in 1 monkey, and simultaneous changes in ALCS, mean pore parameters, and RNFLT occurred in 1 monkey.

Conclusions: A posterior deformation of the ALCS preceded, or was concurrent with, measured axon loss in all early EG eyes. Significant alterations in laminar beams and pores accompanied these early ALCS changes in most EG eyes.

Commercial Relationships: Kevin M. Ivers, None; Nripun Sredar, None; Nimesh B. Patel, None; Lakshmi P. Rajagopalan, None; Hope M. Queener, None; Ronald S. Harwerth, None; Jason Porter, None

Support: NIH Grants R01 EY021783, R01 EY01139, and P30 EY07551

Program Number: 1712

Presentation Time: 12:30 PM - 12:45 PM

Pulse-induced Optic Nerve Head Axial Movement:

Characterization by Phase-sensitive OCT in Humans

Ruikang K. Wang^{1,2}, Lin An¹, Peng Li¹, Murray A. Johnstone².

¹Bioengineering, University of Washington, Seattle, WA;

²Ophthalmology, University of Washington, Seattle, WA.

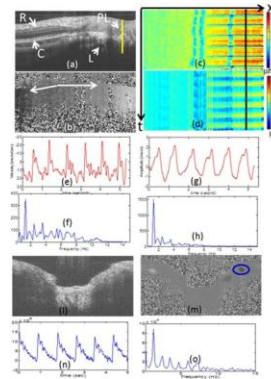
Purpose: To evaluate pulse-induced motion of the human optic nerve head (ONH) using high-speed phase-sensitive spectral domain OCT

Methods: A phase-sensitive OCT system was developed to image the ONH with an imaging speed of 500 kHz A-scan rate. Phase information was extracted from the OCT signals and employed as a sensitive quantitative tool for assessing pulse-induced axial ONH movement. Pulsatile blood flow from the central retinal artery (CRA) was simultaneously imaged permitting correlation with ONH movement. Normal subjects (N=5) participated in the study.

Results: Each subject exhibited pulse-induced ONH axial movement with a mean magnitude of $3.5 \pm 0.8 \mu\text{m}$ and a fundamental frequency of $1.2 \pm 0.2 \text{ Hz}$. ONH movement was 100% negatively correlated with the CRA pulse peak. Figure shows typical results from one subject:

(a) typical structural OCT image encompassing the ONH (temporal-nasal section) and adjacent retina. (b) Corresponding phase-sensitive image. (c) Dynamic ONH velocity map over ~5 sec: the ONH movement exhibits an obvious pulsatile pattern (right side of image). (d) Corresponding displacement map of the ONH, obtained by integrating (c) over the time t. (e) The velocity curve of pulse-induced ONH movement extracted from the position marked by the black line in (c) and the yellow line in (a). Note the y-axis required reversal. (f) Frequency analysis of (e), indicating a fundamental frequency of 1.2 Hz (in this case), and the higher order harmonics (e.g. 2nd and 3rd harmonics) also present. (g) and (h) Corresponding ONH displacement curve (max magnitude = $3.6 \mu\text{m}$) and frequency analysis. (l) and (m) OCT structural image (superior-inferior section) and the corresponding blood flow map, indicating retinal artery measured (circled). (n) and (o) Measured pulsatile blood flow pattern from the CRA (5 sec duration) and the corresponding frequency analysis, indicating 100% correlation with ONH movement.

Conclusions: The high-speed, phase-sensitive OCT system successfully documented pulse-induced axial ONH movement that was 100% negatively correlated with the CRA pulse peak. Characterization of ONH movement permits assessment of mechanical compliance, an important property that may have mechanistic, diagnostic and prognostic significance in management of glaucoma.



Figure

Commercial Relationships: Ruikang K. Wang, National Institutes of Health (F), W.H. Coulter Foundation Translational Research Partnership Program (F), Research to prevent blindness (F), Oregon Health & Science University (P), University of Washington (P); Lin An, None; Peng Li, None; Murray A. Johnstone, Alcon (R), Allergan (R), Allergan (P), Healonics (I), Cascade Ophthalmics (I), Sensimed (R), Ivantis (R), University of Washington (P)

Support: Research to Prevent Blindness Innovative Research Award

252 Lasers; Structure and Function I

Monday, May 06, 2013 11:00 AM-12:45 PM

Exhibit Hall Poster Session

Program #/Board # Range: 1850-1903/B0104-B0157

Organizing Section: Glaucoma

Program Number: 1850 **Poster Board Number:** B0104

Presentation Time: 11:00 AM - 12:45 PM

Narrower Angles Are Associated with Greater Angle Opening After Laser Peripheral Iridotomy

Roland Y. Lee¹, Toshimitsu Kasuga^{1,2}, Qi N. Cui¹, Shan C. Lin¹.

¹Ophthalmology, University of California, San Francisco, San Francisco, CA; ²Ophthalmology, Juntendo University School of Medicine, Tokyo, Japan.

Purpose: To evaluate the association between baseline and laser peripheral iridotomy (LPI) induced opening of anterior chamber angle width.

Methods: Anterior segment optical coherence tomography images captured before and after LPI were analyzed to determine the angle opening distance at $250 \mu\text{m}$ (AOD250), $500 \mu\text{m}$ (AOD500), $750 \mu\text{m}$ (AOD750) from the scleral spur, trabecular-iris space area at $500 \mu\text{m}$ (TISA500) and $750 \mu\text{m}$ (TISA750) from the scleral spur, and angle recess area at $750 \mu\text{m}$ (ARA750) from the scleral spur. Differences in preoperative and postoperative measurements for anterior chamber angle width parameters were compared by paired Student's t-tests. Linear mixed-effects regression models, adjusted for age, sex, preoperative pupil diameter, preoperative central corneal thickness, preoperative anterior corneal curvature, preoperative posterior corneal curvature, and the use of both eyes in the same subject, were used to examine the association between baseline and LPI induced opening of anterior chamber angle width parameters.

Results: Eighty-four eyes of 52 primary angle closure suspects were included in the analysis. AOD250, AOD500, AOD750, TISA500, TISA750, and ARA750 significantly increased following LPI (all $P < 0.0001$). Lower baseline measurements were significantly associated with greater postoperative opening in all anterior chamber angle width parameters (all $P < 0.005$).

Conclusions: Our results showed opening of the anterior chamber angle width after LPI and demonstrated an inverse association between baseline and LPI-induced opening of the anterior chamber angle width, specifically showing that eyes with a more crowded anterior chamber angle undergoing LPI were correlated with a greater magnitude of increase in anterior chamber angle width after the procedure.

Commercial Relationships: Roland Y. Lee, None; Toshimitsu Kasuga, None; Qi N. Cui, None; Shan C. Lin, None

Support: This study was supported by NIH-NEI EY002162 - Core Grant for Vision Research, Research to Prevent Blindness, and That Man May See, Inc.

Program Number: 1851 **Poster Board Number:** B0105

Presentation Time: 11:00 AM - 12:45 PM

Comparison of fluctuations of intraocular pressure before and after selective laser trabeculoplasty in normal tension glaucoma
Naoki Tojo, Keiichi Mitarai, Miyako Oka, Akio Miyakoshi, Atsushi Hayashi. Dept of Ophthalmology and Visual Science, Toyama University Sch of Med, Toyama, Japan.

Purpose: SENSIMED Triggerfish® can measure continuous 24 hours' intraocular pressure (IOP) with a contact lens sensor. We evaluated fluctuations of IOP before and after selective laser trabeculoplasty (SLT) in normal tension glaucoma (NTG) patients
Methods: 10 NTG patients were enrolled in this study (2 males and 8 females). The mean age of patients were 68.8±7.2 years old. All patients were treated with more than two glaucoma eye drops. All patients underwent SLT in 360 degrees. Changes in IOP were monitored with Triggerfish for 24 hours. We compared fluctuations of IOP before and 2 months after SLT with the range and mean deviations of IOP. Corneal thickness and curvature were obtained by anterior segment optical coherence tomography before and after 24-hour IOP measurement

Results: The mean IOP was 13.0±2.7mmHg before SLT and decreased to 11.2±1.9 mmHg after 2 months of SLT (p=0.0098). The range of fluctuation of IOP was 490±103.2mVeq before SLT and 441.7±95.7mVeq after SLT (p=0.77). The mean deviation before SLT was 96.7±32.4mVeq and that after SLT was 109.6±40.7mVeq (p=0.625). Steeper meridian significantly decreased (p=0.0156) after wearing a contact lens of Triggerfish, while flatter meridian showed no significant difference (p=0.453). Corneal thickness showed no significant difference after wearing a contact lens.

Conclusions: SLT significantly decreased IOP, but it did not affect fluctuations of IOP in NTG patients. This is the first study to show changes in fluctuations of continuous IOP for 24hours before and after SLT in NTG patients.

Commercial Relationships: Naoki Tojo, None; Keiichi Mitarai, None; Miyako Oka, None; Akio Miyakoshi, None; Atsushi Hayashi, None

Program Number: 1852 **Poster Board Number:** B0106

Presentation Time: 11:00 AM - 12:45 PM

Diode Cyclophotocoagulation for the Treatment of Refractory Childhood Glaucomas

Lekha Ravindraraj, Sumana S. Kommana, Robert D. Fechtner, Albert S. Khouri. Ophthalmology & Visual Science, University of Medicine & Dentistry of NJ-NJ Medical School, Newark, NJ.

Purpose: To study the efficacy of diode cyclophotocoagulation (CPC) in the treatment of refractory childhood glaucomas.

Methods: A review of records of children with primary congenital glaucoma (PCG) or secondary glaucomas who presented over a 15 year period was conducted. Inclusion: Confirmed diagnosis of childhood glaucomas refractory to other treatments that required CPC

for IOP control. Exclusion: Lack of follow-up (<6 months), treatment not inclusive of CPC. Data on intraocular pressure (IOP), number of glaucoma medications at baseline, 1 year and 2 years after CPC, and laser settings [number/degree of treatment applications, time, & power (mW)] were collected. Means, SD, T-tests, and percent reductions in IOP were calculated.

Results: Of 61 patients (yielding 101 eyes) with childhood glaucomas, a total of 14 patients (7 with PCG and 7 with secondary causes of glaucoma) with 17 eyes (8 PCG and 9 secondary) received 35 CPC's (15 for PCG & 20 for secondary glaucomas). Extent of treatment was: 59% in 3 quadrants, 25% in 4 quadrants, & 16% in 2 quadrants. Mean laser parameters were: count of 22.4 (SD 4.5), power at 1393 mW (SD 346.7), time of 3154 seconds (SD 980.9). Six of the 17 eyes had a previous glaucoma procedure before being treated by CPC. Fifty-three percent (9 of 17 eyes) received CPC only once, while 47% required >1 treatment (with 2, 4, and 2 eyes receiving 2, 3, and >3 CPC's, respectively). There was a significant reduction in IOP (mmHg) from 39.2 at baseline (n=33), to 25.4 (n=22, p<0.001) at 1 year and 29.2 (n=14, p<0.01) at 2 years of follow-up. There was no significant reduction in the number of glaucoma medications (p>0.05) (1.9 at baseline to 2.1 at 1 year and 2.0 at 2 years). Percent IOP reductions at 1 and 2 years are included in Table 1.

Conclusions: CPC significantly reduced IOP in refractory childhood glaucomas. The majority of eyes achieved IOP reductions >20% at 1 and 2 years, however the effect was more robust at 1 year vs 2 years. Multiple CPCs were required in 47% of eyes. Long term follow-up is needed to better characterize CPC efficacy and its potential as an adjunct in the treatment of refractory childhood glaucomas.

	1 Year (n=22)		2 Year (n=14)
>30% Reduction	11	>30% Reduction	5
>20% Reduction	14	>20% Reduction	7
>15% Reduction	18	>15% Reduction	9
>0% Reduction	19	>0% Reduction	12
Mean % Reduction	30.2	Mean % Reduction	24.6

Table 1. Percent reduction in IOP at 1 and 2 years after CPC

Commercial Relationships: Lekha Ravindraraj, None; Sumana S. Kommana, None; Robert D. Fechtner, None; Albert S. Khouri, None

Support: Research to Prevent Blindness, NY, NY

Program Number: 1853 **Poster Board Number:** B0107

Presentation Time: 11:00 AM - 12:45 PM

Change in Intraocular Pressure and Angle of Eyes with Primary Angle Closure Suspects One Year after Laser Peripheral Iridotomy

Dapeng Mou. Beijing Tongren hospital, Beijing, China.

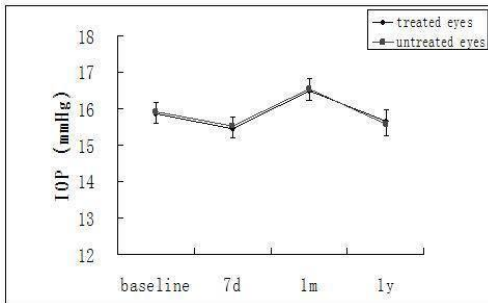
Purpose: To report the change in intraocular pressure (IOP), and anterior chamber angle following laser peripheral iridotomy (LPI) in primary angle closure suspects

Methods: 134 bilateral PACS (non-visibility of the posterior trabecular meshwork for ≥ 180 degrees on gonioscopy) aged 40 years or more diagnosed as bilateral PACS at HandanEye Hospital, China were randomly assigned to undergo LPI in one eye. Gonioscopy and Goldmann applanation tonometry were performed prior to, on day 7 and 12 months post LPI.

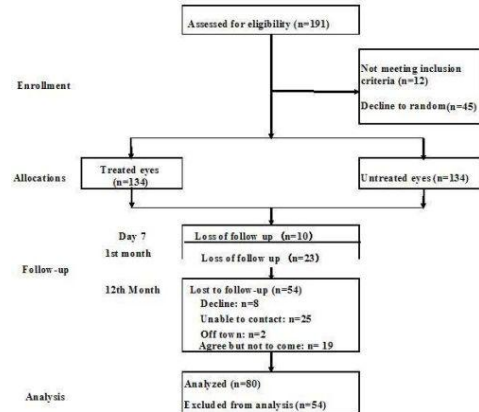
Results: 80 of 134 patients (59.7%) could be followed up at one year. The mean IOP in the treated eyes was 15.9±2.7 mmHg at baseline, 15.4±3.0 mmHg

on day 7; 16.5±2.9 mmHg at one month and 15.5±2.9 mmHg at 12 months; the IOP was very similar to the untreated eyes (p>0.834). One or more quadrants of the angle opened in 93.7% of the LPI treated eyes but 67.0% (53/79) remained closed in two or more quadrants.

Conclusions: Following LPI the IOP was similar in treated and untreated eyes. Two thirds of the treated eyes continued to have non-visibility of the trabecular meshwork over 180 degrees. Further research is needed to determine the full implications of residual closure as well as the need for follow up and treatment in PACS.



Intraocular Pressure (IOP) Changes of Before and After Laser Peripheral Iridotomy in The Treated eye and Fellow Untreated Eye



Flow Chart of Participants in the Trial

Commercial Relationships: Dapeng Mou, None

Support: National "Eleventh Five-Year" Science and Technology Program. The Ministry of Science and Technology of the P.R.C. Grant No. 2007BAI18B08.

Clinical Trial: ChiCTR-TCH-100000820

Program Number: 1854 **Poster Board Number:** B0108

Presentation Time: 11:00 AM - 12:45 PM

The influence of treatment settings for SLT and ALT in the management of open angle glaucoma (OAG): a systematic review and meta-analysis

Sourabh Arora, Karim F. Damji, Ezekiel Weis. University of Alberta, Edmonton, AB, Canada.

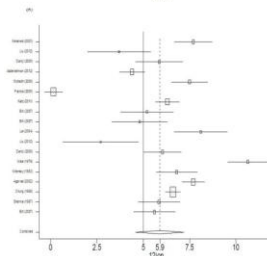
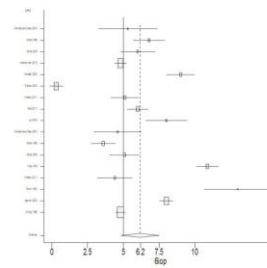
Purpose: To study the relationship between various treatment settings for selective laser (SLT) and argon laser (ALT) trabeculoplasty in the management of OAG

Methods: A comprehensive literature search was performed of MEDLINE and Embase using the PRISMA guidelines. Prospective clinical studies published in English were eligible if they investigated SLT or ALT and reported mean IOP reduction at 6 or 12 months.

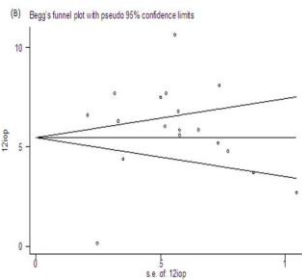
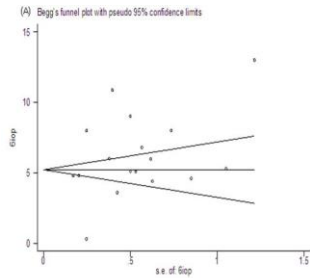
Results: There were 13 eligible studies each for the analysis of SLT and ALT (1,328 cases). The mean power settings reported were 0.79 (0.2 - 1.7) mJ for SLT and 725 (400 - 1500) mW for ALT. Majority of studies reported treatment that was 180 (18/29 study groups) or 360 degrees (8/29 study groups). The summary meta-analysis using a random effects model for both SLT and ALT revealed an IOP reduction at 6 months of 6.16 mm Hg (CI 4.83-7.49, 1,044 cases) and at 12 months of 5.89 mm Hg (CI 4.57-7.20, 1,122 cases). The meta-regression revealed no difference in ALT vs. SLT at 6 months (P=0.459) and 12 months (P=0.262). There was no evidence of publication bias. Meta-regression revealed an association between ALT's minimum power (P < 0.001, P=0.046), maximum power (P < 0.001, P=0.046), and number of spots (P < 0.001, P=0.025) at 6 and 12 months respectively. There was no association with bubbling/blanching level versus IOP at 12 (P=0.931) months for ALT.

SLT pressure reduction is significantly improved (P = 0.001) at 12 months by 2.25 mm Hg if used to a level of occasional or micro bubbling, as opposed to bubbling with every single spot. For SLT, there was no difference in 12 month IOP based on the minimum energy (P=0.127), maximum energy (P=0.863), number of spots (P=0.549), or degrees treated (P=0.451).

Conclusions: Increases in the power settings, number of spots, and degrees treated using ALT resulted in larger IOP reduction at 6 and 12 months. There was no association of IOP reduction with the visual endpoint for treatment with ALT; however with SLT IOP reduction is significantly improved at 12 months if used to a point of occasional or micro bubbling. SLT efficacy does not appear to be influenced by the range of power settings previously reported, or whether treatment is 180 versus 360 degrees.



Meta-analysis of combined SLT and ALT IOP reduction at (A) 6 months and (B) 12 months.



Begg's funnel plot for data reported at (A) 6 months and (B) 12 months.

Commercial Relationships: Sourabh Arora, None; Karim F. Damji, None; Ezekiel Weis, None

Program Number: 1855 **Poster Board Number:** B0109

Presentation Time: 11:00 AM - 12:45 PM

Intraocular Pressure Spikes following Sequential Laser Peripheral Iridotomy for Angle Closure

Jamie Ng^{1,2}, Tian Loon Lee¹, Monisha E. Nongpiur^{1,3}, Wai-Jia Tan², Tin Aung^{1,2}, Shamira Perera¹. ¹Singapore National Eye Centre and Singapore Eye Research Institute, Singapore, Singapore; ²National University Health Systems, Singapore, Singapore; ³Yong Loo Lin School of Medicine, National University of Singapore, Singapore, Singapore.

Purpose: To determine the incidence of intraocular pressure (IOP) spikes within the first 30 minutes after sequential argon-Nd:YAG laser peripheral iridotomy (LPI) in patients with angle closure and to explore risk factors for their occurrence.

Methods: 428 consecutive eyes of 298 patients who had undergone LPI at the Singapore National Eye Centre (SNEC) between June 2011 and August 2011 were reviewed retrospectively. There were 238 primary angle closure suspect (PACS) eyes, 85 primary angle closure (PAC) eyes, 92 primary angle closure glaucoma (PACG) eyes and 13 acute primary angle closure (APAC) eyes. The pre and post-LPI IOP, gonioscopic findings, medications, laser parameters and the need for acute IOP-lowering treatment were recorded.

Results: The proportion of patients with a post-LPI IOP elevation \geq 8mmHg was 10.7% (n=46) and those with a significant IOP spike of \geq 30mmHg was 31 (7.2%). There were no significant differences between those with or without a post-LPI IOP elevation \geq 8mmHg and those with or without a post-LPI IOP of \geq 30mmHg, in terms of age, gender, race, total laser energy utilised and seniority of the physician performing the procedure. Patients who experienced IOP spike \geq 8mmHg were on fewer pre-LPI medications (p=0.009). On logistic regression, patients with APAC had a significantly higher probability of an IOP spike (p=0.003).

Conclusions: There was a low incidence of post-LPI IOP spikes after sequential LPI. The primary diagnosis of APAC was a risk factor, and using pre-procedure ocular hypotensives can potentially reduce their occurrence.

©2013, Copyright by the Association for Research in Vision and Ophthalmology, Inc., all rights reserved. Go to iovs.org to access the version of record. For permission to reproduce any abstract, contact the ARVO Office at arvo@arvo.org.

Commercial Relationships: Jamie Ng, None; Tian Loon Lee, None; Monisha E. Nongpiur, None; Wai-Jia Tan, None; Tin Aung, Alcon (R), Alcon (C), Alcon (F), Allergan (R), Allergan (C), Carl Zeiss Meditec (F), Carl Zeiss Meditec (R), Ellex (F), Ellex (R), Santen (R); Shamira Perera, Carl Zeiss Meditec (R), Allergan (R), Pfizer (R)

Program Number: 1856 **Poster Board Number:** B0110

Presentation Time: 11:00 AM - 12:45 PM

Predictors of Short-Term Intraocular Pressure Response to Selective Laser Trabeculoplasty in Afro-Caribbeans with Glaucoma

Tony Realini. Ophthalmology, WVU Eye Institute, Morgantown, WV.

Purpose: To identify predictors of short-term intraocular pressure (IOP) reduction following selective laser trabeculoplasty (SLT) in Afro-Caribbean eyes with primary open-angle glaucoma (POAG).

Methods: In a prospective cohort study, sixty-one St. Lucians of African descent with POAG underwent without of IOP-lowering drugs followed by bilateral 360 degree SLT. Subjects were re-examined 1 hour, 1 week, 1 month after SLT and then every three months thereafter. IOP was measured by a single examiner using a Perkins tonometer. Short-term IOP response to SLT was defined as the average of IOP readings at months 1 and 3. Putative predictors of this outcome variable included age, gender, prior IOP-lowering medication use (prostaglandin analogues versus all others), baseline IOP, central corneal thickness, cup-disc ratio, and total laser power applied to the eye. A linear regression model was built by first assessing each putative predictor in univariate analysis; those with p<0.1 were included in the multivariate analysis. Right eyes were analyzed primarily; results were confirmed in left eyes.

Results: Mean IOP in 61 right eyes dropped from 21.4 mmHg before SLT to 13.5 mmHg and 14.0 mmHg at 1 and 3 months post-treatment. Univariate predictors of IOP response (p<0.1) included baseline IOP and age. In a multivariate model, both baseline IOP (beta=0.444, p<0.0001) and age (beta=0.0754, p=0.0341) were significant; the model explained less than a third of the total variance (r-squared = 0.32). Results in left eyes were identical.

Conclusions: Baseline IOP and age are significant predictors of IOP response to SLT in Afro-Caribbeans with POAG, although together they account for only a small proportion of the variability in IOP response.

Commercial Relationships: Tony Realini, Lumenis (F), Alcon (C)

Support: American Glaucoma Society Mid-Career Clinician Scientist Grant

Program Number: 1857 **Poster Board Number:** B0111

Presentation Time: 11:00 AM - 12:45 PM

Longitudinal evaluation of selective laser trabeculoplasty repeatability in eyes with pseudoexfoliation glaucoma

Ernesto D. Golez¹, Mark A. Latina^{2,1}. ¹Ophthalmology, Massachusetts Eye and Ear Infirmary, Reading, MA; ²Tufts University School of Medicine, Boston, MA.

Purpose: To examine the repeatability of SLT in patients with pseudoexfoliation glaucoma

Methods: Retrospective, chart review of pseudoexfoliation glaucoma (PXF) patients who underwent initial and/or repeat SLT between January 2001 and March 2012 was performed. Patients with history of prior incisional or laser procedure in the eye were excluded. IOPs, percent IOP reduction and number of glaucoma medications were compared before and after the first and the subsequent laser treatments. The number of laser spots per SLT, and duration of SLT efficacy were documented. If no subsequent laser treatment was

performed, it was noted whether the eye had been controlled medically or undergone surgery.

Results: A total of 79 eyes of 56 patients were included; 24 were males and 32 were females. Of the 79 eyes which underwent SLT #1, 21 (27%) underwent SLT #2 and 5 (6.3%) underwent a SLT #3. Of the remaining eyes after SLT #1, 54% (43/79) had their IOP controlled without additional SLT while 19% (15/79) underwent surgery. Of the remaining eyes after SLT #2, 52% (11/21) had their IOP controlled without additional SLT while 21% (5/21) underwent surgery. After SLT #3, 40% (2/5) of eyes had their IOP controlled without further treatment while 60% (3/5) underwent surgery. The mean laser spots performed was not statistically different for every laser session (SLT #1 63.6±12, SLT #2 60.2±10, and SLT #3 53.8±8). The duration between SLT treatments was a mean of 29±24 months between SLT #1 and #2 and mean of 17±11 months between SLT #2 and #3. Percent IOP reduction after SLT #1 was 39%±18, after SLT #2 was 33%±14 and after SLT #3 was 36%±19. In all 3 procedures, the percent reduction was statistically significant. There was no significant change in the mean number of medications pre and post SLT #1 (from 1.91 to 2.05, p=0.12) and SLT #3 (from 2.00 to 2.20, p=0.37); however the mean number of medications significantly increased pre and post SLT #2 (from 2.19 to 2.67, p<0.05).

Conclusions: SLT was effective in reducing IOP in both initial and repeat treatments in PXFG eyes. The percentage of eyes maintaining IOP control without additional SLT (~50%) and those requiring surgery (~20%) were similar after SLT #1 and #2. Although a small group of patients, 60% of eyes required surgery after SLT #3.

Commercial Relationships: Ernesto D. Golez, None; Mark A. Latina, Lumenis (P), Lumenis (C), Lumenis (F), IOP Inc (C)

Program Number: 1858 **Poster Board Number:** B0112

Presentation Time: 11:00 AM - 12:45 PM

Predictors of Failure with Transscleral Diode Laser Cyclophotocoagulation in the Treatment of Refractory Glaucoma
Samantha Dewundara, Bret A. Hughes, Rominder Momi, Justin Tannir, Chaesik Kim. Department of Ophthalmology, Kresge Eye Institute, Detroit, MI.

Purpose: This study was conducted to evaluate prognostic indicators for failure with transscleral diode laser cyclophotocoagulation (TSDLCP) in the treatment of refractory glaucoma

Methods: This retrospective study analyzed 100 eyes in 100 patients with glaucoma refractory to conventional medical and/or surgical management and subsequently treated with TSDLCP. Failure in treatment was defined as intraocular pressure (IOP) measured < 5 or >22 mmHg, increase in number of antiglaucoma medications and need for additional diode or incisional surgery. Prognostic variables analyzed include patient age, sex, race, diagnosis of diabetes, diagnosis or hypertension, type of glaucoma, number of pre-laser IOP lowering medications used and pre-laser IOP. Data were analyzed using Cox regression and Kaplan-Meier Survival analysis.

Results: Mean patient age was 63±17 years (range 24-89 years). Fifty males and fifty females were studied. With respect to race, 71 African-Americans, 19 Caucasians and 10 other races were studied. Patients had chronic open-angle glaucoma (n=43), chronic angle-closure glaucoma (n=25), neovascular glaucoma (n=22) and other forms of glaucoma (n=10). Forty patients were diagnosed with diabetes mellitus and 72 with hypertension. Average pre-laser IOP was 37 ±12 mmHg. Mean follow up was 12 ± 10 months. Patients received 20 ± 6 laser applications per session, each application lasting 2 seconds in duration, ranging from 180-360 degrees. Total laser energy delivered per eye was 38 ±14 Watts. A success of 45% was noted at mean follow up of 12 months using Kaplan -Meier survival analysis, with a mean post-treatment IOP of 22 ±12mmHg at

12 months (P<0.05). Age, sex, race, diabetes, hypertension, type of glaucoma, number of pre-laser IOP lowering medications used and pre-laser IOP were not prognostic indicators of treatment failure (COX regression analysis, P>0.05).

Conclusions: With significant reductions in IOP, TSDLCP is a safe and effective alternate treatment for refractory glaucoma. Age, sex, race, diabetes, hypertension, type of glaucoma, number of pre-laser IOP lowering medications used and pre-laser IOP do not appear to impact success of treatment.

Commercial Relationships: Samantha Dewundara, None; Bret A. Hughes, None; Rominder Momi, None; Justin Tannir, None; Chaesik Kim, None

Program Number: 1859 **Poster Board Number:** B0113

Presentation Time: 11:00 AM - 12:45 PM

The Relationships between Immediate and Short-term Intraocular Pressure (IOP) Following Selective Laser Trabeculoplasty (SLT), Trabecular Meshwork Pigmentation (TMP), and Laser Power Used

Yotam Weiner¹, Asher Weiner². ¹University of Michigan, Ann-Arbor, MI; ²Ophthalmic Consultants of the Capital Region, Albany, NY.

Purpose: To study the relationships between immediate and early post-SLT IOP, TMP and laser power used.

Methods: A retrospective interventional non-randomized comparative chart review. Main outcome measures were 1-hour IOP elevations and 8-week post-SLT IOP, and their relations to TMP and laser power used. Eyes with primary open angle or normal-tension glaucoma, and ocular hypertension were included. Eyes with pigment dispersion were excluded.

Results: We identified 189 eyes of 189 patients with no previous trabeculoplasty in either eye. Age was 72±12 (mean±SD, range: 28-97) years. Central corneal thickness was 552.4±39.41 (range: 460-669) micron. TMP was 1.3±0.7 (range: 0-4), and SLT power used was 0.82±0.13 (range: 0.5-1.2) mJ. Mean pre-SLT IOP was 18.7±4.7 (range: 11-37) mmHg, reduced to 14.7±3.7 (range: 8-26) mmHg at 8 weeks (p<0.0001). The latter IOP was directly correlated with pre-SLT IOP (p<0.0001, r²=0.389). Neither TMP nor power used alone were correlated with 8-week IOP reduction (%), but the latter was directly correlated with pre-SLT IOP (p<0.0001, r²=0.096), and inversely correlated with TMP/power ratio (p=0.012, r²=0.037). Multiple regression analysis also showed the significant correlation between IOP reduction at 8 weeks, and both pre-SLT IOP (p<0.0001, r²=0.0012) and TMP/power ratio (p=0.0192, r²=0.0012). IOP 1 hour post SLT and Brimonidine 0.1% treatment was 14.5±4.2, (range: 4-30) mmHg. It was significantly lower than pre-SLT IOP (p<0.0001), and directly correlated with it (p<0.0001, r²=0.1749). IOP elevations of >5 mmHg at 1 hour occurred in 4 (2.1%) eyes despite Brimonidine 0.1% treatment. In all 4 eyes, the power used was >0.8 mJ, TMP was <2, and the TMP/power ratio was ≤1.5.

Conclusions: The TMP/power ratio was inversely correlated with SLT efficacy at 8 weeks, that is, we found higher efficacy with higher powers used for a given TMP. Acute IOP elevations were more common with higher powers used, lower TMP, and a lower TMP/power ratio, suggesting that the power used and not the degree of trabecular pigmentation was related to acute IOP elevations. These results may contrast previously published treatment parameters recommendations, and our findings may not apply to eyes with pigment dispersion as these were excluded from our study.

Commercial Relationships: Yotam Weiner, None; Asher Weiner, None

Program Number: 1860 **Poster Board Number:** B0114

Presentation Time: 11:00 AM - 12:45 PM

Aqueous production reduction and aqueous outflow increase in rabbit eyes after ultrasonic cyclocoagulation

Aurelie Begle¹, Florent Aptel², Cyril Lafon³, Jean-Yves Chapelon³, Fabrice Romano¹. ¹EYETECHCARE, Rillieux la Pape, France; ²CHU de Grenoble - Hôpital A. Michallon- Service d'ophtalmologie, Grenoble, France; ³research, U1032 - LabTAU- INSERM, Lyon, France.

Purpose: To study the mechanisms of action of an ultrasonic cyclocoagulation treatment on the reduction of intraocular pressure in rabbit eyes

Methods: Nine eyes of 9 rabbits were insonified with a ring-shaped probe containing 6 miniaturized high-intensity focused ultrasound transducers operating at 21 MHz. The acoustic power was set at 2.45 W, and the exposure duration at 6 sec per transducer. The rabbits were followed for up to 22 days, with regular IOP measurement and ophthalmic examinations (day 0 before treatment, 5, 10 and 21 days after) and then sacrificed to perform histological examinations of the treated eyes (light microscopy, scanning electron microscopy, scanning electronic microscopy after intravascular injection of methacrylate resin)

Results: IOP was reduced from a mean preoperative value of 10.4 ± 1.5 mmHg before treatment to a mean postoperative value of 6.8 ± 1.4 mmHg, 7.2 ± 2mmHg and 7.1 ± 1.7mmHg respectively at 5, 10 and 22 days. No macroscopic abnormalities were found.

In the affected regions, the distal and intermediate parts of the ciliary processes showed acute inflammatory and necrotic changes ranging from stromal edema and vascular congestion. The bi-layered epithelium was degenerated or necrotic and sloughed off in the distal parts of the most affected areas, resulting in decrease of aqueous humor production. Histological examinations performed several weeks after the treatment showed involution of the ciliary processes, with short or absent ciliary processes covered by a non bi-layered epithelium and composed of dysmorphic and probably nonfunctional cells. Light microscopy and scanning electron microscopy of vascular corrosion cast performed after intravascular injection of methacrylate resin shows focal interruption of the ciliary body microvasculature with dimensions comparable to those of lesions observed with light or scanning electron microscopy.

In most animals treated, a fluid space could be seen between the sclera and the ciliary body and between the sclera and the choroid adjacent to treated areas. This aspect therefore likely corresponds to an area where the opening of the space should lead to an increase of the aqueous outflow via the uveoscleral pathway.

Conclusions: Ultrasonic cyclocoagulation using high-intensity focused ultrasound results in dual effect on the dynamics of aqueous humor contributing both to lower IOP.

Commercial Relationships: Aurelie Begle, EYETECHCARE (E); Florent Aptel, EyeTechCare (C); Cyril Lafon, Eye Tech Care (C), Eye Tech Care (P), Eye Tech Care (F); Jean-Yves Chapelon, EyeTakeCare (P), EyeTakeCare (C); Fabrice Romano, Eye Tech Care (I), Eye Tech Care (E), Eye Tech Care (P)

Program Number: 1861 **Poster Board Number:** B0115

Presentation Time: 11:00 AM - 12:45 PM

Comparison of argon laser trabeculoplasty and selective laser trabeculoplasty: a meta-analysis

Audrey M. Paulo¹, Lalatiana H. Razafindrabe², Marie-Josée Fredette^{1,2}. ¹Department of Ophthalmology, Faculty of Medicine, Université Laval, Quebec, QC, Canada; ²CUO (Centre universitaire d'ophtalmologie) / CEVQ (Centre d'excellence sur le vieillissement de Quebec), Centre de recherche du CHU de Quebec, Quebec, QC, Canada.

Purpose: Selective laser trabeculoplasty (SLT) is currently used as an alternative to argon laser trabeculoplasty (ALT); despite the reduction of visible thermal damage with SLT, the superiority of either treatment has not yet been clearly established. This meta-analysis aims to determine if there is a significant difference on intraocular pressure lowering between ALT and SLT at different times post-treatment.

Methods: The electronic search was conducted through Embase, PubMed central, and the Cochrane Central Register of Controlled Trials with a predefined search strategy including strict criteria for inclusion and exclusion. No restriction was applied on language or year of publication. Eligible studies were prospective randomized clinical trials comparing the use of ALT and SLT in patients with ocular hypertension or any form of open-angle glaucoma. Effectiveness of intraocular pressure (IOP) lowering at different times post-treatment and post-retreatment were considered. Selection, data collection and assessment of methodological quality of studies were conducted independently by two reviewers in a standardized way. Analyzes were performed using RevMan software 5.1.

Results: Nine studies, involving 761 eyes treated with laser trabeculoplasty (LT), were included in the meta-analysis. In the context of a first LT, a statistically significant difference in favor of ALT was found when comparing the IOP reduction 1 hour after intervention (weighted mean difference (WMD): 1.13 mmHg [0.06; 2.20]; N=266; P=0.04; I²=0%). No significant difference was observed between the 2 treatments at 1 month (P=0.34), 3 months (P=0.46), 6 months (P=0.26), 12 months (P=0.84) and 24 months (P=0.60). In case of a previous LT, a statistically significant difference in favor of SLT was observed 6 months after retreatment (WMD: -2.15 mmHg [-3.49;-0.82]; N=72; P=0.002; I²=30%). In previous 360° LT, a statistically significant difference in favor of SLT was found 12 months after the retreatment (WMD: -1.94 mmHg [-3.18;-0.69]; N=56; P=0.002; I²=0%).

Conclusions: The meta-analysis did not reveal any significant difference between ALT and SLT within 1 to 24 months post-treatment after an initial intervention. Only a significant difference in the very short term (one hour post-treatment) was found in favor of ALT. For re-treatment, SLT seems to be a better choice as it provided significantly lower IOP at 6 and 12 months post-laser.

Commercial Relationships: Audrey M. Paulo, None; Lalatiana H. Razafindrabe, None; Marie-Josée Fredette, None
Support: Université Laval scholarship

Program Number: 1862 **Poster Board Number:** B0116

Presentation Time: 11:00 AM - 12:45 PM

Selective Laser Trabeculoplasty in the Treatment of Glaucoma in Phakic Versus Pseudophakic Patients

Neil Kalbag, Shriji Patel, Albert S. Khouri, Tamara L. Berezina, Robert D. Fechtner, Amir Cohen. The Institute of Ophthalmology and Visual Science, New Jersey Medical School, Newark, NJ.

Purpose: To compare the intraocular pressure lowering effect of selective laser trabeculoplasty (SLT) for treatment of open-angle glaucoma in phakic versus pseudophakic patients

Methods: A retrospective chart review was performed on 106 eyes of 77 patients who had SLT performed by the same surgeon for the treatment of open-angle glaucoma between 2008 and 2012. All patients were followed for a minimum of 30 days. Patients who required additional laser therapy or surgery during the post-procedure follow up were excluded. Pre and post-procedure intraocular pressures (IOP) were recorded along with pre and post-procedure glaucoma medication lists.

Results: The data for 77 phakic and 29 pseudophakic eyes was examined. Baseline intraocular pressures for phakic and

pseudophakic groups were 21.53 ± 6.86 and 19.58 ± 5.32 respectively, and did not significantly vary from each other ($p = 0.170$). The phakic group experienced a 21.3% reduction in IOP at mean follow up time 258 days, resulting in a post-operative IOP of 16.93 ± 6.29 , while the pseudophakic group experienced a 24.0% reduction in IOP at mean time follow up time 220 days, and post operative IOP of 14.89 ± 4.20 for the pseudophakic group. Postoperative IOP did not significantly differ when comparing the two groups ($p = 0.109$). There was no significant change in medication use in either group.

Conclusions: SLT produced similar long-term intraocular pressure reduction in phakic and pseudophakic patients.

Commercial Relationships: Neil Kalbag, None; Shriji Patel, None; Albert S. Khouri, None; Tamara L. Berezina, None; Robert D. Fechtner, None; Amir Cohen, None

Support: Research to Prevent Blindness, Inc., the New Jersey Lions Eye Research Foundation

Program Number: 1863 **Poster Board Number:** B0117

Presentation Time: 11:00 AM - 12:45 PM

Trans-scleral Selective Laser Trabeculoplasty (SLT) Without a Gonioscopy Lens

Michael Belkin¹, Noa Geffen², Shay Ofir², Audrey Kaplan Messas³, Yaniv Barkana⁴, Avner Belkin², Ehud I. Assia². ¹Goldschleger Eye Research Institute, Tel-Aviv University, Tel-Hashomer, Israel; ²Ophthalmology, Meir Medical Center, Kfar Saba, Israel; ³Ophthalmology, Ein Tal Eye Hospital, Tel Aviv, Israel; ⁴Ophthalmology, Assaf Harofe Medical Center, Tzrifin, Israel.

Purpose: To evaluate whether direct application of SLT irradiation to the perilimbal area is effective in reducing Intraocular Pressure (IOP), eliminating the need for gonioscopy during the procedure.

Methods: A randomized, masked, controlled trial was performed on open angle and pseudoexfoliation glaucoma patients. The control group underwent conventional SLT, delivering 100 laser spots through a gonioscope for 360 degrees of the trabecular meshwork(TM). The trial group underwent irradiation by the same laser at the same irradiation parameters, but instead of delivering the energy through a gonioscopy lens, a similar number of applications were administered all around the limbus on the sclera overlying the TM. IOP was measured and side effects evaluated 1, 7, 30, 60 and 180 days after treatment. No changes were made in the medical regimen.

Results: In the trial group (N=11), IOP decrease from an average of 20.90 mmHg before treatment to 15.89 at 2 months and 15.00 at 6 months. The corresponding numbers for the control group (n=10), were 20.50mmHg, 14.71 and 7 (one patient) respectively. There was no statistical difference between the two groups in IOP reduction [$P = 0.863, 1, 0.387, 0.529, 0.918$ for the IOP on recruitment, 1, 7, 30, 60 and 180 days post SLT respectively, Mann Whitney]. Success, defined as >20% IOP reduction, was attained in 7 patients of either group. There was no statistically significant difference between the groups [$P = 0.757$, Fisher]. One patient in each group showed mild transient inflammatory response.

Conclusions: The effectiveness of trans-scleral SLT depends on the laser energy penetrating a few millimeters into tissues to impact the TM. Laser coherency, lost in tissue transmission, is not required. The mechanism of action of the external laser irradiation studied is probably similar to that of the conventional one. It seems that SLT applied directly to the perilimbal sclera is as efficacious as the conventional procedure and that the use of a gonioscopy lens is not necessary. As the long-term IOP reduction of SLT can be discerned within a few days after treatment, it is likely that the new technique will be as effective as the conventional one. If so, the novel method

will simplify and shorten the SLT procedure considerably and eliminate the corneal and gonioscopy-induced side effects.

Commercial Relationships: Michael Belkin, Alcon (C), Ellex (C), PCT: IL2011/000373 Filed 9/5/2011 Published (P); Noa Geffen, None; Shay Ofir, None; Audrey Kaplan Messas, None; Yaniv Barkana, Sensimed (F); Avner Belkin, None; Ehud I. Assia, Hanita Lenses (C), Biotechnology General (C), APX Technology (I), IOptima (I), VisionCare (C)

Clinical Trial: NCT01384149

Program Number: 1864 **Poster Board Number:** B0118

Presentation Time: 11:00 AM - 12:45 PM

Resident-Performed Selective Laser Trabeculoplasty in Open Angle Glaucoma Patients

Eugene Lowry¹, Daniel Greninger^{4,1}, Travis Porco^{1,2}, Ayman Naseri^{1,3}, Robert L. Stamper¹, Ying Han^{1,3}. ¹Ophthalmology, University of California San Francisco, San Francisco, CA; ²Francis I. Proctor Foundation, University of California San Francisco, San Francisco, CA; ³Ophthalmology, San Francisco Veterans Administration Medical Center, San Francisco, CA; ⁴Ophthalmology, Oregon Health and Science University, Oregon, OR.

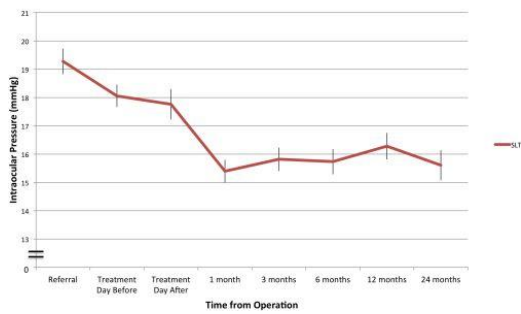
Purpose: To evaluate the efficacy and safety of selective laser trabeculoplasty (SLT) performed by resident ophthalmologists.

Methods: Records of consecutive patients treated with SLT by resident ophthalmologists at the San Francisco Veterans Administration Hospital over a two-year period were reviewed retrospectively. Data including age, indication for treatment, laser settings, pre and postoperative intraocular pressures (IOP), number of eye drop medications, and complications were recorded. Analysis accounted for non-independence of measurements made on eyes in the same patient; change scores were assessed using a clustered Wilcoxon test.

Results: A total of 83 patients underwent 112 SLT operations from November 2009 to December 2011. Average IOP at referral was 19.3. IOP decreased to 18.1 on the day of SLT (p -value 0.024, clustered Wilcoxon signed rank). Mean decrease in postoperative IOP compared to referral was 4.1 (21%) at 3 months and 4.2 (22%) at 24 months. Increased treatment, defined by number of laser shots, was not associated with better IOP control, but was associated with reduced drop requirements ($p = 0.001$, linear regression). There was no significant difference in IOP reduction at 6 months among residents ($p = 0.09$, linear mixed effects regression). There was no significant change in visual acuity 12 months after treatment ($P = 0.54$, clustered Wilcoxon), or with increasing treatment ($P = 0.85$, linear mixed effects regression). Referral IOP was associated with an odds ratio of 1.26 (1.10-1.45), 1.25 (1.11-1.42) and 1.34 (1.16-1.54) for success with each point increase in referral IOP at 3, 6, and 12 months respectively (all p -values <0.01). In a multivariate analysis, referral IOP was the greatest predictor of efficacy, defined as a decrease of IOP > 20%.

Conclusions: We find no evidence that resident performed SLT varies in efficacy or safety among residents or differs from the 20-30% IOP reductions reported in the literature for attending performed SLT. Increasing treatment may lead to less need for topical drops without significant side effects. Patients with higher pre-treatment IOP were most likely to receive benefit from the procedure.

IOP Changes in Patients After Resident Performed SLT



Intraocular pressure at referral, treatment day (before and after treatment) and follow-up appointments. Values are average of all measured patient IOP at each visit time point. Error bars show standard error of the mean for each measurement.

Commercial Relationships: Eugene Lowry, None; Daniel Greninger, None; Travis Porco, NIH NEI (F); Ayman Naseri, Transcend Medical (C); Robert L. Stamper, Transcend (C), Genentech (C); Ying Han, None

Program Number: 1865 **Poster Board Number:** B0119

Presentation Time: 11:00 AM - 12:45 PM

The effect of Selective Laser Trabeculoplasty on IOP changes in the contralateral eye over a two-year followup

Sonia Rana, Justin Tannir, Bret A. Hughes. Kresge Eye Insitute, Detroit, MI.

Purpose: To investigate whether Selective Laser Trabeculoplasty done on one eye affects the IOP of the fellow eye within a two year follow up period.

Methods: A retrospective chart review of patients with Selective Laser

Trabeculoplasty treatment of one eye was performed. Patients were excluded if they had a previous trabeculoplastic, selective or argon, in the treated or fellow eye, additionally patients were excluded if they required additional trabeculoplasty in the followup period, , patients with a history of previous aqueous shunting procedure, uveitic glaucoma, previous trauma, Grade I or Grade 0 angle configuration by Shaffer criteria were excluded.

Results: A total of 22 patient charts were reviewed and analyzed. The time points were divided into pre-treatment (22 patients), 1-3 months (20 patients), 4-9 months (19 patients), 12-15 months (15 patients) and 18-24 months (11 patients). Within the SLT group, there was a statistically significant difference in the pretreatment IOP in compared to the all post-treatment time points. However, the only statistically significant reduction in IOP within the fellow eye group occurred at the first time point of 1-3 months post treatment ($p=.0251$). When comparing the groups, there was a statistically significant difference ($p=.0005$) in the pre-treatment IOP between the treated and untreated eye groups. None of the follow-up time points showed a statistically significant difference between these two groups. During the two year follow-up, 7 of 22 (31.8%) patients had IOP lowering medication changes, 3 of which had an increase in the number of medications and 3 with a decrease; an additional patient had medication restarted and stopped throughout the two year follow-up ultimately leading to a decrease in drops.

Conclusions: The SLT treated eye group showed a statistically significant decrease in IOP at all time points when compared to pretreatment IOP. After SLT, the IOP in the fellow eye showed a statistically significant decrease only in the first 1 to 3 months post

treatment. After this time point, there was no significant difference in IOP between treated and untreated eyes.

Commercial Relationships: Sonia Rana, None; Justin Tannir, None; Bret A. Hughes, None

Program Number: 1866 **Poster Board Number:** B0120

Presentation Time: 11:00 AM - 12:45 PM

Assessment of the Long-Term Outcome of Selective Laser Trabeculoplasty (SLT) in Treatment of Different Glaucoma Types in Patients Receiving Maximum Medicinal Treatment

Eman Elhawy, Camila Zangalli, Daniel M. Shapiro, Lalita Gupta, Michael Hsieh, Abigail Kasprenski, L Jay Katz, George L. Spaeth. Ophthalmology, Wills Eye Institute, Philadelphia, PA.

Purpose: To evaluate efficacy of Selective Laser Trabeculoplasty (SLT) when used as a secondary treatment for glaucoma patients receiving maximum tolerated medicinal therapy

Methods: 88 Glaucoma patients (75 POAG, 6 secondary glaucoma and 7 Normal-Pressure glaucoma) that received three or four medicinal treatments were followed up after treatment with SLT in one, three and five years intervals. Mean IOP was calculated before receiving laser treatments then compared to the IOP measured at 1, 3 and 5 years intervals. A change was defined as a better pressure when more than millimeter drop of IOP was recorded, and as worse when more than one millimeter increase of IOP was recorded. A pressure was referred to as equal when it was the same or changed by one millimeter mercury.

Results: The mean of the baseline IOP for the 88 eyes was 18.35 with a standard deviation of 5.3; the mean IOP 1 year post laser treatment was 16.47 with a standard deviation of 4.87; the mean IOP 3 years post laser treatment was 15.86 with a standard deviation of 6.43; while the mean IOP 5 years post laser treatment was 16.21 with a standard deviation of 6.16.

After 1 year of receiving SLT, 57% (among 83 eyes of patients who reported for follow up) showed a drop in IOP, 17% of patients maintained the same IOP recorded before laser treatment while 27% had higher IOP .

After 3 years of receiving SLT, 48% (among 50 eyes of patients who reported for follow up) showed a drop in IOP, 26% of patients maintained the same IOP recorded before laser treatment while 26% had higher IOP .

At the 5 years follow up visit, 50% (among 14 eyes of patients who reported for follow up) showed a drop in IOP, 29% of patients maintained the same IOP recorded before laser treatment while 21% had higher IOP .

During the follow up 2 eyes required surgery within the first year, an additional five eyes required surgical treatment within the three years following laser, as did an additional five eyes during the five years follow up.

Conclusions: In patients receiving maximal medicinal treatment, SLT showed efficacy in reducing or maintaining IOP for three years.

Commercial Relationships: Eman Elhawy, None; Camila Zangalli, None; Daniel M. Shapiro, None; Lalita Gupta, None; Michael Hsieh, None; Abigail Kasprenski, None; L Jay Katz, Bausch & Lomb (C), Allergan (R), Allergan (C), Allergan (F), Lumenis (R), Lumenis (F); George L. Spaeth, Merck (F), U.S. Patent No. 8,042,946 (P), Pfizer (F)

Program Number: 1867 **Poster Board Number:** B0121

Presentation Time: 11:00 AM - 12:45 PM

Patterned Laser Trabeculoplasty with PASCAL streamline 577

Miho Nozaki, Shuichiro Hirahara, Yuichiro Ogura. Ophthalmology, Nagoya City Univ Med Sch, Nagoya, Japan.

Purpose: Patterned Laser Trabeculoplasty (PLT), the computer-guided laser trabeculoplasty is a newly developed treatment modality using PASCAL® (Topcon Medical Laser Systems, Santa Clara, CA, USA). PLT with PASCAL streamline® (532 nm) has been reported as precise and minimally traumatic treatment, and exhibiting a 24% reduction in intraocular pressure (IOP) (Turati M, et al, Ophthalmic Surg Lasers Imaging, 2010). The purpose of this study is to evaluate the efficacy and safety of the PLT with yellow wavelength PASCAL (PASCAL Streamline 577®) for open-angle glaucoma.

Methods: Eleven eyes of 9 patients with open-angle glaucoma received 577-nm laser treatment with 100-µm spots. Five men and four female (mean age, 65 years) were included and average follow-up period was 6.8 months. Power was titrated for trabecular meshwork blanching at 10 ms and sub-visible treatment was applied with 5-ms pulses. The arc patterns of 66 spots rotated automatically after each laser application so that the new pattern was applied at an untreated position. We evaluated pre- and postoperative IOP, medication score, and laser setting parameter.

Results: Approximately 1,287 laser spots were placed per eye in 16 steps, covering 360° of trabecular meshwork. The IOP significantly decreased from the pretreatment level of 20.5 ± 4.7 to 15.0 ± 2.1 mmHg at one month (p<0.01, t-test) and remained until 6 months (13.4 ± 3.7 mmHg, p<0.05). The IOP reduction rate was 37.2 % at the last examination. There was no significant difference in pre- and postoperative medication score (2.6 and 2.8 respectively). One eye developed transient IOP elevation (9%) after PLT, but there was no eye showed peripheral anterior iris synechia or corneal endothelial damage after PLT.

Conclusions: Our data showed that PLT using 577-nm PASCAL is a safe computer -guided laser treatment, and might be useful to lower the IOP for open-angle glaucoma. A Longer follow-up should be required for future.

Commercial Relationships: Miho Nozaki, None; Shuichiro Hirahara, None; Yuichiro Ogura, None

Program Number: 1868 **Poster Board Number:** B0122

Presentation Time: 11:00 AM - 12:45 PM

Comparison of Selective Laser Trabeculoplasty Outcomes Between Physicians-in-Training and Attending Physicians

Wanda Hu, Simon K. Law, JoAnn A. Giaconi. Jules Stein Eye Institute, Los Angeles, CA.

Purpose: To compare the outcomes of selective laser trabeculoplasty (SLT) performed by ophthalmology residents with those performed by glaucoma attendings in treating open angle glaucoma (OAG).

Methods: This is a retrospective review on patients with OAG (including primary OAG, pseudoexfoliation glaucoma, and pigmentary glaucoma) or OAG suspect who had received SLT performed by second year ophthalmology residents at a Veterans Affairs medical center compared to SLT performed by glaucoma attendings (JAG, SKL) at a tertiary care facility between 1/2008 and 6/2012 with at least 3 months of follow-up. Outcome measures included percent intraocular pressure (IOP) reduction, glaucoma medications, and additional glaucoma medical, laser or surgical therapy.

Results: 43 eyes (43 patients) treated by residents were compared with 68 eyes (68 patients) treated by attendings with mean age of 70.3±11.8 and 69.5±11.8 years, respectively (p=0.742). Attending-treated eyes had a significantly higher proportion of primary SLT compared to resident-treated eyes (25.0% and 2.3%, respectively, p<0.001) and a smaller number of pre-operative glaucoma drops (1.6±1.3, 3.0±1.2, p<0.001) than the resident-treated eyes (Table 1). There were no significant differences between the 2 groups in percent IOP reduction from baseline at all time points after 3 months

(p>0.05). 7.0% of resident-treated eyes and 13.2% of attending-treated eyes experienced an IOP spike (defined as IOP increase > 6 mmHg) within 1 hour of the procedure (p=0.315) (Table 2). There were no significant differences in the rate of additional glaucoma therapy required between attending-treated and resident-treated eyes (36.8%, 39.5%, respectively, p=0.779) and time to requiring additional therapy (14.6 ± 11.2, 14.5 ± 12.0 months, p=0.972). Attending-treated eyes received a significantly greater number of laser spots (128.3±29.7, 99.2±25.9, respectively, p<0.001), and a trend of higher total energy (108.7±29.6, 95.7±43.7, p=0.086) than resident-treated eyes.

Conclusions: SLT performed by residents at a Veterans Affairs facility had similar IOP outcomes when compared to SLT performed by attending physicians at a tertiary care center. Attending physicians tend to use SLT more as a primary treatment.

Table 2. Comparison of Intraocular Pressure Reduction after SLT Between Resident-Treated and Attending-Treated Eyes

Time	Resident-Treated Eyes		Attending-Treated Eyes		P value†
	% IOP Decrease*	n	% IOP Decrease*	n	
2 weeks	14.9 ± 24.6	35	17.4 ± 16.0	47	0.608
6 weeks	16.3 ± 14.6	21	15.8 ± 20.7	49	0.821
3 months	27.3 ± 19.5	16	19.7 ± 18.6	34	0.204
6 months	20.0 ± 20.0	23	17.9 ± 18.6	43	0.658
12 months	15.7 ± 24.6	22	15.5 ± 20.8	35	0.967
18 months	10.3 ± 26.3	18	14.0 ± 20.1	29	0.631
24 months	19.4 ± 22.4	23	11.4 ± 26.4	21	0.287
36 months	17.6 ± 18.4	19	13.1 ± 23.9	11	0.605

IOP = Intraocular pressure

* Mean ± SD

† Two tailed unpaired t-test

Table 1. Baseline Characteristics of Eyes Treated with SLT

Characteristics	Resident-Treated Eyes (n=43)	Attending-Treated Eyes (n=68)	P value
Age (mean ± SD), yrs	70.3 ± 11.8	69.5 ± 11.8	0.742*
Gender			
Male	43 (100%)	41 (60.3%)	<0.001**
Female	0 (0%)	27 (39.7%)	
Cup/Disk ratio ≥ 0.7	36 (83.7%)	56 (82.4%)	0.839**
Baseline IOP (mmHg) (mean ± SD)	18.4 ± 4.1	18.4 ± 0.5	0.935*
Baseline glaucoma medications (mean ± SD)	3.0 ± 1.2	1.6 ± 1.3	<0.001*
SLT as first-line therapy, No. of eyes	1 (2.3%)	17 (25%)	<0.001**
Diagnosis, No. of eyes			
POAG	40 (93.0%)	54 (79.4%)	0.052**
OHT	2 (4.7%)	5 (7.4%)	
PXFG	0 (0%)	7 (10.3%)	
Angle Recession	1 (2.3%)	0 (0%)	
SOAG	0 (0%)	1 (1.5%)	
OAGS	0 (0%)	1 (1.5%)	
Procedure Variables			
No. of Shots (mean ± SD)	99.2 ± 25.9	128.3 ± 29.7	<0.001*
Total Energy (mJ) (mean ± SD)	95.7 ± 43.7	108.7 ± 29.6	0.086*

SLT = Selective laser trabeculoplasty; IOP = Intraocular pressure; SD = standard deviation; POAG = Primary open-angle glaucoma; OHT = Ocular hypertension; PXFG = Pseudoexfoliation glaucoma; SOAG = Secondary open angle glaucoma; OAGS = Open-angle glaucoma suspect

* Two-tailed unpaired t-test

** Chi-squared test

Commercial Relationships: Wanda Hu, None; Simon K. Law, None; JoAnn A. Giaconi, Allergan (C)

Program Number: 1869 **Poster Board Number:** B0123

Presentation Time: 11:00 AM - 12:45 PM

Outcome of Combined Phacoemulsification and Endocyclophotocoagulation in Glaucoma

Faisal A. AIMobarak. Ophthalmology, King Saud University, Riyadh, Saudi Arabia.

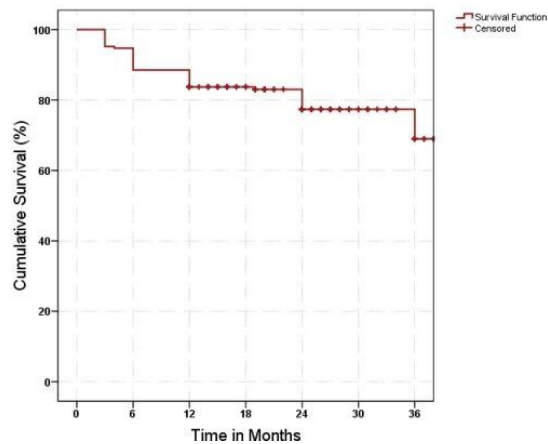
Purpose: To evaluate the outcome of combined phacoemulsification and endocyclophotocoagulation in glaucoma

Methods: 209 eyes of 189 patients who underwent combined phaco-ECP and had a minimum followup of one year were included in this retrospective cohort study. The main outcome measures were the reduction in the intraocular pressure, the change in the number of antiglaucoma medications and the rate of postoperative complications. Kaplan-Meier survival analysis was performed.

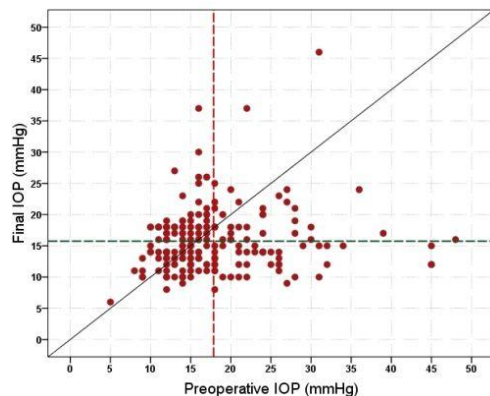
Results: Compared to a mean preoperative pressure of 17.9 mmHg, the IOP decreased by 3, 2 and 1.5 mmHg on 12, 24 and 36 months of

followup. The number of antiglaucoma medications decreased by one over 36 months. The cumulative probability of success was 87.7%, 77.4% and 60.0% on 12, 24 and 36 months postoperatively. There was a slightly positive correlation between the preoperative and postoperative IOP (Spearman's $\rho = 0.13$, $p = 0.04$). The most common complications were fibrinous reaction (21 eyes, 10%), IOP spikes > 30 mmHg (21 eyes, 9.6%) and hyphema (2 eyes, 1%). 7 eyes (3.3%) needed a second glaucoma procedure to control the pressure: 3 shunts, 2 Trabeculectomies and 2 trans-scleral cycloablations.

Conclusions: Phaco-ECP offers a reasonable IOP control with less medications especially on the short term even for eyes that failed filtration procedure. Postoperative complications were few and transient. A small proportion of patients needed a second glaucoma procedure to control the pressure.



Kaplan-Meier survival curve show that the cumulative survival was 87.3%, 77.4% and 69.0% on 12, 24 and 36 months respectively.



Density scatterplot showing slightly positive correlation between the preoperative and postoperative IOP ($\rho = 0.13$, $p = 0.04$). Dashed red line show the mean preoperative IOP while dashed green line show the final mean IOP.

Commercial Relationships: Faisal A. AlMobarak, None

Program Number: 1870 **Poster Board Number:** B0124

Presentation Time: 11:00 AM - 12:45 PM

Laser trabeculoplasty in primates: a morphometric analysis

Tina Damarjian¹, Yang Sun¹, Vincent Gattone^{1,2}. ¹Indiana University, Indianapolis, IN; ²Indiana University, Indianapolis, IN.

Purpose: Several mechanisms have been proposed to describe the modification of outflow facility and the contribution of this process to intraocular pressure (IOP) lowering in glaucomatous eyes treated with laser trabeculoplasty (LTP). Here we investigate the structural changes induced in the eyes of seven treated cynomolgus monkeys to

examine the morphological changes in the trabecular meshwork.

Methods: Laser trabeculoplasty (LTP) was performed on one eye in each of seven cynomolgus monkeys. The treatment was intended to duplicate the procedure as performed in humans. A median of 75 burns of 0.1 sec duration, 50 um size, 900-1400 mw power was applied to the entire circumference of the anterior trabecular meshwork (TM) of each animal. To assess a possible mechanism contributing to this process, analysis of linear and area measurements and calculated volume density changes in randomly selected areas of the filtration angle was done one month following treatment.

Results: One eye of each of the monkeys was treated with LTP demonstrating a significant decrease in IOP (mean IOP reduction 3.5 mmHg $p < 0.001$) and an increase in outflow facility ($p < .001$). This comparison was based on pretreatment levels measured with pneumotometry. There was no significant change in outflow facility in the control eyes. Compared with controls, results demonstrate increased distance from the scleral-ciliary body junction to angle recess and increased thickness of the ciliary body ($p < .05$). While there was no change in the area of corneoscleral TM or Schlemm's canal, the area of the uveal TM also increased ($p < .05$). There was also an increase in interstitial space within the anterior ciliary body ($p < .01$) and the relative area of trabecular spaces within the uveal TM ($p < .05$).

Conclusions: This study shows that consistent IOP modification can be performed in a nonhuman primate model, and via this process demonstrates an increase in outflow facility maybe related to morphological changes. These quantifiable alterations may play a role in the IOP lowering effect of LTP.

Commercial Relationships: Tina Damarjian, None; Yang Sun, None; Vincent Gattone, None

Program Number: 1871 **Poster Board Number:** B0125

Presentation Time: 11:00 AM - 12:45 PM

Long Term Effectiveness and Complications associated with LPI in Treatment of Acute Angle Closure

Alicia Menezes, Sonya B. Shah, Eman Elhawry, Bruno M. Faria, Tao Ming Thomas Chia, Lan Lu, L Jay Katz. Wills Eye Institute, Philadelphia, PA.

Purpose: Acute primary angle closure is an emergent ocular condition often treated with laser peripheral iridotomy (LPI). While numerous studies have examined the outcomes of LPI, many focus predominantly on the Asian population and few have long term follow-up. This study aimed to evaluate the long-term outcomes of LPI after acute primary angle closure in a more diverse population.

Methods: A retrospective chart review was performed from 2002 to 2012. Patients who presented to the Wills Eye Emergency Room with acute primary angle closure and treated with LPI were included.

Those with less than 6 months of follow up were excluded. Ocular exam findings including intraocular pressure (IOP) and visual acuity (VA) were documented at presentation, pre-LPI and at the last follow up visit. The development of complications, need for glaucoma medications and need for further surgery were studied.

Results: Over 10 years, 67 patients presented with primary angle closure attack of which 20 patients and 22 eyes met inclusion criteria. There were 15 females (68%) and 7 males (32%). Patients included 7 Caucasians (32%), 2 African Americans (9%), 6 Asians (27%) and 7 patients of unknown race (32%). The average age was 65. Mean follow-up time was 33 months. Initial mean VA was 1.4 ± 0.7 (LogMAR), and initial mean IOP was $47.5 \text{ mmHg} \pm 14.7 \text{ mmHg}$. All patients were phakic. 19 (86.4%) had nuclear sclerosis. Mean time to LPI was 5 days. Mean pre-LPI VA was 1.2 ± 0.8 and IOP was $26.2 \text{ mmHg} \pm 17.4 \text{ mmHg}$; mean VA at last follow-up was 0.72 ± 0.88 ($p = 0.008$), and IOP was $15.3 \text{ mmHg} \pm 6.5 \text{ mmHg}$ ($p = 0.008$). 4 eyes

ARVO 2013 Annual Meeting Abstracts by Scientific Section/Group – Glaucoma

(18.2%) required cataract extraction, 5 required trabeculectomy (22.7%). None developed retinal tear or detachment. At the last follow-up visit 13 patients (54%) were on glaucoma medications with an average of 2.2 medications being used.

Conclusions: Acute primary angle closure can occur in individuals of diverse races. Female gender and nuclear sclerosis may be predisposing factors. LPI is a safe and effective treatment for acute primary angle closure attack.

Commercial Relationships: Alicia Menezes, None; Sonya B. Shah, None; Eman Elhaway, None; Bruno M. Faria, None; Tao Ming Thomas Chia, None; Lan Lu, None; L Jay Katz, Bausch & Lomb (C), Allergan (R), Allergan (C), Allergan (F), Lumenis (R), Lumenis (F)

Support: Wills Innovation Grant from Wills Eye Institute

Program Number: 1872 **Poster Board Number:** B0126

Presentation Time: 11:00 AM - 12:45 PM

Efficacy of Repeat Selective Laser Trabeculoplasty in African American Patients

Mamta Shah, Babak Eliassi-Rad. Department of Ophthalmology, Boston Univ School of Med, Boston, MA.

Purpose: To evaluate the efficacy of repeat selective laser trabeculoplasty (SLT) in African American patients.

Methods: A retrospective chart review of 50 eyes of 22 African American patients who underwent repeat SLT. Mean intraocular pressure (IOP) was measured after SLT 1 and SLT 2 up to 30 months after each SLT.

Results: SLT 2 was performed 19.0+/-12.9 months after SLT 1. The results are summarized in Table 1. After SLT 1, mean IOP was reduced from 20.5+/-5.10 mmHg to 18.5+/-2.97 mmHg at 6-9 months, 17.8+/-4.25 mmHg at 12-15 months, and 15.4+/-3.06 mmHg at 21-30 months. After SLT 2, mean IOP was reduced from 18.9+/-3.38 mmHg to 16.5+/-5.14 mmHg at 6-9 months (p=0.07), 16.0+/-2.83 mmHg at 12-15 months (p=0.01), and 15.4+/-5.32 mmHg at 21-30 months (p=0.03). The percentage of patients achieving ≥20% IOP reduction from baseline IOP after SLT 1 and SLT 2 is shown in Table 2.

Conclusions: Repeat SLT successfully lowers IOP in African Americans at 12-15 months and 21-30 months.

Mean Intraocular Pressure (IOP) ± STD (mmHg)	SLT 1	SLT 2
Baseline	20.5±5.10	18.9±3.38
6-9 months	18.5±2.97	16.5±5.14
12-15 months	17.8±4.25	16.0±2.83
21-30 months	15.4±3.06	15.4±5.32

Table 1 Summary of Results

	6-9 months	12-15 months	21-30 months
SLT 1	43.7% (n=12)	44.4% (n=18)	30.0% (n=10)
SLT 2	27.3% (n=11)	50.0% (n=8)	42.9% (n=7)

Table 2 Percentage of Eyes Achieving ≥20% Reduction in Intraocular Pressure (IOP) After SLT 1 and SLT 2

Commercial Relationships: Mamta Shah, None; Babak Eliassi-Rad, None

Program Number: 1873 **Poster Board Number:** B0127

Presentation Time: 11:00 AM - 12:45 PM

Effect of Pre-operative Medications on Selective Laser Trabeculoplasty Outcomes

Babak Eliassi-Rad, Mamta Shah. Ophthalmology, Boston University, Boston, MA.

Purpose: To compare the relationship between prostaglandin analogs (PGAs) versus non-prostaglandin analog glaucoma medications on SLT outcome.

Methods: A retrospective chart review of 25 eyes of 25 patients who underwent SLT. All patients were on either 1 PGA medication (latanoprost 0.005% or bimatoprost 0.03%) or 1 non-PGA medication (timolol 0.5%, brimonidine 0.2%, or dorzolamide 2%). Mean intraocular pressure (IOP) was measured before SLT and up to 2 years after SLT.

Results: The patient demographics and results are summarized in Tables 1 and 2 respectively. Baseline mean IOP was 17.7+/-2.5 mmHg for PGA users and 20.1+/-3.1 mmHg for non-PGA users. For PGA users, mean IOP was 16.3+/-5.6 mmHg (p=0.6), 14.3+/-1.7 mmHg (p=0.04), and 12.5+/-1.9 mmHg (p=0.006) at 9-12 months, 21-24 months, and 24-30 months after SLT respectively. For non-PGA users, mean IOP was 14.8+/-3.1 mmHg (p=0.002), 13.3+/-4.2 mmHg (p=0.0004), and 14.6+/-4.0 mmHg (p=0.0009) at 9-12 months, 21-24 months, and 24-30 months after SLT respectively. Mean IOP for PGA users versus non-PGA users was compared at 9-12 months (p=0.6), 21-24 months (p=0.7), and 24-30 months (p=0.3).

Conclusions: Patients using PGAs had a statistically significant reduction in mean IOP 21-24 months and 24-30 months after SLT. Patients using non-PGAs had a statistically significant reduction in mean IOP at 9-12 months, 21-24 months, and 24-30 months after SLT. There was no statistically significant difference in mean IOP between PGA users and non-PGA users at each time point.

Demographics	Frequency
Patients	25
Eyes	25
Male/Female	16/9
Mean Age ± SD (years)	65.8±12.0
Glaucoma Diagnosis	
POAG	20
LTG/OHTN/PXG	4
OAG Suspect/PDG/ARG	1
SLT Eye	
OD	14
OS	11
Glaucoma Medication	
Non-PGA Medication	18
PGA Medication	7

Table 1 Patient Demographics

Time after SLT (months)	PGA Medication	Non-PGA Medication
9-12 months	16.3±5.6 (p=0.6)	14.8±3.1 (p=0.002)
21-24 months	14.3±1.7 (p=0.004)	13.3±4.2 (p=0.0004)
24-30 months	12.5±1.9 (p=0.006)	14.6±4.0 (p=0.0009)

Table 2 Mean Intraocular Pressure (IOP) at 9-12 months, 21-24 months, and 24-30 months after SLT for PGA Medication Users and Non-PGA Medication Users

Commercial Relationships: Babak Eliassi-Rad, None; Mamta Shah, None

Program Number: 1874 **Poster Board Number:** B0128

Presentation Time: 11:00 AM - 12:45 PM

Plateau Iris among American Caucasians, American Chinese, and Mainland Chinese

YINGJIE LI^{1,2}, Ye Elaine Wang^{1,3}, Mary Qiu¹, Dandan Wang^{1,4}, Mingguang He⁴, Shan C. Lin¹. ¹Ophthalmology, University of California San Francisco, San Francisco, CA; ²Ophthalmology, The Third Affiliated Hospital of Nanchang University, Nanchang, China; ³Duke University School of Medicine, Durham, NC; ⁴Ophthalmology, Zhongshan Ophthalmic Center, Sun Yat-sen University, Guangzhou, China.

Purpose: To evaluate the prevalence and common risk factors of plateau iris configuration among American Caucasians, American Chinese, and mainland Chinese subjects using ultrasound biomicroscopy.

Methods: This study included three gender- and age-matched cohorts of 117 American Caucasians, 129 American Chinese and 112 mainland Chinese subjects. One eye was examined per subjects. Eyes with plateau iris configuration were defined as having at least 2 quadrants with the presence of 1) anteriorly directed ciliary body, 2) absent ciliary sulcus, and 3) central flat iris plane. All subjects underwent A-scan biometry and auto-refraction.

Results: Plateau iris configuration was found in 28 (23.9%) American Caucasians, 29 (22.5%) American Chinese, and 23 (20.5%) mainland Chinese subjects. No significant difference in the prevalence of plateau iris configuration was observed among the three cohorts ($P=0.825$, χ^2 test). Spherical equivalent was significantly associated with plateau iris configuration (coefficient 0.233, Hierarchical Cluster Analysis).

Conclusions: The prevalence of plateau iris did not differ among American Caucasians, American Chinese and mainland Chinese subjects. There is a lower rate of plateau iris among myopic eyes compared to emmetropic eyes.

Commercial Relationships: YINGJIE LI, None; Ye Elaine Wang, None; Mary Qiu, None; Dandan Wang, None; Mingguang He, None; Shan C. Lin, None

Support: National Natural Science Foundation of China. Grant No: 81260147.

Program Number: 1875 **Poster Board Number:** B0129

Presentation Time: 11:00 AM - 12:45 PM

Dynamic iris volume characteristics pre and post laser peripheral iridotomy (LPI) in eyes with occludable anterior chamber angles measured with 3 dimensional swept-source Ocular Coherence Tomography (OCT): The Investigating Management of Angle Closure and Treatment (IMPACT) study

Rupert R. Bourne^{1,2}, Laura Sanchez Parra¹, Humma Shahid³, Roger Buckley¹, Shahina Pardhan¹. ¹Vision & Eye Research Unit, Postgraduate Medical Institute, Anglia Ruskin University, Cambridge, United Kingdom; ²Huntingdon Glaucoma Diagnostic & Research Centre, Hinchingsbrooke Hospital, Huntingdon, United Kingdom; ³Ophthalmology, University of Cambridge Hospitals NHS Trust, Cambridge, United Kingdom.

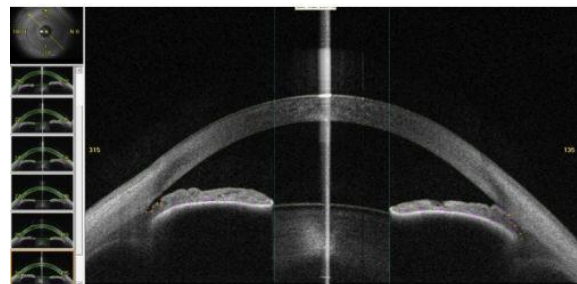
Purpose: Previous studies involving fellow eyes (post-LPI) of patients in which the other eye has suffered acute angle closure (AAC) have reported a gain in iris volume with pharmacological dilation while irises of normal controls lose volume- this 'iris sponge' hypothesis may explain a predisposition of these eyes to AAC. This study investigated the hypothesis that LPI affects iris volume change but in patients with no history of AAC and within the physiological range of pupil size.

Methods: 32 Caucasian patients with bilateral Primary Angle Closure (PAC), Primary Angle Closure Suspect (PACS) or PAC/PACS were recruited. A randomly chosen eye of each patient received LPI. OCT (CASIA) measurements were measured in light (170-200 lux) and dark (0.3-0.5 lux) prior to and 6 weeks after LPI by the same examiner. Change in iris volume between light and dark conditions was measured at each of these 2 timepoints, and association with pre-laser presence of peripheral anterior synechiae (PAS) was explored.

Results: Prior to LPI, total iris volume was greater in light (mean, 36.5 mm³) than in dark conditions (mean, 35.8 mm³; paired t test, $p=0.05$). Following LPI, a similar volume relationship existed (light: mean, 36.4 mm³; dark: mean, 35.5 mm³, $p=0.01$). Light minus dark iris volume change (LDVC) was no different before and after LPI ($p=0.59$). LDVC was not significantly different between eyes with PAS ($n=9$; mean LDVC, 0.61mm³) compared to those without ($n=23$; mean LDVC, 0.75mm³) prior to LPI ($P=0.86$). However, following LPI, eyes with PAS demonstrated negative LDVC values (mean LDVC, -0.49mm³) compared to eyes without PAS in which the relationship was reversed (mean LDVC, 1.54mm³, $P<0.01$).

Conclusions: This study has demonstrated reduction in iris volume in dark conditions within the physiological range of pupil size for a condition (PACS/PAC) which has a much higher prevalence in the population than AAC. The finding that those eyes with PAS exhibited less volume change or an actual increase in iris volume in dark conditions lends support to the 'iris sponge hypothesis', and suggests that there is a spectrum of pathology of dynamic iris behavior in eyes with occludable angles.

Swept-source anterior segment ocular coherence tomography image of the anterior segment demonstrating an open angle at 315 degrees and a closed angle at 135 degrees. Iris volume measurements are displayed in the left-hand panel.



Commercial Relationships: Rupert R. Bourne, Allergan Ltd (F); Laura Sanchez Parra, Allergan Ltd (F); Humma Shahid, None; Roger Buckley, None; Shahina Pardhan, None

Support: Allergan Ltd (unrestricted educational grant)

Clinical Trial: 8955

Program Number: 1876 **Poster Board Number:** B0130

Presentation Time: 11:00 AM - 12:45 PM

Corneal sensitivity and morphology of the corneal subbasal nerve plexus in primary congenital glaucoma

Zisis Gatziooufas^{1,2}, Farhad Hafezi¹, Berthold Seitz². ¹Dpt. of Ophthalmology, University Hospitals of Geneva HUG, Geneva, Switzerland; ²Dpt. of Ophthalmology, Saarland University Medical Center UKS, Homburg/Saar, Germany.

Purpose: To quantify corneal subbasal nerve density and total number of nerve fibers in primary congenital glaucoma (PCG) and evaluate their impact on corneal sensitivity.

Methods: Forty eyes of 26 PCG patients were compared with 40 eyes randomly selected from 40 non-glaucoma patients who populated the control group. Central corneal sensitivity (CCS) was assessed by means of Cochet-Bonnet esthesiometry. Mean subbasal nerve density and total number of nerve fibers were quantified by laser-scanning confocal microscopy (LSCM). Normality of data was assessed by Kolmogorov-Smirnov testing. Differences in parameters were assessed with Student's t test while correlations with CSS with Pearson's correlation.

Results: Significant differences were identified in the mean subbasal nerve density (2108±692µm in PCG, 2642±484µm in controls, p=0.003) and total number of nerve fibers (12.3±4.2 in PCG, 15.4±3.1 in controls, p=0.02). Both groups presented comparable mean CCS and tortuosity. Both groups presented strong correlations between CCS and mean nerve density (r=0.57 in PCG, r=0.67 in controls, all p<0.05), and between CCS and total number of nerve fibers (r=0.55 in PCG, r=0.56 in controls, all p<0.05).

Conclusions: PCG exerts significant changes both in the mean subbasal nerve density and the total number of nerve fibers. However, these changes do not appear to affect central corneal sensitivity.

Commercial Relationships: Zisis Gatziooufas, None; Farhad Hafezi, Schwind (F), Ziemer (F), PCT/CH 2012/000090 (P); Berthold Seitz, None

Program Number: 1877 **Poster Board Number:** B0131

Presentation Time: 11:00 AM - 12:45 PM

Structural and Functional Changes after Intraocular Pressure Reduction in Patients with Glaucoma

Michael Waisbourd, Jeanne Molineaux, Thandeka Myeni, George L. Spaeth, L Jay Katz. Glaucoma Service, Wills Eye Institute, Philadelphia, PA.

Purpose: To determine if there is any relation between structural and functional changes after intraocular pressure (IOP) reduction in patients with glaucoma.

Methods: Patients with glaucoma in whom a pressure-lowering event was to be initiated were included.

All patients received a pressure-lowering intervention - medicines, laser or surgery. Prior to the intervention, they performed a 24-2 SITA standard visual field examination, Spectralis optical coherence tomography (OCT) imaging test (fast retinal nerve fiber layer and macular protocols) and visual evoked potential (VEP) exam using the Diopsys NOVA-VEP Vision Testing System.

For patients with initial IOP ranging between 22-32mmHg, these tests were repeated after 1-2 months, 4-6 months, and 9-12 months after IOP reducing interventions.

For patients with initial IOP ≥33mmHg, after obtaining the baseline examinations (visual field, OCT and VEP), they had their IOP acutely lowered. The studies were then repeated one hour, one day and three months following the acute pressure lowering.

Results: Forty seven patients (58 eyes) were included in the study, 38

patients with initial IOP ranging between 22-32mmHg and 9 patients with initial IOP ≥33mmHg. There was a significant change in IOP over time (P<0.001 for both groups). Change in IOP was significantly associated with change in cup volume (P=0.037) and change in rim area (p=0.032) after the first follow-up visit, for both groups combined. The association between change in IOP and change in VEP amplitude high contrast approached significance after the first follow-up visit in the IOP>33mmHg group (P=0.06). Change in OCT retinal nerve fiber layer over time approached significance in the IOP>33mmHg group (P=0.09).

Conclusions: With a marked reduction of IOP in glaucomatous eyes there were early structural changes confirmed by OCT imaging but no significant changes were noted with functional tests - perimetry and VEP.

Commercial Relationships: Michael Waisbourd, None; Jeanne Molineaux, None; Thandeka Myeni, None; George L. Spaeth, Merck (F), U.S. Patent No. 8,042,946 (P), Pfizer (F); L Jay Katz, Bausch & Lomb (C), Allergan (R), Allergan (C), Allergan (F), Lumenis (R), Lumenis (F)

Support: Allergan horizon grant

Program Number: 1878 **Poster Board Number:** B0132

Presentation Time: 11:00 AM - 12:45 PM

Classification of Retinal Ganglion Cell Defects Seen on Frequency-Domain OCT in the Macula of Patients with Glaucoma

Anastasia Slobodnick^{1,2}, Ali S. Raza^{1,3}, C. Gustavo De Moraes^{2,4}, Christopher C. Teng^{2,5}, Robert Ritch^{2,5}, Donald C. Hood^{2,6}.

¹Psychology, Columbia University, New York, NY; ²Einhorn Clinical Research Center, New York Eye and Ear Infirmary, New York, NY; ³Neurobiology and Behavior, Columbia University, New York, NY; ⁴Ophthalmology, New York University School of Medicine, New York, NY; ⁵Ophthalmology, New York Medical College, Valhalla, NY; ⁶Ophthalmology, Columbia University, New York, NY.

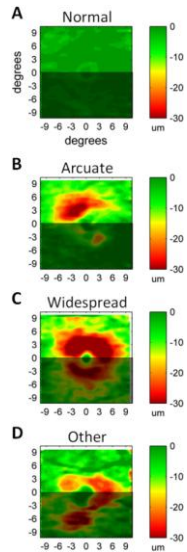
Purpose: To classify patterns of retinal ganglion cell (RGC) defects in glaucoma patients as seen on frequency-domain optical coherence tomography (fdOCT) volume macular scans and to compare these patterns to associated visual fields (VF).

Methods: One eye of 35 glaucoma patients or suspects (inclusion criteria: 24-2 MD of -6 or better) was prospectively tested with fdOCT and 10-2 VFs. The combined RGC and inner plexiform layers (RGC+) of the OCT scans were segmented using a computer-assisted manual segmentation technique.[1,2] RGC+ probability plots [3] (divided into an 8 by 8 grid) were generated. First, a scan was considered abnormal if at least 3 contiguous abnormal squares (at 5%, 2%, 2%) respecting the horizontal midline were present. This criterion yielded 24 abnormal OCT hemifields, similar to the number (26) of abnormal 10-2 VFs yielded by the typical 5%, 5%, 1% criterion. The 24 abnormal OCT hemifields were classified as arcuate-like, widespread, or "other." "Other" included temporal and non-continuous defects. RGC+ thinning plots were obtained by averaging the RGC+ thickness by classification and subtracting the average control thickness.[4] For each OCT group, the means of the associated 10-2 total deviation values were acquired.

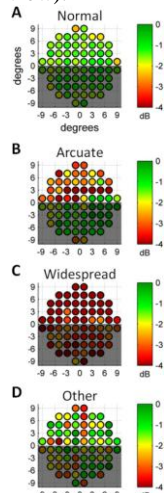
Results: 24 (34%) of the 70 OCT hemifields were abnormal. Of these, 10 (14%) were arcuate-like, 8 (11%) widespread, and 6 (9%) "other." Fig. 1 (field view) shows the average OCT thinning plots for the inferior retinal hemifield and Fig. 2 the averaged associated VFs. For OCTs classified as normal (Fig. 1A), the mean 10-2 VF appeared normal (Fig. 2A). OCTs classified as arcuate exhibited greater thickness loss in the nasal retina (Fig. 1B) and the mean 10-2 VF appeared arcuate (Fig. 2B). For OCTs classified as widespread (Fig.

1C), the mean 10-2 VF also appeared widespread (Fig. 2C). Finally, there was no clear correspondence between OCT (Fig. 1D) and VF (Fig. 2D) for the "other" class, although the sample size was small.

Conclusions: The pattern of RGC defects on OCT could be classified into 4 groups. Except for the "other" category, the average 10-2 VF closely resembled the pattern of OCT RGC+ thinning. 1. Yang et al. Biomed Opt Exp 2011. 2. Raza et al. AO 2011. 3. Hood & Raza. Biomed Opt Exp 2011. 4. Hood et al. TVST 2012.



Average thinning for inferior hemifield OCT classification (field view).



Average visual fields.

Commercial Relationships: Anastasia Slobodnick, None; Ali S. Raza, None; C. Gustavo De Moraes, None; Christopher C. Teng, None; Robert Ritch, None; Donald C. Hood, Topcon, In (F)
Support: NIH grant R01-EY02115

Program Number: 1879 **Poster Board Number:** B0133
Presentation Time: 11:00 AM - 12:45 PM

The investigation of correlation between subfoveal choroidal thickness and sensitivity of visual field in highly myopic glaucoma with peripapillary atrophy optic disc

Kazunori Tamaki¹, Itaru Kimura^{1,2}, Yutaka Imamura³, Yugo Nakazawa¹, Satoshi Watanabe¹, Akira Murakami⁴, Nobuyuki Ebihara¹. ¹Department of Ophthalmology, Juntendo University

Urayasu Hospital, Urayasu City, Japan; ²National Institute of Sensory Organs, Tokyo Medical Center, Tokyo, Japan; ³Department of Ophthalmology, Teikyo University Mizonokuchi Hospital, Kawasaki City, Japan; ⁴Department of Ophthalmology, Juntendo University School of Medicine, Tokyo, Japan.

Purpose: To measure subfoveal choroidal thickness of POAG patients with high myopia, and to investigate the correlation between the choroidal thickness and stage of visual field or MD values, or degree of peripapillary atrophy (PPA).

Methods: 94 eyes from 55 patients (average age 54.0±11.8 years old) diagnosed as POAG including preperimetric glaucoma with spherical equivalent refractive error under -6 diopters were studied. They were classified into 2 groups, one had not the disc with whole surrounding PPA (L-group) and the group which had the disc with whole surrounding PPA (S-group). 42 eyes were S group, and 52 eyes were L group. Subfoveal choroid was imaged with Cirrus HD-OCT (Carl Zeiss Meditec) and its thickness was measured. The correlation were investigated between choroidal thickness and MD value of Humphrey SITA standard (30-2), and the correlation were compared between L and S-group.

Results: There was significantly correlation between MD value and subfoveal choroidal thickness in 94 eyes (r=0.29, p=0.003). In L-group there was more significant correlation between MD value and subfoveal choroidal thickness, and P value rose to 0.378. In S-group no significant correlation was found between MD value and subfoveal choroidal thickness.

Conclusions: It was shown that thinner the subfoveal choroidal thickness was, worse the sensitivity of visual field was, in highly myopic POAG patients totally. Furthermore, it is suggested that there is a group showing good correlation between subfoveal choroidal thickness and the sensitivity of visual field, and a group showing no significant correlation like patients who have whole surrounding PPA.

Commercial Relationships: Kazunori Tamaki, None; Itaru Kimura, None; Yutaka Imamura, None; Yugo Nakazawa, None; Satoshi Watanabe, None; Akira Murakami, SEED (Japan) JP4855782 (P), SEED (Japan) JP5132958 (P); Nobuyuki Ebihara, None

Program Number: 1880 **Poster Board Number:** B0134

Presentation Time: 11:00 AM - 12:45 PM

Structure-Function Relationship between Spectral Domain Optical Coherence Tomography, Heidelberg Retina Tomograph and Flicker Defined Form Perimetry in Patients with Ocular Hypertension and Preperimetric Glaucoma

Ermengarda Marziani¹, Laura de Polo^{1,2}, Erma Collaku¹, Elena Weiszberger¹, Alessandra Acquistapace¹, Andrea Giani¹, Mirella Blini¹, Giovanni Staurenghi¹. ¹Eye Clinic Department of Biomedical and Clinical Science "Luigi Sacco", Luigi Sacco Hospital, Milan, Italy; ²COB, Centro Oculistico Bergamasco, Bergamo, Italy.

Purpose: To assess the correlation between Heidelberg edge perimetry (HEP) and peripapillary retinal nerve fiber layer (RNFL) thickness measured by spectral-domain optical coherence tomography (SD-OCT) Spectralis and by Heidelberg Retina Tomograph III (HRT-III), (Heidelberg Engineering, Heidelberg, Germany).

Methods: The study involved 60 eyes with ocular hypertension (OHT) and/or optic nerve suspicious for glaucoma without visual field damages detectable with the Standard Automated Perimetry (SAP).

All eyes underwent RNFL imaging with Spectralis SD-OCT, topographic imaging HRT-III and Flicker Defined Form Perimetry with HEP.

Cohen's Kappa statistic (k) was used to assess the agreement between SD-OCT and HEP and between HRT and HEP for each of the six RNFL sectors.

Results: Between Spectralis SD-OCT and HEP agreement was fair (0.38) in the nasal sector, good (0.64-0.68) in the superior temporal and inferior temporal sectors and moderate (0.44-0.52) in the superior nasal, inferior nasal and temporal sectors. Between HRT and HEP agreement was slight (0.14-0.16) in the temporal and inferior temporal sectors, fair (0.24-0.34) in the other sectors.

Conclusions: The agreement between HEP and Spectralis SD-OCT was better than HEP and HRT. With Spectralis SD-OCT the strongest correlations were found in the superior and inferior temporal sectors as the ISN'T rule suggests for detecting preperimetric RNFL defects.

Commercial Relationships: Ermengarda Marziani, None; Laura de Polo, None; Erma Collaku, None; Elena Weiszberger, None; Alessandra Acquistapace, None; Andrea Giani, Bayer (C), Novartis (R), Allergan (R); Mirella Blini, None; Giovanni Staurengi, Ocular Instruments (P), GSK (C), Novartis (C), Alcon (C), Allergan (C), Bayer (C), Roche (C), Heidelberg Engineering (C), OD-OS (C), QLT (C), Optos (C)

Program Number: 1881 **Poster Board Number:** B0135

Presentation Time: 11:00 AM - 12:45 PM

Nailfold Hemorrhages and Primary Open-Angle Glaucoma:

More than What Meets the Eye

Kevin Skuran¹, Ryan McCarty¹, Algis Grybauskas¹, Paulius Kuprys¹, John R. Samples³, Paul A. Knepper^{1,2}. ¹Ophthalmology and Visual Sciences, University of Illinois at Chicago, Chicago, IL; ²Ophthalmology, Northwestern University, Chicago, IL; ³Specialty Eye Care, Denver, IL.

Purpose: Vascular dysfunction and microhemorrhages are characteristic of many connective tissue diseases, e.g. scleroderma and systemic lupus erythematosus. The purpose of this study is to evaluate a systemic feature of primary open-angle glaucoma (POAG) with nailfold video capillaroscopy and hyaluronic acid (HA) profiling.

Methods: Nailfold video capillaroscopy using a JH-1004 Capillaroscope was performed on low-tension POAG patients ($n=7$) and on aged-matched normal "control" subjects ($n=7$). Videos were taken of the subject's third and fourth fingers on their non-dominant hand. Videos were analyzed to determine capillary morphology. Capillaries were qualified as normal (hairpin loop), tortuous, bizarre, ramified, bushy, crossed, or widened. Additionally, hemorrhages and avascular areas were recorded, and overall tortuosity was calculated. HA profiling of human serum was completed through glycosaminoglycan (GAG) isolation and HA extraction. GAG isolation was performed on normal and low-tension POAG patient human serum using protease degradation, RNase treatment, DNase treatment, trichloroacetic acid precipitation, and selective alcohol precipitation. HA was extracted from the isolated GAG samples using 0.4M NaCl in 0.1% cetylpyridinium chloride. The isolated HA was run on a 15% TBE gel, and stained with Stains-All. HA ladders of 25kD to 500kD were used to determine the molecular weights and densitometry was performed using Metamorph to determine the relative HA sizes.

Results: Microhemorrhages were observed in all low-tension POAG patients and in only 1 of 7 control subjects ($P<0.001$). There were 35 hemorrhages in 560 capillaries resulting in a 6.3% incidence. POAG subjects had an average tortuosity of 1.6 ± 0.2 while normal subjects had an average tortuosity of 1.7 ± 0.6 . HA concentration tended to decline in POAG serum, with a qualitative difference in low molecular weight HA species observed in POAG patients

Conclusions: In all low-tension POAG patients, microhemorrhages were observed. The direct cause of the microhemorrhages remains undetermined, as there are many possible factors. Such factors include capillary growth regulation, breakdown of support matrix, blood flow velocity, and neurogenic dysfunction. The relative amounts and size of HA described in the HA profiling may provide insight to the capillary growth regulation. Thus, we conclude POAG has systemic features characteristic of connective tissue diseases.

Commercial Relationships: Kevin Skuran, None; Ryan McCarty, None; Algis Grybauskas, None; Paulius Kuprys, None; John R. Samples, None; Paul A. Knepper, None

Support: American Health Assistance Foundation, Research to Prevent Blindness

Program Number: 1882 **Poster Board Number:** B0136

Presentation Time: 11:00 AM - 12:45 PM

Structure Function Relationship: ganglion cell complex assessment by two SD-OCT and standard automated perimetry
Hussam El Chehab, Maxime Delbarre, Redouane Messaoudi, Jean-Remi Fenolland, Marechal Marie, Marlene Francoz, Jean-Marie Giraud, Frank May, Jean-Paul G. Renard. Department of Ophthalmology, Hospital Val de Grace, Paris, France.

Purpose: Investigate relationship between structural damage analyzed by OCT RTVue100 (Optovue, Inc.) and CirrusHD (Carl Zeiss Meditec, Dublin, CA, USA) with functional parameters of standard automated perimetry (SAP).

Methods: 143 eyes of 78 patients (96 early glaucoma, 47 moderate to severe glaucoma) and 43 control eyes were included. They had, the same day, a clinical exam with RTVue100 OCT (7*7 macular grid), CirrusHD OCT (200*200 macular grid), 24°2 and 10°2 SAP (Humphrey SITA-standard).

CirrusHD segmentation includes ganglion cell layer and inner plexiform (GCIPL). RTVue associates retinal nerve fiber layer thereby defining macular ganglion cell complex (GCC). Structural damage parameters analyzed were GCC average thickness, Global and Focal Loss Volume (GLV and FLV) with RTVue, average and minimum GCIPL thickness with CirrusHD. Functional parameters collected were MD, PSD and VFI for 24°2 SAP and MD and PSD for 10°2 SAP.

A Student t-test was performed to compare parameters between groups and a logistic regression analysis calculated Pearson coefficient (r) to study correlation might exist between structural and functional parameters.

Results: Glaucoma group had a significant functional impairment in 24°2 and 10°2 SAP compared to control (MD=-5.6dB±1.1 and PSD=5.9dB±0.7 in 24°2 SAP, $p<0,01$ and MD=-8.3±1.6dB and PSD=7.2dB±1 in 10°2, $p<0,01$).

Logistic regression analysis found a linear correlation between structural and functional parameters.

Glaucoma group correlation coefficients were higher than control group.

OCT RTVue parameters appeared to have higher correlation coefficients with functional indices than those of CirrusHD OCT (r from 0.50 to 0.72 for RTVue and 0.44 to 0.56 for CirrusHD) in 24°2 and 10°2 SAP.

The highest Pearson coefficient with OCT RTVue was between focal damage indices (FLV) and PSD in 24°2 SAP ($r=0.72$). With CirrusHD, it was correlation between minimum GCIPL and PSD in 24°2 SAP ($r=0.56$). Further analysis of macular nerve fibers layer (mNFL) allowed a higher coefficient, $r=0.65$ between mNFL+ average GCIPL and MD of 24°2 SAP.

Correlation coefficients were not different with 24°2 SAP and 10°2 SAP.

Conclusions: This study objectives a structure function relationship between focal structural (FLV and GCIP-L-Min) and functional (PSD) parameter damage with these 2 SD-OCT. If a difference between these OCT may exist, it has to be confirmed by other studies.

Commercial Relationships: Hussam El Chehab, None; Maxime Delbarre, None; Redouane Messaoudi, None; Jean-Remi Fenolland, None; Marechal Marie, None; Marlene Francoz, None; Jean-Marie Giraud, None; Frank May, None; Jean-Paul G. Renard, None

Program Number: 1883 **Poster Board Number:** B0137

Presentation Time: 11:00 AM - 12:45 PM

Structure-Function Mapping: Conviction and Variability in Tracing of Retinal Nerve Fibre Bundles and Comparison to a Computational Model

Jonathan Denniss^{1,2}, Andrew Turpin², Fumi Tanabe³, Chota Matsumoto³, Allison M. McKendrick¹. ¹Optometry and Vision Sciences, The University of Melbourne, Melbourne, VIC, Australia; ²Computing and Information Systems, The University of Melbourne, Melbourne, VIC, Australia; ³Ophthalmology, Kinki University Faculty of Medicine, Osaka, Japan.

Purpose: Maps relating the visual field (VF) to the optic nerve head (ONH) have typically been produced by hand-tracing of nerve fibre bundles in retinal images by single observers. We have published a computational model incorporating biometric parameters as an alternative approach (Denniss et al, IOVS 2012). Here we investigate conviction and variability in nerve fibre tracing, and compare maps produced to the model. We hypothesised that discordance between the methods would be related to uncertainty and variability in tracing.

Methods: VF locations (n=52, 24-2 pattern) were overlaid on composite 490nm scanning laser ophthalmoscope (F-10, Nidek, Japan) retinal images from 10 subjects with varied anatomy (axial length, ONH position). Ophthalmically trained (n=8) and untrained (n=5) observers viewed the images under standardised conditions and manually traced the 1° ONH sector into which nerve fibres from each VF location entered. Observers also recorded the range of sectors into which they were certain the fibre entered. These ranges were scaled for each observer/image to represent conviction in tracing. Traced sectors were compared to 10° sectors predicted by the computational model based on axial length and ONH position.

Results: Across VF locations, variability in tracing fibres was high with median difference between two furthest apart traced sectors for a VF location of 27° (IQR 20-38°) for trained observers and 38° (IQR 28-56°) for untrained observers. Across all traced VF locations, concordance between the model and the range within which observers reported they were certain the fibre entered was 53% for trained and 79% for untrained observers. Across VF locations, conviction in tracing decreased linearly with distance from the ONH (trained: $R^2=0.81$, untrained: $R^2=0.78$, both $p<0.001$). Conviction was inversely correlated with tracing variability (both groups Spearman's $\rho=0.66$, $p<0.001$) and root mean squared differences between traced and model-predicted sectors (Spearman's ρ , trained 0.47, untrained 0.44, both $p<0.001$).

Conclusions: Concordance between traced and model-predicted sectors was moderate, and greater for locations where conviction in tracing was greater. Variability and uncertainty in tracing nerve fibre bundles, particularly further from the ONH, should be taken into account when used to create or as a reference for structure-function maps.

Commercial Relationships: Jonathan Denniss, Heidelberg Engineering GmbH (F); Andrew Turpin, Heidelberg Engineering (F); Fumi Tanabe, None; Chota Matsumoto, None; Allison M. McKendrick, Heidelberg Engineering GmbH (F)

Support: ARC Linkage Project LP100100250, ARC Future Fellowship FT0991326 (to AT), ARC Future Fellowship FT0990930 (to AMM), K.M. Brutton Bequest (to JD)

Program Number: 1884 **Poster Board Number:** B0138

Presentation Time: 11:00 AM - 12:45 PM

Autoregressive Mixed Effects Approach for Modeling Longitudinal Standard Automated Perimetry Data in Glaucoma

Manoj Pathak, Shaban Demirel, Stuart K. Gardiner. Devers Eye Institute, Legacy Research Institute, Portland, OR.

Purpose: Trend analyses are increasingly being performed on perimetry data from patients with glaucoma, for example, trend analyses of the Visual Field Index or pointwise linear regression. However, ordinary least squares (OLS) regression analyses are inappropriate for modeling longitudinal data, and may underestimate true p-values. Models that account for group effects and within-group correlation structure are more suited to longitudinal data. This study examines these methods to model longitudinally collected perimetry data, and determines whether it provides significant improvements over OLS.

Methods: This study used longitudinal data from 168 eyes of 84 subjects with early or suspected glaucoma in the ongoing Portland Progression Project. Data from 1344 visual fields (eight visits per subject) were used. Models were formed to predict Mean Deviation (MD) from age and rim area (from confocal scanning laser ophthalmoscopy). Linear mixed effects models with one level of nesting (subject) or two levels (subject, eye within subject) were examined. An exponential temporal correlation structure with nugget effect was applied to account for same day test-retest variability. Sensitivity at each of the 52 non-blindspot locations (HFA 24-2) was also modeled to determine the performance of the model with pointwise data. Mixed effects models were compared using ANOVA. AICs were also compared against OLS.

Results: For MD, the two level mixed effect model accounting for temporal autocorrelation was significantly better than the two level model not accounting for temporal autocorrelation ($p<0.0001$). The correlation between residuals on the same day was 0.7, decreasing to 0.61 (95% CI [0.47, 0.72]), when one year apart. Two level models significantly improved the model fit compared to one level models ($p<0.0001$). For the pointwise data, two level models were significantly better than single level models ($p<0.0001$) at all visual field locations. For both MD and point wise data, mixed effect models had smaller (better) AICs than OLS regression.

Conclusions: Errors from linear fits of longitudinal data are temporally correlated and OLS regression will underestimate true p-values and overstate the significance of trends. Autoregressive mixed effects models provide a better fit to the test data by accounting for group effects and within-group correlation.

Commercial Relationships: Manoj Pathak, None; Shaban Demirel, Carl Zeiss Meditec (F), Heidelberg Engineering (R), Heidelberg Engineering (F); Stuart K. Gardiner, Allergan (R)

Support: NIH Grants R01 EY020922, R01 EY019674

Program Number: 1885 **Poster Board Number:** B0139

Presentation Time: 11:00 AM - 12:45 PM

Signal-to-Noise Ratios for Structural and Functional Tests in Glaucoma

Cindy L. Blachly, Stuart K. Gardiner, Brad Fortune, Deborah Goren, Michael D. Whitworth, Steven L. Mansberger, Shaban Demirel. Devers Eye Institute, Legacy Health, Portland, OR.

Purpose: The utility of standard automated perimetry (SAP) for monitoring glaucoma is limited by its high variability. Structural tests, such as Optical Coherence Tomography (OCT), may be more

repeatable, since they do not rely on subjective patient responses. However, it is hard to compare techniques in a fair manner due to their different units and dynamic ranges. This study uses a signal-to-noise analysis to compare variability of these techniques on a common scale.

Methods: Longitudinal data were used from 445 eyes of 227 subjects with non-endstage glaucoma enrolled in the ongoing Portland Progression Project. Subjects were tested every six months with SAP (HFA) and OCT (Spectralis) on the same day for a minimum of 5 visits. Only visits with both reliable SAP visual fields ($\leq 15\%$ False Positives, $\leq 30\%$ False Negatives and Fixation Losses) and good quality OCT scans (≥ 15 Quality) were included. Retinal Nerve Fiber Layer Thickness (RNFLT) was assessed from OCT scans after manually refining the delineated layer boundaries in a masked fashion. For each eye, Mean Deviation (MD) from SAP and RNFLT TSNIT average from OCT were regressed against time, and the residuals from the trend over time were calculated. The standard deviation of these residuals was used as a measure of 'Noise'. Three measures of 'Signal' were used: the range of values within the dataset (Range); the change in one year in the most rapidly changing eye based on regression of the series over time ($Slope_{Max}$); and the 10th percentile of these annual changes within the dataset ($Slope_{10}$) to reduce the effect of outliers. As a secondary analysis, the process was repeated using only those sequences where the MD was never worse than -3dB, to reduce the confounding effect of variability increasing with damage in SAP.

Results: For SAP, the noise was 0.58dB. This represented 2.5% of Range, 24.0% of the worst rate $Slope_{Max}$, and 83.2% of $Slope_{10}$. For OCT, the noise was 1.70 μ m, representing 1.8% of Range, 22.9% of $Slope_{Max}$ and 67.4% of $Slope_{10}$. When only relatively healthy eyes ($MD > -3$) were used, the noise for SAP was 2.1% of Range, 20.5% of $Slope_{Max}$ and 71.1% of $Slope_{10}$, while the noise for OCT was 1.8% of Range, 22.3% of $Slope_{Max}$ and 65.9% of $Slope_{10}$.

Conclusions: OCT is slightly less variable than SAP when couched in terms of its dynamic range or the expected rate of change in glaucoma clinical patients. However, the difference between the two is small.

Commercial Relationships: Cindy L. Blachly, None; Stuart K. Gardiner, Allergan (R); Brad Fortune, Heidelberg Engineering, GmbH (F), Carl Zeiss Meditec, Inc (F); Deborah Goren, None; Michael D. Whitworth, None; Steven L. Mansberger, Merck (R), Alcon (C), Allergan (C), Allergan (F), Merck (F), Santen (C), Glaukos (C); Shaban Demirel, Carl Zeiss Meditec (F), Heidelberg Engineering (R), Heidelberg Engineering (F)

Support: NIH Grant EY019674

Program Number: 1886 **Poster Board Number:** B0140

Presentation Time: 11:00 AM - 12:45 PM

Detectability of Visual Field Defects using 0.5 Degree Interval in High Resolution Perimetry and OCT Findings

Takuya Numata¹, Chota Matsumoto¹, Sachiko Okuyama¹, Sonoko Takada¹, Fumi Tanabe¹, Shigeki Hashimoto¹, Mariko Eura¹, Tomoyasu Kayazawa¹, Eiko Koike², Yoshikazu Shimomura¹.

¹Ophthalmology, Kinki University Faculty of Medicine, Osaka-Sayama, Japan; ²Sakai Hospital Kinki University Faculty of Medicine, Sakai, Japan.

Purpose: Visual field testing was performed using 0.5 degree interval in high resolution perimetry to assess detectability of visual field defects which were corresponded to OCT findings. Next, detectability of glaucoma-related visual field defects was investigated using measuring points of various intervals.

Methods: The subjects were 15 eyes of 15 patients with glaucoma and 15 eyes of 15 normal subjects. Octopus 900 Custom test program

was used with the target size 3 and background luminance of 31.4asb. Measuring points were placed on the meridian of 45 degree superior-temporally between the fixation point and the eccentricity of 30 degrees and visual field at each measuring point was assessed three times with the interval of 0.5 degree and high degree visual field profile was obtained. The blind spot was detected using Octopus 900 Custom test with the target size 1, the background luminance of 31.4asb, target luminance of 1000asb, and a grid pattern of 1 degree interval. Visual field was overlapped exactly to fundus findings by matching the blind spot with the visual angle of the fixation point in visual field and the center of the disc and fovea in scanning laser ophthalmoscopy (SLO). The corresponding structural findings were assessed using Cirrus HD-OCT with HD 5 Line Raster (1 line), 9 mm, High Definition Images. In normal eyes, visibility at retinal vessels was examined. In glaucoma cases, visual field profile was obtained using different degree intervals in 17 patterns from 0.5 degree to 8.5 degrees. Mean defect (MD), square root of loss variance (sLV) and maximum sensitivity decline amount in all degree intervals were examined.

Results: In all the normal eyes, visual field testing with 0.5 degree interval presented decreased sensitivity caused by blood vessels by the average and maximum of 1.1dB, and 4dB. In the glaucoma cases, the detectability of visual field defects decreased when measuring points were located at intervals larger than 2 degrees, 3 degrees, and 6 degrees; at the eccentricity smaller than 10 degrees, 10 to 20 degrees, and 20 to 30 degrees, respectively, however, the advanced cases were least affected.

Conclusions: Detectability for glaucoma-related visual field abnormality is greatly affected by the measuring point density. The higher resolution perimetry is desirable at the central visual field.

Commercial Relationships: Takuya Numata, None; Chota Matsumoto, None; Sachiko Okuyama, None; Sonoko Takada, None; Fumi Tanabe, None; Shigeki Hashimoto, None; Mariko Eura, None; Tomoyasu Kayazawa, None; Eiko Koike, None; Yoshikazu Shimomura, None

Program Number: 1887 **Poster Board Number:** B0141

Presentation Time: 11:00 AM - 12:45 PM

The Combined Structure and Function Index as a Predictor of Glaucoma Development

Daniel Meira-Freitas^{1,2}, Renato Lisboa^{1,2}, Andrew J. Tatham¹, Linda M. Zangwill¹, Robert N. Weinreb¹, Christopher A. Girkin³, Jeffrey M. Liebmann⁴, Tammy T. Kuang^{1,5}, Christopher Bowd¹, Felipe A. Medeiros¹.

¹Hamilton Glaucoma Center, Department of Ophthalmology, University of California, San Diego, La Jolla, CA; ²Department of Ophthalmology, Federal University of São Paulo, São Paulo, Brazil; ³Department of Ophthalmology, University of Alabama, Birmingham, AL; ⁴Department of Ophthalmology, New York Eye and Ear Infirmary, New York, NY; ⁵Department of Ophthalmology, Taipei Veterans General Hospital, Taipei, Taiwan.

Purpose: To assess whether baseline combined structure and function index (CSFI) results are predictive of conversion to glaucoma in patients suspected of having the disease.

Methods: The study included 345 glaucoma suspect eyes at baseline followed for an average of 74.8 months in the Diagnostic Innovations in Glaucoma Study (DIGS) and the African Descent and Glaucoma Evaluation Study (ADAGES). All eyes had normal standard automated perimetry (SAP) at baseline. Retinal nerve fiber layer (RNFL) thickness assessment was performed with time domain optical coherence tomography (OCT). Conversion was defined as development of repeatable abnormal SAP or progressive optic disc changes during follow-up. Estimates of the number of retinal ganglion cells were obtained by combining data from SAP and OCT

according to a previously described method. The CSFI was calculated as the age-corrected percent loss of retinal ganglion cells. The association between baseline predictive factors and conversion to glaucoma was investigated with Cox proportional hazards models. Multivariable models were adjusted for age, intraocular pressure and central corneal thickness. The c-index and the modified R² index were used to evaluate and compare predictive abilities of different models.

Results: Fifty-eight (16.8%) eyes converted to glaucoma. Mean baseline CSFI was 14.1% and 0.2% in the converters and nonconverters, respectively. Table 1 shows hazard ratios with 95% confidence interval (CI) for each putative predictive factor for development of conversion. In the multivariable model, higher CSFI was predictive of conversion (adjusted hazard ratio=2.08 per 10% higher; 95%CI: 1.70-2.56; P<0.001). Model including CSFI had superior predictive ability (c-index=0.770; R²=55%) compared to models including standard visual field parameters and OCT average RNFL thickness (c-index from 0.648-0.718; R² from 15-39% - table 2).

Conclusions: Baseline CSFI values were predictive of conversion to glaucoma and performed significantly better than conventional approaches for risk stratification of glaucoma suspects.

Table 1. Univariable and Multivariable Hazard Ratios with 95% Confidence Intervals for the Development of Visual Field Loss or Optic Disc Deterioration

Variables	Univariable	Multivariable [#]
	HR (95% CI)	HR (95% CI)
Age (per decade older)	1.43* (1.11-1.84)	-
IOP (per 1 mmHg higher)	1.02 (0.97-1.07)	-
CCT (per 40µm thinner)	0.86 (0.66-1.12)	-
SAP MD (per 1 dB lower)	1.81* (1.37-2.40)	1.82* (1.37-2.42)
SAP PSD (per 0.2 dB larger)	1.22* (1.05-1.41)	1.20* (1.02-1.40)
SAP VFI (per 1% lower)	1.82* (1.41-2.34)	1.77* (1.37-2.29)
OCT RNFL average thickness (per 10µm thinner)	2.00* (1.59-2.50)	1.96* (1.55-2.48)
wrgc (per 100,000 cells lower)	1.87* (1.55-2.25)	2.03* (1.62-2.53)
CSFI (per 10% higher)	2.03* (1.66-2.50)	2.08* (1.70-2.56)

Abbreviations: HR, Hazard Ratio; CI, Confidence Intervals; IOP, intraocular pressure; CCT, central corneal thickness; SAP, standard automated perimetry; MD, mean deviation; PSD, pattern standard deviation; VFI, visual field index; OCT, optical coherence tomography; RNFL, retinal nerve fiber layer; wrgc, weighted estimate of the number of retinal ganglion cells; CSFI, combined structure and function index.

*Significant at P < 0.05.

[#]Each multivariable models adjusted for Age, IOP and CCT.

Table 2. Predictive ability of each factor as measured by c-index and modified R² index for the multivariable models

Predictive factors	c-index*	R ² (95% CI)*
SAP MD	0.699	28 (14-51)
SAP PSD	0.648	15 (6-34)
SAP VFI	0.688	26 (13-49)
OCT RNFL average thickness	0.718	39 (24-60)
wrgc	0.742	47 (29-66)
CSFI	0.770	55 (39-72)

Abbreviations: SAP, standard automated perimetry; MD, mean deviation; PSD, pattern standard deviation; VFI, visual field index; OCT, optical coherence tomography; RNFL, retinal nerve fiber layer; wrgc, weighted estimate of the number of retinal ganglion cells; CSFI, combined structure and function index.

*The c-index and modified R² index are given for each factor, adjusted for baseline age, baseline intraocular pressure and central corneal thickness.

Commercial Relationships: Daniel Meira-Freitas, None; Renato Lisboa, None; Andrew J. Tatham, None; Linda M. Zangwill, Carl Zeiss Meditec Inc (F), Heidelberg Engineering GmbH (F), Optovue Inc (F), Topcon Medical Systems Inc (F), Nidek Inc (F); Robert N. Weinreb, Aerie (F), Alcon (C), Allergan (C), Altheos (C), Amakem (C), Bausch&Lomb (C), Carl Zeiss-Meditec (C), Genentech (F), Haag-Streit (F), Heidelberg Engineering (F), Konan (F), Lumenis (F), National Eye Institute (F), Nidek (F), Optovue (C), Quark (C), Solx (C), Topcon (C); Christopher A. Girkin, SOLX (F), Heidelberg Engineering (F); Jeffrey M. Liebmann, Alcon Laboratories, Inc. (C), Allergan, Inc. (C), Allergan, Inc. (F), Carl Zeiss Meditec, Inc (F), Heidelberg Engineering, GmbH (F), Topcon Medical Systems,

Inc. (F), National Eye Institute (F), New York Glaucoma Research Institute (F), SOLX, Inc. (C), Bausch & Lomb, Inc (C), Diopsys, Inc. (C), Diopsys, Inc. (F), Merz, Inc. (C), Glaukos, Inc. (C), Quark, Inc. (C); Tammy T. Kuang, None; Christopher Bowd, None; Felipe A. Medeiros, Carl-Zeiss (F), Heidelberg Engineering (F), Topcon (F), Alcon (F), Allergan (F), Sensimed (F), Reichert (F)

Support: National Institutes of Health/National Eye Institute grants EY021818 (F.A.M.), EY11008 (L.M.Z.), EY14267 (L.M.Z.), EY019869 (L.M.Z.); Brazilian National Research Council-CNPq grant 200178/2012-1 (D.M.F); an unrestricted grant from Research to Prevent Blindness (New York, NY); grants for participants' glaucoma medications from Alcon, Allergan, Pfizer, Merck and Santen.

Program Number: 1888 **Poster Board Number:** B0142

Presentation Time: 11:00 AM - 12:45 PM

Reproducibility of In Vivo Lamellar and Pre-lamellar Tissues Measurements with Enhanced Depth Imaging Spectral-Domain Optical Coherence Tomography

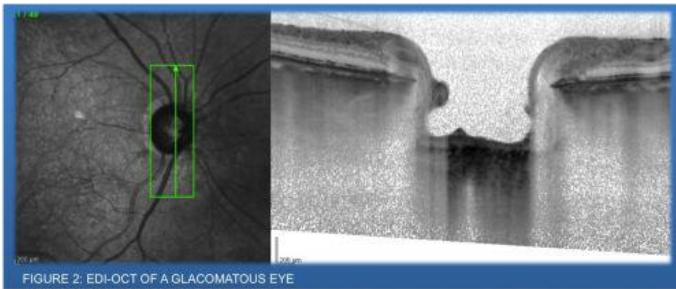
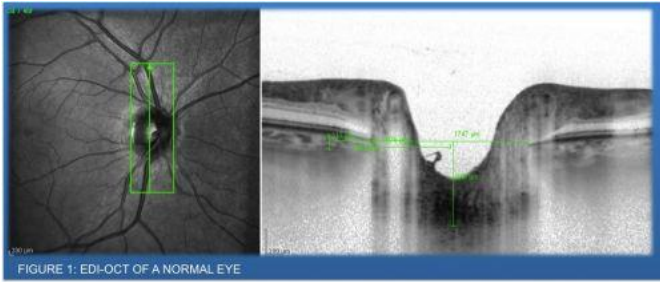
Vitor G. Prado, Paula D. Silva, Paula D. Borba, Igor Matsubara, Augusto Paranhos, Roberto M. Vessani, Tiago S. Prata. Ophthalmology, Federal Univ of Sao Paulo, Sao Paulo, Brazil.

Purpose: To determine the interobserver and intraobserver reproducibility of different optic nerve head (ONH) parameters measurements performed by enhanced depth imaging spectral-domain optical coherence tomography (EDI-OCT) in a population with and without glaucoma.

Methods: We prospectively enrolled glaucomatous patients (glaucomatous optic neuropathy and reproducible visual field defect) and healthy individuals from August 2012 to October 2012. Those with significant media opacity or any ocular disease (besides glaucoma) were excluded. All participants underwent EDI-OCT (SD-OCT; Spectralis®, Wavelength: 870nm; Heidelberg Engineering Co., Heidelberg, Germany). The following ONH parameters were evaluated: lamina cribrosa and pre-lamellar neural tissue thicknesses, scleral canal diameter (Bruch's membrane opening) and cup depth. To examine the inter-observer reproducibility, two independent examiners assessed all images. To examine the intraobserver repeatability, each examiner evaluated each set of images twice. For each EDI-OCT parameter, repeatability and reproducibility were assessed using within-subject standard deviation (Sw) and coefficient of variation (COV; 100%×Sw/overall mean), repeatability coefficient (RC; 1.96×√(2S2w) or 2.77 Sw), intraclass correlation coefficient (ICC; measurement of inter-rater reliability; set for absolute agreement) and Kappa (inter-rater agreement).

Results: A total 19 eyes of 19 patients were included. Overall, all ONH parameters assessed by EDI-OCT showed good repeatability results (Sw range, 4.7 - 19.1 µm; COV range, 0.55% - 7.3%; RC range, 13.1 - 52.9 µm). Judged by the COV, scleral canal diameter had the best and lamina cribrosa thickness had the worst intraobserver repeatability. Judged by the ICC (range, 0.70 - 0.99) and kappa values (range, 0.39 - 0.78), scleral canal diameter and cup depth had the best and lamina cribrosa thickness had the worst interobserver reliability and inter-rater agreement.

Conclusions: Based on manual measurements performed by experienced examiners, most ONH parameters assessed by EDI-OCT showed good intraobserver and interobserver reproducibility. Best results were found for pre-lamellar tissues and landmarks compared to deeper ONH structures, such as the lamina cribrosa.



Commercial Relationships: Vitor G. Prado, None; Paula D. Silva, None; Paula D. Borba, None; Igor Matsubara, None; Augusto Paranhos, Allergan (F), MSD (F); Roberto M. Vessani, ALLERGAN (R); Tiago S. Prata, Allergan (F), Merck (F), Alcon (F), Germed (C)

Program Number: 1889 **Poster Board Number:** B0143
Presentation Time: 11:00 AM - 12:45 PM

The Impact of Lens Vault on Visual Acuity and Refractive Error in Subjects with Angle Closure

Shweta Singhal¹, Stephen Stewart², Monisha E. Nongpiur^{1,3}, Hla M. Htoon^{1,3}, Shamira Perera¹, Tin Aung^{1,4}. ¹Singapore Eye Research Institute and Singapore National Eye Centre, Singapore, Singapore; ²University College London, London, United Kingdom; ³Duke-NUS Graduate Medical School, Singapore, Singapore; ⁴Yong Loo Lin School of Medicine, National University of Singapore, Singapore, Singapore.

Purpose: To investigate the relationship between lens vault (LV) and visual acuity in subjects with angle closure.

Methods: This was a cross-sectional study of 2047 subjects aged 50 years or more who were recruited from a community polyclinic. All participants underwent a standardized ocular examination and anterior segment optical coherence tomography (ASOCT). Customised software was used to measure LV, defined as the perpendicular distance between the anterior pole of the crystalline lens and the horizontal line joining the 2 scleral spurs, on horizontal ASOCT scans. Visual acuity was measured using a logarithm of minimum angle of resolution chart (logMAR chart, Lighthouse Inc, Long Island, New York). Visual acuity was classified as normal (logMAR<0.3), mild impairment (0.3<logMAR<0.6) and moderate/severe impairment (logMAR>0.6). Refraction was measured with an autorefractor machine (Topcon Auto K KR7100D, Topcon Corp, Tokyo, Japan). Spherical equivalent was defined as sphere plus half cylinder. An eye was defined as having angle closure if the posterior pigmented trabecular meshwork was not visualized for at least 180° on gonioscopy.

Results: Complete data on 1453 subjects including 311 with angle closure were available for analysis. Eyes with angle closure were significantly older (p< 0.001), with shorter axial length (AL, p< 0.001) and shallower anterior chamber depth (ACD, p< 0.001).

However, although eyes with angle closure had a significantly greater LV (p< 0.001), there was no significant difference in visual acuity (p=0.14) compared to those with open angles. The majority of angle closure subjects had normal visual acuity or mild visual impairment (85.2%). No significant trend was noted in visual acuity (p=0.12) or spherical equivalent (p=0.63) with increasing magnitude of LV. After adjusting for age, gender, AL, ACD, and spherical equivalent, there was no significant correlation between LV and visual acuity (p = 0.35). Similarly, no significant association was found between LV and spherical equivalent (p=0.06).

Conclusions: No association was found between lens vault and visual acuity or refractive error. Subjects with angle closure may have large LV but good visual acuity.

Commercial Relationships: Shweta Singhal, None; Stephen Stewart, None; Monisha E. Nongpiur, None; Hla M. Htoon, None; Shamira Perera, Carl Zeiss Meditec (R), Allergan (R), Pfizer (R); Tin Aung, Alcon (R), Alcon (C), Alcon (F), Allergan (R), Allergan (C), Carl Zeiss Meditec (F), Carl Zeiss Meditec (R), Ellex (F), Ellex (R), Santen (R)

Support: National Medical Research Council, Singapore and Biomedical Research Council, Singapore

Program Number: 1890 **Poster Board Number:** B0144
Presentation Time: 11:00 AM - 12:45 PM

The optic nerve head: does size matter?

Barbara Zangerl, Elizabeth Y. Wong, Nayuta Yoshioka, Michael P. Hennessy, Michael Kalloniatis. Centre for Eye Health, School of Optometry and Vision Science, The University of New South Wales, Kensington, NSW, Australia.

Purpose: Glaucomatous change, the most common form of optic nerve head (ONH) disease and main cause for vision impairment in aging populations, is intricately linked to disc size. Yet, current methods assessing the ONH are highly subjective and may be unreliable. The disc damage likelihood scale (DDLS), current “gold standard” in glaucoma assessment, relies on size evaluation most commonly obtained by slit lamp exam. We aimed to develop improved methods for this initial step that may aid accurate classification of the ONH and improve glaucoma diagnosis.

Methods: The optic nerve head was visualized by four standard methods: (1) Haag-Streit slit lamp BQ900 in combination with a Volk Super 66D lens (SL), (2) Kowa nonmyd™ WX^{3D} retinal camera at 45° in normal mode (RP), (3) Heidelberg Retina Tomograph (HRT), and (4) Cirrus HD-OCT. Automated calculation with the Cirrus HD-OCT ONH and RNFL OU Analysis function was compared to subjective measurements obtained by experienced clinicians. Statistical analysis was performed to calculate reproducibility and accuracy of the methods.

Results: Intraclinician variation using different methods was typically around 10%, with a maximum of 56%. Interclinician measurements obtained from Cirrus HD-OCT images were most reproducible (variance < 5%) and highly correlated with automated values (R²=0.97, p<0.01), while HRT based disc size showed poor correlation with the automated system (R²=0.80, p<0.01). RP and SL both correlated equally well with the Cirrus ONH size (R²=0.90, p<0.01), but disc size was, on average, smaller with RP (0.15±0.14mm²) and larger with SL (0.38±0.17mm²) resulting in a potential overestimated or underestimation of damage, respectively. While interclinician variance was comparable between HRT and RP (≤28%), SL assessments appeared not easily reproducible (≤58% variance).

Conclusions: ONH assessment based on imaging from the Cirrus HD-OCT resulted in the least stratification between operators and the best correlation to the automated calculation, constituting the most

robust method. However, the required equipment is highly specialized and costly. Based on current results, we propose use of retinal photography as a sustainable alternative. Thus, our results provide a basis to adjust current methods and adopt a unified system for ONH assessments to improve diagnostics for glaucoma and other ONH diseases.

Commercial Relationships: Barbara Zangerl, None; Elizabeth Y. Wong, None; Nayuta Yoshioka, None; Michael P. Hennessy, None; Michael Kalloniatis, None
Support: NHMRC APP1033224

Program Number: 1891 **Poster Board Number:** B0145

Presentation Time: 11:00 AM - 12:45 PM

Predicting standard automated perimetry (SAP) sensitivities from spectral domain optical coherence tomography (SD-OCT) retinal nerve fiber layer thickness (RNFLT) using temporally correlated data

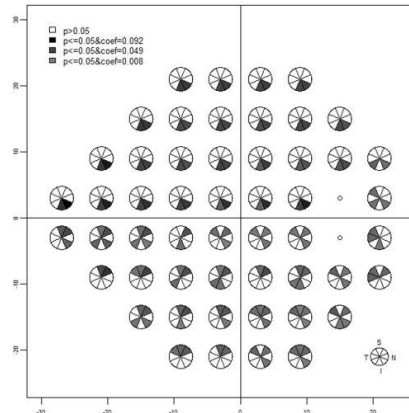
Lisha Deng, Deborah Goren, Manoj Pathak, Shaban Demirel, Stuart K. Gardiner. Discoveries in Sight, Devers Eye Institute, Portland, OR.

Purpose: Cross sectional analyses have been employed to study the association between SAP sensitivities and SD-OCT RNFLT. Longitudinal datasets have only become available recently. Such data provide large sample sizes due to repeat visits per subject while reducing the patient recruitment burden. If correlations between visits are accounted for, this method allows more powerful data analysis, which can be used to assess the structure-function relation.

Methods: 328 eyes of 164 subjects with mild to moderate glaucoma or risk factors for its development were tested for a minimum of 5 visits at six month intervals. SD-OCT circle sweeps (TSNIT Average: Mean 88.02µm, 95% confidence limits 111.52µm - 52.0µm) and SAP 24-2 SITA visual fields (MD: Mean -0.43dB, 95% confidence limits -9.19dB - 2.47dB) were performed. Sensitivity at each of the 52 non-blindspot locations was modeled with a two-level (subject, eye within subject) linear mixed effects model including exponential temporal auto-correlation that accounted for correlations across visits (i.e. over time) and between fellow eyes of an individual. Retinal nerve fibre layer thicknesses (RNFLT) at eight 45° sectors were used to predict visual field sensitivity. Backwards elimination was used to identify the strongest SD-OCT sector predictors of sensitivity for each location by stepwise removal of sectors with negative coefficients or non-significant p-values ($p > 0.05$, one-tailed).

Results: For all visual field locations two-level linear mixed effects models provided good fits to the data. All upper hemifield visual field locations resulted in significant positive coefficients ($p < 0.05$) from inferior and/or inferonasal SD-OCT sectors. Lower hemifield locations were noisier. 25 of the 26 inferior hemifield locations resulted in significant positive coefficients ($p < 0.05$) for the superonasal sector.

Conclusions: Visual field sensitivities can be predicted using two-level linear mixed effects models that account for correlations between eyes and temporal auto-correlation within sequences. As expected, upper hemifield locations were modeled best by inferior and inferonasal RNFL sectors, whereas lower hemifield locations were modeled best by the superonasal sector.



Significant sector predictors of visual field sensitivities

Commercial Relationships: Lisha Deng, None; Deborah Goren, None; Manoj Pathak, None; Shaban Demirel, Carl Zeiss Meditec (F), Heidelberg Engineering (R), Heidelberg Engineering (F); Stuart K. Gardiner, Allergan (R)

Support: NIH Grants R01 EY020922, R01 EY019674

Program Number: 1892 **Poster Board Number:** B0146

Presentation Time: 11:00 AM - 12:45 PM

OPTIC NERVE AND LATERAL GENICULATE BODY IN GLAUCOMA AND ITS ASSOCIATION WITH FUNCTIONAL AN STRUCTURAL OCULAR ALTERATIONS

Augusto Paranhos^{1,2}, Rafael L. Furlanetto¹, Sergio H. Teixeira^{1,2}, Claudio L. Lottenberg^{2,1}, Daniela B. Almeida-Freitas^{2,1}, Edson Amaro^{2,1}. ¹Oftalm-Inst da Visao/EP, Federal Univ of Sao Paulo, Sao Paulo, Brazil; ²Hospital Israelita Albert Einstein, Sao Paulo, Brazil.

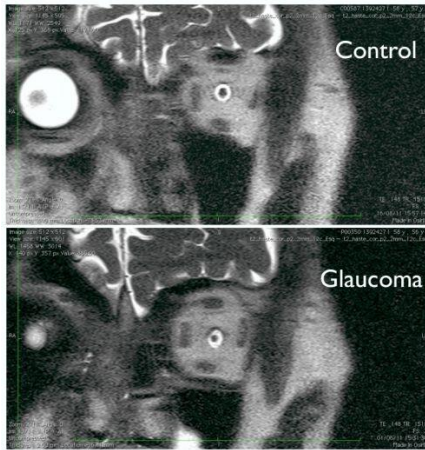
Purpose: To analyze the correlation between 3-Tesla high-speed magnetic resonance imaging (MR) findings of the intraorbital optic nerve and lateral geniculate body (LGB), and structural evaluation of the optic nerve head or visual function assessed by psychophysical tests in glaucomatous patients.

Methods: This was a cross-sectional prospective study including healthy volunteers and glaucoma patients. All participants performed SITA-standard 24-2 automated perimetry (SAP) and frequency doubling perimetry (FDT) (psychophysical tests), optic disc stereophotograph, spectral-domain optical coherence tomography (OCT), confocal scanning laser tomography (HRT), (structural evaluation) and MR. Anatomic-functional correlation was performed with Generalized Linear Models.

Results: 41 glaucoma patients and 12 healthy volunteers were included and 56,86% was female. Mean age was 62,87±0,71 years in glaucoma group and 62,3±6,17 healthy group. There was a significant difference between the height of LGB in glaucoma group (mean: 0.38 mm) and in the control group (mean: 0.41 mm), $p = 0.005$. No significant difference was found regarding base length and area of LGB between the two groups. Regarding orbital segment area of the optic nerve, a significant difference between the two groups was found 5mm from the globe ($P = 0.003$) but not for 10 mm and 15 mm ($P > 0.05$). LGB parameters were not significantly associated with any structural parameter tested (Average OCT RNFL thickness, HRT cup/disk ratio, stereo photo cup/disk ratio) as well as for any functional parameter (SAP MD, SAP VFI and FDT MD). Proximal (5mm) intraorbital optic nerve area was significant correlated with FDT MD ($p = 0.008$) but with no other tested parameter.

Conclusions: Glaucoma patients presented a significant difference in height of LGB as well as a lower area of the proximal (5mm)

intraorbital optic nerve segment. Functional and structural ocular parameters were not well associated with both intraorbital optic nerve segment areas or LGB parameters.



Commercial Relationships: Augusto Paranhos, Allergan (F), MSD (F); Rafael L. Furlanetto, None; Sergio H. Teixeira, None; Claudio L. Lottenberg, None; Daniela B. Almeida-Freitas, None; Edson Amaro, None

Program Number: 1893 **Poster Board Number:** B0147
Presentation Time: 11:00 AM - 12:45 PM

Relationship Between Relative Afferent Pupillary Defect with Pupillography and Ganglion Cell Complex Thickness by Optical Coherence Tomography in Asymmetric Glaucoma

Naoki Ozeki, Kenya Yuki, Daisuke Shiba, Kazuo Tsubota. Keio University, Tokyo, Japan.

Purpose: To evaluate association between the magnitude of relative afferent pupillary defect (RAPD) with pupillography and macular ganglion cell complex thickness (MGCCT) in asymmetric glaucoma.

Methods: We used RAPDx (Konan Medical USA, USA) to evaluate RAPD. The RAPDx is designed to analyze pupil response at multiple, controlled stimulus intensities and multiple color stimuli (white, red, green, blue and yellow). This device records precise amplitude and latency of pupil responses. Inclusion criteria were having optic disc abnormalities and visual field loss with glaucoma. Patients with having retinal disease, optic neuropathy, cornea disease, non-reactive pupils and asymmetric cataract were excluded. MGCCT was measured with spectral domain optical coherence tomography (RS-3000; Nidek, Japan). We evaluated association between asymmetry of the macular MGCCT and RAPDx amplitude and latency of multiple color stimuli (white, red, green, blue and yellow).

Results: Fifty six glaucoma patients (34 males, 22 females; mean age: 62.6 ± 12.0 years; range: 28 - 88 years) were enrolled. Mean MGCCT were 88.9 ± 12.2 (range: 56 - 112) μ m in thicker eyes and 76.3 ± 12.5 (range: 53 - 103) μ m in thinner eyes. The differences of MGCCT (thicker eye - thinner eye) were 12.7 ± 10.8 (range: 1 - 40) μ m. The log-scaled RAPD amplitude were as follows; white 0.37 ± 0.47 , red 0.26 ± 0.78 , green 0.33 ± 0.54 , blue 0.40 ± 0.62 , yellow 0.35 ± 0.56 . The results of linear regression analysis between the log-scaled RAPD amplitude and the MGCCT asymmetry were as follows; white $R^2 = 0.44$ ($p < 0.001$), red $R^2 = 0.29$ ($p < 0.001$), green $R^2 = 0.27$ ($p < 0.001$), blue $R^2 = 0.24$ ($p < 0.001$), yellow $R^2 = 0.25$ ($p < 0.001$). The log-scaled RAPD latency were as follows; white 0.09 ± 0.23 , red -0.01 ± 0.38 , green 0.12 ± 0.39 , blue 0.07 ± 0.54 , yellow -0.04 ± 0.21 . The results of linear regression analysis between the log-scaled RAPD latency and the MGCCT asymmetry were as follows; white $R^2 = 0.07$ ($p = 0.04$), red $R^2 = 0.001$ ($p = 0.76$), green $R^2 =$

0.04 ($p = 0.15$), blue $R^2 = 0.05$ ($p = 0.08$), yellow $R^2 = 0.02$ ($p = 0.25$).

Conclusions: Log-scaled RAPD amplitude had moderate correlation to MGCCT asymmetry, however RAPD latency had weaker relationship to MGCCT asymmetry. White stimulus had stronger relationship to MGCCT asymmetry than other colored stimuli.

Commercial Relationships: Naoki Ozeki, Konan Medical USA (F); Kenya Yuki, None; Daisuke Shiba, Konan Medical USA (F); Kazuo Tsubota, AcuFocus, Inc (C), Allergan (F), Bausch Lomb Surgical (C), Functional visual acuity meter (P), JiNS (P), Kissei (F), Kowa (F), Santen, Inc. (F), Otsuka (F), Pfizer (C), Thea (C), Echo Denki (P), Nidek (F), Ophtecs (F), Wakasa Seikatsu (F), CEPT Company (P)

Support: None in the Support

Program Number: 1894 **Poster Board Number:** B0148

Presentation Time: 11:00 AM - 12:45 PM

Retinotopic-specific changes of cerebral blood flow and grey matter density in visual cortex of patients with glaucoma

Zhang Shaodan^{1,4}, Bo Wang², Yuan Xie³, Chun Zhang⁴, Ningli Wang³. ¹Department of Ophthalmology, The 4th People's Hospital of Shenyang, Shenyang, China; ²State Key Laboratory of Brain and Cognitive Science, Institute of Biophysics, Chinese Academy of Sciences, Beijing, China; ³Beijing TongRen Eye Center, Beijing TongRen Hospital, Capital Medical University, Beijing, China; ⁴Department of Ophthalmology, Peking University Third Hospital, Peking University Health Science Center, Beijing, China.

Purpose: To investigate the impact of glaucoma on the cerebral blood flow (CBF) and grey matter density in patients with primary open angle glaucoma (POAG).

Methods: POAG patients with obvious visual field loss (mean deviation, MD < -6 dB) and best-corrected visual acuity of 20/40 or better were enrolled. Central 5° visual field in bilateral eyes must be reserved. History of cardiovascular diseases and other systemic disorders were excluded. Age and gender matched healthy subjects were enrolled as controls. T1-weighted anatomic images were acquired by a 3-Tesla MRI scanner (Trio; Siemens, Erlangen, Germany). Arterial spin labeling (ASL) MRI were then performed either at baseline or when receiving monocular reversing checkerboard stimulation (8Hz) that presented to the central reserved visual field. The eye with more severe visual field loss was chosen in glaucoma patients, while in controls the study eye was chosen randomly. Grey matter density and cerebral blood flow in the whole brain between groups were compared.

Results: Comparing with controls, significant reduction of grey matter density was observed in the anterior part of calcarine sulcus in patients with POAG, which is considered to be the peripheral retina projection in the visual cortex. Whole brain ASL scanning revealed a decreased regional CBF in the same peripheral retinotopic region in occipital visual cortex of POAG patients at baseline. Monocular central visual field stimulation evoked significant increase of CBF in bilateral occipital poles in both controls and POAG patients. However, the activated voxels were much less in POAG patients than controls.

Conclusions: POAG patients may suffer from retinotopic specific structure and cerebrovascular alterations in the occipital visual cortex. CBF insufficiency may precede the visual field loss and grey matter changes in glaucoma, which, therefore, may be used as a promising indicator for detecting early glaucomatous neurodegeneration. Glaucoma patients may benefit from neuroprotective and vascular regulatory strategies targeting at whole visual pathway.

Commercial Relationships: Zhang Shaodan, None; Bo Wang, None; Yuan Xie, None; Chun Zhang, None; Ningli Wang, None
Support: National Nature Science Foundation of China [grant number, 81100661]; Postdoctoral Science Foundation of China [grant number, 20100480170]; Key Lab Open Foundation of Capital Medical University

Program Number: 1895 **Poster Board Number:** B0149
Presentation Time: 11:00 AM - 12:45 PM
Dynamic iris volume characteristics in the physiological range of pupil size and reproducibility of measurements in eyes with occludable anterior chamber angles: The Investigating Management of Angle Closure and Treatment (IMPACT) study
Humma Shahid¹, Laura Sanchez Parra^{2,3}, Roger Buckley², Shahina Pardhan², Rupert R. Bourne^{1,2}. ¹Ophthalmology, University of Cambridge Hospitals NHS Trust, Cambridge, United Kingdom; ²Vision & Eye Research Unit, Anglia Ruskin University, Cambridge, United Kingdom; ³Huntingdon Glaucoma & Diagnostic Research Centre, Hinchingsbrooke Hospital, Huntingdon, United Kingdom.

Purpose: Previous studies involving fellow eyes of patients in which the other eye has suffered an episode of acute angle closure (AAC) have reported increase in iris volume with pharmacological pupil dilation while normal irises lose volume- this 'iris sponge hypothesis' is thought

to explain the predisposition of these eyes to AAC. This study aimed to investigate physiological changes in iris volume in eyes with occludable angles but no history of AAC using three-dimensional anterior segment ocular coherence tomography (AS-OCT).

Methods: 69 eyes of 35 Caucasian patients with a gonioscopic diagnosis of Primary Angle Closure (PAC), Primary Angle Closure Suspect (PACS) or a combination of both conditions were included. The iris volume, angle opening distance (AOD), angle recess area (ARA), trabecular-iris space area (TISA) and trabecular-iris angle (TIA) were measured in superior, inferior, nasal and temporal meridians using the novel non-contact three-dimensional AS-OCT (CASIA) in dark and light conditions. All images were acquired and evaluated by a single observer. Measurements were repeated to check for intra-observer reliability. Statistical analysis involved a comparison of the change in total iris volume in dark and light conditions. Single and multiple predictor linear regression was performed to determine whether there was a relationship between change in iris volume between light and dark conditions and dimensions of the drainage angle.

Results: The total iris volume in dark conditions was always significantly lower than the volume in light conditions ($P=0.008$). Linear regression analysis showed that the change in iris volume between light and dark conditions was not influenced by differences in angle dimensions ($P>0.05$) in superior, inferior, nasal or temporal meridians. There was no significant interobserver error in iris volume measurements ($P>0.05$).

Conclusions: Three-dimensional anterior segment ocular coherence tomography is a reliable device for iris volume measurement with no significant intra-observer error. Eyes with occludable drainage angles but no history of acute angle closure exhibit a significant reduction in iris volume under physiological dark conditions. This observed change in iris volume is independent of the degree of angle narrowing.

Commercial Relationships: Humma Shahid, None; Laura Sanchez Parra, Allergan Ltd (F); Roger Buckley, None; Shahina Pardhan, None; Rupert R. Bourne, Allergan Ltd (F)
Support: Allergan Ltd

Clinical Trial: 8955

Program Number: 1896 **Poster Board Number:** B0150
Presentation Time: 11:00 AM - 12:45 PM
Comparison of optic disc parameters obtained by simultaneous stereo fundus photography and spectral domain optical coherence tomography

Aiko Iwase¹, Toshiaki Nakagawa³, Makoto Araie². ¹Tajimi Iwase Eye Clinic, Tajimi, Japan; ²Kanto Central Hospital, Tokyo, Japan; ³Kowa, Co. Ltd., Hamamatsu, Japan.

Purpose: Optic disc evaluation from stereo fundus photographs (SFP) by experienced examiners still remain the worldwide standard of glaucoma assessment both in clinical practice and the mass screening of glaucoma, while optic disc morphologic parameters (ODMP) obtained by SD-OCT are going to be widely used in clinical practice. We correlated ODMP obtained using a newly developed simultaneous stereo fundus camera system (Nonmyd WX, Kowa Co. Ltd., Japan: WX) to those obtained using a SD-OCT instrument widely used (Cirrus, Carl Zeiss Meditec, Dublin, CA: Cirrus).

Methods: The study included 29 eyes of 15 glaucoma patients (Age = 68.4 ± 9.4 yrs, MD = -8.6 ± 4.6 dB) who underwent imaging of the optic disc using WX and Cirrus at intervals within 1 month. In WX system, an experienced investigator determined the disc and cup contours viewed using a stereo glass and vertical cup/disc (V-C/D) ratio, disc area (DA) and rim area (RA), and cup volume (CV) were calculated using with 3-dimensional analysis software (VK-2 WX, Kowa) where correction for magnification was done using Gullstrand schematic eye (Optic disc parameters I: ODP1) or by entering refraction and corneal curvature of each eye (ODP2). V-C/D, DA and RA and CV by Cirrus were obtained using ONH analysis.

Results: V-C/D, DA, RA, CV obtained using ODP1 protocol were 0.82 ± 0.06 , 2.32 ± 0.48 mm², 0.83 ± 0.23 mm² and 0.35 ± 0.18 mm³, and those obtained using ODP2 protocol 0.82 ± 0.06 , 2.48 ± 0.53 mm², 0.83 ± 0.27 mm² and 0.40 ± 0.21 mm³, and corresponding figures obtained using Cirrus were 0.79 ± 0.09 , 1.89 ± 0.40 mm², 0.70 ± 0.21 mm² and 0.50 ± 0.33 mm³, respectively. V-C/D, DA and RA obtained using WX were greater ($P=0.000 \sim 0.044$, paired t-test), but CV smaller ($P=0.000$) than those with Cirrus. Spearman's correlation coefficients between ODP1 and Cirrus results were 0.497, 0.793, 0.631, 0.838 ($P<0.005$) for V-C/D, DA, RA and CV, and those between ODP2 and Cirrus results were 0.497, 0.899, 0.713, 0.845 ($P<0.005$). Correlation of Cirrus results to ODP2 was higher than that to ODP1 for DA ($P=0.047$).

Conclusions: ODMP values obtained with Nonmyd WX were well correlated to those with Cirrus and correction for magnification by entering refraction and corneal curvature of each eye improved correlation. V-C/D, DA, RA with the former system were 3.6%, 18.5%, 15.3% greater and CV 43.6% smaller than those with Cirrus.
Commercial Relationships: Aiko Iwase, Carl Zeiss (F), Topcon (F), Kowa (C); Toshiaki Nakagawa, Kowa Company, Ltd. (E); Makoto Araie, Kowa (C), Kowa (R), Zeiss (R), Topcon (R)

Program Number: 1897 **Poster Board Number:** B0151
Presentation Time: 11:00 AM - 12:45 PM
Stereometric parameters of optic disc. Comparison between the Heidelberg Retina Tomograph and Three-Dimensional Optical Coherence Tomography

Claudia Castillo Ayometzi, Francisco Ortega Santana, Alfonso García López. Hosp Nuestra Señora de la Luz, Mexico, Mexico.

Purpose: To study the variability of the stereometric parameters of optic disc between the Heidelberg Retina Tomograph III (HRT III) and Three-Dimensional Optical Coherence Tomography (3D OCT)

in normal subjects and in patients with Primary Open Angle Glaucoma (POAG).

Methods: This cross-sectional study included 18 eyes of normal patients and 35 eyes of POAG patients. Each patient underwent an HRT III examination and 3D OCT Topcon-1000 on the same day. All the examined subjects were older than 47 years. Excluded from the study were eyes with disc area higher than 2.43mm², hazy media, refractive anomalies (myopia higher than 5 diopters or astigmatism higher than 2 diopters) and eyes with other diseases rather than POAG. The analysis concerned the following topographical parameters of the optic nerve: disc area, cup area, rim area, cup volume, rim volume, cup/disc area ratio and linear cup/disc ratio. The means of the variables were calculated for the HRT III and 3D OCT in both groups. A T-test was used to compare the HRT III against 3D OCT.

Results: In normal eyes there was a significant difference ($p < 0.001$) of cup area, cup volume, rim volume, cup/disc ratio and linear cup/ratio between the HRT III and the 3D OCT. In POAG eyes there was a significant difference ($p = < 0.003$) of disc area, cup area, cup/disc area ratio and linear cup/disc ratio. In both groups the 3D OCT overestimate the stereometric parameters of the HRT III.

Conclusions: There is a great variability of the stereometric parameters of optic disc between the Heidelberg Retina Tomograph and Three-Dimensional Optical Coherence Tomography in normal subjects and in patients with Primary Open Angle Glaucoma.

Commercial Relationships: Claudia Castillo Ayometzi, None; Francisco Ortega Santana, None; Alfonso García López, None

Program Number: 1898 **Poster Board Number:** B0152

Presentation Time: 11:00 AM - 12:45 PM

Longitudinal Analysis of Glaucoma Progression by Structure and Function: 7-year Follow-Up by Visual Field (VF) and Optical Coherence Tomography (OCT)

Igor I. Bussel¹, Gadi Wollstein¹, Richard A. Bilonick^{1,2}, Yun Ling^{1,2}, Hiroshi Ishikawa^{1,3}, Jessica E. Nevins¹, Larry Kagemann^{1,3}, Jay S. Duker⁴, Cynthia Mattox⁴, Joel S. Schuman^{1,3}. ¹UPMC Eye Center, Eye and Ear Institute, Ophthalmology and Visual Science Research Center, Department of Ophthalmology, University of Pittsburgh School of Medicine, Pittsburgh, PA; ²Department of Biostatistics, Graduate School of Public Health, University of Pittsburgh, Pittsburgh, PA; ³Department of Bioengineering, Swanson School of Engineering, University of Pittsburgh, Pittsburgh, PA; ⁴New England Eye Center, Tufts Medical Center, Boston, MA.

Purpose: To longitudinally evaluate glaucoma progression by structure and function measurements using VF and OCT in a long-term cohort.

Methods: Sixty eyes (4 healthy, 34 glaucoma suspect, and 22 glaucoma) from 31 subjects followed for an average of 7.4±2.3 years were enrolled to the study. All subjects had ≥5 reliable VF and good quality OCT scans (OCT1, OCT2, Stratus OCT). VF Mean deviation (MD) and OCT mean retinal nerve fiber layer (RNFL) thickness were recorded. A structural equation measurement error model was used to calibrate measurements from multiple OCT devices. VF progression was defined as a decline ≥2dB in MD from baseline, and OCT mean RNFL thinning ≥20µm. Overall trend of VF and OCT progression was also calculated using a linear mixed-effects model and the upper quartile slopes representing rapid progressors were compared.

Results: Qualified subjects had a median of 12 VF and 27 OCT scans. A total of 41 eyes (68.3%) progressed by MD and RNFL criteria with 46.7%, 10.0%, and 11.7% by OCT only, VF only, and both, respectively. From the 7 eyes that progressed by both, 3 eyes progressed by structure and function simultaneously, 3 progressed by OCT before VF, and 1 progressed by VF before OCT. Using the

same progression criteria after 4, 5, 6, and 7 years of follow-up, there was a gradual increase in the number of progressors with all criteria with the agreement between both devices increasing from 6% to 14%. 53% of eyes that were defined as OCT rapid progressors were also labeled as VF rapid progressors.

Conclusions: Though we expected an improved agreement between structure and function in glaucoma progression over the extended follow-up duration, there was only marginal increase in agreement at the tested time points with substantially higher percentage of progression with each modality separately. Therefore, even in an extended follow-up there may be limited detectable correspondence between structural and functional progression.

Commercial Relationships: Igor I. Bussel, None; Gadi Wollstein, Allergan (C); Richard A. Bilonick, None; Yun Ling, None; Hiroshi Ishikawa, None; Jessica E. Nevins, None; Larry Kagemann, None; Jay S. Duker, Carl Zeiss Meditech (F), OptoVue (F), Optos (C); Cynthia Mattox, None; Joel S. Schuman, Carl Zeiss Meditec, Inc. (P)

Support: NIH R01-EY013178, P30 EY008098; Eye and Ear Foundation (Pittsburgh, PA); Research to Prevent Blindness (New York, NY); Doris Duke Charitable Foundation.

Program Number: 1899 **Poster Board Number:** B0153

Presentation Time: 11:00 AM - 12:45 PM

Use of Optical Coherence Tomography in Clinical Practice: Does it Influence the Diagnostic Decision of Glaucoma Specialists and Non-specialists?

Carlos E. Barbosa, Luis G. Biteli, Roberto M. Vessani, Mauro T. Leite, Augusto Paranhos, Tiago S. Prata. UNIFESP, São Paulo, Brazil.

Purpose: To evaluate whether spectral domain optical coherence tomography results influence the diagnostic decision among glaucoma specialists and general ophthalmologists in a clinical setting

Methods: Four glaucoma specialists and seven non-specialists were enrolled in this observational study. The complete clinical data, including intraocular pressure, visual fields (VFs) and stereophotographs, of 10 patients were randomly presented to the examiners and they were required to classify each case in (1) glaucoma, (2) healthy or (3) inconclusive. Later, the SD-OCT results of each case were provided for the examiners, who were required to reassess their diagnosis. The 10 clinical cases consisted of glaucomatous and healthy patients. To be considered glaucomatous, patients had to have evidence of progressive glaucomatous optic neuropathy (GON) with normal VFs or suspicious appearance of the optic disc with peripapillary hemorrhage and normal/inconclusive VFs. Healthy patients had to have suspicious appearance of the optic disc, normal VFs and no evidence of progressive GON for at least 2 years without treatment. The follow-up visits, which were used to confirm the diagnosis, were not presented to the ophthalmologists. Kappa statistics was used to evaluate the agreement between glaucoma specialists and non-specialists

Results: Six glaucoma patients and four healthy individuals were enrolled. The glaucoma specialists were able to detect 33% of glaucoma cases before and 71% after the OCT imaging. Non-specialist were able to detect 40% of glaucoma cases before and 62% after the the OCT imaging. On the other hand, without the aid of SD-OCT, general ophthalmologists tended to misclassify more healthy cases as glaucomatous when compared to glaucoma specialists. The within group agreement for the glaucoma specialists group went from weak agreement ($k=0.19$) to fair agreement ($k=0.31$) after the OCT. The within group agreement for the non-specialists group was weak both before ($k=0.04$) and after ($k=0.07$) the OCT. Using the mode of

the answers in each group, the agreement between specialists and non-specialists went from fair agreement ($k=0.24$) to substantial agreement ($k=0.81$) after the OCT imaging

Conclusions: Ancillary imaging using SD-OCT yielded an increase in the agreement for the diagnostic decision between glaucoma specialists and general ophthalmologists

Commercial Relationships: Carlos E. Barbosa, None; Luis G. Biteli, None; Roberto M. Vessani, ALLERGAN (R); Mauro T. Leite, None; Augusto Paranhos, Allergan (F), MSD (F); Tiago S. Prata, Allergan (F), Merck (F), Alcon (F), Germed (C)

Program Number: 1900 **Poster Board Number:** B0154

Presentation Time: 11:00 AM - 12:45 PM

Bayesian Hierarchical Modelling of Longitudinal Visual Fields to Quantify Glaucoma Progression

Susan R. Bryan^{1,2}, Koenraad A. Vermeer¹, Paul H. Eilers², Hans G. Lemij³, Emmanuel Lesaffre^{2,4}. ¹Rotterdam Ophthalmic Institute, Rotterdam, Netherlands; ²Biostatistics, Erasmus Medical Center, Rotterdam, Netherlands; ³Glaucoma Service, Rotterdam Eye Hospital, Rotterdam, Netherlands; ⁴L-Biostat, KU Leuven, Leuven, Belgium.

Purpose: Evaluation of a longitudinal series of visual fields (VF) provides a method to quantify functional deterioration. Previous research focused on regression models for each location in the eye independently, ignoring that measurements belong to the same eye. To improve predictive ability, a method which explicitly takes into account the hierarchical structure of the data is needed. We propose such a model and evaluate its assumptions.

Methods: We propose the following Bayesian mixed effects model which takes into account the hierarchical structure of the data:

$$y_{ijk}(t) = \beta_0 + \beta_1 * t + b_{0i} + b_{1i} * t + \alpha_{0k(i)} + \alpha_{1k(i)} * t + \varepsilon_{ijk}$$

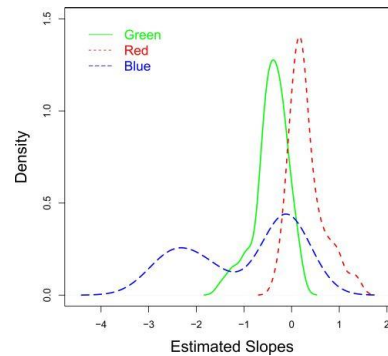
where i corresponds to individual, j to visit, k to location and t represents time. Glaucoma is a progressive disease, and the model takes this latent monotonic nature of the data into account by enforcing a negative slope:

$$\beta_1 * t + b_{1i} * t + \alpha_{1k(i)} * t \leq 0.$$

We used the slopes of 52 locations per eye (excluding blind spot) estimated by linear regression to evaluate possible assumptions for the priors in our model. 134 glaucoma patients from the Rotterdam Eye Hospital were included, with a minimum of 8 years follow-up and at least 15 HFA SITA standard white on white 24-2 fields per person. Both eyes were used in the analysis.

Results: We investigated the slopes estimated from linear regression models considering each location independently. An example of the distribution in 3 different eyes is shown in Figure 1. This shows that the magnitude of the slope is highly variable and the distribution of the slopes sometimes includes positive values (red) and may either be uni-modal (green) or a mixture of distributions (blue).

Conclusions: We proposed a method for modelling the progression of VFs which takes into account the hierarchical structure of the data and uses assumptions based on clinical properties of the data. The distributions of the estimated slopes vary. Hence the need for a mixture versus a particular parametric distribution for the location specific slopes should be considered. Even though some of the estimated slopes are positive, glaucoma is a progressive disease and hence we attribute these positive estimates to measurement error. Including factors which have been shown in the literature to influence measurements, such as test reliability, time of day and season, will take this error into account using our model.



Different distributions of estimated slopes

Commercial Relationships: Susan R. Bryan, None; Koenraad A. Vermeer, Heidelberg Engineering (F), General Hospital Corporation (P); Paul H. Eilers, None; Hans G. Lemij, Carl Zeiss Meditec (C); Emmanuel Lesaffre, Boehringer Ingelheim (F), Boehringer Ingelheim (C)

Program Number: 1901 **Poster Board Number:** B0155

Presentation Time: 11:00 AM - 12:45 PM

Effect of ocular curvature and myopia on retinal blood flow: a theoretical study

Andrea Dziubek¹, Giovanna Guidoboni², Anil N. Hirani³, Alon Harris⁴. ¹Engineering, Science, Mathematics, State University of New York Institute of Technology, Utica, NY; ²Mathematics, Indiana University Purdue University Indianapolis, Indianapolis, IN; ³Computer Science, University of Illinois at Urbana-Champaign, Urbana, IL; ⁴Ophthalmology, Indiana University School of Medicine, Indianapolis, IN.

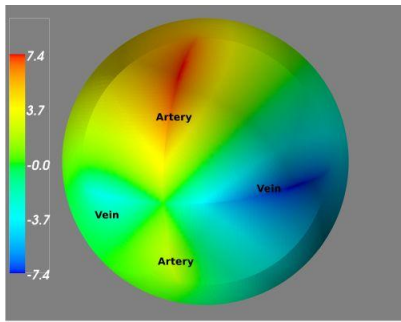
Purpose: Alterations of ocular curvature are involved in myopia, which is considered a risk factor for glaucoma. The mechanism by which myopia contributes to glaucoma remains unclear. In this study we test the hypothesis that blood flow alterations secondary to myopia contribute to glaucomatous optic neuropathy.

Methods: We use a mathematical model describing the blood flow in the retina as the flow of a fluid (blood) through a porous medium (retinal tissue). Distributions of blood velocity and pressure are obtained as the solutions of Darcy's equations via finite elements exterior calculus. Four main arterioles/veins are included as sources/sinks for the flow. We compare the pressure distributions obtained for the case of (1) a flat circular surface and (2) a hemispherical surface, when the same level of blood flow is imposed through the tissue.

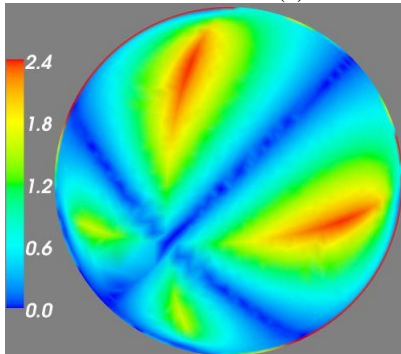
Results: Figure 1 shows the pressure distribution in case (1). The pressure distributions looks similar in both cases, but absolute pressure values differ. For a tissue permeability of $4.165 \text{ mms}^{-1} \text{ kPa}^{-1}$ and overall blood flow of $0.68 \text{ mm}^3 \text{ s}^{-1}$, maximal pressures are 5.0 kPa in case (1) and 7.4 kPa in case (2). Thus, the curved case needs higher pressures than the flat case to attain the same blood flow in the tissue. Also, for the same arterio/venous pressure difference, area of higher curvature experiences reduced blood flow. Figure 2 shows the pressure difference between case (1) and case (2) projected on the two-dimensional plane. The difference is larger when the distance to the arteries/veins is smaller and is least when the distance to the arteries and veins is equal. The maximal pressure difference reaches 32.4%, namely 2.4 kPa.

Conclusions: We computed and compared pressure distributions for retinal blood flow on flat and hemispherical surfaces. Ocular curvature has a noticeable effect in pressure distribution, with differences up to 32.4%. Our model suggests that alterations in ocular

curvature, such as those occurring in myopic eyes, might contribute to glaucomatous damage by reducing retinal blood flow.



Pressure distribution in case (2)



Pressure difference between case (1) and case (2)

Commercial Relationships: Andrea Dziubek, None; Giovanna Guidoboni, None; Anil N. Hirani, None; Alon Harris, MSD (R), Alcon (R), Merck (C), Pharmedica (C), ONO (C), Sucampo (C), Adom (I)

Program Number: 1902 **Poster Board Number:** B0156

Presentation Time: 11:00 AM - 12:45 PM

Relationship between the macular ganglion cell complex thickness and standard automated perimetry in glaucoma

Antonio Ferreras^{1,2}, Blanca Monsalve³, Pilar Calvo⁴, Ana B. Pajarin⁵, Paolo Frezzotti⁶, Paolo Fogagnolo⁷, Michele Figus⁸, Michele M. Iester⁹. ¹Ophthalmology, Miguel Servet University Hospital, Zaragoza, Spain; ²Ophthalmology, University of Zaragoza, Zaragoza, Spain; ³Ophthalmology, Hospital General Universitario Gregorio Marañón, Madrid, Spain; ⁴Ophthalmology, Toronto Western hospital, Toronto, ON, Canada; ⁵Family medicine, Centro de Salud Casablanca, Zaragoza, Spain; ⁶Ophthalmology, University of Siena, Siena, Italy; ⁷Ophthalmology, G.B. Bietti Foundation-IRCCS, Rome, Italy; ⁸Neuroscience, University of Pisa, Pisa, Italy; ⁹Ophthalmology, University of Genoa, Genoa, Italy.

Purpose: To assess the relationship between the macular thickness for the sum of the ganglion cell layer and inner plexiform layer (GCC) measured by spectral-domain optical coherence tomography (OCT) and white-on-white standard automated perimetry (SAP).

Methods: Forty-five healthy controls and 37 glaucoma patients were imaged with Cirrus OCT (Carl Zeiss Meditec, Dublin, Ca). Glaucomatous eyes had intraocular pressure higher than 20 mmHg and abnormal standard automated perimetry (Humphrey Field Analyzer, Carl Zeiss Meditec; 24-2 SITA Standard strategy). Only one eye per participant was randomly included in the statistical analysis. Left eye data were converted to a right eye format. The peripapillary retinal nerve fiber layer (RNFL) thicknesses, the optic nerve head (ONH) parameters and the GCC measurements obtained with Cirrus OCT were included in the study. After checking for a

normal distribution of the variables, Pearson correlations were calculated and compared between the OCT and the SAP parameters. The scatter diagrams and the regression lines were also plotted for the strongest correlations.

Results: Age and central corneal thickness did not differ significantly between the groups. Mean deviation of SAP was -6.86 ± 6.4 dB, in the glaucoma group. All OCT parameters were different between healthy and glaucoma patients except disc area and the RNFL thicknesses at the 3 and 9 clock hour positions. The control group had few mild correlations, while the glaucoma group showed moderate correlations between most OCT parameters and the visual field indices. In the whole population, the strongest correlation was observed between the temporal inferior GCC thickness and the pattern standard deviation (PSD) of SAP (-0.749 , $p < 0.001$). The strongest correlation for the RNFL parameters was found between the RNFL average thickness and the PSD of SAP (-0.677 , $p < 0.001$), while for the ONH parameters was found between the rim area and the PSD of SAP (-0.617 , $p < 0.001$). There were not significant differences between the best correlations of these parameters.

Conclusions: Moderate correlations were observed between the OCT parameters and the indices of SAP in glaucoma patients. The GCC parameters of Cirrus OCT had the strongest correlations with the visual field outcome. This relationship was linear.

Commercial Relationships: Antonio Ferreras, Alcon Laboratories, Inc (R), Allergan, Inc (R), Carl Zeiss Meditec (C), Heidelberg Engineering (F), Instituto Salud Carlos III (F), Novartis (R), Oculus, Inc (F); Blanca Monsalve, None; Pilar Calvo, None; Ana B. Pajarin, None; Paolo Frezzotti, None; Paolo Fogagnolo, None; Michele Figus, None; Michele M. Iester, None

Support: Supported in part by the Instituto de Salud Carlos III grant PI11/01239

Program Number: 1903 **Poster Board Number:** B0157

Presentation Time: 11:00 AM - 12:45 PM

Does Cerebrospinal Fluid Communicate with the Eye?

Emily Mathieu^{1,2}, Neeru Gupta^{2,4}, R. Loch Macdonald^{1,3}, Jinglu Ai^{1,3}, Yeni H. Yucel^{1,2}. ¹Keenan Research Centre at the Li Ka Shing Knowledge Institute, St. Michael's Hospital, Toronto, ON, Canada; ²Ophthalmology & Vision Sciences, Laboratory Medicine and Pathobiology, University of Toronto, Toronto, ON, Canada; ³Surgery, Division of Neurosurgery, St. Michael's Hospital, University of Toronto, Toronto, ON, Canada; ⁴Glaucoma & Nerve Protection Unit, St. Michael's Hospital, Toronto, ON, Canada.

Purpose: It has been suggested that a pressure gradient at the level of the lamina cribrosa between intraocular pressure and cerebrospinal fluid (CSF) may contribute to optic nerve damage in glaucoma. Any relationship between CSF and the eye is largely unknown. The purpose of this study is to determine whether CSF communicates with the eye.

Methods: All procedures adhered to the ARVO Statement for the Use of Animals. 11 mice (male 129SVE) were anesthetized with isoflurane and positioned in a stereotaxic frame (Kopf Instruments, Tujunga, CA). In 7 mice, 3 μ L of a fluorescent nanoparticle tracer, Quantum Dot 655 (QD; Invitrogen, Eugene, OR) was injected into the CSF of the cisterna magna through a suboccipital incision using stereotaxic technique. In controls (n=4) quantum dots were applied to the dura mater and not injected into CSF. Tracer-loaded CSF movement was visualized by *in vivo* hyperspectral imaging of the head and neck region (Maestro; CRI, Woburn, MA) at 20 and 40 minutes and 1, 2 and 6 hours after injection. Mice were sacrificed 6 hours after injection, whole head tissue blocks were fixed in paraformaldehyde, and frozen sections were scanned by hyperspectral imaging, using unmixing algorithms to separate signal

from background (Maestro 2.4 Imaging Software). All sections containing eyes were also imaged with fluorescence microscopy. **Results:** Hyperspectral analysis of head sections showed tracer in one or both eyes of 5 of 7 mice, 6 hours following injection into CSF. Quantum dots were detected in sclera, choroid and retinal tissues by fluorescence microscopy. *In vivo* imaging detected tracer in submandibular lymph nodes in all mice (n=7) after injection into CSF. Control mice (n=4) showed no signal in the eye or submandibular nodes.

Conclusions: There appears to be a communication between the CSF and eye in the mouse. Further studies are needed to elucidate the specific pathways involved and whether this communication is bidirectional. A better understanding of the relationship between these two compartments may help to understand optic nerve injury at the level of lamina cribrosa in glaucoma.

Commercial Relationships: Emily Mathieu, None; Neeru Gupta, None; R. Loch Macdonald, None; Jinglu Ai, None; Yeni H. Yucel, None

Support: Nicky and Thor Eaton Fund (NG), Canadian Institutes of Health Research MOP119432 (NG,YY), NSERC and Vision Science Research Program (EM)

274 Surgery and Laser

Monday, May 06, 2013 2:45 PM-4:30 PM

6B Paper Session

Program #/Board # Range: 2135-2141

Organizing Section: Glaucoma

Program Number: 2135

Presentation Time: 2:45 PM - 3:00 PM

Prospective Randomized Study Comparing ExPRESS to Trabeculectomy: 1 Year Results

Yvonne M. Buys¹, Lilach Drori Wagschal⁴, Yaping Jin², Delan Jinapriya³, Graham E. Trope¹. ¹Ophthalmology & Vision Sciences, University of Toronto, Toronto, ON, Canada; ²Dalla Lana School of Public Health, University of Toronto, Toronto, ON, Canada; ³Ophthalmology, Queen's University, Kingston, ON, Canada; ⁴Ophthalmology, Shaare Zedek Medical Center, Jerusalem, Israel.

Purpose: The ExPRESS device was introduced as an alternative to trabeculectomy with anticipated advantages of improved safety and consistency given the standardized lumen size and less tissue manipulation. Of 5 retrospective and 2 prospective studies, one reported more success with ExPRESS and one lower IOP with trabeculectomy. In addition 2 studies reported lower rates of early hypotony and 1 less choroidals following ExPRESS. We designed a prospective RCT to compare the efficacy and safety of ExPRESS to trabeculectomy.

Methods: This study was registered with the NIH (#NCT01263561). Consenting patients with open-angle glaucoma scheduled for filtration surgery were prospectively randomized to trabeculectomy or ExPRESS both with MMC. Exclusion criteria included; previous ocular incisional surgery (exception of clear cornea phaco or one previous trab), uveitis and vitreous in the A/C. The main outcome was IOP. Secondary outcomes included visual acuity (VA), # of glaucoma meds, complications, corneal pachymetry (CCT), endothelial cell counts (ECC), bleb morphology and additional procedures. Standardized data collection sheets were completed at baseline, day 1, weeks 1 & 2 and months 1, 2, 3, 6 and 12 post-op. A sample size calculation determined that 52 eyes were required to detect a 2 mmHg difference with a power of 80%.

Results: 61 of 64 enrolled patients completed 1-yr F/U (31 ExPRESS, 30 Trab). There were no differences in baseline

characteristics. The mean baseline IOP decreased from 22.6±10.2 and 22.0±6.8 to 11.0±5.5 and 10.0±4.5 at 1-yr in the ExPRESS and Trab groups respectively (p<0.0001). There was no significant difference in IOP between ExPRESS and Trab groups at any time point. Complete success (IOP 5-18 and 20% reduction from baseline without meds) was obtained in 71% ExPRESS and 57% Trab (p=0.24) and qualified success (± meds) in 87% ExPRESS and 93% Trab (p=0.67). 8 (26%) of the ExPRESS and 10 (33%) of the Trab patients were using glaucoma meds at 1-yr (p=0.58). Of the secondary outcomes the only significant difference was visual recovery which was faster in the ExPRESS group.

Conclusions: At 1-yr we found no statistically significant difference between ExPRESS and Trab groups regarding IOP, success rates, # of glaucoma meds, final VA, CCT, ECC, bleb morphology, complications and additional procedures. However, postoperative VA recovery was faster in the ExPRESS group.

Commercial Relationships: Yvonne M. Buys, Alcon Surgical Incorporated (R), Alcon Surgical Incorporated (F), IMED (F); Lilach Drori Wagschal, None; Yaping Jin, None; Delan Jinapriya, Alcon (R); Graham E. Trope, sentsimed (F)

Clinical Trial: NCT01263561

Program Number: 2136

Presentation Time: 3:00 PM - 3:15 PM

SPARC Deficiency Prolongs Bleb Survival In A Mouse Model Of Glaucoma Filtration Surgery By Attenuating Pro-inflammatory and Pro-fibrotic Gene Expression

Tina Wong^{1,2}, Sharon N. Finger², Li-Fong See². ¹Singapore National Eye Centre, Singapore, Singapore; ²Ocular Therapeutics and Drug Delivery, Singapore Eye Research Institute, Singapore, Singapore.

Purpose: Glaucoma filtration surgery (GFS) commonly fails due to scarring at the surgical site. We have previously reported that the SPARC knockout (Sparc^{-/-}) mouse exhibited significantly improved bleb survival in the mouse model of GFS. Besides inhibiting collagen deposition, other possible mechanisms by which SPARC deficiency exerts anti-fibrotic effects are as yet unknown. In the current study, we describe the differential gene expression changes in the early and late phases of subconjunctival wound healing in the SPARC knockout mouse following experimental glaucoma surgery.

Methods: Modified GFS was performed on both WT and Sparc^{-/-} mouse. Surgery was performed on the left eyes only. Bleb tissue and conjunctiva from the contralateral unoperated eye were harvested at Day 2 and Day 7 post-surgery. The unoperated tissue was used as baseline control to calculate the fold change in gene expression after surgery. mRNA expression of extracellular matrix (ECM), ECM-modifying, and pro-inflammatory cytokine genes were quantified using real-time PCR (qPCR) analysis. Cytokine expression was quantified using a multiplexed antibody-based assay (n=15 per genotype per time point).

Results: qPCR analysis indicated that induction of GM-CSF, IL-6, IL-13, TNF- α and MMP-1 mRNA transcripts were significantly reduced at Day 2 post-surgery in the Sparc^{-/-} mouse compared to WT. On Day 7-post-surgery, the induction of Colla1 mRNA transcript was significantly reduced in the Sparc^{-/-} mouse compared to WT. At the protein level, the induction of GM-CSF was profoundly reduced on Day 7 post-surgery in Sparc^{-/-} mice.

Conclusions: Our data suggests that SPARC deficiency is prolongs bleb survival by attenuating the expression of both pro-fibrotic and pro-inflammatory genes in vivo. In addition to the putative direct effect of SPARC on collagen deposition, SPARC may regulate collagen expression by modulating cytokine-induced signaling pathways. Therefore, silencing SPARC may be a promising therapeutic strategy in modulating post-surgical scarring through the

ARVO 2013 Annual Meeting Abstracts by Scientific Section/Group – Glaucoma

abrogation of early inflammation and late fibrogenesis in wound healing.

Commercial Relationships: Tina Wong, 61, 250,006 (P); Sharon N. Finger, None; Li-Fong Seet, PCT/SG2010000382 (P)

Support: National Medical Research Council of Singapore, Translational Clinical Research Grant

Program Number: 2137

Presentation Time: 3:15 PM - 3:30 PM

One year results of intracameral bevacizumab as an adjunct to trabeculectomy in open angle glaucoma patients

Evelien Vandewalle¹, Thierry Zeyen¹, Tine Van Bergen², Leigh Spielberg³, Werner Spileers¹, Ingeborg Stalmans². ¹Ophthalmology, UZ Leuven, Leuven, Belgium; ²Ophthalmology, KU Leuven, Leuven, Belgium; ³Ophthalmology, Rotterdam Eye Hospital, Rotterdam, Netherlands.

Purpose: To investigate the effect of a single intracameral administration of bevacizumab (Avastin®) in terms of clinical outcome following trabeculectomy in patients with either primary open-angle glaucoma (POAG) or normal tension glaucoma (NTG).

Methods: Between April 2009 and November 2010, 144 consecutive, medically uncontrolled glaucoma patients who were scheduled for primary trabeculectomy were included in this prospective, randomized, double-blinded and placebo-controlled study. Patients were divided into POAG and NTG groups, which were then randomized to receive 50 µl of either bevacizumab (25 mg/ml) or placebo (balanced salt solution) in the anterior chamber peroperatively. Patients with NTG also received mitomycin C. The target intraocular pressure (IOP) range was between 6 and 18 mmHg for POAG and between 6 and 14 mmHg for NTG patients. Absolute success was defined as meeting the target IOP without IOP-lowering medications or postoperative interventions. Qualified success was defined as meeting the target IOP with or without either IOP-lowering medications and/or postoperative surgical interventions.

Results: 138 out of 144 randomized patients reached the 1 year follow-up timepoint, 69 of whom received bevacizumab and 69 received placebo. Absolute success in the bevacizumab group was 71% compared to 51% in the placebo group (p=0.02). Qualified success was 87% in the bevacizumab group versus 86% in the placebo group (p=0.99). Needlings were significantly less frequent in the bevacizumab group compared to the placebo group, respectively in 13% versus 35% (p=0.003). Complication rates were low and comparable in both groups.

Conclusions: A single intracameral administration of bevacizumab at the end of trabeculectomy was associated with increased absolute success rates and reduced need for postoperative interventions in order to reach the target IOP.

Commercial Relationships: Evelien Vandewalle, None; Thierry Zeyen, None; Tine Van Bergen, None; Leigh Spielberg, None; Werner Spileers, None; Ingeborg Stalmans, None

Support: Funds for Research in Ophthalmology, Belgium 2009

Clinical Trial: 2009-009038-33

Program Number: 2138

Presentation Time: 3:30 PM - 3:45 PM

Comparison of Phacoemulsification Combined with ab interno Trabeculectomy (AIT), or with Trabeculectomy (Trab), and Phaco Alone for the Management of Cataract and Open-Angle Glaucoma

Marc Toeteberg-Harms¹, Swarup S. Swaminathan¹, Seung Youn Jea¹, Amir Marvasti², Kyuryong Choi¹, Julie Kim¹, Louis R. Pasquale¹, Douglas J. Rhee¹. ¹Harvard Medical School, Massachusetts Eye and

Ear Infirmary, Boston, MA; ²Boston University, School of Medicine, Boston, MA.

Purpose: Eyes with POAG frequently develop cataracts. We evaluated the use of phaco, phaco+AIT, and phaco+trab in this population. We hypothesized that 1) IOP reduction of phaco-trab would be greater than phaco and phaco-AIT, 2) phaco-AIT has a lower complication rate than phaco-trab, and 3) phaco-AIT and phaco-trab would have lower rate of acute IOP elevations (IOP spikes).

Methods: Exclusion criterion of this retrospective case-controlled comparative series was previous incisional glaucoma surgery. Eyes underwent phaco if their IOP was controlled on 2 or less anti-glaucoma medications (AGMs). Eyes received concurrent filtration surgery if their IOP is controlled but requiring >3 AGMs or their IOP is not within the target range. Primary outcome measures were IOP and Kaplan-Meier survival. Primary definition of failure was IOP >21 mmHg or <20% reduction below baseline after 1 month. Secondary outcome measures were AGMs and occurrence of complications; IOP spikes were defined as an elevation >20% over baseline).

Results: 121 eyes underwent phaco, 50 phaco-trab, and 156 phaco-AIT. There were no differences in baseline characteristics. IOP in the phaco group was lower up to 3.5y (P=0.008), for the phaco-AIT up to 3y (P=0.032), and during the entire follow-up period of 6.5y for the phaco-trabs (P=0.020). IOP reduction was highest in the phaco-trab and lowest in the phaco group. AGMs could be reduced in all groups. Besides that, severity and number of complications were higher in the phaco-trab group. Kaplan-Meier survival analysis shows comparable outcomes for all three procedures regardless of definition of failure up to 2y. After 2y, phaco-trab had a greater success rate compared to the phaco and phaco-AIT. Survival time varied between 28.2-33.7m for phaco, between 41.6-45.5m for phaco-trab, and between 22.4-26.6m for phaco-AIT, respectively. IOP spikes occurred in each group within 1m after surgery in 21.5% in the phaco, 44.7% in the phaco-trab, and 8.9% in the phaco-AIT group, respectively. Most IOP spikes were less than 20mmHg.

Conclusions: Phaco-trab had a greater success rate and longer survival time with lower mean IOP. In the first two years the phaco-trab and phaco-AIT are equally effective with highest rate of early complications in the phaco-trab group. Phaco-AIT is reasonable to consider besides phaco-trab.

Commercial Relationships: Marc Toeteberg-Harms, None; Swarup S. Swaminathan, None; Seung Youn Jea, None; Amir Marvasti, None; Kyuryong Choi, None; Julie Kim, None; Louis R. Pasquale, None; Douglas J. Rhee, Alcon (C), Alcon (F), Allergan (C), Aquesys (F), Aquesys (C), Merck (F), Merck (C), Santen (C)

Program Number: 2139

Presentation Time: 3:45 PM - 4:00 PM

Characterization of human ocular fibroblast-subpopulations to prevent fibrosis following fistulating glaucoma surgeries

Thomas Stahnke¹, Marian Löbler², Andreas Wree³, Oliver Stachs¹, Klaus-Peter Schmitz², Rudolf F. Guthoff¹. ¹Department of Ophthalmology, University of Rostock, Rostock, Germany; ²Institute of Biomedical Engineering, University of Rostock, Rostock, Germany; ³Institute of Anatomy, University of Rostock, Rostock, Germany.

Purpose: Fibrotic re-stenosis following fistulating glaucoma surgeries is the major factor for a postoperative decrease in liquid drain. Hence, one of the most important clinical goals is to develop strategies for fibrosis prevention. This study aimed at characterization of fibrotic potential of different primary human ocular fibroblast-subpopulations. Particularly, we focused on the TGF-β pathway. As

this signaling pathway is involved in fibrosis, we investigated its implication in extracellular matrix (ECM) component synthesis and secretion in different ocular fibroblast-subpopulations.

Methods: Human primary fibroblasts from choroidea (hCF), sclera (hSF), Tenon capsule (hTF), and orbital fat tissue (hOF) were isolated and cultured.

For immunocytochemical analysis cells were cultured on coverslips and fixed. Incubation with primary antibodies directed against TGF- β pathway components and ECM proteins was carried out followed by incubation with Cy2 and Cy3 conjugated secondary antibodies. Coverslips were mounted with DAPI-containing mounting medium. To analyze protein lysates 1-D-SDS-PAGE and Western blotting were performed according to the standard protocols. Proteins were transferred to PVDF-membranes and antibodies were used to detect TGF- β pathway components. Targets were analyzed by enhanced chemiluminescence (ECL) detection method followed antibody incubation.

Results: Cytokine TGF- β 1 and the relevant receptors TGF- β -receptor 1 and 2 expression was demonstrated in every fibroblast-subpopulation. Moreover, TGF- β pathway activation could be observed by phosphorylation specific translocation of the downstream mediators (smad 2 and 3) into the nuclei. However, the level of activation and ECM protein synthesis was different between fibroblast-subpopulations with lowest levels in hCF cultures.

Conclusions: Cell culture model of primary ocular fibroblast-subpopulations pave the way for comparative analyzing of fibrotic processes. Moreover, tissue-specific inhibition of cell proliferation, ECM synthesis or transformation into fibrotic active myofibroblasts could be possible. Exploring the influence of TGF- β pathway inhibitors between different fibroblast-subpopulations opens up specific possibilities in cell population dependent prevention of postoperative scarring processes and fibrosis after fistulating glaucoma surgeries.

Commercial Relationships: Thomas Stahnke, None; Marian Löbler, None; Andreas Wree, None; Oliver Stachs, None; Klaus-Peter Schmitz, None; Rudolf F. Guthoff, None
Support: REMEDIS

Program Number: 2140

Presentation Time: 4:00 PM - 4:15 PM

Novel Insight into the Inflammatory and Cellular Responses following Experimental Glaucoma Surgery: a Roadmap for Inhibiting Fibrosis

Li-Fong Seet^{1,3}, Tina Wong^{1,2}. ¹Ocular Therapeutics & Drug Delivery, Singapore Eye Research Institute, Singapore, Singapore; ²Department of Ophthalmology, Yong Loo Lin School of Medicine, National University of Singapore, Singapore, Singapore; ³Department of Research, Duke-NUS Graduate Medical School Singapore, Singapore, Singapore.

Purpose: Failure after glaucoma filtration surgery is attributed to fibrosis at the operated site. To understand the wound healing process after glaucoma filtration surgery, we have developed a mouse model for glaucoma filtration surgery which closely mimics the clinical response. In this study, we describe a systematic analysis of the wound healing response in vivo.

Methods: Modified GFS was performed on mice. Quantitative polymerase chain reaction, antibody-based cytokine assays, flow cytometry, and immunofluorescent analyses were performed to determine gene and cellular changes. Primary subconjunctival fibroblasts were stimulated with TNF- α or TGF- β to assess their involvement in the wound healing process.

Results: Our data revealed that the post-surgical tissue response was separable into two distinguishable phases. The early “acute

inflammatory” phase was characterized by significantly increased transcript expression of Vegfa, Cxcl1, Cxcl5, Ccl2, Ccl3, Ccl4, Gmcsf and specific Mmps as well as greater infiltration of monocytes/macrophages and T cells. The late “fibrotic” phase was characterized by an increased expression of Tgfb2 and extracellular matrix genes as well as a notable reduction of infiltrating inflammatory cells. Significantly more mitotic cells were observed at both time points post-surgery. Subconjunctival fibroblasts may be involved in both phases since they have the capacity to reiterate the in vivo gene expression profiles upon either pro-inflammatory or pro-fibrotic cytokine stimulation.

Conclusions: The wound healing response after GFS is separable into two distinct phases implicating the need for sequential application of therapeutics specifically targeting each phase in order to overcome the long term scarring response.

Commercial Relationships: Li-Fong Seet, PCT/SG2010000382 (P); Tina Wong, 61, 250,006 (P)
Support: NMRC/TCR/002-SERI/2008

Program Number: 2141

Presentation Time: 4:15 PM - 4:30 PM

Excimer Laser Trabeculostomy: Five Year Post-OP Observations

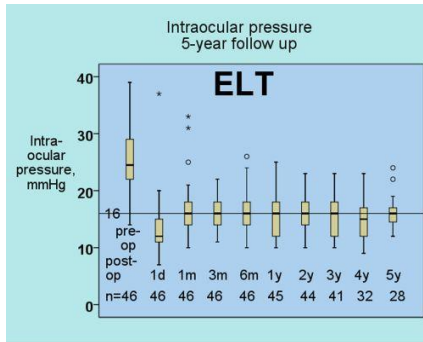
Richard P. Stodtmeister¹, Lea Kleineberg¹, Michael S. Berlin³, Lutz E. Pillunat¹, Ulrich F. Giers². ¹Ophthalmology, University Hospital Carl Gustav Carus, Dresden, Germany; ²Eye Clinic Detmold, Detmold, Germany; ³Glaucoma Institute Beverly Hills, Los Angeles, CA.

Purpose: To evaluate long-term intra-ocular pressure (IOP) lowering efficacy of ELT based on patient observations made over a period of five years. ELT (fiberoptic, ab interno delivery, 308 nm) creates five to ten channels through the trabecular meshwork and inner wall of Schlemm’s canal to lower outflow resistance and thereby lower IOP.

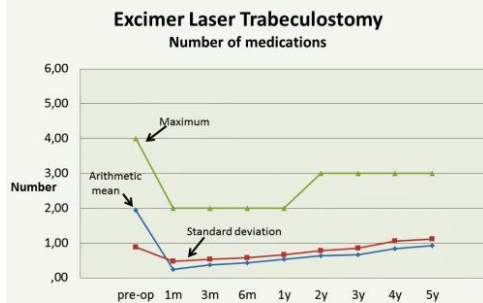
Methods: 46 eyes of 46 patients aged 64 \pm 18 years (mean \pm SD) (M/F: 9/37) participated in this prospective, single site, single surgeon (UG) study. Diagnosis: Primary open-angle glaucoma: 35 eyes; Ocular hypertension: 7; Secondary glaucoma: 2; PEX glaucoma: 2. The IOP was measured by applanation, without wash out, pre-op, 1 day, 1 month (M), 3, 6, 12 M, 2 years (Y), 3, 4, 5 Y post op. Surgical procedure: Following paracentesis, the ELT probe (diameter 0.5 mm) traverses the anterior chamber to contact the trabecular meshwork and excise ten, 200 μ channels into Schlemm’s canal in the lower nasal quadrant. Number of eyes observed at: 1 day post-op: 46; 1 M: 46; 3 M: 46; 6 M: 46; 1 Y: 45; 2 Y: 44; 3 Y: 41; 4 Y: 32; 5 Y: 28.

Results: IOP (mm Hg): pre-op: 25.5 \pm 6.3; post-op 1 day: 13.3 \pm 4.5; 1M: 16.3 \pm 4.3; 3M: 16.0 \pm 2.8; 6M: 16.22 \pm 5.5; 12M: 16.0 \pm 3.8; 2Y: 15.6 \pm 3.0; 3Y: 15.2 \pm 3.7; 4Y: 15.2 \pm 3.4; 5Y: 15.9 \pm 3.0
Statistical tests: ANOVA with repeated measurements and t-tests. SPSS 17.0 (Bonferroni correction). At all times, the IOP values were highly significantly lower than the pre-op values (alpha: p < 0.001). The number of IOP lowering medications also decreased from 1.9 \pm 0.9 pre-op to 0.9 \pm 1.1 at 5 years. There were no intraoperative or postoperative complications.

Conclusions: Significant IOP reduction following ELT, over 35% at all times, has been documented to remain stable in these patients for at least 5 years post op. Additionally, following ELT, the number of IOP lowering medications was significantly reduced.



Boxplots (Minimum,Q1,Median,Q2,Maximum) at the different measurement time points. d=day, m=month, y=year



Number of IOP lowering medications (ordinate) vs the observation time points (abscissa): m=month; y=year

Commercial Relationships: Richard P. Stodtmeister, Novartis (F); Lea Kleineberg, None; Michael S. Berlin, None; Lutz E. Pillunat, None; Ulrich F. Giers, None

276 Imaging II, GL

Monday, May 06, 2013 2:45 PM-4:30 PM
6E Paper Session
Program #/Board # Range: 2149-2155
Organizing Section: Glaucoma

Program Number: 2149
Presentation Time: 2:45 PM - 3:00 PM

Enhancement of Lamina Cribrosa Visibility in Optical

Coherence Tomography Images using Adaptive Compensation

Nicholas G. Strouthidis^{1,2}, Jean Martial Mari³, Sung Chul Park^{4,5}, Michael J. Girard^{2,6}. ¹Glaucoma Research Unit, NIHR Biomedical Research Centre at Moorfields Eye Hospital NHS Foundation Trust and UCL Institute of Ophthalmology, London, United Kingdom; ²Singapore Eye Research Institute, Singapore, Singapore; ³INSERM 1032, Université de Lyon, Lyon, France; ⁴Moise and Chella Safra Advanced Ocular Imaging Laboratory, Einhorn Clinical Research Center, New York Eye and Ear Infirmary, New York, NY; ⁵Department of Ophthalmology, New York Medical College, Valhalla, NY; ⁶In Vivo Biomechanics Laboratory, Department of Bioengineering, National University of Singapore, Singapore, Singapore.

Purpose: To improve the visibility of the lamina cribrosa (LC), including its posterior boundary, in optical coherence tomography (OCT) images of the human optic nerve head (ONH).

Methods: An adaptive compensation algorithm was developed to overcome a

limitation of our standard compensation algorithm, that is the over-amplification of noise at high depth. Such limitation currently hampers our ability to distinguish the posterior LC boundary. In

©2013, Copyright by the Association for Research in Vision and Ophthalmology, Inc., all rights reserved. Go to iovs.org to access the version of record. For permission to reproduce any abstract, contact the ARVO Office at arvo@arvo.org.

adaptive compensation, standard compensation operations are performed until an energy threshold is reached, at which stage the compensation process is stopped to limit noise over-amplification in the inferior (deep) portion of the OCT image. The performance of adaptive compensation was compared to that of standard compensation using OCT images of 3 human ONHs.

Results: Adaptive compensation significantly reduced the intra-layer contrast (a measure of pixel intensity uniformity) in the inferior (deep) portion of the OCT images (from 0.63 ± 0.09 to 0.29 ± 0.03 ; $p < 0.001$), indicating successful removal of noise over-amplification. Furthermore, adaptive compensation significantly increased the interlayer contrast (a measure of boundary visibility) across the posterior LC boundary (from 0.25 ± 0.11 to 0.61 ± 0.28 ; $p < 0.05$), indicating improved posterior LC boundary visibility.

Conclusions: Adaptive compensation provided significant improvement compared to standard compensation by eliminating noise over-amplification at high depth and improving the visibility of the posterior LC boundary. These improvements were performed while maintaining all other benefits of compensation such as shadow removal and contrast enhancement. Adaptive compensation will further help our efforts to characterize in vivo ONH biomechanics for the diagnosis and monitoring of glaucoma.

Commercial Relationships: Nicholas G. Strouthidis, None; Jean Martial Mari, None; Sung Chul Park, None; Michael J. Girard, None

Support: Girard - Singapore Ministry of Education Academic Research Fund Tier 1; Strouthidis acknowledges financial support from the Department of Health through the award made by the National Institute for Health Research to Moorfields Eye Hospital NHS Foundation Trust and UCL Institute of Ophthalmology for a Biomedical Research Centre for Ophthalmology. The views expressed in this publication are those of the authors and not necessarily those of the Department of Health.

Program Number: 2150

Presentation Time: 3:00 PM - 3:15 PM

Peripapillary choroidal volume in eyes with and without primary open-angle glaucoma

Michael Sullivan-Mee¹, Nimesh B. Patel², Denise Pensyl¹, Kathy D. Halverson¹. ¹Optometry, Albuquerque VA Med Center, Albuquerque, NM; ²University of Houston, College of Optometry, Houston, TX.

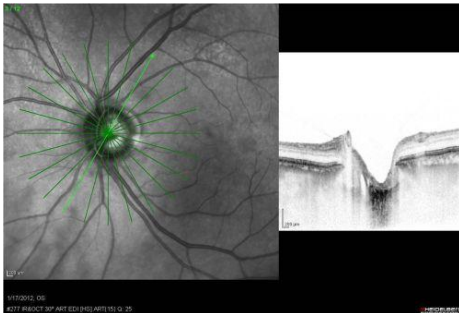
Purpose: To compare peripapillary choroidal volume (PCV) in normal eyes versus eyes diagnosed primary open-angle glaucoma and ocular hypertension.

Methods: We imaged consecutive subjects who were participating in a longitudinal, observational clinical research study and who were diagnosed primary open-angle glaucoma (POAG), ocular hypertension (OH), or normal (NML). Using spectral domain optical coherence tomography with enhanced depth imaging, we acquired twelve 20-degree (approximate 6mm length) radial scans centered on the optic nerve head; each radial scan was separated by 15 degrees. Using a customized Matlab software program, choroidal thickness was quantified for each scan and adjusted for ocular magnification. PCV measures were then calculated using standard linear interpolation techniques. We compared PCV between diagnostic groups using one-way analysis of variance (ANOVA), and we used regression analyses to evaluate relationships between PCV and age, intraocular pressure, ocular pulse amplitude (OPA), central corneal thickness, mean retinal nerve fiber layer thickness (RNFL), visual field indices (mean defect [MD], pattern standard deviation [PSD]), diabetes diagnosis, and glycosylated hemoglobin levels.

Results: We imaged 103 consecutive subjects, obtaining PCV

measures in 191 eyes (86 POAG, 55 OH, 50 NML eyes). Image quality prevented PCV measurement in 15 eyes (7.2%). Overall, PCV demonstrated large inter-individual variability with a 4-fold difference between thinnest and thickest PCV measures. Among all eyes, PCV was significantly thinner ($p < 0.001$) in POAG ($1070 \mu\text{m}^3$) compared to OH ($1276 \mu\text{m}^3$) and NML eyes ($1334 \mu\text{m}^3$) with similar results when right and left eyes were evaluated separately. In multivariate regression analyses, glaucoma diagnosis, age, and ocular pulse amplitude (OPA) were independently associated with PCV (age was inversely related while OPA was directly related). Notably, parameters associated with glaucoma severity (RNFL, MD, PSD) were not independently associated with PCV.

Conclusions: Peripapillary choroidal volume appears to be reduced in eyes with POAG compared to NML and OH eyes. Whether thinner PCV reflects inherent risk for POAG or represents acquired change that occurs as part of the glaucoma pathophysiologic process requires further study.



Commercial Relationships: Michael Sullivan-Mee, None; Nimesh B. Patel, None; Denise Pensyl, None; Kathy D. Halverson, None
Support: K23EY021761

Program Number: 2151
Presentation Time: 3:15 PM - 3:30 PM

Association between Iris Surface Features and Iris Thickness in Asian Eyes

Elizabeth Sidhartha^{1,2}, PREETI GUPTA^{1,2}, Jiemin Liao¹, Yih Chung Tham^{1,2}, Carol Y. Cheung^{1,2}, Tien Y. Wong^{1,2}, Tin Aung^{1,2}, Ching-Yu Cheng^{1,2}. ¹Singapore Eye Research Institute, Singapore, Singapore; ²Department of Ophthalmology, National University of Singapore, Singapore, Singapore.

Purpose: To describe a grading system to assess iris surface features in Asian eyes and to examine the association between iris surface features and iris thickness measured by anterior segment optical coherence tomography (AS-OCT).

Methods: We recruited 50 subjects from the Singapore Malay Eye Study (SiMES), a population-based survey of Singaporean Malays aged 40-80 years. Iris surface features including iris crypts, contraction furrows, and iris color were graded from photographs taken using slit lamp digital camera with standard protocol. We proposed a grading system to assess iris surface features including iris crypts (grade 1-5, by their number and size), furrows (grade 1-3, by their number and circumferential extent), and iris color (grade 1-5, comparing with standard photos, with higher grade denoting darker iris). Intra- and inter-grader agreements between two graders were assessed by weighted kappa (K_w). Vertical and horizontal cross-sections of anterior chamber were imaged using AS-OCT. Iris thickness at $750\mu\text{m}$ (IT_{750}) and $2000\mu\text{m}$ (IT_{2000}) from the scleral spur and maximum central iris thickness (IT_{CM}) were measured using Zhongshan Angle Assessment Program. Associations between iris features and average thickness from the four quadrants were assessed by Spearman's rank correlation (ρ) and generalized estimating

equations to control for inter-eye correlation.

Results: Of the 50 subjects, 75 eyes had complete AS-OCT data and were gradable for iris crypts and color; 64 eyes were graded for furrows. The grading scheme for iris surface features showed good to optimal inter-grader (Crypt $K_w=0.775$, Furrow $K_w=0.836$, Color $K_w=0.718$) and intra-grader (Crypt $K_w=0.919$, Furrow $K_w=0.901$, Color $K_w=0.925$) agreements. Higher crypt grade was significantly correlated with thinner IT_{2000} ($\rho=-0.342$, $p=0.022$). More extensive furrows were correlated with thicker IT_{750} ($\rho=0.453$, $p=0.008$) and IT_{CM} ($\rho=0.250$, $p=0.031$). We did not observe any significant correlations between iris color and iris thickness (all $p > 0.05$).

Conclusions: Iris surface features are clinically observable. Our results show that several iris surface features can be graded from slit lamp photographs and are associated with iris thickness. Irises with larger and more crypts are thinner centrally, and irises with more extensive furrows are thicker peripherally. These findings may have important implications in assessing the risk of angle closure based on iris surface features.

Commercial Relationships: Elizabeth Sidhartha, None; PREETI GUPTA, None; Jiemin Liao, None; Yih Chung Tham, None; Carol Y. Cheung, None; Tien Y. Wong, Allergan (C), Bayer (C), Novartis (C), Pfizer (C), GSK (F), Roche (F); Tin Aung, Alcon (R), Alcon (C), Alcon (F), Allergan (R), Allergan (C), Carl Zeiss Meditec (F), Carl Zeiss Meditec (R), Ellex (F), Ellex (R), Santen (R); Ching-Yu Cheng, None

Support: National Medical Research Council (NMRC) R607/28/2008 and NMRC/NIG/1069/2012.

Program Number: 2152

Presentation Time: 3:30 PM - 3:45 PM

Magnification Errors after Refractive Change by Cataract Surgery on Optic Nerve Head Analysis

Kazuhiko Mori, Tomomichi Nakayama, Yoko Ikeda, Morio Ueno, Haruna Yoshikawa, Yuko Maruyama, Shigeru Kinoshita. Department of Ophthalmology, Kyoto Prefectural Univ of Med, Kamigyo-Ku, Japan.

Purpose: Quantification of the optic disc is influenced by the magnification errors of the refractive status. All ophthalmoscopes have several methods that can be used to compensate for this problem. The purpose of this study was to evaluate the magnification errors after refractive change by cataract surgery on optic nerve head analysis using confocal laser ophthalmoscopy.

Methods: This study was conducted as a retrospective observational case series and involved 14 eyes of 17 glaucoma patients (8 females and 9 males; mean age: 72.0 ± 10.0 years) out of 478 eyes that underwent cataract surgery (including combined procedures with trabeculectomy) between January 2006 and December 2011 at the University Hospital of Kyoto Prefectural University of Medicine. Only the patients who were able to undergo examination of refractive error (RE), corneal curvature radius (CCR), axial length (AL), as well as reliable optic nerve head analysis by use of the Heidelberg Retina Tomograph II (Heidelberg Engineering GmbH, Heidelberg, Germany) during the pre- and postoperative periods were statistically analyzed. Magnification errors after correction by the measured CCR or by the automatic image alignment were evaluated utilizing the optic disc area (DA) and rim area (RA) data of the pre- and postoperative periods. The influence of other ophthalmic factors such as RE and AL on the magnification errors were also evaluated.

Results: The mean postoperative reduction of optic DA was $9.4 \pm 17.4\%$ when the measured CCR were used for each time periods, yet was $10.6 \pm 17.3\%$ for the fixed CCR. On the other hand, the reduction rates of RA were $14.9 \pm 42.6\%$, $10.6 \pm 38.5\%$, and $9.2 \pm 17.8\%$ for the fixed CCR, measured CCR, and automatic image alignment

correction, respectively. However, a certain amount of error still remained after the automatic correction, and a significant correlation was found between the RE and magnification errors (Pearson's correlation coefficient: $R=0.75$, $P=0.0005$).

Conclusions: The measurement of optic DA and RA changed between the pre- and postoperative periods, and was influenced by the refractive error. The existing methods using CCR or image alignment are inadequate for the correction of magnification errors.

Commercial Relationships: Kazuhiko Mori, Ocular Instruments, Inc. (P), Santen Pharmaceutical Co., Ltd. (P); Tomomichi Nakayama, None; Yoko Ikeda, None; Morio Ueno, None; Haruna Yoshikawa, None; Yuko Maruyama, None; Shigeru Kinoshita, Senju Pharmaceutical Co (P), Santen Pharmaceutical Co (P), Otsuka Pharmaceutical Co (C), Alcon (R), AMO (R), HOYA (R)

Program Number: 2153

Presentation Time: 3:45 PM - 4:00 PM

Lamina Cribrosa Reversal after Trabeculectomy : Long-term Follow-up Result

Tae-Woo Kim^{1,2}, Eun Ji Lee^{1,2}, Robert N. Weinreb³.

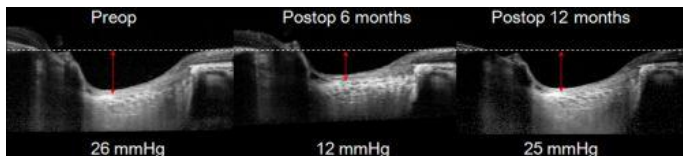
¹Ophthalmology, Seoul National University College of Medicine, Seoul, Republic of Korea; ²Ophthalmology, Seoul National Univ Bundang Hosp, Seongnam, Republic of Korea; ³Ophthalmology, University of California San Diego, La Jolla, CA.

Purpose: To investigate the change in the lamina cribrosa (LC) depth following trabeculectomy up to 2 years.

Methods: The study included 28 eyes of 28 primary open angle glaucoma patients who underwent trabeculectomy and followed up for at least 2 years. Serial horizontal B-scan images of the optic nerve head were obtained from each eye using enhanced depth imaging spectral-domain optical coherence tomography. About 65 B-scans covering the optic discs were obtained before surgery, and at 6 months and ≥ 2 years postoperatively. The pre- and postoperative LC depth (the distance from the Bruch's membrane opening plane to the level of anterior LC surface) was determined on 7 selected B-scan images in each eye and averaged (mean LC depth).

Results: Intraocular pressure (IOP) decreased from 27.4 ± 9.0 mmHg to 9.7 ± 3.1 mmHg at postoperative 6 months ($P < 0.001$) and then increased to 12.7 ± 5.1 mmHg at mean postoperative follow-up of 27.1 ± 3.3 months ($P = 0.001$). The mean LC depth reduced from 625.59 ± 186.33 μm to 499.59 ± 140.56 μm at postoperative 6 months ($P < 0.001$) and then slightly increased to a statistically non-significant level at final follow-up (518.97 ± 133.38 μm). Factors associated with LC depth re-increase were higher IOP at final follow-up ($P = 0.035$), larger IOP fluctuation ($P = 0.007$), higher mean follow-up IOP ($P = 0.022$) and older age ($P = 0.001$).

Conclusions: The LC depth which had been reduced up to postoperative 6 months showed re-displacement in eyes with higher IOP fluctuation, smaller mean LC depth at 6 months and younger age. The data suggest that sustained IOP reduction is essential for preventing re-displacement of the LC after trabeculectomy.



A representative case where the intraocular pressure (IOP) decreased from 26 mmHg to 12 mmHg at postoperative 6 months and then re-elevated to 25 mmHg at postoperative 12 months. Note the decrease of the lamina cribrosa (LC) depth at month 6 and re-displacement of the LC at month 12.

©2013, Copyright by the Association for Research in Vision and Ophthalmology, Inc., all rights reserved. Go to iovs.org to access the version of record. For permission to reproduce any abstract, contact the ARVO Office at arvo@arvo.org.

Commercial Relationships: Tae-Woo Kim, None; Eun Ji Lee, None; Robert N. Weinreb, Aerie (F), Alcon (C), Allergan (C), Altheos (C), Amakem (C), Bausch&Lomb (C), Carl Zeiss-Meditec (C), Genentech (F), Haag-Streit (F), Heidelberg Engineering (F), Konan (F), Lumenis (F), National Eye Institute (F), Nidek (F), Optovue (C), Quark (C), Solx (C), Topcon (C)

Support: National Research Fund Provided by

Program Number: 2154

Presentation Time: 4:00 PM - 4:15 PM

A prospective study on laminar and pre-laminar displacement in patients with chronic progressive glaucoma

Zhongheng Wu, Sayantan Biswas, Christopher K. Leung. CUHK, Hong Kong, Hong Kong.

Purpose: While posterior displacement of the anterior laminar surface (ALS), reduction of neuroretinal rim and thinning of the retinal nerve fiber layer (RNFL) have been reported in experimental glaucoma, longitudinal changes of the laminar cribrosa in patients with chronic glaucoma have not been investigated. This is a 3-year prospective study following pre-laminar and laminar displacement, and pre-laminar tissue thickness (PLTT) in patients with progressive RNFL thinning.

Methods: SD-OCT images of 27 eyes of 20 glaucoma patients (each eye had 6 radial scans centered at the optic disc for each visit) who had been followed 4 monthly for a mean of 47.15 months (range: 35 - 54 months) and had significant RNFL thinning (detected by OCT) were exported for measurement of (1) pre-laminar and (2) laminar displacement and (3) neuroretinal rim width after manually detecting the neural canal opening and the boundaries of anterior laminar and laminar surfaces. The mean values of each parameter were computed from the 6 scans. Progression was defined with reference to the linear regression analysis.

Results: 7 eyes (26.0%) showed pre-laminar displacement [4 had posterior and 3 had anterior displacement (1 had a history of glaucoma surgery)], 12 (44.4%) had laminar displacement [8 had posterior and 4 had anterior displacement (1 had a history of glaucoma surgery)], and 12 (44.4%) had reduction in neuroretinal rim width. All the 7 eyes with pre-laminar displacement also demonstrated corresponding laminar displacement. 3 eyes (11.1%) had thinning of pre-laminar tissue thickness. 9 eyes (33.3%) did not show significant changes in any of the neuroretinal rim and laminar / pre-laminar parameters despite having significant progressive RNFL thinning during the follow-up.

Conclusions: Pre-laminar and laminar displacement can be detected with SD-OCT in chronic glaucoma patients. Progressive RNFL thinning may occur without concomitant laminar and pre-laminar changes.

Commercial Relationships: Zhongheng Wu, None; Sayantan Biswas, None; Christopher K. Leung, Carl Zeiss Meditec (F), Carl Zeiss Meditec (R), Alcon (C), Alcon (R), Alcon (F), Allergan (C), Allergan (R), Tomey (F), Optovue (F)

Program Number: 2155

Presentation Time: 4:15 PM - 4:30 PM

Axonal Transport Deficits Exceed Retinal Nerve Fiber Layer (RNFL) Changes after 3-weeks of Chronic Intraocular Pressure (IOP) Elevation in Young and Old Rats

Carla J. Abbott, Tiffany E. Choe, Claude F. Burgoyne, Brad Fortune. Discoveries in Sight Research Laboratories, Devers Eye Institute and Legacy Research Institute, Legacy Health, Portland, OR.

Purpose: To assess RNFL thickness (RNFLT) and axonal transport patency 3-weeks after chronic IOP elevation in young and old rats.

Methods: Twelve 2-month-old and twelve 9.5-month-old male

Brown-Norway rats were used. Procedures were performed under general anesthesia (ketamine, xylazine, acepromazine 55:5:1 mg/kg IM), except tonometry (TonoLab, iCare) which was measured with topical proparacaine only. IOP was elevated unilaterally by intracameral injections of magnetic microbeads (10µm; Corpuscular Inc.) manipulated into the angle with a magnet. Five baseline IOP measures were collected in trained rats then IOP was measured every other day. RNFLT was measured by SDOCT circle scans (Spectralis, Heidelberg Engineering, GmbH) at baseline (N=21) and at days 7 (N=17), 14 (N=16) and 20 (N=14). Anterograde axonal transport (N=22) was assessed at day 21 by determining the post mortem fluorescence intensity of each superior colliculus 24h after bilateral intravitreal injection of 2µl 1% fluorescent cholera toxin subunit-b. Retinas were evaluated by fluorescence microscopy. Two-way ANOVAs with Bonferroni post-tests were performed.

Results: IOP was elevated in experimental eyes ($p < 0.01$) compared to control but there was no difference ($p > 0.05$) between young and old rats (young mean±s.d.: OD 36.5±4.3, OS 19.2±1.2 mmHg; peak: OD 61.2±6.2, OS 22.8±1.1 mmHg; cumulative difference: 345±90 mmHg.days; old mean: OD 37.5±5.3, OS 18.6±1.2 mmHg; peak: OD 61.9±12.1, OS 22.9±0.8 mmHg; cumulative difference: 366±104 mmHg.days). The experimental eye RNFLT exhibited minimal change from baseline in young rats; day 7: +10.3±15.0% ($p < 0.05$), day 14: -7.2±15.4% ($p > 0.05$), day 20: -7.4±11.8% ($p > 0.05$). Mild RNFL thinning from baseline occurred in old rats; day 7: -4.9±5.6% ($p > 0.05$), day 14: -21.8±9.4% ($p < 0.01$), day 20: -21.4±7.6% ($p < 0.05$). Superior colliculus fluorescence intensity was reduced relative to control by equivalent amounts ($p > 0.05$) in both young (51.4±20.8%, $p < 0.001$) and old (51.7±19.9%, $p < 0.001$) rats, representing a 78% transport deficit. In experimental eyes the RNFL was mostly intact by microscopy despite severely reduced transport to the superior colliculus (Fig.).

Conclusions: Chronic IOP elevation for 3-weeks resulted in severely disrupted anterograde axonal transport in all rats associated with minimal RNFL loss in young rats and mild RNFL loss in old rats.

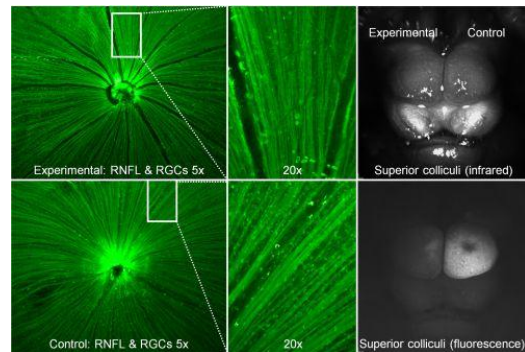


Fig.

Commercial Relationships: Carla J. Abbott, None; Tiffany E. Choe, None; Claude F. Burgoyne, Heidelberg Engineering (F), Heidelberg Engineering (C); Brad Fortune, Heidelberg Engineering, GmbH (F), Carl Zeiss Meditec, Inc (F)

Support: NIH Grant R21EY021211, Legacy Good Samaritan Foundation Grant, Heidelberg Engineering GmbH (equipment)

286 Structure and Function II

Monday, May 06, 2013 2:45 PM-4:30 PM

Exhibit Hall Poster Session

Program #/Board # Range: 2245-2299/B0049-B0103

Organizing Section: Glaucoma

Program Number: 2245 Poster Board Number: B0049

Presentation Time: 2:45 PM - 4:30 PM

Longitudinal Assessment of Retinal Ganglion Cell Degeneration In Vivo

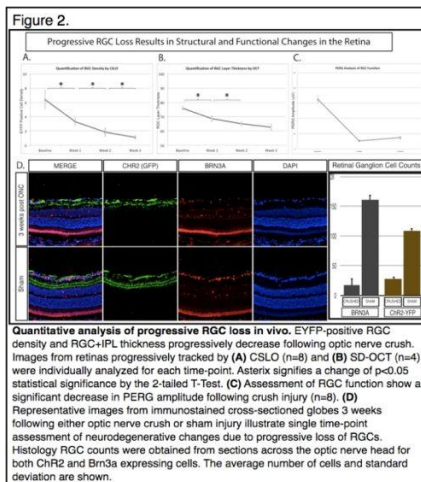
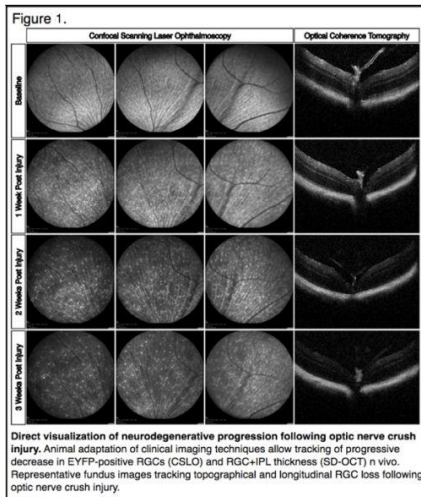
Gustavo C. Munguba, Daisy Lam, Ling Ge, Sanja Galeb, Sinthia Samad, Mary L. Tapia, Andrew Camp, Xiaoli Xing, Richard K. Lee. Ophthalmology, University of Miami BPEI, Miami, FL.

Purpose: To investigate the progressive nature of injury-induced neurodegenerative structural changes occurring following injury to retinal ganglion cell (RGC) axons, including spatial information by taking advantage of recent advances in in-vivo imaging techniques and assess whether structural changes to the RGC+IP layers correlate well with direct assessment of RGC density.

Methods: All animals used in this study were treated in accordance with the ARVO Statement for the Use of Animals in Ophthalmic and Vision Research and were approved by the UM-IACUC. To track degenerative progress in retinas following optic nerve crush (ONC) injury, we used BiopTigen's SD-OCT system and manual segmentation of OCT images. RGC density was measured by confocal laser scanning ophthalmoscope (CSLO) (HRA2; Heidelberg Engineering) and counts were performed using blood vessels as landmarks with which to track anatomically defined progressive RGC loss.

Results: Approximately 50% of RGCs homogeneously distributed throughout the retina of our transgenic line express Thy-1 promoter driven EYFP, labeling RGC dendrites, soma and axons. Static histology studies 3 weeks after optic nerve crush injury show a >70% reduction in the number of Brn3a and GFP positive RGCs present in injured retinas as compared to sham injury control. Unlike histology findings, in vivo density of RGCs expressing EYFP, as tracked by CSLO, progressively decreases as a consequence of ONC injury and can be tracked in a dynamic manner providing both spatial information and nature of progression. RGC+IP layer thickness decreases in response to ONC injury serve as a reliable surrogate structural marker for RGC death. Changes in RGL+IPL thickness heat-maps provide spatial information regarding progressive RGC axonal loss.

Conclusions: In vivo CSLO imaging can track EYFP expression by RGCs, providing dynamic assessment of CNS neuron survival following injury. The use of RGC+IP layer thickness as a surrogate marker for RGC survival is an effective method to follow progressive loss of RGC soma and axons after axonal injury. In vivo visualization of neuron specific gene expression to follow cell survival in a progressive manner may provide a more dynamic view of animal model disease pathophysiology than conventionally used histologic methods. Assessment of RGC density by CSLO is a potentially useful clinical application.



Commercial Relationships: Gustavo C. Munguba, None; **Daisy Lam**, None; **Ling Ge**, None; **Sanja Galeb**, None; **Sinthia Samad**, None; **Mary L. Tapia**, None; **Andrew Camp**, None; **Xiaoli Xing**, None; **Richard K. Lee**, National Eye Institute (F)
Support: F31EY022872

Program Number: 2246 **Poster Board Number:** B0050

Presentation Time: 2:45 PM - 4:30 PM

Lamina Cribrosa Position and Superior Visual Field Loss in Glaucoma

Yiyi Liu^{1,3}, Sung Chul Park^{1,2}, Rafael L. Furlanetto¹, Camila F. Netto¹, Uma J. Damle⁴, Jeffrey M. Liebmann^{1,5}, Robert Ritch^{1,2}.

¹Moise and Chella Safra Advanced Ocular Imaging Laboratory, Einhorn Clinical Research Center, New York Eye and Ear Infirmary, New York, NY; ²Department of Ophthalmology, New York Medical College, Valhalla, NY; ³New York Medical College, Valhalla, NY;

⁴Robert Wood Johnson Medical School, New Brunswick, NJ; ⁵Department of Ophthalmology, New York University School of Medicine, New York, NY.

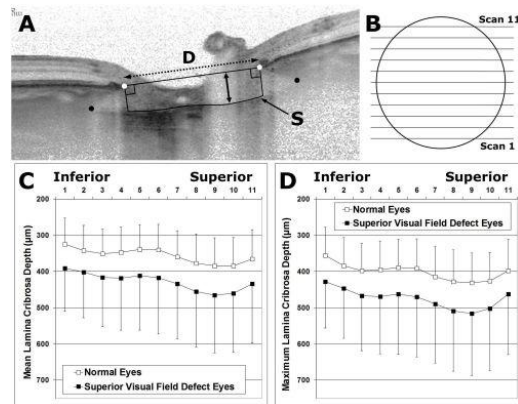
Purpose: To compare the position of the lamina cribrosa (LC) in glaucomatous eyes with superior hemifield visual field defects (VFD) with its position in normal eyes, to see if posterior LC displacement occurs in association with VFD.

Methods: Normal subjects and glaucoma patients with VFD limited to the superior hemifield were recruited. All participants had a complete ophthalmologic examination including standard automated

perimetry and retinal nerve fiber layer (RNFL) thickness measurement using optical coherence tomography (OCT). Serial horizontal enhanced depth imaging (EDI) OCT B-scans of the optic nerve head were obtained from each participant (interval between scans = ~30 µm). After delineating the anterior LC surface, mean and maximum LC depths (reference plane, Bruch’s membrane edges) were measured in 11 equally spaced horizontal B-scans, excluding the LC insertion area under Bruch’s membrane and the scleral rim (**Fig A and B**). Mean and maximum LC depths in each of the 11 B-scans were compared between the 2 groups.

Results: 57 normal eyes (57 subjects; mean age = 56±18 years) and 35 glaucomatous eyes with only superior VFD (35 patients; mean age = 59±17 years; VF mean deviation = -5.9±4.0 dB) were included. The RNFL was significantly thinner in the glaucomatous eyes in both the inferior (59 vs. 95 µm; p<0.01) and in the superior retina (81 vs. 98 µm; p<0.01) compared to the normal eyes. Both mean and maximum LC depths were significantly greater in the glaucomatous eyes in all 11 scans (all p<0.01; **Fig C and D**). Posterior LC displacement in the glaucomatous eyes appeared to be similar between the superior and inferior LC.

Conclusions: We found generalized posterior displacement of the entire central and mid-peripheral LC in the glaucomatous eyes with VFD limited to the superior hemifield, suggesting that detectable LC displacement occurs early in human glaucoma prior to the development of VFD. Studies are needed to elucidate the causal and temporal relationships of peripheral LC deformation with glaucomatous VFD.



(A) White dots = Bruch’s membrane edges; black dots = anterior lamina insertion points; maximum lamina cribrosa (LC) depth = black double arrow; mean LC depth = (area S / length D). (B) The circle indicates the LC. (C and D) Mean and maximum LC depth profiles in the normal and the glaucoma groups.

Commercial Relationships: Yiyi Liu, None; **Sung Chul Park**, None; **Rafael L. Furlanetto**, None; **Camila F. Netto**, None; **Uma J. Damle**, None; **Jeffrey M. Liebmann**, Alcon Laboratories, Inc. (C), Allergan, Inc. (C), Allergan, Inc. (F), Carl Zeiss Meditech, Inc (F), Heidelberg Engineering, GmbH (F), Topcon Medical Systems, Inc. (F), National Eye Institute (F), New York Glaucoma Research Institute (F), SOLX, Inc. (C), Bausch & Lomb, Inc (C), Diopsys, Inc. (C), Diopsys, Inc. (F), Merz, Inc. (C), Glaukos, Inc. (C), Quark, Inc. (C); **Robert Ritch**, None

Support: Allen Adler Research Fund of the New York Glaucoma Research Institute, New York, NY; James Cox Chambers Research Fund of the New York Eye and Ear Infirmary, New York, NY; Peter Crowley Research Fund of the New York Eye and Ear Infirmary, New York, NY

Program Number: 2247 **Poster Board Number:** B0051

Presentation Time: 2:45 PM - 4:30 PM

Between-Subject Differences Account for More Dissociation Between Rim Area and Visual Sensitivity Than Within-Subject Fluctuations

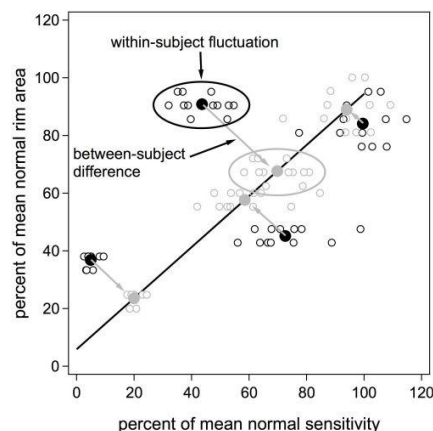
Iván Marín-Franch^{1,2}, *William H. Swanson*¹. ¹School of Optometry, Indiana University, Bloomington, IN; ²Optometry and Visual Science, City University London, London, United Kingdom.

Purpose: The aim of this study was to understand better the dissociation between rim area and visual sensitivity. Under the assumption that the true relationship is linear, we tested the hypothesis that between-subject differences account for more dissociation than within-subject fluctuations.

Methods: We tested the hypothesis independently for the superior-temporal (ST) and the inferior-temporal (IT) sectors. Twelve rim area and visual field examinations were taken for each of 30 eyes of 30 patients with glaucoma followed up over a period of 2 months [Artes et al ARVO 2011, #4148]. We assumed there was no progression. Rim area was expressed as percent normal mm² and sensitivity as percent normal 1 / L. Mean normal values were obtained for 173 visits for 77 eyes of 77 healthy controls. A linear model was fitted that accounted for noise in both sensitivity and rim area. For each patient, we calculated the centroid of the cloud of the 12 recorded rim areas and sensitivities. We corrected for between-subject differences by projecting each patient cloud onto the fitted line (see Figure). For both ST and IT, R^2 values were obtained for: all 360 datapoints (all variability), the 30 centroids (between-subject differences), and the 360 datapoints after correcting for between-subject differences (within-subject fluctuations).

Results: For ST, the R^2 values (and 95% confidence interval) were 23% (17% to 30%) for all variability, 26% (5% to 50%) for between-subject differences, and 86% (83% to 89%) for within-subject fluctuations. For IT, R^2 values were, respectively, 40% (33% to 47%), 45% (19% to 67%), and 87% (84% to 90%). The R^2 values were significantly larger for within-subject fluctuations in both ST and IT (with $\alpha = 0.05$). Adjusting rim area for sector area with quantile regression had no significant effect.

Conclusions: If the true relationship between rim area and visual sensitivity is linear, between-subject differences account for more dissociation than within-subject fluctuations. This result emphasizes the potential of individualized tests and structure-function maps.



Correcting for between-subject differences. Twelve datapoints (open black circles) and corresponding centroids (solid black circles) are shown for each of 4 patients chosen for illustration, as there was little or no overlap between their data clouds. The corresponding projected clouds are shown in gray.

Commercial Relationships: Iván Marín-Franch, None; William H. Swanson, None

Support: R01EY007716. The authors acknowledge Paul H Artes (Dalhousie University, Halifax) and David P Crabb (City University London, UK) for giving us unrestricted access to the 30-patient dataset. The dataset was collected at the Nova Scotia Eye Care Centre in Halifax for research funded by the Glaucoma Research Foundation (San Francisco, CA).

Program Number: 2248 **Poster Board Number:** B0052

Presentation Time: 2:45 PM - 4:30 PM

A Test of a Schematic Model of Glaucomatous Damage of the Macula

*Donald C. Hood*¹, *Ali S. Raza*², *Ilana Traynis*³, *C. Gustavo De Moraes*⁴, *Jeffrey M. Liebmann*^{4,5}, *Robert Ritch*^{5,6}. ¹Psychology and Ophthalmology, Columbia University, New York, NY; ²Neurobiology and Behavior, Columbia University, New York, NY; ³School of Medicine, Tufts University, Boston, MA; ⁴Ophthalmology, NYU School of Medicine, New York, NY; ⁵Einhorn Clinical Research Center, New York Eye & Ear Infirmary, New York, NY; ⁶Ophthalmology, New York Medical College, Valhalla, NY.

Purpose: To test the hypothesis that a recent model [1,2] of glaucomatous damage of the macula, based upon OCT data, predicts the pattern of early defects seen on visual field (VF) tests.

Methods: In a prospective study, 10-2 VFs (2° test grid; HFA II, CZM, Inc.) were obtained from 100 consecutive eyes with glaucomatous optic neuropathy and a reliable 24-2 VF with a mean deviation (MD) better than -6 dB. Thus, 24-2 VFs ranged from 'normal' to mild defects. At each point of the 10-2 VF, the total deviation (TD) values were averaged across eyes and the number of abnormal points (Ncrit) with TD values below a criterion (crit) level of -5, -10, or -15 dB calculated. The data and model are shown in retinal view in figs. 1 and 2, with the location of the points morphed to account for retinal ganglion cell displacement near the fovea [1-3]. In addition, the average TD values of the two regions of the model were compared.

Results: According to the model (fig. 1), most of the inferior macula (within red border) is relatively more vulnerable to damage because it projects largely to the inferior (I) quadrant of the disc, known to be the most common site of glaucomatous damage. The region within the dark gray border encompasses a small portion of the inferior, and the entire superior, macula. This region is relatively less vulnerable because it projects to the temporal (T) quadrant of the disc, known to be less affected by glaucoma. The pattern of both the average TD (fig. 2A) and the Ncrit (see fig. 2B for criterion of -5dB) values showed good agreement with the model. In addition, the average TD value for the red (vulnerable) region was -4.60 dB, significantly ($p < 0.001$; paired t-test) less than the value of -1.36 dB for the gray region.

Conclusions: VF losses of macular sensitivity observed in a prospective study of patients with mild glaucomatous damage conform to the pattern predicted by the model. The vulnerable region of the inferior macula (upper VF) is poorly sampled by the most common VF test (the 24-2 with a 6° grid).[1,2]

1. Hood, Raza et al, TVST, 2012; 2. Hood, Raza et al, PRER, 2012; 3. Raza et al, AO, 2011.

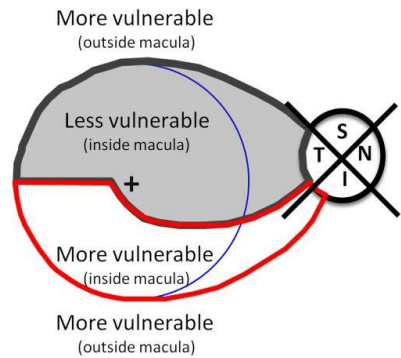


Fig. 1. The model in retinal view.

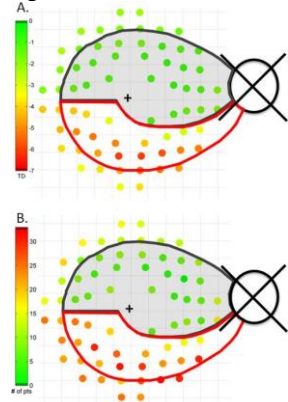


Fig. 2. A. The average TD values (dB) at each location determined with the 10-2 test. B. Same as A for the number of patients with TD values worse than -5 dB. Both panels in retinal view.

Commercial Relationships: Donald C. Hood, Topcon, In (F); Ali S. Raza, None; Ilana Traynis, None; C. Gustavo De Moraes, None; Jeffrey M. Liebmann, Alcon Laboratories, Inc. (C), Allergan, Inc. (C), Allergan, Inc. (F), Carl Zeiss Meditech, Inc (F), Heidelberg Engineering, GmbH (F), Topcon Medical Systems, Inc. (F), National Eye Institute (F), New York Glaucoma Research Institute (F), SOLX, Inc. (C), Bausch & Lomb, Inc (C), Diopsys, Inc. (C), Diopsys, Inc. (F), Merz, Inc. (C), Glaukos, Inc. (C), Quark, Inc. (C); Robert Ritch, None

Support: NIH Grant EY02115

Program Number: 2249 **Poster Board Number:** B0053

Presentation Time: 2:45 PM - 4:30 PM

Ganglion cell complex and peripapillary RNFL alterations in patients with open angle glaucoma

Monica Mosca, Alessandro Rossi, Roberto Sala, Roberto Ratiglia. Eye Clinic, Fondazione IRCCS "Cà Granda - Ospedale Maggiore Policlinico", Milano, Italy.

Purpose: To evaluate ganglion cell complex (GCC) and peripapillary retinal nerve fiber layer (RNFL) damage using Spectral Domain-Optical Coherence Tomography (SD-OCT), and the possible correlation with visual function in POAG with localized visual field defects.

Methods: Cross sectional study on 30 POAG patients (30 eyes) 17 males, 13 females (mean age 66.1±11.9 years) with moderate glaucomatous loss according to Hodapp classification and 30 normal subjects (30 eyes) 10 males, 20 females (mean age 62.2±9.6 years). Complete examination, SAP (Humphrey, 30-2 SITA standard), Cirrus SD-OCT imaging of peripapillary retina and macula were performed. GCC and RNFL thickness values in the retinal areas associated with hemifield localized perimetric defects were compared

with corresponding undamaged areas. Student t-test and Pearson's correlation coefficient (r) between the considered parameters and MD-PSD were used for statistical analysis.

Results: A significant difference ($p < 0.001$) in total mean GCC thickness and total mean RNFL thickness between POAG and control group was found ($59.9 \pm 10.77 \mu\text{m}$ vs $83.63 \pm 6.11 \mu\text{m}$; $61.23 \pm 10.78 \mu\text{m}$ vs $93.06 \pm 8.01 \mu\text{m}$ respectively). In POAG, GCC and RNFL thickness mean values from the retinal areas associated with localized visual field defects were significantly less than in the corresponding perimetrically undamaged areas ($55.23 \pm 10.62 \mu\text{m}$ vs $64.73 \pm 13.06 \mu\text{m}$: $p = 0.003$; $56.55 \pm 9.84 \mu\text{m}$ vs $64.55 \pm 12.11 \mu\text{m}$: $p = 0.007$ respectively). Mean values of the same parameters in the perimetrically undamaged retinal areas of POAG and in the corresponding sectors of control group were significantly different (GCC thickness $64.73 \pm 13.06 \mu\text{m}$ vs $83.23 \pm 7.05 \mu\text{m}$: $p < 0.001$; RNFL thickness $64.55 \pm 12.11 \mu\text{m}$ vs $92.5 \pm 8.03 \mu\text{m}$: $p < 0.001$). Total mean GCC thickness had the stronger correlation with MD and PSD ($r = 0.38$ $p = 0.03$; $r = -0.321$ $p = 0.08$ respectively).

Conclusions: In POAG patients with moderate localized perimetric defects, the new SD-OCT GCC Analysis evaluation could be useful in monitoring the glaucomatous disease and seems to detect earlier than RNFL Analysis the structural damage in accordance with the fact that GCC loss is supposed to occur before that of the RNFL.

Commercial Relationships: Monica Mosca, None; Alessandro Rossi, None; Roberto Sala, None; Roberto Ratiglia, None

Program Number: 2250 **Poster Board Number:** B0054

Presentation Time: 2:45 PM - 4:30 PM

Platelet Function Influences on Disc Hemorrhages in Patients with Open-Angle Glaucoma

Seonghee Shim¹, Joon Mo Kim¹, Chul Young Choi¹, Ki Ho Park².

¹Ophthalmology, Sungkyunkwan University School of Medicine, Kangbuk Samsung Hospital, Seoul, Republic of Korea;

²Ophthalmology, Seoul National University College of Medicine, Seoul, Republic of Korea.

Purpose: To evaluate influences of platelet function on disc hemorrhages in patients with open-angle glaucoma.

Methods: This study included 96 open-angle glaucoma patients with (n=44) and without (n=52) disc hemorrhage. A detailed eye examination including stereo disc photo, red free photo, Humphrey visual field, measurement of RNFL thickness with stratus OCT RNFL thickness, and measurement of collagen/epinephrine (CEPI) closure time with the platelet function analyzer (PFA)-100 system for platelet function assessment were performed in all subjects.

Results: The two groups were closely matched in terms of the mean ages and gender ($p = 0.505$, $p = 0.732$). There was no significant difference on the prevalence of hypertension and diabetes mellitus ($p = 0.133$, $p = 0.164$, respectively). The CEPI closure time was higher in patients with disc hemorrhage than in those without disc hemorrhage (134.48 ± 50.03 vs 105.98 ± 20.31 , $p = 0.001$). The same correlation was observed when platelet function of the two groups were compared by age (Table 1).

Conclusions: Our results indicate that platelet function influences on disc hemorrhages in patients with open-angle glaucoma. The prolonged bleeding due to delayed platelet aggregation time plays the important role in disc hemorrhages observed in open-angle glaucoma patients.

Table 1. Comparison of platelet function between subjects with and without disc hemorrhage by age

	Disc hemorrhage (+) (n=44)	Disc hemorrhage (-) (control) (n=52)	p-value
20-39 years	n=6	n=6	
PFA-100 results			
CEPI closure time (sec)	119.50 (102.25-134.00)	110.00 (96.75-144.50)	0.81
40-59 years	n=25	n=29	
PFA-100 results			
CEPI closure time (sec)	141.72 ± 62.64	112.59 ± 17.66	0.02
60+ years	n=13	n=17	
PFA-100 results			
CEPI closure time (sec)	128.31 ± 26.51	90.76 ± 15.49	<0.001

Data are expressed as mean ± standard deviation (SD), or median (interquartiles).
Independent sample t-tests or Mann-Whitney U tests were used for continuous variables.
PFA: platelet function analyzer, CEPI: collagen/epinephrine

Commercial Relationships: Seonghee Shim, None; Joon Mo Kim, None; Chul Young Choi, None; Ki Ho Park, None

Program Number: 2251 **Poster Board Number:** B0055

Presentation Time: 2:45 PM - 4:30 PM

Diagnostic Innovations in Glaucoma Study (DIGS): Relationship between Disease Severity and Reproducibility of Estimated Number of Retinal Ganglion Cells in Glaucoma

Amir Marvasti^{1,2}, Renato Lisboa^{1,3}, Linda M. Zangwill¹, Robert N. Weinreb¹, Felipe A. Medeiros¹. ¹Hamilton Glaucoma Center, Department of Ophthalmology, University of California, San Diego, San Diego, CA; ²Boston University, School of Medicine, Boston, MA; ³Department of Ophthalmology, Federal Univ of São Paulo, São Paulo, Brazil.

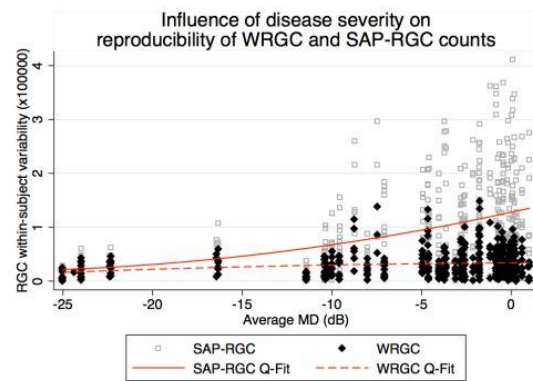
Purpose: To evaluate the influence of disease severity on the reproducibility of estimates of retinal ganglion cell (RGC) counts in a cohort of stable glaucoma patients.

Methods: This study included 55 eyes of 29 glaucoma patients followed for 5 weeks. Subjects were recruited from the Diagnostic Innovations in Glaucoma Study (DIGS). All eyes underwent weekly retinal nerve fiber layer (RNFL) imaging with Spectralis spectral domain optical coherence tomography (SDOCT) and visual field testing with standard automated perimetry (SAP). Estimates of RGC count were obtained from SAP (SAP-RGC) and SDOCT (SDOCT-RGC), and a weighted average (WRGC) was used to obtain a final estimate of the number of RGCs for each eye using structural and functional data. It was assumed that during the 5 weeks of follow-up the disease did not progress and that any change in measurements with retesting represented variability. Absolute differences between baseline and each follow-up were calculated. Intra-class correlation coefficients (ICCs) and weighted least squares (WLS) linear regression analysis were used to evaluate the influence of disease severity, measured by average Mean Deviation (MD), on the reproducibility of RGC count estimates.

Results: The average number of visits per patient was 4.4±0.9. The average MD was -5.07±6.86 dB, ranging from -25.21 to 1.55 dB. The apparently high reproducibility of SAP MD (in dB) in early disease corresponded actually to a large variability when the same data was translated into number of RGCs (SAP-RGC). Both WRGC and SAP-RGC had less variability with worse disease severity; however, WRGC had less variability than SAP-RGC in the entire disease spectrum (Figure). The ICC for the combined structure and function estimate of RGC counts was 0.99, indicating high reproducibility.

Conclusions: Visual field testing, when assessed in terms of RGC counts, shows higher variability in early compared to advanced stages of disease. WRGC, a new index representing a combined structure-function estimate of RGC counts, provides more consistent

reproducibility across the spectrum of disease and shows promise for improving our ability to assess glaucomatous progression.



Quadratic fitted (Q-Fit) lines illustrate WRGC has less variability compared to SAP-RGC in the entire disease spectrum.

Commercial Relationships: Amir Marvasti, None; Renato Lisboa, None; Linda M. Zangwill, Carl Zeiss Meditec Inc (F), Heidelberg Engineering GmbH (F), Optovue Inc (F), Topcon Medical Systems Inc (F), Nidek Inc (F); Robert N. Weinreb, Aerie (F), Alcon (C), Allergan (C), Altheos (C), Amakem (C), Bausch&Lomb (C), Carl Zeiss-Meditec (C), Genentech (F), Haag-Streit (F), Heidelberg Engineering (F), Konan (F), Lumenis (F), National Eye Institute (F), Nidek (F), Optovue (C), Quark (C), Solx (C), Topcon (C); Felipe A. Medeiros, Carl-Zeiss (F), Heidelberg Engineering (F), Topcon (F), Alcon (F), Allergan (F), Sensimed (F), Reichert (F)

Support: NEI EY11008, NEI EY08208, EY021818, EY022039 and participant retention incentive grants in the form of glaucoma medication at no cost from Alcon Laboratories Inc, Allergan, Pfizer Inc, and Santen Inc.

Clinical Trial: NCT00221897

Program Number: 2252 **Poster Board Number:** B0056

Presentation Time: 2:45 PM - 4:30 PM

Acute systemic hemodynamic effects on intraocular pressure in rats with unilateral experimental ocular hypertension

Jonathan C. Li¹, Vivek Kumar Gupta¹, Yuyi You¹, Keith Ng¹, Stuart Graham^{1,2}. ¹Department of Ophthalmology and Visual Sciences, Australian School of Advanced Medicine, Macquarie University, Sydney, NSW, Australia; ²Save Sight Institute, Sydney University, Sydney, NSW, Australia.

Purpose: To evaluate the effects of acute systemic arterial blood pressure (ABP) and central venous pressure (CVP) surges on intraocular pressure (IOP) in ocular hypertensive and normal eyes of rats.

Methods: Unilateral ocular hypertension (OHT) was established in Sprague-Dawley rats by serial weekly intracameral injection of microbeads. Continuous IOP waveform recordings from the anterior chamber were performed using solid-state 1.2F micro-sensors under urethane anesthesia. The effects on IOP during hemodynamic challenges using phenylephrine (PE) (50µg/kg/min i.v.) or rapid isotonic saline loading (20ml/kg over 1 min i.v.) were studied in both eyes.

Results: Over a 10-week period, IOP significantly increased by 53% (P < 0.05) in the unilateral microbead-induced OHT eyes. Both ABP and the IOP were significantly elevated during PE infusion compared to baseline (P < 0.05, Figure 1). A significantly greater IOP increase was found in the experimental OHT eyes compared to contralateral control eyes with maximal increases of 1.46 ± 0.2 mmHg and 0.94 ±

0.1 mmHg respectively ($P < 0.05$). Correspondingly, the OHT eyes had a significantly higher baseline IOP pulse amplitude and also a greater increase in pulse amplitude during PE infusion compared to control eyes ($P < 0.0001$). A rapid and sustained rise in IOP secondary to saline loading was observed in both OHT eyes and control eyes with a significantly greater rise observed among OHT eyes ($P < 0.0001$).

Conclusions: Intravenous administration of PE results in a temporary ABP rise and a transient intraocular hypertensive response. In contrast, surges in CVP results in a more sustained rise in IOP. The response was more pronounced in eyes with experimental glaucoma compared to normal eyes which emphasizes the importance of an intact outflow facility for dampening fluctuations in IOP. The fluid challenge mimics the effects seen in a water drinking test with a greater rise and prolonged recovery time.

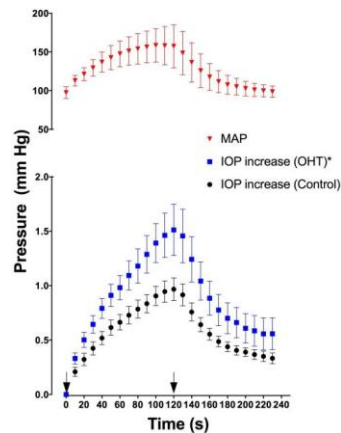


Figure 1. IOP and mean arterial pressure (MAP) during and following IV phenylephrine infusion (50 μ g/kg/min). Start and finish of the infusion over 2 minutes indicated by arrows. IOP rise in OHT eyes was significantly greater than control eyes (values are mean \pm SEM, n=7, * $P < 0.05$).

Commercial Relationships: Jonathan C. Li, None; Vivek Kumar Gupta, None; Yuyi You, None; Keith Ng, None; Stuart Graham, None

Program Number: 2253 **Poster Board Number:** B0057

Presentation Time: 2:45 PM - 4:30 PM

Glaucoma Severity Correlates with Lamina Cribrosa Depth and Thickness

Martha Kim, Karine D. Bojikian, Deana Choi, Mark A. Slabaugh, Philip P. Chen. Ophthalmology, University of Washington School of Medicine, Seattle, WA.

Purpose: To evaluate the correlation between the lamina cribrosa (LC) morphology and glaucoma severity using enhanced depth imaging spectral-domain optical coherence tomography (EDI SD-OCT) and Humphrey visual field test (HVF).

Methods: Optic nerve head B-scans of 103 glaucoma patients were obtained using EDI SD-OCT. Images were analyzed using the Heidelberg Eye Explorer software. LC depth was defined as the greatest distance between the reference plane (the imaginary extension of Bruch's membrane plane) and the anterior border of LC, perpendicular to the reference plane. LC thickness was the distance from anterior border to the posterior border of LC in the center of optic nerve head images of horizontal plane. The two global indices, mean deviation (MD) and pattern standard deviation (PSD) were obtained from HVF.

Results: The mean (\pm standard deviation) values of MD and PSD were -5.4 ± 5.8 dB and 6.2 ± 3.8 dB. The LC depth and the LC

thickness were 540.26 ± 140.39 μ m and 173.23 ± 50.02 μ m. The LC depth showed weak but significant correlation with MD by Pearson correlation test and linear regression analysis (Pearson $\sigma = -0.348$; $P < 0.001$; $r^2 = 0.121$; $P < 0.001$). The LC thickness also correlated with MD (Pearson $\sigma = 0.337$; $P = 0.001$; $r^2 = 0.114$; $P = 0.001$). The PSD showed a similar correlation with the LC depth and the LC thickness. The intraclass correlation coefficients of two observers on performing measurements of the LC depth and the LC thickness showed high reproducibility (0.972 and 0.779).

Conclusions: Glaucoma severity shows a significant correlation with the LC depth and the LC thickness. These measures may be useful in optic nerve head analysis using SD-OCT.

Commercial Relationships: Martha Kim, None; Karine D. Bojikian, None; Deana Choi, None; Mark A. Slabaugh, None; Philip P. Chen, Allergan (C)

Program Number: 2254 **Poster Board Number:** B0058

Presentation Time: 2:45 PM - 4:30 PM

Inter-ethnicity Comparison of Anterior Chamber Biometry and Iris Measurements between Narrow Angle and Open Angle Cohorts Using ASOCT

Ye Elaine Wang^{1,2}, YINGJIE LI^{1,3}, Dandan Wang^{1,4}, Mingguang He⁴, Shan C. Lin¹. ¹Ophthalmology, University of California, San Francisco, San Francisco, CA; ²Duke University School of Medicine, Durham, NC; ³Ophthalmology, Number Third Affiliated Hospital of Nanchang University, Nanchang, China; ⁴State Key Laboratory of Ophthalmology, Zhongshan Ophthalmic Center, Sun Yat-sen University, Guangzhou, China.

Purpose: To assess differences in anterior segment biometry and iris parameters among narrow and open angle American Caucasians, American Chinese and mainland Chinese, in order to elucidate potential inter-ethnic differences in the course of angle closure development.

Methods: Three gender- and age-matched Caucasians, American Chinese, and mainland Chinese cohorts were enrolled. Subjects in each ethnic group were divided into narrow and open angle subgroups. Narrow angles were defined as posterior trabecular meshwork not visible for ≥ 2 quadrants on gonioscopy. ASOCT and customized software were utilized to image and calculate the anterior chamber biometry and iris measurements.

Results: Data from 120, 116, and 116 subjects were available for Caucasian, American Chinese, and mainland Chinese, respectively. The open angle cohort had 96, 80, and 86; while the narrow angle cohort had 24, 36, and 30 Caucasian, American Chinese and mainland Chinese subjects, respectively. After multiple linear regression adjusting for confounders, ethnic Chinese showed significantly smaller anterior chamber width (ACW), anterior chamber depth (ACD), anterior chamber area (ACA), and anterior chamber volume (ACV) in both the open ($p < 0.0001$; $p < 0.0001$; $p = 0.0210$; $p = 0.001$; respectively) and narrow angle cohorts ($p < 0.0001$; $p = 0.0168$; $p = 0.016$; $p = 0.0076$; respectively). For iris measurements, only iris area (Iarea) was found to be significantly greater in both open angle ($p = 0.0098$) and narrow angle ($p = 0.0228$) ethnic Chinese subjects. Iris thickness at 750 μ m from the scleral spur (IT750), and pupil diameter (PD) were only found to be significantly greater in Chinese with open angles ($p = 0.0122$). Iris curvature (Icurv) and lens vault (LV) were not significantly different between Caucasians and Chinese regardless of whether they had narrow or open angle.

Conclusions: Both open and narrow angle ethnic Chinese have smaller ACW, ACD, ACA, and ACV than Caucasians counterparts. This can in part explain the observed difference in the prevalence of angle closure between Chinese and Caucasians. Since within the

narrow angle group, no significant inter-ethnic differences were detected for iris parameters except for iris area, other factors such as iris root insertion location, ciliary body size and angulation, and genetic background may contribute to the increased risk for angle closure in ethnic Chinese.

Commercial Relationships: Ye Elaine Wang, None; YINGJIE LI, None; Dandan Wang, None; Mingguang He, None; Shan C. Lin, None

Program Number: 2255 **Poster Board Number:** B0059

Presentation Time: 2:45 PM - 4:30 PM

Comparison of Regression Analysis in structural and functional monitoring of glaucoma patients

Gijs Thepass¹, Josine van der Schoot¹, Koenraad A. Vermeer¹, Hans G. Lemij^{1,2}. ¹Rotterdam Ophthalmic Institute, Rotterdam Eye Hospital, Rotterdam, Netherlands; ²Glaucoma Service, Rotterdam Eye Hospital, Rotterdam, Netherlands.

Purpose: The agreement between structural and functional measurements in glaucomatous progression is generally poor. For Scanning Laser Polarimetry (SLP), the agreement with functional measurements has been explored relatively little. We wished to explore this in greater detail.

Methods: All eligible eyes of glaucoma patients from the Rotterdam Glaucoma Imaging Study with at least 5 follow-up measurements were enrolled (n=90) in this study. The average time between the first and last visit was 28 months (22-32). The proprietary progression programs for both SLP (GDx ECC, Carl Zeiss Meditec) and Standard Automated Perimetry (SAP) (Humphrey Field Analyzer II, 24-2 white on white SITA test program, Carl Zeiss Meditec) were used (GDx GPA Fast mode and HFA GPA, respectively). The GDx GPA flags any progression as possible or as likely. We also calculated linear regression coefficients for each series of measurements of the SAP Visual Field Index (VFI) and Mean Deviation (MD), and the GDx peripapillary retinal nerve fibre layer thickness (TSNIT average).

Results: All results of the regression analyses are presented in Figs. 1 & 2. None of the tested eyes showed statistically significant progression by HFA GPA, but 5 (6%) eyes showed likely progression by GDx GPA (marked by red triangles in Figs. 1&2). Eight eyes (9%) showed TSNIT average increases (marked by green diamonds in figures 1&2). In our own regression analyses, 52 eyes (58%) showed disease progression by HFA VFI, 60 eyes (67%) by HFA MD and 49 eyes (54%) by GDx TSNIT average. In 31 eyes (34%), there was both structural and functional progression by HFA VFI and TSNIT average (see Figs.). Both structural and functional regression occurred in 18 eyes (20%).

Conclusions: Glaucomatous progression may be detected by SLP and by SAP. There was poor agreement between GDx and HFA progression, regardless of the used analysis. HFA GPA was more conservative than linear regression analysis. One of the limitations of this study is the relatively short average follow-up time. Plots that combine data from both structural and functional test methods (such as in Figs. 1 & 2) may help clinicians appreciate whether structural and functional measurements agree. In case of such agreement, they may feel more confident in their glaucoma management.

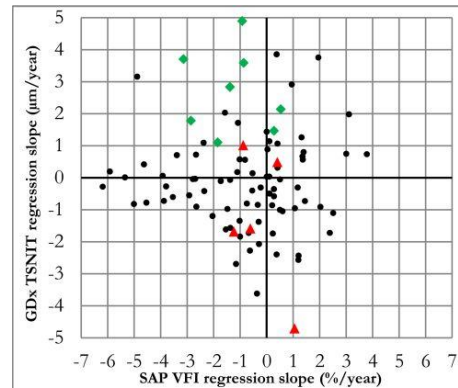


Figure 1. VFI versus TSNIT

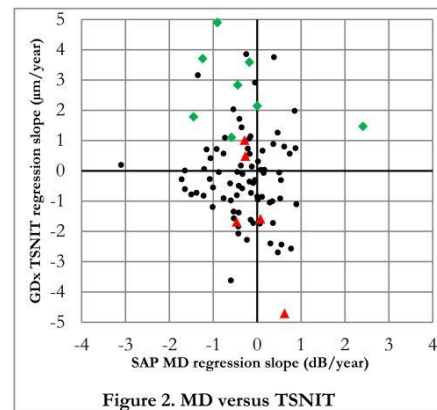


Figure 2. MD versus TSNIT

Commercial Relationships: Gijs Thepass, None; Josine van der Schoot, None; Koenraad A. Vermeer, Heidelberg Engineering (F), General Hospital Corporation (P); Hans G. Lemij, Carl Zeiss Meditec (C)

Clinical Trial: NTR1195

Program Number: 2256 **Poster Board Number:** B0060

Presentation Time: 2:45 PM - 4:30 PM

Evaluation of filtering blebs with transconjunctival oozing by anterior segment optical coherence tomography

Nakashima Kei-Ichi, Toshihiro Inoue, Ayako Fukushima, Hirakawa Saori, Takahiro Kawaji, Hidenobu Tanihara. Department of Ophthalmology, Kumamoto University, Faculty of Life Sciences, Kumamoto, Japan.

Purpose: To evaluate filtering blebs with transconjunctival oozing by anterior segment optical coherence tomography (AS-OCT).

Methods: Cross-sectional study. Forty-eight eyes of 48 patients with filtering blebs after trabeculectomy were examined at Kumamoto University Hospital between August 2011 and November 2012. Transconjunctival oozing was defined as transconjunctival aqueous egress on the bleb without point leak observed by slit-lamp, which was confirmed by digital pressure. Total bleb height, height of internal fluid-filled cavity, bleb wall thickness and bleb wall density were measured by three-dimensional AS-OCT. Age, glaucoma type, postoperative follow-up period, number of topical treatment, intraocular pressure (IOP), bleb vascularity grade classified by Moorfields Bleb Grading System, and bleb parameters of eyes with oozing were compared with eyes without oozing.

Results: Twenty-five eyes (52.1%) of 48 eyes had oozing (25 eyes with digital ocular pressure and 2 eyes without). The average ages were 68.5 ± 10.8 years and 66.8 ± 9.8 years, follow-up periods were

ARVO 2013 Annual Meeting Abstracts by Scientific Section/Group – Glaucoma

549.3 ± 1192.0 days and 600.6 ± 829.0 days, IOPs were 11.2 ± 4.9 mmHg and 14.5 ± 4.2 mmHg, and bleb vascularity grades were 1.2 ± 0.4 and 2.2 ± 1.1 in eyes with oozing and without oozing, respectively. Total bleb heights were 1.08 ± 0.40 and 1.04 ± 0.53 mm, height of internal fluid-filled cavities were 0.37 ± 0.29 and 0.50 ± 0.53 mm, bleb wall thicknesses were 0.71 ± 0.35 and 0.54 ± 0.32 mm, and bleb wall densities were 125.10 ± 35.36 and 162.91 ± 41.33 optical density in eyes with oozing and without oozing, respectively. There were significant differences in IOPs (P = 0.0170), bleb vascularity (P < 0.0001) and bleb wall densities (P = 0.0013) between the two groups, while there were no significant differences in other parameters.

Conclusions: Transconjunctival oozing was associated with IOP control and bleb wall properties.

Commercial Relationships: Nakashima Kei-Ichi, None; Toshihiro Inoue, None; Ayako Fukushima, None; Hirakawa Saori, None; Takahiro Kawaji, None; Hidenobu Tanihara, None
Support: JSPS KAKENHI Grant Number 23390403, 23791993 and 23791994

Program Number: 2257 **Poster Board Number:** B0061
Presentation Time: 2:45 PM - 4:30 PM

Maps Relating OCT Retinal Nerve Fiber Layer to Visual Fields Influence Evaluations of Structure-Function Models
 Ali S. Raza^{1,2}, Donald C. Hood^{1,3}. ¹Psychology, Columbia University, New York, NY; ²Neurobiology and Behavior, Columbia University, New York, NY; ³Ophthalmology, Columbia University, New York, NY.

Purpose: To assess the effect of using a particular map relating optical coherence tomography (OCT) to visual fields (VFs) when evaluating structure-function models.

Methods: Optic disc frequency domain OCT (Topcon, Inc.) volume scans and 24-2 VFs (Zeiss, Inc.) were obtained from 96 eyes of 75 glaucoma patients and suspects (56.4 ± 12.4 yrs, MD -4.0 ± 5.3 dB), 48 eyes of 48 healthy controls (51.4 ± 7.4 yrs, MD -0.2 ± 0.9 dB), and 15 eyes of 11 patients with severe ischemic optic neuropathy (ION; 64.7 ± 10.9 yrs, MD -19.2 ± 7.1 dB). Circumpapillary retinal nerve fiber layer (cpRNFL) measurements were obtained by hand-correcting a segmentation algorithm.¹ Using two maps relating OCT to VFs, Garway-Heath et al. (GH, Fig. 1A)² and Harwerth et al. (H, Fig. 1B),³ structure-function relationships were plotted for both the superior and inferior retina (Fig. 2A). Two models were compared: the Harwerth et al. non-linear model (H-NLM)³ and the Hood and Kardon linear model (HK-LM).⁴ The 8 H-NLM parameters were obtained from the literature³ and are independent of any particular OCT to VF map. Because the 2 HK-LM parameters depend on the map used, they were derived from the control and ION populations (green and red in Fig 2A). Models were evaluated on the independent glaucoma population (without free parameters) using the coefficient of variation of the root mean squared error (CVRMSE), where 0 indicates a perfect model fit.

Results: The residuals for the H-NLM were considerably larger (Fig 2B,C). The HK-LM did better than the H-NLM using the GH map by about a factor of 5 (superior CVRMSE 0.25 vs 1.22; inferior 0.28 vs 1.55; Fig 2B) and the H map by about a factor of 2 to 3 (superior CVRMSE 0.22 vs 0.67; inferior 0.24 vs 0.56; Fig 2C).

Conclusions: Given the H-NLM converts VF and cpRNFL values into ganglion cell counts, it is difficult to understand the model's poorer performance when using the anatomically more defensible GH map. Therefore, further work is needed to determine the accuracy of these derived ganglion cell estimates.

¹Raza et al. *AO* 2011, ²Garway-Heath et al. *IOVS* 2002, ³Harwerth et al. *PRER* 2010, ⁴Hood & Kardon *PRER* 2007

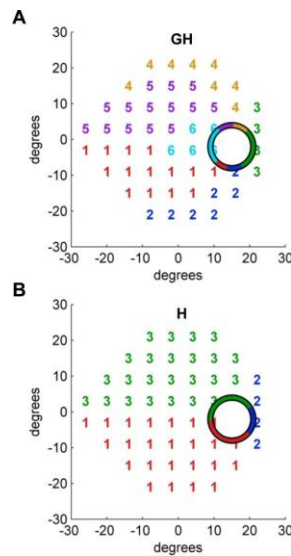


Fig. 1: The GH (A) and H (B) OCT to VF maps.

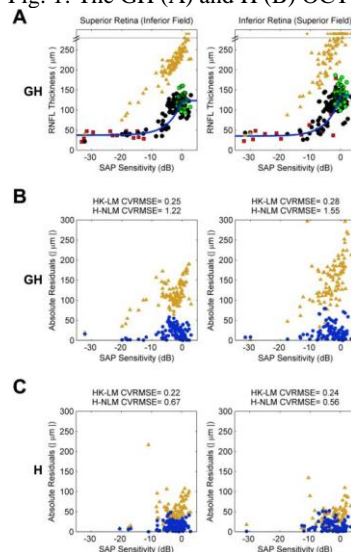


Fig. 2: (A) The HK-LM (blue) and H-NLM (orange Δ) models plotted against the control (green ○), glaucoma (black ●), and ION (red ■) subjects using the GH map. (B) The residuals as in (A). (C) The residuals using the H map.

Commercial Relationships: Ali S. Raza, None; Donald C. Hood, Topcon, In (F)

Support: NIH Grant R01-EY-002115 (DCH) and NSF GRFP DGE-11-44155 (ASR)

Program Number: 2258 **Poster Board Number:** B0062
Presentation Time: 2:45 PM - 4:30 PM

A Novel Method Of Measuring Optic Disc Tilt
 Seng-Chee Loon^{1,2}, Victor Koh^{1,2}, Wan Ling Wong², Xiang LF², Tien Y. Wong^{1,2}, Tin Aung^{3,2}, Paul R. Healey⁴. ¹Ophthalmology, National University Hospital of Singapore, Singapore, Singapore; ²Eye, Singapore Eye Research Institute, Singapore, Singapore; ³Eye, Singapore National Eye Centre, Singapore, Singapore; ⁴Ophthalmology, University of Sydney, Sydney, NSW, Australia.

Purpose: To describe a new method of measuring optic nerve head tilt assessed using the Heidelberg Retinal Tomograph (HRT), and arrive at a definition of optic disc tilt.

Methods: A new program was developed to calculate the horizontal disc tilt from a reference plane using the retinal plane. It estimates the degree of horizontal disc tilt using 35 HRT scans of Chinese eyes with clinically-detectable disc tilt. We applied the same program to 2,927 eyes from the Singapore Malay Eye Study (SiMES), a population study and determine the optimal tilt cut-off based on the area under the receiver operating characteristic curve (AUC) (adjusting for age, gender, diabetes mellitus, hypertension and smoking) for a range of ocular and HRT parameters. Lastly, we apply the program to 300 Malay and 300 Chinese normal eyes which were randomly selected from population studies as controls for comparison to the tilt cases.

Results: The median horizontal disc tilt from the 35 HRT scans of eyes with clinically-detectable disc tilt is 3.8 degrees. The median of optimal cut-offs derived from 2,927 eyes (SiMES) with adjusted AUCs greater than 0.6 from a range of risk factors associated with disc tilt (i.e. glaucoma, IOP) and HRT parameters (i.e. disc area, rim area) is 3.8, which corresponds to the 90th percentile horizontal tilt value of the 216 Malay and 224 Indian control eyes.

Conclusions: We found a method of measuring disc tilt and also correlated the measurements with a population based sample. Based on these measurements, we aim to define the degree of disc tilt which will allow us to classify cases into those which have significant tilt and the severity of tilt. This will allow us to then measure the amount of disc tilt in the population and assess the risk factors and associations with other ocular diseases.

Commercial Relationships: Seng-Chee Loon, None; Victor Koh, None; Wan Ling Wong, None; Xiang LI, None; Tien Y. Wong, Allergan (C), Bayer (C), Novartis (C), Pfizer (C), GSK (F), Roche (F); Tin Aung, Alcon (R), Alcon (C), Alcon (F), Allergan (R), Allergan (C), Carl Zeiss Meditec (F), Carl Zeiss Meditec (R), Ellex (F), Ellex (R), Santen (R); Paul R. Healey, None

Support: NMRC/NIG/2016/2010

Clinical Trial: NMRC/NIG/2016/2010

Program Number: 2259 **Poster Board Number:** B0063

Presentation Time: 2:45 PM - 4:30 PM

Three-Dimensional (3-D) Histomorphometry of Normal Human Optic Nerve Head (ONH) Connective Tissue at physiologic and elevated IOP

Lan Wang¹, Hongli Yang², Massimo A. Fazio¹, Brandon Smith¹, Chad C. Cheetham¹, J Crawford C. Downs¹, Juan Reynaud², Howard Lockwood², Claude F. Burgoyne², Christopher A. Girkin¹. ¹Ophthalmology, Univ of Alabama at Birmingham, Birmingham, AL; ²Discoveries in Sight, Devers Eye Institute, Legacy Research Institute, Portland, OR.

Purpose: To compare the difference of normal human ONH connective tissue structure at physiologic and elevated IOP by 3D histomorphometry.

Methods: 38 eyes from 19 human donors (54±17 years old), collected within 6 hours postmortem underwent aldehyde fixation at 10mmHg IOP in both eyes (7 pairs) or 10 mmHg in the right eye and 45 mmHg in the left eye (12 pairs). The ONH and peripapillary sclera were trephinated and serial sectioned using an automated microtome-based system that yielded serial fluorescent images of the block face as we cut through the ONH at 1.5 µm section thickness; the autofluorescent images were aligned and stacked into a 3D ONH reconstruction with 1.5x1.5x1.5 µm voxel resolution (Downs et al. ISER 2010). The ONH and peripapillary scleral anatomy was delineated in custom software (Downs, Yang et al. IOVS 2007). The 80 Bruch's membrane opening (BMO) points were used to establish a zero reference plane for all measurements. The BMO radius, neural canal depth, lamina cribrosa thickness and depth, and scleral

thickness were calculated and analyzed using mixed effects models with generalized estimation equations.

Results: In adjusted models, IOP elevation from 10 to 45 mmHg resulted in a significant decrease in the posterior scleral canal opening radius (p = 0.028) and posterior lamina insertion radius (p = 0.026). No other significant differences in morphometric parameters were detected (Table 1).

Conclusions: While no significant changes in lamina position were seen, contraction of the posterior neural canal occurs in response to IOP elevation in normal human donor eyes.

	Beta Coefficient	p-value
Lamina Depth	215.969	
Treatment	6.939	0.676
Lamina Thickness	198.208	
Treatment	-19.388	0.113
BMO - Radius	821.390	
Treatment	-11.320	0.481
ASCO - Radius	840.90	
Treatment	-9.720	0.517
ALI - Radius	954.960	
Treatment	12.860	0.529
PSCO - Radius	1048.450	
Treatment	-22.40	0.028*
PLI - Radius	1048.37	
Treatment	-23.150	0.026*
Sclera Thickness	354.530	
Treatment	-13.280	0.518

ASCO: Anterior Sclera Canal Opening; ALI: Anterior Lamina Insertion; PCSO: Posterior Sclera Canal Opening; PLI: Posterior Lamina Insertion. * Significantly different at p<0.05

Commercial Relationships: Lan Wang, None; Hongli Yang, None; Massimo A. Fazio, None; Brandon Smith, None; Chad C. Cheetham, None; J Crawford C. Downs, None; Juan Reynaud, None; Howard Lockwood, None; Claude F. Burgoyne, Heidelberg Engineering (F), Heidelberg Engineering (C); Christopher A. Girkin, SOLX (F), Heidelberg Engineering (F)
Support: NIH RO1: EY 18926-01 (CD, CG), NIH RO1: EY 19333-01 (CD,CG), RPB Physician Scientist Award (CAG), Eyesight Foundation of Alabama (CAG)

Program Number: 2260 **Poster Board Number:** B0064

Presentation Time: 2:45 PM - 4:30 PM

Longitudinal analysis of progression in Korean patients with normal tension glaucoma

Sun Hee Lim, Yeon Ggoch Park, Kyu-Ryong Choi. ophthalmology, Ewha womans university school of medicine, Seoul, Republic of Korea.

Purpose: To evaluate the rate of visual field(VF) progression and changes of retinal nerve fiber layer(RNFL) thickness in Korean patients with normal tension glaucoma(NTG).

Methods: One hundred patients(100 eyes) with NTG, who were being treated with topical antiglaucoma drugs and had been followed for more than 2 years, were studied. All subjects were classified into 3 groups by initial mean deviation(MD): early stage with MD of -6dB or better, moderate stage with MD between -6dB and -12dB, and advanced stage with MD of -12dB or worse. Using Glaucoma change probability analysis(STATPAC2), we determined visual field progression and classified 2 groups: progression and non-progression. To estimate the rate of VF progression of half-of-patients, data were analyzed using Kaplan-Meier survival test. And Linear mixed models were used to estimate the rate of changes in MD(dB/yr) and RNFL thickness(µm/yr) for all subjects.

Results: Forty-two patients were placed in the early stage group,

twenty-four into the moderate stage group, and thirty-four into the advanced stage group. There were significant differences in the baseline MD, baseline PSD and mean MD slope among 3 groups. Mean MD slope in the early stage group (-0.29 ± 0.04 dB/yr) was significantly steeper than that in other groups (moderate stage; -0.33 ± 0.04 dB/yr, severe stage; -0.05 ± 0.08 dB/yr). After 7-8 years, half of patients with NTG showed localized progressions in early or moderate stage groups. In progression group ($n=35$), mean MD slope (-0.41 ± 0.04 dB/yr) was significantly steeper than in non-progression group (-0.11 ± 0.11 dB/yr). In progression group, the proportion of advanced stage was lower (20%) than other stages. The rate of changes of RNFL thickness was steeper in progression group ($-0.97 \pm 0.17 \mu\text{m/yr}$) than non-progression group ($-0.43 \pm 0.05 \mu\text{m/yr}$).

Conclusions: The progression rate of visual field defects, MD slope, and RNFL thickness in patients with NTG differed according to the severity of the initial visual field damage. The progression rate of visual field defects was higher in patients with early or moderate stage than in that with advanced stage.

Commercial Relationships: Sun Hee Lim, None; Yeon Ggoch Park, None; Kyu-Ryong Choi, None

Program Number: 2261 **Poster Board Number:** B0065

Presentation Time: 2:45 PM - 4:30 PM

Symmetry of the Pupillary Light Reflex and its Relationship to Retinal Nerve Fiber Layer Thickness and Visual Field Defect in Subjects With and Without Glaucoma

Dolly S. Chang^{1,2}, Karun S. Arora¹, Michael V. Boland¹, David S. Friedman^{1,2}. ¹Ophthalmology, Wilmer Eye Institute, Johns Hopkins University, Baltimore, MD; ²Epidemiology, Bloomberg School of Public Health, Johns Hopkins University, Baltimore, MD.

Purpose: To assess the relationship between the pupillary light reflex (PLR) and 1) visual field (VF) defect and 2) retinal nerve fiber layer (RNFL) thickness.

Methods: In this prospective case-control study, we enrolled 157 patients with glaucoma (mean age 67 ± 11 , 50% female) and 71 controls (mean age 60 ± 10 , 69% female). Using a pupillometer, we recorded and analyzed pupillary responses to various stimulus patterns (full field, superonasal and inferonasal quadrant arcs). We compared the responses between the two eyes, compared responses to superonasal and inferonasal stimuli within each eye, and calculated the absolute PLR value of each individual eye. We assessed the relationship between PLR, VF and RNFL using Pearson correlation coefficients. For analyses performed at the level of individual eyes, we used mixed effects multi-level modeling to account for between-eye correlations within individuals.

Results: Persons with glaucoma had a more asymmetric pupil response between the two eyes ($p < 0.001$), between superonasal and inferonasal field within the same eye ($p = 0.014$), and also had a smaller amplitude, slower velocity and longer latency of pupil response as compared to controls (all $p < 0.001$). For every 0.3 log unit difference in between-eye asymmetry of PLR there was an average 2.3 dB difference in VF mean deviation ($R^2 = 0.62$, $p < 0.001$, Figure 1) and a $3.7 \mu\text{m}$ difference in RNFL thickness between the two eyes ($R^2 = 0.34$, $p < 0.001$, Figure 2). Greater VF damage and a thinner RNFL for each individual eye were associated with a smaller response amplitude, slower velocity, and longer time to peak constriction and dilation (all $p < 0.001$ after adjusting for age and gender). However, within-eye asymmetry of PLR between superonasal and inferonasal stimulation was not associated with within-eye differences of corresponding locations in VF or RNFL.

Conclusions: When measured precisely the PLR is strongly correlated with visual field functional testing and measurements of

RNFL thickness. Quantitative pupillometry may have a role in the diagnosis and management of optic neuropathies.

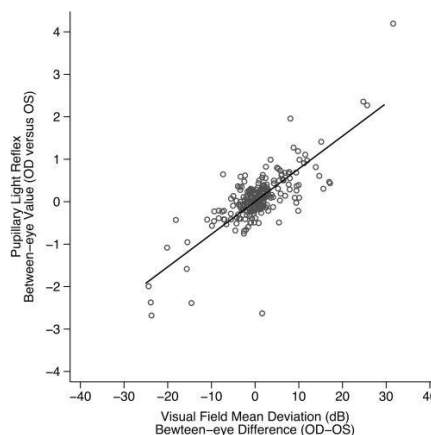


Figure 1. The relationship of between-eye symmetry in pupillary light reflex and visual field defect.

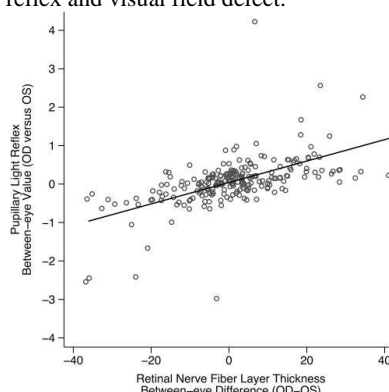


Figure 2. The relationship of between-eye symmetry in pupillary light reflex and retinal nerve fiber layer thickness.

Commercial Relationships: Dolly S. Chang, None; Karun S. Arora, None; Michael V. Boland, None; David S. Friedman, Alcon (C), Bausch & Lomb (C), Merck (C), QLT, Inc (C), Allergan (C), Nidek (C)

Support: 2T32AG000247-16

Program Number: 2262 **Poster Board Number:** B0066

Presentation Time: 2:45 PM - 4:30 PM

Trabeculectomy bleb assessment via three-dimensional anterior segment optical coherence tomography

Takahiro Kawaji, Toshihiro Inoue, Riyo Matsumura, Utako Kuroda, Nakashima Kei-Ichi, Hidenobu Tanihara. Ophthalmology, Kumamoto University, Chuo-ku, Kumamoto, Japan.

Purpose: To evaluate the morphological features of filtering blebs after trabeculectomy by using three-dimensional anterior segment optical coherence tomography (3D AS-OCT).

Methods: This retrospective cross-sectional study evaluated 73 patients who had undergone trabeculectomy with mitomycin C. All blebs were imaged with 3D AS-OCT and analyzed with our custom software. We assessed blebs quantitatively for the following features: bleb height, fluid-filled cavity height, bleb wall thickness, and bleb wall intensity.

Results: The mean (\pm standard deviation [SD]) time period between trabeculectomy and 3D AS-OCT measurement was 22.7 ± 25.5 months; the mean (\pm SD) intraocular pressure (IOP) measured 13.8 ± 3.9 mm Hg at the time of 3D AS-OCT imaging. IOP and the bleb height ($r_s = -0.389$, $P = .0007$) and IOP and the bleb wall intensity (r_s

= 0.399, $P = .0005$) showed statistically significant correlations. Eyes with limbus-based conjunctival flaps had a higher bleb height ($P = .01$), an increased fluid-filled cavity height ($P = .0003$), and a lower bleb wall intensity ($P = .02$) compared with eyes with fornix-based flaps. Bleb wall thickness in these 2 groups did not differ significantly ($P = .17$).

Conclusions: Our 3D AS-OCT imaging, which can evaluate morphological features of trabeculectomy blebs quantitatively and noninvasively, showed that the bleb height and intensity of the bleb wall had significant relationships to the IOP. Limbus-based procedures produced higher blebs, increased fluid-filled cavities, and lower intensity of the bleb wall.

Commercial Relationships: Takahiro Kawaji, None; Toshihiro Inoue, None; Riyo Matsumura, None; Utako Kuroda, None; Nakashima Kei-Ichi, None; Hidenobu Tanihara, None

Support: This work was supported in part by JSPS KAKENHI Grant Number 23390403, 23791993, 23791994.

Program Number: 2263 **Poster Board Number:** B0067

Presentation Time: 2:45 PM - 4:30 PM

Visual and structural prognosis of the untreated fellow eyes of unilateral normal tension glaucoma patients

Hyun-kyung Cho¹, Jongchul Han¹, Wool Suh², Changwon Kee¹.

¹Department of Ophthalmology, Samsung Medical Center, Sungkyunkwan University School of Medicine, Seoul, Republic of Korea; ²Department of Ophthalmology, Hallym Sacred Heart Hospital, College of Medicine, University of Hallym, Anyang, Republic of Korea.

Purpose: To investigate the visual and structural prognosis of the untreated initial non-glaucomatous fellow eyes of unilateral normal tension glaucoma (NTG) patients.

Methods: NTG patients with unilateral visual field (VF) loss and no visual field defect, retinal nerve fiber layer (RNFL) defect or neuroretinal rim (NRR) notching in the fellow eyes and those who had initial non-glaucomatous fellow eyes not treated were included. For the fellow eyes of the 50 subjects, the development of VF defect, RNFL defect, and NRR notching was inspected retrospectively by two observers. Baseline clinical characteristics including initial intraocular pressure (IOP), central corneal thickness, and spherical equivalent were compared between glaucomatous and contralateral eye.

Results: The mean follow-up period was 8.77 ± 2.92 years. Among 50 unilateral NTG patients 5 (10%) patients developed RNFL defect in 5.55 ± 2.69 years and 4 (8%) patients developed NRR notching in 5.17 ± 3.09 years in the fellow eye. Among 6 (12%) patients who had developed either RNFL defect or NRR notching, only 3 (6%) patients developed VF loss in 1.81 years, 3.09 years, and 9.27 years, respectively. Initial IOP was significantly higher (17.20 ± 3.07 mmHg vs 16.58 ± 3.24 mmHg, $p = 0.031$), SE was more myopic (-1.81 ± 2.27 D vs -1.40 ± 2.14 D, $p = 0.025$), and the occurrence of disc hemorrhage ($15/50$ vs $6/50$, $p = 0.049$) was significantly higher in the glaucomatous eye than the contralateral eye.

Conclusions: The incidence of glaucoma development in the fellow eye is rather low, and even glaucoma develops in the fellow eye, it takes quite a long period of time. Therefore, the initial non-glaucomatous fellow eye of the unilateral NTG patient may be observed without treatment until the glaucoma develops.

Commercial Relationships: Hyun-kyung Cho, None; Jongchul Han, None; Wool Suh, None; Changwon Kee, None

Program Number: 2264 **Poster Board Number:** B0068

Presentation Time: 2:45 PM - 4:30 PM

Determinants of angle narrowing after mydriasis

©2013, Copyright by the Association for Research in Vision and Ophthalmology, Inc., all rights reserved. Go to iovs.org to access the version of record. For permission to reproduce any abstract, contact the ARVO Office at arvo@arvo.org.

Syogo Arimura, Yoshihiro Takamura, Takeshi Tomomatsu, Yuji Takihara, Masaru Inatani. Ophthalmology, University of Fukui, Yoshida, Japan.

Purpose: Recent findings indicate lens vault (LV) is a contributing factor for the narrow angle. We analyzed the change of the anterior chamber components after mydriasis noninvasively and accurately using anterior segment optical coherence tomography (ASOCT), and investigated to identify the risk factor of angle narrowing.

Methods: We prospectively conducted angle analysis with AS-OCT before and at 30 minutes after pupil dilation with eye-drops of 0.5% tropicamide and 0.5% phenylephrine hydrochlorid under dark condition (< 1 lux). The parameters included axial length (AL), angle opening distance at 500 or 750 μ m from scleral spur (AOD500, AOD750), angle recess area (ARA), trabecular iris space area (TISA), anterior chamber depth (ACD) and LV. Univariate and multivariate linear regression modeling were performed to assess the relationship between the change of AOD500 (Δ AOD500) and the ocular biometric or systemic parameters (age, height, gender). A stepwise selection regression was used to identify sequentially the contribution of each independent variable.

Results: A total of 103 Japanese subjects (71.5 ± 12.4 years; mean \pm S.D.) were enrolled. After univariate analysis, eyes with more decreased Δ AOD500 showed significantly older age ($P < 0.001$), shorter AL ($P = 0.001$), shorter height ($P = 0.005$), greater LV ($P < 0.001$), and smaller values of AOD500 ($P = 0.021$), AOD750 ($P < 0.001$), ARA ($P = 0.025$), TISA ($P = 0.007$) and ACD ($P = 0.004$). In the multivariate analysis, more decreased AOD500 was significantly associated with older age ($P = 0.013$), greater LV ($P = 0.004$), and smaller AOD500 ($P = 0.004$) and smaller AOD750 ($P = 0.014$). The stepwise linear regression analysis revealed that the strong determinants of Δ AOD500 were LV (partial $R^2 = 0.222$; $P < 0.001$) and age (partial $R^2 = 0.095$; $P < 0.001$). The total of two factors explained 31.7% of the variability of Δ AOD500.

Conclusions: This study revealed that greater LV and older age are independently associated with the angle narrowing after mydriasis. After mydriasis, LV is the primary determinant of angle narrowing.

Commercial Relationships: Syogo Arimura, None; Yoshihiro Takamura, None; Takeshi Tomomatsu, None; Yuji Takihara, None; Masaru Inatani, None

Clinical Trial: UMIN000007791

Program Number: 2265 **Poster Board Number:** B0069

Presentation Time: 2:45 PM - 4:30 PM

Quantification of the filtering bleb's structure using Anterior segment optical coherence tomography

Taiki Kokubun, Satoru Tsuda, Yukihiko Shiga, Yu Yokoyama, Kazuko Omodaka, Ryo Watanabe, Morin Ryu, Shiho Kunimatsu-Sanuki, Hidetoshi Takahashi, Toru Nakazawa. Ophthalmology, Tohoku University Graduate School of Medicine, Sendai, Japan.

Purpose: Trabeculectomy (TLE) is the most common surgical procedure for uncontrolled glaucoma. TLE is the most effective procedure known. Intraocular pressure (IOP) after TLE depends on the bleb's absorption function. In this study, we quantified the bleb's structure and analyzed its function using anterior segment-optical coherence tomography (OCT), specifically the CASIA system (SS-1000; TOMEY, Nagoya, Japan). We also examined the correlation between various parameters of the bleb's structure and IOP after TLE.

Methods: This study included 34 eyes of 30 patients with various types of glaucoma. All patients received TLE with 0.04% MMC from April and August 2012. (mean 69.6 ± 13.6 years, male/female 14/16). All subjects underwent TLE with 0.04% MMC and used three types of eye drops (0.5% Moxifloxacin, 0.1% Betamethasone sodium

phosphate, 0.5% Tranilast). We scanned the bleb just on the scleral flap in 8 directions within a 16mm range, and drew the contour lines of blebs and clefts manually. The correlations between the bleb's parameters (cleft volume, bleb volume, vertical/Horizontal brightness of cleft, and vertical/Horizontal brightness of bleb) and IOP were analyzed at 1W (1 week), 2W (2 weeks), 1M (1 month), and 3M (3 months) after TLE respectively on Spearman's rank correlation coefficient. Similarly, the comparison between IOP after TLE and IOP before TLE was analyzed on the Kruskal Wallis test.

Results: IOP at all measurement points after TLE decreased significantly compared to the IOP before TLE. The IOP at 1W showed a significant correlation with vertical brightness of bleb at 1W, horizontal brightness of bleb at 1W, and cleft volume at 1W ($r=0.40$; $p=0.029$, $r=0.41$; $p=0.037$, and $r=-0.43$; $p=0.027$, respectively). The cleft volume at 1M and 3M, and the vertical brightness of the bleb at 2W correlated with IOP at 3M ($r=-0.67$; $p=0.005$, $r=-0.59$; $p=0.012$, and $r=0.59$; $p=0.034$, respectively).

Conclusions: Bleb's brightness and cleft volume were associated with IOP after TLE. AS-OCT is a useful tool to evaluate the bleb's function in the present and future.

Commercial Relationships: Taiki Kokubun, None; Satoru Tsuda, Kowa (C); Yukihiro Shiga, None; Yu Yokoyama, Kowa Company (C); Kazuko Omodaka, None; Ryo Watanabe, None; Morin Ryu, None; Shiho Kunimatsu-Sanuki, None; Hidetoshi Takahashi, None; Toru Nakazawa, Kowa Company Ltd. (F), Kowa Company Ltd. (C)

Program Number: 2266 **Poster Board Number:** B0070

Presentation Time: 2:45 PM - 4:30 PM

An optical coherence tomographic study of macular ganglion cell layer and inner plexiform layer, and circumpapillary retinal nerve fiber layer in 2 years after a diagnosis of preperimetric glaucoma

Kazuhide Kawase¹, Hiroko Inuzuka^{2,1}, Tetsuya Yamamoto¹.

¹Ophthalmology, Gifu University, Gifu, Japan; ²Ophthalmology, Gifu Municipal Hospital, Gifu, Japan.

Purpose: To elucidate changes of the thickness of macular ganglion cell layer and inner plexiform layer (mGCIPL) and circumpapillary retinal nerve fiber layer (cpRNFL) measured by SD-OCT in 2 years after a diagnosis of preperimetric glaucoma (PPG) in a retrospective manner.

Methods: The PPG was defined as follows: an optic disc with neuroretinal rim thinning, cupping, or a suspicious RNFL defect, absence of visual field defects fulfilling the Anderson's criteria and a refractive error less than 6D. One hundred twenty-one eyes of 121 patients with PPG were subjected. Mean deviation (MD) value from HFA C30-2 program, the mGCIPL thickness and the cpRNFL thickness from SD-OCT (Cirrus HD-OCT 4000) programs Ganglion Cell Analysis, Macula Cube 200x200 and Optic Disc Cube 200x200 at the time of diagnosed PPG and 2 years thereafter were reviewed.

Results: We observed significant decrease of the mGCIPL thickness in all sectors ($p<0.0001$), but no significant decrease in MD value during the 2-year follow-up. We also observed significant decrease in the cpRNFL thickness in the superior, inferior, and temporal sectors ($p<0.0001$, $p<0.0001$, and $p=0.0174$, respectively).

Conclusions: The structural changes were recognized in the macula and circumpapillary retinal nerve fiber in two years after a diagnosis of PPG. SD-OCT is able to detect macular and circumpapillary retinal thinning in two years in PPG patients.

Commercial Relationships: Kazuhide Kawase, None; Hiroko Inuzuka, None; Tetsuya Yamamoto, Alcon Japan (R), Pfizer Japan (R), Senju (R), Santen (R), Kowa (R), Otsuka (R), Pfizer Japan (C), Senju (C), Kowa (C), Otsuka (C)

Program Number: 2267 **Poster Board Number:** B0071

Presentation Time: 2:45 PM - 4:30 PM

Effect of experimental glaucoma on the visual pathway function and superior colliculus glial structure

Melina P. Bordone, Ma.Florencia González Fleitas, Ruth E.

Rosenstein. Department of Human Biochemistry, School of Medicine, University of Buenos Aires/CEFYBO, CONICET., Buenos Aires, Argentina.

Purpose: Classically, glaucoma has been conceived as a disease limited to the eye. However, axons of retinal ganglion cells (RGCs) have extraorbital and intracranial components. In the rat, over 90% of RGCs axons project to the contralateral superior colliculus (SC). We have developed an experimental rat model of glaucoma through weekly intracameral injections of chondroitin sulfate (CS), which mimics central aspects of human glaucoma. The purpose of this work was to study the effects of ocular hypertension on visual pathway function and SC structure.

Methods: Male *Wistar* rats were injected with vehicle or CS in the anterior chamber once a week for 15 weeks. Intraocular pressure (IOP) was assessed with a TonoPen, and flash visual evoked potentials (VEPs) were registered with skull-implanted electrodes. In addition, retinal anterograde transport was examined after an intravitreal injection of β -subunit cholera toxin. An immunohistochemical analysis of Iba1 (microglia activation marker) and glial fibrillary acidic protein (GFAP) levels in the SC were performed. An histochemical analysis of *Griffonia simplicifolia* agglutinin (GSA)-lectin levels was also in the SC were performed.

Results: Ocular hypertension induced a significant decrease in VEP N2-P2 component amplitude at 6 weeks and a further decrease was observed at 15 weeks. Anterograde transport to the SC significantly decreased after 6 weeks of treatment, and was completely abolished at 15 weeks of ocular hypertension. Iba1- immunoreactivity significantly increased in the SC that receives axons from the glaucomatous eye at 6 and 15 weeks of ocular hypertension, which correlated with a significant increase in iba1-positive cell number but not with iba1 expression level/cell. A similar pattern was observed with GSA-lectin levels. A pronounced astroglial response (GFAP levels) was evident in the SC at 15 (but not 6) weeks of hypertension.

Conclusions: These results suggest a "misconnection" between the retina and the superior visual pathway at early stages of ocular hypertension (when the number of RGCs remains unchanged), accompanied by an early microglial response and more delayed astroglial alterations in the SC.

Commercial Relationships: Melina P. Bordone, None;

Ma.Florencia González Fleitas, None; Ruth E. Rosenstein, None

Support: PICT1623 (ANPCyT)- 20020100100678 (UBA)- PIP 1911 (CONICET)

Program Number: 2268 **Poster Board Number:** B0072

Presentation Time: 2:45 PM - 4:30 PM

Non-Invasive Estimation of Intracranial Pressure by Magnetic Resonance Imaging Assisted Orbital Subarachnoid Space Measurement: The Beijing Intracranial and Intraocular Pressure (iCOP) Study

Xiaobin Xie^{2,1}, Ningli Wang¹, Xiaojun Zhang³, Jost B. Jonas⁴, Junfang Xian⁵, Robert Ritch^{6,7}. ¹Beijing Tongren Eye Center, Beijing Tongren Hospital, Capital Medical University, Beijing

Ophthalmology and Visual Sciences Key Laboratory, Beijing, China;

²Ophthalmology, Eye Hospital of China Academy of Chinese

Medical Sciences, Beijing, China; ³Neurology, Beijing Tongren

Hospital, Capital Medical University, Beijing, China;

⁴Ophthalmology, Medical Faculty Mannheim of the Ruprecht-Karls-

University Heidelberg, Mannheim, Germany; ⁵Radiology, Beijing Tongren Hospital, Capital Medical University, Beijing, China; ⁶Einhorn Clinical Research Center, New York Eye and Ear Infirmary, New York, NY; ⁷Department of Ophthalmology, New York Medical College, Valhalla, NY.

Purpose: The orbital subarachnoid space surrounding the optic nerve is continuous with the circulation system for cerebrospinal fluid (CSF) and can be visualized using magnetic resonance imaging (MRI). Patients with increased ICP have a wider than normal orbital CSF space and vice versa. We hypothesized that the orbital subarachnoid space width (OSASW) is correlated with and serves as a surrogate for ICP. Our aim was to develop a method for non-invasive quantitative ICP estimation by MRI-assisted OSASW.

Methods: This clinical inter-method study included consecutive patients aged between 18 and 75 years who underwent lumbar puncture and 3.0-Tesla orbital MRI. The study population was randomly divided into a training group and a test group. The main outcome measure was OSASW at 3, 9, and 15 mm behind the globe. In training group, a non-invasive quantitative ICP assessment method was developed. In test group, the reliability and accuracy of the non-invasive ICP assessment were evaluated.

Results: Seventy-four patients were enrolled into this study. In univariate analysis, lumbar CSF-pressure was significantly associated with the OSASW at all three measurement locations (r ranging from 0.83 to 0.88; $p < 0.0001$) within a lumbar CSF-pressure range 3.7-26.5 mm Hg, with body mass index (BMI; $r = 0.61$; $p < 0.0001$) and with mean arterial blood pressure (MABP; $r = 0.55$; $p < 0.0001$) in the training group. These associations remained statistically significant in multivariate regression. The weighting functions of non-invasive ICP prediction were: Non-invasive ICP = $9.31 \times \text{OSASW} + 0.48 \times \text{BMI} + 0.14 \times \text{MABP} - 19.94$ (OSASW at 3 mm behind the globe); Non-invasive ICP = $16.95 \times \text{OSASW} + 0.39 \times \text{BMI} + 0.14 \times \text{MABP} - 20.90$ (at 9 mm); and Non-invasive ICP = $17.54 \times \text{OSASW} + 0.47 \times \text{BMI} + 0.13 \times \text{MABP} - 21.52$ (at 15 mm). In the independent test group, mean lumbar CSF-pressure (13.6 (5.1) mm Hg) did not differ significantly from mean MRI-derived calculated ICP (OSASW at 3 mm: 12.7 (4.2) mm Hg ($p = 0.07$); at 9 mm: 13.4 (5.1) mm Hg ($p = 0.35$); and at 15 mm: 14.0 (4.9) mm Hg ($p = 0.87$)). The MRI-derived ICP assessment based on the OSASW at 9 mm and at 15 mm had higher reliability and greater accuracy.

Conclusions: MRI-assisted measurement of the OSASW is useful for the non-invasive quantitative estimation of the ICP, if BMI and MABP as contributing parameters are taken into account.

Commercial Relationships: Xiaobin Xie, None; Ningli Wang, None; Xiaojun Zhang, None; Jost B. Jonas, Allergan (C), MSD (C), Alimera (C), CellMed AG (P); Junfang Xian, None; Robert Ritch, None

Support: National Natural Science Foundation of China (81271005), Beijing Natural Science Foundation (7122038) and an Award of Excellent Doctoral Dissertation of Beijing (Beijing YXBS Grant PXM2010_014226_07_000061 and PXM2011_014226_07_000114) and Donation by China Health and Medical Development Foundation

Clinical Trial: ChiCTR-OCC-10001271

Program Number: 2269 **Poster Board Number:** B0073

Presentation Time: 2:45 PM - 4:30 PM

Measurement of minimum rim width (MRW) using Cirrus Optic Nerve Head Volumes in a Chinese Population

Chen-Hsin Sun¹, Tin A. Tun², John Mark S. de Leon², Michael J. Girard^{3,5}, Tin Aung², Nicholas G. Strouthidis^{4,2}. ¹Duke-NUS graduate medical school, Singapore, Singapore; ²Glaucoma, Singapore National Eye Center, Singapore, Singapore;

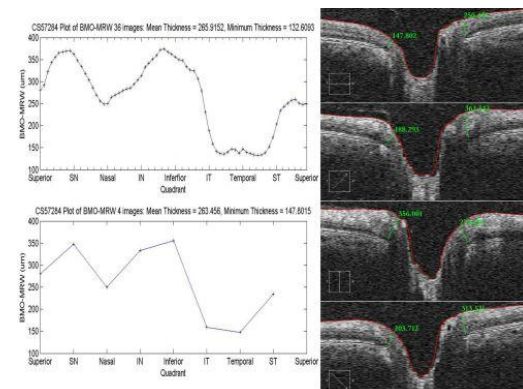
³Bioengineering, National University of Singapore, Singapore, Singapore; ⁴Glaucoma Research Unit, NIHR Biomedical Research Centre at Moorfields Eye Hospital NHS Foundation Trust and UCL Institute of Ophthalmology, London, United Kingdom; ⁵Singapore Eye Research Institute, Singapore, Singapore.

Purpose: The minimum rim width (MRW), the shortest distance between Bruch's membrane opening (BMO) and internal limiting membrane (ILM), has recently been proposed as the most accurate OCT measurement of neuroretinal rim. We describe a method of calculating MRW from Cirrus volumes; we measure MRW in a cohort of normal Singapore Chinese eyes to characterize its distribution.

Methods: 99 right eyes were selected from the Singapore Chinese Eye Study database. Median age was 53 years (range 44 - 76) and 52 subjects were male. Each eye was imaged using the Cirrus OCT system using a standard 4x4x4mm cube acquisition protocol. Within each volume, the ILM and RPE/BM were automatically segmented using the native Cirrus algorithm. 36 interpolated radial B-scans were extracted from each volume. The innermost termination of the RPE/BM signal was assumed to be the BMO, thereby yielding 72 data points per 5 degree increment. We developed an algorithm, coded using Matlab, which measured the shortest distance between the coordinates of each BMO point and the ILM. The extracted MRW measurements were plotted across each eye quadrant to characterize the sectoral distribution of MRW. Mean MRW of each eye was calculated and associations with age were evaluated using linear regression. Furthermore sectoral distribution and mean MRW derived from the 4 'cardinal' B-scans versus 36 B-scans were compared.

Results: The distribution of MRW measurements was consistent with the expected distribution with the rim thickest inferiorly, followed by superior, nasal and temporal sectors. Average of Mean MRW across this cohort was 294um +/- 62um. Linear regression identified that mean MRW decreases with increasing age ($p < 0.05$). Paired T-test of mean MRW computed from 36 B-scans and 4 B-scans showed no statistically significant difference ($p = 0.69$). The plots of sectoral distribution of MRW computed using 36 B-scans demonstrated a similar distribution as MRW computed from 4 B-scans.

Conclusions: It is possible to extract MRW measurements using Cirrus volumes containing automatic segmentations. We demonstrate that the sectoral MRW distribution follows the expected pattern in these eyes and that MRW appears to decrease with age. Our results suggest that MRW derived from 4 cardinal B-scans may be sufficient for assessment for global and sectoral analyses. The utility of this parameter in glaucoma case finding will need to be assessed.



Commercial Relationships: Chen-Hsin Sun, None; Tin A. Tun, None; John Mark S. de Leon, None; Michael J. Girard, None; Tin Aung, Alcon (R), Alcon (C), Alcon (F), Allergan (R), Allergan (C),

Carl Zeiss Meditec (F), Carl Zeiss Meditec (R), Ellex (F), Ellex (R), Santen (R); **Nicholas G. Strouthidis**, None
Support: NGS acknowledges financial support from the UK Department of Health through the award made by the National Institute for Health Research to Moorfields Eye Hospital NHS Foundation Trust and UCL Institute of Ophthalmology for a Biomedical Research Centre for Ophthalmology. The views expressed in this work are those of the authors and not necessarily those of the UK Department of Health.

Program Number: 2270 **Poster Board Number:** B0074
Presentation Time: 2:45 PM - 4:30 PM

Optic nerve head (ONH) connective tissue (CT) deformation within Non-Human Primate (NHP) eyes with moderate to severe (M/S) Experimental Glaucoma (EG)

Galen Williams¹, Ruojin Ren¹, Hongli Yang¹, J Crawford C. Downs², Stuart K. Gardiner¹, Claude F. Burgoyne¹. ¹Discoveries in Sight Research Laboratories, Devers Eye Institute, Portland, OR; ²Ophthalmology, University of Alabama at Birmingham, Birmingham, AL.

Purpose: To characterize ONH CT deformation within 3D histomorphometric reconstructions of 12 M/S EG NHP eyes relative to 9 previously reported early EG (EEG) eyes.¹

Methods: Trephined ONH and peripapillary sclera from both eyes of 12 adult NHPs, (9 - 21 years old) were perfusion fixed at IOP 10 mmHg with one normal, and one M/S EG eye (qualitatively determined by the magnitude of longitudinal change in confocal scanning laser tomography). All eyes were then serial sectioned, 3D reconstructed, 3D delineated and parameterized using our existing techniques¹. Significant between eye differences for each parameter, for each M/S EG eye (compared to its contralateral control), exceeded previously reported maximum physiologic inter-eye differences (PIDmax)² and were compared to the range of EEG eye change.¹ For all parameters, inter-eye differences (Treated eye value subtracted from its contralateral control eye value) were compared between EEG and M/S EG eyes using t-tests.

Results: Post-Bruch's membrane opening (BMO) total prelaminar volume in M/S EG eyes increased from 40 to 578% vs 36 to 188% in the EEG eyes. Lamina posterior deformation ranged from -37 to -437 μm in the M/S EG eyes vs -29 to -184 μm in the EEG eyes. Lamina thickness increased 30 to 113 μm in 3 M/S EG eyes, was unchanged in 6 M/S EG eyes and was thinned 23 to 31 μm in 3 M/S EG eyes compared to increases ranging from 20 to 61 μm in 8 of 9 EEG eyes. Posterior scleral canal opening (PSCO) offset expansion (range, 25 - 33 μm) in M/S EG eyes was less than that in the EEG eyes (range, 30 - 85 μm) with 1 M/S EG eye demonstrating PSCO contraction (64 μm). Between-eye differences of Post-BMO total prelaminar volume are predicted by peak IOP and cumulative IOP difference (p=0.002, p=0.017 respectively).

Conclusions: Global posterior deformation and thickening of the lamina cribrosa increase through NHP M/S EG. However, as previously described in humans and monkeys, the lamina is thinned in the most severely deformed eyes. Taken together, our EEG and M/S EG eye data suggest the lamina thickens in most NHP eyes early in the neuropathy then thins as the neuropathy progresses. The hypothesis that the lamina cribrosa thins first in some eyes is under study using longitudinal SDOCT imaging.

References

1. Yang, et al. IOVS. 2011;52:345-363.
2. Yang, et al. IOVS. 2009;50:224-234.

Parameters	Previously Reported Global Maximum Physiologic Inter-Eye Differences (PIDmax) ¹	Range of Previously Reported Global Between-Eye Differences ² in 8 EEG eyes ³		Range of Global Between-Eye Differences ⁴ in 12 M/S EG eyes		Comparison of Parameter Differences ⁵ Between EEG and M/S EG eyes
		Min ⁶	Max ⁶	Min ⁶	Max ⁶	
Neural Canal Architecture (μm)						
BMO Offset	9	-12	66	12	68	0.385
ASCO Offset	16	17	71	25	66	0.388
AI Offset	18	19	71	19	77	0.246
PI Offset	18	30	139	-21	97	0.152
PSCO Offset	22	30	85	33	64	0.033
ASAS Offset	18	-32	60	21	94	0.721
ASCO Depth	16	-18	-35	19	-31	0.020
AI Depth	20	-35	49	21	112	0.044
PI Depth	20	-28	71	27	158	0.041
PSCO Depth	27	40	-28	43	78	0.846
ASAS Depth	25	-38	-68	40	90	0.049
ONH Connective Tissue (μm)						
Lamina Cribrosa Position	16	-29	-184	-37	-437	0.105
Peripapillary Scleral Position	16	21	59	-47	68	0.134
Lamina Cribrosa Thickness	18	30	61	-31	73	0.062
Scleral Flange Thickness	14	24	54	25	-29	0.831
ASAS Scleral Flange Thickness	20	N/A	N/A	25	36	n/a
Peripapillary Scleral Thickness	6	-32	59	-15	34	0.934
ONH Lamellar Cupping (mm³)						
Post-BMO Total Prelaminar Volume	28%	36%	188%	40%	578%	0.058

ONH Connective Tissue Alterations within 12 Moderate to Severe (M/S) Experimental Glaucoma (EG) eyes

¹ Previously reported values for 9 EEG eyes¹ are included for comparison.
² Minimum values of the range are minimum by magnitude or most negative or both.
³ Maximum values of the range are maximum by magnitude without regard to direction.
⁴ Minimum values of the range are minimum by magnitude without regard to direction.
⁵ Between-eye differences in the EG eye relative to its contralateral normal eye unless previously reported. ⁶ PIDmax²
⁶ t-test comparison of Pooled EEG eyes versus pooled M/S eyes.
 N/A - Data Not Available; BMO - Bruch's Membrane Opening; ASCO - Anterior Scleral Canal Opening; AI - Anterior Lamellar Insertion; PI - Posterior Lamellar Insertion; PSCO - Posterior Scleral Canal Opening; ASAS - Anterior-most aspect of the Subnasal Sclera

Commercial Relationships: Galen Williams, None; Ruojin Ren, None; Hongli Yang, None; J Crawford C. Downs, None; Stuart K. Gardiner, Allergan (R); Claude F. Burgoyne, Heidelberg Engineering (F), Heidelberg Engineering (C)

Support: NIH/NEI R01-EY011610, Legacy Good Samaritan Foundation; Sears Medical Trust; Alcon Research Institute, Heidelberg Engineering, GmbH, Heidelberg, Germany (equipment and unrestricted research support), Reichert Instruments (equipment).

Program Number: 2271 **Poster Board Number:** B0075
Presentation Time: 2:45 PM - 4:30 PM

Reproducibility of Peripapillary Choroidal Thickness Measurements with Enhanced Depth Imaging Spectral-Domain Optical Coherence Tomography

Paula D. Borba, Vitor G. Prado, Paula D. Silva, Igor Matsubara, Tiago S. Prata, Roberto M. Vessani, Augusto Paranhos. DEPARTAMENTO DE OFTALMOLOGIA, Universidade Federal de Sao Paulo, Sao Paulo, Brazil.

Purpose: To investigate the interobserver and intraobserver reproducibility of peripapillary choroidal thickness measurements performed by enhanced depth imaging spectral-domain optical coherence tomography (EDI-OCT) in a population with and without glaucoma.

Methods: We prospectively enrolled glaucomatous patients (glaucomatous optic neuropathy and reproducible visual field defect) and healthy individuals from August 2012 to October 2012. Those with significant media opacity or any ocular disease (besides glaucoma) were excluded. All participants underwent EDI-OCT (SD-OCT; Spectralis®, Wavelength: 870nm; Heidelberg Engineering Co., Heidelberg, Germany). The peripapillary choroid was measured 500μm distant from the inferior margin of the Bruch's membrane opening. To examine the inter-observer reproducibility, two independent examiners assessed all images. To examine the intraobserver reproducibility, each examiner evaluated each set of images twice. The intra-session within-subject standard deviation (Sw), the coefficient of variation (COV; 100%×Sw/overall mean) and the intra-class correlation coefficient (ICC; set for absolute agreement) were calculated.

Results: A total of 10 eyes of 10 patients were included. Mean peripapillary choroidal thickness by graders 1 and 2 were 145.8±41.2 μm and 140.1±30.7 μm, respectively, with a mean difference of 5.7 μm (P=0.73; 95% confidence interval of the difference: -39.9 - 28.4). For the assessment of the intra-observer reproducibility for graders 1 and 2, the mean Sws were 7.3 and 6.3 μm, the mean COVs were 5.6 and 4.8% and the ICCs were 0.96 (95% CI, 0.85 - 0.99) and 0.95 (95% CI, 0.80 - 0.98), respectively.

Conclusions: Based on manual measurement performed by experienced examiners, measurements

of the peripapillary choroidal thickness by EDI OCT showed a high reproducibility among the observers.

Commercial Relationships: Paula D. Borba, None; Vitor G. Prado, None; Paula D. Silva, None; Igor Matsubara, None; Tiago S. Prata, Allergan (F), Alcon (F), Merck (F), Germed (C); Roberto M. Vessani, ALLERGAN (R); Augusto Paranhos, Allergan (F), MSD (F)

Program Number: 2272 **Poster Board Number:** B0076

Presentation Time: 2:45 PM - 4:30 PM

In Vivo Identification of Lamina and Pre-lamina ONH Structures using Enhanced Depth Imaging Spectral-Domain Optical Coherence Tomography

Paula D. Silva, Vitor G. Prado, Paula D. Borba, Igor Matsubara, Roberto M. Vessani, Augusto Paranhos, Tiago S. Prata.

Ophthalmology, Federal University of Sao Paulo, Sao Paulo, Brazil.

Purpose: To investigate the ability of glaucoma specialists to identify different lamina and pre-lamina optic nerve head (ONH) structures using enhanced depth imaging spectral-domain optical coherence tomography (EDI-OCT) in a population with and without glaucoma.

Methods: We prospectively enrolled glaucomatous patients (glaucomatous optic neuropathy and reproducible visual field defect) and healthy individuals from August 2012 to October 2012. Those with significant media opacity or any ocular disease (besides glaucoma) were excluded. All participants underwent EDI-OCT (SD-OCT; Spectralis®, Wavelength: 870nm; Heidelberg Engineering Co., Heidelberg, Germany). We investigated the ability of three glaucoma specialists to identify the following ONH parameters in each EDI-OCT image: anterior and posterior surfaces of the lamina cribrosa, anterior surface of the pre-lamina neural tissue, Bruch's membrane opening (scleral canal diameter), and anterior and posterior margins of the choroid (choroidal thickness) measured 500µm distant from the inferior border of the Bruch's membrane opening. Whenever both eyes were eligible, the right eye was arbitrarily chosen for analysis. Identification of each parameter was graded as easy, difficult or impossible.

Results: A total of 19 eyes of 19 patients were included (mean age, 54.3±25.2 years). Overall, the anterior surface of the pre-lamina neural tissue and the borders of the Bruch's membrane opening were the landmarks most clearly identified (graded as easy in over 90% of the eyes on average). On the other hand, the anterior and posterior surfaces of the lamina cribrosa were clearly identified in less than 35% of the cases on average. Comparing the eyes in which most parameters were easily identified with those that showed poor visibility, the former group was mostly composed by eyes with glaucoma, with larger cup-to-disc ratio (mean of 0.72 vs 0.30; p<0.05) and a thinner pre-lamina neural tissue layer (mean of 188 vs 390 µm; p<0.5).

Conclusions: Most pre-lamina ONH structures could be clearly identified by different glaucoma specialists using EDI-OCT. Identification of deeper structures such as the lamina cribrosa seems to be not always feasible, especially in cases of normal eyes with healthy ONH.

Commercial Relationships: Paula D. Silva, None; Vitor G. Prado, None; Paula D. Borba, None; Igor Matsubara, None; Roberto M. Vessani, ALLERGAN (R); Augusto Paranhos, Allergan (F), MSD (F); Tiago S. Prata, Allergan (F), Alcon (F), Merck (F), Germed (C)

Program Number: 2273 **Poster Board Number:** B0077

Presentation Time: 2:45 PM - 4:30 PM

Descriptive study of the anterior chamber angle using anterior segment Fourier Domain OCT and its relationship to the morphometry of the eye in the normal population

José Ignacio Fernández-Vigo¹, CRISTINA FERNANDEZ-VIGO ESCRIBANO³, Javier García Bella¹, Jose M. Martinez de la Casa¹, Julian Garcia-Feijoo¹, José Fernández-Vigo López².

¹Ophthalmology, Hospital Clinico San Carlos, Madrid, Spain; ²CIOA - Universidad de Extremadura, Badajoz, Spain; ³Centro de Oftalmologia Barraquer, Barcelona, Spain.

Purpose: To measure the anterior chamber angle width with OCT and analyze its relationship with the morphometric variables of the eye in a normal population.

Methods: Prospective study of one eye from 320 consecutive healthy patients. We examined the patients with Pentacam®, IOL Master®, and RTVue® (Optovue, California, USA) anterior segment Fourier Domain OCT (AS-OCT). Images were obtained under standard light conditions, and when the signal strength intensity was greater than 30. Parameters evaluated: age, sex, IOP, refractive error, axial length, pupil diameter and pachymetry. Anterior chamber (AC) parameters examined were: depth, volume and diameter. Angle parameters: nasal and temporal width measured in degrees, angle opening distance (AOD), trabecular iris space area (TISA) and iris thickness; length, thickness and area of the trabecular meshwork (TM). Pearson correlation analysis was performed to study the correlation between the AC angle and the rest of the variables.

Results: 19 patients (6%) were excluded because the angle width could not be measured due to low image quality. The mean values of the population were: age: 45 ± 14.2 years (range 19 to 84), IOP: 15.92 ± 3.8 mmHg (range 8 to 26.4), sphere: -0.4 ± 2.79 diopters (range -6.25 to 6.5), axial length: 23.91 ± 1.51 mm (range 20.03 to 29.14), AC depth: 3.42 ± 0.43 mm (range 2.45 to 4.38), AC diameter: 11.93 ± 0.39 mm (range 11 to 13), iris thickness: 412.6 ± 88.88 microns (range 195 to 910), pupil diameter 2.96 ± 0.62 (1.71 to 5.51). The mean temporal angle width was 38.8 ± 12.7 degrees (range 14.5 to 78.2), AOD: 587.18 ± 261.65 microns, (range 64 to 1440), TISA: 0.201 ± 0.093 mm² (range 0.027 to 0.519). We found a correlation between the angle and the depth of the AC (r = 0.76), with the axial length (r = 0.68), with the spherical refractive error (r = -0.68), with age (R = -0.60), and weakly with the IOP (r = -0.17). Cited correlations were statistically significant (p < 0.05%).

Conclusions: SA Fourier Domain OCT enabled us to analyze and measure the chamber angle in 94% of eyes. We found a strong correlation between the angle width and depth of the AC, spherical refractive error and age, and weak with the IOP.

Commercial Relationships: José Ignacio Fernández-Vigo, None; CRISTINA FERNANDEZ-VIGO ESCRIBANO, None; Javier García Bella, None; Jose M. Martinez de la Casa, None; Julian Garcia-Feijoo, Trancend (C), Ivantis (C), Glaukos (C), MSD (C), Allergan (F), Pfizer (F), Alcon (C), Sensimed (F), Sylentis (F), Bausch and Lomb (C); José Fernández-Vigo López, None

Program Number: 2274 **Poster Board Number:** B0078

Presentation Time: 2:45 PM - 4:30 PM

The Prevalence of Relative Afferent Pupillary Defects in Patients with Normal Visual Fields

Alice Zhang^{1,2}, Lan Lu², Mohsin Ali², Bruno M. Faria², Patricia Martinez², Liang Liang², Huseyin Guzel², Mike A. Tawfik², George L. Spaeth². ¹Jefferson Medical College, Philadelphia, PA; ²Glaucoma Research, Wills Eye Institute, Philadelphia, PA.

Purpose: To determine the frequency with which a relative afferent pupillary defect (RAPD) occurs in patients with glaucoma but without VF loss when tested with SAP.

Methods: A retrospective study: The electronic medical records of

672 patients who presented to the Wills Eye Glaucoma Service from January to May 2012 were reviewed. All patients were included except those with:

- 1) Any condition preventing adequate visualization and examination of the pupil or optic nerve
- 2) Active infection of the anterior or posterior segments of the eye
- 3) Any intraocular surgical or laser procedure within the previous 4 weeks
- 4) Any cause other than glaucoma known to cause an RAPD
- 5) Only one eye, or fixed pupils

Clinical parameters such as VA, IOP, C/D ratio, DDLS, or VF mean defect within 6 months of the documented RAPD testing were tabulated. A documented RAPD was considered a “true” RAPD if it correlated with inter-eye structural asymmetry (such as visual field mean defect, DDLS score, or cup/disc ratio). The visual fields were measured either with Humphrey or Octopus perimetry. Normal VF (Humphrey) was defined as an MD score of -6dB or more positive, WITHOUT any of the following: 3 adjacent data points of <5% with at least one point <1%; PSD significant at <.05 (or 5%); Glaucoma hemifield test “Outside normal limits”. For Octopus, normal VF was defined as an MD score of -0.8 or more negative, with a Bebie curve line not intersecting with the lower confidence limit line.

Results: The analyzed sample size was 152, 28 of whom had visual field via Humphrey and 124 via Octopus. Among 152 analyzed subjects, 89 were RAPD negative, 63 were RAPD positive. Among the 63 positive subjects, 60 subjects had a “true” RAPD. There was high agreement between RAPD and “true” RAPD ($\kappa=0.96$). 85% of the patients (Humphrey testing) had abnormal VF and 93% by Octopus. 55% of patients with abnormal VF (Humphrey) had a positive RAPD; 50% of those with normal VF had a positive RAPD. 39% of patients (Octopus) with abnormal VF had a positive RAPD, while 33% of those with normal VF had a positive RAPD. There was no association between presence of an RAPD and whether or not the field was normal ($p=0.40$ - Humphrey) ($p=0.27$ - Octopus).

Conclusions: Around 1/3 to 1/2 of patients in a tertiary glaucoma practice have a positive RAPD in the absence of a visual field defect being detected by Octopus or Humphrey perimetry.

Commercial Relationships: Alice Zhang, None; Lan Lu, None; Mohsin Ali, None; Bruno M. Faria, None; Patricia Martinez, None; Liang Liang, None; Huseyin Guzel, None; Mike A. Tawfik, None; George L. Spaeth, Merck (F), U.S. Patent No. 8,042,946 (P), Pfizer (F)

Program Number: 2275 **Poster Board Number:** B0079

Presentation Time: 2:45 PM - 4:30 PM

Retinal nerve fiber layer and posterior pole asymmetry analysis by spectral domain-OCT: structure function relationship with visual field sensitivity in glaucoma

Manuele Michelessi¹, Marco Centofanti^{2,1}, Francesco Oddone², Lucia Tanga², Danilo Iannetta¹, Pasquale Pasculli¹, Manuela Ferrazza², Gianluca Manni¹. ¹University of Rome Tor Vergata, Rome, Italy; ²Fondazione G.B. Bietti-IRCCS, Rome, Italy.

Purpose: To evaluate the structure function relationship between visual field (VF) sensitivity by standard automated perimetry (SAP) and retinal nerve fiber layer (RNFL) and macular thickness measured by spectral domain optical coherence tomography (SD-OCT), in glaucomatous patients.

Methods: Seventy-nine eyes of 79 consecutive glaucoma patients were enrolled. All subjects underwent a full eye examination, a SAP test (Humphrey field analyzer, 24-2 SITA standard) and were imaged with Spectralis SD-OCT (Heidelberg Engineering), at the same visit. RNFL scanning protocol and posterior pole asymmetry analysis were performed to obtain peripapillary RNFL and macular thickness,

respectively. Abnormal visual field result (defined as PSD and MD $p<5\%$ and GHT outside normal limits) was used as reference standard. For the RNFL thickness data, six sectors were used to assess the structure function relationship with the VF matching areas. For the macular thickness data, we divided the 64 squares covering the posterior pole area resulting from the scan, in five sectors and we evaluate the relationship with corresponding VF matching area. The global as well as the hemifield data were also used and compared. The VF sensitivity was registered in the dB and 1/L scales and a linear regression analysis using the “least squares” method was used to measure the coefficient of determination (R^2).

Results: For the RNFL/VF relationship, the coefficient of determination (R^2) ranged from 0.09 (nasal VF sector, dB scales) to 0.53 (inferotemporal VF sector, 1/L scale). For the posterior pole/VF relationship, the coefficient of determination ranged from 0.17 (inferonasal VF sector, dB scales) to 0.42 (inferotemporal VF sector, 1/L scale).

Conclusions: Structure function relationship between RNFL thickness and VF sensitivity was moderate and similar to that between posterior pole thickness and VF sensitivity. Inferotemporal VF sector have shown the stronger association with structural corresponding area.

Commercial Relationships: Manuele Michelessi, None; Marco Centofanti, Allergan (R), Pfizer (R), Soft Italia (R), Bausch & Lomb (R), MSD (R); Francesco Oddone, None; Lucia Tanga, Allergan (F), Alcon (F), Merck (F), Bausch & Lomb (F); Danilo Iannetta, None; Pasquale Pasculli, None; Manuela Ferrazza, None; Gianluca Manni, Allergan (F), Alcon (F), Merck (F), Omikron (F), Pfizer (F), Bausch & Lomb (F)

Program Number: 2276 **Poster Board Number:** B0080

Presentation Time: 2:45 PM - 4:30 PM

Rates of functional and structural change are significantly correlated in eyes with early to moderate glaucoma

Shaban Demirel, Lisha Deng, Deborah Goren, Manoj Pathak, Steven L. Mansberger, Brad Fortune, Stuart K. Gardiner. Devers Eye Institute, Legacy Health, Portland, OR.

Purpose: To explore the association between change in visual function and in retinal nerve fiber layer thickness (RNFLT) in participants with early to moderate glaucoma and to test whether regional analyses produce stronger correlations between functional and structural change than global analyses.

Methods: Data from 167 subjects with mild to moderate glaucoma or risk factors for glaucoma were collected at 6-month intervals. Spectral Domain Optical Coherence Tomography (SDOCT) peripapillary circle scans (Spectralis) and Standard Automated Perimetry (Humphrey Field Analyzer: SAP, SITA 24-2) were performed at each visit. All RNFL segmentations were manually refined in a masked fashion and follow-up scans for an eye were aligned to a common baseline. RNFLT data were divided into 45° sectors straddling the principle meridians. Rates of change were calculated per eye for mean deviation (MD), pointwise sensitivity at the 52 non-blindspot locations and RNFLT, both globally and for the RNFLT sectors. The worst eye per subject was selected, based on the rate of MD change (MDR), to increase the spread of rates of change available for analysis.

Results: The mean number of OCT and SAP tests per eye were both 6.3 ± 0.8 (range; 5 to 8) covering 2.9 ± 0.36 yrs. At the most recent visit, mean MD, PSD and global RNFLT were -0.85 ± 2.9 dB, 2.53 ± 2.5 dB and 87.7 ± 14.7 μ m respectively. The mean MDR was -0.34 ± 0.46 dB/yr. The mean pointwise rates of change ranged from -0.65 to -0.03 dB/yr at the different visual field locations, with the nasal field deteriorating significantly faster than the temporal field

($p=0.009$). The mean rate of global RNFLT change was -1.15 ± 1.52 $\mu\text{m}/\text{yr}$. Within OCT sectors the mean rate of RNFLT change ranged from -2.33 to -0.36 $\mu\text{m}/\text{yr}$ and was more rapid in the temporal and superior sectors. The correlation (r) between MDR and global RNFLT change was 0.20 ($p=0.008$). However, MDR was more strongly correlated with rates of RNFLT change within temporal, superotemporal, inferior and inferotemporal sectors than it was with global RNFLT change. The strongest correlation between pointwise visual field change and sectoral RNFLT change was ≈ 0.5 , more than double the correlation between MDR and global RNFLT change.

Conclusions: Rates of functional and structural change in patients with glaucoma are significantly correlated when examined globally but even stronger correlations are observed in regional analyses.

Commercial Relationships: Shaban Demirel, Carl Zeiss Meditec (F), Heidelberg Engineering (R), Heidelberg Engineering (F); Lisha Deng, None; Deborah Goren, None; Manoj Pathak, None; Steven L. Mansberger, Merck (R), Alcon (C), Allergan (C), Allergan (F), Merck (F), Santen (C), Glaukos (C); Brad Fortune, Heidelberg Engineering, GmbH (F), Carl Zeiss Meditec, Inc (F); Stuart K. Gardiner, Allergan (R)

Support: NIH Grant EY019674, Legacy Good Samaritan Foundation

Program Number: 2277 **Poster Board Number:** B0081

Presentation Time: 2:45 PM - 4:30 PM

Pressure Induced Changes in the Human Optic Nerve Head assessed by Immunofluorescent Computed Tomography (ICT)

Donald J. Brown, Geraint J. Parfitt, Korey Reeid, Yilu Xie, James V. Jester. Gavin Herbert Eye Institute, University of California, Irvine, Irvine, CA.

Purpose: Recent evidence suggests increasing the Intra ocular pressure to 50mm Hg, increases the anterior surface area of the lamina cribrosa by 12%. We have developed a novel method (ICT) which enables 3-D quantification of multiple antigens and distinct cell populations in large tissue volumes to validate and expand on these findings in the optic nerve head (ONH).

Methods: Pairs of fresh eyes were obtained from a local eye bank and fixed at either 15 or 50mm Hg overnight in 2% paraformaldehyde/PBS. After fixation, the ONH was carefully dissected and dehydrated through a series of ethanol. The tissue was embedded in butyl-methyl methacrylate and polymerised under UV light at 40C overnight. Tissue blocks were then serially sectioned at 2 μm intervals through a depth of 1mm. Each section was then imaged using non-linear optics to generate second harmonic signals (fibrillar collagen). Then, each section was sequentially immunostained for the cellular markers NCAM and GFAP and for the extracellular matrix components, elastin and type IV collagen. Prior to imaging, DAPI was applied to image cell nuclei. Images were acquired using a 20x/0.75NA objective on a Leica DMI6000B fluorescence microscope and /or a Zeiss 510 Meta coupled to a femtosecond laser. Data sets represent tissue volumes of 4mm X 4mm X 1mm with a voxel resolution of 0.45 X 0.45 X 2 μm . The alignment and 3-D reconstruction of the tissue was performed using Amira software.

Results: ICT reconstructions reveal a layer of elastin immediately anterior to the LC collagen beams. Type IV collagen demonstrated the intricate and torturous vascular bed in the prelaminar layer and peripapillary sclera. Periodic branches from the circle of Zinn-Haller were observed that directly extended into the LC layer. NCAM and GFAP staining, while strongly positive, has not yet been fully reconstructed so the distribution of the LC cell (NCAM positive and GFAP negative) has not yet been determined. However, overall cell density dramatically drops precisely at the anterior surface of the LC.

Conclusions: ICT is an emerging and powerful technique to 3-D visualise distinct cell and matrix distributions in large volumes and that has enabled us to more precisely characterise the structural changes that occur in the ONH in response to IOP. Further analyses will reveal if, for example, the elastin layer and/or vascular bed compresses with increased IOP.

Commercial Relationships: Donald J. Brown, None; Geraint J. Parfitt, None; Korey Reeid, None; Yilu Xie, None; James V. Jester, None

Support: NIH Grant EY19719, Research to Prevent Blindness, Discovery Eye Foundation

Program Number: 2278 **Poster Board Number:** B0082

Presentation Time: 2:45 PM - 4:30 PM

Comparison between peripapillary choroidal thickness and retinal nerve fiber layer (RNFL) damage in healthy, ocular hypertension and glaucomatous eyes

emanuele gerace, Alessandro Cutini, Serena Fragiotta, Marco Marengo, Francesca Verboschi, Carmela Carnevale, Enzo M. Vingolo. Department of Ophthalmology, Sapienza - University of Rome, Rome, Italy.

Purpose: to evaluate the role of the choroid in the different degrees of retinal nerve fiber layer (RNFL) damage in patients affected by ocular hypertension (OH) and primary open angle glaucoma (POAG).

Methods: 117 eyes of 117 patients with POAG or OH (66.8 ± 12.8 years) and 50 healthy subjects (HS) (63.09 ± 21.42 years) were enrolled. Patients were classified into 2 groups according to RNFL classification: 54 eyes within normal limits (WNL) and 48 eyes outside normal limits (ONL). Borderline eyes ($n=15$) were excluded. Peripapillary RNFL thickness was obtained by spectral domain optical coherence tomography (SD-OCT, Heidelberg Engineering). Peripapillary choroidal thickness (CT) was measured from the outer border of the retinal pigment epithelium and the chorio-scleral interface, using enhanced depth imaging mode. CT and RNFL thickness maps were compared between the groups for global (G) and infero-temporal (IT), infero-nasal (IN), supero-temporal (ST), supero-nasal (SN), nasal (N), temporal (T) quadrants. Statistical analysis was performed with Mann-Whitney U test (non-normal distribution), Shapiro-Wilk test ($p<0.05$) or independent Student's t-test (normal distribution). Spearman's rank correlation coefficient was calculated for comparisons.

Results: Mean global CT was 129.23 ± 49.93 μm in POAG/OH eyes and 143.71 ± 40.0 μm in HS ($p=0.04$). There was a negative correlation between CT and age in POAG/OH eyes ($r=-0.48, p<0.0001$) and HS ($r=-0.63, p<0.0001$). In POAG/OH eyes the mean peripapillary CT in the inferior quadrants was significantly thinner than all other quadrants ($p<0.001$). Peripapillary CT in WNL group was significantly thinner than HS in NS, NI and TI quadrants ($p=0.03, p=0.01$ and $p=0.05$ respectively). In ONL group NS, NI, TI, T quadrants and G were significantly less than HS ($p=0.05, p=0.02, p=0.02, p=0.05$ and $p=0.04$ respectively).

Conclusions: In POAG/OH eyes CT in NS, NI and TI quadrants was compromised when compared with HS even if the RNFL thickness was WNL, that suggests that the thinning of the choroid may precede the morphological glaucomatous damage. Moreover in ONL eyes also the T quadrant and global CT were significantly thinner than HS. It could be related with the progression of morphological damage otherwise related to a tendency of eyes with thinner CT to develop a more advanced glaucomatous damage.

Commercial Relationships: emanuele gerace, None; Alessandro Cutini, None; Serena Fragiotta, None; Marco Marengo, None; Francesca Verboschi, None; Carmela Carnevale, None; Enzo M. Vingolo, None

Program Number: 2279 **Poster Board Number:** B0083

Presentation Time: 2:45 PM - 4:30 PM

Comparison of the strengths of ‘moving correlations’ between SD-OCT and SLP nerve fiber layer thickness and standard automated perimetry

Casie Goldman, Shaban Demirel, Cindy L. Blachly, Michael D. Whitworth, Steven L. Mansberger, Stuart K. Gardiner, Deborah Goren. Devers Eye Institute, Legacy Research Institute, Portland, OR.

Purpose: To compare the strength of structure-function correlations between standard automated perimetry (SAP) and retinal nerve fiber layer thicknesses (RNFLT), as measured by either spectral-domain ocular coherence tomography (Corr_{SD-OCT/SAP}) or scanning laser polarimetry (Corr_{SLP/SAP}), at different stages of glaucoma.

Methods: SAP visual fields (SITA Std, 24-2) and RNFLT measures were collected for 400 eyes of 209 participants with early to moderate glaucoma (Mean deviation (MD) mean: -0.31 ± 2.87 ; range: -16.20 to 3.27). To avoid predetermined definitions of disease stage, a rolling binning process was employed that sorted by 6 metrics to stage the disease. These included four functional metrics (MD, Mean sensitivity (MS), number of locations outside normal limits ($p < 5\%$) on the total deviation (TD) probability map, and number of locations on the pattern deviation (PD) probability map) and two structural metrics (mean RNFLT from a circle scan as measured by SD-OCT, mean RNFLT from SLP). For each staging, the first bin was defined as the first 80 observations within the sorted database. Subsequent bins were created for observations 21-100, 41-120, 61-140 etc. This process resulted in 17 overlapping bins specific to each staging. For each bin, Pearson correlation coefficients were calculated between linearized mean sensitivity ($MS_{Lin} = 10^{MS^{*0.1}}$) and RNFLT and compared using Steiger’s test. This process was repeated for the 6 sorting metrics, resulting in 6 distinct stagings.

Results: For all stagings and all bins, Corr_{SD-OCT/SAP} was either equivalent to, or higher than Corr_{SLP/SAP}. When using MD for staging, Corr_{SD-OCT/SAP} values were significantly higher than Corr_{SLP/SAP} for bins with MD ranges -0.88 to 0.2 ($p < 0.001$) and -0.45 to 0.35 ($p = 0.008$). When using TD and PD for staging, Corr_{SD-OCT/SAP} values were significantly higher than Corr_{SLP/SAP} for bins representing eyes with a few defective locations (1-4 abnormal TD locations: $p = 0.033$. 1-3 abnormal PD locations: $p = 0.029$).

Conclusions: Function (MS_{Lin}) correlates significantly more strongly with structure (RNFLT) as assessed by SD-OCT than when assessed by SLP but only during early stages of glaucomatous damage. Correlations between structure and function are similar for SD-OCT and SLP later in the disease process.

Commercial Relationships: Casie Goldman, None; Shaban Demirel, Carl Zeiss Meditec (F), Heidelberg Engineering (R), Heidelberg Engineering (F); Cindy L. Blachly, None; Michael D. Whitworth, None; Steven L. Mansberger, Merck (R), Alcon (C), Allergan (C), Allergan (F), Merck (F), Santen (C), Glaukos (C); Stuart K. Gardiner, Allergan (R); Deborah Goren, None
Support: NIH Grant EY019569 (SD), Legacy Good Samaritan Foundation

Program Number: 2280 **Poster Board Number:** B0084

Presentation Time: 2:45 PM - 4:30 PM

Agreement between the Heidelberg Edge perimetry and the Moorfields regression analysis classifications in healthy and glaucoma individuals

Blanca Monsalve¹, Antonio Ferreras², Miriam Ara², Sofia Otin², Carlos Cortes¹. ¹Ophthalmology, Hospital Univ Gregorio Marañón,

Madrid, Spain; ²Ophthalmology, Miguel Servet University Hospital, Zaragoza, Spain.

Purpose: To evaluate the agreement between the functional classification of Heidelberg Edge perimetry (HEP) and the Moorfields regression classification (MRA) of the Heidelberg retina tomograph 3 (HRT3) in healthy and glaucoma subjects.

Methods: Fifty healthy individuals and 105 open-angle glaucoma patients were consecutive and prospectively selected. All participants underwent at least a reliable HEP (Heidelberg Engineering, Heidelberg, Germany) and were imaged with the HRT3 (Heidelberg Engineering). Eligible subjects for the glaucoma group had to have intraocular pressure higher than 20 mmHg and abnormal HEP. Only one eye from each participant was randomly chosen, unless only one eye met the inclusion criteria. Left eyes were converted to a right eye format. The normative database results of the 6 MRA sectors, obtained after manual outlining of the disc boundaries, were compared with the equivalent 6 functional sectors automatically generated by HEP.

Results: Mean age was 59.34 ± 9.5 years in the control group and 61.11 ± 9.3 years in the glaucoma group. Mean deviation was -5.43 ± 6.1 dB in the glaucoma group. 96% to 100% of the normal eyes were classified as within normal limits (WNL) by both, the HEP and MRA, classifications, while no sector was considered as outside normal limits (ONL). In the glaucoma group, classifications differed less than 10% for the number of patients classified as WNL, borderline and ONL at every sector. Nasal inferior sector was colored as ONL in the 41% of the glaucoma patients for both classifications.

Conclusions: The HEP and MRA classifications had similar diagnostic performance. The agreement between both classifications was excellent for normal subjects and very high for glaucoma patients.

Commercial Relationships: Blanca Monsalve, None; Antonio Ferreras, Alcon Laboratories, Inc (R), Allergan, Inc (R), Carl Zeiss Meditec (C), Heidelberg Engineering (F), Instituto Salud Carlos III (F), Novartis (R), Oculus, Inc (F); Miriam Ara, None; Sofia Otin, None; Carlos Cortes, None

Support: Supported in part by the Instituto de Salud Carlos III grant PI11/01239

Program Number: 2281 **Poster Board Number:** B0085

Presentation Time: 2:45 PM - 4:30 PM

Combining Nerve Fiber Layer and Ganglion Cell Complex Parameters for Glaucoma Diagnosis using Fourier-Domain Optical Coherence Tomography

Xinbo Zhang¹, Ou Tan¹, Rohit Varma^{4,5}, Joel S. Schuman³, David S. Greenfield², David Huang¹. ¹Cassey Eye Institute, Oregon Health & Science University, Portland, OR; ²Bascom Palmer Eye Institute, University of Miami, Miami, FL; ³Ophthalmology, University of Pittsburgh, Pittsburgh, PA; ⁴Ophthalmology, University of Southern California, Los Angeles, CA; ⁵Illinois Eye and Ear Infirmary, University of Illinois at Chicago, Chicago, IL.

Purpose: To define an optical coherence tomography (OCT) based structural diagnostic index (SDI) for glaucoma diagnosis by optimally combining nerve fiber layer (NFL) and ganglion cell complex variables.

Methods: We analyzed the data from participants multi-center longitudinal Advanced Imaging for Glaucoma Study (www.AIGStudy.net). A Fourier-domain OCT system (RTVue) was used to map GCC and NFL thickness 3 times on each study visit. Five types of parameters: overall, superior and inferior average thickness, along with global loss volume (GLV) and focal loss volume (FLV) for both NFL and GCC are used. The study subjects were randomly divided into a training set and a test set. A two-stage

approach was used. First, logistic regression was performed on training set in each parameter type for NFL and GCC to determine optimal weights for NFL and GCC then combine the two parameters into a single one. Next the weight-combined parameters were standardized to the reference values from the normal group. The quadratic and positively truncated form of the standardized parameters from the five types entered a logistic regression to define a single numeric value as the optimal SDI.

Results: The analysis included 197 eyes (99 participants) from normal group; 210 eyes (141 participants) from perimetric glaucoma (PG) group. The training set contains 100 N and 100 PG eyes and the test set contains 97 N and 110 PG eyes. The optimal SDI from the logistic regression developed from the training set included superior and inferior average thicknesses, GLV and FLV, but excluded overall thickness. The area under ROC curve (AROC) for the SDI on the test set is 0.927, significantly better than the AROC for any of the component variables used alone ($p=0.03$). The AROC for component NFL and GCC variables ranged from 0.86 to 0.91.

Conclusions: Combining structural measurements of GCC and NFL from Fourier-domain OCT improved the diagnostic accuracy for glaucoma.

Commercial Relationships: **Xinbo Zhang**, None; **Ou Tan**, Optovue (F), Optovue (P), Carl Zeiss Meditec (P); **Rohit Varma**, Allergan (C), AqueSys (C), Genentech (C), Merck & Co. Inc (C), Replenish (C), Genentech (F), National Eye Institute (F); **Joel S. Schuman**, Carl Zeiss Meditec, Inc. (P); **David S. Greenfield**, National Eye Institute (R), Carl Zeiss Meditec (R), Optovue (R), Heidelberg Engineering (R), Allergan (C), Alcon (C), Merz (C), Quark (C), SOLX (C), Biometric Imaging (C), Senju (C); **David Huang**, Optovue (F), Optovue (I), Optovue (P), Optovue (R), Carl Zeiss Meditec (P)

Support: NIH Grant R01EY013516

Clinical Trial: NCT01314326

Program Number: 2282 **Poster Board Number:** B0086

Presentation Time: 2:45 PM - 4:30 PM

Comparison of Retinal Nerve Fiber Layer and Optic Disk Algorithms with Optical Coherence Tomography with 10 degree of head rotation

Rafael Castañeda Diez, LUIS A. ZARATE, Jesus Jimenez-Roman.

Glaucoma, Asociacion Para Evitar la Ceguera, Mexico City, Mexico.

Purpose: To compare the performance of the retinal nerve fiber layer (RNFL) thickness and optic disk algorithms as determined by optical coherence tomography to detect structural changes when the patient accidentally rotate head.

Methods: Both eyes from 17 control subjects with visual acuity of $> \text{or} = 20/40$, and no ocular pathologic condition. Observation procedures: Two optical coherence tomography algorithms were used: "fast RNFL thickness" and "fast optic disk." All procedure was made by the same observer.

Results: The average RNFL was 102.2 ± 9.15 and 101.67 ± 9.46 in the control and head rotation group, respectively. The average Rim area was 1.42 ± 0.27 and 1.44 ± 0.29 in the control and head rotation group, respectively. The average Disc area was 1.94 ± 0.38 and 1.94 ± 0.40 in the control and head rotation group, respectively. The average C/D Ratio was 0.4682 ± 0.176 and 0.4626 ± 0.177 in the control and head rotation group, respectively. The average Vertical C/D was 0.445 ± 0.166 and 0.441 ± 0.161 in the control and head rotation group, respectively. The average CUP Volume was 0.1588 ± 0.155 and 0.1554 ± 0.156 in the control and head rotation group, respectively. No statistical difference found in RNFL, RIM area, DISC area and Vertical C/D ratio; but found statistical difference in C/D Ratio and CUP Volume.

Conclusions: two of six algorithms present difference when the head is in rotation, it is important to watch the head of the patient during study, especially in elder people (like glaucoma patients).

Commercial Relationships: **Rafael Castañeda Diez**, None; **LUIS A. ZARATE**, None; **Jesus Jimenez-Roman**, None

Program Number: 2283 **Poster Board Number:** B0087

Presentation Time: 2:45 PM - 4:30 PM

Correlation between peripapillary retinal nerve fiber layer thickness and visual field defect in glaucoma

Andre Luiz Silva, Luiz Alberto S. Melo, Moacyr Campos, Ivan M. Tavares. Ophthalmology, Federal University of Sao Paulo, Sao Paulo, Brazil.

Purpose: To evaluate the correlation between peripapillary retinal nerve fiber layer (RNFL) thickness and visual field indices using different spectral-domain optical coherence tomographies (SD-OCT) and visual field perimeters in glaucoma.

Methods: A cross-sectional study was carried out. Primary open-angle glaucoma patients were examined using Spectralis SD-OCT (Heidelberg Engineering, Heidelberg, Germany), Cirrus SD-OCT (Carl Zeiss Meditec, Dublin, CA), RTVue SD-OCT (Optovue, Inc., Fremont, CA), standard automated perimetry (24-2 SITA Standard test, Humphrey Field Analyzer 750, Carl Zeiss Meditec, Dublin, CA), and Frequency Doubling Technology Perimetry (24-2 test, FDT Matrix, Carl Zeiss Meditec, Dublin, CA). The correlation between mean peripapillary RNFL thickness and visual fields indices was analyzed using Spearman rank correlation test.

Results: A total of 44 eyes of 25 patients were included in the study. The mean (standard deviation) peripapillary RNFL thickness obtained by Spectralis, Cirrus, and RTVue were $74.7 (15.9) \mu\text{m}$, $72.4 (12.5) \mu\text{m}$, and $93.7 (17.4) \mu\text{m}$, respectively. The mean (standard deviation) standard automated perimetry Mean Deviation (MD) index was $-6.61 (7.12) \text{dB}$. The RNFL thickness obtained by Spectralis and Cirrus showed similar, moderate correlations with visual field indices (Table). The correlation between RNFL thickness obtained by RTVue and visual field indices were weaker than those obtained by Spectralis and Cirrus OCT (Table).

Conclusions: Moderate correlations between peripapillary RNFL thickness and visual field indices were found in glaucoma patients. The correlation between RNFL thickness obtained by RTVue and visual field indices were weaker than those obtained by Spectralis and Cirrus OCT.

Table. Correlation between mean peripapillary retinal nerve fiber layer thickness and perimetric indices

Perimetry	Optical Coherence Tomography		
	Spectralis $r (P)$	Cirrus $r (P)$	RTVue $r (P)$
SAP			
MD	0.54 (<0.001)	0.51 (0.001)	0.32 (0.04)
PSD	-0.48 (0.002)	-0.46 (0.003)	-0.30 (0.06)
VFI	0.57 (<0.001)	0.53 (0.001)	0.33 (0.03)
FDT Matrix			
MD	0.67 (<0.001)	0.52 (0.001)	0.41 (0.01)
PSD	-0.46 (0.003)	-0.27 (0.13)	-0.24 (0.15)

r = Spearman rank correlation coefficient

SAP = Standard automated perimetry

MD = Mean Deviation; PSD = Pattern Standard Deviation

VFI = Visual Field Index

FDT = Frequency Doubling Technology Perimetry

Commercial Relationships: **Andre Luiz Silva**, None; **Luiz Alberto S. Melo**, None; **Moacyr Campos**, None; **Ivan M. Tavares**, None
Support: CAPES-PRODOC, Ministry of Education of Brazil.

Program Number: 2284 **Poster Board Number:** B0088

Presentation Time: 2:45 PM - 4:30 PM

Relationship between the mean deviation of the visual field (Humphrey) and the analysis of the retinal fiber layer thickness of the optical coherence tomography (Stratus OCT) for moderates and severes glaucomatous eyes

Idriss Badat¹, Edouard Dumas de La Roque¹, Martial Mercie¹, Benedicte Tougeron¹, Nasser Yani¹, Nadia Bouamama¹, Julie Morin², Pierre Ingrand¹, Michèle Boissonnot¹, Nicolas Levezuel¹. ¹Service d'ophtalmologie, CHU La Milétrie, Poitiers, France; ²Département d'ophtalmologie, Hôpital Rosemond-Maisonnette, Montréal, QC, Canada.

Purpose: To evaluate the capacity of optical coherence tomography Stratus (OCT) and its role in discriminating moderate versus severe glaucoma by the study of retinal nerve fiber layer thickness.

Methods: This comparative study includes sixty-six glaucomatous eyes (42 moderates and 24 severes). Eyes were separated in two groups according to Hodapp classification, based on the visual field white-white SITA Standard (Swedish Interactive Threshold Algorithms) 24.2. The peri-papillary retinal nerve fiber layer thickness was measured by the stratus OCT using the protocol Fast RNFL Thickness. The studied Oct parameters used were the global average thickness (global mean), and the thickness of the retinal fiber layers on the four meridian lines. The OCT parameters were then compared with the mean deviation (MD) of the visual field.

Results: The global average thickness of the retinal nerve fiber layer is respectively 64.73 μm +/- 9.87, 54.14 +/- 9.98 for the moderate and the severe glaucomatous eyes with a significant difference of $p=0.0007$. The thickness of the retinal fiber layers on the four meridian quadrants were found significantly different between the two groups ($p=0.05$) for the temporal, superior and inferior meridian. The global mean and the inferior and temporal meridian lines showed the most important areas under the ROC curve (respectively 0.766 0.785 and 0.780) for the moderate glaucoma against the severe ones. The threshold of 44 μm for the temporal quadrant has an ability of discrimination of 76% of specificity and sensibility.

Conclusions: OCT of optic nerve fiber layer is a very interesting discrimination tool for moderate to severe glaucoma. It gives estimation of nerve fiber layer thickness at which the disease risks to progress to a more severe stage. It complements well the visual field and combined to it, helps to the evaluation of the severity of glaucoma and its management even for advanced cases.

Commercial Relationships: Idriss Badat, None; Edouard Dumas de La Roque, None; Martial Mercie, None; Benedicte Tougeron, None; Nasser Yani, None; Nadia Bouamama, None; Julie Morin, None; Pierre Ingrand, None; Michèle Boissonnot, None; Nicolas Levezuel, None

Program Number: 2285 **Poster Board Number:** B0089

Presentation Time: 2:45 PM - 4:30 PM

Myopia in Primary Angle Closure Glaucoma

Kailing Yong¹, Tianxia Gong², Monisha E. Nongpiur^{1,3}, Hwee Kuan Lee², Li Cheng², Shamira Perera¹, Tin Aung^{1,4}. ¹Singapore National Eye Centre and Singapore Eye Research Institute, Singapore, Singapore; ²Bioinformatics Institute, A*STAR (Agency for Science, Technology and Research), Singapore, Singapore; ³Duke-NUS Graduate Medical School, Singapore, Singapore; ⁴Yong Loo Lin School of Medicine, National University of Singapore, Singapore, Singapore.

Purpose: To evaluate the prevalence of myopia and to assess ocular biometric parameters in subjects with primary angle closure.

Methods: The study recruited 460 subjects, which included 152 primary angle closure suspects (PACS), 80 primary angle closure

(PAC), 174 primary angle closure glaucoma (PACG) and 54 subjects with acute primary angle closure (APAC). A-scan biometry (US-800; Nidek Co. Ltd, Tokyo, Japan) was used to obtain measurements of anterior chamber depth (ACD), axial length (AL), lens thickness (LT) and vitreous length (VL). Refraction was measured with an autorefractor (Canon RK-5 Auto Ref-Keratometer; Canon Inc. Ltd., Tokyo, Japan), and refractive status was categorized as myopia (<-0.50D), emmetropia (-0.50D to +0.50D) and hyperopia (>+0.50).

Results: The mean age of the subjects was 65.6 years (SD \pm 8.8), 64.8% were female and the majority of subjects were Chinese (92%). Amongst all subjects with angle closure, 23% had myopia and 51.1% had hyperopia. Overall, 9.6% of angle closure subjects had moderate and high myopia (<-2.0D). The lowest proportion of myopic patients was in the PACS sub-group (10.5%). While the myopic angle closure subjects had statistically longer AL ($p=0.02$ and $p<0.001$) and VL ($p=0.03$ and $p<0.001$) than the emmetropic and hyperopic subjects, there was no statistical difference in ACD ($p=0.44$) and LT ($p=0.46$) between the different refractive status groups.

Conclusions: Almost a quarter of subjects with angle closure were myopic with 9.6% having moderate to high myopia. Myopic angle closure may be mediated through a shallow anterior chamber as ACD did not vary with refractive status, but myopic angle closure subjects had longer VL and AL. We advocate gonioscopy in all patients irrespective of refractive status, as a significant proportion of angle closure patients may be myopic.

Commercial Relationships: Kailing Yong, None; Tianxia Gong, None; Monisha E. Nongpiur, None; Hwee Kuan Lee, None; Li Cheng, None; Shamira Perera, Carl Zeiss Meditec (R), Allergan (R), Pfizer (R); Tin Aung, Alcon (R), Alcon (C), Alcon (F), Allergan (R), Allergan (C), Carl Zeiss Meditec (F), Carl Zeiss Meditec (R), Ellex (F), Ellex (R), Santen (R)

Support: National Medical Research Council, Singapore and Biomedical Research Council, Singapore

Program Number: 2286 **Poster Board Number:** B0090

Presentation Time: 2:45 PM - 4:30 PM

Comparison between deviation map of circumpapillary retinal nerve fiber layer and macular ganglion cell-inner plexiform layer measurements using high-definition optical coherence tomography in the detection of early glaucoma

Yun Jeong Choi^{1,2}, Mi Jeung Kim^{1,2}, Kyoung Nam Kim^{1,2}, Jin Wook Jeoung^{1,2}, Ki Ho Park^{1,2}, Dong Myung Kim^{1,2}. ¹Ophthalmology, Seoul National University College of Medicine, Seoul, Republic of Korea; ²Ophthalmology, Seoul National University Hospital, Seoul, Republic of Korea.

Purpose: To compare the sensitivity and specificity of the deviation map of circumpapillary retinal nerve fiber layer (cpRNFL) and macular ganglion cell-inner plexiform layer (GCIPL) measurements using high-definition optical coherence tomography (Cirrus HD-OCT) for discriminating between healthy control and early glaucoma patients.

Methods: We prospectively enrolled 171 early glaucoma patients confirmed by two reliable visual field tests (mean deviation > -6 dB) and 114 healthy control subjects. Abnormal cpRNFL and macular GCIPL deviation maps corresponding to visual field defects represented as red ($P < 1\%$) or yellow ($P < 5\%$) superpixels were used to calculate the sensitivity and specificity (%). We used three different criteria for deviation map abnormality: a cluster of three or more contiguous yellow in the same hemifield on the deviation map, including one or more red ones (criteria 1); a cluster of five or more yellow superpixels, including three or more red (criteria 2); a cluster of ten or more yellow superpixels, including five or more red (criteria 3). Sensitivity differences were determined by McNemar test.

Results: The early glaucoma detection sensitivities of the cpRNFL deviation map were 92.7% (95% confidence interval (CI): 88.5 - 96.9%) for criteria 1, 90.1% (95% CI: 85.7 - 94.5%) for criteria 2, and 88.0% (95% CI: 83.1 - 92.9%) for criteria 3. The specificities were 54.4% (95% CI: 45.1 - 63.7%), 64.9% (95% CI: 56.0 - 73.8%), and 76.3% (95% CI: 68.4 - 84.2%), respectively. The sensitivities of the macular GCIPL deviation map were 90.4% (95% CI: 86.1 - 94.7%) for criteria 1, 87.4% (95% CI: 82.5 - 92.3%) for criteria 2, and 85.1% (95% CI: 79.8 - 90.4%) for criteria 3. The specificities were 59.6% (95% CI: 50.5 - 68.7%), 69.3% (95% CI: 60.7 - 77.9%), and 76.3% (95% CI: 68.4 - 84.2%), respectively. The sensitivity difference between the cpRNFL and macular GCIPL deviation maps was not statistically significant for any of the three abnormality criteria ($P > 0.05$).

Conclusions: The deviation map of macular GCIPL measurement by Cirrus HD-OCT showed similar early glaucoma detection sensitivities to that of the cpRNFL deviation map. On this basis, the macular GCIPL deviation map can be considered to be a complementary glaucoma diagnostic test.

Commercial Relationships: Yun Jeong Choi, None; Mi Jeung Kim, None; Kyoung Nam Kim, None; Jin Wook Jeoung, None; Ki Ho Park, None; Dong Myung Kim, None

Program Number: 2287 **Poster Board Number:** B0091

Presentation Time: 2:45 PM - 4:30 PM

Reproducibility of the measurement of Optic Nerve Head Hemoglobin levels

Carmen Mendez-Hernandez¹, Ignacio Rodriguez-Uña¹, Paula Arribas Pardo¹, Federico Saenz-Frances¹, Manuel González-de-la-Rosa², Jose M. Martinez de la Casa¹, Enrique Santos-Bueso¹, Julian Garcia-Feijoo¹. ¹Glaucoma, Instituto de Investigación Sanitaria San Carlos (IdISSC) Fundación de Investigación Biomédica del Hospital Clínico San Carlos, Madrid, Spain; ²Hospital Universitario de Canarias., La Laguna, Spain.

Purpose: To evaluate the intraobserver, interobserver, within and between-session reproducibility of the measurement of Optic Nerve Head (ONH) Hemoglobin levels using colour analysis by Laguna ONhE (Optic Nerve Hemoglobine) program.

Methods: Observational prospective study of 29 eyes (11 hypertensive and glaucomatous; 18 healthy eyes). Two investigators obtained two retinographies (Canon non-mydratic retinal camera CD-DGi, Canon Inc., Tokyo, Japan) in two testing sessions three weeks apart and analyzed the images using the Laguna ONhE (Optic Nerve Hemoglobine). The following parameters were quantified: ONH Hemoglobin concentration in its whole extent and in vertical disk diameter, disc-cup ratio and GDF (Glaucoma Discriminant Function). Agreement was illustrated using Bland-Altman plots and reproducibility was assessed comparing the intraclass correlation coefficients (ICC).

Results: In session 1, investigator 1 found mean levels of ONH Hemoglobin of 67.94 +/- 8.70% in healthy eyes and of 57.90 +/- 5.36% in hypertensive and glaucomatous eyes. Correspondent values for investigator 2 were 68.27 +/- 8.52% and 57.83 +/- 4.88%, respectively. ONH Hemoglobin concentration measurements, in its whole as well as in the vertical diameter, showed the highest ICCs (All above 0.9). Variability was greater for GDF (ICC>0.8) and cup-disc ratio (ICC>0.71).

Conclusions: The measurement of ONH Hemoglobin concentration using the Laguna ONhE program shows high reproducibility both in glaucomatous and non-glaucomatous ONHs.

Commercial Relationships: Carmen Mendez-Hernandez, None; Ignacio Rodriguez-Uña, None; Paula Arribas Pardo, None; Federico Saenz-Frances, None; Manuel González-de-la-Rosa,

Haag Streit (P), Oculus (P); Jose M. Martinez de la Casa, None; Enrique Santos-Bueso, None; Julian Garcia-Feijoo, Trancend (C), Ivantis (C), Glaukos (C), MSD (C), Allergan (F), Pfizer (F), Alcon (C), Sensimed (F), Sylentis (F), Bausch and Lomb (C)

Support: Instituto de Investigación Sanitaria San Carlos (IdISSC). Fundación Investigación Biomédica del Hospital Clínico San Carlos. Fondo de Investigación Sanitaria. Instituto de Salud Carlos III.

Clinical Trial: PI09/90933

Program Number: 2288 **Poster Board Number:** B0092

Presentation Time: 2:45 PM - 4:30 PM

Macular Ganglion Cell Imaging Study: Glaucoma Diagnostic Accuracy of Spectral-Domain Optical Coherence Tomography
Jin Wook Jeoung¹, Yun Jeong Choi¹, Seok Hwan Kim², Ki Ho Park¹, Dong Myung Kim¹. ¹Department of Ophthalmology, Seoul National University Hospital, Seoul National University College of Medicine, Seoul, Republic of Korea; ²Department of Ophthalmology, Seoul National University Boramae Hospital, Seoul, Republic of Korea.

Purpose: To evaluate the diagnostic accuracy of macular ganglion cell-inner plexiform layer (GCIPL) measurements using high-definition optical coherence tomography (Cirrus HD-OCT) ganglion cell analysis algorithm for detecting early, moderate and severe glaucoma.

Methods: One hundred and twenty normal subjects and 215 glaucoma patients (128 patients with early glaucoma, 50 with moderate glaucoma, and 37 with severe glaucoma) were enrolled from the Macular Ganglion Cell Imaging Study. Macular GCIPL, peripapillary retinal nerve fiber layer (RNFL) thickness, and optic nerve head (ONH) parameters were measured in each subject. Areas under the receiver operating characteristic curves (AUROCs) were calculated and compared. Based on the internal normative database, the sensitivity and specificity for detecting early, moderate, and severe glaucoma were calculated.

Results: There was no statistically significant difference between the AUROCs for the best OCT parameters. For detecting early glaucoma, the sensitivity of the Cirrus GCIPL parameters ranged from 28.1% to 75.2% and that of the Cirrus RNFL parameters ranged from 6.3% to 57.0%. For the early glaucoma group, the best parameter from the GCIPL generally had a higher sensitivity than those of the RNFL and ONH parameters with comparable specificity ($P < 0.01$, McNemar's test).

Conclusions: There were no significant differences between the AUROCs for Cirrus GCIPL, RNFL and ONH parameters, indicating that these maps have similar diagnostic potentials for glaucoma. For detecting early glaucoma, the macular GCIPL parameters had generally higher sensitivities than the OCT RNFL parameters with comparable specificities.

Commercial Relationships: Jin Wook Jeoung, None; Yun Jeong Choi, None; Seok Hwan Kim, None; Ki Ho Park, None; Dong Myung Kim, None

Program Number: 2289 **Poster Board Number:** B0093

Presentation Time: 2:45 PM - 4:30 PM

Relationship between Axonal Subtypes and Size of Retinal Nerve Fiber Bundles

Ye Zhou^{1,2}, Xiaopeng Zhao², Xiang-Run Huang^{2,1}. ¹Biomedical Engineering, University of Miami, Miami, FL; ²Ophthalmology, Miller School of Medicine, University of Miami, Miami, FL.

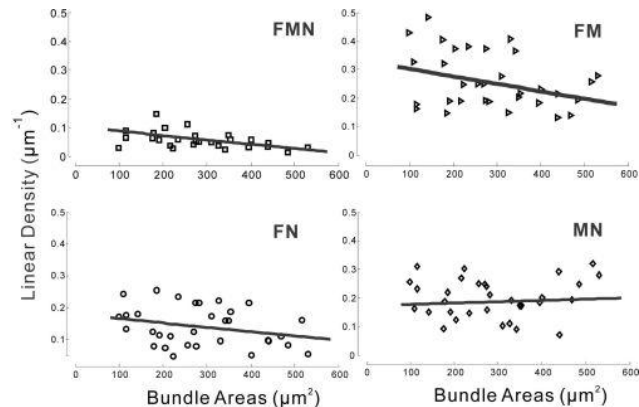
Purpose: The axons of retinal ganglion cells (RGCs) consist of cytoskeletal components, including actin filaments (F-actin), microtubules (MTs) and neurofilaments (NFs). In this study, we classified axonal subtypes based on the relative contents of these components and studied the relationship between each subtype and

the sizes of retinal nerve fibers bundles. Knowledge gained will be useful for understanding selective damage of the nerve fiber bundles in glaucoma.

Methods: Normal Wistar rats were used in this study. Whole-mounted retinas were simultaneously stained with fluorescence to label F-actin, MTs and NFs. Strands of these components, running along the axons, were identified by confocal imaging of the tissues. To determine the relative content of cytoskeletal components, lines across cytoskeletal strands were defined within nerve fiber bundles. Intensity profiles along the lines were obtained for each cytoskeletal component. Axons were classified by relative intensities of these components. For instance, axons with intensely stained F-actin, MTs and NFs were classified as FMN subtype. A linear density of each subtype was calculated as the number of the subtype found along a line divided by the line length. Bundle size was determined by multiplying bundle width with its thickness. The density was studied for different sizes of nerve fiber bundles.

Results: Normal axons could be classified as the subtypes of FMN, FM, FN, and MN, in which three or two cytoskeletal components were nearly colocalized. Also there were subtypes, F, M, N, of which one structure dominated the content of axons. The linear densities of the axonal subtypes, FMN, FM and FN, decreased with increasing of the bundle size, while the density of MN did not change very much with the bundle size.

Conclusions: Normal axons of retinal ganglion cells contain different proportions of cytoskeletal components. Because cytoskeleton provides support for axonal structure and function, the lower cytoskeletal density in larger nerve fiber bundles may offer an explanation of selectively greater loss of large nerve fiber bundles found in glaucomatous eyes.



Commercial Relationships: Ye Zhou, None; Xiaopeng Zhao, None; Xiang-Run Huang, None

Support: NIH grant R01-EY019084 and Center Grant P30-EY014801, American Health Assistance Foundation G2008-033, and an unrestricted grant to the University of Miami from Research to Prevent Blindness, Inc.

Program Number: 2290 **Poster Board Number:** B0094

Presentation Time: 2:45 PM - 4:30 PM

DETERMINATION OF OPTIC DISC HEMOGLOBIN QUANTITY IN OCULAR HYPERTENSION, COMPARED WITH OPTICAL COHERENCE TOMOGRAPHY

Paula Arribas Pardo¹, Julian Garcia-Feijoo¹, Manuel González-de-la-Rosa², Ignacio Rodríguez-Uña¹, Clara Berrozpe Villabona¹, Federico Saenz-Frances¹, Jose M. Martínez de la Casa¹, Enrique Santos-Bueso¹, Carmen Mendez-Hernandez¹. ¹Glaucoma. Instituto de Investigación Sanitaria San Carlos (IdISSC) Fundación de Investigación Biomédica del Hospital Clínico San Carlos, Madrid,

©2013, Copyright by the Association for Research in Vision and Ophthalmology, Inc., all rights reserved. Go to iovs.org to access the version of record. For permission to reproduce any abstract, contact the ARVO Office at arvo@arvo.org.

Spain., Madrid, Spain; ²Hospital Universitario de Canarias., La Laguna, Spain.

Purpose: To determine the diagnostic capacity of a new method for measuring hemoglobin

(Hb) levels at the optic nerve head (ONH), Laguna ONhE (Optic Nerve Hemoglobine) compared with optical coherence tomography (OCT Spectralis) in ocular hypertension (OHT).

Methods: OHT eyes (n=40) and healthy eyes (n=44) underwent a transversal study using TOP G1 perimetry, OCT Spectralis and optic disc retinographies acquired with a non-mydratic fundus camera (Canon non-mydratic retinal camera CD-DGi, Canon Inc., Tokyo, Japan). Laguna ONhE program was used to calculate the Hb amount of the ONH. Area under the receiver operating characteristic curves (AUC) and correlation between structural and functional parameters were determined (Spearman Rho).

Results: The greatest AUC corresponded to Laguna ONhE parameters GDF (Glaucoma Discrimination Function) (0.844 CI 95% 0.762- 0.926), Hemoglobin concentration in the vertical optic disc axis (8 & 20 Sector) (0.817 CI 95% 0.726- 0.907) and C/D Estimated Ratio (0.806 CI 95% 0.714- 0.898), versus the ones obtained for OCT Retinal Nerve Fiber Layer Thickness (RNFL) (0.577 CI 95% 0.439- 0.715).

Conclusions: Discrimination between OHT and controls is better made with Laguna ONhE program than OCT Spectralis in ocular hypertension eyes.

Commercial Relationships: Paula Arribas Pardo, None; Julian Garcia-Feijoo, Trancend (C), Ivantis (C), Glaukos (C), MSD (C), Allergan (F), Pfizer (F), Alcon (C), Sensimed (F), Sylentis (F), Bausch and Lomb (C); Manuel González-de-la-Rosa, Haag Streit (P), Oculus (P); Ignacio Rodríguez-Uña, None; Clara Berrozpe Villabona, None; Federico Saenz-Frances, None; Jose M. Martínez de la Casa, None; Enrique Santos-Bueso, None; Carmen Mendez-Hernandez, None

Support: Instituto de Investigación Sanitaria San Carlos (IdISSC). Fundación Investigación Biomédica del Hospital Clínico San Carlos. Fondo de Investigación Sanitaria. Instituto de Salud Carlos III.

Clinical Trial: PI09/90933

Program Number: 2291 **Poster Board Number:** B0095

Presentation Time: 2:45 PM - 4:30 PM

The Relationship Between Morphological Changes and Reduction of Active Areas of Aqueous Outflow in Eyes with Primary Open Angle Glaucoma

Elliot D. Cha, Rui Jin, Haiyan Gong. Ophthalmology, Boston University School of Medicine, Boston, MA.

Purpose: The aim of this study was to identify morphological differences between active and non-active areas of outflow in normal human eyes and to further identify additional structural changes that lead to reductions in active areas of aqueous outflow in primary open angle glaucoma (POAG).

Methods: Four POAG and four normal human eyes were perfused for 30 minutes at 15mmHg to establish a stable baseline outflow facility. The anterior chamber of each eye was exchanged (5mL) and perfused with a fixed volume (200µL) of fluorescent microspheres to visualize the outflow patterns. All eyes were perfusion-fixed. Fluorescent tracer distribution in episcleral veins (EV) and trabecular meshwork (TM) were imaged and analyzed on a global scale. All eyes were then dissected and further categorized into no, low, and high tracer regions. Distribution of tracer throughout the outflow pathway was imaged and analyzed by confocal microscopy in frontal sections and specific morphological changes associated with each flow type were further analyzed using both light and electron microscopy.

Results: Outflow facility was significantly lower in POAG eyes compared to normal eyes ($p < 0.05$). Areas of active outflow were segmental in normal eyes and significantly reduced in POAG eyes ($p < 0.05$). Interestingly, the remaining active flow areas of POAG eyes were predominantly in the nasal quadrant. High and low tracer regions for both normal and POAG eyes showed similar outflow morphology, with a discontinuous basement membrane (BM) along the inner wall endothelium of Schlemm's canal (SC), open SC, and open spaces between trabecular beams. Regions of normal eyes exhibiting no tracer showed a narrower SC and denser extracellular matrix (ECM) in the TM compared to high tracer regions. Regions devoid of tracer in POAG eyes were associated with a collapsed SC, more continuous and thicker BM along the inner wall of SC, and increased ECM beneath the inner wall and in the TM.

Conclusions: Morphological differences were found that consistently distinguished active and non-active areas of outflow in normal eyes. Having the ability to distinguish these areas has permitted us to identify the features that accompany the reduction of active flow area in POAG. Equally important, these features were not found in remaining active areas of outflow.

Commercial Relationships: Elliot D. Cha, None; Rui Jin, None; Haiyan Gong, None

Support: NIH Grant EY018712 & EY022634, Massachusetts Lions Eye Research Fund

Program Number: 2292 **Poster Board Number:** B0096

Presentation Time: 2:45 PM - 4:30 PM

A Novel Rat Model to Study the Role of Intracranial Hypotension in Optic Neuropathy

Uttio Roy Chowdhury, Bradley H. Holman, Cheryl R. Hann, Cindy K. Bahler, Michael P. Fautsch. Ophthalmology, Mayo Clinic, Rochester, MN.

Purpose: Retrospective studies from our laboratory have identified low cerebrospinal fluid pressure (CSFP) as a risk factor for glaucoma. The low CSFP will presumably be reflected in a proportionally lowered intracranial pressure (ICP). Unfortunately, there are no existing animal models to investigate the role of ICP and the glaucoma phenotype. In the current study, we developed a rat model that can be used to manipulate ICP, and eventually be used to study the role of ICP on optic neuropathy.

Methods: Brown Norway rats ($n=3$, retired breeders, age >8 months, weight > 300 g) were surgically implanted with a 20 gauge cannula into the lateral ventricle. The cannula was held in place by dental cement and secured to the skull with 4 screws. An external 3 mm port was connected to PE60 tubing protected by a flexible metal tether. The tether was connected to a swivel mount that enabled movement within the cage. The tubing was attached to a pressure transducer connected to a computer that recorded ICP in real-time. An artificial CSF syringe column was attached in series and positioned at head-level. Lowering of the column enabled manual reduction of ICP. After completion of data collection, rats were sacrificed and processed for histological analysis. Daily ICP was calculated by averaging 24 hours of consecutive data.

Results: Rats undergoing manual manipulation resulting in chronic depression of ICP showed no signs of apparent discomfort during length of experiments which lasted up to 3 months. Baseline ICP for rats was 4.1 ± 1.0 mmHg ($n=3$). Lowering of artificial CSF column by 2-cm below head level reduced ICP to 2.4 ± 1.3 mmHg ($n=3$), nearly 50% below baseline levels. Histological studies confirmed correct cannula placement and indicated minimal invasive damage to brain tissues.

Conclusions: We have developed a unique and viable rat model to study the effect of reduced intracranial ICP on optic neuropathies.

Commercial Relationships: Uttio Roy Chowdhury, None; Bradley H. Holman, None; Cheryl R. Hann, None; Cindy K. Bahler, None; Michael P. Fautsch, None

Support: American Health Assistance Foundation; Research to Prevent Blindness and Mayo Foundation

Program Number: 2293 **Poster Board Number:** B0097

Presentation Time: 2:45 PM - 4:30 PM

Effect of Pupil Dilation on Angle Metrics Obtained from Spectral-Domain Optical Coherence Tomography (SD-OCT)
Xiaojing Pan, Vikas Chopra, Brian A. Francis, Zhou Yuan Zhang, Muneeswar Nittala, Jyotsna Maram, Lyndsey V. Fou, Peggy W. Romano, Cullen J. Barnett, Srinivas Sadda. Doheny Eye Institute, University of Southern California, Los Angeles, CA.

Purpose: PURPOSE: To evaluate the effect of pupil dilation on anterior chamber angle (ACA) measurements obtained by spectral-domain optical coherence tomography (SD-OCT).

Methods: METHODS: A total of 40 eyes from 20 healthy, normal subjects underwent anterior segment OCT imaging using a Cirrus SD-OCT according to an IRB-approved protocol. For each eye, 5-line raster scans of the inferior angle were performed under 3 pupillary conditions: pupil constricted under standard room lighting, physiologic mydriasis in a darkened room, and after pharmacologic mydriasis. The inferior angle Schwalbe's line-angle opening distance (SL-AOD) and the Schwalbe's line-trabecular-iris space area (SL-TISA, measured 500 microns posteriorly from Schwalbe's line) were computed for each eye and pupillary condition. Measurements were performed by masked certified reading center graders using customized grading software. Differences in measurements between different pupillary conditions were compared.

Results: RESULTS: Among the twenty subjects, 11 were female, and 9 were male. The mean age was 29.8 years and the majority was of Asian-descent (65%). SL-AOD under pupillary constriction to room light measured 0.87 ± 0.31 mm, but measured smaller under physiologic mydriasis (0.75 ± 0.29 mm) and larger under pharmacologic mydriasis (0.9 ± 0.38 mm) ($P=0.01$). Analogously, SL-TISA under pupillary constriction to room light measured 0.33 ± 0.14 mm², but measured smaller under physiologic mydriasis (0.29 ± 0.13 mm²) and larger under pharmacologic mydriasis (0.34 ± 0.17 mm²) ($P=0.03$). Compared to pupil constriction to light, the mean SL-AOD decreased 0.54 mm and SL-TISA decreased 0.46 mm² respectively under physiologic mydriasis in the dark ($P < 0.001$). Compared to physiologic mydriasis, the mean SL-AOD increased 0.15 mm and SL-TISA increased 0.05 mm² respectively after pharmacologic mydriasis ($P < 0.05$).

Conclusions: CONCLUSIONS: Anterior chamber angle metrics differed significantly based on the lighting condition and the state of pupillary dilation. Whereas physiologic mydriasis appeared to make measurements smaller, pharmacologic mydriasis made measurements slightly larger. Accounting for the state of the pupil and standardizing the lighting condition would appear to be of importance for future studies of the angle.

Commercial Relationships: Xiaojing Pan, None; Vikas Chopra, Allergan, Inc. (C); Brian A. Francis, Allergan (F), Merck (F), Neomedix (C), Endoptiks (C), Lumenis (F); Zhou Yuan Zhang, None; Muneeswar Nittala, None; Jyotsna Maram, None; Lyndsey V. Fou, None; Peggy W. Romano, None; Cullen J. Barnett, None; Srinivas Sadda, Allergan (C), Genentech (C), Regeneron (C), Optos (C), Carl Zeiss Meditec (C), Optos (F), Carl Zeiss Meditec (F), Optovue (F)

Program Number: 2294 **Poster Board Number:** B0098

Presentation Time: 2:45 PM - 4:30 PM

Structure and function in multifocal pupillographic objective perimetry (mfPOP)

Maria Kolic^{1,2}, Allan Y. Chain³, Andrew C. James^{1,2}, Ted Maddess^{1,2}, Corinne F. Carle^{1,2}. ¹ARC CoE in Vision Science, Australian National University, Canberra City, ACT, Australia; ²Eccles Institute of Neuroscience, Australian National University, Canberra, ACT, Australia; ³ANU Medical School, Australian National University, Canberra City, ACT, Australia.

Purpose: To compare correlations between peripapillary retinal nerve fibre layer (RNFL) thicknesses and visual field changes detected using SAP and multifocal pupillographic objective perimetry (mfPOP) in glaucoma.

Methods: Structure-function correlations were computed for data from 25 glaucoma and 25 normal subjects tested using SAP thresholds and fields derived from three mfPOP stimulus protocols: 1) LumBal: luminance-balanced bright yellow stimuli on a 10 cd/m² yellow background; 2) Lum+Col: 150 cd/m² green stimuli on 10 cd/m² red; and 3) Lum+ColBal = Lum+Col but with luminance balancing. Field data were grouped in arcuate clusters according to Stratus OCT sectors. Pearson correlation coefficients (r) by test region and arcuate cluster were calculated between mfPOP or SAP deviations and RNFL deviations from normative data.

Results: The strongest correlations were observed in the superior-superotemporal sector in severe glaucoma eyes: $r=0.94$ and $r=0.90$ for the mfPOP LumBal and Lum+Col protocols respectively (both $n=16$, $p<0.05$). Correlations across all test-points in both SAP and mfPOP were strongest in eyes with severe glaucoma (SAP MD<-12dB): SAP $r=0.56$, LumBal $r=0.55$, Lum+Col $r=0.52$, Lum+ColBal $r=0.41$ (all $n=192$, $p<0.05$). No significant correlation was observed in normal subjects for mfPOP or SAP. For all patient eyes taken together SAP correlations were higher than mfPOP, however scatterplots of mfPOP/RNFL deviations were quite linear while SAP data saturated.

Conclusions: For both methods the largest correlations with RNFL thickness corresponded to the inferior nasal field of more severely damaged eyes. Head to head comparison of mfPOP and SAP showed similar structure/function relationships.

Commercial Relationships: Maria Kolic, SeeingMachines Ltd (E); Allan Y. Chain, None; Andrew C. James, Seeing Machines, Inc (P); Ted Maddess, Seeing Machines (F), Seeing Machines (P), EyeCo (I); Corinne F. Carle, AU2012/905171 (P)

Support: Australian Research Council through the ARC Centre of Excellence in Vision Science (CE0561903)

Program Number: 2295 **Poster Board Number:** B0099

Presentation Time: 2:45 PM - 4:30 PM

Continuous Likelihood Ratios for Glaucoma Diagnosis Using the Combined Index of Structure and Function

Tammy Tung-Mei Kuang^{1,2}, Renato Lisboa^{1,3}, Andrew J. Tatham¹, Linda M. Zangwill¹, Robert N. Weinreb¹, Jeffrey M. Liebmann^{4,5}, Christopher A. Girkin⁶, Naira Khachatryan¹, Naama Hammel¹, Felipe A. Medeiros¹. ¹Department of Ophthalmology, Hamilton Glaucoma Center, California, CA; ²Department of Ophthalmology, Taipei Veterans General Hospital, Taipei, Taiwan; ³Department of Ophthalmology, Federal University of São Paulo, São Paulo, Brazil; ⁴School of Medicine, New York University, New York, NY; ⁵Department of Ophthalmology, Einhorn Clinical Research Center, New York Eye and Ear Infirmary, New York, NY; ⁶School of Medicine, University of Alabama, Birmingham, AL.

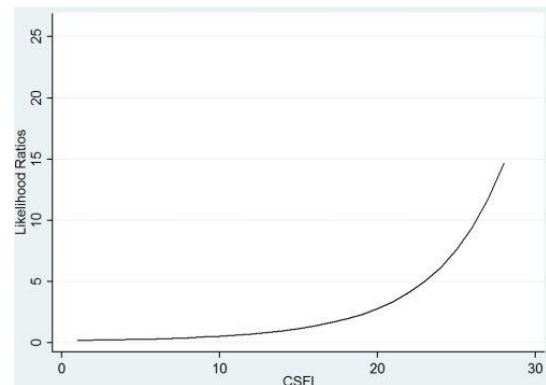
Purpose: To evaluate the ability of a combined index of structure and function (CSFI) to diagnose glaucoma using a new methodology for calculating continuous likelihood ratios (LRs).

Methods: This was an observational cohort study that included 937

eyes of 624 subjects recruited from the Diagnostic Innovations Glaucoma Study (DIGS) and the African Descent and Glaucoma Evaluation Study (ADAGES). Eyes were classified as having glaucoma if they had previous progressive optic nerve change and/or reproducible visual field damage. The control group was composed of eyes from healthy subjects recruited from the general population, regardless of visual field and optic disc status. All eyes underwent retinal nerve fiber layer imaging with Spectralis spectral domain optical coherence tomography (SDOCT) and standard automated perimetry (SAP). Estimated number of retinal ganglion cells (RGCs) were obtained from SDOCT and SAP and a weighted average (WRGC) was used to obtain the final estimate of number of RGCs for each eye. The CSFI was calculated as the percent loss of RGCs obtained by subtracting estimated from age-expected RGC numbers. Continuous LRs for glaucoma diagnosis were estimated for WRGC estimates and CSFI using a new methodology based on estimating the tangents to the Receiver Operating Characteristic (ROC) curve.

Results: Three hundred ninety nine eyes of 240 subjects were included in the control group and 538 eyes of 384 patients in the glaucoma group. The median of mean deviation was -3.5 dB (range -27.5 to 2.0 dB) for the glaucoma group. The number of WRGC was 1,078,000±195,000 in the control group and 596,000±217,000 in the glaucoma group ($P<0.0001$). CSFI was -3.7 ± 12.3 in the control group and 34.7 ± 23.3 in the glaucoma group ($P<0.001$). Continuous LRs were calculated for each specific value of WRGC and CSFI. Lower WRGC estimates and larger CSFI values were associated with larger LRs for glaucoma diagnosis. CSFI values larger than 26 were associated with large effects on post-test probability of disease, that is, LRs greater than 10.

Conclusions: The methodology allowed estimation of continuous LRs for glaucoma diagnosis for specific values of WRGC estimates and CSFI values. Calculation of continuous LRs may facilitate the incorporation of results of diagnostic tests into clinical decision-making for glaucoma diagnosis.



Graph of Likelihood Ratios against Combined Index of Structure and Function

Commercial Relationships: Tammy Tung-Mei Kuang, None; Renato Lisboa, None; Andrew J. Tatham, None; Linda M. Zangwill, Carl Zeiss Meditec Inc (F), Heidelberg Engineering GmbH (F), Optovue Inc (F), Topcon Medical Systems Inc (F), Nidek Inc (F); Robert N. Weinreb, Aerie (F), Alcon (C), Allergan (C), Altheos (C), Amakem (C), Bausch&Lomb (C), Carl Zeiss-Meditec (C), Genentech (F), Haag-Streit (F), Heidelberg Engineering (F), Konan (F), Lumenis (F), National Eye Institute (F), Nidek (F), Optovue (C), Quark (C), Solx (C), Topcon (C); Jeffrey M. Liebmann, Alcon Laboratories, Inc. (C), Allergan, Inc. (C), Allergan, Inc. (F), Carl Zeiss Meditec, Inc (F), Heidelberg Engineering, GmbH (F), Topcon Medical Systems, Inc. (F), National Eye Institute (F), New York

ARVO 2013 Annual Meeting Abstracts by Scientific Section/Group – Glaucoma

Glaucoma Research Institute (F), SOLX, Inc. (C), Bausch & Lomb, Inc (C), Diopsys, Inc. (C), Diopsys, Inc. (F), Merz, Inc. (C), Glaukos, Inc. (C), Quark, Inc. (C); **Christopher A. Girkin**, SOLX (F), Heidelberg Engineering (F); **Naira Khachatryan**, None; **Naama Hammel**, None; **Felipe A. Medeiros**, Carl-Zeiss (F), Heidelberg Engineering (F), Topcon (F), Alcon (F), Allergan (F), Sensimed (F), Reichert (F)

Support: Supported by National Eye Institute grants U10EY14267, EY019869, EY021818, EY022039 and EY08208, EY11008, and EY13959 and Eyesight Foundation of Alabama; Alcon Laboratories Inc.; Allergan Inc.; Pfizer Inc.; Merck Inc.; Santen Inc.; and the Edith C. Blum Research Fund of the New York Glaucoma Research Institute, New York, NY. Supported by an unrestricted grant from Research to Prevent Blindness, New York, New York

Clinical Trial: NCT00221923

Program Number: 2296 **Poster Board Number:** B0100

Presentation Time: 2:45 PM - 4:30 PM

The Geometric Factors related to Central Visual Field Defect in Normal Tension Glaucoma

Hyungyu Yoo, Marvin Lee, Jaehong Ahn. Department of Ophthalmology, Ajou University School of Medicine, Suwon, Republic of Korea.

Purpose: To investigate the relationship between the ocular geometric factors measured by optic disc stereophotographs (ODP) and central visual field (VF) defect in normal tension glaucoma (NTG) patients.

Methods: This retrospective study included eighty-eight eyes of 88 NTG patients with mild VF defect (MD > -6.0dB). NTG patients were divided into two subgroups, according to VF tests: the central VF-invading and central VF-sparing groups. Optic nerve head (ONH) parameters including disc dimensions, peripapillary atrophy (PPA) and distance between fovea and disc margin (DFD) were obtained by ODP and retinal nerve fiber layer thickness (RNFLT) was measured by Stratus optical coherence tomography (OCT).

Results: Intraocular pressure was not different between groups but ocular pulse amplitude was higher in invading group (2.91 vs 2.43 mmHg, $p=0.017$) DFD of invading group (3.642 ± 0.401 mm) was shorter than sparing group (3.877 ± 0.278 mm) ($p=0.002$). The sparing group had more vertically oval ONH ($p=0.023$) and wider temporal PPA width ($p=0.031$). The RNFLT of invading group was thinner in temporal and inferior quadrants, but thicker in superior quadrant than that of sparing group. In a multiple linear regression analysis, DFD was the only geometric factor associated with degree of central VF involvement ($p=0.002$). DFD was positively correlated with temporal RNFLT in sparing group ($r=0.484$, $p<0.001$) but not in invading group ($r=-0.080$, $p=0.631$).

Conclusions: The central VF defect appears to be related with shorter DFD in the patients with mild NTG. It may suggest that the eyes with shorter DFD tends to manifest earlier central VF defect because they may have less structural reservoir resisting glaucomatous damage related to parafoveal involvement.

Commercial Relationships: Hyungyu Yoo, None; Marvin Lee, None; Jaehong Ahn, None

Program Number: 2297 **Poster Board Number:** B0101

Presentation Time: 2:45 PM - 4:30 PM

EVALUATION OF OPTIC NERVE HEAD FOR DIAGNOSIS OF GLAUCOMA IN CADAVER EYES WITHOUT PRIOR HISTORY

Srinivasan Senthilkumari¹, Mohan Neethu², Radhakrishnan Santhi³, Subbiah Ramaswami Krishnadas⁴, Veerappan Muthukkaruppan⁵.

¹Department of Ocular Pharmacology, Aravind Medical Research

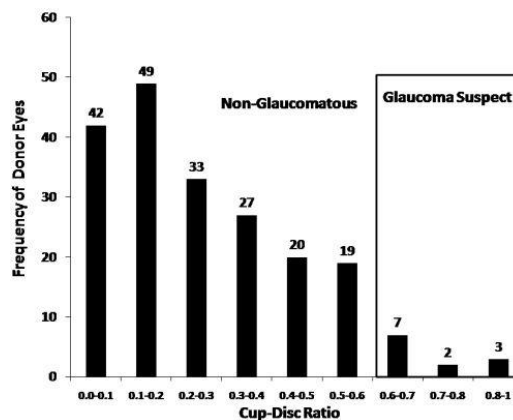
Foundation, Madurai, India; ²Glaucoma Clinic, Aravind Eye Hospital, Madurai, India; ³Department of Pathology, Aravind Medical Research Foundation, Madurai, India; ⁴Glaucoma Clinic, Aravind Eye Hospital, Madurai, India; ⁵Department of Immunology and Cell Biology, Aravind Medical Research Foundation, Madurai, India.

Purpose: Human tissues are important in vision research since they serve as a “Proof of Concept” for the findings derived from experimental models for age-related ocular diseases including glaucoma. The unique anatomy of human aqueous outflow tract makes it a mainstay for glaucoma research. The present study was to develop methods to identify glaucoma by examining the optic nerve head (ONH) of donor eyes, especially when information on preexisting ocular disease was unavailable in India.

Methods: The ONH of the donor eyes was evaluated under stereomicroscope for cup-disc ratio (CDR) and focal rim thinning was noted. The vertical diameter of the cup and disc was also measured using a pre-calibrated eye piece micrometer. The eyes suspected of glaucoma were subjected to histological analysis to confirm the presence of specific glaucomatous changes.

Results: A total of 202 eyes from 119 donors (68 males & 51 females, 42 to 96 years) were evaluated for glaucoma. Among them, 190 (94%) eyes showed CDR in the range of 0.0 to 0.6 and the remaining eyes CDR more than 0.6. The calculated mean CDR of non-glaucomatous and the glaucoma-suspect groups were found to be 0.3 ± 0.16 and 0.62 ± 0.27 respectively and it was significantly different ($p=0.0003$). Out of 12 eyes suspected for glaucoma, seven eyes from five donors showed specific glaucomatous changes by histology. The prevalence of glaucoma was 4.2% among the donors studied.

Conclusions: The present study described a simple method of screening fresh donor eyes for selecting those with glaucoma features using CDR and histological analysis. This method would help us to obtain biologically active human ocular tissues for glaucoma research on gene expression, ultra structural/ proteome changes and outflow mechanism.



Commercial Relationships: Srinivasan Senthilkumari, None; Mohan Neethu, None; Radhakrishnan Santhi, None; Subbiah Ramaswami Krishnadas, None; Veerappan Muthukkaruppan, None

Support: Aravind Medical Research Foundation - In-House Funding, INDIA

Program Number: 2298 **Poster Board Number:** B0102

Presentation Time: 2:45 PM - 4:30 PM

Diagnostic power of the new colorimetry photographic device (Laguna ONHe) in glaucomatous and hypertensive eyes:

comparative study with Spectralis optical coherence tomography and HRT III confocal tomography

Ignacio Rodriguez-Uña¹, Carmen Mendez-Hernandez¹, Manuel González-de-la-Rosa², Federico Saenz-Frances¹, Paula Arribas Pardo¹, Jose M. Martinez de la Casa¹, Julian Garcia-Feijoo¹.

¹Glaucoma, Instituto de Investigación Sanitaria San Carlos (IdISSC) Fundación de Investigación Biomédica del Hospital Clínico San Carlos, Madrid, Spain; ²Hospital Universitario de Canarias, La Laguna, Spain.

Purpose: Assessing the diagnostic power of the new device, Laguna ONhE, in the measurements of Optic Nerve Head Hemoglobin (ONHH) versus Spectralis optical coherence tomography (OCT) and confocal tomography (HRT III) in hypertensive and glaucomatous eyes.

Methods: Hypertensive (n=36), glaucomatous (n=66) and healthy (n=65) eyes were evaluated using Spectralis OCT, HRT III and non-mydiatic retinography of the Optic Nerve Head (ONH). ONHH was measured using Laguna ONhE software. Areas under ROC curve were calculated and correlation between those parameters with greater diagnostic power was investigated with Spearman Rho coefficient.

Results: The area under ROC curve for Glaucoma Discriminant Function (GDF) index calculated with Laguna ONhE was 0.756 (95% CI: 0.674-0.838). With OCT, the area for retinal nerve fiber layer thickness (RNFLT) was 0.741 (95% CI: 0.654-0.828). With HRT, two parameters were studied: Glaucoma Probability Score (GPS) and vertical cup-disc ratio. The values for the area under the curve were 0.742 (95% CI: 0.656-0.828) and 0.738 (95% CI: 0.652-0.824), respectively.

GDF showed the best correlation with GPS of the HRT (-0.609, p<0.01), higher in severe glaucomatous eyes (-0.675) than in early (-0.519) or moderate (-0.450) glaucomatous eyes. GDF correlation with the RNFLT determined by OCT was 0.446 (p<0.01), all glaucomatous eyes considered.

Conclusions: ONHH concentration correlates with Spectralis OCT and HRT III parameters, with similar diagnostic power. The new colorimetry photographic device, Laguna ONhE, might be useful in structural diagnosis of glaucoma.

Commercial Relationships: Ignacio Rodriguez-Uña, None; Carmen Mendez-Hernandez, None; Manuel González-de-la-Rosa, Haag Streit (P), Oculus (P); Federico Saenz-Frances, None; Paula Arribas Pardo, None; Jose M. Martinez de la Casa, None; Julian Garcia-Feijoo, Tracend (C), Ivantis (C), Glaukos (C), MSD (C), Allergan (F), Pfizer (F), Alcon (C), Sensimed (F), Sylentis (F), Bausch and Lomb (C)

Support: Instituto de Investigación Sanitaria San Carlos (IdISSC). Fundación Investigación Biomédica del Hospital Clínico San Carlos. Fondo de Investigación Sanitaria. Instituto de Salud Carlos III
Clinical Trial: PI09/90933

Program Number: 2299 **Poster Board Number:** B0103

Presentation Time: 2:45 PM - 4:30 PM

Three-dimensional quantitative analysis of collagen fibre architecture in human peripapillary sclera

Jacek K. Pijanka¹, Thomas Sorensen², Thao D. Nguyen³, Harry Quigley⁴, Craig Boote¹.

¹Structural Biophysics, School of Optometry and Vision Sciences, Cardiff University, Cardiff, United Kingdom; ²Diamond Light Source, Didcot, United Kingdom; ³The Department of Mechanical Engineering, The Johns Hopkins University, Baltimore, MD; ⁴Glaucoma Centre of Excellence, Wilmer Ophthalmological Institute, Johns Hopkins University School of Medicine, Baltimore, MD.

Purpose: The collagen fibre architecture of the peripapillary sclera has a significant influence on the optic nerve head (ONH) biomechanics and may therefore be important in glaucoma. Our purpose was to obtain the first quantitative 3D maps of collagen fibre architecture in the human peripapillary sclera.

Methods: 6 mm diameter peripapillary scleral buttons were removed post-mortem from three left normal Caucasian human donor eyes aged 74-79 years with no history of glaucoma. Six 150 µm thick serial sections were obtained for each button using a cryo-microtome. Wide angle x-ray scattering was used to quantify the orientation (Fig. 1), mass distribution and degree of anisotropy (Table 1) of preferentially aligned collagen fibres at 0.5 mm intervals across each section. Second harmonic generation multiphoton microscopy provided visual confirmation of the collagen fibre alignment.

Results: Consistent with previous findings by our lab and others, a ring of fibres was noted circumscribing the ONH, in which the degree of fibre alignment varied with circumferential position (Fig. 1). New quantitative depth-profiling of the fibre anisotropy revealed that the circumferential fibre ring structure was concentrated in the mid stromal depth (Fig. 1 and Table 1). Meridional fibre bands were also noted anchoring superiorly and inferiorly into the peripapillary fibre ring and radiating obliquely into the mid-posterior sclera. This feature was also more evident in the mid-stromal depth (Fig. 1).

Conclusions: The anisotropic collagen fibre architecture of the human peripapillary sclera exhibits marked depth-dependency. This may represent a mechanical adaptation designed to protect the ONH from pressure elevations by more effectively reinforcing the peripapillary tissue at its insertion point with the lamina cribrosa.

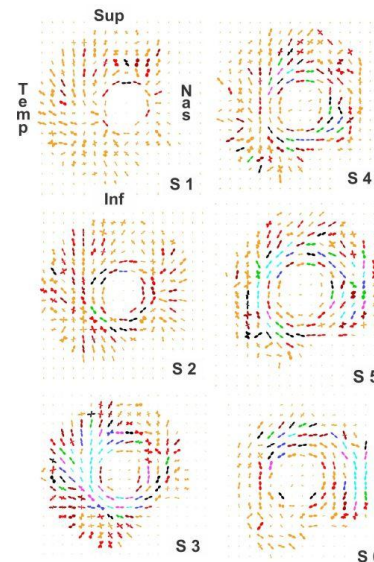


Fig. 1: Polar vector maps of collagen fibre alignment as a function of tissue depth in the peripapillary sclera and ONH of a normal human eye. The plots have been scaled down by the following factors: orange(1), red(2), brown (3), black(4), green(5), blue(6), purple(7), turquoise(10). Interval between data points:0.5 mm. Section 1 represents the inner 150 µm of tissue, adjacent to choroid.

Sections	Depth (µm)	Mean anisotropy
1 (inner)	900 - 750	0.54
2	750 - 600	0.64
3	600 - 450	0.68
4	450 - 300	0.63
5	300 - 150	0.56
6 (outer)	150 - 0	0.42

Table 1: Mean fibre anisotropy (expressed as proportion of preferentially aligned fibres) in the peripapillary sclera per section (n=3 eyes).

Commercial Relationships: Jacek K. Pijanka, None; Thomas Sorensen, None; Thao D. Nguyen, None; Harry Quigley, Sensimed (C), Genetech (C), Merck (C), Sucampo (C); Craig Boote, None
Support: Fight For Sight 501917

302 Clinical Studies/Trials

Tuesday, May 07, 2013 8:30 AM-10:15 AM

6B Paper Session

Program #/Board # Range: 2619-2625

Organizing Section: Glaucoma

Program Number: 2619

Presentation Time: 8:30 AM - 8:45 AM

The United Kingdom Glaucoma Treatment Study (UKGTS): baseline characteristics and main outcomes

David F. Garway-Heath¹, Gerassimos Lascaratos¹, Catey Bunce¹, David P. Crabb², Richard A. Russell², Ameet Shah¹, Katsuyoshi Suzuki¹, Edward White¹, Francesca Amalfitano¹. ¹NIHR Biomedical Research Centre at Moorfields Eye Hospital NHS Foundation Trust and UCL Institute of Ophthalmology, London, United Kingdom; ²Department of Optometry and Visual Science, City University, London, United Kingdom.

Purpose: Medical IOP reduction is the standard initial treatment for open angle glaucoma (OAG), yet no randomized placebo-controlled study of medical IOP reduction has been undertaken previously.

Methods: The United Kingdom Glaucoma Treatment Study (UKGTS) is the first randomized, double-masked, placebo-controlled, multi-centre medical treatment trial for OAG. 516 newly-diagnosed (previously untreated) patients with OAG were prospectively recruited at 10 UK centres between 2007 and 2010. The observation period was 2 years, with subjects monitored by visual field (VF) testing, quantitative imaging, optic disc photography and tonometry at 11 visits. Eligible patients were assigned by concealed telephone allocation to treatment with latanoprost 0.005% or placebo. The primary outcome measure was time to VF deterioration within 24 months, based on Humphrey VF Analyzer GPA criteria.

Results: Mean (±SD) subject age was 66(±11) years and 52.9% were male. The baseline mean IOP (±SD) was 18.9±4mmHg in the better mean deviation (MD) eyes (median [IQR] MD -1.27dB [-2.37, -0.19]) and 19.9±4.6mmHg in the worse MD eyes (median [IQR] MD -3.30dB [-5.60, -1.98]). Survival analysis showed a significant difference in the time from baseline to confirmed VF progression between the two treatment groups (p=0.0012) (Fig.1). The adjusted hazard ratio by site was 0.498 (95% CI 0.332, 0.747). The median (IQR) MD slope for all eyes with reliable VFs on at least 5 visits was 0.17 (-0.34 to 0.51) dB/year and -0.05 (-0.70 to 0.49) dB/year for the latanoprost and placebo groups, respectively (p=0.0003). The mean IOP reduction from the pre-allocation visit to the first visit post-

treatment allocation was greater in the latanoprost group (4.5mmHg) as compared to the placebo (0.6mmHg). 127 patients who did not reach an endpoint failed to complete 2 years' follow-up 24.6%.

Conclusions: The UKGTS is the first randomized, placebo-controlled trial to show the efficacy of medical treatment in reducing VF deterioration in OAG. The observation period was short (2 years) compared to most trials; the analysis of deterioration velocity and inclusion of quantitative imaging has the potential to reduce the number of patients and/or duration required for subsequent clinical trials and will be modelled in subsequent analyses.

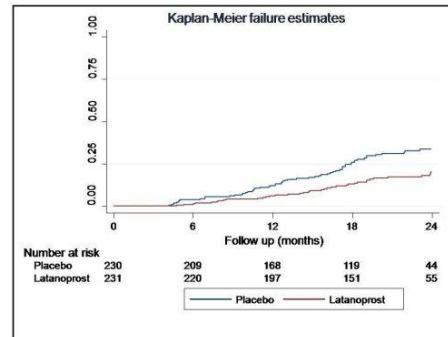


Figure 1

Commercial Relationships: David F. Garway-Heath, Moorfields MDT (P), Carl Zeiss Meditec (F), Heidelberg Engineering (F), Reichert Technologies (F), Ziemer Ophthalmic Systems AG (F), Pfizer Inc (F), Allergan (F), Allergan (C), Allergan (R), Alcon (C), Alcon (R), Bausch & Lomb (R), Merck (R), Santen (R), Quark (C), Teva (C), Topcon (F), OptoVue (F); Gerassimos Lascaratos, None; Catey Bunce, None; David P. Crabb, Allergan Inc. (R), Moorfields MDT (P); Richard A. Russell, None; Ameet Shah, None; Katsuyoshi Suzuki, None; Edward White, None; Francesca Amalfitano, None

Support: Supported by an unrestricted Investigator-Initiated Research Grant from Pfizer, Inc. The research also was supported by the National Institute for Health Research Biomedical Research Centre at Moorfields Eye Hospital NHS Foundation Trust and UCL Institute of Ophthalmology. The views expressed are those of the author(s) and not necessarily those of the NHS, the NIHR or the Department of Health. Equipment loans were made by Heidelberg Engineering GmbH, Carl Zeiss Meditec, Inc, and OptoVue, Inc. The trial sponsor was Moorfields Eye Hospital NHS Foundation Trust. The funding organizations had no role in the design or conduct of this research.

Clinical Trial: ISRCTN96423140

Program Number: 2620

Presentation Time: 8:45 AM - 9:00 AM

Canadian Glaucoma Study 4: Neuroretinal Rim Area Change in Patients with Visual Field-based Endpoints and Interventions

Rizwan Malik^{1,6}, Neil O'Leary^{1,7}, Frederick S. Mikelberg², Gordon A. Balazsi³, Raymond P. LeBlanc¹, Mark R. Lesk⁴, Marcelo T. Nicoletti¹, Graham E. Trope⁵, Balwantray C. Chauhan¹.

¹Ophthalmology and Visual Sciences, Dalhousie University, Halifax, NS, Canada; ²Ophthalmology and Visual Sciences, University of British Columbia, Vancouver, BC, Canada; ³Ophthalmology, McGill University, Montreal, QC, Canada; ⁴Université de Montréal, Montreal, QC, Canada; ⁵Ophthalmology and Visual Sciences, University of Toronto, Toronto, ON, Canada; ⁶NIHR Biomedical Research Centre for Ophthalmology at Moorfields Eye Hospital NHS Foundation Trust and UCL Institute of Ophthalmology, London, United Kingdom; ⁷Centre for Biostatistics, Institute of Population

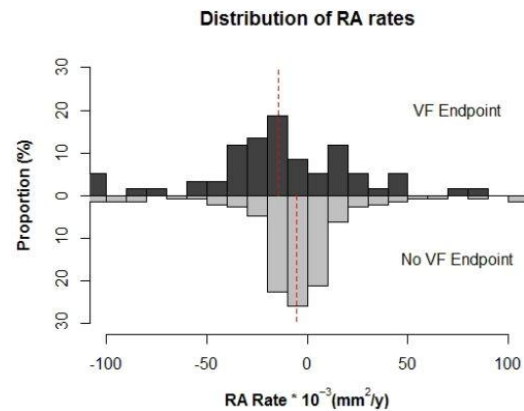
Health, School of Medicine, University of Manchester, Manchester, United Kingdom.

Purpose: (1) To compare rates of neuroretinal rim area (RA) change in patients with and without a visual field (VF) endpoint in the Canadian Glaucoma Study (CGS). (2) To determine whether IOP intervention after the VF endpoint had an impact on RA change.

Methods: Patients were treated to achieve a target IOP and examined at 4-month intervals with standard automated perimetry and confocal scanning laser tomography (CSLT). Patients reaching a VF endpoint defined by repeatable progression based on total deviation change probability analysis underwent an additional $\geq 20\%$ IOP reduction (Canadian Glaucoma Study Group. *Canadian Glaucoma Study I. Can J Ophthalmol.* 2006; 41: 566-75). RA rates were computed with robust linear regression only when ≥ 4 examinations were available and compared for patients with and without a VF endpoint. For patients with endpoints, the change in RA rate was computed (RA rate post-intervention - RA rate pre-intervention).

Results: Of the 258 enrolled patients, 206 (80%) had sufficient follow-up to compute RA rates. The median (interquartile range, IQR) baseline age, follow-up and number of CSLT examinations was 68 (58, 75) years, 6 (5, 7) years, and 15 (12, 19) respectively. The median (IQR) RA rate prior to a VF endpoint of $-14 (-32, 11) \times 10^{-3} \text{ mm}^2/\text{year}$ (n=59) was significantly worse (P=0.02, **see figure**), compared to that in patients with no endpoint: $-5 (-14, 5) \times 10^{-3} \text{ mm}^2/\text{year}$ (n=147). In 43 patients with sufficient follow-up before and after IOP-lowering intervention, the median change (95% CI) in RA rate was $8 (-10, 24) \times 10^{-3} \text{ mm}^2/\text{year}$.

Conclusions: Prior to the VF endpoint, patients with VF progression had a median RA rate that was nearly 3 times worse compared to those without progression. After the endpoint, IOP intervention did not have a statistically significant impact on the subsequent RA rate.



Distribution of RA rates prior to the first VF endpoint, in patients with and without a VF endpoint.

Commercial Relationships: Rizwan Malik, NIHR Moorfields Biomedical Research Centre (F), Special Trustees of Moorfields Eye Hospital (F); Neil O'Leary, None; Frederick S. Mikelberg, None; Gordon A. Balazsi, None; Raymond P. LeBlanc, None; Mark R. Lesk, None; Marcelo T. Nicolela, Allergan Inc (F), Alcon (F); Graham E. Trope, sensimed (F); Balwantray C. Chauhan, None

Support: Canadian National Institute for the Blind, Allergan Canada Inc., Merck Frosst Canada, Pfizer Canada Inc.

Clinical Trial: NCT00262626

Program Number: 2621

Presentation Time: 9:00 AM - 9:15 AM

A Randomized, Phase II Study of Trabodenoson (INO-8875) in Adults with Ocular Hypertension (OHT) or Primary Open-Angle Glaucoma (POAG)

Jonathan S. Myers¹, Kenneth N. Sall², Harvey DuBiner³, Chaim Brickman⁴, N. Slomowitz⁴, William McVicar⁴, Rudolf Baumgartner⁴.
¹Glaucoma, Wills Eye Institute, Philadelphia, PA; ²Sall Research Medical Center, Inc., Artesia, CA; ³Eye Care Center Management, GA, Morrow, GA; ⁴Inotek Pharmaceutical Corporation, Lexington, MA.

Purpose: The efficacy and tolerability of trabodenoson, a highly-selective adenosine-1 agonist, were assessed following monocular topical application in subjects with OHT or POAG.

Methods: Adults who signed informed consent and met enrollment criteria underwent a 4-day placebo run-in period. Subjects in Part 1 were randomized to placebo or 50-200 µg of trabodenoson BID for 14 days and in Part 2 to placebo or 500 µg of trabodenoson BID for 28 days. Masked-IOP measurements and safety assessments were performed before, during and after the treatment period.

Results: 144 subjects were randomized to placebo or trabodenoson. The most consistent decreases in IOP were noted at the 500 µg dose [N=67: 33 placebo - baseline (mean pre-dose) 27.1±2.9 (SD) mmHg; 34 active - baseline (mean pre-dose) 26.2±2.4 (SD) mmHg]. Day 14 and Day 28 mean diurnal IOP changes were computed by averaging the changes from baseline (Day 1 8AM) at 8AM, 10AM, 12PM, 4PM and 8PM (12 hrs post dose). By Day 14, the 500 µg cohort had achieved a significant reduction in mean diurnal IOP compared to placebo (median $\Delta = -4.9 \pm 2.9$ (SD) mmHg [p=0.01]) with a further decrease by Day 28 (median $\Delta = -6.5 \pm 2.5$ (SD) mmHg [p<0.001]). Day 28 subgroup analyses for subjects with: OHT (N=13, median $\Delta = -6.3 \pm 2.4$ mmHg, p=0.003), POAG (N=20, median $\Delta = -6.6 \pm 2.6$ mmHg, p=0.005), baseline IOP ≥ 25 mmHg (N=21, median $\Delta = -7.2 \pm 2.5$ mmHg, p<0.001); and subjects requiring wash out of glaucoma medication(s) prior to randomization (N=11, median $\Delta = -7.2 \pm 2.7$ mmHg, p=0.002) all showed significant reductions in mean diurnal IOP.

All doses were well-tolerated. External eye examinations indicated post-randomization hyperemia rates for the placebo and 500 µg cohorts were unchanged from baseline. These hyperemias were transient (<4 hr), generally mild, self-limited and not associated with anterior chamber cells or flare in either cohort. All other safety data including electrocardiograms were unremarkable. Increases in systemic exposure to Trabodenoson were dose-related with no evidence of accumulation in plasma.

Conclusions: Trabodenoson was well-tolerated, safe, and resulted in significant IOP reductions in adults with OHT or POAG.

Diurnal IOP Change (Δ) from Baseline (mmHg); 500 µg Trabodenoson Cohort						
	Day 14- All	Day 28- All	Day 28- OHT	Day 28- POAG	Day 28-IOP >25 mmHg	Day 28- washouts
N	34	34	13	20	21	11
Baseline \pm SD	26.2 \pm 2.4	26.2 \pm 2.4	26.3 \pm 2.7	26.1 \pm 2.2	27.3 \pm 2.2	27.4 \pm 2.2
Median Δ \pm SD	-4.9 \pm 2.9	-6.5 \pm 2.5	-6.3 \pm 2.4	-6.6 \pm 2.6	-7.2 \pm 2.5	-7.2 \pm 2.7
P value vs placebo	P=0.01	P<0.001	p=0.003	p=0.005	p<0.001	p=0.002

Commercial Relationships: Jonathan S. Myers, Alcon (R), Allergan (C), Allergan (R), Inotek (F), Inotek (C), Merck (R), Sucampo (C); Kenneth N. Sall, None; Harvey DuBiner, Alcon (R); Chaim Brickman, Inotek Pharmaceuticals Corporation (E); N. Slomowitz, Inotek Pharmaceutical Corp (E); William McVicar, Inotek Pharmaceuticals (E); Rudolf Baumgartner, Inotek Pharm Corp (E)

Clinical Trial: NCT01123785

Program Number: 2622

Presentation Time: 9:15 AM - 9:30 AM

Association of poor eyedrop instillation technique and faster rate of visual field progression in patients under chronic glaucoma medical therapy

Jimena Schmidt^{1,2}, Andres Gerhard^{1,2}, Militza Sanchez², Pablo Musa¹, David S. Friedman³, Eugenio A. Maul^{1,2}. ¹Ophthalmology Department, Pontificia Universidad Catolica de Chile, Santiago, Chile; ²Ophthalmology Department, Hospital Sotero del Rio, Santiago, Chile; ³Ophthalmology Department, Wilmer Eye Institute/John Hopkins, Baltimore, MD.

Purpose: To study the association of eyedrop instillation technique and previous rate of visual field progression (VFP) in patients under chronic glaucoma medical therapy.

Methods: We conducted a retrospective review of visual fields (VF) from patients that participated in a randomized controlled trial (RCT) comparing success of 2 eyedrop instillation techniques (NCT01417689). All participants were on chronic (>= 1 year), bilateral ocular hypotensive therapy.

Eligibility criteria included >= 6 previous VFs at the time of enrollment and having non-missing data for the baseline evaluation of the RCT.

After censoring the first 2 VFs to reduce noise induced by learning, VFP was estimated using linear regression to estimate the the slope of Mean Deviation in dB/year.

The variables correlated with rate of VFP were: Total success, defined as getting the drop in the eye using only one eyedrop; and number of eyedrops spent during instillation dichotomized using different cut-offs.

Given that most of the patients had 2 eligible eyes, generalized estimating equations were used to estimate the associations.

Results: The 228 patients enrolled in the RCT had data for baseline eyedrop instillation evaluation of which 134 patients (239 eyes) had >=6 previous VFs.

Mean age (sd) was 73.9 (7.5) years, 58% were women. Included eyes had a mean (sd) of 9.8 (SD 2.3) previous exams.

While 99% of the eyes managed to get a drop in the eye, only 164 (69%) did so spending only one drop (Total success). Patients that achieved total success at baseline had a mean rate of VFP of -0.52dB/year versus -0.67 dB/year in those that did not. (p=0.12). For the association of number of drops spent to VFP, the cutoff that achieved the greatest contrast and significance was >=3 drops spent. The 24 eyes (10%) that spent 3 or more drops had a mean rate of progression of 0.91dB/year while those that spent <3 drops had a mean rate of VFP of 0.52 dB/year. (p=0.05)

Conclusions: Our data suggests that patients spending more drops per instillation attempt might be at risk of progressing faster. This association could be mediated by decreased adherence and needs confirmation in prospective studies.

Commercial Relationships: **Jimena Schmidt**, None; **Andres Gerhard**, None; **Militza Sanchez**, None; **Pablo Musa**, None; **David S. Friedman**, Alcon (C), Bausch & Lomb (C), Merck (C), QLT, Inc (C), Allergan (C), Nidek (C); **Eugenio A. Maul**, None

Program Number: 2623

Presentation Time: 9:30 AM - 9:45 AM

Non-adherence in glaucoma and its association with satisfaction of glaucoma and medication information

Heidi Cate^{1,2}, Debi Bhattacharya², Allan Clark³, Richard Fordham³, Richard Holland³, David C. Broadway¹. ¹Glaucoma Research Unit, Ophthalmology, Norfolk and Norwich University Hospital Foundation Trust, Norwich, United Kingdom; ²School of Pharmacy, University of East Anglia, Norwich, United Kingdom; ³Norwich

Medical School, University of East Anglia, Norwich, United Kingdom.

Purpose: Medication non-adherence can lead to visual field loss, unnecessary additional prescribing and/or intervention. Patient satisfaction with medicines information is associated with improved adherence, however, the relationship between adherence and glaucoma information provision is unclear. The study aimed to determine if patients treated with travoprost were more adherent if satisfied with both medication-related and glaucoma information.

Methods: Patients newly prescribed travoprost were given a Travalert Dosing Aid® from which 8 months of daily adherence data were collected. The mean % adherence rate for each month was calculated and month 7 and 8 mean % adherence combined. Participants received either standard care (control) or additional medication and glaucoma related information by trained glaucoma support assistants (GSAs) (intervention). Satisfaction with received information (SIMS) was measured at 2 and 8 months for both groups. At 2 months, the intervention group also rated the glaucoma information received from the GSAs.

Results: 208 patients (106 control and 102 intervention) were included. There was no significant difference in adherence between the groups at any time point or at month 7 and 8 combined (p=0.703). There was no correlation between adherence and SIMS score at month 8 for the total cohort (r=-0.015 p=0.883). However, SIMS scores were higher in the intervention group (p<0.001) at months 2 and 8 (Table). More than 80% (n=70) of intervention patients considered the GSA service improved their knowledge of glaucoma (87%), confidence with therapy (85%), and drop administration (87%). There was a positive correlation between satisfaction with glaucoma information received from the GSAs and adherence in the intervention group (r=0.243 p=0.022).

Conclusions: The mean control adherence rate was higher than expected, which may have contributed to the absence of a demonstrable difference between the two groups. However, intervention participants demonstrated raised satisfaction levels with GSA delivered glaucoma and medication-related information relative to standard care. Although this study did not appear to improve adherence, a GSA service did improve patient satisfaction with medication and glaucoma-related information which may have the potential to improve adherence.

	Control		Intervention		Mann-Whitney U (Mean Rank)
	Median (IQ)	Mean (SD)	Median (IQ)	Mean (SD)	
Month 2	10.0 (8.0, 14.0)	10.46 (4.28) n=92	15.0 (13.0, 17.0)	14.17 (3.43) n=76	Z=-5.604 p>0.001 (65.55 - 107.43)
Month 8	11.0 (8.0, 14.0)	10.91 (4.28) n=85	16.0 (11.8, 17.0)	13.93 (4.05) n=74	Z=-4.529 p>0.001 (64.81 - 97.45)

Comparison of SIMS scores between intervention and control groups at month 2 and month 8.

Commercial Relationships: **Heidi Cate**, None; **Debi Bhattacharya**, None; **Allan Clark**, None; **Richard Fordham**, None; **Richard Holland**, None; **David C. Broadway**, None

Support: This abstract presents independent research commissioned by the National Institute for Health Research (NIHR) under its Research for Patient Benefit (RfPB) Programme (Grant Reference Number PB-PG-1207-14119). The views expressed are those of the authors and not necessarily those of the NHS, the NIHR or the Department of Health.

Clinical Trial: ISRCTN89683704

Program Number: 2624

Presentation Time: 9:45 AM - 10:00 AM

Protective effects of JNK inhibition in retinal ganglion cells and in retinal ischemia/reperfusion injury

Byung-Jin Kim¹, Yang Liu¹, Sean Silverman¹, Robert J. Wordinger¹, Richard T. Libby², Iok-Hou Pang¹, Abbot F. Clark¹. ¹The North Texas Eye Research Institute, Univ of North Texas Hlth Sci Ctr, Fort Worth, TX; ²Department of Ophthalmology, University of Rochester Medical Center, Rochester, NY.

Purpose: The JNK (cJun N-terminal kinase) signaling pathway plays an important role in neuronal pathophysiology. Using JNK inhibitor SP600125, we examined involvement of the JNK pathway in cultured retinal ganglion cell (RGC) death and in mouse retinal ischemia/reperfusion (I/R) injury.

Methods: The in vitro effects of several JNK inhibitors were evaluated in cultured adult rat retinal cells enriched in RGCs. Cytotoxicity was induced by glutamate or trophic factor withdrawal. Survival of RGCs was assessed by counting Thy-1 positive cells. Retinal I/R was induced in female C57BL/6J mice by raising the intraocular pressure to 120 mmHg for 60 min followed by reperfusion. SP600125 (5, 15, 30 mg/kg) was administered intraperitoneally once daily for 28 days starting at 2 h prior to injury. At various time points after I/R, phosphorylation of JNK and cJun was examined by immunoblotting of retinal proteins. The thickness of retinal layers and cell numbers in the ganglion cell layer (GCL) were examined using H&E stained retinal cross sections, and retinal function was measured by scotopic ERG.

Results: SP600125 dose-dependently and significantly ($p < 0.05$) protected against glutamate- and trophic factor withdrawal-induced cultured RGC cell death. In the I/R model, phosphorylation of JNK and cJun in the retina was significantly ($p < 0.05$) increased at 1 h after injury. I/R injury significantly ($p < 0.05$) decreased the thickness of retinal layers, including the whole retina ($-23.2 \pm 5.7\%$), inner plexiform layer ($-38.0 \pm 6.7\%$), and inner nuclear layer ($-25.1 \pm 7.4\%$) and cell numbers in the GCL ($-30.0 \pm 5.6\%$). Importantly, administration of all three doses of SP600125 protected against all these degenerative morphological changes ($p < 0.05$). In addition, SP600125 significantly ($p < 0.05$) protected against I/R-induced reduction in b-wave amplitude at 3, 7, 14, 21 and 28 days after injury.

Conclusions: Our results demonstrated involvement of the JNK pathway in retinal degeneration in both in vitro and in vivo models and suggest that JNK inhibitors may be a useful therapeutic strategy for neuroprotection in the retina.

Commercial Relationships: Byung-Jin Kim, None; Yang Liu, None; Sean Silverman, None; Robert J. Wordinger, None; Richard T. Libby, None; Iok-Hou Pang, None; Abbot F. Clark, Alcon Research, Ltd. (F)

Support: DOD (Department of Defense) grant, W81XWH-10-2-0003

Program Number: 2625

Presentation Time: 10:00 AM - 10:15 AM

Topical administration of MRZ-99030, a β -amyloid aggregation modulator, protects retinal ganglion cells and axons in a rodent model of glaucoma

Andreas Gravius¹, Kai-Uwe Klein¹, Leonard A. Levin², Wolf Lagreze³, Nico Wegener¹, Wojciech Danysz¹. ¹Merz Pharmaceuticals, Frankfurt, Germany; ²McGill University, Montreal, QC, Canada; ³University of Freiburg, Freiburg, Germany.

Purpose: Topical administration of MRZ-99030, a β -amyloid aggregation modulator, protects retinal ganglion cells and axons in a rodent model of glaucoma
MRZ-99030 is a small molecule with neuroprotective activity via

modulation of β -amyloid (A β) aggregation. This compound inhibits A β -induced toxicity in multiple in vitro and in vivo models and is currently under Phase I clinical development. The neurotoxic peptide A β has recently been implicated in retinal ganglion cell (RGC) apoptosis in glaucoma, with evidence of caspase-3-mediated abnormal amyloid precursor protein processing, increased expression of A β in RGCs and optic nerves in experimental glaucoma and increased A β in the ganglion cell layer of glaucoma patients. Some forms of aggregated A β are able to induce significant RGC apoptosis in vivo and in vitro. Interestingly, it has been shown that targeting different components of the A β formation and aggregation pathway can effectively reduce glaucomatous RGC apoptosis in vivo and therefore raises the possibility of neuroprotection in glaucoma. Based on these findings, we assessed the neuroprotective potential of MRZ-99030 after topical administration in a commonly used rodent model of glaucoma

Methods: Ocular hypertension was induced in Brown Norway rats by two injections of hypertonic saline into the episcleral veins. This results in increase of intraocular pressure, with progressive loss of RGCs and axonal degeneration. Topical administration of MRZ-99030 3 times daily for 6 weeks, followed by counting of previously retrograde-labelled RGCs in whole-mounts and assessment of optic nerve sections. All experiments were done with the identity of the topical solution masked. In addition, retina concentrations of MRZ-99030 were assessed in rats and monkeys for evaluation of PK/PD relationship.

Results: MRZ-99030 dose-dependently and significantly reduced loss of RGCs compared to vehicle control with a maximal effect size of 95%. Also axonal degeneration was significantly decreased in drug-treated eyes. Pharmacokinetic studies revealed sufficient retina concentrations of MRZ-99030 above in vitro affinity in both rats and monkeys.

Conclusions: Modulation of A β aggregation may be a promising avenue for neuroprotection and axoprotection in glaucoma.

Commercial Relationships: Andreas Gravius, Merz Pharmaceuticals (E); Kai-Uwe Klein, Merz Pharmaceuticals GmbH (E); Leonard A. Levin, Quark (C), Inotek (C), Merz (C), Wisconsin Alumni Research Foundation (P), Cytodefense (I), Teva (C), Allergan (C); Wolf Lagreze, Merz (C), Allergan (C); Nico Wegener, Merz Pharmaceuticals (E); Wojciech Danysz, Merz Pharmaceuticals (E)

304 Perimetry I

Tuesday, May 07, 2013 8:30 AM-10:15 AM

6E Paper Session

Program #/Board # Range: 2630-2636

Organizing Section: Glaucoma

Program Number: 2630

Presentation Time: 8:30 AM - 8:45 AM

Visual fields in patients with glaucoma: variability, outliers, and the power to detect change

Paul H. Artes^{1,2}, Neil O'Leary¹, Balwantray C. Chauhan^{1,2}, Marcelo T. Nicolela^{1,2}, Lesya Shuba^{1,2}, Paul E. Rafuse^{1,2}. ¹Ophthalmology and Visual Sciences, Dalhousie University, Halifax, NS, Canada; ²Nova Scotia Eye Care Centre, Capital Health, Halifax, NS, Canada.

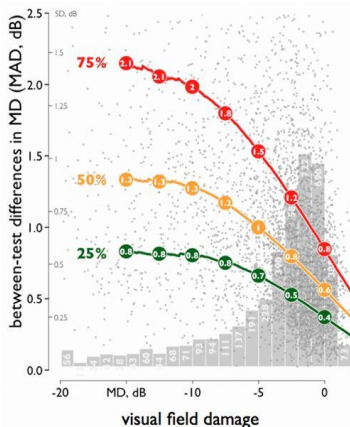
Purpose: To report on visual field variability, outliers, and the ability to detect change over time in a large dataset of patients followed at the QEII Eye Care Centre in Halifax, Nova Scotia.

Methods: Visual field series (SITA Standard 24-2 test, Humphrey Field Analyzer) were analyzed from all patients who had undergone 5+ examinations over 2+ years. Variability over time was estimated

by the median absolute deviation (MAD) of differences in Mean Deviation (MD) between consecutive tests, and related to the median MD of the series using quantile regression. Outliers were determined with MM-estimation, a regression technique that iteratively determines "robustness weights" to reduce the impact of suspect observations on the estimated rate of change and its statistical significance. We classified observations with weights <0.5, <0.05, and <0.001 as suspect, probable, and definite outliers.

Results: Visual field series were analyzed from 2,200 patients (4,160 eyes; n=36,600 exams; median age [interquartile range, IQR], 66 [57,74] years; MD, -2.4 [-5.3, -0.9] dB; follow-up, 7 [5, 10] years; 8 [6, 11] exams). Suspect, probable, and definite outliers were present in 13%, 7%, and 5% of visual field series. On average, the MD difference between consecutive tests was 0.6 dB in eyes with near-normal visual fields (median MD of series, 0.0 dB) and 1.3 dB in eyes with moderately advanced damage (median MD, -10.0 dB, Fig. 1). However, the within-series variability varied more than 2-fold between patients, from 0.8 dB (25th percentile) to 2.0 dB (75th percentile).

Conclusions: Visual field series from patients followed in clinical practice often contain outliers which violate the assumptions of ordinary-least-squares (OLS) regression. Robust regression techniques should be used routinely to estimate rates of change over time and to alert clinicians to suspect data. Variability over time varies more than 2-fold between patients with similar visual field damage, underscoring the importance of determining the significance of change based on individualized rather than population-based criteria.



Quantile regression curves of visual field variability in a clinical population of patients with glaucoma.

Commercial Relationships: Paul H. Artes, Heidelberg Engineering, Germany (C), Haag-Streit AG, Switzerland (C), Carl Zeiss Meditec, Germany (C), Optovue Inc, CA, USA (C), Peridata GmbH, Germany (F); Neil O'Leary, None; Balwantray C. Chauhan, None; Marcelo T. Nicolela, Allergan Inc (F), Alcon (F); Lesya Shuba, None; Paul E. Rafuse, None
Support: Glaucoma Research Foundation, San Francisco (PHA); Canadian Institutes of Health Research MOP-11357 (BCC)

Program Number: 2631

Presentation Time: 8:45 AM - 9:00 AM

Enhancement of a Risk Calculator to Assess Rates of Visual Field Progression in Treated Glaucoma Patients using Topographic Analysis

Rafael L. Furlanetto^{1,2}, C. Gustavo De Moraes¹, Anastasia Slobodnick³, Jeffrey M. Liebmann^{1,3}, Robert Ritch^{1,4}. ¹Einhorn

Clinical Research Center, New York Eye and Ear Infirmary, New York, NY; ²Department of Ophthalmology, Federal University of Sao Paulo, Sao Paulo, Brazil; ³New York University School of Medicine, New York, NY; ⁴Department of Ophthalmology, New York Medical College, Valhalla, NY.

Purpose: We recently developed and validated a model to objectively predict rates of visual field (VF) progression in patients with treated glaucoma. Despite its good performance in predicting final mean deviation (MD), the model does not take into account the localized nature of glaucomatous disease and progression, and hence is unable to predict sectorial VF deterioration. We aimed to enhance our prediction model by adding VF topographical information and validate it in a subset of glaucoma patients.

Methods: Data from 367 eyes with treated open-angle glaucoma (reference population) was used to develop the topographic model. All patients had at least 8 reliable VF SITA-Standard tests. Pointwise linear regression analysis was used to calculate the global and localized rates of VF sensitivity change. For VF topographic analysis, we used 6 VF sectors from the Garway-Heath (GH) structure-function map. Multivariable analysis, adjusted for follow-up time, was performed including known risk factors for glaucomatous VF progression. For each VF sector, we obtained one equation to predict sectorial rates of VF progression (decibels [dB]/year). To validate the model, each equation was tested on an independent validation population (50 eyes, 50 glaucoma patients) with similar characteristics as the reference population. Our outcome measures were the difference and correlation between predicted and observed rates of progression for each GH VF sector.

Results: There was a moderate correlation between predicted and observed topographic rates of progression (Table 1). The mean (95%CI) difference between observed and predicted values were -0.379 (-0.3092 to 0.158), 0.2247 (0.026 to 0.4234), 0.00494 (-0.1681 to 0.1780), 0.2851 (0.1271 to 0.4431), 0.1996 (0.04488 to 0.3544) and 0.05057 (-0.08542 to 0.1866) in the superior, superior-nasal, central, temporal, inferior-nasal and inferior sectors, respectively (all $r \geq 0.40$; $P < 0.05$). The parameter estimates of each variable differed based on the VF sector (Table 2).

Conclusions: Our enhanced prediction model is accurate in estimating glaucomatous progression in different VF sectors. This model may be helpful for clinicians in assessing areas of greater risk of progression and estimating the rate of progression in each VF sector as opposed to global indices.

Table 1: Calibration and Correlation Between Predicted and Observed Topographic Rates of Progression

Garway-Heath VF Sector	Calibration*			Spearman's Correlation Coefficient (r)
	< 10%	< 20%	< 50%	
Superior	0.22	0.22	0.46	0.412
Superior-Nasal	0.54	0.6	0.74	0.521
Central	0.4	0.5	0.62	0.4
Temporal	0.5	0.54	0.62	0.504
Inferior-Nasal	0.54	0.56	0.72	0.457
Inferior	0.48	0.5	0.64	0.429

VF=visual field

*Percentage difference between predicted and observed slopes.

Table 2: Risk Factor Beta-Coefficients for Each Visual Field (VF) Sector

Garway-Heath VF Sector	Risk Factors for VF Progression								Weighted Initial Damage	
	XFG	β-PPA	DH	Mean IOP	Peak IOP	CCT	MD 1 st VF	Time		Age
Superior	-0.270	0.094	-0.227	-0.002	-0.031	0.001	-0.022	0.044	-0.004	-0.013
Superior-Nasal	-0.334	-0.048	-0.438	0.004	-0.039	0.000	-0.046	0.048	-0.006	-0.121
Central	-0.103	-0.022	-0.213	-0.021	-0.005	0.001	-0.002	0.043	-0.007	0.039
Temporal	-0.184	0.032	0.080	-0.003	-0.017	0.000	0.001	0.018	-0.008	0.090
Inferior-Nasal	-0.166	-0.013	-0.312	-0.025	-0.021	0.000	-0.020	0.045	-0.003	-0.127
Inferior	-0.178	-0.050	-0.192	-0.018	-0.024	0.000	-0.011	0.025	-0.003	-0.051

XFG=exfoliative glaucoma; PPA=peripapillary atrophy; DH=disc hemorrhage; IOP=intraocular pressure; CCT=central corneal thickness; MD=mean deviation

Commercial Relationships: Rafael L. Furlanetto, None; C. Gustavo De Moraes, None; Anastasia Slobodnick, None; Jeffrey M. Liebmann, Alcon Laboratories, Inc. (C), Allergan, Inc. (C), Allergan, Inc. (F), Carl Zeiss Meditech, Inc (F), Heidelberg Engineering, GmbH (F), Topcon Medical Systems, Inc. (F), National Eye Institute (F), New York Glaucoma Research Institute (F), SOLX, Inc. (C), Bausch & Lomb, Inc (C), Diopsys, Inc. (C), Diopsys, Inc. (F), Merz, Inc. (C), Glaukos, Inc. (C), Quark, Inc. (C); **Robert Ritch**, None

Support: Supported by the James Cox Chambers Research Fund of the New York Eye and Ear Infirmary, New York, NY; and the Edith C. Blum Foundation, New York, NY.

Program Number: 2632

Presentation Time: 9:00 AM - 9:15 AM

Key predictors of visual field test reliability

Jason Ho¹, Sally Ameen¹, Laura Crawley¹, Eduardo M. Normando^{1,2}, M Francesca Cordeiro^{1,2}, Philip A. Bloom^{1,3}, Faisal Ahmed¹.

¹Glaucoma Research Unit, Western Eye Hospital, London, United Kingdom; ²Glaucoma & Retinal Degeneration Research Group, UCL Institute of Ophthalmology, London, United Kingdom; ³Ophthalmology Unit, The Hillingdon Hospital, London, United Kingdom.

Purpose: Patient reliability is of key importance in helping clinicians interpret visual fields (VF) for accurate glaucoma diagnosis and progression monitoring.

We investigate which patient factors predict poor VF test reliability according to standard indices of Fixation loss (FL), False-negatives (FN) and False-positives (FP).

Methods: We conducted a 14-year (1998-2012) retrospective review of 34304 Humphrey 24-2 visual field tests from 8532 patients at a single tertiary referral centre. Corresponding clinical data was collated from a Medisoft database. Each VF test was analysed individually.

Standard criteria were used to assess VF test reliability: FL<25%, FP<25% and FN<33%. Multivariate binomial logistic regression analysis determined which clinical factors correlate with VF reliability. Subgroup analysis was performed for: (i) patients with >3 VF tests and (ii) VF tests with recorded visual acuity data.

Results: 26.25% of VFs were unreliable. Mean patient age was 65. Standard reliability indices (FL, FN, FP) independently demonstrate good correlation (p=0.00).

Age, greater mean deviation, an established glaucoma diagnosis, using >1 glaucoma medication and having fewer prior VF tests, all negatively correlate with the likelihood of VF test reliability (p<0.03).

VF tests performed at shorter intervals are less likely to be reliable (Odds Ratio 1.03, p=0.015). Sex, presence of cataract and ARMD are not significant predictors. Worse visual acuity is independently associated with more unreliable VF tests.

Conclusions: Older patients with worse vision, more advanced

glaucoma and fewer prior VF tests are less likely to yield reliable VF results and testing at shorter intervals does not necessarily increase reliability.

These factors can aid clinical decisions to improve resource utilisation of visual field tests in busy glaucoma practices.

Commercial Relationships: Jason Ho, None; Sally Ameen, None; Laura Crawley, None; Eduardo M. Normando, None; M Francesca Cordeiro, application (P); Philip A. Bloom, International Glaucoma Association (S), UKISCRS (S), Ophthalmology Section, RSM (S); Faisal Ahmed, None

Program Number: 2633

Presentation Time: 9:15 AM - 9:30 AM

A New Index to Monitor Central Field Progression in Glaucoma

Gustavo De Moraes^{1,2}, Rafael L. Furlanetto^{1,2}, Jeffrey M. Liebmann^{1,2}, Robert Ritch^{1,2}. ¹Ophthalmology, New York Eye and Ear Infirmary, New York, NY; ²Ophthalmology, New York University Medical Center, New York, NY.

Purpose: The visual field index (VFI) summarizes global visual field (VF) data and was developed to monitor glaucoma progression using 24-2 SITA fields.[1] We applied the same principles and statistical procedures to develop a new parameter, the central field index (CFI), to monitor 10-2 VF progression.

Methods: The CFI was developed by calculating age-corrected defect depth at test points obtained during 10-2 examinations. The sensitivities at these points were scored as percentages similar to the method described for the VFI: 100 - [(| total deviation | ÷ age-corrected normal threshold) x 100].[1] Based on a published estimate of the spatial magnification present in the occipital cortex,[2] a weighting procedure was performed in which the 4 central-most points were allotted a greater weight (x3.5) than the remaining 64 points (x1.5). Therefore, the CFI is the mean of all weighted scores in percent. To validate this, we performed mixed linear model testing for the association between the CFI and various known risk factors for glaucoma progression in a sample of 176 eyes (142 patients) with established glaucoma and at least 5 10-2 VFs. To determine whether the CFI was affected by cataract - as is known to occur with mean deviation (MD) - we conducted a pilot evaluation comparing rates of CFI change (%/yr) in 3 groups of patients: 1) eyes with cataract, 2) pseudophakic eyes, and 3) eyes in which cataract surgery was performed in the middle of the series.

Results: We were able to generate CFI values for the entire sample based on the description above. The mean rate of CFI change of the entire sample was -1.35%/yr (95% CI, -1.66 to -1.05 %/yr). Risk factors for faster CFI progression were worse baseline CFI (P<0.001), older age (P=0.014), and higher peak IOP (P=0.050). There was no significant difference in slopes of CFI progression among the 3 groups (P=0.98) whereas MD slopes differed significantly (P=0.001).

Conclusions: We have developed and validated a new index to monitor central field progression that is minimally affected by the presence or removal of cataract and which correlates significantly with known risk factors for glaucoma progression. This has important implications for glaucoma management.

1. Bengtsson B, Heijl A. Am J Ophthalmol. 2008.

2. Levi DM, Klein SA, Aitsebaumo AP. Vision Res 1985.

Commercial Relationships: Gustavo De Moraes, None; Rafael L. Furlanetto, None; Jeffrey M. Liebmann, Alcon Laboratories, Inc. (C), Allergan, Inc. (C), Allergan, Inc. (F), Carl Zeiss Meditech, Inc (F), Heidelberg Engineering, GmbH (F), Topcon Medical Systems, Inc. (F), National Eye Institute (F), New York Glaucoma Research Institute (F), SOLX, Inc. (C), Bausch & Lomb, Inc (C), Diopsys, Inc.

ARVO 2013 Annual Meeting Abstracts by Scientific Section/Group – Glaucoma

(C), Diopsys, Inc. (F), Merz, Inc. (C), Glaukos, Inc. (C), Quark, Inc. (C); **Robert Ritch**, None

Support: John and Dorothy Roberts Research Fund of the New York Glaucoma Research Institute, New York, NY; the James Cox Chambers Research Fund of the New York Eye and Ear Infirmary; and the Edith C. Blum Foundation, New York, NY.

Program Number: 2634

Presentation Time: 9:30 AM - 9:45 AM

Determinants of Visual Field Reliability

Pradeep Y. Ramulu, Michael V. Boland, Jiangxia Wang, Li Xu, Jamie Brown, David S. Friedman. Ophthalmology, Wilmer Eye Inst/Johns Hopkins, Baltimore, MD.

Purpose: To determine the influence of visual field (VF) test parameters on VF reliability.

Methods: Reliability was determined for each VF in eyes with at least 5 VF tests. Reliability was judged by: (1) the difference (residual) between the measured (actual) and predicted VF MD, and (2) the presence of a residual MD more than 2 standard deviations outside the norm for the studied eye. Predicted VF MD was calculated in models incorporating baseline MD, MD of each study period VF, time from baseline VF date, and the number of annual VFs. Studied predictors of VF reliability included percentage of false negatives, false positives and fixation losses, test duration, time of VF testing, day of VF testing, and season of year.

Results: 1,778 eyes in 1,047 patients were examined, and mean duration between the first and last VFs was 5.1 years. False positives were associated with a greater measured MD than predicted (+1.05 dB/10% false positives, $p < 0.001$) while false negatives were associated with a lower measured MD than predicted (-0.40 dB/10% false negatives, $p < 0.001$). Fixations losses were not associated with residual MD (+0.02 dB/10% fixation losses, $p = 0.07$), while longer test duration was associated with a lower measured MD than predicted (-0.34 dB/extra minute of testing, $p < 0.001$). Residual MD also increased in winter as compared to non-winter months ($p \leq 0.02$), but did not vary by time of day or day of week ($p > 0.05$). The odds of a VF demonstrating a residual MD at least two standard deviations outside the norm for the studied eye increased with greater test duration (Odds Ratio [OR]=2.07, $p < 0.001$), false positive percentage (OR=1.26/10% increase, $p = 0.004$), and false negative percentage (OR=1.51/10% increase, $p < 0.001$), but was not associated with the percentage of fixation losses, time of day, day of week, or season of year ($p > 0.1$ for all).

Conclusions: False positives, false negatives and test duration are the most significant predictors of VF reliability, and should be the primary clinical criteria for determining whether or not a VF result can be considered reliable. Fixation losses do not significantly predict VF reliability independent of other factors and may not have significant meaning in determining whether a VF result can be trusted. False positives are associated with the greatest difference between measured and predicted VF MD, and even modest amounts of false positives should be recognized as potentially producing significant errors.

Commercial Relationships: Pradeep Y. Ramulu, None; Michael V. Boland, None; Jiangxia Wang, None; Li Xu, None; Jamie Brown, None; David S. Friedman, Alcon (C), Bausch & Lomb (C), Merck (C), QLT, Inc (C), Allergan (C), Nidek (C)

Support: K23018595, Research to Prevent Blindness Special Scholar Grant, Doris Duke Foundation

Program Number: 2635

Presentation Time: 9:45 AM - 10:00 AM

Rates of Glaucomatous Visual Field Change in a Large Clinical Population

Balwantray C. Chauhan, Paul E. Rafuse, Lesya Shuba, Marcelo T. Nicoleta, Paul H. Artes. Ophthalmology & Visual Sciences, Dalhousie University, Halifax, NS, Canada.

Purpose: To determine the rate of glaucomatous visual field change in > 2,000 patients followed clinically in a tertiary eye care centre.

Methods: All patients with glaucoma or suspected glaucoma, with ≥ 5 standard automated perimetry exams (24-2 SITA) and ≥ 2 years follow-up were included in the analysis. Rates of Mean Deviation (MD) change were derived in one randomly selected eye with robust linear regression analysis. The proportion of patients with “fast” (worse than -1 dB/yr) and “catastrophic” (worse than -2 dB/yr) progression was computed as well as the relationship between baseline MD and baseline age on MD rate. To determine whether MD rate statistics depended on the number of exams, the sample was divided into quintiles based on an approximately equal number of exams to ensure the MD rate statistics were independent.

Results: There were 2,198 patients in this study with a median (interquartile range, IQR) baseline age of 65.7 (57.0, 74.0) years, baseline MD of -2.4 (-5.3, -0.84) dB and follow-up of 7.2 (4.9, 10.2) years with 8 (6, 11) exams. The mean (SD) and median (IQR) MD rates were -0.16 (0.63) dB/yr and -0.06 (-0.31, 0.11) dB/yr respectively. There were 124 (5.6%) patients with fast and 33 (1.5%) patients with catastrophic progression (Figure). Baseline MD correlated poorly with MD rate ($r = -0.23$, $P = 0.27$), however, advancing baseline age was statistically significantly associated with a worse MD rate ($r = -0.20$, $P < 0.01$). MD rate statistics depended on the number of examinations, with the proportion of fast progressors varying from 2.4 to 9.2% and catastrophic progressors from 0.2 to 3.9% (Table). The median MD rate worsened with an increasing number of exams.

Conclusions: (1) There was a significantly stronger association between advancing age and worse MD rate compared to that between baseline MD and MD rate; (2) MD rate statistics are influenced by the number of exams, with a lower exam frequency yielding a higher proportion of patients with faster progression.

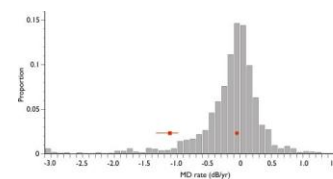


Figure. MD rate distribution in 2,198 patients with ≥ 5 exams. Red circle and squares represent the median and 5th percentile of the distribution, respectively with their 95% confidence intervals.

Table. MD rate statistics for study population divided into quintiles

Quintile	Number of patients	Number of exams	Median MD rate (dB/yr)	Fast progressors (%)	Catastrophic progressors (%)
1	436	5	-0.03	9.2	3.9
2	349	6	-0.05	7.2	2.6
3	490	7.8	-0.03	5.7	0.8
4	466	9.11	-0.06	4.3	0.4
5	457	>12	-0.11	2.4	0.2

Commercial Relationships: Balwantray C. Chauhan, None; Paul E. Rafuse, None; Lesya Shuba, None; Marcelo T. Nicoleta,

Allergan Inc (F), Alcon (F); Paul H. Artes, Heidelberg Engineering, Germany (C), Haag-Streit AG, Switzerland (C), Carl Zeiss Meditec, Germany (C), Optovue Inc, CA, USA (C), Peridata GmbH, Germany (F)

Support: Canadian Institutes of Health Research MOP-11357

Program Number: 2636

Presentation Time: 10:00 AM - 10:15 AM

The Effect of Stimulus Size on the Relation between Sensitivity and Variability in Perimetry

Stuart K. Gardiner¹, Deborah Goren¹, Casie Goldman¹, William H. Swanson², Shaban Demirel¹. ¹Discoveries In Sight Laboratories, Devers Eye Institute, Portland, OR; ²School of Optometry, Indiana University, Bloomington, IN.

Purpose: Variability increases as sensitivity declines in clinical automated perimetry, complicating analysis and interpretation of results. It has been suggested that using Size V stimuli reduces variability, steepening Frequency-of-Seeing (FOS) curves by summing responses from more retinal ganglion cells (RGCs). However, this has largely been assessed indirectly, using clinical perimetry to estimate sensitivity and test-retest variability. These are influenced by the algorithm used, not just by physiologic variability. In this study, we measure FOS curves in damaged areas, examining the effect of stimulus size.

Methods: FOS curves were recorded at four locations in 16 subjects with moderate to advanced glaucoma. The method of constant stimuli was used, with 35 presentations at each of 7 contrasts, on an Octopus perimeter controlled using the Open Perimetry Interface. The false positive rate was estimated based on 25 catch trials. The false negative rate was assumed to be 5%. A cumulative Gaussian curve was fit to the response probabilities at each location, with two free parameters: mean (50% detection, “sensitivity”) and standard deviation (SD, “variability”). This was repeated using Size III and Size V stimuli. SD was regressed against sensitivity using a generalized estimating equation (GEE) model to account for intra-subject correlations.

Results: Sensitivities were higher for Size V stimuli, $p < 0.001$. Plots of variability against sensitivity were well-described by a linear relation. With SD & sensitivity (Sens) expressed in dB, for Size III stimuli $SD = 10.02 - 0.32 * Sens$ ($R^2 = 0.73$), and for Size V stimuli $SD = 10.84 - 0.33 * Sens$ ($R^2 = 0.67$). Combining data, variability for a given sensitivity did not differ significantly between stimulus sizes III and V ($p = 0.105$, GEE regression).

Conclusions: Testing the same location in a subject’s field with Size V stimuli instead of Size III increases sensitivity and hence decreases variability. However for a given sensitivity, variability appears constant between these two stimulus sizes. This is consistent with both sensitivity and variability being determined solely by the number of remaining RGCs at that location. Modifying the stimulus size while keeping contrast fixed, instead of modifying contrast for a fixed stimulus size, could result in variability being more constant across disease stages in glaucoma.

Commercial Relationships: Stuart K. Gardiner, Allergan (R); Deborah Goren, None; Casie Goldman, None; William H. Swanson, None; Shaban Demirel, Carl Zeiss Meditec (F), Heidelberg Engineering (R), Heidelberg Engineering (F)
Support: NIH Grant R01 EY020922

326 Biomechanics

Tuesday, May 07, 2013 11:00 AM-12:45 PM
6B Paper Session

Program #/Board # Range: 3154-3160
Organizing Section: Glaucoma

Program Number: 3154

Presentation Time: 11:00 AM - 11:15 AM

Temporal Relationships in Structural Changes of the Optic Nerve Head and Macula in Experimental Glaucoma in Non-Human Primates

Nimesh B. Patel, Ronald S. Harwerth. College of Optometry, University of Houston, Houston, TX.

Purpose: Assessment of structural changes in the retina and optic nerve head (ONH) with spectral domain optical coherence tomography (SD OCT) is important for the diagnosis and management of glaucoma. The present study was undertaken to investigate the temporal relationships of structural changes using a model of laser-induced glaucoma in rhesus monkeys, which parallels structural and functional defects in patients.

Methods: Unilateral Argon laser treatments were used to scar the trabecular meshwork and elevate the intraocular pressures in six monkeys. SD OCT transverse retinal scaling was calculated using a three surface schematic eye that incorporated individual ocular biometry measures. Radial and raster scans centered on the ONH and raster scans centered on the macula were used for morphological analysis of total retinal thickness and ONH cupping. Retinal nerve fiber layer (RNFL) area measures, both with and without removal of major retinal vascular, were determined from elliptical scan paths 550 μ m from the ONH rim margin.

Results: The earliest changes were in the ONH parameters. The maximum cup depth, increased linearly with increase in cumulative IOP ($R^2 = 0.09$, $p = 0.03$). In addition, an exponential decrease in neuroretinal rim (NRR) volume also occurred early ($R^2 = 0.78$, $p < 0.01$). The decrease in NRR volume occurred prior to a change in global RNFL area, and the relationship was best described by an exponential model ($R^2 = 0.64$, $p < 0.01$). The percentage vascular contribution to the RNFL increased with decreasing area ($R^2 = 0.64$, $p < 0.01$), but the overall vessel area decreased with increasing stages of glaucoma ($R^2 = 0.33$, $p < 0.01$). A later decrease in macular volume in a central 3 mm circular zone was linearly correlated with the temporal RNFL area ($R^2 = 0.61$, $p < 0.01$).

Conclusions: Early structural changes in the ONH morphology were correlated to the cumulative IOP, which supports a biomechanical paradigm for the initial neuronal damage in glaucoma. Subsequent structural neuropathologic alterations represent a cascade from NRR volume to RNFL area and macular thinning. These results suggest that different aspects of neuropathy should be assessed with advancing stages in the progression of glaucoma.

Commercial Relationships: Nimesh B. Patel, None; Ronald S. Harwerth, None
Support: NIH Grant R01 EY001139, K23 EY021761, P30 EY007551

Program Number: 3155

Presentation Time: 11:15 AM - 11:30 AM

Racial variation in the structure of the lamina cribrosa and sclera within 3-D fluorescent reconstructed optic nerve heads (ONH) from normal human donor tissue

Christopher A. Girkin¹, Massimo A. Fazio¹, Hongli Yang², Lan Wang¹, Brandon Smith¹, Chad C. Cheetham¹, Claude F. Burgoyne², J Crawford C. Downs¹. ¹Ophthalmology, Univ of Alabama at Birmingham, Birmingham, AL; ²Devers Eye Institute, Portland, OR.

Purpose: To examine associations between morphometric variations in the structure of the lamina cribrosa and sclera with age and race [African descent (AD), European Descent (ED)] within histologic 3-D fluorescent reconstructions of normal human donor ONHs.

Methods: The trephinated ONH and peripapillary sclera from 26 normal human donor eyes with clinical records fixed at physiologic IOP were serial sectioned using an automated microtome-based system that yielded serial fluorescent images of the block face as we cut through the ONH at 1 μ m section thickness (Downs JC et al, ISER 2010). We aligned and stacked the autofluorescent images to create a 3-D ONH reconstruction with a voxel resolution of 1x1x1 μ m and

then delineated the ONH and peripapillary sclera according to guidelines set for histomorphometric ONH delineations (Downs, Yang, et al. IOVS 2007). Associations with age and race and significant interactions were determined for key morphometric parameters using mixed effects models with generalized estimating equations.

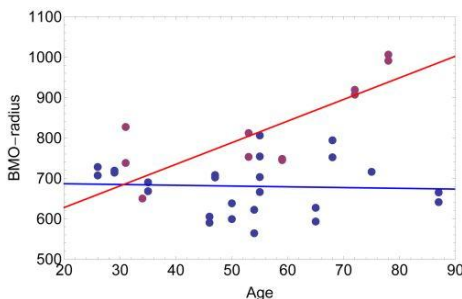
Results: In adjusted models (table), the peripapillary sclera ($p=0.0032$) and lamina cribrosa ($p=0.00026$) were thinner in eyes from AD donors, which also exhibited a deeper posterior lamina insertion (PLI) (p -value: 0.026). There was significant age-associated enlargement in Bruch's membrane opening (BMO) along with all neural canal landmarks within AD group (Figure).

Conclusions: Significant variations in ONH ultrastructure associated with age and across racial groups are present, which are likely to result in different biomechanical behavior with age and between racial groups.

Table: Beta Coefficients and associated p-values from mixed effects models

	Beta Coefficient	p-value
Laminar Thickness		
Age	0.625	0.14
Race (ED)	44.8	0.00026
Scleral Thickness		
Age	0.024	0.997
Race (ED)	100.8	0.0032
BMO - Radius		
Age	4.96	0.013
Race (ED)	149.8	0.252
Age x Race	-5.22	0.013
ASCO - Radius		
Age	4.38	0.015
Race (ED)	128.1	0.274
Age x Race	-4.63	0.019
PLI		
Age	1.25	0.112
Race (ED)	74.3	0.026

Figure: Scatter plot of BMO radius and age across racial strata (blue line – ED, Red line – AD).



Commercial Relationships: Christopher A. Girkin, SOLX (F), Heidelberg Engineering (F); Massimo A. Fazio, None; Hongli Yang, None; Lan Wang, None; Brandon Smith, None; Chad C. Cheetham, None; Claude F. Burgoyne, Heidelberg Engineering (F), Heidelberg Engineering (C); J Crawford C. Downs, None
Support: NIH Grants: R01EY019333-01, R01 EY018926-01, Research to Prevent Blindness, EyeSight Foundation of Alabama

Program Number: 3156

Presentation Time: 11:30 AM - 11:45 AM

Racial Differences in Mechanical Strain in the Posterior Human Sclera

Massimo A. Fazio^{1,2}, Rafael Grytz¹, Luigi Bruno², Jeffrey S. Morris³, Christopher A. Girkin², J Crawford C. Downs². ¹Ophthalmology, The University of Alabama in Birmingham, Birmingham, AL;

²Mechanical Engineering, University of Calabria, Cosenza, Italy;

³Department of Biostatistics, The University of Texas MD Anderson Cancer Center, Houston, TX.

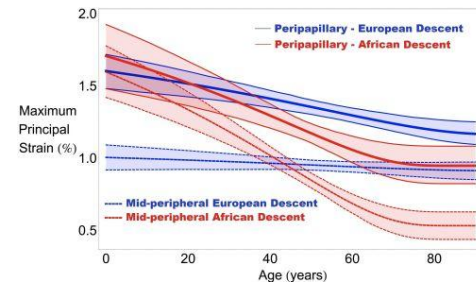
©2013, Copyright by the Association for Research in Vision and Ophthalmology, Inc., all rights reserved. Go to iovs.org to access the version of record. For permission to reproduce any abstract, contact the ARVO Office at arvo@arvo.org.

Purpose: To establish racial differences in the mechanical behavior of peripapillary and mid-peripheral human sclera in normal eyes from donors of African (AD) and European (ED) descent.

Methods: Twenty-nine pairs of normal eyes from human donors (9 AD, 20 ED) aged 0 to 90 years old were mechanically inflated tested within 48 hours post mortem as follows. The intact posterior scleral shell of each eye was pressurized from 5 to 45 mmHg while the full-field three-dimensional displacements of the scleral surface were measured using laser speckle interferometry. Under the assumption of tissue incompressibility, mean maximum principal (tensile) strain was computed within the peripapillary and mid-peripheral regions surrounding the optic nerve head (ONH). The peripapillary and mid-peripheral regions were defined as a ~9 degree-wide-band adjacent to the ONH and the band of equal surface area immediately outside the peripapillary region, respectively.

Results: The posterior sclera stiffened significantly faster with age in both regions of the AD eyes compared to ED donors (Figure; $p<0.01$). The sclera in both regions stiffened significantly with age in the AD eyes, while only peripapillary region stiffened significantly with age in the ED eyes ($p<0.001$).

Conclusions: These results indicate 1) the peripapillary sclera is subjected to significantly higher tensile strain than the mid-peripheral sclera, independent of race, 2) AD eyes showed a more rapid stiffening with age than ED eyes, and 3) while the mid-peripheral region doesn't significantly stiffen with age in the ED eyes, a rapid and significant stiffening of the mid-peripheral sclera is present in the AD eyes. These significant racial differences in scleral biomechanics may contribute to the increased susceptibility of AD persons to glaucoma.



Maximum principal scleral strain plotted by race and age for both the peripapillary and mid-peripheral regions (mean \pm 95% CI). Scleral strains decrease with age in the AD group in both the peripapillary and mid-peripheral regions ($p<0.001$) and at a faster rate than in the ED eyes. Only strains in the peripapillary region exhibited a significant change with age in the ED eyes ($p<0.001$). Maximum principal (tensile) strain was significantly higher in the peripapillary region than in the mid-peripheral region for both groups at all ages ($P<0.001$)

Commercial Relationships: Massimo A. Fazio, None; Rafael Grytz, None; Luigi Bruno, None; Jeffrey S. Morris, None; Christopher A. Girkin, SOLX (F), Heidelberg Engineering (F); J Crawford C. Downs, None
Support: NIH Grants R01-EY18926, R01-EY19333; Legacy Good Samaritan Foundation

Program Number: 3157

Presentation Time: 11:45 AM - 12:00 PM

Peripapillary Sclera (ppS) and Lamina Cribrosa (LC) 3D Strain Mapping in High- and Normal-tension Glaucoma Patients following IOP Lowering by Trabeculectomy (TE)

Michael J. Girard^{1,2}, Nicholas G. Strouthidis^{3,2}. ¹Bioengineering, National University of Singapore, Singapore, Singapore; ²Singapore

Eye Research Institute, Singapore, Singapore; ³Glaucoma Research Unit, NIHR Biomedical Research Centre at Moorfields Eye Hospital NHS Foundation Trust and UCL Institute of Ophthalmology, London, United Kingdom.

Purpose: To experimentally measure and compare ppS and LC strains (deformations) in the eyes of high- and normal-tension glaucoma patients following IOP-lowering by TE.

Methods: 3 high-tension (pre-TE IOP: 27.7 ± 7.2 mmHg; post-TE IOP: 13.3 ± 3.2 mmHg) and 3 normal-tension (pre-TE IOP: 11.7 ± 2.5 mmHg; post-TE IOP: 7.0 ± 2.6 mmHg) glaucoma patients were imaged (1 treated eye per patient) using optical coherence tomography (OCT; Heidelberg Spectralis) (< 5 days) before and (< 5 weeks) after TE. At each imaging session an OCT scan of the ONH was acquired ($384 \times 496 \times 145$ voxels) and averaged 9 times to reduce noise. In each post-TE OCT volume, 4 groups of tissues were manually segmented: the pre-laminar tissue, the choroid, the ppS and the LC. Segmentations were conducted only when tissue was visible as detected from the OCT signal. Full-thickness segmentation of the LC and ppS could not be achieved. Segmented ONHs were meshed and each comprised approximately 50,000 tetrahedrons and 5,000 nodes. For each ONH, a 3D tracking algorithm was applied to both post- and pre-TE OCT volumes to extract IOP-induced 3D displacements (referenced to the plane of Bruch's membrane opening) at the defined nodes. Displacements were filtered, then smoothed to remove noise. 3D strains (1st principal component) were then computed from the displacements and averaged in the ppS and LC for each ONH. Here, strains represent the amount of deformation relief following TE.

Results: Following IOP lowering and for all ONHs, LC strains ($4.2 \pm 3.3\%$) were on average higher than those of the ppS ($1.9 \pm 0.7\%$). No statistical difference was observed when comparing ppS strains from high-tension glaucoma ($2.1 \pm 0.5\%$) to those from normal-tension glaucoma ($1.9 \pm 1.0\%$). Similarly, no statistical difference was observed when comparing LC strains from high-tension glaucoma ($5.1 \pm 4.9\%$) to those from normal-tension glaucoma ($3.3 \pm 1.3\%$).

Conclusions: Our data suggest that TE in normal-tension glaucoma patients can relieve ppS and LC strains of the same order as those relieved in high-tension glaucoma patients. Our data also suggest a wide patient-to-patient variability in ONH biomechanical properties. We believe that in vivo measurements of ppS and LC strains could become powerful predictors of glaucoma progression. More patients are needed to strengthen the outcome of this work.

Commercial Relationships: Michael J. Girard, None; Nicholas G. Strouthidis, None

Support: Singapore Ministry of Education Academic Research Funds Tier 1 (MJAG); NGS acknowledges financial support from the UK Department of Health through the award made by the National Institute for Health Research to Moorfields Eye Hospital NHS Foundation Trust and UCL Institute of Ophthalmology for a Biomedical Research Centre for Ophthalmology. The views expressed in this work are those of the authors and not necessarily those of the UK Department of Health

Program Number: 3158

Presentation Time: 12:00 PM - 12:15 PM

IOP Elevation Reduces the Waviness of the Load Bearing Collagen Fibers in the Lamina Cribrosa

Ian A. Sigal^{1,2}, Jonathan L. Grimm¹, Ning-Jiun Jan^{1,2}, Richard A. Bilonick^{1,3}, Gadi Wollstein^{1,4}, Larry Kagemann^{1,2}, Hiroshi Ishikawa^{1,2}, Joel S. Schuman^{1,2}, Katherine A. Davoli¹, Kira L. Lathrop^{1,2}. ¹Ophthalmology, University of Pittsburgh, Pittsburgh, PA; ²Bioengineering, University of Pittsburgh, Pittsburgh, PA; ³Biostatistics, University of Pittsburgh, Pittsburgh, PA; ⁴McGowan

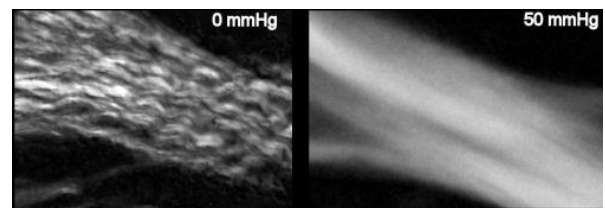
Institute for Regenerative Medicine, University of Pittsburgh, Pittsburgh, PA.

Purpose: Collagen fiber waviness, or crimp, is the primary cause of the nonlinear response of the load-bearing tissues of the eye, and is therefore central to determine the effects of IOP and sensitivity to elevated IOP. Despite the critical importance of fiber crimp in biomechanics, it has not been measured in ocular tissues. Our goal was to measure the crimp of the lamina cribrosa trabeculae and determine how it changes as IOP increases.

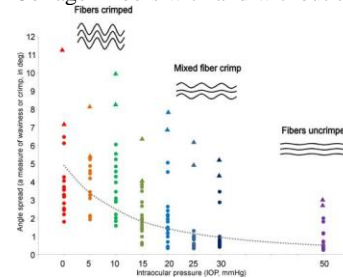
Methods: Sixteen eyes of eight young sheep (<2 years) were obtained from the local abattoir within two hours of sacrifice and kept at 4°C until fixation. Eyes were fixed at 0 (no cannula), 5, 15, 20, 30 or 50 mmHg by infusing 10% formalin through a cannula inserted into the anterior chamber connected to a reservoir. Eyes were then immersed in 10% formalin and IOP maintained for 24 hours. Following fixation the ONH and surrounding sclera were excised and cryosectioned coronally (30µm). Digital photographs were obtained (20x objective, 0.5 NA, 0.5 reducer, Olympus DP26-CU camera, 8 bit greyscale, 0.345µm/pix), stitched into mosaics and were analyzed using custom routines to determine local variations in collagen fiber orientation longitudinal to lamina cribrosa trabeculae as a measure of waviness (Figure 1). A minimum of 14 lamina trabeculae were selected for measurement in each eye, with two of these intentionally of trabeculae suspected to have particularly high crimp.

Results: There was substantial waviness at low IOPs, decreasing with IOP (Figure 2). Very low waviness (angle spread below 1°) first appeared at an IOP of 15 mmHg. Even at an elevated of 30 mmHg some trabeculae still retained moderate waviness (3-4°). An exponential model fit to the log-transformed waviness as a function of IOP demonstrated that as IOP increases there was a significant decrease in waviness ($p < 0.0001$) and in the spread of the waviness itself.

Conclusions: Our results show that the collagen fibers of the lamina trabeculae are substantially crimped at low IOPs. Increases in IOP stretch the fibers, reducing crimp, first in some trabeculae, and eventually in all of them. To the best of our knowledge this is the first report of experimental measurements of crimp in ocular tissues.



Collagen fibers with and without crimp



Waviness as a function of IOP. Each point is a measurement in a trabecula. Deliberate measurements of high crimp are triangles. Dotted line shows the exponential model fit

Commercial Relationships: Ian A. Sigal, None; Jonathan L. Grimm, None; Ning-Jiun Jan, None; Richard A. Bilonick, None; Gadi Wollstein, Allergan (C); Larry Kagemann, None; Hiroshi Ishikawa, None; Joel S. Schuman, Carl Zeiss Meditec, Inc. (P);

Katherine A. Davoli, None; **Kira L. Lathrop**, PCT/US2012/027268 (P)
Support: NIH P30 EY008098; Eye and Ear Foundation (Pittsburgh, PA); Research to Prevent Blindness.

Program Number: 3159

Presentation Time: 12:15 PM - 12:30 PM

IOP Exposure Determines Scleral Shell Strain Changes in Nonhuman Primate (NHP) Experimental Glaucoma

J Crawford C. Downs¹, Massimo A. Fazio¹, Michael J. Girard², Claude F. Burgoyne³. ¹Ophthalmology, University of Alabama at Birmingham, Birmingham, AL; ²Bioengineering, National University of Singapore, Singapore, Singapore; ³Devers Eye Institute, Legacy Research Institute, Portland, OR.

Purpose: To determine the time course of alterations in scleral shell mechanical behavior induced by exposure to chronic IOP elevations.

Methods: Posterior scleral shells from 5 bilaterally normal and 10 unilateral experimental glaucoma NHPs and were pressurized from 5 to 45 mmHg and the resulting full-field, three-dimensional, scleral surface deformations were measured using laser speckle interferometry. Scleral strain (local tissue deformation) was calculated directly from displacements. Maximum principal strain was averaged for a ~15 degree-wide-band adjacent to the ONH, and the relative difference in mean strain was calculated between contralateral eyes and compared with differential cumulative IOP exposure during the study period. The relationship between the difference in scleral strain and the difference in cumulative IOP exposure in contralateral eyes was assessed using statistical models, and the Akaike Information Criterion was used to determine whether a linear or nonlinear functional form provided the best fit of the hypothesized relationship, if present.

Results: Relative differential scleral tensile strain was significantly associated with differential cumulative IOP exposure in contralateral eyes. The linear model showed that relative differential mean posterior scleral tensile strain decreases with increasing differential cumulative IOP exposure ($p=0.035$). However, the quadratic statistical model fit significantly better than the linear model, and revealed a more complex relationship (AIC, $p=0.0196$; Figure).

Conclusions: These results show that scleral remodeling occurs in response to chronic IOP elevation, and the resulting mechanical behavior is dependent on the differential cumulative IOP exposure over time (a dose effect). As differential cumulative IOP exposure increases, the eye with the higher IOP exposure softens initially, resulting in a temporarily higher scleral tensile strains, but then stiffens significantly thereafter to exhibit lower mean tensile strains than the contralateral eye with lower IOP exposure ($p<0.0001$).

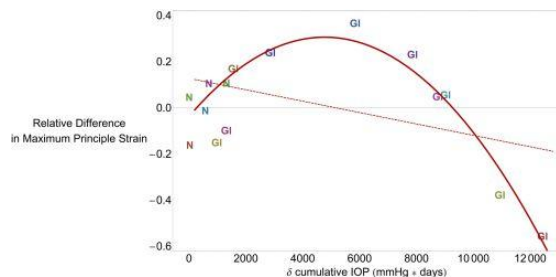


Figure. Linear and nonlinear statistical models showing the significant relationship between relative differential mean posterior scleral tensile strain and differential cumulative IOP exposure in NHPs. N, bilaterally normal NHPs; GI, NHPs in which one eye was exposed to chronically elevated IOP.

Commercial Relationships: **J Crawford C. Downs**, None; **Massimo A. Fazio**, None; **Michael J. Girard**, None; **Claude F. Burgoyne**, Heidelberg Engineering (F), Heidelberg Engineering (C)
Support: NIH Grants EY011610, EY018926, EY019333

Program Number: 3160

Presentation Time: 12:30 PM - 12:45 PM

Optic Nerve Head (ONH) Lamina Cribrosa Insertion Migration and Pialization in Moderate and Severe Non-human Primate (NHP) Experimental Glaucoma (EG)

Hongli Yang¹, Ruojin Ren¹, Galen Williams¹, Howard Lockwood¹, J Crawford C. Downs², Stuart K. Gardiner¹, Claude F. Burgoyne¹.

¹Discoveries in Sight Research Laboratories, Devers Eye Institute and the Legacy Research Institute, Portland, OR; ²Ophthalmology, University of Alabama at Birmingham, Birmingham, AL.

Purpose: To characterize the morphology of the lamina cribrosa insertion into the neural canal wall in moderate to severe (M/S) EG NHP eyes relative to their contralateral controls. M/S EG eye data were then compared to previously reported early EG (EEG) and bilateral normal eye data.

Methods: In 19 NHPs, laser-induced chronic IOP elevations were unilaterally induced until confocal scanning laser ophthalmoscopy demonstrated either the onset (EEG: 9 eyes) or progression of ONH surface change to qualitatively determined moderate to severe levels (M/S EG: 10 eyes). Fellow control eyes and both eyes of 6 bilateral normal NHPs, were classified as normal (N). ONHs from all 25 animals were perfusion fixed, digitally reconstructed and 3D delineated. Anterior Lamina Insertion Position (ALIP), Posterior Lamina Insertion Position (PLIP), Lamina Insertion Length (LIL) were calculated for each ONH. Treatment effects were assessed by generalized estimating equations. Inter-eye differences were pooled into 3 groups (N-N, EEG-N and M/S EG-N) and box-whisker plots generated.

Results: ALIP was significantly posterior in the M/S EG eyes compared with N eyes and EEG eyes (both $p<0.01$, M/S EG: Mean \pm SD = -75 ± 38 μ m, EEG -32 ± 28 μ m, N -20 ± 16 μ m). PLIP was significantly posterior in the M/S EG eyes compared with N eyes ($p=0.01$, M/S EG -29 ± 92 μ m, N 40 ± 23 μ m) but not significantly different from EEG (-2 ± 24 μ m, $p=0.34$). LIL in M/S EG was not different from N eyes although it was significantly increased in EEG eyes compared to N eyes ($p<0.01$). Individual animal inter-eye differences (EG - N eye) for ALIP and PLIP were larger in M/S EG than EEG (Fig 2). LIL increased in all 9 EEG eyes (14-47 μ m), while it was increased only in 5 M/S EG eyes (4-65 μ m) and decreased in 5 M/S EG eyes (15-52 μ m) (relative to their respective control eyes).

Conclusions: ALI and PLI both migrate outward as the NHP eye becomes progressively damaged by EG. LIL decreases in a subset of M/S EG eyes are consistent with lamina thinning through the course of EG progression as previously described in human glaucoma. Outward ALI and PLI migration is consistent with physical trauma and/or remodeling of the lamina beams that include retrolamina septal recruitment (Roberts et al, IOVS, 2009).

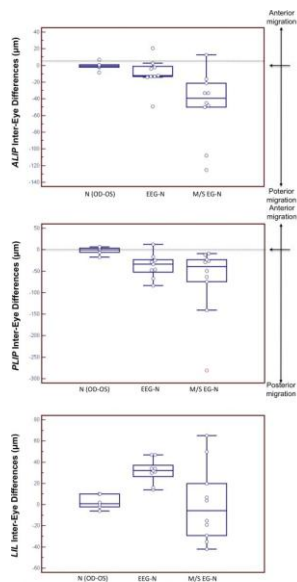
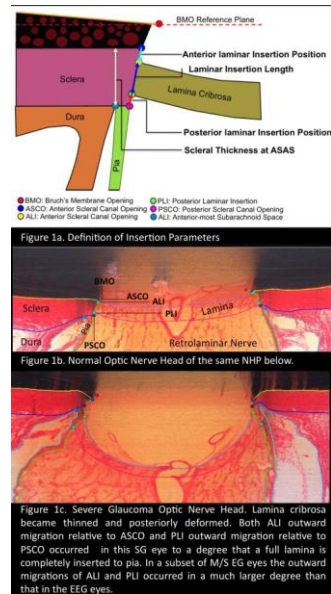


Figure 2. Box and whisker plots of ALIP, PLIP, LIL inter-eye Differences (Normal animals: OD eye value subtracted from OS eye values; EG animals: Glaucoma eye value subtracted from normal eye value) for N-N, EEG-N and M/S EG-N groups. Blue circles are individual inter-eye differences.

Commercial Relationships: Hongli Yang, None; Ruojin Ren, None; Galen Williams, None; Howard Lockwood, None; J Crawford C. Downs, None; Stuart K. Gardiner, Allergan (R); Claude F. Burgoyne, Heidelberg Engineering (F), Heidelberg Engineering (C)
Support: NIH/NEI R01-EY011610

347 Trabecular Meshwork II

Tuesday, May 07, 2013 11:00 AM-12:45 PM

Exhibit Hall Poster Session

Program #/Board # Range: 3526-3567/D0255-D0296

Organizing Section: Glaucoma

Program Number: 3526 **Poster Board Number:** D0255

Presentation Time: 11:00 AM - 12:45 PM

Ageing of Schlemm’s canal in primary open angle glaucoma in hereditary and non-hereditary cases

Teruhiko Hamanaka¹, Tetsuro Sakurai², Akira Matsuda³, Akira Murakami³. ¹Ophthalmology, Japanese Red Cross Medical Ctr, Shibuya-Ku, Japan; ²Center of General Education, Tokyo University of Science, Suwa, Suwa, Japan; ³Ophthalmology, Juntendo University, Tokyo, Japan.

Purpose: In ARVO 2011, we reported that the length of Schlemm’s canal (SC) was significantly shorter in the eyes of hereditary POAG (group A) than that of non-hereditary POAG (group B) patients (p=0.000). This time, we investigated whether the size of SC and SC endothelium (SCE) change according to aging by dividing patients’ specimens into two groups (A and B).

Methods: Trabeculectomy (TLE) specimens from 58 eyes in group A (58±14 y) and 64 eyes in group B (63±16 y) were processed for light microscopy of thrombomodulin (TM) immunohistochemical staining and transmission electron microscopy (TEM). TM staining patterns were investigated by measuring the length of negative TM areas of the inner wall of SC. SCE of 10 TLE specimens from patients before the age of 40 and 15 TLE specimens from those aged over 70 from both groups were observed by TEM. This study was approved by the IRB in Japanese Red Cross Medical Center.

Results: There was no correlation between the size of SC and aging in both groups (p=0.0543, 0.3965 in groups A and B, respectively). TM staining was strongly positive in Sondermann’s canal, while it tended to be weak and sometimes discontinuous in the normal sized SC. Local negative TM staining areas of the inner wall of SC were observed in the eyes of both groups. The ratio of negative TM staining areas of the inner wall of SC/the total length of SC (RNTM) was significantly higher in group B (19.3%) compared to group A (4.9%) (p=0.0001303). RNTM in group B became significantly higher than that in group A after the fifth decade of life (over 50: p=0.001, over 60: p=0.0003, over 70: p=0.0099). TEM observation revealed that degeneration and dropout of SCE in the inner wall were frequently observed in the eyes of those aged over 70 but not in the eyes of those before 40 years old in both groups.

Conclusions: Different TM staining patterns in SC may reflect functional differences in SCE for aqueous outflow. The function of SCE in group B may be more affected according to aging. Degeneration and dropout of SCE observed in older eyes of both groups may be one of the reasons for the increasing risk factor of POAG occurrence or worsening of IOP control according to aging.
Commercial Relationships: Teruhiko Hamanaka, None; Tetsuro Sakurai, None; Akira Matsuda, None; Akira Murakami, SEED(Japan) JP4855782 (P), SEED(Japan) JP5132958 (P)
Support: None in the Support field

Program Number: 3527 **Poster Board Number:** D0256

Presentation Time: 11:00 AM - 12:45 PM

A magnetic bead-based method for mouse trabecular meshwork cell isolation

Weiming Mao, Yang Liu, Robert J. Wordinger, Abbot F. Clark. Cell Biology & Anatomy, UNT Health Science Center, NTERI, Fort Worth, TX.

Purpose: Glaucoma is a leading cause of visual impairment worldwide. The most important risk factor of glaucoma is elevated intraocular pressure (IOP). In primary open angle glaucoma (POAG) patients, damage to the trabecular meshwork (TM) causes ocular hypertension. The mouse model has been widely used for glaucoma research. However, due to the extreme small size of the mouse eye, it is very difficult to dissect pure mouse TM (MTM) tissues and establish MTM cell strains. To circumvent these problems, we took the advantage of the phagocytic property of TM cells, and developed

a novel magnetic bead-based method that enables us to isolate pure MTM cells.

Methods: After anesthesia, 1 μ l magnetic beads (2.0-2.9 μ m in diameter) were intracamerally injected into one of the BLAB/c mouse eyes. To study the localization of the beads, mice were sacrificed 1-7 days post-injection, and eyes were enucleated for transmission electron microscopy (TEM). To isolate MTM cells, anterior segments were dissected from 10-15 sterilized mouse eyes 7 day post-injection. The tissues were digested with collagenase A for 2 to 4 hours. MTM cells were purified with a strong magnetic field as well as repeated washings. Purified MTM cells were cultured serially from 96-well plates to 25 cm flasks, and were further characterized.

Results: TEM studies showed that the magnetic beads located specifically in the mouse TM, but not in corneal or scleral fibroblast cells. Cultured MTM cells were spindle-like and they did not tend to grow into clusters that are usually seen in fibroblast cell cultures. These TM cells expressed TM markers including collagen IV, laminin, and α -smooth muscle actin, as shown by immunocytochemistry studies. Similar to human TM cells, MTM cells treated with 100 nM dexamethasone also showed the formation of cross-linked actin networks (about 2-fold increase, $n=5$ or 6, $p<0.001$) and induction of myocilin, as revealed by immunofluorescent staining and western immunoblotting, respectively.

Conclusions: The magnetic bead-based method is effective in the isolation of pure MTM cells with minimal requirement of micro-dissection techniques. This will be a useful tool for TM cell isolation from small animals for glaucoma research.

Commercial Relationships: Weiming Mao, None; Yang Liu, None; Robert J. Wordinger, None; Abbot F. Clark, Alcon Research, Ltd. (F)

Support: None.

Program Number: 3528 **Poster Board Number:** D0257

Presentation Time: 11:00 AM - 12:45 PM

Live Imaging of Actin Structure in Human Trabecular Meshwork

Jeremy Hwang, Jose M. Gonzalez, James C. Tan. Ophthalmology, University of Southern California, Los Angeles, CA.

Purpose: To characterize the in-situ organization of live filamentous actin (F-actin) in viable ex-vivo human trabecular meshwork (TM) using 2-photon excitation fluorescence microscopy (TPEF).

Methods: Human corneoscleral donor rim tissue was cut into 30 degree wedges and transduced with adenovirus carrying a red fluorescence-conjugated F-actin marker (LifeAct). Tissues were incubated with virus in serum-free DME for 2h at 37°C and 8% CO₂ and then overnight in complete medium. Live tissue was then analyzed with TPEF in situ at 24, 48 and 72h post-transduction. Some tissues were co-incubated with Calcein AM, a cytosolic intravital dye used to identify living cells. Some tissues (untreated and transduced) were fixed and labeled with Alexa-488-conjugated phalloidin for comparison.

Results: In contrast to phalloidin-labeled fixed tissue, where cellular F-actin labeling was cortical at membrane edges and punctate in cytosolic and perinuclear regions, LifeAct-transduced TM cells showed a more diffuse intracellular F-actin pattern. Similar to phalloidin-labeled F-actin, LifeAct fluorescence was observed wrapped around or stretched across trabecular beams. LifeAct colocalized with F-actin. LifeAct expressing cells co-labeled with Calcein indicating viability. In these co-labeled cells, LifeAct had a more cortical distribution compared with the diffusely cytosolic distribution of Calcein. LifeAct expression was seen in the uveal meshwork and the superficial corneoscleral meshwork. Expression

was patchy, likely due to a dependence on transduction efficiency, cellular viability and the functional barrier properties of the TM.

Conclusions: Changes in actin structure in the TM alter aqueous outflow facility and intraocular pressure. Modulating actin structure thus has therapeutic implications for glaucoma. We characterize a new system for studying actin dynamics in viable human TM tissue. A combined approach involving TPEF, LifeAct and phalloidin labeling may be useful for analyzing the effect of potential glaucoma therapies.

Commercial Relationships: Jeremy Hwang, None; Jose M. Gonzalez, None; James C. Tan, None

Support: National Institutes of Health, Bethesda, MD (grant numbers: EY020863 (JCHT); EY03040 (Doheny Vision Research Institute Imaging Core); 1S10RR024754 (USC Multiphoton Core); Kirchgessner Foundation Research Grant (JCHT); Career Development Award from Research to Prevent Blindness (JCHT); and an unrestricted grant from the Research to Prevent Blindness, Inc., New York, New York.

Program Number: 3529 **Poster Board Number:** D0258

Presentation Time: 11:00 AM - 12:45 PM

Dynamic Re-establishment of the Actin Cytoskeleton Impacts the Mechanotransducing Pathway in Human Trabecular Meshwork Cells

Paul Russell¹, Sara M. Thomasy¹, Christopher J. Murphy^{1,2}.

¹Department of Surgical and Radiological Sciences, University of California Davis, Davis, CA; ²Department of Ophthalmology and Vision Science, University of California, Davis, Davis, CA.

Purpose: After treatment of human trabecular meshwork (HTM) cells with Latrunculin B (Lat B), an actin cytoskeleton disruptor, there is a transient increase in the Young's modulus (YM) or stiffness of HTM cells. This increase in YM was reported on hydrogels with moduli similar to normal (5 kPa) and glaucomatous (75 kPa) meshwork as well as on hard surfaces (>1 GPa). The increase was approximately 4 fold over the base line YM on the hard surfaces at 90 minutes post recovery. The increases were less for the hydrogels. Recently, the proteins Yes-associated protein (YAP) and transcription coactivator with PDZ-binding motif (TAZ) were reported to be the mechanotransducers of extracellular alterations. The purpose of this study was to investigate gene expression changes in YAP and TAZ and other proteins in the mechanotransducing pathway during the dynamic changes occurring with the rearrangement of the actin cytoskeleton after Lat B treatment.

Methods: HTM cells were treated with 2 μ M Lat B or vehicle for 30 minutes. The cells were washed and placed in serum containing medium for 1 hour. RNA was then harvested and quantitative PCR was done to determine mRNA expression of several genes.

Results: There was a significant increase in YAP/TAZ mRNA in HTM cells on the 75 kPa hydrogels compared to cells on the 5 kPa hydrogels or the tissue culture plastic (TCP). Addition of Lat B resulted in a significant decrease of YAP mRNA on both hydrogels, but no change on the TCP. TAZ mRNA was also significantly decreased on the 75 kPa hydrogels, but was not altered on either the 5 kPa hydrogels or the TCP. The protein 14-3-3 σ associates with YAP/TAZ and sequesters them in the cytoplasm. The mRNA for 14-3-3 σ was increased on both hydrogels compared to TCP and was significantly increased with Lat B treatment on the hydrogels but not altered on TCP. Connective tissue growth factor, whose mRNA expression is directed by YAP, was down regulated on the hydrogels with Lat B treatment but not altered on TCP.

Conclusions: During the dynamic reassembly of the actin cytoskeleton after Lat B treatment, there were substantial alterations in the signaling pathway involving the mechanotransducers

YAP/TAZ. If the HTM cells are merely grown on TCP, this alteration was not observed. These data highlight the need to conduct experiments on substrates that mimic the compliances measured in normal or glaucomatous HTM.

Commercial Relationships: Paul Russell, None; Sara M. Thomasy, None; Christopher J. Murphy, Ocular Services On Demand (I), Ocular Services On Demand (C), Platypus Technologies LLC (I), Imbed LLC (I), EyeKor LLC (I), Allergan (C), Genentech (C), Sarcodex (C), Covance (C)

Support: NIH Grants Ey019475, EY019970 and P30EY12576, a grant from National Glaucoma Research, a program of the American Health Assistance Foundation and an unrestricted grant from the Research to Prevent Blindness

Program Number: 3530 **Poster Board Number:** D0259

Presentation Time: 11:00 AM - 12:45 PM

Imaging the Effects of Prostaglandins on Cultured Trabecular Meshwork Cells by Coherent Anti-Stokes Raman Scattering (CARS)

David A. Ammar¹, Omid Masihzadeh¹, Malik Y. Kahook¹, Tim C. Lei². ¹Ophthalmology, Univ of Colorado Denver School of Medicine, Aurora, CO; ²Electrical Engineering, Univ of Colorado Denver, Denver, CO.

Purpose: To non-destructively monitor morphological changes to the lipid membranes of living primary cultures of human trabecular meshwork cells (hTMC) without the application of exogenous label.

Methods: hTMC were imaged using a non-linear optical technique, coherent anti-Stokes Raman scattering (CARS), after treatment with a commercial formulation of latanoprost. Untreated cells and cells treated with vehicle containing the preservative benzalkonium chloride (BAK) were imaged as controls. Cells were fixed, stained with the fluorescent lipid dye Nile Red and imaged by conventional confocal microscopy to verify lipid membrane structures.

Results: Analysis of CARS images of hTMC treated for 24 hours with 0.5 µg/ml latanoprost revealed multiple intracellular lipid membranes absent from untreated or BAK-treated hTMC. Treatment of hTMC with sodium fluoride or ouabain, agents shown to cause morphological changes to hTMC, also did not induce formation of intracellular lipid membrane.

Conclusions: CARS microscopy detected changes in living hTMC morphology that was validated by subsequent histological stain. Prostaglandin-induced changes to hTMC involved rearrangement of lipid membrane within these cells. These in vitro results identify a novel biological response to a class of anti-glaucoma drugs, and further experiments are needed to establish how this effect is involved in the hypotensive action of prostaglandins in vivo.

Commercial Relationships: David A. Ammar, U.S. Patent Application #13/700,682 (P); Omid Masihzadeh, U.S. Patent Application #13/700,682 (P); Malik Y. Kahook, Alcon (C), Allergan (C), Merck (C), B&L (C), Glaukos (C), Ivantis (C), ClarVista Medical (P), Dose Medical (P), AMO (P), Genentech (F), Regeneron (F); Tim C. Lei, U.S. Patent Application #13/700,682 (P)

Support: Supported by a State of Colorado Bioscience Discovery Evaluation Grant and by NIH DK095232. Core grant support from NIH/NCRR S10RR025447 and NIH/NCRR Colorado CTSI Grant Number UL1 RR025780.

Program Number: 3531 **Poster Board Number:** D0260

Presentation Time: 11:00 AM - 12:45 PM

Transforming Growth Factor-β2 (TGF-β2) Induces Expression of Biologically Active Bone Morphogenetic Protein-1 (BMP1) in Human Trabecular Meshwork Cells

Tara Tovar-Vidales^{1,2}, Ashley M. Fitzgerald^{1,2}, Abbot F. Clark^{1,2}, Robert J. Wordinger^{1,2}. ¹Cell Biology & Anatomy, University of North Texas Hlth Sci Ctr, Fort Worth, TX; ²North Texas Eye Research Institute, University of North Texas Hlth Sci Ctr, Fort Worth, TX.

Purpose: Previous studies have shown that TGF-β2 increases the deposition of extracellular matrix (ECM) in the trabecular meshwork (TM), which may account for increased aqueous humor outflow resistance in glaucoma. However, there are limited studies on the factors that regulate the processing of TGF-β2 and ECM proteins into their mature form. Bone morphogenetic protein 1 (BMP1) is an enzyme responsible for the cleavage and maturation of growth factors and ECM proteins. The purpose of this study was to determine whether: (a) cultured human TM cells express BMP1, (b) BMP1 expression is regulated by TGF-β2, (c) BMP1 is biologically active, and (d) BMP1 regulates LOX activity.

Methods: Primary human TM cell strains were grown until confluent, and total RNA and conditioned medium (CM) were isolated and subjected to qPCR and Western immunoblotting for BMP1. BMP1 immunolocalization was performed in 3 pairs of normal (NTM) and 3 pairs of glaucomatous (GTM) human donor eyes. Human TM cells were treated with or without TGF-β2 (5ng/ml) for 6, 12, 24 and 48 hours in serum free medium. qPCR (NTM=3) was used to determine BMP1 mRNA expression and Western immunoblotting (NTM=3; GTM=2) was used to determine BMP1 protein expression. BMP1 protein secretion was measured in CM of TM cell cultures (NTM=5; GTM=5). BMP1 activity was measured (NTM=3) in TM cells treated with TGF-β2 or with a combination of TGF-β2 /UK383367 at 1, 3, and 5 µM for 24 hours. Lysyl oxidase (LOX) enzyme activity (NTM=3) was evaluated by WB in TM cells treated with BMP1 or with a combination of BMP1/LOX activity inhibitor β-aminopropionitrile (BAPN) for 48 hours.

Results: Human TM cells expressed mRNA and protein for BMP1. Exogenous TGF-β2 increased mRNA expression at all time points for 6, 12, and 24 hours compared with their controls (p<0.05). GTM BMP1 secretion in the CM were increased compared to NTM (p<0.05). An ELISA showed TGF-β2 induced BMP1 secretion compared to their controls in all cell strains (p<0.05). BMP1 stimulated LOX enzymatic activity in TM cells.

Conclusions: BMP1 is expressed in the human TM. TGF-β2 induction of BMP1 may be responsible for increased processing of growth factors and ECM proteins into their mature forms resulting in TM stiffness and resistance to ECM degradation. BMP1 may be involved in normal TM function as well as the pathogenesis of glaucoma.

Commercial Relationships: Tara Tovar-Vidales, None; Ashley M. Fitzgerald, None; Abbot F. Clark, Alcon Research, Ltd. (F); Robert J. Wordinger, None

Support: NIH Grant EY017374 (RJW)

Program Number: 3532 **Poster Board Number:** D0261

Presentation Time: 11:00 AM - 12:45 PM

Dexamethasone induces stress fiber re-arrangement through non-canonical Wnt signaling in trabecular meshwork cells

Yong Yuan, Chia-Yang Liu, Winston W. Kao. Ophthalmology, University of Cincinnati, Cincinnati, OH.

Purpose: Dexamethasone (DEX) regulates aqueous humor outflow by inducing a re-organization of the cytoskeleton to form cross-linked actin networks (CLAN) in the trabecular meshwork (TM) cells. Myosin Light Chain Kinase (MLCK) has been demonstrated to play an important role in this process, but the upstream components of the pathway leading to MLCK activation are still not clearly defined. Attempts were made to determine if non-canonical Wnt

signaling mediates the DEX-induced cytoskeletal changes in TM cells.

Methods: Primary TM cells were treated with 100 nM DEX in low serum medium. The medium was changed every 3 days. After 7-10 days of culture, the cells were harvested and subjected to molecular biology analysis for the expression of Wnt ligands by degenerate PCR and real-time qRT-PCR. Morphology and immunofluorescence analysis were also performed for stress fiber (phalloidin stain), MLC-P and Wnt5a. Lentivirus-based shRNA against non-canonical Wnt receptor (ROR2) was used to determine the role of non-canonical Wnt signaling in DEX induced cytoskeleton changes.

Results: DEX induced stress fiber re-arrangement in TM cells. Increased level of myosin light chain phosphorylation was observed in DEX-treated cells. Non-canonical Wnt ligand (Wnt5a) was up-regulated by DEX as demonstrated by real time qRT-PCR and immunostaining. Knockdown ROR2, the receptor of non-canonical Wnt signaling, abolished the effects of DEX on the formation of CLAN and the increased phosphorylation of MLC seen in DEX-treated TM cells.

Conclusions: Our data suggests that DEX induces the up-regulation of non-canonical Wnt ligand Wnt5a. Wnt 5a activates myosin light kinase through non-canonical Wnt receptor ROR2. Given the similarities between DEX-induced glaucoma and primary open angle glaucoma, our results provided mechanism of action for applying ROCK inhibitor to treat primary open-angle glaucoma.

Commercial Relationships: Yong Yuan, None; Chia-Yang Liu, None; Winston W. Kao, None

Support: NIH/NEI EY013755, NIH RO1 EY21501, Research to Prevent Blindness, Ohio Lions Eye Research Foundation

Program Number: 3533 **Poster Board Number:** D0262

Presentation Time: 11:00 AM - 12:45 PM

Proteomic Analysis of Trabecular Meshwork Extracellular Matrix

Vasanth Rao¹, Rupalatha Maddala², Nikolai P. Skiba².

¹Ophthalmology & Pharmacology, Duke University Medical Center, Durham, NC; ²Ophthalmology, Duke University Medical Center, Durham, NC.

Purpose: The role of extracellular matrix (ECM) synthesis, turnover and organization in influencing aqueous humor outflow through the trabecular pathway and intraocular pressure, has been heavily contested. However, there is not much by way of a comprehensive analysis of trabecular meshwork (TM) tissue ECM proteins in the literature. Here we provide the ECM protein composition of porcine TM tissue analyzed by Synapt G2 mass spectrometry.

Methods: TM tissue extracted from freshly enucleated porcine eyes was minced and digested with dispase, and homogenized in high salt Tris buffer solution. The 7000 g pellet derived from the tissue homogenate was dissolved in 2 M urea buffer and stirred overnight. The 14,000 g supernatant from urea dissolved tissue specimens was separated by gradient SDS-PAGE (4-15% acrylamide) and proteins stained using GelCode blue. Distinct protein bands from SDS-PAGE gels were extracted, digested in-gel with trypsin and identified by mass spectrometric analysis using a Synapt G2 Water system.

Results: The procedure described above produced consistent results (n=4) with respect to extracting predominantly (>80%) ECM proteins from the TM tissue. Additionally, Synapt G2 mass spectrometry-based proteomics analysis of the ECM enriched fraction from TM tissue revealed the presence of Perlecan, Collagen $\alpha 1$, Collagen $\alpha 3$, Prolargin, Biglycan, Decorin, Fibromodulin, Thrombospondin-1, EGF-containing fibulin-1, Mimecan, sushi-repeat-containing proteins (SRPX1 and 2), Fibulin-5, Fibulin-1, C1q/TNF-related proteins, Lumican, Fibronectin, Laminin, Type VI collagen, Galectin-

1, Matrilin-2, Tenascin XB, Nidogen-2, Periostin, Podocan and other ECM and ECM-associated proteins as some of the predominant proteins. Based on these reproducible observations, the effects of elevated intraocular pressure (50 mm Hg) on the ECM composition of porcine TM tissue are being assessed by quantitative proteomics analysis to identify alterations in specific ECM proteins.

Conclusions: This study provides a reproducible protocol for the extraction of ECM proteins from TM tissue and comprehensive data on the identification and composition of ECM proteins in the TM tissue, as evaluated using proteomics analysis.

Commercial Relationships: Vasanth Rao, None; Rupalatha Maddala, None; Nikolai P. Skiba, None
Support: EY018590;EY012201

Program Number: 3534 **Poster Board Number:** D0263

Presentation Time: 11:00 AM - 12:45 PM

Microspheres (MS) Perfused into the Anterior Chamber (AC) enter the Lumen of Cylindrical Structures Spanning Schlemm's canal (SC)

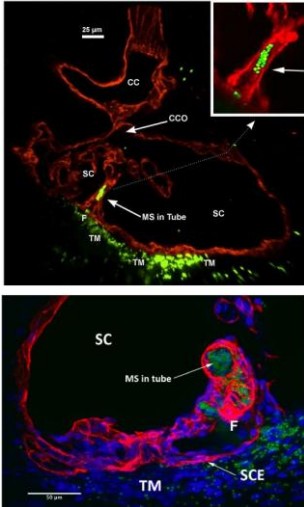
Elizabeth Martin^{1,2}, Nicolette Orkney², Murray A. Johnstone². ¹Univ of Washington Sch of Med, Seattle, WA; ²Ophthalmology, University of Washington, Seattle, WA.

Purpose: Previous reports document cylindrical tube-like structures arising from funnel-shaped regions (F) of the inner wall of SC endothelium (SCE) to attach to SC external wall. We hypothesized that these structures function as flow conduits and if so MS perfused into the AC will be carried into their lumen by flowing aqueous.

Methods: Nemestrina monkey eyes (n=14) Preliminary perfusions with fluorescent MS; sizes: 15 μ m, 10 μ m, 8 μ m, 5 μ m, 2 μ m, 1 μ m. Final perfusions of 2 μ m (n=1) or 1 μ m MS (n=4) for mean of 23 min at mean IOP of 24 mmHg. SC dilation with Healon GV, a viscoelastic. Tissue fixed in 4% paraformaldehyde. Radial 250-500 μ m limbal segments cut. Segments evaluated with dissecting and fluorescent microscope for presence of cylindrical structures spanning SC. IHC using DAPI (20) or PI (7) for nuclei and CD31 for labeling of SC & CC endothelium(27). Imaging with confocal microscopy; processing with Fiji and Imaris.

Results: No spheres present in tubes perfused at 15, 10, 8 or 5 μ m. In 1 eye perfused with 2 μ m MS with 48 segments examined, MS were present in 2 (5%) of 40 tubes. In 4 eyes perfused with 1 μ m MS, 231 total segments were examined (Mean: 14.4 per quadrant). A total of 293 tubes were visualized (Mean: 18.3 tubes/quadrant, 1.27 tubes/segment). MS were present in 27 tubes (9.2% of total). Confocal imaging depth limitations resulted in regional tube image capture as follows: Of 27 tubes imaged, 8 spanned completely from SCE to SC external wall, 23/27 had both the funnel and the cylindrical region present, while 12/27 had a distal attachment of the tube to either the external wall of SC (6) or a septa at a collector channel ostia (CCO) (6). MS present in: funnel 17; cylindrical area 19; distal end 8; all three areas 2.

Conclusions: MS perfused into the AC are carried into the funnel and along the lumen of cylindrical tube-like structures arising from SC inner wall. Aqueous would not actively flow into and carry MS through a blindly ending tube without an outlet. One may reasonably conclude MS are carried into the lumen by actively flowing aqueous that passes into SC through the tubular conduits.



Green microspheres enter funnels and cylindrical regions of tubules spanning SC. Red is CD31, a label for SC and CC endothelium. Blue is DAPI that stains nuclei. See abstract for other callouts.

Commercial Relationships: Elizabeth Martin, None; Nicolette Orkney, None; Murray A. Johnstone, Alcon (R), Allergan (R), Allergan (P), Healonics (I), Cascade Ophthalmics (I), Sensimed (R), Ivantis (R), University of Washington (P)

Program Number: 3535 **Poster Board Number:** D0264

Presentation Time: 11:00 AM - 12:45 PM

Benzalkonium Chloride is Cytotoxic While Preservative-free Tafluprost is Cytoprotective in Human Trabecular Meshwork Cells

Caitlin A. Chang¹, Cindy M. Hutnik². ¹Faculty of Medicine and Dentistry, University of Western Ontario, London, ON, Canada; ²Ophthalmology, Ivey Eye Institute, London, ON, Canada.

Purpose: The use of the preservative benzalkonium chloride (BAK) in topical ophthalmic medications is controversial. It is effective as an antimicrobial and antifungal compound, and is the most frequently used preservative in topical ophthalmic medications. However, as BAK adversely affects the surface of the eye and reduces patient comfort and compliance, there is interest in alternative or preservative-free formulations. Tafluprost is the first preservative-free PGA, has good tolerability and safety, and its IOP-lowering effect is comparable to that of other PGAs. Like other PGAs, it acts on the prostaglandin F2 α receptor, which is known to have anti-apoptotic effects. The purpose of this study was to investigate the effect of BAK toxicity and tafluprost in primary human trabecular meshwork (HTM) cells, and to study the cytoprotective effect of tafluprost in HTM cells stressed with BAK. Our objective was to determine whether BAK or tafluprost have an in vitro cytotoxic effect on primary HTM cells, and if BAK-tafluprost co-incubation attenuates BAK cytotoxicity.

Methods: Primary HTM cells were treated with various BAK and tafluprost free acid concentrations over multiple exposure times, and cell viability was measured with the 3-(4,5-dimethylthiazol-2-yl)-2,5-diphenol tetrazolium bromide (MTT) assay. HTM cells were co-treated with BAK and tafluprost free acid for 30 min and cell viability was assessed.

Results: BAK treatment induced a time- and dose-dependent reduction in HTM cell viability. Tafluprost treatment did not significantly affect cell viability. Co-treatment of BAK with tafluprost showed an increase in cell viability as compared to BAK treatment alone.

Conclusions: These results demonstrate that BAK is harmful to the health of the HTM cells, and its use in topical ophthalmic medications should perhaps be re-evaluated. Tafluprost is both safe and cytoprotective for the HTM. The finding that tafluprost has a positive effect on HTM cell viability, with minimal or no negative effects, further supports the merits of the use of preservative-free ophthalmic medications in the treatment of glaucoma. Further clinical investigations are needed to clarify whether BAK reduces the efficacy of anti-glaucoma medications and whether tafluprost may provide additional benefits for glaucoma patients besides lowering IOP.

Commercial Relationships: Caitlin A. Chang, None; Cindy M. Hutnik, None

Program Number: 3536 **Poster Board Number:** D0265

Presentation Time: 11:00 AM - 12:45 PM

Expression of Stem Cell Markers in the Bovine Corneal Endothelium, Insert Region and Trabecular Meshwork

Wing Yan Yu¹, Carl M. Sheridan², Ian Grierson², Amy C. Lo^{1,3}, Sai Hung David Wong^{1,3}. ¹Department of Ophthalmology, The University of Hong Kong, Pokfulam, Hong Kong; ²Department of Eye and Vision Science, The University of Liverpool, Liverpool, United Kingdom; ³Research Centre of Heart, Brain, Hormone and Healthy Aging, The University of Hong Kong, Pokfulam, Hong Kong.

Purpose: Previous studies suggest that adult stem/progenitor cells (SPCs) reside in the human trabecular meshwork insert region (TMI) at the posterior limbus, where the corneal endothelium (CE) joins the trabecular meshwork (TM). They may supply new cells for regenerating the CE and TM. However, the existence of SPCs in these architecturally different regions of non-primate species have not been investigated. In this study, we aimed to examine the localization of the SPCs in the bovine anterior chamber angle, which provides a large tissue model for research.

Methods: Fresh bovine eyes were obtained from the abattoir within 6 hours post mortem. The anterior segment was fixed in 4% formaldehyde, paraffin embedded and cut into serial 5 μ m-thick sections. The expression of stem cell markers in the CE, TMI and TM was assessed by immunohistochemistry. These markers included ABCG2, Ankyrin G, Nestin, Oct4, Pax6, Sox2, STRO-1 and Telomerase. Parallel immunocytochemical studies on SPCs isolated from the bovine CE and TM using sphere culture were also carried out.

Results: Positive immunofluorescence of ABCG2, Nestin, Oct4, Pax6, Sox2, STRO-1 and telomerase were observed in the CE, TM and in isolated cells located within the TMI. These cells were found in deeper layers just beneath the very end of the peripheral CE and they seemed to be continuous with the anterior TM. However, Ankyrin G staining was only restricted to the TMI. SPCs isolated from the CE and TM respectively showed positive immunoreactivity with all the stem cell markers mentioned.

Conclusions: SPCs are present in the bovine anterior chamber angle despite the anatomical structural difference to human. Positive immunostaining observed in the entire CE and TM may be due to the relative young age of the animals. Nevertheless, the exclusive Ankyrin G staining and robust expression of a panel of stem cell markers in the TMI provide strong evidence that the bovine TMI house SPCs which may be comparable to those observed in human.

Commercial Relationships: Wing Yan Yu, None; Carl M. Sheridan, None; Ian Grierson, Polyphotonix UK (C), Bausch and Lomb (C); Amy C. Lo, None; Sai Hung David Wong, None

Support: University Development Fund and the Seed Funding for Basic Research from The University of Hong Kong

Program Number: 3537 **Poster Board Number:** D0266

Presentation Time: 11:00 AM - 12:45 PM

Metabolic Dependence of Conventional Outflow Facility in Mice
Alexandra Boussommier Calleja¹, W Daniel Stamer³, C R. Ethier^{1,2}, Darryl R. Overby¹. ¹Bioengineering, Imperial College London, London, United Kingdom; ²Biomedical engineering, Georgia Institute of Technology, Atlanta, GA; ³Ophthalmology, Duke University, Durham, NC.

Purpose: Conventional aqueous humor outflow is considered to be a process independent of cellular metabolism. In particular, previous studies have shown outflow facility to be relatively unaffected by metabolic poisons or changes in temperature (after accounting for temperature effects on perfusion media viscosity). Our goal was to determine whether conventional outflow facility in mice is similarly independent of cellular metabolism.

Methods: Enucleated eyes from C57BL/6 mice were perfused within 3 hrs of death at sequential pressures (4, 8, 15, 25 mmHg) while submerged in isotonic saline under temperature control. Conventional outflow facility was calculated as the slope of the best-fit linear regression of flow rate vs. pressure. One group of paired eyes was perfused with PBS + 5.5 mM glucose, with one eye at 20°C and the fellow eye at 35°C. A second group was perfused similarly, but with PBS + a metabolic poison (2 mM sodium azide) + 10 mM dideoxy-D-glucose.

Results: Eyes perfused at 35°C without poison had a 2.49±0.86 fold higher conventional facility vs. eyes perfused at 20°C (0.0069±0.0021 vs. 0.0171±0.0028 µl/min/mmHg; N = 6 vs. 6; p = 4 x 10⁻⁵; Mean±SD). Importantly, this temperature-dependent increase was significantly larger than the predicted 1.39-fold increase based on viscosity change alone (p=4 x 10⁻³). In contrast, eyes perfused with metabolic poison showed a 1.52±0.81 fold increase in facility with increasing temperature (0.0087±0.0035 vs. 0.0132±0.0046; N = 7 vs. 5; p=0.107), which was not significantly different from the expected viscosity change (p=0.346).

Conclusions: In these preliminary experiments, a metabolic poison eliminated the temperature-dependent increase in conventional outflow facility in mouse eyes. In contrast to past data from perfused human cadaver eyes (VanBuskirk, AJO 1974 77:565), our data in mice suggest that conventional outflow depends partially on cellular metabolism. These differences could reflect underlying species differences, differences in perfusion methodology or post mortem time.

Commercial Relationships: Alexandra Boussommier Calleja, None; W Daniel Stamer, Allergan (F), Alcon (F), Acucela (C), Aerie (C), Cytokinetics (C); C R. Ethier, None; Darryl R. Overby, Allergan, Inc. (F), Allergan, Inc. (C)

Support: National Glaucoma Research, a Program of the American Health Assistance Foundation

Program Number: 3538 **Poster Board Number:** D0267

Presentation Time: 11:00 AM - 12:45 PM

Schlemm's Canal (SC) Inner Wall Pores Correlate with Segmental Outflow in Human Eyes

C R. Ethier^{1,2}, Sietse T. Braakman², Arthur T. Read³, Darren W. Chan³, Darryl R. Overby². ¹Biomedical Engineering, Georgia Institute of Technology, Atlanta, GA; ²Bioengineering, Imperial College, London, United Kingdom; ³Ophthalmology and Vision Science, University of Toronto, Toronto, ON, Canada.

Purpose: Non-uniform drainage of aqueous humor (AH) through the trabecular meshwork (TM) likely influences outflow resistance, and SC inner wall (IW) pore density may influence local AH flow. Here we test whether regions of segmental outflow coincide with high IW

pore density.

Methods: This study extends data from ARVO 2012. We labeled TM outflow patterns by perfusing 2 pairs of normal human enucleated eyes at 8 mmHg/37 °C with mock AH containing fluorescent microspheres. All eyes were fixed by immersion. IW/TM in outflow tissue wedges was examined by en face confocal microscopy and 4-7 150x50µm regions-of-interest (ROIs) with either high or low fluorescent tracer intensity were identified per wedge. Average tracer fluorescence intensity integrated over the JCT region was measured in each ROI. IW pore density (n) and diameters (D) were then measured in the same ROIs by scanning electron microscopy, and 5 IW pore metrics were computed in each ROI: $P^k = nD^k$, for k = 0...4. Note P₀ = pore density; P₁ = nD-product, indicating strength of the funneling effect; P₂, P₃ and P₄ are proportional to IW porosity, local fluid conductance from Sampson's law and from Poiseuille's law, respectively. Data were analyzed by ANCOVA with Bonferroni correction, as required.

Results: All eyes had normal facility. Unlike pressure-fixed eyes, these immersion-fixed eyes had more paracellular [B] vs intracellular [I] pores (54% B pores). Tracer intensity correlated with total pore density (p=0.02). For I pores, P_k did not depend on tracer intensity for any k = 0...4, indicating that I pores did not co-localize with regions of high flow. However, for B pores, P_k was correlated with tracer intensity for all k=0...4, with p < 0.004 for all pore metrics.

Conclusions: B, but not I, pores co-localize with regions of high tracer representing segmental outflow, supporting the hypothesis that B pores are involved in fluid transport across the IW of SC. The very strong correlation between inner wall B pore metrics and tracer intensity is consistent with local outflow patterns being controlled by an interaction between flow through the JCT and across the IW. Further, our data are consistent with B pores being the "normal" AH route across the IW at lower pressures, with I pores providing a secondary route at higher pressures.

Commercial Relationships: C R. Ethier, None; Sietse T. Braakman, None; Arthur T. Read, None; Darren W. Chan, None; Darryl R. Overby, Allergan, Inc. (F), Allergan, Inc. (C)
Support: National Glaucoma Research, a program of the American Health Assistance Foundation (DRO); NIH grant EY019696 (DRO; CRE); Royal Society Wolfson Merit Research Award (CRE)

Program Number: 3539 **Poster Board Number:** D0268

Presentation Time: 11:00 AM - 12:45 PM

Transcriptional Profiling of Human Schlemm's Canal Cells Following Latanoprost, Bimatoprost and Prostaglandin F2alpha (PGF2α) Treatment

Nelson S. Winkler¹, Uttio Roy Chowdhury², Michael P. Fautsch².

¹Mayo Medical School, Rochester, MN; ²Ophthalmology, Mayo Clinic, Rochester, MN.

Purpose: Prostaglandin analogs lower intraocular pressure (IOP) by modulating the trabecular outflow pathway and are used as first line drugs for treating ocular hypertension. However, the mechanism of action of these drugs is largely unknown. The current study was undertaken to identify differential gene expression patterns in human Schlemm's canal cells following treatment with latanoprost, bimatoprost and PGF2α.

Methods: Three confluent primary human Schlemm's canal cell lines (provided by Dr. Dan Stamer, Duke University) were incubated with DMEM containing latanoprost-free acid (100nM), bimatoprost-free acid (1 µM), and PGF2α (100nM). DMEM containing vehicle (ethanol) was used as the control. Following 2, 6 and 12 hour incubations, total RNA was isolated from each cell line. Total RNA (100 ng) was reverse transcribed, column purified, and in vitro transcribed generating biotin-labeled cRNA. The in vitro transcribed

products were fragmented and used to probe Affymetrix GeneChip Human Genome U133 Plus 2.0 arrays. A total of 54 Affymetrix GeneChip Human Genome U133 Plus 2.0 arrays were probed. Following normalization, differentially regulated gene sequences that had >1.5-fold change in gene expression were considered significant. Real-time PCR was used to verify accuracy of the microarrays.

Results: A total of 15 genes were upregulated and 2 genes were downregulated at all timepoints, in all cell lines, and under all treatments. Among the upregulated genes, *NR4A3* and *RCAN1* were elevated greater than 4.5-fold. Many of the differentially regulated genes are associated with metabolic pathways and ion transport systems suggesting that treatment with the prostaglandin analogs may result in increased metabolic functions and overall better cell health.

Conclusions: Treatment with PGF₂ α and its analogs cause differential expression of gene targets involved in functionally concentric pathways suggesting that common signaling mechanisms are utilized by all three drugs in human Schlemm's canal cells.

Commercial Relationships: Nelson S. Winkler, None; Uttio Roy Chowdhury, None; Michael P. Fautsch, None

Support: NIH grants EY07065 and EY21727; Research to Prevent Blindness and Mayo Foundation

Program Number: 3540 **Poster Board Number:** D0269

Presentation Time: 11:00 AM - 12:45 PM

Microparticle Delivery of Matrix Metalloproteinase-3 to Trabecular Meshwork Cells

Beatrice Yue¹, Sanja B. Turturro¹, Suhair Sunoqrot², Hongyu Ying¹, Seungpyo Hong². ¹Ophthalm & Vis Sciences, Univ of Illinois at Chicago, Chicago, IL; ²Departments of Biopharmaceutical Sciences and Bioengineering, University of Illinois at Chicago, Chicago, IL.

Purpose: To test the feasibility of using microparticles for slow and sustained release of active matrix metalloproteinase-3 (MMP-3) to degrade extracellular matrix (ECM) elements such as fibronectin in cultured human trabecular meshwork (TM) cells. Accumulation of ECM materials in the TM is believed to be a contributing factor to intraocular pressure elevation, a major risk factor/cause of primary open angle glaucoma.

Methods: β -casein, with molecular weight (26 kDa) and hydrophobicity similar to those of the active MMP-3 fragment (19.2 kDa), was used for the initial testing. β -casein (2.2 mg) was encapsulated into poly(lactic-co-glycolic acid) (PLGA) microparticles following a double emulsion procedure. The protein amount encapsulated into the microparticles was measured by Bradford protein assay and the encapsulation efficiency was determined. The release test was conducted in Dulbecco's Eagle's minimum essential medium (DMEM) without or with the presence of human TM cells. Encapsulation of active MMP-3 (5 μ g) into PLGA microparticles was subsequently carried out. Human TM cells pretreated with 100 nM of dexamethasone (DEX, to induce fibronectin expression) were set up as an assay platform for MMP-3. The fibronectin degradation or reduction of fibronectin levels was used as an indicator of the enzyme activity.

Results: The encapsulation efficiency for β -casein was around 53%. The release test showed a slow and sustained release of β -casein over 20 days. The encapsulation efficiency for MMP-3 was estimated to be approximately 50%. The release medium collected from MMP-3-microparticle treated cultures, compared to that from empty- and β -casein-microparticle controls, markedly reduced the fibronectin staining in DEX-pretreated TM cells. The MMP-3 released to the culture medium was found active, still capable of degrading fibronectin after 9 days of incubation.

Conclusions: This study demonstrated the feasibility of

encapsulating MMP-3 into polymeric microparticles and the potential of delivering active enzyme to TM cells.

Commercial Relationships: Beatrice Yue, None; Sanja B. Turturro, None; Suhair Sunoqrot, None; Hongyu Ying, None; Seungpyo Hong, None

Support: Grants EY018828 and EY005628 (to B.Y.J.T.Y.) and core grant EY001792 from the National Eye Institute, Bethesda, Maryland.

Program Number: 3541 **Poster Board Number:** D0270

Presentation Time: 11:00 AM - 12:45 PM

CLINICAL EFFICACY OF ULTRASONIC CIRCULAR CYCLO COAGULATION IN REFRACTORY GLAUCOMA. PRELIMINARY RESULTS

Paolo Fogagnolo¹, Maurizio Digiumi², Emanuele Maggiolo², Luca M. Rossetti². ¹Fondazione GB Bietti-IRCCS, Rome, Italy; ²University Eye Clinic, San Paolo Hospital, Milan, Italy.

Purpose: To report the preliminary data of clinical efficacy and safety of Ultrasonic Circular Cyclo Coagulation (UC3) in refractory glaucoma.

Methods: 11 patients were treated in our centre as a part of the multicenter Eye-Must study. 7 patients had previous trabeculectomies, 3 diode coagulation of ciliary body, 2 valve implant; 3 penetrating keratoplasty, 2 trauma, 2 retinal detachment. All patients were under maximum-tolerated topical treatment; 5 cases also received Diamox. Corneal edema was present in 4 patients. Treatment was performed in peribulbar anaesthesia in all cases; a partial coagulation of 6 fixed zones was obtained by means of a single-step procedure lasting about 2 minutes. Follow-up visits were performed at day 1, 7, 28. Data at month 3, 6, 9, 12 will be provided.

Results: Baseline IOP was 27.1 \pm 4.6 mm Hg. IOP at day 1, 7, and 28 was respectively 20.8 \pm 5.7, 18.6 \pm 6.1, 17.9 \pm 3.7 mm Hg; this corresponded to a mean reduction of 23%, 31%, 29%.

At day 7, Diamox was discontinued in all patients except one (for this patient, it was reduced); no change in topical treatment was necessary in any patient.

Treatment was well-tolerated in all cases. No major intra- or post-operative complications occurred. Mild conjunctival hyperemia was present at day 1 in all cases; 1 case had a mild corneal abrasion. At day 7, all side effects had resolved. At month 1, corneal edema disappeared in 3 patients, and reduced in 1. No patients required any other surgical procedure.

Conclusions: Based on our preliminary data, UC3 is a secure and effective treatment in refractory glaucoma.

Commercial Relationships: Paolo Fogagnolo, None; Maurizio Digiumi, None; Emanuele Maggiolo, None; Luca M. Rossetti, None
Clinical Trial: NCT01592955

Program Number: 3542 **Poster Board Number:** D0271

Presentation Time: 11:00 AM - 12:45 PM

EFFECT OF CELLULAR AND PLASMA FIBRONECTIN ISOFORMS ON NORMAL HUMAN TRABECULAR MESHWORK CELLS

Wanda E. Medina-Ortiz^{1,2}, Robert J. Wordinger^{1,2}, Abbot F. Clark^{1,2}. ¹Cell Biology and Anatomy, Univ of North Texas Hlth Science Ctr, Fort Worth, TX; ²NTERI, Univ of North Texas Hlth Science Ctr, Fort Worth, TX.

Purpose: The expression of cellular (cFN) and plasma (pFN) fibronectin isoforms are induced by TGF- β 2 in human trabecular meshwork (HTM) cultured cells. Expression of specific FN isoforms can alter ECM homeostasis, ECM-cell interactions, and gene expression. Our purpose is to determine cFN levels in HTM tissues

and to explore the impact of FN isoforms on HTM cells by studying changes in adhesion, cytoskeletal organization and gene expression. **Methods:** Differences between cFN levels in normal (NTM) and glaucomatous (GTM) tissues were obtained by immunohistochemistry. NTM cell strains were cultured for 24-48 hrs on surfaces coated with cFN or pFN, and the responses were compared to PBS controls. Changes in formation and redistribution of F-actin fibers and adhesion proteins were analyzed by phalloidin staining, Western immunoblots, and immunocytochemistry. Gene expression changes were analyzed using PCR arrays.

Results: GTM tissues exhibited significantly greater cFN levels (1.7-fold, $p < 0.05$). NTM strains exposed to both FN isoforms showed increased F-actin formation and redistribution; however, the F-actin pattern and distribution was different between cFN and pFN. Similarly, adhesion molecules such as talin, vinculin, paxillin and integrin beta 1 were increased and redistributed. Both FN isoforms changed gene expression, including alpha-smooth muscle actin-2, metalloproteases and their inhibitors, inflammatory cytokines, and TGF- β related genes.

Conclusions: Our results show that GTM tissues expressed more cFN and that NTM cells respond differently depending on the FN isoform. The relationship between TGF- β 2 modulation of FN isoform expression and the effect of FN isoforms on NTM cells suggests that this type of ECM remodeling may contribute to the TM changes associated with glaucoma.

Commercial Relationships: Wanda E. Medina-Ortiz, None; Robert J. Wordinger, None; Abbot F. Clark, Alcon Research, Ltd. (F)

Support: NIH Grant RO1 EY017374

Program Number: 3543 **Poster Board Number:** D0272

Presentation Time: 11:00 AM - 12:45 PM

Decrease of nuclear Yes-associated protein (YAP) with human trabecular meshwork (HTM) cell passage

Joshua Morgan¹, Christopher J. Murphy^{1,2}, Paul Russell¹.

¹Veterinary Medicine: Surgical and Radiological Sciences, University of California, Davis, Davis, CA; ²School of Medicine: Department of Ophthalmology and Vision Sciences, University of California, Davis, Davis, CA.

Purpose: YAP is a transcriptional coactivator with roles in proliferation and cell survival. YAP has recently been implicated in mechanotransduction, with cells grown on stiffer substrates exhibiting increased nuclear localization and transcriptional activity by this protein. Among YAP's transcription targets are numerous genes associated with glaucoma such as transforming growth factor- β and connective tissue growth factor. The expression of these genes with disease would be consistent with more nuclear localization of YAP as a result of the elevated stiffness found in the glaucomatous HTM. We wished to quantify the nuclear localization of YAP as a function of passage number and presence of serum in cultured HTM cells as a baseline for future studies on the impact of substratum stiffness.

Methods: HTM cells from four donors were maintained in DMEM/F12 + 10% serum. For each passage, cells were plated at 100,000 cells/35 mm tissue culture plastic (TCPS) dish and allowed to attach overnight. The following day the media was replaced with media \pm serum. After 3 days, the cells were fixed and permeabilized with 4% formaldehyde and 0.5% Triton. The cells were labeled with rabbit anti-YAP and counterstained with DAPI. The cells were imaged and the YAP nuclear contrast ratio (NCR), defined as the ratio of the YAP staining intensity in the nucleus or in the adjacent cytosol, was quantified.

Results: In cells from all four donors there was substantial nuclear

labeling of YAP and this was not influenced by the presence or absence of serum. The average nuclear contrast ratio decreased with passage from around 1.8 in earlier passages to $\sim 1.2 - 1.4$ at terminal passage (12-14), indicating that even in senescence YAP was not totally excluded from the nucleus of HTM cells. The decrease in nuclear labeling of YAP was mirrored by a decrease in cell density, consistent with the role of YAP in proliferation.

Conclusions: In culture, HTM cells cultured on TCPS express YAP and the localization is not influenced by the presence or absence of serum. A decrease in NCR is observed with increasing cell passage. With YAP targets including multiple genes believed to be important in glaucoma and the published observations of the elevated stiffness of the glaucomatous HTM and the stiffness-dependent nuclear localization of YAP, this protein represents a novel potential target for pharmacological intervention in glaucoma.

Commercial Relationships: Joshua Morgan, None; Christopher J. Murphy, Ocular Services On Demand (I), Ocular Services On Demand (C), Platypus Technologies LLC (I), Imbed LLC (I), EyeKor LLC (I), Allergan (C), Genentech (C), Sarcodex (C), Covance (C); Paul Russell, None

Support: NIH Grant EY019475, NIH Grant EY019970, NIH Grant EY12576, and an unrestricted grant from Research to Prevent Blindness

Program Number: 3544 **Poster Board Number:** D0273

Presentation Time: 11:00 AM - 12:45 PM

Three-dimensional structure of the mouse ciliary muscle, its innervation and connections to the outflow tissues and choroid

Elke Luetjen-Drecoll¹, Ozan Tektas¹, Darryl R. Overby². ¹Dept. of Anatomy II, University of Erlangen Nurnberg, Erlangen, Germany; ²Bioengineering, Imperial College London, London, United Kingdom.

Purpose: To determine the functional morphology of the mouse ciliary muscle and outflow pathways, focusing on the connections between the ciliary muscle, trabecular meshwork (TM), Schlemm's canal (SC) and choroid.

Methods: Immunohistochemical studies of histological sections and whole mounts using antibodies against α -SM-Actin, elastin, and the neuronal markers: vesicular acetylcholine transporter (VACHT), nitric oxide synthase (NOS), vasoactive intestinal peptide (VIP), tyrosine hydroxylase (TH) as well as semi- and ultrathin serial sections in sagittal and tangential planes were performed in eyes of BALB/c- and C57BL/6 mice.

Results: The mouse TM, similar to human TM, contains an elastic fiber network present within the TM lamellae and juxtacanalicular TM (JCT). Elastic fibers are located at the center of the TM lamellae, which are continuous with the anterior surface of the ciliary body/iris stroma. The JCT consists of around four layers of TM cells and surrounding connective tissue including the elastic fiber network. The network is connected to SC inner wall endothelium and JCT cells. The mouse ciliary muscle consists of mainly longitudinally oriented, branching smooth muscle cells, laterally connected to each other by junctional complexes. Anteriorly, the muscle cells form elastic tendons inserting into the subendothelial elastic net and into the elastic fibers at the center of the TM lamellae. Posteriorly, the elastic tendons of the ciliary muscle insert into the elastic net of the choroid and into the basement membrane of the choriocapillaris. Ciliary muscle fibers are surrounded by VACHT-positive varicosities. No staining for NOS, VIP or TH was seen within the ciliary muscle. TM cells (most of them staining for α -SM-Actin) were in contact with VACHT- and TH-positive varicosities.

Conclusions: In mice, as in human, the cholinergic innervated ciliary muscle forms elastic tendons inserting anteriorly into the TM and inner wall of SC and posteriorly into the choroid.

Contraction of the mouse ciliary muscle may act to open SC, pull the ciliary body/iris inwardly, and potentially increase outflow facility.

Commercial Relationships: **Elke Luetjen-Drecoll**, None; **Ozan Tektas**, None; **Darryl R. Overby**, Allergan, Inc. (F), Allergan, Inc. (C)

Program Number: 3545 **Poster Board Number:** D0274

Presentation Time: 11:00 AM - 12:45 PM

Prdx6 abates the process of senescence and restores trabecular meshwork cell integrity by regulating Telomerase, p16 and p21 Expression

Nigar Fatma¹, Eri Kubo², Bhavana Chhunchha¹, W Daniel Stamer³, Dhirendra P. Singh¹. ¹Ophthalmology and Visual Sciences, Univ of Neb Med Center, Omaha, NE; ²Ophthalmology, Kanazawa Medical University, Kanazawa, Japan; ³Ophthalmology, Duke Eye Center, Duke University, Durham, NC.

Purpose: Normal functioning of Trabecular Meshwork (TM) is vital in regulating intraocular pressure (IOP). Glaucomatous TM cells contain increased levels of extracellular matrix (ECM) and oxidative DNA and protein adducts, and undergo senescence, suggesting a role for oxidative stress. Peroxiredoxin 6 (Prdx6) provides cytoprotection from oxidative stress. Using human TM cells facing oxidative stress as a model *in vitro*, we tested the hypothesis that Prdx6 overexpression is protective in glaucomatous or aging TM cells.

Methods: pGFP-Prdx6 and/or pGRN145-hTERT (ATCC) or mutant plasmids were overexpressed in TM cells from normal and glaucomatous human subjects of different ages and different passages and were exposed to H₂O₂ (0-200µM). Prdx6 fused to TAT transduction domain was also used to deliver Prdx6 to assess cytoprotection. Cell viability, cell proliferation, lipid peroxidation (LPO) were measured by MTS assay, BrdU incorporation and LPO assay kit, respectively. Reactive oxygen species (ROS) were quantified using H2DCF dye. Real-time PCR and Western analysis assessed the level of Prdx6, telomerase reverse transcriptase (TERT), ECM proteins and senescence markers, p16 and p21. β-galactosidase staining was done for senescence markers. 8-OHdG assay was used for oxidative DNA damage. Telomerase activity and TGFβs were assessed by Telomerase and Emax assays kits, respectively.

Results: Glaucomatous or aging cells, or cells facing oxidative stress showed reduced Prdx6 expression. Such cells had increased expression of ECM proteins; *asm-actin*, fibronectin, thrombospondin1, TGase2, PAI1, tropomyosin, p16, p21; and reduced expression and activity of telomerase, hTERT. Glaucomatous cells bore increased ROS and active TGFβ1 and 2 and LPO adducts. The abnormalities were reversed in cells overexpressing Prdx6; having significantly reduced β-galactosidase staining, with increased proliferation/cell division and telomerase activity.

Conclusions: The study shows Prdx6's ability reverse the senescence process of glaucomatous TM cells by increasing telomerase activity, and argues a role for oxidative damage in replicative senescence. Since loss of Prdx6 expression in TM cells is causally related to TM cells etiopathogenesis, development of Prdx6 expression-based therapeutics may delay or prevent TM cell dysfunction, representing a novel therapeutic strategy for glaucoma.

Commercial Relationships: **Nigar Fatma**, None; **Eri Kubo**, None; **Bhavana Chhunchha**, None; **W Daniel Stamer**, Allergan (F), Alcon (F), Acucela (C), Aerie (C), Cytokinetics (C); **Dhirendra P. Singh**, None

Support: NIH Grant EY013394

Program Number: 3546 **Poster Board Number:** D0275

Presentation Time: 11:00 AM - 12:45 PM

©2013, Copyright by the Association for Research in Vision and Ophthalmology, Inc., all rights reserved. Go to iovs.org to access the version of record. For permission to reproduce any abstract, contact the ARVO Office at arvo@arvo.org.

ADAMTS4 activity and TIMP3 levels are modulated in trabecular meshwork cells with decreased hyaluronan synthesis

Kate E. Keller, Yong-Feng Yang, Ying Ying Sun, Ted S. Acott.

Ophthalmology, Casey Eye Institute - OHSU, Portland, OR.

Purpose: Accumulating evidence supports a role for hyaluronan (HA) in regulating matrix metalloproteinase (MMP) expression, cellular localization and activity. Here, we analyzed ADAMTS4 (a disintegrin and metalloproteinase with thrombospondin motifs-4) mRNA expression, protein levels and enzyme activity in trabecular meshwork (TM) cells with depleted HA. The amount of TIMP3, the tissue inhibitor of ADAMTS4, was also assessed.

Methods: Two methods were used to reduce HA concentration: 1 mM 4-methylumbelliferone (4MU) or previously characterized short hairpin RNAi silencing (shRNA) lentivirus targeted to each individual HA synthase (HAS) gene (shHAS1, shHAS2 and shHAS3). Vehicle control and shControl, which does not target any known gene, were also included. Primary porcine TM cells were subjected to 4MU treatment for 48 or 72 hours. For infection, lentivirus was incubated for 3 days and then cells were changed to serum-free media for a further 48 or 72 hours. ADAMTS4 mRNA levels were determined by quantitative RT-PCR and protein levels in RIPA cell lysates were analyzed by Western immunoblotting. A fluorometric ADAMTS4 activity assay was used to quantitate enzyme activity. Cells were fixed and immunostained for confocal microscopy.

Results: ADAMTS4 mRNA levels decreased with all treatments, but protein levels were not significantly altered. ADAMTS4 activity was significantly decreased with all treatments at 48 and 72 hours. TIMP3 protein levels were reduced with shHAS infection, but increased with 4MU treatment. TIMP3 was immunolocalized in the cytoplasm and at PILS (podosome or invadopodia-like structures), areas of focal ECM degradation. TIMP3 also colocalized with clusters of ADAMTS4-stained vesicles. There seemed to be a higher degree of colocalization of TIMP3 and ADAMTS4 in 4MU-treated cells.

Conclusions: ADAMTS4 activity appears to be dependent on HA concentration. Since HA concentration decreases in aged eyes and is reduced even further in POAG patients, the ability of TM cells to focally remodel ECM via ADAMTS4 may be compromised, which in turn could adversely affect aqueous outflow.

Commercial Relationships: **Kate E. Keller**, None; **Yong-Feng Yang**, None; **Ying Ying Sun**, None; **Ted S. Acott**, None

Support: EY019643, EY008247, EY003279, EY010572, and an unrestricted grant from Research to Prevent Blindness

Program Number: 3547 **Poster Board Number:** D0276

Presentation Time: 11:00 AM - 12:45 PM

MECHANICAL STRESS ACTIVATES AUTOPHAGY IN TRABECULAR MESHWORK CELLS

Ping Xu, Kristine M. Porter, Nalla Thambi Jeyabalan, Paloma B.

Liton. ophthalmology, Duke university, Durham, NC.

Purpose: To investigate the activation of autophagy with mechanical stress in trabecular meshwork (TM) cells.

Methods: Confluent cultures of human and porcine TM cells were subjected to static mechanical stress (30% stretching) for up to 16 hours. Autophagy dynamics was monitored by confocal microscopy using AdtfLC3; immunoblotting, by monitoring the LC3-I to LC3-II conversion; and electron microscopy. Protein expression levels were quantified by WB analysis using specific antibodies against Atgs, LAMP1, p62, LC3B, CTSB, p70S6K and pp70S6K. mRNA expression levels of beclin, Atg4, Atg5, Atg7, LC3, LAMP1, and LAMP2 were monitored by qPCR. Rapamycin, bafilomycin A1, chloroquine, and 3-MA were used to pharmacologically modulate the autophagic pathway. Activation of autophagy was also evaluated in

enucleated whole globe porcine eyes subjected to perfusion pressures of 10, 20, and 40mmHg

Results: Western-blot analysis showed increased levels of the autophagosome marker LC3-II in porcine and human TM cells as early as 30 minutes post-stretching compared to non-stretched cultures (1.35±0.07 fold). Elevated LC3-II peaked at 3 hours of continuous stretching (2.23±0.51 fold) and gradually decreased at 16 hours, concurrent with decreased levels of Atg12 (0.32±0.07 fold), a protein regulating LC3 lipidation. No changes in the mRNA levels for the genes tested were observed. The increase in LC3-II in the mechanically stressed cultures was prevented with the autophagy inhibitor 3-MA. Confocal microscopy showed increased number of autophagolysosomes (8.9±1.1 versus 5.5±0.7 autophagosome/cell, p=0.0001), indicating the proper maturation of nascent autophagosomes. This data was confirmed by electron microscopy. A significant increase in LC3-II protein levels was also observed in the outflow pathway of whole globe porcine eyes subjected for one hour to perfusion pressure of 40 mmHg compared to eyes perfused at 10 mmHg.

Conclusions: Our results clearly indicate that autophagy is rapidly induced in TM cells in response to mechanical stress. Based on this, we hypothesize that autophagy is part of an integrated response to mechanical challenge, allowing cells to cope with a continuously changing physical environment. We further hypothesize that this response mechanism is impaired in glaucoma, as a result of a decrease in the autophagic capacity with chronic oxidative stress and/or aging.

Commercial Relationships: Ping Xu, None; Kristine M. Porter, None; Nalla Thambi Jeyabalan, None; Paloma B. Liton, None
Support: NIH-R01EY020491, NIH-R21EY019137, NIH-P30EY005722, AHAF G2012022, and Research to Prevent Blindness.

Program Number: 3548 **Poster Board Number:** D0277

Presentation Time: 11:00 AM - 12:45 PM

DIMINISHED AUTOPHAGIC CAPACITY OF GLAUCOMATOUS TRABECULAR MESHWORK CELLS

Kristine M. Porter, Ping Xu, W Daniel Stamer, Paloma B. Liton.
Ophthalmology-DUMC 3802, Duke Eye Center, Durham, NC.

Purpose: To evaluate the autophagic capacity in non-glaucomatous and glaucomatous trabecular meshwork (TM) cells.

Methods: Experiments were performed in primary cultures and transformed cell lines of non-glaucomatous and glaucomatous human TM cells grown to confluence under normal culture conditions. mRNA and/or protein expression levels of components of the autophagic lysosomal pathway (Atg3, Atg4, Atg5, Atg12, Beclin, p62, cathepsin D, cathepsin B, LAMP1, and TFEB) were quantified by qPCR and WB analyses, respectively. Autophagy dynamics were evaluated by monitoring the LC3-I to LC3-II conversion. Intralysosomal oxidized material, lysosomal content (LTR), and senescence-associated-β-galactosidase (SA-β-gal, FDG) were monitored by flow cytometry.

Results: Primary cultures of glaucomatous TM cells demonstrated decreased lysosomal content, but increased intralysosomal oxidized material and SA-β-gal activity compared to non-glaucomatous TM cells (LTR: 82±38.9 RFU versus 197.01±59.688; AF: 27.73±0.87 RFU versus 22.92±1.308; FDG: 89.38±18.68 versus 17.32±2.73; p<0.05). We also found a significant down-regulation of mRNA expression of LC3 (0.77 ± 0.06 fold), ATG4 (0.02 ± 0.001 fold), ATG7 (0.51 ± 0.07) and LAMP1 (0.33 ± 0.04) in glaucomatous compared to non-glaucomatous TM cells. However, no changes in the mRNA levels of beclin, LAMP2, and Atg5 were observed. At the protein level, glaucomatous TM cells showed a significant decrease

(>50 %) in the content of the lysosomal marker LAMP1, the lysosomal enzymes cathepsin B and cathepsin D, as well as the autophagosome marker LC3-II compared to control cells. A decrease in LC3-II and LAMP1 was also confirmed in the transformed glaucomatous cell line compared to the control cell line.

Conclusions: Our results indicate that (1) TM cells isolated from the glaucomatous outflow pathway retain in vitro the senescence phenotype observed in glaucomatous outflow tissue in vivo; and (2) glaucomatous TM cells display diminished autophagic capacity, characterized by lower levels of key protein participants of the autophagic lysosomal pathway, including LC3-II. Autophagy has been shown by our laboratory to be activated in response to oxidative and mechanical stress; therefore, we hypothesize that such diminished autophagic capacity in glaucomatous TM cells jeopardizes their ability to respond to stress, possibly contributing to the loss in cellularity observed in the outflow pathway in glaucoma.

Commercial Relationships: Kristine M. Porter, None; Ping Xu, None; W Daniel Stamer, Allergan (F), Alcon (F), Acucela (C), Aerie (C), Cytokinetics (C); Paloma B. Liton, None

Support: SUPPORT: NIH-R01EY020491, NIH-R21EY019137, NIH-EY022359, NIH-P30EY005722, AHAF G2012022, and Research to Prevent Blindness

Program Number: 3549 **Poster Board Number:** D0278

Presentation Time: 11:00 AM - 12:45 PM

Overexpression of SPARC Upregulates Gremlin and Proteoglycans Opticin & Decorin

Swarup S. Swaminathan, Dong-Jin Oh, Douglas J. Rhee. Dept. of Ophthalmology, Massachusetts Eye & Ear Infirmary, Boston, MA.

Purpose: We have shown that overexpression of Secreted Protein Acidic and Rich in Cysteine (SPARC), a matricellular protein known to modulate extracellular matrix (ECM) content, leads to increased intraocular pressure in human tissue. We thus attempted to identify potential mechanisms by which SPARC may induce ocular hypertension. Proteoglycans were the main targets investigated due to their role in ECM homeostasis. Bone morphogenetic protein-4 (BMP-4) and gremlin were also assessed due to their known modulation of TGF-β2 signaling.

Methods: Primary human trabecular meshwork (TM) cultures were derived from separate donors aged 12, 42, 44, 47, 57, 68, and 70 using a previously published protocol. TM cultures were allowed to grow to confluence at 37C in 10% CO2 atmosphere and then allowed 2-3 days to differentiate. For adenovirus infection, human TM cells were incubated in 2% FBS media with multiplicity of infection (MOI) 25 of Ad5.control or Ad5.hSPARC for 18 hours, after which 10% FBS media of an equal volume with 2% media were added for another 24 hours. TM cultures were incubated in serum-free media for 24 hours. Cultured TM cells were lysed in 1x radioimmunoprecipitation assay (RIPA) buffer or 1x Lysis Buffer with protease inhibitors. The serum-free conditioned media and cell lysates were then analyzed by immunoblot assays using antibodies against versican V0, versican V1, collagen XVIII, chondroitin-6-sulfate, decorin, opticin, fibromodulin, lumican, gremlin, and BMP-4.

Results: Immunoblot assays demonstrated that SPARC overexpression significantly upregulated opticin (25.87 ± 9.44%; n=4, p=0.038) and decorin (16.36 ± 3.43%; n=4, p=0.004). SPARC overexpression did not affect the levels of versican V0, versican V1, lumican (n=4), fibromodulin, collagen XVIII, and chondroitin-6-sulfate (n=3). Interestingly, SPARC overexpression significantly upregulated gremlin (32.32 ± 7.18%; n=3, p=0.012) but had no effect on BMP-4 level (n=4).

Conclusions: This study suggests that SPARC may modulate intraocular pressure through the proteoglycans opticin and decorin, as

well as gremlin. Decorin has been shown to be upregulated by TGF- β 2, and has also been found within SD plaque material in glaucomatous eyes. Both decorin and opticin are known regulators of collagen fibrillogenesis, which may affect aqueous humor outflow. Thus, SPARC may serve as an essential node in the TGF- β 2-mediated pathogenesis of primary open-angle glaucoma.

Commercial Relationships: Swarup S. Swaminathan, None; Dong-Jin Oh, None; Douglas J. Rhee, Alcon (C), Alcon (F), Allergan (C), Aquesys (F), Aquesys (C), Merck (F), Merck (C), Santen (C)

Support: Howard Hughes Medical Institute Medical Research Fellowship (SSS), NIH R01 EY 019654-01 (DJR), and NIH EY 014104 (MEEI Vision-Core Grant)

Program Number: 3550 **Poster Board Number:** D0279

Presentation Time: 11:00 AM - 12:45 PM

Multimodal Microscopy of Aqueous Drainage Channels in Live Mice

Jose M. Gonzalez, James C. Tan. Ophthalmology, University of Southern California, Los Angeles, CA.

Purpose: To non-invasively analyze the aqueous humor drainage channels of live mice by multimodal 2-photon excitation fluorescence (TPEF) imaging.

Methods: Anesthetized mice were carefully positioned so that the eye and corneoscleral limbus were accessible to a microscope objective (63X) on an objective inverter for upright TPEF microscopy. TPEF (850nm) was used to generate collagen-associated second harmonic generation (SHG) that was captured through a narrowband filter (425nm (+/- 10nm)). Wild-type C57BL/6 and BALB/c, and transgenic TIE-2-GFP (Tunica interna endothelial cell kinase, or Angiopoietin-1 receptor; BALB/c) and Prox1-GFP (lymphatic endothelial nuclear transcription factor; C57BL/6) mice were studied. RFP-conjugated dextran (70kDa) was injected intravenously prior to enucleation. For F-actin labeling, eyes were enucleated, fixed, permeabilized and incubated with Alexa-568-conjugated phalloidin overnight. Some eyes were frozen for histology.

Results: SHG revealed loosely arranged fine collagen fibrils in the conjunctival stroma. Just deep to the conjunctiva, sclera was identifiable by coarse collagen bands. In the intervening space were episcleral vessels (diameter < 5um) with phalloidin-labeled walls. Deep (5-10um) to this, lay a network of parallel interconnecting channels resembling an intrascleral plexus. The plexus was cell-lined, labeled with phalloidin and created scleral SHG signal voids. Yet deeper to the external surface (extending 15-40um), collector channels that were perpendicular and connected to the intrascleral plexuses opened via discrete ostia into a large channel (>100um in diameter) of Schlemm's Canal. Walls of collector channels and ostia labeled with phalloidin. These findings were confirmed by 3D reconstructions and histology. Dextran-RFP and Prox1-GFP were associated with intrascleral aqueous veins and Tie-2-GFP were associated with episcleral vessels.

Conclusions: Multimodal TPEF that exploited transgenic fluorescence was used to analyze the distal aqueous drainage channels with reference to collagen SHG in mice. 3D reconstruction provided stunning views of the in situ drainage tissue. Combined, these approaches could yield unique insights into mouse aqueous humor outflow biology.

Commercial Relationships: Jose M. Gonzalez, None; James C. Tan, None

Support: NIH EY020863; EY03040; 1S10RR024754; Kirchgessner Foundation Research Grant; Career Development Award from RPB; unrestricted RPB grant

Program Number: 3551 **Poster Board Number:** D0280

Presentation Time: 11:00 AM - 12:45 PM

Transcriptional Co-regulatory Patterns Associated with TNF α Treatment of Trabecular Meshwork Cells

Lauren Hayashi¹, Dongseok Choi², Kathryn Carr², Mary J. Kelley¹, Ted S. Acott¹. ¹Ophthalmology, Casey Eye Institute, Oregon Health and Science University, Portland, OR; ²Public Health and Preventive Medicine, Oregon Health and Science University, Portland, OR.

Purpose: TNF α is a key mediator of therapeutic effects of laser trabeculoplasty on glaucoma. In trabecular meshwork (TM) cells, matrix metalloproteinases initiate extracellular matrix (ECM) turnover in response to TNF α . To further understand this remodeling and its effects on aqueous humor outflow resistance, studies were conducted to identify transcription factor binding sites and regulatory pathways involved in TM gene expression patterns after TNF α treatment.

Methods: Primary porcine TM cells were treated with recombinant human TNF α (10ng/ml). Purified RNA was collected for gene expression profiling after 12, 24, and 48 hrs. After normalizing, Significance Analysis of Microarrays was used to identify differentially expressed genes with statistical significance defined as a q-value of less than 5%. TIGHTCLUST cluster analysis was used to group significant genes by temporal expression patterns. Fifty clusters were identified. Clusters up regulated at 24 and 48 hrs were evaluated using Metacore transcription factor network algorithms and the presence of pathway start or end nodes were determined. Clusters down regulated at 24 and 48 hrs were analyzed similarly. All resulting networks were assessed for ECM regulation themes.

Results: Genes in clusters down regulated by TNF α at 24 hrs implicate the canonical SMAD and non-canonical ERK TGF- β pathway, Wnt pathway and versican transcription. For TNF α treated clusters up regulated at 24 hrs, it appears carboxy terminal binding protein 1 (CtBP1) and APC sequester β -catenin, produced via JNK and c-Jun, mark it for ubiquitination and repress the Wnt pathway. TGF- β is up regulated through the non-canonical JNK pathway and could bind CD44-anchored SMAD2 or -3. CD44 may also bind hyaluronan, strengthening the cellular response to BMP-7. By 48 hrs BMP-7 is up regulated, antagonizing TGF- β , while CtBP still prevents β -catenin from activating the Wnt pathway. Meanwhile versican, Wnt, thrombospondin 1, fibronectin and fibrillin are associated with genes down regulated at 48 hrs after TNF α treatment.

Conclusions: Wnt and TGF- β contribute to ECM components and intraocular pressure (IOP) regulation. Previously we showed Wnt is active at 12 hrs (Hayashi, et al. ARVO 2012; 3250/A95.). By 24 hrs Wnt and some TGF- β pathways are deactivated. Full repression of TGF- β occurs by 48 hrs. Wnt is an early response mechanism while TGF- β has longer term effects on the ECM.

Commercial Relationships: Lauren Hayashi, None; Dongseok Choi, None; Kathryn Carr, None; Mary J. Kelley, None; Ted S. Acott, None

Support: NIH grants EY019935, EY008247, EY003279, EY010572 and Research to Prevent Blindness

Program Number: 3552 **Poster Board Number:** D0281

Presentation Time: 11:00 AM - 12:45 PM

Characterization of Sirtuin family protein expression in human trabecular meshwork cells

Ayan Chatterjee, Sarah S. Oh, Guadalupe Villarreal, Douglas J. Rhee. Department of Ophthalmology, Massachusetts Eye and Ear Infirmary, Cambridge, MA.

Purpose: The Sirtuin (Sirt) family of proteins is a group of NAD⁺-dependent deacetylases that have been associated with the regulation of aging in mammals. Their expression profile in human trabecular meshwork (TM) cells at baseline and under conditions associated with glaucoma pathogenesis have not yet been characterized. We examined whether the Sirt family of proteins would be expressed at detectable levels in primary cultured human TM cells and whether their expression profile may be altered in response to treatment with TGF- β 2 or dexamethasone.

Methods: Human TM tissues were isolated and primary TM cells were established from cadaveric donors ranging in age from 42 to 69. TM cell cultures were maintained in Dulbecco's modified Eagle medium (DMEM) containing 20% fetal bovine serum, 1% L-glutamine (2 mM), and gentamicin (10 μ g/mL) at 37°C in 10% CO₂ atmosphere. All experiments used TM cells in the fourth to fifth passage. TM cells were treated with either 3 ng/mL TGF- β 2 or equal volumes of 4 mM HCl vehicle, added directly to the culture media. TM cells were treated with 100 nM dexamethasone or equal volumes of 0.004% ethanol vehicle, added directly to the culture media. Integrated band intensities were calculated from immunoblots using LiCor Image Studio software and normalized using β -actin. Student t-tests were used for statistical analyses.

Results: All seven Sirt family proteins were detectable by immunoblot in human TM tissues (n=4) and also in cultured TM cells (n=4). Sirt family protein expression levels did not change significantly in 24-hour TGF- β 2-treated TM cells versus control cells (n=4). However, Sirt3 protein levels were increased by 20.02 \pm 4.68% (n=4; p=0.0052) in 24-hour dexamethasone-treated cells versus control cells. No other Sirt proteins showed statistically significant changes due to treatment with the specified conditions.

Conclusions: Our findings suggest that all seven Sirt family proteins are expressed in human TM. The baseline Sirt family expression profile does not change in response to 24-hour TGF- β 2 treatment but does change in response to dexamethasone treatment. In cultured human TM cells, 24-hour dexamethasone treatment increases Sirt3 protein levels.

Commercial Relationships: Ayan Chatterjee, None; Sarah S. Oh, None; Guadalupe Villarreal, None; Douglas J. Rhee, Alcon (C), Alcon (F), Allergan (C), Aquesys (F), Aquesys (C), Merck (F), Merck (C), Santen (C)

Support: Howard Hughes Medical Institute Student Research Fellowship, NIH R01 EY 019654-01 (DJR), and NIH EY 014104 (MEEI Vision-Core Grant)

Program Number: 3553 **Poster Board Number:** D0282

Presentation Time: 11:00 AM - 12:45 PM

In situ 3D Distribution of Filamentous Actin in Mouse Trabecular Meshwork

James C. Tan, Jose M. Gonzalez, MinHee K. Ko. Ophthalmology, Univ of Southern California, Los Angeles, CA.

Purpose: To determine the 3-dimensional distribution of filamentous (F-actin) in the mouse trabecular meshwork (TM) and ciliary muscle (CM) by multimodal 2-photon excitation fluorescence (TPEF) imaging.

Methods: Enucleated C57BL/6 and BALB/c eyes were fixed, permeabilized and incubated with Alexa-568-conjugated phalloidin to label F-actin. The limbus of the eye faced down on coverglass, allowing imaging by inverted TPEF using a 63X objective. Excitation wavelength of 850nm was used in combination with a narrowband filter (425nm \pm 10nm) for collagen-associated second harmonics generation (SHG), and wideband filter (635nm \pm 45nm) for red fluorescence. Corresponding frozen sections were labeled with phalloidin and antibodies against classic smooth muscle epitopes

(calponin, caldesmon, and α -smooth muscle actin (ASMA)) to identify CM.

Results: Collagen SHG imaging permitted localization of Schlemm's canal (SC) with reference to sclera in situ. With deeper scanning through SC, a structure was encountered with phalloidin labeling, consistent with TM or SC inner wall endothelium. Scanning through this structure showed phalloidin-associated fluorescence in an apparent cortical distribution in cells for 10-15 μ m before intensely phalloidin-labeled finger-like projections were encountered. These projections looked like muscle fibers, appeared to intermingle with labeled cells in the TM, and were oriented perpendicular to SC. Sagittal views of thin frozen sections revealed low intensity phalloidin labeling in the TM adjacent to SC, but phalloidin labeling in the CM was intense. Calponin, caldesmon and ASMA labeling in the TM was sparse and of low intensity, but labeling in the CM was intense and co-localized with phalloidin labeling.

Conclusions: Phalloidin F-actin labeling in the TM and CM of the intact mouse eye could be visualized by TPEF. TPEF and immunohistochemistry indicate an organization of TM sandwiched between SC and CM, wherein CM bundles appear to intermingle or insert into the TM region in mice.

Commercial Relationships: James C. Tan, None; Jose M. Gonzalez, None; MinHee K. Ko, None

Support: NIH EY020863; EY03040; 1S10RR024754; Kirchgessner Foundation Research Grant; RPB Career Development Award; unrestricted grant from the RPB

Program Number: 3554 **Poster Board Number:** D0283

Presentation Time: 11:00 AM - 12:45 PM

Effects of Calcitonin Gene Related Peptide on Bovine Trabecular Meshwork and Ciliary Muscle

Dai Ogino, Shun Watanabe, Yusuke Ohta, Kota Fujiwara, Takeshi Yoshitomi. Department of Ophthalmology, Akita University, Akita-shi, Japan.

Purpose: Calcitonin Gene Related Peptide (CGRP) localizes to trabecular meshwork (TM) and ciliary muscle (CM). Intracameral injection of CGRP increases the outflow facility in cat. Substance P (SP) co-localizes with CGRP in many nerve fibers. The purpose of this study is to investigate the effect of CGRP and SP on the contractility of bovine TM and CM by measurement of isometric tension recording methods.

Methods: Bovine eyes were obtained from a local slaughterhouse. A small piece of specimens were carefully dissected from an excised ciliary muscle bundle and trabecular meshwork. The preparation was vertically mounted in a small organ bath through which solution flowed at a constant rate. The tension was isometrically recorded using a U-gauge transducer.

Results: CGRP (30 nM) relaxed both bovine TM and CM which were precontracted by carbachol (2 μ M), while SP (1 μ M) had no effect. Pretreatment with CGRP 8-37 (100 nM), selective competitive antagonist at CGRP receptors, significantly attenuated the relaxation response on TM and CM.

Conclusions: Various agents may modulate the contractility of trabecular meshwork and may be actively involved in the regulation of intraocular pressure. We revealed that CGRP have a relaxing effect on contracted bovine TM and CM. These results indicate that CGRP binding sites are in bovine TM and CM. CGRP may have an important role to control aqueous humor dynamics.

Commercial Relationships: Dai Ogino, None; Shun Watanabe, None; Yusuke Ohta, None; Kota Fujiwara, None; Takeshi Yoshitomi, Santen (F), Pfizer (F), Alcon (F)

Program Number: 3555 **Poster Board Number:** D0284

Presentation Time: 11:00 AM - 12:45 PM

Stem Cells from Trabecular Meshwork Home to Damaged TM Tissue in vivo

Yiqin Du, Hongmin Yun, Enzhi Yang, Joel S. Schuman.

Ophthalmology, University of Pittsburgh, Pittsburgh, PA.

Purpose: We recently described a population of multipotent stem cells present in human trabecular meshwork (TM) tissue which can differentiate to functional TM cells in vitro and in vivo (Du et al, IOVS 2012; 53:1566). This study explored the hypothesis that these human trabecular meshwork stem cells (TMSCs) when introduced into the eye can home to damaged trabecular meshwork (TM) and will repair the tissue damage.

Methods: Human TMSCs were isolated and passaged as previously reported. Damage was produced in a 180° arc of the TM of adult C57BL/6 mice by laser photocoagulation using a 532nm green laser. After laser damage, 50,000 of either TMSCs or fibroblasts from human corneal stroma were injected into mouse anterior chamber. Cells were prelabeled with DiO before injection. Intraocular pressure (IOP) was measured regularly for 2 weeks after cell injection. DiO labeled cells were detected by confocal microscope on tissue wholemounts and cryosections. Expression of stem cell marker MUC1 or differentiated TM cell marker CHI3L1 was examined by immunostaining on wholemount or cryosections. Transmission electron microscopy was used to compare the TM with TMSC- and fibroblast-transplantation.

Results: Injection of human TMSCs did not increase recipient mouse IOP. Injected TMSCs localized specifically to the damaged TM region but not the unwounded TM or other normal tissues. In contrast, injected fibroblasts were detected in the TM, cornea and iris. Some injected TMSCs maintained expression of MUC1, whereas some differentiated into TM cells with expression of CHI3L1. TM tissue damage by laser photocoagulation was repaired by injected TMSCs. The damage to the TM was not recovered in mice with fibroblasts transplantation.

Conclusions: Human TMSCs have the ability to home to damaged TM tissue and adopt a TM phenotype, with the possibility of repairing damaged TM tissue. This opens a door for stem cell-based therapy for glaucoma.

Commercial Relationships: **Yiqin Du**, None; **Hongmin Yun**, None; **Enzhi Yang**, None; **Joel S. Schuman**, Carl Zeiss Meditec, Inc. (P)

Support: NIH Grants EY016415, P30-EY008098, Eye & Ear Foundation of Pittsburgh, Research to Prevent Blindness, an anonymous philanthropic donation.

Program Number: 3556 **Poster Board Number:** D0285

Presentation Time: 11:00 AM - 12:45 PM

Identification of TGF-β2-induced Proinflammatory Cytokines Secreted from Cultured Trabecular Meshwork Cells

Miyuki Inoue, Toshihiro Inoue, Tomokazu Fujimoto, Nanaka Awai-Kasaoka, Hidenobu Tanihara. Department of Ophthalmology, Kumamoto University, Faculty of Life Sciences, Kumamoto, Japan.

Purpose: To identify TGF-β2-induced proinflammatory cytokines secreted from trabecular meshwork cells.

Methods: Cultured human trabecular meshwork cells were treated with vehicle (control), 1.0, 2.5, or 5.0 ng/ml human recombinant TGF-β2 for 24 hours after over-night serum starvation, and conditioned media were collected. Levels of interleukin (IL)-1α, IL-1β, IL-6, IL-8, IL-10, monocyte chemoattractant protein (MCP)-1, tumor necrosis factor (TNF)-α, platelet-derived growth factor (PDGF)-AA, PDGF-AB/BB, and vascular endothelial growth factor (VEGF) were simultaneously determined by multiplex immunoassay. Each experiment was conducted in triplicate. The data were analyzed using

the Dunnett's multiple comparison test.

Results: IL-1α, IL-1β, TNF-α and VEGF were undetectable in any of the conditioned media. The mean levels (±SD) of IL-6, IL-8, IL-10, MCP-1, PDGF-AA and PDGF-AB/BB in the control condition were 6.8 ± 0.2, 3.0 ± 0.6, 1.8 ± 0.1, 19.3 ± 0.6, 1.2 ± 0.1 and 1.0 ± 0.2 pg/ml, respectively. After stimulation with TGF-β2, the levels of IL-6, IL-8 and PDGF-AA were significantly increased (P <0.001 for each) compared with control, while the levels of IL-10, MCP-1, PDGF-AB/BB were not different among conditions. The IL-6 levels were significantly increased by 4.2, 4.3 and 4.6 times after stimulation with 1.0, 2.5 and 5.0 ng/ml TGF-β2, respectively compared with control. The corresponding values for IL-8 were 1.9, 2.1 and 2.4. For PDGF-AA, those values were 5.9, 17.6 and 30.5, and the increase was dose-dependent (P <0.001).

Conclusions: TGF-β2 induced IL-6, IL-8 and PDGF-AA secretions from trabecular meshwork cells, suggesting that TGF-β2 may induce secondary proinflammatory responses in aqueous outflow tissues and thereby modulate glaucoma pathology.

Commercial Relationships: **Miyuki Inoue**, None; **Toshihiro Inoue**, None; **Tomokazu Fujimoto**, None; **Nanaka Awai-Kasaoka**, None; **Hidenobu Tanihara**, None

Support: JSPS KAKENHI Grant Number 23390403 and 23791994

Program Number: 3557 **Poster Board Number:** D0286

Presentation Time: 11:00 AM - 12:45 PM

Type I collagen-induced Epithelial Mesenchymal Transition-like Phenomenon in Trabecular Meshwork Cells

Ayako Fukushima, Eri Takahashi, Tomokazu Fujimoto, Sachi Kojima, Toshihiro Inoue, Hidenobu Tanihara. Ophthalmology, Kumamoto University, Kumamoto, Japan.

Purpose: To investigate the effects of type I collagen (Col I) on monkey trabecular meshwork (TM) cells.

Methods: TM cells were cultured on Col I-coated or uncoated dish in serum-free medium for 48 hours. Cell lysates were subjected to western blot assays with antibodies against epithelial or mesenchymal markers. Cell-cell adhesion was stained for β-catenin and images were gained by confocal fluorescence microscopy. The migratory ability was evaluated by the wound healing assay. Confluent monolayer was scratched by sterile tip and photographed at each time, and evaluated by the measuring the migration from the edge. The blots were quantified using Image J.

Results: TM cells showed epithelial-like island appearance on uncoated dish, and the same cells on Col I-coated dish demonstrated scattering phenotype. Western blot analysis showed the increased expression of mesenchymal markers (fibronectin (p=0.015), α-SMA (p=0.043), and phospho Smad2 (p=0.027)) induced by Col I. In contrast, similar experiments revealed decreased expression of an epithelial marker, occludin, under the stimulant of Col I. Confocal images of staining with β-catenin revealed linear staining at the cell-cell borders in TM cells on uncoated dish, and Col I-coating disrupted it. In addition, Col I enhanced cell motility in TM cells compared to controls (uncoated dish) (p=0.0053). Further, JNK inhibitor, SP600125, inhibited Col I-induced changes of mesenchymal phenotype, up-regulation of fibronectin (p=0.036) and high motility (p=0.0021).

Conclusions: Our findings indicated that the occurrence of EMT-like phenomenon caused by extracellular matrix in TM cells, suggesting the contribution of this phenomenon to the aberrant status in aqueous humor flow of glaucomatous eyes.

Commercial Relationships: **Ayako Fukushima**, None; **Eri Takahashi**, None; **Tomokazu Fujimoto**, None; **Sachi Kojima**, None; **Toshihiro Inoue**, None; **Hidenobu Tanihara**, None

Support: MEXT 12017015

Program Number: 3558 **Poster Board Number:** D0287

Presentation Time: 11:00 AM - 12:45 PM

Smad3 phosphorylation promotes Transforming Growth Factor- β 2 mediated expression of endothelin-1 in human trabecular meshwork cells

Cynthia L. Von Zee^{1,2}, Jonathan D. Lautz^{1,3}, Kelly Langert^{1,2}, Evan B. Stubbs^{1,2}. ¹Research Service (151), Loyola University Medical Center, Maywood, IL; ²Ophthalmology, Loyola University Chicago Stritch School of Medicine, Maywood, IL; ³Program in Neuroscience, Loyola University Chicago Stritch School of Medicine, Maywood, IL.

Purpose: In human trabecular meshwork (TM) cells, Transforming Growth Factor (TGF)- β 2 markedly enhances synthesis and secretion of the vasoactive peptide endothelin-1 (ET-1), in part, through activation of the canonical (Smad) signaling pathway. Here, we determined the role of Smad3 signaling in facilitating TGF- β 2 mediated enhancement of ET-1 expression in human TM cells.

Methods: Transformed human TM cells (GTM3) cultured in serum-free media were incubated in the absence or presence of Specific Inhibitor of Smad3 (SIS3; 10 μ M) followed by treatment with TGF- β 2 (5 ng/ml) for 30 min, 1h, 6h, or 24h. Relative changes in preproendothelin (ppET)-1 mRNA content and Smad3 phosphorylation were quantified by quantitative real-time PCR (qRT-PCR) and Western blot, respectively.

Results: Human TM cells cultured in the presence (5 ng/ml, 24h) of TGF- β 2 exhibit a marked, time-dependent, and sustained induction of Smad3 phosphorylation, compared to vehicle controls. Pre-treatment with SIS3 (30 min) attenuated Smad3 phosphorylation induced by TGF- β 2 (30 min). In marked contrast, Smad3 phosphorylation was enhanced in GTM3 cells treated (1h) with SIS3 prior to incubation with TGF- β 2 (6h, 24h). GTM3 cells treated with TGF- β 2 alone exhibited a marked (>9-fold), time-dependent significant increase in ppET-1 mRNA content by 6h. By comparison, GTM3 cells pre-treated (1h) with SIS3 followed by TGF- β 2 (6h, 24h) exhibited further enhancement of ppET-1 mRNA content compared to TGF- β 2 treated controls.

Conclusions: The selective inhibitor SIS3 effectively attenuates short-term (30 min) Smad3 phosphorylation. However, SIS3 enhances chronic, long-term (6h, 24h) Smad3 phosphorylation by TGF- β 2. Enhanced Smad3 phosphorylation markedly augments TGF- β 2 mediated increases in ppET-1 mRNA content in human TM cells. Elevated levels of TGF- β 2 present in AH of POAG patients may increase ET-1 synthesis in human TM cells by promoting activation of Smad3 signaling.

Commercial Relationships: Cynthia L. Von Zee, None; Jonathan D. Lautz, None; Kelly Langert, None; Evan B. Stubbs, None

Support: Department of Veterans Affairs (C3638R, B3756-F, C7506M), the Illinois Society for the Prevention of Blindness, the Midwest Eye Banks, and the Richard A. Peritt Charitable Foundation

Program Number: 3559 **Poster Board Number:** D0288

Presentation Time: 11:00 AM - 12:45 PM

Quantitative study of the trabecular meshwork and its relationship to the morphometry of the eye in the normal population using an anterior segment Fourier Domain OCT

José Fernández-Vigo López¹, José Ignacio Fernández-Vigo², CRISTINA FERNANDEZ-VIGO ESCRIBANO³, Jose M. Martinez de la Casa², Julian Garcia-Feijoo². ¹Ophthalmology, CIOA - UNIVERSIDAD DE EXTREMADURA, Madrid, Spain; ²Ophthalmology, Hospital Clinico San Carlos, Madrid, Spain; ³Centro de Oftalmología Barraquer, Barcelona, Spain.

Purpose: To study the size of the trabecular meshwork (TM) with anterior segment Fourier Domain OCT, and analyze its relationship with the morphometric variables of the eye in a normal population.

Methods: Prospective study of one eye from 320 consecutive healthy patients. We examined the patients with Pentacam®, IOL Master®, and anterior segment RTVue® (Optovue, California, USA) Fourier Domain OCT (AS-OCT). Images were obtained under standard light conditions, and when the signal strength intensity was greater than 30. Parameters evaluated included: age, sex, IOP, refractive error, axial length, pupil diameter and pachymetry. Anterior chamber (AC) parameters examined: depth, volume and diameter. Angle parameters examined: nasal and temporal width measured in degrees, angle opening distance (AOD), trabecular iris space area (TISA) and iris thickness; length, thickness and area of the trabecular meshwork (TM). Pearson correlation analysis was performed to study the correlation between the TM size and the rest of the variables.

Results: 37 patients (11.7%) were excluded because the TM could not be identified due to low image quality. The mean values of the population were: age: 45 \pm 14.2 years (range 19 to 84), IOP: 15.92 \pm 3.8 mmHg (range 8 to 26.4), sphere: -0.4 \pm 2.79 diopters (range -6.25 to 6.5), axial length: 23.91 \pm 1.51mm (range 20.03 to 29.14), AC depth: 3.42 \pm 0.43 mm (range 2.45 to 4.38), AC diameter: 11.93 \pm 0.39 mm (range 11 to 13), iris thickness: 412.6 \pm 88.88 microns (range 195 to 910), pupil diameter 2.96 \pm 0.62 (1.71 to 5.51), pachymetry: 549.01 \pm 32.96 microns (range 471 to 643). The mean temporal angle width was 38.8 \pm 12.7 degrees (range 14.5 to 78.2), AOD: 587.18 \pm 261.65 microns, (range 64 to 1440), TISA: 0.201 \pm 0.093 mm² (range 0.027 to 0.519). The mean area of TM was 0.067 \pm 0.023 mm² (range 0.023 to 0.126), with an average length of 536 \pm 130 microns (range 271 to 879) and an average thickness of 170 \pm 33 microns (range 83 to 267). There was no significant correlation between the TM size and any of the variables studied (r < 0.13). Cited correlations were statistically significant (p < 0.05%).

Conclusions: SA Fourier Domain OCT enabled us to analyze and measure the MT in 88.3% of eyes. Our results suggest that the TM size is not related with any ocular or general parameter studied.

Commercial Relationships: José Fernández-Vigo López, None; José Ignacio Fernández-Vigo, None; CRISTINA FERNANDEZ-VIGO ESCRIBANO, None; Jose M. Martinez de la Casa, None; Julian Garcia-Feijoo, Trancend (C), Ivantis (C), Glaukos (C), MSD (C), Allergan (F), Pfizer (F), Alcon (C), Sensimed (F), Sylentis (F), Bausch and Lomb (C)

Program Number: 3560 **Poster Board Number:** D0289

Presentation Time: 11:00 AM - 12:45 PM

Caveolins modulate ECM turnover by Trabecular Meshwork cells

Mini Aga, Kate E. Keller, John M. Bradley, Ted S. Acott. Ophthalmology, Casey Eye Institute, Oregon Health & Science University, Portland, OR.

Purpose: Caveolins (CAVs) are the principal structural components of caveolae. One role of CAVs is the endocytosis and recycling of extracellular matrix (ECM) components. SNPs identified near the CAV1/CAV2 gene loci, have been associated with primary open-angle glaucoma. Therefore, CAV-silencing lentivirus was generated to evaluate ECM uptake in TM cells and to measure the effect on outflow facility.

Methods: Studies were conducted using cultured primary human and porcine TM cells and perfused anterior segments. Short hairpin CAV1 and CAV2 silencing (shRNA) and control lentivirus were generated. Effects of CAV silencing on podosome- or invadopodia-like structures (PILS) component localization and ECM degradation were determined by confocal microscopy. Perfused anterior segments

were subjected to CAV shRNA to determine the effect on outflow facility.

Results: Both CAV1 and CAV2 colocalized with cortactin at PILS, areas of focal ECM degradation. Interestingly CAVs also colocalized with various ECM components including fibronectin (FN) and MMP2. CAV silencing effectively reduced protein expression of their respective CAVs in TM cells. A distinct increase in FN fibrils was observed upon CAV silencing as compared to control. Modest FN uptake vesicles were associated with CAV1 or CAV2 at 30 and 90 minutes after exposing TM cells to exogenous Rhodamine-labeled FN (rhodFN), and associated more strongly with clathrin and RAB7. CAV1 or CAV2 silencing also resulted in decreased expression of integrin beta1. Increased matrix degradation was observed in both CAV1 and CAV2 knockdown cells. MMP2 was colocalized with CAVs in TM cells. More ADAMTS4 vesicles were observed in CAV2-silenced cells and clustering of ADAMTS4-stained vesicles was seen in CAV1 knockdown cells. Outflow facility increased significantly in CAV1-silenced anterior segments, whereas a significant decrease was observed with CAV2-silenced eyes.

Conclusions: CAVs are co-localized with numerous ECM components at PILS in TM cells. CAV silencing changed the ECM composition and organization at PILS, which may explain in part the observed changes in outflow facility in perfusion culture following CAV silencing.

Commercial Relationships: Mini Aga, None; Kate E. Keller, None; John M. Bradley, None; Ted S. Acott, None
Support: NIH EY008247, EY003279, EY010572, EY019643, Research to Prevent Blindness

Program Number: 3561 **Poster Board Number:** D0290

Presentation Time: 11:00 AM - 12:45 PM

Artificial Simulation of Conventional Aqueous Humor Outflow Dynamics

EUN KYOUNG KIM, Edward R. Chu, Aleksandr Yelenskiy, Jose M. Gonzalez, James C. Tan. Department of Ophthalmology, Doheny Eye Institute, Keck School of Medicine, University of Southern California, Los Angeles, CA.

Purpose: To construct and test an artificial system to simulate, measure and better understand conventional outflow dynamics.

Methods: We constructed an artificial perfusion model with the following key components: 1) 50ul glass syringe on a microsyringe pump (representing aqueous inflow), 2) modified small caliber 35G needle to provide resistance (trabecular meshwork (TM) resistor), 3) 1-way valve (Schlemm's canal inner wall endothelium (SCIW) barrier), and 4) distal fluid column (episcleral venous pressure (EVP)), all connected in series via rigid tubing with 3 intervening pressure transducers (PT). PT#1 (representing intraocular pressure (IOP)) was connected between pump and needle, PT#2 (tissue pressure) between needle and valve, PT#3 (EVP) between valve and column. Needle resistance, pump flow rate calibration and valve cracking (opening) pressure were characterized separately. A voltage feedback loop between the pump and PT#1 was set up via an analogue voltage controller that allowed pump flow rate to vary automatically to maintain a pre-set constant perfusion pressure. Flow rate and all pressure data were simultaneously sampled at millisecond intervals and viewed in real time in LabChart software.

Results: Adjusted for valve cracking pressure, consistent pumping did not start until the pressure in PT#1 exceeded PT#3 (PT#1>PT#3), indicating no measureable outflow at IOP below EVP. For PT#1<PT#3, PT#1 equaled PT#2, but once PT#1>PT#3, PT#1 gradually exceeded PT#2 with the differential between PT#1 and PT#2 increasing with pressure, consistent with the effect of needle (TM) resistance. Once outflow was established when PT#1

(IOP)>PT#3 (EVP), increasing fluid column height so that PT#3>PT#1 caused the pump to stop, reflecting outflow cessation. In the absence of a valve (SCIW), a pressure differential could not be maintained between PT#1 (IOP) and PT#3 (EVP). In the absence of needle (TM) resistance, unrestricted pumping (outflow) occurred once PT#1 (IOP)>PT#3 (EVP).

Conclusions: The artificial model simulated physiological characteristics that may be predicted of the conventional outflow pathway. Physical features of system components could be altered, and effects of this observed and quantified directly. This model provides a platform for simulating and understanding physiological and pathological aspects of aqueous dynamics and improving analytical approaches for live animal studies.

Commercial Relationships: EUN KYOUNG KIM, None; Edward R. Chu, Edison Pharmaceuticals (F); Aleksandr Yelenskiy, None; Jose M. Gonzalez, None; James C. Tan, None

Support: I have no grants or support

Program Number: 3562 **Poster Board Number:** D0291

Presentation Time: 11:00 AM - 12:45 PM

Trabecular Meshwork Cell Expression of Two Novel Mucin Genes Located in the MHC Class I Locus

M Elizabeth Fini, Shinwu Jeong. USC Institute for Genetic Medicine, Keck School of Medicine of USC, Los Angeles, CA.

Purpose: Mucins, characterized by tandem repeats that serve as sites for O-glycosylation, are important to ocular surface health. Two novel mucin genes, PBMUCL1 (MUC22) and PBMUCL2 (HCG22), were recently identified in a mucin gene cluster within the MHC Class I locus on chromosome 6 (Hu Genet 129:117, 2011). We investigated expression in cells of the anterior segment.

Methods: We used two immortalized human cell lines: HCLE from corneal limbal epithelium and TM-1 from trabecular meshwork (TM). We also used primary TM cell lines isolated from human corneal rims. Cells were untreated or treated with agents linked to ocular hypertension: IL-1beta (10 ng/ml), the glucocorticoid (GC) triamcinolone acetonide (TA; 100 ng/ml), and TGF-beta (10 ng/ml). RT-PCR was used to determine mRNA expression. Statistical significance was determined by use of Student's t-test. FLAG or GFP-tagged cDNAs were cloned in the pcDNA3.1+ vector and expressed in TM-1 cells followed by fluorescence microscopy, subcellular fractionation and/or western blotting.

Results: HCLE cells express PBMUCL1 but not PBMUCL2; TM cells express both. IL-1 stimulates expression of both genes in TM cells, while TA inhibits basal and IL-1-stimulated expression. TGF-beta also inhibits expression. Conceptual translation indicates that PBMUCL1 mRNA encodes a plasma membrane-associated protein of 174 kDa and PBMUCL2 mRNA encodes a secreted protein of 26kDa. A cloned variant of PBMUCL1 cDNA with a truncated mucin repeat region (57 kDa), tagged with GFP (27 kDa) and expressed in TM-1 cells, enriches in the plasma membrane, migrating at ~ 200 kDa on westerns. FLAG-tagged PBMUCL2 cDNA is expressed as a ~40 kDa cytoplasmic form and a ~67 kDa secreted form. O-glycosylation predicted by sequence analysis explains the larger than expected sizes.

Conclusions: The expression of mucins by TM cells has not previously been considered to our knowledge. These experiments confirm that the novel mucin genes, PBMUCL1 (MUC22) and PBMUCL2 (HCG22), are regulated by agents associated with ocular hypertension and encode proteins translated in TM cells. Interestingly, an association between the MHC class I locus and ocular hypertension was reported more than 35 years ago (Science 194:1427, 1976). The presence of a mucin layer that collapses with tissue fixation would help reconcile the discrepancy between

measured outflow resistance and observed size of outflow pathway spaces.

Commercial Relationships: M Elizabeth Fini, None; Shinwu Jeong, None

Support: NIH Grant R01-EY09828; NIH Grant P30-EY003040; Research to Prevent Blindness unrestricted grant to Doheny Eye Institute

Program Number: 3563 **Poster Board Number:** D0292

Presentation Time: 11:00 AM - 12:45 PM

Effect of NaHS, a fast-releasing Hydrogen sulfide donor on Aqueous Humor Outflow in Porcine Trabecular Meshwork

Ya Fatou Njie-Mbye¹, Jenaye Robinson¹, Anita Okpobiri¹, Madhura Chitnis¹, Catherine A. Opere², Sunny E. Ohia¹. ¹Pharmaceutical Sciences, TX Sthrn Univ-Coll of Pharm & Hlth Sci, Houston, TX; ²Department of Pharmacy Sciences, Creighton University, Omaha, NE.

Purpose: Evidence from our laboratory demonstrates that hydrogen sulfide (H₂S) (using sodium hydrosulfide, NaHS as a generator of H₂S in biological tissues) can produce pharmacological effects in mammalian ocular tissues such as a decrease in intraocular pressure (IOP) in normotensive rabbits. In the present study we tested the hypothesis that the observed IOP-lowering effect of NaHS is mediated by an increase in aqueous humor outflow in porcine trabecular meshwork.

Methods: Porcine ocular anterior segments explants containing only the trabecular meshwork were mounted on a perfusion chamber and perfused with Dulbecco's Modified Eagle's Medium (DMEM) at constant pressure of 7.35 mmHg and maintained at 37°C, 5% CO₂. Once aqueous humor outflow was stable (~ 3 hours), ocular anterior segment explants were administered with different concentrations of NaHS (0.1 nM - 10 μM), and outflow was monitored for an additional 4 hours. Vehicle (0.1% saline) was run in parallel.

Results: The fast releasing H₂S donor, NaHS (0.1 nM - 10 μM) produced a concentration-dependent increase in aqueous humor outflow in ocular anterior segment explants. For instance, administration of NaHS (100 nM) caused a significant (*p*<0.01) enhancement [145 ± 14.61 % of basal (mean ± SE)] of aqueous humor outflow which lasted for an hour.

Conclusions: NaHS can increase aqueous humor outflow in porcine trabecular meshwork indicating a pharmacological role for H₂S in the regulation of IOP.

Commercial Relationships: Ya Fatou Njie-Mbye, None; Jenaye Robinson, None; Anita Okpobiri, None; Madhura Chitnis, None; Catherine A. Opere, None; Sunny E. Ohia, None
Support: NIH Grant EY022215-01

Program Number: 3564 **Poster Board Number:** D0293

Presentation Time: 11:00 AM - 12:45 PM

ZONULAR LIGAMENT DYSPLASIA IN BEAGLES WITH HEREDITARY PRIMARY OPEN ANGLE GLAUCOMA (POAG)

Leandro B. Teixeira¹, Erin M. Scott¹, Simone Iwabe³, Richard R. Dubielzig¹, Andras M. Komaromy^{2,3}. ¹Pathobiological Science, UW-Madison Sch of Vet Med, Madison, WI; ²College of Veterinary Medicine, Michigan State University, East Lansing, MI; ³School of Veterinary Medicine, University of Pennsylvania, Philadelphia, PA.

Purpose: To characterize the microscopic and ultrastructural morphology of the anterior uvea of Beagles with autosomal recessively inherited POAG due to a G661R missense mutation in the ADAMTS10 gene.

Methods: Four animals were analyzed, a 6-month old (6m/+) and a 3-year old (3y/+) non-affected dog heterozygous for ADAMTS10

mutation, and two age-matched affected dogs homozygous for the mutation (6m-/-; 3y-/-G); the older affected dog showed clinical signs of glaucoma. Animals were enucleated and globes processed for histology and transmission electron microscopy (TEM).

Results: Grossly the 3y-/-G animal presented markedly irregular ciliary processes. Both homozygous animals presented with thick and homogenous eosinophilic, PAS-positive and Masson's trichrome blue, proteinaceous material carpeting the ciliary body surface, consistent with collapsed dysplastic zonular ligaments. TEM showed a thick mat of dysplastic zonular ligament fibrils associated with markedly irregular and reduplicated basement membranes carpeting the surface of the ciliary body epithelium. The 3y-/-G animal also presented moderate disruption of the collagen fibers in the core of the trabecular meshwork beams. All animals presented normal scleral collagen.

Conclusions: The lesions are consistent with previously described zonular ligament dysplasia of terrier dog breeds affected by a mutation in ADAMTS17. Mutations in both ADAMTS10 and ADAMTS17 are responsible human Weill-Marchesani syndrome. The zonular and TM collagen lesions suggest the mutation impacts the metabolism of these proteins in the ocular tissues. Histological and TEM features of the trabecular meshwork are compatible with POAG and support the use of these animals as POAG model.

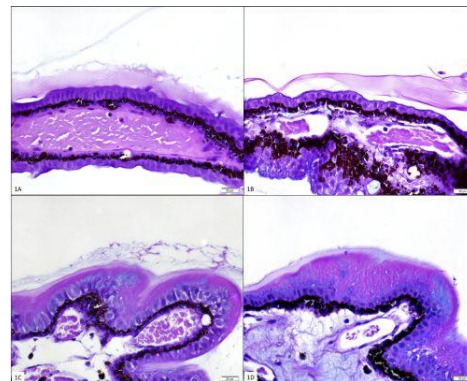


Fig. 1. Ciliary epithelium. A. 6m/+ B. 3y/+ Normal ciliary epithelium and zonules protein carpeting the epithelium surface. C. 6m/- and D. 3y-/-G. Homogenous, multi-laminated and eosinophilic proteinaceous material carpeting the ciliary body epithelium interpreted as collapsed dysplastic zonules. Alcian-blue PAS.

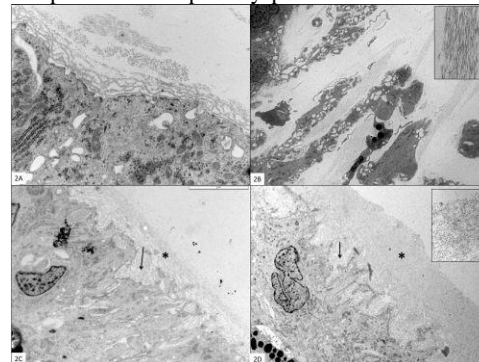


Fig. 2. TEM. A. 6m/+ and B. 3y/+. Normal epithelial cells with associated zonules and zonular fibers (2B inset). C. 6m/- and D. 3y-/-G. Epithelial cells with markedly duplicated basement membranes (arrow) and thick mat of dysplastic zonular fibrils carpeting the cell surface (* and 2D inset).

Commercial Relationships: Leandro B. Teixeira, None; Erin M. Scott, None; Simone Iwabe, None; Richard R. Dubielzig, OSOD, LLC (I), Allergan (C); Andras M. Komaromy, None
Support: University of Pennsylvania Research Foundation, NIH grant P30EY001583, and an unrestricted gift from Edward Sheppard and family.

Program Number: 3565 **Poster Board Number:** D0294

Presentation Time: 11:00 AM - 12:45 PM

Overexpression of GPR158, an Orphan Member of G Protein-Coupled Receptor Family C, Mimics Effects of Glucocorticoids on Trabecular Meshwork Cells

Nitin L. Patel¹, Tatsuo Itakura¹, M Elizabeth Fini^{1,2}. ¹Institute for Genetic Medicine, Keck School of Medicine of USC, Los Angeles, CA; ²Cell & Neurobiology, Keck School of Medicine of USC, Los Angeles, CA.

Purpose: Administration of glucocorticoids (GCs) causes spiking of intraocular pressure in a subset of patients due to a reduction in aqueous outflow facility. GPR158 is expressed in trabecular meshwork (TM) cells of the conventional outflow pathway and transcription is stimulated by GCs (ARVO, Patel et al., 2011). We investigated the possible role of GPR158 in controlling TM cellular activities known to be affected by GCs.

Methods: We used the immortalized TM-1 cell line and primary TM cells isolated from discarded human eye tissue. GPR158 cDNA was cloned into two mammalian expression vectors: pcDNA 3.1(+) and pEGFP-C1, the latter generates C-terminus GFP fusion with GPR158. TM barrier function was quantified using the In Vitro vascular permeability assay, which measures permeability of a confluent cell monolayer to FITC-dextran.

Results: Similar to treatment with GCs, transient overexpression of GPR158 in TM cells increased the rate of cell proliferation (4-fold), and significantly enhanced TM barrier function. Conversely, siRNA knockdown of endogenous GPR158 inhibited cell proliferation (barrier function studies in progress). GPR158 overexpression was accompanied by elevated expression of cyclin D1 and the intercellular tight junction proteins, ZO-1 and occludin. Both endogenous and overexpressed GPR158 protein localized to punctate structures in the nucleus of TM cells. Significantly, overexpressed GPR158 protein was shifted entirely to the plasma membrane when TM cells were treated with inhibitors of clathrin-mediated endocytosis (concanavalin A or chlorpromazine). Mutation of a nuclear localization signal (NLS) in the 8th helix of GPR158 also shifted the protein out of the nucleus, but not to the plasma membrane, instead found within discrete vesicles under the plasma membrane. These results suggest that newly synthesized GPR158 traffics to the plasma membrane of TM cells, where it is rapidly internalized in endocytic vesicles for translocation to the nucleus. Importantly, GPR158 stimulation of TM cell proliferation was completely abrogated by failure to translocate to the nucleus (barrier function studies in progress).

Conclusions: TM cell overexpression of nuclear localized GPR158 mimics the effects of GCs. Pharmaceutical-assisted retention of GPR158 at the plasma membrane may be a novel strategy to treat GCs-induced ocular hypertension.

Commercial Relationships: Nitin L. Patel, None; Tatsuo Itakura, None; M Elizabeth Fini, None

Support: NIH grants R01-EY09828, P30-EY003040; Unrestricted grant from Research to Prevent Blindness to Doheny Eye Institute

Program Number: 3566 **Poster Board Number:** D0295

Presentation Time: 11:00 AM - 12:45 PM

Extracellular Matrix Gene Expression Profiling of High and Low Flow Areas of Human Trabecular Meshwork

Janice A. Vranka, Kate E. Keller, Ted S. Acott. Ophthalmology, Casey Eye Inst/Oregon Hlth & Sci Univ, Portland, OR.

Purpose: Several studies have shown that aqueous humor outflow is segmental, rather than uniform, around the circumference of the trabecular meshwork (TM). Extracellular matrix (ECM) composition is thought to not only vary in localized areas of high or low outflow, but also to respond differently to external stimuli thus affecting relative outflow rates. The purpose of this work was to identify ECM genes that display segmental differences in expression levels and which change in response to increased pressure in both low and high flow areas of the TM.

Methods: Human donor eyes were perfused at 1x and 2x pressure in vitro using anterior segment perfusion organ culture. Fluorescent amine-modified microspheres (200nm diameter) were injected into anterior segments during perfusion. Relative intensity of fluorescence was used to visualize and separate low and high flow areas of the TM. RNA was isolated and quantitative PCR arrays were used to identify ECM and adhesion gene differences in high and low flow areas of the TM from respective regions of perfused eyes.

Results: Differences in fold regulation of ECM genes, including MMPs, proteoglycans, integrins, and cell adhesion molecules were seen when comparing low and high flow areas of the TM both at physiological and elevated pressures. MMPs and SPARC were among the genes that were up-regulated in high flow regions under physiological conditions. At 2x pressure versican was one of the major genes up-regulated in high flow regions, in comparison with low flow regions at the same pressure conditions. A variety of genes were down-regulated in high flow regions in comparison with low flow regions at both 1x and 2x pressures, including integrins, cell adhesion molecules and collagens. Among the multiple genes that changed in strictly low or strictly high flow regions in response to elevated pressures were versican and SPARC, whose expression levels were inversely correlated to each other. This suggests a differential response to increased pressure in low and high flow regions of the TM.

Conclusions: Here we have shown differences in mRNA levels of several ECM genes in low and high flow areas of the TM at physiological and elevated pressures. These results provide further evidence for segmental differences in ECM composition that may in turn influence aqueous outflow resistance in the TM.

Commercial Relationships: Janice A. Vranka, None; Kate E. Keller, None; Ted S. Acott, None

Support: NIH EY008247 (TSA), EY010572 (TSA), EY019643 (KEK)

Program Number: 3567 **Poster Board Number:** D0296

Presentation Time: 11:00 AM - 12:45 PM

Oxidative Stress Impacts On Barrier Function of Porcine Angular Aqueous Plexus Cell Monolayers

Yuan Lei¹, W Daniel Stamer², Jihong Wu¹, Xinghuai Sun³. ¹Research Centre, Eye and ENT hospital, Shanghai, China; ²Ophthalmology, Duke University, Durham, NC; ³Ophthalmology, Eye and ENT hospital, Shanghai, China.

Purpose: Our goal was to model aging and to investigate the effects of oxidative stress on angular aqueous plexus (AAP) endothelial cells isolated from porcine eyes. AAP is the porcine equivalent of human Schlemm's canal (SC). Our hypothesis is that oxidative stress would impact AAP cell barrier function.

Methods: Cells were differentially isolated from porcine outflow tissues using puromycin treatment. Cultures of porcine AAP cells were grown for 2 weeks in physiological (5% O₂) or hyperoxic

conditions (40% O₂). Cell growth rate, size, transendothelial electrical resistance (TEER), hydraulic conductivity (HC) were measured. The expression of ageing marker SA-galactosidase was monitored, and the expression levels of cytoskeletal and barrier proteins such as F-actin, phospho-myosin light chain (phospho-MLC), occludin, claudin, ZO-1, beta-catenin and VE-cadherin were measured by immunofluorescence staining and western blot analysis.

Results: Our data showed that chronic hyperoxia inhibited cell growth rate from day 3 onward, the cell size increased by $18.2\% \pm 5.1\%$, and cells stained positive for SA-gal. Hyperoxia resulted in a significant increase of TEER compared with the control group from day 10 onward ($p < 0.05$, $n = 6$). When perfused in the basal-to-apical direction, at 4 mmHg, HC of AAP cells was 1.97 ± 0.12 and 1.54 ± 0.13 uL/mmHg/min/cm² in control and hyperoxia group, respectively ($p < 0.05$, $n = 6$). Upon examining cells more closely by immunofluorescence staining, stressed cells expressed a greater abundance of F-actin, phospho-MLC, occludin, claudin-5, beta-catenin and VE-cadherin comparing to the control group ($n = 6$). At the site of cell-cell contact, we also observed increased expression of F-actin, beta-catenin and VE-cadherin. Western blot confirmed an overall higher level of expression of phospho-MLC, occludin, claudin-5, ZO-1, beta-catenin and VE-cadherin in the high oxygen group compared with control.

Conclusions: Chronic exposure of AAP cells to oxidative stress decreased cell monolayer permeability and up-regulated cytoskeletal and cell-cell adhesion protein expression; suggesting that with age and increased oxidative stress, resistance at the level of Schlemm's canal in humans also increases.

Commercial Relationships: Yuan Lei, None; W Daniel Stamer, Allergan (F), Alcon (F), Acucela (C), Aerie (C), Cytokinetics (C); Jihong Wu, None; Xinghuai Sun, None

379 Perimetry II

Tuesday, May 07, 2013 2:45 PM-4:30 PM

Exhibit Hall Poster Session

Program #/Board # Range: 3914-3966/D0202-D0254

Organizing Section: Glaucoma

Program Number: 3914 **Poster Board Number:** D0202

Presentation Time: 2:45 PM - 4:30 PM

A method to identify the edge of visual field scotoma; the estimation of prediction error of the visual field sensitivity is large at the steep 'edge' of scotoma

Yuka Aoyama, Hiroshi Murata, Mayumi Tahara, Mieko Yanagisawa, Chihiro Mayama, Ryo Asaoka. University of Tokyo Graduate School of Medicine, Tokyo, Japan.

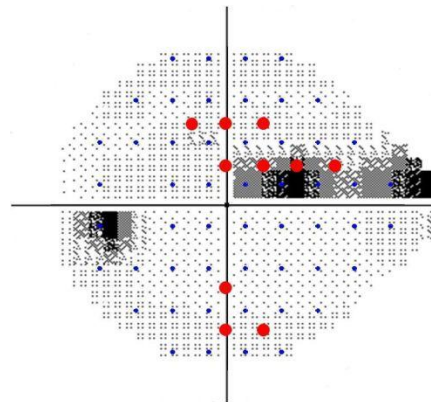
Purpose: Humphrey 24-2 visual field (VF) test grid has a spatial gap, since each test point is located six degrees apart. The purpose of this study was to create a method to identify the edge of VF scotoma and to investigate the relationship between the steepness of the 'edge' of scotoma and the prediction error of VF sensitivity.

Methods: Eleven clinically stable glaucomatous patients with reliable VFs were recruited. Then, using the latest VFs (Humphrey 24-2) of these patients, the gradient of the plane on the hill of vision from the sensitivity of adjacent four/three points is calculated, so that the 'edge' of VF damage is identified. Next, VF measurement was carried out, adding ten test points at the centre of adjacent four/three points (red circle, Figure 1) where the gradient of the plane is largest (Full threshold, Custom mode). The VF measurements were performed using two approaches; random target presentation of 62 test points together and showing ten added points following or prior (randomly selected) to 52 (24-2) points. Each measurement with each

approach was repeated twice (in total four measurement for a patient) in a same visit. Then, the absolute value of the difference between the measured sensitivity of the added ten test points and the average of the sensitivities of surrounding three/four test points were calculated. Finally, the relationship between the gradient of sensitivity plane and the absolute difference was investigated using the multiple level modeling (MLM).

Results: MLM revealed significant relationship between the absolute difference and the gradient of plane with all of the four measurements ($p < 0.05$).

Conclusions: The discrepancy between the estimated sensitivity from the surrounding test points and the actually measured sensitivity at the gap in the 24-2 grid became large where the edge of scotoma is steep. It may be advantageous to increase the spatial information by carrying out additional measurement at these areas, in order to estimate scotoma more accurately.



Commercial Relationships: Yuka Aoyama, None; Hiroshi Murata, None; Mayumi Tahara, None; Mieko Yanagisawa, None; Chihiro Mayama, None; Ryo Asaoka, None

Program Number: 3915 **Poster Board Number:** D0203

Presentation Time: 2:45 PM - 4:30 PM

Exploration of the Dynamic Range of the Moorfields MDT to Assess Suitability to Monitor Glaucoma

Marco A. Miranda¹, Gay M. Verdon-Roe¹, Ciara Bergin¹, Tony Redmond¹, David P. Crabb², David F. Garway-Heath¹. ¹National Institute for Health Research (NIHR) Biomedical Research Centre, Moorfields Eye Hospital NHS Foundation Trust and UCL Institute of Ophthalmology, London, United Kingdom; ²Optometry and Visual Science, City University London, London, United Kingdom.

Purpose: To compare the dynamic range between stimuli employed in Standard Automated Perimetry, SAP, and in the Moorfields Motion Displacement Test, MMDT.

Methods: Frequency-of-seeing curves (FOS) were obtained from data collected at 8 locations of the visual field (VF) in 23 subjects with a range of pointwise sensitivities (0 - 35dB on the Humphrey VF analyzer, Carl Zeiss Meditec., SITA-Standard). Four locations of the VF in one eye per subject were tested. The method of constant stimuli was used for both SAP- and MMDT-like stimuli with 15 bins and 8 presentations per bin used to build the FOS curve. SAP was performed using Goldmann size III stimuli presented for 200msec. For the MMDT, vertical lines of areas ranging from 0.27 to 6.10mm², depending on eccentricity, oscillated for 600msec. Both types of stimuli were presented on an EIZO GS521 monochromatic monitor (0.17mm/pixel) using the MMDT software (v.1.8.3). The Psignifit toolbox (v.3.0) was used to plot the curves and estimate the 50%-seen threshold. Results were analyzed using a multiple linear regression

analysis (least squares).

Results: SAP and MMDT thresholds were calculated from 184 FOS curves with truncation effects observed less frequently in SAP (7 cases) than in MMDT (19 cases). MMDT thresholds were measured across the range of SAP sensitivities from 36.8 to 7.8dB. The relationship between the two scales is significantly dependent (adjusted $R^2 = 0.76$, p -value = 0.003; Figure 1) on the MMDT stimulus area and can be described by the formula:

$$Threshold_{SAP} = -0.65 \times Threshold_{MMDT} - 0.63 \times stimulus\ area + 36.61 \text{ (Eq.1)}$$

Conclusions: A strong linear association between the values obtained with SAP and the MMDT was observed. Motion displacement threshold increased as VF sensitivity reduced. Although truncation of the FOS curves was more frequent with the MMDT, thresholds derived from staircase, as in clinical perimetry, would be more robust at this end of the scale. The results suggest that the MMDT has the potential to be used for monitoring glaucoma deterioration.

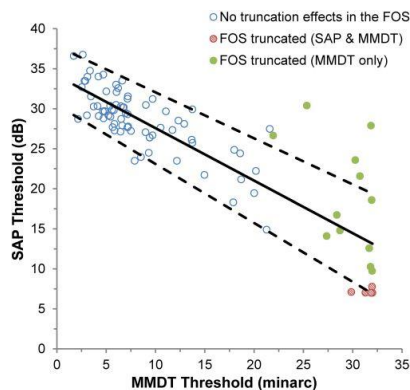


Figure 1: Relationship between thresholds (measured or projected 50%-seen level on the FOS curve) obtained with SAP (vertical axis) and the MMDT (horizontal axis) at the 8 locations tested. Solid line represents the multiple linear regression line (Eq.1) and dashed lines represent the 95% confidence intervals of the equation.

Commercial Relationships: Marco A. Miranda, None; Gay M. Verdon-Roe, Moorfields MDT (P); Ciara Bergin, Moorfields MDT (P); Tony Redmond, None; David P. Crabb, Allergan Inc. (R), Moorfields MDT (P); David F. Garway-Heath, Moorfields MDT (P), Carl Zeiss Meditec (F), Heidelberg Engineering (F), Reichert Technologies (F), Ziemer Ophthalmic Systems AG (F), Pfizer Inc (F), Allergan (F), Allergan (C), Allergan (R), Alcon (C), Alcon (R), Bausch & Lomb (R), Merck (R), Santen (R), Quark (C), Teva (C), Topcon (F), OptoVue (F)

Support: Funded by the NIHR Moorfields Biomedical Research Centre and the Special Trustees of Moorfields Eye Hospital (code: ST 10 05 D)

Program Number: 3916 **Poster Board Number:** D0204

Presentation Time: 2:45 PM - 4:30 PM

Reclaiming the Periphery - Frequency of Seeing for Static Automatic Perimetry on Peripheral Isopters for Patients with Glaucoma and Healthy Controls

Vera M. Mønter^{1,2}, David P. Crabb², Paul H. Artes¹. ¹Optometry and Visual Science, City University London, London, United Kingdom; ²Ophthalmology and Visual Sciences, Dalhousie University, Halifax, NS, Canada.

Purpose: Clinical visual field (VF) tests often focus on the central 30°; an area that neglects more than 80% of a person’s overall VF. However, vision in the far periphery is important for mobility, balance and guidance of attention. Our goal is to establish an

automatic kinetic test for the peripheral VF (PVF), complementing standard automated perimetry of the central 30°. We test the hypothesis that there is a consistent relation between responses to static and kinetic stimuli in glaucoma patients and healthy controls allowing us to link both approaches.

Methods: PVFs of 15 patients (Mean age: 60 years, MD: -7.2 dB) with glaucoma and 15 controls (Mean age: 39 years) were examined with a fully automated kinetic test on the Octopus 900 (HAAG-STREIT). Stimuli with intensity of 15 dB (IIIe) were presented moving at 5°/sec along 16 meridians (Fig1). The median response of three presentations was chosen to define the isopter. As a global measure for PVF defects we defined the mean isopter radius deviation (MIR dev) - the difference of the MIR and the MIR of the age matched normative isopter (Vonthein et al., 2007). For a subgroup of 7 patients and 11 controls frequency of seeing (FOS) curves to size III static stimuli (200ms) were measured at five locations on the isopter (Fig1). Psychometric functions were fitted to determine the sensitivity (50% seeing).

Results: The FOS showed a lower sensitivity for static [median (m): 11.8 dB, 95% CI: 11.3, 12.2] than expected from the kinetic stimuli (15 dB). The difference in sensitivity was similar for controls [m: 12.1 dB, 95% CI: 11.4, 12.7] and glaucoma patients [m: 11.3 dB, 95% CI 10.8, 11.9] (Fig2) and was independent of location, age and eccentricity. MIR dev and MD of the central VF were not closely related [$r^2 = 0.35$].

Conclusions: FOS data reveals a consistent difference between static and kinetic sensitivity in glaucoma patients and controls at isopter locations. Despite the different measurement acquisition, both approaches can therefore be combined to measure the peripheral and central VF. A difference in the extent of VF loss in central and peripheral areas may explain the low association between MIR dev and MD in glaucoma patients.

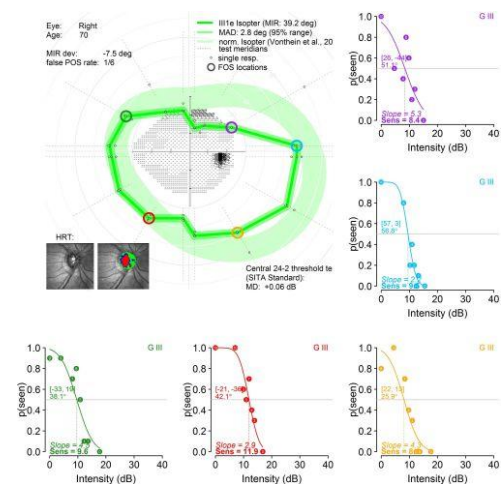
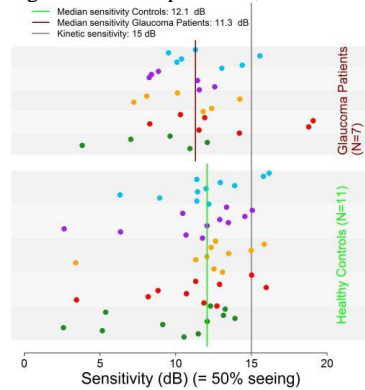


Fig1: Case example: PVF, CVF and FOS.



Commercial Relationships: Vera M. Mönter, None; David P. Crabb, Allergan Inc. (R), Moorfields MDT (P); Paul H. Artes, Heidelberg Engineering, Germany (C), Haag-Streit AG, Switzerland (C), Carl Zeiss Meditec, Germany (C), Optovue Inc, CA, USA (C), Peridata GmbH, Germany (F)

Program Number: 3917 **Poster Board Number:** D0205

Presentation Time: 2:45 PM - 4:30 PM

Mechanisms Underlying Frequency-Doubling Technology (FDT) in Glaucoma

Michele D. Lee¹, James Wielaard¹, Jennifer H. Acton^{1,3}, Sucharita Boddu¹, Sung Chul Park², Jeffrey M. Liebmann^{1,2}, Roland Smith¹.

¹Ophthalmology, New York University, New York, NY;

²Ophthalmology, New York Eye and Ear Infirmary, New York, NY;

³School of Optometry and Visual Sciences, Cardiff University, Wales, United Kingdom.

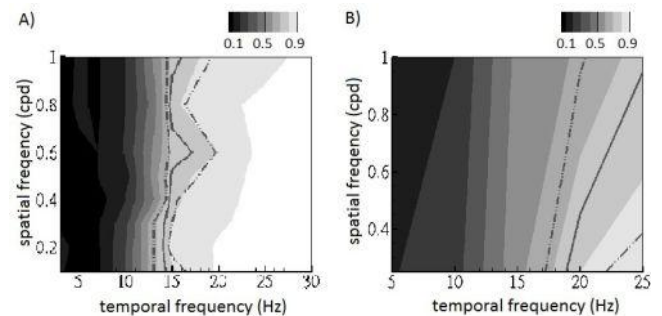
Purpose: The mechanism of the frequency doubling illusion (FDI) and FDT remain uncertain. FDT perimetry such as the Humphrey Matrix FDT (Carl Zeiss Meditec) uses flickering gratings that presumably elicit the FDI for enhanced detection of glaucoma, but has not definitely been shown superior to the current reference standard, SITA-SAP. Patients supposedly perceive the FDI in the test, but this is not verified. To better understand FDT, we present a study comparing the perception of the FDI in normal subjects and subjects with glaucoma.

Methods: We examined 8 normal subjects (19-31 years) and 8 subjects with mild to moderate primary open-angle glaucoma (26-86 years). Experiments consisted of a monocular two-alternative forced-choice task. A high-contrast counterphase grating of varied spatial and temporal frequencies was briefly presented, followed by 2 static matching stimuli at veridical and doubled spatial frequencies. The task was to choose the one best resembling the counterphase grating. Static stimuli were viewed centrally and presented in a random order.

Results: Average psychometric functions are shown in Fig 1. Perception of the FDI by normal subjects shows little dependence on spatial frequency; subjects with glaucoma show some dependence. Strikingly, subjects with glaucoma perceive the FDI at much higher temporal frequencies than normal subjects. Although our data are preliminary, this result seems significant, as the mean frequencies are approximately 2 standard deviations apart.

Conclusions: Our results imply that individuals with glaucoma are less subject to the FDI than normal subjects, as they maintain "correct" perception over a broader temporal frequency range. However, perception of the FDI in general tends to be accompanied by enhanced contrast perception. This suggests that the diminished perception of the FDI by patients with glaucoma results from impaired contrast threshold relative to normal subjects; this may be the mechanism for glaucoma detection by FDT. This interesting

observation merits further investigation, with future observations including age-matched controls and careful perimetric testing of the FDI itself in search of early diagnosis of glaucoma.



Psychometric functions averaged for normal subjects (A) and subjects with glaucoma (B). Lighter shades represent a higher probability of seeing the illusion. Solid lines represent 0.75 probability of seeing the illusion; dashed lines represent ± 1 SD.

Commercial Relationships: Michele D. Lee, None; James Wielaard, None; Jennifer H. Acton, None; Sucharita Boddu, None; Sung Chul Park, None; Jeffrey M. Liebmann, Alcon Laboratories, Inc. (C), Allergan, Inc. (C), Allergan, Inc. (F), Carl Zeiss Meditec, Inc (F), Heidelberg Engineering, GmbH (F), Topcon Medical Systems, Inc. (F), National Eye Institute (F), New York Glaucoma Research Institute (F), SOLX, Inc. (C), Bausch & Lomb, Inc (C), Diopsys, Inc. (C), Diopsys, Inc. (F), Merz, Inc. (C), Glaukos, Inc. (C), Quark, Inc. (C); Roland Smith, None
Support: Research to Prevent Blindness (MDL, New York University Department of Ophthalmology), NEI R01 EY021470 (RTS)

Program Number: 3918 **Poster Board Number:** D0206

Presentation Time: 2:45 PM - 4:30 PM

The Effects of Trabeculectomy on the Fast and Slow Components of Visual Field Rates

Parham Azarbod^{1,2}, Kouros Nouri-Mahdavi², Esteban Morales², Fei Yu², Abdelmonem Afifi², Anne L. Coleman², Joseph Caprioli².

¹Ophthalmology, Moorfields Eye Hospital, London, United Kingdom; ²Ophthalmology, Jules Stein Eye Institute, Los Angeles, CA.

Purpose: To investigate the effects of trabeculectomy on the fast and slow components of visual field (VF) rates using two pointwise regression techniques.

Methods: Open-angle glaucoma patients with five or more reliable visual fields prior to and following trabeculectomy were included. Pointwise VF location rates were determined by using exponential and linear regressions. The visual field rates were partitioned into a faster and a slower component using a technique described recently. The rates (regression slope) of the identified locations within each of the two components were then analyzed for changes between the preoperative and postoperative periods. The "units" for Pointwise Exponential Regression (PER) rates prior to and post trabeculectomy were "%/year" and for linear regressions were "dB/year". The findings were then compared with the effects of surgery on the MD (using linear regression) of the visual fields.

Results: Seventy eight patients (96 eyes) were analyzed. The average follow up and number of visual fields (+SD) were 5.3 (± 3.01) years and 11.29 (± 8.67) prior to and 5.97 (± 2.82) years and 10.15 (± 5.46) post trabeculectomy, respectively. The average (\pm SD) fast rate with PER prior to surgery was 31.5 (± 32.8) %/year (-1.26 ± 1.42 dB/year with linear regression) and this slowed to 5.6 (± 35.8) %/year (-0.24 ± 1.10 dB/year with linear regression) ($p < 0.001$) after trabeculectomy.

ARVO 2013 Annual Meeting Abstracts by Scientific Section/Group – Glaucoma

The average (\pm SD) slow rate with PER before surgery was -8.6 (± 17.8) %/year ($+0.54 \pm 1.32$ dB/yr; using linear regression) and this increased to 5.0 (± 18.8) %/year (-0.09 ± 1.02 dB/year; using linear regression) ($p < 0.001$) after surgery. The MD rate of decay also showed a slowing down from -0.58 (± 1.26) dB/year to 0.20 ± 1.193 dB/year ($p < 0.001$)

Conclusions: Trabeculectomy has a differential effect on the slow and fast components of VF's. The progression rate of the fast component of VF decay is significantly slowed while the slow component rate is slightly increased. These differential effects of filtration surgery may be diminished or masked when global indices are used to assess outcomes, and could lead to an underestimation of the beneficial effects of surgical treatment of glaucoma.

Commercial Relationships: Parham Azarbod, None; Kouros Nouri-Mahdavi, Allergan (C); Esteban Morales, None; Fei Yu, None; Abdelmonem Affifi, None; Anne L. Coleman, None; Joseph Caprioli, Allergan Inc. (C), Allergan Inc. (F), Allergan Inc. (R)

Program Number: 3919 **Poster Board Number:** D0207

Presentation Time: 2:45 PM - 4:30 PM

The Effect of Eccentricity on the Test-Retest Characteristics of Standard Automated Perimetry in Glaucoma

Sarah L. Bishop¹, Yuan-Hao (Derek) Ho¹, Deborah Goren², John G. Flanagan^{1,3}. ¹School of Optometry and Vision Sciences, University of Waterloo, Waterloo, ON, Canada; ²Devers Eye Institute, Legacy Research Institute, Portland, OR; ³Ophthalmology and Vision Science, University of Toronto, Toronto, ON, Canada.

Purpose: To study the effect of perimetric eccentricity on the test-retest characteristics in participants with early to moderate glaucoma.

Methods: The sample consisted of 161 participants with early ($n=135$) to moderate ($n=26$) glaucoma. Each participant was experienced at perimetry and underwent 2 standard automated perimetry tests (SAP) within 8 weeks, using the Heidelberg Edge Perimeter (HEP; ASTAStd, size III, 24-2). The visual field was divided into 3 zones (central 10°, 10-16°, and 16-25°) with each zone additionally divided into upper and lower hemifields (6 zones in total). All blindspot locations were removed and 0dBs were additionally removed in consideration of the floor effect. Threshold values were analyzed as a function of concentric zone, hemifield and visit. Test/ re-test characteristics (taken as visit 1 - visit 2) for each zone and hemifield were analyzed using scatter plots and Bland and Altman (B-A) plots. Effects of visual field location, hemifield and visit were analyzed with repeated measures ANOVA ($p < 0.05$).

Results: There was a significant effect by zone ($p < 0.001$), sensitivity reducing with eccentricity, but not between visits ($p = 0.434$). There was also a significant difference between hemifields, with the lower hemifields showing higher sensitivity ($p < 0.001$), but no interaction between hemifield and visit ($p = 0.639$). The mean of differences (MoD) between visits ranged between -0.02 and -0.15 dB, showing a small, but non-significant learning effect. The B-A limits of agreement (1.96 SD of the MoD) were greatest in the most peripheral zone (C10°: ± 5.15 ; 10-16°: ± 4.68 ; 16-25°: ± 5.80), although there was no significant interaction for Zone x Visit. The upper hemifield showed the largest limits of agreement (e.g. U16-25°: ± 6.02 vs. L16-25°: ± 5.45). There was a significant interaction for Zone x Visit x Hemifield ($p = 0.002$). Additionally, when looking at defect depth per zone, there were more abnormal locations at all defect depths in the 16-25° zone. However, when corrected for the number of locations per zone there was surprisingly an equal chance of detecting defect within each zone.

Conclusions: As expected, sensitivity reduced with eccentricity and the upper hemifield gave the lowest sensitivity and worst

repeatability. The likelihood of finding defect in early glaucoma was equal across zones when corrected for the number of locations tested.

Commercial Relationships: Sarah L. Bishop, Carl Zeiss Meditec (F); Yuan-Hao (Derek) Ho, None; Deborah Goren, None; John G. Flanagan, Heidelberg Engineering (C), Heidelberg Engineering (R), Heidelberg Engineering (F), Carl Zeiss Meditec (C), Carl Zeiss Meditec (R), Carl Zeiss Meditec (R), Alcon Pharmaceuticals (R), Alcon Pharmaceuticals (R), Optovue Inc (F), Optovue Inc (F), Photon etc (F), Photon etc (F)

Program Number: 3920 **Poster Board Number:** D0208

Presentation Time: 2:45 PM - 4:30 PM

Assessing the Reliability of Humphrey Visual Field Testing in an Urban Population

Manal H. Peracha, Bret A. Hughes, Justin Tannir, Rominder Momi, Anju Goyal, Mark S. Juzych, Chaesik Kim, Melanie McQueen, Alicia M. Eby, Farvah Fatima. Kresge Eye Institute, Wayne State University, Grosse Ile, MI.

Purpose: The purpose of this study was to assess the reliability of Humphrey visual field testing based on the three reliability indices defined by Humphrey Instruments, Inc. In addition, the study aims to assess the correlation between visual field reliability with severity of glaucoma, visual acuity, intraocular pressure, pupil diameter, and number of medications.

Methods: This was a retrospective comparative study. Medical records were reviewed to determine patient reliability in Humphrey automated visual field testing. Three hundred seventy-eight randomly selected electronic patient charts were evaluated, including patients with and without glaucoma, providing 1,091 visual field tests. Reliability criteria were established by Humphrey Instruments, Inc. as less than 20% fixation losses or less than 33% false negative errors or false positive errors.

Results: Overall, patients performed reliably in 52% of visual field tests. The most common cause of poor reliability was fixation loss, with 43% of patient tests deemed unreliable due to a fixation loss rate greater than 20%. False positive responses (1.7%) and false negative responses (4.2%) were much less common causes of poor reliability. There was a statistically significant difference between visual field reliability and severity of glaucoma ($p < 0.0001$). Fifty-four percent of patients with mild glaucoma ($MD > -7$ db) and 50% of patients with moderate glaucoma ($-15 < MD < -7$ db) were significantly more reliable compared to 29% with severe glaucoma ($MD < -15$), ($p < 0.0001$). There was a significant difference between reliability and visual acuity and number of glaucoma medications ($p < 0.05$), however, there was not a statistical difference between reliability and IOP ($p = 0.06$).

Conclusions: A significantly higher number of Humphrey visual field tests were reliable in the mild to moderate glaucoma groups compared with the severe group within this population of patients. The majority of unreliable fields were due to fixation losses. Increased severity of glaucoma correlated with reduced reliability. Decreased visual acuity, higher numbers of glaucoma medications, and decreased pupil size were also associated with reduced reliability; however, IOP was not significantly associated with glaucoma severity.

Commercial Relationships: Manal H. Peracha, None; Bret A. Hughes, None; Justin Tannir, None; Rominder Momi, None; Anju Goyal, None; Mark S. Juzych, None; Chaesik Kim, None; Melanie McQueen, None; Alicia M. Eby, None; Farvah Fatima, None

Program Number: 3921 **Poster Board Number:** D0209

Presentation Time: 2:45 PM - 4:30 PM

Visual Field Progression Rate of Different Glaucomatous Optic Disc Phenotypes in Progressive Open-Angle Glaucoma

Jong Rak Lee, Kyoung Sub Lee, Michael S. Kook. Ophthalmology, Asan medical center, Seoul, Republic of Korea.

Purpose: To investigate and compare visual field (VF) progression rate of different VF regions according to glaucomatous optic disc phenotypes (Nicollela & Drance classification) in open-angle glaucoma (OAG) patients with baseline intraocular pressure (IOP) in normal statistical range ($\geq 70\%$) experiencing VF progression assessed by Humphrey VF analyzer

Methods: OAG patients with VF progression by event-based analysis and a minimum of 5 VF tests over at least 2 years were initially classified as focal, concentric, myopic, senile sclerotic groups according to optic disc appearance as described by Nicollela and Drance. After adjusting covariates- age, sex, laterality, spherical equivalent (SE), baseline/mean follow-up IOP, baseline VF global indices, using linear mixed-effects model, VF progression rate was evaluated with respect to mean thresholds of overall and regional clusters in central 10 and peripheral 10 to 24 degrees, and compared among different groups. VF Progression rate was defined significant with negative slope having following significance level ($p < 0.05$ for overall, $P < 0.025$ for central and peripheral clusters).

Results: 121 eyes (58 focal, 22 concentric, 41 myopic) were included in the analysis with a mean follow-up period of 6.1 years and a mean number of VF tests of 6.3. Myopic group was younger (42.5 years) and more myopic (-5.0 D) than focal (55.5 years, -0.7 D) and concentric (53.7 years, -1.1 D) groups, but other demographic factors were not significantly different among the groups. All groups showed significant rate of VF progression over time ($P < 0.025$). In overall VF area, concentric group showed faster VF progression (-0.54 dB/year) than focal (-0.44 dB/year) or myopic (-0.36 dB/year) groups. In central 10 degrees, focal group showed fastest VF progression rate (-0.55 dB/year) whereas concentric group showed fastest progression rate (-0.57 dB/year) in peripheral 10 to 24 degrees. Among various covariates, age ($p < 0.01$) and initial MD ($P < 0.01$) were associated with faster VF progression rate at all clusters. Myopic group showed slowest progression rate in both central and peripheral area (-0.35 dB/year).

Conclusions: In progressive patients with OAG, glaucomatous optic disc classification based on phenotypes may be useful in terms of predicting VF progression rate at different VF areas (central vs. peripheral).

Commercial Relationships: Jong Rak Lee, None; Kyoung Sub Lee, None; Michael S. Kook, None

Program Number: 3922 **Poster Board Number:** D0210

Presentation Time: 2:45 PM - 4:30 PM

Useful Diagnostic Tool for Progressive Visual Acuity Decrease in Glaucoma Patients

Takeshi Yabana, Kazuko Omodaka, Mai Takahashi, Noriko Himori, Morin Ryu, Kazuichi Maruyama, Toru Nakazawa. Tohoku university, Sendai, Japan.

Purpose: Macular retinal thickness, especially at the temporal side of the optical disc, is sometimes associated with a progressive decrease of visual acuity in glaucoma patients. The purpose this present study was to develop a simple and useful tool for the analysis of visual acuity that is associated with visual function of the Humphrey field analyzer (HFA) or macular retinal thickness in glaucoma patients.

Methods: This study involved 60 eyes of 34 patients with open-angle glaucoma. Measurements of the retinal nerve fiber layer (RNFL), the ganglion cell complex (GCC), and the ganglion cell layer plus inner plexiform layer (GCL+IPL) in all eyes were obtained by use of an optical coherence tomography (OCT) macular map (3D-OCT2000; TOPCON Corporation, Tokyo, Japan). To retrieve reliable threshold values, the total deviation (TD) and the pattern deviation (PD) were

collected by use of the HFA SITA-standard 10-2 program.

Spearman's rank correlation coefficient analysis was used to investigate the correlation between visual acuity and macular retinal thickness of each grid (2i four quarters) at the site of the macular area, and the correlation with visual acuity and each 68 points of the HFA parameters.

Results: OCT macula map findings showed that visual acuity correlated with the thickness of the RNFL ($r = -0.31 \sim -0.54$) and the GCC ($r = -0.31 \sim -0.50$) at the nasal side of the upper area of fovea. Moreover, the GCL+IPL ($r = -0.31 \sim -0.51$) in the papillomacular bundle was found to be correlated with visual acuity. The HFA results showed that visual acuity was in accordance with TD ($r = -0.39 \sim -0.56$), the measured threshold values ($r = -0.36 \sim -0.55$), and PD ($r = -0.23 \sim -0.50$), which were in accordance with the papillomacular bundle area.

Conclusions: In the glaucoma patients involved in this study, visual acuity was found to be strongly correlated with macular retinal thickness or visual function of HFA in the papillomacular bundle area. These findings indicate that the combined quantitative analysis of these examinations is a useful diagnostic tool for the possible progressive visual acuity decrease in glaucoma patients.

Commercial Relationships: Takeshi Yabana, None; Kazuko Omodaka, None; Mai Takahashi, None; Noriko Himori, None; Morin Ryu, None; Kazuichi Maruyama, None; Toru Nakazawa, Kowa Company Ltd. (F), Kowa Company Ltd. (C)

Program Number: 3923 **Poster Board Number:** D0211

Presentation Time: 2:45 PM - 4:30 PM

Simulated visual field using macular RNFLT in patients with glaucoma

Mai Takahashi, Kazuko Omodaka, Noriko Himori, Morin Ryu, Toru Nakazawa. Ophthalmology, Tohoku University Graduate School of Medicine, Sendai, Japan.

Purpose: Measurement of macular retinal nerve fiber layer thickness (mRNFLT) with optical coherence tomography (OCT) has become an important tool to diagnose glaucoma in its early stages and to detect decreased visual acuity in glaucoma patients. We investigated, in detail, the correlation between structure and function in the macula, and whether we could simulate the visual field with mRNFLT data.

Methods: This study comprised 60 eyes of 34 patients with open angle glaucoma. To assess macular function, threshold, total deviation (TD), and pattern deviation (PD) from the Humphrey field analyzer (HFA, SITA-standard, 10-2 program) were used. To assess macular structure, we analyzed thickness data for the mRNFLT, ganglion cell complex (GCC), and ganglion cell layer plus inner plexiform layer (GCL+IPL) from an OCT map of the macula (3D-OCT2000, Topcon, signal > 50). An analysis was performed with Spearman's coefficient of correlation to determine both the significance of the correlation between the HFA parameters and macular thickness at each of 68 test points (corresponding to the one grid of an OCT macular map), and also the formula for simulation. We then calculated a simulated threshold for each test point with the formula from the correlation between the thresholds and mRNFLT from the linear regression analysis.

Results: For most test points, macular function and the layer-by-layer structure were significantly correlated. The levels of coefficient correlation in the significantly correlated test points were: threshold ($r = 0.26 \sim 0.87$) \geq TD ($r = 0.27 \sim 0.87$) $>$ PD ($r = 0.24 \sim 0.69$) for function, and RNFL: ($r = 0.35 \sim 0.87$) \geq GCC ($r = 0.28 \sim 0.85$) $>$ GCL+IPL ($r = 0.24 \sim 0.81$) for structure. The simulated grayscale map of the visual field based on the formula of the regression line between the mRNFLT and the threshold was very similar to the actual visual fields. There was a

ARVO 2013 Annual Meeting Abstracts by Scientific Section/Group – Glaucoma

significant correlation between the average simulated threshold of each of the 68 test points and the MD of the actual visual fields ($r=0.76$, $p<0.0001$).

Conclusions: There was a significant correlation between structure and function in the macular area. The simulated visual fields generated from mRNFLT accurately reproduced the actual visual fields. Such a simulation of macular function generated from OCT parameters may be useful for glaucoma assessment in patients.

Commercial Relationships: Mai Takahashi, None; Kazuko Omodaka, None; Noriko Himori, None; Morin Ryu, None; Toru Nakazawa, Kowa Company Ltd. (F), Kowa Company Ltd. (C)

Program Number: 3924 **Poster Board Number:** D0212

Presentation Time: 2:45 PM - 4:30 PM

Temporal summation varies with visual field eccentricity for perimetric stimuli scaled to the area of complete spatial summation

Padraig J. Mulholland^{1,2}, Tony Redmond^{3,2}, Margarita B. Zlatkova¹, David F. Garway-Heath², Roger S. Anderson^{1,2}. ¹School of Biomedical Sciences, University of Ulster, Coleraine, United Kingdom; ²NIHR Biomedical Research Centre at Moorfields Eye Hospital NHS Foundation Trust and UCL Institute of Ophthalmology, London, United Kingdom; ³School of Optometry and Vision Sciences, Cardiff University, Cardiff, United Kingdom.

Purpose: Previous studies have found the limit of complete temporal summation (critical duration) to remain constant across the visual field, but these studies did not account/control for changes in spatial summation with increasing visual field eccentricity. We wished to investigate temporal summation as a function of visual field eccentricity with a standard perimetric stimulus and a stimulus scaled to the area of complete spatial summation (Ricco's area).

Methods: Achromatic temporal and spatial summation functions were generated for five healthy subjects (median age 29 years, range 24-47), at 5°, 10° and 15° eccentricity in four diagonal visual field meridians. A Goldmann III stimulus (0.43° diameter) was used for temporal summation experiments and a 200msec stimulus was used for spatial summation experiments. Temporal summation experiments were repeated with a stimulus equal in size to Ricco's area at each test location. Ricco's area and the critical duration were estimated from the respective functions using an iterative two-phase regression technique. All stimuli were presented on a gamma-corrected achromatic CRT monitor running at 121 Hz with an adapting field of luminance 10 cdm⁻².

Results: Ricco's area was larger at greater visual field eccentricities (0.34 log units, $\chi^2(2) = 19.9$, $p<0.005$). There were negligible differences in critical duration measurements across the range of eccentricities investigated with a Goldmann III stimulus (0.067 log units, $\chi^2(2) = 3.32$, $p = 0.19$). Median (IQR) critical duration values at 5°, 10° and 15° eccentricity with the scaled stimulus were 35.4 msec (26.2, 44.3), 45.2 msec (34.6, 67.6) and 64 msec (42.8, 90) respectively. This increase was statistically significant (0.26 log units, $\chi^2(2) = 9.03$, $p = 0.011$). Post-hoc Wilcoxon signed-rank analysis with Bonferroni correction reported a significant increase in critical duration estimates between 5° and 15° when examined using the scaled stimulus ($z = -2.80$, $p = 0.005$).

Conclusions: The critical duration increases with visual field eccentricity when the stimulus is scaled to the localized Ricco's area. This may have implications for perimetric thresholds in regions where a Goldmann III stimulus equals or is smaller than Ricco's area.

Commercial Relationships: Padraig J. Mulholland, None; Tony Redmond, None; Margarita B. Zlatkova, None; David F. Garway-Heath, Moorfields MDT (P), Carl Zeiss Meditec (F), Heidelberg Engineering (F), Reichert Technologies (F), Ziemer Ophthalmic

Systems AG (F), Pfizer Inc (F), Allergan (F), Allergan (C), Allergan (R), Alcon (C), Alcon (R), Bausch & Lomb (R), Merck (R), Santen (R), Quark (C), Teva (C), Topcon (F), OptoVue (F); **Roger S. Anderson**, None

Support: Department of Employment and Learning Northern Ireland (DEL) PhD Studentship, NIHR Moorfields Biomedical Research Centre

Program Number: 3925 **Poster Board Number:** D0213

Presentation Time: 2:45 PM - 4:30 PM

Feasibility of the Moorfields Motion Displacement Test for community based glaucoma screening

CARMEN GONZALEZ-ALVAREZ^{1,2}, Ramos Antonio Manuel², James Loughman^{1,3}. ¹Department of Optometry, Dublin Institute of Technology, Dublin, Ireland; ²Departamento de Ciencias de Saude, Universidade de Lurio, Nampula, Mozambique; ³African Vision Research Institute, University of ZwaZulu Natal, Durban, South Africa.

Purpose: 285 million people are visually impaired worldwide. 90% of the world's visually impaired live in developing countries. One of the major causes of visual impairment is glaucoma. The Moorfields Motion Displacement Test (MMDT) is a novel glaucoma screening device, designed specifically for community based screening in developing countries. The current study was designed to determine the effect of education level and computer experience on MMDT repeatability.

Methods: 164 participants, from Nampula, Mozambique, were recruited to the study. Participants were stratified according to education level (primary vs tertiary) and experience of computer use (no experience vs experience). The subject's task was to indicate the presence of horizontal displacement of the white line stimuli using a computer mouse. Threshold was determined using the minimum displacement perceived. Variables measured were global probability of true damage (PTD), testing time (TT) false positives (FP). PTD measured in percentage is calculated between each field location and the number of unseen responses. Global PDT is the sum of PDT of each location. The visual field test was conducted twice, and results compared device repeatability.

Results: The mean age of the study group was 31 ± 11 (range = 15 - 56). 54 % of participants reported experience of computer use, while 46% participants reported university level education. Independent samples t test revealed no difference in PTD between computer subgroups for either the initial or repeat test ($P = 0.84$ and 0.97 respectively), or for education subgroups ($P = 0.25$ and 0.57 respectively). Paired T test analysis reveals no difference between PTD1 and PTD2 for any subgroup ($P = 0.06$ to 0.79). A statistically significant positive correlation was found between repeat PTD measures for all subgroups ($r 0.91$ to 0.98 ; $P < 0.01$ for all). Bland Altman analysis reveals good repeatability for all subgroups.

Conclusions: The MMDT is a repeatable visual field device that could be implemented in community glaucoma screening programmes. The device has many advantages including its portability, affordability, and short testing time. It is easy to understand and to perform, robust to optical blur and to cataract, and therefore can be performed without near correction. The current results validate its general repeatability for all sectors of society likely to be encountered in developing communities.

Commercial Relationships: CARMEN GONZALEZ-ALVAREZ, None; Ramos Antonio Manuel, None; James Loughman, None

Program Number: 3926 **Poster Board Number:** D0214

Presentation Time: 2:45 PM - 4:30 PM

Obstacle crossing in patients with glaucoma in different lighting conditions

Amy C. Scarfe, Matthew A. Timmis, Rupert R. Bourne, Daryl R. Tabrett, Shahina Pardhan. Vision and Eye Research Unit (VERU), Postgraduate Medical Institute, Anglia Ruskin University, Cambridge, United Kingdom.

Purpose: To assess the adaptive gait of patients with peripheral visual field loss due to glaucoma when crossing obstacles of varying heights, in two different light conditions.

Methods: Three-dimensional kinematic data were collected from twenty-five glaucoma (73.2 ± 8.3 years) and twenty-three normally sighted control participants (71.6 ± 6.9 years). Participants walked up to and stepped over either a low (5 cm) or high (10 cm) floor based obstacle in both bright (800 lx) and dim (8 lx) lighting conditions. Movement patterns of both the lead and trail limb were analysed. Peripheral visual field loss among the glaucoma group was confirmed using Humphrey 30-2 SITA standard tests.

Results: Statistically significant between-group differences were observed in vertical foot clearance for the high obstacle, in bright light condition ($p=0.022$) and also for the low obstacle in dim light condition ($p=0.022$); this difference approached statistical significance for the low obstacle, in bright light condition ($p=0.056$). Across conditions, glaucoma patients lifted their lead foot 10% higher over the obstacle compared to normally sighted controls. Glaucoma patients also lifted the toe of their trail limb 12% higher than the normally sighted controls and the velocity with which their lead and trail foot crossed the obstacle was 5% slower than the visual normals; however these were not statistically significant. Within the key kinematic variables analysed there was considerable overlap between the distributions of the two groups. This overlap was likely due to the range in severity and location of peripheral visual field loss in the glaucoma group.

Conclusions: In comparison to normally sighted controls, glaucoma patients exhibit moderate adaptations in gait when performing an obstacle crossing task. These subtle differences may indicate that glaucoma patients adopt a cautious approach to mobility tasks that present a high risk of falling.

Commercial Relationships: Amy C. Scarfe, None; Matthew A. Timmis, None; Rupert R. Bourne, Allergan Ltd (F); Daryl R. Tabrett, None; Shahina Pardhan, None

Support: NHS Cambridgeshire, UK (Flexibility and Sustainability Funding)

Program Number: 3927 **Poster Board Number:** D0215

Presentation Time: 2:45 PM - 4:30 PM

Acute Intraocular Pressure Elevation in Mice Results in Diminished Scotopic and Photopic Contrast Sensitivity

Benjamin J. Frankfort, Meike E. van der Heijden, Cameron S. Cowan, Samuel M. Wu. Ophthalmology, Baylor College of Medicine, Houston, TX.

Purpose: To assess the relationship between acute elevations of intraocular pressure (IOP) and visual contrast sensitivity in mice.

Methods: Baseline scotopic and photopic contrast sensitivities were determined on peak spatiotemporal frequency (spatial frequency = 0.08 cyc/deg; temporal frequency = 2 deg/sec; speed = 25 cyc/sec) for five (5) C57Bl6 female mice with an established optokinetic-based technique. IOP was then elevated experimentally in one eye via a single anterior chamber injection of highly cohesive sodium hyaluronate (Healon 5, Abbott Medical Optics, Inc.). After post-operative measurement of IOP with a rebound tonometer (Tonolab) mice were immediately dark-adapted. Following two hours of dark-adaptation contrast sensitivity was assessed with the same technique under scotopic and then photopic conditions. IOP and contrast

sensitivity were sequentially measured on post-operative days 1, 2, 3, 4, and 6. T-tests and repeated measures ANOVAs with cutoffs of $p < 0.05$ were conducted in SPSS version 21 (IBM).

Results: IOP is elevated to approximately 35 mmHg following a single injection of sodium hyaluronate but decreases to baseline after about 2 days. When IOP is elevated, both scotopic and photopic contrast sensitivities are markedly reduced. Both scotopic and photopic contrast sensitivities recover as IOP normalizes. There is a mild delay in both scotopic and photopic contrast sensitivity recovery which is more prominent under photopic conditions.

Conclusions: Acute IOP elevation results in decreased scotopic and photopic contrast sensitivity in mice. IOP normalizes faster than contrast sensitivity recovers.

Commercial Relationships: Benjamin J. Frankfort, None; Meike E. van der Heijden, None; Cameron S. Cowan, None; Samuel M. Wu, None

Support: NIH Grant EY021479; NIH Grant EY019908; NIH Grant EY004446

Program Number: 3928 **Poster Board Number:** D0216

Presentation Time: 2:45 PM - 4:30 PM

Smoothing Algorithms for Pointwise Visual Field Predictions in Glaucoma

Esteban Morales¹, Parham Azarbod¹, Abdelmonem Afifi², Fei Yu², Anne L. Coleman³, Kouros Nouri-Mahdavi¹, Joseph Caprioli¹.

¹Ophthalmology, University of California, Los Angeles, Los Angeles, CA; ²Biostatistics, University of California, Los Angeles, Los Angeles, CA; ³Epidemiology, University of California, Los Angeles, Los Angeles, CA.

Purpose: The study was conducted to compare four threshold smoothing techniques for predicting the rates of visual field (VF) worsening in glaucoma.

Methods: 798 patients with primary open-angle glaucoma and 6 or more years of follow-up were included. Thresholds at each VF location for the first four years or first half of the follow-up time (whichever was greater) were smoothed with clusters defined by the Glaucoma Hemifield Test (GHT), the Garway-Heath clusters, nearest neighbor weighting (NN), and weighting by the correlation of rates of all other VF locations. Thresholds for smoothed locations were regressed with a pointwise exponential model. VF predictions derived from the exponential regression were compared with average of the actual VF thresholds at the final two follow-up visits. Since there is no formal statistical test to assess the statistical significance of the difference in root mean square (RMS) values among four approaches for model prediction, the approaches were simply ranked by the RMS values with smaller RMS value indicating better model prediction.

Results: The average (\pm SD) follow-up time and number of visual field exams used for the smoothing and prediction were 4.1 (\pm 1.3) years and 8.1 (\pm 2.4), respectively. The average (\pm SD) follow-up time for the final two visits was 8.3 (\pm 2.2) years. The RMS values of the differences between the observed and the predicted thresholds at last follow up for each VF location was 11.8 dB for the GHT clusters, 12.4 dB for the correlation weighting, 12.4 dB for the Garway-Heath clusters, 12.5 dB for the NN weighting, and 12.6 for the raw (unsmoothed) values.

Conclusions: Although the differences among the pointwise VF predictions with the four smoothing techniques and the unsmoothed predictions is not large, the GHT method improved the predictions of final threshold values more than other methods, while the use of the raw values provided the worst predictions. It is worth considering using GHT clustering to improve the accuracy of pointwise predictions of VF outcomes in glaucoma.

Commercial Relationships: Esteban Morales, None; Parham Azarbod, None; Abdelmonem Affi, None; Fei Yu, None; Anne L. Coleman, None; Kouros Nouri-Mahdavi, Allergan (C); Joseph Caprioli, Allergan Inc. (F), Allergan Inc. (C), Allergan Inc. (R)

Program Number: 3929 **Poster Board Number:** D0217
Presentation Time: 2:45 PM - 4:30 PM
Performance of the Visual Field Index in Patients with Advanced Field Loss

Meera Ramanathan¹, Jun Mo Lee¹, Nila Cirineo¹, Abdelmonem Affi², Esteban Morales¹, Fei Yu^{1,2}, Kouros Nouri-Mahdavi¹, Anne L. Coleman^{1,3}, Joseph Caprioli¹. ¹Ophthalmology, Jules Stein Eye Institute, University of California at Los Angeles, Los Angeles, CA; ²Biostatistics, Karin Fielding School of Public Health, University of California at Los Angeles, Los Angeles, CA; ³Epidemiology, Karin Fielding School of Public Health, University of California at Los Angeles, Los Angeles, CA.

Purpose: The purpose of this study is to explore the relationship between the Visual Field Index (VFI) and the visual field mean deviation (MD), determined by analyzing the change in VFI (Δ VFI) with change in MD (Δ MD) in patients with advanced damage.

Methods: The MD and VFI values obtained from visual field tests conducted on 176 eyes of 168 glaucoma patients having an MD around -20dB were studied. A total of 535 exams from 1984 to 2011 with MD values within the range of -16dB to -24dB were included. Two divisions were made with the first having serial MDs all less than or greater than -20 dB and the second with serial MDs crossing -20 dB. The relationship of Δ VFI with Δ MD was evaluated.

Results: The means (\pm SD) for the Δ VFI are 6.47 (\pm 9.17) corresponding to MDs on either side of -20dB and 15.41 (\pm 7.64) corresponding to MDs crossing -20dB ($p < 0.0001$). For Δ VFI/ Δ MD, these values are 6.47 (\pm 9.17) when the range of MD falls on either side of -20 dB, and 8.12 (\pm 6.78) when the range of MD crosses the -20 dB value ($p < 0.00026$).

Conclusions: The value of the VFI becomes highly variable with MDs crossing -20dB in comparison to those VFIs corresponding to MDs on either side of -20dB. The reason for this effect is the change from use of pattern deviation to total deviation values in calculation of VFI at the MD boundary of -20dB. The development of methods to measure visual field rates that are free from this boundary effect would be desirable.

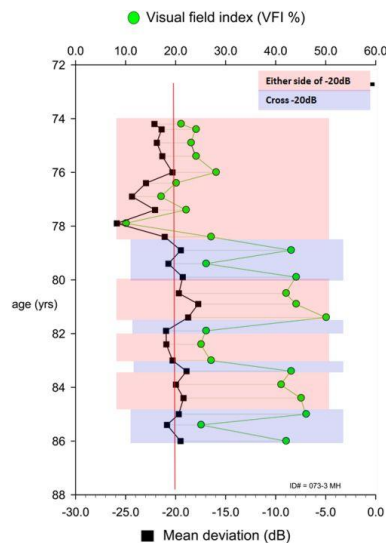


Figure 1. This plot is an example of a given patient's pattern of MD progression and corresponding VFI fluctuation.

©2013, Copyright by the Association for Research in Vision and Ophthalmology, Inc., all rights reserved. Go to iovs.org to access the version of record. For permission to reproduce any abstract, contact the ARVO Office at arvo@arvo.org.

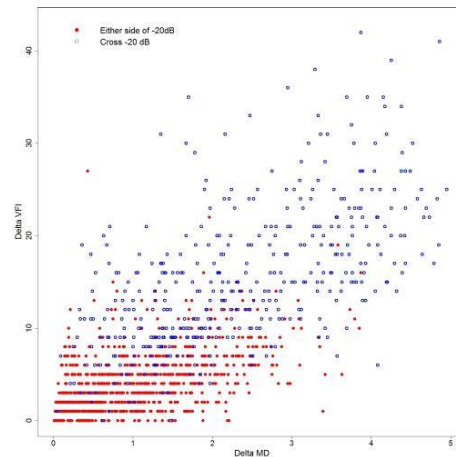


Figure 2. A representation of the relationship between Δ VFI and Δ MD for the 176 eyes in the study.

Commercial Relationships: Meera Ramanathan, None; Jun Mo Lee, None; Nila Cirineo, None; Abdelmonem Affi, None; Esteban Morales, None; Fei Yu, None; Kouros Nouri-Mahdavi, Allergan (C); Anne L. Coleman, None; Joseph Caprioli, Allergan Inc. (C), Allergan Inc. (F), Allergan Inc. (R)

Program Number: 3930 **Poster Board Number:** D0218

Presentation Time: 2:45 PM - 4:30 PM
The Relationship Between Visual Acuity, Intraocular Pressure, and Rates of Visual Field Progression Using 10-2 Perimetry
 Carly J. Seidman¹, C. Gustavo De Moraes^{1,2}, Rafael L. Furlanetto², Jeffrey M. Liebmann^{1,2}, Robert Ritch^{2,3}. ¹New York University School of Medicine, New York, NY; ²Einhorn Clinical Research Center, New York Eye and Ear Infirmary, New York, NY; ³Ophthalmology, New York Medical College, New York, NY.

Purpose: Randomized glaucoma trials (RCTs) have used automated perimetry to measure visual field (VF) changes to determine outcomes, concluding that intraocular pressure (IOP) plays a key role in glaucoma onset and progression. Although 50% of retinal ganglion cells are located in the macula, this area is underrepresented in conventional perimetry. Given the lack of information in the literature regarding central vision loss and IOP, we investigated the association between rates of best corrected visual acuity (BCVA) loss, 10-2 progression, and IOP in patients with established glaucoma.

Methods: This observational cohort study included patients with glaucomatous optic neuropathy and reproducible VF defects on SITA-Standard 24-2 tests. All patients had paracentral VF damage and were followed with 24-2 and 10-2 perimetry. Patients with fewer than 5 10-2 VF during follow-up were excluded. We investigated the association between IOP and changes of BCVA (LogMAR) and tested the association between rates of 10-2 mean deviation (MD) progression and decline in BCVA. Mixed linear models were used for statistical analysis.

Results: 176 eyes (142 patients, mean age, 60.7 \pm 10.6) followed for 5.2 \pm 4.4 years were included. Mean baseline BCVA was 0.19 \pm 0.2 (=20/30 Snellen). The mean rate of 10-2 MD progression was -0.47 \pm 0.6 dB/yr. The mean rate of LogMAR increase was 0.013 \pm 0.03 units/year, translating to a decline in BCVA from 20/30 to 20/40 during follow-up. Variables significantly associated with decline of BCVA were worse baseline MD ($P < 0.001$), follow-up IOP ($P = 0.024$), baseline IOP ($P = 0.001$), peak IOP ($P = 0.017$), and worse baseline BCVA ($P < 0.001$). BCVA change was significantly associated with MD rates of progression ($P < 0.001$).

Conclusions: This is the first study to demonstrate that IOP reduction

prevents not only conventional perimetric progression as shown in RCT but also slows the rate of BCVA deterioration and central field loss in glaucoma. Clinicians should not overlook changes in BCVA even if 10-2 VFs remain stable.

Commercial Relationships: **Carly J. Seidman**, None; **C. Gustavo De Moraes**, None; **Rafael L. Furlanetto**, None; **Jeffrey M. Liebmann**, Alcon Laboratories, Inc. (C), Allergan, Inc. (C), Allergan, Inc. (F), Carl Zeiss Meditech, Inc (F), Heidelberg Engineering, GmbH (F), Topcon Medical Systems, Inc. (F), National Eye Institute (F), New York Glaucoma Research Institute (F), SOLX, Inc. (C), Bausch & Lomb, Inc (C), Diopsys, Inc. (C), Diopsys, Inc. (F), Merz, Inc. (C), Glaukos, Inc. (C), Quark, Inc. (C); **Robert Ritch**, None

Support: Paul and Ellen Richman Research Fund of the New York Glaucoma Research Institute; Edith C. Blum Foundation

Program Number: 3931 **Poster Board Number:** D0219

Presentation Time: 2:45 PM - 4:30 PM

Temporal filtering of longitudinal visual field data

*Chris A. Johnson*¹, *Carrie K. Doyle*^{1,2}, *Trina Eden*^{1,2}, *Michael Wall*^{2,3}. ¹Ophthalmology & Visual Sci, University of Iowa, Iowa City, IA;

²Neurology, University of Iowa, Iowa City, IA; ³Neurology, Veterans Administration, Iowa City, IA.

Purpose: To determine whether low pass filtering (3 temporal bin smoothing) of longitudinal visual field data would influence the ability to detect progressive glaucomatous damage.

Methods: One eye of one hundred and eight patients with a clinical diagnosis of glaucoma (MD mean at baseline = -6.73, SD = 4.45, Max = -0.12, Min = -19.94) underwent automated perimetric testing with the Humphrey Field Analyzer 24-2 stimulus pattern, a size III target and the SITA standard threshold estimation strategy. Testing was performed every six months, with two initial baseline visual field measures. To be eligible for the study, participants were required to have at least five additional visual field tests beyond the initial baseline measurements. Mean Deviation (MD) and Pattern Standard Deviation (PSD) are often used as clinical methods of monitoring glaucomatous visual field progression, as is the visual field index or VFI which is based on MD. Linear regression was used to assess the filtered and unfiltered data sets.

Results: We found minimal differences in the slope of linear regression results for filtered versus unfiltered MD (Unfiltered mean = -0.446, SD = 0.703, max = 0.869, min = -2.45; Filtered mean = -0.316, SD = 0.597, Max = 0.919, Min = -2.17) or PSD (Unfiltered mean = 0.102, SD = 0.410, Max = 2.25, Min = -0.958; Filtered mean = 0.044, SD = 0.436, Max = 2.099, Min = -0.977) or in the goodness of fit for the regression evaluations.

Conclusions: Although previous investigations of procedures to minimize variability for longitudinal visual field data sets (e.g. low pass filtering and one-omitting and three-omitting analysis methods) have reported modest improvements in the ability to determine glaucomatous visual field changes, our findings revealed no difference between filtered and unfiltered data sets in assessing visual field change. This may be due to our use of global indices (MD and PSD) that provide a composite evaluation of all visual field locations tested (reducing variability) rather than individual points or small groups of points evaluated in prior studies, and the use of empirical visual field data rather than simulated results.

Commercial Relationships: **Chris A. Johnson**, Lundbeck (C), Ivantis (C), Jaeb Center (C), AEGIS (C), Acufocus (C), Haag Streit (C); **Carrie K. Doyle**, None; **Trina Eden**, None; **Michael Wall**, None

Support: Veterans Administration Merit Review Grant

Program Number: 3932 **Poster Board Number:** D0220

Presentation Time: 2:45 PM - 4:30 PM

Influence of prior information on Bayesian estimators of visual field progression

Andrew J. Anderson. Optometry & Vision Sciences, The University of Melbourne, Parkville, VIC, Australia.

Purpose: Progression of visual field damage in glaucoma is often assessed by linear regression of the summary index mean deviation (MD). Bayesian estimators allow likely progression rates in the population (the prior distribution) to constrain rate estimates for individuals. We examined the benefits of having a prior distribution accounting for one of progression's major risk factors - whether intraocular pressure (IOP) is treated - to gauge the maximum benefit expected from developing priors for other glaucoma risk factors.

Methods: Our *prior distribution* was derived from published clinical data from either treated (Canadian Glaucoma Study: matched-prior condition) or untreated (Early Manifest Glaucoma Trial; unmatched-prior condition) patients with primary open angle glaucoma, each fitted with a modified hyperbolic secant. We simulated series of MD values (2 fields per year for 6 years) with true underlying rates of progression (R) drawn from the same distribution as the prior for the matched-prior condition. The standard deviation of MD values was 1.0 dB. We estimated progression rates (r) for subsets of each series (2 through 11 visual field assessments) through linear regression, and determined the likelihood of obtaining this estimate as a function of a range of true underlying progression rates (the *likelihood function* for the conditional probability $r|R$). The maximum likelihood estimate of rate was calculated from the most likely value of the *posterior distribution* formed by the product of the prior distribution and the likelihood function.

Results: For short (4) visual field series, the matched-prior condition, unmatched-prior condition and linear regression gave median errors (r minus R) of 0.02, 0.20 & 0.00 dB/year, respectively. Positive predictive values for determining rapidly progressing (= worse than -1 dB/year) rates in the simulated patient cohort were 0.46, 0.42 and 0.38, with negative predictive values of 0.93, 0.94 and 0.95. For more extended series (7 fields) the magnitude of the differences between techniques decreased, although the order was unchanged.

Conclusions: Performance shifts in Bayesian estimators of visual field progression are modest even when prior distributions do not adequately reflect large risk factors, such as IOP treatment.

Commercial Relationships: **Andrew J. Anderson**, None

Support: Australian Research Council Future Fellowship FT120100407

Program Number: 3933 **Poster Board Number:** D0221

Presentation Time: 2:45 PM - 4:30 PM

The relationship between visual acuity and central visual field on vision related quality of life in advanced glaucomatous patients

*Mizu Okamoto*¹, *Hiroshi Murata*¹, *Makoto Araie*^{1,2}, *Hiroyo Hirasawa*¹, *Chihiro Mayama*¹, *Ryo Asaoka*¹. ¹Ophthalmology, University of Tokyo school of Medicine, Tokyo, Japan; ²Kanto Central Hospital, Tokyo, Japan.

Purpose: To investigate the relationship between visual acuity and central visual field on vision related quality of life (VRQOL) in advanced glaucomatous patients.

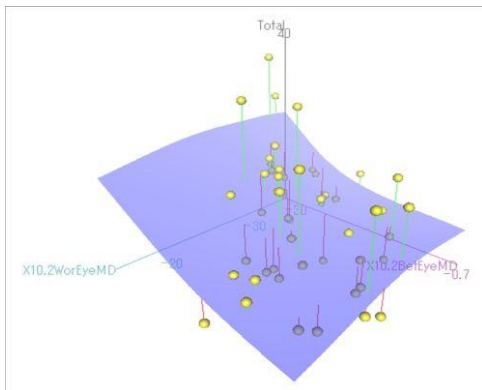
Methods: We conducted hearing investigation using the 'Sumi questionnaire' (Sumi et al. Ophthalmol. 2003;110:332-339) on 50 advanced glaucomatous patients who had mean deviation(MD) less than -15dB (Humphrey 24-2 SITA Standard program) at least in one eye.

VRQOL score in each task (Word/Walk/Move/Eat) was calculated as the sum of scores of all questions of the task, we have calculated total

and itemized. Visual field (VF) was measured using Humphrey SITA Standard program(10-2). The impact of MD of better eye (MD-bet), MD of worse eye (MD-wor), VA(LogMAR VA) of better eye (VA-bet) and VA of worse eye (VA-wor) were compared using the correlation coefficients. Furthermore, partial regression was used to estimate the direct impact of a variable, in relationship with another variable.

Results: The correlation coefficient of each VRQOL score (Total/Word/Walk/Move/Eat) was (-0.39/-0.42/-0.37/-0.34/-0.17(MD-bet)), (-0.24/-0.27/-0.35/-0.12/-0.11(MD-wor)), (0.57/0.40/0.37/0.21/0.17(VA-bet)), (0.34/0.28/0.37/0.11/0.02(VA-wor)), respectively. In the comparison between better and worse eyes, the partial correlation coefficient of each VRQOL score (Total/Word/Walk/Move/Eat) was (-0.34/-0.25/-0.32/-0.13/-0.32(MD-bet)), (-0.08/-0.21/0.05/-0.03/-0.07(MD-wor)), (0.32/0.25/0.18/0.18/0.50(VA-bet)), (0.12/0.24/0.01/-0.07/0.11(VA-wor)), respectively. In the comparison between MD-bet and VA-bet, the partial correlation coefficient of each VRQOL score (Total/Word/Walk/Move/Eat) was (-0.36/-0.31/-0.30/-0.13/-0.31(MD-bet)) and (0.34/0.31/0.14/0.13/0.53(VA-bet)), respectively.

Conclusions: The result of partial correlation analysis revealed the direct effect of worse eye on VRQOL was smaller than that of better eye, except for the task of Word. Both of MD-bet and VA-bet are closely related to VRQOL scores.



Commercial Relationships: Mizu Okamoto, None; Hiroshi Murata, None; Makoto Araie, Kowa (C), Kowa (R), Zeiss (R), Topcon (R); Hiroyo Hirasawa, None; Chihiro Mayama, None; Ryo Asaoka, None

Program Number: 3934 **Poster Board Number:** D0222

Presentation Time: 2:45 PM - 4:30 PM

Cluster-Based Trend Analysis of Visual Field Progression in Low Tension and High Tension Open-Angle Glaucoma

Iman Goharian, David S. Greenfield, Mitra Sehi. Bascom Palmer Eye Institute, Palm Beach Gardens, FL.

Purpose: To investigate cluster-based characteristics of visual field progression in low tension glaucoma (LTG) and high tension open-angle glaucoma (HTG) using 2 trend-based analysis methods.

Methods: Records of glaucoma patients with ≥ 30 months of follow-up and ≥ 6 standard automated perimetry (SAP) tests were reviewed. Inclusion required age ≥ 40 years, visual acuity $\geq 20/40$ and reliable SAP. LTG was defined as untreated IOP ≤ 21 mmHg, no history of IOP > 21 mmHg, open iridocorneal angles, reproducible glaucomatous SAP abnormality and corresponding optic nerve damage. The 2 groups were matched for age, follow-up time and baseline MD. SAP test locations were grouped into 10 clusters based on the topographic distribution of the RNFL. Progression was determined using: A) Corrected Cluster Trend Analysis (CCTA; EyeSuite, Haag-Streit,

Switzerland), defined as progression rate (dB/yr) in mean pattern deviation (PD) values of each cluster at $p < 0.01$; B) Pointwise Linear Regression Analysis (PLR; ProgressorTM, UK) defined as pointwise progression rate at $p < 0.01$ in ≥ 1 location in each cluster. Random effect models, ANOVA, and regression analyses were performed.

Results: 70 eyes (35 LTG, 35 HTG) were enrolled. Patients with LTG and HTG had similar age (71.5 ± 8.9 ; 72.0 ± 9.0 yrs; $p = 0.79$), follow-up time (60.9 ± 22.4 ; 64.3 ± 29.2 mos; $p = 0.58$), treated IOP (14.4 ± 2.9 ; 14.6 ± 3.9 mmHg; $p = 0.78$), baseline MD (4.5 ± 4.0 ; -4.4 ± 4.0 dB; $p = 0.91$), and rate of loss in MD (0.33 ± 0.57 ; -0.15 ± 0.72 dB/yr; $p = 0.27$). The rate of loss in square root of loss variance (sLV) was worse in LTG (0.27 ± 0.38 dB; $p = 0.01$) vs HTG (0.03 ± 0.39 dB). More LTG eyes were classified as progressors compared with HTG eyes using CCTA (26 vs 17; $p = 0.048$) and PLR (27 vs 16; $p = 0.01$). The number of progressing LTG eyes in inferior arcuate cluster was higher than the number of progressing HTG eyes (12 vs 4; $p = 0.03$) but was similar ($p > 0.05$) in all other clusters using CCTA. The cluster-based rates of loss were steeper in LTG in inferior arcuate (0.17 ± 0.43 dB/yr; $p = 0.03$) and inferior paracentral clusters (0.33 ± 0.62 dB/yr; $p = 0.02$) vs HTG (0.01 ± 0.28 and -0.04 ± 0.67 dB/yr) using CCTA. Both methods agreed on 25 LTG and 16 HTG progressors, and 2 LTG and 0 HTG non-progressors ($\kappa = 0.40$; $p = 0.01$).

Conclusions: Paracentral and arcuate clusters progress faster and more frequently in LTG compared with HTG and should be monitored more closely.

Commercial Relationships: Iman Goharian, None; David S. Greenfield, National Eye Institute (R), Carl Zeiss Meditec (R), Optovue (R), Heidelberg Engineering (R), Allergan (C), Alcon (C), Merz (C), Quark (C), SOLX (C), Biometric Imaging (C), Senju (C); Mitra Sehi, Allergan, Inc. (C)

Support: NIH R01 EY013516 (Advanced Imaging for Glaucoma Study), P30EY014801 (University of Miami core grant)

Clinical Trial: NCT01314326

Program Number: 3935 **Poster Board Number:** D0223

Presentation Time: 2:45 PM - 4:30 PM

The Evaluation of Driving Performance in Glaucoma Patients Using Binocular or Monocular Visual Field Parameters

chayin chen. Ophthalmology, Chang Gung Memorial Hospital, Pu Zih City, Chia-yi, Taiwan.

Purpose: To identify the association of clinical visual field parameters and driving performance in glaucoma patients.

Methods: Fifty-one glaucoma patients with visual acuity at least 20/40 of better eye and visual field loss for at least one eye were recruited. The parameters in Humphrey 30-2 monocular visual field test and binocular Esterman visual field test (EVFT) were correlated with National Eye Institute Vision Function Questionnaire. Fisher's exact test was used to determine if there are nonrandom associations between driving performance and visual field defects.

Results: The mean Esterman efficiency score and mean monocular visual field mean deviation of better eye were 93.43 ± 10.49 and -8.37 ± 7.01 dB, respectively. Patients in group of Esterman efficiency score < 90 or monocular visual field test mean deviation < -10.0 dB of better eye, subjectively experienced statistically significant difficulty in driving at night or in difficult conditions (e.g. bad weather, rush hour, freeway, or city traffic), when compared with that in Esterman efficiency score > 90 or mean deviation > -10.0 dB (driving at night in EVFT group: 80% (score ≤ 90) versus 33.3% (score > 90) with fisher's test $P = 0.012$, or in Humphrey test group: 66.7% (MD ≤ -10) versus 32.4% (MD > -10 ; fisher's test $P = 0.033$); driving in difficult conditions in EVFT group: 80% (score ≤ 90) versus 33.3% (score > 90) with fisher's test $P = 0.012$, or in Humphrey

ARVO 2013 Annual Meeting Abstracts by Scientific Section/Group – Glaucoma

test group: 66.7% (MD≤-10) versus 30.3% (MD>-10) with fisher’s test P= 0.027). However, under the condition of driving in familiar places during the daytime, there is no statistically significant difference in Humphrey test groups (P=0.079).

Conclusions: We described that binocular EVFT also could perform a valuable tool in assessing driving performance in glaucoma patients. This study revealed the tendency of driving difficulty in dark or difficult conditions in glaucoma patients with moderate to severe visual field loss (binocular Esterman efficiency score < 90 or monocular visual field test mean deviation < -10 dB in better eye).

Commercial Relationships: chayu in chen, None
Support: Chang Gung Memorial Hospital Grant

Program Number: 3936 **Poster Board Number:** D0224
Presentation Time: 2:45 PM - 4:30 PM

Unusual Cause of High Fixation Loss Rate during Standard Automated Perimetry Testing

Tamara L. Berezina, Eileen Buroff, Albert S. Khouri, Amir Cohen, Robert D. Fechtner. Ophthalmology, UMDNJ-New Jersey Medical School, Newark, NJ.

Purpose: Fixation loss rate is one of the visual field test reliability indices. High fixation loss rate is usually attributed to poor patient performance in maintaining regard of the fixation target. The aim of this work is to present an unusual mechanism of high fixation losses during visual field examination and a simple resolution.

Methods: We identified three otherwise alert patients noted to be accumulating a high fixation loss rate during monitored testing using Humphrey Field Analyzer (Carl Zeiss Meditec) Program 24-2. Every usual effort (including repeated patient instruction and repositioning) was made in order to reduce excessive fixation loss, but without success. Rhythmic head movements were noticed and the operator confirmed the presence of chewing gum in the mouth of each of these patients. Testing was repeated several minutes after chewing gum was removed with immediate resolution of the high fixation loss rate. We attempted to replicate these visual field testing conditions in three healthy volunteers instructed to chew gum during testing.

Results: Visual field tests of three glaucoma patients prior to the moment when chewing gum in the mouth was identified were considered unreliable due to fixation loss that was as high as 82.7±9.3%. Visual field retest performed after the chewing gum was removed became reliable: fixation loss decreased to 6.3±5.7% (p=0.011 vs. the test with chewing gum in the mouth). Three healthy volunteers did not demonstrate difference in fixation loss rate with and without having chewing gum in the mouth (0.67±0.33% vs. 0.33±0.58%, p=0.42).

Conclusions: For some individuals, the pattern or magnitude of spontaneous movements resulting from chewing gum during visual field examination causes significant increase in reported fixation loss rate. This phenomenon appears sensitive to the individual’s technique of gum chewing. Clinicians should be aware of this possible cause of high fixation loss and the simple remedy; remove chewing gum prior to visual field testing.

Commercial Relationships: Tamara L. Berezina, None; Eileen Buroff, None; Albert S. Khouri, None; Amir Cohen, None; Robert D. Fechtner, None

Program Number: 3937 **Poster Board Number:** D0225
Presentation Time: 2:45 PM - 4:30 PM

Glaucoma Monitoring with Frequency Doubling Perimetry in the Groningen Longitudinal Glaucoma Study

Christiaan Wesselink¹, Nomdo M. Jansonius^{1,2}. ¹Dept. of Ophthalmology, University Medical Center Groningen, Groningen,

Netherlands; ²Dept. of Epidemiology, Erasmus Medical Center, Rotterdam, Netherlands.

Purpose: To determine the suitability of frequency doubling perimetry (FDT) for glaucoma monitoring.

Methods: One hundred twenty six eyes of 126 glaucoma patients were included. Patients were followed prospectively with the Humphrey Field Analyzer (HFA; 30-2 SITA) and FDT (C20-1 full threshold) in the Groningen Longitudinal Glaucoma Study, an observational cohort study. The rate of progression (ROP) was calculated. We used the mean deviation (MD) for HFA and the number of test locations with p < 1% in the total deviation probability plot for FDT. Patients were stratified in three equally sized groups (tertiles; slow, average and fast progressors) based on their ROP, for both HFA and FDT.

Results: On average 8.1 HFA and 4.5 FDT tests were available after a mean follow-up (identical for HFA and FDT) of 6.4 years. The mean (SD) HFA MD at baseline was -7.9 (6.4) dB; the mean (SD) number of abnormal FDT test locations at baseline was 6.1 (4.5). The mean (SD) HFA ROP was -0.28 (0.55) dB/yr and the mean (SD) FDT ROP was 0.12 (0.50) abnormal test locations per year. There was a highly significant association between HFA and FDT ROP (chi-squared test: p<0.001; see figure).

Conclusions: Using frequency doubling perimetry for the monitoring of glaucoma patients can give some insight in disease progression. This suggests that FDT can be used in patients who cannot be reliably tested with standard automated perimetry.

FDT Rate of Progression	Fast	4	16	22
	Average	17	16	9
	Slow	21	10	11
	Slow	Average	Fast	
	HFA			
	Rate of Progression			

Commercial Relationships: Christiaan Wesselink, None; Nomdo M. Jansonius, None

Program Number: 3938 **Poster Board Number:** D0226
Presentation Time: 2:45 PM - 4:30 PM

Comparison of Web-based Perimetry and office-based Humphrey Visual Field (HVF) in Patients with Glaucoma

Jing Hou^{1,2}, Sean K. Wang³, Jeremy D. Keenan², Brian Chon², Nita Subramanian², Tsontcho Ianchulev⁴, Robert L. Stamper², Robert Chang³, Ying Han². ¹OPHTHALMOLOGY, People's Hospital, Peking University, Beijing, China; ²OPHTHALMOLOGY, University California, San Francisco, San Francisco, CA; ³OPHTHALMOLOGY, Stanford University, Palo Alto, CA; ⁴Transcend Medical, Palo Alto, CA.

Purpose: To compare a new online Perimetry (Peristat) with Humphrey visual field (HVF) for patients with mild, moderate and severe glaucoma.

Methods: Seventy-seven glaucoma patients with 129 eyes and 15 controls with 15 eyes were enrolled from the University of California, San Francisco and Stanford University. All subjects performed 24-2 SITA-standard HVF (Carl Zeiss Meditec, Dublin,

ARVO 2013 Annual Meeting Abstracts by Scientific Section/Group – Glaucoma

CA) and Peristat (www.KeepYourSight.org) in the office within 3 months. A reliable field for both tests was defined as fixation loss, false positive and false negative $\leq 33\%$. The severity of glaucoma was classified based on Hodapp-Anderson-Parrish criterion. The agreement between Peristat and HVF was graded per eye and per quadrant with Cohen's Kappa. HVF defect in each quadrant was defined as clusters of ≥ 3 adjacent points with $P \leq 5\%$ on the pattern deviation plot or ≥ 2 adjacent points with $P \leq 1\%$. Peristat defect in each quadrant was defined as clusters of ≥ 3 adjacent points with ≥ 6.7 dB loss from background or ≥ 2 adjacent points with ≥ 10 dB loss. An abnormal eye was identified if there was ≥ 1 abnormal quadrant.

Results: Fifty-nine glaucoma patients with 78 eyes and 15 controls with 15 eyes obtained reliable HVF and Peristat tests. The numbers of eyes with mild, moderate and severe glaucoma were 47 (60.3%), 17 (21.8%), and 14 (17.9%), respectively.

When fields were analyzed per quadrant, of the 312 quadrants, Cohen's Kappas between the two tests for mild, moderate and severe glaucoma were 0.135 (95% Confidence Interval (CI): 0.011 to 0.259), 0.239 (95% CI: 0.089 to 0.390), and 0.301 (95% CI: 0.074 to 0.529), respectively.

When fields were analyzed per eye, Cohen's Kappas between the two tests for mild, moderate and severe glaucoma were 0.30 (95% CI: 0.119 to 0.486), 0.75 (95% CI: 0.524 to 0.978), and 0.86 (95% CI: 0.677 to 1.047), respectively. The sensitivity and specificity of Peristat to identify glaucomatous eye were 82.4% and 93.3% for moderate glaucoma, and 92.9% and 93.3% for severe glaucoma, respectively.

Conclusions: Web-based Peristat has a good to very good agreement with HVF to identify eyes with moderate and severe glaucoma. The spatial correlation between Peristat and HVF is fair for those eyes. Given that Peristat has high sensitivity and specificity to identify eyes with moderate to severe glaucoma, it could be a good glaucoma-screening tool.

Commercial Relationships: Jing Hou, None; Sean K. Wang, None; Jeremy D. Keenan, None; Brian Chon, Transcend Medical (C); Nita Subramanian, None; Tsontcho Ianchulev, Transcend Medical (E), Wavetec Medical (C), Corinthian Medical (C); Robert L. Stamper, Transcend (C), Genentech (C); Robert Chang, None; Ying Han, None

Program Number: 3939 **Poster Board Number:** D0227

Presentation Time: 2:45 PM - 4:30 PM

Adaptation abnormalities in Primary Open-Angle Glaucoma

Shira Radner, Robert Ennis, Barry Lee, Mitchell W. Dul, Qasim Zaidi. Graduate Department of Biological and Vision Sciences, SUNY State College of Optometry, New York, NY.

Purpose: Dynamic color and brightness adaptation are crucial for visual functioning. Does the effect of Glaucoma on retinal ganglion cells compromise these functions? Zaidi, Ennis, Cao, & Lee (Neural locus of color afterimages. *Current Biology*, 22(3), 220 - 224, 2012) used psychophysics and in vivo single-cell recordings to show that ganglion cells are the adaptation locus for color afterimages at moderate intensities. We used the same procedure to test the hypothesis that adaptation is weaker in patients with glaucoma (POAG) compared with age-matched controls.

Methods: On a CRT at a distance of 83 cm, a 4° central disk was divided into two halves. Beginning and ending at mid-grey, sinusoidal half-cycles slowly modulated the colors of the hemi-disks for 16 sec at 1/32 Hz to opposite ends of the cardinal axes (red-green, yellow-violet and white-black) that respectively isolate parvo, konio and magno ganglion cells (Sun, Smithson, Lee, and Zaidi, *Specificity of cone inputs to macaque retinal ganglion cells. J. Neurophysiology*, 95: 837-849, 2006). Observers perceived the difference between the

two colors as first increasing and then decreasing to identity, followed by increasing and decreasing differences between the complementary colors forming an afterimage. Due to ganglion cell adaptation, the identity point preceded the end of the physical modulation, and the physical contrast at that point estimated the magnitude of adaptation. A second 2° circle was presented as a clock with a central dot as the fixation point, at either the central location or peripherally at 8° left, right, top or bottom. Observers used the clock to report the time of the identity point and a button press to report the end of the afterimage. We measured identity points and afterimage durations for the affected eyes of 13 POAG patients and 15 age-matched controls. The 5 fixation locations times the 3 cardinal axes were presented in random order, with 3 repetitions.

Results: In 14 out of the 15 comparisons (locations x colors), mean identity points were later for glaucoma patients than for controls (probability of chance occurrence $< .0001$). All observers reported prolonged afterimages, but the measurements were noisier, and differences in duration were not significant.

Conclusions: Neural adaptation is slower in glaucoma patients for all three classes of retinal ganglion cells.

Commercial Relationships: Shira Radner, None; Robert Ennis, None; Barry Lee, None; Mitchell W. Dul, None; Qasim Zaidi, None

Support: EY007556, EY007716, EY013312, EY007716, T35EY020481

Program Number: 3940 **Poster Board Number:** D0228

Presentation Time: 2:45 PM - 4:30 PM

Accuracy of sensitivities measured by perimetry at damaged locations in subjects with glaucoma

Deborah Goren¹, Shaban Demirel¹, Casie Goldman¹, William H. Swanson², Stuart K. Gardiner¹. ¹Devers Eye Institute, Legacy Research Institute, Portland, OR; ²School of Optometry, Indiana University, Bloomington, IN.

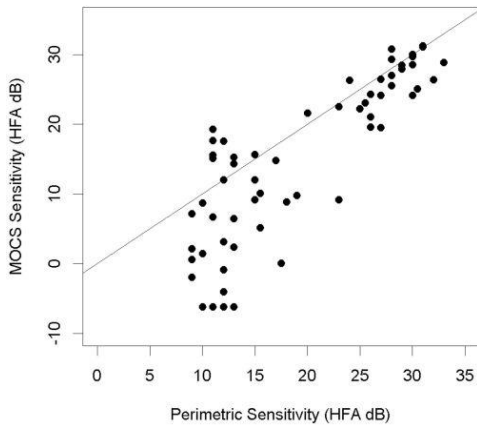
Purpose: Responses from primate retinal ganglion cells (RGCs) stimulated by perimetric stimuli saturate at contrasts beyond ≈ 15 -20dB. Increasing contrast further should not appreciably increase the response besides effects of scattered light. If this holds true in humans, sensitivities from automated perimetry (SAP) in areas of significant damage would be essentially random, and so uninformative of the true threshold. We sought to assess the relation between SAP estimates and the true sensitivities at such damaged locations.

Methods: 16 subjects with moderate to advanced glaucoma were recruited. For each subject, four visual field locations were chosen. Two of these had sensitivities between 6dB and 18dB on both of their last two clinic visits (averaged to give "perimetric sensitivity"), two were positioned to aid spatial uncertainty. The method of constant stimuli (MOCS) was used to generate Frequency-of-Seeing curves at each location using an Octopus perimeter externally controlled by the Open Perimetry Interface. 35 presentations were made at each of 7 intensities centered on the perimetric sensitivity, including the brightest available stimulus (equivalent to 3.75dB on the Humphrey Field Analyzer) at the two damaged locations. 25 blank catch trials were used to measure the false positive rate. A cumulative Gaussian curve was fit to the response probabilities at each location to estimate threshold (50% detection). The significance of the correlation between MOCS and perimetric sensitivities was determined using generalized estimating equations.

Results: Among the 32 damaged locations tested (perimetric sensitivities 9-16dB), the correlation between MOCS and perimetric sensitivities was 0.173 ($p=0.101$). At 17 of these locations, the brightest stimulus was detected on $<50\%$ of presentations, indicating

that true sensitivity was in fact below 3.75dB. Perimetry overestimated MOCS sensitivity at most locations. Above 16dB, a significant correlation was seen ($r=0.837$, $p<0.001$).

Conclusions: Below around 16dB, perimetric sensitivities are only weakly informative about the true functional status. They tended to overestimate true sensitivity, by a random amount. The effective dynamic range of standard perimetry may be limited by RGC saturation, not just the maximal luminance of the perimeter.



Perimetry underestimates FOS curve sensitivity. The line represents equality.

Commercial Relationships: Deborah Goren, None; Shaban Demirel, Carl Zeiss Meditec (F), Heidelberg Engineering (R), Heidelberg Engineering (F); Casie Goldman, None; William H. Swanson, None; Stuart K. Gardiner, Allergan (R)
Support: NIH Grant: RO1 EY020922 (SKG)

Program Number: 3941 **Poster Board Number:** D0229

Presentation Time: 2:45 PM - 4:30 PM

Reduced Central Visual Field Sensitivity in Glaucoma Patients With Normal 10-2 Visual Fields Compared to Healthy Controls

Lyne Racette, Amber N. Goad, Linda S. Morgan, Joni S. Hoop, Jennifer Eikenberry, Darrell WuDunn, Brian C. Samuels, Ariel Tying, Anh-Danh T. Phan. Eugene & Marilyn Glick Eye Inst, Indiana University, Indianapolis, IN.

Purpose: To determine whether changes in central visual function exist in glaucoma patients who present with abnormal peripheral visual fields, but who still have normal central visual fields based on global indices.

Methods: Twenty-three eyes were included: 11 patients with primary open-angle glaucoma (POAG) and 12 healthy controls. Patients had a clinical diagnosis of POAG, abnormal Standard Automated Perimetry (SAP) 24-2 and normal SAP 10-2 results. Controls had healthy eyes based on a complete ophthalmological examination and normal SAP 24-2 and 10-2 results. Abnormality on the 24-2 tests was defined as an "Outside Normal Limits" outcome on the Glaucoma Hemifield Test and/or a Pattern Standard Deviation (PSD) value triggered at <10% or worse. Abnormality on the 10-2 tests was defined as a PSD triggered at <5% or worse. Two-tailed t-tests were used to compare the groups on the 24-2 foveal threshold and on the following 10-2 parameters: Mean Deviation (MD), PSD, total number of abnormal Total Deviation (TD) and Pattern Deviation (PD) points (points triggered at either 5%, 2%, or 1%), and the number of TD and PD points triggered at <1%. The Levene test was used to determine whether t-tests for equal or unequal variance were performed. Alpha was set at 0.05.

Results: POAG patients were older than controls (67.3 ± 9.3 yrs; 54.1 ± 8.9 yrs; $p = 0.002$) and had significantly lower foveal

thresholds (34.3 ± 1.9 dB; 36.9 ± 2.3 dB; $p = 0.01$). This may be due to the significant difference in age between the groups (foveal thresholds are not age-corrected). No significant differences were found between the groups for visual acuity and refraction. POAG patients had significantly worse MD values than controls (-1.6 ± 2.6 dB; 0.34 ± 0.9 dB; $p = 0.04$), higher PSD values (1.4 ± 0.1 dB; 1.1 ± 0.2 dB; $p = 0.001$), a higher total number of abnormal PD points (7.2 ± 2.6 ; 3.5 ± 3.0 ; $p = 0.01$), and a higher number of PD points triggered at <1% (1.4 ± 1.1 ; 0.4 ± 0.7 ; $p = 0.02$). No significant differences were found in total number of abnormal TD points (15.6 ± 24.2 dB; 0.8 ± 1.3 dB; $p = 0.07$) and number of TD points triggered at <1% (7.2 ± 19.5 ; 0.1 ± 0.3 ; $p = 0.25$).

Conclusions: Normal 10-2 results differ in POAG patients compared to normals, with evidence of subtle loss in central visual function in glaucoma patients.

Commercial Relationships: Lyne Racette, None; Amber N. Goad, None; Linda S. Morgan, None; Joni S. Hoop, None; Jennifer Eikenberry, None; Darrell WuDunn, Merck (R), Alcon (R); Brian C. Samuels, Merck & Co., Inc (F), Merck & Co., Inc (C), ICHE (C); Ariel Tying, None; Anh-Danh T. Phan, None
Support: Indiana University Health Values Fund VFR-353; Indiana University Biomedical Research Grant; Indiana University EMPOWER grant

Program Number: 3942 **Poster Board Number:** D0230

Presentation Time: 2:45 PM - 4:30 PM

Linear, Tobit and Nonlinear Exponential Regression Modeling of Visual Field Data

Colleen Kummer¹, Gideon J. Zamba³, Trudy L. Burns¹, Paul Romitti¹, Paul H. Artes², Carrie K. Doyle⁵, Chris A. Johnson⁴, Michael Wall⁴. ¹Epidemiology, University of Iowa, Iowa City, IA; ²Dalhousie University, Halifax, NS, Canada; ³Biosstatistics, University of Iowa, Iowa City, IA; ⁴Ophthalmology, University of Iowa, Iowa City, IA; ⁵VA Health Care System, Iowa City, IA.

Purpose: This glaucoma progression statistical modeling study compared the goodness-of-fit of linear, nonlinear exponential, and tobit regression models of longitudinal visual field series data to determine an appropriate model for analysis of these data.

Methods: Visual field data for 52 locations (blind spot locations excluded) in each of 96 glaucomatous eyes, one/subject, were collected using the Humphrey Field Analyzer II 24-2. The Goldmann size III stimuli were used with 24-2 SITA Standard. The dataset included visual field exams at 9 time points taken every 6 months over 4 years. Locations with ≥ 8 floor (0dB) sensitivity values were excluded. Maximum likelihood was used for the estimation of model parameters and the Akaike information criterion (AIC) was computed. Models with the lowest AIC were determined to be the best fitting for that location. The Wilcoxon Signed Rank test was used to determine if the pairwise differences in AIC values between the normal linear, nonlinear exponential, and the tobit regression models were significant within each subject. The R statistical software package was used.

Results: Of the 4740 visual field locations, the tobit regression model fit the data as well or better than the normal model in 99.98% of locations (88.5% the AICs were the same, 11.5% the tobit AIC was lower). Across all subjects, the difference in AIC generated by the normal model and the tobit model was significantly, positively correlated with the number of floor observations (Spearman $r=0.99$, $p<0.0001$) indicating that as more 0dB values are present, the advantage of fitting the tobit model increases. Examination of intra-subject differences in AIC, showed that the tobit regression model fit significantly better in 41.7% of subjects. These subjects had significantly lower mean defect (MD) at baseline ($p<0.0001$); with a

ARVO 2013 Annual Meeting Abstracts by Scientific Section/Group – Glaucoma

MD=-10.3 on average for those in which the tobit model fit better, and MD=-4.3 on average in those with no significant difference between the normal linear and tobit models.

Conclusions: Our results show that these visual field location data were best fit by the tobit model when floor observations are recorded. The tobit model is particularly useful for subjects with advanced disease such as seen in progressive glaucoma. Increased precision in modeling may contribute to accurate and early detection of visual field change and consequently early treatment to preserve visual function.

Commercial Relationships: Colleen Kummet, None; Gideon J. Zamba, None; Trudy L. Burns, None; Paul Romitti, None; Paul H. Artes, Heidelberg Engineering, Germany (C), Haag-Streit AG, Switzerland (C), Carl Zeiss Meditec, Germany (C), Optovue Inc, CA, USA (C), Peridata GmbH, Germany (F); Carrie K. Doyle, None; Chris A. Johnson, Lundbeck (C), Ivantis (C), Jaeb Center (C), AEGIS (C), Acufocus (C), Haag Streit (C); Michael Wall, None
Support: Veterans Affairs Rehabilitation R&D Merit Review Grant

Program Number: 3943 **Poster Board Number:** D0231

Presentation Time: 2:45 PM - 4:30 PM

Automated stimulus choice in condensed grids for assessment of visual field defects

Luke X. Chong¹, Allison M. McKendrick¹, Andrew Turpin².

¹Department of Optometry and Vision Sciences, The University of Melbourne, Parkville, VIC, Australia; ²Department of Computing and Information Systems, The University of Melbourne, Parkville, VIC, Australia.

Purpose: A condensed stimulus grid improves spatial characterisation of visual field (VF) defects (Schiefer et al IOVS 2010). We define a new algorithm that autonomously selects locations for stimulus presentations within a dense grid to improve characterisation of VF defects. We hypothesised our algorithm would provide more accurate estimates of threshold for all locations than linear interpolation of a less dense grid.

Methods: Each location in our grid runs a ZEST-like procedure, with seed locations initially presented twice, and subsequent trials taking place at the mid-point of the two locations with the highest gradient (estimated threshold/distance). After each presentation, locations that have had no presentations are updated based on a weighting of spatial relationships determined from a database of 297 VFs. The total number of presentations was limited to be comparable to existing procedures.

The algorithm was tested using computer simulation on 54 empirical VFs (HFA 24-2). A 5x5 (25 locations) grid of 24-2 points was selected from each field, from which every second location was omitted to create a 3x3 (9 locations) grid. Omitting locations models a coarser VF grid where the intermediate values are known. Three results were compared: 1) Our algorithm run on all 25 locations; 2) our procedure for the 3x3 grid with untested locations being "interpolated estimates"; 3) the input thresholds as estimates on the 3x3 grid with untested locations being "interpolated from true-fields". Procedures were compared to the input VF to determine error. Simulations were repeated 200 times with stochastic patient responses. Locations derived from interpolation were compared to corresponding measured locations in the 5x5 grid for analysis.

Results: The median absolute error (MAE) was lower in the 5x5 grid compared to the interpolated 3x3 grid (2.57dB vs 3.15dB, Wilcoxon $P < 0.05$). The interpolated true field had lower MAE than the 5x5 grid (1.50dB vs 2.57dB, Wilcoxon $P < 0.05$). The interquartile ranges for the 5x5 grid, "interpolated estimates" and "interpolated from true-fields" were 1.76dB, 3.52dB and 2.50dB respectively.

Conclusions: This procedure shows potential to automatically

choose additional locations to test within areas of loss without increasing test time. Simulations suggest testing locations spaced closer together provides more accurate information about a scotoma than interpolating across a coarser grid.

Commercial Relationships: Luke X. Chong, None; Allison M. McKendrick, Heidelberg Engineering GmbH (F); Andrew Turpin, Heidelberg Engineering (F)

Support: Melbourne Research Scholarship, ARC FT0990930, ARC FT0991326

Program Number: 3944 **Poster Board Number:** D0232

Presentation Time: 2:45 PM - 4:30 PM

NOVEL TECHNIQUE: A PUPILLOMETER-BASED OBJECTIVE CHROMATIC PERIMETRY

Ygal Rotenstreich¹, Alon Skaat¹, Ifat Sher-Rosenthal¹, Andrew F. Kolker², Elkana Rosenfeld¹, Shlomo Melamed¹, Michael Belkin¹.

¹Goldschleger Eye Research Institute, Sheba Medical Center, Tel Hashomer, Israel; ²Department of Ophthalmology, George Washington University, Washington, DC.

Purpose: Quantification of the pupil response to chromatic light stimuli can be used to assess rod, cone, and melanopsin-containing ganglion cell activity. Here we developed a novel objective perimetry technique based on the pupil response to multifocal chromatic stimuli in normal subjects and in patients with glaucoma and retinitis pigmentosa (RP).

Methods: A computerized infrared video pupillometer was used to record changes in pupil diameter in response to short- and long-wavelength stimuli (peak 485 nm and 620 nm, respectively) size V, at light intensities of 15-100 cd-s/m² and duration of 1000 ms at different points of the visual field. The RP patient group included 16 eyes of 8 patients and the normal group included 18 eyes of 11 subjects. The glaucoma patient group included 22 eyes of 11 patients and the normal group included 38 eyes of 19 subjects.

Results: Significantly reduced pupillary responses were obtained in RP patients under testing conditions that emphasized rod contribution (short-wavelength stimuli at 40 cd-s/m²) in nearly all perimetric locations ($P < 0.05$). The glaucoma group showed significantly reduced pupillary responses under testing conditions that emphasized ganglion cell contribution (short-wavelength stimuli at high intensity) in all perimetric locations ($P < 0.05$) as well as reduced pupillary responses under conditions that emphasized rod contribution mostly in nasal areas ($p < 0.05$). By contrast, both patient groups demonstrated nearly normal pupillary responses under testing conditions that emphasized cone cell contribution (long-wavelength stimuli at high intensity) in majority of perimetric locations.

Conclusions: This study demonstrates the feasibility of using pupillometer-based chromatic perimetry for objectively assessing visual field defects and retinal function in patients with retinal dystrophies and glaucoma. Furthermore, this method may be used to distinguish between the damaged cells underlying the visual field defect.

Commercial Relationships: Ygal Rotenstreich, PCT/L2010/00624 (P), Sheba Medical Center (P); Alon Skaat, None; Ifat Sher-Rosenthal, None; Andrew F. Kolker, None; Elkana Rosenfeld, None; Shlomo Melamed, Solx (F), Eyetechnicare (F), Ioptima (F), Allergan (F); Michael Belkin, Alcon (C), Ellex (C), PCT: IL2011/000373 Filed 9/5/2011 Published (P)

Support: Claire and Amade Martier fund research grant, Israeli Ministry of Absorption grant

Clinical Trial: NCT01021982

Program Number: 3945 **Poster Board Number:** D0233

Presentation Time: 2:45 PM - 4:30 PM

Longitudinal analysis of Glaucoma Suspects from the Erlangen glaucoma registry (EGR): Influence of neuroretinal rim area and visual field indices on Progression

Hohberger Bettina, Folkert K. Horn, Anselm G. Junemann, Robert Laemmer. University Erlangen, Erlangen, Germany.

Purpose: The aim of this study was to investigate the long-term follow up of glaucoma suspects, recruited from the Erlangen glaucoma registry to detect parameters, indicating disease progression. For this purpose visual fields and the neuroretinal rim area (quantified with the HRT) were compared between two cohorts: with and without perimetric progression.

Methods: 329 glaucoma suspect eyes were included (177 OHTs, 152 preperimetric open angle glaucomas, preOAG). All patients are members of the Erlangen glaucoma registry (ISSN 2191-5008, CS-2011) for 8 to 20 years. The clinical database (NCT00494923) allows longitudinal observation of exactly defined glaucoma patient groups over two decades. The protocol was approved by the Local Ethics Committee (3457). All had annual complete ophthalmological examinations, including Octopus (protocol G1) and HRT. In our study, information from 5 years of consecutive clinical-instrumental evaluation of the glaucoma suspects separated 2 groups: Patients without and with glaucoma progression. Progression was defined using perimetric event analysis, confirmed at least once. In order to investigate the progress per year individually, linear regression analyses were done using 6 data sets before progression occurred. In the non-progressive group, the most recent 5 years were evaluated. In addition, annual results were compared with t-test ($\alpha = 0.05$).

Results: 38 (11,5 %; 5 OHT; 22 preOAG) of the total cohort showed perimetric glaucoma progression. This progressive group showed significant higher MD as the non-progressive group at baseline of the present observation period. SLV was higher in the progressive group at all time-points of examinations. This difference reached level of significance 2 years before visual field losses occurred. The area of the neuroretinal rim was significant different between both subgroups 5 years before perimetric field defects occurred, with no significant decrease in the course.

Conclusions: Findings in the present ‘suspect’ cohort of the EGR show the prognostic value of an increasing sLV for conversion to ‘perimetric’ glaucoma. Therefore, reduced area of neuroretinal rim values and elevated sLV must be considered as indicators for glaucoma progression.

Commercial Relationships: Hohberger Bettina, None; Folkert K. Horn, None; Anselm G. Junemann, None; Robert Laemmer, None
Support: SFB 539 (1997 - 2009)

Clinical Trial: NCT00494923

Program Number: 3946 **Poster Board Number:** D0234

Presentation Time: 2:45 PM - 4:30 PM

Relationship between Target Speed and Simple Visual Reaction Time Measured at the Location of Kinetic Threshold using Automated Kinetic Perimetry

Tomoyasu Kayazawa¹, Chota Matsumoto¹, Sachiko Okuyama¹, Shigeki Hashimoto¹, Eiko Koike², Hiroki Nomoto¹, Fumi Tanabe¹, Mariko Eura¹, Takuya Numata¹, Yoshikazu Shimomura¹.

¹Department of Ophthalmology, Kinki University Fac, Osaka-Sayama City, Japan; ²Department of Ophthalmology, Sakai Hospital Kinki University Fac, Sakai City, Japan.

Purpose: There have been several reports in which the relationships between target speed and simple visual reaction time (RT) in kinetic perimetry were investigated. In those previous studies, the RT was measured at the locations of sufficient suprathreshold. Such RT may not necessarily equal the RT at the location of kinetic threshold (KT). In this study, we measured the RT at the location of KT to investigate

the relationship between the target speed and RT.

Methods: Five normal eyes of 5 subjects (2 males, 3 females; range of age: 31-38 years) were tested using the Goldmann kinetic perimetry program in Octopus 900 with the target luminance and size of III/4e, I/4e, I/3e, I/2e and I/1e, and with ten kinds of target speed from 1°/s to 10°/s. First, the response point for each kinetic target was measured along the meridians of 135° and 225°. After that, the target was moved perpendicularly from the point 1° outside of the response point on the meridians at each target speed. When there was a response, the same target was presented from 1° farther outside, and the outermost response point was determined as KT for each target speed. Next, RT of each target at the location of KT was measured using the “RT-vector” procedure. If the target was not seen, the target was moved inward 1° by 1° until there was a response.

Results: The RTs measured at the locations of KT were 708.5 ms (1°/s), 604.8 ms (2°/s), 462.0 ms (3°/s), 402.3 ms (4°/s), 414.8 ms (5°/s), 418.5 ms (6°/s), 385.8 ms (7°/s), 366.3 ms (8°/s), 366.3 ms (9°/s) and 349.0 ms (10°/s) with target of I/4e. It was also observed with target of III/4e, I/3e, I/2e and I/1e that the RT increased as the target speed decreased between 1° and 10°/s.

Conclusions: If we correct KT with RT in automated kinetic perimetry, RT should be evaluated at the same speed as the target speed used actually.

Commercial Relationships: Tomoyasu Kayazawa, None; Chota Matsumoto, None; Sachiko Okuyama, None; Shigeki Hashimoto, None; Eiko Koike, None; Hiroki Nomoto, None; Fumi Tanabe, None; Mariko Eura, None; Takuya Numata, None; Yoshikazu Shimomura, None

Program Number: 3947 **Poster Board Number:** D0235

Presentation Time: 2:45 PM - 4:30 PM

A novel system to detect the progression of glaucomatous visual field damage: aggregating the results of point-wise analysis with the binomial test

Hiroshi Murata, Ayako Karakawa, Hiroyo Hirasawa, Chihiro Mayama, Makoto Aihara, Ryo Asaoka. Ophthalmology, University of Tokyo, Tokyo, Japan.

Purpose: To create a novel system to detect the progression of glaucomatous visual field (GVF) damage by carrying out the binomial test on the result of point-wise analysis on visual field (VF).

Methods: Ninety-nine eyes of 59 open angle glaucoma patients (53±12 years, mean±sd) who underwent more than 15 VFs (Humphrey Field Analyzer, SITA standard, 30-2), were retrospectively collected. 15 VFs (6.0±1.5 years), excluding the first VF, were used for the analysis. Using the total deviation (td) of each point on the 2nd to 16th VF (VF2-16), linear regression analysis was carried out. The numbers of the test points with $p < 0.025, 0.05, 0.075$ and 0.1 were calculated to perform binomial test (one-side) and then the median value of the p values was calculated. A VF was defined as “progressive” if the median value was < 0.025 (“point-wise method”). Similarly, the progression analysis was carried out using VF2-6 to VF2-15. Then these probabilities were calculated; both of VF2-16 and prior VFs were “progressive”: sensitivity, both of VF2-16 and prior VFs were “non-progressive”: sensitivity, and VF2-16 was “non-progressive” however prior VFs were “progressive”: false positive. Same probabilities were calculated using the conventional MD slope method.

Results: The specificity and false positive rates with the point-wise method (42±24, 8±10%) outperformed MD slope (38±25, 18±13%, $P < 0.05$), while the specificities were not significantly different (96±2 and 96±3% $p = 0.95$).

Conclusions: It was suggested that the point-wise method may be

able to detect the progression of GVF earlier than the MD slope method.

Commercial Relationships: Hiroshi Murata, None; Ayako Karakawa, None; Hiroyo Hirasawa, None; Chihiro Mayama, None; Makoto Aihara, Ono pharmaceutical company (F), Pfizer (F); Ryo Asaoka, None

Program Number: 3948 **Poster Board Number:** D0236

Presentation Time: 2:45 PM - 4:30 PM

Relationship between Corneal Hysteresis and Visual Field Progression in Glaucoma and Ocular Hypertensive Eyes

Marta Pazos¹, Alfonso Anton^{1,2}, Maria Jesus López-Valladares³, Valentín Tinguaro Díaz-Alemán⁴, Monica Fallon². ¹Ophthalmology. Glaucoma., Hospital de l'Esperança. Parc de Salut Mar., Barcelona, Spain; ²Glaucoma. Research., Institut Català de la Retina., Barcelona, Spain; ³Ophthalmology. Glaucoma., Complexo Hospitalario Universitario de Santiago de Compostela, Santiago de Compostela, Spain; ⁴Ophthalmology. Glaucoma., Hospital Universitario de Canarias, Tenerife, Spain.

Purpose: To investigate if glaucomatous visual field progression is associated to corneal hysteresis parameters measured by the Ocular Response Analyzer (ORA).

Methods: One hundred glaucomatous and ocular hypertensive (OHT) patients previously analyzed for an ORA reproducibility study were prospectively evaluated in the basis of their standard follow-up care in the glaucoma clinic. Only patients with 3 years follow-up and a minimum of 5 Humphrey Standard 24-2 visual fields (VF) were included. Guided Progression Analyzer (GPA) Visual Field Index (VFI) rate of progression (significant trend at p<0.05) and/or Progression Analysis Probability of events (three contiguous points significantly changing in at least two consecutive tests) were used to detect VF progression.

Results: 59 eyes (31 Glaucoma and 28 OHT, mean age 70.69±11.87 y; mean MD -2.95±4.7 dB; mean number of VF 8±2.45; mean follow-up time 4.10 ±0.64 y) met the enrolment criteria. The glaucoma group had significantly lower central corneal thickness (CCT) (531.42±30.9 vs 559.07±26.57µm, p<0.01) and lower corneal resistance factor (CRF) (9.16±1.61 vs 11.59±1.83, p<0.01) but not significantly different corneal hysteresis (CH) (8.66±2.16 vs 9.72±2.26, p=0.07) compared with the OHT group. The mean global VFI rate of progression was -0.57 ± 1.22 dB/year (Glaucoma:-1.05±1.5 vs OHT: -0.03±0.4 dB/year; p<0.01). Seventeen eyes reached a progression endpoint (2 in the OHT group and 15 in the Glaucoma group). Progressing eyes had greater baseline cup-to-disc ratio (0.66±0.2 vs 0.51±0.23; p<0.05), lower CCT (530±36.34 vs 550.4±36.3 µm; p<0.05) and lower CRF (9.31±1.27 vs; 10.72±2.25; p<0.05) but not significantly different CH (8.34±2.5 vs 9.50±2.1; p=0.07) compared with non-progressing eyes. Rate of progression, among progressing eyes, was significantly greater with decreasing CRF (r2 0.04, p<0.001).

Conclusions: Thinner CCT and lower CRF were associated with progressive field worsening in glaucomatous and OHT eyes.

Commercial Relationships: Marta Pazos, None; Alfonso Anton, ALCON (F), SANTEN (C), MSD (C), THEA (C), TRANSCEND (C), ALCON (R), ALLERGAN (R), SANTEN (R); Maria Jesus López-Valladares, Allergan Inc (F), MSD (Merck Sharp and Dohme Spain) (R); Valentín Tinguaro Díaz-Alemán, None; Monica Fallon, None

Program Number: 3949 **Poster Board Number:** D0237

Presentation Time: 2:45 PM - 4:30 PM

Expert Evaluation of Visual Field Change in Glaucoma Correlates Better With the Measured Fast Component of Visual Field Loss

Nila Cirineo¹, Kouros Nouri-Mahdavi¹, Jun Mo Lee¹, Meera Ramanathan¹, Esteban Morales¹, Fei Yu^{1,2}, Abdelmonem Afifi², Anne L. Coleman^{1,3}, Joseph Caprioli¹. ¹Ophthalmology, Jules Stein Eye Institute, Los Angeles, CA; ²Biostatistics, School of Public Health at UCLA, Los Angeles, CA; ³Epidemiology, School of Public Health at UCLA, Los Angeles, CA.

Purpose: This study was conducted to compare the assessment of decay in serial visual fields (VF) based on subjective expert evaluation and rates of fast and slow components determined by pointwise exponential regression.

Methods: Five thousand one hundred eighty seven Humphrey visual field exams from 378 patients with primary open angle glaucoma were evaluated by a glaucoma subspecialist for determination of progression. Serial of VFs were evaluated by an expert for changes using score of 1 (most likely progression) to 5 (least likely) for change and 1 (no change) to 6 (very fast) for rate of changes. Pointwise exponential regression (PER) was used to measure the fast and slow components of VF deterioration. The qualitative and quantitative methods were then compared.

Results: The correlation coefficient (r) between the fast component and expert evaluation was -0.268 (p<0.0001) and for the slow component -0.156 (p=0.002). Figure 1 shows the relationship between the calculated rate of decay and the score of likelihood of progression for the fast and slow components. Figure 2 shows the relationship between the calculated rate of decay and scored rate of decay based on expert evaluation.

Conclusions: Expert qualitative evaluation of VF series for change and rates of changes correlate more closely with the fast component of VF decay than the slow component of VF decay.

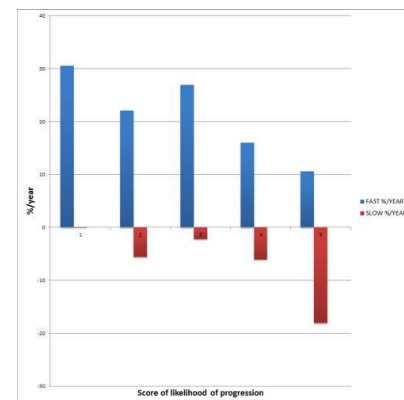


Figure 1

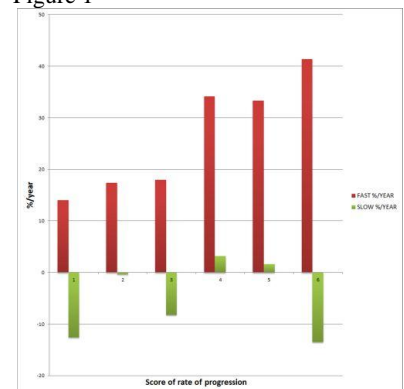


Figure 2

Commercial Relationships: Nila Cirineo, None; Kouros Nouri-Mahdavi, Allergan (C); Jun Mo Lee, None; Meera Ramanathan, None; Esteban Morales, None; Fei Yu, None; Abdelmonem Affifi, None; Anne L. Coleman, None; Joseph Caprioli, Allergan Inc. (F), Allergan Inc. (C), Allergan Inc. (R)

Program Number: 3950 **Poster Board Number:** D0238

Presentation Time: 2:45 PM - 4:30 PM

Noise-Corrected Event Analysis of Automated Visual Fields

David W. Richards, Zia Khan. Ophthalmology, Univ of South Florida Coll of Med, Tampa, FL.

Purpose: To develop a rigorous method for the determination of a Visual Field “Event”, defined as “a statistically significant sudden change in the overall sensitivity of an automated visual field (VF)”.

Methods: We previously developed a method for detection of VF progression (Richards et.al. ARVO 2011 Program # 4155) by accounting for the “noise” at every location within a VF, based on transformation of variable to approximate a Gaussian distribution. Once the pointwise noise has been so defined for a series of VF’s, a sudden change in overall sensitivity (“Event”) may be determined by treating an existing series of Zeiss-Humphrey Sita-Standard 24-2 VF’s as a 52-dimensional normal distribution and computing the 52-dimensional Chi-square value for a new VF, based on the established means and variances, and requiring $p < 0.05$. We tested this method by analyzing 92 VF’s of 10 eyes of 10 patients and comparing results with modified Parrish-Hodapp-Anderson (PHA) criteria (AAO BCSC 2011-2012 Section 10 p 77) for: Case 1, Deepening of existing scotoma; Case 2, Depression of a point adjacent to existing scotoma; Case 3, Depression of a previously normal point; and Case 4, Depression of two adjacent normal points.

Results: Results for all 4 cases are significant at $p < 0.05$ level by Mann Whitney U Test.

Case 1: Criterion of 7 db is too weak; deepening by >10 db is needed.

Case 2: Criterion of 9 db is too strong; deepening by 5 db is sufficient.

Case 3: Criterion of 11 db is too strong; deepening by 7 db is sufficient.

Case 4: Criterion of 5 db is too weak; deepening by 6 db is needed.

Conclusions: Transformation of variable and accounting for pointwise noise of a series of VF’s permit, for the first time, computation of a precise statistical measure of an “Event” when a new VF is obtained. Previously used criteria, such as PHA, while reasonable estimates, may not always be reliable.

Commercial Relationships: David W. Richards, None; Zia Khan, None

Program Number: 3951 **Poster Board Number:** D0239

Presentation Time: 2:45 PM - 4:30 PM

Detection of Functional Defect in Early Glaucoma using Standard Automated Perimetry and Flicker Defined Form Perimetry

Yuan-Hao (Derek) Ho¹, John G. Flanagan^{1,2}. ¹School of Optometry and Vision Science, University of Waterloo, Waterloo, ON, Canada; ²Department of Ophthalmology & Vision Science, University of Toronto, Toronto Western Hospital, Toronto, ON, Canada.

Purpose: To compare the detection of functional loss in early glaucoma using standard automated perimetry and flicker defined form perimetry.

Methods: 156 early-moderate glaucomatous subjects were recruited (average age: 62.6 ± 11.0 ; 75 male, 78 OD). Humphrey Field Analyzer (HFA) SITASd 24-2 classified subjects as 130 early glaucoma eyes and 26 moderate glaucoma eyes using a modified Hodapp criteria (MD: -2.12 ± 2.04 dB; PSD: 2.56 ± 1.78 dB). The Heidelberg Edge

Perimetry (HEP) was used to perform both standard automated perimetry (HEP-SAP) and flicker defined form perimetry (HEP-FDF). Of note is that both forms of perimetry share the identical normative database. Participants were tested at 3 visits within a 3 month period, including HFA SITASd 24-2 (visit 1), HEP-SAP ASTASd 24-2 (visit 2&3) and HEP-FDF ASTASd 24-2 (all visits). Unreliable visual fields were excluded from the study.

Results: The HEP-FDF gave more defects (2514 PD less than 5%, 1568 less than 1%, 1357 less than 0.5%; MS: 13.33 ± 6.34 dB) than HEP-SAP (1817 PD less than 5%, 833 less than 1%, 647 less than 0.5%; MS: 27.89 ± 3.91 dB). Test re-test characteristics were similar for both HEP-FDF ($r=0.82$, MoD=-0.43, CoR=7.47) and HEP-SAP ($r=0.75$, MoD=-0.15, CoR=5.45) in our study. Test time was significantly ($p < 0.001$) longer for HEP-FDF (463.12 ± 150.97 sec) than HEP-SAP (353.19 ± 75.84 sec), due to the larger number of field defects detected by HEP-FDF.

Conclusions: Visual field defects were detected earlier by HEP-FDF when compared to HEP-SAP in early glaucoma. Both tests gave similar test-retest characteristics. There was a similar test time for similar amounts of defect. The greater the defect the longer the test time.

Commercial Relationships: Yuan-Hao (Derek) Ho, None; John G. Flanagan, Heidelberg Engineering (C), Heidelberg Engineering (R), Heidelberg Engineering (F), Carl Zeiss Meditec (C), Carl Zeiss Meditec (R), Carl Zeiss Meditec (R), Alcon Pharmaceuticals (R), Alcon Pharmaceuticals (R), Optovue Inc (F), Optovue Inc (F), Photon etc (F), Photon etc (F)

Support: Heidelberg Engineering GmbH

Program Number: 3952 **Poster Board Number:** D0240

Presentation Time: 2:45 PM - 4:30 PM

Comparing performance of the Flicker-Defined Form (FDF) stimulus and Standard Automated Perimetry (SAP) using the Heidelberg Edge Perimeter (HEP) in patients newly referred with suspect glaucoma

Csilla Ajtony¹, Gnanapragasam Nithyanandarajah¹, Rupert R. Bourne^{1,2}. ¹NIHR Biomedical Research Centre at Moorfields Eye Hospital NHS Foundation Trust, UCL Institute of Ophthalmology, London, United Kingdom; ²Vision & Eye Research Unit, Postgraduate Medical Institute, Anglia Ruskin University, Cambridge, United Kingdom.

Purpose: To compare the performance of Heidelberg Edge Perimeter (HEP) Flicker-Defined Form (FDF) and Standard Automated Perimetry (SAP) strategies to Humphrey SAP, in terms of reliability, duration of test and agreement between tests.

Methods: Consecutive new glaucoma suspects referred to a hospital’s glaucoma service received all 3 tests. A screening pre-test familiarised patients to the FDF stimulus followed by HEP-SAP and HEP-FDF tests. Agreement between tests was analysed using visual fields of patients with normal optic discs as judged by experienced optic disc graders using optic disc photographs.

Results: 137 patients (50 men, 57 women) with non-glaucomatous optic discs were included (average age, 61.1 years [SD, 9.9 years], range 22-89 years). 30 patients who performed unreliable HEP-FDF visual fields were excluded. Significantly lower values for test duration time compared to HFA-SAP (HEP-FDF: mean 276.3 seconds, SD 77.2 s; HEP-SAP: mean 214.9 s, SD 37.9 s; HFA-SAP: mean 307.1 s, SD 47.9 s). Among the reliability indexes, Fixation Losses were significantly fewer with the HEP-FDF (mean %, 1.19, SD 4.21; HEP-SAP: mean 5.21, SD 16.25; HFA-SAP: mean, 14.87, SD 23.69). False Positive values (%) for HFA-SAP (mean 2.66; SD 4.62) were significantly higher than both HEP-FDF (mean 0.75; SD 1.17), or HEP-SAP (mean 0.79; SD 3.01). The mean False Negative

ratios for HEP-FDF, HEP-SAP and HFA-SAP visual fields were 7.1 (SD 10.7), 3.9 (SD 8.0), 1.9 (SD 3.7), respectively. Significantly higher values for Mean Deviation (HEP-FDF: mean, -2.69, SD 2.59; HEP-SAP: mean, -0.52, SD 1.45; HFA-SAP: mean -0.64, SD 1.78; $p < 0.001$) and Pattern Standard Deviation (HEP-FDF: mean 2.16, SD 1.13; HEP-SAP: mean, 1.53, SD, 0.91; $p < 0.001$) were found in HEP-FDF tests.

Conclusions: The FDF test is intended for early detection of glaucomatous visual fields. Tests using this instrument were associated with higher false negative values than HEP-SAP and HFA-SAP. However, patients performed better on the HEP-FDF in terms of fewer fixation losses and lower false positive rates. Additionally test duration was faster with the HEP-FDF. Higher MD values were found with HEP-FDF visual fields than both HEP-SAP and HFA-SAP strategies, but PSD more closely agreed with HFA-SAP when testing these patients with normal optic nerves.

Commercial Relationships: Csilla Ajtony, None; Gnanapragasam Nithyanandarajah, None; Rupert R. Bourne, Allergan Ltd (F)

Program Number: 3953 **Poster Board Number:** D0241

Presentation Time: 2:45 PM - 4:30 PM

Eye Movement Perimetry in Glaucoma Patients

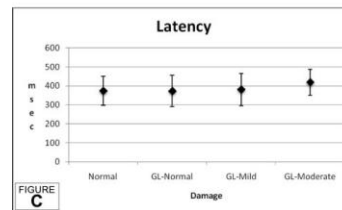
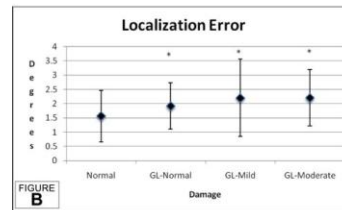
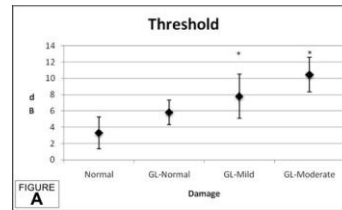
Alice Xu¹, David E. Warren², Carrie K. Doyle^{3,4}, Andrew Papendieck¹, Matthew J. Thurtell^{3,4}, Michael Wall^{3,4}. ¹Carver College of Medicine, Iowa City, IA; ²Department of Neurology, University of Iowa, Iowa City, IA; ³Iowa City VA Health Care System, Iowa City, IA; ⁴Department of Ophthalmology, University of Iowa, Iowa City, IA.

Purpose: We have developed a new perimetry test that evaluates two novel eye movement measures in addition to visual threshold. We hypothesized that optic nerve damage seen in glaucoma patients will result in increased visual threshold, reduced saccadic accuracy, and lengthened saccadic latency when compared with normals.

Methods: 19 glaucoma patients (56 to 78 years) had visual thresholds tested at 3 test locations based on Standard Automated Perimetry (SAP)-determined visual loss: normal sensitivity (+2 to -2dB on total deviation plot), mild visual loss (-3 to -6dB), and moderate loss (-7 to -16dB). 29 age-matched ocular healthy subjects (49 to 74 years) were tested at 3 test locations based on eccentricity: central (3, -3), middle (3, 9), and peripheral (-21, 3). Frequency of seeing curves were constructed using a circular light gray stimulus presented on a dark gray background. Size was varied and location presentation randomized. An EyeLink1000 infrared camera recorded saccadic eye movements to the stimulus. Using threshold and suprathreshold data from frequency of seeing curves, we compared visual threshold (50% seen stimulus), saccadic accuracy (measured as localization error—the distance between recorded final eye position and stimulus position), and saccadic latency (time taken to initiate a saccade to the stimulus) between glaucoma patients and normals matched in eccentricity. Differences among groups were assessed using ANOVA.

Results: Glaucoma patients had higher visual thresholds (Threshold, graph A, $p < .001$) and decreased saccadic accuracy (Localization Error, graph B, $p = .008$) as compared with normals. Eye movement perimetry also showed reduced saccadic accuracy for test locations that SAP considered as normal sensitivity. Threshold increased and localization error increased in this order: normals, glaucoma normal sensitivity, glaucoma mild damage, and glaucoma moderate damage. Saccadic latency measures showed no significant differences between normals and glaucoma patients (Latency, graph C, $p = .12$).

Conclusions: Eye movement perimetry shows a significant increase in saccadic localization error with increasing glaucomatous damage; saccadic latencies, however, did not significantly change.



Diamond designates mean value for normals and glaucoma test locations of normal or mild or moderate damage. Bars designate 1SD. Stars designate statistical significance.

Commercial Relationships: Alice Xu, None; David E. Warren, None; Carrie K. Doyle, None; Andrew Papendieck, None; Matthew J. Thurtell, None; Michael Wall, None

Support: Veterans Affairs Rehabilitation R&D Merit Review Grant

Program Number: 3954 **Poster Board Number:** D0242

Presentation Time: 2:45 PM - 4:30 PM

The ability of Moorfields Motion displacement visual field test to discriminate different stages of glaucoma

Robert L. Stamper, Orathai Chansanti, Nita Subramanian. Ophthalmology, Univ California-San Francisco, San Francisco, CA.

Purpose: To determine if the Moorfield Motion Displacement Test (MMDT) can classify different stages of glaucoma, based on automated static perimetry (AVF) test results.

Methods: After informed consent was obtained, MMDT was performed in 270 patients (422 eyes) who had automated static perimetry done in the preceding year. We used The Enhanced Suprathreshold algorithm 99.5 pandora, which took approximately 2 minutes per eye. Patients were excluded if they had unreliable results in either AVF or MMDT. Criteria of exclusion were fixation loss > 25%, false positive > 33% and false negative > 33%. We classified the glaucoma patients into two groups depending on whether the mean deviation (MD) of the AVF was better than -6.00 or worse, according to the glaucoma staging system (GSS). We also analyzed the group of normal visual field in order to find the specificity. We compared 2 parameters from HVF to percentage of damage (PTD) from MMDT. One was MD vs PTD and other was VFI vs PTD. The scores on the MMDT were analyzed in a masked fashion and compared to the MD. A PTD of 70% was chosen as the cutoff point. We also reviewed the topographic pattern of visual field in both HVF and MMDT in a masked fashion.

Results: There were 213 eyes where MD was better than -6.00 and 57 eyes with MD of -6.00 and worse. Specificity was relatively low: 90.4% of 136 eyes with normal automated static perimetry were also normal by MMDT. Sensitivity was high for moderate to advanced

glaucoma; 98.9% of 57 eyes with moderate to advanced glaucoma had an abnormal MMDT. 76.6% of 77 eyes with early glaucoma (MD-1 to -5.99) had abnormal MMDT. However, there was some overlap. Receiver operator characteristic curves are in process and will be presented.

Conclusions: The MMDT was quite sensitive in detecting moderate to advanced glaucomatous visual field damage. However, using a 70% normal cutoff for the MMDT, the specificity was somewhat low. If an appropriate cutoff score for MMDT can be found that maintains the high sensitivity but improves the specificity, the MMDT might be an effective screening tool.

Commercial Relationships: Robert L. Stamper, Transcend (C), Genentech (C); Orathai Chansanti, None; Nita Subramanian, None

Support: NIH Core Grant; Research to Prevent Blindness; Fortisure Foundation

Program Number: 3955 **Poster Board Number:** D0243

Presentation Time: 2:45 PM - 4:30 PM

Detection of Glaucomatous Progression Comparing SITA Standard and Matrix Perimetry

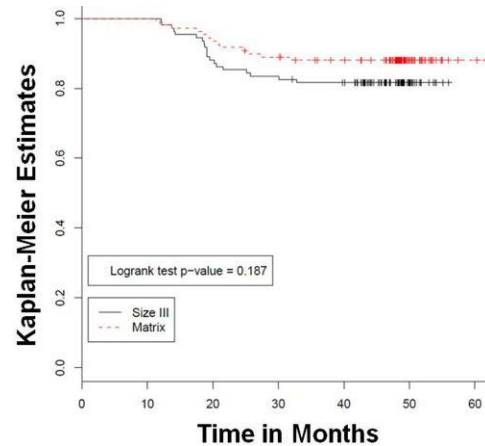
Michael Wall^{1,2}, Carrie K. Doyle^{1,2}, Trina Eden^{1,2}, Chris A. Johnson², Gideon J. Zamba³. ¹Iowa City VA Health Care System, Iowa City, IA; ²Ophthalmology and Visual Sciences, University of Iowa, Carver College of Medicine, Iowa City, IA; ³Biostatistics, University of Iowa, College of Public Health, Iowa City, IA.

Purpose: The Humphrey Matrix may be more sensitive in detecting glaucomatous visual field loss compared to SITA-Standard. Therefore, it may be a good candidate to determine disease progression in glaucoma patients. Our aim was to test the hypothesis automated perimetry using the Humphrey Matrix would determine progression before SITA-Standard Size III.

Methods: Sixty normal subjects and 120 glaucoma patients were tested twice at baseline and every six months for 4 years with SITA-Standard size III and Matrix. We used a method of pointwise linear regression, PLRA2. With this approach, a glaucoma patient is defined as progressing if a significant slope was detected at the same test location in three of four consecutive visual field examinations with confirmed progression in two or more test locations. The 60 normals followed longitudinally were used to calculate specificity. Kaplan-Meier curves were used to compare the tests.

Results: SITA-Standard testing detected visual field progression at a higher rate than the Humphrey Matrix (Figure). Using a slope of -1.0 dB per year at a p = 0.05 significance level, the hit rate/specificity ratios of size III were 18% and 100% and for Matrix were 12% and 97.7%.

Conclusions: SITA-Standard size III testing may identify glaucomatous visual field progression earlier than testing with the Humphrey Matrix.



Commercial Relationships: Michael Wall, None; Carrie K. Doyle, None; Trina Eden, None; Chris A. Johnson, Lundbeck (C), Ivantis (C), Jaeb Center (C), AEGIS (C), Acufocus (C), Haag Streit (C); Gideon J. Zamba, None

Support: Veterans Affairs Rehabilitation R&D Merit Review Grant

Program Number: 3956 **Poster Board Number:** D0244

Presentation Time: 2:45 PM - 4:30 PM

Personalizing the Frequency and Timing of Testing to Check for Glaucoma Progression: a Novel Approach

Mariel Lavieri¹, Jonathan Helm³, Gregory Schell¹, Mark Van Oyen¹, David C. Musch², Joshua D. Stein². ¹Industrial and Operations Engineering, University of Michigan, Ann Arbor, MI; ²Department of Ophthalmology and Visual Sciences, University of Michigan, Ann Arbor, MI; ³Kelley School of Business, Indiana University, Bloomington, IN.

Purpose: To determine whether it is possible to significantly improve detection of disease progression in patients with open angle glaucoma (OAG) by using personalized, dynamically-adjusted schedules of visual field (VF) testing and intraocular pressure (IOP) measurements.

Methods: A Kalman filter was used to model the disease dynamics of a large group of patients with mild to advanced OAG based on VF and IOP readings obtained sequentially over time. As additional VF and IOP tests are performed on each patient, the filter updates our knowledge about each patient's disease dynamics. Parameterization and validation of the models was performed using >5 years of longitudinal data of IOP measurements and VF testing from patients who were enrolled in the Collaborative Initial Glaucoma Treatment Study (CIGTS) and the Advanced Glaucoma Intervention Study (AGIS). The model then forecasts each patient's disease dynamics into the future while incorporating the uncertainty associated with those forecasts. Logistic regression was used to model the relationship between the current and future disease dynamics and OAG progression. We developed an algorithm which combines the Kalman filter learning capabilities and the logistic regression predictive power to determine personalized schedules of VF and IOP testing for each patient. Our algorithm was compared against fixed interval schedules for obtaining VFs and IOP measurements from the trials.

Results: A total of 571 participants (571 eyes) with OAG were evaluated. Compared to yearly intervals of checking VFs and IOPs, our approach using the Kalman filter achieved a 27% increase of efficiency in detecting OAG progression (p<0.0001) and detected OAG progression 63% sooner (i.e. reduced diagnostic delay) (p<0.0001) using the same number of tests per patient.

Conclusions: Dynamic and personalized schedules for obtaining IOP and VF measures using a Kalman filter approach can improve the likelihood of detecting OAG progression and identifying OAG progression sooner than fixed interval examination schedules.

Performance Measures	Fixed Interval Testing (IOP / VF)			Kalman Filter Algorithm
	1 year	1.5 years	2 years	
# Tests per Patient (IOP / VF)	4.71	3.44	2.78	4.57
Detection Efficiency (detection of progression at first point of progression)	0.55	0.32	0.30	0.82
Diagnostic Delay (months)	2.38	5.43	7.34	1.47

Table 1: Performance of the Kalman filter algorithm compared to fixed interval testing to detect OAG progression based on the data from the CIGTS and AGIS clinical trials.

Commercial Relationships: Mariel Lavieri, 13/668,280 (P); Jonathan Helm, 13/668,280 (P); Gregory Schell, 13/668,280 (P); Mark Van Oyen, Univ. of Michigan 13/668,280 (P); David C. Musch, Glaukos (C), AqueSys (C), InnFocus (C), Pfizer (F), DigiSight Technologies (C); Joshua D. Stein, University of Michigan - time to next glaucoma test algorithm patent (P)
Support: NSF 1161439

Program Number: 3957 **Poster Board Number:** D0245
Presentation Time: 2:45 PM - 4:30 PM

Comparison of perimetric results with the Humphrey and Mon-CV3 perimeters

Jesus Jimenez-Roman, Claudia Riveros, LUIS A. ZARATE, Mauricio Turati, Felix Gil Carrasco. Glaucoma, APEC, Mexico, Mexico.

Purpose: Standard perimetry has become the usual procedure for evaluating glaucoma visual field defects. Early detection is vital in glaucoma because it is a treatable disease with irreversible visual loss. The standard automated perimetry is not selective for any ganglion cells. Our objective was to compare the perimetric results obtained with Humphrey perimetry and Mon CV3, in patients with open angle glaucoma, pseudoexfoliation glaucoma, normal-tension glaucoma and suspected glaucoma.

Methods: Standard perimetry has become the usual procedure for evaluating glaucoma visual field defects. Early detection is vital in glaucoma because it is a treatable disease with irreversible visual loss. The standard automated perimetry is not selective for any ganglion cells. Our objective was to compare the perimetric results obtained with Humphrey perimetry and Mon CV3, in patients with open angle glaucoma, pseudoexfoliation glaucoma, normal-tension glaucoma and suspected glaucoma.

Results: Our study included 29 patients, (55 eyes), 13 women (44.82%) and 16 men (55.17%). Mean age was 61 years. We recorded 22 patients with primary open-angle glaucoma (75.8%), 3 patients with pseudoexfoliation glaucoma (10.3%), 1 patient with normal tension glaucoma (2.9%) and 3 with suspected glaucoma (10.3%). Below is the percentage of abnormal results in each test, related with the global indices mean deviation (MD). For SITA-Standard 57.1% (16/28), SITA-Fast 100% (27/27), STAT-24 55.5% (10/18), FAST-24 93.9% (31/33). The average time to perform the Mon-CV3 test was 280 seconds compared with an average time of over 308 seconds on the Humphrey. No statistical difference was found during time to perform both perimetric tests.

Conclusions: Both perimetric test show similar time to perform the study.

Commercial Relationships: Jesus Jimenez-Roman, None; Claudia Riveros, None; LUIS A. ZARATE, None; Mauricio Turati, None; Felix Gil Carrasco, None

Program Number: 3958 **Poster Board Number:** D0246

Presentation Time: 2:45 PM - 4:30 PM

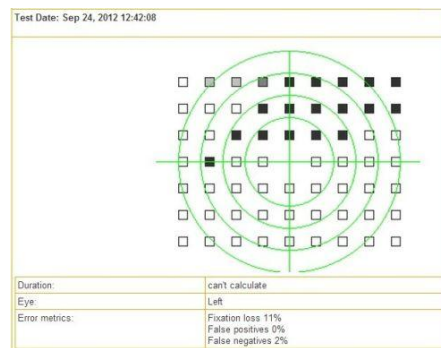
Clinical Utility of Web-based Office and Home Peristat for the Detection of Visual Field Defects in Patients with Glaucoma
 Sean K. Wang¹, Jing Hou², Sean Ianchulev², Brian Chon², Ying Han², Robert Chang¹. ¹Stanford University, Stanford, CA; ²University of California, San Francisco, San Francisco, CA.

Purpose: To investigate the performance of a new virtual perimetry device for online office-based and home-based detection of scotomas. This is a pilot study to characterize the reliability, sensitivity and specificity of self-administered Peristat screening and compare to office-based testing under clinical supervision.

Methods: Nineteen patients undergoing routine examinations for glaucoma were enrolled from the University of California, San Francisco Medical Center and the Byers Eye Institute at Stanford University. All patients performed Peristat testing under two sets of conditions: once in the office under clinical supervision and once individually at home. Visual field results from each tested eye were divided into four quadrants, each of which was independently scored as normal or abnormal. A quadrant was defined as abnormal if it contained a cluster of ≥ 3 adjacent points with ≥ 6.7 dB loss from background or ≥ 2 adjacent points with ≥ 10 dB loss from background. Peristat findings were deemed reliable for tests with ≤ 33% rate for false positives, false negatives, and fixation loss.

Results: Of the 19 enrolled patients, 11 (57.9%) obtained valid results for both office- and home-based Peristat. A total of 16 eyes represented 64 visual field quadrants, 52 (81.3%) of which consistently identified possible defects as abnormal or within normal range. For 3 (4.7%) quadrants, normal office-based findings were subsequently graded as abnormal at home. For 9 (14.1%) quadrants, abnormal office-based findings were subsequently graded as normal at home. Comparing all office versus home Peristat quadrants, the Cohen's kappa coefficient was 0.750. No significant difference was observed between the groups with respect to fixation loss (p = 0.2225), false negatives (p = 0.1093), or false positives (p = 0.3519) during the tests.

Conclusions: Self-administered home-based Peristat shows comparable efficacy in detecting scotomas as office-based testing under clinical supervision. Peristat has the potential to be used as a self-administered home screening perimetric test.



Online Peristat identifies scotomas by interrogating four quadrants of a visual field.

Commercial Relationships: Sean K. Wang, None; Jing Hou, None; Sean Ianchulev, transcend medical (E), keepyoursight foundation (S); Brian Chon, Transcend Medical (C); Ying Han, None; Robert Chang, None

Program Number: 3959 **Poster Board Number:** D0247

Presentation Time: 2:45 PM - 4:30 PM

A novel method to predicting quality of visual life and identifying essential visual field locations

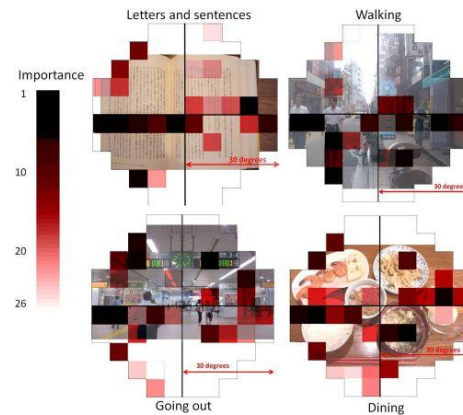
Hiroyo Hirasawa¹, Hiroshi Murata¹, Yuka Aoyama¹, Makoto Araie², Chihiro Mayama¹, Makoto Aihara^{3,1}, Ryo Asaoka¹. ¹Ophthalmology, University of Tokyo Graduate School of Medicine, Tokyo, Japan; ²Kanto Central Hospital, the Mutual Aid Association of Public School Teachers, Tokyo, Japan; ³Shirato Eye Clinic, Tokyo, Japan.

Purpose: The purpose was to perform comparative evaluation of the several machine learning algorithm to predict quality of visual life (QoVL) in glaucomatous patients. Furthermore, we aimed to identify important visual field (VF) test points for QoVL considering the inter-relationship among visual acuity (VA) and VF test points.

Methods: QoVL score was surveyed in 164 glaucoma patients using the 'Sumi questionnaire' (Ophthalmology 2003;110:332-339). The relationship between VAs of better/worse eye, total deviation (TD) values of all of the test points on integrated binocular visual field (IVF), and the general and each QoVL score (letters/sentences, walking, going out, dining) were investigated using four machine learning algorithm: the Random Forest (RF), Gradient Boosting machine (Boost), Support vector machine (SVM) and Feed forward neural network (NNET). For comparison, multiple regression (MR) method was also investigated. The cross validation was carried out using the one leave out method and the prediction errors of those four methods were compared. Then the contributing IVF test points for the general and each QoVL scores were determined using the algorithm with tightest prediction error.

Results: The prediction errors from RF, Boost, NNET and SVM were 1.97, 1.96, 2.59 and 2.23, respectively, which were significantly smaller compared to that from MR (3.38). Thus, we adopted RF for the following analyses. The important VF test points for general QoVL score existed widely around the horizontal line and some points existed at peripheral area (Figure 1). Specific test points were chosen for each QoVL task (Figure 2); VF test points along the horizontal line were chosen for the letters/sentences, and walking. In addition, peripheral points in the left hemi-field were chosen for letters/sentences, and peripheral inferior hemi-field was chosen for the walking. For going out, test points just beneath the horizontal line in the left hemifield and also those in the peripheral superior hemi-field was chosen. For dining, the selected test points were scattered widely in peripheral areas.

Conclusions: Accurate prediction of QoVL was obtained by analyzing TDs on IVF and VA simultaneously using the RF method and also important VF test points were identified using the prediction system. It would be beneficial to pay attention to these VF locations for clinicians and patients of glaucoma.



Commercial Relationships: Hiroyo Hirasawa, None; Hiroshi Murata, None; Yuka Aoyama, None; Makoto Araie, Kowa (C), Kowa (R), Zeiss (R), Topcon (R); Chihiro Mayama, None; Makoto Aihara, Ono pharmaceutical company (F), Pfizer (F); Ryo Asaoka, None

Program Number: 3960 **Poster Board Number:** D0248

Presentation Time: 2:45 PM - 4:30 PM

Effect of Exposure to Computer Simulated Visual Field Test on Variability of Test Results

Justin Hellman¹, S Taylor Smith¹, Jimena Schmid^{2,3}, Andres Gerhard^{2,3}, Militza Sanchez^{2,3}, Felipe Mellado², Eugenio A. Maul^{2,3}, Pradeep Y. Ramulu¹. ¹University Of Chicago Pritzker School of Medicine, Chicago, IL; ²Ophthalmology, Pontificia Universidad Catolica de Chile, Santiago, Chile; ³Ophthalmology, Hospital Sotero del Rio, Santiago, Chile; ⁴Johns Hopkins Wilmer Eye Institute, Baltimore, MD.

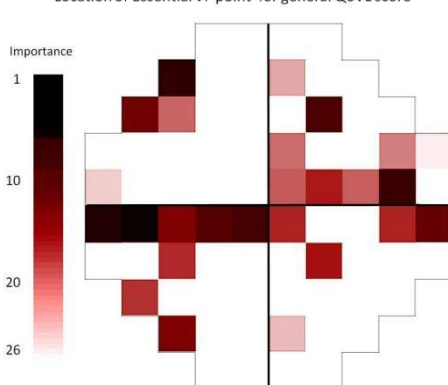
Purpose: To evaluate the efficacy of a computer simulated visual field test in reducing visual field variability and improving visual field test reliability indexes in perimetric novices

Methods: This randomized controlled trial enrolled patients newly referred to a glaucoma clinic for visual field (VF) testing and evaluation. Eligibility criteria included age 18 years or greater and no more than 1 previous VF test examination during the past 4 years. Patients were randomized to intervention or control groups. The intervention group received computer simulated visual field tests (CSVF) before completing a 24-2 Sita Standard VF test (Humphrey Field Analyzer II, Carl Zeiss Meditec, Dublin, CA) in 2 separate sessions 1-2 weeks apart, while control subjects completed two 24-2 Sita Standard VF tests without any prior preparation. Right eyes were tested first in both standard and computer-simulated VFs. The main study outcome was absolute difference in mean deviation of the first and second Sita Standard VF exam. Secondary outcomes included false positive responses, false negative responses and proportion of unreliable exams. Analyses were conducted separately for right and left eyes.

Results: Sixty-two patients completed study procedures, including 31 randomized to standard therapy and 31 randomized to the intervention. Mean age (sd) was 69 (10) years and 71% of the participants were female. Absolute difference between first and second VF MD (sd) for right eyes was 2.3 (3.1) dB in the control group and 1.4 (2.0) dB in the intervention group (p=0.17). For left eyes the effect of training went in the opposite direction, with an absolute first to second VF MD difference of 1.9 (2.3) dB and 2.4 (3.0) dB in the control and intervention group respectively. (p=0.44)

Conclusions: Computer simulated visual field training did not achieve a statistically significant effect on the variability of an initial

Location of Essential VF point for general QoVL score



ARVO 2013 Annual Meeting Abstracts by Scientific Section/Group – Glaucoma

set of 2 visual fields obtained shortly after glaucoma or glaucoma suspect diagnosis. However, we observed a trend towards a positive effect in right eyes that were tested first, suggesting that further refinement may be able to increase the accuracy of VF results. Future methods may also need to minimize fatigue, which may explain the observed trend towards a greater variability in left eye testing.

Commercial Relationships: Justin Hellman, None; S Taylor Smith, None; Jimena Schmidt, None; Andres Gerhard, None; Militza Sanchez, None; Felipe Mellado, None; Eugenio A. Maul, None; Pradeep Y. Ramulu, None

Support: Pritzker School of Medicine Scholarship and Discovery Innovation Award

Clinical Trial: NCT01669031

Program Number: 3961 **Poster Board Number:** D0249

Presentation Time: 2:45 PM - 4:30 PM

Persistence of Glaucoma Therapy and Visual Field Progression

John Mark S. de Leon¹, Desmond T. Quek², Hla M. Htoon¹, Ecosse L. Lamoureux³, Tin Aung^{1, 2}. ¹Singapore Eye Research institute, Singapore, Singapore; ²Glaucoma, Singapore National Eye Center, Singapore, Singapore; ³Ophthalmology, University of Melbourne, Melbourne, VIC, Australia.

Purpose: To determine the longitudinal association of visual field (VF) progression with persistency in a cohort of patients who were commenced on glaucoma medical therapy.

Methods: Pharmacy records were examined retrospectively for patients who commenced glaucoma mono-therapy from October 2005 to September 2006 until 3 years later (Quek DTL et al, Arch Ophthalmol 2011). A patient was defined as persistent over this sample period if he/she had refilled the prescription for the same medication ≤ 90 days after the previous prescription had lapsed. For this study, only patients with ≥ 5 reliable VF data (SITA 24-2, Carl Zeiss Meditec, Dublin, CA) over the next few years were included. VF progression was analysed using point-wise linear regression (Progressor, Medisoft, Ltd, Leeds, U.K.) and defined using two criteria: (a) ≥ 2 adjacent progressing points (slope $p < 0.01$) in one hemi-field and (b) ≥ 3 progressing points (slope $p < 0.01$) (adjacent or non-adjacent). The mean number of progressing points; and the average slopes of progressing points and the entire VF were also determined.

Results: 320 persistent (PS) and 2461 non-persistent (NP) patients were identified. After excluding eyes with < 5 reliable VF data, 140 eligible patients (28 PS and 112 NP) were studied. The majority of patients in both groups were Chinese and there was no inter-group difference for mean age (63.7 ± 13.5 and 59.9 ± 11.1 years for PS and NP respectively; $p=0.13$). The mean follow-up periods were 54.8 ± 7.8 vs. 53.3 ± 11.5 months ($p=0.9$) for the PS and NP groups respectively. Overall, there were 1/28 (3.6%) and 12/112 (10.7%) subjects who progressed in the PS and NP groups ($p=0.47$) using criterion A; and 1/28 (3.6%) and 11/112 (9.82%, $p=0.46$) using criterion B. The mean number of progressing points (0.32 ± 0.19 vs. 0.73 ± 0.17 , $p=0.27$), the average slope of progressing points (-0.33 ± 0.82 vs. -0.80 ± 1.47 dB/yr, $p=0.11$) and the average slope of the entire VF (0.12 vs. -0.2 dB/yr, $p=0.4$) were similar for both groups. A multivariate model, adjusted for age and gender, showed that the slope of progressing points was associated with non-persistence ($p=0.04$).

Conclusions: There were small but appreciable differences in VF progression rates between PS and NP glaucoma subjects. Non-persistent patients were more likely to have steeper progression of visual field points.

Commercial Relationships: John Mark S. de Leon, None; Desmond T. Quek, None; Hla M. Htoon, None; Ecosse L.

Lamoureux, None; Tin Aung, Alcon (R), Alcon (C), Alcon (F), Allergan (R), Allergan (C), Carl Zeiss Meditec (F), Carl Zeiss Meditec (R), Ellex (F), Ellex (R), Santen (R)

Program Number: 3962 **Poster Board Number:** D0250

Presentation Time: 2:45 PM - 4:30 PM

Finding Patterns in Glaucomatous Visual Field Loss: Components, Prototypes, and Archetypes

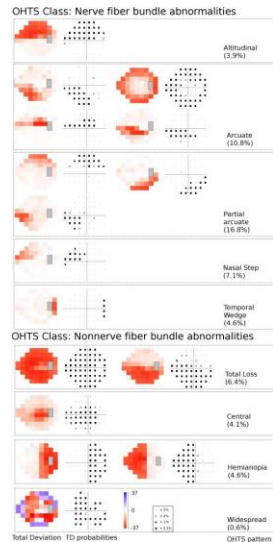
Tobias Elze¹, Louis R. Pasquale², Lucy Q. Shen², Angela Turalba², Teresa C. Chen², Douglas J. Rhee², Janey L. Wiggs², Cynthia Grosskreutz², Stacey Brauner², Peter Bex¹. ¹Schepens Eye Research Institute, Harvard Medical School, Boston, MA; ²Massachusetts Eye and Ear Infirmary, Boston, MA.

Purpose: Glaucomatous visual field loss follows characteristic patterns which are related to the retinal nerve fiber geometry. Over the past decades, numerous mostly qualitative classification schemes for the patterns have been proposed. Here, we try to find quantitative mathematical models for the classification of glaucomatous functional damage.

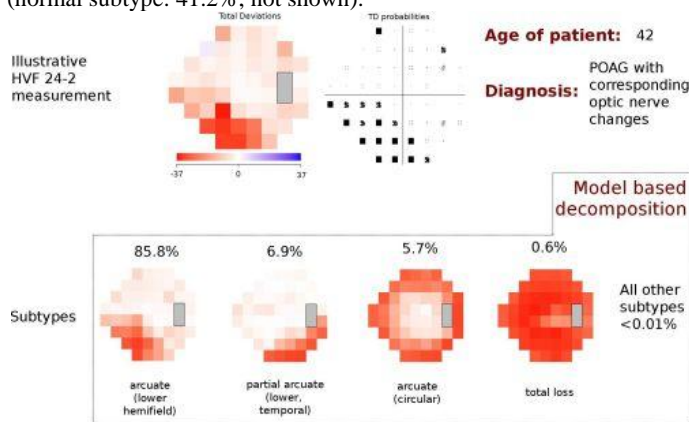
Methods: We apply the statistical learning procedures Independent Component Analysis (ICA), Cluster Analysis (CIA), and Archetypal Analysis to a set of 13,231 reliable ($FL \leq 33\%$, $FN \leq 20\%$) Humphrey Visual Fields (HFV 24-2) of glaucoma patients or suspects from a large clinical glaucoma practice. Left eye locations were mirrored for data analysis to match right eye locations. No repeated measurements over same eye and patient were included. We compare our mathematical classification schemes to the 17 patterns defined in the Ocular Hypertension Treatment Study (OHTS; Keltner et al., Arch. Ophthalmol. 121, 2003, 643-50).

Results: ICA and CIA yielded patterns not consistent with clinical observations. However, when patterns of visual field loss are learned on the convex hull of the data space (Archetypal Analysis), they closely resemble the clinically derived visual field classification scheme of OHTS. In our solution with 17 subtypes, 16 of them match the exact definitions of patterns given in OHTS (Fig. 1), while the remaining subtype represents the normal visual field. Unlike the OHTS scheme, however, our approach can serve as a framework to quantify the various subtypes of glaucomatous visual field loss. Fig. 2 illustratively shows that the model we proposed can be used to decompose any HVF 24-2 into these 17 subtypes quantitatively.

Conclusions: We show that typical patterns observed by clinical practitioners can be extracted by purely mathematical procedures that are agnostic to the ophthalmological background. Our approach can serve as an adjunct to global indices and provides a way to objectively quantify functional loss in glaucoma.



Archetype analysis patterns vs. OHTS classification: The 16 abnormal subtypes. Each box contains those subtypes which match the OHTS pattern given on the right of the box. The % values denote the weight of the subtypes in the box relative to all 17 subtypes (normal subtype: 41.2%; not shown).



Illustrative HVF 24-2 and its decomposition into subtypes.

Commercial Relationships: Tobias Elze, None; Louis R. Pasquale, None; Lucy Q. Shen, None; Angela Turalba, None; Teresa C. Chen, None; Douglas J. Rhee, Alcon (C), Alcon (F), Allergan (C), Aquesys (F), Aquesys (C), Merck (F), Merck (C), Santen (C); Janey L. Wiggs, None; Cynthia Grosskreutz, Novartis Institutes for BioMedical Research (E); Stacey Brauner, None; Peter Bex, Adaptive Sensory Technology, LLC (S), Rapid Assessment of Visual Sensitivity (P)
Support: NIH Grant R01 EY018664

Program Number: 3963 **Poster Board Number:** D0251

Presentation Time: 2:45 PM - 4:30 PM

Getting the timing right: Clustered volley stimulus presentation for multifocal pupil perimetry in glaucoma

Corinne F. Carle^{1,2}, Andrew C. James^{1,2}, Maria Kolic^{1,2}, Rohan W. Essex^{1,3}, Ted Maddess^{1,2}. ¹ARC Centre of Excellence in Vis. Science, The Australian National University, Canberra, ACT, Australia; ²Eccles Institute of Neuroscience, The Australian National University, Canberra, ACT, Australia; ³Ophthalmology Dept, The Canberra Hospital, Garran, ACT, Australia.

Purpose: Multifocal pupillographic perimetry (mfPOP) is being developed as an objective method of assessing patients' visual fields in various disorders. The purpose of this study is to assess a new mfPOP stimulus presentation method in glaucoma, and to compare luminance stimuli presented using this method with those also utilising red/green color-exchange.

Methods: 20 subjects with open-angle glaucoma and 24 age-matched subjects with normal vision were tested twice using three 6-minute mfPOP stimulus protocols. Stimuli of 33 ms duration were presented in each of 44 test-regions per eye within a 60° field. Presentations occurred at mean intervals of 4 s in each of these regions, either in a continuous series across all regions as in previous studies, or in spatially clustered volleys. One protocol (*OldLum*) used the older continuous presentation method and comprised **yellow** luminance stimuli on a 10 cd/m² **yellow** background. The remaining two protocols used the new Clustered Volley (CV) method and either the same yellow luminance stimuli (*CVLum*), or **green** stimuli of the same luminance as the other two protocols on a 10 cd/m² **red** background (*CVLum+Col*). We report the mean of ROC outputs (AUC) for the single- and two-worst performing regions in each eye.

Results: In Severe eyes (*n*=7) and using pupillary constriction amplitudes, *CVLum* produced the best diagnostic accuracy (AUC=1.00±0.00), somewhat better than *OldLum* (AUC=0.93±0.04) and *CVLum+Col* (AUC=0.92±0.04). In Moderate (*n*=13) and Mild (*n*=13) eyes *CVLum+Col* produced the best AUCs of 0.85±0.05 and 0.67±0.07 respectively. (7 fellow eyes showed no signs of disease.) Use of pattern deviations produced a small improvement in Mild eyes (AUC=0.69±0.07), the best result for this group however was obtained using constriction latencies and *CVLum* (AUC=0.79±0.05).

Conclusions: Higher diagnostic accuracy was achieved using the new Clustered Volley method. Luminance stimuli in this format were more accurate in Severe eyes, color-exchange stimuli performing better in less damaged eyes.

Commercial Relationships: Corinne F. Carle, AU2012/905171 (P); Andrew C. James, Seeing Machines, Inc (P); Maria Kolic, SeeingMachines Ltd (E); Rohan W. Essex, None; Ted Maddess, Seeing Machines (F), Seeing Machines (P), EyeCo (I)

Support: Australian Research Council through ARC C of E in Vision Science CE0561903

Program Number: 3964 **Poster Board Number:** D0252

Presentation Time: 2:45 PM - 4:30 PM

Glaucoma alters rapid contrast adaptation

Jia Jia Lek, Algis J. Vingrys, Allison M. McKendrick. Optometry and Vision Sciences, The University of Melbourne, Melbourne, VIC, Australia.

Purpose: The visual system quickly and efficiently adapts to changes in contrast, often with changes in fixation. The neurobiological mechanisms underpinning contrast adaptation are located at multiple sites within the visual pathways, with a key site at the retinal ganglion cell (RGC) dendrites. Early degenerative changes to RGC dendrites are a feature of glaucoma; hence we hypothesised that functional measures of contrast adaptation may be abnormal early in the disease. This study investigates if the magnitude and timecourse of recovery due to fast contrast adaptation is altered in glaucoma using a contrast detection task. We also explored whether facilitation and masking adaptation effects on contrast discrimination are altered in glaucoma.

Methods: 15 people with glaucoma (mean age±SD: 66yrs±7) and 17 controls (62yrs±6), all with normal standard automated perimetry (SAP) measures within the central 4° participated. Central contrast detection and discrimination thresholds were measured for briefly presented (94ms) Gabor patches (1°x1°, 2cpd) with and without

ARVO 2013 Annual Meeting Abstracts by Scientific Section/Group – Glaucoma

adaptation to patterns (1s, 2cpd, 50%contrast). The magnitude and timecourse of detection threshold elevation post-adaptation was assessed for varying interstimulus intervals (ISI: 47, 106, 200, 400, 600, 1000ms) between the adaptor and target. The magnitude of discrimination threshold changes was assessed for varying contrast relationships using targets below (30%), equivalent (50%) or above (70%) the adaptor.

Results: Unadapted contrast detection ($p < 0.0001$) and discrimination ($p < 0.0001$) thresholds were elevated in the glaucoma group. Contrast detection thresholds (normalised to unadapted thresholds) of the glaucoma group were less affected by adaptation for ISIs: 47, 106, 200ms ($p = 0.02$), returning to unadapted threshold earlier (~200ms) than controls (~400ms). Contrast discrimination data (normalised to unadapted thresholds) demonstrated similar between group facilitation effects for targets below ($p = 0.3$) and above ($p = 0.21$) the adaptor. The glaucoma group showed less masking when the target was equivalent to the adaptor ($p = 0.023$).

Conclusions: The glaucoma group demonstrated elevated macular contrast detection and discrimination thresholds without adaptation. Reduced adaptation effects in the form of masking immediately post-adaptor indicate altered fast contrast adaptation in glaucoma. These findings imply central vision abnormalities in natural visual experiences that are not captured by SAP.

Commercial Relationships: Jia Jia Lek, None; Algis J. Vingrys, None; Allison M. McKendrick, Heidelberg Engineering GmbH (F)
Support: Australia Postgraduate Award and ARC FT0990930

Program Number: 3965 **Poster Board Number:** D0253

Presentation Time: 2:45 PM - 4:30 PM

Weighting of Visual Field Mean Deviation according to Test-Retest Variability of Pointwise Thresholds

Nariman Nassiri, Simon K. Law, Anne L. Coleman, Joseph Caprioli, Kouros Nouri-Mahdavi. Ophthalmology, Jules Stein Eye Institute/UCLA, Los Angeles, CA.

Purpose: To determine whether a 'corrected' mean deviation (MD) index weighted according to test-retest variability of the visual field (VF) test locations at baseline, regardless of topographic location, would improve detection of glaucoma progression or prediction by reducing longitudinal noise in visual field series.

Methods: 274 glaucoma eyes (207 patients) with ≥ 6 SITA-standard VF exams over at least 3 years of follow-up were reviewed. Out of the above cohort, 84 eyes with three or more locations marked as "X" on GPA follow-up printouts were selected. 'Corrected' MD for each visual field exam was calculated weighting the threshold at each test location based on the test-retest variability of the baseline threshold as reported by Heijl et al. (AJO 1989). Linear regression analysis (LRA) of MD and 'corrected' MD against time was carried out for the entire follow-up period and the root mean square (RMS) of residuals from the MD and 'corrected' MD fits were compared. For comparison of predictive performance, 33 eyes with at least 10 VF exams and 6 years of follow-up were selected and LRA was performed on the first half of data and the observed-minus-predicted values at the end of follow-up were compared.

Results: The 84 study eyes were followed for 8.5 ± 2.4 years and had an average of 10.8 ± 2.8 VF exams. The average (\pm SD) MD was $-4.2 (\pm 4.5)$ dB at baseline. The median (IQR) decay rate was $-0.16 (-0.42$ to $0.06)$ dB/year for MD and $-0.14 (-0.37$ to $0.05)$ dB/year for 'corrected' MD ($p < 0.007$). LRA of MD (vs. 'corrected' MD) against time detected worsening (i.e. decay rate < 0 dB with $p < 0.05$) in 26 (31%) vs. 19 (23%) eyes, and improvement (decay rate > 0 dB with $p < 0.05$) in 1 (1%) vs. 4 (5%) eyes, respectively ($p < 0.001$). The median RMS of residuals was 1.06 and 1.04 dB for the MD and 'corrected' MD, respectively ($p = 0.03$). The difference between

observed and predicted MD (median 1.3, IQR: -0.8 to 5.1 dB) was smaller than the difference between observed and predicted 'corrected' MD (median: -4.8 , IQR: -6.3 to -1.4 dB) ($p = 0.027$ for the difference in the absolute values).

Conclusions: Weighting of the global index MD according to test-retest variability of VF locations at baseline did not improve detection of glaucoma progression or its prediction. Other weighting strategies need to be explored especially in cohorts with advanced glaucoma where significant long-term variability is expected.

Commercial Relationships: Nariman Nassiri, None; Simon K. Law, None; Anne L. Coleman, None; Joseph Caprioli, Allergan Inc. (F), Allergan Inc. (C), Allergan Inc. (R); Kouros Nouri-Mahdavi, Allergan (C)

Support: Partially Supported by Research to Prevent Blindness

Program Number: 3966 **Poster Board Number:** D0254

Presentation Time: 2:45 PM - 4:30 PM

Initial Central versus Peripheral Visual Field Defects in Normal Tension Glaucoma Patients: Clinical Characteristics and Progression rates

Myungwon Lee¹, Hyun-kyung Cho², Jeongmin Lee³, Changwon Kee².

¹Department of Ophthalmology, Dankook University Hospital, Cheonan, Republic of Korea; ²Department of Ophthalmology, Samsung Medical Hospital, Seoul, Republic of Korea; ³Department of Ophthalmology, Yonseiplus Eye Center, Sunghnam, Republic of Korea.

Purpose: To investigate the clinical characteristics and progression rates of the initial central visual field (VF) defect compared with the initial peripheral VF defect in normal tension glaucoma (NTG) patients.

Methods: Among NTG patients showing a single hemifield defect and who performed more than 5 reliable standard VF tests, medical records of the initial central VF defects (involvement of ≥ 3 adjacent points with $P < 5\%$ within the central 12° of fixation, one point with a $P < .01$ within the central 6° of fixation) (group 1, $n = 32$) or peripheral VF defects (no VF abnormality within the central 6° of fixation) (group 2, $n = 34$) were retrospectively analyzed. The changes of mean thresholds of the 10 zones of the glaucoma hemifield test, central 6° and 12° of fixation, peripheral zones other than central 6° and 12° of fixation, and the entire superior or inferior hemifield were inspected. Linear mixed effect model with unequal random effect variances was employed. Covariates such as age, gender, initial intraocular pressure, mean deviation (MD), pattern standard deviation (PSD), and visual field index (VFI) were controlled.

Results: There were no significant differences between the two groups in age, gender, follow-up period, ocular factors including baseline/mean treated intraocular pressure, and systemic factors including systolic or diastolic blood pressure/perfusion pressure, mean ocular perfusion pressure (MOPP) (all $p > 0.05$) (MOPP: 91.03 ± 10.24 mmHg in group 1 and 94.91 ± 10.36 mmHg in group 2, $p = 0.131$). There were no significant differences in baseline MD and PSD ($p > 0.05$) but a significant difference in VFI (90.74 ± 6.13 in group 1 and 95.36 ± 4.03 in group 2, $p = 0.001$). The progression rates between the two groups were not significantly different in all zones we investigated (all $p > 0.05$) (for the entire hemifield; -0.606 dB/yr in group 1 and -0.565 dB/yr in group 2).

Conclusions: Baseline characteristics and the progression rates of the initial central and peripheral VF defect in NTG patients were not significantly different except for the VFI. It is assumed that the pathogenesis of the central and peripheral VF defect may not be different in NTG.

Commercial Relationships: Myungwon Lee, None; Hyun-kyung Cho, None; Jeongmin Lee, None; Changwon Kee, None

402 New Ideas

Wednesday, May 08, 2013 8:30 AM-10:15 AM

6B Paper Session

Program #/Board # Range: 4009-4015

Organizing Section: Glaucoma

Program Number: 4009

Presentation Time: 8:30 AM - 8:45 AM

Glucose-induced Temporary Visual Recovery in Human**Glaucoma: A Prospective, Double-blind, Randomised Study**

Robert J. Casson, Glyn Chidlow, Andreas Ebnetter, Guoge Han, Jolly Gilhotra, John P. Wood. SA Institute of Ophthalmology, SA Inst of Ophthalmol, Adelaide Univ, Adelaide, SA, Australia.

Purpose: We have previously shown that elevated vitreal glucose levels provide robust neuroprotection against acute and chronic experimental retinal ischemia, and experimental glaucoma. In vitro, the effect is mediated by glycolytic energy supply and the pentose phosphate pathway. In this early translational study, we hypothesised that elevated vitreal glucose levels could temporarily improve psychophysical parameters of visual function in patients with primary open-angle glaucoma (POAG).

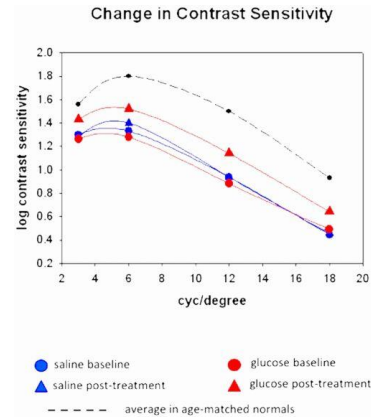
Methods: In a preliminary study on non-diabetic patients scheduled for vitrectomy, we showed that intensive topical application of glucose (50% glucose 5 minutely for 1 hour) significantly elevated the vitreous glucose concentration in pseudophakic but not phakic patients.

We then conducted a double-blind, randomized crossover study on 28 pseudophakic eyes of 15 patients with POAG but no other ocular pathology. The main outcome measure was change from baseline in contrast sensitivity (CS) at 12 cycles/degree (using the CSV-1000). CS at 3, 6, and 18 cycles/degree, and the logarithm of the minimum angle of resolution (logMAR) visual acuity (VA) were secondary outcomes.

Topical saline was used as a control, with a washout interval of 2-3 weeks. Patients randomly received either glucose/saline or saline/glucose. We applied the same glucose-dosing regimen as per the preliminary study, measuring CS, logMAR VA, refraction, intraocular pressure (IOP), and central corneal thickness (CCT) at baseline and 15-30 minutes after drops. The effect of treatment was modeled by linear regression using a generalized estimating equation approach to parameter estimation.

Results: There were no adverse effects. Saline had negligible effect on visual function. The mean change from baseline after glucose treatment on the CS at 12 cycles/degree was 0.25 log units (95% C.I. 0.09 -0.42) greater than saline ($P = 0.003$). CS was also significantly enhanced compared to controls at 3, 6, and 18 cycles/degree ($P < 0.000$; $P = 0.006$; $P = 0.042$). The mean change in logMAR VA was 2 letters (95% C.I. 0.7 -3.3) greater after glucose ($P = 0.002$). The glucose treatment had no significant effect on refraction, IOP, or CCT.

Conclusions: Intensive topical glucose reached the vitreous in pseudophakes, and improved the mean CS and VA in a group of pseudophakic patients with POAG, suggesting possible temporary neurorecovery at the level of the retina.



Commercial Relationships: Robert J. Casson, None; Glyn Chidlow, None; Andreas Ebnetter, None; Guoge Han, None; Jolly Gilhotra, None; John P. Wood, None
Support: Ophthalmic Research Institute of Australia
Clinical Trial: ACTRN12612001134819

Program Number: 4010

Presentation Time: 8:45 AM - 9:00 AM

Radiation Treatment Does Not Protect the Rat Optic Nerve from Elevated Intraocular Pressure (IOP)-Induced Injury

Elaine C. Johnson, William Cepurna, John C. Morrison. Ophthalmology, Casey Eye Institute-OHSU, Portland, OR.

Purpose: Sublethal irradiation has been shown to powerfully protect the optic nerve from elevated IOP-induced injury in the DBA/2j mouse genetic glaucoma model (Howell et al, PMID 22426214). The purpose of this study is to determine if the same treatment provides neuroprotection in an experimentally-induced glaucoma model in the rat.

Methods: At 6 weeks following head-only irradiation (10 Gy), episcleral vein injection of hypertonic saline was used to elevate IOP unilaterally in Brown Norway rats (N=28) as well as in a group of non-irradiated control rats (N=27). IOP was measured three times weekly using a TonoLab tonometer in awake animals. At 5 weeks post-injection, optic nerve cross-sections were graded using an injury scale ranging from 1 (normal) to 5 (>50% axon degeneration). Statistical analyses utilized t-test, linear regression and 2 way ANOVA.

Results: For the radiation and control glaucoma model nerves, the mean (\pm SEM) injury grades were not significantly different (3.65 ± 0.30 and 3.55 ± 0.32 , respectively). This mean injury grade is approximately equivalent to 35% of optic nerve axons in the process of degeneration. Analysis of IOP levels above uninjected fellow eye values showed that mean (radiation: 7.0 ± 1.3 mmHg; control: 5.4 ± 1.2 mm Hg) and peak (radiation: 16.9 ± 2.0 mmHg; control: 18.5 ± 2.2 mm Hg) were not different between the two glaucoma model groups. Linear regression analysis of either mean or peak IOP to injury grade revealed no significant difference in the regression lines, although in both cases the best fit was to peak IOP ($R^2 = 0.80$ radiation, 0.66 control). 2-way ANOVA of nerves grouped by either mean or peak IOP range did not reveal any significant differences in optic nerve injury grade between radiation and control glaucoma model nerve groups with equivalent IOP exposures. For both mean and peak IOP analyses, radiation treatment had no overall effect on injury grade, while the effect of IOP level was extremely significant ($p < 0.0001$).

Conclusions: In contrast to previous observations in the DBA/2j mouse genetic glaucoma model, head-only irradiation does not

protect the optic nerve from injury from chronic experimentally-induced IOP elevation in the rat.

Commercial Relationships: Elaine C. Johnson, None; William Cepurna, None; John C. Morrison, None

Support: Medical Research Foundation of Oregon, Research to Prevent Blindness

Program Number: 4011

Presentation Time: 9:00 AM - 9:15 AM

Estrogen Pathway Polymorphisms in Relation to Primary Open Angle Glaucoma: A Gender-Specific Analysis from Patients in the United States

Louis R. Pasquale^{1,2}, Stephanie Loomis¹, Brian Yaspan³, Jae H. Kang², Robert N. Weinreb⁶, Julia E. Richards⁷, Michael A. Hauser⁴, Jonathan L. Haines⁵, Janey L. Wiggs¹. ¹Ophthalmology, Mass Eye & Ear Infirmary, Boston, MA; ²Medicine, Brigham and Women's Hospital, Boston, MA; ³Genentech, Inc, San Francisco, CA; ⁴Ophthalmology, Duke University, Durham, NC; ⁵Center for Human Genetics Research, Vanderbilt University, Nashville, TN; ⁶Ophthalmology, UCSD, San Diego, CA; ⁷Ophthalmology and Visual Sciences, University of Michigan, Ann Arbor, MI.

Purpose: Altered estrogen metabolism has been strongly implicated in the pathogenesis of primary open-angle glaucoma (POAG). We assessed the association between a panel of estrogen metabolism single nucleotide polymorphisms (SNPs) in relation to POAG using a gender specific approach.

Methods: We included 3,146 POAG cases and 3,487 controls from the combined Glaucoma Genes and Environment (GLAUGEN) study and NEI Glaucoma Human Genetics Collaboration (NEIGHBOR) consortium in this analysis. We assembled all SNPs from the estrogen metabolism pathway available on the Illumina 660W-Quad array platform. We assessed whether this aggregate of SNPs was associated with POAG overall and then by gender using the Pathway Analysis by Randomization Incorporating Structure (PARIS) analysis software package in our combined dataset. In secondary analysis we assessed associations between estrogen SNP pathway and POAG in women stratified by intraocular pressure (IOP) ≥ 22 mm Hg (HPG) or IOP < 22 mm Hg (NPG) at diagnosis. In addition, we determined which SNPs in the pathway accounted for any significant associations.

Results: The estrogen SNP pathway was not associated with POAG, NPG or HPG overall ($p \geq 0.11$). While the estrogen SNP pathway was not associated with POAG in males (permuted $p=1.0$) it was associated with POAG among women (permuted $p=0.02$). Among women, the estrogen SNP pathway was associated with HPG only (permuted $p=0.004$). The association between the estrogen SNP pathway and HPG in women was driven by polymorphisms in the following genes in the pathway: *COMT*, *ESR1*, *AKR1C4*, *ESR2*, *CYP1A2*, *CYP3A4*, *SRDSA1* on autosomes and *STS* on the X chromosome. The *COMT* SNPs showed the strongest association with POAG across the spectrum of IOP (permuted $p < 0.001$ for HPG and $p=0.01$ for NTG) among women.

Conclusions: The estrogen SNP pathway was strongly associated with HPG in women. These data provide insight regarding how common variants in the estrogen metabolism pathway contribute to POAG in women.

Commercial Relationships: Louis R. Pasquale, None; Stephanie Loomis, None; Brian Yaspan, Genentech (E); Jae H. Kang, None; Robert N. Weinreb, Aerie (F), Alcon (C), Allergan (C), Altheos (C), Amakem (C), Bausch&Lomb (C), Carl Zeiss-Meditec (C), Genentech (F), Haag-Streit (F), Heidelberg Engineering (F), Konan (F), Lumenis (F), National Eye Institute (F), Nidek (F), Optovue (C), Quark (C), Solx (C), Topcon (C); Julia E. Richards, None; Michael A. Hauser,

None; Jonathan L. Haines, Arctic Dx (I), AMD genes (P); Janey L. Wiggs, None

Support: NEI R01 EY015473; HG004728; HG005259; EY015872-05S1; EY019126-02S1

Program Number: 4012

Presentation Time: 9:15 AM - 9:30 AM

A Novel Device for Clinical Measurement of Corneal Elasticity

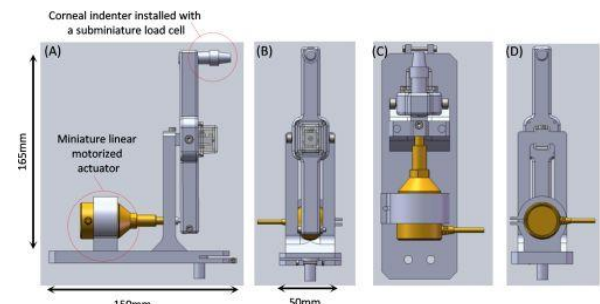
Christopher K. Leung¹, Cong Ye¹, Match Ko², Leo Leung², David Lam². ¹Ophthalmology and Visual Sciences, The Chinese University of Hong Kong, Hong Kong, Hong Kong; ²Mechanical Engineering, Hong Kong University of Science and Technology, Hong Kong, Hong Kong.

Purpose: The investigation of corneal biomechanics has been obfuscated by the lack of an instrument that can measure corneal elasticity. We have validated the principle of corneal indentation for measurement of corneal elastic modulus (E) in a silicone model of cornea, in porcine eyes (ex vivo testing) and rabbit eyes (in vivo testing). In this study, we designed and built a prototype for measurement of corneal E in glaucoma patients.

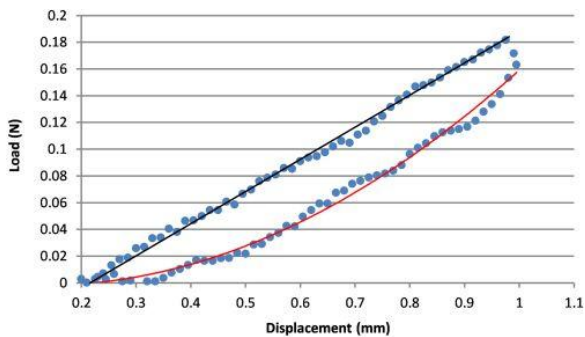
Methods: The prototype device is portable and designed to fit into a slit-lamp (Fig.1). It has 2 key components: (1) a corneal indenter with a subminiature load cell for measurement of the load, and (2) a miniature linear motorized actuator that propels the indenter and measures the displacement of corneal indentation. The load displacement data are transmitted to a notebook computer via Bluetooth to allow visual display of the load displacement curve. 30 eyes of 15 glaucoma/suspect patients were recruited for measurement of IOP (dynamic contour tonometry), CCT, corneal curvature (K) and corneal E (3 consecutive measurements) in the same visit. The test-retest variability of corneal E was evaluated and the association between IOP and corneal E was examined with linear mixed model.

Results: The mean IOP, CCT and K were 18.5 ± 4.2 mmHg, 560.5 ± 35.2 μ m, and 43.8 ± 1.6 D, respectively. Corneal E was derived from the load displacement curve (Fig.2), taking individual K and CCT in the calculation. The corneal E ranged between 0.41 and 0.89 MPa (mean: 0.63 ± 0.11 MPa). The ICC was 0.837 (95% CI: 0.727 - 0.913). There was a significant correlation in corneal E between fellow eyes ($r=0.619$, $p=0.015$) and the corneal E was positively associated with IOP ($p=0.017$) (with adjustment of correlation between fellow eyes).

Conclusions: This study provides an unprecedented documentation of corneal E in human eyes in vivo. Corneal E is often reported with little attention to the preload (the IOP). Our finding indicates that corneal elastic modulus should always be interpreted with IOP.



A prototype corneal indentation device for clinical measurement of corneal elastic modulus.



The loading portion of the load displacement curve (black line) is essentially linear and is used to calculate corneal elastic modulus (the tangent modulus). The unloading portion is non-linear (red line) and the area bounded by the loading and unloading curves represents corneal hysteresis.

Commercial Relationships: Christopher K. Leung, Carl Zeiss Meditec (F), Carl Zeiss Meditec (R), Alcon (C), Alcon (R), Alcon (F), Allergan (C), Allergan (R), Tomey (F), Optovue (F); Cong Ye, None; Match Ko, NON-DESTRUCTIVE MEASUREMENT OF MECHANICAL PROPERTIES OF AN ELLIPSOIDAL SHELL (US 61/457,784) (P); Leo Leung, NON-DESTRUCTIVE MEASUREMENT OF MECHANICAL PROPERTIES OF AN ELLIPSOIDAL SHELL (US 61/457,784) (P); David Lam, The Hong Kong University of Science and Technology (P)
Support: Innovation and Technology Fund (Hong Kong)

Program Number: 4013

Presentation Time: 9:30 AM - 9:45 AM

A Potential Role for the Hypothalamic Orexin System in Mediating Intraocular Pressure Fluctuations

Brian C. Samuels¹, Nathan Hammes¹, Philip L. Johnson², Anantha Shekhar^{3,4}. ¹Department of Ophthalmology, Eugene & Marilyn Glick Eye Inst, Ind Univ, Indianapolis, IN; ²Department of Anatomy, Indiana University, Indianapolis, IN; ³Department of Psychiatry, Indiana University, Indianapolis, IN; ⁴Clinical and Translational Sciences Institute, Indiana University, Indianapolis, IN.

Purpose: We have recently shown that chemical stimulation of the dorsomedial/perifornical hypothalamus (DMH/PeF) evokes increases in intraocular pressure (IOP), intracranial pressure (ICP), and the translamellar pressure gradient. The DMH/PeF region receives strong direct and indirect projections from the suprachiasmatic nucleus and has extensive efferent projections to autonomic sympathetic relays. Therefore, the DMH/PeF neurons are ideally situated to modulate circadian fluctuations in IOP. Orexins are a novel class of neuropeptides that play a key role in regulating circadian behaviors as well as neuroendocrine and autonomic functions. Given that orexin containing neurons are located almost exclusively in the DMH/PeF region, we hypothesize that fluctuations in IOP and ICP are regulated, at least in part, by these orexin containing neurons. To test this hypothesis, we examined the effect of a systemically administered orexin 1 receptor antagonist, SB334861 (Tocris), on the increases in IOP and ICP following chemical stimulation of the DMH/PeF with the GABA-A receptor antagonist bicuculline methiodide (BMI).

Methods: The cisterna magna space of isoflurane-anesthetized Sprague-Dawley rats (250-300g; n=18) was cannulated for continuous monitoring of ICP. The ICP line was then connected to high sensitivity pressure transducer attached to a PowerLab data acquisition system (AD Instruments). An iCareLab tonometer was used to record IOP every 2 minutes throughout the experiment. Rats received an injection of SB334861 (30mg/kg, i.p.) or vehicle 30

minutes prior to stereotaxic microinjection of BMI (30pmol/75nL) into the DMH/PeF region. The resulting increases in IOP and ICP were then recorded and differences between treatment groups determined by t-test with significance set at $P \leq 0.05$.

Results: Compared to vehicle control, pretreatment with the SB334861 attenuated the maximum increase in IOP (13.1 ± 1.9 vs 7.7 ± 1.0 mmHg; $p=0.03$) but not ICP (5.0 ± 0.5 vs 3.9 ± 0.7 mmHg; $p=0.19$) following chemical stimulation.

Conclusions: These data are the first to support the hypothesis that orexin neurons located in the DMH/PeF region play a role in mediating circadian fluctuations in IOP, a previously unrecognized function of these specific neurons. Further, these neurons may provide a novel target for future glaucoma therapies aimed at reducing circadian fluctuation of IOP.

Commercial Relationships: Brian C. Samuels, Merck & Co., Inc (F), Merck & Co., Inc (C), ICHE (C); Nathan Hammes, None; Philip L. Johnson, None; Anantha Shekhar, Indiana University (P)
Support: NIH KL2 TR000163; (A. Shekhar, PI)

Program Number: 4014

Presentation Time: 9:45 AM - 10:00 AM

Pulse-induced Trabecular Meshwork (TM) Movement in Humans: Characterization by Phase-sensitive OCT (PhS-OCT)

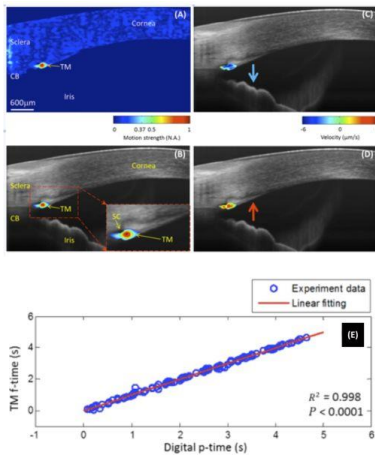
Murray A. Johnstone², Peng Li¹, Tueng T. Shen^{1,2}, Ruikang K. Wang¹. ¹Bioengineering, University of Washington, Seattle, WA; ²Ophthalmology, University of Washington, Seattle, WA.

Purpose: Aqueous flows from Schlemm's canal (SC) to the aqueous veins by cyclic pulsatile mechanisms that depend on TM movement. TM movement is dependent on biomechanical properties that become abnormal in glaucoma. We hypothesized that PhS-OCT could detect and measure pulse-induced TM movement in human subjects.

Methods: 10 subjects, 20 eyes; sex F/M, 6/4; mean age \pm SD, 37 ± 12 ; heart rate \pm SD 70 ± 11 . A PhS-OCT system measured TM movement with a sensitivity to tissue motion at the nanometer (nm) scale. A digital pulsometer signal was synchronized with the PhS-OCT data acquisition system through triggers. Analysis involved correlation of timing and phase lag of the digital pulse and the TM tissue wave, TM velocity measurements, relationships of TM motion to heart rate and age, strength mapping of the TM velocity wave, correlation of harmonics of the 1st 9 pulse-induced motion waves and correlation between digital and CRA pulse waves.

Results: Digital pulse peaks and TM pulse wave minima were highly correlated $R^2 = 0.998$, $P < 0.0001$. Frequency components of the harmonic waves were also highly correlated. ($R^2 = 0.996$, $P < 0.0001$). Energy of TM motion was contained primarily in the 1st 4 harmonic waves (80%). The tissue phase lag was negatively correlated with heart rate ($P < 0.05$), but not age. Velocity of maximal TM motion toward and away from SC was $\sim 3 \mu$ /sec. The digital and CRA pulse were almost in phase (0.08 sec. delay).

Conclusions: PhS-OCT imaging detected and measured TM movement that was highly correlated with the cardiac pulse. TM motion strength, harmonics and velocity were characterized. PhS-OCT may provide a sensitive clinical tool for monitoring development and progression of aqueous outflow system biomechanical changes leading to pressure elevation in glaucoma.



Spatial characterization of TM motion. (A) Normalized strength mapping of the ocular tissue motion around the corneo-scleral limbus; (B) isolated TM strength mapping superimposed on the corresponding structural cross-section, enlarged view of the area marked by the dashed red square in (B). (C) and (D) isolated TM velocity cross-sections superimposed on the structural cross-section, respectively corresponding to the downward velocity toward the AC and the upward velocity toward SC external wall. (E) Linear correlation between the TM pulse peak (f-time) and the digital pulse peak (p-time) in seconds (s) from time 0.

Commercial Relationships: Murray A. Johnstone, Alcon (R), Allergan (R), Allergan (P), Healonics (I), Cascade Ophthalmics (I), Sensimed (R), Ivantis (R), University of Washington (P); Peng Li, None; Tueng T. Shen, None; Ruikang K. Wang, National Institutes of Health (F), W.H. Coulter Foundation Translational Research Partnership Program (F), Research to prevent blindness (F), Oregon Health & Science University (P), University of Washington (P)

Program Number: 4015

Presentation Time: 10:00 AM - 10:15 AM

A quantitative approach to the analysis of visual field defect location and its relationship to measures of disability

Michael V. Boland, Pradeep Y. Ramulu, Karun S. Arora, Joan L. Jefferys, David S. Friedman. Wilmer Eye Institute, Johns Hopkins University, Baltimore, MD.

Purpose: To determine, using a quantitative method, whether the location of visual field loss is related to measures of disability

Methods: The Salisbury Eye Evaluation was a population-based study of elderly residents of Salisbury, Maryland. Participants underwent visual field (VF) testing and were evaluated for measures of disability including driving status, reading speed, mobility course speed, walking speed, stair climbing rate, and the Activities of Daily Vision Scale (ADVS.) Between 409 and 487 participants with some VF loss completed measures of disability and bilateral VF testing. As a quantitative measure of the distribution of VF, we calculated the first order moment of the linear scale threshold values from an integrated binocular VF. This moment is analogous to the center of mass of a physical object. To more completely capture the distribution of vision, we calculated the second and third order central moments of the linearized threshold values. These values are comparable to the concepts of variance and skewness in statistics. All three moments were calculated along both the vertical and horizontal axes of the VF. Logistic and log-linear models were used to assess the relationship between the moments and the measures of disability.

Results: Using the first order moment along the vertical axis as a measure of inferior v. superior vision loss, the likelihood of not

driving (OR 1.59, CI 1.15 to 2.20), scoring 79 or less on the ADVS (OR 2.11, CI 1.40 3.18), or reading ≤ 90 words per minute (OR 1.40, CI 1.07 to 1.83) were all worse with inferior VF loss (center of remaining VF shifted superior) as compared to superior VF loss. Reading speed declined by 10.7 words per minute (CI -16.7 to -4.6) for each degree the center of remaining vision was displaced upward by inferior VF loss. Using the second order moment along the horizontal axis as a measure of central v. peripheral VF loss, the risk of not driving, of scoring poorly on the ADVS, and reading speed were all worse with both central and peripheral vision loss but only reading speed was significantly more affected by central vision loss.

Conclusions: A set of objective, quantitative measures of the location of VF loss show that while multiple measures of disability are affected by the location of vision loss in the vertical direction, only reading speed is significantly more affected by inferior VF loss. **Commercial Relationships:** Michael V. Boland, None; Pradeep Y. Ramulu, Tissue Banks International (C); Karun S. Arora, None; Joan L. Jefferys, None; David S. Friedman, Alcon (C), Bausch & Lomb (C), Merck (C), QLT, Inc (C), Allergan (C), Nidek (C) **Support:** Research to Prevent Blindness

423 Ocular Blood Flow; Surgery and Wound Healing

Wednesday, May 08, 2013 8:30 AM-10:15 AM

Exhibit Hall Poster Session

Program #/Board # Range: 4442-4496/D0182-D0236

Organizing Section: Glaucoma

Program Number: 4442 **Poster Board Number:** D0182

Presentation Time: 8:30 AM - 10:15 AM

Retinal Nerve Fiber Layer Thickness is Correlated to Retrobulbar Blood Flow in Glaucoma Patients of African Descent

Anne Schroeder¹, Alon Harris¹, Brent A. Siesky¹, Leslie A. Tobe¹, Nathaniel J. Kim¹, Annahita Amireskandari¹, Brian M. Marek¹, Lyne Racette¹, George J. Eckert², Ariel Tyring¹. ¹Ophthalmology, Indiana University School of Medicine, Indianapolis, IN; ²Division of Biostatistics, Indiana University School of Medicine, Indianapolis, IN.

Purpose: To examine the relationship between retinal nerve fiber layer (RNFL) thickness and retrobulbar blood flow in open angle glaucoma (OAG) patients of African descent (AD) and European descent (ED) over three years.

Methods: 67 patients with OAG (18 AD, 49 ED) were assessed for RNFL thickness as measured by optical coherence tomography (OCT) and blood flow velocities and vascular resistive index (RI) in the ophthalmic artery (OA), central retinal artery (CRA) and nasal (NPCA) and temporal (TPCA) posterior ciliary arteries using color Doppler imaging (CDI). Pearson correlations were calculated to evaluate the associations between measurements at baseline and between the changes in measurements between baseline and 3 years with $p < 0.05$ considered statistically significant.

Results: In patients of AD, change in average RNFL thickness was significantly correlated with change in TPCA end diastolic velocity (EDV) ($r = -0.77$, $p = 0.01$) and change in TPCA RI ($r = 0.69$, $p = 0.04$). Change in inferior RNFL thickness was also correlated with change in TPCA EDV ($r = 0.79$, $p = 0.01$), change in temporal RNFL thickness was positively correlated with change in CRA EDV ($r = 0.55$, $p = 0.13$) and change in NPCA EDV ($r = 0.78$, $p = 0.01$). Change in superior RNFL thickness was significantly correlated with change in TPCA RI ($r = 0.68$, $p = 0.04$) and significantly correlated with change in CRA RI ($r = 0.82$, $p = 0.005$) over three years. In patients of ED, these correlations were weak and did not reach statistical significance ($r = -$

0.07 to 0.16, $p > 0.05$) with the exception of the correlation between temporal RNFL thickness and CRA EDV ($r = -0.34$, $p = 0.03$). There were statistically significant differences in the strength of correlations between AD and ED groups for each relationship ($p < 0.005$).

Conclusions: In this cohort of patients with OAG, changes in retrobulbar blood flow velocities and vascular resistance were correlated with changes in RNFL thickness in patients of AD. These relationships were not found in OAG patients of ED. This suggests that OAG patients of AD and ED may have differences in the vascular contribution to their glaucomatous damage.

Commercial Relationships: Anne Schroeder, None; Alon Harris, MSD (R), Alcon (R), Merck (C), Pharmedica (C), ONO (C), Sucampo (C), Adom (I); Brent A. Siesky, None; Leslie A. Tobe, None; Nathaniel J. Kim, None; Annahita Amireskandari, None; Brian M. Marek, None; Lyne Racette, None; George J. Eckert, None; Ariel Tying, None

Support: NIH 1R21EY022101-01A1, Grant from Pfizer Pharmaceuticals Inc.

Program Number: 4443 **Poster Board Number:** D0183

Presentation Time: 8:30 AM - 10:15 AM

Changes in Retinal Blood Flow are Strongly Correlated to Changes in Optic Nerve Head Morphology in Patients of African Descent

Leslie A. Tobe¹, Alon Harris¹, Brent A. Siesky¹, Lyne Racette¹, Darrell WuDunn¹, Annahita Amireskandari¹, Nathaniel J. Kim¹, Andrew H. Huck¹, Ariel Tying¹, Miriam Zalish². ¹Ophthalmology, Indiana University School of Medicine, Indianapolis, IN; ²Ophthalmology, Kaplan Medical Center, Rehovot, Israel.

Purpose: To examine the relationship between changes in retinal blood flow and changes in optic nerve head (ONH) morphology in open-angle glaucoma (OAG) patients of African descent (AD) and European descent (ED) over three years.

Methods: 68 patients with OAG (17 AD; 51 ED) were assessed for retinal blood flow using confocal scanning laser Doppler and ONH morphology using Heidelberg retinal tomography and optical coherence tomography. Total (mean) retinal capillary blood flow was divided into superior and inferior temporal areas and mean retinal flow for each area was determined. Pearson correlations were calculated to evaluate the associations between measurements at baseline and between the changes in measurements between baseline and 3 years with $p < 0.05$ considered statistically significant.

Results: In OAG patients of AD, change in superior mean retinal blood flow was strongly, negatively and significantly correlated with change in cup/disc (C/D) area ratio ($r = -0.78$, $p = 0.020$) and cup area ($r = -0.75$, $p = 0.0283$) and strongly and positively correlated with rim area ($r = 0.74$, $p = 0.0328$) and vertical integrated rim area ($r = 0.86$, $p = 0.0241$) over three years. In OAG patients of ED, these correlations were weak and did not reach statistical significance ($r = 0.19$, $p = 0.2529$; $r = -0.17$, $p = 0.2876$; $r = 0.20$, $p = 0.2086$; $r = -0.05$, $p = 0.7804$). The difference in strength of correlations between AD and ED groups was also statistically significant for each relationship ($p < 0.0052$; $p < 0.0083$; $p < 0.0143$; $p < 0.0001$). In OAG patients of AD, change in inferior mean retinal blood flow was also strongly, negatively and significantly correlated with change in C/D area ratio ($r = -0.88$, $p = 0.0156$) and linear C/D ratio ($r = -0.86$, $p = 0.0265$) over three years. In OAG patients of ED, these correlations were weak and did not reach statistical significance ($r = -0.06$, $p = 0.6923$; $r = -0.05$, $p = 0.7584$). Similar to superior mean blood flow, the differences in each correlation comparison between AD and ED groups was statistically significant ($p < 0.0001$; $p < 0.0001$).

Conclusions: In OAG patients of AD, changes in retinal blood flow were strongly correlated with glaucomatous ONH morphological

changes after 3 years. OAG patients of ED had weak correlations, suggesting OAG patients of AD may have a stronger vascular component involved in their glaucoma pathology compared to OAG patients of ED.

Commercial Relationships: Leslie A. Tobe, None; Alon Harris, MSD (R), Alcon (R), Merck (C), Pharmedica (C), ONO (C), Sucampo (C), Adom (I); Brent A. Siesky, None; Lyne Racette, None; Darrell WuDunn, Merck (R), Alcon (R); Annahita Amireskandari, None; Nathaniel J. Kim, None; Andrew H. Huck, None; Ariel Tying, None; Miriam Zalish, None
Support: NIH 1R21EY022101-01A1, Grant from Pfizer Pharmaceuticals Inc.

Program Number: 4444 **Poster Board Number:** D0184

Presentation Time: 8:30 AM - 10:15 AM

Comparison of Nebulized dorzolamide/timolol fixed combination Mist vs Drops on Retrobulbar Blood Flow, Intraocular Pressure in Glaucoma Patients

Ruta Barsauskaite¹, Alon Harris², Ingrida Januleviciene¹, Lina Siaudvytyte¹, Vaida Diliene¹, Brent Siesky². ¹Eye Clinic, Lithuanian University of Health Sciences, Kaunas, Lithuania; ²Eugene and Marilyn Glick Eye Institute, Indiana University School of Medicine, Indianapolis, IN.

Purpose: To evaluate intraocular pressure (IOP), retrobulbar blood flow (RBF) parameters and ocular side effects with use of topical dorzolamide/timolol fixed combination (DTFC) drop vs nebulized DTFC mist in primary open-angle glaucoma (POAG) patients.

Methods: 15 POAG patients were included in a prospective, open-label, cross-over study. RBF was measured using Color Doppler imaging in the ophthalmic (OA) and central retinal (CRA) arteries, assessing peak-systolic (PSV) and end-diastolic (EDV) velocities and calculated resistance index (RI). After baseline timolol measurements (IOP and RBF), patients were randomly assigned for the application of DTFC drops or mist for the first treatment and were crossed-over to the alternative formulation on the second visit. DTFC mist/drops were applied to the experimental eye and examinations were performed after 15 and 60 min. DTFC mist was applied 6 times for 30 sec using a misting device. The level of significance $p < 0.05$ was considered significant.

Results: DTFC mist significantly increased PSV and EDV after 15 and 60 min in both arteries (respectively, OA: PSV 12.5% and 9.6% ($p = 0.01$), EDV 25.8% and 23.1% ($p = 0.03$); CRA: PSV 11.5% and 8.7% ($p < 0.05$); EDV 32% and 21.6% ($p < 0.02$)). DTFC drops had similar effects on CRA PSV and EDV after 15 min and 60 min (respectively, PSV 8.1% and 9.6% ($p < 0.02$); EDV 17.1% and 23% ($p < 0.03$)) but a statistically significant effect in OA PSV and EDV was seen only after 15 min (9% and 21.4%, $p < 0.02$). DTFC mist reduced CRA RI after both time points (8.5% and 10.2%, $p < 0.04$). Both formulations showed significant decreases in IOP after 15 and 60 min with IOP decreasing by 5.7% ($p = 0.01$) after 15 min and 10.2% ($p = 0.002$) after 60 min using DTFC mist, and by 4% ($p = 0.01$) and 9.3% ($p < 0.001$) after using DTFC drops. All patients reported ocular irritation after drop application and 1 patient complained of general weakness after mist treatment.

Conclusions: Mist of nebulized DTFC reduced IOP and increased blood flow in the OA and the CRA, without causing ocular irritation as compared to traditional DTFC drop methodology.

Commercial Relationships: Ruta Barsauskaite, None; Alon Harris, MSD (R), Alcon (R), Merck (C), Pharmedica (C), ONO (C), Sucampo (C), Adom (I); Ingrida Januleviciene, Pharmedica (F), Alcon (C), MSD (C), Santen (C); Lina Siaudvytyte, None; Vaida Diliene, None; Brent Siesky, None
Clinical Trial: P2-21/2010

Program Number: 4445 **Poster Board Number:** D0185

Presentation Time: 8:30 AM - 10:15 AM

Ocular Hemodynamic Changes after Trabeculectomy in Pseudoexfoliative and Primary Open-Angle Glaucoma

Vaida Diliene¹, Alon Harris², Ingrida Januleviciene¹, Lina Siaudvytyte¹, Ruta Barsauskaite¹, Brent Siesky². ¹Eye Clinic, Lithuanian University of Health Sciences, Kaunas, Lithuania; ²Eugene and Marilyn Glick Eye Institute, Indiana University School of Medicine, Indianapolis, IN.

Purpose: To evaluate the effects of trabeculectomy on ocular hemodynamic parameters in pseudoexfoliative (PXG) and primary open-angle glaucoma (POAG) and to analyze serum antiphospholipid antibody levels (APLAs) in PXG.

Methods: 30 open-angle glaucoma patients were included in the prospective study. Intraocular pressure (IOP), ocular perfusion pressure (OPP), blood pressure (BP) and pulsatile ocular blood flow (POBF) were measured 1 day before and 1 month after trabeculectomy. Retrobulbar blood flow (RBF) was measured using Color Doppler imaging in the ophthalmic (OA), central retinal (CRA) and temporal short posterior ciliary (tSPCA) arteries, assessing peak-systolic (PSV), end-diastolic (EDV) velocities and calculated resistance index (RI). Venous blood samples were taken from PXG patients, IgG APLAs levels were assessed. The level of significance was $p < 0.05$.

Results: IOP decreased significantly in both groups after trabeculectomy (from 30.1(7.2) to 15.0(5.1) mmHg in PXG; from 29.1(7.7) to 13.1(5.5) mmHg in POAG, $p < 0.05$). OPP increased significantly from 38.9(10.3) to 55.5(8.6) in PXG and from 40.9(11.0) to 56.7(8.9) in POAG, $p < 0.05$. Both groups showed significant increase in CRA PSV after surgery (from 8.75(2.27) to 9.79(2.31) in PXG; from 8.55(2.59) to 10.11(2.64) in POAG, $p < 0.05$), though significant decrease in RI was observed only in POAG, $p < 0.05$. Both groups showed significant increase in POBF (from 13.09(3.41) to 18.81(5.70) in PXG; from 11.89(5.79) to 19.29(9.02) in POAG, $p < 0.05$). 10 PXG patients had normal APLAs levels 8.7(2.9) GPLU/mL and 4 patients had borderline/increased 22.6(7.1) GPLU/mL. Patients with higher APLAs levels had lower IOP (28.8(4.9)), higher OPP (41.63(8.23)) compared to patients that had normal APLAs, $p > 0.05$. Patients with normal APLAs levels showed significant decrease in IOP (from 30.7(8.1) to (15.2(5.9)), and increases in POBF (from 13.24(3.69) to 19.94(5.03)), CRA PSV (from 8.78(2.39) to 9.46(2.17)) and tSPCA PSV (from 7.61(2.15) to 8.35(1.98)), $p < 0.05$.

Conclusions: Trabeculectomy resulted in a statistically significant decrease in IOP and increase in ocular blood flow. Effects of trabeculectomy in PXG patients were significantly less than in patients with POAG. Patients with normal APLAs levels had a significant increase in ocular hemodynamics compared to patients with higher APLAs. Further studies are needed to analyze APLAs effects in different patients groups.

Commercial Relationships: Vaida Diliene, None; Alon Harris, MSD (R), Alcon (R), Merck (C), Pharmalight (C), ONO (C), Sucampo (C), Adom (I); Ingrida Januleviciene, Pharmalight (F), Alcon (C), MSD (C), Santen (C); Lina Siaudvytyte, None; Ruta Barsauskaite, None; Brent Siesky, None

Clinical Trial: BC-LSMU(R)-246

Program Number: 4446 **Poster Board Number:** D0186

Presentation Time: 8:30 AM - 10:15 AM

Systemic Blood Pressure and Ocular Perfusion Pressure Affect Macular Thickness in Glaucoma Patients of African Descent

Brian M. Marek¹, Alon Harris¹, Brent A. Siesky¹, Leslie A. Tobe¹, Ariel Tyring¹, Annahita Amireskandari¹, Nathaniel J. Kim¹, Joshua G. Paschall¹, George J. Eckert², Lyne Racette¹. ¹Ophthalmology, Indiana Univ. Sch. of Medicine, Indianapolis, IN; ²Division of Biostatistics, Indiana Univ. Sch. of Medicine, Indianapolis, IN.

Purpose: To evaluate the differences between glaucoma patients of African descent (AD) and European descent (ED) with respect to the relationship between the change in either systemic blood pressure or ocular perfusion pressure and macular thickness over three years.

Methods: 76 patients with open-angle glaucoma (OAG) (18 of AD; 58 of ED) were assessed at baseline and three year follow up for systolic (SBP) and diastolic (DBP) blood pressure using automated ambulatory measurements and OPP, which was calculated using the following equation: $OPP = 2/3[DBP + 1/3(SBP - DBP)] - IOP$. Systolic (SPP), diastolic (DPP) and mean (MPP) perfusion pressures were also calculated as SBP-IOP, DBP-IOP and mean arterial pressure-IOP, respectively. Macular structure was measured by optical coherence tomography. Pearson correlations were calculated to evaluate the associations between measurements at baseline and between the changes in measurements between baseline and three years.

Results: In patients of AD, change in inner superior and inferior macular thickness were strongly, negatively and significantly correlated with change in SPP ($r = -0.86$, $p = 0.0098$; $r = -0.93$, $p = 0.0007$), DPP ($r = -0.93$, $p = 0.0011$; $r = -0.94$, $p = 0.00050$), OPP ($r = -0.90$, $p = 0.0033$; $r = -0.92$, $p = 0.0012$), MPP ($r = -0.90$, $p = 0.0029$; $r = -0.95$, $p = 0.0003$), SBP ($r = -0.83$, $p = 0.0085$; $r = -0.82$, $p = 0.0093$), and MAP ($r = -0.81$, $p = 0.0108$; $r = -0.75$, $p = 0.028$) over three years. In patients of ED, these correlations were weak and did not reach statistical significance ($r = 0.02$ to 0.21 , $p > 0.05$). Also in patients of AD, change in outer inferior macular thickness was positively correlated with change in MAP ($r = 0.72$, $p = 0.0403$), SBP ($r = 0.71$, $p = 0.0477$) and DBP ($r = 0.71$, $p = 0.0457$). In patients of ED, these correlations were weak and non-significant ($r = 0.06$ to 0.16 , $p > 0.05$). There was a statistically significant difference in strength of correlations between AD and ED groups for each of the above relationship ($p < 0.0151$).

Conclusions: OAG patients of AD descent have a significantly stronger correlation between changes in OPP and BP and change in macular thickness than those of ED, with the association being more prominent in the inner portions of the retina. This suggests that in OAG patients of AD, vascular parameters may play a larger role in the structural changes observed in the glaucomatous eye.

Commercial Relationships: Brian M. Marek, None; Alon Harris, MSD (R), Alcon (R), Merck (C), Pharmalight (C), ONO (C), Sucampo (C), Adom (I); Brent A. Siesky, None; Leslie A. Tobe, None; Ariel Tyring, None; Annahita Amireskandari, None; Nathaniel J. Kim, None; Joshua G. Paschall, None; George J. Eckert, None; Lyne Racette, None

Support: NIH 1R21EY022101-01A1, Grant from Pfizer Pharmaceuticals Inc.

Program Number: 4447 **Poster Board Number:** D0187

Presentation Time: 8:30 AM - 10:15 AM

Retinal and Macular Morphology is Correlated with Retrobulbar Vascular Resistance in Diabetic Patients with Glaucoma

Austin L. Gerber¹, Alon Harris¹, Brent A. Siesky¹, George J. Eckert³, Ingrida Januleviciene², Nathaniel J. Kim¹, Annahita Amireskandari¹, Brian M. Marek¹, Leslie A. Tobe¹, Andrew H. Huck¹.

¹Ophthalmology, Indiana Univ School of Med, Indianapolis, IN; ²Eye Clinic, Lithuanian University of Health Sciences, Kaunas, Lithuania; ³Division of Biostatistics, Indiana Univ School of Med, Indianapolis, IN.

Purpose: To examine the relationship between changes in retinal and macular morphology and retrobulbar blood flow in diabetic and non-diabetic patients with open angle glaucoma (OAG) after three years.

Methods: 68 patients (15 diabetic, 53 non-diabetic) with OAG were assessed for retinal nerve fiber layer (RNFL) thickness and macular morphology using optical coherence tomography (OCT) and retrobulbar blood flow in the ophthalmic artery (OA), central retinal artery (CRA) and nasal (NPCA) and temporal (TPCA) posterior ciliary arteries using color Doppler imaging (CDI) at baseline and three years follow up. Pearson correlations were calculated to evaluate the associations between measurements at baseline and between the changes in measurements between baseline and 3 years.

Results: In OAG patients with diabetes, change in OA resistive index (RI) was strongly and negatively correlated with change in average RNFL thickness ($r=-0.93$, $p=0.02$), inner superior macular thickness ($r=-0.85$, $p=0.03$), outer inferior macular thickness ($r=-0.97$, $p=0.03$), inner nasal macular thickness ($r=-0.85$, $p=0.03$), outer temporal macular thickness ($r=-0.95$, $p<0.01$) and macular volume ($r=-0.90$, $p=0.01$) and change in NPCA RI was strongly and negatively correlated with change in temporal RNFL thickness ($r=-0.90$, $p=0.04$), inner nasal macular thickness ($r=-0.84$, $p=0.03$), inner temporal macular thickness ($r=-0.84$, $p=0.03$) and macular volume ($r=-0.83$, $p=0.04$) with statistical significance over three years. In OAG patients without diabetes, these correlations were weak and did not reach statistical significance ($r=-0.32$ to 0.02 , $p>0.05$). There was a statistically significant difference in strength of correlations between groups for each relationship ($p<0.01$). In diabetic patients, change in CRA EDV was correlated with change in superior and inferior RNFL thickness ($r=-0.89$, $p=0.05$; $r=-0.72$, $p=0.19$). Other correlations between CRA and NPCA PSV and EDV were weak ($r=-0.57$ to 0.33) in both diabetics and non-diabetics and only statistically significant in non-diabetics (diabetics $p>0.05$, non-diabetics $p<0.01$).

Conclusions: Changes in vascular resistance were strongly correlated with deterioration of the RNFL and macula in OAG patients with diabetes. This suggests that diabetics may have a stronger vascular component to their glaucomatous progression than non-diabetics.

Commercial Relationships: Austin L. Gerber, None; Alon Harris, MSD (R), Alcon (R), Merck (C), Pharmalight (C), ONO (C), Sucampo (C), Adom (I); Brent A. Siesky, None; George J. Eckert, None; Ingrida Januleviciene, Pharmalight (F), Santen (C), Alcon (C), MSD (C); Nathaniel J. Kim, None; Annahita Amireskandari, None; Brian M. Marek, None; Leslie A. Tobe, None; Andrew H. Huck, None

Support: ADA; Grant 1-12-IN-20, Grant from Pfizer Pharmaceuticals Inc.

Program Number: 4448 **Poster Board Number:** D0188

Presentation Time: 8:30 AM - 10:15 AM

Blood pressure induced dynamic blood flow autoregulation in the optic nerve head of early experimental glaucoma

Lin Wang, Chelsea Piper, Grant Cull, Claude F. Burgoyne. Devers Eye Institute, Legacy Research Institute, Portland, OR.

Purpose: Dynamic autoregulation (dAR) refers to a transient blood flow (BF) response to the sudden perfusion pressure changes induced by altering either blood pressure (BP) or intraocular pressure (IOP). The purpose of the study was to test a hypothesis that dAR capacity in the optic nerve head (ONH) is compromised after chronic IOP elevation in non-human primate (NHP) experimental glaucoma (EG).

Methods: In one eye of each 12 NHPs, trabecular meshwork was photocoagulated by laser to induce chronic IOP elevation. The fellow eye was served as control (Ctl). After IOP elevation, ONH dAR in both eyes was assessed biweekly. Under general anesthesia, BF was recorded continuously by a Laser Speckle Flowgraphy (Softcare,

Japan). BP was registered continuously through an arterial line. BP cuffs were placed around the two arms and one thigh. The cuffs were inflated before the starting of BF recording and were simultaneously released after first ten seconds of BF recording to induce a rapid BP drop (ranging from 12 to 23 mmHg) to evoke the dAR response in ONH. The BF measurements continued for an additional 50 seconds (Fig 1). Retinal nerve fiber layer thickness (RNFLT) was measured by Spectral Domain Optical Coherence Tomography at the end of each test. The experimental endpoint was defined as approximately 12% RNFLT loss in the EG eye. dAR parameters were extracted from BF recordings, including: 1) Basal BF-before the cuff release; 2) maximal BF decrease (%) from basal BF; 3) Tr-the amount of time it took to the maximal BF decrease, 4) Kr-the slope of dAR descending curve. The mean between-eye differences of the parameter were compared (Paired Student T-test).

Results: The average IOP was 29 ± 1 mmHg in EG eyes and 13 ± 3 mmHg in Ctl ($p<0.001$) two to six weeks after laser treatment. The cuff deflation induced 17 ± 3 mmHg of BP drop for EG eyes and 16 ± 3 mmHg for Ctl eyes ($P=0.09$). All four dAR parameters were significantly changed in EG eyes compared to control eyes (Table).

Conclusions: These subtle but significant early hemodynamic changes in EG eye suggest that chronic IOP elevation has a significant impact on the vascular system in the ONH, which manifest as compromised BF autoregulation and basal BF increase. These parameters may be further tested in human glaucoma to identify earlier signs of impaired vascular system in ONH.

Fig 1

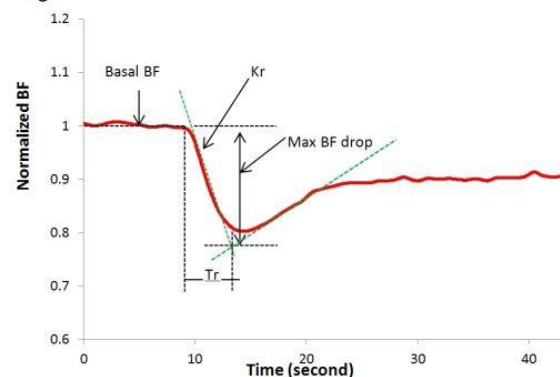


Table	Basal BF	Max BF	Tr	Kr
Ctl	10.05 ± 1.6	$11.15\% \pm 1.5\%$	3.30 ± 0.8	-0.41 ± 0.1
EG	11.69 ± 1.6	$16.21\% \pm 4.7\%$	3.96 ± 0.4	-0.53 ± 0.2
P-value	0.003	0.006	0.03	0.03

Commercial Relationships: Lin Wang, None; Chelsea Piper, None; Grant Cull, None; Claude F. Burgoyne, Heidelberg Engineering (F), Heidelberg Engineering (C)

Support: NIH Grant EY19939; Legacy Good Samaritan Foundation, Portland OR; unrestricted research fund from Pfizer Inc.

Program Number: 4449 **Poster Board Number:** D0189

Presentation Time: 8:30 AM - 10:15 AM

The NO donor, isorbide-5-mononitrate alone or combined with timolol, latanoprost or dorzolamide ameliorates intraocular pressure and ocular hemodynamic in an experimental model of glaucoma in rabbits

Francesco Impagnatiello¹, Barbara Giambene², Francesca Fabrizi³, Elena Bastia¹, Fernando Galassi², Emanuela Masini³. ¹Nicox Research Institute, Bresso, Milan, Italy; ²Eye Clinic, University of Florence, Florence, Italy; ³Preclinical and Clinical Pharmacology, University of Florence, Florence, Italy.

Purpose: Ocular hypertension is the major risk factor in glaucoma. However, other risk factors of vascular origin have been identified. Nitric oxide (NO) signalling seems to play a crucial role, being involved in the regulation of aqueous humour (AH) outflow and ocular hemodynamics. We studied the effects on intraocular pressure (IOP) and retrobulbar hemodynamic following 28 days daily topical dosing with isosorbide-5-mononitrate (ISMN, 0.5%), either alone or combined with the β -blocker, timolol (0.5%), the prostaglandin F₂ α agonist, latanoprost (0.05%) and the carbonic anhydrase inhibitor, dorzolamide (2%) in an experimental rabbit model of glaucoma.

Methods: Ocular hypertension was obtained by the injection of carborer (0.1%, 0.1ml) in the anterior chamber of New Zealand White rabbits. IOP was measured using a Tono-Pen. Retrobulbar hemodynamics of the ophthalmic artery was assessed using Color Doppler Imaging. The examinations were performed prior to drug treatment (baseline) and 7, 14, 21 and 28 days thereafter. Furthermore, cGMP content in AH was monitored throughout the experimental period to address the extent of NO signalling pathway activation.

Results: On average, IOP rose from 13.4 \pm 2.0 mmHg at baseline to 38.9 \pm 4.0 mmHg one week post carborer injection and remained stable thereafter. Timolol, latanoprost, and dorzolamide lowered IOP (on average 20-30%, p<0.001) at all time points post dose. ISMN, albeit less effectively, also lowered IOP in this model and the effect was additive when co-administered with timolol, latanoprost or dorzolamide. Similarly, carborer increased the resistivity index of the ophthalmic artery from 0.48 \pm 0.02 (basal) to 0.62 \pm 0.03 (one week post carborer, p<0.05). ISMN reversed this effect when administered alone or combined with timolol, latanoprost or dorzolamide. Consistent with the above findings, NO markers i.e. cGMP and nitrate were increased in AH following ISMN treatment.

Conclusions: ISMN by re-establishing physiologic NO signaling in target ocular tissues, ameliorates the effects of current treatments on IOP and ocular hemodynamics.

Commercial Relationships: Francesco Impagnatiello, Nicox Research Institute (C); Barbara Giambene, None; Francesca Fabrizi, Nicox Research Institute (F); Elena Bastia, Nicox Research Institute (E); Fernando Galassi, None; Emanuela Masini, Nicox Research Institute (F)

Program Number: 4450 **Poster Board Number:** D0190

Presentation Time: 8:30 AM - 10:15 AM

Effects of diverse Nitric Oxide donation on ocular hemodynamic and intraocular pressure in normotensive rabbits

Elena Bastia¹, Francesco Impagnatiello¹, Daniela Miglietta¹, Barbara Giambene², Emanuela Masini³, Nicoletta Almirante¹.

¹Nicox Research Institute, Bresso, Milan, Italy; ²Eye Clinic, University of Florence, Florence, Italy; ³Preclinical and Clinical Pharmacology, University of Florence, Florence, Italy.

Purpose: There is evidence that nitric oxide (NO) is involved in the regulation of intraocular pressure (IOP) and ocular hemodynamics. We previously reported that NO donation incorporated into IOP lowering agents enhances IOP lowering activity and improves ocular perfusion of parent compounds. In an attempt to correlate IOP lowering properties with functional NO potency, we studied the effects on IOP and ocular hemodynamic of novel NO donors characterized by increasing NO donating capacity.

Methods: New Zealand White (NZW) rabbits were used. Novel NO donating compounds diversifying for one nitrate group (NCX 583) or two nitrate groups in vicinal (NCX 548) and distal (NCX 604) relationships were investigated. Isosorbide-5-mononitrate (ISMN) was used for comparison. The compounds were characterized with respect to their functional vascular effects as well as IOP lowering

following topical dosing. NO-mediated vasorelaxant activity was tested in isolated norepinephrine (NE)-precontracted rabbit aortic rings. IOP was measured using a pneumatonomer prior to drug dosing and at 30, 60, 120, 180, 240 and 360 min thereafter. Ophthalmic artery hemodynamic was studied using Color Doppler Imaging.

Results: Likewise ISMN (EC₅₀=9.6 \pm 2.9 μ M) NCX 583, NCX 548 and NCX 604 showed vasorelaxant activity with an estimated potency of 2.5 \pm 0.6, 0.12 \pm 0.04 and 3.1 \pm 0.9 μ M, respectively, thus indicating different NO release depending on the chemical nature of the compounds. NCX 583 (1%) and NCX 604 (1%) lowered IOP to similar extent as ISMN (1%) reaching 10% reduction of IOP from basal value within 30-60 min post dosing. In contrast, the vicinal dinitrate derivative, NCX 548 (1%) was the most active reaching a maximum of 25% reduction of IOP compared to vehicle. Similarly, compounds also lowered the resistivity index of the ophthalmic artery.

Conclusions: Data show that NO donation leads to IOP lowering and enhanced ocular perfusion. The magnitude of the effect appears to depend on the functional potency of the NO donors. Overall modulation of NO is a target of interest for the development of innovative IOP lowering agents

Commercial Relationships: Elena Bastia, Nicox Research Institute (E); Francesco Impagnatiello, Nicox Research Institute (C); Daniela Miglietta, Nicox Research Institute (E); Barbara Giambene, None; Emanuela Masini, Nicox Research Institute (F); Nicoletta Almirante, Nicox Research Institute (E)

Program Number: 4451 **Poster Board Number:** D0191

Presentation Time: 8:30 AM - 10:15 AM

Association between waveform changes in optic nerve head circulation and retinal nerve fiber layer thickness in normal-tension glaucoma patients compared to healthy subjects, measured by laser speckle flowgraphy

Yukihiro Shiga, Yu Yokoyama, Toshifumi Asano, Shigeto Maekawa, Satoru Tsuda, Naoko Aizawa, Kazuko Omodaka, Morin Ryu, Toru Nakazawa. Ophthalmology, Tohoku University, Sendai, Japan.

Purpose: To use laser speckle flowgraphy (LSFG) to evaluate differences between normal subjects and patients with normal-tension glaucoma (NTG) in waveform analysis parameters (skew, blowout time (BOT), flow acceleration index (FAI), and acceleration time index (ATI)) of blood flow in the optic nerve head (ONH). Additionally, to evaluate the correlation of these LSFG parameters with an objective examination.

Methods: 78 NTG patients and 22 age-matched normal subjects (59.37 \pm 6.65, 57.32 \pm 7.42, respectively) were included in this case-control study. We measured ONH circulation with LSFG just after recording intraocular pressure (IOP) and systemic blood pressure. Microcirculation in the capillary area of the ONH was evaluated with LSFG parameters calculated using the equipped software (LSFG Analyzer, ver. 3.0.43.0, Softcare Ltd, Fukuoka, Japan). Average circumpapillary retinal nerve fiber layer thickness (cpRNFLT) was measured with Stratus OCT, and the visual field was examined with a Humphrey Field Analyzer (HFA, 30-2 SITA standard). Eyes with NTG were divided into three groups based on the progression of visual field defects.

Results: There were no significant differences in IOP or systemic blood pressure between the normal subjects and the NTG patients. In the ONH, the waveform analysis parameters of skew and FAI were significantly lower in the NTG patients compared to the controls (skew: NTG 11.61 \pm 1.87 AU, Control 13.11 \pm 1.48 AU, p<0.001; FAI: NTG 0.96 \pm 0.41 AU; control 2.29 \pm 0.67 AU, p<0.001). The parameter of ATI was significantly higher (NTG: 32.37 \pm 3.68 AU;

control: 29.98 ± 2.14 AU, $p=0.004$). The data for skew, ATI, and FAI were significantly correlated to the cpRNFLT ($r=0.39$, -0.31 , and 0.70 , respectively, $p<0.01$).

Conclusions: In the NTG patients, the waveform peak for ONH blood flow shifted to the posterior compared the control subjects. LSFG waveform analysis parameters indicated the level of glaucomatous damage in NTG patients. These results may help the diagnosis of NTG, as well as research on its pathogenesis.

Commercial Relationships: Yukihiko Shiga, None; Yu Yokoyama, Kowa Company (C); Toshifumi Asano, None; Shigeto Maekawa, None; Satoru Tsuda, Kowa (C); Naoko Aizawa, None; Kazuko Omodaka, None; Morin Ryu, None; Toru Nakazawa, Kowa Company Ltd. (F); Kowa Company Ltd. (C)

Support: None in the Support field

Program Number: 4452 **Poster Board Number:** D0192

Presentation Time: 8:30 AM - 10:15 AM

Analysis of the Correlation Between Peripapillary Choroidal Thickness and the Nerve Fiber Layer Damage in Primary Open Angle Glaucoma Patients

Nimesh Patel¹, Chandrasekharan Krishnan^{2,1}. ¹Tufts University School of Medicine, Boston, MA; ²New England Eye Care Center, Boston, MA.

Purpose: To examine the relationship between peripapillary choroidal thickness, nerve fiber layer thickness and visual field loss in asymmetric Primary Open Angle Glaucoma patients.

Methods: 124 eyes of 62 Primary Open Angle Glaucoma (POAG) patients seen at New England Eye Center between September 2009 and August 2011 were analyzed. Nerve fiber layer thickness measurements were obtained via Cirrus OCT (Carl Zeiss Meditec, Inc). Humphrey visual fields (Carl Zeiss Meditec, Inc) were performed and Mean Deviation data was used for analysis. Peripapillary choroidal thickness measurements were obtained via Cirrus OCT high definition raster scanning in four quadrants (superior, inferior, temporal and nasal) at distances 500 μ m, 1000 μ m and 1500 μ m from the optic nerve. A single sub-foveal measurement was also obtained. Interocular differences (OD-OS) in choroidal thickness were then compared to interocular differences in nerve fiber layer thickness and visual field mean deviation to see whether these variables were correlated.

Results: There was no statistically significant correlation (Pearson's correlation coefficient, Sig 2-tailed value) found in regards to interocular differences in peripapillary choroidal thickness and interocular differences in nerve fiber layer thickness or mean deviation in visual field in any of the four quadrants or in the subfoveal region (sig two-tailed <0.05) in this group of POAG patients.

Conclusions: Based on the results of this study, changes in peripapillary choroidal thickness do not seem to correlate with nerve fiber layer thickness or with visual field damage in patients with primary open angle glaucoma.

Commercial Relationships: Nimesh Patel, Research to Prevent Blindness (F); Chandrasekharan Krishnan, None

Support: Research to Prevent Blindness Funding

Program Number: 4453 **Poster Board Number:** D0193

Presentation Time: 8:30 AM - 10:15 AM

Change in intraocular pressure is a major determinant of retinal vein pulsation properties

William Morgan¹, Martin Hazelton², Brigid Betz-Stablein², Philip House¹, Yu Dao-Yi¹. ¹Lions Eye Institute, Nedlands, WA, Australia; ²Institute of Fundamental Sciences, Massey University, Palmerston North, New Zealand.

Purpose: The force required to induce venous pulsation is a significant predictor of glaucoma progression. It is not known whether alterations in intraocular pressure affect these vein pulsation properties.

Methods: Glaucoma and suspect patients had two retinal vein ophthalmodynamometric force (ODF) measurements at least 40 days apart. All subjects had Humphrey visual fields, scanning laser tomography, central corneal thickness (CCT) and IOP recorded at the initial visit. The time intervals between ODF measurements and age were calculated. The upper and lower hemiview ODF was measured. The change in ODF and change in IOP was calculated. Data from each eye was analysed using a linear mixed model with random factors to account for left and right eye, upper and lower correlation.

Results: Thirty two subjects fulfilled the criterion (20 females). The mean time interval between measurements was $14.3 (\pm 9.9)$ months and mean age was $60 (\pm 11)$ years. Multivariate linear regression analysis demonstrated that change in mean ODF was significantly associated with change in intraocular pressure (coefficient = 0.55 mmHg/mmHg, $p=0.0009$). Other parameters: central corneal thickness ($p=0.31$), initial IOP ($p=0.79$), hemi-neuroretinal rim area ($p=0.26$), age ($p=0.66$), mean hemifield defect ($p=0.33$) and time interval ($p=0.38$) were not significantly associated with change in ODF.

Conclusions: Change in ODF is strongly associated with change in IOP such that a reduced

intraocular pressure is associated with a subsequent reduction in venous ODF. This implies that favourable changes in central retinal vein properties are occurring when intraocular pressure is reduced.

Commercial Relationships: William Morgan, National Health and Medical Research Council (F); Martin Hazelton, None; Brigid Betz-Stablein, None; Philip House, None; Yu Dao-Yi, None

Support: NHMRC project grant 1020367

Clinical Trial: ACTRN12608000274370

Program Number: 4454 **Poster Board Number:** D0194

Presentation Time: 8:30 AM - 10:15 AM

Nonphysiologic nocturnal blood pressure dipping in Primary Open Angle Glaucoma (POAG) and Normal Pressure Glaucoma (NPG) patients

Karin R. Pillunat, Cosima Hermann, Olga Furashova, Eberhard Spoerl, Lutz E. Pillunat. Dept of Ophthalmology, Univ Clinic Carl Gustav Carus Dresden, Dresden, Germany.

Purpose: In order to evaluate whether nonphysiologic nocturnal blood pressure dipping is associated with visual field indices in POAG and NPG patients.

Methods: 29 patients suffering from POWG (IOP > 22 mmHg) and 22 patients suffering from NTG (IOP < 21 mmHg) were included in a prospective clinical trial. 24 hour blood pressure was measured (Bosch&Sohn GmbH). According to WHO criteria a mean arterial blood pressure (MAP) dipping less than 10% and more than 20% was considered as nonphysiologic dipping, a MAP-dipping between 10% and 20% was considered as physiologic dipping. Visual field tests were only taken from right eyes with the Humphrey 30-2 SST program. A mean deviation (MD) of more than -6 dB was considered as early, a MD between -6 dB and -12 dB as moderate and a MD of less than -12 dB as severe glaucomatous loss. For statistical analysis the Chi²-test was used. A p-value less than 0,05 was considered as statistically significant.

Results: 45% of the patients showed nonphysiologic MAP dipping. MD of less than -6 dB was seen in 57% of these cases. 55% however showed physiologic MAP dipping. MD of less than -6 dB was seen only in 35% of physiological dippers. The difference between visual

ARVO 2013 Annual Meeting Abstracts by Scientific Section/Group – Glaucoma

field indices between nonphysiological and physiological dippers was statistically significant ($p=0.05$). 58% of POAG patients and 27% of NTG patients were nonphysiologic MAP dippers.

Conclusions: Nonphysiologic nocturnal blood pressure dipping is associated with more advanced visual field defects especially in POAG but also in NPG patients. Therefore also in POAG patients diurnal blood pressure monitoring has to be regarded as an important diagnostic tool.

Commercial Relationships: Karin R. Pillunat, None; Cosima Hermann, None; Olga Furushova, None; Eberhard Spoerl, None; Lutz E. Pillunat, None

Clinical Trial: NCT01503996

Program Number: 4455 **Poster Board Number:** D0195

Presentation Time: 8:30 AM - 10:15 AM

Relation of Spontaneous Retinal Venous Pulsation and Disc Hemorrhage in Open Angle Glaucoma

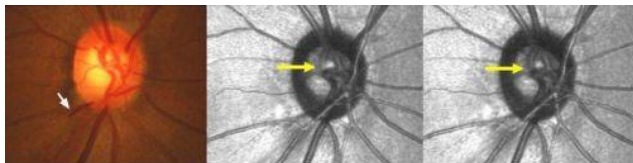
Mijin Kim^{1,2}, Tae-Woo Kim^{1,2}, Robert N. Weinreb³, Eun Ji Lee^{1,2}, Je Hyun Seo⁴, Ki Ho Park¹, Dong Myung Kim¹. ¹Ophthalmology, Seoul National University Bundang Hospital, Seongnam, Gyeonggi-do, Republic of Korea; ²Ophthalmology, Seoul National University College of Medicine, Seoul, Republic of Korea; ³Hamilton Glaucoma Center and Department of Ophthalmology, University of California San Diego, La Jolla, CA; ⁴Pusan National University Yangsan Hospital, Yangsan, Republic of Korea.

Purpose: To investigate the relationship of disc hemorrhage (DH) and spontaneous venous pulsation (SVP) in open angle glaucoma (OAG).

Methods: Fifty-six eyes of 56 patients with DH on the day of movie recording, and 118 eyes of 118 patients in whose eyes DH has not been observed for at least 4 years were included. The SVP was assessed using a movie tool provided by confocal scanning laser ophthalmoscope (Spectralis HRA, Heidelberg Engineering, Heidelberg, Germany). The frequency of SVP was compared between patients with and without DH. Logistic regression analysis was used to determine the factors associated with the occurrence of DH.

Results: The frequency of SVP in overall patients with OAG was 60.3%, and the presence of SVP was not significantly associated with DH by logistic analysis (OR, 0.698; $P = 0.200$). Greater visual field mean deviation (OR, 1.100; $P = 0.024$), lower untreated intraocular pressure (OR, 0.888; $P = 0.013$), and the tendency to cold hands (OR, 2.796; $P = 0.022$) showed association with DH.

Conclusions: In consecutive patients with OAG, presence/absence of SVP was not associated with DH. This finding suggests that the occurrence of DH may be independent of increase in retrolaminar venous resistance.



(Left) Disc photograph of a patient with disc hemorrhage in inferotemporal area of the optic nerve (white arrow). (Middle) Video frame of the minimum diameter of central retinal vein (CRV) identified using a confocal scanning laser ophthalmoscope. (Right) Video frame maximum diameter of CRV. Note the difference of the diameter of the CRV indicated with yellow arrow.

Commercial Relationships: Mijin Kim, None; Tae-Woo Kim, None; Robert N. Weinreb, Aerie (F), Alcon (C), Allergan (C), Altheos (C), Amakem (C), Bausch&Lomb (C), Carl Zeiss-Meditec

(C), Genentech (F), Haag-Streit (F), Heidelberg Engineering (F), Konan (F), Lumenis (F), National Eye Institute (F), Nidek (F), Optovue (C), Quark (C), Solx (C), Topcon (C); Eun Ji Lee, None; Je Hyun Seo, None; Ki Ho Park, None; Dong Myung Kim, None

Program Number: 4456 **Poster Board Number:** D0196

Presentation Time: 8:30 AM - 10:15 AM

Optic Nerve Capillaries Blood Oxygenation in Normal and Primary Open-Angle Glaucoma Subjects

Vasile Diaconu, Van Loc Tran. Ecole D'optometrie, University of Montreal, Montreal, QC, Canada.

Purpose: Open-angle glaucoma was defined as a neurodegenerative disease, characterized by high intraocular pressure (IOP), progressive retinal cell death, with subsequent visual field loss (Flammer and Drance, 1984). Elevated IOP has been identified as one of the major risk factors for glaucomatous optic nerve damage and current treatment of glaucoma aims to reduce IOP to prevent visual loss (Heijl et al., 2002). However, an adequate IOP control cannot prevent the disease progression in all patients. The aim of the present study was to explore the optic nerve capillaries blood oxygenation in healthy subjects and patients with open-angle glaucoma.

Methods: The normal blood oxygenation of the optic nerve's capillaries has been estimated in 35 healthy subjects from a laboratory database. The blood oxygenation of the optic nerve's capillaries has been also estimated in 16 eyes of 8 glaucoma patients, under treatment with different topical medication, to maintain lower IOP. A non-invasive retinal oximeter, with a multichannel spectroscopy technique has been used to measure the optic nerve's blood oxygenation (Diaconu 1009). The blood oxygenation has been evaluated from three specific locations from the optic nerve papilla, representing an area of 0.5 mm in diameter. An experimental session consisted of 20 consecutive measurements in an interval of 10 seconds for each investigated area.

Results: The results from the present study suggest a homogeneous blood oxygenation in the optic nerve capillary area structures of the normal subject. For a 95% confidence interval, the normal optic nerve's blood oxygenation is in the range, from 59% to 72.75%. The papilla of the glaucomatous subjects could include areas, where the blood oxygenation rate is either lower or higher compared to the normal blood oxygenation values. However the papilla of the optical nerve of four glaucomatous patients participating in the study presents blood oxygenation within the limits of the normal range.

Conclusions: The present study suggests that the blood oxygenation measurements at the level of the capillary structures in the area of the optical nerve could provide insight into the evolution of glaucoma.

Commercial Relationships: Vasile Diaconu, None; Van Loc Tran, None

Program Number: 4457 **Poster Board Number:** D0197

Presentation Time: 8:30 AM - 10:15 AM

Reduced Retinal Blood Flow is Associated with Thinner Retinal Nerve Fiber Layer in Glaucomatous Eyes with Single Hemifield Damage

Mitra Sehi¹, Iman Goharian¹, Ranjith Kumar Konduru², Ou Tan³, Sowmya Srinivas², Srinivas R. Sadda², David Huang³, David S. Greenfield¹. ¹Ophthalmology, Bascom Palmer Eye Institute, University of Miami, Palm Beach Gardens, FL; ²Ophthalmology, Doheny Eye Institute, University of Southern California, Los Angeles, CA; ³Ophthalmology, Casey Eye Institute, Oregon Health and Science University, Portland, OR.

Purpose: To examine the hypotheses that retinal blood flow (RBF) is significantly reduced in the abnormal visual hemifield of glaucomatous eyes with single-hemifield damage; and that there are

significant associations between reduced retinal sensitivity (RS) in abnormal hemifield, and RBF, retinal nerve fiber layer thickness (RNFL) and ganglion cell complex thickness (GCC) in the corresponding hemisphere.

Methods: Glaucomatous eyes with visual field loss confined to a single hemifield underwent Spectral-domain optical coherence tomography (SDOCT), Doppler SDOCT and standard automated perimetry (SAP). Using Dual Angle Protocol, a double-circle scanning pattern was applied to measure the venous BF. Disc photos were registered with Doppler images to identify the veins. RBF was derived from the recorded Doppler frequency shift and the calculated angle between the beam and the vessel. Total and hemispheric RBF values were calculated. Average, superior and inferior RNFL and GCC were measured. Shapiro-Wilk Test, ANOVA with Tukey HSD and regression analyses were performed.

Results: 30 eyes (age 61.5±9.2 yrs) were included. Mean RS was reduced in abnormal hemifield compared with the normal hemifield (22.5±7.1 vs 28.5±2.0dB, p<0.001). Mean RBF was reduced in retinal hemisphere associated with abnormal hemifield vs the opposite hemisphere (15.3±5.4 vs 19.3±8.4 μL/min, p=0.03). The RNFL was thinner in corresponding abnormal hemisphere vs the opposite hemisphere (87.0±20.2 vs 103.7±20.6μm, p=0.002). The GCC was thinner in corresponding abnormal hemisphere vs the opposite hemisphere (80.6±10.3 vs 83.6±10.1μm, p=0.04). The RBF was associated with RNFL (r=0.41, p=0.02) and GCC (r=0.43, p=0.02), but not with the RS in 1/lambert or dB (r=0.31, p=0.09; r=0.30, p=0.10 respectively) in corresponding abnormal hemisphere and abnormal hemifield.

Conclusions: In glaucomatous eyes with single-hemifield damage, retinal blood flow is significantly reduced in the hemisphere associated with abnormal hemifield. These findings emphasize the role of retinal blood flow in the pathogenesis of glaucoma.

Commercial Relationships: Mitra Sehi, Allergan, Inc. (C); Iman Goharian, None; Ranjith Kumar Konduru, None; Ou Tan, Optovue (F), Optovue (P), Carl Zeiss Meditec (P); Sowmya Srinivas, None; Srinivas R. Sadda, Regeneron (C), Genentech (C), Allergan (C), Carl Zeiss Meditec (C), Optos (C), Carl Zeiss Meditec (F), Optovue (F), Optos (F); David Huang, Optovue (F), Optovue (I), Optovue (P), Optovue (R), Carl Zeiss Meditec (P); David S. Greenfield, National Eye Institute (R), Carl Zeiss Meditec (R), Optovue (R), Heidelberg Engineering (R), Allergan (C), Alcon (C), Merz (C), Quark (C), SOLX (C), Biometric Imaging (C), Senju (C) **Support:** NIH R01 EY013516, P30EY014801, An unrestricted grant from Research to Prevent Blindness, New York, New York **Clinical Trial:** NCT01314326

Program Number: 4458 **Poster Board Number:** D0198

Presentation Time: 8:30 AM - 10:15 AM

Optic Nerve Head Label-free Microangiography: OCT-based Correlation of Microstructure and Microvasculature in Normal & Open Angle Glaucoma Subjects

Lin an¹, Peng Li¹, Murray A. Johnstone², Ruikang K. Wang^{1,2}.

¹Bioengineering, University of Washington, Seattle, WA;

²Ophthalmology, University of Washington, Seattle, WA.

Purpose: To determine the feasibility of correlating optic nerve head (ONH) structure with functioning microvasculature in the ONH and scleral rim using a 3D OCT imaging technique.

Methods: OMAG, a label-free OCT vascular imaging procedure, operating at 842 nm central wavelength was modified to image ONH microstructure and microcirculations. Human subjects (7) [Normal Eyes (10), OAG (4); Mean age (35)] participated in this pilot study. OMAG acquired 3D volumetric datasets from each subject, providing simultaneous structural and microvascular images of the ONH.

©2013, Copyright by the Association for Research in Vision and Ophthalmology, Inc., all rights reserved. Go to iovs.org to access the version of record. For permission to reproduce any abstract, contact the ARVO Office at arvo@arvo.org.

Results: The tissue organization and functional blood flow as acquired by OMAG appear similar among the normal subjects. The typical images acquired from one normal subject are shown in Fig 1: Rows (80, 180, 400 and 600μm depth); Columns (a-j=structure, b-k=microvasculature; c-l=merged). (a-c) NFL capillaries branching from retinal artery. (d-f) ONH vessels enter from level of choroid to supply prelaminar layer. (g-i) lamina cribrosa (LC) is continuous with sclera. Vessels penetrate sclera to supply LC capillaries; vascular pattern mirrors LC beam architecture. (j-l), deeper LC and vascular pattern persist, less regular organizational pattern than in (g-i). Large vessels are visible at external edge of scleral rim in region of circle of Zinn-Haller. Fig. 2: Typical images acquired from one glaucoma subject's ONH: (a -b) cross-sectional structure & corresponding vascular images (temporal-nasal section), indicating thinning of prelaminar layer. (c-d) enface views of the LC, 100μm below the ONH surface; LC-porous structure (c) is visible; unlike Fig. 1g pore architecture is compressed & non-uniform. In Fig. 2d, unlike Fig. 1h, capillaries mirroring LC beam architecture are absent, presumably dropping out & leaving large CRA vessels visible in this deep cup.

Conclusions: OMAG can provide detailed images of functioning capillaries as well as larger vessels that supply ONH tissue beds. Correlation between simultaneous structural and blood flow images provided in vivo evidence of mutual relationships. OAG eyes had a striking loss of vasculature, particularly in the lamina cribrosa. The non-invasive label-free technology should prove beneficial clinically in identifying and monitoring vascular components of mechanisms associated with ONH damage in glaucoma.

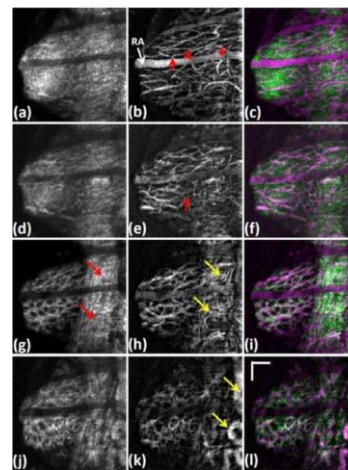


Fig.1

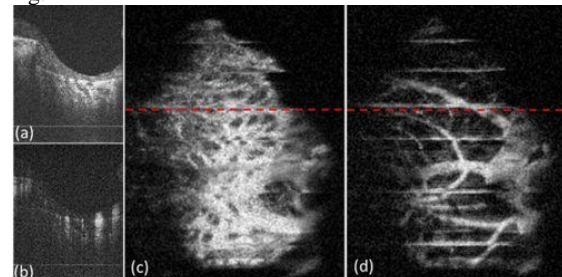


Fig.2

Commercial Relationships: Lin an, None; Peng Li, None; Murray A. Johnstone, Alcon (R), Allergan (R), Allergan (P), Healonics (I), Cascade Ophthalmics (I), Sensimed (R), Ivantis (R), University of Washington (P); Ruikang K. Wang, National Institutes of Health (F), W.H. Coulter Foundation Translational Research Partnership

Program (F), Research to prevent blindness (F), Oregon Health & Science University (P), University of Washington (P)
Support: W.H. Coulter Foundation Translational Research Partnership Program and Research to Prevent Blindness Innovative Research Award

Program Number: 4459 **Poster Board Number:** D0199

Presentation Time: 8:30 AM - 10:15 AM

Effect of Cerebrospinal Fluid Pressure on Central Retinal Artery Hemodynamics: a Mathematical Model

Lucia Carichino¹, Giovanna Guidoboni¹, Annahita Amireskandari², Brent Siesky², Alon Harris². ¹Mathematics, Indiana University Purdue Univ, Indianapolis, IN; ²Ophthalmology, Indiana University Sch of Medicine, Indianapolis, IN.

Purpose: To investigate the influence of cerebrospinal fluid pressure (CSF-p) on central retinal artery (CRA) hemodynamics. This investigation is motivated by several studies that suggested low CSF-p as a possible risk factor for glaucoma. In particular, there is evidence of lower CSF-p in normal-tension glaucoma subjects.

Methods: A mathematical model is developed to simulate the effect of CSF-p on CRA hemodynamics. The model incorporates a description of the lamina cribrosa (LC) deformation and the blood flow in the CRA. The LC is modeled as a homogeneous linearly elastic circular plate of constant finite thickness, which deforms under the combined action of intraocular pressure (IOP), CSF-p and scleral tension. The CRA is modeled as a fluid-structure interaction system. The walls of the CRA deform under the action of an external pressure that varies along the vessel length to include CSF-p, IOP and the compression induced by LC deformation. Numerical simulations are performed at constant IOP=15mmHg and constant mean arterial pressure 62mmHg, while the CSF-p is varied in the range between 1 and 30mmHg.

Results: As CSF-p increases, the CRA blood velocity (v) and flow rate (Q) predicted by the mathematical model show a complex behavior, see Figure 1 and 2. The CRA hemodynamic response can be divided in three phases. In phase A and C the system is dominated by the trans-LC pressure gradient. More precisely, in phase A the trans-LC pressure gradient decreases with CSF-p elevation, leading to an increase in v and Q, while in phase C the gradient increases with CSF-p elevation, leading to a decrease in v and Q. In phase B the trans-LC pressure gradient is small enough to be overcome by the scleral tension. This leads to a less steep decrease in v and Q when compared with phase C, which results from the direct action of elevated CSF-p on the pre-laminar CRA segment.

Conclusions: Low CSF-p has been associated with primary open angle glaucoma (POAG). The exact mechanisms responsible for this association remain unclear. Our model suggests that the contribution of CSF-p alterations to POAG pathophysiology might be mediated by secondary retinal blood flow changes.

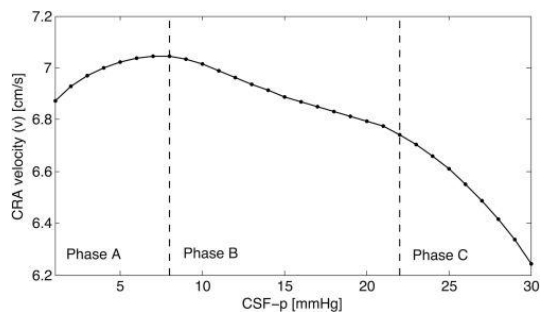


Figure 1. Response of CRA velocity to CSF-p elevations.

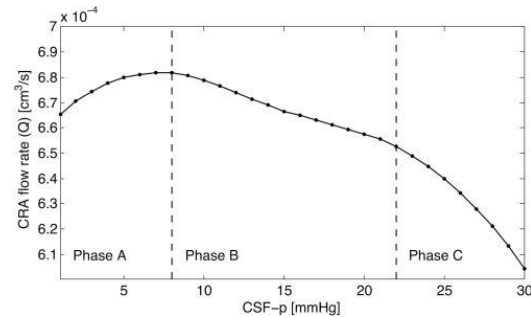


Figure 2. Response of CRA flow rate to CSF-p elevations.

Commercial Relationships: Lucia Carichino, None; Giovanna Guidoboni, None; Annahita Amireskandari, None; Brent Siesky, None; Alon Harris, MSD (R), Alcon (R), Merck (C), Pharmalight (C), ONO (C), Sucampo (C), Adom (I)

Support: Indiana University Collaborative Research Grant, NSF-DMS 1134731, NSF-DMS 1224195, NIH: 1R21EY022101-01A1

Program Number: 4460 **Poster Board Number:** D0200

Presentation Time: 8:30 AM - 10:15 AM

The effect of anthocyanins and ginkgo biloba extract treatment in patients with open-angle glaucoma depending on the presence of diabetes mellitus

Yong Woo Lee¹, Seonghee Shim¹, Joon Mo Kim¹, Chul Young Choi¹, Ki Ho Park². ¹Ophthalmology, Sungkyunkwan University School of Medicine, Kangbuk Samsung Hospital, Seoul, Republic of Korea; ²Ophthalmology, Seoul National University College of Medicine, Seoul, Republic of Korea.

Purpose: Anthocyanins and ginkgo biloba extract (GBE) are considered beneficial for various vascular disease. This study was performed to evaluate the effect of anthocyanins and GBE on visual function in patients with open-angle glaucoma depending on the presence of diabetes mellitus (DM).

Methods: Retrospective study by chart review of 410 individuals (271 men and 139 women) with open-angle glaucoma who were treated with anthocyanins (n = 184) / GBE (n = 116) or no medication (n = 110). Humphrey Visual Field (HVF) test, logarithm of the minimal angle of resolution best-corrected visual acuity (logMAR BCVA), and intraocular pressure, blood pressure, and fasting blood glucose were determined before and at the end of treatment. Data was divided into two groups, depending on presence of DM, and change of visual function parameters in each group were analyzed.

Results: In the open-angle glaucoma patients without DM (n=254), the mean change of logMAR BCVA was -0.07(±0.24) in anthocyanins treatment group, 0.004(±0.06) in GBE group and 0.05(±0.20) in control (p<0.001). In the open-angle glaucoma patients with DM (n=156), the mean change of logMAR BCVA was -0.03(±0.15) in anthocyanins treatment group, 0.03(±0.08) in GBE group and 0.06(±0.09) in control (p=0.005). Other changes in visual function parameters were not consistently correlated with anthocyanins or GBE treatment.

Conclusions: Systemic administration of anthocyanins appeared to be helpful in improving BCVA in some individuals with open-angle glaucoma regardless of diabetes mellitus.

Table 1. Changes (after-before) in best corrected visual acuity (logMAR), visual field indices in the patients without diabetes mellitus.

	Anthocyanins (n=8)	Ginkgo Biloba Extract (n=9)	Control (n=8)	p-value [†]	p-value [‡]
Change of mean BCVA logMAR*	-0.07±0.24	0.00±0.16	0.05±0.20	<0.001	0.014
Change of ICD (dB) [†]	0.71±0.74	0.73±0.34	0.06±0.97	0.34	0.929
Change of PSD (dB) [†]	-0.01±0.83	-0.22±0.54	0.25±0.14	0.53	0.437

*Mean ± SD
[†] One-way ANOVA
[‡] Independent sample t-test between anthocyanins and ginkgo biloba extract

Table 2. Changes (after-before) in best corrected visual acuity (logMAR), visual field indices in the patients with diabetes mellitus.

	Anthocyanins (n=14)	Ginkgo Biloba Extract (n=20)	Control (n=26)	p-value [†]	p-value [‡]
Change of mean BCVA logMAR*	-0.03±0.15	0.03±0.18	0.06±0.19	0.005	0.063
Change of ICD (dB) [†]	0.73±0.36	0.76±0.87	1.35±0.77	0.824	0.888
Change of PSD (dB) [†]	-0.24±0.42	0.55±0.73	-0.18±0.16	0.295	0.163

*Mean ± SD
[†] One-way ANOVA
[‡] Independent sample t-test between anthocyanins and ginkgo biloba extract

Commercial Relationships: Yong Woo Lee, None; Seonghee Shim, None; Joon Mo Kim, None; Chul Young Choi, None; Ki Ho Park, None

Program Number: 4461 **Poster Board Number:** D0201

Presentation Time: 8:30 AM - 10:15 AM

A theoretical investigation of the relationship between intraocular pressure, cerebrospinal fluid pressure, arterial blood pressure, blood flow autoregulation and retinal hemodynamics
 Giovanna Guidoboni¹, Alon Harris², Simone Cassani¹, Lucia Carichino¹, Annahita Amireskandari², Brent A. Siesky².

¹Mathematics, Indiana University Purdue Univ, Indianapolis, IN;

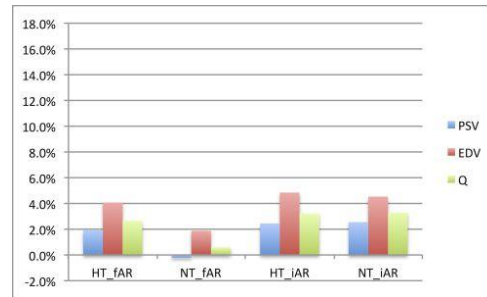
²Ophthalmology, Indiana University School of Medicine, Indianapolis, IN.

Purpose: Alterations in intraocular pressure (IOP), cerebrospinal fluid pressure (CSF-p), arterial blood pressure (BP), and blood flow autoregulation (AR) have been suggested as possible risk factors for glaucoma. The goal of this study is to investigate whether and to what extent these factors influence retinal hemodynamics, as a first step towards a deeper understanding of how they might contribute to glaucoma pathophysiology.

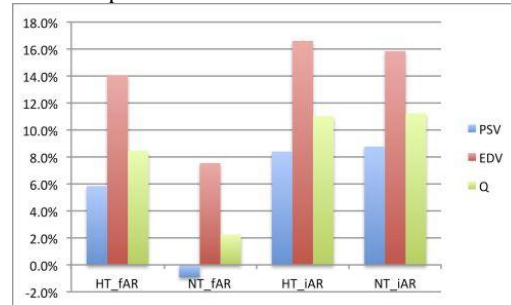
Methods: A mathematical model of the retinal circulation is used as a “virtual lab” to isolate the contributions of IOP, CSF-p, BP and AR on retinal hemodynamics. The model describes the retinal vascular bed as a network of five compartments: central retinal artery (CRA), arterioles, capillaries, venules, and central retinal vein (CRV). The blood flow is driven by systemic pressures, and is regulated by variable resistances accounting for nonlinear effects due to AR, and compression of the lamina cribrosa on CRA and CRV (which depends on IOP, CSF-p, and scleral tension). Velocities, pressures and volumetric flows are computed using the model for (1) IOP=15mmHg (baseline) and 24 mmHg (elevated IOP); (2) CSF-p = 7mmHg (baseline) and 5 mmHg (low CSF-p); (3) BP = 120/80mmHg (normotensive-NT) and 145/85mmHg (hypertensive-HT); and (4) functional AR (fAR) and impaired AR (iAR).

Results: Variations in peak systolic velocity (PSV), end diastolic velocity (EDV), and mean retinal blood flow (Q) in the CRA predicted by the model are reported in Fig1 and Fig2. Variations are computed as percent differences with respect to the values obtained for baseline IOP and CSF-p. When CSF-p is low (Fig1), the variations in PSV and Q remain below 3.3% for both NT and HT, and both fAR and iAR cases, while the variations in EDV reach 4.8% for HT_iAR. When IOP is elevated (Fig2), the variations in PSV and Q remain below 11.2% for both NT and HT, and both fAR and iAR cases, while the variations in EDV reach 16.6% for HT_iAR. In both panels, the case NT_fAR shows variations of smallest magnitudes.

Conclusions: Our mathematical model suggests that retinal blood flow is nonlinearly modulated by IOP, CSF-p, BP, and AR. Specifically, alterations in CRA blood flow are affected by low CSF-p and elevated IOP in different ways and are more pronounced in patients with systemic hypertension.



Low CSF-p case



Elevated IOP case

Commercial Relationships: Giovanna Guidoboni, None; Alon Harris, MSD (R), Alcon (R), Merck (C), Pharmalight (C), ONO (C), Sucampo (C), Adom (I); Simone Cassani, None; Lucia Carichino, None; Annahita Amireskandari, None; Brent A. Siesky, None
Support: NSF/DMS grants 1134731 and 1224195, the NIH grant 1R21EY022101-01A1, the Indiana University Collaborative Research Grant fund of the Office of the Vice President for Research

Program Number: 4462 **Poster Board Number:** D0202

Presentation Time: 8:30 AM - 10:15 AM

Effect of Trabeculectomy on Retinal Hemodynamics: Mathematical Modeling of Clinical Data

Simone Cassani¹, Giovanna Guidoboni¹, Ingrida Januleviciene³, Lucia Carichino¹, Brent Siesky², Leslie A. Tobe², Annahita Amireskandari², Alon Harris². ¹Mathematics, Indiana University Purdue Univ, Indianapolis, IN; ²Ophthalmology, Indiana University Sch of Medicine, Indianapolis, IN; ³Eye Clinic Of Lithuanian University of Health Sciences, Kaunas, Lithuania.

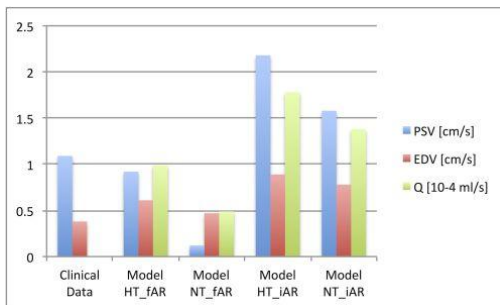
Purpose: To investigate the effect of trabeculectomy (TB) on retinal hemodynamics and to study how this relationship may be influenced by arterial blood pressure and blood flow autoregulation (AR).

Methods: A mathematical model of the retinal circulation is used to predict alterations in retinal blood flow associated with reductions of intraocular pressure (IOP) following TB. The model describes the retinal vascular bed as a network of five lumped compartments: central retinal artery (CRA), arterioles, capillaries, venules, and central retinal vein (CRV). The blood flow is driven by systemic pressures, and is regulated by variable resistances accounting for nonlinear effects due to AR, and IOP-induced compression of the lamina cribrosa on CRA and CRV. Peak systolic velocity (PSV), end diastolic velocity (EDV), and mean blood volumetric flow (Q) in the CRA are computed with the mathematical model for (i) IOP=28.7 mmHg and 13.1 mmHg, corresponding to IOP levels before and after

TB; (ii) systolic and diastolic blood pressures SBP/DBP = 120/80 mmHg and 143/84 mmHg, representing normotensive (NT) and hypertensive (HT) subjects; and functional AR (fAR) or impaired AR (iAR). The model predictions are compared with the clinical data collected in a study involving 49 patients, examining the blood flow pre and post TB.

Results: The clinical data show that PSV and EDV increase from 7.81 ± 2.51 cm/s and 2.39 ± 0.94 cm/s to 8.90 ± 2.66 cm/s and 2.77 ± 1.14 after TB, while IOP decreases from 28.7 ± 7.9 mmHg to 13.1 ± 5.8 mmHg. The mean values of SBP/DBP are 143/84 mmHg, as for the HT case of the mathematical model. The amounts by which PSV and EDV increase are reported in the Figure and are compared with model predictions. The increases in Q predicted by the model are also reported in the Figure. The case HT_fAR is the closest to the clinical data, and shows that PSV increases more than EDV. On the contrary, in NT_fAR, EDV increases more than PSV, suggesting that the levels of arterial blood pressure strongly influence the results. When AR is impaired, the increases in PSV, EDV and Q are much more pronounced than in the case of functional AR.

Conclusions: Our mathematical model suggests that CRA blood flow is increased secondarily to TB. Specifically our model reveals the relative impact of alterations in blood pressure and dysfunctional regulation of CRA hemodynamics on changes in retinal blood flow following TB.



Commercial Relationships: Simone Cassani, None; Giovanna Guidoboni, None; Ingrida Januleviciene, Pharmalight (F), Alcon (C), MSD (C), Santen (C); Lucia Carichino, None; Brent Siesky, None; Leslie A. Tobe, None; Annahita Amireskandari, None; Alon Harris, MSD (R), Alcon (R), Merck (C), Pharmalight (C), ONO (C), Sucampo (C), Adom (I)

Support: Indiana University Collaborative Research Grant, NSF-DMS 1224195, NSF-DMS 1134731, NIH: 1R21EY022101-01A1

Program Number: 4463 **Poster Board Number:** D0203

Presentation Time: 8:30 AM - 10:15 AM

Effect of intraocular pressure and arterial blood pressure on oxygen saturation levels in the retina: a theoretical model

Julia Arciero¹, Alon Harris², Giovanna Guidoboni¹. ¹Mathematics, Indiana Univ-Purdue Univ Indianapolis, Indianapolis, IN; ²Ophthalmology, Indiana University, Indianapolis, IN.

Purpose: Open-angle glaucoma (OAG) is characterized by progressive retinal ganglion cell death and visual field loss. Although elevated intraocular pressure (IOP) is the primary risk factor for OAG, several studies have shown that impaired perfusion and oxygen delivery to retinal ganglion cells may contribute to OAG pathophysiology. In this study, a mathematical model is used to predict blood oxygen saturation in the retina as IOP and mean arterial pressure (MAP) are varied and to assess conditions that may lead to normal or impaired oxygenation.

Methods: A theoretical model is used to simulate oxygen delivery to the retina via five compartments of blood vessels. Oxygen is assumed

to be delivered by large arterioles (LA), small arterioles (SA), and capillaries (C); oxygen exchange by small venules (SV) and large venules (LV) is neglected. A Krogh cylinder model is used in which each oxygen-delivering vessel runs along the axis of a cylinder representing the exclusive tissue region it supplies. The oxygen demand is assumed to be constant, and the decline in oxygen flux must equal the rate of oxygen consumption, by the conservation of mass. Oxygen saturation levels in the five compartments are predicted for a wide range of MAP (80, 100, and 160 mmHg) while IOP is held at a control (15 mmHg) or elevated (25 mmHg) level.

Results: Model predictions suggest that an isolated measure of oxygen saturation is not sufficient for distinguishing between the multiple factors that influence blood oxygen levels, including IOP and MAP. For example, a MAP of 80 mmHg and IOP of 15 mmHg yield nearly identical model predictions of oxygen saturation in venules as a MAP of 100 mmHg and IOP of 25 mmHg (Fig. 1A-1B). Oximetry data from patients typically indicate a blood oxygen saturation of 90-100% in arterioles and 50-75% in venules (Figure 2). Thus, oximetry data provide direct clinical measures of oxygen saturation, but do not provide a direct identification of the factors that may alter oxygen saturation levels.

Conclusions: Oximetry measures provide important indications of tissue oxygenation, but this study also motivates the need for theoretical models to guide the differentiation and identification of the most relevant factors to consider in order to treat OAG most successfully.

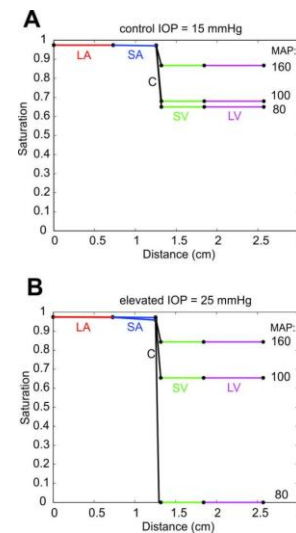


Figure 1.

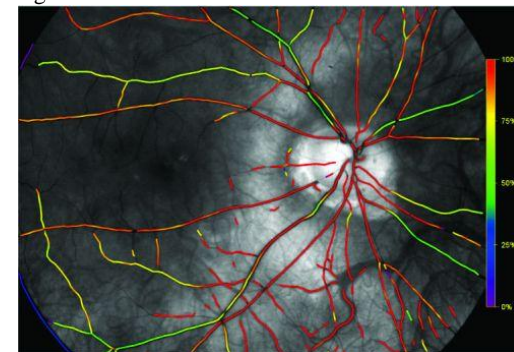


Figure 2.

Commercial Relationships: Julia Arciero, None; Alon Harris, MSD (R), Alcon (R), Merck (C), Pharmedica (C), ONO (C), Sucampo (C), Adom (I); **Giovanna Guidoboni**, None
Support: NSF-DMS 1224195

Program Number: 4464 **Poster Board Number:** D0204

Presentation Time: 8:30 AM - 10:15 AM

Retinal Oximetry in Early Primary Open Angle Glaucoma

Scott D. Lawrence, Pooja D. Jani, Kyle Billow, Jean-Claude Mwanza, Iryna A. Falkenstein. Ophthalmology, Univ of North Carolina at Chapel Hill, Chapel Hill, NC.

Purpose: To determine if there is a difference in retinal oxygen saturation in eyes diagnosed with early primary open angle glaucoma (POAG) versus normal eyes.

Methods: This was a prospective observational study. Twenty eyes (13 patients) diagnosed with early POAG (visual field mean deviation < -6 dB; mean, -2.83 ± 1.19 dB) underwent retinal oximetry measurement. Twenty normal eyes (20 patients) served as controls. Optic disc-centered images were obtained with the Oxymap T1 retinal oximeter (Oxymap, Reykjavik, Iceland) for all patients. Mean retinal oxygen saturation was calculated for each eye globally and by quadrant (inferonasal, IN; superonasal, SN; inferotemporal, IT; superotemporal, ST) using a modified ring algorithm developed at our institution. Glaucoma patients also underwent Humphrey visual field, 24-2 testing and peripapillary retinal nerve fiber layer (RNFL) measurement using spectral domain optical coherence tomography. Retinal oxygen saturation levels were compared between groups using general linear model analysis after adjusting for age. The correlation between retinal oxygen saturation, RNFL and visual field mean deviation was assessed with Pearson correlation.

Results: Oxygen saturation in venules (SvO₂) was higher in eyes diagnosed with early POAG compared to normal eyes (mean, $61.94 \pm 2\%$ vs $51.39 \pm 2\%$, $p = 0.002$). SvO₂ was also elevated in each quadrant in the early POAG group (IN, $p < 0.001$; SN, $p = 0.03$; IT, $p = 0.005$; ST, $p = 0.03$). The mean arteriovenous difference was lower in early POAG eyes ($28.9 \pm 2\%$ vs $37.84 \pm 2\%$, $p = 0.001$) and in all quadrants. There was no difference in mean ($p = 0.39$) or quadrant (all $p > 0.05$) arteriolar oxygen saturation between groups, and there was no correlation between mean retinal oxygen saturation and mean RNFL thickness ($r = 0.06$) or visual field mean deviation ($r = 0.08$).

Conclusions: Patients with early POAG have significantly elevated SvO₂ and decreased arteriovenous difference in retinal oxygen saturation compared with normal eyes. These preliminary findings suggest decreased retinal oxygen utilization and metabolism in eyes with mild glaucomatous changes.

Commercial Relationships: Scott D. Lawrence, None; Pooja D. Jani, None; Kyle Billow, None; Jean-Claude Mwanza, None; Iryna A. Falkenstein, None

Support: Unrestricted grant from Research to Prevent Blindness

Program Number: 4465 **Poster Board Number:** D0205

Presentation Time: 8:30 AM - 10:15 AM

Optic nerve head basal blood flow increases early and then progressively decreases in non-human primate experimental glaucoma

Grant Cull, Chelsea Piper, Claude F. Burgoyne, Lin Wang. Devers Eye Institute, Legacy Research Institute, Portland, OR.

Purpose: To study the effect of chronic elevated IOP on optic nerve head (ONH) basal blood flow (bBF) in Non-human Primate (NHP) experimental glaucoma (EG) at progressive stages of retinal nerve fiber layer thickness (RNFLT) loss.

Methods: In six adult NHPs, two needles were inserted into the anterior chamber of each eye: one connected to a saline reservoir to

set the IOP at 10 mmHg; the other recording the actual IOP. Three or more baseline (BL) ONH bBF measurements (excluding large vessels), in units of mean blur rate (MBR) and RNFLT were measured by Laser Speckle Flowgraphy and Spectral Domain Optical Coherence Tomography, respectively. Chronic IOP elevation in the EG eye was induced by laser treatment of the trabecular meshwork with the contralateral eye serving as control (CTL). Bi-weekly ONH bBF and RNFLT measurements were obtained throughout the follow-up period. NHPs were sacrificed when EG eye RNFLT was 40 - 62% thinner than BL. ONH bBF measurements for both eyes were split in 4 groups based on RNFLT loss in the treatment eye: 1) BL (before laser treatment), 2) RNFLT loss <10%, 3) RNFLT loss between 10% and 40%, and 4) RNFLT loss >40. A repeated measure ANOVA and post hoc LSD test assessed EG vs CTL eye ONH bBF change within and between groups.

Results: Mean (\pm SD) post-laser IOP was 13.5 ± 2.7 mmHg in the CTL eyes and 32 ± 3.8 mmHg in the EG eyes. During the early stage of EG (RNFLT loss <10%), ONH bBF was significantly increased compared with its BL value ($p=0.01$ *). As RNFLT decreased further (10-40%), bBF returned to being statistically insignificant from BL ($p=0.6$). Significant ONH bBF reduction developed ($p<0.0001$ *) once the RNFLT loss was greater than 40%. There was no significant bBF change in the CTL eyes at any stage compared with BL (Fig.1). There was a significant interaction between stage of RNFLT and eyes ($p<0.0001$).

Conclusions: ONH bBF increases early and then progressively decreases in NHP EG. The early ONH bBF increase may be the result of autoregulation-induced vasodilation that is a response to the challenges of IOP elevation or may itself be evidence for autoregulation dysfunction. Later ONH bBF decreases is likely the result of reduced metabolic demand or autoregulatory capability.

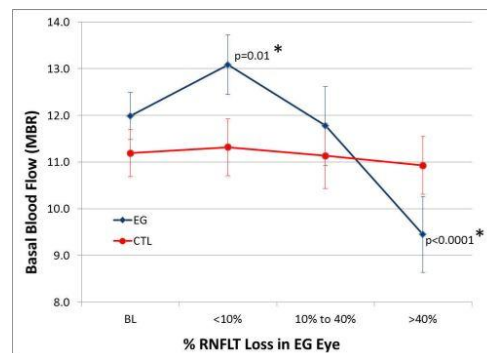


Figure 1 shows ONH bBF (MBR) for the EG and CTL eyes in the 6 NHP at progressive stages of RNFLT loss compared with BL.

Commercial Relationships: Grant Cull, None; Chelsea Piper, None; Claude F. Burgoyne, Heidelberg Engineering (F), Heidelberg Engineering (C); Lin Wang, None
Support: NIH Grant EY19939

Program Number: 4466 **Poster Board Number:** D0206

Presentation Time: 8:30 AM - 10:15 AM

Correlation between papillomacular bundle thickness (PMBT) and optic nerve blood flow in primary open-angle, including normal-pressure, glaucoma

Wataru Kobayashi¹, Kazuko Omodaka¹, Kyosuke Togashi², Morin Ryu¹, Tetsuya Yuasa², Toru Nakazawa¹. ¹Ophthalmology, Tohoku University, Sendai, Japan; ²Bio-Systems Engineering, Yamagata University, Yonezawa, Japan.

Purpose: To determine the relationship, in glaucoma patients, between PMBT and logMAR best corrected visual acuity (BCVA), as

well as the relationship between PMBT and optic nerve blood flow.

Methods: We studied 50 eyes of 27 patients with primary open-angle glaucoma, including normal-pressure glaucoma. We used two methods to measure PMBT, both using optical coherence tomography (3D-OCT2000, TOPCON, Japan). The first method used built-in program of 3D-OCT2000 to measure retinal nerve fiber layer thickness (RNFLT) and ganglion cell complex thickness (GCCT) in a square 10-degree area centered on the macula. The second method used a new program to measure a rectangular area (1.5mm wide and 9.0mm long) centered on the mid-point of the optic nerve disc and the macula, sub-divided into three parts along its length. In the middle part of this rectangular section, we measured RNFLT and GCCT with software for the automatic analysis of NFLT developed by Yamagata University. Additionally, we measured optic nerve blood flow with Laser Speckle Flowgraphy (LSFG-NAVI, Softcare, Japan). We divided the optic nerve into superior (S), temporal (T), inferior (I), and nasal (N) quadrants and measured MA (mean MBR in all areas), MT (mean MBR in the tissue area), and MV (mean MBR in the vessel area) in each quadrant. The Spearman coefficient of correlation was calculated to determine the relationship among RNFLT, GCCT, logMAR BCVA, and optic nerve blood flow.

Results: There was a significant correlation between RNFLT ($r=-0.48$) and GCCT ($r=-0.56$) in the central 10 degrees of the macula and logMAR BCVA. Similarly, there was a significant correlation between RNFLT ($r=-0.56$) and GCCT ($r=-0.50$) in the middle part of the new rectangular section we measured and logMAR BCVA. Moreover, there was a significant correlation between RNFLT ($r=0.39$) and GCCT ($r=0.39$) in the central 10 degrees of the macula and temporal MT. Similarly, there was a significant correlation between RNFLT ($r=0.37$) and GCCT ($r=0.52$) in the middle part of the rectangular section and temporal MT. The highest coefficient of correlation was between GCCT and temporal MT ($r=0.52$).

Conclusions: There is a significant correlation among RNFLT, GCCT, and logMAR BCVA, and also among RNFLT, GCCT, and temporal MT in glaucoma patients with low PMBT. Our findings may indicate that temporal MT relates closely to low PMBT.

Commercial Relationships: Wataru Kobayashi, None; Kazuko Omodaka, None; Kyosuke Togashi, None; Morin Ryu, None; Tetsuya Yuasa, None; Toru Nakazawa, Kowa Company Ltd. (F), Kowa Company Ltd. (C)

Program Number: 4467 **Poster Board Number:** D0207

Presentation Time: 8:30 AM - 10:15 AM

Optic Nerve Head Morphology and Retrobulbar Blood Flow; Differences between Glaucoma Patients with and without Diabetes

Joshua G. Paschall, Alon Harris, Brent A. Siesky, Leslie A. Tobe, Annahita Amireskandari, Nathaniel J. Kim, Chi-Wah R. Yung, Brian M. Marek, Darrell WuDunn, John Abrams. Ophthalmology, Indiana University School of Medicine, Indianapolis, IN.

Purpose: To evaluate retrobulbar blood flow in relation to optic nerve head (ONH) morphology over time in open-angle glaucoma (OAG) patients with and without diabetes.

Methods: 77 patients (17 diabetic, 60 non-diabetic) with OAG were assessed for ONH morphology utilizing Heidelberg retinal tomography and optical coherence tomography (cup/disc (C/D) ratio, cup shape, cup depth, disc area, rim area, rim width, rim volume, height variation contour). Retrobulbar blood flow was measured using Color Doppler imaging (CDI) in the ophthalmic artery (OA), central retinal artery (CRA) and nasal (NPCA) and temporal (TPCA) posterior ciliary arteries. Pearson correlations were calculated to evaluate the associations between measurements at baseline and between the changes in measurements between baseline and 3 years.

Results: Changes in OA peak systolic velocity (PSV), end-diastolic velocity (EDV), and resistive index (RI) in OAG patients with diabetes strongly correlated ($r=-0.95$ to 0.78) with changes in multiple ONH parameters, and were significantly different compared to OAG patients without diabetes ($p<0.0043$). Changes in CRA PSV and EDV were more strongly correlated in diabetics with ONH changes than non-diabetics ($r=-0.78$ to -0.56 ; $r=0.43$ to 0.31 ; $p<0.0023$). Changes in NPCA EDV were strongly and significantly correlated ($r=-0.87$ to -0.59 ; $p=0.02$ to 0.25) with ONH changes in diabetics and weakly correlated in non-diabetics ($r=0.34$ to 0.18) with significant differences between groups ($p<0.002$). NPCA RI changes strongly correlated with ONH changes in diabetics ($r=-0.91$ to -0.72), and weakly correlated in non-diabetics ($r=0.35$ to -0.14) with significant differences between groups ($p<0.001$).

Conclusions: In this cohort of OAG patients, changes in ONH morphology were strongly correlated to retrobulbar blood flow changes in diabetics. This data indicates that changes in ONH morphology may be more influenced by ocular blood flow in for OAG patients with diabetes.

Commercial Relationships: Joshua G. Paschall, None; Alon Harris, MSD (R), Alcon (R), Merck (C), Pharmalight (C), ONO (C), Sucampo (C), Adom (I); Brent A. Siesky, None; Leslie A. Tobe, None; Annahita Amireskandari, None; Nathaniel J. Kim, None; Chi-Wah R. Yung, None; Brian M. Marek, None; Darrell WuDunn, Merck (R), Alcon (R); John Abrams, ADOM (I) **Support:** American Diabetes Association grant 1-12-IN-20 and Pfizer Pharmaceuticals, Inc

Program Number: 4468 **Poster Board Number:** D0208

Presentation Time: 8:30 AM - 10:15 AM

Glaucoma Patients with Diabetes Have Increasing Vascular Resistance in the Ophthalmic and Central Retinal Arteries Compared to Glaucoma Patients without Diabetes

Nathaniel J. Kim, Alon Harris, Brent A. Siesky, Annahita Amireskandari, Joshua G. Paschall, Darrell WuDunn, Louis B. Cantor, Chi-Wah R. Yung, Leslie A. Tobe, John Abrams. Ophthalmology, Indiana University School of Medicine, Indianapolis, IN.

Purpose: To examine differences in ophthalmic artery (OA) and central retinal artery (CRA) blood flow velocities and vascular resistance between diabetic and non-diabetic patients with open angle glaucoma (OAG) after three years.

Methods: 82 patients (17 diabetic, 65 non-diabetic) with OAG were assessed at baseline and three years follow up for retrobulbar blood flow and vascular resistance (RI) using color Doppler imaging in the OA and CRA. Repeated measures analysis of covariance was used to compare the baseline and three year measurements. All measures had 95% confidence intervals with $p<0.05$ considered statistically significant.

Results: Diabetic OAG patients had significantly increased OA RI and CRA RI compared to non-diabetic OAG patients ($p<0.0126$ and $p<0.0063$ respectively). Diabetic patients had higher OA RI and CRA RI [mean (95% CI)] at three years [$x=0.808$ (0.833, 0.779); $x=0.731$ (0.757, 0.702)] than at baseline [$x=0.744$ (0.773, 0.712); $x=0.682$ (0.716, 0.645)]. The differences between three-year values from baseline for OA RI and CRA RI were statistically significant [$\Delta=0.084$, (0.135, 0.039), $p<0.0001$; $\Delta=0.057$ (0.104, 0.016), $p<0.0060$]. Non-diabetic patients had higher OA RI and lower CRA RI at three years [$x=0.774$ (0.790, 0.757); $x=0.710$ (0.725, 0.695)] than at baseline [$x=0.755$ (0.769, 0.741); $x=0.716$ (0.731, 0.700)]. The difference between three-year values from baseline for OA RI was statistically significant [$\Delta=0.021$, (0.041, 0.002), $p<0.0312$]. However, the difference between three-year values from baseline for

CRA RI was not statistically significant [$\Delta=-0.005$ (0.012, -0.022), $p<0.5327$]. Changes in OA and CRA peak systolic velocity and end diastolic velocity, from which RI was derived, after three years were not statistically significant ($p>0.05$).

Conclusions: Diabetic patients with OAG had significantly increased OA and CRA vascular resistance compared to non-diabetic OAG patients after three years. Diabetes is known to have systemic vascular manifestations, which may be reflected in their glaucoma pathophysiology. Our data suggests that diabetic patients with OAG may have more ocular vascular contributions to the glaucoma disease process compared to non-diabetic OAG patients.

Commercial Relationships: Nathaniel J. Kim, None; Alon Harris, MSD (R), Alcon (R), Merck (C), Pharmedlight (C), ONO (C), Sucampo (C), Adom (I); Brent A. Siesky, None; Annahita Amireskandari, None; Joshua G. Paschall, None; Darrell WuDunn, Merck (R), Alcon (R); Louis B. Cantor, Allergan, Inc (C), Allergan, Inc (R), Alcon, Inc (R), Merck, Inc (R), QLT, Inc (C), QLT, Inc. (I); Chi-Wah R. Yung, None; Leslie A. Tobe, None; John Abrams, ADOM (I)

Support: ADA: Grant 1-12-IN-20; Pfizer Pharmaceuticals Inc.

Program Number: 4469 **Poster Board Number:** D0209

Presentation Time: 8:30 AM - 10:15 AM

Changes in Retinal Blood Flow Correlate More Strongly with Changes in Optic Nerve Head Morphology in Glaucoma Patients with Diabetes Compared to Glaucoma Patients without Diabetes

Annahita Amireskandari, Alon Harris, Brent A. Siesky, Nathaniel J. Kim, Brian M. Marek, Joshua G. Paschall, Louis B. Cantor, Yara P. Catoira-Boyle, John Abrams, Leslie A. Tobe. Ophthalmology, Indiana Univ Sch of Medicine, Northville, MI.

Purpose: To evaluate the impact of retinal blood flow on optic nerve head morphology in open-angle glaucoma (OAG) patients with and without diabetes mellitus (DM).

Methods: 66 patients with OAG (14 with DM; 52 without DM) were assessed at baseline and 3 year follow up for retinal capillary blood flow using confocal scanning laser Doppler and ocular structure using Heidelberg retinal tomography and optical coherence tomography. Pearson correlations were calculated to evaluate the associations between measurements at baseline and between the changes in measurements between baseline and 3 years.

Results: Change from baseline to 3 years in the amount of zero blood flow in the superior retina significantly correlated with the change in maximum cup depth in patients with DM ($r=-0.91$, $p=0.0298$), but this change was not significant in those without DM ($p=0.8087$); and was significantly different between groups ($p<0.0000$). Change in inferior zero pixel blood flow was significantly correlated with the change in cup to disc (C/D) area ratio ($r=-0.92$, $p=0.0273$), and C/D vertical ratio ($r=0.9$, $p=0.0353$) in diabetic patients, but not in non-diabetics ($p>0.05$), with significant differences between groups ($p<0.0001$). Change in superior mean retinal flow was significantly correlated with change in cup area ($r=-0.30$, $p=0.0498$), cup volume ($r=-0.36$, $p=0.0178$) and rim volume ($r=0.35$, $p=0.0193$) in patients without DM, but not in diabetics ($p>0.05$), with a significant difference between the 2 groups ($p<0.0101$). The change in inferior mean flow significantly correlated with the change in cup area ($r=0.97$, $p=0.0029$), C/D area ratio ($r=0.96$, $p=0.0070$), linear C/D ratio ($r=0.93$, $p=0.0172$), rim area ($r=-0.97$, $p=0.0036$) and rim volume ($r=-0.95$, $p=0.0084$) in diabetics, but not in non-diabetics ($p>0.05$); with a significant difference between groups ($p\leq 0.0001$).

Conclusions: In this cohort of patients with OAG, changes in retinal capillary blood flow correlated more strongly with changes in optic nerve head morphology in patients with DM than in those without DM. This data suggests that changes in retinal blood flow may play a

larger role in optic nerve head morphology in OAG patients with DM.

Commercial Relationships: Annahita Amireskandari, None; Alon Harris, MSD (R), Alcon (R), Merck (C), Pharmedlight (C), ONO (C), Sucampo (C), Adom (I); Brent A. Siesky, None; Nathaniel J. Kim, None; Brian M. Marek, None; Joshua G. Paschall, None; Louis B. Cantor, Allergan, Inc (C), Allergan, Inc (R), Alcon, Inc (R), Merck, Inc (R), QLT, Inc (C), QLT, Inc. (I); Yara P. Catoira-Boyle, None; John Abrams, ADOM (I); Leslie A. Tobe, None

Support: American Diabetes Association Grant: 1-12-IN-20 and a grant from Pfizer Pharmaceuticals, Inc.

Program Number: 4470 **Poster Board Number:** D0210

Presentation Time: 8:30 AM - 10:15 AM

Systemic Blood Pressure and Ocular Perfusion Pressure affect Retrobulbar Blood Flow Differently in Glaucoma Patients of European and African Descent

Ariel Tyring, Alon Harris, Brent A. Siesky, Lyne Racette, Yara P. Catoira-Boyle, Annahita Amireskandari, Nathaniel J. Kim, Joshua G. Paschall, Brian M. Marek, Leslie A. Tobe. Ophthalmology, Indiana University School of Medicine, Indianapolis, IN.

Purpose: To examine differences in the relationship between systemic blood pressure (BP) and ocular perfusion pressure (OPP) with localized ocular blood flow in the central retinal artery (CRA) and ophthalmic artery (OA) in glaucoma patients of European descent (ED) and African descent (AD).

Methods: 75 patients with open-angle glaucoma (OAG) (19 of AD, 56 of ED) were assessed at baseline and after three years follow up. Blood flow velocities and vascular resistance were assessed using color Doppler imaging (CDI). Systolic (SBP) and diastolic (DBP) blood pressure were measured using automated ambulatory measurements, intraocular pressure (IOP) was measured using Goldmann tonometry, and OPP was calculated using the following equation: $OPP=2/3[\text{mean arterial pressure (MAP)}]-IOP$. Systolic (SPP), diastolic (DPP) and mean (MPP) perfusion pressures were also calculated as SBP-IOP, DBP-IOP and mean arterial pressure-IOP respectively. Pearson correlations were calculated to evaluate the associations between measurements at baseline and between the changes in measurements between baseline and 3 years with p values <0.05 considered statistically significant.

Results: Changes in SBP, MAP, SPP were more strongly correlated to CRA peak systolic blood flow velocity (PSV) and end diastolic velocity (EDV) in OAG patients of AD versus ED [$r=-0.38$ to -0.47 (AD); $r=0.23$ to 0.17 (ED)] with statistically significant differences between groups in every parameter ($P=0.0110$ to 0.0330). In patients of ED, changes in OA EDV positively correlated with changes in SBP ($r=0.45$, $p=0.0013$), MAP ($r=0.43$, $p=0.0025$), SPP ($r=0.41$, $p=0.0040$), OPP ($r=0.31$, $p=0.0365$), and MPP ($r=0.35$, $p=0.0147$) over three years. These same relationships were negative and not statistically significant for patients of AD ($p>0.05$). The differences between the groups were statistically significant for each correlation ($p<0.0413$; $p<0.0368$; $p<0.0356$; $p<0.0490$; $p<0.0416$, respectively).

Conclusions: In OAG patients of AD, CRA blood flow was more strongly correlated to blood pressure and perfusion pressure than in OAG patients of ED. OA changes were more strongly correlated to ED than AD OAG patients. This indicates that retinal blood flow may not be sufficiently autoregulated during changing blood and perfusion pressure in OAG patients of AD.

Commercial Relationships: Ariel Tyring, None; Alon Harris, MSD (R), Alcon (R), Merck (C), Pharmedlight (C), ONO (C), Sucampo (C), Adom (I); Brent A. Siesky, None; Lyne Racette, None; Yara P. Catoira-Boyle, None; Annahita Amireskandari,

None; **Nathaniel J. Kim**, None; **Joshua G. Paschall**, None; **Brian M. Marek**, None; **Leslie A. Tobe**, None
Support: NIH: 1R21EY022101-01A1 and Pfizer Pharmaceuticals

Program Number: 4471 **Poster Board Number:** D0211

Presentation Time: 8:30 AM - 10:15 AM

Retinal Oximetry in Primary Open-Angle Glaucoma: Differences in Patients of African and European Descent

Brent A. Siesky, Alon Harris, Lyne Racette, Louis B. Cantor, Leslie A. Tobe, Yara P. Catoira-Boyle, Chi-Wah R. Yung, Darrell WuDunn, James M. Beach. Ophthalmology, Indiana Univ Sch of Medicine, Zionville, IN.

Purpose: To determine whether retinal blood vessel oxygen saturation is different in patients with open-angle glaucoma (OAG) of African (AD) and European (ED) descent.

Methods: During a single study visit, retinal oxygen saturation in eight AD (Age 65.9±8.2, 6 female, 2 male) and 13 ED (Age 72.5±8.2; 4 male, 9 female) patients with OAG was measured in retinal blood vessels with a spectrophotometric retinal oximeter in darkness. Oxygen tension (PO₂) was calculated from oxygen saturation values. Intraocular pressure (IOP), ocular perfusion pressure (OPP), calculated as 2/3 mean arterial pressure-IOP, and 24-2 sita standard visual fields were analyzed. Statistical analysis was performed using two-tailed student's t-test of unequal variance, with p<0.05 considered statistically significant.

Results: Mean oxygen saturation in retinal arteries was 89.9% ±8.9% in OAG patients of AD and 94.7% ±7.9% in OAG patients of ED (p=0.25). Mean oxygen saturation in venules was 65.5% ±10.7% in persons of AD compared to 58.3% ± 20.5% in ED (p=0.33). The mean arteriovenous difference in oxygen saturation was significantly lower in persons of AD (24.4% ± 9.3%) than in those of ED (36.4% ± 14.1%); (p=0.03). No significant differences were found in IOP (AD: 15.5 ±2.7; ED: 14.3 ±4.3); (p=0.47) or visual field mean deviation (AD: -7.55 ±7.9; ED: -4.67 ±7.53); (p=0.43) or pattern standard deviation (AD: 6.48 ±4.66; ED: 4.63 ±3.66); (p=0.39). Additionally, OPP was not significantly different between groups (AD: 45.75 ±5.82; ED: 51.04 ±6.36); (p=0.08).

Conclusions: OAG patients of AD present with significantly decreased arteriovenous difference in retinal oxygen saturation compared to OAG patients of ED. These differences were observed despite similar IOP, visual field defects and OPP. These data suggest that retinal oxygen metabolism is affected differently in OAG patients of AD compared to ED and may possibly be related to impaired vascular autoregulation and blood flow.

Commercial Relationships: **Brent A. Siesky**, None; **Alon Harris**, MSD (R), Alcon (R), Merck (C), Pharmalight (C), ONO (C), Sucampo (C), Adom (I); **Lyne Racette**, None; **Louis B. Cantor**, Allergan, Inc (C), Allergan, Inc (R), Alcon, Inc (R), Merck, Inc (R), QLT, Inc (C), QLT, Inc. (I); **Leslie A. Tobe**, None; **Yara P. Catoira-Boyle**, None; **Chi-Wah R. Yung**, None; **Darrell WuDunn**, Merck (R), Alcon (R); **James M. Beach**, Oximap (I)

Support: NIH: 1R21EY022101-01A1 and Pfizer pharmaceuticals

Program Number: 4472 **Poster Board Number:** D0212

Presentation Time: 8:30 AM - 10:15 AM

Systemic Blood Pressure and Ocular Perfusion Pressure Affects Blood Flow to the Optic Nerve Head in Glaucoma Patients with Diabetes

Andrew H. Huck¹, Alon Harris¹, Brent A. Siesky¹, Leslie A. Tobe¹, Nathaniel J. Kim¹, Annahita Amireskandari¹, Brian M. Marek¹, Ingrida Januleviciene², Barbara M. Wirostko³, George J. Eckert⁴.

¹Ophthalmology, Indiana University School of Medicine, Indianapolis, IN; ²Ophthalmology, Lithuanian University of Health

Sciences, Kaunas, Lithuania; ³Ophthalmology, University of Utah, Park City, UT; ⁴Division of Biostatistics, Indiana University School of Medicine, Indianapolis, IN.

Purpose: To examine the relationship between systemic blood pressure (BP) and ocular perfusion pressures (OPP) with blood flow in the temporal (TPCA) and nasal (NPCA) short posterior ciliary arteries in open-angle glaucoma (OAG) patients with and without diabetes mellitus (DM).

Methods: 75 patients with OAG (17 with DM; 58 without DM) were assessed at baseline and three year follow-up for BP, OPP and blood flow velocities and vascular resistance in the TPCA and NPCA using color Doppler imaging (CDI). Systolic (SBP) and diastolic (DBP) blood pressure (ambulatory) were measured and OPP was calculated as: $OPP = \frac{2}{3}[DBP + \frac{1}{3}(SBP - DBP)] - \text{intraocular pressure (IOP)}$. Systolic (SPP), diastolic (DPP) and mean (MPP) perfusion pressures were also calculated as SBP-IOP, DBP-IOP and mean arterial pressure (MAP)-IOP, respectively. Pearson correlations were calculated to evaluate the associations between measurements at baseline and between the changes in measurements between baseline and three years.

Results: In OAG patients with DM, changes in SBP, MAP, SPP, OPP and MPP strongly correlated to changes in TPCA end diastolic velocity (EDV) [$r = 0.88$ to 0.80 (DM); $r = 0.07$ to -0.03 (non-DM)] and resistive index (RI) [$r = 0.76$ to 0.53 (DM); $r = -0.14$ to -0.19 (non-DM)] compared to non-DM OAG patients with statistically significant differences between groups [$p < 0.0006$; $p < 0.0148$]. In OAG patients with DM, changes in DBP, DPP, OPP and MPP were also strongly correlated to changes in TPCA peak systolic velocity (PSV) [$r = 0.77$ to 0.74 (DM); $r = 0.13$ to 0.02 (non-DM); between groups ($p < 0.0042$)].

In OAG patients with DM, changes in SBP, DBP, MAP, SPP, DPP, OPP and MPP strongly correlated to changes in NPCA EDV [$r = 0.82$ to 0.35 (DM); $r = -0.07$ to -0.37 (non-DM); between groups ($p < 0.0351$)]. Changes in SBP, MAP, SPP, and MPP were also correlated to changes in NPCA PSV [$r = 0.70$ to 0.48 (DM); $r = 0.00$ to -0.11 (non-DM); between groups ($p < 0.0445$)].

Conclusions: In OAG patients with diabetes, changes in short posterior ciliary artery blood flow were strongly correlated to changes in BP and OPP. These correlations were weak for OAG patients without diabetes and the differences between groups were statistically significant. This data suggests that OAG patients with diabetes may have impaired vascular autoregulation during fluctuations in systemic BP and OPP.

Commercial Relationships: **Andrew H. Huck**, None; **Alon Harris**, MSD (R), Alcon (R), Merck (C), Pharmalight (C), ONO (C), Sucampo (C), Adom (I); **Brent A. Siesky**, None; **Leslie A. Tobe**, None; **Nathaniel J. Kim**, None; **Annahita Amireskandari**, None; **Brian M. Marek**, None; **Ingrida Januleviciene**, Pharmalight (F), Santen (C), Alcon (C), MSD (C); **Barbara M. Wirostko**, Jade Therapeutics (P), Jade Therapeutics (I), Jade Therapeutics (E), Altheos Inc. (C), Merck (C), SKS Ocular (C), USTAR (F); **George J. Eckert**, None

Support: ADA: Grant 1-12-IN-20 and Pfizer Pharmaceuticals

Program Number: 4473 **Poster Board Number:** D0213

Presentation Time: 8:30 AM - 10:15 AM

Effects of Rho Kinase Inhibitor on mRNAs Associated with Glaucoma Progression in Human Trabecular Meshwork Cells Following Oxidative Stress

Hideki Mochizuki, Junko Hirata, Yoshiaki Kiuchi. Ophthalmology and Visual Science, Hiroshima University, Hiroshima, Japan.

Purpose: Oxidative stress occurs in glaucoma and is known to increase two pro-inflammatory cytokines, IL-6 and IL-8, in human

trabecular meshwork (HTM) cells after an oxidative challenge. IL-6 and IL-8 have been linked to the process of cellular senescence. Chronic exposure to these cytokines, which occurs in glaucoma, may damage HTM cells. Rho kinase (ROCK) inhibitor is in a novel class of intraocular pressure reducing drugs. The purpose of this study was to determine if ROCK inhibitor influences IL-6 and IL-8 mRNA expression in HTM cells.

Methods: Primary HTM cell cultures were obtained from three donor corneas (n=3). Cells were used prior to the 7th passage. Cells were serum starved for 24 hours and treated with 300 μM hydrogen peroxide (H₂O₂) for 3 hours in the presence of 25 μM Y-27632. These cells were compared with cells without Y-27632. Selected mRNAs (IL-6, IL-8, and myocilin) from the cells were analyzed using relative quantitative PCR.

Results: H₂O₂ increased IL-6 mRNA expression 1.76-3.31-fold. Y-27632 suppressed this increase by 0.83-1.28-fold. IL-8 mRNA was increased 5.96-11.58-fold with H₂O₂ treatment, and this increase was reduced to 2.43-6.13-fold with Y-27632. The effect of Y-27632 on myocilin mRNA was not consistent and depended on the individuality of donors.

Conclusions: Y-27632 reduced IL-6 and IL-8 mRNA expression following oxidative stress in HTM cells. These results suggest that ROCK inhibitor may protect HTM cells from the cellular senescence process due to pro-inflammatory cytokines associated with glaucoma. ROCK inhibitor may provide an additional benefit other than intraocular pressure reduction in glaucoma patients.

Commercial Relationships: Hideki Mochizuki, None; Junko Hirata, None; Yoshiaki Kiuchi, None

Program Number: 4474 **Poster Board Number:** D0214

Presentation Time: 8:30 AM - 10:15 AM

Burden of care associated with Childhood Glaucoma: 4 year study

Jacey Hanna, Lekha Ravindraraj, Robert D. Fechtner, Albert S. Khouri. Ophthalmology, The Institute of Ophthalmology and Visual Science, New Jersey Medical School, Newark, NJ.

Purpose: To evaluate the burden of care associated with managing childhood glaucoma upon diagnosis and during first 4 years of care.

Methods: Records of children with primary congenital glaucoma (PCG) or secondary glaucomas (secondary to systemic conditions such as neurofibromatosis, Sturge-Weber, other; ocular conditions such as uveitis or post childhood cataract) who presented over a 15 year period to the New Jersey Medical School were reviewed. Data on interventions undergone in each eye at every year throughout the first four years of management after initial diagnosis was collected. This included (1) total number of exams under anesthesia (EUA) (2) glaucoma procedures (P), including other procedures undergone secondary to the patient's glaucoma such as cataract extractions, pars plana vitrectomies, or penetrating keratoplasties and (3) all office and emergency department visits (V) related to the patient's glaucoma.

Results: A total of 60 patients (101 eyes) diagnosed with and managed for childhood glaucoma were included. Of those, a total of 23 patients were identified that included data up to four years after initial diagnosis. These consisted of 10 patients with PCG (a total of 19 eyes), and 13 patients with secondary glaucoma (a total of 20 eyes). The mean age at presentation was 41.1 months (ranging from birth to 216 months) and 35.1 months (ranging from birth to 240 months) in the PCG and secondary glaucoma groups respectively. Combined, the mean number of total interventions (EUAs, V, and P) per patient (39 eyes of 23 patients) at each of the four years since diagnosis was 8.9, 5.7, 4.6, and 4.8. The mean number of interventions per patient in each of the two groups each year is included in Table 1.

©2013, Copyright by the Association for Research in Vision and Ophthalmology, Inc., all rights reserved. Go to iovs.org to access the version of record. For permission to reproduce any abstract, contact the ARVO Office at arvo@arvo.org.

Conclusions: Childhood glaucomas pose significant burden of care on families and care givers at diagnosis and during the first 4 years of treatment. This burden was highest the first year after diagnosis, but persisted during the 4 years included in this study.

	Mean Number of Interventions per Patient				
	YEAR 1	YEAR 2	YEAR 3	YEAR 4	TOTAL
PRIMARY GLAUCOMA (N=10)					
EUA	3.9	2.1	2	1.2	9.2
V	2.1	0.3	1	0.8	4.2
P	3.4	3.1	2.5	4	13
TOTAL	9.4	5.5	5.5	6	26.4
SECONDARY GLAUCOMA (N=13)					
EUA	2.5	1.2	1.1	0.4	5.1
V	2.2	0.7	0.2	0.4	3.5
P	3.8	4	2.5	3.1	13.4
TOTAL	8.4	5.8	3.8	3.8	22.0

TABLE 1. Burden of care per patient for PCG and Secondary Glaucoma for 4 Years

Commercial Relationships: Jacey Hanna, None; Lekha Ravindraraj, None; Robert D. Fechtner, None; Albert S. Khouri, None

Support: Research to Prevent Blindness, NY, NY

Program Number: 4475 **Poster Board Number:** D0215

Presentation Time: 8:30 AM - 10:15 AM

Evaluation of surface free energy of Aurolab Aqueous Drainage Implant (AADI) and its influence on cell adhesion property, in comparison with Baerveldt Implant

Chidambaranathan Gowri Priya¹, Karuppasamy Sivakumar², Manju Pillai³, Subbiah Ramaswami Krishnadas⁴, Ravilla D. Sriram⁵, Veerappan Muthukkaruppan⁶. ¹Department of Immunology and Stem Cell Biology, Aravind Medical Research Foundation, Dr. G. Venkataswamy Eye Research Institute, Madurai, India; ²Polymer Division, Aurolab, Madurai, India; ³Glaucoma Clinic, Aravind Eye Hospital and Postgraduate Institute of Ophthalmology, Madurai, India; ⁴Glaucoma Clinic, Aravind Eye Hospital and Postgraduate Institute of Ophthalmology, Madurai, India; ⁵Aurolab, Madurai, India; ⁶Department of Immunology and Stem Cell Biology, Aravind Medical Research Foundation, Dr. G. Venkataswamy Eye Research Institute, Madurai, India.

Purpose: Aurolab Aqueous Drainage Implant (AADI), is a relatively cost-effective non-valved glaucoma drainage device indicated in refractory glaucoma management in the developing world. This study was carried out to both evaluate the surface free energy of AADI and its influence on the adhesion of human Tenon fibroblast, and to compare it with Baerveldt implants.

Methods: The surface free energy of AADI and Baerveldt implants were measured using a contact angle meter with five different standards - water, formamide, diiodomethane, ethylene glycol and 1-bromonaphthalene. The human Tenon fibroblast cultures were established using the Tenon's capsule obtained during routine cataract surgery from three donors, who had given prior written consent. The implants were attached to the culture dishes using single component silicone and tested for toxicity. After growing the fibroblasts in these dishes for 72 hours and staining with cell tracker green, their adhesion onto the implants was quantified in fluorescent microscope.

Results: The surface free energy of AADI (15.8mJ/m²) was identified to be higher than Baerveldt (13.2 mJ/m²). Adhesion of Tenon fibroblasts corresponded well to the surface free energy and was more profound on AADI while it was less on Baerveldt implants.

Conclusions: The above results indicate that due to higher surface

ARVO 2013 Annual Meeting Abstracts by Scientific Section/Group – Glaucoma

energy and cell adhesion property, AADI might attract more fibroblasts and fibrous encapsulation compared to Baerveldt, which warrants further investigation on the clinical outcome.

Table of contact angle values and related parameters for AADI and Baerveldt Implant

Contact Angle*					
Implant	Water	Formamide	Diiodomethane	Ethylene glycol	1-Bromonaphthalene
AADI	106.9±7.6	103±2.4	76.9±15.1	96.5±4.2	69.7±3.8
Baerveldt	112.7±2.4	103.8±1.0	85.8±3.7	99.6±1.6	75.5±5.2
Work of Adhesion					
AADI	49.1	53.2	56.6	46.1	52.5
Baerveldt	43.5	48.2	51.8	41.7	47.9
Interfacial Free energy					
AADI	39.5	20.7	10	17.6	6.8
Baerveldt	42.5	23.1	12.2	19.4	8.8

*A minimum of five contact angle readings were measured using each standard and the other parameters were derived from average of the contact angle values.

Commercial Relationships: Chidambaranathan Gowri Priya, None; Karuppasamy Sivakumar, Aurolab (E); Manju Pillai, None; Subbiah Ramaswami Krishnadas, None; Ravilla D. Sriram, Aurolab (E); Veerappan Muthukkaruppan, None
Support: AMRF-Aurolab Research Grant (2012-2013)

Program Number: 4476 **Poster Board Number:** D0216

Presentation Time: 8:30 AM - 10:15 AM

Targeting specific TGF- β signaling pathways to prevent bleb fibrosis after glaucoma drainage device surgery

Christian K. Vorwerk¹, Vladislavs Sokalskis², Alexander Zabelyshenskiy², Hagen Thieme¹, Lars Choritz^{1,2}. ¹Dept of Ophthalmology, Otto von Guericke University, Magdeburg, Germany; ²Dept of Ophthalmology, University Medical Center, Mainz, Germany.

Purpose: Bleb fibrosis is one of the major reasons for failed filtering surgery in glaucoma patients. Antifibrotic substances like Mitomycin C and 5-fluorouracil are successfully used to prevent bleb failure, however because of their modes of action they can have potentially vision-threatening side effects. The aim of this study was to investigate in vitro the potential of two drugs targeting specific signaling pathways downstream of the TGF- β receptor to prevent Tenon fibroblast proliferation, migration and myofibroblast transdifferentiation.

Methods: Primary cultures of human Tenon's Fibroblasts (HTF), stimulated with TGF- β 2 (1ng/ml), were treated with different concentrations of either Imatinib, Rapamycin or vehicle (control). Proliferation was determined indirectly via repeated measurement of cell viability using resazurin dye. Migration was measured with a scratch wound healing assay, whereas myofibroblast transdifferentiation was assessed by alpha-smooth muscle expression (α SMA) using qPCR.

Results: Both Imatinib and Rapamycin significantly inhibited TGF- β -induced HTF proliferation. While Rapamycin showed a dose dependent effect at a concentration as low as 10-11 mol/l ($p < 0.05$); (maximal effect at 10-8 mol/l ($p < 0.001$), $IC_{50} = 3.8 \times 10^{-11}$ mol/l) and no toxicity up to 10-6 mol/l, Imatinib was only effective at 10-8 mol/l and caused a loss of cells above 10-6 mol/l. Migration was not affected by Rapamycin, while Imatinib dose dependently inhibited HTF migration above 10-7 mol/l. Neither drug inhibited α SMA in TGF- β -stimulated HTF.

Conclusions: Imatinib and Rapamycin both inhibit TGF- β -induced HTF proliferation, but have differential effects on HTF Migration while leaving myofibroblast transdifferentiation unaffected. Both drugs may have some benefit in prevention of bleb fibrosis after filtering surgery. More importantly, pharmacological targeting of specific pathways of TGF- β pleiotrophic effects in vivo may lead to a better understanding of the underlying pathomechanisms of bleb fibrosis after glaucoma drainage devices surgery.

©2013, Copyright by the Association for Research in Vision and Ophthalmology, Inc., all rights reserved. Go to iovs.org to access the version of record. For permission to reproduce any abstract, contact the ARVO Office at arvo@arvo.org.

Commercial Relationships: Christian K. Vorwerk, None; Vladislavs Sokalskis, None; Alexander Zabelyshenskiy, None; Hagen Thieme, None; Lars Choritz, None

Program Number: 4477 **Poster Board Number:** D0217

Presentation Time: 8:30 AM - 10:15 AM

Retrospective study of congenital glaucoma surgical treatment
 Hector Bello Lopez Portillo, Jesus Jimenez-Roman, Mauricio Turati-Acosta, Magdalena García-Huerta, Rafael Castañeda Diez, Felix Gil Carrasco, Cristina Isida Llerandi. Asociacion para Evitar la Ceguera en Mexico, Mexico, Mexico.

Purpose: To study efficacy of surgical treatment for congenital glaucoma and compare different surgical techniques

Methods: Review of patients records from 2000 to 2011 in Hospital "Dr. Luis Sánchez Bulnes" from Asociación para Evitar la Ceguera en México.

Results: 79 patients with congenital glaucoma between 2000 and 2011 were included; 80 % of cases less than a year old, sex distribution was 62% male and 38% female. 158 eyes where included in study, most utilized procedure was goniotomy en 126 cases, 35.71% where qualified as success, 60.31% failed an 3.96 there was no report. Ahmed valve implat was de second mos utilized procedurce in 64 of cases 51.56% success, 45.31% failed , finally trabeculotomy was made in 62 cases 45.16 success, 51.61% failed.

Conclusions: Most used surgical treatment was Goniotomy Best success rate was in Ahmed Valve Implant group

Commercial Relationships: Hector Bello Lopez Portillo, None; Jesus Jimenez-Roman, None; Mauricio Turati-Acosta, None; Magdalena García-Huerta, None; Rafael Castañeda Diez, None; Felix Gil Carrasco, None; Cristina Isida Llerandi, None

Program Number: 4478 **Poster Board Number:** D0218

Presentation Time: 8:30 AM - 10:15 AM

Intraocular Pressure Reduction of Modified 360-degree Suture Trabeculotomy in Intent-to-treat Eyes

Daisuke Shiba, Takeshi Ono, Naoki Ozeki, Kenya Yuki, Kazuo Tsubota. Ophthalmology, Keio University, Shinjuku-ku, Japan.

Purpose: To investigate intraocular pressure (IOP) lowering effect of modified 360-degree suture trabeculotomy (S-LOT).

Methods: All eyes for which we intended to operate S-LOT at Keio university hospital from February 2010 through January 2012 were included to the present retrospective study. Main outcome measures were rate of threading through 360-dgree of Schlemm canal, IOP, medications and complications. The ends of 5-0 nylon suture were rounded like a matchstick head by cautery. In cases unable to thread through 360-degree, we cut as much trabecular meshwork as possible by the same 5-0 nylon suture.

Results: Thirty six glaucomatous eyes of 33 patients were included to the study. All eyes were followed at least 6 months. Mean age was 59.4+/- 19.6, and 9 eyes were of female. 360-degree threading was possible in 26 eyes (72.2%). The mean IOP dropped from 33.2 +/- 9.0mmHg preoperatively to 16.5 +/- 5.9mmHg at one month ($p < 0.01$), 14.4+/- 4.2mmHg at 6 months ($p < 0.01$) and 13.3+/- 5.1mmHg at 12 months ($p < 0.01$). Medications were 3.9 +/- 1.3 preoperatively, 0.66 +/- 1.2 at one month, 0.45 +/- 0.9 at 6 months and 0.46 +/- 1.0 at 12 months. There was no severe complication.

Conclusions: Modified 360-degree suture trabeculotomy was safe and effective surgery.

Commercial Relationships: Daisuke Shiba, Konan Medical USA (F); Takeshi Ono, None; Naoki Ozeki, Konan Medical USA (F); Kenya Yuki, None; Kazuo Tsubota, AcuFocus, Inc (C), Allergan (F), Bausch Lomb Surgical (C), Functional visual acuity meter (P), JiNS (P), Kissei (F), Kowa (F), Santen, Inc. (F), Otsuka (F), Pfizer

(C), Thea (C), Echo Denki (P), Nidek (F), OphTECS (F), Wakasa Seikatsu (F), CEPT Company (P)

Program Number: 4479 **Poster Board Number:** D0219

Presentation Time: 8:30 AM - 10:15 AM

Evaluation of Dose Effect of ALK-5 Inhibitor and Controlled Delivery with Novel Pentablock Polymer in Glaucoma Filtration Surgery

Hiroshi Nakamura^{1,2}, *Jeffrey J. Dunmire*¹, *Vijaykumar Sutariya*^{2,3}, *Michael Hewit*², *Daniel Wehrung*², *Sulabh Patel*⁴, *Ashim K. Mitra*⁴.

¹Ophthalmology, Summa Health System, Akron, OH;

²Pharmaceutical sciences, Northeast Ohio Medical University, Rootstown, OH; ³Pharmaceutical sciences, University of South Florida, Tampa, FL; ⁴Pharmaceutical sciences, University of Missouri-Kansas City, Kansas City, MO.

Purpose: It was demonstrated that activin receptor-like kinase 5 (ALK-5) inhibitors are effective to improve filtering bleb survival after glaucoma filtration surgery (GFS) in the rabbit model. The purpose of this study is to evaluate the dose effect of the inhibitor, including drug concentration in blebs. In addition, a novel pentablock polymer was examined for controlled delivery of the inhibitor for GFS.

Methods: Tablets containing 2.5 (n=6), 5.0 (9), 10.0 (10) and 20.0 (6) mg of ALK-5 inhibitor were placed at the surgical site of GFS in the rabbit model. At post-surgical day 6, the filtering blebs were photographed and then collected. Reverse phase HPLC with UV detection was performed to measure the inhibitor concentration in the bleb. In order to investigate new controlled delivery of the inhibitor for GFS, thermoreversible gel consisting of a pentablock PEG-PCL-PLA-PCL-PEG polymer (25% w/v) containing the inhibitor at the concentration of 50 µg/µl was prepared. During rabbit GFS (n=3), 0.1 ml of the gel was injected into subconjunctival space at the surgical site after conjunctival sutures. Eyes were observed at least twice per week following surgery until the time of bleb failure. At the end of the observation period, the eyes were enucleated and fixed, and the blebs were histologically examined.

Results: The concentration of ALK-5 inhibitor in the filtering bleb at day 6 was varied, and no statistical difference was observed among four different amounts of the inhibitor. On the other hand, the size of filtering bleb at day 6 was significantly larger with increasing amount of the inhibitor (p<0.05). In GFS using the inhibitor with thermoreversible gel, filtering blebs survived until day 14, 23 and 25, which is improved bleb survival compared to our previous data from GFS with tablets (12-19 days) containing the same amount of inhibitor. In two of 3 rabbits, backward flow of the gel into the anterior chamber was observed just after subconjunctival injection. In two of 3 rabbits, aqueous humor leakage from filtering blebs was observed at the end of post-surgical observation. In hematoxylin-eosin staining, a thinner conjunctival epithelium was observed.

Conclusions: The inhibitor amount in tablets did not affect its concentration in blebs but did affect the bleb size. The pentablock polymer may provide a novel controlled drug delivery system in GFS.

Commercial Relationships: *Hiroshi Nakamura*, None; *Jeffrey J. Dunmire*, None; *Vijaykumar Sutariya*, None; *Michael Hewit*, None; *Daniel Wehrung*, None; *Sulabh Patel*, None; *Ashim K. Mitra*, None

Support: NIH R01EY020916

Program Number: 4480 **Poster Board Number:** D0220

Presentation Time: 8:30 AM - 10:15 AM

The effect of steroid and matrix metalloproteinase inhibitor on bleb survival in an experimental animal model

©2013, Copyright by the Association for Research in Vision and Ophthalmology, Inc., all rights reserved. Go to iovs.org to access the version of record. For permission to reproduce any abstract, contact the ARVO Office at arvo@arvo.org.

Alastair Lockwood^{1,2}, *Abeer Mohamed Ahmed*^{1,2}, *Ashkan Khalili*^{1,2}, *Sahar Awwad*^{1,2}, *Garima Sharma*^{1,2}, *Steve Brocchini*^{1,2}, *Peng T. Khaw*¹. ¹NIHR Moorfields Biomedical Research Centre, London, United Kingdom; ²UCL School of Pharmacy, University College London, London, United Kingdom.

Purpose: The perioperative application of a sustained release matrix metalloproteinase inhibitor (MMPi) is a potential non-toxic alternative to mitomycin C (MMC) for prolonging bleb survival in glaucoma surgery. Steroids are another class of anti-inflammatory that may enhance anti-scarring efficacy. We aimed to determine whether the combination of dexamethasone and ilomastat were able to prolong bleb survival in an experimental animal model.

Methods: A randomised, prospective, masked, single observer in vivo study over 30 days was conducted. Glaucoma filtration surgery was performed on 18 New Zealand White rabbits. The rabbits received perioperatively one of three potential subconjunctival treatments, randomised according to a Latin Square design: one dexamethasone implant 2 mm diameter (1 mg) and one ilomastat implant 2 mm (1 mg), MMC soaked sponges 0.2 mg/mL for 3 minutes (positive control) and sterile water group, water applied as per MMC (negative control). Success was determined according to a clinical observation of bleb survival.

Results: Four of the six rabbits treated with ilomastat / dexamethasone combination maintained the appearance of a bleb until day 30. Of those that did not, one developed an endophthalmitis in the first week post surgery and the other failed on day 27. The sterile water treated group failed at a median of 18 days (range 12 - 21). Of the MMC treated group one animal had a bleb that failed at day 27.

Conclusions: Dexamethasone / ilomastat implants do appear to prolong bleb survival in this animal model.

Commercial Relationships: *Alastair Lockwood*, None; *Abeer Mohamed Ahmed*, Steve Brocchini (WO09/063222) (P), Peng Khaw (WO09/063222) (P); *Ashkan Khalili*, University College London (P); *Sahar Awwad*, None; *Garima Sharma*, None; *Steve Brocchini*, None; *Peng T. Khaw*, University College Moorfields (P) **Support:** Medical Research Council G801650, Fight for Sight, Freemasons Grand Charity, NIHR Biomedical Research Centre for Ophthalmology, Helen Hamlyn Trust

Program Number: 4481 **Poster Board Number:** D0221

Presentation Time: 8:30 AM - 10:15 AM

Attenuation of Glaucoma Filtration Surgery-induced Scarring by an FDA-approved Histone Deacetylase Inhibitor, Suberoylanilide Hydroxamic Acid (SAHA)

Ajay Sharma, *Jacob W. Brubaker*, *Marcos Reyes*, *Jason T. Rodier*, *Ashish Tandon*, *Rajiv R. Mohan*. Mason Eye Institute, University of Missouri, Columbia, MO.

Purpose: Glaucoma filtration surgery (GFS) is frequently used to treat glaucoma. Postoperative scar due to excessive wound healing is a major complication resulting in the failure of treatment. We found SAHA highly potent to inhibit corneal scarring in vivo without toxicity. This study tested the hypothesis that topical SAHA application following GFS is effective and safe to treat postoperative GFS-induced scarring.

Methods: Twelve New Zealand White rabbits underwent GFS to create a conjunctival flap using a beaver blade and a sclerotomy was performed. Animals received single intraoperative application of sponge soaked SAHA or balanced saline solution (BSS). The intraocular pressure (IOP) was measured using applanation tonometer with the animals under topical anesthesia. Clinical examination was performed to evaluate the general appearance, bleb score (1-4) and any toxicity of the treated eyes. On postoperative day 14, rabbits

were sacrificed and the eyes were enucleated together with the conjunctiva to preserve the bleb and snap frozen in optimal cutting temperature (OCT) fluid. The tissues were sectioned and stained with hematoxylin and eosin (H&E), for α -smooth muscle actin (SMA), a myofibroblast marker and F actin, a marker for activated fibroblasts.

Results: Intraoperative topical SAHA treatment showed notably less fibrosis in ocular tissue compared to the untreated control (up to 60%). An increased mean bleb score and normal intraocular pressure were observed in rabbits that received SAHA treatment indicating successfully functioning filtering bleb. H&E histology data revealed an overall decrease in the area of fibrotic deposit. Detection of larger blebs with aqueous pores and less fibrosis at the scleral flap demonstrated SAHA's effective anti-fibrotic response.

Immunostaining detected a decrease in SMA+ and F-actin+ cells (quantification and statistical analyses are underway). There were no apparent clinical signs of toxicity in the eyes of SAHA treated rabbits.

Conclusions: The intraoperative topical SAHA application significantly decreases postoperative fibrosis and improves the outcome of GFS. Larger animal study is warranted.

Commercial Relationships: Ajay Sharma, None; Jacob W. Brubaker, None; Marcos Reyes, None; Jason T. Rodier, None; Ashish Tandon, None; Rajiv R. Mohan, None
Support: RO1EY17294 (RRM) BX00035701 (RRM)

Program Number: 4482 **Poster Board Number:** D0222

Presentation Time: 8:30 AM - 10:15 AM

Surgical Outcomes of Augmented MMC Trabeculectomy After Failed Seton Surgery

Jose A. Paczka^{1,3}, Luz A. Giorgi-Sandoval^{2,3}, Miriam A. Ramos-Hernandez¹, Jesus Jimenez-Roman^{2,3}, Arie Merikansky².

¹Oftalmologia, University of Guadalajara, Guadalajara, Mexico;

²Oftalmologia, Asistencia e Investigacion en Glaucoma, A.C.,

Guadalajara, Mexico; ³Glaucoma, Global Glaucoma Institute, Guadalajara, Mexico.

Purpose: To determine surgical rates in a consecutive series of cases of glaucoma treated with secondary trabeculectomy (supplemented with mitomycin C - MMC) in a setting of Ahmed glaucoma valve (AGV) failure.

Methods: In this retrospective non-comparative analysis, 24 consecutive cases affected by a mixture of glaucomas which failed after being surgically treated with AGV were assessed. In all cases, MMC (0.5 mg / 5 minutes of trans-operative subconjunctival exposure) supplemented the action of a "safe" trabeculectomy as a mean to control pressure. Using standard definition of surgical success / failure, Kaplan-Meier survival analysis was used to estimate surgical outcomes in cases which were followed up for at least 12 months.

Results: Medical chart information derived from twenty four eyes of 20 patients (13 females, 7 males; mean age: 57.6 \pm 11.3 years) was included in the analysis. All eyes had received an AGV as a primary procedure to treat different types of glaucoma. A diversity of reasons was evaluated by the treating surgeon to decide for a new glaucoma intervention. Cumulative causes of AGV failure included tube / plate exposure (n = 11), refractory hypertensive phase (n = 7), endothelium / lens tube contact (n = 4), miscellaneous (n = 8). Pre-trabeculectomy mean IOP was 16.8 \pm 6.9 mm Hg. Overall success rate with secondary trabeculectomy was 96% and 92%, at the 6-month and 12-month post-operative moments, respectively. Mean post-operative IOP was 11.4 \pm 2.4 mm Hg (P = 0.001) and 13.5 \pm 3.3 mm Hg (P = 0.001) after 6 and 12 months after trabeculectomy, respectively. Cumulative complication rate was 12%.

Conclusions: Our findings demonstrated that secondary

trabeculectomy supplemented with MMC is a very good surgical alternative to treat diverse types of AGV failure when this procedure was used as a primary operation.

Commercial Relationships: Jose A. Paczka, None; Luz A. Giorgi-Sandoval, None; Miriam A. Ramos-Hernandez, None; Jesus Jimenez-Roman, None; Arie Merikansky, None

Program Number: 4483 **Poster Board Number:** D0223

Presentation Time: 8:30 AM - 10:15 AM

Influence of endothelin-1 in aqueous humor on IOP and filtration surgery outcome

Lars Choritz^{1,2}, Benjamin Mahmoodi¹, Maren Machert¹, Norbert Pfeiffer¹, Hagen Thieme². ¹Ophthalmology, University Medical Center, Mainz, Germany; ²Ophthalmology, University Clinic, Otto von Guericke University, Magdeburg, Germany.

Purpose: In a previously published study, we found a significant correlation between endothelin-1 in the aqueous humor of glaucoma patients obtained during cataract surgery or trabeculectomy and immediately pre-operative intraocular pressure. The aim of this chart-review study was to assess, whether the previously recorded ET-1 concentrations had any influence on IOP development or surgical outcome during up to five years of follow-up.

Methods: Clinical records of the patients enrolled in the original study were reviewed, post surgical IOP development, number of 5-FU treatments, bleb revisions, further glaucoma surgeries, glaucoma medications and complications were compared between patients with high (above median) and low (below median) ET-1 concentrations in aqueous humor.

Results: Of the 56 glaucoma patients originally enrolled, 51 came into our clinic for further consultations. Median follow-up time was 24 months (range 1 to 59 months). There were no significant differences in IOP at any time point during follow-up. In the subpopulation of patients who had undergone trabeculectomy (n=36), both groups needed the same number of 5-FU injections (5.5 \pm 3.7 high vs. 5.1 \pm 3.1 low, p=0.74), needlings (0.2 \pm 0.7 vs. 0.2 \pm 0.7, p=0.82) and suture lyses (0.4 \pm 0.8 vs. 0.3 \pm 0.7, p=0.65) during the post-operative phase. Complication rates and number of revision procedures were equally low in both groups, although all 4 recorded bleb revisions were necessary in the high ET-1 group. At the end of follow-up, the number of glaucoma medications was not significantly different (0.3 \pm 0.8 vs. 0.2 \pm 0.5, p=0.88).

Conclusions: ET-1 concentrations in aqueous humor do not appear to have any influence on long term outcome or IOP development after filtration surgery. While several animal models as well as our previous clinical study suggest a role for ET-1 in IOP control by inducing contraction of trabecular meshwork (TM), this influence on IOP development is likely reduced once the TM has been shunted. Its predictive value for long term outcome of filtering surgery therefore is limited.

Commercial Relationships: Lars Choritz, None; Benjamin Mahmoodi, None; Maren Machert, None; Norbert Pfeiffer, Sensimed AG (F), Sensimed AG (R), MSD (F), MSD (R), Alcon (F), Allergan (F), Novartis (F), Novartis (R), Bayer (F), Heidelberg Engineering (F), Bausch&Lomb (F), Boehringer-Ingelheim (F), Carl Zeiss Meditec (F), Chibret (F), Nidek (F), Pfizer (F), Santen (F), Santen (R), Topcon (F), Ivantis Inc (F), Ivantis Inc (R); Hagen Thieme, None

Program Number: 4484 **Poster Board Number:** D0224

Presentation Time: 8:30 AM - 10:15 AM

A NEW TECHNIQUE FOR GLAUCOMA SURGERY: SCOROLLI TRABECULECTOMY

ARVO 2013 Annual Meeting Abstracts by Scientific Section/Group – Glaucoma

Lucia Scorolli¹, Enrico Meduri², Antonio De Leo⁵, Renato Pieralberto Meduri³, Edina Zere⁴, Pier Paolo Piccaluga³, Sergio Zaccaria Scalinci¹. ¹Ophthalmology, S Orsola Malpighi Hospital Bologna, Bologna, Italy; ²Medical School, University of Sophia, Sophia, Bulgaria; ³IE Business School, Madrid, Spain; ⁴Ophthalmology, University La Sapienza, Rome, Italy; ⁵Molecular Pathology, University of Bologna, Bologna, Italy.

Purpose: Prospective study to value the efficacy of Scorolli trabeculectomy, a new technique using only low cost material. It aims to reduce the complications of classic trabeculectomy in open angle glaucoma: hyphema, inflammation of the anterior chamber, excessive filtration leading to hypotonia, reduced or abolished anterior chamber, choroidal detachment and endophthalmitis. It is performed with an association of deep sclerectomy and light trabeculectomy with a new artificial maintenance of the spaces.

Methods: Patients resistant to therapy or other filtering surgeries in 110 pseudophakic eyes (A group) followed for 1,6 year (A group) and in 42 phakic eye (C group) followed for 1,6 year. The control group is 35 patients (group B) treated with deep sclerectomy adding T-flux valve or Aquaflow type plant collagen. All patients were obliged to maximal therapy and often resistant to other surgery. Authors have valued average age, preoperative and postoperative intraocular pressure for 1,6 year and so Humphrey computerized visual fields and preoperative and postoperative best corrected visual acuity.

Results: Complete success if intraocular pressure is ≤ 15 mm Hg without therapy, partial success if intraocular pressure is ≤ 18 mmHg with or without therapy, failure success if intraocular pressure is > 18 mm Hg, with or without therapy.

Group A and C have never had patients with intraocular pressure > 15 mm Hg without therapy.

Visual fields have had no significative differences between preoperative and postoperative, even though subjective improvements are declared. No significative differences between preoperative and postoperative Best Corrected Visual acuities.

Conclusions: Excellent technique, light difficulty in learning curve, strongly reduction of postoperative inflammation in anterior chamber, no a-ipotalamia, flat blab, no choroidal detachments, possible surgery in outpatients, strong maintenance of low intraocular pressure over time, very limited cost.

Commercial Relationships: Lucia Scorolli, None; Enrico Meduri, None; Antonio De Leo, None; Renato Pieralberto Meduri, None; Edina Zere, None; Pier Paolo Piccaluga, None; Sergio Zaccaria Scalinci, None

Program Number: 4485 **Poster Board Number:** D0225

Presentation Time: 8:30 AM - 10:15 AM

Functional and anatomic outcomes following endocyclophotocoagulation (ECP) surgery for neo-vascular glaucoma as compared to routine glaucoma care

Kyle V. Marra¹, Sushant Wagley², Ahmed F. Omar³, Jorge G. Arroyo¹. ¹Beth Israel Deaconess Medical Center, Boston, MA; ²College of Human Medicine - Michigan State University, East Lansing, MI; ³Joslin Diabetes Center, Boston, MA.

Purpose: To compare outcomes after treatment of neovascular glaucoma (NVG) with combination pars plana vitrectomy (PPV), endoscopic panretinal photocoagulation (PRP), and endocyclophotocoagulation (ECP) versus case-matched control patients with NVG who received routine glaucoma care.

Methods: In this retrospective, consecutive, age-matched study, all patients were seen at the Beth Israel Deaconess Medical Center with severe NVG. One group of patients were treated with PPV/PRP/ECP (ECP group, n=17) while another case-matched control group

received routine glaucoma care (control group, n=18). Outcome measures included visual acuity, intraocular pressure (IOP), post-operative regression of iris neovascularization, complication rates, and the number of required anti-glaucoma medications.

Results: Post-operative visual acuity deterioration by two or more lines was recorded in 11.1% of ECP cases and 11.8% of control cases. Mean IOP was significantly reduced (39.2 to 14.4 mmHg; $p=0.005$) within the ECP group while such significant reduction was not seen within the control group (30.8 to 22.7 mmHg; $p=0.126$). In case-matched between-group analysis, the IOP drop in the ECP group was also significant ($p=0.013$) when compared to the IOP drop in the control group. Disappearance of postoperative iris neovascularization was noted in the 80.0% of ECP cases versus 54.5% of control cases. The mean number of anti-glaucoma medications was also significantly reduced (3.1 to 0.9; $p=0.003$) within the ECP group, with no significant change within the matched cases of the control group (1.58 to 1.81; $p=0.952$). This change in number of glaucoma medications was significant ($p=0.010$) in between-group analysis of matched cases.

Conclusions: PPV followed by endoscopic PRP and ECP appeared to stabilize IOP more quickly and for a longer duration than other standard treatments for NVG. ECP also seemed to reduce the need for glaucoma medications better than other standard treatments for patients with NVG. These results suggest that more long-term investigation of ECP for NVG is warranted.

Commercial Relationships: Kyle V. Marra, None; Sushant Wagley, None; Ahmed F. Omar, None; Jorge G. Arroyo, None

Program Number: 4486 **Poster Board Number:** D0226

Presentation Time: 8:30 AM - 10:15 AM

Efficacy of Catheter Assisted 360° Trabeculectomy in Primary Congenital Glaucoma (PCG)

Erika Wandel¹, Dipali Dave¹, Monisha Mandalaywala Vora², Craig H. Marcus³, Robert F. Rothman³, Tamiesha Frempong¹, Daniel D. Hayes², Allison Angelilli², Janet B. Serle^{1,3}. ¹Ophthalmology, Mount Sinai Hospital, New York, NY; ²Ophthalmology, North Shore-Long Island Jewish Health System, Manhasset, NY; ³Glaucoma Consultants of Long Island, Bethpage, NY.

Purpose: To assess the efficacy of catheter assisted 360° trabeculectomy in PCG patients.

Methods: Retrospective review of all primary congenital glaucoma patients treated between June 2008 and November 2012 at 2 sites. Parameters analyzed included intraocular pressure, number of pre- and post-op glaucoma medications, cup-to-disc ratio. Failure was defined as the need for additional surgery. Paired t-test was performed to determine whether surgery was successful in reducing the intraocular pressure (IOP).

Results: 18 eyes from 11 patients were identified that underwent catheter assisted 360° trabeculectomy for PCG. At the time of surgery, patients were (mean \pm SD) 5.2 ± 2.6 months of age and post-operative follow up was 1.7 ± 1.7 years. Mean IOP was reduced ($p < 0.05$) by 15.2 ± 10.1 mmHg, and remained consistently reduced over the 1.7 ± 1.7 follow up years. 6 eyes showed a decrease in the cup to disc ratio. The number of glaucoma medications decreased from 1.2 ± 1.1 prior to surgery to 0.7 ± 0.9 medications after surgery. The reduction of glaucoma medications remained steady throughout follow up. No ocular or systemic complications were reported postoperatively. 22% (4/18) of the eyes required additional surgery. In these 4 patients glaucoma drainage devices were the subsequent procedure.

Conclusions: Catheter assisted 360° trabeculectomy effectively reduced intraocular pressure in 94% of eyes included in the study. Surgery was successful in 78% of the eyes, and was associated with a

reduction in topical glaucoma therapy in patients with congenital glaucoma over nearly a 2 year follow-up.

Commercial Relationships: Erika Wandel, None; Dipali Dave, None; Monisha Mandalaywala Vora, None; Craig H. Marcus, None; Robert F. Rothman, None; Tamiesha Frempong, None; Daniel D. Hayes, None; Allison Angelilli, None; Janet B. Serle, Acorn (F), Aerie (F), Forest Research Institute (C), Ono (C), Sucampo (C), Fovea (F)

Program Number: 4487 **Poster Board Number:** D0227

Presentation Time: 8:30 AM - 10:15 AM

Ahmed glaucoma valve FP7 and FP8 in pediatric glaucoma: A randomized clinical trial

Bruno L. Esporcatte, Camila F. Netto, Thais Tanno, Luiz Alberto S. Melo, Ivan M. Tavares, Christiane Rolim de Moura. Glaucoma, Federal University of São Paulo, São Paulo, Brazil.

Purpose: To compare the results of two models of Ahmed Glaucoma Valve (AGV) (New World Medical, Rancho Cucamonga, CA) implants (FP7 and FP8) in patients with pediatric glaucoma.

Methods: A prospective, randomized, clinical trial was carried out. Patients with primary or secondary pediatric glaucoma who previously underwent anti-glaucoma surgery were enrolled. The patients were randomly allocated to receive either FP7 or FP8 AGV model and were examined under general anesthesia just before and 6 months after glaucoma implant surgery.

Results: A total of 8 patients (8 eyes) received FP7 implants and 7 patients (7 eyes) received FP8 implants. The mean (standard deviation) age of the FP7 and FP8 groups was 4.9 (3.8) years and 4.7 (2.9) years, respectively. No statistically significance differences in intraocular pressure, axial length, corneal diameter and limbus-plate distance were found between groups at the 6-month postoperative visit ($p > 0.05$, Table).

Conclusions: There is no significant difference in the 6-month follow-up of anti-glaucoma surgery using FP7 and FP8 AGV model in pediatric glaucoma.

Table. Comparison of FP7 and FP8 Ahmed Glaucoma Valve models in pediatric glaucoma

Variable	Preoperative visit		6-month postoperative visit		P*
	Ahmed Glaucoma Valve Model		Ahmed Glaucoma Valve Model		
	FP7	FP8	FP7	FP8	
IOP, mmHg	Mean (SD) 25.4 (6.7)	Mean (SD) 28.6 (10.1)	Mean (SD) 19.3 (8.4)	Mean (SD) 15.8 (3.9)	0.45
Axial length, mm	25.3 (3.0)	28.0 (2.4)	25.2 (2.9)	29.7 (1.2)	0.25
Corneal diameter, mm	13.4 (2.2)	13.5 (1.0)	13.1 (1.0)	13.6 (1.0)	0.77
Plate-limbus distance, mm	9.9 (0.4)	9.9 (0.4)	9.3 (1.2)	8.7 (1.2)	0.35

* Analysis of Covariance (ANCOVA) adjusted for preoperative values

SD = standard deviation; IOP = intraocular pressure

Commercial Relationships: Bruno L. Esporcatte, None; Camila F. Netto, None; Thais Tanno, None; Luiz Alberto S. Melo, None; Ivan M. Tavares, None; Christiane Rolim de Moura, None
Support: Coordenação de Aperfeiçoamento de Pessoal de Nível Superior (CAPES)

Clinical Trial: nct01494974

Program Number: 4488 **Poster Board Number:** D0228

Presentation Time: 8:30 AM - 10:15 AM

A model to measure surgical outflow using a two-tubed experimental glaucoma drainage device

Craig Ross, Dan Nguyen, Surinder S. Pandav, Yu Qin Li, Jonathan G. Crowston, Michael A. Coote. Centre for Eye Research Australia, University of Melbourne, Royal Victorian Eye and Ear Hospital, East Melbourne, VIC, Australia.

Purpose: Engineering modelling suggests that the key determinant of success in glaucoma surgery is the hydraulic conductivity of the bleb or peri-implant capsule. However, previous experimental models of glaucoma surgery relied on indirect measures of surgical success such as bleb appearance or intraocular pressure in animals with

normal trabecular outflow. We wished to develop a method to directly measure fluid outflow into rabbit implant capsules after experimental glaucoma surgery. We present a refinement and extension of the model we reported recently in IOVS.

Methods: An experimental glaucoma drainage device (GDD) was developed with similar physical dimensions to the Paediatric Molteno implant, except with two tubes. Implants were fabricated using a 3D-printer and tubes attached with medical-grade silicone adhesive. Devices were implanted into the right eyes of 17 New Zealand White rabbits, with one tube inserted into the anterior chamber and the other occluded and left under the conjunctiva. After one (n=5) or four (n=5) weeks, the anterior chamber tube was tied off and the second tube cannulated and connected to a pressure transducer-controlled syringe pump. Outflow into capsules at 12mmHg was measured for 5 minutes. In another group (n=7), there was no connection to the anterior chamber and capsule outflow was measured four weeks after surgery without aqueous exposure.

Results: There was a significant decline in capsule outflow between one and four weeks after surgery, from 2.46 +/- 0.80 to 0.67 +/- 0.16 $\mu\text{L}/\text{min}$ at 12mmHg (mean + SD). However, four-week post-surgery capsules without aqueous drainage demonstrated greater outflow than capsules with fluid exposure, at 3.00 +/- 2.10 $\mu\text{L}/\text{min}$ at 12mmHg. One-way ANOVA: $p < 0.05$.

Conclusions: Two-tubed experimental GDDs allow for accurate and simplified recording of the outflow into capsules, the main determinant of success in glaucoma filtration surgery. The conductivity of implant capsules declines significantly by four weeks after surgery in the rabbit, however this does not occur in the absence of aqueous drainage. These results provide direct evidence that aqueous drainage itself is problematic to maintaining the function of glaucoma surgery in the rabbit. Additionally, the use of a 3D-printer allows for prototyping implants with differing physical characteristics, and by testing their efficacy one can adopt an informed design process.

Commercial Relationships: Craig Ross, None; Dan Nguyen, None; Surinder S. Pandav, None; Yu Qin Li, None; Jonathan G. Crowston, None; Michael A. Coote, None

Program Number: 4489 **Poster Board Number:** D0229

Presentation Time: 8:30 AM - 10:15 AM

Comparison of Early Post-Operative Challenges in P200 Ex-PRESS Shunts and Conventional Trabeculectomies

Maheen Haque, Bret A. Hughes, Justin Tannir, Rominder Momi, Chaesik Kim. Kresge Eye Institute/Wayne State University, Detroit, MI.

Purpose: To evaluate and compare post-operative outcomes for P200 Ex-PRESS shunts and conventional trabeculectomies in achieving intraocular pressure (IOP) control in patients with primary open angle glaucoma (POAG).

Methods: This is a retrospective chart review of 30 eyes of 24 patients with POAG who underwent P200 Ex-PRESS shunt placement or conventional trabeculectomy for IOP control by one surgeon (B. Hughes, Detroit, MI). Patients were evaluated prior to surgery and clinical diagnosis was recorded. Best corrected visual acuity (BCVA), IOP, and number of glaucoma medications were followed prior to and following surgery. Postoperative complications were followed for both groups. Patients excluded from analysis included those with a history of neovascular or uveitic glaucoma and those who underwent cataract extraction at or within 6 months of glaucoma surgery.

Results: There were 30 eyes of 24 patients with a mean age of 72 years in the P200 Ex-PRESS group and 64.7 years in the conventional trabeculectomy group. Average length of followup was

13.2 months in the P200 Ex-PRESS group and 25.9 months in the conventional trabeculectomy group ($p < 0.05$). A trend towards better recovery of visual acuity was seen in the P200 Ex-PRESS group but there was not a statistically significant difference in visual acuity between the two groups at any time during the post-operative period. The mean postoperative IOP was found to be lower at all time points for patients in both groups, but was found to be significantly lower in the P200 Ex-PRESS group at 6-9 months ($p < 0.05$). Patients in both groups used less glaucoma medications after surgery but this was not a statistically significant difference. While there were no statistically significant differences in the complications between the two groups, there was a higher incidence of early postoperative hypotony (46.7%, $p = .25$) and choroidal effusion (26.7%, $p = .11$) in the P200 Ex-PRESS group. More patients underwent surgical revision in the trabeculectomy group (26.7%, $p = .33$)

Conclusions: There is a significant decrease in postoperative IOP in both groups. However, there is a statistical trend for lower IOP in patients who undergo surgery with a P200 Ex-PRESS shunt. There is a higher incidence of early postoperative complications in the P200 Ex-PRESS shunt group but more patients require revisional surgery after a conventional trabeculectomy.

Commercial Relationships: Maheen Haque, None; Bret A. Hughes, None; Justin Tannir, None; Rominder Momi, None; Chaesik Kim, None

Program Number: 4490 **Poster Board Number:** D0230

Presentation Time: 8:30 AM - 10:15 AM

Comparison of surgical outcomes of Express Shunt and Ahmed Valve in Neovascular Glaucoma

Huseyin Kadikoy, Bret A. Hughes, Justin Tannir, Rominder Momi. Ophthalmology, Kresge Eye Institute, Royal Oak, MI.

Purpose: Neovascular glaucoma is potentially devastating form of secondary glaucoma, which have a guarded visual prognosis. In the advanced stages of neovascular glaucoma surgical management is often required to manage elevated intraocular pressure. The use of express shunt and glaucoma drainage implant are two procedures often considered in managing patients who are refractory to medical therapy. IOP outcomes, decrease in need for glaucoma drops and surgical complications for with either procedure were explored.

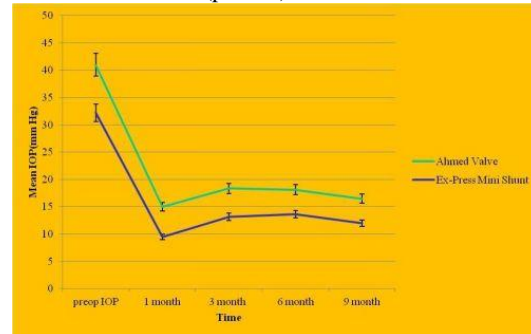
Methods: A retrospective comparative case series of Ahmed Valve and Ex-Press Shunt performed by three glaucoma surgeons. Patients with less than 3 post operative visits or more than one glaucoma surgery have been excluded. Pre-operative visual acuity (VA), intra- and post-operative complications, pre and post surgical IOP and glaucoma medications have been recorded.

Results: 21 Neovascular glaucoma patients with Ahmed Valve vs. 6 Ex-Press Mini shunt were included in the study. Mean patient age was 70 years. Mean follow up time was 14 months for Ahmed Valve and 9.4 months for Ex-Press Mini Shunt. 2 out of 23 Ahmed Valve patients required repeat excisional surgery but no Ex-Press Mini Shunt patients required repeat surgery. These patients have been excluded from study. 2 out of 21 Ahmed Valve patients had hyphema, 1 Ahmed Valve patient had chroidal effusion. Ex-Press shunt patients required less glaucoma drops than Ahmed Valve patients ($p = 0.011$) Figure 1. Mean IOP decrease in Ahmed Valve vs. Express Shunt was statistically not different. ($p = 0.22$) Figure 2.

Conclusions: Our data suggests that Ex-Press shunt might be as or even more efficous in the treatment of neovascular glaucoma. Ex-Press shunt and Ahmed Valve lowered the IOP similarly. In addition, Ex-Press shunt patients required less glaucoma medications overall. Further research including recruitment of more patients and data points is required to confirm the role of express shunt in neovascular glaucoma.



Mean (IOP) before and after surgery in both the Ahmed Valve and Ex-Press Mini shunt ($p = 0.22$).



Mean number of pre- and postoperative glaucoma medications after Ahmed Valve and Ex-Press Mini Shunt. Ex-Press shunt required less number of medications ($p = 0.011$)

Commercial Relationships: Huseyin Kadikoy, None; Bret A. Hughes, None; Justin Tannir, None; Rominder Momi, None

Program Number: 4491 **Poster Board Number:** D0231

Presentation Time: 8:30 AM - 10:15 AM

A Novel Minimally Invasive Drainage Implant (the MIDI-Arrow): One-Two Year Follow Up

Paul F. Palmberg¹, Juan F. Batlle³, Rachel Alburquerque³, Adalgisa Corona-Peralta³, Isabelle Riss⁴, Richard Parrish¹, Esdras Arrieta², Jean-Marie A. Parel². ¹Biophysics (Ophthalmology), University of Miami, Miami, FL; ²Ophthalmology, University of Miami, Miami, FL; ³Centro Laser, Santo Domingo, Dominican Republic; ⁴Pole Ophthalmologique, Clinique Mutualiste, Pessac, France.

Purpose: To evaluate the safety and IOP lowering efficacy of a novel micro-lumen glaucoma drainage device used with MMC application and placed under a conjunctival flap.

Methods: Single site, single surgeon (JB) prospective single arm study in 23 eyes of 23 mixed-race adult subjects with POAG. 9 eyes underwent combined procedures and 14 had implantation alone. All eyes received an intraoperative wide application under the subconjunctival flap of 0.4 mg/ml MMC for 3 minutes (technique of Khaw). Subjects were seen at 1 day, 1 week, 1, 3, 6, 9, 12 and 24 months.

Results: The mean IOP fell from a baseline of 24.0 +/- 5.4 mm Hg to 10.5 +/- 2.8 at 12 months (range 6-18, N=23) and to 10.2 +/- 2.0 at 2 years (N=10). Glaucoma meds fell from an average of 2.2 +/- 1.0 to 0.3 at 12 months. Complete success, defined as an IOP >5 and <21, and a greater than 20% reduction in IOP without medical therapy, was 91%, and modified success (with medication) was 96% at one year. One subject required bleb needling at 90 days, and was at 10 mm Hg off meds at 2 years. 21 of 23 subjects had a wide, low profile ischemic bleb at 1 year. Complications included 2 subjects with transient shallow anterior chamber, 2 (combined cases) with transient

ARVO 2013 Annual Meeting Abstracts by Scientific Section/Group – Glaucoma

choroidal detachment, 2 with transient hypotony after day one, none with chronic hypotony or maculopathy. The mean HVF MD was -15.6 +/- 13.3 at baseline and -15.5 +/- 13.3 at 1 year. There was no change in mean ETDRS Va at one year. No tube exposure, migration, or blockage, and no bleb infection was encountered.

Conclusions: The MIDI-arrow replaces a scleral flap with an 8.5 mm small internal diameter (62 u) flexible tube implanted through a 3 mm needle track. The implant is made of the biocompatible material SIBS, poly(styrene-block-isobutylene-block-styrene). At 2 ul / min flow, the tube has a trans-scleral pressure drop of 5 mm Hg, avoiding hypotony problems. We believe that the success is attributable to minimal inflammation associated with only a needle track entry. The needle track which starts 3 mm posterior to the limbus (technique of Felix Gil) and small size of the tube appear to obviate the need for a patch graft to protect the tube as the lid margin does not rub over that location. The operation appears to require only rare post-operative intervention. An FDA trial of this device should begin soon.



Bleb at two years

Commercial Relationships: Paul F. Palmberg, AqueSys (C), Innovia (C), Aurolab (unpaid) (C), Aeon (DSMB) (R); Juan F. Batlle, Innovia LLC (C), Innovia LLC (F), OptiMedica Corporation (C), OptiMedica Corporation (F), PPI LLC (P), AqueSys (C), AqueSys (F), Reflow Biomedical Technologies (I), STAAR Surgical Co. (C), Emmetrope Ophthalmics, LLC (C), Croma (C); Rachel Albuquerque, Innovia LLC (C), Innovia LLC (F), AqueSys (C), AqueSys (F); Adalgisa Corona-Peralta, None; Isabelle Riss, None; Richard Parrish, AqueSys, Inc (C), Aerie Pharmaceuticals, Inc (C), Bausch + Lomb (C), Glaukos Corporation (C), InnFocus, Inc (C), Innolene LLC (R), Merck & Co, Inc (C), Vitalspring Technologies, Inc (I), Alimera Sciences, Inc (C); Esdras Arrieta, None; Jean-Marie A. Parel, CROMA (F), InnFocus (F), Abeamed (F), University of Miami (P)

Support: Study supported by Innovia; Ophthalmic Biophysics Laboratory University of Miami

Clinical Trial: 002-2007

Program Number: 4492 **Poster Board Number:** D0232

Presentation Time: 8:30 AM - 10:15 AM

Surgical Outcomes in First 25 Canaloplasties and Impact of Growing Experience on Complications

Elisabeth P. Aponte, Jonathan Eisengart. Ophthalmology, Cleveland Clinic Cole Eye Institute, Cleveland, OH.

Purpose: To review the first 25 canaloplasties of a glaucoma specialist and determine how a single surgeon's growing experience in this procedure affects surgical time, complications and early outcomes.

Methods: We retrospectively reviewed the medical records of all patients who underwent canaloplasty by a single surgeon since 2010. Canaloplasties were divided into 2 equal groups of 12, based on the date of surgery, an "early group" G1 and a "late group" G2.

Results: 25 canaloplasties were found during this review. One early canaloplasty was converted to trabeculectomy intraoperatively and excluded from IOP outcomes. The remaining 24 canaloplasties were divided into G1 and G2. The average preoperative IOP in G1 was 21.26 mmHg on an average of 2.8 medications while that of G2 was 21 mmHg (P=0.88) on 2.54 medications (P=0.42). In G1, 8 of 12 canaloplasties had successful placement of tensioning suture after canalization with stent compared to 11 of 12 in G2. Perforation of the trabeculo-Desemet's membrane occurred in 5 patients in G1 and 4 in G2, with 3 in each group being microperforations with no further intraoperative consequence. Combined phaco-canaloplasty averaged 54 and 52.6 minutes in G1 and G2, respectively (P=0.73). IOP on day 1 were 17.9 mmHg and 13.3 mmHg, in G1 and 2, respectively without glaucoma medications (P=0.17). At 1 month, IOPs were 15.5 mmHg (mean = 0.25 medications) and 14.18 mmHg (on no medication) in G1 and G2, respectively (P=0.43). Visual acuity was equal or better than 20/40 at day 1 in 5 of 12 patients in G1 and 8 of 12 patients in G2. Early post-operative complications included 5 hyphemas in G1 and 4 in G2, which all but 1 resolved during the first week. Hypotony (IOP < 6) was found in 1 patient in each group at day 1. Four small flat blebs were seen in G1 at 1 month and five in G2. The average final IOP in G1 was 18.5 mmHg on 1.9 medications and 14.83mmHg (P=0.09) in G2 on no medication (P<0.0001).

Conclusions: Canaloplasty in both the early and late groups resulted in a significant decrease in IOP and need for glaucoma medications. More patients in the later group had successful retention of tensioning suture after canalization with stent and visual acuity better than 20/40 at day 1. IOP at day 1 and final follow-up were also lower in the late group although not statistically significant. Intraoperative time and early complications were comparable between the 2 groups.

Commercial Relationships: Elisabeth P. Aponte, None; Jonathan Eisengart, None

Support: Research to Prevent Blindness

Program Number: 4493 **Poster Board Number:** D0233

Presentation Time: 8:30 AM - 10:15 AM

Review of the Success Rate of an Intraoperative Modified Bleb Revision Technique

Priya Gupta, Karun S. Arora, Chun-Hao Lee, David S. Friedman. Wilmer Eye Institute, Johns Hopkins Hospital, Baltimore, MD.

Purpose: Needling of a scarred trabeculectomy is often performed in the office using a slit lamp microscope as an alternative to additional surgery to lower intraocular pressure (IOP). However, the success rate in an office setting is relatively low (31% after 6 months in one study).

The authors used a modified bleb revision technique in the operating room, providing control and immediate feedback. To our knowledge, the success rate of this technique has not previously been described. The purpose of this study is to perform a retrospective chart review to determine the success rate of this procedure.

Methods: The modified technique involves placing a 25 gauge infusion cannula in the anterior chamber. As fibrotic adhesions within the bleb are lysed with a 25 gauge needle, the continuous infusion of balanced salt solution from the anterior chamber provides immediate bleb elevation, indicating flow. A subconjunctival injection of 5-fluorouracil is given at the conclusion of each case. A retrospective chart review was performed for patients undergoing the intraoperative modified bleb revision technique in the setting of a failed trabeculectomy due to scarring at the Wilmer Eye Institute at Johns Hopkins University between 8/1/10 and 2/28/12. Data was collected and analyzed from the three clinic visits prior to the procedure, as well as data from post-operative day 1, week 1, month 1, month 3, month 6, and month 12.

Results: 25 eyes of 22 patients were identified. The mean IOP at the visit prior to the procedure was 21.72 +/- 6.52 and subjects were using an average of 2.1 +/- 1.4 medication classes. The mean IOP reduction at each time point was 8.58 +/- 8.14, 7.96 +/- 9.51, 9.24 +/- 7.33, 7.83 +/- 6.87, 5.86 +/- 8.08, and 6.26 +/- 5.82 respectively. The % reduction in IOP at the post-operative time points was 40.6 +/- 35.4, 36.8 +/- 39.6, 38.8 +/- 26.7, 32.8 +/- 22.2, 25.6 +/- 36.7 and 30.1 +/- 27.8. At day 1, no subjects were taking glaucoma medications. At subsequent time points, the reduction in medication classes was 1.4, 1.0, 1.0, 1.5 and 0.8 respectively. Of the 24 patients that had an IOP target set pre-operatively, 60.9%, 56.5%, 60.0%, 45.5%, and 63.2% were within the target IOP at the respective time points.

Conclusions: The modified technique of bleb needling may provide a successful method to lower IOP in the setting of a previous trabeculectomy, thus preventing additional surgery and preserving conjunctiva.

Commercial Relationships: Priya Gupta, None; Karun S. Arora, None; Chun-Hao Lee, None; David S. Friedman, Alcon (C), Bausch & Lomb (C), Merck (C), QLT, Inc (C), Allergan (C), Nidek (C)

Program Number: 4494 **Poster Board Number:** D0234

Presentation Time: 8:30 AM - 10:15 AM

Clinical and Tomographic Findings in Filtering Blebs Undergoing Digital Compression

Miriam A. Ramos-Hernandez², Miriam A. Ramos-Hernandez², Elia Chavez², Luz A. Giorgi-Sandoval¹, Jose A. Paczka^{1,2}. ¹Asistencia e Investigacion en Glaucoma, A.C., Guadalajara, Mexico; ²Instituto de Oftalmologia y Ciencias Visuales, Guadalajara, Mexico.

Purpose: To investigate clinical and tomographic profile of filtering blebs of eyes requiring digital compression to decrease intraocular pressure (IOP) as compared to blebs spontaneously achieving adequate IOP

Methods: We prospectively assessed 13 eyes which underwent primary mitomycin C augmented trabeculectomy and required continuous digital compression (DC) to achieve target IOP; 18 additional operated eyes (equivalent type of filtering surgery) not requiring digital compression (NRDC) to reach adequate level of IOP were also included in the study. All cases underwent clinical photography and anterior segment tomography (Cirrus anterior segment module of optical coherence tomography; Carl Zeiss Meditec; San Leandro, California, U.S.A.). Filtering bleb photographs and tomographic images were assessed by the same investigator (JAP) in a masked fashion. Würzburg filtering bleb score was used for clinical assessment. A novel weighted score for tomographic analysis was also applied.

Results: Thirteen eyes from 9 patients (mean age: 64.5 ± 8.2 years) belonging to the DC group had a mean IOP (13.4 ± 5.1 mm Hg) that was not significantly different to the mean value of IOP (14.1 ± 4.7 mm Hg, P > 0.05) of 18 eyes from 15 patients (mean age: 69.8 ± 4.9 years) of NRDC group. Mean scores derived from the Würzburg classification were not different between groups (8.5 ± 2.7. vs. 9.1 ± 3.2; DC vs. NRDC, respectively). In contrast, the tomographic score of the DC group (4.0 ± 2.6) was significantly different to the one obtained after scoring the NRDC group (7.6 ± 1.6, P = 0.01).

Conclusions: The current study suggests that structural findings of filtering blebs derived from anterior segment OCT (tomographic score) seems to perform better than clinical assessment to differentiate among blebs of different capacities of filtration.

Commercial Relationships: Miriam A. Ramos-Hernandez, None; Miriam A. Ramos-Hernandez, None; Elia Chavez, None; Luz A. Giorgi-Sandoval, None; Jose A. Paczka, None

Program Number: 4495 **Poster Board Number:** D0235

Presentation Time: 8:30 AM - 10:15 AM

Cyclodialysis incidence in anterior segment surgery in an Ophthalmology Referral Center

Rodrigo Bolanos¹, Alejandro Navas³, Enrique O. Graue-Hernández³, Arturo J. Ramirez-Miranda³, Jasbeth Ledesma Gil². ¹Research Unit, Inst of Ophthal Conde de Valenciana, Mexico City, Mexico; ²Glaucoma, Instituto de Oftalmologia Conde de Valenciana, Mexico DF, Mexico; ³Cornea An Refractive Surgery, Instituto de Oftalmologia Conde de Valenciana, Mexico DF, Mexico.

Purpose: To determine the distribution of visual acuity and its associated factors in a population with high proportion of indigenous people.

Methods: Chart review of patients with anterior segment surgery and diagnosis of cyclodialysis between 2001 and 2007 were obtained.

Retrospective case series, observational study. STATA 8.0 was used for graphics and descriptive statistics.

Results: 54 files with cyclodialysis diagnosis were recolected, 18 were excluded. 36 were analyzed, 15 male and 21 female. The causes were: 21 due to trabeculectomy, 7 extracapsular cataract surgery, 4 phacoemulsification, 2 combination of trabeculectomy and phacoemulsification and 2 Ahmed valvular implantation. Average intraocular pressure was 4 mmHg (0-10 mmHg). The incidence of cyclodialysis is 0.5 per 100 cases. Visual acuity varied from 20/20 to no light perception. Mean age was 56.57 years (7-84 years).

Conclusions: The incidence of cyclodialysis is 0.5 per 100 cases during the study period.

Commercial Relationships: Rodrigo Bolanos, Institute Ophthalmology (P); Alejandro Navas, None; Enrique O. Graue-Hernández, None; Arturo J. Ramirez-Miranda, Carl Zeiss Meditec (R); Jasbeth Ledesma Gil, None

Program Number: 4496 **Poster Board Number:** D0236

Presentation Time: 8:30 AM - 10:15 AM

Optimal administration route of bevacizumab after glaucoma filtration surgery

Karolien P. Hollanders¹, Tine Van Bergen¹, Davine Sijnave¹, Sarah Van de Velde¹, Evelien Vandewalle¹, Lieve K. Moons², Ingeborg Stalmans¹. ¹neuroscience, lab of ophthalmology, KULeuven, Leuven, Belgium; ²biology, KULeuven, Leuven, Belgium.

Purpose: Glaucoma filtration surgery (GFS) frequently leads to surgical failure due to excessive postoperative wound healing. We previously showed that bevacizumab was able to improve surgical outcome in a rabbit model of GFS. However, the most optimal route of administration of bevacizumab is still unknown. Therefore, the current study was designed to investigate the effect on postoperative scarring of a single subconjunctival, intracameral or intravitreal injection of bevacizumab.

Methods: The effect of bevacizumab (AvastinTM, Genentech) was investigated in a mouse model of GFS in C75Bl/6 mice. Immediately after surgery, mice were divided in 3 groups (n=10 per group) and received a subconjunctival (SC), intracameral (IC) or intravitreal (IV) injection. In all groups, one eye was injected with bevacizumab (1 µl; 25 µg) and the other eye was used as a negative control and received an injection of NaCl (1 µl; 0.9%). Treatment outcome was studied by clinical investigation of bleb area and bleb survival every other day. Mice were killed on postoperative day 14 and immunohistological analysis of angiogenesis (CD31) and collagen deposition (Sirius Red) were performed.

Results: In the mouse model of GFS, treatment using a SC, IC, IV injection of bevacizumab significantly improved surgical outcome by increasing bleb area with 53 ± 5 % (P<0.001); with 45 ± 3 %

($P=0.004$) and with $49 \pm 4\%$ ($P<0.001$), respectively, compared to negative control. Bleb survival improved only after SC injection compared to NaCl ($P=0.04$); all blebs survived until day 14 after SC bevacizumab injection, whereas only 62.5% of the NaCl treated eyes survived ($P=0.04$). No significant effects on bleb survival were seen after IC and IV injection. In all groups, blood vessel density was significantly reduced after bevacizumab treatment at 14 days after surgery with $36 \pm 4\%$ ($P<0.001$); with $31 \pm 1\%$ ($P<0.001$) and with $34 \pm 4\%$ ($P<0.001$), respectively. All administration routes of bevacizumab significantly diminished collagen deposition with $27 \pm 4\%$ ($P<0.001$); with $27 \pm 1\%$ ($P<0.001$) and with $27 \pm 2\%$ ($P<0.001$), respectively, compared to negative control.

Conclusions: This study shows that a subconjunctival injection of bevacizumab had the largest effect on surgical outcome compared to intracameral and intravitreal injection.

Commercial Relationships: Karolien P. Hollanders, None; Tine Van Bergen, None; Davine Sijnave, Amakem therapeutics (F); Sarah Van de Velde, Amakem Therapeutics (F); Evelien Vandewalle, None; Lieve K. Moons, None; Ingeborg Stalmans, None

424 Genetics I

Wednesday, May 08, 2013 11:00 AM-12:45 PM

6B Paper Session

Program #/Board # Range: 4497-4503

Organizing Section: Glaucoma

Program Number: 4497

Presentation Time: 11:00 AM - 11:15 AM

Genome-wide Association Study and Meta-Analysis of Intraocular Pressure in Primary Open-Angle Glaucoma Cases and Controls in the NEIGHBOR, GLAUGEN and AMD-MMAP Studies

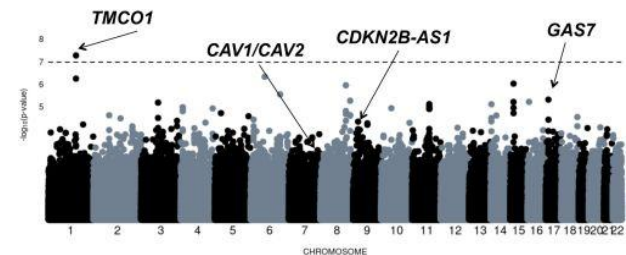
Sayoko E. Moroi¹, Ayse B. Ozel², David M. Reed¹, Kari E. Branham¹, Michael A. Hauser³, Louis R. Pasquale⁴, Janey L. Wiggs⁴, Julia E. Richards¹, Jun Z. Li². ¹Ophthalmology & Visual Sciences, Univ of Michigan-Kellogg Eye Ctr, Ann Arbor, MI; ²Human Genetics, University of Michigan, Ann Arbor, MI; ³Center for Human Genetics, Duke University School of Medicine, Durham, NC; ⁴Department of Ophthalmology, Harvard Medical School, Massachusetts Eye and Ear Infirmary, Boston, MA.

Purpose: Intraocular pressure (IOP), a major risk for glaucoma, is influenced by both genetic and environmental factors. We performed a genome-wide association study (GWAS) to discover common genetic variants associated with IOP.

Methods: We assessed the association between single nucleotide polymorphisms (SNPs) and IOP from primary open-angle glaucoma (POAG) cases and controls in more than 6,000 subjects of European ancestry, who are part of the NEIGHBOR (NEI Glaucoma Human genetics collaBORation) consortium, the GLAUGEN (Glaucoma Genes and Environment) study, and the University of Michigan subset of AMD-MMAP MI (Age-related Macular Degeneration-Michigan, Mayo, AREDS and Philadelphia) studies. There were 466,573 SNPs shared across studies. When there were IOP values for both eyes, the maximum IOP was used. The association between IOP and genotypes was tested with a linear regression additive model adjusted for age, gender, and principal component (PC) scores. Treated IOPs were adjusted by dividing by 0.7, an approach confirmed in a subset of patients with pre- and post-treatment IOP values. We also performed a candidate gene association analyses for IOP using the following previously reported IOP related and glaucoma genes: TMCO1, CDKN2B-AS1, GAS7 and CAV1/CAV2.

Results: This dataset included 1,931 cases and 2,199 controls from NEIGHBOR, 820 cases and 343 controls from GLAUGEN, and 128 cases and 870 controls from the Michigan cohort of AMD-MMAP. While no signal achieved genome-wide significance in individual studies, a meta-analysis identified that IOP was associated with TMCO1 (rs7518099-G, $p = 6.5E-8$). Focused analyses of TMCO1, CDKN2B-AS1, GAS7, and CAV1/CAV2 revealed association signals that are consistent across the three studies and replicated the previously reported association in both effect size and direction. In the NEIGHBOR dataset, the association at TMCO1 was stronger in males than in females; and the effects at CDKN2B-AS1 and CAV1/CAV2 were stronger in the younger subjects.

Conclusions: Our meta-analysis identified significant association between IOP and TMCO1. In addition, the previously reported genes of CDKN2B-AS1, GAS7, and CAV1/CAV2 revealed association signals consistent in both effect size and direction with previous reports. Our results add to the GWAS evidence that these genes are involved in IOP regulation.



Commercial Relationships: Sayoko E. Moroi, Merck (F), Wolters Kluwer (F); Ayse B. Ozel, None; David M. Reed, None; Kari E. Branham, Arctic DX (P); Michael A. Hauser, None; Louis R. Pasquale, None; Janey L. Wiggs, None; Julia E. Richards, None; Jun Z. Li, None

Support: NEI R01 EY015473; HG004728; HG005259; EY015872-05S1; EY019126-02S1

Program Number: 4498

Presentation Time: 11:15 AM - 11:30 AM

Molecular mechanisms in Primary Glaucoma: POAG-associated variant disrupts microRNA regulation of CDKN2B expression

Terry Gaasterland^{1,2}, Amy N. Dubinsky³, Albert R. La Spada^{3,8}, Kaweh Mansouri^{4,10}, Karl H. Willert^{8,9}, Douglas E. Gaasterland⁵, Michael A. Hauser⁶, Louis R. Pasquale⁷, Janey L. Wiggs⁷, Robert N. Weinreb¹⁰. ¹Institute for Genomic Medicine, Univ of California San Diego, La Jolla, CA; ²Marine Biology Research Division, Univ of California San Diego, La Jolla, CA; ³Department of Pediatrics, Univ of California San Diego, La Jolla, CA; ⁴University of Geneva, Geneva, Switzerland; ⁵Ophthalmology, Potomac, MD; ⁶Department of Medicine, Duke University, Durham, NC; ⁷Massachusetts Eye and Ear Institute, Harvard, Cambridge, MA; ⁸Cellular and Molecular Medicine; Neurosciences, Univ of California San Diego, La Jolla, CA; ⁹Sanford Consortium for Regenerative Medicine, La Jolla, CA; ¹⁰Hamilton Glaucoma Center, Univ of California San Diego, La Jolla, CA.

Purpose: To evaluate functional consequences of SNP rs3217992—which is associated with increased susceptibility to optic nerve degeneration in glaucoma in the NEIGHBOR study. One of 17 such SNPs in chromosome 9p21, its odds ratio indicates risk. It occurs in the 3' untranslated region (UTR) of CDKN2B, encoded in an intron of CDKN2B-AS. CDKN2B inhibits cell-cycle progression via CDK4. We hypothesize the minor allele disrupts binding of a microRNA which regulates CDKN2B expression and modulates cell-cycle progression, with effect in glaucoma.

Methods: With our microRNA (miR) seed site detection algorithm ZoomMiR, we identified microRNA candidates. ZoomMiR finds all 6 to 8 base complementary matches to initial bases of every miR archived in miRbase. In CDKN2B, it found 5 seeds. SNP rs3217992 is in a predicted seed sequence for miR-138-2*. HapMap showed the SNP is in separate haplotypes from protective SNPs. GENSAT, dbEST, GEO and miRbase queries showed CDKN2B is expressed in eye and glia; and miR-138-2*, in brain. To determine to what extent the alleles and a disrupted seed sequence affect miR-138-2* ability to target CDKN2B, we used a dual-luciferase reporter assay. We used quantitative PCR to measure CDKN2B, CDKN2A, and miR levels in human neural progenitors (NP), in neurons derived from human induced pluripotent stem cells, and in selected mouse tissues.

Results: miR-138-2* effectively targets a luciferase reporter transcript engineered to contain 100 bases surrounding the risk SNP in its 3' UTR. Disrupting the seed increased reporter activity, demonstrating this mutation/change negatively affected miR-138-2* ability to target the reporter transcript. Importantly, introducing the minor allele into the construct likewise increased reporter activity, strongly suggesting this risk allele—through the action of miR-138-2*—alters the stability of CDKN2B transcript. Furthermore, CDKN2B and miR-138-2*, but not CDKN2A, are expressed in human NP, neurons and mouse retina. As revealed by database queries, CDKN2B is expressed in glial cells and miR-138 precursor, in glial stem cells, and this SNP in CDKN2B has been shown as protective in glioma.

Conclusions: Our results support a model in which CDKN2B regulation by miR-138-2* is important, especially in glia, and is impaired by SNP rs3217992. This molecular mechanism may underlie primary glaucoma and have implications in glia-related diseases.

Commercial Relationships: Terry Gaasterland, None; Amy N. Dubinsky, None; Albert R. La Spada, None; Kaweh Mansouri, Sensimed AG, Switzerland (C); Karl H. Willert, None; Douglas E. Gaasterland, None; Michael A. Hauser, None; Louis R. Pasquale, None; Janey L. Wiggs, None; Robert N. Weinreb, Aerie (F), Alcon (C), Allergan (C), Altheos (C), Amakem (C), Bausch&Lomb (C), Carl Zeiss-Meditec (C), Genentech (F), Haag-Streit (F), Heidelberg Engineering (F), Konan (F), Lumenis (F), National Eye Institute (F), Nidek (F), Optovue (C), Quark (C), Solx (C), Topcon (C)
Support: NIH Grants EY022306-01 EY021237-02 EY020678-01

Program Number: 4499

Presentation Time: 11:30 AM - 11:45 AM

Runs of Homozygosity Across the Whole Genome Suggests two Novel Genes in Primary Congenital Glaucoma

Subhabrata Chakrabarti¹, Sriparna Ganguly³, Meha Kabra¹, Anil K. Mandal², Sirisha Senthil¹, Inderjeet Kaur¹, Partha P. Majumder^{4,3}.

¹Brien Holden Eye Research Centre, LV Prasad Eye Institute, Hyderabad, India; ²Jasti V Ramanamma Childrens Eye Care Centre, L V Prasad Eye Institute, Hyderabad, India; ³Department of Human Genetics, Indian Statistical Institute, Kolkata, India; ⁴National Institute of Biomedical Genomics, Kalyani, India.

Purpose: Primary congenital glaucoma (PCG) is largely attributed to mutations in the *CYP1B1* gene that are globally structured on intragenic haplotypes. These mutations account for 20-50% of cases in different populations worldwide while the contributions of other genes in the remaining cases are yet unknown. Based on the premise of large regions of homozygosity harboring the *CYP1B1* mutations, we aimed to identify the missing genetic determinants in the *CYP1B1*-negative PCG cases using runs of homozygosity (ROH) across the whole genome.

Methods: Initially, an algorithm (based on 'R' program) was devised

to identify regions within each chromosome where the homozygote genotype frequencies differed significantly across the 90,000 single nucleotide polymorphisms (SNPs) between the PCG cases devoid of *CYP1B1* mutations (n=131) and ethnically matched normal controls (n=130). Genotyping of these SNPs were accomplished by a combination of microarray and resequencing. Test of proportions were calculated for the consecutive markers harboring the associated SNPs that exhibited homozygosity. Further, haplotypes were generated with the flanking SNPs to the associated variant observed through ROH and analyzed using the Haploview software (version 4.2) that uses an EM algorithm. Using online databases (NCBI and Seattle SNPs) putative gene(s) harboring the risk haplotypes were identified.

Results: We identified multiple genomic regions across different chromosomes, wherein stretches of 7, 6 and 5-loci were significant (Z score >= 1.96). Further, test of proportions among cases and controls indicated that only 7 regions were significant (p < 0.01) with uninterrupted stretches of consecutive SNPs. Of these, two regions on chromosomes 19 (33 kb) and 21 (4.25 kb) exhibited the largest stretches that were associated with PCG. Haplotype analysis using 10,000 permutation tests indicated major risk haplotypes on chromosomes 19 (C-C-G-G-G-A; p=0.006) and 20 (C-C-A-C-A-T; p=0.001). Bioinformatic analysis further demonstrated that the ROH on chromosomes 19 and 20 lay within the *KLHL26* and the *TSHZ2* genes, respectively.

Conclusions: Based on ROH approach, we identified two novel candidate genes in PCG that have been earlier implicated in regulating aqueous humor outflow (*KLHL26*) and embryonic development (*TSHZ2*).

Commercial Relationships: Subhabrata Chakrabarti, None; Sriparna Ganguly, None; Meha Kabra, None; Anil K. Mandal, None; Sirisha Senthil, None; Inderjeet Kaur, None; Partha P. Majumder, None

Support: Australia India Strategic Research Fund

Program Number: 4500

Presentation Time: 11:45 AM - 12:00 PM

Genetic factors and pathways affecting retinal nerve fiber layer thickness

Cristina Venturini^{1,2}, Pirro G. Hysi², Abhishek Nag², Ekaterina Yonova², Jie Jin Wang^{3,4}, Tien Y. Wong^{5,6}, Paul R. Healey⁴, Paul Mitchell⁴, Christopher J. Hammond², Ananth C. Viswanathan^{7,8}.

¹Genetics, UCL, Institute of Ophthalmology, London, United Kingdom; ²Twin Research & Epidemiology Research, King's College London, London, United Kingdom; ³Centre for Eye Research Australia (CERA), Department of Ophthalmology, University of Melbourne, Melbourne, NSW, Australia; ⁴Department of Ophthalmology, University of Sydney Centre for Vision Research, Sydney, NSW, Australia; ⁵Epidemiology and Public Health, National University of Singapore, Singapore, Singapore; ⁶Singapore Eye Research Institute, Singapore, Singapore; ⁷Glaucoma Service, Moorfield Eye Hospital, London, United Kingdom; ⁸NIHR Biomedical Research Centre, Moorfield Eye Hospital and UCL Institute of Ophthalmology, London, United Kingdom.

Purpose: The Retinal nerve fiber layer (RNFL) thickness is used in the diagnosis of glaucoma and the assessment of progression or stability. Despite the known high heritability of RNFL thickness, the genes affecting this trait have not been extensively investigated. The aim of this study was to investigate genetic factors and pathways underlying RNFL thickness.

Methods: We carried out a genome wide association study (GWAS) on a panel of 2,617,903 SNPs imputed on the bases of the 1000 Genome for 964 individuals over the age of 49 years from the Blue

Mountain Eye Study with quantitative measurements for RNFL thickness for the right eye. The regression analysis was corrected for age and sex. We also performed enrichment analysis with DAVID bioinformatics resources to extract putative biological mechanisms associated with the genes of interest.

Results: No genome-wide significant results were obtained after multiple testing corrections. However, there are some strongly suggestive association signals. The first one is at rs1154119 on SLC25A21 on chromosome 14 ($\beta=0.04$, $p\text{-value}=2.41 \times 10^{-7}$). This gene is part of the solute carrier family 25 and it is involved in transporting C5-C7 oxodicarboxylates across the inner membranes of mitochondria. Another suggestive association signal was found at rs2493383 ($\beta=0.01$, $p\text{-value}=1.67 \times 10^{-6}$), which lies on SNX6 (chromosome 14). This gene is involved in several stages of intracellular trafficking and it promotes lysosomal degradation of Cdkn1B. Enrichment analysis shows an involvement of neuronal activity. The most significant pathway was axon guidance ($p\text{-value}=0.003$).

Conclusions: This study identified new suggestive association signals on chromosome 14 (SLC25A21 and SNX6) for retinal nerve fiber layer thickness. SNX6 promotes lysosomal degradation of Cdkn1B. This gene belongs to the same gene family of Cdkn2B which was previously associated with glaucoma and glaucoma endophenotypes such as vertical cup/disc ratio. Enrichment analysis appears to confirm the role of the genetic signals identified in this study in the determination of ganglion cell layer morphology and hence RNFL thickness.

Commercial Relationships: Cristina Venturini, None; Pirro G. Hysi, None; Abhishek Nag, None; Ekaterina Yonova, None; Jie Jin Wang, None; Tien Y. Wong, Allergan (C), Bayer (C), Novartis (C), Pfizer (C), GSK (F), Roche (F); Paul R. Healey, None; Paul Mitchell, Novartis (R), Bayer (R); Christopher J. Hammond, None; Ananth C. Viswanathan, None

Program Number: 4501

Presentation Time: 12:00 PM - 12:15 PM

The role of SIX6 in primary open-angle glaucoma

Michael A. Hauser^{1,2}, Megan Ulmer¹, Yangfan Liu³, Erica Davis³, Nicholas Katsanis³, Yutao Liu¹, Louis R. Pasquale⁴, Janey L. Wiggs⁴, Allison E. Ashley-Koch¹, R Rand Allingham². ¹Medicine, Duke Univ Medical Center, Durham, NC; ²Ophthalmology, Duke Univ Medical Center, Durham, NC; ³Cell Biology, Duke University, Durham, NC; ⁴Ophthalmology, Harvard Medical School, Boston, MA.

Purpose: To identify sequence variants within and near the SIX6 gene, to assess their association with primary open angle glaucoma (POAG), and to perform functional testing.

Methods: Meta-analysis of the NEIGHBOR and GLAUGEN datasets have identified a region on chromosome 14q23 that is significantly associated with POAG risk (top SNP rs10483727, $p\text{-value}=3.9 \times 10^{-11}$, OR= 1.32) as well as POAG quantitative endophenotypes involving optic nerve measurements. This locus contains the homeobox gene SIX6, which is known to play a role in ocular development. To identify potential causal variants, we sequenced the exons and flanking regions of the SIX6 locus in 262 POAG cases and 279 POAG controls. Variants identified are currently being functionally tested: morpholino antisense oligonucleotides for targeted knockdown have been injected into developing zebrafish embryos. Phenotypic rescue is underway with SIX6 mRNAs containing variants identified in human patients.

Results: We identified six nonsynonymous changes in the SIX6 gene, including five novel variants (Glu93Gln, Glu129Lys, His141Asn (rs33912345), Leu205Arg, Thr212Met, and Ser242Ile). Using an allele-based chi-squared test, rs33912345 was significant

associated with POAG ($p\text{-value}=0.0005$, OR=1.54). We replicated this association, using a logistic regression model adjusted for age and gender, in a larger case-control dataset consisting of 482 POAG cases and 433 POAG controls ($p\text{-value}=0.005$, OR=1.40). We performed ordered subset analysis case-control (OSACC), a method for performing a series of stratified analyses, using an important quantitative POAG risk factor, intraocular pressure. Rs33912345 showed increased evidence of association (permutation $p\text{-value}=0.00008$, OR=1.71) in a subset of 206 cases with elevated intraocular pressure ($>27\text{mmHg}$). Rs33912345 also displays strong association with POAG risk after imputation of genotypes in the NEIGHBOR/GLAUGEN dataset of 3166 cases and 3391 controls ($p\text{-value}=4.2 \times 10^{-10}$). Preliminary results of SIX6 knockdown in the zebrafish show reduced eye size.

Conclusions: The SIX6 gene contains multiple variants highly associated with POAG status. Both common and rare variants may confer disease risk for POAG.

Commercial Relationships: Michael A. Hauser, None; Megan Ulmer, None; Yangfan Liu, None; Erica Davis, None; Nicholas Katsanis, None; Yutao Liu, None; Louis R. Pasquale, None; Janey L. Wiggs, None; Allison E. Ashley-Koch, None; R Rand Allingham, New World Medical (C)

Support: EY13315, EY019126, HG005259, HG004728

Program Number: 4502

Presentation Time: 12:15 PM - 12:30 PM

A genome-wide association study of intra-ocular pressure identifies a novel association in the gene FAM125B in the TwinsUK cohort

Abhishek Nag¹, Pirro G. Hysi¹, Cristina Venturini^{2,1}, Ekaterina Yonova¹, Katie M. Williams¹, Christopher J. Hammond¹.

¹Department of Twin Research, King's College London, London, United Kingdom; ²Institute of ophthalmology, University College London, London, United Kingdom.

Purpose: Glaucoma is a major cause of visual impairment and the second leading cause of blindness in the world. Efforts to dissect the genetic basis of glaucoma have revealed that common genetic variants in several genes determine susceptibility to glaucoma and its endophenotypes. We performed a genome-wide association study in the TwinsUK cohort (all of confirmed Caucasian ancestry) of intra-ocular pressure (IOP), used as the endophenotype for glaucoma.

Methods: The study was carried out in a sample of 2774 subjects with mean age of 56.5 years. IOP was measured using Ocular Response Analyser (ORA-Reichert®, Buffalo, NY), a non-contact air-puff tonometer. The mean IOP was 15.6 mmHg (s.d. = 3.26, range = 7-38). Subjects were genotyped using two genotyping platforms from Illumina: 300K Duo for part of the samples and HumanHap610-Quad array for rest of the samples. Whole genome imputation of the genotypes was performed on the basis of HapMap2. Association testing was performed using Merlin that implements a score-test based method to adjust for the family structure in the subjects.

Results: IOP was significantly associated with rs2286886 at 9q33.3 ($\beta = 0.56$, $p = 3.6 \times 10^{-8}$), which was directly genotyped in FAM125B (Homo sapiens family with sequence similarity 125, member B). Two other SNPs at 9q33.3 (rs2286885 and rs10819167) were also significantly associated with IOP ($p < 5 \times 10^{-8}$). Adjustment for central corneal thickness (CCT) improved the significance of association for rs2286886 ($p = 1.01 \times 10^{-9}$).

Conclusions: This study has identified genome-wide significant associations between SNPs in FAM125B and IOP. FAM125B codes for a component of the membrane complex involving trafficking of ubiquitinated proteins, similar to the Caveolin genes which have been

ARVO 2013 Annual Meeting Abstracts by Scientific Section/Group – Glaucoma

associated with POAG. Replication of this locus, and further examination of FAM125B's possible role in glaucoma, is required.
Commercial Relationships: **Abhishek Nag**, None; **Pirro G. Hysi**, None; **Cristina Venturini**, None; **Ekaterina Yonova**, None; **Katie M. Williams**, None; **Christopher J. Hammond**, None

Program Number: 4503

Presentation Time: 12:30 PM - 12:45 PM

Identification of further novel genome wide significant loci for open angle glaucoma blindness utilizing the Australian and New Zealand Registry of Advanced Glaucoma

Jamie E. Craig¹, Alex W. Hewitt^{2,1}, Stuart Graham³, Paul R. Healey⁴, Robert J. Casson⁵, Paul Mitchell⁶, John Landers¹, Stuart MacGregor⁶, David A. Mackey², Kathryn P. Burdon¹.

¹Ophthalmology, Flinders University, Bedford Park, Adelaide, SA, Australia; ²Ophthalmology, Lions Eye Institute, Perth, WA, Australia; ³Ophthalmology, Macquarie University, Sydney, NSW, Australia; ⁴Ophthalmology, Sydney University, Sydney, NSW, Australia; ⁵Ophthalmology, Adelaide University, Adelaide, SA, Australia; ⁶Queensland Institute of Medical Research, Brisbane, QLD, Australia.

Purpose: The pathogenesis of glaucoma, the leading cause of irreversible blindness remains poorly understood. There is a strong genetic basis for open angle glaucoma (OAG), and replicated susceptibility genes have been identified through genome wide association studies (GWAS). Using severely affected cases enhances genetic power to detect associations, and in a previous GWAS of individuals with advanced visual field loss from OAG we found strong associations at chromosome 1q24 (TMCO1) and 9p21 (CDKN2B-AS1). Using further cases recruited through the Australian and New Zealand Registry of Advanced Glaucoma (ANZRAG) we aimed to perform an extended study doubling the size, with the aim of identifying further common susceptibility loci for glaucoma blindness.

Methods: 1184 cases recruited through ANZRAG met entry criteria, which are advanced field loss due to OAG with either visual acuity worse than 20/200, severe global field loss, or field loss involving central fixation in the worst eye. These samples were genotyped on Illumina OmniExpress arrays and compared to 2761 examined controls from the Blue Mountains Eye Study, and 4642 unexamined controls from the publicly available Wellcome Trust Case Control Consortium, and the Illumina iControl databases. Following data cleaning and removal of genetic outliers by principal components analysis, association analysis was conducted in PLINK.

Results: Genome wide significant associations ($p < 10^{-8}$) were identified at 9 loci. As expected, the previously identified regions (CDKN2B-AS1, 9p21, OR 1.46, $p=2 \times 10^{-15}$, and TMCO1, 1q24, OR 1.56, $p=1.6 \times 10^{-14}$) remained strongly associated. We also confirmed SIX1/SIX6 on chromosome 14q23 at genome wide significance (OR 1.29, $p=5 \times 10^{-9}$). Single nucleotide polymorphisms (SNPs) at a further 6 loci were associated at the level of genome wide significance (4p12, $p=3.1 \times 10^{-20}$; 1q32, $p=5 \times 10^{-15}$; 4p16, $p=4 \times 10^{-10}$; 7p21, $p=1.3 \times 10^{-8}$; 3p12, $p=1.7 \times 10^{-8}$; 7q31, $p=2 \times 10^{-8}$). Further analysis and replication studies are ongoing. Genes at several of these loci are strong functional candidates for OAG.

Conclusions: The use of extreme phenotypes is a successful and cost-effective strategy to identify genes contributing to OAG blindness. These discoveries are likely to be of importance in directing future glaucoma research in risk profiling, and developing novel therapeutic targets.

Commercial Relationships: **Jamie E. Craig**, None; **Alex W. Hewitt**, None; **Stuart Graham**, None; **Paul R. Healey**, None; **Robert J. Casson**, None; **Paul Mitchell**, Novartis (R), Bayer (R);

John Landers, None; **Stuart MacGregor**, None; **David A. Mackey**, None; **Kathryn P. Burdon**, None
Support: NHMRC, ORIA

442 Surgery and Wound Healing

Wednesday, May 08, 2013 11:00 AM-12:45 PM

Exhibit Hall Poster Session

Program #/Board # Range: 4743-4797/D0127-D0181

Organizing Section: Glaucoma

Program Number: 4743 **Poster Board Number:** D0127

Presentation Time: 11:00 AM - 12:45 PM

Prospective evaluation of medical therapy to prevent the hypertensive phase following implantation of a glaucoma drainage device

Helen L. Kornmann, Allen Kwong, JoAnn A. Giaconi, Joseph Caprioli, Simon K. Law. Ophthalmology, Jules Stein Eye Institute, Los Angeles, CA.

Purpose: Glaucoma drainage devices (GDD) are frequently used to control intraocular pressure (IOP) in complicated or refractive glaucomas. After implantation, the IOP typically undergoes a hypertensive phase (HP). The reason for this transient rise in IOP is poorly understood and can cause further damage to the optic nerve. The purpose of this study was to prospectively investigate the effectiveness of glaucoma medical therapy in preventing the HP following a GDD procedure.

Methods: Patients who underwent a GDD procedure were monitored every week for 1 month and every month for 6 months postoperatively. HP was defined as an IOP > 21 mmHg during the first 3 months after surgery. Patients were randomized to receive aqueous suppressants (including beta-blockers, alpha-agonists, or carbonic anhydrase inhibitors) when the postoperative IOP was > 10 mmHg (early-treatment group) or when the postoperative IOP was > 17 mmHg (standard-treatment group). Outcome measures included the occurrence of HP and IOP control.

Results: 53 eyes (50 patients) received a GDD, with a mean age of 64.1 ± 13.8 years and 49.1% of patients Caucasian. Preoperative IOP was 26.3 ± 8.6 mmHg. HP was observed in 20 eyes (38.8%) with average peak IOP of 28.7 ± 6.6 mmHg. There were no significant differences between the early-treatment group ($n=26$ eyes) and standard-treatment group ($n=27$ eyes) with regard to the occurrence of HP (34.6% and 40.7%, respectively) or the average peak IOP (27.1 ± 5.9 and 31.0 ± 7.5 mmHg, respectively). No eyes in the early-treatment group and two eyes in standard-treatment group required additional glaucoma surgery within 6 months postoperatively. Medical therapy initiated prior to the development of HP was not associated with hypotony (defined as IOP < 6 mmHg) or maculopathy.

Conclusions: Medical therapy with topical aqueous suppressants initiated before the expected HP is comparable to standard treatments used to reduce the occurrence of HP after GDD procedure. It is not associated with hypotony even if the therapy was initiated when the postoperative IOP was already low. The effect of early treatment did not differ significantly between starting the topical therapy when the postoperative IOP was in the low versus high teens.

Commercial Relationships: **Helen L. Kornmann**, None; **Allen Kwong**, None; **JoAnn A. Giaconi**, Allergan (C); **Joseph Caprioli**, Allergan Inc. (F), Allergan Inc. (C), Allergan Inc. (R); **Simon K. Law**, None

Support: Research to Prevent Blindness (RPB), Inc., New York, New York

Clinical Trial: NCT00869141

Program Number: 4744 **Poster Board Number:** D0128

Presentation Time: 11:00 AM - 12:45 PM

High Intensity Focused Ultrasound (HIFU) in patients with Refractory Glaucoma

Shlomo Melamed, Modi Goldenfeld, Daniel Cotlear, Alon Skaat. Goldschleger Eye Institute, Sheba Medical Center, Ramat Gan, Israel.

Purpose: To evaluate Efficacy and Safety of High Intensity Focused Ultrasound (HIFU) in patients with Refractory Glaucoma.

Methods: Our study is a prospective study of 20 eyes of 20 patients with Refractory Glaucoma.

HIFU is a new technology for Cyclophotocoagulation, utilizing a novel miniature probe with 6 piezoceramic transducers emitting ultrasound energy focused on the ciliary body and processes. All patients had an IOP of at least 30 mm Hg with maximally tolerated medical treatment and at least one invasive glaucoma surgery. All eyes were treated with HIFU delivered through 6 high-frequency transducers operating at 21 MHz and emitting for 6 seconds each. Complete Ophthalmic examination was performed before Rx and at 1 day, 1 week, 1, 3 and 6 months.

Results: Intraocular pressure was reduced by 42.6 % ($P < 0.01$) from a mean preoperative value of 36.4 ± 2.8 mm Hg to a mean postoperative value of 27.8 ± 4.3 , 18.6 ± 3.6 and 20.9 ± 5.3 mm Hg at 1 day, 1 week and 3 months, respectively. No major intraoperative or postoperative complications were observed.

Conclusions: HIFU is a very safe and effective novel methodology for reducing IOP in Refractory Glaucoma cases.

Commercial Relationships: Shlomo Melamed, Solx (F), Eyetechnicare (F), Ioptima (F), Allergan (F); Modi Goldenfeld, None; Daniel Cotlear, None; Alon Skaat, None

Clinical Trial: NCT01338467

Program Number: 4745 **Poster Board Number:** D0129

Presentation Time: 11:00 AM - 12:45 PM

Ahmed Glaucoma Valve versus Gold Micro Shunt (GMS) implants - Five years Results of a Prospective Randomized Clinical Trial

Iris Moroz, Shlomo Melamed, Oded Sagiv, Guy J. Ben Simon, Modi Goldenfeld, Alon Skaat. Goldschleger Eye Institute, Tel Hashomer, Israel.

Purpose: To report 5-year outcomes of Ahmed Glaucoma Valve (AGV) implantation Compared with the Gold Micro Shunt (GMS) implants (20 μ GMS and 40 μ GMS-Plus) in the treatment of refractory glaucoma.

Methods: Comparative prospective interventional clinical trial. A total of 32 eyes of 32 patients with refractory glaucoma were prospectively assigned to either AGV or GMS implantation. All procedures were performed by a single surgeon at the Glaucoma Service of Goldschleger Eye Institute between January 2006 and July 2007. Kaplan-Meier survival with success defined as intraocular pressure (IOP) > 5 mmHg and < 22 mmHg and at least 20% reduction from preoperative IOP (with or without antiglaucoma medications). Secondary outcome measures included intraocular pressure, visual acuity, number of glaucoma medications and comparison between 20 μ GMS and 40 μ GMS-Plus subgroups.

Results: At the end of the follow up period, the AGV group had a significantly reduced final mean IOP of 17.3 ± 1.7 mmHg (vs. pre IOP of 33.5 ± 4.1 mmHg, $P = 0.004$) - a reduction of a mean 16.1 ± 4.0 mmHg, without a significant change in the final mean number of 2 ± 0.5 medications (vs. 2.5 ± 0.4 pre-op, $P = 0.43$). The GMS group had a significantly reduced final mean IOP of 20.2 ± 1.8 mmHg (vs. pre IOP of 31.1 ± 1.2 mmHg, $P = 0.0001$) - a reduction of a mean

10.9 ± 2.2 mmHg, without a significant change in the final mean number of 2.6 ± 1.5 medications (vs. 3.0 ± 0.2 pre-op, $P = 0.24$). The cumulative successes for the AGV group was 0.78 and for the GMS group was 0.67 with a similar rate of success based on the Kaplan-Meier survival functions ($P = 0.83$).

Conclusions: No difference was shown in the success rate between the AGV and GMS during 5 years of prospective follow-up. Both procedures were associated with similar IOP reduction and use of supplemental medical therapy at 5 years.

Commercial Relationships: Iris Moroz, None; Shlomo Melamed, Solx (F), Eyetechnicare (F), Ioptima (F), Allergan (F); Oded Sagiv, SOLX Ltd, Boston, Massachusetts, USA (F); Guy J. Ben Simon, None; Modi Goldenfeld, None; Alon Skaat, None

Support: SOLX Inc

Clinical Trial: NCT00382395

Program Number: 4746 **Poster Board Number:** D0130

Presentation Time: 11:00 AM - 12:45 PM

Graft-free Ahmed valve implantation through a 6mm scleral tunnel

Kailun Jiang¹, Gdih Gdih². ¹The Ottawa Hospital, Ottawa, ON, Canada; ²University of Manitoba, Winnipeg, MB, Canada.

Purpose: To evaluate the safety, efficacy, and cost benefit to the health care system of Ahmed glaucoma valve (AGV) tube implantation through a 6mm scleral tunnel (graft-free technique).

Methods: Retrospective chart review (12-month follow-up) from a single clinical setting. Preoperative ocular medications, intraocular pressure (IOP), and visual acuity were compared to values recorded at each follow-up exam. The 95% confidence interval for fractional survival at any particular time was calculated using the Kaplan-Meier method. Failure was defined as:

1. IOP < 6 mmHg or IOP > 21 mmHg on 2 consecutive visits after 3 months
2. Additional surgical intervention to control IOP
3. No light perception (NLP)

Eye banks across Canada were surveyed for cost incurred by the health care system for providing scleral tissue used in conventional AGV implantation.

Results: 84 eyes were implanted using the graft-free method with a success rate of 89.7% at 6-month. 6 eyes failed: 3 NLP, 1 persistent hypotony, 1 secondary AVG, 1 AGV extraction. The rate of hypotony peaked at 36% on post-operative-day (POD) 1, reducing to 20% by POD10 and 1.2% by 3 months. Clinical flat anterior chamber developed in 9.5% of eyes. 10% of eyes experienced a hypertensive phase (mean IOP= 27.22 mmHg). Preoperatively, eyes received on average 3 units of glaucoma medication. Postoperatively, 22 eyes required no medication for IOP control. Of the eyes requiring postoperative glaucoma medication, 40.5% restarted during week 3-4; an additional 23.8% of eyes were restarted 5-6 weeks post-operatively. By 6-month eyes were on average using 1.2-units of glaucoma medication. Hyphema was the most common (24%) early postoperative complication. The rate of conjunctival dehiscence within the first year is 1.2%. 4 eye banks from 4 provinces were surveyed for cost data. The cost of sclera ranged from \$116 to \$300 CAD. Using the graft-free technique, the cost of our surgical unit, excluding the cost of the valve, is 217% (\$1872 CAD) less than that of the conventional scleral-graft method. This reflects the reduced number of instruments and OR time required for the graft-free method.

Conclusions: Our data suggests that the safety and efficacy of a 6mm scleral tunnel is comparable to conventional scleral-graft method. The graft-free scleral tunnel not only removes the risk of prion

transmission, it simplifies and reduces procedural time and is a cost effective alternative to scleral-graft methods.

Commercial Relationships: Kailun Jiang, None; Gdih Gdih, None

Program Number: 4747 **Poster Board Number:** D0131

Presentation Time: 11:00 AM - 12:45 PM

The PLGA implant as an antimitotic delivery system after experimental trabeculectomy

Ignacio Rodriguez-Agirretxe^{1,2}, Sandra Vega³, Elena Vecino⁴, Javier Mendicutte², Fabiola Eder², Tatiana M. Suarez-Cortes³, Arantxa Acera³. ¹Glaucoma, ICQO, Bilbao, Spain; ²Glaucoma, Donostia Hospital, San Sebastian, Spain; ³Biofalmik SL, Derio, Spain; ⁴Cellular Biology, University of the Basque Country, Leioa, Spain.

Purpose: To investigate the effect of poly (lactic-co-glycolic acid) (PLGA) implants loaded with mitomycin C (MMC) and with different adjuvant treatments after glaucoma filtration surgery (GFS), in comparison to standard treatments.

Methods: Forty-two New Zealand White rabbits underwent bilateral GFS and received different treatments (left eye): topical MMC (group 1); topical 5-fluorouracil (5-FU) (group 2); PLGA implant (group 3); MMC-loaded and -coated PLGA implant (group 4); MMC-loaded and 5-FU-coated PLGA implant (group 5); subconjunctival bevacizumab (group 6); MMC loaded PLGA implant and subconjunctival bevacizumab (group 7) and no treatment (right eye of all animals) (group 8). Intraocular pressure (IOP) and filtering bleb were evaluated at 0, 1, 5, 7, 14, 21 and 28 days after GFS. Histology was performed to examine the conjunctiva, sclerotomy, filtering bleb and persistence of the implant.

Results: The best hypotensive results were achieved in the MMC-loaded and -coated PLGA implant group (group 4), which presented the lowest IOP values on days 1, 5, 7, 14 and 28 after GFS.

Excluding the implant groups, bleb survival was superior to controls in groups 1, 2 and lower in group 6. Group 7 presented greater extension, height and vascularization of the bleb. Epithelial thinning and lymphoplasmacytic infiltrate were observed in groups 1, 2, 4, 5 and 7. The rates of closure of the sclerotomy and bleb were 100% and 76% respectively and implant persistence was 95%.

Conclusions: MMC-loaded and -coated implants have optimal surgical results, followed by topical MMC application. In this experimental model, bevacizumab may be antagonistic to MMC.

Commercial Relationships: Ignacio Rodriguez-Agirretxe, None; Sandra Vega, BIOFALMIK S.L. (E); Elena Vecino, None; Javier Mendicutte, None; Fabiola Eder, None; Tatiana M. Suarez-Cortes, Biofalmik S.L. (E); Arantxa Acera, BIOFALMIK SL (E)

Support: Spanish Ministry of Science and innovation (PPT-010000-2009-30) and Grupos Consolidados Gobierno Vasco (IT437-10).

Program Number: 4748 **Poster Board Number:** D0132

Presentation Time: 11:00 AM - 12:45 PM

Corneal Endothelial Cells Loss After Trabeculectomy For Glaucoma

Juan A. Dios^{1,2}, Maybee E. Delgado², Vania V. Castro³.

¹Ophthalmology, Clinica Ricardo Palma, Lima, Peru;

²Ophthalmology, Hospital Alberto Sabogal Sologuren, Callao, Peru;

³Ophthalmology, Hospital Nacional Arzobispo Loayza, Lima, Peru.

Purpose: To study corneal endothelial cells changes after trabeculectomy with mitomycin C, performed for uncontrolled glaucoma and determine risk factors associated to adverse results.

Methods: Prospective, observational evaluation of changes in density and shape of the corneal endothelial cells in 59 eyes of 53 patients, who underwent trabeculectomy, in an academic center, during a one-year period. Intracameral anesthesia was not used, hyaluronic acid was injected to the anterior chamber to maintain it formed, and

removed it during the surgery. Central corneal endothelial cells were studied with specular microscopy at baseline and 1, 7, 15, 30, 60 and 120 days after surgery. Intraocular pressure (IOP), lens status, and presence of complications were analyzed. Statistical significance was evaluated with the Mann Whitney U test.

Results: Mean endothelial cell density (ECD) decreased 464 cells/mm² (17.86%) 30 days post surgery compared to baseline; and 563 cells/mm² (21.67%) at 120 days, these changes were statistically significant (p <0.001). Patients who achieved Total Success (IOP <18 mm Hg postoperatively) showed no significant decrease (17.01%) of ECD, in contrast to those with Partial Success or Failure (26.08% and 29.4%; p <0.001).

Greater ECD reduction was observed in patients with post-surgery hyphema or flat anterior chamber, compared with patients without complications (-1059 vs. -456 cells/mm²; p <0.001). ECD was also reduced in pseudophakic patients compared to those without prior cataract surgery (-571 vs. -405 cells/mm²; p <0.001).

Coefficient of variation (CoV) was statistically significant increased in nearly all patients, independent of the IOP value, complications and lens status.

Conclusions: Statistically significant ECD loss was observed in eyes after trabeculectomy with mitomycin C for glaucoma. The severity of this loss was associated with post-surgical time, poorly controlled IOP after trabeculectomy, post-operative complications (such as flat anterior chamber), and prior cataract surgery.

CoV was statistically increased in nearly all patients without risk factor associated. Our data supports the consideration of risk factors for corneal damage in deciding surgical management for glaucoma, trying to avoid surgical complications.

	Patients Number (%)	ECD Decrease At 120 days Median (%)	P (U-Mann Whitney) ECD	CoV Increase At 120 days (Median)	P (U-Mann Whitney) CoV
Total Success	46 (77.97%)	-441.02 (17.01%)	0.006	11.04	<0.001
Partial Success	7 (11.88%)	-750.14 (26.08%)	<0.001	19.85	<0.001
Failure	6 (10.17%)	-994.50 (29.4%)	<0.001	12.06	<0.001

Changes in endothelial cells density, related to postoperative intraocular pressure

Complications	Number (%)	ECD Pre surgery Median	ECD 120 days Median	ECD Variation Median	p (U-Mann Whitney)
None	22/59 (37.29%)	2647.67	2191.36	-456.31	0,018
Encapsulated bleb	0/59 (0)	-	-	-	-
Flat bleb	29/59 (49.15%)	2464	1968.41	-495.59	0,011
Shallow AC	1/59 (1.69%)	2598	1025	-1573	<0,001
Choroidal Detachment	2/59 (3.39%)	1864.5	1194.5	-470	0,013
Hemovitreus	1/59 (1.69%)	3780	1025	-2735	<0,001
Hphema	3/59 (5.08%)	2562.33	1503	-1059	<0,001
Seidel	5/59 (8.47%)	2172.4	2031.4	-141	0,103

Changes in endothelial cell density relative to postoperative trabeculectomy complications

Commercial Relationships: Juan A. Dios, None; Maybee E. Delgado, None; Vania V. Castro, None
Support: None in the Support field below.

Program Number: 4749 **Poster Board Number:** D0133

Presentation Time: 11:00 AM - 12:45 PM

Comparison of surgical outcomes between 360 degree catheter assisted and traditional 180 degree trabeculotomy in patients with congenital glaucoma

Monisha Mandalaywala Vora^{1,3}, Craig H. Marcus^{1,2}, Robert F. Rothman^{1,2}, Daniel D. Hayes^{1,2}, Allison Angelilli^{1,2}.

¹Ophthalmology, North Shore Long Island Jewish Medical Center, Great Neck, NY; ²Glaucoma Consultants of Long Island, Lake Success, NY; ³Hofstra School of Medicine, Lake Success, NY.

Purpose: To compare operative outcomes of patients after 360 degree catheter assisted with traditional trabeculotomy through 12 months follow up.

Methods: Retrospective, nonrandomized, comparative study of patients with congenital glaucoma seen by the Glaucoma Consultants of Long Island who underwent 360 degree catheter assisted or 180 degree trabeculotomy to control intraocular pressure (IOP) between April 2000 and July 2012. All surgeries were performed by one of the listed authors.

Results: We included 14 separate eye surgeries of 8 patients who underwent 360 degree trabeculotomy, and 7 eye surgeries of 5 patients who underwent 180 degree trabeculotomy. All 12 patients were followed for a minimum of 12 months. The absolute length of follow up was 7.4 (± 2.1) years in the 180 group and 1.3 (± 1.4) years in the 360 group. One patient had a 360 degree procedure in one eye and 180 degree in the fellow eye. No differences were found with respect to age at diagnosis ($P=0.02$) or at surgery ($P=0.49$), gender ($P=0.26$), right versus left eye ($P=1.00$). The mean percentage reduction in IOP from preop values at 12 months after surgery was 54.7% (± 19.4) for the 360 group compared with 49.6% (± 14.1) for the 180 group ($P = 0.70$). A higher percentage of patients treated with 360 versus 180 (57.1% vs. 35.7%) required postop medications, although this did not attain significance ($P=0.39$). Hyphema (7.1%) was the most common postop complication seen in patients undergoing 180-degree trabeculotomy. No complications were reported in the 360 degree group. Of the 14 surgeries in the 180 group, 5 required reoperation, which included Baerveldt glaucoma implant (2), a repeat 180 degree trabeculotomy followed by a trabectome (1), and deep sclerostomy/viscocalanostomy (2). Of the 7 surgeries included in the 360 group, 1 required reoperation (goniotomy). Failure was based on the absolute number of reoperations, since this may be more predictive in this population as compared to adults.

Conclusions: In our small study sample, both 360 degree catheter assisted and traditional 180 degree trabeculotomy achieve significant IOP reduction at 12 months for patients with congenital glaucoma. In our sample, 360 degree trabeculotomy had lower rates of reoperation as compared to the traditional 180. However, these results need to be confirmed by a prospective, randomized, longitudinal study.

Commercial Relationships: Monisha Mandalaywala Vora, None; Craig H. Marcus, None; Robert F. Rothman, None; Daniel D. Hayes, None; Allison Angelilli, None

Program Number: 4750 **Poster Board Number:** D0134

Presentation Time: 11:00 AM - 12:45 PM

Long term Intraocular Pressure Control Using Combined Endoscopic Cyclophotocoagulation (ECP) And Phacoemulsification in the Treatment of Mild to Moderate Glaucoma - 5 Year Results

Michael J. Siegel¹, Whitney Boling⁵, Omar S. Faridi⁶, Chirag K. Gupta³, Mark S. Juzych^{1,2}, Matthew Citron^{3,4}, Marc J. Siegel^{3,4}, Les I. Siegel^{3,4}. ¹Ophthalmology, Kresge Eye Institute, Detroit, MI; ²School of Medicine, Wayne State University, Detroit, MI; ³Ophthalmology, William Beaumont Hospital, Royal Oak, MI; ⁴Ophthalmology, Glaucoma Center of Michigan, Southfield, MI; ⁵Internal Medicine, Detroit Medical Center, Detroit, MI; ⁶Ophthalmology, Eye Physicians & Surgeons, PC of Connecticut, Milford, CT.

Purpose: The purpose of this study is to evaluate the long-term efficacy of Phacoemulsification combined with Endoscopic Cyclophotocoagulation in the treatment of mild-moderate glaucoma.

Methods: This was a retrospective, case-controlled, non-industry sponsored interventional study at one center from 2004-2012. Inclusion criteria included mild to moderate glaucoma of any type with or without medical therapy. Main outcome measures included intraocular pressure, glaucoma medication use and complications. Patients were excluded if they had severe glaucoma, prior phacoemulsification, cyclodestructive, filtering, or tube-shunt procedures. Evaluation was performed from baseline up to 66 months.

Results: The Mean baseline IOP in 261 eyes of 163 patients was 17.27 mmHg (± 0.29 SE). The mean IOP was significantly reduced at every time point from baseline to 66 months with the average IOP at month 66 (n=47) being 13.63 mmHg (± 0.41 SE). At baseline the mean number of glaucoma medications was 1.27 (± 0.35 SE) (median 1.00; range 1-4). After Phaco/ECP the number of medications to control IOP was significantly reduced at every time point from baseline to 66 months with the mean number of medications at 66 months (n=47) being 0.19 (± 0.05 SE). The number of eyes that had IOP spikes ≥ 10 mmHg within the first postoperative month was minimal. 21 eyes (8.3%) had 1 IOP spike, and 5 eyes (1.7%) had 2 IOP spikes.

Conclusions: This study shows a significant reduction in IOP from baseline up to 66 months with an average reduction in IOP of 21.1%. After undergoing ECP at the time of cataract surgery, patients on topical medication are 10.5 times more likely to be off of medications at 66 months from when compared to baseline. At 66 months, 60% of patients were able to maintain or decrease IOP without any increase in medication use and 50% of patients were able to achieve a minimum of 10% reduction of IOP with no increase in utilization of IOP lower medications. Although this study has limitations due to its retrospective and non-comparative nature, these results show effective control of IOP with less dependence on topical medications. Thus, ECP is a safe and simple procedure to use at the time of cataract surgery for the long-term control of mild-moderate glaucoma.

Commercial Relationships: Michael J. Siegel, None; Whitney Boling, None; Omar S. Faridi, None; Chirag K. Gupta, None; Mark S. Juzych, None; Matthew Citron, None; Marc J. Siegel, None; Les I. Siegel, None

Program Number: 4751 **Poster Board Number:** D0135

Presentation Time: 11:00 AM - 12:45 PM

Longitudinal Study of Corneal Endothelial Damage After Anterior Tube Shunt Surgery

Koichi ONO¹, Teruhiko Hamanaka², Satoshi Kimura¹. ¹Department of Ophthalmology, Juntendo Tokyo Koto Geriatric Medical Center, Juntendo University School of Medicine, Koto-ku, Japan; ²Department of Ophthalmology, Japanese Red Cross Medical Center, Shibuya-ku, Japan.

Purpose: To investigate the changes of corneal endothelial density (CED) at the central cornea and to determine risk factors.

Methods: Data on corneal endothelial density were reviewed for 49 patients (49 eyes, 241 measurements) who underwent anterior tube shunt surgery by a single surgeon at a single center. In addition to the age at surgery and sex, the type of tube used (Molteno vs. Baerveldt), postoperative period, length of tube in the anterior chamber, angle between tube and the corneal endothelium, tube insertion site (anterior vs. posterior to Schwalbe's line), and jet flow of aqueous humor (yes vs. no) were considered as risk factors for a decrease of central CED. Tube length and angle were measured by anterior

segment optical coherence tomography (AS-OCT). The tube insertion site was observed by gonioscopy and AS-OCT. We assumed that jet flow of aqueous humor would start just after release of the tube ligature (7-0 nylon) with an argon laser. Mixed-effect multiple linear regression analysis was employed to analyze unbalanced panel data. Institutional review board approval was obtained from the Japanese Red Cross Medical Center and this study was consistent with the Declaration of Helsinki.

Results: The mean postoperative period (\pm standard deviation) was 4.6 (\pm 2.9) years, with a mean of 4.9 (\pm 2.4) CED measurements. After adjusting for other variables, CED decreased significantly every year after surgery (β : -115.1 per year, 95% confidence interval (CI): -142.0 to -88.2). Factors associated with CED reduction were tube ligature release (β : -245.9, 95%CI: -417.1 to -74.7), tube angle (β : -16.2 per 1 degree with narrowing, 95%CI: -31.1 to -1.3), and tube position (β : -445.5, 95%CI: -829.7 to -61.3). In contrast, the age, sex, tube, and tube length did not show a statistically significant association with CED reduction.

Conclusions: Anterior tube shunt surgery is associated with a decrease of CED. Peripheral cell loss due to rubbing the cornea with a tube could stimulate endothelial migration and reduce the central CED. Jet flow of aqueous humor could also contribute to CED reduction.

Commercial Relationships: Koichi ONO, None; Teruhiko Hamanaka, None; Satoshi Kimura, None

Program Number: 4752 **Poster Board Number:** D0136

Presentation Time: 11:00 AM - 12:45 PM

Outcomes of combined glaucoma tube shunt and fluocinolone acetonide implant placement in uveitic patients compared to outcomes in uveitic and open angle glaucoma patients with glaucoma tube shunt placement alone

Daniel B. Moore, Sanjay Asrani. Ophthalmology, Duke Eye Center, Durham, NC.

Purpose: To determine whether the outcomes of patients with uveitic glaucoma were different when a fluocinolone acetonide implant was combined with an Ahmed glaucoma valve (AV) ("FA/AV") when compared to outcomes among patients with uveitic glaucoma or primary open angle glaucoma in whom an AV alone was placed ("uveitic AV" and "OAG AV", respectively).

Methods: A retrospective review was conducted of consecutive patients evaluated at the Duke Eye Center between 2009-2012. The primary outcome measure was surgical success, defined as intraocular pressure (IOP) between 5 and 18 mmHg and greater than 20% reduction of IOP at two consecutive visits without the need for additional IOP lowering, surgical procedure or removal of AV. Secondary outcome measures included IOP and number of glaucoma medications at the preoperative visit and postoperative months 1, 6, 12 and 24. Patients were excluded if they had undergone previous glaucoma surgery or if the AV was placed in the pars plana.

Results: A total of 95 eyes (22 FA/AV, 27 uveitic AV, 46 OAG AV) were included in the study. The mean time of surgical success was significantly greater in uveitic FA/AV (630 \pm 54 days) compared to uveitic AV (433 \pm 61 days) and OAG AV (375 \pm 51 days) ($p=0.0025$). There were no significant IOP or medication differences between the two uveitic groups at any post-operative visit. When compared to OAG AV, uveitic FA/AV had a significantly greater decrease in IOP at postop month 12 ($p=0.021$), while uveitic AV had a significantly greater decrease in IOP at all postoperative visits ($p<0.05$ all time points). There were significantly fewer medications required in uveitic AV as compared to OAG AV at 12 and 24 months postop ($p=0.033$ and 0.05). Inadequate IOP control was the predominant cause of failure in all groups.

Conclusions: FA combined with AV in eyes with uveitic glaucoma had a longer duration of surgical success than patients with uveitic glaucoma or OAG treated with AV insertion alone. Further, following AV placement, eyes with uveitic glaucoma had greater IOP control on fewer medications than eyes with OAG. These data should compel further investigation evaluating the expanded use of steroid implants in selected glaucomatous eyes undergoing placement of a drainage device.

Commercial Relationships: Daniel B. Moore, None; Sanjay Asrani, None

Program Number: 4753 **Poster Board Number:** D0137

Presentation Time: 11:00 AM - 12:45 PM

The effect of aqueous humour protein content and viscosity on equilibrium pressure under the scleral flap in trabeculectomies

Amir Samsudin^{1,2}, Ian Eames³, Steve Brocchini^{2,4}, Peng T. Khaw².

¹University of Malaya, Kuala Lumpur, Malaysia; ²NIHR Biomedical Research Centre at Moorfields Eye Hospital NHS Foundation Trust and UCL Institute of Ophthalmology, London, United Kingdom;

³UCL Department of Mechanical Engineering, London, United Kingdom;

⁴UCL School of Pharmacy, London, United Kingdom.

Purpose: To look at the influence of aqueous humour protein content and viscosity, which may increase in anterior chamber inflammation, on equilibrium pressure under the scleral flap in trabeculectomies.

The influence of suture numbers and scleral flap shapes was also investigated

Methods: Normal and uveitic aqueous humour were represented by plain BSS, BSS containing 300 mg/ 100 ml of albumin and BSS containing 3000 mg/ 100 ml of albumin. Porcine corneoscleral rims were mounted on a Barron artificial anterior chamber and chamber pressure was measured using a pressure transducer. 4 mm x 4 mm partial thickness scleral flaps and 0.75 mm diameter sclerostomies were created, followed by re-suturing of the flap with either 2 or 4 sutures, as in a trabeculectomy. Equilibrium pressure in the chamber was noted. The square scleral flaps were also compared with 4 mm x 3 mm rectangular and 4 mm x 4 mm triangular flaps. In all cases, $n = 8$. Statistical analysis involved the unpaired t-test and one-way ANOVA. $p < 0.05$ was considered statistically significant

Results: The relative viscosities were 1.02, 1.04 and 1.12 respectively, compared to 1.00 for distilled water [$p < 0.001$]). Equilibrium pressures were higher with 4 sutures than with 2 sutures ($p = 0.047$). There were no significant differences in equilibrium pressure between the different fluids and the different scleral flap shapes ($p > 0.05$)

Conclusions: Equilibrium pressures under the scleral flap are affected by the number of sutures but not by the different aqueous humour protein contents and viscosities encountered in anterior chamber inflammation, or by typical scleral flap shapes and sizes

Commercial Relationships: Amir Samsudin, None; Ian Eames, None; Steve Brocchini, None; Peng T. Khaw, University College Moorfields (P)

Support: Ministry of Higher Education, Malaysia; National Institute for Health Research (NIHR) Biomedical Research Centre at Moorfields Eye Hospital NHS Foundation Trust and UCL Institute of Ophthalmology, UK

Program Number: 4754 **Poster Board Number:** D0138

Presentation Time: 11:00 AM - 12:45 PM

Outcomes of Pars Plana Baerveldt Glaucoma Drainage Implant in Boston Type 1 Keratoprosthesis Surgery

Eun S. Huh, Ahmad A. Aref, Thasarat S. Vajaranant, Jose De la Cruz, Felix Y. Chau, Maria S. Cortina. Ophthalmology, Univ of Illinois Eye & Ear Infirmary, Chicago, IL.

Purpose: Glaucoma drainage implantation (GDI) in conjunction with Boston Type 1 Keratoprosthesis (KPro) placement is a surgical option in controlling postoperative glaucoma. The Ahmed FP-7 glaucoma drainage device implant (AGI; New World Medical, Inc., Rancho Cucamonga, California, USA) has been used with highest frequency in this patient population, as reported in literature. We hypothesize that combined pars plana vitrectomy with placement of a Baerveldt glaucoma drainage device implant (BGI; Abbott Laboratories, Inc., Abbott Park, Illinois, USA) in KPro patients is similarly effective compared to a pars plana placed AGI.

Methods: A retrospective review of 106 patients who underwent KPro from April 2007 to September 2012 was performed. Preoperative and postoperative parameters collected and analyzed included: visual acuity, intraocular pressure (IOP), number of glaucoma medications to achieve IOP control, and postoperative complications.

Results: Eleven and twelve eyes that underwent combined KPro and pars plana placed BGI or AGI, respectively, were identified. Seventy-five percent of the BGI eyes and 100% of the AGI eyes had preoperative diagnosis of glaucoma. Table 1 shows the preoperative and postoperative parameters of the AGI and BGI eyes.

Average follow-up was 9.6 months (± 9.5 , range, 1.8-35.8 months) for the BGI group and 34.2 (± 15.9 , range, 12.7-67.4 months) months for the AGI group. Two of the AGI eyes required subsequent BGI placement, with one also requiring cyclophotocoagulation (CPC), for better IOP control. Two eyes required AGI and KPro explantation, one due to fungal endophthalmitis from a corneal ulcer and the other due to hypotony from tractional retinal detachment. One of the BGI eyes required subsequent CPC for optimal IOP control. There were no erosions of the tube or plate in either AGI or BGI groups.

Conclusions: For the management of glaucoma in KPro patients, posteriorly placed pars plana BGI in conjunction with KPro has low rates of postoperative complications, including the need for additional glaucoma surgery.

TABLE 1: Comparison of AGI and BGI	
Preoperative visual acuity (logMAR)	2
Preoperative IOP (mmHG)	21
Preoperative number of medications	2
Postoperative visual acuity (logMAR)	0
Postoperative IOP (mmHG)	14
Postoperative number of medications	2

Commercial Relationships: Eun S. Huh, None; Ahmad A. Aref, None; Thasarat S. Vajaranant, None; Jose De la Cruz, alcon (C), amo (C); Felix Y. Chau, None; Maria S. Cortina, None

Program Number: 4755 **Poster Board Number:** D0139

Presentation Time: 11:00 AM - 12:45 PM

The Effect of Trabeculectomy on Astigmatism

Heleen Delbeke, Ingeborg Stalmans, Evelien Vandewalle, Thierry Zeyen. Ophthalmology, University hospitals Leuven, Leuven, Belgium.

Purpose: To investigate the change in corneal astigmatism after trabeculectomy.

Methods: Between January and April 2012 patients who underwent a primary trabeculectomy were included in this prospective study. We

measured visual acuity (VA), automated keratorefractometry, and intraocular pressure (IOP) pre- and postoperatively at month 1, 3 and 6. Changes in astigmatism were quantified using the vector analysis described by Cravy (Ophthalmic Surgery 1979; 10: 38-49). A Friedman test and a linear model for longitudinal measures were used to compare changes in refraction and IOP. A binomial test was used to compare the proportion of eyes with a shift of astigmatism with- or against the rule (WTR or ATR).

Results: Fifty two eyes (51 patients) were included. The mean (\pm SD) IOP decreased from 17.5 ± 5.41 mmHg preoperatively to 9.7 ± 3.96 mmHg after 6 months ($p < 0.001$). The mean logMAR VA was 0.17 ± 0.22 preoperatively and 0.14 ± 0.14 after 6 months ($p = 0.9$). After 6 months 32/47 eyes showed a shift of astigmatism WTR ($p = 0.02$). The median difference in cylinder after 6 months for all the eyes was $+0.5D$ (range 0-4D) ($p = 0.004$). The mean axis of the positive cylinder changed from $169^\circ \pm 148^\circ$ to $135^\circ \pm 146^\circ$ after 6 months ($p = 0.12$). The mean spherical equivalent changed from $-0.47D \pm 2.27D$ to $-0.07D \pm 1.93D$ ($p = 0.15$).

Conclusions: Trabeculectomy induced a small but statistically significant shift of astigmatism with the rule after 6 months. Spherical equivalent didn't change compared with preoperatively. Most often glasses will not need to be changed after trabeculectomy.

Commercial Relationships: Heleen Delbeke, None; Ingeborg Stalmans, None; Evelien Vandewalle, None; Thierry Zeyen, None **Clinical Trial:** NCT01711190

Program Number: 4756 **Poster Board Number:** D0140

Presentation Time: 11:00 AM - 12:45 PM

Initial Results of Treatment of Advanced Glaucoma with Ahmed Wing Valve

Jennifer Oakley¹, Cara Capitena¹, David W. Richards¹, William E. Layden². ¹University of South Florida, Tampa, FL; ²University Glaucoma Center, Tampa, FL.

Purpose: To compare the surgical and visual outcomes of standard Ahmed valve with a new "wing" Ahmed valve in the treatment of advanced glaucoma. The plate of the wing valve has a surface area of approximately 450 mm-sq compared to a surface area of 180 mm-sq for the standard Ahmed valve.

Methods: This was a retrospective nonrandomized comparative trial of 30 consecutive patients who underwent implantation of the Ahmed wing valve compared with an equal number of age and sex matched controls who had standard Ahmed valve implantation. All procedures were performed by a single surgeon (WEL). We compared vision and intraocular pressures preoperatively and at intervals of one day, one week, two weeks, six weeks, 10 to 12 weeks, 5 to 7 months, and 10 to 14 months. We also compared complication rates between the two groups.

Results: By Students t-test, requiring $p < 0.05$, intraocular pressures were statistically similar at all intervals except on postoperative day one when average IOP was 15 with the wing valve and 10.5 with the standard Ahmed valve ($p = 0.044$). At the 10 to 14 month time point, average IOP with the wing valve was 15 compared to 19 with the standard valve, although this was not statistically significant ($p = 0.099$). The number of major complications (exposed valve with revision, explanted valve, or second valve implant) was 6 for the wing valve and 5 for the standard valve.

Conclusions: Despite the larger surface area, the wing valve did not produce a statistically significant lower IOP at the one year time point. The rate of complications was similar.

Commercial Relationships: Jennifer Oakley, None; Cara Capitena, None; David W. Richards, None; William E. Layden, None

Program Number: 4757 **Poster Board Number:** D0141

Presentation Time: 11:00 AM - 12:45 PM

Comparison of the outcomes of Trabectome with Trabeculotomy with deep Sclerectomy - Ab Interno vs Ab Externo approach
MASAHIRO MAEDA^{1,2}, **Natsu Kondo**², **Kazunori Onuki**², **Asato Hasegawa**³. ¹University of California, Irvine, Irvine, CA; ²Gifu Red Cross Hospital, Gifu, Japan; ³Social Insurance Chukyo Hospital, Nagoya, Japan.

Purpose: To evaluate the outcomes of Trabectome and Trabeculotomy with deep Sclerectomy in Japanese patients.

Methods: This study is retrospective, non-randomized matched pair study. 20 eyes which had undergone trabeculotomy with deep Sclerectomy (TDS) were included in the study. 20 eyes from the Trabectome database were selected as the study group. Matching criteria included age, combined surgery performed such as phacoemulsification and type of glaucoma. The outcome measures recorded are intraocular pressure (IOP), glaucoma medications before and after surgery and the occurrence of post-operative secondary surgeries if any.

Results: At 12 months, mean pre-operative IOP and glaucoma medications were reduced from 27.5 ± 10.6 mmHg and 2.8 ± 1.0 to 15.7 ± 2.8 mmHg ($p < 0.01$) and 1.3 ± 1.3 ($p < 0.01$) respectively in Trabectome group. No patient required subsequent glaucoma surgeries. In TDS group, mean pre-operative IOP and glaucoma medications were reduced from 26.4 ± 7.9 mmHg and 3.1 ± 1.2 to 13.5 ± 3.7 mmHg ($p < 0.01$) and 2.1 ± 1.0 ($p < 0.01$) respectively at 12 months. One patient was required to undergo another trabeculectomy. There was no statistical significant difference between both groups in IOP ($p = 0.06$) and medications ($p = 1.0$) at 12 months.

Conclusions: Both TDS and Trabectome successfully lower IOP and the need for glaucoma medications. Trabectome is a viable alternative to TDS in Adult Japanese patients.

Commercial Relationships: MASAHIRO MAEDA, None; Natsu Kondo, None; Kazunori Onuki, None; Asato Hasegawa, None

Program Number: 4758 **Poster Board Number:** D0142

Presentation Time: 11:00 AM - 12:45 PM

Comparison of Surgical Outcomes of the Ex-PRESS Glaucoma Filtration Device with Mitomycin C in Phakic and Pseudophakic Eyes

Sarwat Salim, Jim Wan, Haiming Du. Ophthalmology, Hamilton Eye Institute, Memphis, TN.

Purpose: To compare the surgical outcomes of the Ex-PRESS glaucoma filtration device with mitomycin C in phakic and pseudophakic eyes.

Methods: This was a retrospective comparative case series of 76 eyes (40 phakic eyes and 36 pseudophakic eyes) that underwent placement of the Ex-PRESS glaucoma filtration device under a partial-thickness scleral flap for uncontrolled glaucoma. All pseudophakic eyes had prior clear-corneal phacoemulsification. All eyes received intraoperative mitomycin C at the time of Ex-PRESS implantation. The primary outcome measures were intraocular pressure, number of postoperative glaucoma medications, and surgical success. Surgical success was defined as intraocular pressure between 5 and 18 mmHg, with or without glaucoma medications, and without further glaucoma surgery or loss of light perception vision. Secondary outcome measures were intraoperative and postoperative complications.

Results: Average follow-up was 32.3 ± 7.9 (range, 15-47) months for phakic eyes and 29.0 ± 8.8 (range, 14.3-47) months for pseudophakic eyes. No significant difference was observed between phakic and pseudophakic eyes in mean intraocular pressure, change from baseline intraocular pressure, or adjunctive use of glaucoma

medications at 33 months follow-up. Surgical success by Kaplan-Meier survival analysis at 33 months was 80.00% for phakic eyes and 80.65% for pseudophakic eyes ($P = 0.94$). Reasons for surgical failure included increased IOP (three eyes, 3.9%), persistent hypotony with maculopathy (one eye, 1.3%), and further surgery (four eyes, 5.3%).

Conclusions: Surgical outcomes after insertion of the Ex-PRESS glaucoma filtration device were similar in phakic and pseudophakic eyes after prior clear-corneal phacoemulsification

Commercial Relationships: Sarwat Salim, Alcon (C); Jim Wan, None; Haiming Du, None

Program Number: 4759 **Poster Board Number:** D0143

Presentation Time: 11:00 AM - 12:45 PM

Ex-press mini-implant in the management of ocular hypertension secondary to silicon oil tamponade

Nicola Cardascia, Francesco Cantatore, Paolo Ferreri, Francesco Boscia, Luigi Sborgia, Giovanni Alessio. Ophthalmology, Università di Bari A Moro, Bari, Italy.

Purpose: To compare the success of patients with ocular hypertension, secondary to pars plana vitrectomy and silicon oil tamponade, who had an Ex-press mini glaucoma shunt device implantation (Alcon Laboratories, Inc. Fort Worth, Texas, USA) to those who had conventional trabeculectomy.

Methods: Retrospective study. The records of 10 eyes of 10 consecutive subjects who had Ex-press implants and 9 eyes of 9 consecutive controls who had trabeculectomy procedures were reviewed. Success was defined as an intraocular pressure (IOP) reduction in patients who did not require further glaucoma surgery in the eye of note.

Results: IOP reduced of 10.3 ± 9.7 mmHg (range -31 to 3) in the Ex-press group and of 13.9 ± 11.4 mmHg (range -35 to -4) in the trabeculectomy group. The difference in the percentage of IOP reduction between the standard trabeculectomy group (42.7%) and the Ex-PRESS group (35.9%) was statistically not significant ($P = .72$).

Conclusions: The Ex-PRESS device is at least as effective as the standard trabeculectomy in lowering the IOP of patients with hypertension secondary to pars plana vitrectomy and silicon oil tamponade. Even if the data further suggest that the Ex-PRESS device does not result in an overall greater percentage reduction in IOP than with trabeculectomy, this does not reach statistical significance.

Commercial Relationships: Nicola Cardascia, None; Francesco Cantatore, None; Paolo Ferreri, None; Francesco Boscia, None; Luigi Sborgia, None; Giovanni Alessio, None

Program Number: 4760 **Poster Board Number:** D0144

Presentation Time: 11:00 AM - 12:45 PM

Prospective morphological subconjunctive analysis by spectral domain optical coherence tomography of blebless glaucoma surgeries

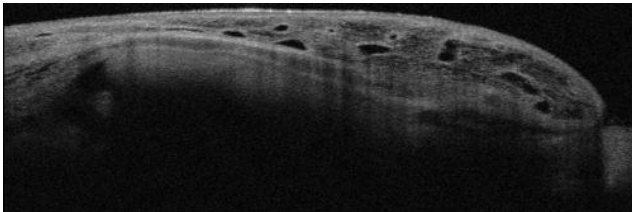
J. Aritz Urcola^{1,2}, *Cristian Dalmasso*¹, *Javier Cabrerizo*¹, *Amaia Latorre*³. ¹Ophthalmology, Hospital Universitario Araba, Vitoria-Gasteiz, Spain; ²Ophthalmology, Begitek Clínica Oftalmológica, Donostia-San Sebastián, Spain; ³Research and development, Hospital Universitario Araba, Vitoria-Gasteiz, Spain.

Purpose: To provide by prospective spectral-domain anterior segment optical coherence tomography (AS-OCT) assessment, morphological details of blebless filtering glaucoma surgeries (nonpenetrating deep sclerectomy (NPDS) and combined phacoemulsification + NPDS) and analyze the correlation of intraocular pressure (IOP) reduction with any of the OCT parameters.

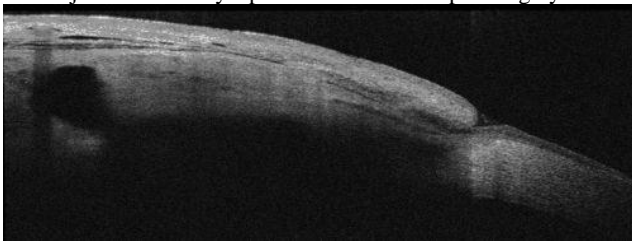
Methods: A total of 111 eyes were included in this study. All surgeries were performed with antimetabolite agent (mitomycin C 0.2 mg/ml) avoiding any scleral implant. 69 NPDS and 42 combined phacoemulsification + NPDS. IOP and morphological bleb features were prospectively analyzed by AS-OCT in 1 week, 1, 3, 6 and 12 months follow-up. Blebs were imaged with a commercially available AS-OCT system and the presence or absence of 3 qualitative parameters was analyzed: subconjunctival microcysts (SMC), posterior episcleral fluid (PEF) and anterior episcleral fluid (AEF).

Results: Postsurgical prospective analysis by AS-OCT of the bleb morphological features at each time point shows statistical differences in the frequency of these parameters. Presence of SMC, PFE decays progressively in first 6 months (from 82.7% and 85.3% in first week to 28.9% and 51.1% in 6 month follow-up respectively); whereas presence of AEF shows a converse evolution beyond the third month. It is present only in 4.8% of surgeries in first week and in 77.8% of cases in 6 month follow-up. Intraocular pressure and medication use reduction in all eyes were significantly decreased from baseline (IOP 23.8 ± 7.4 mm Hg) at every time point ($p < .001$) with a mean IOP of 15.5 ± 4.3 mm Hg in 12 month postoperative follow up. Nevertheless, greater IOP reduction levels were not statistically correlated with any of the 3 qualitative bleb parameters analyzed in each of the follow-up.

Conclusions: AS-OCT is a useful tool for the assessment of the filtering function in blebless glaucoma surgeries as NPDS and phacoemulsification + NPDS. Morphological features of the filtering bleb changes dynamically in the first months of the glaucoma surgery and to monitor by new imaging techniques permits a comprehensive study of the ocular tissues responses to the wound healing process.



Subconjunctival microcyst present at first week postsurgery



Fluid accumulation posterior to scleral flap edge present at first month postsurgery

Commercial Relationships: J. Aritz Urcola, None; Cristian Dalmasso, None; Javier Cabrerizo, None; Amaia Latorre, None
Support: Gobierno Vasco N0 exp 2011111135

Program Number: 4761 **Poster Board Number:** D0145

Presentation Time: 11:00 AM - 12:45 PM

Refractive outcome after phacoemulsification following trabeculectomy

Oliver L. Yeh, Philip P. Chen. Ophthalmology, University of Washington, Seattle, WA.

Purpose: To evaluate postoperative refraction in patients undergoing phacoemulsification after trabeculectomy

Methods: We reviewed the records of 86 eyes (72 patients) with glaucoma previously treated by trabeculectomy which subsequently

underwent phacoemulsification by one surgeon (PC) between November 1999 and December 2011. Preoperative, intraoperative, and postoperative data were collected, including intraocular pressure (IOP) and refraction, ophthalmic biometry, predicted refraction, and postoperative refraction.

Results: The mean patient age at phacoemulsification was 67.5 ± 12.9 years, with a mean time between trabeculectomy and phacoemulsification of 73 ± 98 months. The mean IOP was 12.0 ± 5.7 mmHg preoperatively on 0.5 ± 1.1 medications, and 11.4 ± 4.4 mmHg on 0.7 ± 1.1 medications at month 6 postoperatively. The median visual acuity was 20/40 preoperatively, and 20/20 at month 6 postoperatively. The average difference between the last postoperative manifest refraction and the predicted refraction was $+0.025D$. The difference between manifest and predicted refraction was $> 1D$ in 37 eyes (large-difference, or LDiff group). The only significant pre- or intra-operative risk factor for LDiff was preoperative IOP, which was lower in the LDiff group (10.6 ± 4.6 vs 13.3 ± 6.4 mmHg, $P = .041$). Non-significant risk factors included age, preoperative refraction, number of preoperative glaucoma medications, axial length, type of biometry, formula used for intraocular lens calculation, and presence of an IOP spike postoperatively.

Conclusions: Lower pre-operative intraocular pressure is associated with a larger difference in final refraction in eyes having phacoemulsification after trabeculectomy.

Commercial Relationships: Oliver L. Yeh, None; Philip P. Chen, Allergan (C)

Support: D. Franklin Milam M.D. Fellows Support Fund; unrestricted grant from Research to Prevent Blindness

Program Number: 4762 **Poster Board Number:** D0146

Presentation Time: 11:00 AM - 12:45 PM

Long Term Outcomes of Filtration Surgery for Normal-Tension Glaucoma with Visual Field Progression at Low Intraocular Pressure

Scott K. Schultz, Shawn M. Iverson, Wei Shi, Joyce C. Schiffman, David S. Greenfield. Ophthalmology, Bascom Palmer Eye Institute, Palm Beach Gardens, FL.

Purpose: The purpose of this study was to examine the long-term outcome of glaucoma filtration surgery for progressive normal-tension glaucoma (NTG) at low intraocular pressure (IOP).

Methods: A retrospective chart review was conducted to identify NTG patients that underwent trabeculectomy with mitomycin C (MMC) between February 2006 and October 2010 for progressive visual field (VF) loss with preoperative intraocular pressure ≤ 15 mmHg during the 12-month period prior to surgery. All eyes had evidence of glaucomatous optic neuropathy and progressive VF loss, uncontrolled IOP on maximum medical therapy, and minimum postoperative follow-up of 12 months. Exclusion criteria consisted of age ≤ 18 , recorded IOP > 22 mmHg, ocular disease other than glaucoma, or prior incisional surgery except uncomplicated cataract extraction. Failure was defined as IOP reduction $< 20\%$ below baseline (criteria 1), $< 30\%$ (criteria 2), or $< 40\%$ (criteria 3) on two consecutive follow-up visits after 3 months, reoperation for glaucoma, or loss of light perception, and was assessed using Kaplan-Meier survival analyses.

Results: Thirty eyes of 28 patients (mean age 73 ± 8.7 years) were enrolled with a mean follow-up period of 50 ± 31 mos. Mean postoperative IOP (8.3 ± 3.2 mmHg) and number of medications (0.6 ± 1.00) at final follow-up was significantly ($p < 0.001$) reduced compared to prior to surgery (13.2 ± 1.4 mmHg and 2.5 ± 1.2 , respectively). The cumulative probability of failure during 5 years of follow-up was 35% (criteria 1), 46%, (criteria 2), and 65% (criteria

3). Hypotony (IOP ≤ 5 mmHg on two consecutive follow-up visits after 3 months) was observed in 10 eyes. One eye developed clinical evidence of chorioretinal folds in the macula. Mean change in logMAR visual acuity in eyes (n=10) with hypotony (-0.14 ± 0.18), was not significantly different ($p=0.37$) than eyes (n=20) without hypotony (-0.04 ± 0.28). Other complications included CME (3), bleb leakage (2), endophthalmitis (1), blebitis (1), corneal edema (1), and choroidal effusion (1).

Conclusions: Trabeculectomy with MMC is an effective method for achieving long-term IOP reduction of 20-40% in NTG eyes with progression at low IOP. Hypotony is a common postoperative occurrence but did not result in a significantly greater degree of vision loss compared to the patients without hypotony in this series.

Commercial Relationships: Scott K. Schultz, None; Shawn M. Iverson, None; Wei Shi, None; Joyce C. Schiffman, None; David S. Greenfield, National Eye Institute (R), Carl Zeiss Meditec (R), Optovue (R), Heidelberg Engineering (R), Allergan (C), Alcon (C), Merz (C), Quark (C), SOLX (C), Biometric Imaging (C), Senju (C)

Program Number: 4763 **Poster Board Number:** D0147

Presentation Time: 11:00 AM - 12:45 PM

Corneal Endothelial Cell Density and Filtration Surgery in Patients with Posner-Schlossman Syndrome

Yuko Maruyama¹, Kazuhiko Mori¹, Morio Ueno¹, Yoko Ikeda¹, Kazuichi Maruyama², Shigeru Kinoshita¹. ¹Ophthalmology, Kyoto Prefectural Univ of Med, Kyoto, Japan; ²Ophthalmology, Tohoku University Graduate School of Medicine, Sendai, Japan.

Purpose: In some cases of Posner-Schlossman syndrome (PSS), corneal endothelial cell (CEC) density in the afflicted eye was lower than that of the healthy eye. Trabeculectomy (TLE) is necessary for controlling intraocular pressure (IOP) that cannot be managed with drug medications. The purpose of this present study was to analyze the correlation between percentage of CEC reduction and necessity of TLE in patients with PSS.

Methods: This study involved 19 eyes of 19 glaucoma patients (10 females, 9 males; mean age: 51.5 ± 20.7 years; mean follow-up: 2.6 ± 1.6 years) diagnosed as PSS at the glaucoma and uveitis clinic of Kyoto Prefectural University of Medicine, Kyoto, Japan. PSS was diagnosed based on having recurrent unilateral episodes of elevated intraocular pressure, mild anterior chamber inflammation with a few keratic precipitates and excluding other uveitic diseases. We retrospectively investigated the patient data of CEC density measured by specular microscopy. CEC reduction rate in the afflicted eye was defined as follows: (healthy-eye CEC density - afflicted-eye CEC density) / healthy-eye CEC density $\times 100$ (%). The cases were divided into 2 groups in relation to mean CEC reduction rate (CEC_RR high or CEC_RR low group), and the rate of patients who required TLE were then compared in these 2 groups. The frequency of events, such as IOP elevation or inflammatory attack, between 1-year pre- and postoperative periods in the cases that required filtering surgery was also compared.

Results: Of the 19 patients, there were 9 cases of CEC_RR high (CEC reduction $> 23.3\%$) and 10 cases of CEC_RR low (CEC reduction $< 23.3\%$). Seven cases (78%) required TLE in the CEC_RR high group, while only 1 case (10%) in the CEC_RR low group ($p=0.0055$, Fisher's exact test). The frequency of inflammatory events was reduced to 0.2 ± 0.1 times/year in the period of the following surgery, while 4.9 ± 0.5 times/year in the period of preceding surgery ($p<0.0001$, Student's t-test).

Conclusions: The findings of this study show that the cases of high corneal endothelial cell reduction rate tend to be drug resistant and require trabeculectomy.

Commercial Relationships: Yuko Maruyama, None; Kazuhiko Mori, Ocular Instruments, Inc. (P), Santen Pharmaceutical Co., Ltd. (P); Morio Ueno, None; Yoko Ikeda, None; Kazuichi Maruyama, None; Shigeru Kinoshita, Senju Pharmaceutical Co (P), Santen Pharmaceutical Co (P), Otsuka Pharmaceutical Co (C), Alcon (R), AMO (R), HOYA (R)

Program Number: 4764 **Poster Board Number:** D0148

Presentation Time: 11:00 AM - 12:45 PM

A Comparison of Sequential Glaucoma Drainage Device Implantation versus Cyclophotocoagulation Following Failure of a Primary Drainage Device

Joshua Levinson, Annette Giangiacomo, Allen D. Beck, Paul B. Pruet, Anastasios Costarides. Ophthalmology, Emory University, Atlanta, GA.

Purpose: To compare implantation of a sequential glaucoma drainage device (GDD) with trans-scleral cyclophotocoagulation (CPC) for intraocular pressure (IOP) control following failure of a primary GDD.

Methods: A retrospective chart review was performed for all patients who underwent GDD implantation at a single institution over ten years. Patients who required an additional GDD and/or CPC were identified and included for analysis. Success was defined as an absence of all of the following: loss of light perception, reoperation for glaucoma, and IOP >21 or < 6 at two consecutive visits after an initial three month period.

Results: Thirty-two patients had a sequential GDD implanted, and 21 patients underwent CPC. These patients were statistically similar in regards to age, sex, race, glaucoma diagnosis, and number of previous incisional surgeries. The GDD cohort had a significantly lower pre-operative IOP (27.8 vs 33.2 mmHg, $p=0.0275$) and better LogMAR visual acuity (0.94 vs 1.41, $p=0.0299$). The mean length of follow-up was 37.9 months for the GDD group and 46.3 months for the CPC group. Both procedures significantly reduced IOP between the pre-operative and final visits. IOP decreased 40.7% ($p<0.0001$) in the GDD group and 56.3% ($p<0.0001$) in the CPC group. Success occurred in 62.5% (20 of 32) of the GDD group and 52.4% (11 of 21) of the CPC group. In survival analysis of the GDD and CPC groups, mean survival time was 61.5 and 62.2 months, respectively ($p=0.873$). There were 2 cases of endophthalmitis (2 of 32, 6.3%) in the GDD group, and none in the CPC group. Both cases were associated with exposure of the GDD through the conjunctiva. Corneal decompensation and/or graft failure was more likely to occur in patients undergoing additional GDD implantation (9 of 31, 29.0% vs 1 of 19, 5.3%, $p=0.011$).

Conclusions: The implantation of a sequential GDD and CPC are both effective means of reducing IOP in patients with refractory glaucoma following the failure of an initial GDD. CPC has traditionally been used in eyes that are considered poor candidates for surgery or those with poor visual potential. CPC after primary GDD failure warrants further investigation for use in eyes with preserved vision as it may provide similar IOP-lowering effects without exposing patients to the risks associated with intraocular surgery and implantation of an additional foreign body.

Commercial Relationships: Joshua Levinson, None; Annette Giangiacomo, None; Allen D. Beck, None; Paul B. Pruet, None; Anastasios Costarides, None

Program Number: 4765 **Poster Board Number:** D0149

Presentation Time: 11:00 AM - 12:45 PM

Retrobulbar Shunt (RS) for Encapsulated Blebs

Sylvia L. Groth¹, William E. Sponset². ¹University of Minnesota Medical School, Minneapolis, MN; ²University of Texas - San

ARVO 2013 Annual Meeting Abstracts by Scientific Section/Group – Glaucoma

Antonio, Biomedical Engineering; WESMDPA Glaucoma Service, San Antonio, TX.

Purpose: Loss of filtration with fibrotically encapsulated blebs has been a longstanding clinical dilemma, eventually affecting up to 20% of eyes undergoing traditional tube shunt procedures. In this series of eyes with encapsulated blebs refractory to other therapy a new wide-bore silicone secondary shunt resembling a “French drain” was implanted to deliver entrapped aqueous from the impervious bleb into the retrobulbar space. This study evaluates the efficacy of this new retrobulbar shunt (RS).

Methods: 13 eyes with chronic bleb encapsulation and uncontrolled ocular hypertension underwent implantation of an RS silicone retrobulbar shunt. The device was used in tandem with existing Ahmed or Baerveldt tube shunts. A unique arrowhead flange locked the implant into the bleb, further secured via tabbed eyelets, directing the tubing into the retrobulbar space.

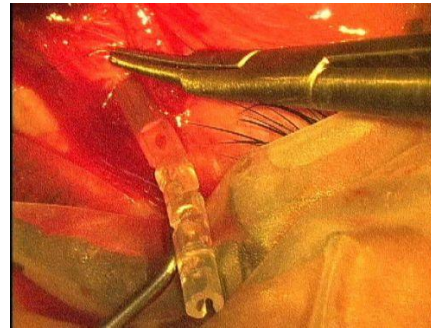
IOP and antiglaucoma medications were compared with pre-op levels 1 wk, 1 mo, 2 mo, 6 mo, 12 mo and 18 mo post-op (paired t-test).

Results: There were 5M/8F of mean age 61.5±2.9 yrs. Mean pre-op IOP was 31.5±2.8 mmHg on 2.7 ±0.4 medications. Mean IOP at the 6 post-op intervals was 10.9, 12.9, 13.3, 12.9, 14.0 and 16.5 (mean Δ-15.0 mm Hg (-48%); P=0.01), using 0, 0, 0.33, 0.18, 0.43 and 0.5 medications (mean Δ -2.2 meds (-81%); P=0.01). Viscoelastic reformations were required for several eyes post-op.

Conclusions: Encapsulated blebs have compromised glaucoma treatment for thousands of patients, a majority of whom were left with few effective alternative therapeutic options. With insertion of this retrobulbar shunt, the previously redundant bleb can be converted into a compressible cystern, resurrecting seton function by allowing transfer of aqueous into the retrobulbar space. Orbital fat acts as a one-way flow modulator for the multiple drainage ports in the large-bore RS silicone tubing. Since the original small-tubed ±valved shunt remains in situ, there is minimal risk of hypotony or hyphema. The high sulcus RS surgical insertion also minimizes risks of exposure or infection. Among these 13 eyes the RS was highly effective in substantially reducing IOP and medication requirement.



RS tube before implantation (above) and placed atop an Ahmed tube shunt in the orientation it would occupy in the eye (below). Note the large relative diameter of the RS tube.



RS in the bleb being sutured down before inserting posterior end into retrobulbar space.

Commercial Relationships: Sylvia L. Groth, None; William E. Sponsel, New World Medical (P)

Program Number: 4766 **Poster Board Number:** D0150

Presentation Time: 11:00 AM - 12:45 PM

The outcome of two different tube ligation methods in Baerveldt implant surgery

Shuri Kawamorita¹, Teruhiko Hamanaka¹, Tetsuro Sakurai².

¹Japanese Red Cross Medical Center, Tokyo, Japan; ²Tokyo University of Science Suwa, Nagano, Japan.

Purpose: We retrospectively investigated the complications and results of two different tube ligation methods: releasable suture ligation using 8-0 polyglactin (group A) and unreleasable suture ligation using 7-0 nylon (group B), three months after Baerveldt implant surgery.

Methods: After excluding the eyes with combined surgery of trabeculectomy (24 eyes), stent methods (1 eye) and complication of tube or plate exposure (5 eyes), 70 eyes of 67 patients were used for this study. The surgery was performed by a single surgeon (TH). Groups A and B were composed of 20 eyes of 18 patients and 50 eyes of 49 patients, respectively. In group A, the tube was ligated within 5 mm before the plate. In group B, the tube was ligated 2 mm from the tip of the tube and inserted into the anterior chamber, and then the tube was released using an argon laser when the intraocular pressure (IOP) exceeded 21 mmHg. Ocular hypertension, hypotension and cilio-choroidal detachment were reviewed for three months after the surgery. This study was approved by the IRB of the Japanese Red Cross Medical Center.

Results: High IOP occurred significantly more often in group B (p=0.035), but the success rates did not differ significantly between the two groups (p=0.389).

Conclusions: Both ligation methods were revealed to be useful, but the unreleasable suture method should not be used for eyes with severely advanced glaucoma.

Group	HYP0 during 3M	HYP0 at 3M	OHT during 3M	OHT at 3M	CCD at 3M	Success: eyes (rate)
A	5 (25%)	0 (0%)	7 (35%)	0 (0%)	2 (10%)	19 (95%)
B	14 (28%)	1 (2%)	32 (64%)	3 (6%)	0 (0%)	40 (80%)
p value	1.000	1.000	0.035	1.000	0.079	0.389

results

Commercial Relationships: Shuri Kawamorita, None; Teruhiko Hamanaka, None; Tetsuro Sakurai, None

Program Number: 4767 **Poster Board Number:** D0151

Presentation Time: 11:00 AM - 12:45 PM

Tube Shunt versus Trabeculectomy Surgery in Patients with Glaucoma Associated with Ocular Inflammation

Cecilia S. Lee, Aaron Y. Lee, Anjali Bhorade, Humeyra Karacal. Ophthalmology, Washington University in St. Louis, St. Louis, MO.

Purpose: To compare the surgical outcomes of tube shunt versus trabeculectomy with antimetabolite surgery in patients with glaucoma associated with ocular inflammation.

Methods: We retrospectively reviewed charts of all patients with a diagnosis of uveitic or steroid induced glaucoma at Washington University at St. Louis. Included patients were those with uveitis or steroid use prior to glaucoma onset, a primary tube shunt or trabeculectomy surgery, and ≥ 3 months follow-up after surgery. Cox regression model and Kaplan Meier survival analysis were conducted to determine risk of surgical failure with respect to time in the tube vs. trabeculectomy groups. Surgical failure was defined as IOP > 21 mmHg at >2 consecutive post-operative visits, any additional glaucoma procedures, loss of light perception, and complications secondary to hypotony. Covariates included were age, race, gender, pre-operative IOP, pre-operative number of glaucoma medications, perioperative use of steroids or systemic immunosuppressants, anterior segment involving uveitis, and combined surgery with cataract extraction.

Results: Of the 509 patient charts reviewed, 58 eyes of 42 patients (mean age of 55 years) met inclusion criteria. Median follow-up time was 85.0 months (5.8 - 200.6 months). There were 30 cases of tube shunts (53%) (16 Ahmed, 14 Baerveldt) and 28 cases of trabeculectomy with mitomycin (47%) (2 with Ex-Press shunts). The two most common etiologies of ocular inflammation were idiopathic (33, 55.9%), followed by sarcoidosis (12, 20.3%). Demographics and pre- and post-operative variables are displayed in Table 1. After controlling for covariates with p<0.1 (anterior involving uveitis, combined surgery, and race), tube shunts trended towards a 44.4% lower risk of surgical failure (HR: 0.56 95% CI: 0.21 to 1.49) and had a lower sustained risk of time to failure compared to the trabeculectomy group (Figure 1).

Conclusions: Tube shunt surgeries may have a lower risk of surgical failure compared to trabeculectomy surgery in patients with glaucoma associated with ocular inflammation.

	Tube Shunt (n = 30)	Trabeculectomy (n = 28)	p value
Mean age (years)	56.3	53.5	0.51
Female gender (n, %)	27 (90.0%)	20 (71.4%)	0.10
African American Race (n, %)	20 (66.7%)	10 (35.7%)	0.03*
Right eye (n, %)	15 (50%)	15 (53.6%)	0.80
Mean pre-op IOP (mmHg)	32.4	32.2	0.95
Mean post-op IOP (mmHg)	14.0	13.0	0.44
Mean # pre-op medications	3.37	3.04	0.18
Mean # post-op medications	1.30	0.96	0.34

Table 1. Demographics and pre- and post-operative variables in tube shunt vs. trabeculectomy surgery groups. (Post-operative IOP was defined as mean IOP at 2 consecutive visits 1-year post-op; *p < 0.05)

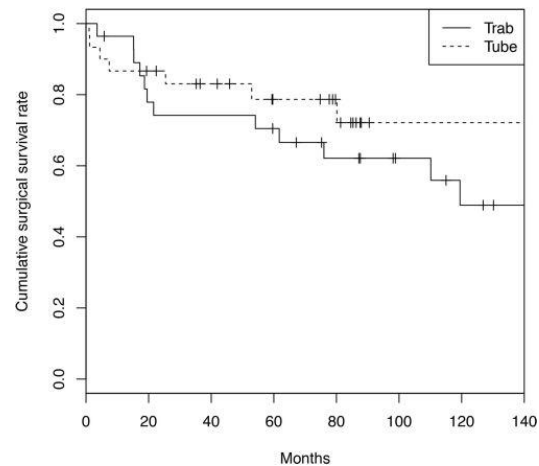


Figure 1. Kaplan-Meier survival curve showing the proportion of surgical survival in the tube shunt versus trabeculectomy groups.

Commercial Relationships: Cecilia S. Lee, None; Aaron Y. Lee, Cogent 14 Productions LLC (threeplus.org) (P); Anjali Bhorade, None; Humeyra Karacal, None

Support: Unrestricted Grant from Research to Prevent Blindness and the NIH Vision Core Grant P30 EY02687

Program Number: 4768 **Poster Board Number:** D0152

Presentation Time: 11:00 AM - 12:45 PM

Foreign Body Reaction in Glaucoma Drainage Implant Surgery

Kyoung In Jung, Chankee Park. Department of Ophthalmology and Visual Science, Seoul St. Mary's Hospital, College of Medicine, The Catholic University of Korea, Seoul, Republic of Korea.

Purpose: To investigate the histopathology of the foreign body reaction (FBR), and the effect of aqueous humor on it in glaucoma drainage implant surgery

Methods: A glaucoma drainage device (Ahmed glaucoma valve) was implanted into 20 New Zealand white rabbits. We monitored the histopathology of blebs at microscopic levels from 2-days to 8-weeks postoperatively. Hematoxylin and eosin staining, Masson's trichrome staining, anti-actin and α -smooth muscle immunofluorescence staining, and anti-proliferating cell nuclear antigen immunohistochemistry were performed. To observe effects of aqueous humor on FBR, we designed two implant models. One group received a plate with a tube placed in the anterior chamber (experimental group), while the other received the plate cut from the tube (control group).

Results: Foreign body giant cells were found along the inner border of blebs, and the innermost layer of bleb demonstrated a densely packed collagenous stratum in both groups. The number of foreign body giant cells was suppressed in the experimental group compared to the control group (P < 0.001). Fibroblast division was more active in the experimental group than in the control group. Masson's trichrome staining demonstrated that the innermost avascular collagenous layer was much thicker in the experimental group than in the control group (P = 0.021). The extent of α -SMA staining was greater in the experimental group than in the control group.

Conclusions: In the aqueous humor environment, wound healing around a glaucoma drainage implant revealed the unique FBR with the relatively small number of foreign body giant cells and reinforced fibrotic encapsulation.

Commercial Relationships: Kyoung In Jung, None; Chankee Park, None

Program Number: 4769 **Poster Board Number:** D0153

Presentation Time: 11:00 AM - 12:45 PM

An Engineering Model for Predicting the Aqueous Humor Flow Rate through the Natural Pathway Following Glaucoma Surgeries

Joseph Nelly Sugu Sugira, Matthew J. Rickard. College of Engineering, California Baptist University, Riverside, CA.

Purpose: To predict the aqueous humor flow rate through the natural pathway following glaucoma surgeries for various pre and post-operative conditions.

Methods: An engineering model has been developed for predicting the post-operative aqueous humor flow through the natural and surgically created pathways, where the latter can be a subconjunctival route initiated in glaucoma surgery such as a tube procedure (valve or valveless), a trabeculectomy, or a scleral mini-shunt operation. The model solves for the fluid flow parameters via analogy by solving equations commonly used in electrical circuit analysis. With the exception of the Ahmed Valve, the model assumes all resistances to be independent of the pressure differential across the resistor and all resistances are assumed unchanged with time. A steady outflow is assumed, which is driven by IOP (ignoring special behavior of the uveoscleral outflow). Resistance through the natural pathway, which is assumed to be the same both pre- and post-operative, is calculated using pre-operative IOP and by assuming all flow to pass through the natural pathway prior to surgery. To approximate the resistance of the Ahmed Valve (New World Medical, Model FP7), data was collected from a gravity-driven in vitro experiment using a low-flow liquid flow meter (Sensirion Inc.) and a pressure sensor (Honeywell).

Results: For a pre- and post-operative IOP of 30 mmHg and 10 mmHg, respectively, 13% of the total flow is predicted through the natural pathway post-operation for any external path procedure (valve/valveless tube, trabeculectomy, scleral mini-shunt, etc.), based on the assumptions of an episcleral venous pressure and aqueous humor flow rate of 7 mmHg and 2.5 μ L/min, respectively. For a post-operative IOP of 15 mmHg (all other conditions unchanged), 34% is predicted through the natural pathway. For the Ahmed Valve in the above 10 and 15 mmHg cases, the pressure downstream of the valve is predicted to be 1.6 and 7.1 mmHg, respectively. Since our model assumes the resistance in the natural pathway (TM, Schlemm's canal, collector channels) to be unchanged pre- and post-operation, our prediction of flow maintained in the natural path is further increased if that resistance is reduced during surgery.

Conclusions: Our engineering model predicts that the aqueous humor outflow through the natural pathway following Glaucoma surgery can be significant.

Commercial Relationships: Joseph Nelly Sugu Sugira, None; Matthew J. Rickard, None

Program Number: 4770 **Poster Board Number:** D0154

Presentation Time: 11:00 AM - 12:45 PM

Tube Exposures in Glaucoma Drainage Devices

Paramdeep S. Mand, Philip P. Chen, Mark A. Slabaugh. Ophthalmology, University of Washington, Seattle, WA.

Purpose: Tube exposure can be a devastating complication of glaucoma drainage devices (GDDs), but information on the causes of this complication is lacking. We examined patients who underwent repair of tube exposures at a tertiary hospital in hopes to help identify those patients at risk and to conjecture possible causes of exposure.

Methods: Retrospective chart review was completed in order to perform this case-control study. The charts of consecutive patients who underwent repair for exposure of tubes of glaucoma drainage devices from 5/2001-5/2012 and controls matched for time of follow-up since GDD surgery to time of implant exposure were analyzed. Clinical data and outcomes were collected. Statistical analysis was

performed using SPSS (Chicago, IL 2011), and statistical significance was set at $p < 0.05$.

Results: A total of 23 eyes with a GDD with tube erosions and 26 controls were identified. The mean age of those with tube exposures was 49.3 ± 20.9 vs. 60.9 ± 14.3 for the control group ($p=.032$). Number of previous surgeries in the study group was 3.6 ± 1.5 vs. 1.7 ± 2.1 for the control group ($p=.001$). Number of previous surgeries with a conjunctival incision was 2.5 ± 1.1 in the tube exposure group and 0.6 ± 0.6 in the control group ($p<.001$). The number of topical medications after surgery was 3.0 ± 1.9 in the study group and 1.7 ± 2.1 in the control group ($p=.038$).

Conclusions: This study suggests that a higher number of previous surgeries and postoperative topical medications place patients with a GDD at risk of having exposure of the draining tube.

Commercial Relationships: Paramdeep S. Mand, None; Philip P. Chen, Allergan (C); Mark A. Slabaugh, None

Support: Research to Prevent Blindness

Program Number: 4771 **Poster Board Number:** D0155

Presentation Time: 11:00 AM - 12:45 PM

THE EFFECT OF ADJUVANT MITOMYCIN C IN AHMED GLAUCOMA VALVE SURGERY FOR REFRACTORY GLAUCOMA

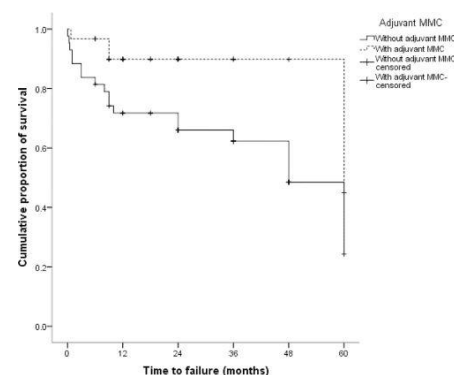
Melissa Tien, Leonard W. Yip, Elizabeth Poh Ying Wong, Vernon Yong, Hon Tym Wong, Boon Ang Lim. Ophthalmology, National Healthcare Group Eye Institute, Tan Tock Seng Hospital, Singapore, Singapore.

Purpose: To describe the efficacy and safety of adjuvant Mitomycin C (MMC) with glaucoma drainage device surgery in refractory glaucoma.

Methods: Retrospective case control study. Consecutive cases of Ahmed valve glaucoma (AGV) surgery performed during the study period were included. Surgery with or without adjuvant MMC was surgeon practice dependent. Patients' records were reviewed for clinical and demographic factors, treatments, intraocular pressure (IOP), visual acuity and any complications.

Results: A total of 74 eyes that underwent AGV implantation in Tan Tock Seng Hospital, Singapore, from 1st January 2001 to 31st December 2009 for refractory glaucoma. We found a statistically significant difference in success rates between patients receiving MMC and those without ($p=0.011$), with the MMC treated group being 4.86 times more likely to have success as compared to the non-MMC group (95% C.I: 1.45 - 16.34). There was no significant difference in complication rates between treatment groups.

Conclusions: The use of adjuvant MMC in AGV implantation is effective in improving overall surgical success in patients with refractory glaucoma.



Kaplan Meier Survival Curves: comparing treatment groups with and without MMC at 5 years

Commercial Relationships: Melissa Tien, None; Leonard W. Yip, None; Elizabeth Poh Ying Wong, None; Vernon Yong, None; Hon Tym Wong, None; Boon Ang Lim, None
Clinical Trial: 2008/00509

Program Number: 4772 **Poster Board Number:** D0156

Presentation Time: 11:00 AM - 12:45 PM

Repairing filtration bleb leakage with FocalSeal® in rabbit model

Tatsuo Nagata¹, Yukinori Harada¹, Hiroyuki Kondo¹, Mikki Arai^{2,3}, Akihiko Tawara¹. ¹Ophthalmology, University of Occupational and Environmental Health, Japan, Fukuoka, Japan; ²Arai Eye Clinic, Fukuoka, Japan; ³Schepens Eye Research Institute, Harvard Medical School, Boston, MA.

Purpose: The bleb leakage is regarded as a risk of bleb infection, which is one of the most serious complications after filtration surgery. There is no perfect way to stop the bleb leakage. Present study evaluated to close bleb leaks with a hydrogel sealant (FocalSeal®) in rabbits.

Methods: A fornix-based full-thickness filtration surgery with 24 gauge indwelling catheter and intraoperative mitomycin C was performed in each one eye of 6 New Zealand albino rabbits. After 1 week of the surgery, we perforated the bleb to make a 1.5 mm hole in the each filtration bleb. In three rabbits, the hole was covered using FocalSeal® with blue green light for 40 seconds. In the other three rabbits, we left the holes open. We checked the leakage with trypan blue. After 2 weeks of the first surgery, we checked the leakages of the six rabbits. After three weeks of the first surgery, the eyes were enucleated and examined histologically. In addition, we checked the intraocular pressures of both eyes with tonopen® for three weeks.

Results: In the three rabbits with FocalSeal® application, the bleb leaking stopped after the treatment, although the others did not stop bleb leakage. The intraocular pressures of the eyes closed with FocalSeal® were always lower compared with those of the non-closed bleb leak group. On histological examinations, the holes were closed with covering of the conjunctival epithelial cell in FocalSeal® group, though the holes were open in the other group. By Masson's trichrome, PCNA and α -SMA immunohistochemical staining, the bleb holes closed with FocalSeal® accompanied less inflammatory cells than the just perforated holes did.

Conclusions: In this study, the bleb leaks could be functionally closed with FocalSeal®. The results suggest that the bleb leak closure with FocalSeal® can be an additional way of it in the filtration surgery of human glaucoma.

Commercial Relationships: Tatsuo Nagata, None; Yukinori Harada, None; Hiroyuki Kondo, None; Mikki Arai, None; Akihiko Tawara, None

Program Number: 4773 **Poster Board Number:** D0157

Presentation Time: 11:00 AM - 12:45 PM

Ultrasound biomicroscopy findings after suprachoroidal cypass implant for glaucoma: one year follow-up

ELISA GONZALEZ PASTOR, Marta C. Bermudez, LAURA MORALES-FERNANDEZ, Jose M. Martinez de la Casa, Julian Garcia-Feijoo. Glaucoma, Hospital Clinico San Carlos, madrid, Spain.

Purpose: To evaluate the suprachoroidal space after CyPass (CP) implantation in patients with uncontrolled POAG.

Methods: Prospective observational study. Inclusion criteria: Patients with POAG who were candidates for glaucoma surgery (uncontrolled IOP on medical therapy). 24 eyes of 24 consecutive patients were included and underwent ab interno CP implantation. The CP (Transcend medical, CA) is a 6.25 mm long tube with a through lumen (outer diameter: 0.51 mm) designed to communicate

between the anterior chamber and the supraciliary space allowing the aqueous to reach the suprachoroidal space. UBM exams (UBM 840; Zeiss-Humphrey) were performed at 2 and 6 months and one year postop. Hourly scans of the angle and the pars plana were taken, radial and transversal scans of the area where the CP was implanted were also performed. We evaluated the presence of suprachoroidal fluid (hypoechoic space between the choroid and sclera) and peri-CP fluid (hypoechoic space between the CP and the surrounding tissue) with radial scans and the pars plana indentation by the CP (transversal scan). Study visits included measurements of IOP, however the UBM examiner has blinded to the IOP. Non parametric test were used to compare continuous variables, the Chi-square test was used to compare categorical variables.

Results: Baseline IOP: 20.9 SD 5.7. Mean number of topical drugs: 2.33 SD 0.7. Mean IOP at one month (all patients untreated): 15.4 SD 4.2. Mean IOP at six months: 14.95 SD 3.3. Mean number of drugs: 0.7 SD 0.9. Mean IOP at one year: 17.6 SD 3.4. Mean number of drugs: 1.1 SD 1.0. UBM detected fluid in the suprachoroidal space in 100% of the patients at two months (5 in four quadrants and all the other in the quadrant where the CP was implanted). At six months 54% (5 in four quadrants, 8 in one) and 33% at one year (only one patient had liquid in four quadrants). 100% had fluid around the CP at two months and 91.6% at six months. At one year only 13% had peri-CP fluid. Pars plana indentation was found in 6 patients in all exams. However transversal scans of the distal end of the CP could not be obtained in 3 patients.

Conclusions: UBM allowed us to detect peri-CP and suprachoroidal fluid short-term after CP implantation. The displacement of the dispositive or the scarring of the suprachoroidal space may be reasons for explaining lower effect of Cypass over time in some patients.

Commercial Relationships: ELISA GONZALEZ PASTOR, None; Marta C. Bermudez, None; LAURA MORALES-FERNANDEZ, None; Jose M. Martinez de la Casa, None; Julian Garcia-Feijoo, Trancend (C), Ivantis (C), Glaukos (C), MSD (C), Allergan (F), Pfizer (F), Alcon (C), Sensimed (F), Sylentis (F), Bausch and Lomb (C)

Program Number: 4774 **Poster Board Number:** D0158

Presentation Time: 11:00 AM - 12:45 PM

Complementary effects of bevacizumab and MMC in the improvement of surgical outcome after glaucoma filtration surgery

Tine Van Bergen¹, Karolien P. Hollanders¹, Davine Sijnave¹, Sarah Van de Velde¹, Evelien Vandewalle¹, Lieve K. Moons², Ingeborg Stalmans¹. ¹Lab of Ophthalmology, KU Leuven, Leuven, Belgium; ²Department of Biology, Zoological Institute, KU Leuven, Leuven, Belgium.

Purpose: Mitomycin-C (MMC) serves as the gold standard to reduce scar formation. It has impacted the success rate of glaucoma filtration surgery (GFS), but carries a risk of vision threatening complications. Antifibrotic agents, such as bevacizumab, also can improve surgical outcome. In this study, we first compared the effect of MMC versus bevacizumab on the surgical outcome of GFS. Secondly, we investigated the complementary effects of MMC and anti-VEGF therapy.

Methods: The effect of bevacizumab and MMC on surgical outcome was investigated in a mouse model of GFS. Immediately after surgery, mice were allocated into three groups (n=5/group). The 1st group received a subconjunctival (SC) injection of bevacizumab (1 μ l; 25 μ g); the 2nd group was treated during surgery with MMC (sponge soaked with MMC 0.02% for 2 minutes). Group 3 received a combination of MMC and a SC bevacizumab injection. Treatment outcome was studied by clinical investigation of bleb area every other

day. (Immuno)stainings were performed to study angiogenesis (CD31) and fibrosis (Sirius Red) on postoperative day 14. Vascular endothelial growth factor (VEGF) levels after MMC treatment were measured in rabbit aqueous humor (AH) samples by ELISA.

Results: SC injection of bevacizumab and MMC application were equally effective in improving surgical outcome. In both groups, bleb area was improved with $53 \pm 4\%$ ($P=0.17$) and blood vessel density ($37 \pm 4\%$; $P=0.44$) and fibrosis ($22 \pm 3\%$; $P=0.88$) were equally reduced after both treatments. Remarkably, one day after surgery, VEGF levels were significantly increased with $97 \pm 4\%$ in the AH of MMC-treated eyes ($P=0.04$). As compared to MMC monotherapy, combination of MMC and bevacizumab was able to increase bleb area with $18 \pm 6\%$ ($P=0.02$) by an additional reduction of angiogenesis ($54 \pm 4\%$; $P=0.002$) and fibrosis ($32 \pm 5\%$; $P=0.01$).

Conclusions: This study elucidates the potential benefit of bevacizumab to improve glaucoma surgery, in combination with the currently used antimetabolic agents. Our data indeed suggest that bevacizumab together with MMC may have complementary effects, due to upregulation of VEGF after MMC treatment.

Commercial Relationships: Tine Van Bergen, None; Karolien P. Hollanders, None; Davine Sijnave, Amakem therapeutics (F); Sarah Van de Velde, Amakem Therapeutics (F); Evelien Vandewalle, None; Lieve K. Moons, None; Ingeborg Stalmans, None

Program Number: 4775 **Poster Board Number:** D0159

Presentation Time: 11:00 AM - 12:45 PM

Ultrasonic Circular Cyclo Coagulation in patients with Primary Open-Angle Glaucoma: a Multicenter Clinical Trial

Florent Aptel¹, Philippe Denis², Jean-Francois J. Rouland³, Jean-Philippe Nordmann⁴, Yves M. Lachkar⁵, Jean-Paul G. Renard⁶, Eric Sellem⁷, Christophe Baudouin⁴, Alain M. Bron⁸. ¹Grenoble University Hospital, Grenoble, France; ²Hôpital de la Croix-Rousse, Hospices Civils de Lyon, Lyon, France; ³Hôpital Claude Huriez, CHRU de Lille, Lille, France; ⁴Centre Hospitalier National des Quinze-Vingts, Paris, France; ⁵Institut du glaucome, Fondation Hôpital Saint-Joseph, Paris, France; ⁶Hôpital d'Instruction des Armées du Val de Grâce, Paris, France; ⁷Centre Ophtalmologique Kléber, Lyon, France; ⁸Dijon University Hospital, Dijon, France.

Purpose: To evaluate the efficacy and safety of the Ultrasonic Circular Cyclo Coagulation (UC3) procedure.

Methods: Prospective non comparative interventional clinical study performed in 9 French glaucoma centers. Forty-two eyes of 42 patients with primary open-angle glaucoma (POAG), intraocular pressure (IOP) > 21 mmHg, an average of 1.65 failed previous surgeries and an average of 3.2 hypotensive medications were insonified with a therapy probe comprising 6 piezoelectric transducers. The 6 transducers were activated, 18 patients (group 1) were treated with a 4 seconds exposure time for each shot and 24 patients (group 2) with a 6 seconds exposure time. Complete ophthalmic examinations were performed before the procedure, and at 1 day, 1 week, 1, 2, 3, 6 and 12 months after. Primary outcomes were surgical success (defined as IOP reduction from baseline $\geq 20\%$ and IOP > 5mmHg) at the last follow-up visit, and vision-threatening complications. Secondary outcomes were mean IOP at each follow-up visits compared to baseline, medication use, complications, and re-interventions.

Results: IOP was significantly reduced in both groups ($p<0.05$), from a mean preoperative value of 28.6 ± 4.7 mmHg in group 1 and 28.1 ± 8.6 mmHg in group 2 to a mean value of 16.1 ± 2.8 mmHg in group 1 and 16.7 ± 4.4 mmHg in group 2 at last follow-up. Success (IOP reduction >20%) was achieved in 12 of 18 (67%) eyes of the group 1 and in 17 of 24 (71%) eyes of the group 2 at last follow-up. Four

patients were re-treated. No major intra- or post-operative complications occurred.

Conclusions: Ultrasonic Circular Cyclo Coagulation seems to be an effective and well-tolerated method to reduce intraocular pressure in patients with POAG.

Commercial Relationships: Florent Aptel, EyeTechCare (C); Philippe Denis, EyeTechcare (C), Alcon (C), Thea (C), Allergan (C), MSD (C); Jean-Francois J. Rouland, Thea (R), EyeTechcare (R); Jean-Philippe Nordmann, None; Yves M. Lachkar, None; Jean-Paul G. Renard, None; Eric Sellem, ALCON (C), ALLERGAN (C), MSD (C), THÉA (C), EYETECHCARE (C); Christophe Baudouin, None; Alain M. Bron, Allergan (C), Bausch Lomb (C), Horus (F), Théa (C)

Clinical Trial: NCT01338467

Program Number: 4776 **Poster Board Number:** D0160

Presentation Time: 11:00 AM - 12:45 PM

The Effect of Early Post-op Anti-Hypertensive Agents on the Hypertensive Phase following Ahmed FP 7 Glaucoma Valve Implantation, a Retrospective Review

Brenton Finklea, Ankur Gupta, Sandra M. Johnson. Ophthalmology, University of Virginia, Charlottesville, VA.

Purpose: This study investigates the effects of the early implementation of glaucoma medications on the incidence and severity of the hypertensive phase, as well the effect on long term intraocular pressure (IOP) control in patients status post Ahmed glaucoma valve implantation.

Methods: This is a retrospective, non-comparative case series of Ahmed glaucoma implant surgeries performed at the University of Virginia, between September 2008 and January 2012. To date, 75 patients have met inclusion criteria, of which 63 completed a minimum of 90 days of follow up. Absolute IOP as well as percentage relative to pre-operative baseline were recorded. Patients are divided into two groups. The Conventional Treatment Group (CTG) (n=44) included patients in whom glaucoma medications were initiated at the onset of the hypertensive phase (IOP >21 mmHg in the first 8 weeks post-op). The Interventional Treatment Group (ITG) (n=19) are patients in whom glaucoma medications are initiated at IOP <21 mmHg.

Results: CTG and ITG were similar with respect to age and gender distribution. Preoperative average IOP was similar between the CTG and ITG (35.3 vs 33.1) though number of pre-op medications were fewer in the CTG (3.23 vs 4.11). At post-op month 3, the absolute IOP and percentage of baseline for the CTG and ITG were 16.81/54% and 18.85/61%, respectively. At post-op month 6, these indices for the CTG and ITG were 20.69/59% and 17.82/54%, respectively. Patients in the ITG were given more glaucoma medications than those in the CTG at post-op month 3 (2.38 vs 1.19). At 6 months, there was a smaller difference in medications between the ITG and CTG (2.29 vs 1.73). Overall, 31.6% of patients in the ITG experienced a hypertensive phase, compared with 64% of patients in the CTG.

Conclusions: In this sampling, a significantly lower percentage of the ITG experienced a hypertensive phase compared to the CTG. In addition, the 6 month IOP was lower in the ITG, suggesting a positive impact of early introduction of glaucoma medications postoperatively for Ahmed glaucoma valve implantation. The ITG did continue to require 0.56 more glaucoma medications than the CTG at 6 months, but this is a slight decrease from the preoperative difference of 0.88. Further statistical analysis will be presented, as well as data on patients in our study who continue to meet end points.

Commercial Relationships: Brenton Finklea, None; Ankur Gupta, None; Sandra M. Johnson, Merck (C), Aquesys (C), SOLX (C)

Program Number: 4777 **Poster Board Number:** D0161
Presentation Time: 11:00 AM - 12:45 PM

A comparative study of combined trabeculectomy with ECCE/PCIOL versus Ex-press Shunt with ECCE/PCIOL

Farvah Fatima^{1,2}, Bret A. Hughes^{1,2}, Rominder Momi^{1,2}, Justin Tannir^{1,2}, Mark S. Juzych^{1,2}, Chaesik Kim^{1,2}, Manal H. Peracha^{1,2}, Alicia M. Eby^{1,2}, Melanie McQueen^{1,2}. ¹Wayne State University School of Medicine, Detroit, MI; ²Kresge Eye Institute, Detroit, MI.

Purpose: To compare the success rates of trabeculectomy with ECCE/PCIOL versus Ex-press shunt implantation with ECCE/PCIOL in glaucoma patients.

Methods: This was a retrospective comparative study that included 204 eyes of 183 patients with the underlying diagnosis of glaucoma. A total of 103 eyes which received trabeculectomy with ECCE/PCIOL and 101 eyes which were implanted with the Ex-press shunt and had ECCE/PCIOL were analyzed. Two criteria were used to determine the rate of surgical success. The stringent Criteria 1 defined success as 4mmHg < intraocular pressure < 19mmHg, use of less than one medication post-operatively, and no further glaucoma surgeries. The lenient Criteria 2 defined success as 4mmHg < intraocular pressure < 21mmHg, use of less than two medications post-operatively, and no further glaucoma surgeries.

Results: The mean follow-up time was 28±18 months for the trabeculectomy with ECCE/PCIOL with a range from 0 to 67 months. The mean follow-up time was 5.6±4.8 months for the Ex-press shunt with ECCE/PCIOL with a range from 0 to 28 months. The surgery success as defined by Criteria 1 had a statistically significant difference, with the mean length of success being 13.53 months for the trabeculectomy and 15.5 months for the Ex-press shunt (p-value of 0.0124). The surgery success as defined by Criteria 2 also had a statistically significant difference, with the mean length of success being 20.56 months for the trabeculectomy and 24.72 months for the Ex-press shunt (p-value of 0.0087).

Conclusions: Both the trabeculectomy and Ex-press shunt are effective procedures for lowering intraocular pressures. However, when using both stringent and lenient criteria for success, the Ex-press shunt with ECCE/PCIOL had a statistically significant higher success rate when compared to the trabeculectomy with ECCE/PCIOL.

Commercial Relationships: Farvah Fatima, None; Bret A. Hughes, None; Rominder Momi, None; Justin Tannir, None; Mark S. Juzych, None; Chaesik Kim, None; Manal H. Peracha, None; Alicia M. Eby, None; Melanie McQueen, None

Program Number: 4778 **Poster Board Number:** D0162
Presentation Time: 11:00 AM - 12:45 PM

Efficacy and Safety of Intracameral Triesence™ Use in Glaucoma Surgery

Michael Koval, Marlene R. Moster, Kathryn B. Freidl, Michael J. Pro, Jonathan S. Myers. Glaucoma, Wills Eye Institute, Philadelphia, PA.

Purpose: To evaluate the efficacy and safety of intracameral Triesence™ (Triamcinolone injectable suspension) use in trabeculectomy, tube shunt, or combined phacoemulsification-trabeculectomy.

Methods: This is an analysis of 77 consecutive, eligible patients enrolled for a randomized clinical trial from April 2009 to July 2011 at the Wills Glaucoma Service, Philadelphia. Patients undergoing standard surgical technique were randomized to Triesence™ or

balanced saline solution. They were followed on post-operative day 1 (POD1), week 1, month 1, 3, and 6. Outcome measures were visual acuity (VA), comfort, bleb grading with the Indiana Bleb Appearance Grading Scale (IBAGS), intraocular pressure (IOP), cataract, AC inflammation, and medication use. AC inflammation was assessed at both the slit lamp and with the KOWA FM 500 laser flare meter. Complications were recorded. Success was defined as IOP ≤ 21mmHg and 20% IOP reduction. Failure was inability to meet above criteria, IOP < 5mmHg, or the need for repeat glaucoma surgery. Mixed effects linear regression with square root transformation to meet assumptions of normality and constant variance was used for the IOP and other outcomes.

Results: There were no significant differences between treatment groups on any of the patient characteristics (age, race, sex, diagnosis, nerve health, cataract, IOP and VA). Mean IOP was higher in the Triesence™ arm on Day 1, but this difference did not reach statistical significance. No significant differences in IOP were observed at any time points between the groups. Among the outcome measures recorded, dry eye scores were lower in the Triesence™ arm at Month 1 while flare scores were higher in the Triesence™ arm on Day 1 but lower at Month 1. No other significant differences in outcome measures were observed. The rate of complications was higher in the Triesence™ arm on Day 1. There were no significant differences in medication use between the two groups.

Conclusions: Intracameral Triesence™ use showed no difference at 6 months in AC inflammation, flare, VA, IOP, or comfort when compared to controls. There were no differences in cataract, complications beyond day 1, or medications needed. This study found no evidence to support the use of Triesence™ in routine glaucoma surgeries such as trabeculectomy, tube shunt, or other combined procedures.

Commercial Relationships: Michael Koval, None; Marlene R. Moster, Alcon (C), Alcon (F), Allergan (F), Allergan (C), Merck (F), Merck (C), Mobius (F), Aeon (F), Aerie (F), Ista (F), iScience (F), Solex (C), Bausch and Lomb (F); Kathryn B. Freidl, None; Michael J. Pro, Alcon (C); Jonathan S. Myers, Alcon (R), Allergan (C), Allergan (R), Inotek (F), Inotek (C), Merck (R), Sucampo (C)
Support: Alcon investigator initiated grant
Clinical Trial: NCT00853905

Program Number: 4779 **Poster Board Number:** D0163
Presentation Time: 11:00 AM - 12:45 PM

Acute Intra-ocular Pressure (IOP) Changes Following Cataract Surgery With and Without Trabectome™ Ab-interno Trabeculectomy

Asher Weiner¹, Yotam Weiner². ¹Ophthalmic Consultants of the Capital Region, Albany, NY; ²Undergraduate, University of Michigan, Ann-Arbor, MI.

Purpose: To determine whether the use of Trabectome™ may help protect eyes at risk from acute IOP elevations during the immediate post-operative period following cataract surgery.

Methods: A retrospective interventional non-randomized comparative chart review. Main outcome measures were IOP 3-4 hours and 20 hours following surgery. Brimonidine 0.1% was used in all eyes at the end of surgery, following the 3-4 hour IOP check, and before the 20-hour IOP check.

Results: We identified 62 eyes of 62 patients with no previous surgery in either eye that underwent IOP measurement 3-4 hours following surgery in an attempt to find and treat acute post-operative IOP elevations in eyes with glaucomatous or suspicious optic nerves. One surgeon (AW) performed combined cataract with Trabectome™ surgery (C+T group) in 31 eyes, and cataract surgery alone (C group) in the remaining 31 eyes. In the C+T and C groups, IOP before

surgery was 16.2 ± 3.6 (mean \pm SD, range: 8-24) mmHg and 14.6 ± 2.7 (range: 11-22) mmHg, respectively ($p=0.059$). IOP was measured 3.5 ± 0.7 (range: 2.4-5.7) hours and 3.7 ± 0.6 (range: 2.6-5.0) hours following end of surgery, respectively ($p=0.1$), and it was 13.5 ± 6.3 (range: 6-32) mmHg and 19.8 ± 8.2 (range: 6-48) mmHg, respectively, significantly lower in the C+T group ($p=0.001$). IOP >21 mmHg was found in 2 (6.5%) eyes and 10 (32.3%) eyes, respectively, significantly less in the C+T group ($p=0.010$). Twenty hours following surgery, IOP was 12.1 ± 5.5 (range: 5-29) mmHg and 18.0 ± 5.5 (range: 11-32) mmHg, respectively, significantly lower in the C+T group ($p=0.0001$). Compared to pre-surgery IOP, the 3-4-hour and 20-hour IOP decreased in the C+T group by $15.2 \pm 35.6\%$ (range: (-69.5)-88.2%), and by $22.6 \pm 33.7\%$ (range: (-72.2)-70.6%), respectively. In contrast, IOP increased in the C group by $35.2 \pm 45.3\%$ (range: (-60.0)-150.0%) and by $24.1 \pm 38.7\%$ (range: (-27.8)-136.4%), respectively. The difference between the groups was significant at both time points ($p<0.0001$). IOP change was not correlated with central corneal thickness, cataract density or phacoemulsification cumulative dissipated energy (CDE).

Conclusions: Compared to cataract surgery alone, combined cataract with Trabectome™ surgery may help protect eyes at risk from acute IOP elevations during the first 20 hours following surgery, even in the presence of Brimonidine 0.1% treatment.

Commercial Relationships: Asher Weiner, None; Yotam Weiner, None

Program Number: 4780 **Poster Board Number:** D0164

Presentation Time: 11:00 AM - 12:45 PM

Patients presenting with severe glaucomatous visual field defect benefit from both surgical and medical treatment

Eugenio J. Maul de la Puente, Jaime A. Tapia, Alan Kastner.
Ophthalmology, Universidad Catolica, Santiago, Chile.

Purpose: To compare the outcome of surgical and medical therapy in patients with severe glaucomatous visual field damage at presentation.

A severe visual field defect at presentation has been considered an indication for primary surgery (1).

Methods: A retrospective chart review of patients presenting to our clinic over a 5-year period (2007-2011) with open angle glaucoma (OAG), severe visual field damage (Mean Deviation < -20 dB [2]) in at least one eye and ≥ 1 year of follow-up was conducted.

Outcomes compared across groups included proportion of patients with a 3dB loss in the mean deviation (MD) and proportion patients with a 2-line loss of visual acuity.

Results: Of 70 patients presenting with severe visual field loss in at least one eye, 49 (54 eyes) had ≥ 1 year of follow-up. Thirteen (24%) and 41 (76%) eyes received initial surgical and medical treatment respectively.

Mean age at presentation (SD) was 67.5 (11.8) years and median follow-up 2.9 years (Interquartile Range, IQR=2.0-4.9).

The surgical and medical treatment groups were comparable with respect to baseline age (66.8 vs 67.7 years), MD (-26.0 vs -25.5 dB) and logMar best corrected visual acuity (0.29 vs 0.25). The surgical group had longer follow-up (5.1 (2.7) vs 3.1 (1.66) years, p -value=0.02) and a higher number of visual field tests (7.1 (5.0) vs 4.3 (2.8) tests, p -value=0.07)

The proportion of eyes experiencing a 3-dB MD loss was 14% and 0% in the surgical and medical treatment group respectively (p -value=0.3).

The proportion of eyes experiencing a 2-line loss of visual acuity was 29% and 27% in the surgical and medical treatment groups respectively. ($P=1$)

Conclusions: The present study showed comparable visual outcomes

in eyes presenting with severe visual field damage treated with surgery or medically. It may provide insight to the risk faced by patients with advanced glaucoma enrolling in clinical trials exploring treatment alternatives (3).

1. King AJ et al.: Treating patients with advanced glaucoma - should we reconsider current practice. *Brit J Ophthalmol* 2011; 95: 1185-92

2. Mills RP et al.: Categorizing the end stage glaucoma from prediagnosis to end stage disease. *Amer. J Ophthalmol* 2006; 141:24-30

3. Leighton P et al.: The willingness of patients presenting with advanced glaucoma to participate in a trial comparing primary medical vs primary surgical treatment. *Eye* 2012; 26:300-6

Commercial Relationships: Eugenio J. Maul de la Puente, None; Jaime A. Tapia, None; Alan Kastner, None

Program Number: 4781 **Poster Board Number:** D0165

Presentation Time: 11:00 AM - 12:45 PM

EXPERIENCE IN THE USE OF THE EXPRESS DEVICE WITHOUT MYTOMICIN C IN PATIENTS WITH PRIMARY OPEN ANGLE GLAUCOMA

Cristina G. Isida Llerandi, Hector Bello Lopez Portillo, Rafael Castañeda Diez, Magdalena García-Huerta, Felix Gil Carrasco, Jesus Jimenez-Roman, Mauricio Turati-Acosta, LUIS A. ZARATE.
Glaucoma, Asociación para Evitar la Ceguera en México, Coyoacan, Mexico.

Purpose: To evaluate the efficacy in the control of the intraocular pressure (IOP) with the Express device without the use of Mytomicin C in patients with Primary Open Angle Glaucoma (POAG).

Methods: Prospective, cross sectional and experimental study. 23 eyes of 22 patients with diagnosis of POAG were included. The diagnosis of POAG was made by means of complete ophthalmological examination which included slit lamp examination, IOP measurement by Goldmann Tonometry, 24-2 Sita standard Visual fields, and optical coherent tomography of the optic nerve and nerve fiber layer analysis. Device implantation was performed by conventional trabeculectomy technique with no use of Mytomicin C. Posterior to the surgery all patients were treated with topical steroids and antibiotic. The IOP was measured the first and third day post surgery and then every week on first month and then monthly until sixth month. Bleb characteristics and complications were also evaluated as well as complementary procedures needed.

Results: 23 eyes (22 patients) 4 male and 18 female. Mean age was 66 years. Mean basal tonometry was 17.21 mmHg and mean final IOP 13.82 mmHg. Postsurgical complications included Seidel in seven patients (30.43%), flat anterior chamber and choroidal detachment was found in two patients (8.69%). One patient had surgical failure who required maximal topical medication (4.34%). Ten patients (43.47%) required needling with 5 fluorouracil application. We found conjunctival retraction in one patient (4.34%) that did not require and additional procedure.

Conclusions: The Express device is useful in the surgical management in patients with POAG because low complications incidence was obtained as well as good IOP control. Larger population of patients should be evaluated to obtain more concluding results.

Commercial Relationships: Cristina G. Isida Llerandi, None; Hector Bello Lopez Portillo, None; Rafael Castañeda Diez, None; Magdalena García-Huerta, None; Felix Gil Carrasco, None; Jesus Jimenez-Roman, None; Mauricio Turati-Acosta, None; LUIS A. ZARATE, None

Program Number: 4782 **Poster Board Number:** D0166

Presentation Time: 11:00 AM - 12:45 PM

Investigation of the filtration surgery with FocalSeal® in rabbit's eyes

Yukinori Harada¹, Tatsuo Nagata¹, Mikki Arai^{2,3}, Akihiko Tawara¹.

¹Department of Ophthalmology, University of Occupational & Environmental Health, Kitakyushu, Japan; ²Arai Eye Clinic, Fukuoka, Japan; ³Schepens Eye Research Institute, Harvard Medical School, Boston, MA.

Purpose: FocalSeal® (FS) is an absorbable polyethylene glycol based synthetic hydrogel. A blue-green light makes FS harden by photopolymerization. The aim of this study was to investigate the efficacy of the intra-operative using FS for glaucoma filtration surgery in rabbit's eyes.

Methods: There were two groups in this study. The first group included 9 rabbits. The conjunctiva in the left eyes was incised from limbus and the sclera was revealed, and FS was spread above the sclera, and then, after photopolymerization the conjunctiva was closed. In the right eyes, the conjunctiva was incised and simply closed (control). In the other group (6 rabbits included), a fornix-based filtration surgery with silicone tube sutured under the scleral flap was done in the left eye of 6 rabbits. In 3 of them, the seat of hardened FS was placed over the filtration site. In the other 3 eyes, the seat was not placed. Intraocular pressure measurements and bleb evaluations using ultrasound biomicroscopy (UBM) were performed. Six eyes from 3 rabbits in the first group were each enucleated 2, 4, 6 weeks after the surgery. In the second group, the left eyes of 6 rabbits were enucleated 4 weeks after surgery. Histopathologic evaluations of the surgical area were done in all enucleated eyes.

Results: In the first group, FS was remained in the subconjunctival spaces with inflammatory cells 2 weeks after the surgery. There was no FS observed in 4 weeks after the surgery, although there was a small subconjunctival space. In 6 weeks after the surgery, there were more Masson trichrome staining-positive collagen deposits in the subconjunctival tissues in the control than in the FS treated eyes. In the second group, postoperative IOPs of the FS treated eyes were lower than that of non-treated eyes, although there was no significant difference. The subconjunctival filtration spaces were detected by both UBM and histopathology in the FS treated eyes, but not in the control eyes. There was no remarkable difference in the immunohistochemical staining by anti- α -SMA antibody between FS and control. By anti-Vimentin antibody staining, the connective tissues of the bleb in the control eyes stained stronger than those in the FS treated eyes.

Conclusions: FocalSeal® used in the subconjunctival space could be a useful adjunctive substance to keep the filtering route in glaucoma filtration surgeries in rabbits.

Commercial Relationships: Yukinori Harada, None; Tatsuo Nagata, None; Mikki Arai, None; Akihiko Tawara, None

Program Number: 4783 **Poster Board Number:** D0167

Presentation Time: 11:00 AM - 12:45 PM

Long-term results after Ahmed glaucoma valve implantation for different types of glaucoma

Olga Furashova, Karin R. Pillunat, Eberhard Spoerl, Lutz E. Pillunat. Ophthalmology, University Hospital, Dresden, Germany.

Purpose: To present long-term outcomes of Ahmed glaucoma valve implantation in patients with different types of glaucoma.

Methods: Retrospective chart review of 214 patients (214 eyes) with different types of glaucoma, who underwent Ahmed valve implantation (model FP7, New World Medical, Rancho Cucamonga, CA). Surgical success was defined as an IOP reduction of more than 20% and additionally between 5 and 21 mmHg at 1,2,3 and 4 years after surgery.

Results: Among the 214 eyes were 32.2% suffering from

neovascular glaucoma (NVG), 28.5% suffering from primary open angle glaucoma (POAG), 10.7% suffering from congenital glaucoma, 7.9% suffering from uveitic glaucoma, 3.7% suffering from pseudoexfoliative glaucoma, 1.9% suffering from angle closure glaucoma and 23% suffering from other secondary types of glaucoma. Mean IOP preoperative was 38.6±11.2 mmHg. After 1 year follow-up, the success rate was 92.3% (167 of 181 eyes) with mean IOP 14.7±5.0 mmHg (p<0.001; t-test for paired samples); by 2 years, the success rate was 93.6% (147 of 157 eyes) with mean IOP 14.3±4.7 mmHg (p<0.001; t-test for paired samples). At 3 and 4 years after implantation success rates were 95.2% (119 of 125 eyes) with mean IOP 14.0±4.7 mmHg (p<0.001; t-test for paired samples) and 92.3% (84 of 91) with mean IOP 14.0±4.6 mmHg (p<0.001; t-test for paired samples) respectively.

At four years, the success rate in the POAG group was significantly higher than that in the NVG group (96% vs. 75%, p=0.04 by Chi2-test). Preoperative history of cyclocryocoagulation/cyclophotocoagulation was not a significant risk factor for surgical failure of Ahmed valve implantation (97% success rate in the group with previous cyclocryocoagulation/cyclophotocoagulation vs. 93% in the group without these; p=0.410 by Chi2-test).

Conclusions: Ahmed glaucoma valve implantation is a safe and successful procedure for decompensated glaucoma. Long-term success rates are depending on the type of glaucoma. A history of cyclocryocoagulation or cyclophotocoagulation seems not to be a risk factor for failure after Ahmed valve implantation.

Commercial Relationships: Olga Furashova, None; Karin R. Pillunat, None; Eberhard Spoerl, None; Lutz E. Pillunat, None
Clinical Trial: NCT01741961

Program Number: 4784 **Poster Board Number:** D0168

Presentation Time: 11:00 AM - 12:45 PM

Efficacy of Goniosynechialysis for Chronic Angle-Closure Glaucoma

Guoping Qing, Dapeng Mou. Beijing Tongren Eye Center, Beijing Tongren Hospital, Beijing, China.

Purpose: To evaluate the intraocular pressure (IOP) lowering efficacy of goniosynechialysis (GSL) for chronic angle-closure glaucoma (CACG) using a simplified slit lamp technique.

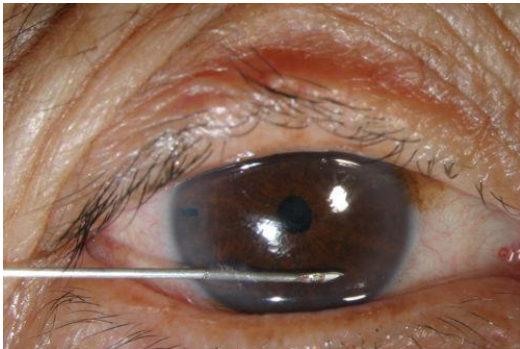
Methods: Patients with CACG was treated randomly with either anterior chamber(AC) paracentesis-guided limited GSL under biomicroscope with a needle or anti-glaucoma medication after laser peripheral iridotomy (LPI). All patients underwent ophthalmologic examinations including measurement of VA, BCVA, and IOP, biomicroscopy; fundus examination; and gonioscopy followed by GSL in the surgery group and prescription of anti-glaucoma medication in the control group.

Results: Forty-four patients (28 men, 14 women) were identified as having CACG with an initial mean IOP of 27.1 ± 6.7 mmHg (range, 25-37) in the surgery group and 26.8±7.4mmHg (range, 23-41) in the control group. No statistical difference was identified between the average initial IOP of the two groups. Six month after the treatment, the mean IOP in the surgery group decreased to 16.3 ± 2.8 mmHg (range, 14-19) without antiglaucoma medication. Meanwhile, the average IOP in the control group was 17.3 ± 2.4 mmHg (range, 13-20) without an average of 1.4 antiglaucoma eydrops (range, 1-3). Both groups have a significant decrease in IOP after the treatment. Nevertheless, the surgery group had statistically lower IOP and more decrease in IOP than that of the control group, identified with paired sample T test. AC bleeding was the most common complication of the AC paracentesis guided GSL, which occurred in 59.1% of the cases(13 /22) and was absorbed thin several days without special

ARVO 2013 Annual Meeting Abstracts by Scientific Section/Group – Glaucoma

care. No visual field deterioration or visual impairment was discerned in both groups.

Conclusions: The novel slit lamp procedure, AC paracentesis guided limited GSL lowers the IOP in patients with CACG, though it may lead to mild AC bleeding.



Under biomicroscope, the needle tip was advanced into the inferior AC angle over the iris plane, with the bevel at the front side. To dissect the closed angle, the needle tip pushed the iris root backward and drag it down from the trabecular meshwork surface.

Commercial Relationships: Guoping Qing, None; Dapeng Mou, None

Clinical Trial: ChiCTR-TRC-11001455

Program Number: 4785 **Poster Board Number:** D0169

Presentation Time: 11:00 AM - 12:45 PM

Imaging of Surgical Blebs using Spectral Domain Optical Coherence Tomography

Giovanni Milano^{1,2}, Marta Raimondi^{1,2}, Sara Lanteri^{1,2}, Sara Lombardo^{1,2}, Alice Chandra Verticchio Vercellin^{1,2}, Carlo Alberto Cutolo^{1,2}, Laura Bossolesi^{2,1}, Gemma C. Rossi^{2,1}. ¹University Eye Clinic, University of Pavia, Pavia, Italy; ²Fondazione IRCCS Policlinico San Matteo, pavia, Italy.

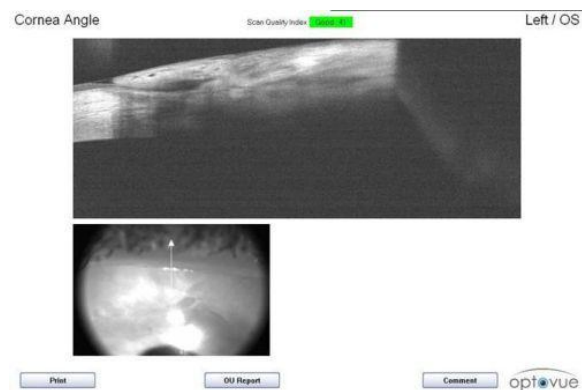
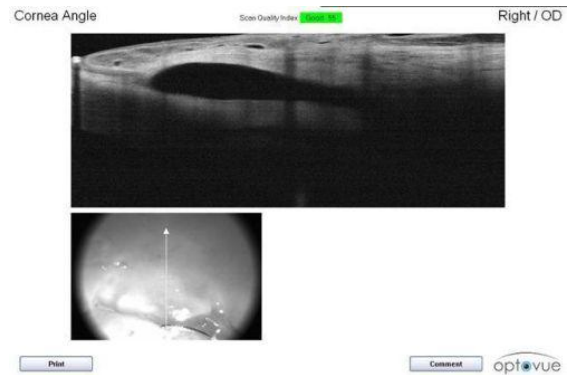
Purpose: To evaluate blebs after glaucoma surgery using spectral domain OCT (SDOCT)

Methods: Cross-sectional study involving the last 21 eyes submitted to glaucoma surgery at the University Eye Clinic of Pavia (Italy) and with a mean follow-up of 5.5±5.3 months. In 13 cases the chosen procedure was a trabeculectomy, with Mitomycin C (MMC) 0.3% used in 9 of them. In 5 cases a filtering device Ex-PRESS 200 was inserted after treatment with MMC 0.3% and in 3 cases a previously failed filtering glaucoma procedure was revised inserting the biodegradable collagen implant iGen (Life Spring Biotech Co, Taipei, Taiwan) on the top of the scleral flap. The blebs were imaged using the SDOCT iVue (Optovue Inc, Fremont, Ca, U.S.A.). A masked observer assessed the ability of iVue in visualizing structures relating to successful filtration: bleb wall thickening, bleb cavity, hyporeflexive spaces in bleb wall, scleral flap.

Results: Post-op intraocular pressure (IOP) was lower in patients submitted to trabeculectomy with MMC (9.3±3.4 mmHg) with a significant difference only compared to trabeculectomy without MMC (p=0.01). In these patients elements of filtration were pointed out in a greater proportion of cases (91.7%) as compared to trabeculectomy (81.2%), insertion of filtering device (75%) and revision of filtration (75%). If we divide all cases on the basis of IOP independently to surgical procedure, filtration is more evident if IOP ≤ 10 mmHg (85.4%) as compared to cases with IOP > 10 mmHg (77.7%).

Conclusions: SDOCT can provide useful evidence of filtration in the bleb up to the scleral flap. The morphological features can be

correlated to IOP. Trabeculectomy with MMC 0.3% can provide good filtration and control of IOP. However SDOCT cannot give information under the scleral flap due to limited deep tissue penetration.



Commercial Relationships: Giovanni Milano, Alcon (R); Marta Raimondi, None; Sara Lanteri, None; Sara Lombardo, None; Alice Chandra Verticchio Vercellin, None; Carlo Alberto Cutolo, None; Laura Bossolesi, None; Gemma C. Rossi, None

Program Number: 4786 **Poster Board Number:** D0170

Presentation Time: 11:00 AM - 12:45 PM

Fibrovascular ingrowth - a common cause of Glaucoma Drainage Device failure in refractory pediatric glaucoma

Irene Tung, Inna Marcus, Warakorn Thiamthat, Eniolami Dosunmu, Sharon F. Freedman. Duke Eye Center, Durham, NC.

Purpose: Glaucoma drainage devices (GDDs) for refractory pediatric glaucoma can fail to control intraocular pressure (IOP) by several mechanisms. In addition to encapsulation, fibrovascular ingrowth can limit outflow in valved Ahmed GDDs. This study evaluates initial GDD failure and subsequent GDD placement for refractory pediatric glaucoma.

Methods: Ongoing, retrospective review of all patients having >2 GDDs for refractory pediatric glaucoma, >6mos follow up, single surgeon, 1/1995-8/2012. Data collected included glaucoma diagnosis, age at surgery, surgical interventions, pre-/post-operative IOP and medications, complications. Failure defined as IOP>21mmHg (or clinically inadequate), and/or IOP-reducing surgery/devastating complication

Results: Included to date are 33 eyes (27 patients) having >two GDDs. Glaucoma diagnoses included congenital/infantile (n=13eyes), aphakic (n=10eyes), uveitic (n=5eyes), and other (n=5eyes). Average age at second GDD was 10.6±7.3yrs, with mean IOP 30±12mmHg, on 3±1 medications. Initial GDDs implanted were: Ahmed (New World Medical, Inc., Rancho Cucamonga, CA, n=28),

Baerveldt (Abbott Medical Optics, Abbott Park, IL, n=5). Fibrovascular ingrowth-sometimes unsuspected, and confirmed under anesthesia by bleb needling-was documented at second GDD surgery in 13/33 eyes (39%), and only in Ahmed GDDs [models S2 (n=4), FP7 (n=4), S3 (n=3), unspecified (n=2)]. Mean time to failure of initial Ahmed GDDs by fibrous ingrowth was 70 months (range 11-153). Second GDDs placed were: Ahmed (same location/replacing Ahmed, n=8; different location, n=13); Baerveldt (same location/replacing Ahmed, n=6; different location, n=6). Failure of second GDDs occurred in 15/33 eyes (45%): 10/15 (67%) underwent third GDD surgery, 3/15 (20%) had endoscopic laser cycloablation, and 2/15 (13%) suffered retinal detachment.

Conclusions: Published studies report failure of Ahmed models S2 and S3 from fibrovascular valve chamber ingrowth, but similar reports for the newer FP7 model are lacking. This study documents fibrovascular ingrowth of Ahmed FP7 GDDs in pediatric glaucoma. Fibrovascular ingrowth commonly causes Ahmed GDD failure in refractory pediatric glaucoma, and may be under-diagnosed.

Commercial Relationships: Irene Tung, None; Inna Marcus, None; Warakorn Thiamthath, None; Eniolami Dosunmu, None; Sharon F. Freedman, Pfizer, Inc. (C)

Program Number: 4787 **Poster Board Number:** D0171

Presentation Time: 11:00 AM - 12:45 PM

Association of Aqueous Humor Dynamic Markers in Glaucoma With Canaloplasty Surgery

David M. Reed, Jesse L. Gilbert, Sayoko E. Moroi. Ophthalmology & Visual Sciences, University of Michigan, Ann Arbor, MI.

Purpose: This retrospective case series was designed to examine markers that may be predictive of canaloplasty outcomes. We hypothesize that the potential markers include: fluorescein diffusion into the anterior chamber, blood reflux in the anterior chamber, and episcleral venous drainage.

Methods: This study is a retrospective case series of 16 consecutive patients, who underwent canaloplasty surgery by a single surgeon. These patients were enrolled in an IRBMED approved protocol to review medical records for clinical research. During the process of the surgical technique, the surgeon incorporated fluorescein canalography as part of the canaloplasty procedure to evaluate these potential markers. High definition video was recorded on the majority of cases. The fluorescein diffusion, blood reflux, and fluorescein outflow pattern are being analyzed. These dynamic data will be correlated with the short-term canaloplasty results.

Results: There were 4 females and 12 males, with a mean age and SD of 60 +/-19 years. The pre-operative mean maximum IOP within three clinic visits prior to surgery was 21 +/- 8.6 mmHg (range 12 - 45 mmHg). The glaucoma diagnoses included: juvenile glaucoma and open-angle forms of glaucoma. The final post-op IOP was 11 +/- 3.4 mmHg (range 2 - 15.5 mmHg). The functional evaluation of fluorescein diffusion, blood reflux, and fluorescein outflow will be demonstrated. These functional markers will be quantified and tested for association with the short-term canaloplasty results.

Conclusions: As suggested by Grieshaber et al (IOVS 51:498-504, 2010), functional evaluation of aqueous humor dynamic outflow may be helpful in assessing surgical outcome of canaloplasty.

Commercial Relationships: David M. Reed, None; Jesse L. Gilbert, None; Sayoko E. Moroi, Merck (F), Wolters Kluwer (F) **Support:** NIH Grant EY007003, Research to Prevent Blindness Unrestricted Grant

Program Number: 4788 **Poster Board Number:** D0172

Presentation Time: 11:00 AM - 12:45 PM

The effect of the Hydrus trabecular shunt on endothelial cell count: a double blind prospective randomized clinical study
Antonio M. Fea, Giulia Consolandi, Giulia Pignata, Paola Maria Loredana Cannizzo, Marco Dal Vecchio, Francesco Gallozzi, Carlo Lavia, Teresa Rolle, Federico M. Grignolo. Ophth/I Clinica Oculistica, Universita di Torino, Torino, Italy.

Purpose: One of the major complications of glaucoma tube surgery is the endothelial cell loss. Recently trabecular micro-shunts have been proved effective in reducing intraocular pressure in conjunction with cataract surgery, but there are no reports on their potential side effects on the endothelium.

Methods: In a double masked prospective randomized clinical study, endothelial cell count of patients undergoing cataract surgery (controls) or cataract and Hydrus stent (Ivantis) implant (cases) was performed at baseline and 3 months after surgery. Patients with an endothelial cell density lower than 1500 or with endothelial guttae were excluded. Endothelial cell evaluation was performed with a Konan Cellchek XL. The percentual change of the preoperative and postoperative CD, SD, CV and SA was compared between the two groups using unpaired Student t-test. All surgery was performed by the same surgeon (AF)

Results: A total of 24 patients were included in the study using a 2:1 randomization criterion (8 controls: 16 cases). Two patients were excluded because of cornea guttata. Cases and controls had comparable pre-operative endothelial parameters (CD: controls: 2373+/-114 cases: 2495+/-80; SD: controls: 145+/-16 cases: 163+/-11; CV: controls: 33.4+/-2.7 cases: 39+/-1.9; SA: controls: 53+/-3.3 cases:56+/-2.4). The percentual decrease in cell density between groups (cases: 16,6&+/- 17.2 controls: 12%+/-12.1)after surgery was not significantly different (p=0.5).

Conclusions: The Percentual CD reduction in both groups is comparable to the data reported in the literature. The implant of the Hydrus device in conjunction of cataract surgery does not seem to significantly affect the endothelial cell count in the short term. Long term studies are warranted.

Commercial Relationships: Antonio M. Fea, Glaukos (C), Ivantis (F); Giulia Consolandi, None; Giulia Pignata, None; Paola Maria Loredana Cannizzo, None; Marco Dal Vecchio, None; Francesco Gallozzi, None; Carlo Lavia, None; Teresa Rolle, THEA (C); Federico M. Grignolo, None **Clinical Trial:** NCT01539239

Program Number: 4789 **Poster Board Number:** D0173

Presentation Time: 11:00 AM - 12:45 PM

Comparison short term post operative hypotony rates of 23 gauge versus 25 gauge needle size in the formation of a cornea-scleral track for Baerveldt tube insertion into the anterior chamber

Kirithika Muthusamy, Jason Cheng, Keith Barton, K Sheng Lim, Laura Beltran-Agullo. Glaucoma, Moorfields Eye Hospital, London, United Kingdom.

Purpose: To compare immediate post operative entry site leak and hypotony rates of using two different size needles (23 and 25 gauge) in the formation of a track for insertion of a Baerveldt tube into the anterior chamber.

Methods: Retrospective case note review of 58 patients who had Baerveldt tube implants in 2 tertiary glaucoma units. There were 2 groups being compared. Group 23G had 29 patients that were part of the primary tube versus trabeculectomy (PTVT) study and used the 23 gauge needle to form the track before insertion of the tube. The second group, 25G group, had 27 patients which were routine tube implant patients, where the surgeon's preference of a 25 gauge needle was used. Visual acuity (VA), intraocular pressure (IOP), post

operative complications and number of IOP drops were recorded at 1 day, 1 week, 1 month and 3 months after surgery.

Results: Four patients (14%, $P < 0.001$) in the 23G group had hypotony within the first week, compared with none in the 25G group. Two of these four eyes, in the 23G group, had anterior bleb formation and leaking from around the tube entry site, one other eye had shallowing of the anterior chamber with no anterior bleb or leak and the fourth eye had no sequelae from the hypotony. One eye in the 25G group had a shallowing of the anterior chamber at 1 week, but maintained the IOP at 9mmHg, with no leak or anterior bleb seen. There was also an additional hypotony in the 25G group at 3 months, after removal of the supramid stent.

The mean IOP in the 23G group was lower than the 25G group at all time points. In the 23G group, the mean IOP was 21.5mmHg at pre-op, 16.9mmHg at day 1, 15mmHg at week 1, 17.7mmHg at month 1 and 18.5mmHg at month 3. The mean IOP in the 25G group was lower, with 26.4mmHg pre-operatively ($P=0.002$), 23.3mmHg at day 1 ($P=0.004$), 20.9mmHg at week 1 ($P=0.008$), 18.3mmHg at month 1 ($P=0.744$), and 17.1mmHg at month 3 ($P=0.337$).

Conclusions: The wider 23 gauge needle track, for Baerveldt tube entry, results in lower mean IOP within the first week, although at 1 and 3 months post operatively, the IOP difference is no longer statistically significant. However, this is also at the expense of a higher hypotony rate, entry site leak and shallow anterior chamber.

Commercial Relationships: Kirithika Muthusamy, None; Jason Cheng, None; Keith Barton, AqueSys (I), Ophthalmic Implants (PTE) Ltd (I), Merck (F), Refocus (F), Alcon (C), AqueSys (C), Ivantis (C), Refocus (R), Thea (C), Alimera (C); K Sheng Lim, None; Laura Beltran-Agullo, None

Program Number: 4790 **Poster Board Number:** D0174

Presentation Time: 11:00 AM - 12:45 PM

IOP-lowering and Safety Associated with Opening Gold Micro Shunt's Windows

Nicolas Cadet, Paul Harasymowycz. Ophthalmology, Universite de Montreal, Montreal, QC, Canada.

Purpose: To determine the intraocular pressure-lowering effect and safety of opening the Gold Micro Shunt's (GMS) windows.

Methods: The study is a case series that studied 5 subjects, among which there were three with primary open-angle glaucoma, one with aphakic glaucoma and one with neovascular glaucoma. It looks retrospectively at the safety of opening the GMS' windows and its effect on the IOP and number of glaucoma eyedrops. Among the research subjects, there were 4 males and 1 female, aged between 56 and 81 (average age 70). Four of the subjects were Caucasian and one was Hispanic. They had undergone 0 to 4 surgeries before GMS implantation. The GMS has 8 closed windows upon implantation. Four of these windows were opened in all five patients. Average follow-up post GMS implantation was 3 years.

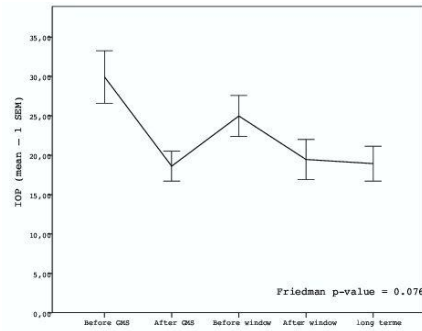
The GMS was implanted in each patient. The IOP (using a Goldmann tonometer) and number of glaucoma medications were recorded before and after the implantation of the GMS, as well as before and after the opening of the GMS' windows with a Titanium-Sapphire (Ti-Sap) laser. Patients were assessed for complications arising from implanting the GMS and opening its windows.

Results: Implantation of the GMS was associated with an average decrease in IOP of 37.0% ($p=0.076$). The average IOP before window-opening was 24.9 and after window opening, it was 17.6. The IOP thus dropped a further 29.3% ($p=0.055$) on average after the opening of the GMS' windows. The windows were opened an average 6.4 months after GMS implantation. IOP dropped 2.3 to 10.7% per window opened (average 7.3%). Long-term IOP at follow-ups remained lower than pre-GMS levels in all patients. The IOP

reduction post window opening lasted throughout follow-up, i.e. from 17 to 42 months (average 30 months). The number of glaucoma drops for each patient did not decrease after opening the GMS' windows.

One patient developed transitory cystoid macular edema after GMS implantation that resolved with a course of NSAID drops. No complication arose from the opening of the GMS' windows.

Conclusions: Our study suggests that opening the GMS' windows is safe and is associated with a substantial and sustained reduction in IOP. In the future, conducting similar studies with larger cohorts and longer follow-up would make it possible to obtain more data.



Average IOP of the 5 patients versus time

Commercial Relationships: Nicolas Cadet, None; Paul Harasymowycz, Allergan (C), Alcon (C), Merck (C), SOLX (C), Pfizer (R), Novartis (R), Bausch and Lomb (R), AMO (R)

Program Number: 4791 **Poster Board Number:** D0175

Presentation Time: 11:00 AM - 12:45 PM

Persistent hypotony associated to the use of immunosuppressive therapy in glaucoma drainage implants

Susana Duch, Oana Stirbu, Elena Milla, Oscar Buchacra Castellano. Ophthalmology- Glaucoma, Institut Condal d'Oftalmologia, Barcelona, Spain.

Purpose: To describe the histopathology of non-valved implants in three cases of persistent postoperative Hypotony after the restrictive tube ligature was released, in patients under long term immunosuppressive therapy.

Methods: Human tissue study of surgical pathology specimens with clinicopathological correlation

Results: The macroscopic appearance of the capsules, 3 and 4 months postoperatively, was immature and loose. Microscopic examination disclosed extremely irregular and loose tissue, its thickness measuring from 0.02 to 0.6mm, depending on the place of the capsule that was studied. The withdrawal of the immunosuppressive therapy did not allow the rebuilding of new capsules, and implant exchange with a valved device was needed, in order to recover IOP.

Conclusions: The use of chronic immunosuppressants may interfere with the capsule formation around the plates in non-valved drainage devices. Thus, in these cases valved implants might be safer.

Commercial Relationships: Susana Duch, None; Oana Stirbu, None; Elena Milla, None; Oscar Buchacra Castellano, None

Program Number: 4792 **Poster Board Number:** D0176

Presentation Time: 11:00 AM - 12:45 PM

Retrospective review of patients with refractory glaucoma treated with Transcleral Diode Laser Cyclophotocoagulation

Vikas Tah², Saruban Pasu¹, Sanjay Shah¹. ¹Glaucoma, St Helier Hospital, London, United Kingdom; ²Oxford Eye Hospital, Harrow, United Kingdom.

Purpose: To report the efficacy and safety of cyclodiode laser therapy in the management of refractory glaucoma over a 5 year period in a single centre at St Heliers Hospital in Sutton of London .

Methods: A retrospective review was undertaken of patients who at undergone transcleral diode laser cyclophotocoagulation at St Helier Hospital. Records were obtained from the theatre log book and patient notes then tracked and reviewed.

Laser settings were recorded, along with visual acuities, intraocular pressure (IOP) and initiation of pressure lowering drops.

Complications were noted along with comorbidities over a 5 year period.

Results: 96 eyes were treated between March 2000 - October 2007. Mean age 70 years old. 61% were male. Mean settings: 40.1 shots, 1500mW power and 1500ms duration. Mean energy delivered was 90.2 Joules.

Primary outcome of success was IOP between 5 and 21mmHg or a 30% reduction from baseline. At 6 month review 66% were successful, at 1 year 83% and at 2 and 5 years 80%.

The IOP reduction was 52% at 1 week, 40% at 1 and 6 months, 53% at 1 year, 56% at 2 years and 45% at 5 years. 18 (37%) eyes saw 6/60 or better prior to treatment. Of these, 2 lost vision of 2 lines or more.

Overall, there was a 32% drop in the number of glaucoma medications over the 5 year period. 19 patients were on oral acetazolamide pre treatment, 10 of which remained on oral acetazolamide post treatment. 1 patient developed post procedure anterior uveitis (on a background of fuchs heterochromic cyclitis), while two patients were hypotonous at the 5 year follow up.

Conclusions: Cyclodiode remains a useful adjunctive treatment for refractory glaucoma. Our review showed a sustained decrease in IOP and reduction in the use of IOP-lowering drops following treatment. Our data was comparable to that of the UK National Cyclodiode Laser Survey 2011. Historically used only in non-seeing eyes, we have shown it can be safely and effectively used in sighted patients. Conclusion: We propose that cyclodiode may be safely used in seeing and non-seeing eyes, and suggest its use be considered on a case-by-case basis, offered as a potential lower risk treatment in higher risk patients.

Commercial Relationships: Vikas Tah, None; Saruban Pasu, None; Sanjay Shah, None

Program Number: 4793 **Poster Board Number:** D0177

Presentation Time: 11:00 AM - 12:45 PM

Comparison of IOP and postoperative complications in patients undergoing tube shunt or trabeculectomy surgery for uveitis-related intraocular pressure elevation

Umair Iqbal, Manpartap Bal, Ralf R. Buhrmann, Chloe C. Gottlieb. University of Ottawa Eye Institute, Ottawa, ON, Canada.

Purpose: To compare rates of successful IOP reduction and complications in patients with uveitis-related intraocular pressure elevation undergoing tube shunt or trabeculectomy surgery.

Methods: Patients were identified by an electronic search of one surgeon's billing records for glaucoma surgical procedure codes. Inclusion criteria were: trabeculectomy or tube shunt surgery with diagnosis of uveitic glaucoma or elevated intraocular pressure associated with uveitis. A chart review was conducted and data tabulated for age, surgery type, complications and IOP at 6 months and 1 year. Eyes lost to follow-up were excluded from the analysis.

Results: Data were collected from 28 eyes of 26 patients of whom 14 were male (53.8%) and 12 (46.2%) were female. The mean age at the time of surgery was 53.5 ± 16.5 years (range 23-89 years). Most eyes underwent trabeculectomy surgery with MMC (23 eyes, 82.1%) while an aqueous tube shunt was implanted in 5 eyes (17.9%). Four eyes (80%) had Baerveldt valve implanted and 1 (20%) had Ahmed

valve implantation. Data was collected at 6 months and 1 year. At 6 months, 21 eyes (91.3%) in the trabeculectomy group met the success criteria of IOP ≤21mmHg while 4 eyes (80%) met the success criteria in tube shunt group. By 1 year, 5 eyes (2 trabeculectomies and 3 tubes) were lost to follow-up and tube shunt failed in 1 eye which required a second operation. Therefore, 19 eyes (90.5%; 21 eyes) in trabeculectomy group met the success criteria of IOP ≤21mmHg while 1 eye (50%, 2 eyes) in tube shunt group met the success criteria. Moreover, within the trabeculectomy group, 9 eyes (39.1%; 23 eyes) at 6 months required one or multiple post-op needling procedures to control IOP and by 1 year no additional needling was required in the remaining 21 eyes. Bleb leaks occurred in 4 eyes (17.4%, 23 eyes) at 6 months.

Conclusions: In the patients studied, trabeculectomy with MMC was the most common type of surgical treatment. By the end of 6 months, 91.3% eyes met success criteria in trabeculectomy group compared to 80% eyes in tube group. These numbers decreased to 90.5% and 50% respectively by 1 year. Complications also occurred after trabeculectomy which required needling or leak repairs to control IOP. No such complications threatening IOP control occurred in the tube shunt group.

Commercial Relationships: Umair Iqbal, None; Manpartap Bal, None; Ralf R. Buhrmann, None; Chloe C. Gottlieb, Novartis (C), Allergan (F)

Program Number: 4794 **Poster Board Number:** D0178

Presentation Time: 11:00 AM - 12:45 PM

Comparison between Endothelial Cell Loss After MICS Phaco with ExPress Implant and MICS Phaco Safe-Trabeculectomy
Romeo Altafini, Simonetta Morselli. Ophthalmology Unit, San Bassiano Hosp, Bassano del Grappa, Vicenza, Italy.

Purpose: To evaluate corneal endothelial cell loss after phaco with ExPress implant compared to phaco trabeculectomy

Methods: Forty eyes of forty patients affected by cataract and open angle glaucoma were randomized to Micro incision cataract surgery (MICS) phaco with Express P50 implant under scleral flap (group 1) or MICS safe-phacotrabeculectomy (group 2) after informed consent. All patients were operated by two-site surgery. There were no statistically significant differences in age, sex, anterior chamber depth and axial length. Non contact corneal specular microscopy (Tomey 3000 tm) was performed in all eyes before and 1st, 3rd, 6th months after surgery. Endothelial cell density (CCD), coefficient of variation in cell size (CV) and percentage of hexagram cells (HEX) between the two groups were considered before and after surgery. Mean endothelial cell count was measured in the central corneal area and in the superior area close to Express implant and close to trabeculectomy site. One-way analysis of variance (ANOVA) was used to analyze endothelial cell loss differences between two groups.

Results: The mean preoperative endothelial cell density in group 1 (ECD) was 2144 cells/mm² ± 267 (SD) and was 2203 ± 269 cells/mm² in the group 2 (P=.431). The mean postoperatively endothelial cell loss was 8.8% at the 1st month, 10.5% at 3rd month and 12.6 % at 6th month in group 1 and 8% at 1st month, 10.2% at 3rd month and 12.3 % at 6th month in the group 2. The differences were not statistically significant between the two groups (P >.05). The superior area, close to Express implant and close to trabeculectomy site, showed the higher decrease in endothelial cell density. Endothelial cell loss was 18.5% in the group 1 and 18.2% in the group 2 after six months. The percentage of hexagonal cells and coefficient of variation in cell size were not different between the two groups preoperatively or postoperatively. The difference was not statistically significant

Conclusions: Our results suggest that endothelial cell loss is due to

surgical trauma even in central and superior area in both group. In our study the implant of P50 Express is safe and effective as mini-trabeculectomy and there were no statistically significant endothelial cell loss after Express P50 implanted.

Commercial Relationships: Romeo Altafini, None; Simonetta Morselli, None

Support: None in the Support field below

Program Number: 4795 **Poster Board Number:** D0179

Presentation Time: 11:00 AM - 12:45 PM

The relationship between skin phototype and trabeculectomy outcome

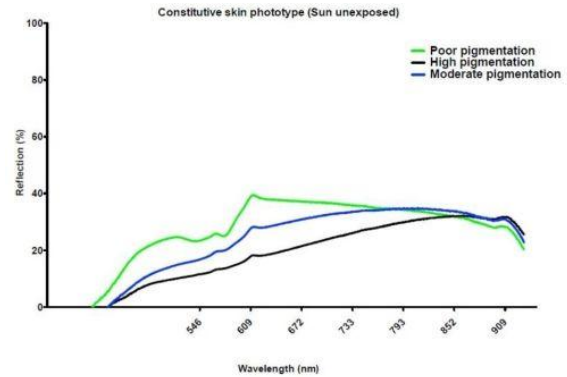
Jonathan C. Clarke^{1,2}, Ming-Yueh Lee^{1,3}, Ashkan Khalili², Sumit Dhingra^{1,2}, Catey Bunce², Peng T. Khaw^{1,2}. ¹Glaucoma Service, Moorfields Eye Hospital, London, United Kingdom; ²NIHR Biomedical Research Centre for Ophthalmology, Moorfields Eye Hospital and UCL Institute of Ophthalmology, London, United Kingdom; ³Kuala Lumpur Hospital, Kuala Lumpur, Malaysia.

Purpose: Identification of risk factors for glaucoma drainage surgery (trabeculectomy) failure determines the level of perioperative augmentation with antimetabolites. Spectrophotometers measure the reflectance from skin from a light source giving the individuals phototype. They are non-invasive and acquire information rapidly. 680nm reflectance is reduced in pigmented skin types. They may help quantify the risk of future surgical failure.

Methods: Patients who had previously completed a randomized controlled trial of intraoperative 5FU versus placebo were invited to participate in a follow up study. Sun unexposed (constitutional) and sun exposed (facultative) phototypes were measured under standard conditions. Cox regression analysis was performed to assess the association between time to reach trial failure criteria for intraocular pressure control during follow-up and skin reflectance at 680nm wavelength.

Results: Skin phototype of 24 patients was measured. The averages of 5 readings of constitutional and facultative measurements were taken. Examples of the skin phototype curves are shown in figure 1. Mean constitutional value was 40.3% reflectance (range 15.1-50.9), and mean facultative value was 35.5% reflectance (range 7.7-47.7). An association with failure criteria of >17mmHg on 2 consecutive follow up visits was identified with constitutional (HR 0.95 (95% CI 0.90-0.99)) and facultative (HR 0.94 (95% CI 0.90-0.99)) measurements. For failure definition of >21mmHg on 2 consecutive visits also identified associations with failure for both constitutional (HR 0.91 (95% CI 0.86-0.97)) and facultative (HR 0.92 (95% CI 0.87-0.98)) measurement. However, following adjustment for ethnic origin, the effect is not found to be significant.

Conclusions: We have identified an association between lower skin reflectance measurements and surgical outcome. The role of ethnic origin however is complex and requires further investigation. Non-invasive spectrophotometers can measure properties in the skin that are predictive for future outcomes in glaucoma surgery.



Commercial Relationships: Jonathan C. Clarke, None; Ming-Yueh Lee, None; Ashkan Khalili, University College London (P); Sumit Dhingra, None; Catey Bunce, None; Peng T. Khaw, University College Moorfields (P)

Support: The research was funded by the National Institute for Health Research (NIHR) Biomedical Research Centre based at Moorfields Eye Hospital NHS Foundation Trust and UCL Institute of Ophthalmology. The MRC 5-FU trial was funded by the Medical Research Council of Great Britain, grant number G 9330070

Program Number: 4796 **Poster Board Number:** D0180

Presentation Time: 11:00 AM - 12:45 PM

Rosmarinic Acid Suppresses Responses By Fibroblasts Contributing To Fibrosis Following Glaucoma Filtration Surgery

Jayter S. Paula¹, Carolina Modulo¹, Marco Andrey C. Frade², Peter Reinach¹, Eduardo M. Rocha¹. ¹Department of Ophthalmology, FMRP - USP, Ribeirao Preto, Brazil; ²Internal Medicine Department, FMRP - USP, Ribeirao Preto, Brazil.

Purpose: Tenon's fibroblast proliferation and myofibroblast differentiation are contributors to the excessive subconjunctival scarring that occurs frequently after glaucoma filtration surgery. Rosmarinic acid (RA) is a natural polyphenol that has anti-fibrotic activities, found in many herbs. We reported that RA was able to control neovascularization, but not fibrosis, related to healing process in an experimental glaucoma surgery model (ARVO, 2012). Thus, the objective of this study was to determine if RA could suppress proliferation and differentiation of rabbits Tenon's capsule fibroblasts (RTF).

Methods: RTF obtained from New Zealand rabbits were cultured in Dulbecco's modified Eagle's medium (DMEM). The dose dependent effects of RA (i.e. 0.3, 1.0 and 3.0 μ M, for 12 h) on third passage cell proliferation were determined with the MTT assay in triplicate after 48 h. Immunofluorescence of alpha smooth muscle actin (alpha-SMA) assessed myofibroblast differentiation. Real-time reverse transcription polymerase chain reaction evaluated type I alpha I collagen (COL1A1) gene expression.

Results: Only 1.0 μ M (-10.5%; $p=0.035$) and 3.0 μ M (-24.1%; $p=0.014$) RA suppressed proliferation after 48 h. On the other hand, at all RA concentrations, myofibroblast differentiation declined by 18.4% to 32.5%, compared to control. Moreover, COL1A1 mRNA expression also declined with RA treatments ($p=0.002$).

Conclusions: RA suppressed RTF proliferation and transdifferentiation as well as COL1A1 gene expression. As RA treatment was previously associated with lower neovascularization *in vivo*, it remains an open question whether or not fibroblasts suppression by RA could control subconjunctival angiogenesis observed after glaucoma surgery.

ARVO 2013 Annual Meeting Abstracts by Scientific Section/Group – Glaucoma

Commercial Relationships: Jayter S. Paula, None; Carolina Modulo, None; Marco Andrey C. Frade, None; Peter Reinach, None; Eduardo M. Rocha, None
Support: FAPESP # 2012/00622-9

Program Number: 4797 **Poster Board Number:** D0181

Presentation Time: 11:00 AM - 12:45 PM

Incidence and success rates of trabeculectomy with ExPress mini shunt following failed canaloplasty

Jacob W. Brubaker, Mahmoud A. Khaimi. Ophthalmology, Dean McGee Eye Institute, University of Oklahoma, Oklahoma City, OK.

Purpose: Canaloplasty, utilizing superior conjunctiva and sclera, could potentially compromise successful dissection and long-term success of a future trabeculectomy. This paper investigates the circumstances and incidence of canaloplasty failures and the success of subsequent trabeculectomy with ExPress mini shunt.

Methods: A retrospective review was performed investigating the total number of patients requiring trabeculectomy with ExPress shunt following canaloplasty, performed at one center, over a four-year period. Patient's age, sex, type of glaucoma, and preoperative characteristics, including intraocular pressure (IOP), number of glaucoma drops, and visual acuity were analyzed. The time to canaloplasty failure, response to Nd:Yag goniotomy, IOP, and subsequent trabeculectomy success were evaluated. Final IOP, vision, and glaucoma drop requirements were recorded.

Results: A total of 417 patients with a previous canaloplasty were found over the four-year period. A total of 21 trabeculectomies with ExPress shunt were performed in patients with a previously failed canaloplasty. This represents an incidence of 5%. Patient demographics included an average age at the time of canaloplasty of 70.9 years, preoperative IOP of 26.2, and 2.4 glaucoma drops. Average time to failure was 229 days (69 to 405 days). Nd:Yag goniotomy was performed at an average of 77 days postoperatively (21 to 215 days). Time from goniotomy to trabeculectomy was an average of 121 days (43 to 207). The average preoperative IOP prior to trabeculectomy with ExPress shunt was 34 mmHg on an average of 2.3 drops. The final average IOP with an average follow-up of 10 months was 13.5 mmHg using an average of 0.2 drops.

Conclusions: In this series the failure rate of canaloplasty was low. After review of the literature, this study demonstrates for the first time that, in those patients requiring trabeculectomy with ExPress shunt, the previous canaloplasty surgery did not prevent subsequent success.

Commercial Relationships: Jacob W. Brubaker, None; Mahmoud A. Khaimi, iScience (C)

Support: Research to prevent blindness

443 Imaging III, GL

Wednesday, May 08, 2013 11:00 AM-12:45 PM

Exhibit Hall Poster Session

Program #/Board # Range: 4798-4852/D0237-D0291

Organizing Section: Glaucoma

Program Number: 4798 **Poster Board Number:** D0237

Presentation Time: 11:00 AM - 12:45 PM

Glaucoma progression detection using a Bayesian-fuzzy logic approach applied to 3D spectral domain optical coherence tomography optic nerve head images

Akram Belghith, Christopher Bowd, Robert N. Weinreb, Andrew J. Tatham, Atsuya Miki, Felipe A. Medeiros, Linda M. Zangwill.

Department of Ophthalmology-0946, Hamilton Glaucoma Center, La Jolla, CA.

Purpose: To detect glaucomatous changes in the optic nerve head (ONH), we proposed a novel fuzzy Bayesian detection scheme (FBDS), which aims to classify the 3D Spectralis SD-OCT images of the ONH into "non-progressing" and the "progressing" glaucoma classes.

Methods: We formulated the detection of glaucomatous change between baseline image and follow up images as a missing data problem. We proposed the use of a Bayesian approach to model the a priori we have on the change detection map. We used the Markov Random Field Model (MRF) to handle the spatial dependency of changed pixels. To accommodate the presence of false positive detection, the estimated change detection map is then used to classify a 3D spectralis SDOCT image into the "non-progressing" and "progressing" glaucoma classes based on a novel fuzzy logic classifier. An independent training set, which consists of 10 normal eyes, 5 non-progressing eyes and 10 progressing eyes, was used to train the fuzzy logic classifier. Progression was defined as the presence of one or more changed follow-ups. Diagnostic accuracy was estimated using 117 eyes of 75 participants from the UCSD Diagnostic Innovations in Glaucoma Study (DIGS). Sensitivity was estimated in 27 eyes classified as progressing by standardized assessment of stereophotographs by 2 independent graders and/or by designation as "likely progression" based on visual field Guided Progression Analysis (mean follow-up 4 years, 4 tests). Specificity was estimated using 50 stable glaucoma eyes (imaged once a week for 5 consecutive weeks) and using 40 healthy eyes (mean follow-up 3 years, 3 tests). We compared the FBDS method to a Support vector Machine SVM with the whole image difference between the baseline and a follow up as input, and to 2 alternative FBDS methods, one without the MRF prior and one with a threshold classifier.

Results: Sensitivity in progressors, specificity in stable Glaucoma eyes and specificity in normals, obtained with different methods, are presented in Table1.

Conclusions: The FBSD method with use of the MRF as prior and the fuzzy classification results in high specificity in both normal and stable glaucoma eyes (94% and 92% respectively) while maintaining good sensitivity.

	FBDS	SVM	FBDS without MRF prior	FBDS with a threshold classifier
Sensitivity in progressors	64%	63%	55%	58%
Specificity in Stable Glaucoma Eyes	92%	69%	82%	85%
Specificity in normals	94%	83%	86%	87%

Commercial Relationships: Akram Belghith, None; Christopher Bowd, None; Robert N. Weinreb, Aerie (F), Alcon (C), Allergan (C), Altheos (C), Amakem (C), Bausch&Lomb (C), Carl Zeiss-Meditec (C), Genentech (F), Haag-Streit (F), Heidelberg Engineering (F), Konan (F), Lumenis (F), National Eye Institute (F), Nidek (F), Optovue (C), Quark (C), Solx (C), Topcon (C); **Andrew J. Tatham**, None; **Atsuya Miki**, NIDEK (C); **Felipe A. Medeiros**, Carl-Zeiss (F), Heidelberg Engineering (F), Topcon (F), Alcon (F), Allergan (F), Sensimed (F), Reichert (F); **Linda M. Zangwill**, Carl Zeiss Meditec Inc (F), Heidelberg Engineering GmbH (F), Optovue Inc (F), Topcon Medical Systems Inc (F), Nidek Inc (F)
Support: P30EY022589, R01EY022039

Program Number: 4799 **Poster Board Number:** D0238

Presentation Time: 11:00 AM - 12:45 PM

Changes in Anterior Segment Morphology after Laser Iridotomy in Asian Indian Eyes: A Source Swept Anterior Segment Optical Tomography Study

Rajesh Sasikumar, Trupti Patil, Sathi A. Devi, Dhanraj Rao, Ramgopal Balu, Narendra K. Puttaiah, Bhujang K. Shetty.

GLAUCOMA AND RESEARCH, NARAYANA NETHRALAYA, Bangalore, India.

Purpose: To evaluate changes in anterior chamber parameters and factors that determine the extent of angle opening after laser peripheral iridotomy (LPI) in Asian Indian eyes with angle closure.

Methods: In this prospective, non-comparative cohort study, patients with angle closure disease who were scheduled for LPI were enrolled. Under standardized dark room conditions, anterior chamber parameters before and 1 week after LPI were compared using the source-swept anterior segment coherence tomography (Casia SS-1000 OCT; Tomey, Nagoya, Japan). Parameters measured using the built-in software included anterior chamber volume (ACV), iris volume (IV), anterior chamber depth (ACD), angle opening distance at 500 μm (AOD500) anterior to the scleral spur, trabecular-iris space area 500 (TISA500), and trabecular iris angle (TIA500). A scan biometry (Lens Star, Haag Streit, USA) was used to measure axial length (AL) and lens thickness (LT). Multivariate linear regression analysis was performed for predictors of percentage change in mean angle opening distance (AOD500).

Results: Sixty six eyes (66 subjects) were analyzed; 8 eyes were excluded due to poor scleral spur visibility. The mean age was 57.9 ± 9.4 years; majority were women (57%). Post LPI, the mean angle width (modified Shaffer grading) increased from 1.03 (95% C.I, 0.83-1.23) to 2.83 (95% C.I, 2.54-3.11) ($p < 0.0001$), with a corresponding increase in ACV from 104.7 ± 27.9 to 111.9 ± 24.0 mm³ ($p < 0.001$); there was no change in ACD, LT or IV ($p > 0.5$). While the TIA increased significantly in all quadrants ($p < 0.001$), AOD500 increased only in the temporal and inferior quadrants. ARA500 increased only in the superior quadrant ($P < 0.01$), while TISA showed significant changes in the nasal and inferior quadrants ($p < 0.001$). While LT ($\beta = -0.49$, $p = 0.03$) and ACD ($\beta = 0.60$, $p = 0.005$) were associated with Δ AOD500 in the univariate analysis, none of the parameters showed association in the multivariate analysis.

Conclusions: In this cohort of angle closure subjects, LPI caused a significant increase in the angle width in all quadrants. While ACV showed change after LPI, other variables did not show consistent change and there was no change in ACD or IV.

Commercial Relationships: Rajesh Sasikumar, None; Trupti Patil, None; Sathi A. Devi, None; Dhanraj Rao, None; Ramgopal Balu, None; Narendra K. Puttaiah, None; Bhujang K. Shetty, None

Program Number: 4800 **Poster Board Number:** D0239

Presentation Time: 11:00 AM - 12:45 PM

Intersubject correlation between circumpapillary distribution of retinal nerve fiber layer and retinal vessels: comparison between optical coherence tomography and scanning laser polarimetry

Ivania Pereira¹, Stephan Holzer¹, Hemma Resch¹, Barbara Kiss¹, Georg Fischer², Clemens Vass¹. ¹Ophthalmology & Optometry, Medical University Vienna, Vienna, Austria; ²Center for Medical Statistics Informatics and Intelligent Systems, Section for Medical Information Management and Imaging, Medical University Vienna, Vienna, Austria.

Purpose: To assess circumpapillary retinal vessel thickness (cRVT) profiles and correlate them with retinal nerve fiber layer (RNFL) thickness measured by high resolution optical coherence tomography (HR-OCT) and scanning laser polarimetry (SLP).

Methods: A sample of 106 healthy volunteers underwent complete

ophthalmologic examination, including HR-OCT scanning (Cirrus® Carl Zeiss Meditec Inc.) and SLP (GDx-VCC® and GDx-ECC® Carl Zeiss Meditec Inc.). A proprietary software was developed in MATLAB® (Version R2009b, The Mathworks Inc.) for individual manual assessment of the optic disc (OD) border and cRVT, using the SLO image from Cirrus HR-OCT centered in the OD. For each measurable vessel, we established a line connecting its center point at the OD border with the OD center. The angle between this line and a horizontal line passing through OD center was determined. Individual cRVT measurements were convoluted with a Gaussian window, generating a cRVT profile dependent on the number of sectors measured in each device (256 sectors for HR-OCT or 64 sectors for both GDxVCC and GDxECC). Intersubject variability was determined using MATLAB.

Results: The median values for intersubject correlation between cRVT and RNFL thickness and the numbers of significant sectors as measured with Cirrus HR-OCT, GDx-ECC and GDx-VCC were 0.255 (186/256 sectors statistically significant), 0.192 (32/64) and 0.195 (33/64). 90% percentiles of the intersubject correlation were 0.400, 0.355 and 0.336, respectively.

Conclusions: Both SLP methods (GDx-VCC and GDx-ECC) yield comparable results regarding the intersubject correlation of the cRVT profile and the RNFL with about 50% of the sectors showing significant correlation. However, regarding the HR-OCT, our data showed a tendency towards a better correlation which was statistically significant in 70% of the sectors. Based on our results, up to 25% of the interindividual variation of the RNFL thickness might be explained by the variation of the cRVT.

Commercial Relationships: Ivania Pereira, None; Stephan Holzer, None; Hemma Resch, None; Barbara Kiss, None; Georg Fischer, None; Clemens Vass, None

Support: WWTF - LS11-046

Program Number: 4801 **Poster Board Number:** D0240

Presentation Time: 11:00 AM - 12:45 PM

Topographic Correlation between Ganglion Cell-Inner Plexiform Layer and Circumpapillary Retinal Nerve Fiber Layer Defect using Spectral Domain Optical Coherence Tomography

Ki Ho Park^{1,2}, Ko Eun Kim^{1,2}, Jin Wook Jeoung^{1,2}, Seok Hwan Kim^{1,3}, Dong Myung Kim^{1,2}. ¹Ophthalmology, Seoul National University College of Medicine, Seoul, Republic of Korea; ²Ophthalmology, Seoul National University Hospital, Seoul, Republic of Korea; ³Ophthalmology, SMG-SNU Boramae Medical Center, Seoul, Republic of Korea.

Purpose: To investigate the topographic correlation between ganglion cell-inner plexiform layer (GCIPL) and circumpapillary retinal nerve fiber layer (cpRNFL) defect in patients with localized RNFL defects using spectral domain (Cirrus) optical coherence tomography (OCT)

Methods: Fifty-four eyes of 54 patients showing localized RNFL defects on red-free RNFL photographs (angular width less than 30 degrees) were included. The angular location of the defect (angle α) and the angular width of the defects were measured from the RNFL photograph. The cpRNFL and GCIPL thickness measurements and deviation map analysis from normative database were performed by OCT (Figure 1). Topographic associations between angle α , clock-wise positions of cpRNFL defect, and GCIPL defect were evaluated.

Results: Topographic associations between clock-wise positions of cpRNFL defect and 6 sectors of GCIPL were: localized RNFL defect at 7 o/c \rightarrow defect at all inferior sectors; 8 o/c \rightarrow inferior and inferotemporal sectors; 10, 11 o/c \rightarrow all superior sectors (Figure 2). Six sectors showed different distribution of angle α ; however, there was overlap in range of angle α between adjacent sectors. Minimum

angle α in eyes showing defects in inferonasal, inferior, inferotemporal, superotemporal, superior, and superonasal sectors were 296.3, 284.3, 272.7, 48.7, 45.3, and 43.1 degrees, respectively. Maximum angle α in eyes showing defects were 340.3, 323.6, 312.8, 96.3, 76.4, and 58.2 degrees, respectively. The average angle α in eyes showing defects were 320.6, 308.0, 296.3, 68.2, 56.8, and 49.9 degrees, respectively.

Conclusions: Topographic correlation between cpRNFL and GCIPL defect can be obtained from patients with localized RNFL defects using angle α on red-free RNFL photographs and cpRNFL and GCIPL thickness deviation maps. The results reflect the topographic location of retinal ganglion cell death associated with the clock hour location of cpRNFL loss in vivo.

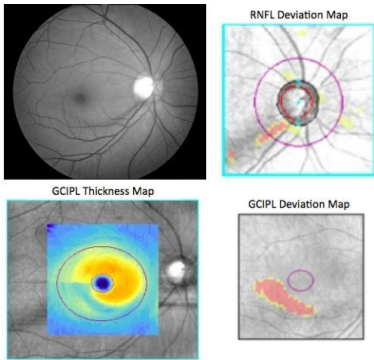


Figure 1

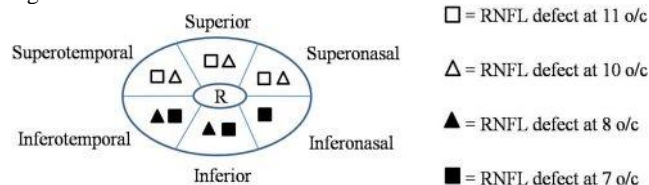


Figure 2

Commercial Relationships: Ki Ho Park, None; Ko Eun Kim, None; Jin Wook Jeoung, None; Seok Hwan Kim, None; Dong Myung Kim, None

Program Number: 4802 **Poster Board Number:** D0241

Presentation Time: 11:00 AM - 12:45 PM

Detecting Glaucomatous Structural Changes in Glaucoma Suspect Eyes Using a Cohort of Stable Glaucoma Patients

Naama Hammel¹, Linda M. Zangwill¹, Atsuya Miki¹, Sonia Jain², Feng He², Naira Khachatryan¹, Jeffrey M. Liebmann^{3,4}, Christopher A. Girkin³, Felipe A. Medeiros¹, Robert N. Weinreb¹. ¹Hamilton Glaucoma Center, Department of Ophthalmology, University of California, San Diego, La Jolla, CA; ²Department of Family and Preventive Medicine, University of California, San Diego, La Jolla, CA; ³New York University School of Medicine, New York, NY; ⁴Department of Ophthalmology, Einhorn Clinical Research Center, New York Eye and Ear Infirmary, New York, NY; ⁵School of Medicine, University of Alabama, Birmingham, AL.

Purpose: To establish normative test-retest variability limits for Spectralis SD-OCT retinal nerve fiber layer thickness (RNFLT) measurements using a cohort of stable glaucoma patients, and to evaluate whether changes exceeding these limits are associated with the development of glaucomatous visual field damage in a group of glaucoma suspects.

Methods: In order to estimate the 95 and 99 percentile variability limits, a group of stable glaucoma patients with repeatable visual field damage underwent weekly Spectralis SD-OCT testing over a

period of approximately 5 weeks. Fifty-five eyes of 29 stable glaucoma patients were included to compute the “95%change” and “99%change” (progression, improvement or both) criteria. Glaucoma suspects, defined as subjects having glaucomatous optic neuropathy based on stereo-photograph review or ocular hypertension without repeatable visual field damage at baseline, and ≥ 3 Spectralis SD-OCT visits were included. Eyes were classified as converts or non-converts based on the development of repeatable (3x) visual field damage. Glaucoma Suspect eyes were classified as having a repeatable RNFLT change if ≥ 2 visits change exceeded the 95% and/or 99% change cut-offs; otherwise eyes were considered as not changing.

Results: 474 eyes of 312 glaucoma suspects included had a median of 4 SD-OCT visits (range 3 to 11) over a median of 2.3 years. Seventy-nine eyes (16.6%) were classified as converts and 395 eyes (83.4%) were classified as non-converts. Of the 90 patients who met 99% progression criteria for global RNFLT 22 (27.85%) were converts and 68 (75.56%) non-converts. Of the 21 patients who met the 99% progression criteria for RNFLT Superior 4 (19%) were converts and 17 (81%) non-converts. Of the 81 patients who met the 99% progression criteria for RNFLT Inferior 15 (18.52%) were converts and 66 (81.48%) non-converts. Significant associations were observed between visual field conversion and global RNFL thinning exceeding the 95% and 99% cut-offs (odds ratios= 1.69 (95% CI 1.006, 2.84) and 1.84 (95% CI 1.05, 3.22) respectively). There were no significant associations between VF conversion and sectoral RNFL thinning.

Conclusions: The development of visual field damage was associated with global RNFL thinning established using limits derived from SD-OCT testing of stable glaucoma eyes.

Commercial Relationships: Naama Hammel, None; Linda M. Zangwill, Carl Zeiss Meditec Inc (F), Heidelberg Engineering GmbH (F), Optovue Inc (F), Topcon Medical Systems Inc (F), Nidek Inc (F); Atsuya Miki, NIDEK (C); Sonia Jain, None; Feng He, None; Naira Khachatryan, None; Jeffrey M. Liebmann, Alcon Laboratories, Inc. (C), Allergan, Inc. (C), Allergan, Inc. (F), Carl Zeiss Meditec, Inc (F), Heidelberg Engineering, GmbH (F), Topcon Medical Systems, Inc. (F), National Eye Institute (F), New York Glaucoma Research Institute (F), SOLX, Inc. (C), Bausch & Lomb, Inc (C), Diopsys, Inc. (C), Diopsys, Inc. (F), Merz, Inc. (C), Glaukos, Inc. (C), Quark, Inc. (C); Christopher A. Girkin, SOLX (F), Heidelberg Engineering (F); Felipe A. Medeiros, Carl-Zeiss (F), Heidelberg Engineering (F), Topcon (F), Alcon (F), Allergan (F), Sensimed (F), Reichert (F); Robert N. Weinreb, Aerie (F), Alcon (C), Allergan (C), Altheos (C), Amakem (C), Bausch&Lomb (C), Carl Zeiss-Meditec (C), Genentech (F), Haag-Streit (F), Heidelberg Engineering (F), Konan (F), Lumenis (F), National Eye Institute (F), Nidek (F), Optovue (C), Quark (C), Solx (C), Topcon (C)

Support: Supported by National Eye Institute grants U10EY14267, EY019869, EY021818, EY022039 and EY08208, EY11008, and EY13959 and Eyesight Foundation of Alabama; Alcon Laboratories Inc.; Allergan Inc.; Pfizer Inc.; Merck Inc.; Santen Inc.; and the Edith C. Blum Research Fund of the New York Glaucoma Research Institute, New York, NY, Supported by an unrestricted grant from Research to Prevent Blindness, New York, New York; Christopher A. Girkin: EyeSight Foundation of Alabama, Research to Prevent Blindness

Clinical Trial: NCT00221923

Program Number: 4803 **Poster Board Number:** D0242

Presentation Time: 11:00 AM - 12:45 PM

Evaluation of retinal nerve fiber layer retardation, thickness and birefringence along the major nerve fiber bundles measured with polarization sensitive OCT

Stefan Zotter¹, Michael Pircher¹, Teresa Torzicky¹, Bernhard Baumann¹, Philipp K. Roberts^{2,1}, Ivania Pereira², Stephan Holzer², Clemens Vass², Ursula Schmidt-Erfurth², Christoph K. Hitzenberger¹. ¹Center for Med. Phys. and Biomed. Eng., Medical University of Vienna, Vienna, Austria; ²Department of Ophthalmology and Visual Sciences, Medical University of Vienna, Vienna, Austria.

Purpose: To evaluate the retinal nerve fiber layer (RNFL) retardation, thickness and birefringence along the major nerve fiber bundles within healthy human subject using polarization sensitive OCT (PS-OCT).

Methods: For this study a recently presented PS-OCT system was used. The instrument provides a maximum scan field of 40° x 40° and operates at an A-scan rate of 70kHz. Currently 10 eyes of 5 healthy subjects are included in the study. 3D measurements of the optic disc area were performed and RNFL retardation, thickness and birefringence maps were generated for each dataset. For quantitative analysis seven evaluation boxes were placed manually along the large nerve fiber bundles superior and inferior to the optic disc. The mean retardation, thickness and birefringence was calculated within these boxes and plotted against the distance from the center of the optic disc. The resulting curves were averaged for all eyes included in the study.

Results: The mean RNFL retardation within our study group started at a value of 37.2° superior at 5° eccentricity from the center of the optic disc (37° inferior) and decreased to 24.2° at 12° eccentricity (23.6° inferior). The mean RNFL thickness superior at 5° eccentricity was measured to be 163.6µm (175.7µm inferior) and decreased to 127.9µm (123.2µm inferior) at 12° eccentricity. The mean birefringence exhibited a value of 0.147°/µm superior to the optic disc at 5° eccentricity (0.14°/µm) and remained widely constant along the major nerve fiber bundle. The mean birefringence at 12° eccentricity was 0.138°/µm superior and 0.141°/µm inferior.

Conclusions: The mean RNFL retardation, thickness and birefringence were evaluated along the large nerve fiber bundles within the human retina. We found that the retardation and thickness decreases with eccentricity from the optic disc whereas the birefringence remains widely constant. Further measurements on a larger study population are planned to support these findings.

Commercial Relationships: Stefan Zotter, Canon Inc. (F); Michael Pircher, Canon Inc. (F), Canon Inc. (F); Teresa Torzicky, Canon (F); Bernhard Baumann, Canon Inc. (F); Philipp K. Roberts, Canon Inc. (F); Ivania Pereira, None; Stephan Holzer, None; Clemens Vass, None; Ursula Schmidt-Erfurth, Alcon (C), Bayer Healthcare (C), Novartis (C); Christoph K. Hitzenberger, Canon Inc. (F), Canon Inc. (C)

Program Number: 4804 **Poster Board Number:** D0243

Presentation Time: 11:00 AM - 12:45 PM

In-Vivo Microstructural Anatomy of Parapapillary Atrophy: Beta-Zone and Gamma- Zone

Yi Dai¹, Jost B. Jonas², Haili Huang¹, Min Wang¹, Xinghuai Sun¹.

¹Ophthalmology, EYE & ENT Hospital, Shanghai, China;

²Ophthalmology, Medical Faculty Mannheim of the Ruprecht-Karls-University, Heidelberg, Germany.

Purpose: To examine the morphologic features of parapapillary atrophy by using enhanced depth imaging optical coherence tomography (EDI-OCT) and color fundus photographs.

Methods: The clinical observational comparative study included 80 normal eyes of 46 subjects and 80 eyes of 46 patients with primary open-angle glaucoma. Both groups did not vary significantly in axial length (P=0.19) and refractive error (P=0.22). Color fundus photographs and horizontal cross-sectional B-scan images obtained

by EDI-OCT were examined. On the EDI-OCT images, we measured a gamma zone defined as the region between the temporal disc margin to the beginning of Bruch's membrane, and a beta zone defined as Bruch's membrane without retinal pigment epithelium.

Results: Gamma zone (mean area: 1.09±1.83 mm²) was significantly associated with longer axial length (P<0.001; standardized coefficient beta: 0.59), longer vertical disc diameter (P<0.001; beta: 0.32), older age (P<0.001; beta: 0.22), and absence of glaucoma (P=0.003; beta: -0.20). Beta zone (mean area: 0.83±0.59 mm²) was associated with longer axial length (P<0.001; beta: 0.29), longer vertical disc diameter (P=0.002; beta: 0.24), older age (P=0.01; beta: 0.19), and presence of glaucoma (P<0.001; beta: 0.34).

Conclusions: In addition to associations with older age, increasing myopia and larger disc size, EDI-OCT defined gamma zone of parapapillary atrophy was associated with absence of glaucoma, while EDI-OCT defined beta zone was associated with the presence of glaucoma. Differentiation between both beta zone and gamma zone may clinically be useful.

Commercial Relationships: Yi Dai, None; Jost B. Jonas, Allergan (C), MSD (C), Alimera (C), CellMed AG (P); Haili Huang, None; Min Wang, None; Xinghuai Sun, None

Support: National Science Foundation of China (81170838), and Shanghai Science and Technology Commission (11PJ1402100)

Program Number: 4805 **Poster Board Number:** D0244

Presentation Time: 11:00 AM - 12:45 PM

Comparison of birefringence-related data between scanning laser polarimetry (GDx) and polarization sensitive optical coherence tomography (PS-OCT)

Clemens Vass¹, Ivania Pereira¹, Stefan Zotter², Stephan Holzer¹, Hemma Resch¹, Michael Pircher², Christoph K. Hitzenberger². ¹Dept of Ophthalmology, Medical University of Vienna, Vienna, Austria; ²Center for Medical Physics and Biomedical Engineering, Medical University of Vienna, Vienna, Austria.

Purpose: To compare the retardation of the retinal nerve fiber layer (RNFL) measured with the scanning laser polarimeter GDx-VCC and GDx-ECC (Carl Zeiss Meditec Inc.) with the retardation as measured with polarization sensitive optical coherence tomography (PS-OCT).

Methods: A sample of 8 healthy volunteers, 13 glaucoma suspects and 5 early glaucoma patients underwent complete ophthalmologic examination, including visual field testing, GDx-VCC and GDx-ECC and PS-OCT. Early glaucoma was defined as glaucomatous optic neuropathy with a visual field mean deviation (VF-MD) of -4 dB or better. The definition of glaucoma suspect was based on the suspect appearance of the optic disc while VF was normal. PS-OCT was measured with a system operating at 70kHz A-scan rate (scan angle 30°x30° or 40°x40°, scan pattern 1024x250 A-scans). We compared the average retardation of the superior and inferior sectors. The thickness values of the GDx were converted to degree of retardation for comparison using the published fixed conversion factor. When converting the data we furthermore took into account for the different wavelengths of the GDx and our PS-OCT.

Results: For the mean values (deg.) and standard deviations of the three different measurements please see the table. For GDx-ECC, GDx-VCC and PS-OCT we found statistically significant differences between the healthy and the suspect groups (p<0.05). There was also a small but statistically significant difference between the retardation found with the GDx and the PS-OCT, the latter giving slightly higher values (p<0.05).

Conclusions: The retardation values given by the GDx and the PS-OCT are comparable as are the differences between the groups.

	Healthy	Suspects	Early glaucoma
Age	49.5	60.2	59.9
PS-OCT superior	20.84 (± 2.35)	17.36 (± 3.68)	16.71 (± 6.60)
PS-OCT inferior	22.36 (± 1.80)	18.37 (± 3.30)	16.94 (± 4.40)
GDx-ECC superior	19.01 (± 1.20)	16.06 (± 1.60)	14.87 (± 4.05)
GDx-ECC inferior	18.57 (± 2.07)	15.34 (± 2.08)	13.14 (± 2.64)
GDx-VCC superior	19.53 (± 0.93)	16.22 (± 1.71)	14.98 (± 4.05)
GDx-VCC inferior	19.22 (± 2.23)	15.53 (± 2.26)	12.86 (± 3.02)

Commercial Relationships: Clemens Vass, None; Ivania Pereira, None; Stefan Zotter, Canon Inc. (F); Stephan Holzer, None; Hemma Resch, None; Michael Pircher, Canon Inc. (F), Canon Inc. (C); Christoph K. Hitzenberger, Canon Inc. (F), Canon Inc. (C)

Program Number: 4806 **Poster Board Number:** D0245

Presentation Time: 11:00 AM - 12:45 PM

Agreement between Clinical versus Automated Disc Damage Likelihood Scalw (DDLs) Staging in Asian Indian eyes

Premnath Gnanewaran, Sathi A. Devi, Ramgopal Balu, Dhanraj Rao, Narendra K. Puttaiah, Rohit Shetty, Rajesh Sasikumar. Glaucoma, Narayana Nethralaya, Bangalore, India.

Purpose: To determine the agreement between clinical versus automated Disc Damage Likelihood Scale (DDLs) staging and if it was affected by disc size.

Methods: In this prospective observational study, consecutive subjects who were diagnosed to have glaucoma or ocular hypertension were enrolled. DDLs staging was done clinically by stereo-biomechanography after measuring optic disc size and rim/disc ratio. Using appropriate corrective factors for measuring disc size, the discs were categorized into small, average and large discs. The Kowa Nonmyd WX retinal camera (Kowa Optimed, Nagoya, Japan) was used for stereoscopic fundus imaging; a single examiner then stereoscopically observed and marked the outline of the optic disc and cup; the built-in software then calculated the DDLs staging. Agreement between the 2 methods and for evaluating effect of disc size was assessed using weighted kappa (categorical data) and reliability was measured using intraclass correlation coefficient (ICC). We also assessed intra-observer reproducibility of the automated staging in 30 eyes.

Results: 68 eyes (36 patients) were enrolled; the mean age was 49.8 ± 16.9 years and majority were men (64%). The two methods showed good agreement ($\kappa=0.81$, 95% C.I. 0.74-0.88) and repeatability ($r=0.97$, 95% C.I. 0.96-0.98). Moderate sized discs showed very good agreement ($r=0.85$, 95% C.I. 0.77-0.93), while large discs showed moderate agreement ($r=0.69$, 95% C.I. 0.53-0.83). Intra-observer reproducibility was very good for the automated staging ($r=0.97$, 95% C.I. 0.97-0.99).

Conclusions: Automated DDLs staging showed good agreement with clinical staging and could be used as an alternative tool in diagnosis; disc size did not appear to be a major determinant.

Commercial Relationships: Premnath Gnanewaran, None; Sathi A. Devi, None; Ramgopal Balu, None; Dhanraj Rao, None; Narendra K. Puttaiah, None; Rohit Shetty, None; Rajesh Sasikumar, None

Program Number: 4807 **Poster Board Number:** D0246

Presentation Time: 11:00 AM - 12:45 PM

Multiple linear regression analysis between circumpapillary retinal nerve fiber layer thickness profiles measured with scanning laser polarimetry and retinal blood vessel thickness, optic disc parameters and age

Hemma Resch¹, Ivania Pereira¹, Stephan Holzer¹, Barbara Kiss¹, Georg Fischer², Clemens Vass¹. ¹Ophthalmology and Optometry, Medical University of Vienna, Austria, Vienna, Austria; ²Center for Medical Statistics Informatics and Intelligent Systems, Section for

Medical Information Management and Imaging, Medical University of Vienna, Austria, Vienna, Austria.

Purpose: Variations of the normal quantity and distribution of retinal nerve fiber layer (cRNFL) thickness may compromise accurate glaucoma diagnosis. Following the idea that vessels mark regions of thicker cRNFL, the purpose of the present work is to correlate cRNFL with circumpapillary retinal vessel thickness (cRVT) together with optic disc (OD) size and shape as well as age.

Methods: cRNFL thickness values of 106 healthy subjects were measured using scanning laser polarimetry (SLP), (GDx-ECC © Carl Zeiss Meditec Inc.) and OD HR-OCT scans (Cirrus® Carl Zeiss Meditec Inc.) were obtained. A proprietary software was developed in MATLAB® (Version R2009b, The Mathworks Inc.) for manual identification of the OD contour and assessment of the cRVT at OD border, using the SLO image from Cirrus HR-OCT centered in the OD. The angle of the intersection between a horizontal line passing through the OD center and a line between OD center and the center point of each vessel measured was calculated. cRVT data were convoluted with a Gaussian window, generating a 64-sector profile dependent on the 64 sectors for GDxECC. Intersubject correlations were calculated using SPSS Software Package (version 17.0). In a stepwise multiple linear regression analysis we used cRVT, OD area (ODA), OD vertical to horizontal diameter ratio (VHR) and age as independent and cRNFL thickness as dependent variables for each of the 64 sectors. The significance level was $p < 0.05$.

Results: 52 out of 64 sectors had a significant intersubject correlation in multiple linear regression analysis. cRVT, ODA, VHR and age were included either alone or together with other variables in 30/64, 16/64, 14/64, 17/64 sectors with a maximum regression coefficient (Rmax) of 0.51, 0.31, 0.27 and 0.35. Both cRVT and VHR, ODA and age, cRVT and age were included in 11/64, 1/64 and 12/64 with Rmax of 0.55, 0.33 and 0.44.

Conclusions: In multiple linear regression we found significant impact of one or more of the investigated independent variables on the cRNFL in 80% of the sectors. The single most important variable was the cRVT, significantly contributing to the cRNFL in 47% of the sectors. The cRVT profile together with age and other OD parameters, as ODA and VHR might explain up to 30% of the interindividual variation of the cRNFL thickness profiles.

Commercial Relationships: Hemma Resch, None; Ivania Pereira, None; Stephan Holzer, None; Barbara Kiss, None; Georg Fischer, None; Clemens Vass, None

Support: WWTF - LS11-046

Program Number: 4808 **Poster Board Number:** D0247

Presentation Time: 11:00 AM - 12:45 PM

Influence of Anterior Segment Biometric Parameters on the Anterior Chamber Angle Width in Eyes with Angle Closure and Open Angle

Takaaki Matsuki^{1,2}, Fumitaka Hirose^{1,2}, Takanori Kameda^{1,2}, Yasuhiko Hiram^{1,2}, Yasuo Kurimoto^{1,2}. ¹Ophthalmology, Kobe City Medical Center General Hospital, Kobe, Japan; ²Ophthalmology, Inst of Biomed Research and Innovation, Kobe, Japan.

Purpose: Primary angle-closure glaucoma is a significant cause of blindness in Asia. Assessment of angle configuration is important for the prevention and treatment of primary angle closure. The purpose of this study is to investigate the associations between anterior chamber angle width and other anterior segment biometric parameters, and to identify the major predictors of anterior chamber angle width in eyes with angle closure and open angle.

Methods: We used anterior segment optical coherence tomography (AS-OCT) to examine 118 eyes of 118 angle closure patients (27 men and 91 women with a mean age of 71.1 ± 8.3 years) and 34 eyes

of 34 primary open angle glaucoma patients (17 men and 17 women with a mean age of 67.7 ± 7.7 years) under dark and light conditions. After measuring the angle opening distance 500 (AOD500), anterior chamber depth (ACD), iris thickness (IT), iris convexity (IC), pupil diameter (PD), anterior chamber width (ACW), and crystalline lens rise (CLR), we performed univariate analyses and multivariate regression analyses for the AOD500 for each group.

Results: Results: In angle closure group, the explanatory variables relevant to the AOD500 were ACD, IT, IC, PD, and ACW under both dark and light conditions (In the dark: standard coefficients (β) 0.518, -0.399, -0.281, -0.261, and -0.223, respectively, $p < 0.01$ for all, adjusted $R^2 = 0.473$ In the light: β 0.413, -0.166, -0.401, -0.333, and -0.210, respectively, $p < 0.01$ for all except IT ($p < 0.05$), adjusted $R^2 = 0.413$). In open angles group, the explanatory variables relevant to the AOD500 were ACD, IT, IC, and ACW under the dark conditions, and ACD, IT, IC, and PD under the light conditions (In the dark: β 0.578, -0.558, -0.480, and -0.262, respectively, $p < 0.01$ for all, adjusted $R^2 = 0.851$ In the light: β 0.397, -0.317, -0.588, and -0.235, respectively, $p < 0.01$ for all, adjusted $R^2 = 0.828$).

Conclusions: This study quantitatively confirmed that ACD was one of the major predictors of the anterior chamber angle width under both dark and light conditions and especially under the dark conditions, IT was stronger factor rather than IC whether eyes with angle closure or open angle. Therefore this study showed that the same anterior segment anatomical or physiological principles exist between eyes with angle closure and eyes with open angle.

Commercial Relationships: Takaaki Matsuki, None; Fumitaka Hirose, None; Takanori Kameda, None; Yasuhiko Hirami, None; Yasuo Kurimoto, HOYA (F), Santen (F), Senju (F), Abott (F), Alcon (F)

Program Number: 4809 **Poster Board Number:** D0248

Presentation Time: 11:00 AM - 12:45 PM

Scan quality can affect Scanning Laser Polarimetry outcomes

Alice Chandra Verticchio Vercellin^{1,2}, Giovanni Milano^{1,2}, Sara Lombardo^{1,2}, Marta Raimondi^{1,2}, Sara Lanteri^{1,2}, Carlo Alberto Cutolo^{1,2}, Laura Bossolesi^{2,1}, Gemma C. Rossi^{2,1}. ¹University of Pavia, Pavia, Italy; ²Policlinico San Matteo Pavia, Pavia, Italy.

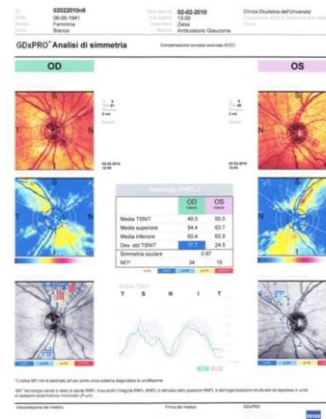
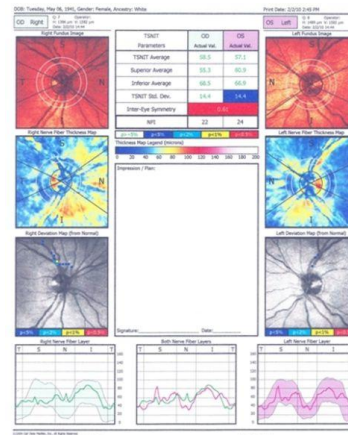
Purpose: To compare scanning laser polarimetry (GDx) with variable corneal compensation (VCC) versus enhanced corneal compensation (ECC) and to correlate GDx structural data with functional data of Standard Automated Perimetry (SAP).

Methods: 339 eyes of 182 glaucoma suspects were included and screened by the glaucoma unit of the University Eye Clinic of Pavia (Italy). Patients were submitted to complete ophthalmic examination, standard automated perimetry (SAP), scanning laser polarimetry with GDx-VCC and GDx-ECC. Quality image (Q), typical scan score (TSS), nerve fibers index (NFI), nerve fibers layer average thickness in a band around the optic nerve head (TSNIT average) and in the upper (TSNIT sup) and lower sector (TSNIT inf) provided by VCC and ECC were taken into account and compared using Wilcoxon signed-rank test. Correlation between GDx and perimetric global indexes MD, PSD was evaluated with Pearson correlation index. The same statistics tests were applied to a smaller group of 118 eyes characterized by a scanning laser polarimetry of optimal quality (Q>7 and TSS>80 both with VCC and ECC).

Results: ECC provides better quality images than VCC: 204 images out of 339 (60%) were of good quality (Q>7) with VCC and 325 out of 339 (96%) with ECC. 140 images out of 339 (41%) were atypical (TSS<80) with VCC but only 20 out of 339 with ECC (6%). In both groups ECC versus VCC constantly displays lower TSNIT thickness and higher NFI and structure/function correlation was only poor to moderate, better for ECC parameters and above all for NFI. In the

selected group of 118 patients the difference ECC/VCC reduces and there is an increase of the structure/function correlation for VCC parameters particularly for TSNIT inferior and average.

Conclusions: ECC provides better quality images than VCC and probably reproduces a more reliable RNFL structure model than VCC. ECC points out lower RNFL thickness and higher NFI and reveals a better correlation to perimetric indexes as compared to VCC. GDx-ECC could improve early glaucoma diagnosis. Considering a poor to moderate structure/function correlation even with GDx-ECC, a correct diagnosis of glaucomatous optic neuropathy still requires an evaluation of structure and function of the optic nerve.



Commercial Relationships: Alice Chandra Verticchio Vercellin, None; Giovanni Milano, Alcon (R); Sara Lombardo, None; Marta Raimondi, None; Sara Lanteri, None; Carlo Alberto Cutolo, None; Laura Bossolesi, None; Gemma C. Rossi, None

Program Number: 4810 **Poster Board Number:** D0249

Presentation Time: 11:00 AM - 12:45 PM

A New Marker for Detecting Retinal Ganglion Cell Apoptosis

Jacky Man Kwong Kwong¹, Celia Hoang¹, Reshil M. Torrevillas¹, Joseph Caprioli¹, Richard W. Yee², Brian D. Gray³, Jeffrey A. Mattis³, Koon Y. Pak³. ¹Ophthalmology, Jules Stein Eye Institute, UCLA, Los Angeles, CA; ²Cizik Eye Clinic, University of Texas, Health Science Center, Houston, TX; ³Molecular Targeting Technologies, Inc., West Chester, PA.

Purpose: To detect retinal ganglion cell (RGC) apoptosis using molecular probes comprising, bis(zinc(II)-dipicolylamine) (Zn-DPA) conjugated with fluorescent dyes, in N-methyl-D-aspartate (NMDA)-induced excitotoxicity in rats.

Methods: Adult Wistar rats, 3 months old, were given unilateral intravitreal injection of 3 μ L of 40mM neutralized NMDA in 0.1M phosphate buffered saline. Groups of animals were euthanized at 2, 4, 6, 9, 12, 24 and 48 hours after injection and their eyes were enucleated (N=4 per group). One hour prior to euthanasia, 3 μ L of 1mM Zn-DPA conjugated with either fluorescein (Zn-DPA480) or rhodamine (Zn-DPA550) was intravitreally injected. Zn-DPA binds to the anionic membrane of cells undergoing apoptosis and necrosis. For quantitative analysis, TdT-mediated biotin-dUTP nick end labeling (TUNEL) and immunohistochemistry of beta-tubulin (RGC marker) and vimentin (Muller cell marker) were performed on retinal sections. Prelabeling of RGC with retrograde dyes including fluorogold and DTMR was performed and the retinal flatmount was examined using fluorescence microscopy.

Results: Remarkable fluorescence labeling of Zn-DPA480 and Zn-DPA550 was observed in the cells in the RGC layer from 2 hours up to 24 hours after NMDA injection. There was absence of Zn-DPA labeling at 48 hours post-injection and with all controls. At 4 hours post-injection, 53.1 \pm 10.1% of Zn-DPA 480 positive were beta-tubulin positive while 16.4 \pm 9.0% of Zn-DPA480 positive cells were vimentin positive. Prelabeling of fluorogold and DTMR confirmed that the majority of Zn-DPA480 and Zn-DPA550 positive cells found in retinal flatmount were RGCs. The TUNEL positive cells appeared at 4 hours and the number peaked at 18 hours post-injection but disappeared at 48 hours. At 4 hours post-injection, 90.1 \pm 4.6% of Zn-DPA480 positive cells were TUNEL positive while over 96.4 \pm 3.5% of TUNEL positive cells were Zn-DPA480 positive.

Conclusions: Our findings demonstrate that intravitreal injection of fluorescent Zn-DPAs labels RGCs undergoing apoptosis suggesting the potential as an imaging probe for tracking degenerating retinal neurons in vivo.

Commercial Relationships: Jacky Man Kwong Kwong, MTTI (P); Celia Hoang, None; Reshil M. Torrevillas, None; Joseph Caprioli, Allergan Inc. (F), Allergan Inc. (C), Allergan Inc. (R); Richard W. Yee, MTTI (P), Allergan (R); Brian D. Gray, Molecular Targeting Technologies, Inc (E), Molecular Targeting Technologies, Inc (P); Jeffrey A. Mattis, Molecular Targeting Technologies, Inc. (E); Koon Y. Pak, Molecular Targeting Technologies, Inc. (E), Molecular Targeting Technologies, Inc. (I), Molecular Targeting Technologies, Inc. (P)

Support: None in the Support

Program Number: 4811 **Poster Board Number:** D0250

Presentation Time: 11:00 AM - 12:45 PM

Pupil-based detection of asymmetric glaucomatous damage - comparison of the Konan RAPDx pupillograph, swinging flashlight method, and magnifier-assisted swinging flashlight method

Mohsin Ali^{1,2}, Lan Lu¹, Patricia Martinez¹, Bruno M. Faria¹, Lalita Gupta¹, Alice Zhang^{1,2}, Eileen Hwang¹, Marlene R. Moster¹, George L. Spaeth¹. ¹Glaucoma Service, Wills Eye Institute, Philadelphia, PA; ²Jefferson Medical College, Philadelphia, PA.

Purpose: Afferent pupillary defect (APD) testing is most commonly performed using the swinging flashlight method (SFM). The magnifier-assisted SFM (MA-SFM), which involves holding a +20-diopter lens in front of the eye being examined, has previously been found to increase the sensitivity of APD detection. Pupillography devices, such as the Konan RAPDx, may also allow for improved APD detection, while providing objective measurements of pupil response parameters. This study aims to compare the ability of the RAPDx pupillograph with the SFM and MA-SFM in the detection of asymmetric glaucomatous damage.

Methods: 118 patients presenting to the glaucoma service underwent

full clinical examinations and APD testing with the SFM, MA-SFM, and RAPDx pupillograph. Each test was performed by separate examiners who were blinded to the patient's clinical information and to the results of the other tests. Using the SFM and MA-SFM, an apparently positive APD was defined by the presence of immediate or delayed pupillary dilation. Using the RAPDx pupillograph, an apparently positive APD was defined by a calculated index of defect, Amp_c, greater than 0.2 (representing the negative log of the difference between the amplitudes of constriction in one eye versus the other). An APD (positive SFM, positive MA-SFM, or Amp_c > 0.2) was considered "corroborated" when there was a difference of (a) ≥ 1 Disc Damage Likelihood Scale unit between both eyes or (b) ≥ 0.1 cup/disc ratio between both eyes.

Results: 22/118 (18.6%) patients were unable to complete pupillography testing for reasons such as ptosis and irregular or fixed pupils. 39/118 patients were excluded because of retinal disease or insufficient clinical data. Apparent APDs were detected in 15/57 (26.3%), 35/57 (61.4%), and 35/57 (61.4%) by the SFM, MA-SFM, and RAPDx, respectively. "Corroborated" APDs were found in 9/57 (15.8%), 21/57 (36.8%), and 22/57 (38.6%) by the SFM, MA-SFM, and RAPDx, respectively. Clinically detected asymmetry in disc damage was missed in 28/57 (49.1%), 12/57 (21.1%), and 12/57 (21.1%) by the SFM, MA-SFM, and RAPDx, respectively.

Conclusions: The RAPDx pupillograph and MA-SFM are useful tools in the detection of asymmetric glaucomatous damage and are able to detect apparent and "corroborated" APDs more often than the SFM.

Commercial Relationships: Mohsin Ali, None; Lan Lu, None; Patricia Martinez, None; Bruno M. Faria, None; Lalita Gupta, None; Alice Zhang, None; Eileen Hwang, None; Marlene R. Moster, Alcon (C), Alcon (F), Allergan (F), Allergan (C), Merck (F), Merck (C), Mobius (F), Aeon (F), Aerie (F), Ista (F), iScience (F), Solex (C), Baush and Lomb (F); George L. Spaeth, Merck (F), U.S. Patent No. 8,042,946 (P), Pfizer (F)

Program Number: 4812 **Poster Board Number:** D0251

Presentation Time: 11:00 AM - 12:45 PM

Effect of Laser Peripheral Iridotomy on Trabecular-Iris Surface Area Over 360 Degrees in Primary Angle Closure

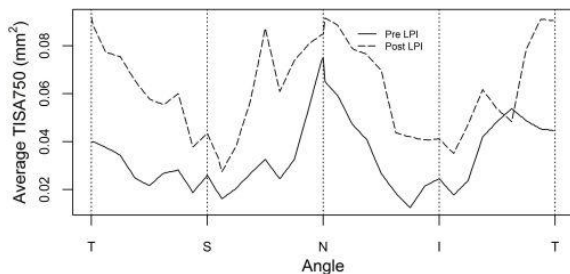
Donna Nguyen¹, Nicholas P. Bell^{1,2}, Lauren S. Blieden^{1,2}, Laura A. Baker², Alice Z. Chuang¹, Robert M. Feldman^{1,2}. ¹Ophthalmology and Visual Science, The University of Texas Health Science Center at Houston, Houston, TX; ²Robert Cizik Eye Clinic, Houston, TX.

Purpose: Trabecular-iris surface area 750 (TISA750) is a measurement commonly used to characterize the anterior chamber angle depth. By using Swept Source Fourier domain anterior segment optical coherence tomography (FD ASOCT), TISA750 can now be calculated every 1.4 degrees over the entire circumference of the anterior chamber angle. Clinically, it is believed that the entire angle deepens after laser peripheral iridotomy (LPI); however, this has never been quantitatively measured. The purpose of this study is to evaluate the effect of LPI on TISA750 over the entire angle circumference in primary angle closure (PAC) eyes.

Methods: Thirteen consecutive eyes with PAC and Spaeth gonioscopy grades A or B scheduled for LPI were included. LPIs were placed temporally. Eyes were imaged in both 2D and 3D modes using the Angle Analysis Scan on the CASIA SS-1000 ASOCT (Tomey, Nagoya, Japan) preoperatively and 3 months postoperatively. An experienced reader using the Anterior Chamber Analysis and Interpretation software (ACAI, Houston, Texas) identified the scleral spur landmarks (SSLs) on the higher resolution 2D images (both horizontal and vertical scans). The ACAI software automatically transferred the SSLs to the same location on the 3D

images and then interpolated SSLs for the rest of the angle. These were confirmed or adjusted by the reader. Average TISA750 was calculated for each location at each time point based on these SSLs. **Results:** Thirteen eyes of 7 patients were evaluated. The average age was 59.4 (\pm 10.6) years. Eight of the LPIs were within 20 degrees inferotemporal to the horizontal meridian and 5 were within 20 degrees superotemporal to the horizontal meridian. Overall, average TISA750 increased from 0.033 mm² to 0.062 mm² post-LPI and was greater than the pre-LPI TISA750 at all locations except 30-40 degrees below the horizontal meridian. Figure 1 shows the average TISA750 pre- and post-LPI.

Conclusions: The clinical impression of circumferential angle deepening after LPI is confirmed quantitatively. TISA750 increases over the entire circumference of the angle with the exception of 30-40 degrees below the horizontal meridian. We hypothesize that the lack of deepening in this location may be related to post-LPI iris thickening inferior to the area of the LPI. This deserves further study.



Average TISA750 Pre- and Post-LPI

Commercial Relationships: Donna Nguyen, None; Nicholas P. Bell, None; Lauren S. Blieden, None; Laura A. Baker, None; Alice Z. Chuang, None; Robert M. Feldman, Tomey Corporation (F) **Support:** NEI Vision Core Grant P30EY010608; Challenge Grant to the University of Texas Medical School at Houston from Research to Prevent Blindness, New York, NY; and the Hermann Eye Fund, Houston, TX. The Casia SS-1000 FD-ASOCT was loaned to Robert M Feldman, MD by the Tomey Corporation.

Program Number: 4813 **Poster Board Number:** D0252

Presentation Time: 11:00 AM - 12:45 PM

The Prevalence of Spectral Domain Optical Coherence Tomography Artifact Patterns in Different Subtypes of Open Angle Glaucoma and Normal Eyes

Neda Baniasadi, Eleftherios I. Paschalis, Teresa C. Chen. Ophthalmology, Massachusetts Eye & Ear Infirmary/Harvard Medical School, Boston, MA.

Purpose: To determine the prevalence of different types of spectral domain optical coherence tomography (SD-OCT) scan artifacts for four different types of open angle glaucoma (OAG): primary OAG (POAG), normal tension glaucoma (NTG), pseudoexfoliation glaucoma (PXG), and pigmentary glaucoma (PDG), and compare with normal controls.

Methods: SD-OCT (Heidelberg Engineering, Heidelberg, Germany) retinal nerve fiber layer (RNFL) scan printouts were evaluated for three patterns of artifacts: 1) algorithm failure: misidentification of the RNFL borders, 2) poor signal, or signal strength <15 dBm, 3) scan de-centration. The prevalence of each type of artifacts was determined for four subtypes of OAG and for normal patients.

Results: The study population consisted of 256 eyes of 256 patients: 91 patients with OAG, 28 with NTG, 45 with PXG, 12 with PDG, and 80 without glaucoma. The prevalence of good scans was 49.21% (n=126), algorithm failure was 21.87% (n=56), de-centration was 7.03% (n=18), and poor signal was 13.28% (n=34). For scans with

two types of artifacts, we could detect combined algorithm failure and poor signal in 7.03% (n=18), algorithm failure and de-centration in 0.39% (n=1), and poor signal and de-centration in 0.39% (n=1). Two eyes (0.78%) had three types of artifacts. There were no significant differences in the prevalence of artifacts between different subtypes of OAG and normal eyes. (p >0.05)

Conclusions: This study reveals that the prevalence of SD-OCT artifacts is high, with the algorithm failure being the most common artifact. There were no significant differences in the prevalence of artifacts among all studied subtypes of OAG.

Commercial Relationships: Neda Baniasadi, None; Eleftherios I. Paschalis, None; Teresa C. Chen, None

Program Number: 4814 **Poster Board Number:** D0253

Presentation Time: 11:00 AM - 12:45 PM

Evaluation of segmented macular scans by spectral domain optical coherence tomography in glaucoma

Maxime Delbarre, Hussam El Chehab, Marlene Francoz, Jean-Remi Fenolland, Marechal Marie, Jean-Marie Giraud, Frank May, Jean-Paul G. Renard. Department of Ophthalmology, Hôpital du Val-de-Grâce, Paris, France.

Purpose: The aim of this study is to evaluate the glaucoma discriminating ability of macular layers measured by spectral domain optical coherence tomography (Cirrus HD-OCT, Carl Zeiss Meditec (CZM), Dublin, CA, USA).

Methods: This study concerns 252 eyes of 120 glaucoma patients treated for primary open angle glaucoma (POAG) (164 early POAG, 44 moderate POAG and 44 advanced POAG) and 337 eyes of 148 normal control subjects. Every patient underwent a visual field testing (Humphrey Field Analyser, SITA-Standard 24-2, CZM), and SD-OCT imaging (Cirrus HD-OCT) in the macular (Ganglion Cell Analysis (GCA), macular cube 200x200) and optic nerve head regions (optic disc cube 200x200).

OCT macular scans were segmented into macular nerve fibre layer (mNFL), ganglion cell layer with inner plexiform layer (GCIPL) and ganglion cell complex (GCC) (mNFL + GCIPL). Glaucoma discriminating ability was assessed using the area under the receiver operator characteristic curve (AUC) for all macular parameters and mean circumpapillary retinal nerve fibre layer (cpRNFL).

Results: There is a statistically significant difference between glaucomatous eyes and control eyes for every parameters (p <0.05). Parameters with the best AUCs in the early POAG group were the minimum GCIPL (0.747 (Se = 46.4%, Sp = 89.9%)), average GCIPL (0.716 (Se = 52.4%, Sp = 84.3%)), GCC (0.710 (Se = 86.0%, Sp = 47.5%)), cpRNFL (0.704 (Se = 39.0% sp = 92.42%)), minimum mNFL (0.673 (Se = 28.0%, Sp = 92.6%)) and average mNFL (0.655 (Se = 31.0%, Sp = 95.0%))

Parameters with the best AUCs in the moderate POAG group were the minimum GCIPL (0.864 (Se = 65.9%, Sp = 92.3%)), GCC (0.858 (Se = 47.7%, Sp = 94.9%)), cpRNFL (0.853 (Se = 36.6% sp = 99.0%)), average GCIPL (0.838 (Se = 13.6%, Sp = 98.5%)), average mNFL (0.820 (Se = 79.5%, Sp = 76.0%)) and minimum mNFL (0.815 (Se = 59.1%, Sp = 95.2%)).

Parameters with the best AUCs in the advanced POAG group were the minimum GCIPL (0.938 (Se = 86.4%, Sp = 93.5%)), GCC (0.928 (Se = 68.2%, Sp = 97.3%)), minimum mNFL (0.920 (Se = 63.6%, Sp = 97.6%)), average GCIPL (0.908 (Se = 50.0% sp = 98.5%)), cpRNFL (0.854 (Se = 52.4 %, Sp = 100.0%)) and average mNFL (0.854 (Se = 52.4 %, Sp = 100.0%)).

Conclusions: The minimum macular GCIPL is a new index obtained with the GCA algorithm of Cirrus-HD OCT. It seems to have an excellent ability to detect glaucoma at every stage with a better performance than peripapillary RNFL.

Commercial Relationships: Maxime Delbarre, None; Hussam El Chehab, None; Marlene Francoz, None; Jean-Remi Fenolland, None; Marechal Marie, None; Jean-Marie Giraud, None; Frank May, None; Jean-Paul G. Renard, None

Program Number: 4815 **Poster Board Number:** D0254

Presentation Time: 11:00 AM - 12:45 PM

A Novel Technology to Detect and Visualize Macular Retinal Nerve Fiber Layer (RNFL) Loss in Glaucoma Using Spectral Domain Optical Coherence Tomography

Laura de Polo^{1,2}, Alessandro Invernizzi¹, Mariano Cozzi¹, Mirella Blini¹, Giovanni Staurenghi¹. ¹Hospital Luigi Sacco, Milano, Italy; ²COB, Centro Oculistico Bergamasco, Bergamo, Italy.

Purpose: To test a new method for the detection and visualization of macular RNFL loss in eyes affected by glaucoma at different stages (mild, moderate and severe) confirmed against standard automated perimetry.

Methods: 20 eyes of 20 patients (mean age 69±9 years old) were enrolled into the study. 10 eyes were normal and 10 were affected by a glaucomatous field defect at different stages (MD from -4 to -15 dB) confirmed performing a Humphrey 24-2 SITA standard visual field.

All eyes underwent retinal nerve fiber layer (RNFL) imaging with Spectralis SD-OCT (Heidelberg Engineering, Heidelberg, Germany). Each patient underwent the standard RNFL analysis by Spectralis SD-OCT.

In addition we performed a dense volume scan consisting in 391 horizontal sections within a 20X15 degree rectangle centered on the fovea. Averaging was set to 16 frames. B-scans were separated by 11 microns intervals.

Using the incorporated analysis software (Heidelberg Eye Explorer version 5.7.0.1) we obtained transversal scan images showing the RNFL.

Results: In normal eyes Spectralis SD-OCT revealed hyperreflective arched shaped bundles from the temporal periphery above and below the fovea to the optic disc, sparing a horizontal line passing through the fovea and the optic disc. The papillo-macular bundle could also be appreciated.

In glaucomatous eyes at early and moderate stage the hyperreflective bundles were not visible in the area corresponding to the visual field defect. In eyes at advanced stage of the disease, the RNFL was so reduced that the whole area appeared darker. In these patients no hyperreflectant lines were detectable, suggesting a wide loss of RNF corresponding to visual field loss.

Conclusions: The study shows that our dense volume scan protocol associated with the new transversal section provided by the Spectralis OCT software, is able to identify retinal fiber bundles in normal eyes and can detect RNFL loss, from early to advanced stage of glaucoma. This defects visualization follows the same visual field damage shape respecting anatomical RNFL distribution. The increased acquisition speed, could make this new approach a useful tool in clinical practice.

Commercial Relationships: Laura de Polo, None; Alessandro Invernizzi, None; Mariano Cozzi, None; Mirella Blini, None; Giovanni Staurenghi, Ocular Instruments (P), GSK (C), Novartis (C), Alcon (C), Allergan (C), Bayer (C), Roche (C), Heidelberg Engineering (C), OD-OS (C), QLT (C), Optos (C)

Program Number: 4816 **Poster Board Number:** D0255

Presentation Time: 11:00 AM - 12:45 PM

In vivo imaging of lamina cribrosa pore and optic nerve head geometry in normal human eyes

Amitabha S. Bhakta, Danica J. Marrelli, Nripun Sredar, Kevin M. Ivers, Nimesh B. Patel, Hope M. Queener, Jason Porter. College of Optometry, University of Houston, Houston, TX.

Purpose: To distinguish structural changes in the lamina cribrosa and optic nerve head (ONH) in glaucoma, it is important to understand the variability in ONH morphology present in normal eyes. Toward this goal, we have examined anterior lamina cribrosa pore and ONH geometry in vivo in normal subjects.

Methods: Spectral domain optical coherence tomography (Spectralis HRA+OCT) radial scans (48, 20° B-scans with Enhanced Depth Imaging) centered on the ONH were acquired in dilated fellow eyes of 17 normal human subjects (24-66 years old). Bruch's membrane opening (BMO), the anterior lamina cribrosa surface (ALCS) and internal limiting membrane (ILM) were manually segmented. BMO area, mean ALCS radius of curvature ([RoC], or mean radius of a thin plate spline surface fit to marked ALCS points), mean ALCS depth (ALCSD) from the BMO plane and prelaminar tissue volume (i.e., volume within the BMO from the ILM to the ALCS) were calculated. Images of ALCS pores acquired with an adaptive optics scanning laser ophthalmoscope (AOSLO) were transformed from 2D to 3D using the thin plate spline surface. ALCS pore area, elongation and nearest neighbor distance (NND) were calculated. Ocular biometry was measured (LENSTAR) to scale image data.

Results: The coefficients of variation (CV) for all ONH parameters across right eyes ranged from 15-23%. Mean BMO area, ALCS RoC, ALCSD and prelaminar tissue volume were 1.89 ± 0.43 mm², 3.72 ± 0.82 mm, 364.6 ± 89.3 μm and 0.997 ± 0.157 mm³, respectively. Most ONH parameters were similar between fellow eyes. Mean percent differences in BMO area, mean ALCS RoC, mean ALCSD, and prelaminar tissue volume were 10.2 ± 6.9%, 21.4 ± 26.2%, 7.8 ± 10.2% and 6.1 ± 4.4%, respectively. The CVs for ALCS pore parameters across all right eyes were larger (16-30%). Mean ALCS pore area, elongation and NND were 2349 ± 683 μm², 2.12 ± 0.36 and 75.7 ± 14.4 μm, respectively. Laminar pore parameters showed increased variability between fellow eyes. Mean percent differences in ALCS pore area, elongation and NND were 29.5 ± 18.8%, 17.1 ± 14.1% and 22.5 ± 20.3%, respectively. There were no significant correlations between axial length and any analyzed ONH or laminar pore parameters.

Conclusions: Between fellow eyes most ONH parameters were similar, whereas laminar pore geometry varied greatly for most subjects. These normative data will serve as a basis for differentiating ONH structural changes in glaucoma.

Commercial Relationships: Amitabha S. Bhakta, None; Danica J. Marrelli, Allergan (R), Alcon Laboratories (R), Merck (R), Carl Zeiss Meditec (R); Nripun Sredar, None; Kevin M. Ivers, None; Nimesh B. Patel, None; Hope M. Queener, None; Jason Porter, None

Support: NIH Grants R01 EY021783, K23 EY021761 and P30 EY07551, University of Houston College of Optometry

Program Number: 4817 **Poster Board Number:** D0256

Presentation Time: 11:00 AM - 12:45 PM

Frequency of Abnormal Retinal Nerve Fiber Layer and Ganglion Cell Layer SDOCT Scans in Healthy Eyes and Glaucoma Suspects in a Prospective Longitudinal Study

Shawn M. Iverson¹, Mitra Sehi¹, William J. Feuer², Wei Shi², David S. Greenfield¹. ¹Glaucoma, University of Miami, Palm Beach Gardens, FL; ²Ophthalmology, University of Miami, Miami, FL.

Purpose: To examine the frequency of abnormal retinal nerve fiber layer thickness (RNFLT) and ganglion cell complex (GCC) measurements among healthy eyes and glaucoma suspects (GS) in a prospective longitudinal study.

Methods: Normal and GS eyes with ≥ 24 month follow-up were included. Healthy eyes had no significant ocular history except uncomplicated cataract extraction and had 2 normal standard automated perimetry (SAP) exams, defined as glaucoma hemifield test within normal limits (WNL) and mean and pattern standard deviation at $p > 5\%$, prior to enrollment. GS consisted of eyes with ocular hypertension (IOP ≥ 24 mmHg) and normal optic discs and SAP; or glaucomatous optic neuropathy but normal SAP; or confirmed perimetric glaucoma in the fellow eye. Spectral-domain optical coherence tomography (SDOCT; Optovue Inc, Fremont, CA) was performed annually in normal and biannually in GS eyes. At each visit ≥ 3 scans with signal strength index ≥ 40 were acquired and the best scan was chosen for analysis. One eye was randomly selected for inclusion. Average, superior, inferior and sectoral RNFLT, and average, superior and inferior GCC parameters with $p > 5\%$ were classified as “Within Normal Limits; WNL” and $p < 1\%$ were classified as “outside normal limits; ONL”.

Results: 23 normal and 74 GS eyes were enrolled and followed up for 41.6 ± 9.5 months. At baseline, 100% of normal and 91% of GS eyes had all RNFLT parameters classified as WNL, and 91% of normal and 88% of GS eyes had all GCC parameters classified as WNL. Among eyes with a WNL baseline RNFLT classification, no normal eyes and 22 (33%) GS eyes subsequently developed ONL classification consisting of abnormal average RNFLT ($n=5$), hemifield RNFLT ($n=5$) or sectoral RNFLT ($n=21$). Among eyes with a WNL baseline GCC classification, no normal eyes and 8 GS eyes (12%) subsequently developed an ONL classification consisting of average GCC ($n=4$), superior GCC ($n=5$) or inferior GCC ($n=5$). The rates of loss for all RNFLT and GCC parameters were similar ($p > 0.05$) between the 2 groups. No eyes developed abnormal SAP during follow-up.

Conclusions: Specificity in this sample of healthy eyes was very high for RNFLT (100%) and GCC (91%) parameters. It is unclear whether the high detection rate for abnormal sectoral RNFLT among GS eyes represents false positives or more sensitive early detection of disease progression.

Commercial Relationships: Shawn M. Iverson, None; Mitra Sehi, Allergan, Inc. (C); William J. Feuer, Abbott Medical optics (F), New World Medical (F); Wei Shi, None; David S. Greenfield, National Eye Institute (R), Carl Zeiss Meditec (R), Optovue (R), Heidelberg Engineering (R), Allergan (C), Alcon (C), Merz (C), Quark (C), SOLX (C), Biometric Imaging (C), Senju (C)

Support: R01EY013516, P30EY014801

Clinical Trial: NCT01314326

Program Number: 4818 **Poster Board Number:** D0257

Presentation Time: 11:00 AM - 12:45 PM

Inner Nuclear Layer (INL) Cystoid Spaces (Lacunae) Observed in Experimental Glaucoma and Axotomy in Non-Human Primates (NHPs)

T Michael Nork^{1,2}, Carol A. Rasmussen^{1,2}, James N. Ver Hoeve^{1,2}, Christopher J. Murphy^{3,2}, Michael W. Neider^{1,2}, Charlene B. Kim^{1,2}, Brian J. Christian⁴. ¹Ophthal & Visual Sciences, Univ of Wisconsin-Madison, Madison, WI; ²Ocular Services On Demand (OSOD), LLC, Madison, WI; ³Surgical Radiol Sci-Sch of Veterinary Medicine, Univ California--Davis, Davis, CA; ⁴Covance, Inc, Madison, WI.

Purpose: To use *in vivo* optical imaging to document the presence of INL lacunae in NHP eyes that have undergone hemi-endodiathermy axotomy and/or laser trabecular meshwork destruction (LTD) to induce experimental glaucoma.

Methods: 4 cynomolgus macaques underwent hemi-endodiathermy axotomy (ARVO 2011, #2460). 3 rhesus macaques first underwent hemi-axotomy followed 3 months later by LTD of the same eye. 6

additional cynomolgus macaques had LTD only. All of the animals were imaged with SD-OCT (either a Zeiss Cirrus™ or Heidelberg Spectralis™). The 3 rhesus and the 6 LTD-only cynos were also imaged with adaptive optics (AO) (Imagine Eyes rtx1™)—4 areas centered 8 degrees from the fovea, 2 superior and 2 inferior. At the time of AO imaging, the 3 rhesus had been glaucomatous for 4 months with average intraocular pressures (IOPs) of 40, 50 and 51 mmHg. The LTD for the 6 cynos had been performed between 3 and 9 years prior to imaging and their IOPs on the day of imaging ranged from 11 to 43 mmHg.

Results: Lacunae were evident only in the inferior (axotomized) portion of all 4 of the non-glaucomatous cynos. Histology confirmed that these spaces were at the level of the INL. Amongst the glaucomatous animals, lacunae were identified by SD-OCT in 2 of the 3 rhesus and 4 of the 6 cynos. With AO on these same animals, lacunae were found in 1 of the 3 rhesus and 3 of the 6 cynos. AO imaging and *en face* views with the SD-OCT showed that the lacunae had a patchy distribution. Lacunae were not found in any of the control eyes.

Conclusions: Lacunae within the INL are a common feature in both rhesus and cynomolgus macaque eyes that have lost retinal ganglion cells as the result of endodiathermy axotomy and/or experimental glaucoma. Although evident with both SD-OCT and AO, lacunae were found in more animals with the SD-OCT probably because it scanned the entire macula, whereas the AO was limited to 4 degree fields of view. The patchy distribution of the lacunae is reminiscent of the irregular nature of visual field loss in humans with glaucoma and other optic neuropathies. Future studies are needed to determine the time course, distribution and association, if any, with IOP of this anatomic feature. If present in human eyes, this finding could have implications for diagnosing and possibly monitoring treatment of patients with optic neuropathies.

Commercial Relationships: T Michael Nork, None; Carol A.

Rasmussen, None; James N. Ver Hoeve, OSOD, LLC (C), Covance, Inc (F); Christopher J. Murphy, Ocular Services On Demand (I), Ocular Services On Demand (C), Platypus Technologies LLC (I), Imbed LLC (I), EyeKor LLC (I), Allergan (C), Genentech (C), Sarcodex (C), Covance (C); Michael W. Neider, None; Charlene B. Kim, None; Brian J. Christian, None

Support: NIH Grant P30 EY016665, Research to Prevent Blindness

Program Number: 4819 **Poster Board Number:** D0258

Presentation Time: 11:00 AM - 12:45 PM

Computational discovery of optic nerve head phenotypes

Mark Christopher¹, Li Tang², John H. Finger², Todd E. Scheetz^{2,1}, Michael D. Abramoff^{2,3}. ¹Biomedical Engineering, University of Iowa, Iowa City, IA; ²Ophthalmology and Visual Sciences, University of Iowa, Iowa City, IA; ³Veterans Affairs, University of Iowa, Iowa City, IA.

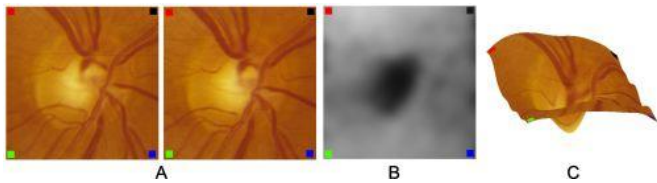
Purpose: To apply computational methods in the discovery of 3D optic nerve head (ONH) structural phenotype features for detecting and monitoring glaucoma damage, and the discovery of new phenotype-genotype associations.

Methods: A subset of participants ($n=370$) from the Ocular Hypertension Treatment Study was selected on the basis of availability of simultaneous stereo fundus images. A stereo correspondence algorithm, optimized for fundus images, was applied to the set of stereo fundus pairs to produce a disparity map that quantitatively measured the ONH structure for each subject (Figure 1). Principal component analysis (PCA) was applied to the disparity maps to extract computational 3D ONH structural features. The first 25 principal components, or features, were retained and examined individually in building a predictive regression model for horizontal

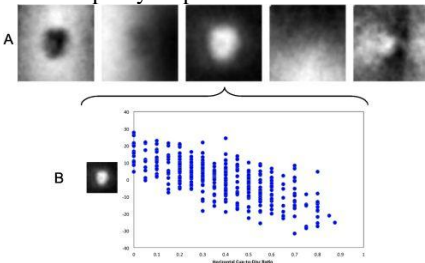
cup-to-disc ratio (HCDR). The relationship between the ONH features and demographic variables gender, age and ethnicity were also examined. In all cases, Bonferroni correction was used to adjust for multiple hypothesis testing.

Results: Five of the 25 computational 3D ONH features were significantly associated (corrected $p < 0.05$) with HCDR, the association for a single ONH feature is shown in Figure 2. Combined, these features explained 65% of the variance in HCDR in the subjects. Significant associations were also found between the features and ethnicity, while suggestive associations were found with age and gender.

Conclusions: Using computational methods, we generated a set of structural features for quantifying the 3D shape of the ONH. These statistically independently features had significant association with and predictive power for HCDR, a clinically important measurement used to diagnose and monitor glaucoma. Intriguing associations of ONH phenotype features were also found with ethnicity, age and gender. Future work will explore the power of applying these features to detect and track glaucoma.



A: A stereo fundus pair cropped around the ONH. B: The disparity map of the stereo pair. C: A 3D rendering of the ONH structure based on the disparity map.



A: The top five computational 3D ONH structural features derived from PCA. The features are shown in decreasing order of explained variance in ONH structure, from left to right. B: The relationship between the third 3D ONH structural feature and HCDR measurements for each subject. This feature was significantly ($p < 1e-16$) associated with HCDR.

Commercial Relationships: Mark Christopher, None; Li Tang, None; John H. Fingert, None; Todd E. Scheetz, None; Michael D. Abramoff, IDx LLC (E), IDx LLC (I), University of Iowa (P)

Program Number: 4820 **Poster Board Number:** D0259

Presentation Time: 11:00 AM - 12:45 PM

The Effect of Image Quality on the Reliability of Nerve Fiber Layer Measurements with Fourier-Domain OCT

Ou Tan¹, Xinbo Zhang¹, Nils A. Loewen², Joel S. Schuman², David S. Greenfield³, Rohit Varma⁴, David Huang¹. ¹Ophthalmology, Oregon Health & Science Univ, Portland, OR; ²Ophthalmology, University of Pittsburgh School of Medicine, Pittsburgh, PA; ³Ophthalmology, Bascom Palmer Eye Institute, Miami, FL; ⁴Ophthalmology, University of Southern California and Doheny Eye Institute, Los Angeles, CA.

Purpose: To determine if image quality affects the reliability of peripapillary retinal nerve fiber layer (NFL) thickness.

Methods: One hundred and nineteen normal and 136 glaucomatous

eyes were scanned with optical nerve head (ONH) scan using RTVue Fourier-domain optical coherence tomography (OCT) system (Optovue, Fremont, CA). Each eye was scanned 3 times every visit. Normal subjects were scanned every 6 month and glaucoma subjects every 6 months. Scans from the earliest available 2 visits in the multicenter Advanced Imaging for Glaucoma study (www.AIGStudy.net) were used. Overall NFL thickness was obtained using RTVue 6.1.0.4 software. Marginal signal strength, defined as signal strength index (SSI) between 35 and 45, was detected using the automated RTVue software. Axial or transverse image cropping artifacts were detected using an automated software developed by coauthor Tan. The scans were classified as “weak-signal” (SSI=35-45), “cropped” (cropping artifact detected), or “clean” (SSI>45 and no image cropping). The reliability of NFL measurement was assessed by inter-subject variance in normal eyes, intra-visit repeatability, and inter-visit reproducibility, all evaluated by pooled standard deviation.

Results: In the normal group, clean scans had significantly smaller inter-subject variance ($p < 0.001$ and $p = 0.01$, F-test) in overall NFL thickness than cropped and weak-signal scans (Table 1). Cropped and weak-signal scans had poorer reproducibility and repeatability than clean scans ($p < 0.001$ for all comparisons by F-test, Table 2).

Conclusions: Excluding low quality scans (SSI<45, cropping artifacts) may improve the reliability of glaucoma diagnosis and monitoring by OCT NFL thickness measurements. Automated software to detect image cropping may be useful.

Sub-dataset	Cropped	Weak-Signal	Clean
Normal (# eyes)	28	56	117
Glaucoma (# eyes)	66	106	120
Normal (AVG±SD)	104.1±13.5	100.9±11.1	100.9±8.4
Glaucoma (AVG±SD)	85.6±12.5	82.4±12.5	82.7±12.8

Table 1: Image Quality Effects on Population Distribution of Overall NFL Thickness

	Cropped	Weak-Signal	Clean
Normal Intra-visit (µm)	3.09	2.32	1.51
Glaucoma Intra-visit (µm)	5.48	3.73	1.60
Normal Inter-visit (µm)	6.43	4.92	2.91

Pooled standard deviation

Table 2 Image Quality Effects on Repeatability and Reproducibility

Commercial Relationships: Ou Tan, Optovue (F), Optovue (P), Carl Zeiss Meditec (P); Xinbo Zhang, None; Nils A. Loewen, None; Joel S. Schuman, Carl Zeiss Meditec, Inc. (P); David S. Greenfield, National Eye Institute (R), Carl Zeiss Meditec (R), Optovue (R), Heidelberg Engineering (R), Allergan (C), Alcon (C), Merz (C), Quark (C), SOLX (C), Biometric Imaging (C), Senju (C); Rohit Varma, Allergan (C), AqueSys (C), Genentech (C), Merck & Co. Inc (C), Replenish (C), Genentech (F), National Eye Institute (F); David Huang, Optovue (F), Optovue (I), Optovue (P), Optovue (R), Carl Zeiss Meditec (P)

Support: NIH R01 EY013516, Optovue

Clinical Trial: NCT01314326

Program Number: 4821 **Poster Board Number:** D0260

Presentation Time: 11:00 AM - 12:45 PM

Combining Optical Coherence Topography measurements using the ‘Random Forest’ decision tree classifier improves the diagnosis of glaucoma

Koichiro Sugimoto, Hiroshi Murata, Hiroyo Hirasawa, Chihiro Mayama, Makoto Aihara, Ryo Asaoka. Department of Ophthalmology, University of Tokyo Graduate School of Medicine, Tokyo, Japan.

Purpose: To examine whether combining Optical Coherence Topography measurements using the ‘Random Forest’ decision tree method improves the diagnosis of glaucoma

Methods: SD-OCT (Topcon 3D OCT-2000) and perimetry (Humphrey Field Analyzer, SITA standard, 24-2 or 30-2 test pattern) measurements were conducted in 293 eyes of 179 subjects with glaucoma or suspected glaucoma. Visual field (VF) damage was used a ‘gold-standard’ to classify glaucomatous eyes. VF damage was defined as a pattern standard deviation (PSD) value, or, a Glaucoma Hemifield Test (GHT) result, outside normal limits. In total 224 out of 293 eyes (76.5%) had glaucomatous VF damage. The ‘Random Forest’ method was then used to analyze the relationship between the presence/absence of glaucomatous VF damage and the following variables: age, gender, right or left eye, plus 238 different OCT measurements (including axial length). The area under the receiver operating characteristic curve (AROC) was then derived using the probability of glaucoma as suggested by the proportion of votes in this Random Forest classifier. For comparison, four AROCs were derived based on individual OCT thickness measurements of: (i) the macular retinal nerve fiber layer (m-RNFL) alone, (ii) the mean circumpapillary retinal nerve fiber layer (cp-RNFL) alone, (iii) the ganglion cell layer + inner plexiform layer (GCL + IPL) alone, and (iv) rim area alone.

Results: The AROC from the combined Random Forest classifier (0.90) was significantly larger than the AROCs based on individual measurements of m-RNFL (0.86), cp-RNFL (0.77), GCL + IPL (0.80), and rim area (0.78).

Conclusions: Evaluating OCT measurements using the Random Forest method provides an accurate diagnosis of glaucoma.

Commercial Relationships: *Koichiro Sugimoto*, None; *Hiroshi Murata*, None; *Hiroyo Hirasawa*, None; *Chihiro Mayama*, None; *Makoto Aihara*, Ono pharmaceutical company (F), Pfizer (F); *Ryo Asaoka*, None

Program Number: 4822 **Poster Board Number:** D0261

Presentation Time: 11:00 AM - 12:45 PM

Comparison of Gonioscopy with Cirrus and Visante Optical Coherence Tomography (OCT) for Anterior Chamber Angle Assessment in Glaucoma Patients

Cindy X. Hu, Camila Zangalli, Anand Mantravadi, Mohsin Ali, Bruno M. Faria, Jesse Richman, Sheryl S. Wizov, Reza Razeghinejad, Marlene R. Moster, L Jay Katz. Glaucoma Research, Wills Eye Institute, Philadelphia, PA.

Purpose: Assessment of the anterior chamber angle is essential in the management of narrow-angle and closed-angle glaucomas. Gonioscopic grading, the gold standard, is a semiquantitative assessment and results may vary between clinicians. Biometric analysis with OCT may provide a more objective assessment. In this prospective study, we aimed to compare gonioscopy with Cirrus and Visante OCT for determination of angle closure risk.

Methods: Gonioscopy grading using Spaeth Classification and determination of angle closure risk were performed on one eye for 39 phakic patients by 3 glaucoma specialists. Images of this same angle

using both Cirrus and Visante OCT were obtained and graded. Inter-rater agreement for gonioscopy and imaging using Kendall’s coefficient of concordance (W) and Cohen’s kappa (K) was determined.

Results: Of these 39 patients, 54% were female, 64% were Caucasian and average age was 60. Most patients were diagnosed with narrow-angle (48%) or primary open angle (34%) glaucoma. Gonioscopy demonstrated substantial agreement in angle grade (W=0.78) and angle closure risk assessment (W=0.83) between the 3 specialists. Cirrus and Visante showed substantial agreement in determining if the angle was open or closed (K=0.73), but only fair agreement with gonioscopy (Cirrus K=0.37, Visante K=0.44).

Conclusions: Cirrus and Visante OCT had good agreement with each other, but only fair agreement with gonioscopy for angle assessment.

Commercial Relationships: *Cindy X. Hu*, None; *Camila Zangalli*, None; *Anand Mantravadi*, None; *Mohsin Ali*, None; *Bruno M. Faria*, None; *Jesse Richman*, none (P); *Sheryl S. Wizov*, None; *Reza Razeghinejad*, None; *Marlene R. Moster*, Alcon (C), Alcon (F), Allergan (F), Allergan (C), Merck (F), Merck (C), Mobius (F), Aeon (F), Aerie (F), Ista (F), iScience (F), Solex (C), Bausch and Lomb (F); *L Jay Katz*, Bausch & Lomb (C), Allergan (R), Allergan (C), Allergan (F), Lumenis (R), Lumenis (F)

Support: Wills Eye Institute Innovation Grant #11-003, American Glaucoma Society Mentoring for Advancement of Physician-Scientists (MAPS) Grant

Program Number: 4823 **Poster Board Number:** D0262

Presentation Time: 11:00 AM - 12:45 PM

In Vivo Structure of the Schlemm’s Canal and the Collector Channels in Eyes with Chronic Angle-Closure Glaucoma Compared to Normal Eyes

Camila F. Netto¹, Sung Chul Park^{1, 2}, Wendy A. Kirkland¹, Rafael L. Furlanetto¹, Yiyi Liu^{1, 3}, Jeffrey M. Liebmann^{1, 4}, Robert Ritch^{1, 2}.

¹Moise and Chella Safra Advanced Ocular Imaging Laboratory, Einhorn Clinical Research Center, New York Eye and Ear Infirmary, New York, NY; ²Department of Ophthalmology, New York Medical College, Valhalla, NY; ³New York Medical College, Valhalla, NY; ⁴Department of Ophthalmology, New York University School of Medicine, New York, NY.

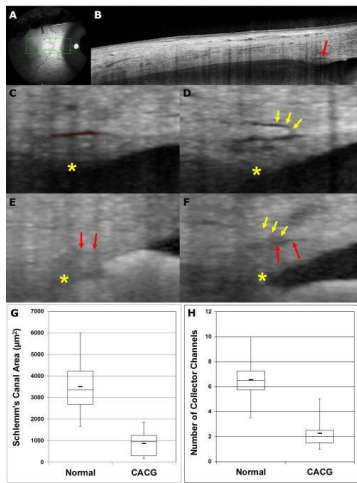
Purpose: To characterize in vivo structure of the Schlemm’s canal (SC) and the collector channels (CC) in eyes with chronic angle-closure glaucoma (CAG) compared to normal eyes.

Methods: Serial horizontal enhanced depth imaging optical coherence tomography (EDI OCT) B-scans were obtained in the nasal and temporal limbal areas from CAG patients and normal subjects (81 scans per 15x5 degree rectangle; interval between scans, ~35 μ m; **Fig A and B**). The cross-sectional area of the SC was measured in each EDI OCT B-scan (**Fig C**). After three-dimensional SC reconstruction, SC volume was calculated for each eye. The CCs connected to SC (**Fig D**) were counted.

Results: Nine CAG eyes (9 patients; mean age, 72 \pm 10 years) and 11 normal eyes (11 subjects; mean age, 28 \pm 5 years) were included. In CAG eyes, the SC and CC were mostly obliterated in the areas with high peripheral anterior synechiae (PAS; **Fig E**) and were mostly open but smaller than those in normal eyes in the areas with no or low PAS (**Fig F**). The mean cross-sectional SC area was significantly smaller in the CAG than in the normal eyes (863 \pm 611 μ m² vs. 3512 \pm 1228 μ m²; p<0.001; **Fig G**), as was the SC volume (0.005 \pm 0.003 mm³ vs. 0.020 \pm 0.006 mm³; p<0.001). The number of the CCs was significantly smaller in the CAG than in the normal eyes (2.3 \pm 1.3 vs. 6.5 \pm 1.6; p<0.001; **Fig H**).

Conclusions: SC appears smaller and connected to fewer open CCs

in CACG eyes than in normal eyes. In CACG eyes, circumferential aqueous flow is compromised in areas with high PAS.



(A) 15x5 degree rectangle for 81 serial horizontal EDI OCT B-scans. (B) A horizontal EDI OCT B-scan of the limbus and sclera (red arrow = Schlemm's canal [SC]). (C) SC was delineated (red dotted line) to measure its cross-sectional area (asterisk = scleral spur). (D) Yellow arrows = collector channel. (E) Obliterated SC (red arrows). (F) Open but small SC (red arrows) and CC (yellow arrows). (G and H) Box-and-whisker plot for the SC area and the number of collector channels in the CACG and the normal eyes.

Commercial Relationships: Camila F. Netto, None; Sung Chul Park, None; Wendy A. Kirkland, None; Rafael L. Furlanetto, None; Yiyi Liu, None; Jeffrey M. Liebmann, Alcon Laboratories, Inc. (C), Allergan, Inc. (C), Allergan, Inc. (F), Carl Zeiss Meditech, Inc (F), Heidelberg Engineering, GmbH (F), Topcon Medical Systems, Inc. (F), National Eye Institute (F), New York Glaucoma Research Institute (F), SOLX, Inc. (C), Bausch & Lomb, Inc (C), Diopsys, Inc. (C), Diopsys, Inc. (F), Merz, Inc. (C), Glaukos, Inc. (C), Quark, Inc. (C); Robert Ritch, None

Support: Shiela Evers Research Fund of the New York Glaucoma Research Institute, New York, NY; James Cox Chambers Research Fund of the New York Eye and Ear Infirmary, New York, NY; American Glaucoma Society MAPS Award; Peter Crowley Research Fund of the New York Eye and Ear Infirmary, New York, NY

Program Number: 4824 **Poster Board Number:** D0263

Presentation Time: 11:00 AM - 12:45 PM

Stereo digital photography demonstrates excellent reproducibility with stereo slide film for the evaluation of glaucomatous optic disc features

Faazil Kassam², Sourabh Arora¹, Chris J. Rudnisky¹, Gordon Douglas², Marianne C. Edwards¹, Karin Verstraten², Beatrice K. Wong³, Karim F. Damji¹. ¹Ophthalmology, University of Alberta, Edmonton, AB, Canada; ²Ophthalmology, University of Calgary, Calgary, AB, Canada; ³Ophthalmology, Loma Linda University, Loma Linda, CA.

Purpose: To determine the sensitivity, specificity, and reproducibility of stereo digital photography in detecting optic nerve head features of glaucoma

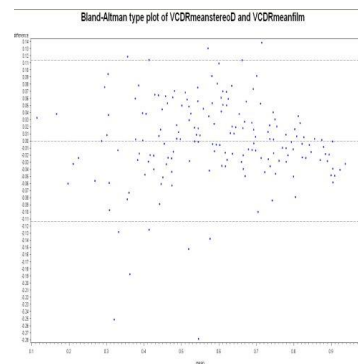
Methods: 192 eyes with glaucomatous, suspicious, or normal optic nerves were imaged to produce stereoscopic digital photographs (Secure Diagnostic Imaging) and stereo slide film images. The primary observation of interest was the vertical cup-to-disc ratio (VCDR); secondary features assessed were disc hemorrhage and notching. Images were graded by each of 4 glaucoma specialists in a

random order. The mean from all 4 specialists was used to combine VCDR evaluations into a single grade. VCDR was reviewed for images in which the standard deviation of the mean was >0.2. For disc hemorrhage and notching, the majority opinion was used for the final grade; in cases without a majority, the final grading was determined via consensus discussion. Weighted kappa was calculated to identify the reproducibility of digital imaging using film as the gold standard. A Bland-Altman (BA) plot was used to analyze the agreement between formats for VCDR. Sensitivity, specificity, and area under ROC curve (AUC) were also calculated for disc hemorrhage and notching.

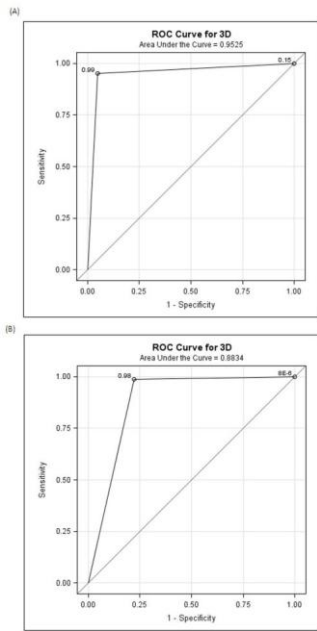
Results: There were 192 eyes imaged using both formats. The overall mean VCDR for digital and film was 0.588±0.068 vs. 0.593±0.068, respectively. The weighted kappa between film and digital was 0.781 (95% CI 0.740-0.823). The BA plot demonstrated fairly random distribution of points above and below a mean difference of 0, although there was less variability for higher cup-disc ratios, suggesting better agreement for larger VCDR. Sensitivity and specificity of digital imaging to detect notching was 95.2% and 95.2% respectively with an AUC=0.953. For disc hemorrhage, sensitivity and specificity were 77.8% and 98.9% respectively with an AUC=0.883. For disc hemorrhage, weighted kappa was 0.767 (95% CI 0.546-0.988). For notching, weighted kappa was 0.868 (95% CI 0.784-0.952).

Conclusions: Digital stereoscopic imaging demonstrates excellent reproducibility in comparison to stereo slide film when evaluating 3 important features of glaucoma: VCDR, notching and disc hemorrhage

Acknowledgement: Abshir Moalin provided technical assistance



BA plot correlation between formats for VCDR



ROC curves for digital imaging detecting notching (A) and disc hemorrhage (B) compared to film

Commercial Relationships: Faazil Kassam, None; Sourabh Arora, None; Chris J. Rudnisky, Secure Diagnostic Imaging (I); Gordon Douglas, None; Marianne C. Edwards, None; Karin Verstraten, None; Beatrice K. Wong, None; Karim F. Damji, None

Support: Capital Health Alberta, Canada Glaucoma Clinical Research Council

Program Number: 4825 **Poster Board Number:** D0264

Presentation Time: 11:00 AM - 12:45 PM

Comparison of Cirrus spectral-domain optical coherence tomography (OCT) -measured macula ganglion cell-inner plexiform layer (GCIPL) thickness and circumpapillary retinal nerve fiber layer (cpRNFL) thickness-deviation maps for detection of localized retinal nerve fiber layer (RNFL) defects in glaucoma

Yu Jeong Kim¹, Mijeung Kim^{1,2}, Ki Ho Park^{1,2}, Jin Wook Jeoung^{1,2}, Yun Jeong Choi², Kyoung Nam Kim², Dong Myung Kim^{1,2}.

¹Ophthalmology, Seoul National University College of Medicine, Seoul, Republic of Korea; ²Ophthalmology, Seoul National University Hospital, Seoul, Republic of Korea.

Purpose: To evaluate and compare the abilities of Cirrus spectral-domain optical coherence tomography (OCT)-measured macula ganglion cell-inner plexiform layer (GCIPL) thickness- and circumpapillary retinal nerve fiber layer (cpRNFL) thickness-deviation maps for detection of localized RNFL defects in glaucoma.

Methods: This cross-sectional comparative study included 58 eyes of 58 glaucoma subjects with localized RNFL defects, as well as 80 normal control subjects. Based on their internal normative databases, the sensitivity and specificity of GCIPL and cpRNFL thickness-deviation maps for detection of localized RNFL defects were calculated.

Results: According to abnormality criteria 1 — a cluster of at least three superpixels at the 5% abnormality level (yellow) including at least one superpixel at the 1% level (red) — the sensitivity of the deviation map was 84.62% (95% confidence interval, 74.27 - 91.46) for GCIPL and 89.74% (80.27 - 95.15) for cpRNFL ; the specificity was 68.75% (57.29 - 78.39) for GCIPL and 61.25 (49.67 - 71.74) for

cpRNFL. These results showed no significant difference in the GCIPL and cpRNFL sensitivities or specificities. According to abnormality criteria 2 — a cluster of at least five superpixels at the 5% level including at least three superpixels at the 1% level — and abnormality criteria 3 — a cluster of at least ten superpixels at the 5% level including at least five superpixels at the 1% level — there were no significant differences shown between GCIPL and cpRNFL in the abilities for detecting localized RNFL defects.

Conclusions: Based on their normative databases, comparisons with the GCIPL and cpRNFL parameters showed no significant difference in sensitivity or specificity, indicating that they offer similar diagnostic abilities for detection of localized RNFL defects.

Commercial Relationships: Yu Jeong Kim, None; Mijeung Kim, None; Ki Ho Park, None; Jin Wook Jeoung, None; Yun Jeong Choi, None; Kyoung Nam Kim, None; Dong Myung Kim, None

Program Number: 4826 **Poster Board Number:** D0265

Presentation Time: 11:00 AM - 12:45 PM

Does reduction in retinal nerve fiber layer (RNFL) birefringence precede change in RNFL thickness in glaucoma?

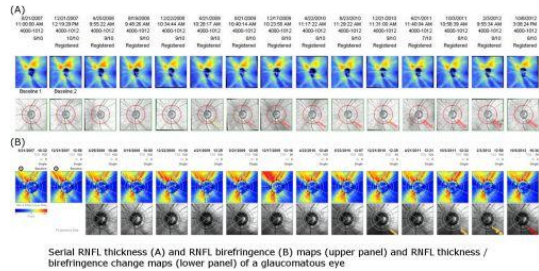
Guihua Xu, Yun Ting Jeffrey Tse, Christopher K. Leung. The Chinese University of Hong Kong, HongKong, China.

Purpose: Previous experimental studies suggest that loss of RNFL birefringence measured with scanning laser polarimetry (SLP) is evident before reduction in RNFL thickness measured with optical coherence tomography (OCT) after optic nerve injury. However, clinical data corroborating this observation is still lacking. In this prospective study, we compared the performance of SLP and OCT RNFL map analyses in detecting RNFL progression in glaucoma patients.

Methods: 248 eyes of 151 glaucoma patients were followed at 4-month intervals for RNFL imaging with SLP (GDx ECC) and OCT (Cirrus HD-OCT) for ≥ 36 months. Only images meeting the quality criteria (signal strength ≥ 8 for OCT; quality score ≥ 8 for SLP) and collected during the same visits were included for progression analysis. RNFL progression was evaluated by the Guided Progression Analysis (GPA) using serial RNFL birefringence (SLP) and RNFL thickness maps (OCT). Progression was defined when there were more than 5 pixels encoded in red in the RNFL change map (i.e. repeatable reduction in RNFL birefringence / thickness greater than the test-retest variability). The RNFL change maps in the latest follow-up were exported to a computer for measurement of area of change.

Results: The mean follow-up time was 62.7 months (range: 36.1-82.8 months). 29 eyes (11.7%) of 27 patients (17.9%) had RNFL thickness progression detected by OCT alone whereas only 8 eyes (3.2%) of 8 patients (5.2%) had RNFL birefringence progression detected by SLP ($p < 0.001$, Fisher exact test). 7 eyes of 7 patients had RNFL progression detected by both instruments. Notably, all eyes had RNFL thickness progression prior to RNFL birefringence progression. The area of RNFL thickness and RNFL birefringence progression ranged between 0.34 and 3.12 mm², (mean, 1.20 \pm 0.67 mm²), and between 1.12 and 4.23 mm², (mean, 2.41 \pm 1.32 mm²), respectively. The inferotemporal sector was the most frequent location where progression was detected by both SLP and OCT.

Conclusions: Both SLP and OCT can detect RNFL progression. In glaucoma, reduction in RNFL thickness detected by OCT occurs before reduction in RNFL birefringence detected by SLP.



Commercial Relationships: Guihua Xu, None; Yun Ting Jeffrey Tse, None; Christopher K. Leung, Carl Zeiss Meditec (F), Carl Ziess Meditec (R), Alcon (C), Alcon (R), Alcon (F), Allergan (C), Allergan (R), Tomey (F), Optovue (F)

Program Number: 4827 **Poster Board Number:** D0266
Presentation Time: 11:00 AM - 12:45 PM

Glaucoma Clinician (GC) Color Stereophoto (CSphoto) Rim Estimation Compared to Colocalized Spectral Domain Optical Coherence Tomography (SDOCT) Minimum Rim Measurements

Robert M. Kinast, Ruojin Ren, Helen Koenigsman, Hongli Yang, Stuart K. Gardiner, Juan Reynaud, Steven L. Mansberger, Brad Fortune, Shaban Demirel, Claude F. Burgoyne. Discoveries in Sight Research Laboratories, Devers Eye Institute, Legacy Research Institute, Portland, OR.

Purpose: To compare GC CSphoto neuroretinal rim width (RW_{GC}) and area (RA_{GC}) to colocalized SDOCT minimum rim width (MRW_{SDOCT}) and area (MRA_{SDOCT}) in 53 eyes of 53 glaucoma and glaucoma suspect patients.

Methods: For each eye, same day CSphotos and SDOCT data sets (Spectralis, Heidelberg Engineering) were colocalized using the SDOCT IR image. Bruch’s membrane opening (BMO) and the internal limiting membrane (ILM) were hand delineated within the SDOCT data sets and MRW_{SDOCT}/MRA_{SDOCT} were calculated based on the minimum distance between BMO and the ILM within 12 sectors based on the fovea - BMO_{centroid} (FoBMO) axis (Figure 1). Five GCs independently delineated the disc (DM) and rim margin (RM) within the colocalized CSphotos generating RW_{GC} and RA_{GC} estimates within the same FoBMO sectors. For each sector of each eye, the magnitude of each GC RW and RA estimate as well as their difference from MRW_{SDOCT} and MRA_{SDOCT} were recorded. Generalized estimating equations were used to assess the significance of GC versus SDOCT differences accounting for inter-clinician correlations for the same eye.

Results: Between GC differences in mean RW_{GC} and mean RA_{GC} (Figure 1) were substantial. While mean RW_{GC} was significantly larger than BMO-MRW ($p \leq 0.003$) in every FoBMO segment and RA_{GC} was greater than MRA_{SDOCT} superior nasally, RA_{GC} was less than MRA_{SDOCT} (Figure 1) inferior temporally. GC versus SDOCT discordance for both RW and RA (Figure 1) were substantial in all quadrants.

Conclusions: SDOCT/CSphoto colocalization and a common, FoBMO-based regionalization strategy has allowed the first precise comparisons between glaucoma clinician and SDOCT rim assessment. Variability among the five GCs in this study was substantial and lead to wide GC versus SDOCT discordance. The source and clinical importance of these differences are under study.

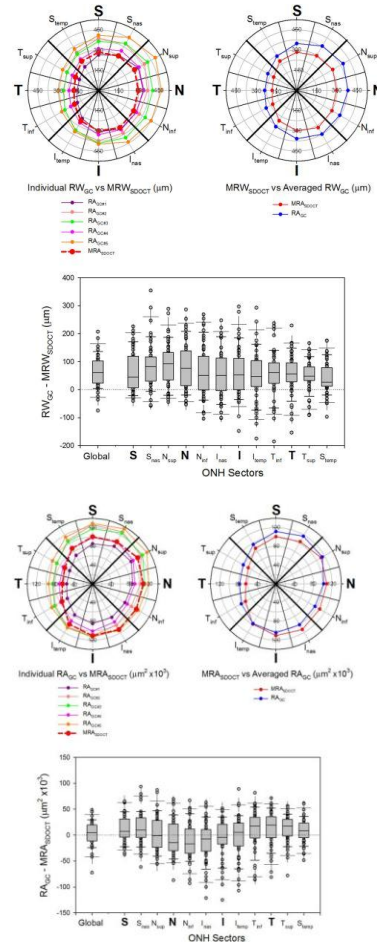


Figure 1. Five GC’s individual and averaged RW_{GC} and RA_{GC} compared to colocalized MRW_{SDOCT} and MRA_{SDOCT} . Variability plots of GC and SDOCT differences organized by 12 sectors based on the FoBMO axis.

Commercial Relationships: Robert M. Kinast, None; Ruojin Ren, None; Helen Koenigsman, None; Hongli Yang, None; Stuart K. Gardiner, Allergan (R); Juan Reynaud, None; Steven L. Mansberger, Merck (R), Alcon (C), Allergan (C), Allergan (F), Merck (F), Santen (C), Glaukos (C); Brad Fortune, Heidelberg Engineering, GmbH (F), Carl Zeiss Meditec, Inc (F); Shaban Demirel, Carl Zeiss Meditec (F), Heidelberg Engineering (R), Heidelberg Engineering (F); Claude F. Burgoyne, Heidelberg Engineering (F), Heidelberg Engineering (C)

Support: NIH/NEI R01-EY021281; NIH/NEI R01-EY-019674; Legacy Good Samaritan Foundation; Sears Medical Trust; Alcon Research Institute; Heidelberg Engineering, GmbH, Heidelberg, Germany (equipment and unrestricted research support); Reichert Instruments (equipment)

Program Number: 4828 **Poster Board Number:** D0267
Presentation Time: 11:00 AM - 12:45 PM

Ability of spectral domain optical coherence tomography to diagnose preperimetric glaucoma

Chandrasekhar Garudadri, Harsha L. Rao, Uday Addepalli, Shashikant Chaudhary, Tukaram Kumbar, Sirisha Senthil. Glaucoma, L V Prasad Eye Institute, Hyderabad, India.

Purpose: To evaluate the ability of optic nerve head (ONH), retinal nerve fiber layer (RNFL) and ganglion cell complex (GCC)

parameters of spectral domain optical coherence tomograph (SDOCT) in detecting preperimetric glaucoma.

Methods: We studied 261 eyes of 197 subjects referred to a tertiary eye care center by general ophthalmologists as glaucoma suspects based on optic disc appearance.

All participants underwent comprehensive eye examination including visual fields, ONH, RNFL and GCC imaging with the commercially available SDOCT. The visual fields (VF) evaluated by standard automated perimetry were normal in all eyes. Two glaucoma experts masked to clinical, VF and imaging information independently classified the optic nerves into glaucoma and non-glaucoma groups based on digital optic disc photographs.

Ability of SDOCT parameters to discriminate glaucoma (preperimetric) eyes from non-glaucoma (control) eyes was evaluated by areas under the receiver operating characteristic curves (AUC), sensitivities at fixed specificities of 80% and 95%, and likelihood ratios (LR).

Results: Experts classified 68 eyes of 60 patients as glaucomatous and 193 eyes of 137 subjects as controls. Age and VF characteristics were comparable between the groups. All SDOCT parameters were significantly different between the glaucomatous and control groups. ONH, RNFL and GCC parameters with best AUCs to differentiate preperimetric glaucoma from control eyes were inferior neuroretinal rim area (0.708), inferior quadrant RNFL thickness (0.713) and global loss volume (0.702) respectively. Sensitivities at 95% specificity for all these parameters were below 27%. LRs of outside normal limits category of the RNFL and GCC parameters were between 2.2 and 5.9, and within normal limits category were between 0.6 and 0.8. LRs of borderline category of SDOCT parameters were between 1 and 2.

Conclusions: Diagnostic abilities of ONH, RNFL and GCC parameters of SDOCT in preperimetric glaucoma were poor. This indicates a need for improvements in the current analysis algorithms of SDOCT for detection of preperimetric glaucoma.

Commercial Relationships: Chandrasekhar Garudadri, Optovue (F); Harsha L. Rao, Allergan (C); Uday Addepalli, None; Shashikant Chaudhary, None; Tukaram Kumbar, None; Sirisha Senthil, None

Support: Hyderabad Eye Research Foundation

Program Number: 4829 **Poster Board Number:** D0268

Presentation Time: 11:00 AM - 12:45 PM

A novel alignment and subtraction technique for the detection of glaucoma progression

Elizabeth D. Marlow^{1,2}, Margaret M. McGlynn², Nathan M. Radcliffe². ¹New York University School of Medicine, New York, NY; ²Ophthalmology, Weill Cornell Medical College, New York, NY.

Purpose: Identification of features of glaucoma progression informs clinical management. While flicker chronoscopy is useful, a dynamic view is not always possible. Auto-alignment and subtraction of serial optic nerve photos (ASSOP) was used to generate static representations of differences between baseline and follow-up images that may be valuable for identifying glaucomatous change.

Methods: Subtraction maps were generated from auto-aligned (EyeIC, Narbeth, PA) baseline and follow up images using Adobe Photoshop software. They demonstrate progressive retinal nerve fiber layer (RNFL) defects, optic disc hemorrhage (DH), neuroretinal rim loss (RL), and peripapillary atrophy (PPA). A masked glaucoma specialist identified features of progression on subtraction map first, then assessed feature strength by comparison with original images using flicker. Control images with no progression and parallax-only images were included.

Results: Seventy-six eyes of 71 patients were used to generate subtraction maps that detected glaucoma progression in 87% of DH (n=31, Sensitivity (Se) 84%, Specificity (Sp) 98%) and 84% of PPA (n=32, Se 81%, Sp 98%) cases. The lowest rates of detection were seen with RL (67%, n=31, Se 65%, Sp 98%). The subtraction technique was most sensitive for detecting parallax (41 of 40, Se 98%, Sp 94%). All features of glaucoma progression appeared equally strong in flicker and subtraction images. However, parallax was stronger in 13% of subtraction maps overall and in 50% of images containing RNFL defects in particular. Among control images selected for absence of features of glaucomatous change (n=11) in original flicker images, no features were detected on subtraction maps.

Conclusions: ASSOP reliably detects features of glaucoma progression with a single static image. Parallax identification may also be facilitated. Future investigations should determine an algorithm that can be uniformly applied to any set of temporally-spaced and aligned images to create a subtraction map yielding the highest quality visualization of change.

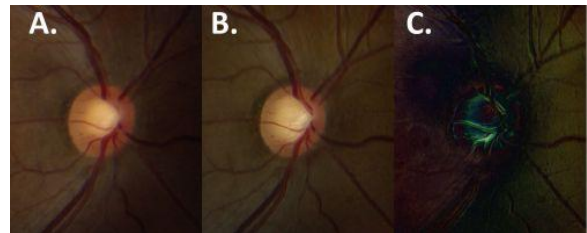


Figure 1. Baseline (A), follow-up (B) and subtraction image (C), demonstrating neuroretinal rim loss in both the follow up and subtraction images.

Commercial Relationships: Elizabeth D. Marlow, None; Margaret M. McGlynn, None; Nathan M. Radcliffe, Allergan Inc (C), Iridex (C), Alcon (C), Merge Healthcare (C), Carl Zeiss Meditec, Inc (C)

Support: This work was supported by the Seth Sprague Educational & Charitable Foundation, by Research to Prevent Blindness and by The American Glaucoma Society through the Mentoring for Advancement of Physician-Scientists award program.

Program Number: 4830 **Poster Board Number:** D0269

Presentation Time: 11:00 AM - 12:45 PM

Glaucoma discrimination of ganglion cell complex measurements with two SD-OCT

Marlene Francoz, Hussam El Chehab, Jean-Remi Fenolland, Maxime Delbarre, Jean-Marie Giraud, Frank May, Jean-Paul G. Renard. Military Hosp of Val-de-Grace, Paris, Paris, France.

Purpose: To use macular retinal ganglion cell analysis from Cirrus HD-OCT (Carl Zeiss Meditec, Dublin, CA) and RTVue-OCT (Optovue Inc., Fremont, USA) and evaluate their diagnostic ability in glaucoma.

Methods: A total of 167 eyes were enrolled in 3 groups: (1) early open angle glaucoma patients (n=65); (2) moderate-to-advanced open angle glaucoma patients (n=46); (3) normal subjects (n=56). All patients underwent a complete examination including biomicroscopy and 24-2 automated perimetry. Each eye had macular analysis using the macular cube 200x200 and GCA algorithm from Cirrus HD and macular map with GCC algorithm from RTVue. Macular layers (mNFL, GCL-IPL and GCC) and their parameters (average, minimum and 6 sectoral thicknesses) obtained with Cirrus HD were analyzed as GCC thickness and parameters (average, inferior, superior, FLV and GLV) obtained with RTVue. Glaucoma discriminating ability was assessed using area under the receiver

operator characteristic curve (AUC) for all parameters. Each eye underwent circumpapillary RNFL (cpRNFL) analysis using Optic disc cube 200x200 from Cirrus HD and ONH program from RTVue.

Results: Average thickness with Cirrus HD was, respectively for group 1, 2 and 3, $27.9 \pm 6.6 \mu\text{m}$, $21.3 \pm 6.0 \mu\text{m}$ and $33.0 \pm 5.5 \mu\text{m}$ for mNFL; $65.6 \pm 7.4 \mu\text{m}$, $57.8 \pm 13.1 \mu\text{m}$ and $80.3 \pm 9.9 \mu\text{m}$ for GCL-IPL; and $93.4 \pm 11.8 \mu\text{m}$, $79.1 \pm 17.9 \mu\text{m}$ and $101.5 \pm 20.1 \mu\text{m}$ for GCC ($p < 0.01$ between each group). Average GCC with RTVue was $75.7 \pm 10.7 \mu\text{m}$, $72.6 \pm 9.7 \mu\text{m}$ et $93.9 \pm 7.7 \mu\text{m}$, for group 1, 2 and 3 respectively ($p < 0.05$). Sensitivity and specificity were from 82 to 93 % for all Cirrus HD macular parameters and were from 75 to 96 % for all RTVue macular parameters. AUCs from Cirrus HD macular parameters were 0.836 to 0.925 and from RTVue macular parameters were 0.878 to 0.949. These values were compared to the discriminating ability of cpRNFL parameters from each OCT.

Conclusions: The two OCT macular ganglion cell analysis showed similar glaucoma diagnostic ability and were comparable with that of cpRNFL

Commercial Relationships: Marlene Francoz, None; Hussam El Chehab, None; Jean-Remi Fenolland, None; Maxime Delbarre, None; Jean-Marie Giraud, None; Frank May, None; Jean-Paul G. Renard, None

Program Number: 4831 **Poster Board Number:** D0270

Presentation Time: 11:00 AM - 12:45 PM

Enhanced Depth Imaging Optical Coherence Tomography of Trabecular Outflow Pathway

Anum Butt¹, Sung Chul Park^{2,3}, Rafael L. Furlanetto², Wendy A. Kirkland², Camila F. Netto², Mohammed Al-Jumayli², Jeffrey M. Liebmann^{2,4}, Robert Ritch^{2,3}. ¹Department of Ophthalmology, The Aga Khan University, Karachi, Pakistan; ²Moise and Chella Safra Advanced Ocular Imaging Laboratory, Einhorn Clinical Research Center, New York Eye and Ear Infirmary, New York, NY; ³Department of Ophthalmology, New York Medical College, Valhalla, NY; ⁴Department of Ophthalmology, New York University School of Medicine, New York, NY.

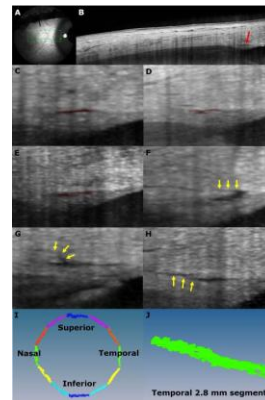
Purpose: To assess the usefulness of enhanced depth imaging optical coherence tomography (EDI OCT) for evaluating *in vivo* microarchitecture of the trabecular outflow pathway.

Methods: Serial horizontal EDI OCT B-scans were obtained in the nasal and temporal limbal areas from one eye of normal subjects (81 scans per 15x5 degree rectangle; interval between scans, ~35 μm ; **Fig A and B**). The intra- and inter-observer reproducibility of the Schlemm's canal (SC) cross-sectional area measurement was evaluated using 40 randomly selected EDI OCT scans (8 scans per each of 5 normal eyes). Analysis was based on 3 independent series of re-evaluations made by two observers. The microarchitecture of SC and collector channel (CC) was assessed. For one eye, serial EDI OCT was performed in a radial fashion in every clock hour and 3-dimensional image of the entire SC circumference was reconstructed.

Results: Eleven normal eyes (11 subjects; mean age, 28 ± 5 years) were included. The SC cross-sectional area measurement by the two observers showed excellent intra- (ICC [intraclass correlation coefficient] = 0.830 for observer 1 and 0.886 for observer 2) and inter-observer (ICC = 0.793) reproducibility (all $p < 0.001$). SC was continuous in the scanned area in all eyes. The cross-sectional shape of SC varied considerably among regions with intermittent bifurcation (**Fig C-E**). Most CCs were connected to the outer wall of the SC and their locations varied from the medial to the lateral ends of SC (**Fig F-H**). The entire SC circumference was successfully reconstructed 3-dimensionally (**Fig I and J**).

Conclusions: EDI OCT is useful for evaluating the *in vivo* microarchitecture of the trabecular outflow pathway. This has

implications for the development of new drugs and techniques to reduce intraocular pressure.



(A) 15x5 degree rectangle for 81 serial horizontal EDI OCT B-scans. (B) A horizontal EDI OCT B-scan of the limbus and sclera (red arrow = Schlemm's canal [SC]). (C-E) SC of various shapes (red dotted lines). (F-H) Collector channels of various locations (yellow arrows). (I and J) 3-dimensionally reconstructed SC (entire circumference and temporal 2.8-mm segment, respectively).

Commercial Relationships: Anum Butt, None; Sung Chul Park, None; Rafael L. Furlanetto, None; Wendy A. Kirkland, None; Camila F. Netto, None; Mohammed Al-Jumayli, None; Jeffrey M. Liebmann, Alcon Laboratories, Inc. (C), Allergan, Inc. (C), Allergan, Inc. (F), Carl Zeiss Meditech, Inc (F), Heidelberg Engineering, GmbH (F), Topcon Medical Systems, Inc. (F), National Eye Institute (F), New York Glaucoma Research Institute (F), SOLX, Inc. (C), Bausch & Lomb, Inc (C), Diopsys, Inc. (C), Diopsys, Inc. (F), Merz, Inc. (C), Glaukos, Inc. (C), Quark, Inc. (C); **Robert Ritch**, None

Support: Ralph and Sylvia Ablon Research Fund of the New York Glaucoma Research Institute, New York, NY; James Cox Chambers Research Fund of the New York Eye and Ear Infirmary, New York, NY; American Glaucoma Society MAPS Award; Peter Crowley Research Fund of the New York Eye and Ear Infirmary

Program Number: 4832 **Poster Board Number:** D0271

Presentation Time: 11:00 AM - 12:45 PM

Automated Flicker Chronoscopy for the Identification of Preperimetric Glaucomatous Progression

Nathan M. Radcliffe, Joshua R. Ehrlich, Fabiana Q. Silva, Zeba Syed. Ophthalmology, Weill Cornell Medical College, New York, NY.

Purpose: To describe eyes with preperimetric glaucomatous progression identified by automated alternation flicker (AAF), and to characterize visual field and optical coherence tomography (OCT) findings among these eyes.

Methods: In this cross-sectional investigation, baseline and follow-up optic nerve head photographs were obtained and used to create AAF images. Two masked graders (FS and NR) determined which eyes had evidence of glaucomatous structural progression. Eyes were included if they had a normal result on Humphrey Field Analyzer 24-2 SITA standard automated perimetry and a normal or borderline retinal nerve fiber layer (RNFL) thickness on OCT after the follow-up digital photograph. All interim and subsequent visual field and OCT results were reviewed for each eye to evaluate for progression and fluctuation of these parameters.

Results: Of 407 individuals considered for inclusion in this study, 115 met photographic and visual field inclusion criteria. Twenty eyes with structural progression were identified using AAF, with 18 of the

ARVO 2013 Annual Meeting Abstracts by Scientific Section/Group – Glaucoma

eyes (90%) demonstrating neuroretinal rim loss and six (30%) developing RNFL defects. While all study eyes had normal visual fields at the time of follow-up photography, 7 (35%) developed subsequent abnormal fields. Eleven eyes (55%) underwent visual field fluctuation; nine eyes had at least one abnormal field prior to the normal field, while three had normalization after visual field progression. Five eyes (25%) with normal or borderline OCTs at the time of follow-up photography developed subsequent OCT abnormalities. Six eyes (30%) had OCT fluctuation; five had at least one abnormal OCT prior to the normal or borderline OCT, and one had normalization after an OCT abnormality.

Conclusions: AAF may allow for early detection of structural injury in glaucoma, prior to the onset of visual field and OCT abnormalities. In patients with preperimetric photographic progression, visual field and OCT findings often become abnormal or fluctuate.

Commercial Relationships: Nathan M. Radcliffe, Allergan Inc (C), Iridex (C), Alcon (C), Merge Healthcare (C), Carl Zeiss Meditec, Inc (C); Joshua R. Ehrlich, None; Fabiana Q. Silva, None; Zeba Syed, None

Support: This work was supported by the Seth Sprague Educational & Charitable Foundation, by Research to Prevent Blindness, and by The American Glaucoma Society through the Mentoring for Advancement of Physician-Scientists award program.

Program Number: 4833 **Poster Board Number:** D0272

Presentation Time: 11:00 AM - 12:45 PM

Developments in Optical Coherence Tomography Imaging in a Rat Model of Glaucoma

Jean-Remi Fenolland^{1,2}, Céline Boucher², Markus A. Mayer³, William H. Rostene², Christophe Baudouin^{2,4}, Alexandre Denoyer^{2,4}.

¹Ophthalmology, Val de Grace Military Hospital, Paris, France;

²Team S12, Vision Institute, UPMC University Paris 6; UMRS968 INSERM; UMR7210 CNRS, Paris, France; ³Pattern Recognition Lab, University of Erlangen-Nuremberg, Nuremberg, Germany;

⁴Quinze-Vingts National Ophthalmology Hospital, Paris, France.

Purpose: Optical Coherence Tomography (OCT) is a powerful imaging procedure widely used in clinical practice. In research, however, no accurate optical solution was available to perform OCT in rats. Moreover, there was no tool to assist the researcher in measuring in vivo the thickness of retinal layers, especially the nerve fiber layer (RNFL). This study aimed to evaluate OCT imaging of anterior and posterior segments and to develop an automated segmentation of retinal layers in a rat model of glaucoma.

Methods: Twenty male Long Evans rats with surgically induced glaucoma were followed during 2 months. OCT Envisu™ and its acquisition software InVivoVue Clinic (Biotigen corporation, SC, USA) were used. Imaging was performed with a new optical system fitted to rat eye characteristics. For the anterior segment imaging, a dedicated telecentric lens was used. Acquisitions were performed at the corneal apex for anterior chamber depth (ACD) measurement. Animal was then moved using stereotaxic device toward the limbus in order to measure the iridocorneal angle (ICA). For retinal imaging, 1-mm diameter circle scans centered on the optic nerve were performed. Axial and lateral resolutions were of 2 μm and 5 μm respectively. An innovative semi-automatic segmentation of retinal layers was developed through OCTSEG software.

Results: Corneal stromal thickness was 116±18 μm and epithelial thickness was 44±7 μm. ACD was 0.75±0.05 mm and AIC was measured at 11.4±3°, further confirming the absence of angle closure and consistently with what obtained by UltraBio Microscopy. At the posterior pole, 2-month ocular hypertension was found to be associated with significant RNFL thinning as compared to normotensive control eyes (25.4 ± 1.8 μm vs 29.1 ± 1.3 μm

respectively, P<0.001), which was considered as an early stage of glaucomatous neuropathy.

Conclusions: OCT may become an indispensable tool to evaluate chronic glaucoma models in animal. Anterior segment OCT can precise the corneal/iridocorneal changes and thus the true mechanism of hypertension on the one hand. Retinal imaging and automated layer segmentation is a new and only way to monitor in vivo the retinal changes on the other hand. Here we also report that it could detect an early thinning of the RNFL in our glaucoma model, further emphasizing the importance of this imaging process in animal research.

Commercial Relationships: Jean-Remi Fenolland, None; Céline Boucher, None; Markus A. Mayer, None; William H. Rostene, None; Christophe Baudouin, None; Alexandre Denoyer, None

Program Number: 4834 **Poster Board Number:** D0273

Presentation Time: 11:00 AM - 12:45 PM

Optic disc and neuroretinal rim area measurements with spectral-domain optical coherence tomography and confocal scanning laser ophthalmoscopy in myopic eyes

Kunliang Qiu. JSIEC, Shantou, Afghanistan.

Purpose: To compare optic disc and neuroretinal rim area measurements from spectral-domain optical coherence tomography (SD-OCT) to those from confocal scanning laser ophthalmoscopy in myopic eyes.

Methods: One hundred sixty-five eyes from 165 healthy subjects with mean spherical equivalent -5.24 ± 4.2 D (range, -15.75 to -1.00 D) were analyzed. Optic disc measurements including disc area, rim area, cup volume were obtained with an optical coherence tomograph (Cirrus SD-OCT; Carl Zeiss Meditec Inc., Dublin, CA) and a confocal scanning laser ophthalmoscope (Heidelberg Retina Tomograph, HRT 2; Heidelberg Engineering, GmbH, Dossenheim, Germany). Bland-Altman plots were used to evaluate the agreement for each optic disc parameter. The effect of myopia status on difference of disc measurements between two instruments was evaluated by linear regression analysis.

Results: The median (range) axial length (AL) was 25.6 mm (23.08-28.12 mm). Mean HRT disc area were larger than SD-OCT measurements (P < 0.001) and the difference was positively associated with axial length measurements. HRT rim area was larger than Cirrus measurements (P < 0.001) and the difference was not affected by myopia status. HRT cup volume were significantly smaller than Cirrus measurements (P < 0.001).

Conclusions: HRT overestimated optic disc area and rim area as compared to SD-OCT. A portion of the difference in HRT and SD-OCT optic disc measurements is due to myopia status. Disc parameters from the two devices are not interchangeable.

Commercial Relationships: Kunliang Qiu, None

Program Number: 4835 **Poster Board Number:** D0274

Presentation Time: 11:00 AM - 12:45 PM

Association of vascular risk factors with structural glaucomatous progression by flicker chronoscopy

Margaret M. McGlynn, Joshua R. Ehrlich, Elizabeth D. Marlow, Fabiana Q. Silva, Nathan M. Radcliffe. Weill Cornell Medical College, New York, NY.

Purpose: Identification of progression and modification of risk factors are important for management of glaucoma. We used serial flicker chronoscopy images to determine the relationship between vascular risk factors and structural glaucomatous progression.

Methods: Two glaucoma fellowship-trained ophthalmologists, masked to temporal sequence, independently graded serial flicker chronoscopy images from one eye of a cohort of glaucoma patients

for features of structural progression in this retrospective cohort study. After adjudication, simple and multiple logistic models were constructed to determine variables associated with increased odds of progression, including intraocular pressure (IOP), systolic and diastolic blood pressure (BP) and ocular perfusion pressure (OPP). **Results:** Seventy-two eyes of 72 patients were included for analysis. Patients with any form of structural progression (n=40) were older (67.0 vs. 58.8 years; $p = 0.005$), had thinner corneas (528.0 vs. 554.1 microns; $p = 0.08$), had been followed for longer (38.5 vs. 25.1 months; $p < 0.001$) and had lower mean diastolic BP (71.8 vs. 76.5 mm Hg; $p = 0.02$) than patients with no progression (n=32). Simple logistic models were constructed and central corneal thickness (CCT) (OR = 0.8 per 10 μm , 95% confidence interval (CI) 0.8, 1.0, $P < 0.03$), and mean diastolic BP (OR = 0.2 per 10 mm Hg, 95% CI 0.1, 0.6, $P < 0.006$) were associated with progressive retinal nerve fiber layer (RNFL) loss, with both CCT and mean diastolic BP significant in the multivariable model ($p=0.01$ and 0.009, respectively). For progressive neuroretinal rim loss, simple logistic models revealed associations with duration of follow-up (OR = 1.0 per 6 months, 95% CI 1.0, 1.1, $P < 0.02$) and mean diastolic BP (OR = 0.4 per 10 mm Hg, 95% CI 0.2, 0.8, $P < 0.01$) with both terms being significant in the multivariable model ($p=0.006$ and 0.003, respectively).

Conclusions: This study is the first to use structural progression and flicker chronoscopy to identify vascular glaucoma risk factors. Older age, thinner corneas, and lower mean diastolic BP were associated with progression. By multivariable analysis, CCT was associated with RNFL loss, while diastolic BP was associated with both RNFL and neuroretinal rim loss. These findings suggest that diastolic BP may be an independent risk factor for glaucomatous progression which may have implications for future management and screening. **Commercial Relationships:** Margaret M. McGlynn, None; Joshua R. Ehrlich, None; Elizabeth D. Marlow, None; Fabiana Q. Silva, None; Nathan M. Radcliffe, Allergan Inc (C), Iridex (C), Alcon (C), Merge Healthcare (C), Carl Zeiss Meditec, Inc (C)

Support: This work was supported by the Seth Sprague Educational & Charitable Foundation, by Research to Prevent Blindness and by The American Glaucoma Society through the Mentoring for Advancement of Physician-Scientists award program.

Program Number: 4836 **Poster Board Number:** D0275

Presentation Time: 11:00 AM - 12:45 PM

Optic nerve head analysis using confocal scanning laser ophthalmoscopy and spectral-domain optical coherence tomography

Gloria Roberti¹, Francesco Oddone¹, Lucia Tanga¹, Manuele Michelessi², Daniele De Geronimo¹, Marco Centofanti^{1,2}, Gianluca Manni^{1,2}. ¹IRCCS Fondazione GB Bietti, Rome, Italy; ²DSCMT, University of Rome Tor Vergata, Rome, Italy.

Purpose: to compare the diagnostic accuracy of optic nerve head (ONH) analysis using two different devices, confocal scanning laser ophthalmoscopy and spectral-domain optical coherence tomography and the agreement between tests.

Methods: forty-six glaucomatous patients and 58 healthy subjects underwent a complete ophthalmological examination, visual field testing by standard automated perimetry (Humphrey Field Analyzer Carl Zeiss Meditec) and ONH assessment by confocal scanning laser ophthalmoscopy Heidelberg Retina Tomograph 3 (HRT3, Heidelberg Engineering, GmbH) and spectral-domain optical coherence tomography RTVue-100 (Optovue Inc.).

HRT3 and RTVue-100 were performed in random order within the same session. Areas under the receiver operating characteristic curve, AUROCs, were calculated for ONH global parameters (rim area, RA, rim volume, RV, cup volume, CV, cup area, CA, Cup/Disc ratio,

C/Dr) to compare their diagnostic accuracy.

The differences of all global ONH parameters between the two devices were plotted against their means to evaluate their agreement (Bland-Altman plots).

ONH sectorial analysis was considered to determine the sector with highest sensitivity considering normative classifications. The Kappa statistic was used to quantify and evaluate the agreement between sector analysis.

Results: for both devices RA, RV, and C/Dr had good diagnostic accuracy (RTVue-100 AUROCs=0.89;0.92;0.88 and HRT3 AUROCs= 0.83; 0.84; 0.83) while CA had fair diagnostic accuracy (RTVue-100 AUROC=0.74 and HRT3 AUROC=0.76). HRT3 CV had fair diagnostic accuracy and RTVue-100 CV had very poor diagnostic accuracy.

CV Bland-Altman plot showed the highest mean difference between the instruments.

HRT3 infero-temporal (IT) sector had the highest sensitivity (80.43%) while for Rtvue-100 the supero-temporal (ST) sector had the highest sensitivity (76.1%). The agreement between all sectors was fair (ST, $k=0.34$, supero-nasal $k=0.23$, infero-nasal, $k=0.21$) while it was moderate for the IT ($k=0.41$).

Conclusions: this study suggests that ONH global parameters have good diagnostic accuracy, except for CV RTVue-100 which is the only one not to be interchangeable between these two devices, while ONH sectorial analysis has good sensitivity but fair agreement between these instruments.

Commercial Relationships: Gloria Roberti, None; Francesco Oddone, None; Lucia Tanga, Allergan (F), Alcon (F), Merck (F), Bausch & Lomb (F); Manuele Michelessi, None; Daniele De Geronimo, None; Marco Centofanti, Allergan (R), Pfizer (R), Sooft Italia (R), Bausch & Lomb (R), MSD (R); Gianluca Manni, Allergan (F), Alcon (F), Merck (F), Omikron (F), Pfizer (F), Bausch & Lomb (F)

Program Number: 4837 **Poster Board Number:** D0276

Presentation Time: 11:00 AM - 12:45 PM

A Tree Classification Method for Identifying Normal Eyes, Non-Progressing Glaucoma Eyes, and Progressing Glaucoma Eyes from Spectral Domain OCT RNFL Thickness Measurements

Michael H. Goldbaum, Siamak Yousefi, Akram Belghith, Linda M. Zangwill, Felipe A. Medeiros, Robert N. Weinreb, Daniel Meira-Freitas, Nima Hatami, Christopher Bowd. Ophthalmology, University of California at San Diego, La Jolla, CA.

Purpose: To discriminate between normal eyes, non-progressing glaucoma eyes and progressing glaucoma eyes from longitudinal series of SD-OCT measurements (retinal nerve fiber layer [RNFL] thickness measured in 6 sectors and average RNFL thickness). We propose a binary classification to 1) discriminate normal from glaucoma eyes and 2) distinguish between non-progressing and progressing glaucoma eyes, using seven-dimensional RNFL measurements as input features. The final outcome assigned eyes to one of three classes: "Normal", "Non-progressing" or "Progressing".

Methods: A Bayesian classifier was trained on three separate Spectralis RNFL image series from normal eyes, non-progressing glaucoma eyes and progressing glaucoma eyes. The dataset included 73 images from 20 normal participants (mean follow-up 3 years, 3 tests), 331 images from 20 non-progressing glaucoma patients (imaged once a week for 5 consecutive weeks) and 81 images from 20 progressing glaucoma patients from the UCSD Diagnostic Innovations in Glaucoma Study (DIGS). Progression was defined by standardized assessment of stereophotographs and/or by designation as "likely progression" based on SAP Guided Progression Analysis (mean follow-up 4 years, 4 tests). 80% of each dataset was selected

for classifier training and the remaining non-overlapping 20% was used for testing. First, images of normal eyes were separated from images of glaucoma eyes (non-progressing and progressing) then, non-progressors were separated from progressors. Classification was repeated 100 times and each time the samples were randomly permuted before dividing the dataset for training and testing. Confusion matrices representing specificity and sensitivity were computed.

Results: Specificity for classifying all images from normal eyes was 80% and sensitivity for classifying all images from glaucoma eyes was 79%. Specificity for identifying images from non-progressing glaucoma eyes was 93% and sensitivity for identifying images from progressing glaucoma eyes was 80%.

Conclusions: Tree classification using a Bayesian strategy showed high specificity in normal eyes and high sensitivity in glaucoma eyes, with good accuracy for separating non-progressing from progressing glaucoma eyes.

Commercial Relationships: Michael H. Goldbaum, None; Siamak Yousefi, None; Akram Belghith, None; Linda M. Zangwill, Carl Zeiss Meditec Inc (F), Heidelberg Engineering GmbH (F), Optovue Inc (F), Topcon Medical Systems Inc (F), Nidek Inc (F); Felipe A. Medeiros, Carl-Zeiss (F), Heidelberg Engineering (F), Topcon (F), Alcon (F), Allergan (F), Sensimed (F), Reichert (F); Robert N. Weinreb, Aerie (F), Alcon (C), Allergan (C), Altheos (C), Amakem (C), Bausch&Lomb (C), Carl Zeiss-Meditec (C), Genentech (F), Haag-Streit (F), Heidelberg Engineering (F), Konan (F), Lumenis (F), National Eye Institute (F), Nidek (F), Optovue (C), Quark (C), Solx (C), Topcon (C); Daniel Meira-Freitas, None; Nima Hatami, None; Christopher Bowd, None

Support: NIH Grants RO1EY022039, RO1EY011008, RO1EY021818, P30EY022589; Research to Prevent Blindness; David & Marilyn Dunn Fund

Clinical Trial: NTC00221897

Program Number: 4838 **Poster Board Number:** D0277

Presentation Time: 11:00 AM - 12:45 PM

Utilization of Novel Technology to Improve Accuracy and Efficiency of Assessing Progression of Glaucomatous Changes in Serial Fundus Photos

Ozgur Ozkan¹, Reginald Barnes², Bethany Markowitz¹.

¹Ophthalmology, University of South Carolina/Palmetto Health, Columbia, SC; ²Ophthalmology, Georgetown University/Washington Hospital Center, Washington, DC.

Purpose: Color fundus photos are used to assess for glaucomatous changes to the optic nerve head. Alternating Animation Flicker (AAF) is a novel technology that automatically and precisely aligns two images of the same fundus. The software then alternates between the two images to create an animation such that differences appear as motion. This study compares accuracy and time to assessment (TTA) for progression of optic nerve head changes evaluated with AAF compared to traditional side-by-side fundus photos.

Methods: Eight residents were shown five side-by-side serial, color fundus images of optic nerves heads and six animated gif's of AAF's generated from color fundus images focusing on the optic nerves heads of glaucoma patients. Both sets of images contained similarly graded difficulty-level images and one non-progressive nerve head that had no glaucomatous changes. All participating residents were given identical instructions to note any glaucomatous changes (including cup-to-disc ratio changes, notching, Drance hemorrhages, retinal nerve fiber layer changes, etc.). Times were recorded from initial side-by-side images viewed and from the animated gif presented to completion of written findings. Written responses were graded by giving one point for each glaucomatous change accurately

identified.

Results: The average number of correctly identified glaucomatous changes by side-by-side analysis was 2.375 (SD=1.49) out of 12 (19.8%) for the ophthalmology residents' readings. In comparison, the mean number of correctly identified changes utilizing AAF was 8 (SD=1.41) out of 11 (72.7%), correlating to a 2.7 fold increase in accuracy ($P < 1.45 \times 10^{-6}$). See table 1.

The mean TTA by traditional analysis was 22.5 sec (SD=4.8 sec). The mean TTA using AAF generated animated gif's was 14.9 sec (SD=2.4 sec). The overall improvement in time to completion of assessment was 7.6 seconds or a 66.2% time savings ($P < 3.4 \times 10^{-6}$). See table 2.

Conclusions: Evaluations of fundus photos remain the gold standard for evaluating optic nerve changes in glaucoma. Multiple studies have already shown significant inter-observer variability in evaluating side-by-side serial fundus photos.

Alternating Animation Flicker (AAF) significantly improved the accuracy and efficiency of residents in their analysis of glaucomatous changes over time in fundus photographs.

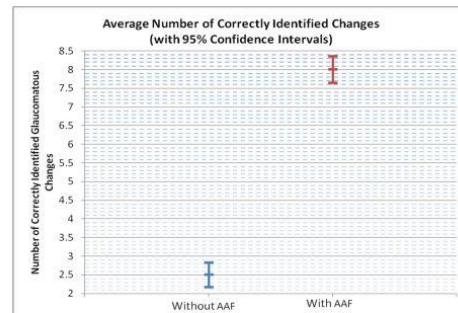


Chart 1

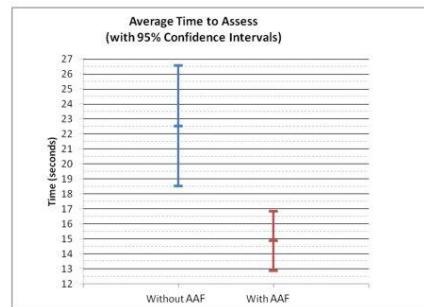


Chart 2

Commercial Relationships: Ozgur Ozkan, EyeIC, Inc (F); Reginald Barnes, EYEIC, Inc (F); Bethany Markowitz, None

Program Number: 4839 **Poster Board Number:** D0278

Presentation Time: 11:00 AM - 12:45 PM

Objective Assessment of Glaucoma Suspect Comparing Different Imaging Techniques

Eduardo M. Normando^{1,2}, Lisa A. Turner¹, Faisal Ahmed², Philip A. Bloom², M Francesca Cordeiro^{1,2}. ¹Glaucoma & Retinal Neurodegeneration Research Group, Visual Neuroscience, UCL Institute of Ophthalmology, London, United Kingdom; ²Western Eye Hospital, Imperial College Healthcare Trust, London, United Kingdom.

Purpose: Despite the development and establishment of state-of-the-art retinal imaging technology, there are few good clinical studies assessing objective changes in patients with glaucoma suspect. The aim of this study was to prospectively assess, using different objective imaging parameters, the retinal anatomical features of

patients with glaucoma suspect.

Methods: 60 patients referred from general practitioners with a high risk factor for glaucoma were assessed at the Western Eye Hospital in London. 60 healthy were also assessed as control. Patients were assessed with Heidelberg Retinal Tomography (HRT3), and Spectral Domain Optical Coherence Tomography (SD-OCT) as well as Humphrey Visual Field (HVF) repeatedly from the first visit up to eighteen months follow-up. OCT Thickness map, OCT posterior pole analysis, OCT RNFL thickness profile, HRT stereometric Parameters, Moorefield Regression Analysis (MRA), GPS Classification along with a custom image analysis was used to compare retinal features and optic nerve head structures. Repeated imaging was performed in all patients.

Results: 70% of patients with glaucoma suspect showed retinal abnormalities at the OCT with a superotemporal and inferotemporal thinning of the peripapillary retina beyond the OCT RNFL and HRT scanning area. 54% had abnormal RNFL thickness profile compared to healthy subjects. 60% of the patients showed abnormal MRA which was in keeping with GPS classification. All healthy subjects had no pathological findings. Custom designed image analysis showed consistency between OCT and HRT findings.

Conclusions: This study shows that state-of-the-art imaging technology increases the sensitivity and specificity in early diagnosis for glaucoma when different imaging devices are used simultaneously. Recognisable modification in patients with glaucoma suspect occurs when both HRT and OCT are used. It confirms that early modifications in retinal structure are assessable but only when a multi-platform approach is applied.

Commercial Relationships: Eduardo M. Normando, None; Lisa A. Turner, None; Faisal Ahmed, None; Philip A. Bloom, International Glaucoma Association (S), UKISCRS (S), Ophthalmology Section, RSM (S); M Francesca Cordeiro, application (P)

Program Number: 4840 **Poster Board Number:** D0279

Presentation Time: 11:00 AM - 12:45 PM

Evaluation of Inner to Outer Retina Area Ratio for Detection of Glaucoma with Macular OCT Imaging

Navid Amini^{1,4}, Nila Cirineo¹, Shane Knipping¹, Hamid Hosseini¹, JoAnn A. Giaconi¹, Simon K. Law¹, Thomas Chou³, Luminita A. Vese², Joseph Caprioli¹, Kouros Nouri-Mahdavi¹. ¹Ophthalmology, Jules Stein Eye Institute at UCLA, Los Angeles, CA; ²Department of Mathematics, UCLA, Los Angeles, CA; ³Department of Biomathematics, UCLA, Los Angeles, CA; ⁴UCLA Wireless Health Institute, Los Angeles, CA.

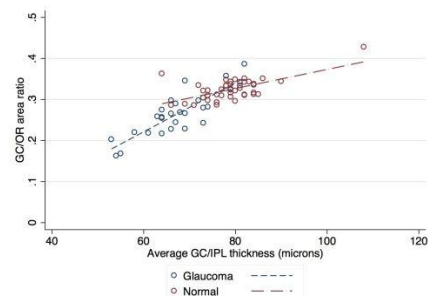
Purpose: To determine whether the inner to outer retina (OR) area ratio can improve detection of glaucoma with macular SD-OCT imaging as compared to ganglion cell/inner plexiform layer (GC/IPL) thickness measurements.

Methods: Forty-one normal subjects and 27 glaucoma patients from the UCLA OCT Imaging Study were included. Macular images were obtained (posterior pole algorithm, Spectralis SD-OCT) and the raw data files were exported for automatic segmentation of retinal layers using 3-D contextual information (Iowa OCT Explorer). Properties of the derivative of surface and thickness functions were exploited to locate the foveal center in MATLAB. The B-scan passing through the foveal center was used for computing the total area of inner and outer retina layers in the central 4.8mm of the scan. Average ganglion cell/inner plexiform layer (GC/IPL) measurements were also obtained (Macular Cube 200x200, Cirrus HD-OCT). Logistic regression and area under the ROC curves (AUCs) were used to compare models. Performance of ganglion cell complex and GC/IPL to OR (GCC/OR vs. GC/OR) area ratios were also compared.

©2013, Copyright by the Association for Research in Vision and Ophthalmology, Inc., all rights reserved. Go to iovs.org to access the version of record. For permission to reproduce any abstract, contact the ARVO Office at arvo@arvo.org.

Results: The median (IQR) MD was -3.9 (-6.3 to -2.5) dB and 0 (-0.8 to 0.4) dB in glaucoma and normal subjects, respectively. The corresponding mean GC/OR area ratios were 0.27 (±0.05) and 0.33 (±0.03). GC/OR area ratio was not related to age or axial length in normal subjects (p>0.05). GC/IPL thickness and GC/OR ratio were highly correlated (p<0.001) in normal (R²=0.39) and glaucoma subjects (R²=0.74). AUCs for detection of glaucoma were similar for GC/IPL (0.90) or GC/OR area ratio (0.88) when adjusted for age and axial length. GC/OR area ratio and its interaction with average GC/IPL were found to be significantly predictive of glaucoma (p=0.005 and 0.009, respectively) when added to GC/IPL. This improved the predictive performance of the logistic regression compared to GC/IPL alone (AUC for the combined model=0.93; p=0.09 for comparison to GC/IPL model). The results were similar when GCC/OR area ratio was used.

Conclusions: GC/OR area ratio does not vary as a function of age or axial length in normal subjects. Adding GC/OR area ratio to GC/IPL thickness in multivariate predictive models can potentially improve detection of glaucoma.



Correlation of the macular GC/OR area ratio with average GC/IPL thickness.

Commercial Relationships: Navid Amini, None; Nila Cirineo, None; Shane Knipping, None; Hamid Hosseini, None; JoAnn A. Giaconi, Allergan (C); Simon K. Law, None; Thomas Chou, None; Luminita A. Vese, None; Joseph Caprioli, Allergan Inc. (C), Allergan Inc. (F), Allergan Inc. (R); Kouros Nouri-Mahdavi, Allergan (C)

Support: Gerald Oppenheimer Family Foundation Center for the Prevention of Eye Disease Endowment Fund (KNM) and American Glaucoma Society's Early Clinician-Scientist Award (KNM)

Program Number: 4841 **Poster Board Number:** D0280

Presentation Time: 11:00 AM - 12:45 PM

The Magnitude and Direction of Mismatch between Bruch's Membrane Opening (BMO) and Anterior Scleral Canal Opening (ASCO) within Spectral Domain Optical Coherence Tomography (SD-OCT) Optic Nerve Head (ONH) Scans of Ocular Hypertension and Glaucoma Patients

Christy A. Hardin, Hongli Yang, Ruojin Ren, Lin He, Stuart K. Gardiner, Brad Fortune, Shaban Demirel, Claude F. Burgoyne. Discoveries in Sight Research Laboratory, Devers Eye Institution and Legacy Research Institute, Portland, OR.

Purpose: To assess the magnitude and direction of mismatch between BMO and ASCO within SDOCT ONH scans of 131 ocular hypertension and glaucoma patients.

Methods: Both eyes of 131 patients (aged 33-90) underwent SDOCT (Heidelberg Spectralis, 870nm) ONH imaging (48 high-resolution, ONH centered, radial B-scans). Data from one eye per patient was chosen based on optimal scan quality. BMO and ASCO were manually delineated within each SDOCT data set (Figure 1) and 12 ONH sectors were established based on the Foveal-BMOcentroid

(FoBMO) axis. Eyes without visible BMO or ASCO in any sector were eliminated from the study. The direction and magnitude of the BMO-ASCO centroid axis was determined and the mean BMO and ASCO radii were quantified for each of the 12 sectors. The average BMO and ASCO radii and the distribution of differences (ASCO-BMO) among all 131 eyes were analyzed by sector.

Results: All sectors showed significant mismatch ($p < 0.001$) between BMO-ASCO except the inferior temporal and temporal inferior sectors (Fig 2a). Mismatch between BMO and ASCO was greatest in the nasal superior, nasal, superior nasal, nasal inferior, and superior sectors (Mean difference \pm SD: 145 ± 87.5 , 135 ± 94.0 , 127 ± 72.5 , 113 ± 90.1 , 96 ± 57.4 , respectively) with substantial variation across eyes and locations (Fig 2b).

Conclusions: This is the first characterization of SDOCT detected BMO-ASCO mismatch in eyes of glaucoma patients. Our data suggest that in the subset of eyes that could be studied, the frequency and magnitude of BMO-ASCO mismatch is greatest in the superior and nasal sectors, however in some eyes it extends along the superior nasal- inferior temporal axis or less commonly involves all 12 segments of BMO. Since the ASCO and BMO are connected by the Border Tissues of Elshnig (BTE), ASCO-BMO mismatch contributes to the regional location of “internally oblique” and “externally oblique” BTE as previously described by Strouthidis, et al, IOVS 2009 and Reis, et al, Ophthalmology. 2012. The implications of these findings for cross-sectional and longitudinal studies of SDOCT ONH imaging are under study.

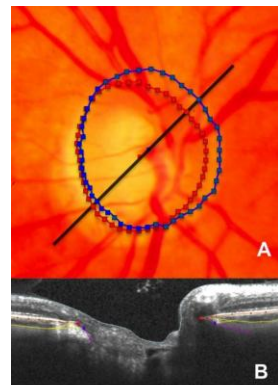
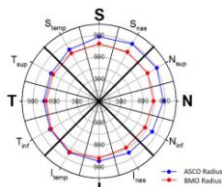


Figure 1. The disc photograph (A) and SD OCT B-scan (B) appearance of Bruch's Membrane Opening (BMO) – Anterior Sclera Canal Opening (ASCO) mismatch. (A) Colocalized disc photograph with BMO line in red and ASCO line in blue. Blue line marks the orientation of SDOCT radial B scan section. (B) Representative delineated B-scan highlighted in panel A. Light blue lines: the internal limiting membrane (ILM), orange lines: Bruch's membrane/retinal pigment epithelium (BM/RPE), red points: the Bruch's membrane opening (BMO), blue points: the anterior lamina sclera canal opening (ASCO), yellow lines: anterior sclera surface, purple line: neural boundary.



2a Mean ASCO and BMO Radii (μm)

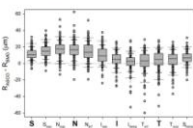


Figure 2. (a) Comparison of co-localized SDOCT Bruch's Membrane Opening (BMO) and Anterior Sclera Canal Opening (ASCO) radii using 12 radial B-scan registration. The upper polar plot shows the mean BMO and ASCO data from 131 patients are regionalized into 12 sectors by using radial B-scans. The red circles and lines represent BMO radii while the blue circles and lines represent ASCO radii. (b) The lower box plot shows individual difference between BMO and ASCO mean radii over the 12 regionalized sectors. The circles are the $R_{BMO} - R_{ASCO}$ difference of each individual eye for each sector. The lower and upper limits of the box indicate a 1SD. The horizontal lines inside the box is the median value while the horizontal short lines outside the box represent 25%, 75% and 95% quantiles respectively.

Commercial Relationships: Christy A. Hardin, None; Hongli Yang, None; Ruojin Ren, None; Lin He, None; Stuart K. Gardiner, Allergan (R); Brad Fortune, Heidelberg Engineering, GmbH (F), Carl Zeiss Meditec, Inc (F); Shaban Demirel, Carl Zeiss Meditec (F), Heidelberg Engineering (R), Heidelberg Engineering (F); Claude F. Burgoyne, Heidelberg Engineering (F), Heidelberg Engineering (C)
Support: NIH/NEI R01-EY021281; NIH/NEI R01-EY-019674

Program Number: 4842 **Poster Board Number:** D0281
Presentation Time: 11:00 AM - 12:45 PM
Variability of the Foveal-Bruch's Membrane Opening centroid (FoBMO) axis angle in patients with ocular hypertension and early glaucoma

Luke Reyes, Ruojin Ren, Juan Reynaud, Hongli Yang, Stuart K. Gardiner, Brad Fortune, Shaban Demirel, Claude F. Burgoyne. Discoveries in Sight Research Laboratories, Devers Eye Institute, Legacy Research Institute, Portland, OR.

Purpose: To determine the range and measurement variability of the FoBMO angle relative to the horizontal meridian of the acquired image frame (AIF) in 191 eyes of patients with glaucoma and high-risk ocular hypertension.

Methods: Spectral domain optical coherence tomography (SDOCT, Heidelberg Engineering) scans were obtained in 191 patients (46 -90 years of age, using a pattern of 48 radial 30° B-scans centered on the optic nerve head (ONH). In the data from one eye per patient, the BMO was delineated within every other radial B-scan (24 total) and its centroid was determined. The fovea was then independently marked within the corresponding infrared reflectance image by two delineators and then re-marked by one delineator to measure inter and intra-delineator variability. The linear distance between the BMO centroid and fovea and the angle between FoBMO and the AIF horizontal (negative below, positive above) were calculated for each delineation of each eye.

Results: The average FoBMO axis was $-6.4 \pm 4.0^\circ$ relative to the AIF horizontal (range -16° to $+6.4^\circ$, Figure 1). The average FoBMO distance was $4365 \pm 280 \mu\text{m}$ (range 3599 to 5200 μm). The FoBMO axis was ≥ 10 degrees below the AIF horizontal in 21% of eyes and equal to or above the AIF horizontal in 6% of eyes. Delineation of the FoBMO axis angle was highly correlated within a delineator ($R^2=0.86$) and between delineators ($R^2=0.90$). Bland-Altman limits-of-agreement for intra- and inter-delineator repeatability, respectively, were 2.7° and 3.4° for FoBMO axis angle and $368 \mu\text{m}$ and $432 \mu\text{m}$ for FoBMO distance.

Conclusions: The range of FoBMO axis angles within this cohort is substantial and similar to a recent report (Patel, OVS 2012). These results indicate that the FoBMO axis measured using this method is sufficiently repeatable to permit reliable analysis of 30° ONH sectors oriented to this landmark. Because the FoBMO axis influences axon bundle paths and is an anatomical reference shared by nearly all human eyes, using it (rather than the AIF axes) to regionalize ONH data may personalize the interpretation of SDOCT ONH imaging.

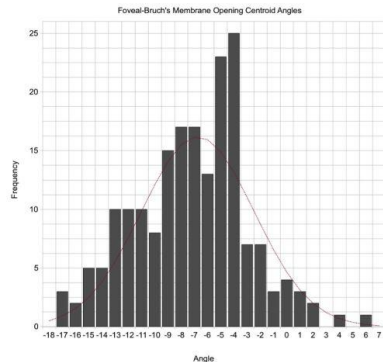


Figure 1: Distribution of Foveal-Bruch's Membrane Opening centroid (FoBMO) axis angles

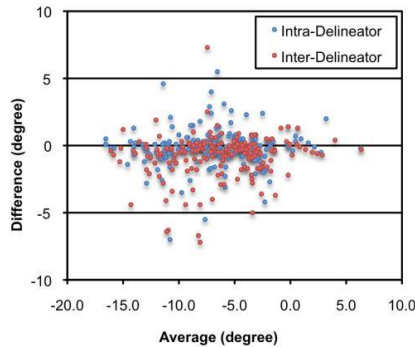


Figure 2: Bland-Altman plot of variability in delineating FoBMO axis angles

Commercial Relationships: Luke Reyes, None; Ruojin Ren, None; Juan Reynaud, None; Hongli Yang, None; Stuart K. Gardiner, Allergan (R); Brad Fortune, Heidelberg Engineering, GmbH (F), Carl Zeiss Meditec, Inc (F); Shaban Demirel, Carl Zeiss Meditec (F), Heidelberg Engineering (R), Heidelberg Engineering (F); Claude F. Burgoyne, Heidelberg Engineering (F), Heidelberg Engineering (C)
Support: NIH/NEI R01-EY021281; NIH/NEI R01-EY-019674; Legacy Good Samaritan Foundation; Sears Medical Trust; Alcon Research Institute, Heidelberg Engineering, GmbH, Heidelberg, Germany (equipment and unrestricted research support), Reichert Instruments (equipment).

Program Number: 4843 **Poster Board Number:** D0282

Presentation Time: 11:00 AM - 12:45 PM

Quadratic Bayesian Pattern Detection for Detecting Glaucomatous Change in Follow-up SD-OCT RNFL Thickness Measurements

Siamak Yousefi, Akram Belghith, Michael H. Goldbaum, Linda M. Zangwill, Felipe A. Medeiros, Robert N. Weinreb, Renato Lisboa, Christopher Bowd. Ophthalmology, Hamilton Glaucoma Center, La Jolla, CA.

Purpose: We proposed a quadratic Bayesian pattern detector to detect change from longitudinal series of SD-OCT measurements, including retinal nerve fiber layer (RNFL) thickness measured in 6 sectors and average RNFL thickness (a total of 7 input dimensions), in stable and progressing glaucoma eyes.

Methods: A quadratic Bayesian pattern detection method was employed to detect change in the seven-dimensional vector of SD-OCT based-RNFL thickness measurements, by comparing baseline to follow-up exams, from a longitudinal series. Spectralis RNFL image series were obtained from non-progressing glaucoma eyes and progressing glaucoma eyes which correspond to no-change and change, respectively. The dataset included 331 images from 20 non-

progressing glaucoma patients (imaged once a week for 5 consecutive weeks) and 81 images from 20 progressing glaucoma patients from the UCSD Diagnostic Innovations in Glaucoma Study (DIGS). Progression was defined by standardized assessment of stereophotographs and/or by designation as “likely progression” based on SAP Guided Progression Analysis (mean follow-up 4 years, 4 tests). Two normative databases were generated from 90% of the data in the original datasets by calculating the norm 1 distance between the RNFL measurements from the baseline and each follow-up exam, for each group. The quadratic Bayesian pattern detector was trained based on the normative datasets and then was tested using ten-fold cross-validation to evaluate the accuracy of change detection. For testing, for each subject, each follow-up exam was compared to the baseline exam separately. If more than half of the follow-up exams showed progression based on the trained Bayesian pattern detector, the eye was classified as progressed, otherwise, the eye was classified as non-progressed. Sensitivity and specificity were computed based on this rule.

Results: The diagnostic accuracies were: 80% sensitivity in progressors and 78% specificity in non-progressors.

Conclusions: A Bayesian pattern detection method was developed that could detect glaucomatous progression from baseline and follow-up images. This method provided reasonable specificity to detect stable eyes and sensitivity to detect progressing eyes, with the potential to improve accuracy by increasing number of samples in the normative database.

Commercial Relationships: Siamak Yousefi, None; Akram Belghith, None; Michael H. Goldbaum, None; Linda M. Zangwill, Carl Zeiss Meditec Inc (F), Heidelberg Engineering GmbH (F), Optovue Inc (F), Topcon Medical Systems Inc (F), Nidek Inc (F); Felipe A. Medeiros, Carl-Zeiss (F), Heidelberg Engineering (F), Topcon (F), Alcon (F), Allergan (F), Sensimed (F), Reichert (F); Robert N. Weinreb, Aerie (F), Alcon (C), Allergan (C), Altheos (C), Amakem (C), Bausch&Lomb (C), Carl Zeiss-Meditec (C), Genentech (F), Haag-Streit (F), Heidelberg Engineering (F), Konan (F), Lumenis (F), National Eye Institute (F), Nidek (F), Optovue (C), Quark (C), Solx (C), Topcon (C); Renato Lisboa, None; Christopher Bowd, None

Support: NIH R01EY022039, NIH R01EY011008, NIH R01EY021818, NIH P30EY022589, Research to Prevent Blindness.

Clinical Trial: NCT00221897

Program Number: 4844 **Poster Board Number:** D0283

Presentation Time: 11:00 AM - 12:45 PM

A method for mapping retinal nerve fiber layer birefringence

Juan Reynaud, Brad Fortune. Discoveries in Sight Research Laboratories, Devers Eye Institute and Legacy Research Institute, Portland, OR.

Purpose: We have shown that RNFL retardance, measured by scanning laser polarimetry (SLP), declines prior to RNFL thickness measured by spectral domain optical coherence tomography (SDOCT) using global average peripapillary scan locations for non-human primates (NHP) with experimental glaucoma (EG). These results are consistent with the hypothesis that axonal cytoskeletal disruption precedes axon bundle thinning within the RNFL during the course of glaucomatous neurodegeneration. An important step forward in testing this hypothesis is to develop a method for mapping RNFL birefringence beyond the conventional peripapillary scan locations.

Methods: SLP scans (GDxVCC, Carl Zeiss Meditec, Inc) and SDOCT cube scans consisting of 290 horizontal raster lines (Spectralis, Heidelberg Engineering, GmbH) were acquired longitudinally in NHPs with EG. Custom software was developed to

rapidly co-localize pairs of reflectance images and derive birefringence maps.

Results: Fig1 demonstrates each step of the method and an example of glaucomatous change in RNFL birefringence.

Conclusions: We developed software to rapidly and effectively co-localize the reflectance image from SLP scans to the reflectance image from SDOCT scans and to derive RNFL birefringence maps from the retardance and thickness values, respectively. Registration of scans over time and across instruments reduces noise in longitudinal series of sectoral data.

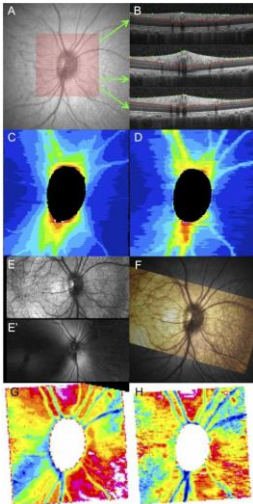


Fig1: Focal RNFL birefringence changes can be followed longitudinally (by sector and eccentricity). (A) Infrared reflectance image acquired during baseline SDOCT cube scan; red lines indicate position of 290 raster scans. (B) Examples of individual B-scans with RNFL segmentations (red and green lines) from positions indicated by green arrows. (C) RNFL thickness map for baseline derived from data in panels A&B. (D) RNFL thickness map for final time point; note mild decrease in thickness. (E) Infrared reflectance image obtained from the baseline SLP scan and (E') corresponding RNFL retardance map. (F) Colocalization step to register SLP scan to SDOCT scan: the SLP reflectance image is pseudo-colored, scaled, translated and rotated to optimize match. This step enables calculation of birefringence (nm retardance per μm thickness) and derivation of maps for (G) baseline and (H) final time point demonstrating birefringence changes in this eye.

Commercial Relationships: Juan Reynaud, None; Brad Fortune, Heidelberg Engineering, GmbH (F), Carl Zeiss Meditec, Inc (F)
Support: NIH R01-EY019327 (BF); Legacy Good Samaritan Foundation; Heidelberg Engineering, GmbH, Heidelberg, Germany (equipment and unrestricted research support); Carl Zeiss Meditec, Inc. (equipment).

Program Number: 4845 **Poster Board Number:** D0284

Presentation Time: 11:00 AM - 12:45 PM

The Prevalence of Cirrus SD-OCT Ganglion Cell Segmentation Errors in High Myopes

Tessa Johung¹, Jonathan D. Oakley², Daniel Russakoff², Sonny Sabhlok¹, Felix Li³, Robert Chang¹. ¹Stanford University, Stanford, CA; ²Voxeleron, Pleasanton, CA; ³Dept. of Ophthalmology and Visual Sciences, Chinese University of Hong Kong, Hong Kong, China.

Purpose: To investigate the prevalence of sectoral value differences due to segmentation errors in macular Ganglion cell-inner plexiform layer (GCIPL) scans using SD-OCT in glaucomatous and highly

myopic eyes.

Methods: 174 Cirrus HD-OCT macula scans were obtained from 77 patients. 96 eyes had high myopia ($> -5\text{D}$ acuity) and were glaucoma suspects. 78 were defined as glaucomatous, having progressive visual field defects in more than one examination. GCIPL analysis was performed using the Cirrus 6.0 software and custom Septem retinal segmentation software. All thickness measurements were compared and sectors differing by more than 10 microns were manually reviewed by an expert observer. Cirrus review was performed on the instrument; Septem review using a Matlab GUI. A sector error was counted whenever either an error of more than 10 microns was seen.

Results: For Cirrus, 27 eyes (15.5%) reported at least one sector error. The Septem algorithm had only 6 such instances (3.4%). The chi-square test reports a significant difference in the prevalence of errors between the algorithms ($p < 0.001$). Figure 1 shows example GCIP maps. Figure 2 shows their underlying segmentations.

Conclusions: The prevalence of errors in GCIP Cirrus thickness maps in the study is high (15.5%). Algorithms are improving, as is evidenced by the low error rate using Septem (3.4%). For current commercial devices, the emphasis on clinical judgment when assessing glaucomatous damage in such populations remains.

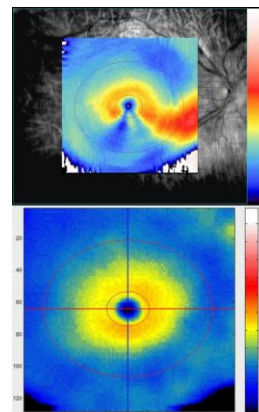


Figure 1: On the left is the GCIPL thickness map from the Cirrus 6.0 software. On the right that generated by Septem. Each colorbar reports thicknesses in microns. Note that the Cirrus map shows two apparent arcuate defects, but each should be turning toward the optic nerve, on the right of the image, to be real (this eye is OD). The Septem map shows no such defects.

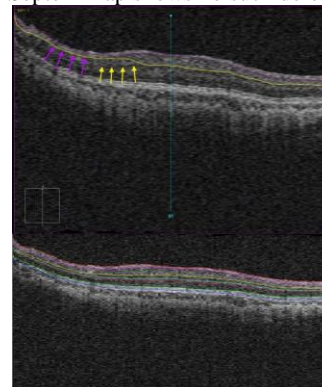


Figure 2: The top image shows a vertical B-scan from the OCT and Cirrus segmentations. It is positioned to pass through an apparent arcuate defect (Figure 1). The left side is inferior; the right side superior. Below, is the result from Septem, here showing all seven segmented layers. Each has the posterior of the RNFL and IPL reported in magenta and yellow, respectively. The error in the Cirrus

result appears to stem from the posterior of the IPL boundary identifying instead the posterior of the RNFL. Arrows show where the RNFL (magenta arrows) and IPL (yellow arrows) should be.

Commercial Relationships: Tessa Johung, None; Jonathan D. Oakley, Voxeleron LLC (E); Daniel Russakoff, Voxeleron (E); Sonny Sabhlok, None; Felix Li, None; Robert Chang, None

Program Number: 4846 **Poster Board Number:** D0285

Presentation Time: 11:00 AM - 12:45 PM

Optic disc morphology parameters in primary open angle glaucoma in Japanese using a stereo fundus camera - The Glaucoma Stereo Analysis Study (GSAS)

Yu Yokoyama¹, Masaki Tanito², Koji Nitta³, Maki Katai⁴, Yasushi Kitaoka⁵, Kazuko Omodaka¹, Satoru Tsuda¹, Toshiaki Nakagawa⁶, Toru Nakazawa¹. ¹Department of Ophthalmology, Tohoku university, Sendai-shi, Japan; ²Department of Ophthalmology, Shimane University Faculty of Medicine, Izumo-shi, Japan; ³Department of Ophthalmology, Fukui-ken Saiseikai Hospital, Fukui-shi, Japan; ⁴Department of Ophthalmology, Sapporo Teishin Hospital, Sapporo-shi, Japan; ⁵Department of Ophthalmology, St. Marianna University School of Medicine, Sapporo-shi, Japan; ⁶Research & Development Section, Electronics & Optics Division, Kowa Company, Ltd, Nagoya-shi, Japan.

Purpose: To assess physical parameters of optic disc morphology in primary open angle glaucoma with a stereo fundus camera.

Methods: The Glaucoma Stereo Analysis Study (GSAS), a cross sectional multicenter collaborative study, enrolled 187 criteria-eligible eyes with primary open angle glaucoma from 187 subjects (male: female = 100: 87, age = 62 ± 9, range: 30-80). The diagnosis of glaucoma was based on glaucomatous fundus appearances and the corresponding visual field defects. The data included best-corrected visual acuity, refractive error, intraocular pressure, mean deviation (MD) as measured with the Humphrey field analyzer (HFA, SITA standard 30-2), and MD slope, as determined by more than six reliable HFA results were collected retrospectively. Exclusion criteria included 1) a history of intraocular surgery other than for cataracts or glaucoma, 2) any history of intraocular surgery in the previous three years, 3) most recent MD < -12 dB. If both eyes met the inclusion criteria, the eye with more advanced glaucoma was selected. The optic disc imaged with a commercially available stereo fundus camera (nonmydWX, Kowa Company, Ltd., Japan) was three-dimensionally analyzed using newly developed software to calculate the various optic disc parameters. Mean rim decentring was defined as (superotemporal rim area - inferotemporal rim area)/(superotemporal rim area + inferotemporal rim area). The Spearman rank correlation coefficient was used to assess correlations in the data.

Results: The quantitative disc parameters in this study were as follows: vertical disc width, 1.86 ± 0.23 mm; horizontal disc width, 1.66 ± 0.28 mm; vertical cup-to-disc ratio (C/D), 0.82 ± 0.08; horizontal C/D, 0.74 ± 0.09; superior rim-to-disc ratio (R/D), 0.08 ± 0.06; inferior R/D, 0.04 ± 0.05; mean cup depth, 0.20 ± 0.09mm; maximum cup depth, 0.52 ± 0.19 mm; and disc tilt angle, 10.5 ± 12.5 degrees. Mean rim decentring was 0.30 ± 0.42 and the absolute value of rim decentring was 0.45 ± 0.27. There were negative correlations between disc tilt angle and age (r = -0.30, p < 0.0001) or refractive error (r = -0.36, p < 0.0001).

Conclusions: We were able to obtain basic data set of GSAS. The nonmydWX system made it possible to perform quantitative analyses of the optic disc in glaucoma.

Commercial Relationships: Yu Yokoyama, Kowa Company (C); Masaki Tanito, Kowa Company, Ltd. (F), Kowa Company, Ltd. (C);

Koji Nitta, Kowa (C); Maki Katai, Kowa Company, Ltd. (F); Yasushi Kitaoka, Kowa Company, Ltd. (F), Kowa Company, Ltd. (C); Kazuko Omodaka, None; Satoru Tsuda, Kowa (C); Toshiaki Nakagawa, Kowa Company, Ltd. (E); Toru Nakazawa, Kowa Company Ltd. (F), Kowa Company Ltd. (C)

Program Number: 4847 **Poster Board Number:** D0286

Presentation Time: 11:00 AM - 12:45 PM

Glaucoma Assessment using Retinal Topography by Scanning Laser Ophthalmoscope Imaging

Maarten Huijbregtse, Dirk De Brouwere, Michiel Mensink. i-Optics BV, The Hague, Netherlands.

Purpose: A 3D topographic reconstruction of the retinal surface can be a helpful aid in diagnosing and monitoring the occurrence and progression of retinal pathologies like glaucoma. In this study, we used a compact confocal Scanning Laser Ophthalmoscope (cSLO) to assess the presence of glaucoma in a mixed group of subjects through retinal topography of the optic nerve head.

Methods: For this study, a zero-dilation compact cSLO (EasyScan, i-Optics, The Netherlands) was modified to acquire stacks of retinal images at different focal depths. The confocal nature of the camera enables the 3D reconstruction of the retinal surface from a depth-resolved image stack after image registration. Besides ten healthy eyes, ten glaucomatous eyes were recruited. Subjects were excluded from the study when the optical media were unclear. The 45 degree nasal field was imaged twice for all eyes. Reconstructed topographic maps were rendered and presented to two experienced glaucoma graders.

Results: Both graders referred the glaucomatous eyes with a strong agreement to the diagnosis as communicated in each patient's medical record. Sensitivity and specificity were in line with the outcomes known in the standard practice for glaucoma diagnosis. Additionally, no significant difference could be observed when comparing the two different topographic reconstructions taken in each eye.

Conclusions: The results indicate that retinal topography can be implemented in a compact cSLO camera, in a precise enough manner to use it for diagnosing and monitoring glaucoma. We believe this will allow healthcare providers to prevent progression of visual loss in glaucomatous patients with treatments in the early stages of the pathology.

Commercial Relationships: Maarten Huijbregtse, i-Optics BV (E); Dirk De Brouwere, i-Optics bv (E); Michiel Mensink, i-Optics bv (I), i-Optics bv (P), i-Optics bv (S)

Support: Dutch Innovation Funding IK11055

Program Number: 4848 **Poster Board Number:** D0287

Presentation Time: 11:00 AM - 12:45 PM

Macular Retinal Ganglion Cell Complex Thickness and Its Relationship to the Retinal Nerve Fiber Layer in Non-Human Primates with Ocular Hypertension

Kaveh Azartash, James A. Burke. Biological Sciences, Allergan, Irvine, CA.

Purpose: Imaging studies in glaucoma patients show that chronically elevated intraocular pressure (IOP) leads to a thinning of both the retinal nerve fiber layer around the optic nerve (RNFL) and the macular ganglion cell complex (mGCC) thickness (nerve fiber layer + retinal ganglion cell + inner plexiform layer). This study examined the relationship between the mGCC thickness and the RNFL thickness in non-human primates (NHPs) with chronic ocular hypertension (OHT) using a semi-automatic software for quantifying mGCC and RNFL thickness. Specifically the diagnostic sensitivity and repeatability of mGCC thickness vs. RNFL thickness was

evaluated.

Methods: Twelve Cynomolgus monkeys weighing 5.3 ± 1.6 kg and with approximately 15 ± 4.2 years of age were used in this study. Animals had unilateral chronic OHT that was induced by circumferential laser treatment to the trabecular meshwork in one eye (OD) for approximately 9.5 ± 2.3 years. RNFL thickness and mGCC thickness were measured bilaterally using optical coherence tomography (Bioptigen Inc., Durham, 27560). A semi-automated algorithm was utilized by three randomized and masked delineators to delineate the retinal layers. Both delineation and data acquisition were performed twice for repeatability measures. Statistical analysis was performed to compare the significance of mGCC thickness vs. that of RNFL thickness. OS (naïve eye) was used as a control for each subject and statistical significance was analyzed in OD (OHT eye) vs. OS for both mGCC and RNFL.

Results: Both Cohen's d value and the effective size coefficient indicate a larger degree of separation in mGCC vs. RNFL. mGCC showed Cohen's d value and effective size coefficient of 2.13 and 0.73 respectively where RNFL had 1.31 and 0.54 for Cohen's d and effective size. A larger chi-square value -17.38 vs. 8.24- for GCC vs. RNFL respectively, also revealed a larger difference in the log likelihood between mGCC thickness when compared with that of RNFL. Correlation coefficient of 0.76 suggest an acceptable repeatability b/w the two mGCC measurements.

Conclusions: This study suggests that mGCC is more affected when compared to RNFL in NHPs with chronic OHT eyes. Additionally mGCC thickness measurements exhibit high potentials to be a good alternative or a complementary measurement to RNFL thickness assessment in the clinical evaluation of glaucoma.

Commercial Relationships: Kaveh Azartash, Allergan (E); James A. Burke, Allergan, Inc (E)

Program Number: 4849 **Poster Board Number:** D0288

Presentation Time: 11:00 AM - 12:45 PM

Longitudinal Measurements In Vivo of Retinal Nerve Fiber Layer Thickness (RNFLT) and Retinal Ganglion Cell (RGC) Density after Optic Nerve Transection (ONT) in Rat

Tiffany E. Choe, Carla J. Abbott, Kendra Young, Brad Fortune.

Discoveries in Sight, Devers Eye Inst, Legacy Health, Portland, OR.

Purpose: To determine the relationship between RNFLT and RGC density measured in vivo after unilateral ONT.

Methods: Eighteen adult male Brown-Norway rats were studied. All procedures were performed under anesthesia (ketamine:xylazine:acepromazine, 55:5:1 mg/kg IM). Two baseline measurements of peripapillary RNFLT were obtained by SDOCT (Spectralis, Heidelberg Engineering) then repeated weekly for 1 month after either unilateral ONT (N=11) or sham surgery (N=7). RGCs were labeled by retrograde transport from the superior colliculus of fluorescently conjugated cholera toxin B (CTB) 48 hours prior to surgery (N=15; bilateral saline injections in N=3 ONT controls). RGC density measurements were obtained by confocal scanning laser ophthalmoscopy (Spectralis) at baseline (1 hour prior to surgery) and weekly for 1 month (N=15). Fluorescence microscopy of whole-mount retinae was performed post mortem to measure RGC density and to evaluate reactivity of microglia (anti-Iba1) and astrocytes (anti-GFAP). Statistics included two-way ANOVA for repeated measures with Bonferroni corrected post-hoc comparisons and Deming linear regression.

Results: RNFLT decreased after ONT ($p < 0.0001$) by 16%, 28% and 34% at weeks 2, 3 and 4. RGC density decreased after ONT ($p < 0.0001$) by 24%, 69%, 84% and 91% at weeks 1, 2, 3 and 4. In vivo measures of RNFLT and RGC density were strongly correlated ($R = 0.83$, $p < 0.0001$). RGC density measured in vivo at week 4 and

post mortem by microscopy were strongly correlated ($R = 0.92$, $p < 0.0001$). RNFLT and RGC density did not change in sham operated or their fellow control eyes and there was no difference between these groups for post mortem RGC density ($p = 0.62$). In the fellow eyes of the ONT-operated group that had bilateral CTB labeling of RGCs, RNFLT increased by 24%, 68% and 49% at weeks 2, 3 and 4 ($p < 0.0001$), but it did not change in fellow ONT-eyes that did not receive CTB. Microgliosis was clearly evident in the RNFLT of the ONT-fellow eyes that had CTB, far exceeding that observed in eyes of any other group. Astrocyte changes were not observed in any group.

Conclusions: In vivo measurements of RNFLT and RGC density are strongly correlated and can be used to monitor longitudinal changes after optic nerve injury. Microgliosis occurred in fellow eyes of ONT operated rats if CTB was used to label their RGCs, causing increased RNFLT.

Commercial Relationships: Tiffany E. Choe, None; Carla J. Abbott, None; Kendra Young, None; Brad Fortune, Heidelberg Engineering, GmbH (F), Carl Zeiss Meditec, Inc (F)

Support: NIH Grant R21EY021311; Legacy Good Samaritan Foundation Grant; Heidelberg Engineering, GmbH (equipment)

Program Number: 4850 **Poster Board Number:** D0289

Presentation Time: 11:00 AM - 12:45 PM

In Vivo Dimensions of Schlemm's Canal and Number of Collector Channels in the Nasal and Temporal Areas of Normal Eyes

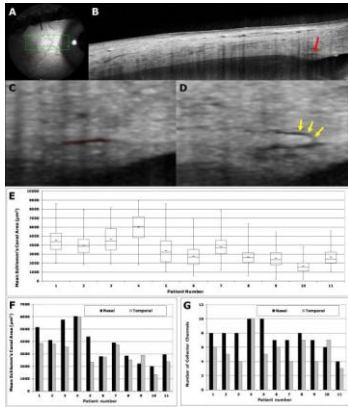
Wendy A. Kirkland¹, Sung Chul Park^{1,2}, Rafael L. Furlanetto¹, Camila F. Netto¹, Yiyi Liu^{1,3}, Jeffrey M. Liebmann^{1,4}, Robert Ritch^{1,2}. ¹Moise and Chella Safra Advanced Ocular Imaging Laboratory, Einhorn Clinical Research Center, New York Eye and Ear Infirmary, New York, NY; ²Department of Ophthalmology, Valhalla, NY; ³New York Medical College, Valhalla, NY; ⁴Department of Ophthalmology, New York University School of Medicine, New York, NY.

Purpose: To determine if differences exist in the dimensions of Schlemm's canal (SC) and the number of collector channels (CCs) between the nasal and temporal areas of normal eyes using *in vivo* enhanced depth imaging optical coherence tomography (EDI OCT).

Methods: Serial horizontal EDI OCT B-scans were obtained in the nasal and temporal limbal areas from one eye of each normal subjects (81 scans per 15×5 degree rectangle; interval between scans, ~ 35 μ m; **Fig A and B**). The cross-sectional area of SC was measured in each EDI OCT B-scan (**Fig C**). After three-dimensional SC reconstruction, SC volume was calculated for the nasal and temporal areas. The CCs connected to the SC (**Fig D**) were counted in these areas. SC measurements and CC counting were performed by an independent observer, who was masked to the clinical information of the examined eyes.

Results: Eleven normal eyes (11 subjects; mean age, 28 ± 5 years) were included. The cross-sectional area of SC varied considerably within (mean of coefficients of variation of all eyes = 36%) and among the eyes (coefficient of variation of means of all eyes = 35%) (**Fig E**). The mean cross-sectional SC area was significantly greater nasally than temporally (3837 ± 1397 μ m² vs. 3188 ± 1204 μ m²; $p = 0.034$; **Fig F**), as was the SC volume (0.011 ± 0.004 mm³ vs. 0.009 ± 0.003 mm³; $p = 0.034$). The SC cross-sectional area and volume were greater temporally than nasally in only one eye. The number of the CCs was significantly greater nasally than temporally (7.5 ± 1.7 vs. 5.5 ± 2.0 ; $p = 0.004$; **Fig G**).

Conclusions: SC is larger with more CCs nasally than temporally in normal eyes. This may have important implications for the development of treatments that target the trabecular outflow pathway.



(A) 15x5 degree rectangle for 81 serial horizontal EDI OCT B-scans. (B) A horizontal EDI OCT B-scan of the limbus and sclera (red arrow = Schlemm's canal [SC]). (C) SC was delineated (red dotted line) to measure its cross-sectional area. (D) Yellow arrows = collector channel. (E) Box-and-whisker plot for the SC cross-sectional area in 11 normal eyes (error bar = minimum and maximum values). (F and G) Mean SC area and the number of collector channels in 11 normal eyes.

Commercial Relationships: Wendy A. Kirkland, None; Sung Chul Park, None; Rafael L. Furlanetto, None; Camila F. Netto, None; Yiyi Liu, None; Jeffrey M. Liebmann, Alcon Laboratories, Inc. (C), Allergan, Inc. (C), Allergan, Inc. (F), Carl Zeiss Meditech, Inc (F), Heidelberg Engineering, GmbH (F), Topcon Medical Systems, Inc. (F), National Eye Institute (F), New York Glaucoma Research Institute (F), SOLX, Inc. (C), Bausch & Lomb, Inc (C), Diopsys, Inc. (C), Diopsys, Inc. (F), Merz, Inc. (C), Glaukos, Inc. (C), Quark, Inc. (C); **Robert Ritch**, None

Support: Joseph and Geraldine LaMotta Research Fund of the New York Glaucoma Research Institute, New York, NY; James Cox Chambers Research Fund of the New York Eye and Ear Infirmary, New York, NY; American Glaucoma Society MAPS Award; Peter Crowley Research Fund of the New York Eye and Ear Infirmary, New York, NY

Program Number: 4851 **Poster Board Number:** D0290

Presentation Time: 11:00 AM - 12:45 PM

The macular retinal layer thickness in glaucoma patients

Yoshiaki Kiuchi, Ulfah Rimayanti, Miftahul Akhyar Latief.
Ophthalmology & Visual Science, Hiroshima University, Hiroshima, Japan.

Purpose: The development of Optical Coherent Tomography (OCT) enables the thickness of the retinal nerve fiber layer (NFL), the ganglion cell layer and the inner plexiform layer (GCL+IPL) and the outer retinal layer (ORL) in the macular area to be evaluated separately. The purpose of this study was to determine the relationships among these three (NFL, GCL+IPL and ORL) OCT parameters in glaucoma patients.

Methods: The parameters of the OCT were determined using the Topcon 3D OCT-2000 instrument. We compared the average thickness of the NFL, GCL+IPL and ORL in the macular area between subjects with glaucoma and normal controls. The relationships between the macular OCT parameters were determined using the regression analyses and the Akaike information criterion. The significance of the differences in the thicknesses of the OCT macular parameters of normal eyes and glaucomatous eyes was determined using t tests. A P value <0.05 was considered to be statistically significant.

Results: Eighty-four glaucoma patients and 36 normal control subjects were studied. The NFL and GCL+IPL thicknesses in the normal group were significantly thicker than those in the glaucoma group (all P <0.0001). The outer retinal layer in glaucoma patients was thinner than that in normal subjects. However, the P values did not reach the level of significance (P=0.062). The relationships between the NFL of the macular area and the GCL+IPL were determined by third-order regression models. Changes in the average thickness of the NFL preceded changes in the average thickness of the GCL + IPL.

Conclusions: Glaucoma mainly damages the inner-retinal layer in the macular area. There is a possibility that the loss of the outer retinal layer may be caused by glaucoma. Our results also suggest that the damage of the NFL preceded the damage of the GCL + IPL.

Commercial Relationships: Yoshiaki Kiuchi, None; Ulfah Rimayanti, None; Miftahul Akhyar Latief, None

Program Number: 4852 **Poster Board Number:** D0291

Presentation Time: 11:00 AM - 12:45 PM

A comparison of retinal nerve fiber layer quadrant thickness between glaucomatous and glaucoma suspect eyes

Alicia M. Eby, Rominder Momi, Justin Tannir, Bret A. Hughes, Anju Goyal, Aman Shukairy, Chaesik Kim, Manal H. Peracha, Farvah Fatima, Melanie McQueen. Kresge Eye Institute, Wayne State University School of Medicine, Detroit, MI.

Purpose: To investigate the quantifiable difference in retinal nerve fiber layer (RNFL) thickness in both the superior and inferior domains of the optic nerve between glaucomatous eyes and glaucoma suspect eyes using Optical Coherence Tomography (OCT) data.

Methods: This was a retrospective chart review of 236 eyes of 236 patients with established diagnosis of glaucoma (Group 1) and 134 eyes of 134 patients diagnosed as glaucoma suspect (Group 2). For both study groups the variables collected included age, sex, race, visual acuity (VA), intraocular pressure (IOP), cup-to-disc (CD) ratio, VF mean deviation (MD), pattern standard deviation (PSD), and OCT parameters including RNFL thickness in each quadrant, cup area and rim area. Exclusion criteria included age > 75 years old and date of service between VF and OCT testing > 3 months. 84% of the patients had stringent reliability indices using the 10% cutoff rates for false-negative and false-positive responses, as well as fixation losses. Paired and unpaired t-test, Chi-square test were used to analyze data.

Results: In our study, 88% of patients were African American, 9% Caucasian, and 3% identified as other. There was a statistically significant difference between Group 1 and Group 2 in terms of age (70±15 vs 63±13, p<.0001), CD ratio (.69±.12 vs .60±.17, p<.0001), medications (1.8±1.2 vs .2±.5, p<.0001), VF MD (-11.2±9.6 vs -4.3±5.6, p<.0001), VF PSD (5.2±3.4 vs 3.1±2.9, p<.0001), and logmar visual acuity (.40±.61 vs .15±.24, p<.0001), respectively. There was no difference in gender or IOP (16.0±5.6 vs 16.5±3.6, p=.35). However, there was a significant difference between Group 1 and Group 2 with respect to superior NFL (80.5±25.9 vs 108.5±22.9, p<.0001) and inferior NFL (84.3±39.8 vs 117.4±22.6, p<.0001), respectively.

Conclusions: There was a statistically significant difference in both superior and inferior RNFL between glaucoma and glaucoma suspect eyes. We propose that the use of RNFL thickness, especially the superior and inferior quadrants, be a potential tool incorporated into the screening, evaluation and staging of disease states in glaucoma as well as glaucoma suspect patients.

Commercial Relationships: Alicia M. Eby, None; Rominder Momi, None; Justin Tannir, None; Bret A. Hughes, None; Anju Goyal, None; Aman Shukairy, None; Chaesik Kim, None; Manal

H. Peracha, None; **Farvah Fatima**, None; **Melanie McQueen**, None

Support: Research to prevent blindness

459 Neuroprotection

Wednesday, May 08, 2013 2:45 PM-4:30 PM
6B Paper Session

Program #/Board # Range: 4938-4944

Organizing Section: Glaucoma

Program Number: 4938

Presentation Time: 2:45 PM - 3:00 PM

Ocular Hypotensive and Neuroprotective Effects of Agmatine

Samin Hong. Ophthalmology, Yonsei University College of Medicine, Seoul, Republic of Korea.

Purpose: Agmatine, a primary polyamine and putative neuromodulator, is known to have neuroprotective effects on various neuronal damages in the central nervous system. In this investigation, it was assessed whether agmatine effectively lowers the intraocular pressure (IOP) and rescues the injured retinal ganglion cells (RGCs) in a wide range of experimental models..

Methods: Agmatine, a primary polyamine and putative neuromodulator, is known to have neuroprotective effects on various neuronal damages in the central nervous system. In this investigation, it was assessed whether agmatine effectively lowers the intraocular pressure (IOP) and rescues the injured retinal ganglion cells (RGCs) in a wide range of experimental models.

Results: In a chronic ocular hypertensive rat model, IOP was significantly increased (about a 50% increase over the baseline IOP) and well maintained until 12 weeks. Topically administered agmatine powerfully lowered IOP to approximately 30% of its pretreatment level. EVC caused about 55% loss of RGCs in the control group, but agmatine appeared to attenuate this RGC loss to around 20%. Meanwhile, in a transient ocular ischemic mouse model, MCAO induced apoptosis to mostly the whole cells in the entire retinal layer, but topically/systemically administered agmatine significantly reduced the proportion of apoptotic cells.

Conclusions: Agmatine appeared to effectively lower IOP and rescue RGCs in a chronic ocular hypertensive rat model and decreased retinal damage in a transient ocular ischemic mouse model. Although the precise mechanisms underlying these effects have not been well established yet, it is possible that agmatine offers a powerful new ocular hypotensive and neuroprotective agent for patients suffering from glaucoma.

Commercial Relationships: *Samin Hong*, None

Program Number: 4939

Presentation Time: 3:00 PM - 3:15 PM

The Jigsaw Effect: Clinical Evidence for CNS Control of Visual Field Loss in Chronic Glaucoma

William E. Sponsel^{1,2}, *Nancy Satsangi*³, *Matthew A. Reilly*¹, *Sylvia L. Groth*⁴, *Stuart J. McKinnon*⁵. ¹Biomedical Engineering, University of Texas - San Antonio, San Antonio, TX; ²Madison Square Bldg Ste 306, WESMDPA, San Antonio, TX; ³School of Medicine, University of Texas Health Science Center - San Antonio, San Antonio, TX; ⁴School of Medicine, University of Minnesota, Minneapolis, MN; ⁵Ophthalmology and Neurobiology, Duke University, Durham, NC.

Purpose: To statistically assess the tendency for the conservation of the binocular visual field in patients with moderate to severe glaucomatous field loss in both eyes. The goal of this work was to determine whether chronic bilateral visual field degeneration can be explained on a bilaterally independent ocular pathologic basis, or if

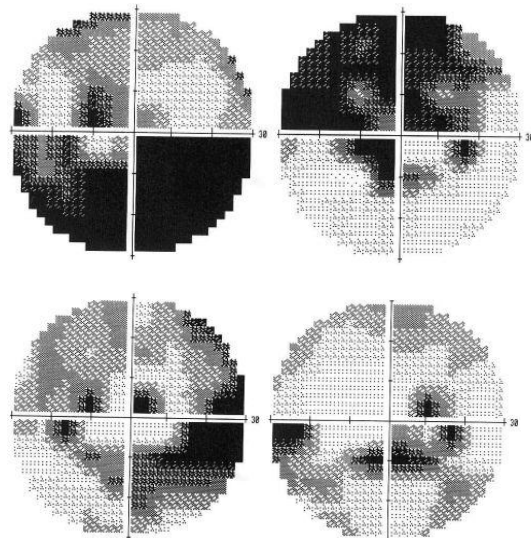
the mathematical evidence indicates that the CNS must help direct the process in an integrated bilateral manner.

Methods: Case control study. Subjects: 47 patients with stabilized chronic progressive glaucoma undergoing Humphrey Visual Field 30-2 testing were evaluated. One single-session paired set of left (OS) and right (OD) eye visual fields was assessed for each individual. Each OS visual field locus was paired with either (a) its directly comitant OD locus, or (b) a random non-comitant OD locus of equal eccentricity from fixation. Mean threshold values were calculated for the 76 loci of each eye of all 47 subjects. The mean value for the higher of each of the paired individual comitant locus values (HCD) from both eyes, using combinations (b) and (c), were similarly calculated for all subjects, using all 76 points OU, running 10,000 iterations for (b), and compared by paired t-test.

Results: Global mean thresholds were 14.73 OS and 15.80 dB OD; mean 15.27 OU, ~5 dB lower than the better of the paired loci ($p < 0.000000001$). Mean threshold for direct HCD pairings (a) was 20.55, versus 20.10 (range 19.9-20.2) for (b) ($p = 0.0002$). Mirrored field pairings confirmed that anatomic symmetry factors could not account for the observed differences.

Conclusions: A very strong tendency for optimizing the binocular visual field, in a manner that defies simple anatomic symmetry considerations, was observed. Direct inspection of the paired visual fields of these patients provides insights into this phenomenon, displaying the interlocking, mutually asymmetric jigsaw-like character of many bilateral scotomata.

It is known that focal axonal injury in one eye may be accompanied by increased activity in the contralateral retinal glia and geniculate layers receiving comitant visual information from the fellow non-injured eye (see Bodeutsch et al, J Neurobiol 1999, Penagis et al, Eur J Neurosci 2005, Dai et al, Exp Eye Res 2009). Focal bilateral compensation of this kind may be involved in the conservation of the binocular visual field in patients with chronic progressive glaucoma.



Commercial Relationships: *William E. Sponsel*, New World Medical (P); *Nancy Satsangi*, None; *Matthew A. Reilly*, None; *Sylvia L. Groth*, None; *Stuart J. McKinnon*, Merz (F)

Program Number: 4940

Presentation Time: 3:15 PM - 3:30 PM

AAV-Mediated Neurotrophin-4 Is Neuroprotective In Murine Model Of Microbead-Induced Glaucoma with Neurotrophin Expression in the Visual Pathway

Anna M. Demetriades, Lihua Guo, Chendong Pan. Glaucoma Research Laboratory, Weill Cornell Medical College, New York, NY.

Purpose: To determine if an adeno-associated viral (AAV2) vector with a CAG promoter expressing neurotrophin-4 (NT4) is neuroprotective in the murine model of microbead-induced ocular hypertension and the extent to which NT4 is expressed in the visual pathway.

Methods: Polystyrene microbeads were injected into the anterior chamber of adult mice to elevate intraocular pressure (IOP). An intravitreal injection containing 1×10^9 vector genomes of either AAV.NT4.HA or AAV.Null was administered into the same eye. Intraocular pressure was measured by TonoLab tonometry at weekly intervals. Mice were sacrificed at four weeks and retinal ganglion cell (RGC) loss was quantified. Enzyme-linked immunosorbent assay (ELISA) and HA immunohistochemistry was performed to determine NT4 expression in the visual pathway.

Results: Increased IOP was confirmed in microbead-injected eyes by tonometer. Uninjected control eyes had a mean RGC count of 3065 ± 410 cells/mm² (n=15). At four weeks, microbead-injected eyes that received AAV.NT4.HA demonstrated 2141 ± 85 cells/mm² (n=8) and microbead-injected eyes that received AAV.Null demonstrated 1547 ± 89 cells/mm² (n=10). Thus, microbead-injected eyes treated with AAV.NT4.HA contained over 135% increase in viable RGCs at four weeks compared to eyes treated with AAV.Null (p<0.005).

Compared to uninjected mice (n=5), intravitreal AAV.NT4.HA resulted in increased NT4 levels (ng NT4/mg total protein) in the retina (3.7 vs. 0.002), optic nerve (19.8 vs. 0.04), lateral geniculate nucleus (0.1 vs. 0.002) and superior colliculus (0.1 vs. 0.004). There was no increase in NT4 levels in the visual cortex. HA immunohistochemistry confirmed NT4 expression in RGCs, lateral geniculate nucleus and superior colliculus but not in the visual cortex.

Conclusions: Intravitreal AAV.NT4 results in NT4 expression from RGCs to their synapses in the lateral geniculate nucleus and superior colliculus and has neuroprotective effects on RGC survival. Increased NT4 expression has no effect on IOP, which is consistent with NT4-induced neuroprotection in an environment of elevated IOP. Intravitreal AAV.NT4 may represent a promising treatment for glaucoma targeting the neurodegenerative aspect of this disease.

Commercial Relationships: Anna M. Demetriades, None; Lihua Guo, None; Chendong Pan, None

Support: Fight for Sight, American Glaucoma Society, Research to Prevent Blindness, Inc.

Program Number: 4941

Presentation Time: 3:30 PM - 3:45 PM

The Effect of Modulators of Microtubule Stability on Dendritic Morphology in Cultured Retinal Ganglion Cells

Rachel Chong¹, Barbara Lorber¹, Keith R. Martin^{1,2}. ¹John Van Geest Centre for Brain Repair, University of Cambridge, Cambridge, United Kingdom; ²NIHR Biomedical Research Centre, University of Cambridge, Cambridge, United Kingdom.

Purpose: Microtubule instability is strongly associated with dendritic degeneration in several neurodegenerative diseases. Simplification of retinal ganglion cell (RGC) dendritic trees and synaptic stripping have been observed as early injury responses in experimental glaucoma models. Our hypothesis is that promoting microtubule stability with Taxol may have a beneficial effect on RGC dendrites after injury. We therefore aimed to develop a model to study the effect of RGC microtubule stabilisation.

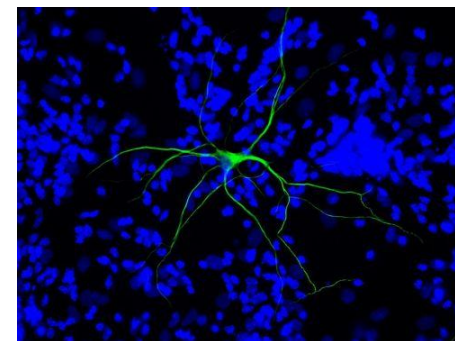
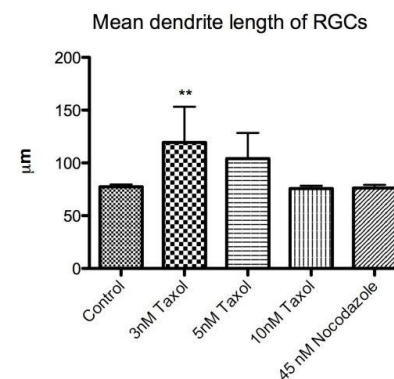
Methods: A dissociated mixed primary retinal cell culture system was used to test the effect of 3, 5 and 10 nM Taxol, a microtubule-stabiliser, and 45 nM Nocodazole, a microtubule-destabiliser, on

RGCs taken from postnatal day 8 (P8) male Sprague-Dawley rats. Immunocytochemistry (ICC) was used to identify RGCs (BIII-tubulin) and label the somatodendritic compartment (MAP-2). Image processing software (ImageJ) was used to compare dendrite length, number of branch-points and Sholl analysis of RGCs exposed to the above conditions.

Statistical analysis was done using the D'Agostino & Pearson test of normality to determine the distribution of dendrite characteristics from the control group, before the Kruskal-Wallis one-way analysis of variance was used to evaluate the significance of inter-group differences.

Results: Co-localisation of MAP-2 with BIII-tubulin enabled clear visualisation of RGC dendrites in dissociated primary mixed retinal cell cultures from P8 Sprague-Dawley rats (Fig 1). Mean RGC dendrite length was significantly increased in cells that were treated with 3 nM Taxol ($119.5 \pm 33.69 \mu\text{m}$) when compared with the drug-free control group ($77.48 \pm 2.08 \mu\text{m}$, p < 0.01, Fig 2). There was no significant difference in maximum dendrite length, number of branch-points and Sholl analysis between the treated and untreated groups. Nocodazole, a microtubule destabiliser, did not have a significant effect on dendritic length in this system.

Conclusions: Degeneration of RGC dendrites occurs early in experimental glaucoma. This is the first study to suggest that a low concentration of Taxol increases the mean dendrite length of cultured RGCs. In on-going work we are investigating if this effect is also evident in *in vivo* experimental models of glaucoma, and if preservation or re-establishment of synaptic connectivity is possible.



P8 RGC dendritic tree seen on ICC; MAP-2 (green), DAPI (blue).

Commercial Relationships: Rachel Chong, None; Barbara Lorber, None; Keith R. Martin, None

Support: Jukes Glaucoma Research Fund (UK), Cambridge NIHR Biomedical Research Centre (UK), Agency for Science Technology and Research (Singapore)

Program Number: 4942

Presentation Time: 3:45 PM - 4:00 PM

Enhanced retinal ganglion cell survival in glaucoma by hypoxic postconditioning after disease onset

Yanli Zhu¹, Lihong Zhang¹, Chia-Wen Chiang², Jeff Gidday¹.

¹Neurosurgery, Washington Univ Sch of Med, St Louis, MO;

²Radiology, Washington Univ Sch of Med, St. Louis, MO.

Purpose: We showed previously, in an inducible mouse model of open-angle glaucoma, that retinal ganglion cell (RGC) soma and axons could be robustly protected if preconditioned with repetitive systemic hypoxia prior to intraocular pressure (IOP) elevation, reflecting the presence of innate epigenetic mechanisms capable of enhancing RGC survival in this disease (Zhu Y et al., *Mol Med* 2012). The present study was undertaken to determine whether exposing mice to repetitive hypoxia after glaucoma onset ("postconditioning") could provide similar RGC protection.

Methods: The IOP in one eye of adult male C57Bl/6 mice was chronically elevated to 20±2 mmHg by episcleral vein ligation (Zhu Y et al., *Mol Med* 2012; Zhu Y et al., *IOVS* 2013). Starting 3 d after IOP elevation, mice were exposed for 1 h to systemic hypoxia (11% oxygen), and this exposure was repeated seven times over the ensuing 3 wks (at 2-day or 3-day intervals); matched, randomized controls not postconditioned with hypoxia were also studied in parallel. After 3 wks of sustained intraocular hypertension, visual acuity was assessed bilaterally by optokinetic tracking. Thereafter, animals were sacrificed for RGC soma quantification in retinal flat mounts, and RGC axon quantification in postlaminal optic nerves, by NeuN and SMI32 immunohistochemistry, respectively.

Results: In untreated controls, RGC soma loss was 20±2% (*p=0.002 vs. fellow eye), axon loss in the postlaminal optic nerve was 19±2% (*p <0.001 vs. fellow eye), and visual acuity was reduced 41% (*p=0.008 vs. baseline) after 3 wks of disease. However, in the postconditioned cohort, which exhibited the same magnitude of IOP elevation as untreated controls, RGC soma loss was only 8±2% (*p=0.002 vs. untreated controls), RGC axon loss was only 7±2% (*p <0.001 vs. untreated controls), and visual acuity was only reduced 11% (p=0.106 vs. untreated controls).

Conclusions: Robust morphologic (>60% improvement) and functional (>72% improvement) protection of RGC soma and axons can be achieved after disease onset, and independent of IOP, by the protracted activation of endogenous cytoprotective mechanisms secondary to repetitive hypoxic stress. Thus, physiologic or pharmacologic stressors that induce and maintain epigenetic-based protective responses may serve as novel therapeutic strategies for enhancing RGC survival in patients with open-angle glaucoma.

Commercial Relationships: Yanli Zhu, None; Lihong Zhang, None; Chia-Wen Chiang, None; Jeff Gidday, None

Support: NIH EY018607 (JMG)

Program Number: 4943

Presentation Time: 4:00 PM - 4:15 PM

Neuroprotection from excitotoxic RGC death: is there a role for MMPs?

Lies De Groef, Manuel A. Salinas-Navarro, Eline Dekeyster, Kim Lemmens, Djoere Gaublot, Inge Van Hove, Lieve K. Moons.

Department of Biology, Laboratory for Neural Circuit Development and Regeneration, KU Leuven, Leuven, Belgium.

Purpose: Multiple studies in glaucoma patients and animal models, have reported differential expression and activity of matrix metalloproteinase (MMPs). These data have led to the hypothesis that MMPs are involved in glaucoma pathogenesis. However, their *in vivo* functions remain poorly understood. Here, we investigate the contribution of MMPs to retinal ganglion cell (RGC) death in the excitotoxic mouse retina and reveal that MMP-2, -3 and -9 deficient

mice are -at least partially- protected from excitotoxic RGC death.

Methods: Excitotoxic RGC death was induced via intravitreal injection of 20 mM NMDA, both in wild type and MMP-2, -3 or -9 deficient mice (N>5). Expression of MMPs was examined via immunohistochemistry and Western blot. RGC survival was assessed by quantifying the number of survival RGCs after Brn3a immunostaining on whole mounted retinas using a custom-made automated routine.

Results: MMP-9 is expressed by RGCs and microglia and also shows strong immunoreactivity in the inner limiting membrane. MMP-2 and -3, on the other hand, have a macroglial origin and are expressed throughout all layers of the mouse retina. At 24 hours post NMDA injection (24hpi), a strong upregulation of MMP-3 and -9 expression is seen, whereas MMP-2 levels only increase modestly.

MMP-9 deficiency protects retinas from NMDA-induced RGC death. Also in MMP-2^{-/-} and MMP-3^{-/-} mice, RGC death is attenuated.

Whereas only 17.0±0.05% of the RGCs survive in wild type mice at 24hpi, RGC survival is increased to 34.01±0.01% and 33.99±0.05% in, respectively, MMP-2^{-/-} and MMP-3^{-/-} animals. We are currently analyzing time-dependent cellular changes within the excitotoxic retina and investigating possible underlying mechanisms.

Conclusions: MMP-2, -3 and -9 deficiency reduces RGC death in an excitotoxic mouse glaucoma model. For MMP-9, this is in accordance to what has been shown in an optic nerve ligation glaucoma model and most likely related to anoikis of RGCs. On the other hand, for MMP-2 and -3, this neuroprotective effect might be related to modulation of the glial reactivity accompanying RGC degeneration, as suggested by their glial expression pattern.

Commercial Relationships: Lies De Groef, None; Manuel A. Salinas-Navarro, None; Eline Dekeyster, None; Kim Lemmens, None; Djoere Gaublot, None; Inge Van Hove, None; Lieve K. Moons, None

Support: IWT

Program Number: 4944

Presentation Time: 4:15 PM - 4:30 PM

TrkB Receptor Agonists as Neuroprotective Molecules in Glaucoma -Effect of 7,8 Dihydroxyflavone

Stuart Graham^{1,2}, Yuyi You¹, Jonathan C. Li¹, Vivek Kumar Gupta¹.

¹Australian School of Advanced Medicine, Macquarie University, Sydney, NSW, Australia; ²Save Sight Institute, Sydney University, Sydney, NSW, Australia.

Purpose: Tropomyosin related kinase B (TrkB) receptor activation through neurotrophic factors plays an important role in the protection of retinal ganglion cells (RGCs) in glaucoma. We recently reported that TrkB receptor signalling is regulated by Shp2 phosphatase under ocular hypertensive conditions. A novel flavanoid 7,8 Dihydroxyflavone (DHF) is a high-affinity TrkB agonist that provokes receptor dimerization and autophosphorylation and activation of downstream signalling *in vivo*, here we examine the structural, functional and molecular effects of administration of this compound on the retina, ganglion cell layer (GCL) and optic nerve in experimental glaucoma.

Methods: A unilateral chronic ocular hypertensive model was established by weekly microbead injections in adult SD rats (n=16). One group of rats was administered 7,8 DHF intraperitoneally for 20 weeks (n=8). Electroretinogram (ERG) and scotopic threshold response (STR) were performed to assess retinal function. Changes in retinal morphology were evaluated by H & E staining. The optic nerve was examined for atrophic changes. The molecular effects of 7,8 DHF on retinal TrkB receptor and its downstream signalling were assessed *ex vivo* in retinal organ cultures followed by western blotting.

Results: While ERG was unchanged in both groups, administration of 7,8 DHF prevented selective loss of STR in the ocular hypertensive eyes ($p < 0.01$). No perceptible differences were detected in the scotopic ERG recordings. A structural protection against rarefaction of GCL was also observed by qualitative assessment and optic nerve morphology was conserved. Molecular analysis of the rat retinas upon 7,8 DHF treatment revealed a robust activation of the retinal TrkB receptor ($p < 0.05$) and its downstream Akt and Erk survival signalling pathways.

Conclusions: This study demonstrates for the first time that the natural flavanoid 7,8 DHF could stimulate the TrkB receptor signalling in the retina. Administration of this natural flavanoid derivative significantly reduces the RGC structural and functional loss and optic nerve damage elicited by experimental glaucoma.

Commercial Relationships: Stuart Graham, None; Yuyi You, None; Jonathan C. Li, None; Vivek Kumar Gupta, None

Support: MQNS, ORIA Research Grant

511 Intraocular Pressure

Thursday, May 09, 2013 8:30 AM-10:15 AM

Exhibit Hall Poster Session

Program #/Board # Range: 5615-5663/C0001-C0049

Organizing Section: Glaucoma

Program Number: 5615 **Poster Board Number:** C0001

Presentation Time: 8:30 AM - 10:15 AM

Postural change in intraocular pressure between sitting and lying body positions - a direct comparison of its measurement with an unmodified Goldmann applanation tonometer, Tonopen XL, pneumatonometer, and HA-2 hand-held applanation tonometer yaniv barkana. ¹Ophthalmology, Assaf Harofe Medical Center, Beer Yaakov, Israel; ²Ophthalmology, Tel Aviv University, Tel Aviv, Israel.

Purpose: The magnitude of change in intraocular pressure (IOP) with change in body posture is not routinely considered in clinical glaucoma practice. It has been reported using different tonometers with very different results. This study presents a direct comparison of 4 tonometers in measuring postural IOP change.

Methods: In healthy subjects, IOP was measured OU in with a Goldmann applanation tonometer (GAT) while sitting, then using the same GAT with the subject in the left lateral decubitus position after lying for 15 minutes, using a novel system comprising a motorized bed and modified slit-lamp table. On the next day, sitting IOP was measured in one eye using GAT, and in random order Tonopen XL and pneumatonometer. Then subjects lay down, and IOP was measured with these tonometers and also hand-held GAT (HA-2) after lying for 15 minutes and 45 minutes, supine except with GAT.

Results: Enrolled were 19 subjects, 10 males and 9 females, with mean age 33.0 ± 12.4 years. On day 1, sitting GAT IOP (mmHg) was 13.7 ± 3.0 OD and 13.6 ± 2.8 OS ($p = 0.7$), and lying GAT IOP was 17.8 ± 3.5 OD and 18.1 ± 3.2 OS ($p = 0.3$ for inter-eye postural IOP change). The coefficient of determination for right-left eye pairs of postural IOP difference was 0.453. On day 2, postural change after lying 15 minutes as measured with GAT, Tonopen, pneumatonometer, and HA-2 was 4.9 ± 2.6 , 1.6 ± 1.8 , 4.2 ± 2.0 and 3.1 ± 2.7 , respectively. After lying 45 minutes it decreased to 3.3 ± 2.1 , 1.1 ± 4.3 , 3.1 ± 2.5 , and 2.6 ± 3.3 , respectively; this IOP decrease was statistically significant for GAT and pneumatonometer. In some subjects there was nearly no postural change in IOP, while in some IOP rose by 8-10 mmHg. 95% limits of agreement showed poor agreement between GAT and the other 3 tonometers in measured sitting and lying IOP and postural IOP change.

Conclusions: Average postural IOP change was similar when measured with GAT and pneumatonometer, smaller with hand-held GAT, and much smaller with Tonopen. This change significantly decreased during lying between the 15 and 45 minute timepoints. Inter-subject variability in postural IOP was remarkable, consistent with previous reports, suggesting the importance of this parameter in clinical glaucoma practice. Inter-device agreement was poor and similar to previous reports.

Commercial Relationships: yaniv barkana, Sensimed (F)

Support: The current study was supported by a grant from Sensimed, Switzerland

Program Number: 5616 **Poster Board Number:** C0002

Presentation Time: 8:30 AM - 10:15 AM

A new Tonometer-the Corvis ST Tonometer Clinical Comparison with Non-contact, and Goldmann Applanation Tonometers

Jiaxu Hong, JianJiang Xu, Anji Wei, Sophie X. Deng, Xinghuai Sun. Ophthalmology, Eye & Ear, Nose, Throat Hospital, Shanghai, China.

Purpose: To compare intraocular pressure (IOP) measurements obtained using Topocon non-contact tonometer (NCT), Goldmann applanation tonometer (GAT), and Corvis ST (CST), a newly developed tonometer with features of visualization and measurement of the corneal deformation response to an air pulse. A secondary objective was to assess the agreement among the devices.

Methods: Fifty-nine participants with a mixture of glaucoma patients (36 cases with 36 eyes) and control volunteers (23 cases with 23 eyes) were enrolled. The IOP measurements were obtained with the CST, NCT, and GAT by two experienced clinicians. IOP values were compared. Repeatability and reproducibility were assessed by the coefficient of variation and intraclass correlation coefficient. Device agreement was calculated by Bland-Altman analysis.

Results: Mean IOP for all examined eyes was 18.9 ± 5.8 mmHg for CST, 21.3 ± 6.8 mmHg for NCT, and 20.3 ± 5.7 mmHg for GAT. There was a statistically significant difference in IOP measured among different tonometers. However, correlation analysis showed a high correlation between each pair of these three devices (All $P < 0.001$). The CST displays the best repeatability and reproducibility. Bland-Altman analysis revealed a bias between CST and GAT, CST and NCT, and GAT and NCT of -1.3, -2.4, and -1.1 mmHg, with 95% limits of agreement of -6.2 to 3.5 mmHg, -10.1 to 5.2 mmHg, and -8.3 to 6.2 mmHg, respectively.

Conclusions: Although the CST may significantly underestimate IOP in relation to GAT and NCT, it offers an alternative method for measuring IOP. The IOP measurements taken with each device may not be interchangeable.

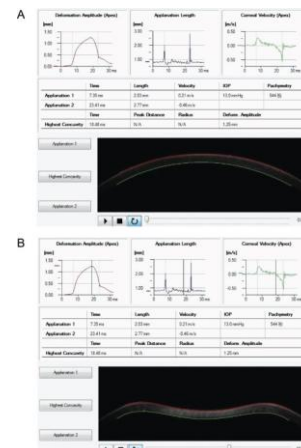


Figure 1. Intraocular pressure measurement by Corvis ST (CST). (A)

Real-time information of a participant recorded immediately upon an air impulse. (B) Real-time information of a participant recorded at the highest concavity, indicating the biggest deformation amplitude of the cornea.

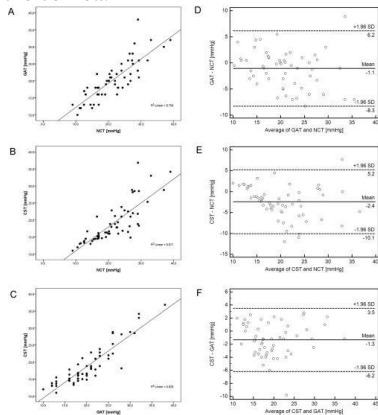


Figure 2. Correlation among different IOP measurement devices. Significant positive correlations were noted (A) between CST and NCT ($\rho = 0.871$; $P < 0.001$), (B) between CST and GAT ($\rho = 0.896$; $P < 0.001$), (C) and between GAT and NCT ($\rho = 0.839$; $P < 0.001$). Bland-Altman scatterplot showing the agreement among different IOP measurement devices: (D) between a Corvis ST tonometer (CST) and a Goldmann applanation tonometer (GAT). (E) between CST and Non-contact tonometer (NCT). (F) between GAT and NCT. **Commercial Relationships:** Jiayu Hong, None; JianJiang Xu, None; Anji Wei, None; Sophie X. Deng, None; Xinghuai Sun, None

Support: This work was supported by grants from the Key Clinic Medicine Research Program, the Ministry of Health, China (2010-2012); Doctoral Fund, the Ministry of Education, China; National Science and Technology Research Program, the Ministry of Science and Technology, China (2012BAI08B01); National Natural Science Foundation of China (81170817, 81200658); Scientific Research Program, Science and Technology Commission of Shanghai Municipality, Shanghai (11231200602, 11DZ2260900).

Program Number: 5617 **Poster Board Number:** C0003

Presentation Time: 8:30 AM - 10:15 AM

Intraocular pressure characteristics of subjects with either exfoliation syndrome or exfoliative glaucoma as determined with the Water Drinking Test: preliminary findings

Mehmet C. Mocan¹, Burcu Kasim¹, Ersin Muz¹, Mehmet Orhan¹, Murat T. Irkeç¹, Dimitrios G. Mikropoulos², Anastasios-Georgios P. Konstas². ¹Department of Ophthalmology, Hacettepe Univ School of Medicine, Ankara, Turkey, ²1st Department of Ophthalmology, AHEPA Hospital, Thessaloniki, Greece.

Purpose: To investigate intraocular pressure (IOP) characteristics of subjects with either untreated exfoliation syndrome (XFS), or treated exfoliative glaucoma (XFG) undergoing the Water Drinking Test (WDT).

Methods: Prospective observational study undertaken at a university setting. We investigated subjects with untreated XFS with in-office IOP measurements of < 21 mmHg (group A), medically treated XFG patients whose in-office IOP levels were < 21 mmHg (group B), and normal controls (group C). All subjects underwent a standard WDT test. The IOP was measured before and four times after water ingestion at 15 minute intervals. Maximum IOP (IOPmax), mean IOP (IOPmean), the IOP increase (IOPinc) from baseline IOP to IOPmax and percentage of IOP fluctuation (IOPfluct) during the WDT were calculated and compared across the 3 groups. The one-way analysis

of variance (ANOVA) test or the Kruskal-Wallis test was used for comparisons. The study was powered to detect an IOP difference of 1.0 ± 1.0 mmHg with a β error of 0.10 and an α error of 0.05.

Results: Sixty eyes of sixty age-matched subjects (20 eyes per group) were recruited for the study. There were no differences between the 3 groups for age, sex, visual acuity, central corneal thickness and in-office IOP level. All IOP measurements evaluated at 15 min intervals as well as IOPmax (25.2 ± 4.3 mmHg; 18.2 ± 3.1 mmHg; 19.6 ± 2.5 mmHg), IOPmean (22.7 ± 3.6 mmHg; 16.5 ± 3.0 mmHg; 18.1 ± 2.5 mmHg), IOPinc (9.3 ± 3.6 mmHg; 4.1 ± 1.8 mmHg; 3.8 ± 1.3 mmHg) and IOPfluct (60.4 ± 25.1 %; 31.5 ± 17.8 %; 24.8 ± 9.7 %) were significantly greater in the XFG group ($p < 0.001$ for all parameters studied) compared to the XFS and the control groups. None of the IOP parameters evaluated in the study were found to be significantly different in XFG patients who were treated with monotherapy compared with those on multiple medications ($p > 0.1$ for all parameters). WDT results of patients treated with prostaglandin analogues were similar to those treated with other agents ($p > 0.5$ for all parameters).

Conclusions: Medically treated XFG patients, but not XFS subjects, demonstrate significant IOP elevation during WDT indicative of impaired trabecular outflow facility. WDT may be of clinical value in assessing IOP characteristics in XFG.

Commercial Relationships: Mehmet C. Mocan, None; Burcu Kasim, None; Ersin Muz, None; Mehmet Orhan, None; Murat T. Irkeç, None; Dimitrios G. Mikropoulos, MERCK (R); Anastasios-Georgios P. Konstas, Alcon (F), Allergan (C), MSD (C), Nicox (C)

Program Number: 5618 **Poster Board Number:** C0004

Presentation Time: 8:30 AM - 10:15 AM

Investigation of the Effect of Gonioscopy on Intraocular Pressure
Ardalan Aminlari, Christine Callahan, Ingrid U. Scott, George C. Papachristou, Joanna Olson. Ophthalmology, Penn State Hershey Eye Center, Hershey, PA.

Purpose: Intraocular pressure (IOP) measurements taken during ophthalmologic examinations affect clinical decision-making. For example, IOP is an important factor in deciding whether or not to start, discontinue, or continue IOP-lowering agents. Gonioscopy (an examination of the drainage system of the eye) is a procedure performed commonly by ophthalmologists, especially in patients suspected or known to have glaucoma. To date, there are no published data regarding the potential effect of gonioscopy on IOP. The purpose of the current study is to investigate whether gonioscopy has an effect on IOP.

Methods: The study protocol was approved by the Penn State College of Medicine Institutional Review Board. All study participants were recruited from the Penn State Hershey Eye Center glaucoma clinic. Participants were consented according to the IRB protocol. Baseline IOP of study participants was measured in each eye using Goldmann applanation. Gonioscopy was performed on participants' study eye only. The study eye was determined by alternating between right and left eyes of consecutive study participants. At 1 and 5 minutes after gonioscopy completion, participants' IOP was measured in each eye using Goldmann applanation. Participants' fellow eyes, which did not undergo gonioscopy, served as control eyes. Change in IOP between the baseline and 1-minute measurements, and between the baseline and 5-minute measurements, were compared between study and control eyes.

Results: The study included 18 participants. Nine (50%) were male. Average age was 71 (+13) years. There was no significant difference in central corneal thickness between the study and control eyes (552 and 553 microns, respectively). There was no significant difference

in IOP between study and control eyes at baseline, 1 minute and 5 minutes. Both study and control eyes showed a significant decrease in IOP between baseline vs. 1 minute, and baseline vs. 5 minutes.

Conclusions: Although both the study and the control eyes showed a significant downward trend in IOP with repeated measurements, there was no difference in the magnitude of IOP reduction between the study and control eyes. Thus, there does not appear to be a significant effect of gonioscopy on IOP measurement.

Commercial Relationships: Ardan Aminlari, None; Christine Callahan, None; Ingrid U. Scott, None; George C. Papachristou, None; Joanna Olson, None

Program Number: 5619 **Poster Board Number:** C0005

Presentation Time: 8:30 AM - 10:15 AM

Diurnal Non-Clinic-Measured Intraocular Pressure Profile in Primary Angle-Closure Glaucoma Patients

Shaoying Tan, Nafees B. Baig, Clement C. Tham. Ophthalmology and Visual Sciences, The Chinese University of Hong Kong, Hong Kong, Hong Kong.

Purpose: Single intraocular pressure (IOP) measurement in clinic cannot reflect IOP fluctuation and its peak level during daily life. In this study, the diurnal IOP profiles in clinic and non-clinic environments were investigated and compared in patients with primary angle-closure glaucoma (PACG).

Methods: Twenty-six eyes from 26 PACG patients under regular medical treatments were included in this study. IOP was measured by Rebound self-measured tonometry daily at 8:00, 12:00, 16:00, 20:00 and 24:00 for 1 week under patients' routine activities. Goldmann applanation tonometer was used to verify the IOP measurement on the same tested eye in clinic on the recruitment day, the middle of the week, and the last day.

Results: Variable patterns of diurnal IOP profiles were observed among the PACG patients under medical treatment. Their IOPs were well controlled within 21 mmHg (range: 5.8-20.93mmHg). The mean of diurnal IOP profile shows highest in the morning and gradually decreases throughout the day. The frequency of peak IOP occurred in the early morning was 44% and most lowest IOP happened in the late evening was 36%. The differences between mean of diurnal non-clinic IOP and clinic-measured IOP were 1.28 ± 0.86 mmHg (mean \pm S.D.). The 95% limits of agreement were -6.20 - 3.64 mmHg.

Conclusions: Diurnal IOP was stably maintained in most of PACG patients under medical treatments. Highest IOP was observed in the morning. The peak diurnal IOP in non-clinic environment could be predicted from the mean clinic IOPs.

Commercial Relationships: Shaoying Tan, None; Nafees B. Baig, None; Clement C. Tham, Aeon Astron Corporation (F), Alcon Laboratories, Inc. (C), Alcon Laboratories, Inc. (R), Alcon Laboratories, Inc. (F), Allergan, Inc. (C), Allergan, Inc. (R), Bausch & Lomb (C), Icare Finland (F), Merck & Co., Inc. (C), Merck & Co., Inc. (R), Pfizer, Inc. (C), Pfizer, Inc. (R), Pfizer, Inc. (F), Santen Pharmaceutical Co., Ltd. (C), Santen Pharmaceutical Co., Ltd. (R), Santen Pharmaceutical Co., Ltd. (F), Sensimed (F)

Program Number: 5620 **Poster Board Number:** C0006

Presentation Time: 8:30 AM - 10:15 AM

The Effect of Child Delivery Process on the Intraocular Pressure in Healthy Women

Amit Meshi¹, Sharon Armarnik¹, Haggai Kaneti², Fani Segev¹, Ehud I. Assia^{1,3}, Noa Geffen¹. ¹Ophthalmology, Meir Medical Center, Kfar-Saba, Israel; ²Obstetrics and Gynecology, Meir Medical Center, Kfar-Saba, Israel; ³Ein-Tal, Tel Aviv, Israel.

Purpose: To investigate the effect of vaginal child delivery on the intraocular pressure (IOP) in healthy women.

Methods: Open, prospective, non-randomized, single center clinical trial, enrolling healthy pregnant women candidates for vaginal delivery at their acceptance to the delivery room. Medical, ophthalmic and obstetric histories were obtained at enrollment and biomicroscopic examination using a portable slit lamp was performed. Heart rate (HR), blood pressure (BP) and IOP (in 1 randomly selected eye, using a Tonopen XL) were measured at enrollment, during the 1st (latent and active phases), 2nd and 3rd stages of the delivery and at 24, 48 hours postpartum. The average of 3 IOP measurements (variance<5%) was calculated. Labor position and drugs were documented.

Results: Thirty healthy Caucasian women were recruited. Average age was 31.5 years (range 19-41). Mean gestational age was 39.2 weeks. The mean number of pregnancies and deliveries was 3 and 2.2, respectively. Four women had dropped-out from the study due to an unplanned conversion to cesarean section. Fourteen women required induction of labor with oxytocin and one underwent vacuum-assisted delivery. All women received epidural anesthesia. Twenty two women were in supine position, 3 in left decubitus position and 1 in right decubitus position. The mean IOP (\pm standard deviation) measured on admission, during the latent and active phases of the 1st stage of delivery, during the 2nd and 3rd stages of delivery and 24, 48 hours post-delivery were 11.8 ± 3.6 mm Hg, 11.9 ± 3.3 mm Hg, 11.8 ± 2.9 mm Hg, 12.1 ± 3.1 mm Hg, 12.2 ± 4.0 mm Hg, 11.9 ± 2.4 mm Hg and 13.2 ± 2.3 mm Hg, respectively ($P > 0.05$). Mean HR and BP remained stable during all stages of delivery.

Conclusions: To the best of our knowledge this is the first time that the impact of the modern labor on the IOP was investigated. The IOP changes documented during vaginal delivery under an epidural anesthesia were within the physiologic diurnal variation range. IOP changes during labor probably have no clinical significance in healthy women and should not serve as an indication for changes in the planned management of labor.

Commercial Relationships: Amit Meshi, None; Sharon Armarnik, None; Haggai Kaneti, None; Fani Segev, None; Ehud I. Assia, Hanita Lenses (C), Biotechnology General (C), APX Technology (I), IOPTima (I), VisionCare (C); Noa Geffen, None
Clinical Trial: NCT01174342

Program Number: 5621 **Poster Board Number:** C0007

Presentation Time: 8:30 AM - 10:15 AM

Association of Epidural Steroid Injections(s) with Intraocular Pressure Elevation

Deepti Saini¹, Ingrid U. Scott¹, Christine Callahan¹, John Paul Malayil², Jason Gillon¹, Jill Eckert². ¹Ophthalmology, Penn State Milton S. Hershey Medical Center, Hershey, PA; ²Pain Management, Penn State Milton S. Hershey Medical Center, Hershey, PA.

Purpose: To investigate whether epidural steroid injection(s) (ESI) are associated with an elevation in intraocular pressure (IOP).

Methods: Retrospective, consecutive case series. The study protocol was approved by the Penn State College of Medicine Institutional Review Board. Medical records were reviewed of all patients who received at least one ESI in the Penn State Pain Management Clinic between 1/1/2002 and 12/31/2011, and had at least one ocular evaluation at the Penn State Hershey Eye Center within 4 months prior to ESI and at least one ocular evaluation in the Penn State Hershey Eye Center within 4 months after ESI. The main outcome measure of the study is IOP elevation post-ESI (defined as $\geq 30\%$ mmHg increase from baseline mean IOP or any addition of IOP-lowering medication or laser/surgical intervention post-ESI). Statistical analysis was performed using a Cox regression model.

Results: The study included 67 patients (120 eyes) with a mean age of 74 years. Of these patients, 44 (66%) had a documented history of

glaucoma or ocular hypertension at the time of first ESI, and 12 patients (18%) had a history of being glaucoma suspects. Post-ESI, 11 patients (16%) demonstrated an IOP increase of $\geq 30\%$ from baseline IOP (n=8, 11%) or were treated with an increase in IOP-lowering medications (n=7, 10%) or both (n=2, 3%). Baseline factors significantly associated with post-ESI IOP elevation include age >70 years, history of oral or inhaled steroid use, and use of IOP-lowering medication. Eight of the 11 (73%) patients who demonstrated a $\geq 30\%$ increase from baseline IOP and/or were treated with an increase in IOP-lowering medication had received multiple ESI, while only 18/56 (32%) patients who did not have a $\geq 30\%$ IOP elevation and/or increase in IOP-lowering medication had received multiple ESI. Factors not significantly associated with IOP elevation post-ESI include, but are not limited to, gender, history of IOP-lowering laser or surgery, history of steroid eye drop/intraocular injection, and location of ESI.

Conclusions: Corticosteroids administered via epidural injection may be associated with IOP elevation. We recommend prospective studies to investigate this association further, as well as to better elucidate baseline patient characteristics that might be predictive of post-ESI elevation and how long after an ESI a rise in IOP may occur.

Commercial Relationships: Deepti Saini, None; Ingrid U. Scott, None; Christine Callahan, None; John Paul Malayil, None; Jason Gillon, None; Jill Eckert, None

Program Number: 5622 **Poster Board Number:** C0008

Presentation Time: 8:30 AM - 10:15 AM

Relationship between Central Corneal Thickness and Intraocular Pressure in Indigenous Africans in Nigeria

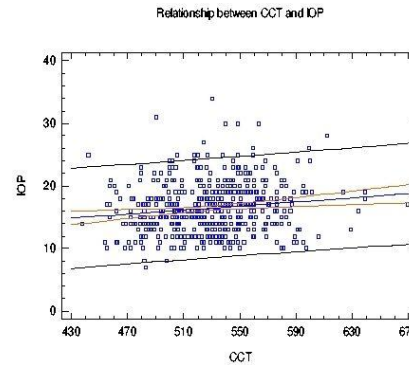
Nwamalubia N. Nzelu- Egwuonwu.¹ ophthalmology, mass medical mission, lagos, Nigeria; ²ophthalmology, mass medical mission, lagos, Nigeria.

Purpose: To determine the relationship between Central Corneal Thickness (CCT) and Intraocular pressure (IOP) in indigenous Africans in Nigeria

Methods: A population - based cross - sectional study was carried out on indigenous Africans in a selected population in Lagos State, Nigeria. After obtaining written informed consent, all participants underwent detailed evaluation including medical and ocular history and examination. The central corneal thickness was determined with AccuPach VI Ultrasound Pachymeter and IOP by the Perkins handheld applanation tonometer. All measurements of IOP and CCT were taken between 10.00am and 1pm to control for diurnal variation. The measurement of both the CCT and IOP were carried out by a single examiner to minimize inter-observer error. Data was analyzed using the Epi Info Statistical software (Epi Info 3.5.1 for Windows, 2008) and SPSS (version 10.0) programme. A p- value of ≤ 0.05 was considered significant.

Results: A total of 968 eyes of 484 eligible participants were analyzed in this study. Multiple regression analysis showed a significant positive correlation between CCT and IOP in the study population (p = 0.002). The linear regression formula for this study was: $IOP = 7.87 + (0.016 \text{ CCT}) \text{ mmHg}$. This indicates that a rise in CCT of 10 μm leads to an increase in IOP of about 0.16 mmHg.

Conclusions: Central corneal thickness could result in systematic error in the measurement of IOP by applanation tonometry in the study population. The CCT should therefore, be considered in the management of glaucoma in indigenous Africans in Nigeria.



Commercial Relationships: Nwamalubia N. Nzelu- Egwuonwu, None

Support: mmm grant

Program Number: 5623 **Poster Board Number:** C0009

Presentation Time: 8:30 AM - 10:15 AM

Refined IOP measurement with rebound tonometry in the rabbit

Hong Zhang^{1,2}, Dong Yang^{1,3}, Craig Ross¹, Jonathan P. Wigg¹, Surinder S. Pandav¹. ¹Ophthalmology, Ctr for Eye Resrch Australia, East Melbourne, VIC, Australia; ²Royal Victorian Eye and Ear Hospital, Melbourne,, VIC, Australia; ³Harbin Medical University, Harbin, China.

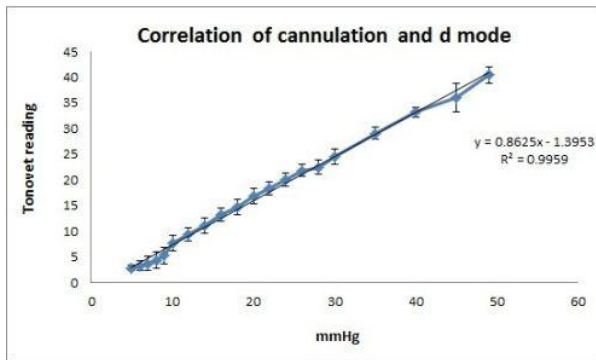
Purpose: An animal model for glaucoma research requires accurate and reproducible measurements of intraocular pressure (IOP). The induction-impact (rebound) Tonovet tonometer provides a non-invasive method of measuring IOP. Although rabbit models are often used in drug-related and surgical glaucoma research, IOP measurement by Tonovet has not been fully validated in this species. We aim to design a standardized method of IOP measurement with the rebound tonometer in rabbit.

Methods: All experimental procedures complied with the ARVO Statement for the Use of Animals in Ophthalmic and Vision Research. IOP was set and measured manometrically in generally anesthetized rabbits (n=8) after anterior chamber cannulation through the peripheral cornea. The 26-gauge needle used for anterior chamber cannulation was connected to a pressure transducer-controlled syringe pump from Harvard Apparatus. IOP was raised in 5mmHg steps from 5 to 50 mmHg using an open stopcock method. The IOP was measured with the TonoVet in both “p” and “d” modes by taking four to six readings at each point by two independent observers. IOP was measured by orienting the tonovet in horizontal or vertical positions. TonoVet measurements were compared with the corresponding manometric measurements. The differences between IOP of left and right eye, ages of rabbits were also compared.

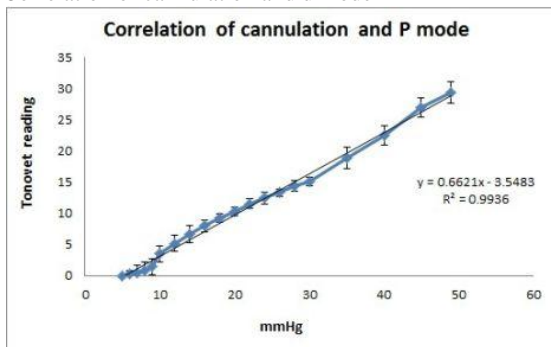
Results: The position of the tonovet handle makes no difference to IOP measurements. TonoVet readings correlated well with manometric IOP (“d” mode: r(2) coefficient = 0.9966; “p” mode: r(2) coefficient = 0.9941). No significant differences were observed when comparing right and left eyes (t-test, p>0.05). The TonoVet had a tendency to underestimate IOP compared to anterior chamber cannulation. TonoVet readings obtained with “d” mode were closer to manometric IOP than those obtained with the “p” mode, although conversion formulae were possible to calculate for both modes. IOP recover at day 3 after cannulation. Younger rabbits have lower IOP compared with older rabbits (P< 0.01).

Conclusions: The TonoVet is a reliable and precise tool for the measurement of IOP in rabbits. The measured IOP tended to underestimate at IOP values from 5 to 50 mmHg. To compensate for this systematic error and calculate the actual IOP, correction factors

were needed. The “d” mode is more useful than “p” mode in measuring rabbit IOP.



Correlation of cannulation and d mode



correlation of cannulation and p mode

Commercial Relationships: Hong Zhang, None; Dong Yang, None; Craig Ross, None; Jonathan P. Wigg, None; Surinder S. Pandav, None

Support: Key (Key grant) Project of Chinese Ministry of Education ; Foundation for the New Century Talents by the Educational Committee of Heilongjiang Province No.1251--NCET—011;Supported by Doctoral Fund of Ministry of Education of China

Program Number: 5624 **Poster Board Number:** C0010

Presentation Time: 8:30 AM - 10:15 AM

IOP measurement with I-CARE Rebound TONOMETER, PNEUMOTONOMETER and TONOPEN IN SEDATED CHILDREN with glaucoma and controls

Fatemah T. Al-Shamlan¹, Jonathan Song^{1,2}, Deepak P. Edward^{1,2}, Ibrahim Al Jadaan¹, Sami A. Al Shahwan¹, Jose Morales¹, Arif O. Khan¹, Saleh Al-Mesfer¹, Abdulaziz H. Awad¹, Shahira Al Turkmani¹.

¹king khalid eye specialist hospital, Riyadh, Saudi Arabia;

²Ophthalmology, Wilmer Eye Institute/Johns Hopkins University, Baltimore, MD.

Purpose: To prospectively compare IOP measurements with the I-Care rebound tonometer with the Tonopen(Tp) and Pneumotonometer(Pm) in children under sedation and correlate measurements with the corneal diameter.

Methods: Subjects: Children (under 5 years of age) with glaucoma (excluding those who underwent corneal surgery) (N=42), undergoing sedated eye exam and a control group without glaucoma (n=18) undergoing a sedated exam. The IOP was measured by three instruments: I-Care, Pm and Tp and the horizontal corneal diameter (Cd) recorded during the same sedated examination.

Results: The age of the control group was 26.33 months+/- 13.9(range 10-60 months). The mean Cd was average10.8+/-1.2mm (range 9-13 mm)

IOP measured by I-Care, Pm and Tp in control were 13.9+/-3.38 mm Hg (range 8-20.), 15.9+/- 4.27mmHg (range 10- 27) and 14.76+/- 3.25mmHg (range 10-21) respectively.Using Bland- Altman testing, the mean difference +/- 2 SD between the Tp and Pm was (-7.79, 5.44) with a correlation of 0.725 (p=.001). The mean difference +/- 2 SD between Tp and I care was (-5.06, 6.72) with a correlation of 0.620 (p=.008). The mean difference +/- 2 SD between Pm and I-care (-4.58, 8.59) with a correlation of 0.615 (p=.009).

The Cd correlation with the IOP measured by I-care, Pm and Tp using Spearman’s correlation was as follows: 0.108 (p= .679), 0.120 (p= .645) and 0.139 (p= .594).In the glaucoma group the age was 12.7+/-1.5mmHg (range 8-17 mm). IOP measurements by I care, Pm and TP were 18.15+/-5.9 mm Hg, (range 8.1-31.5), 19.9+/- 6.7mmHg (7.5- 35.5) and 20.5+/-7.6 mmHg (range 5-43) respectively. Using Bland-Altman testing the mean difference +/- 2 SD between Tp and Pm was (-7.4, 8.76) with a correlation of 0 .835 (p=0.00). The mean difference +/- 2 SD between Tp and I-care was (-8.39, 13.10) with a correlation of 0.702 (p=.000). The mean difference +/- 2 SD between Pm and Icare (-8.57, 11.98) with a correlation of 0.607 (p=.000).The Cd correlation with the IOP taken by I-care, Pm, and Tp, using Spearman’s correlation was as follows: 0.003(p= .984),-0.100 (p= .529), -0.012(p= .940)

Conclusions: IOP measurements using the three tonometers were comparable in both groups undergoing sedated eye exam. I-care IOP measurements appears to be least effected by corneal diameter.

Commercial Relationships: Fatemah T. Al-Shamlan, None; Jonathan Song, None; Deepak P. Edward, None; Ibrahim Al Jadaan, None; Sami A. Al Shahwan, None; Jose Morales, None; Arif O. Khan, None; Saleh Al-Mesfer, None; Abdulaziz H. Awad, None; Shahira Al Turkmani, None

Clinical Trial: 1231-P

Program Number: 5625 **Poster Board Number:** C0011

Presentation Time: 8:30 AM - 10:15 AM

Twenty-Four-Hour Habitual Intraocular Pressure in Young, Myopic, Untreated Open- Angle Glaucoma Patients

Jeong D. Dawoon, Kook S. Michael, Lee Kyong sub, Lee Jong Rak. ophthalmolgy, Asan medical center, Seoul, Republic of Korea.

Purpose: To characterize the 24-hour rhythm of intraocular pressure (IOP) in young, myopic, untreated open-angle glaucoma (OAG) patients with normal baseline IOP in the habitual position

Methods: Sixty-four young, myopic OAG eyes, ages 18 to 40 years, with moderate to severe myopia (≤-3 diopters) and 56 age-matched young, emmetropic (≥-1.5 diopters) OAG eyes (control group) with normal baseline IOP were prospectively recruited and underwent 24-hour measurement of IOP and systemic blood pressure (BP) in the habitual position. In the wake period, IOP and BP were measured in the sitting position while they were measured in the supine position followed by sitting position after a 5-minute rest in the sleep period

Results: In young, myopic OAG group, the average habitual IOP was higher than the control group in both diurnal and nocturnal period (P=0.01, 0.02, respectively). In both myopic and control OAG groups, the average nocturnal IOP in the supine position was higher than the average diurnal IOP in the sitting position. However, the magnitude of this IOP elevation during nocturnal period was significantly less in the myopic group than in the control group (0.2 mmHg vs. 1.2 mmHg, P<0.001). In both myopic and control OAG groups, the average diurnal IOP in the sitting position was higher than the average nocturnal IOP in the sitting position. There was no difference in the 24-hour rhythms of mean arterial BP between the two groups

Conclusions: In the habitual body position, young, myopic OAG

eyes with normal baseline IOP exhibit higher 24-hour IOP at both diurnal and nocturnal period than the age-matched emmetropic eyes. IOP increases at night in both OAG groups, but the magnitude of the increase is significantly less in the myopic group than in the control group. The difference in globe size may result in less pronounced nocturnal habitual IOP elevation in young, myopic glaucomatous eyes

Commercial Relationships: Jeong D. Dawoon, None; Kook S. Michael, None; Lee Kyong sub, None; Lee Jong Rak, None

Program Number: 5626 **Poster Board Number:** C0012

Presentation Time: 8:30 AM - 10:15 AM

24-HOUR INTRAOCULAR PRESSURE RHYTHM IN YOUNG HEALTHY SUBJECTS EVALUATED WITH CONTINUOUS MONITORING USING CONTACT LENS SENSOR

Christophe Chiquet^{1,2}, Benjamin Mottet^{1,2}, Florent Aptel^{1,2}, Ralitsa Hubanova¹, Jean-Louis Pépin², Jean-Paul Romanet¹. ¹Department of Ophthalmology, University Hospital, CHU Grenoble, Grenoble, France; ²Lab Hypoxia and Physiopathology, INSERM U1042, Joseph Fourier University, Grenoble, France.

Purpose: To evaluate 24-h intraocular pressure (IOP) rhythm reproducibility during repeated continuous 24-h IOP monitoring with non-contact tonometry (NCT) and a contact lens sensor (CLS) in healthy subjects

Methods: Subjects were housed in a sleep laboratory and underwent four 24-h sessions of IOP measurements over a 6-month period. After randomized attribution, the IOP of the first eye was continuously monitored using the CLS Sensimed TriggerFish® and the IOP of the fellow eye was measured hourly using the Pulsair Intellipuff non-contact tonometer. Two sessions with NCT measurements in one eye and CLS measurements in the fellow eye, one session with CLS measurements in only one eye, and one session with NCT measurements in both eyes were performed. A nonlinear least-squares dual harmonic regression analysis was used to model the 24-h IOP rhythm. Comparison of acrophase, bathyphase, amplitude, the midline estimating statistic of rhythm (MESOR), IOP values, IOP changes and agreement were evaluated in the three tonometry methods.

Results: A significant nyctohemeral IOP rhythm was found in 31 out of 36 sessions (86%) using NCT and in all sessions (100%) using CLS. Hourly awakening during NCT IOP measurements did not significantly change the mean phases of the 24-h IOP pattern evaluated using CLS in the contralateral eye. Throughout the sessions, intraclass correlation coefficients (ICCs) of the CLS acrophase (0.6 [0-0.9]; $p=0.03$), CLS bathyphase (0.7 [0.1-0.9]; $p=0.01$), NCT amplitude (0.7 [0.1-0.9]; $p=0.01$) and NCT MESOR (0.9 [0.9-1]; $p<0.01$) were significant. The highest numbers of hourly IOP values ($n=18$) and hourly IOP changes ($n=9$) with fair to good agreement in a 24-h cycle were obtained using NCT and CLS, respectively. When performing NCT measurements in one eye and CLS measurements in the contralateral eye, the IOP change at each time point normalized from the first measurement (9:00 AM) were not symmetric individually or within the population.

Conclusions: The CLS is an accurate and reproducible method to characterize the nyctohemeral IOP rhythm in healthy subjects but does not estimate the absolute IOP value in millimeters of mercury corresponding to the relative variation of the electrical signal measured.

Commercial Relationships: Christophe Chiquet, None; Benjamin Mottet, None; Florent Aptel, EyeTechCare (C); Ralitsa Hubanova, None; Jean-Louis Pépin, None; Jean-Paul Romanet, None

Support: Association de Recherche et de Formation en Ophtalmologie (ARFO, Grenoble).

Program Number: 5627 **Poster Board Number:** C0013

Presentation Time: 8:30 AM - 10:15 AM

Randomized Clinical Investigation to Assess the Efficacy of SENSIMED Triggerfish® Continuous IOP Monitoring

Milko E. Iliev¹, John Thygesen², Evelien Vandewalle³, Julian Garcia-Feijoo⁴, Salvador Garcia-Delpech⁵. ¹Ophthalmology, University of Bern, Bern, Switzerland; ²Ophthalmology, Copenhagen University Hospital, Glostrup, Denmark; ³Ophthalmology, University Hospitals Leuven, Leuven, Belgium; ⁴Ophthalmology, Instituto de Investigación Sanitaria HCSC, Universidad Complutense, Madrid, Spain; ⁵Ophthalmology, Hospital Universitario y Politécnico la Fe, Valencia, Spain.

Purpose: The need of a reliable intraocular pressure (IOP) monitoring in glaucoma patients is widely recognized. The new contact lens based sensor Triggerfish® (TF) uses an embedded strain gauge to detect circumferential changes in corneal periphery as a result of IOP change, and records fluctuations from baseline in Millivolts. The purpose of this study was to assess the correlation of TF readings with the IOP values of two clinically established tonometers, the Goldmann applanation (GAT) and the ICare PRO rebound tonometer

Methods: This was a multi-center, randomized, clinical trial. Patients with primary open-angle glaucoma were randomized into eight device groups and a control group. For the device groups, the randomly selected eye was assessed by continuous TF monitoring (Sensimed AG, Lausanne, Switzerland) for 3, 6, 9, 12, 15, 18, 21 or 24 hours and by tonometry before and after TF installation and every 3 h after TF removal until the end of 24-h period. The fellow eyes -as well as both eyes of patients in the control group- were assessed by ICare PRO and GAT at 3-h intervals over 24 hours. Paired comparisons were done between TF and tonometry measurements on fellow eyes in parallel and on the same eye at different time points during a 24-h period

Results: Fifty-nine eligible patients were enrolled in five centers, 11 in the control and 48 in the eight device groups. Mean age was 64.8 ± 10.8 y and 42.4% of patients were female. The regression modeling demonstrated that change in TF readings did not correlate and was not a predictor of change in IOP as measured by either GAT or ICare PRO tonometers. Within subject mean correlations (Pearson) between TF and tonometers in the fellow eye were low ($r=0.22$ for GAT, and $r=0.06$ for ICare PRO), and between the two tonometers were moderate ($r=0.47$ in the study, and $r=0.51$ in the fellow eye). Correlations were strong between study/fellow eye for the same tonometer (GAT, $r=0.69$; ICare PRO, $r=0.60$). Inclusion of blood pressure, refraction, axial length, corneal thickness, topography, and hysteresis did not change the above results

Conclusions: Changes in Triggerfish® signal cannot be related to changes in IOP as measured by clinical tonometry. This may be due to the difference in methodology, detection via central versus peripheral cornea, or other reasons. It is still poorly understood how to integrate the TF readings in our clinical practice.

Commercial Relationships: Milko E. Iliev, None; John Thygesen, None; Evelien Vandewalle, None; Julian Garcia-Feijoo, Trancend (C), Ivantis (C), Glaukos (C), MSD (C), Allergan (F), Pfizer (F), Alcon (C), Sensimed (F), Sylentis (F), Bausch and Lomb (C); Salvador Garcia-Delpech, None

Support: Sponsored by SENSIMED AG, Lausanne, Switzerland
Clinical Trial: NCT01319604

Program Number: 5628 **Poster Board Number:** C0014

Presentation Time: 8:30 AM - 10:15 AM

Single versus Multiple Measurements for Comparing Group Intraocular Pressure

Brian Chon^{1,2}, Gerard Smits³, Shan C. Lin², Sean Ianchulev^{2,3}.

¹School of Medicine, Duke University, Durham, NC; ²Department of Ophthalmology, University of California San Francisco, San Francisco, CA; ³Transcend Medical, Menlo Park, CA.

Purpose: In glaucoma studies, mean IOP is often the primary outcome used as evidence of efficacy during therapeutic intervention. The objective of this study is to explore the incremental clinical utility from diurnal IOP measurements versus reduced IOP sampling strategies. Specifically, this study aimed to determine to what extent using a single random IOP measurement (SRM) instead of diurnal (3) measurements (DM), affects estimates of group mean IOP and proportion of patients above or below a target IOP.

Methods: IOP data were used from subjects enrolled in the COMPASS FDA clinical study of the CyPass suprachoroidal Micro-Stent. Sets of data, representing varying “study sizes,” were generated by sampling with replacement from a database of 470 records with complete (3 measures) diurnal IOP data. Resampling was performed 2000 times for each study size (range: 25-1000). The average bias for the point estimate of the sample mean using a SRM compared with using DM was examined. The confidence interval of the point estimate of the IOP mean from each method was also compared. In addition to resampling, the base sample was used to determine differences in outcomes when a SRM vs DM based on various cut points (e.g., IOP <21). All programming was performed in SAS version 9.2.

Results: For all sample sizes tested, there was no consistent directional difference in mean IOP using SRM or DM. The confidence interval around the mean IOP estimate was reduced with increasing sample size for both endpoints. For study sizes of 50, 100, 300 and 500 patients, 95% of the time the SRM was within 0.50, 0.36, 0.21 and 0.16 mmHg of the DM. The DM estimates fewer patients reaching an IOP target than SRM, for targets ≤ 18-25 mmHg and ≥ 28 mmHg and greater.

Conclusions: Using a SRM can accurately estimate a group’s mean IOP from multiple measurements. The CI of the group mean IOP estimate is reduced, more precise, with larger sample sizes. In analyses of proportions of patients reaching an IOP target (IOP ≤ or ≥ a target level), using SRM will overestimate the proportion of patients that reach or exceed a target. Depending on outcomes of interest, it may be practical in future studies to use a SRM to approximate the DM.

Commercial Relationships: Brian Chon, Transcend Medical (C); Gerard Smits, Transcend Medical (C); Shan C. Lin, None; Sean Ianchulev, transcend medical (E), keepyoursight foundation (S)

Clinical Trial: NCT01085357

Program Number: 5629 **Poster Board Number:** C0015

Presentation Time: 8:30 AM - 10:15 AM

Ocular Hypertension Profile after Pterygium Excision

Maria Husain, Anhtuan Nguyen, Kundandeep Nagi. Ophthalmology, University of Texas Health Science Center, San Antonio, TX.

Purpose: The occurrence of steroid induced ocular hypertension (OHTN) is a well known phenomenon, though not clearly studied after pterygium surgery. This study aimed to look at the post-operative IOP profile and associated ocular hypertension or glaucoma after pterygium excision.

Methods: A retrospective chart review yielding 83 post pterygium excision eyes were included in the study. Demographic factors, visual acuity, pre and post-operative intraocular pressure (IOP), surgical technique, length and type of steroid use were recorded. Our endpoint was the development of ocular hypertension and/or glaucoma; in addition, we anticipate comparing these patients with age and sex matched post-operative cataract controls.

Results: The average age of the all subjects was 55 (range 28-86). Among patients that developed OHTN (n=14, 16.9%) or glaucoma (n=1, 1.2%), the average age was 55.3 (range 35-79), and 33% were female. Those that developed OHTN had an average post-op IOP increase of 13.57 mmHg (STDEV 6.17, p<0.001) compared to nonresponders, occurring an average of 70.2 days post-op. The patient that developed glaucoma had a 19 mmHg increase in IOP postoperatively, occurring 170 days post-op. Subjects that developed increased IOP had a longer course of topical steroids compared to those that did not respond (144.92 days vs. 98.41 days, p=0.053); this difference approached statistical significance. An average of 1.60 IOP lowering medications was needed to treat the IOP, and no surgical intervention was required. 6 (35.29%) eyes that underwent amniotic membrane graft developed OHTN/glaucoma, and 9 (13.64%) eyes that had conjunctival autografting developed OHTN (p = .039).

Conclusions: Similar to literature examining post-operative IOP rises, our study finds that post-operative pterygium excision patients are at a significant risk to developing ocular hypertension. Development of a standard dosing regimen may blunt the incidence of vision threatening eye complications.

Commercial Relationships: Maria Husain, None; Anhtuan Nguyen, None; Kundandeep Nagi, None

Program Number: 5630 **Poster Board Number:** C0016

Presentation Time: 8:30 AM - 10:15 AM

IOP lowering effect of prostanoid FP and EP3 receptor dual agonist on mouse eyes

Reiko Yamagishi¹, Kazufumi Nagai³, Shinsaku Yamane³, Makoto Aihara^{2,1}. ¹Dept of Ophthalmology Sch of Med, University of Tokyo, Bunkyo-ku, Japan; ²Shirato eye clinic, Tokyo, Japan; ³ONO PHARMACEUTICAL CO., LTD., Osaka, Japan.

Purpose: We previously reported that the IOP-lowering effect by the stimulation of FP receptor involved EP3 receptor stimulation through the EP3 receptor. In this study, we made a comparison closely between FP receptor and FP/EP3 receptor dual agonist. Moreover, we examined the effect of FP/EP3 receptor dual agonist on IOP reduction in order to confirm the involvement of EP3 receptor. For elucidation of the mechanism of IOP reduction, we performed similar experiments using C57BL6 mice (WT), FP receptor deficient mice (FPKO), EP3 receptor deficient mice (EP3KO) and WT pre-treated with NSAIDs (WT + NSAIDs).

Methods: A single drop with 3 μL aliquots of 0.003% ONO-AG-241 (=ONO, FP/EP3 dual agonist), or 0.005% latanoprost (=LAT, FP agonist), were topically applied into randomly selected one of two eyes in ddY mouse. We measured IOP over time with a micro needle method. IOP reduction was evaluated by the difference between IOP of the treated eye and that of the contralateral control eye. Further, we measured IOP in WT, FPKO, EP3KO, and WT+NSAIDs at 2 and 8 hours after instillation.

Results: Significant IOP reductions were observed at 2 (17.1±2.1%; p< 0.01) and 4 (13.0±2.9%; p< 0.01) hours after LAT instillation, but not at 6 and 8 hours. ONO showed similar but prolonged IOP lowering effect at 2 (16.1±4.0%; p< 0.01), 4 (16.6±2.0%; p< 0.01), 6 (13.7±2.2%; p< 0.01) and 8 (10.5±2.1%; p< 0.01) hours after instillation.

Two hours after instillation of LAT, IOP reduction in WT, FPKO, EP3KO and WT+NSAIDs were 15.0±0.7%, 1.5±1.0%, 11.2±0.6%, and 12.9±0.6%, respectively. The IOP reduction induced by LAT in FPKO was significantly decreased compared to WT. (p<0.05) IOP reduction by ONO in WT, FPKO, EP3KO and WT+NSAIDs were 15.4±0.7%, 9.4±0.9%, 11.4±1.0%, and 11.2±0.6%, respectively. The IOP reduction induced by ONO showed no difference among all

types of mice. Eight hours after instillation, LAT induced no IOP reduction in all types of mice. However, ONO still reduced IOP in WT, FPKO, EP3KO and WT+NSAIDs, which were $11.6 \pm 0.7\%$, $9.0 \pm 0.7\%$, $4.1 \pm 0.5\%$, and $5.6 \pm 0.7\%$, respectively. The IOP reduction at 8 hours after ONO instillation in EP3KO mice was significantly decreased in WT mice. ($p < 0.05$)

Conclusions: FP/EP3 receptor dual agonist induced significant and prolonged IOP reduction compared to latanoprost in mouse eyes. IOP-lowering effect of FP/EP3 receptor dual agonist may involve endogenous PG production and EP3 receptor stimulation.

Commercial Relationships: Reiko Yamagishi, None; Kazufumi Nagai, ONO PHARMACEUTICAL CO.,LTD (E); Shinsaku Yamane, ONO PHARMACEUTICAL CO., LTD. (E); Makoto Aihara, Ono pharmaceutical company (F), Pfizer (F)

Program Number: 5631 **Poster Board Number:** C0017

Presentation Time: 8:30 AM - 10:15 AM

Sub-chronic IOP lowering effect of AMA0076 and Y-39983 in Dutch Belted rabbits

Sarah Van de Velde¹, Tine Van Bergen¹, Davine Sijnave¹, Karolien P. Hollanders¹, Evelien Vandewalle¹, Lieve K. Moons², Dirk Leysen³, Ingeborg Stalmans¹. ¹Lab of Ophthalmology, KULeuven, Leuven, Belgium; ²Biology, Zoölogical Institute, KULeuven, Leuven, Belgium; ³Amakem Therapeutics, Diepenbeek, Belgium.

Purpose: To investigate IOP lowering efficacy of rho kinase (ROCK) inhibitors, AMA0076 and Y-39983, after sub-chronic treatment.

Methods: Dutch Belted rabbits (5 rabbits/concentration) were treated daily with a single topical dose of AMA0076 (0.05, 0.1 and 0.4%) or Y-39983 (0.025, 0.05 and 0.1%) in a masked fashion for 14 days. Saline was used as control in the contralateral eye. IOP was measured before, 3 and 7 hours after administration of the treatment. AMA0076 is a locally acting ROCK inhibitor, developed by Amakem Therapeutics, to reduce side effects such as hyperemia otherwise seen after administration of a ROCK inhibitor.

Results: Mean baseline IOP before the start of the experiment (day 0) was 21.02 ± 0.42 and 20.69 ± 0.39 mmHg for AMA0076 and Y-39983, respectively. Significant IOP reduction was observed in all AMA0076 and Y-39983 treatment groups. A maximal IOP reduction of 39 and 35% was reached with AMA0076 0.1% and Y-39983 0.05%, respectively. Initially, IOP returned to baseline values (day 0) 24 hours after administration of AMA0076. After 3 days of treatment with AMA0076 a sustained IOP lowering effect was present, IOP did not return to baseline values (day 0), but remained significantly lower for all concentrations of AMA0076 ($p < 0.05$). Treatment with Y-39983 did not show this sustained IOP decrease. As a result of this sustained IOP lowering effect smaller IOP fluctuations were observed in animals treated with AMA0076 compared to Y-39983. Hyperemia was observed with all concentrations of Y-39983 whereas only mild hyperemia was induced after administration of AMA0076 0.4% (highest concentration used).

Conclusions: Once daily treatment of rabbits with ROCK inhibitor AMA0076 resulted in IOP reduction that was more sustained and associated with smaller peak-trough fluctuations than Y-39983.

Commercial Relationships: Sarah Van de Velde, Amakem Therapeutics (F); Tine Van Bergen, None; Davine Sijnave, Amakem therapeutics (F); Karolien P. Hollanders, None; Evelien Vandewalle, None; Lieve K. Moons, None; Dirk Leysen, Amakem NV (E); Ingeborg Stalmans, Amakem (F), Amakem (C), Amakem (R)

Support: IWT Baekeland Amakem Therapeutics

Program Number: 5632 **Poster Board Number:** C0018

©2013, Copyright by the Association for Research in Vision and Ophthalmology, Inc., all rights reserved. Go to iovs.org to access the version of record. For permission to reproduce any abstract, contact the ARVO Office at arvo@arvo.org.

Presentation Time: 8:30 AM - 10:15 AM

Altered expression of TGFβ1 and MMP-9 results in elevated intraocular pressure in mice

Anuja Siwakoti¹, Jennifer Robertson², Judith A. West-Mays².

¹Medical Sciences, McMaster University, Hamilton, ON, Canada;

²Pathology and Molecular Medicine, McMaster University, Hamilton, ON, Canada.

Purpose: Extracellular matrix (ECM) remodeling is thought to have profound effects on tissue architecture and associated function. It is important to study the contributions of TGFβ1 and MMP-9, two genes that are known to regulate the dynamics of the ECM and suspected to control aqueous outflow. Our lab has previously shown that overexpression of TGFβ, which stimulates matrix accumulation, results in altered morphology, cataracts and ocular hypertension in rodents. We have also demonstrated that TGFβ-induced cataracts can be mitigated through inhibition of the matrix metalloproteinases (MMP): MMP-2 and MMP-9. In the current study, we investigated how the loss of MMP-9 expression affects the TGFβ-induced changes in intraocular pressure (IOP).

Methods: The expression of a TGFβ1 transgene, under control of the αA-crystallin promoter, was used to target TGFβ expression to the anterior chamber of the mouse eye (J. Clin. Invest., 101, 625-634, 1998). The TGFβ1 transgenic mice were then bred onto a MMP-9 knockout (KO) background. Transgenic, KO and wild type littermates aged 1 month to 4 months were used. IOP was measured using the Tonolab rebound tonometer. The animals were sacrificed and eyes were enucleated. The eyes were processed and paraffin sectioned for histological and immunofluorescence studies. Immunofluorescence was performed to detect αSMA, collagen IV and N-cadherin molecules.

Results: Our results demonstrate that lens-specific expression of TGFβ1 in mice results in significant increase in IOP accompanied by altered morphology of the anterior segment. TGFβ1 transgenic mice bred onto the MMP-9 KO background exhibited a further increase in IOP. Interestingly, MMP-9 KO animals (without the TGFβ1 transgene), which exhibited normal angle morphology, had increased IOP levels compared to their wild-type littermates.

Conclusions: These results indicate that alterations in expression levels of the extracellular matrix remodelling molecules, TGFβ1 and MMP-9, can impact the regulation of IOP. In particular, the loss of MMP-9 expression resulted in increased IOP levels, in the absence of any overt morphological changes. Further investigation into the mechanisms of MMP-9 activity in the anterior angle may give clues to how extracellular matrix remodeling participates in ocular hypertension and glaucoma.

Commercial Relationships: Anuja Siwakoti, None; Jennifer

Robertson, None; Judith A. West-Mays, None

Support: American Health Assistance Foundation

Program Number: 5633 **Poster Board Number:** C0019

Presentation Time: 8:30 AM - 10:15 AM

Sustained Delivery of Travoprost from a Biodegradable Hydrogel Punctum Plug for the Treatment of Glaucoma

Abbe Miller, Charles D. Blizzard, Amar S. Sawhney, Michael Bassett, Peter Jarrett, Arthur Driscoll, Monica O'Connor, Doug Molla, Steve Takach. Ocular Therapeutix, Inc., Bedford, MA.

Purpose: To formulate 1, 2 and 3-month sustained release travoprost from biodegradable hydrogel punctum plugs for the treatment of glaucoma.

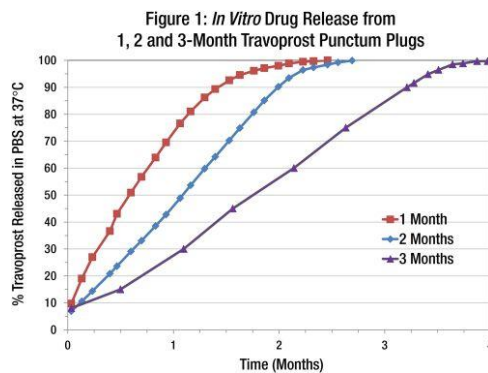
Methods: Travoprost was encapsulated in various formulations of polylactide microparticles (PM), which were dry blended and suspended in a multi-arm polyethylene glycol (PEG) precursor solution conjugated with fluorescein and injected into small bore

ARVO 2013 Annual Meeting Abstracts by Scientific Section/Group – Glaucoma

tubing prior to cross-linking. The travoprost in the PM/hydrogel matrix was dried in tubing and cut into plugs. Drug release rate from the respective formulations was assessed in PBS at pH 7.4 at 37 C until complete dissolution. The 3-month formulation was evaluated for plug visualization through the tissue in a canine model under illumination with a blue light and yellow filter.

Results: Sustained release of travoprost via PEG hydrogel punctum plugs was confirmed in vitro for each of the three formulations tested (Figure 1). Additionally, each formulation released a daily dose (based on in vitro release data) exceeding that administered by commercially available travoprost eye drops. Visualization and retention of the plug was confirmed in vivo (Figure 2).

Conclusions: 1, 2 and 3-month sustained release of travoprost from biodegradable punctum plugs is feasible, and can deliver travoprost into the tear fluid at therapeutic levels. Plug retention is a key attribute to achieve clinical success, and confirmation of plug presence can be done by physicians and patients for monitoring. In recent clinical trials, the 1- and 2-month formulations demonstrated a reduction of intraocular pressure (IOP) in patients with glaucoma and ocular hypertension comparable to commercially available topical prostaglandin analogs.



Commercial Relationships: Abbe Miller, Ocular Therapeutix, Inc. (E); Charles D. Blizzard, Ocular Therapeutix, Inc. (E); Amar S. Sawhney, Ocular Therapeutix (E); Michael Bassett, Ocular Therapeutix (E); Peter Jarrett, Ocular Therapeutix (E); Arthur Driscoll, Ocular Therapeutix (E); Monica O'Connor, Ocular Therapeutix (E); Doug Molla, Ocular Therapeutix (E); Steve Takach, Ocular Therapeutix (E)

Program Number: 5634 **Poster Board Number:** C0020
Presentation Time: 8:30 AM - 10:15 AM
Assessment of Intervisit IOP Control in Eyes with Advanced Glaucoma

©2013, Copyright by the Association for Research in Vision and Ophthalmology, Inc., all rights reserved. Go to iovs.org to access the version of record. For permission to reproduce any abstract, contact the ARVO Office at arvo@arvo.org.

Priya Patel, Nicole Pritz, Robert D. Fechtner, Albert S. Khouri. New Jersey Medical School, Newark, NJ.

Purpose: The Advanced Glaucoma Intervention Study (AGIS) provided evidence more than a decade ago that low intraocular pressure (IOP) was associated with reduced progression of visual field defects. The aim of this study was to evaluate the extent of intervisit control of IOP with current treatments of patients with advanced glaucoma.

Methods: Medical records of consecutive patients with a diagnosis of advanced primary open angle glaucoma (POAG) at New Jersey Medical School between 06/2012 and 11/2012 were reviewed. Inclusion: POAG with documented cup-to-disc ratio ≥ 0.8 and visual field abnormalities in both hemifields and/or loss within 5° of fixation in at least one hemifield as tested with standard automated perimetry, >9 office visits. Exclusion: Glaucoma other than POAG, mild to moderate POAG, <9 office visits. Data on IOP, ocular medications, lens status, and ophthalmic surgeries (incisional and laser) were collected. IOP was categorized into one of four groups (Excellent <14, Good 14-17.5, Fair 18-21, Poor >21 mmHg; consistent with AGIS). Effect of lens status and glaucoma surgery was analyzed. Percentages, means, paired t-tests, and chi-square analyses were used.

Results: 493 time points were collected for 50 eyes (28 patients). Mean age was 65 years (range: 46 to 88 years). The numbers of time points that fell within the various categories were: Excellent 173/493 (35%), Good 179/493 (36%), Fair 75/493 (15%), Poor 66/493 (13%). When further grouped into time points < or ≥ 18 mmHg, glaucoma surgery and lower mean number of medications were statistically significantly higher in time points with IOP <18 mmHg. The number of time points < 18 mmHg was higher for pseudophakic eyes, but this did not reach statistical significance (Table 1).

Conclusions: In eyes with advanced POAG, IOP control below 18 mmHg was achieved in about 70% of office visits, and was more often seen in eyes after glaucoma surgery. Rigorous IOP control remains a challenge in advanced POAG more than a decade after AGIS recommendations.

	IOP < 18	IOP ≥ 18	p
Phakic	68% (239/353)	32% (114/353)	p = 0.07
Pseudophakic	77% (77/100)	23% (23/100)	
No Glaucoma Surgery	68% (178/263)	32% (85/263)	p = 0.05
Glaucoma Surgery	76% (174/230)	24% (56/230)	
Mean Number Medications	1.5	2.2	p < 0.001

Commercial Relationships: Priya Patel, None; Nicole Pritz, None; Robert D. Fechtner, None; Albert S. Khouri, None
Support: Research to Prevent Blindness, NY, NY

Program Number: 5635 **Poster Board Number:** C0021
Presentation Time: 8:30 AM - 10:15 AM
Short duration intraocular pressure patterns detected by a contact lens sensor for 24-hour recording
 Kaweh Mansouri^{1, 2}, Robert N. Weinreb², Rene Goedkoop³, Mona Moshtaghi², Syril Dorairaj^{4, 2}, Ali Tafreshi², John H. Liu². ¹Glaucoma sector, Division of Ophthalmology, University of Geneva, Geneva, Switzerland; ²Department of Ophthalmology, Hamilton Glaucoma Center, University of California, San Diego, La Jolla, CA; ³Sensimed

AG, Lausanne, Switzerland; ⁴Department of Ophthalmology, Mayo clinic, Jacksonville, FL.

Purpose: To demonstrate the ability of a contact lens sensor (CLS) to record short duration intraocular pressure (IOP) patterns.

Methods: A single-center, prospective, open label study was designed to record 24-hour IOP patterns using a CLS in healthy subjects and patients with primary open angle glaucoma (POAG). Following ophthalmic examination, eligible subjects stayed at the sleep laboratory during the 24-hour IOP recording. The CLS (Triggerfish®, Sensimed AG, Switzerland) measures the circumferential changes of the cornea at the corneoscleral junction. Short duration efficacy of the CLS was defined as recording the known phenomenon of IOP increase when going from a wake (sitting) to a sleep state in the recumbent position (W/S slope, interval 1 hr before and after sleep) and to assess the ocular pulse frequency (OPF) relative to the measured heart rate. The OPF was read from CLS output by two blinded observers. The accuracy of the CLS to detect OPF had to be $\geq 70\%$ for the CLS output interval (30 seconds every 5 minutes) concurrent to that of the heart rate interval (pulse over 6 consecutive minutes, 3 times during sleep). Accuracy of detecting the OPF was reached if the lower margin of the 95.25% confidence interval (CI) was $\geq 75\%$.

Results: Twenty-nine eligible participants (27 healthy subjects and 2 glaucoma patients), were included in the analysis. The mean age was 33.7 ± 13.8 years, and 48% were female. The mean W/S slope was significantly positive (56.9 ± 40.5 ; $p < 0.0001$). Only one participant (3.4%) had a negative W/S slope. The two observers were in agreement for 84% of OPF plots from the CLS output (evaluable 44% and non-evaluable 40%, respectively). There was no agreement between observers for 16% of plots. Plots were not evaluable because patients were woken up for other measurements. The proportion of accurate OPF plots was 86.5% (45 out 52; 95.25% CI of 75% - 93.2%). Given the predefined lower margin being within the CI, the CLS was accurate in detecting a short duration IOP pattern, the OPF.

Conclusions: The CLS is capable of recording short duration IOP patterns, the W/S slope and the OPF, indicating that the CLS output represents the effect of the IOP changes on the corneoscleral junction.

Commercial Relationships: Kaweh Mansouri, Sensimed AG, Switzerland (C); Robert N. Weinreb, Aerie (F), Alcon (C), Allergan (C), Altheos (C), Amakem (C), Bausch&Lomb (C), Carl Zeiss-Meditec (C), Genentech (F), Haag-Streit (F), Heidelberg Engineering (F), Konan (F), Lumenis (F), National Eye Institute (F), Nidek (F), Optovue (C), Quark (C), Solx (C), Topcon (C); Rene Goedkoop, Sensimed AG (E); Mona Moshtaghi, None; Syril Dorairaj, None; Ali Tafreshi, None; John H. Liu, Allergan (F), Alcon (F), Aerie (F), Sensimed (F), Bausch + Lomb (F)

Support: Sensimed AG

Clinical Trial: NCT01390779

Program Number: 5636 **Poster Board Number:** C0022

Presentation Time: 8:30 AM - 10:15 AM

Intraocular pressure after phacoemulsification in glaucoma patients

Karine D. Bojikian^{1,2}, Mark A. Slabaugh¹, Philip P. Chen¹.

¹Ophthalmology, University of Washington, Seattle, WA;

²Ophthalmology, Universidade Federal de Sao Paulo, Sao Paulo, Brazil.

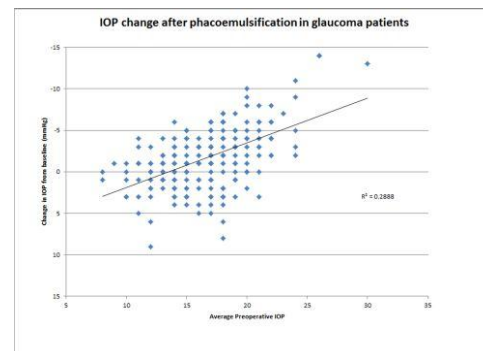
Purpose: To investigate the relationship between preoperative factors and intraocular pressure (IOP) reduction after phacoemulsification in glaucoma patients.

Methods: Retrospective review of consecutive glaucoma patients without prior incisional glaucoma surgery undergoing

phacoemulsification between January 1997 and October 2011, who had at least one year of follow-up. Pertinent clinical information prior to surgery was recorded. This included demographic information, diagnosis subtypes, mean preoperative IOP, postoperative IOP at 1 year, glaucoma medications, disease severity indices, ophthalmic biometry and treatment measures. Statistical analysis was performed using Spearman's correlation and 2-tailed paired Student t test.

Results: We included 219 eyes of 219 patients. The average age was 74.17 ± 9.86 years, 127 (58%) were female, and 163 (74%) were Caucasian. Visual field mean deviation was -5.59 ± 6.75 (mean \pm S.D.) while pattern standard deviation was 4.19 ± 3.19 . The mean preoperative IOP was 16.42 ± 3.56 mmHg, and the postoperative IOP at 1 year was 14.82 ± 3.43 mmHg. The mean pre-operative number of medications was 1.86 ± 1.03 and the mean post-operative number of medications was 1.88 ± 1.09 . Intraocular pressure reduction at 1 year after surgery was not related to age, sex, type of glaucoma, preoperative refraction, axial length, anterior chamber depth, gonioscopy grade, central corneal thickness, preoperative number of medications, previous laser procedures, or visual field parameters ($P = 0.147-0.964$). However 1-year postoperative IOP was strongly associated with the mean preoperative IOP ($P < 0.001$) (Figure).

Conclusions: A modest IOP reduction occurred after phacoemulsification in glaucoma patients. The IOP reduction was proportional to the mean preoperative IOP; higher mean preoperative IOP was associated with a greater reduction in IOP.



Commercial Relationships: Karine D. Bojikian, None; Mark A. Slabaugh, None; Philip P. Chen, Allergan (C)

Support: Unrestricted educational grant from Research to Prevent Blindness

Program Number: 5637 **Poster Board Number:** C0023

Presentation Time: 8:30 AM - 10:15 AM

24-hour intraocular pressure (IOP) fluctuation profile before and after laser peripheral iridotomy in newly diagnosed subjects with primary angle closure

Baskaran Mani^{1,2}, Tin Aung^{1,2}. ¹Singapore Eye Research Institute, Singapore, Singapore; ²Ophthalmology, Yong Loo Lin School of Medicine, National University of Singapore, Singapore, Singapore.

Purpose: To evaluate the 24-hour circadian intraocular pressure (IOP) fluctuation profile before and after laser peripheral iridotomy (LPI) in newly diagnosed subjects with primary angle closure (PAC) using a contact lens based IOP sensor.

Methods: Seven newly diagnosed primary angle closure subjects from a glaucoma clinic underwent diurnal IOP profiling with Goldmann applanation tonometry (GAT at 8 am, 10 am, 12 noon and 2 pm), gonioscopy and 24-hour IOP profiling using a contact lens based IOP sensor (Sensimed Triggerfish™, Lausanne, Switzerland) before and after LPI. Mean GAT IOP and GAT IOP fluctuation (Maximum IOP - Minimum IOP) were compared using Wilcoxon

rank sum test. Serial measurement analysis of the time-weighted average of 24-hour IOP fluctuation (in arbitrary units) and comparison between specific times of the day were performed using non-parametric methods.

Results: The mean age of study participants was 65 (± 5.6) years and most of the subjects were of Chinese origin (6/7) and female (5/7). Mean baseline GAT IOP was 23.29 (± 0.49) mm Hg. The angle remained closed in 3/7 (42.9%) subjects even after LPI. Comparing pre and post LPI, there was no difference in mean diurnal GAT IOP [19.66 (± 2.09) vs 16.7 (± 3.57) mm Hg, $p=0.25$], or mean GAT IOP fluctuation [6.86 (± 2.67) vs 5.29 (± 1.89), $p=0.58$]. For both pre and post LPI 24-hour IOP profiling with the IOP sensor, we found nocturnal and morning IOP peaks compared to evening measurements (Figure 1, $p<0.0001$, Kruskal Wallis test). Using serial measurement analysis, there was no significant change in median IOP fluctuations after LPI overall ($p=0.25$) or during specific times of the day ($p=0.48$); however, morning IOP profile showed a trend of less IOP fluctuation after LPI (Figure 1).

Conclusions: Nocturnal and morning peaks in IOP were found in newly diagnosed PAC subjects. Morning IOP peaks were lower after LPI.

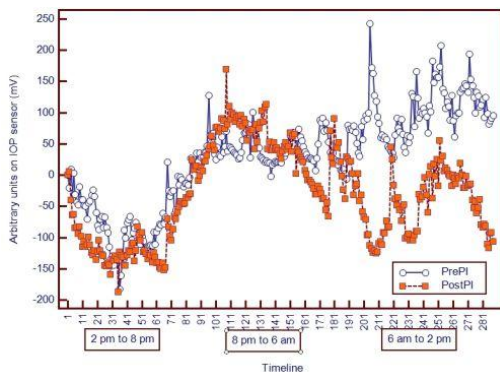


Figure 1: 24-hour IOP fluctuation profile before and after LPI
Commercial Relationships: Baskaran Mani, None; Tin Aung, Alcon (R), Alcon (C), Alcon (F), Allergan (R), Allergan (C), Carl Zeiss Meditec (F), Carl Zeiss Meditec (R), Ellex (F), Ellex (R), Santen (R)

Support: Singhealth Foundation Research Grant - SHF/FG428P/2010

Program Number: 5638 **Poster Board Number:** C0024

Presentation Time: 8:30 AM - 10:15 AM

Effects of Different Sleeping Postures on Intraocular Pressure and Ocular Perfusion Pressure in Healthy Young Subjects

Chungkwon Yoo, Tae-Eun Lee, Yong Y. Kim. Department of Ophthalmology, Korea University College of Medicine, Seoul, Republic of Korea.

Purpose: We conducted this study to investigate how changing recumbent postures among supine, lateral decubitus, and prone with head turn positions influences intraocular pressure (IOP) in healthy subjects, and to assess how ocular perfusion pressure (OPP) changes in such postural alterations of body and head.

Methods: This study included twenty healthy young Korean subjects. IOP and blood pressure measurements were taken with the subjects in the sitting position and the recumbent positions including supine, right lateral decubitus, left lateral decubitus, prone with right head turn, and prone with left head turn positions. IOP was measured using Icare® tonometer in both eyes 5 minutes after assuming each position in a randomized sequence. OPP was calculated using the formulas based on the mean blood pressure adjusted for the height of
©2013, Copyright by the Association for Research in Vision and Ophthalmology, Inc., all rights reserved. Go to iovs.org to access the version of record. For permission to reproduce any abstract, contact the ARVO Office at arvo@arvo.org.

the eye over the heart. The eye on the lower side in the lateral decubitus or prone-with-head-turn position was termed as a dependent eye. Main outcome measures were difference in IOP and OPP of the dependent and non-dependent eyes during changes of sleeping positions of body and head.

Results: Mean IOP of right and left eyes while sitting was significantly lower than that measured in each recumbent position (all, $P<0.001$). OPPs in both eyes were significantly higher in all recumbent positions than in sitting position (all, $p<0.001$). Mean IOP of the dependent eyes was higher than that of the non-dependent eyes in the lateral decubitus positions, and also in the prone positions with head turns (all, $P<0.001$). No significant inter-eye difference in OPP was found in all the positions. Compared among IOPs measured in the recumbent positions, mean IOP of the dependent eye in the lateral decubitus position or in the prone position with head turn was significantly higher than that of the ipsilateral eye in the supine position (all, $P<0.001$).

Conclusions: All sleeping positions of head and body resulted in an elevation of IOP and an increase in the calculated OPP compared with the sitting position in healthy young subjects. The postural change from supine to lateral decubitus or prone-with-head-turn position increased IOP of the dependent eyes without significant alteration in OPP in healthy awake subjects. Further research is needed under nocturnal conditions in a sleep laboratory.

Commercial Relationships: Chungkwon Yoo, None; Tae-Eun Lee, None; Yong Y. Kim, None

Support: a Grant K1131751 from Korea University

Program Number: 5639 **Poster Board Number:** C0025

Presentation Time: 8:30 AM - 10:15 AM

Intraocular pressure and central corneal thickness in 91,000 patients

Shilpa Desai¹, Julie Schallhorn¹, Steven C. Schallhorn², Yvonne Ou¹.
¹Ophthalmology, USCF, San Francisco, CA; ²Optical Express, San Diego, CA.

Purpose: To study the relationship between central corneal thickness (CCT) and intraocular pressure (IOP) in a healthy population.

Methods: This study is a retrospective chart review of 91,024 patients (174,666 eyes) who underwent pre-operative pachymetry and IOP measurement before refractive surgery. Patients with glaucoma were excluded. Central corneal thickness was measured using a standard pachymetry instrument. IOP was measured using non-contact tonometry. A multivariable regression analysis was performed to determine the relationship between CCT and IOP, and association with other covariates.

Results: The study population ranged from ages 18 to 72 (mean age = 38.6 ± 11.9 years). Myopic patients represented 83% of the study population. The refractive errors ranged from -12.125 diopters (D) to +6.125 D. Among myopic patients the average refractive error was -3.21 ± 1.9 D, while among hyperopic patients the average refractive error was $+1.91 \pm 0.80$ D. The average CCT measurement was 546 ± 33 μm , ranging from 410 to 700 μm . The average IOP was 15.2 ± 2.9 mmHg, ranging from 9 to 27 mmHg. A statistically significant linear relationship was found between IOP and CCT ($p < 0.0001$). Controlling for age, average keratometry, and mean spherical equivalent, it was found that for every 10 μm change in CCT, measured IOP changed by 0.3 mmHg.

Conclusions: This is the largest study of healthy eyes to identify a linear relationship between CCT and IOP. This data suggests that a correction of IOP measurement can be made based on CCT.

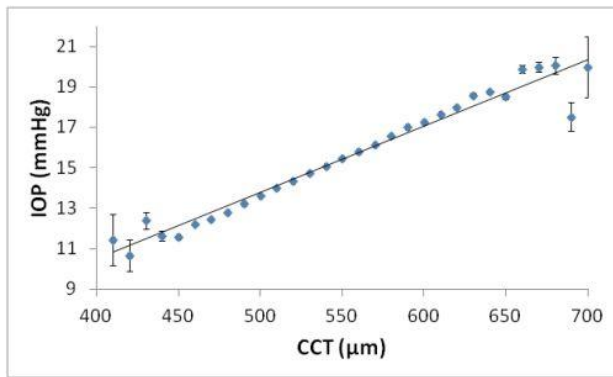


Figure 1: Linear relationship between intraocular pressure (IOP) and central corneal thickness (CCT), controlling for age, average keratometry, and mean spherical equivalent.

Commercial Relationships: Shilpa Desai, None; Julie Schallhorn, None; Steven C. Schallhorn, AMO (C), Allergan (C); Yvonne Ou, None

Program Number: 5640 **Poster Board Number:** C0026

Presentation Time: 8:30 AM - 10:15 AM

Spectral analysis of intraocular pressure pulse wave for early prediction of glaucoma

Magdalena Widlicka¹, D Robert Iskander², Patrycja Krzyzanowska-Berkowska³, Malgorzata A. Kowalska¹. ¹Institute of Physics, Wrocław University of Technology, Wrocław, Poland; ²Institute of Biomedical Engineering and Instrumentation, Wrocław University of Technology, Wrocław, Poland; ³Department of Ophthalmology, Wrocław Medical University, Wrocław, Poland.

Purpose: To evaluate the efficacy of spectral analysis of intraocular pressure pulse wave for discriminating healthy eyes from open and close glaucomatous eyes as well as glaucoma suspect eyes.

Methods: A prospective study including 262 adults (185 F & 77 M) was set at the Glaucoma Clinic, Department of Ophthalmology, Wrocław Medical University. Age matched control group (CG) consisted of 62 healthy adults (44 F and 18 M). Patients were classified in 3 groups: diagnosed primary open angle glaucoma patients (129) (POAG), primary angle-closure glaucoma patients (20) (PACG) and glaucoma suspect patients (51) (SG). Subjects underwent ophthalmologic examination including medical history, best corrected visual acuity measurement, slit-lamp biomicroscopy, dilated fundus examination, corneal ultrasound pachymetry, corneal topography, and intraocular pressure measurement with dynamic contour tonometry (DCT, Pascal). Patients with systemic medical history were excluded. The project was approved by the institution's Ethics Committee and adhered to the Tenets of the Declaration of Helsinki. DCT time series were saved and analyzed with custom written software that included signal preprocessing, filtering and spectral analysis. Unlike previous attempts of analyzing dynamic measurements of ocular pulse (Evans et al, Graefes Arch Clin Exp Ophthalmol, 2002; Bozić et al, Curr Eye Res, 2012), a novel energy content spectral analysis, which takes into account non-stationarity of considered time series, was applied. Spectral content up to the 6th harmonic of the pressure pulse wave was considered. The energy ratio of spectral bins located around the 6th and 1th harmonic was chosen as a discriminating parameter. Statistical analyses included standard descriptive statistics and one-way ANOVA.

Results: The group average energy ratio normalized to that of CG was 23.38, 5.59 and 1.39 for the SG, POAG and PACG, respectively. Significant differences ($p < 0.05$) were found between SG and all other

groups, POAG and CG, POAG and PACG but not between CG and PACG.

Conclusions: Spectral analysis techniques that take into account the non-stationary character of the DCT signals could prove to be useful for discriminating/classifying certain types of glaucomatous eyes and for predicting early glaucoma.

Commercial Relationships: Magdalena Widlicka, Grant of Polish Ministry of Science (F); D Robert Iskander, Eaglet Eye (F), Eaglet Eye (I); Patrycja Krzyzanowska-Berkowska, None; Malgorzata A. Kowalska, None

Support: Grant of Polish Ministry of Science, number NN518423336

Program Number: 5641 **Poster Board Number:** C0027

Presentation Time: 8:30 AM - 10:15 AM

Intraocular pressure measured by tonometry and a contact lens sensor in patients with open angle glaucoma

Katrin Lorenz¹, Rene Goedkoop², Marcel M. Keilani¹, Nele Berssenbruegge¹, Christina A. Korb¹, Joanna Wasielica-Poslednik¹, Norbert Pfeiffer¹. ¹Department of Ophthalmology, University Medical Center Mainz, Mainz, Germany; ²Sensimed AG, Lausanne, Switzerland.

Purpose: To investigate the relationship between 24-hour intraocular pressure (IOP) fluctuation pattern as measured by repeated, specific-point-in-time tonometry (TM) and continuous recording with a contact lens sensor (CLS) in patients with primary open angle glaucoma (POAG).

Methods: A single center, prospective, randomized, controlled, open, crossover observational study was designed to investigate the relationship between the nycthemeral IOP pattern as measured by conventional TM every 2 hours and the CLS (Triggerfish®, Sensimed, Lausanne, Switzerland). For IOP measurement the Goldmann applanation tonometry (GAT) was used for erect and the Perkins for supine measurements. Following baseline examination, patients with POAG were hospitalized for 48 hours. Eyes were randomized to TM and CLS for the first session (S1) and the reverse for S2 on the subsequent day. Relationships between TM and CLS were computed within each patient separately and summarized over all patients.

Results: Eleven eligible patients were analyzed. Mean age was 70.3 ± 7.8 years, 33.3% were female. Mean baseline GAT IOP was symmetric for both eyes for both sessions (S1: 14.9 ± 3.4 and 14.5 ± 2.4 mmHg; S2: 15.6 ± 3.1 and 13.8 ± 2.4). In S1 the correlation between TM and the CLS was 0.40 ± 0.22 (Spearman, $p = 0.0011$) and in S2 -0.20 ± 0.29 (ns). GAT-CLS correlations differed between S1 and S2 ($p < 0.001$). In S1 the correlation was positive for all patients, 45% low (< 0.4) and 55% moderate to high correlation (≥ 0.4). Mean 24-hour IOP in S2 was 12.9 ± 1.4 mmHg, similar to that of S1 (14.3 ± 2.6 mmHg, ns), whereas the mean 24-hour CLS output was significantly lower in S2 (17.0 ± 159.5 arbitrary units (AU)) as compared to in S1 (93.4 ± 193.6 AU; ($p < 0.0001$, Wilcoxon Signed-rank test). The correlation for TM between eyes and sessions was 0.18 ($p = 0.28$) and for CLS 0.42 ($p = 0.002$). Between sessions the TM correlation between eyes was negative, low and moderate to high in 40%, 10% and 50% of patients, respectively. Similarly the CLS correlation was 0%, 30% and 70%.

Conclusions: The 24-hour IOP as measured by repeated TM and continuous CLS in the contralateral eye correlate inconsistently. At the moment we do not know whether this is due to a small correlation between GAT and CLS or due to fluctuation of IOP between days. The 24-hour IOP measurement between eyes and sessions appears to be less reliable when using repeat TM as compared to the use of the CLS.

Commercial Relationships: Katrin Lorenz, Sensimed AG (F), Sensimed AG (R), MSD (R), Ivantis Inc (F), Ivantis Inc (R), Bayer (R); Rene Goedkoop, Sensimed AG (E); Marcel M. Keilani, None; Nele Berssenbrugge, None; Christina A. Korb, None; Joanna Wasielica-Polednik, None; Norbert Pfeiffer, Sensimed AG (F), Sensimed AG (R), MSD (F), MSD (R), Alcon (F), Allergan (F), Novartis (F), Novartis (R), Bayer (F), Heidelberg Engineering (F), Bausch&Lomb (F), Boehringer-Ingelheim (F), Carl Zeiss Meditec (F), Chibret (F), Nidek (F), Pfizer (F), Santen (F), Santen (R), Topcon (F), Ivantis Inc (F), Ivantis Inc (R)
Support: Sensimed AG research grant
Clinical Trial: NCT01391078

Program Number: 5642 **Poster Board Number:** C0028
Presentation Time: 8:30 AM - 10:15 AM
Characterization of Vav2/3-deficient mice with spontaneous IOP elevation
Keiko Fujikawa¹, Kaoru Inoue¹, Takae Koshiyama², Reiko Yamagishi³, Makoto Aihara^{3,4}. ¹Hokkaido University Graduate School of Health Science, Sapporo, Japan; ²Hokkaido University Graduate School of Medicine, Sapporo, Japan; ³University of Tokyo Graduate School of Medicine, Tokyo, Japan; ⁴Shirato Eye Clinic, Tokyo, Japan.

Purpose: We previously described that deficiency of Vav proteins leads to an ocular phenotype in mice similar to human angle closure glaucoma, which shows early onset of iridocorneal angle changes and elevated intraocular pressure (IOP). The Vav proteins are the best-characterized guanine nucleotide exchange factors for Rho GTPases, which regulate actin cytoskeleton, migration, adhesion, and involved in rhythm. We demonstrate more precise analysis of Vav2/3-deficient and Vav2-deficient phenotype, particularly of IOP, and of influence on circadian rhythm. In the end, we aim to evaluate spontaneously IOP-elevated mouse model for human glaucoma investigation.

Methods: We used the microneedle methods to measure IOPs of Vav2/3-deficient mice at 14, 20, 22 week and Vav2-deficient mice at 13 and 21 week respectively every 2 weeks. Concerning the 24-hour circadian rhythm, twice (day and night) IOP measurements with TonoLab rebound tonometer were carried out on Vav2/3, Vav2, and Vav3-deficient mice (Vav2/3KO, Vav2KO, Vav3KO) for 5 days. IOP elevation of Vav2/3KO and Vav2KO mice was evaluated compared to those of age-matched wild type mice. Differences between any groups were regarded as significant when they indicate above wild type IOP+2×S.D. With frozen sectioning samples, anterior ocular chamber and optic nerve head degeneration were examined.

Results: With microneedle methods, 29.4%(5/17) of Vav2/3KO and 33.3%(4/12) of Vav2KO mice show IOP elevation, respectively. Among Vav2/3KO and Vav2KO mice, IOPs of elevated-IOP groups indicated 28.8 ± 6.9 and 19.8 ± 1.9 mmHg, while those of non elevated-IOP groups were 15.4 ± 1.2 and 15.6 ± 0.8 mmHg, respectively. In elevated-IOP groups of Vav2/3 and Vav2 KO mice, iridocorneal angle closures, optic nerve head cupping, and thinner of nerve fiber layer were demonstrated. In addition, some of elevated-IOP mice showed leucoma of cornea, buphthalmos, and phthisis bulbi. Once IOP elevated, mice continuously maintain its high level of IOP until at least 28 week-old ages. Investigation of the IOP circadian rhythm in Vav2/3KO, Vav2KO and Vav3KO mice, reveals two-phases with IOP elevation at night similar to that of normal mice.

Conclusions: Vav2/3 and Vav2-deficient mice show ocular hypertension due to ocular anterior chamber abnormalities and consequently cause glaucomatous optic neuropathy. Therefore, as an

animal model of spontaneous ocular hypertension, Vav-deficient mice serve a valuable tool.

Commercial Relationships: Keiko Fujikawa, None; Kaoru Inoue, None; Takae Koshiyama, None; Reiko Yamagishi, None; Makoto Aihara, Ono pharmaceutical company (F), Pfizer (F)
Support: Grants-in-Aid for scientific research from the Ministry of Education, Culture, Sports, Science and Technology in Japan (No.22390312)

Program Number: 5643 **Poster Board Number:** C0029
Presentation Time: 8:30 AM - 10:15 AM
First implantation of a telemetric, intraocular pressure sensor in patients with glaucoma

Niklas Plange, Antonis Koutsonas, Peter Walter. Dept of Ophthalmology, RWTH Aachen University, Aachen, Germany.

Purpose: To investigate safety and intraocular pressure (IOP) measurement of a telemetric intraocular pressure sensor in patients with glaucoma.

Methods: 5 patients with glaucoma were included in a prospective single-center clinical trial (follow-up 3 months-1 year). The ring-shaped telemetric IOP sensor (ARGOS, Implants Ophthalmic Products GmbH, Hannover, Germany) is a miniature device with eight pressure-sensitive capacitors included in a single substrate Application-Specific Integrated Circuit (ASIC) combined with a circular micro coil antenna. The device is completely encapsulated in silicone rubber with an outside diameter of 11.3 mm. A reader unit uses a high frequency magnetic field for power and data transmission.

Results: The implantation of the telemetric pressure sensor was successfully performed in the ciliary sulcus at the end of a planned cataract surgery with implantation of an intracapsular lens. The sensor was implanted using a 5.5 mm clear corneal incision. Three patients had a significant sterile anterior chamber inflammation 2 days after surgery that resolved 7 days later following intensive anti-inflammatory treatment. In all patients, IOP measurement was successfully performed at all visits. All patients successfully performed home self-tonometry after a short instruction.

Conclusions: Despite an early postoperative anterior chamber inflammation in some patients, the IOP sensor was well tolerated in all patients during follow-up. For the first time, continuous IOP monitoring using a non-contact intraocular pressure sensor seems possible in glaucoma patients. The variability of IOP values using the ARGOS sensor compared to Goldmann applanation tonometry has yet to be evaluated.

Commercial Relationships: Niklas Plange, Implants Ophthalmic Products (F); Antonis Koutsonas, None; Peter Walter, Novartis (R), Bayer (R), Second Sight (R), Bayer (F), Novartis (F)
Clinical Trial: DRKS00003335

Program Number: 5644 **Poster Board Number:** C0030
Presentation Time: 8:30 AM - 10:15 AM
Comparison of Rebound Tonometer Icare-Pro and Goldmann Handheld Applanation Tonometer in Congenital Glaucoma

LAURA MORALES-FERNANDEZ, Lara Borrego, Jose M. Martinez de la Casa, Federico Saenz-Frances, Julian Garcia-Feijoo. GLAUCOMA, HOSPITAL CLINICO, Madrid, Spain.

Purpose: To establish the reproducibility of the new rebound tonometer Icare-Pro, and its correlation with the Goldmann Handheld Applanation Tonometer (Perkins) in pediatric patients diagnosed with primary congenital glaucoma.

Methods: Using both tonometers, the IOP was prospectively determined in 78 eyes of 40 patients with congenital glaucoma examined under anaesthesia (short age: 8 to 88 months). Corneal

curvature, central corneal thickness (CCT), and axial length were also measured in each patient.

Results: There was a good correlation between IOP readings obtained by the GAT and the Icare-Pro ($r=0.796$, $p<0.001$). Icare readings were midly higher than GAT measurements (mean IOP difference $-0.36 + 3.95$ mmHg, $p=0.40$). A Bland-Altman plot indicated the 95% limits of agreement between the two methods were 7.4 to -8.1 mm Hg (slope= 0.017 ; $p=0.919$). In terms of pachymetry, in this group of patients, the two tonometers behaved in a similar way, without correlation observed between IOP measurements and central corneal thickness.

Conclusions: The new rebound tonometer Icare-Pro shows a high reproducibility and excellent correlation in their measurements with the Goldmann handheld applanation tonometer in children with congenital glaucoma.

Commercial Relationships: LAURA MORALES-FERNANDEZ, None; Lara Borrego, None; Jose M. Martinez de la Casa, None; Federico Saenz-Frances, None; Julian Garcia-Feijoo, Trancend (C), Ivantis (C), Glaukos (C), MSD (C), Allergan (F), Pfizer (F), Alcon (C), Sensimed (F), Sylentis (F), Bausch and Lomb (C)

Program Number: 5645 **Poster Board Number:** C0031

Presentation Time: 8:30 AM - 10:15 AM

The Effect of the Automated Visual Field Examination on Intraocular Pressure (IOP) in Patients with Glaucoma

Sonya Makhni¹, Dipali Dave¹, Matthew Karl², Janet B. Serle¹.

¹Mount Sinai School of Medicine, New York, NY; ²SUNY Downstate College of Medicine, Brooklyn, NY.

Purpose: To evaluate the effect of the automated visual field examination on the intraocular pressure (IOP) in glaucoma suspects and glaucoma patients.

Methods: An ongoing prospective study has enrolled 40 patients (80 eyes) with mean age of 64 ± 13.5 years. Enrollment criteria included glaucoma or glaucoma suspects, clinical monitoring for >1 month, and no change in clinical management from previous month. Patients underwent Humphrey Visual Field (HVF) SITA 24-2 examination as part of routine care. Goldmann applanation tonometry was performed 1 hour prior to the HVF, and 15 minutes and 1 hour following completion of the field (referred to as IOP1, IOP2, and IOP3). Univariate chi-square analysis was conducted to evaluate for statistical significance of IOP changes.

Results: Patients (40 patients, 80 eyes) were (mean \pm SD) 64 ± 13.5 years of age, on 2.5 ± 1.6 prescribed glaucoma medications, and had a mean visual field index (VFI) of 86 ± 17.7 on HVF testing; 22 patients had undergone at least one surgical and/or laser glaucoma treatment in the past. Mean IOP1, IOP2, and IOP3 were found to be constant across all time points for both eyes, at 13.5 ± 0.02 , 13.4 ± 0.22 , and 13.4 ± 0.39 mmHg, respectively. The mean change in IOP from IOP1 to IOP2 was: -0.12 ± 2.8 mmHg, from IOP2 to IOP3: 0.00 ± 1.9 mmHg, and from IOP2 to IOP3: 0.00 ± 2.3 mmHg. Increases in intraocular pressure of >2 mm Hg (4.2 ± 1.2 mmHg) from IOP1 to IOP2 were noted in 23% of patients (9 patients, 10 eyes). Of these eyes, 7 showed reductions of greater than 2 mmHg from IOP1 to IOP3.

Age, gender, number of medications, severity of glaucoma, as well as number and type of surgical procedures previously performed did not result in any significant effects on IOP.

Conclusions: In this patient population, most of whom had mild glaucoma, no significant changes in eye pressure following the HVF were found. IOP can be measured soon after performing visual field testing, as is the common practice.

Commercial Relationships: Sonya Makhni, None; Dipali Dave, None; Matthew Karl, None; Janet B. Serle, Acorn (F), Aerie (F), Forest Research Institute (C), Ono (C), Sucampo (C), Fovea (F)
Support: NEI Core Grant EY001867; Unrestricted grant from RPB; Mount Sinai School of Medicine student research grant

Program Number: 5646 **Poster Board Number:** C0032

Presentation Time: 8:30 AM - 10:15 AM

Ocular Indications of Partial Penetrance in Mice Heterozygous for NBCe1 (Slc4a4)

Michael F. Romero^{1,2}, Heather L. Holmes¹, Uttio Roy Chowdhury³, Cheryl R. Hann³, Min-Hwang Chang¹, Michael P. Fautsch³, An-Ping Chen¹. ¹Physiology & Biomedical Engineering, Mayo Clinic College of Medicine, Rochester, MN; ²Nephrology & Hypertension, Mayo Clinic College of Medicine, Rochester, MN; ³Ophthalmology, Mayo Clinic College of Medicine, Rochester, MN.

Purpose: Recessive human mutations in the electrogenic Na⁺-bicarbonate cotransporter (NBCe1, Slc4a4) cause severe proximal renal tubular acidosis (pRTA) as well as bilateral glaucoma and cataracts. Although heterozygous carriers (parents and siblings) make some amount of the mutant form of NBCe1 protein, they have been considered asymptomatic. In 2007 a nbce1-knockout (NUL) mouse was reported; yet, analysis of these mice did not include ocular parameters. Our study sought to investigate the impact of nbce1-knockout (NUL) and heterozygosity (HET, +/-) on the eye.

Methods: Breeding pairs of HET-nbce1 mice were obtained from Dr. Gary Shull (U Cinc., OH) to generate NUL, HET and wild-type (WT) mice. Intraocular pressure (IOP) in non-anaesthetized mice (2 wk - 12 mo) was measured using a handheld rebound Tonometer (iCare). IOP was repeated in 5-6 animals (n) per genotype, R and L eye, while keeping time of day constant; "N" is the total number of IOP points. Since NUL's die by 18d, we sacrificed and performed histological studies before 18 d. We also examined ocular histology of mice >10 mo.

Results: IOP measurements indicate that young (2wk-3mo) WT (14.5 ± 1.3 mmHg; N=53) and HET (14.9 ± 1.1 mmHg; N=64) mice are similar (mean \pm SD). IOP's for NUL's were erratic, but histology revealed NUL's had no anterior chamber (AC), indicating a more severe phenotype than humans with recessive NBCe1 mutations. Ocular histology of young HETs was similar to young WTs. A second IOP-series in older mice (10-12 mo) showed that HETs had developed elevated IOP: WT (15.5 ± 1.1 , N=118) and HET (19.7 ± 2.0 , N=104). Histologically, older WTs and HETs had normal AC and angles. Surprisingly, the HET retinas were missing several layers: outer plexiform layer (OPL), outer nuclear layer (ONL) and rods. Significant cellular debris was present between the inner nuclear layer and the retinal pigmented epithelium (RPE).

Conclusions: Allelic variations in the NBCe1 gene may be a contributor to age-related onset of elevated IOP with concurrent retinal degeneration.

Commercial Relationships: Michael F. Romero, None; Heather L. Holmes, None; Uttio Roy Chowdhury, None; Cheryl R. Hann, None; Min-Hwang Chang, None; Michael P. Fautsch, None; An-Ping Chen, None

Support: EY017732 (MFR), EY021727 (MPF, MFR); AHA-SDG2640146 (MC); Research to Prevent Blindness (MPF); and Mayo Foundation

Program Number: 5647 **Poster Board Number:** C0033

Presentation Time: 8:30 AM - 10:15 AM

Microbead Occlusion Model of Glaucoma in Non-Human Primates

Wendi S. Lambert, Brian J. Carlson, David J. Calkins. Vanderbilt Eye Institute, Vanderbilt University Med Center, Nashville, TN.

Purpose: We established an acute model of glaucoma in rodents using intracameral injection of microbeads to obstruct aqueous humor outflow and induce ocular hypertension (OHT). While rodent models of glaucoma have been and continue to be extremely informative, important differences in structure and function exist between rodents and primates. Inducing OHT in non-human primates (NHP) would allow us to better understand how these differences influence glaucoma pathology and progression. The purpose of this study was to establish an acute NHP model of glaucoma by injecting microbeads into the anterior chamber of squirrel monkeys.

Methods: OHT was induced in Bolivian squirrel monkeys (SMs) via bilateral injection of 15µm or 30µm polystyrene microbeads into the anterior chamber. Intraocular pressure (IOP) was measured weekly in anesthetized SMs and 2 to 3 times weekly in awake SMs using a restraint tube system. SMs received topical Xalatan, an IOP-lowering drug, once daily two weeks post-injection.

Results: Bilateral injection of 50µl of 15µm microbeads increased IOP in anesthetized SMs 27.8% from 16.58 ± 0.47 mmHg to 21.20 ± 0.52 mmHg after 6 days ($p=0.002$, $n=3$). Xalatan treatment for 2 days lowered IOP 30.6% compared to OHT ($p<0.001$) and 11.3% compared to baseline ($p=0.181$). Stopping Xalatan treatment increased IOP 32.4% compared to OHT+Xalatan and 17.5% compared to baseline ($p<0.031$). Weekly anesthetic events to measure IOP resulted in weight loss in most SMs. To address this we developed a physical restraint system to measure IOP in awake SMs. Using this system, injection of 40µl of 30µm microbeads elevated awake IOP 20.6% from 16.63 ± 0.22 mmHg to 19.98 ± 0.28 mmHg over 10 days ($p<0.001$, $n=3$). Xalatan treatment for 4 days lowered IOP 8.2% compared to OHT ($p=0.010$); however IOP was still elevated compared to baseline (10.4%, $p=0.040$). Stopping Xalatan treatment increased IOP to 9.3% compared to OHT+Xalatan and 20.6% compared to baseline ($p<0.042$).

Conclusions: Microbead injection induced OHT in SMs that was alleviated with Xalatan treatment. Multiple anesthetic events produced weight loss in the majority of SMs, so a physical restraint system and training paradigm to measure IOP in awake SMs was developed. Using this model of glaucoma in SMs, we can develop a more complete view of disease progression, which in turn could provide new therapeutic targets and treatment options for patients.

Commercial Relationships: Wendi S. Lambert, QLT Inc. (F); Brian J. Carlson, QLT, Inc. (F); David J. Calkins, QLT, Inc (F), Allergan (F), QLT, Inc (C), Allergan (C)

Support: Melza and Theodore Barr and Glaucoma Research Foundations (DJC), AHAF (DJC), NEI Grant (5R01EY017427-03) (DJC), Research to Prevent Blindness Inc., Departmental Unrestricted Grant (DJC), and NEI Core Grant (5P30EY008126-19) (DJC)

Program Number: 5648 **Poster Board Number:** C0034

Presentation Time: 8:30 AM - 10:15 AM

The Role Of Ageing In Experimental Glaucoma

T H Khanh Vu^{1,2}, Kin-Sang Cho¹, Martine M. Jager², Dong F. Chen¹. ¹Ophthalmology, Schepens Eye Research Institute, Boston, MA; ²Ophthalmology, Leiden University Medical Center, Leiden, Netherlands.

Purpose: A number of degenerative retinal diseases are age-related, including glaucoma. It is believed that basic differences exist in the immunological microenvironment of eyes from young and old individuals. In addition, emerging studies report that the immune system plays an important role in glaucoma. Therefore, we studied whether old mice, presumably harboring a low level of age-related

ocular para-inflammation, were more sensitive to neurodegeneration after IOP elevation than young mice.

Methods: Elevation of IOP was induced by anterior chamber (AC) injection of microbeads (MB), while controls received an injection of phosphate buffered saline (PBS). Twelve weeks-old C57BL/6J mice injected with MB or PBS were compared with 12 months-old mice injected with MB or PBS. IOP was measured on day 2, 7, 10, 14, 17, 21, and 24. At 4 weeks post-injection, all mice were sacrificed and retinal ganglion cell (RGC) quantification was performed by βIII-tubulin immunofluorescence staining in retinal sections. In addition, ocular immune responses were evaluated by detecting anti-Hsp responding T cells with an IFN-γ enzyme-linked immunosorbent spot and fluorescence-activated cell sorting assay.

Results: A single injection of MB in the AC resulted in a significant IOP elevation that lasted approximately 3 weeks in both young and old mice. Control mice with PBS injection showed no significant change in IOP. Remarkably, aged mice exhibited an increased loss of RGCs as compared to young mice after MB injection, while in controls; no significant difference was noted in the number of RGCs between young and old mice. Higher levels of Hsp27-specific CD4+ T cells were seen subsequent to MB injection in both young and aged mice when compared to age-matched control mice who received a PBS injection. More importantly, significantly higher levels of Hsp27-specific CD4+ T cells were present in aged mice compared to young mice in both normal and ocular hypertensive (OHT) groups.

Conclusions: IOP elevation induced a higher degree of RGC loss in aged mice that is accompanied by higher levels of Hsp27-specific CD4+ T cells under both normal and OHT conditions, than in young mice. We propose that the immunological microenvironment of the eye contributes critically to the enhanced neurodegeneration following IOP elevation in old mice. Therefore, understanding age-related inflammatory changes in the retina may lead to a better knowledge of the pathogenesis of glaucoma in the elderly.

Commercial Relationships: T H Khanh Vu, None; Kin-Sang Cho, None; Martine M. Jager, None; Dong F. Chen, GlaxoSmithKline (F), Patent/Schepens Eye Research Institute (P)

Support: Stichting Glaucoomfonds, Stichting Nederlands Oogheelkundig Onderzoek, Oogfonds, Prins Bernhard Cultuurfonds

Program Number: 5649 **Poster Board Number:** C0035

Presentation Time: 8:30 AM - 10:15 AM

Establishment of the ocular hypertension model using the common marmoset

Masamitsu Shimazawa¹, Shinsuke Nakamura¹, Miki Miwa², Kazuhiro Tsuruma¹, Makoto Aihara³, Katsuki Nakamura², Hideaki Hara¹.

¹Molecular Pharmacology, Department of Biofunctional Evaluation, Gifu Pharmaceutical University, Gifu, Japan; ²Department of Behavioral and Brain Sciences, Primate Research Institute, Kyoto University, Inuyama, Japan; ³Department of Ophthalmology, University of Tokyo School of Medicine, Tokyo, Japan.

Purpose: We established an experimental glaucoma model in the common marmoset (*Callithrix jacchus*).

Methods: Chronic intraocular pressure (IOP) elevation was induced by laser trabeculoplasty twice at 2-week intervals in the left eyes of 4 common marmosets. IOP was measured before and at 4, 7, 8, 11, 13 weeks after first laser treatment, and ophthalmoscopic examinations were also performed. At 13 weeks after laser treatment, each eye was enucleated, and retinal cross-sections and optic nerve were prepared for histological examination.

Results: IOP was persistently elevated to over 30 mmHg in laser-treated eyes during 13 weeks in 3 marmosets, but IOP in one marmoset was transiently increased to 26.6 mmHg at 7 weeks and then declined to normal level in the fellow eye. In ophthalmoscopy,

deepened and enlarged optic disc cupping, depending on the extent of IOP elevation and duration, were observed in laser-treated eyes of 3 marmosets with persistent IOP elevation, but there was no apparent change in the optic disc in the laser-treated eye of one marmoset with transient IOP elevation. Histological examination showed marked atrophy with deepened and enlarged cupping of optic disc, thinning of retinal nerve fiber layer and retinal ganglion loss in the retina, and axonal atrophy and loss in the optic nerve, depending on the extent of IOP elevation and duration.

Conclusions: We succeeded in producing an experimental glaucoma model in the common marmoset, and this model may be useful in elucidating the pathophysiological mechanism for glaucoma.

Commercial Relationships: Masamitsu Shimazawa, None; Shinsuke Nakamura, None; Miki Miwa, None; Kazuhiro Tsuruma, None; Makoto Aihara, Ono pharmaceutical company (F), Pfizer (F); Katsuki Nakamura, None; Hideaki Hara, None
Support: This study was supported in part by Grant-in-Aid for Scientific Research (C) (No. 23592612) and (B) (No. 22390321) from the Ministry of Education, Culture, Sports, Science, and Technology, Japan, by Takeda Science Foundation, and by the Cooperative Research Program of Primate Research Institute, Kyoto University (2010 and 2011).

Program Number: 5650 **Poster Board Number:** C0036

Presentation Time: 8:30 AM - 10:15 AM

Intraocular pressure in chronic users of low-dose oral corticosteroids for connective tissue disease

beatriz gomes^{1,2}, Marcony R. Santhiago¹, Haroldo Moraes¹. ¹Federal University of Rio de Janeiro, Rio de Janeiro, Brazil; ²Bonsucesso Federal Hospital, Rio de Janeiro, Brazil.

Purpose: Patients with connective tissue disease (CTD) were shown to have a stronger ocular hypertensive response to steroids than healthy controls. Although a clinically significant intraocular pressure (IOP) rise might be expected in patients with CTD on high-dose systemic corticosteroid therapy, the effects of low-dose therapy remain unknown. The authors aimed to assess whether low-dose chronic systemic corticosteroid therapy for CTD has clinically significant ocular hypertensive effects.

Methods: In this observational controlled study, 86 patients with CTD were grouped according to corticosteroid therapy. Group 1 was comprised of patients with CTD on use of low-dose oral corticosteroid for at least 6 months and group 2 included CTD patients without use of corticosteroid therapy. Group 3 was comprised of healthy controls. Low-dose was defined as a daily dosage up to 10mg of prednisone or its equivalent. The main outcomes were IOP and diagnosis of glaucoma.

Results: In all the 3 groups, the IOP were within the normal range. The mean IOP was 13.1 ± 2.7 mmHg in CTD corticosteroid group (Group 1); 13.7 ± 2.7 mmHg in CTD group without corticosteroid therapy (Group 2); and 13.1 ± 1.6 mmHg in control group (Group 3). No significant differences in IOP were observed between the 3 groups ($P=0.50$) Furthermore, no significant differences were found in terms of prevalence of glaucoma (15% in Group 1; 14% in Group 2; and 5% in Group 3; $P=0.54$).

Conclusions: Low-dose systemic corticosteroid therapy has no clinically significant ocular hypertensive effects in patients with CTD.

Commercial Relationships: beatriz gomes, None; Marcony R. Santhiago, None; Haroldo Moraes, None

Program Number: 5651 **Poster Board Number:** C0037

Presentation Time: 8:30 AM - 10:15 AM

Changes in intraocular pressure measurements and corneal biomechanical properties in eyes with glaucoma using prostaglandin analogues

MARIA JOSE MONTERO, Oscar D. Albis-Donado, Jesus Jimenez-Roman. Glaucoma, APEC, Mexico city, Mexico.

Purpose: To measure intraocular pressure changes with applanation tonometry (AT), dynamic contour tonometry (DCT) and ocular response analyzer (ORA) in eyes with glaucoma treated with prostaglandin analogues (PGA)

Methods: Intraocular pressure (IOP) was measured using AT, DCT and ORA in 38 glaucoma eyes at baseline and after 3 weeks of treatment with PGA. Baseline mean difference in IOP between tonometers was compared to differences with treatment. Paired samples T test was used for pre and post-treatment comparisons. Central Corneal Thickness (CCT), corneal hysteresis (CH) and corneal resistance factor (CRF) were also measured and analysed using SPSS version 19

Results: Eyes treated with PGAs have lower IOP than at baseline, but each tonometry method shows a different mean amount of IOP lowering. Baseline and treated mean IOPs were different among the 3 tonometers, mean change in IOP as measured by AT was -1.21 mmHg, -1.26 mmHg with DCT and 3 mmHg with ORA. Corneal hysteresis increases an average of 0.83 mmHg while corneal thickness decreases an average of 7.8 microns, corneal resistance factor does not experience a significant change with prostaglandin analogue treatment

Conclusions: AT and DCT seem to be less affected by corneal biomechanical changes induced by PGAs, whereas ORA measurements show an artifactual larger effect of PGAs on IOP; corneal hysteresis increases significantly post treatment with this kind of drugs. Corneal thickness decreases with prostaglandin analogue treatment

Commercial Relationships: MARIA JOSE MONTERO, None; Oscar D. Albis-Donado, None; Jesus Jimenez-Roman, None

Program Number: 5652 **Poster Board Number:** C0038

Presentation Time: 8:30 AM - 10:15 AM

Effect on intraocular pressure after intravitreal injection of anti-vascular endothelial growth factor agents in eyes with neovascular age related macular degeneration

Junglim Kim¹, Jeongmin Lee². ¹busan paik hospital, Busan, Republic of Korea; ²Yonseiplus eye center, Seoul, Republic of Korea.

Purpose: To report the rate of intraocular pressure (IOP) elevation associated with repeated intravitreal injections of anti-vascular endothelial growth factor (VEGF) agents and to determine if sustained elevation of IOP after injection was predicted using IOP one hour after injection.

Methods: The charts of 259 eyes undergoing intravitreal injection with anti-VEGF agents for neovascular age-related macular degeneration (AMD) were reviewed for history of glaucoma, total number of injections and changes in IOP. Sustained IOP elevation was defined as IOP ≥ 22 mmHg and a change from baseline of ≥ 6 mmHg recorded on at least two consecutive visits and lasting ≥ 30 days. Data were analyzed independently for two groups according to difference between baseline IOP and IOP one hour after injection (1) more than 6 mmHg and (2) less than 6 mmHg.

Results: Of the 259 eyes receiving injections with bevacizumab and/or ranibizumab, 4.25% (n=11 eyes) had sustained IOP elevation. The rate of sustained elevation IOP was 4.72% (5/106) for the eyes receiving only bevacizumab, 2.68% (3/112) for the eyes receiving only ranibizumab and 7.32% (3/41) for eyes undergoing bevacizumab and ranibizumab. The rates of glaucoma and sustained IOP elevation are high in the group which is more than 6 mmHg

difference between baseline IOP and IOP one hour after injection (6.67% vs. 0.65% respectively, $p=0.008$, 9.52% vs. 0.63% respectively, $p=0.001$).

Conclusions: Sustained IOP elevations can occur undergoing intravitreal anti-VEGF treatment for neovascular AMD. It suggests the possibility of a heightened risk for further elevation of IOP in patients with pre-existing glaucoma who receive either bevacizumab or ranibizumab. AMD eyes that receive intravitreal anti VEGF injections need to be monitored for IOP changes, especially those in which is more than 6 mmHg difference between baseline IOP and IOP one hour after injection. Prospective studies are needed to verify these results and better understand the implications of these findings. **Commercial Relationships:** Junglim Kim, None; Jeongmin Lee, None

Program Number: 5653 **Poster Board Number:** C0039

Presentation Time: 8:30 AM - 10:15 AM

INTRAOULAR PRESSURE CHANGES BY CONTINUOUS RECORDING THROUGH TRIGGERFISH CONTACT LENS APPLICATION IN PATIENTS UNDERGOING WATER DRINKING TEST: CORRELATION WITH GOLDMANN READINGS IN CONTRALATERAL EYE

Nicola Ungaro¹, Giovan Battista Scazzi¹, Maria Francesca Giacosa¹, Maria Grazia Tardini², Giacomo Bacchi¹, Stefano A. Gandolfi².

¹Azienda Ospedaliera Universitaria di Parma, Parma, Italy;

²Università degli studi di Parma, Parma, Italy.

Purpose: To evaluate the changes of intraocular pressure (IOP) through Triggerfish contact lenses (LAC) after water drinking test (WDT) and their correlations with IOP changes recorded with Goldmann Tonometry (GAT)

Methods: Retrospective analysis of ten healthy glaucoma suspect subjects. First, The IOP was recorded in both eyes with standard GAT, then the Triggerfish LAC, which is able to measure changes in corneal curvature that are related to IOP, was applied into a random eye. Hereinafter was administered the WDT: 10 mL/kg of water in 5 min. After 15 min we started to measure IOP with GAT in the fellow eye, every 15 min for 90 min, while LAC recorded data every 5 min during all this period of time; the changes in IOP were compared to baseline recorded before the WDT. Similarly the records obtained in the two eyes with the two methods were compared with each other **Results:** Data are shown in Table 1. The t test analysis of changes in IOP recorded with GAT was significant in four points compared to baseline (tab. 1). IOP changes measured with LAC were significant in two points compared to baseline (tab. 1). The comparison of the pressure recordings obtained with the two methods was carried out with the Pearson coefficient. To reduce the individual variability was considered the mean of values measured from both the Goldmann and the Triggerfish in all the timepoints of the curve. It was found a good correlation between the two methods ($P = 0.989$)

Conclusions: Both methods showed a significant change in IOP after the WDT. The analysis of the means of values in all timepoints of the two instruments showed a good correlation proving that there is a relationship between the changes in IOP measured by Goldmann and changes in corneal curvature measured by Triggerfish LAC. Further studies are needed to eventually establish an algorithm that exactly correlates the corneal curvature changes recorded with Triggerfish LAC with IOP changes measured with GAT

Table 1

	TIMEPOINTS (MEANS)						
	T ₀₀	T ₀	T ₀₋₁₅	T ₀₋₃₀	T ₀₋₄₅	T ₀₋₆₀	T ₀₋₇₅
GAT (mmHg)	12,6	14,5	15,4	15,2	14,6	12,8	12,3
LAC (mV)		-0,89	-0,895	-0,285	-0,685	-3,36	-4,05

	T-TEST BETWEEN TIMEPOINTS AND BASELINE					
	T ₀₀ -T ₀	T ₀₀ -T ₀₋₁₅	T ₀₀ -T ₀₋₃₀	T ₀₀ -T ₀₋₄₅	T ₀₀ -T ₀₋₆₀	T ₀₀ -T ₀₋₇₅
GAT P value	0,0002	0,00054	0,00037	0,00189	0,33089	0,23393
LAC P value	0,19809	0,03134	0,00926	0,07208	0,2569	-

LEGEND	
T ₀₀	Baseline value, before (for GAT) or after (for LAC) the WDT
T ₀	Measurement after 15 minutes from WDT
T ₀₋₁₅	Measurement after 30 minutes from WDT
T ₀₋₃₀	Measurement after 45 minutes from WDT
T ₀₋₄₅	Measurement after 60 minutes from WDT
T ₀₋₆₀	Measurement after 75 minutes from WDT
T ₀₋₇₅	Measurement after 90 minutes from WDT

Commercial Relationships: Nicola Ungaro, None; Giovan Battista Scazzi, None; Maria Francesca Giacosa, None; Maria Grazia Tardini, None; Giacomo Bacchi, None; Stefano A. Gandolfi, SENSIMED (R), ALLERGAN (R), ALCON (R), ALLERGAN (F), ALCON (F), GLAUKOS (F), IVANTIS (F)

Program Number: 5654 **Poster Board Number:** C0040

Presentation Time: 8:30 AM - 10:15 AM

Comparison of the Cellular Response to Overnight Contact Lens Wear on the Sclera and Cornea

John G. Flanagan^{1,2}, Aphrodite D. Stavropoulos^{1,5}, Doerte Luensmann^{2,3}, Cameron K. Postnikoff⁴, Maud Gorbet^{4,3}. ¹Dept of Ophthal & Vision Sci, Univ of Toronto, Toronto Western Hosp, Toronto, ON, Canada; ²School of Optometry and Vision Science, Univeristy of Waterloo, Waterloo, ON, Canada; ³Centre for Contact Lens Research, Univeristy of Waterloo, Waterloo, ON, Canada; ⁴Systems Design Engineering, Univeristy of Waterloo, Waterloo, ON, Canada; ⁵Institute of Medical Sciences, Univeristy of Toronto, Toronto, ON, Canada.

Purpose: To investigate the overnight inflammatory response to a hydrogel carrier material designed for a 24-hour intraocular pressure (IOP) monitoring device mounted on the superior, scleral bulbar conjunctiva, and compare it to overnight lens wear on the cornea.

Methods: Eight participants were recruited to a sleep lab for 3 non-consecutive visits. The 1st visit consisted of overnight sleep (8 hrs) with no contact lens in place (baseline); the 2nd visit consisted of overnight sleep with a hydrogel contact lens fitted bilaterally to the cornea; and the 3rd visit consisted of overnight sleep with a hydrogel contact lens placed bilaterally on the superior, scleral bulbar conjunctiva, beneath the upper lid. Immediately upon awakening, participants had the lenses removed and their eyes washed using a non-contact irrigation system. The expression of the C3a receptor (C3aR), CD95 (Fas, cell death inducing receptor), CD54 (ICAM-1), CD66b (degranulation marker), and CD45 (Pan leukocyte marker) on polymorphonuclear leukocytes (PMN) was evaluated by flow cytometry for each visit and is reported as arbitrary fluorescent units (AFU).

Results: Flow cytometric analysis of PMN revealed a significant decrease in the expression of C3aR after overnight contact lens wear on the cornea (13 ± 7 AFU, $p < 0.01$) as compared to overnight lens wear over the sclera (42 ± 23 AFU) and no lens wear (35 ± 11 AFU). A reduction in CD54 expression was observed for overnight lens wear over the sclera and the cornea (25 ± 6 AFU, $p \leq 0.03$; 26 ± 8 AFU, $p > 0.05$) when compared to baseline (37 ± 12 AFU). For all visits, CD95 remained at background levels and there was no significant difference in CD66b expression.

Conclusions: These results suggest that overnight lens wear on the cornea alters the expression of C3aR, a receptor important in the regulation of the leukocyte inflammatory response mediated by complement activation. PMN response to overnight contact lens wear on the superior, scleral bulbar conjunctiva was similar to the control condition with no contact lens. Silicone hydrogel contact lenses, approved for overnight wear on the cornea, may be safely mounted on the scleral bulbar conjunctiva and presents a promising carrier material for a 24-hour IOP monitoring device.

Commercial Relationships: John G. Flanagan, Heidelberg Engineering (C), Heidelberg Engineering (R), Heidelberg Engineering (F), Carl Zeiss Meditec (C), Carl Zeiss Meditec (R), Carl Zeiss Meditec (R), Alcon Pharmaceuticals (R), Alcon Pharmaceuticals (R), Optovue Inc (F), Optovue Inc (F), Photon etc (F), Photon etc (F); **Aphrodite D. Stavropoulos**, None; **Doerte Luensmann**, Alcon (R); **Cameron K. Postnikoff**, CIBA Vision (F); **Maud Gorbet**, CIBA Vision/Alcon (F)
Support: Glaucoma Research Society of Canada, Peterborough K.M. Hunter Award

Program Number: 5655 **Poster Board Number:** C0041

Presentation Time: 8:30 AM - 10:15 AM

Are thinner corneas associated with reduced hysteresis?

Trupti Patil, Rajesh Sasikumar, Sathi A. Devi. Glaucoma, Narayana Nethralaya, Bangalore, India.

Purpose: To determine the relationship between central corneal thickness (CCT) and corneal biomechanical properties in Asian Indian eyes with glaucoma.

Methods: In this prospective observational comparative study, glaucoma patients on treatment were assigned to two groups based on CCT; CCT < 500 μ (group A) and >500 μ (group B). Goldman applanation tonometry (GAT) was measured in all using a single calibration checked device. Corneal hysteresis (CH), corneal resistance factor (CRF), corneal-compensated IOP (IOPcc), and Goldmann-correlated IOP (IOPg) were measured using the Ocular Response Analyzer (ORA). The deformation amplitude (DA) of the cornea was measured using the CorVis non-contact tonometer. Pearson's correlation coefficient was used to evaluate correlation between parameters. Univariate and multivariate regression analysis was used to determine the relationship between the various parameters

Results: A total of 107 eyes (76 patients) were enrolled; 60 eyes had CCT < 500 μ . Majority had open angle glaucoma (62%). The average CCT of group A was 474.7 \pm 18.7 μ compared to that of group B (534.6 \pm 24.1 μ) (p<0.01). The average CH (7.29 mm Hg in group A vs 7.68 mmHg in group B, p>0.05) and DA (1.01mm vs 1.04mm, p>0.05) was not significantly different, but CRF (8.34mm Hg vs 9.43 mm Hg) showed significant difference (p=0.03). CH showed a weak positive relationship with CCT in both groups (r=0.22-0.25, p<0.05). Univariate analysis with CH as the dependent variable in group A showed significant association with CCT, IOPcc, CRF and GAT (p<0.05) in group A; only IOPcc and CRF showed association in multivariate analysis.

Conclusions: CH, which measures viscous damping of cornea was not significantly different between the two groups; CH and DA do not appear to be influenced by CCT. CRF was significantly different between the two groups, suggestive of reduced overall resistance in thinner cornea.

Commercial Relationships: Trupti Patil, None; Rajesh Sasikumar, None; Sathi A. Devi, None

Program Number: 5656 **Poster Board Number:** C0042

Presentation Time: 8:30 AM - 10:15 AM

©2013, Copyright by the Association for Research in Vision and Ophthalmology, Inc., all rights reserved. Go to iovs.org to access the version of record. For permission to reproduce any abstract, contact the ARVO Office at arvo@arvo.org.

Continuous intraocular pressure monitoring with a wireless contact lens and ocular telemetry sensor in patients with open angle glaucoma: pilot study

Claudia Cortes Alcocer^{1,2}, Jesus Jimenez-Roman¹, Felix Gil Carrasco¹, Fernando Del Real². ¹Glaucoma, APEC, Mexico City, Mexico; ²Universidad La Salle, Mexico City, Mexico.

Purpose: To report our initial clinical results with a wireless ocular telemetry sensor (OTS) (Sensimed AG, Switzerland) for continuous intraocular pressure (IOP) monitoring in patients with open angle glaucoma.

Methods: A prospective, observational study. We included 6 patients with clinical diagnosis of open angle glaucoma. All patients underwent a complete ophthalmologic examination, best corrected visual acuity, gonioscopic examination, intraocular pressure (Goldman applanation tonometer), visual field testing and optic nerve examination with stereoscopic photograph. We performed a conventional IOP 24-h monitoring with Goldman applanation tonometer during diurnal period (8:00 am to 5:00 pm) and Perkins applanation and Schiotz indentation tonometry in nocturnal period (8:00 pm to 6:00 am) The OTS is a disposable silicone contact lens with an embedded micro-electromechanical system, which measures changes in corneal curvature induced by variations in IOP. An antenna, mounted around the eye, receives the data and it is transmitted to a recorder. Patients were asked to fill a tolerability and comfort form in which they grade their level of ocular comfort an some symptoms on a 10 grade scale.

Results: A successful signal was recorder in all of our patients. The mean age was 65.5 \pm 7.3 years, 75% were female. The highest signals were recorded during the nocturnal period and we found that this peaks correlate with the time were the highest IOP values were measured in the conventional IOP monitoring. The mean of the mayor variation recorded was 55.5 μ m \pm 8.8 μ m. Prolonges Peaks (>1 hr) were observed in all patient occurring outside office hours. No serious adverse events were reported. Average patient score for comfort was 6.5 and the most frequent symptoms were itching from the antenna patch, foreign body sensation, and redness.

Conclusions: We found a positive correlation between the conventional 24-h IOP monitoring and the contact lens monitoring. Intraocular pressure fluctuations were detected and recorded successfully with the Triggerfish device. This OTS has the potential to improve clinical approach and assessment of glaucoma patients because static IOP measurements obtained in diurnal or nocturnal testing only estimates a portion of the 24-h IOP and do not reflect the dynamic nature of IOP.

Commercial Relationships: Claudia Cortes Alcocer, None; Jesus Jimenez-Roman, None; Felix Gil Carrasco, None; Fernando Del Real, None

Program Number: 5657 **Poster Board Number:** C0043

Presentation Time: 8:30 AM - 10:15 AM

Development of an implantable system for measuring intraocular pressure in rats

Christopher L. Passaglia¹, Simon Bello², Radouil T. Tzekov^{3,4}, Sharad S. Malavade³. ¹Chemical and Biomedical Engineering, University of South Florida, Tampa, FL; ²Electrical Engineering, University of South Florida, Tampa, FL; ³Ophthalmology, University of South Florida, Tampa, FL; ⁴Roskamp Institute, Sarasota, FL.

Purpose: To devise a method of continuously recording the intraocular pressure of a rat's eye in order to monitor pressure changes induced by experimental glaucoma or other processes on a 24-hr basis.

Methods: The system consists of a small custom-designed pressure sensor connected directly to the anterior chamber of the eye via a

cannula and fine-bore tubing. The pressure sensor was fabricated by removing the plunger of a 1ml syringe, cutting the syringe down in length, and gluing over the cut end a thin plastic film which acts as a diaphragm. A small semiconductor strain gauge was then glued to the outside surface of the diaphragm and sealed. The leads of the strain gauge were connected to an electronic circuit consisting of a small battery, a Wheatstone bridge, an amplifier, and a filter. The pressure signal sensed by the circuit will ultimately be transmitted wirelessly to a receiver, but for testing purposes was sent to a data acquisition board for analysis and display. The syringe and connective tubing were filled with artificial aqueous humor, and the tubing was tunneled subcutaneously from an incision in the scalp to the eye orbit and out a small hole in the conjunctiva near the limbus. Due to the small dimensions of the rat eye, a special cannula and surgical procedure was developed to penetrate the cornea and maintain the cannula in place without damaging the iris or other internal structures.

Results: The system was tested by applying hydrostatic and hydrodynamic pressure directly to the sensor at first and then indirectly via a second cannula in the rat eye. Pressure amplitude was varied by randomly altering the height of a saline bath connected to a manometer in parallel with the sensor. The height variations caused an injection or aspiration of fluid through the cannula, which deflected the sensor diaphragm and generated a stable pressure voltage signal that was detectable up to 80 mmHg with a resolution of <0.5mmHg.

Conclusions: The results show that it is possible to cannulate the anterior chamber of the rat eye and directly record intraocular pressure for a prolonged period of time with a pressure sensor that is implantable in a rat, which paves the way for chronic studies in awake animals.

Commercial Relationships: Christopher L. Passaglia, None; Simon Bello, University of South Florida (E), University of South Florida (P); Radouil T. Tzekov, None; Sharad S. Malavade, None

Program Number: 5658 **Poster Board Number:** C0044

Presentation Time: 8:30 AM - 10:15 AM

24-hour IOP monitoring with the SENSIMED Triggerfish contact lens: effect of sleep position and assessment of upward drift

Laura Beltran-Agullo¹, Jason Cheng¹, Yvonne M. Buys^{1,2}, Farzana Jahan³, John G. Flanagan^{1,2}, Colin M. Shapiro^{3,1}, Naheed Hossain³, Sonja Simon-Zoula⁴, Graham E. Trope^{1,2}. ¹Ophthalmology, Toronto Western Hospital, Toronto, ON, Canada; ²University of Toronto, Toronto, ON, Canada; ³Sleep Research Unit, Toronto Western Hospital, Toronto, ON, Canada; ⁴Sensimed AG, Lausanne, Switzerland.

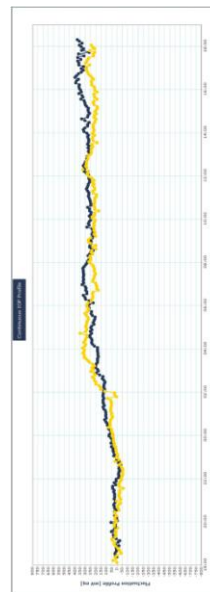
Purpose: To determine the difference in relative IOP measured by the SENSIMED Triggerfish (TF) in flat compared to 30 degree head-up sleeping positions in patients with glaucoma and describe an IOP “drift” phenomenon observed after 24h monitoring session.

Methods: Patients with progressive POAG or NTG (defined as a new or recurrent optic disc haemorrhage) were included in this prospective, randomized, cross-over comparative study. IOP fluctuation was monitored for 24hr using the TF sensor in 2 separate sessions. Patients were randomly assigned to sleep flat one night and 30 degree head-up the other. TF IOP-monitoring curves in arbitrary units were obtained. Comparisons of IOP (measured by applanation tonometry), corneal central thickness (CCT) and spheric equivalent before the sensor fitting and after its removal were performed. Sleep period was defined as 22-6h. Mean TF outputs between sleep positions were compared. A potential association between IOP change from baseline and last mean TF values before sensor removal

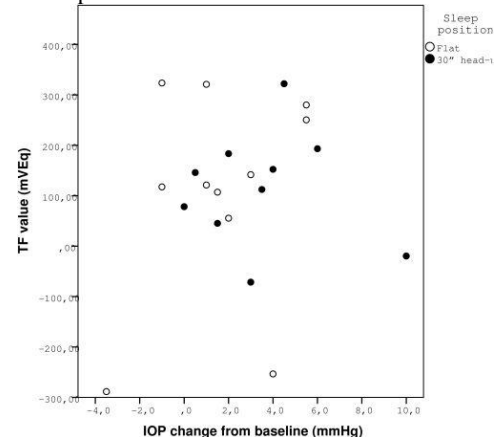
(17-18h) was studied.

Results: Twelve subjects were included in the study. One subject withdrew consent after the first session and was excluded from the analysis. Mean hourly TF values during sleep from 22-6h were significantly higher in 5 of 11 subjects in flat position ($p < 0.05$). However, no differences in overall mean hourly TF values between positions were found ($p > 0.05$ for each interval). A marked increase from baseline in the TF output ($>100\text{mVEq}$) over 24 hours was detected (“DRIFT” phenomenon, fig.1) in 8 of 11 subjects with a mean \pm SD increase of $106,9 \pm 208,2$ mVEq and in 6 of 11 subjects with a mean of $81,33 \pm 153,03$ mVEq in flat and head-up position, respectively. An IOP increase of $1,6 \pm 2,8$ mmHg ($p = 0.08$) in flat and $2,8 \pm 3,0$ mmHg ($p=0,006$) in head-up position after 24h was found. No significant correlation was found between IOP change and last mean TF values (17-18h) before sensor removal (fig.2). The sensor caused a myopic shift ($p < 0.05$) but no significant increase in CCT was found.

Conclusions: Sleep position seems to affect the IOP as measured by TF in some patients with progressive glaucoma. However, the upward drift in TF output detected in more than 50% of the subjects needs to be taken into account when interpreting TF output. Further studies are required to establish whether this drift is an artefact or real.



TF output with drift



Commercial Relationships: Laura Beltran-Agullo, None; Jason Cheng, None; Yvonne M. Buys, Alcon Surgical Incorporated (R), Alcon Surgical Incorporated (F), IMED (F); Farzana Jahan, Sensimed Triggerfish (F); John G. Flanagan, Heidelberg Engineering (C), Heidelberg Engineering (R), Heidelberg Engineering (F), Carl Zeiss Meditec (C), Carl Zeiss Meditec (R), Carl Zeiss Meditec (R), Alcon Pharmaceuticals (R), Alcon Pharmaceuticals (R), Optovue Inc (F), Optovue Inc (F), Photon etc (F), Photon etc (F); Colin M. Shapiro, Triggerfish (F); Naheed Hossain, Sensimed Triggerfish (F); Sonja Simon-Zoula, Sensimed AG (E); Graham E. Trope, Sensimed (F)
Support: Sensimed AG, Lausanne, Switzerland.
Clinical Trial: NCT01351779

Program Number: 5659 **Poster Board Number:** C0045

Presentation Time: 8:30 AM - 10:15 AM

The Effect of Intravitreal Kenolog on Intraocular Pressure in Patients with Glaucoma

Melanie McQueen, Justin Tannir, Rominder Momi, Bret A. Hughes, Anju Goyal, Mark S. Juzych, Chaesik Kim, Alicia M. Eby, Farvah Fatima, Manal H. Peracha. Kresge Eye Institute, Wayne State University School of Medicine, Detroit, MI.

Purpose: Intravitreal triamcinolone acetonide (Kenolog) injections are used to treat a broad spectrum of retinal diseases causing macular edema. The purpose of this study was to determine the effect of intravitreal kenolog injection on intraocular pressure (IOP) in patients with glaucoma, glaucoma suspect or without glaucoma.

Methods: Retrospective chart review of Kresge Eye Institute patients that had received intravitreal kenolog injection. Patients were subdivided into three groups: patients with diagnosis of glaucoma, glaucoma suspect, and patients without glaucoma. Each group was assessed for IOP measurements prior to injection. Subsequent measurements were taken at 1-2, 3-5, and 6-9 months post injection.

Results: Data was collected from 81 patients who had kenolog injections between 2006 and 2012. There were 52 females and 29 males. Average patient age was 60 years. There were 60 (74%) patients without glaucoma, 11 (14%) with glaucoma and 10 (12%) glaucoma suspects. One to two months post injection, IOP increased in 60.3% of the non-glaucoma group (0.87 ± 5.95 mmHg), 38.5% of the Glaucoma group (1.23 ± 9.30) and 57.1% of the Glaucoma Suspect group (1.14 ± 4.10). Within this time period there was one occurrence of acute angle closure requiring surgical intervention in the glaucoma group. Three to five months post injection IOP remained elevated in 44% of the non-glaucoma group (-0.31 ± 4.60), 50% of Glaucoma group (6.29 ± 12.61), and 60% of Glaucoma Suspect (2.2 ± 4.21). Lastly, at six to nine months the IOP remained elevated in 59.1% of non-glaucoma (1.8 ± 6.24), 25% Glaucoma (-3.38 ± 4.57) and 60% of Glaucoma suspect (1.8 ± 4.32). There was no statistically significant difference in IOP change among groups. In addition, there was no significant difference between the pre-injection and post-injection IOP in any of the groups.

Conclusions: Although there were incidences of elevation in IOP post injection in all three groups, upon comparison there was no significant difference among the glaucoma, glaucoma suspect or non-glaucoma patients.

Commercial Relationships: Melanie McQueen, None; Justin Tannir, None; Rominder Momi, None; Bret A. Hughes, None; Anju Goyal, None; Mark S. Juzych, None; Chaesik Kim, None; Alicia M. Eby, None; Farvah Fatima, None; Manal H. Peracha, None

Program Number: 5660 **Poster Board Number:** C0046

Presentation Time: 8:30 AM - 10:15 AM

©2013, Copyright by the Association for Research in Vision and Ophthalmology, Inc., all rights reserved. Go to iovs.org to access the version of record. For permission to reproduce any abstract, contact the ARVO Office at arvo@arvo.org.

COMPARATIVE AGREEMENT AMONG THREE METHODS OF TONOMETRY: GOLDMANN APPLANATION, TRANSPALPEBRAL, AND DYNAMIC CONTOUR

LUIS A. ZARATE¹, Magdalena García-Huerta¹, Rafael Castañeda Diez¹, Mauricio Turati¹, Felix Gil Carrasco¹, Jesus Jimenez-Roman¹, Jose A. Paczka². ¹GLAUCOMA, ASOCIACION PARA EVITAR LA CEGUERA EN MEXICO, Mexico, Mexico; ²Glaucoma, 3. Asistencia e Investigacion en Glaucoma, A.C, Guadalajara, Mexico.

Purpose: To investigate agreement of intraocular pressure (IOP) as measured by the Goldmann applanation tonometer (GAT), the Pascal dynamic contour tonometer (DCT), and Diaton transpalpebral tonometer (DTT).

Methods: Device agreement was calculated by Bland-Altman analysis in 77 eyes of 40 individuals (mean age 58.9 ± 13 years) with a mixed diagnosis of glaucoma suspicion and primary open-angle glaucoma. All measurements were performed in a random order by the same clinician according to standard procedures.

Results: Mean IOPs \pm S.D. were 14.4 ± 2.9 mm Hg (GAT), 18.8 ± 3.2 mm Hg (DCT; $P = 0.005$, ANOVA), and 15.1 ± 3.1 mm Hg (DTT). Bland-Altman analysis demonstrated that, on average, DCT IOP measurements overestimated in approximately 3 mm Hg, values derived from GAT and DTT, although agreement was fairly good.

Conclusions: All methods of tonometry were adequate to measure IOP in our sample. Agreement among devices was considered good; nevertheless, DCT values of IOP were significantly higher as compared to the other two assessed methods.

Commercial Relationships: LUIS A. ZARATE, None; Magdalena García-Huerta, None; Rafael Castañeda Diez, None; Mauricio Turati, None; Felix Gil Carrasco, None; Jesus Jimenez-Roman, None; Jose A. Paczka, None

Program Number: 5661 **Poster Board Number:** C0047

Presentation Time: 8:30 AM - 10:15 AM

Hemofiltration impact on intraocular pressure in patients with end stage renal disease without any evidence of glaucoma

RUTH GEORGINA NAVARRETE ORTEGA¹, RUTH GEORGINA NAVARRETE ORTEGA¹, Hector Perez Grovas^{1,2}. ¹GLAUCOMA, HOSPITAL NUESTRA SEÑORA DE LA LUZ, México, City, Mexico; ²NEFROLOGY, INSTITUTO NACIONAL DE CARDIOLOGIA "IGNACIO CHAVEZ", México, City, Mexico.

Purpose: PURPOSE: To determine the intraocular pressure (IOP) changes in patients with renal replacement therapy by hemofiltration.

Methods: METHODS: 15 patients of 32.5 ± 12 years, with more than 2 months in hemofiltration, steady, without any antihypertensives drugs, and no primary open glaucoma precedent. Tonopen readings of IOP were obtained sequentially 30 minutes before hemofiltration treatment, at 60, 90, 120 and 240 minutes during the procedure and 30 minutes after the treatment. The hemofiltration prescription was with an ordinary FMC-4008H machine, polisulfona F80 filter, and 4 hours long.

Results: RESULTS: The mean basal intraocular pressure was 17.3 ± 4 mmHg for the right eye and 17.0 ± 4 mmHg for the left eye.

According to the Tonopen readings of IOP during the treatment it was found for the right eye 16.7 ± 5 mmHg at 60 minutes, 17.7 ± 5 mmHg at 90 minutes, 17.1 ± 4 mmHg at 120 minutes, 16.6 ± 4 mmHg at 240 minutes and $14.6 \pm 4^*$ mmHg after hemofiltration. And for the left eye were 16.9 ± 4 at 60 minutes, 19.2 ± 3 , at 90 minutes, 17.1 ± 3 at 120 minutes, 17.4 ± 4 at 240 minutes and $15.1 \pm 4^*$ after hemofiltration treatment. Statistical ANOVA was used. There were no statistical significant changes of intraocular pressure during the treatment. Indeed at the end of the treatment it was found a statistical significant decrease of IOP ($p = 0.005$), in contrast with the other time of measure.

Conclusions: CONCLUSIONS: Hemofiltration treatment decreased IOP after 30 minutes of renal replacement therapy.

Commercial Relationships: RUTH GEORGINA NAVARRETE ORTEGA, None; RUTH GEORGINA NAVARRETE ORTEGA, None; Hector Perez Grovas, None
Support:

Clinical Trial:

Program Number: 5662 **Poster Board Number:** C0048

Presentation Time: 8:30 AM - 10:15 AM

Central Corneal Thickness and IOP Response to Topical Ocular Hypotensive Medication in the Low-pressure Glaucoma Treatment Study

Christopher C. Teng^{1,2}, Gustavo De Moraes^{1,2}, Jeffrey M. Liebmann², David S. Greenfield³, Robert Ritch^{1,4}, Theodore Krupin^{5,6}. ¹Ophthalmology, Einhorn Clinical Research Center, New York Eye & Ear Infirmary, New York, NY; ²Ophthalmology, NYU School of Medicine, New York, NY; ³Ophthalmology, Bascom Palmer Eye Institute, Palm Beach Gardens, FL; ⁴Ophthalmology, New York Medical College, Valhalla, NY; ⁵Ophthalmology, Feinberg School of Medicine, Northwestern University, Chicago, IL; ⁶The Chicago Center for Vision Research, Chicago, IL.

Purpose: The Ocular Hypertension Treatment Study (OHTS) showed that IOP response to medical therapy was associated with central corneal thickness (CCT) and that eyes with thinner corneas have a more substantial IOP lowering than those with thick corneas. We aimed to investigate whether CCT correlated with IOP response to topical ocular hypotensive medication in the Low-pressure Glaucoma Treatment Study (LoGTS).

Methods: 253 LoGTS participants were analyzed. The groups were divided into tertiles based on CCT, and the 85 patients with the thickest corneas (Group A) and 85 patients with the thinnest corneas (Group B) were compared. Various parameters were analyzed, including mean IOP during the diurnal curve prior to treatment, follow up IOP peak, trough, mean and fluctuation, absolute and percent IOP reduction, and mean deviation (MD) rate of progression (dB/yr).

Results: As expected, Group A had a thicker CCT than Group B (580.2±23.4 vs. 508.6±20.6 microns, p<0.001). During the diurnal curve, Group A had a higher mean IOP than Group B (16.1±2.3 vs. 15.3±2.6, p=0.05). Follow up mean IOP was lower in Group B than Group A (13.4±2.4 vs. 14.4±2.1 mmHg, p=0.005) as was IOP trough during follow up (10.9±2.4 vs. 11.7±2.5, p=0.037). There was no difference in IOP peak during follow up (p=0.179), IOP fluctuation (p=0.277), absolute IOP reduction (p=0.41) or percent IOP reduction (p=0.20). There was no difference in the mean deviation slopes between Group A and B (-0.14±0.82 vs. -0.26±1.01, p=0.38).

Conclusions: Unlike the OHTS findings, there was no correlation between IOP response to medical therapy and CCT in eyes with low pressure glaucoma.

Commercial Relationships: Christopher C. Teng, None; Gustavo De Moraes, None; Jeffrey M. Liebmann, Alcon Laboratories, Inc. (C), Allergan, Inc. (C), Allergan, Inc. (F), Carl Zeiss Meditec, Inc (F), Heidelberg Engineering, GmbH (F), Topcon Medical Systems, Inc. (F), National Eye Institute (F), New York Glaucoma Research Institute (F), SOLX, Inc. (C), Bausch & Lomb, Inc (C), Diopsys, Inc. (C), Diopsys, Inc. (F), Merz, Inc. (C), Glaukos, Inc. (C), Quark, Inc. (C); David S. Greenfield, National Eye Institute (R), Carl Zeiss Meditec (R), Optovue (R), Heidelberg Engineering (R), Allergan (C),

Alcon (C), Merz (C), Quark (C), SOLX (C), Biometric Imaging (C), Senju (C); Robert Ritch, None; Theodore Krupin, None
Support: Allergan, Inc., Irvine, California; the Chicago Center for Vision Research, Chicago, Illinois; Research to Prevent Blindness, Inc., New York, NY; Corinne Graber Research Fund of the New York Glaucoma Research Institute, New York, NY. Study medications were provided by Allergan, Inc.; Dr. De Moraes is the Edith C. Blum Foundation Research Scientist, New York Glaucoma Research Institute, New York, NY.

Clinical Trial: NCT00317577

Program Number: 5663 **Poster Board Number:** C0049

Presentation Time: 8:30 AM - 10:15 AM

Comparison of Intraocular Pressure Measurements Using a Tono-Pen with Ocufilm + Cover Versus Examination Glove Fingertip Cover

Daniel Apple, Bethany Markowitz. Ophthalmology, University of South Carolina School of Medicine, Columbia, SC.

Purpose: To compare intraocular pressure (IOP) measurements taken with a Tono-Pen XL (Reichert Technologies) using Ocufilm + covers (Reichert Technologies) to measurements taken using the fingertip of a Criterion Pure Nitrile examination glove (Henry Schein Medical).

Methods: Subjects without glaucoma, known ocular pathology, history of intraocular surgery, or trauma were recruited into this study. Proparacaine was applied to both eyes of subjects seated in an upright position. IOP was obtained in the right eye immediately followed by the left eye using Ocufilm + covers. After resting for 5 minutes, proparacaine was reapplied and the IOP was measured in the same fashion using the fingertip of a nitrile examination glove. A single operator measured the IOP in each eye, and only measurements with a 95% confidence interval noted by the Tono-pen were accepted.

Results: The IOP of 12 eyes was studied. The average right eye IOP when checked with Ocufilm and gloves was 13 mmHg using both methods with a standard deviation of 2.8 mmHg and 5.5 mmHg respectively and an average difference of 0. The average left eye IOP was 14.5 mmHg when checked with Ocufilm covers with a standard deviation of 2.4 mmHg. Using gloves, the average left eye IOP was 15.0 mmHg with a standard deviation of 5.1 mmHg. The average difference was 0.5 mmHg. The absolute IOP difference between Ocufilm covers and gloves was 4.3 mmHg (range 1-9 mmHg) for the right eye and 4.5 mmHg (range 1-8 mmHg) for the left eye.

Conclusions: The IOP measurements varied when taken with Ocufilm and fingertips in the same eye with an average difference of approximately 4 mmHg. Variability within the glove tip measurements is evidenced by a standard deviation nearly twice the amount of that the Ocufilm when performed on the same subjects. Also of note, the subjects of this study noted significant increase in time required to obtain an acceptable measurement with 95% confidence interval while using the nitrile glove. Not only were multiple attempts more commonly required, but measurements themselves were more lengthy. Time required for measurements was not objectively monitored during this study. From this preliminary study, we conclude that glove tips should not be relied on for clinical decision making; however, further study involving more subjects and timing of measurements would be beneficial to further explore this topic further.

Commercial Relationships: Daniel Apple, None; Bethany Markowitz, None

523 Structure/Function

Thursday, May 09, 2013 10:30 AM-12:15 PM

6B Paper Session

Program #/Board # Range: 5914-5920

Organizing Section: Glaucoma

Program Number: 5914

Presentation Time: 10:30 AM - 10:45 AM

Relationships among Visual Cortex Metabolism, Retinal Morphology and Visual Function in Early and Advanced Glaucoma

Kevin C. Chan^{1,2}, Ian P. Conner¹, Zaid Safiullah², Seong-Gi Kim^{3,2}, Gadi Wollstein¹, Joel S. Schuman^{1,2}. ¹UPMC Eye Center, Eye and Ear Institute, Ophthalmology and Visual Science Research Center, Department of Ophthalmology, University of Pittsburgh, Pittsburgh, PA; ²Department of Bioengineering, University of Pittsburgh, Pittsburgh, PA; ³Department of Radiology, University of Pittsburgh, Pittsburgh, PA.

Purpose: Glaucoma is a neurodegenerative disease of the visual system. Although recent reports indicate the involvement of the visual brain, apart from the eye, in glaucoma, its underlying pathophysiological mechanisms remain largely unknown. This study evaluated the visual cortical metabolism in association with structural and functional ophthalmic clinical measurements in early and advanced glaucoma.

Methods: 5 early (age=68.0±4.6 yrs) and 5 advanced glaucoma patients (age=68.2±3.5 yrs) underwent proton magnetic resonance spectroscopy (1H-MRS) of both left and right primary visual cortex using a 3 Tesla MRI scanner. Peak integrals of visual brain metabolites [N-acetylaspartate (NAA), creatine (Cr), choline (Cho), glutamate/glutamine complex (Glx), myo-inositol (Ins)] were determined from 1H-MRS using the syngo MR software. The global averages of clinical spectral-domain OCT measurements [peripapillary retinal nerve fiber layer (pRNFL) thickness; macular ganglion cell/inner plexiform layer (mGCL+IPL) thickness; cup-to-disc ratio (c/d)] and Humphrey visual field (VF) pattern standard deviation (PSD) were also obtained in each eye of the same patients. The OCT and VF parameters averaged between both eyes or in the worst eye alone were compared with brain metabolite peak integrals relative to Cr. Mann-Whitney tests were also performed between early and advanced glaucoma.

Results: Significant differences were obtained in all OCT and VF measurements between early and advanced glaucoma (p<0.05). In 1H-MRS, Cho:Cr in the visual cortex was lower in advanced glaucoma than in early glaucoma (p<0.05). Positive correlations were found when comparing pRNFL with Cho:Cr and Ins:Cr, mGCL+IPL with Cho:Cr and Ins:Cr, and c/d with Glx:Cr (p<0.05); whereas negative correlations were observed when comparing pRNFL with Glx:Cr, c/d with Cho:Cr and Ins:Cr, and PSD with Cho:Cr (p<0.05). No apparent correlation was found between NAA:Cr and clinical parameters (p>0.05).

Conclusions: The current results indicated the close associations between visual brain metabolisms and structural and functional clinical ophthalmic findings in glaucoma. These changes were detected prior to alterations in neuronal integrity marker NAA:Cr and may be a sensitive means to assess glaucoma. They also suggested the involvement of cholinergic and glutamatergic neurotransmission systems in the mechanisms of glaucoma in visual cortex.

Commercial Relationships: Kevin C. Chan, None; Ian P. Conner, None; Zaid Safiullah, None; Seong-Gi Kim, None; Gadi Wollstein, Allergan (C); Joel S. Schuman, Carl Zeiss Meditec, Inc. (P)

Support: NIH Grant P30-EY008098; Eye and Ear Foundation (Pittsburgh, PA); Research to Prevent Blindness

Program Number: 5915

©2013, Copyright by the Association for Research in Vision and Ophthalmology, Inc., all rights reserved. Go to iovs.org to access the version of record. For permission to reproduce any abstract, contact the ARVO Office at arvo@arvo.org.

Presentation Time: 10:45 AM - 11:00 AM

The relationship between cup/disc ratio and estimated number of retinal ganglion cells

Andrew J. Tatham¹, Robert N. Weinreb¹, Linda M. Zangwill¹, Jeffrey M. Liebmann², Christopher A. Girkin³, Felipe A. Medeiros¹.

¹Hamilton Glaucoma Center, University California San Diego, La Jolla, CA; ²Department of Ophthalmology, New York Eye and Ear Infirmary, New York, NY; ³Department of Ophthalmology, University of Alabama, Birmingham, AL.

Purpose: To investigate the relationship between cup/disc ratio (CDR) and estimates of retinal ganglion cell (RGC) number derived from spectral domain optical coherence tomography (SD-OCT) and standard automated perimetry (SAP).

Methods: A cross-sectional study of 336 eyes of 209 subjects from the African Descent and Glaucoma Evaluation Study (ADAGES) and the Diagnostic Innovations in Glaucoma Study (DIGS). The study included 156 healthy eyes, 53 glaucoma suspects and 127 eyes with glaucoma tested with SAP, Cirrus SD-OCT and stereoscopic optic disc photography within 6 months. CDR was determined from stereoscopic photographs by two or more experienced masked graders. Severity of glaucoma was defined using the Hodapp-Anderson-Parrish classification. The number of RGCs in each eye was estimated using a previously published model that combines estimates of RGC number from SAP sensitivity thresholds and SD-OCT retinal nerve fiber layer thickness measurements.

Results: The mean estimated RGC count was 1,062,105 in healthy eyes, 828,062 in glaucoma suspects, 778,888 in early glaucoma, 483,176 in moderate glaucoma, and 228,229 in advanced glaucoma. Healthy eyes had a mean vertical CDR of 0.45 ± 0.15 compared to 0.80 ± 0.16 in glaucomatous eyes. The relationship between estimated RGC counts and vertical CDR was best represented using a 3rd degree polynomial regression model, including age and optic disc area, which accounted for 83.6% of the variation in estimated RGC counts (Figure 1). The non-linear relationship between the RGC estimates and CDRs indicated that eyes with a large CDR would require loss of large numbers of RGCs for a small increase in CDR.

Conclusions: The relationship between estimated RGC counts and CDR suggests that assessment of change in CDR is an insensitive method for evaluation of progressive neural losses in glaucoma. Even relatively small changes in CDR may be associated with large losses of RGCs, especially in eyes with large CDRs.

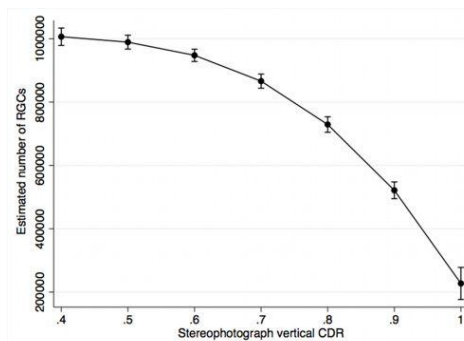


Figure 1. The relationship between estimated number of retinal ganglion cells (RGCs) and vertical CDR as fitted by the polynomial regression model. Results are for age and optic disc area corresponding to average values in the sample.

Commercial Relationships: Andrew J. Tatham, None; Robert N. Weinreb, Aerie (F), Alcon (C), Allergan (C), Altheos (C), Amakem (C), Bausch&Lomb (C), Carl Zeiss-Meditec (C), Genentech (F), Haag-Streit (F), Heidelberg Engineering (F), Konan (F), Lumenis (F),

ARVO 2013 Annual Meeting Abstracts by Scientific Section/Group – Glaucoma

National Eye Institute (F), Nidek (F), Optovue (C), Quark (C), Solx (C), Topcon (C); **Linda M. Zangwill**, Carl Zeiss Meditec Inc (F), Heidelberg Engineering GmbH (F), Optovue Inc (F), Topcon Medical Systems Inc (F), Nidek Inc (F); **Jeffrey M. Liebmann**, Alcon Laboratories, Inc. (C), Allergan, Inc. (C), Allergan, Inc. (F), Carl Zeiss Meditec, Inc (F), Heidelberg Engineering, GmbH (F), Topcon Medical Systems, Inc. (F), National Eye Institute (F), New York Glaucoma Research Institute (F), SOLX, Inc. (C), Bausch & Lomb, Inc (C), Diopsys, Inc. (C), Diopsys, Inc. (F), Merz, Inc. (C), Glaukos, Inc. (C), Quark, Inc. (C); **Christopher A. Girkin**, SOLX (F), Heidelberg Engineering (F); **Felipe A. Medeiros**, Carl-Zeiss (F), Heidelberg Engineering (F), Topcon (F), Alcon (F), Allergan (F), Sensimed (F), Reichert (F)

Support: NIH/NEI Grants EY021818, EY11008, EY14267, EY019869

Clinical Trial: NCT00221923

Program Number: 5916

Presentation Time: 11:00 AM - 11:15 AM

Machine Classifier Clustering of Ocular Structure Measurements Poorly Corresponds with Longitudinal Functional Performance in Glaucoma

Jessica E. Nevins¹, David Danks^{2,3}, Gadi Wollstein¹, Hiroshi Ishikawa^{1,4}, Larry Kagemann^{1,4}, Ian A. Sigal^{1,4}, Joel S. Schuman^{1,4}.

¹UPMC Eye Center, Eye and Ear Institute, Ophthalmology and Visual Science Research Center, Department of Ophthalmology, University of Pittsburgh, Pittsburgh, PA; ²Department of Philosophy, Carnegie Mellon University, Pittsburgh, PA; ³Institute for Human & Machine Cognition, Pensacola, FL; ⁴Department of Bioengineering, Swanson School of Engineering, University of Pittsburgh, Pittsburgh, PA.

Purpose: Structure and function measurements are both used to assess glaucomatous damage. The purpose of this study was to evaluate the association between longitudinal structural and functional measurements.

Methods: 5330 visits from 694 healthy, glaucoma suspect, and glaucomatous eyes were used. Each eye had at least two visits with visual field (VF) tests and at least two ocular imaging devices obtained in each visit: scanning laser polarimetry (GDx with enhanced corneal compensation and with variable corneal compensation), confocal scanning laser ophthalmoscopy (HRT), time-domain (Stratus) and spectral-domain (RTVue) optical coherence tomography. Four different machine learning classifier methods were used to cluster the eyes based on all structural parameters. Two methods (k-means and k-medoids) find compact, convex clusters defined by center points in parameter space. The other two methods (hierarchical agglomerative and divisive) build clusters through iterative grouping and splitting, and so can yield complex, non-convex clusters. These clusters were tested for correlation with functional measurements from VF tests.

Results: The mean baseline age of the study population was 59.2 (range: 16.5-85.1) years with a mean follow-up length of 5.0 (0.4-7.8) years and a mean of 8 (2-24) visits. Clustering within each device was stable with a minimal correlation coefficient =0.85 and half the correlations >0.95 by comparing clusters created when using all the data compared to subsamples of the data. Clustering between devices was highly correlated with a minimal correlation coefficient =0.80 and over half the correlations >0.90. There was poor correspondence with predicting the VF measurements at the next visit or the rates of VF measurement change with a maximum correlation =0.50 and over half the correlations <0.30.

Conclusions: The presence of structural changes was confirmed by the good agreement among clusters based on structure, regardless of

the algorithm used for clustering. Nevertheless, structure clusters were dissociated from longitudinal functional changes. It is unknown if this is because of a lack of association between structure and function or because different clusterings are needed between them.

Commercial Relationships: **Jessica E. Nevins**, None; **David Danks**, None; **Gadi Wollstein**, Allergan (C); **Hiroshi Ishikawa**, None; **Larry Kagemann**, None; **Ian A. Sigal**, None; **Joel S. Schuman**, Carl Zeiss Meditec, Inc. (P)

Support: NIH R01-EY013178, P30 EY008098; Eye and Ear Foundation (Pittsburgh, PA); Research to Prevent Blindness (New York, NY).

Program Number: 5917

Presentation Time: 11:15 AM - 11:30 AM

Posterior Lamina Cribrosa Displacement at Different Stages of Glaucoma

Sung Chul Park^{1,2}, Rafael L. Furlanetto¹, Camila F. Netto¹, Yiyi Liu^{1,3}, Yungtai Kung^{1,3}, Sandra Fernando-Sieminski⁴, Jeffrey M.

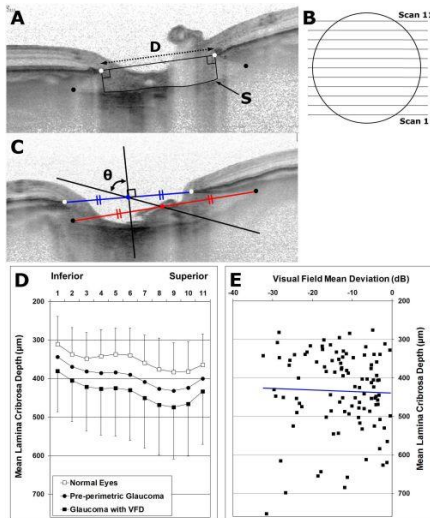
Liebmann^{1,5}, Robert Ritch^{1,2}. ¹Moise and Chella Safra Advanced Ocular Imaging Laboratory, Einhorn Clinical Research Center, New York Eye and Ear Infirmary, New York, NY; ²Department of Ophthalmology, New York Medical College, Valhalla, NY; ³New York Medical College, New York, NY; ⁴Ross Eye Institute, State University of New York at Buffalo, Buffalo, NY; ⁵Department of Ophthalmology, New York University School of Medicine, New York, NY.

Purpose: To compare in vivo lamina cribrosa (LC) position between normal subjects and patients with glaucoma at different stages.

Methods: Normal subjects and glaucoma patients at various disease stages were recruited. All participants had a complete ophthalmologic examination including standard automated perimetry (SAP; 24-2 SITA-standard, Humphrey Field Analyzer). Serial horizontal enhanced depth imaging optical coherence tomography (EDI OCT) B-scans of the optic nerve head were obtained from each participant (interval between scans, ~30 μ m). After delineating the anterior LC surface, mean LC depth (reference plane, Bruch's membrane edges) was measured in 11 equally spaced horizontal B-scans for one eye of each participant, excluding the LC insertion area under Bruch's membrane and the scleral rim (Fig A and B). Mean LC depth was compared among 1) normal eyes, 2) glaucomatous eyes with no visual field defects (VFD) (pre-perimetric glaucoma), and 3) glaucomatous eyes with VFD. Age, intraocular pressure (IOP) and angle of lateral LC displacement (Fig C) were recorded.

Results: 62 normal eyes (mean age, 55 \pm 17 years), 43 pre-perimetric glaucoma eyes (mean age, 61 \pm 17 years), 104 glaucomatous eyes with VFD (mean age, 59 \pm 17 years; mean VF mean deviation [MD], -12.9 \pm 8.2 dB) were included. Mean LC depth was significantly different among the glaucoma with VFD, pre-perimetric glaucoma, and normal groups (434 \pm 102, 395 \pm 74, and 351 \pm 70 μ m, respectively), before and after controlling for age, IOP and angle of lateral LC displacement (all p<0.03). Mean LC depth was significantly greater in the same order in all 11 scans after controlling for age, IOP and angle of lateral LC displacement (all p<0.04; Fig D). Among glaucomatous eyes with VFD, mean LC depth had no significant correlation with VF MD (p=0.14; Fig E).

Conclusions: In human glaucoma, posterior displacement of the central and mid-peripheral LC occurs mostly at earlier stages of glaucoma before the development of VFD detectable in SAP.



(A) White dots = Bruch's membrane edges; black dots = anterior LC insertion points; mean LC depth = (area S/length D). (B) The circle indicates the LC. (C) Angle of lateral LC displacement (θ) was measured in the horizontal midline scan of the LC. Blue dot = midpoint between the 2 Bruch's membrane edges. Red dot = midpoint between the 2 anterior LC insertion points. (D) Mean LC depth profiles. (E) Scatterplot of mean LC depth vs. VF MD.

Commercial Relationships: Sung Chul Park, None; Rafael L. Furlanetto, None; Camila F. Netto, None; Yiyi Liu, None; Yungtai Kung, None; Sandra Fernando-Sieminski, None; Jeffrey M. Liebmann, Alcon Laboratories, Inc. (C), Allergan, Inc. (C), Allergan, Inc. (F), Carl Zeiss Meditec, Inc (F), Heidelberg Engineering, GmbH (F), Topcon Medical Systems, Inc. (F), National Eye Institute (F), New York Glaucoma Research Institute (F), SOLX, Inc. (C), Bausch & Lomb, Inc (C), Diopsys, Inc. (C), Diopsys, Inc. (F), Merz, Inc. (C), Glaukos, Inc. (C), Quark, Inc. (C); **Robert Ritch**, None

Support: Gloria Rubin and Michael Fux Research Fund of the New York Glaucoma Research Institute, New York, NY; James Cox Chambers Research Fund of the New York Eye and Ear Infirmary, New York, NY; American Glaucoma Society MAPS Award; Peter Crowley Research Fund of the New York Eye and Ear Infirmary, New York, NY

Program Number: 5918

Presentation Time: 11:30 AM - 11:45 AM

Relating retinal ganglion cell (RGC) function and retinal nerve fiber layer (RNFL) retardance to progressive loss of RNFL thickness (RNFLT)

Brad Fortune, Grant Cull, Juan Reynaud, Claude F. Burgoyne. Discoveries in Sight Research Laboratories, Devers Eye Institute and Legacy Research Institute, Legacy Health, Portland, OR.

Purpose: To relate RGC functional loss and RNFL retardance changes to progressive loss of RNFLT.

Methods: N=36 rhesus macaques with unilateral experimental glaucoma (EG) each had ≥ 3 baseline (BL) measurements of peripapillary RNFLT (Spectralis SDOCT, Heidelberg Engineering, GmbH), retardance (GDxVCC, Carl Zeiss Meditec, Inc) and multifocal electroretinography (mfERG, VERIS, Electro-Diagnostic Imaging, Inc). mfERG responses were high-pass filtered (>75 Hz) to measure high- and low-frequency component (HFC and LFC) amplitudes, including LFC peaks N1, P1 and N2. Chronic unilateral intraocular pressure (IOP) elevation was induced by trabecular

meshwork laser; alternating bi-weekly testing continued (SDOCT one week, SLP and mfERG the next). The measurement noise (95% confidence interval, CI) of each parameter was determined by bootstrapping all BL observations. Onset of RNFLT change was defined as the first of two sequential observations below the noise limit.

Results: Post-laser follow-up was 9 ± 7 months; mean and peak IOP were 18 ± 5 and 39 ± 12 mmHg in EG eyes, 11 ± 2 and 17 ± 6 mmHg in fellow control eyes (CTL). At the final available time point, RNFLT had decreased from BL by $13 \pm 13\%$, retardance by $19 \pm 11\%$ and the mfERG HFC by $29 \pm 17\%$ ($p < 0.0001$ each); CTL eyes changed by $+0.3 \pm 3\%$ ($p = 0.44$), $+0.7 \pm 6\%$, ($p = 0.45$) and $-6 \pm 14\%$ ($p = 0.01$), respectively. Retardance and HFC were correlated with RNFLT at the final time point ($R^2 = 0.57$, $p < 0.0001$ and $R^2 = 0.37$, $p < 0.0001$, respectively) but none of the LFC amplitudes were correlated with RNFLT (N1: $R^2 = 0.08$, $p = 0.1$; P1: $R^2 = 0.04$, $p = 0.3$; N2: $R^2 = 0.08$, $p = 0.1$). A linear model was most appropriate (F-test, $p \geq 0.6$ each) to relate relative loss (final:BL) of each parameter to RNFLT loss; the resultant slope was > 0 for retardance (0.65 , $p < 0.0001$) and HFC (0.72 , $p = 0.001$) but not for any LFC parameter; the Y-intercept was significantly negative for retardance (-11% , 95% CI: -7% to -15%) and mfERG HFC (-20% , 95% CI: -13% to -27%). Onset of RNFLT change occurred in 25/36 EG eyes and 0/36 CTL eyes; at the prior test session (median 8 days earlier), retardance was reduced by $17 \pm 10\%$ and HFC by $28 \pm 13\%$ below BL ($p < 0.0001$ each).

Conclusions: RGC axonal cytoskeletal disruption and specific RGC functional changes, as measured by RNFL retardance and mfERG, respectively, are present at the onset of RNFLT change in EG and correlate with its progressive loss beyond onset.

Commercial Relationships: Brad Fortune, Heidelberg Engineering, GmbH (F), Carl Zeiss Meditec, Inc (F); **Grant Cull**, None; **Juan Reynaud**, None; **Claude F. Burgoyne**, Heidelberg Engineering (F), Heidelberg Engineering (C) **Support:** NIH R01-EY019327 (BF), R01-EY011610 (CFB); Glaucoma Research Foundation (BF); American Health Assistance Foundation (BF); Legacy Good Samaritan Foundation; Heidelberg Engineering, GmbH, Heidelberg, Germany (equipment and unrestricted research support); Carl Zeiss Meditec, Inc. (equipment).

Program Number: 5919

Presentation Time: 11:45 AM - 12:00 PM

Why ISNT Rim Area Greater for Superior Optic Disc?

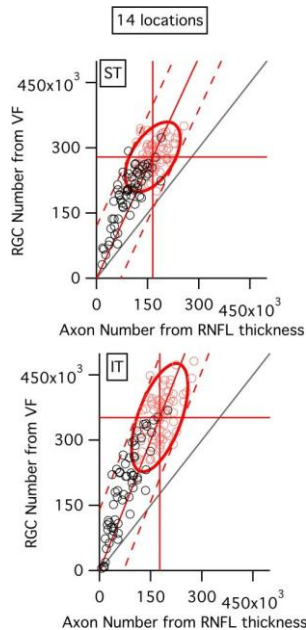
William H. Swanson¹, Victor Malinovsky¹, Mitchell W. Dul². ¹School of Optometry, Indiana University, Bloomington, IN; ²SUNY College of Optometry, State University of New York, New York, NY.

Purpose: Histological data show greater retinal ganglion cell (RGC) density in superior than inferior retina (Curcio & Allen 1990 JCN 300:5), but neuroretinal rim area and retinal nerve fiber layer (RNFL) thickness are not greater for superior optic disc. The hypothesis was that this can be accounted for by macular visual field projection to inferior temporal (IT) but not superior temporal (ST) optic disc sectors (Hood et al, 2012 TVST 1:3).

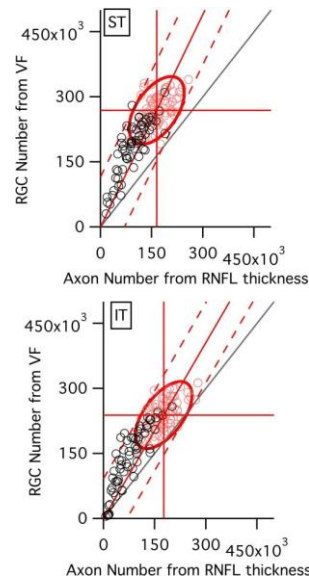
Methods: One eye each of 61 patients with glaucoma and 71 age-similar control subjects was tested with HRT-III for rim area, Stratus OCT 3.4 for RNFL thickness, and 24-2 SITA Standard for visual field (VF) sensitivities. ST and IT optic disc sectors were defined by the 2002 Garway-Heath map (IOVS 43:2213), and estimates of RGCs from VF and RNFL values were derived with the 2007 Harwerth model (IOVS 48:763). Bivariate Gaussian ellipses at $p = 0.90$ characterized control data, and tangents yielded confidence limits for patients. Each sector maps to 14 VF locations: the first 13 locations are mirror images across the horizontal midline, and the 14th location is at 4° for IT and 21° for ST.

Results: Controls had equal rim areas for ST and IT (0.21 mm²), and lower RNFL thickness for ST than IT (127 ± 26 vs. 136 ± 26 μm), yielding fewer RGCs for ST: 165 ± 38 vs. 176 ± 39 × 10³ (t = -3.3, p < 0.002). With 14 locations, VF also yielded fewer RGCs for ST: 279 ± 38 vs. 352 ± 58 × 10³ (t = -17, p < 0.0001). With 13 locations, ST yielded more RGCs than IT: 269 ± 36 vs. 239 ± 36 × 10³ (t = +11, p < 0.0001). The 14th location provided an average of 10 × 10³ RGCs for ST and 113 × 10³ RGCs for IT. In both cases, patient data fell within the confidence limits, and above the line of equality (i.e., RGC estimates were greater for VF than RNFL).

Conclusions: Ganglion cell estimates from perimetry agreed with histological findings of greater ganglion cell density in superior retina, for 13 locations per sector but not 14 locations. This result underscores the role of mapping the macula to the optic disc in structure-function analyses.



RGC estimates for 14 visual field locations per sector. Circles show estimates of RGCs for VF & RNFL. Red circles show control data, ellipses are confidence limits at p=0.90, red horizontal and vertical lines are means. Black diagonal line for equality, red diagonal lines for linear mean (solid) and confidence limits (dashed).



RGC estimates for 13 visual field locations per sector, rest as in Figure 1.

Commercial Relationships: William H. Swanson, None; Victor Malinovsky, None; Mitchell W. Dul, None
Support: NIH Grant R01EY007716

Program Number: 5920

Presentation Time: 12:00 PM - 12:15 PM

Retinal venous pulsatility is reduced in regions of nerve fibre layer loss in glaucoma

Mojtaba Golzan¹, William Morgan², Stuart Graham¹. ¹Macquarie University, Sydney, NSW, Australia; ²Lions Eye Institute, University of Western Australia, Perth, NSW, Australia.

Purpose: Loss of spontaneous retinal venous pulsatility (SRVP) has been described as a new risk factor for glaucoma and its progression. In this study we investigate the magnitude of local SRVP's and retinal venous pulsation pressure (VPP) and correlate these with glaucomatous damage in the same region.

Methods: 20 subjects with primary open angle glaucoma were studied. SRVP amplitude of superior and inferior hemiretinal veins was measured in all patients using the Dynamic Vessel Analyzer (DVA, Imedos). Ophthalmodynamometry (OcuDyn - Perth, WA) was performed to measure VPP in veins with absent visible pulsations. Sectoral RNFL thickness was recorded using Spectralis OCT (Heidelberg). Raw SRVP recordings were passed through a low pass filter (cut of frequency; 5Hz). For each individual, mean SRVP amplitude and then amplitude normalized for IOP (i.e. SRVP/IOP) were plotted against local RNFL thickness (superior and inferior sectors). VPP measurements were also plotted against SRVP amplitude and RNFL thickness.

Results: SRVP was detectable and recordable from hemi-retinal veins in all subjects using the DVA, even though no visible SRVP was present in many cases (using 60D lens). Mean SRVP amplitude for all subjects was 3.9±2.2 μm. SRVP amplitude correlated with RNFL thickness (r₂=0.55), and when normalised for IOP was strongly correlated, with larger SRVP amplitudes observed in thicker RNFL (RNFL=108.1SRVP +42.4, r₂=0.7). An inverse relationship occurred when comparing VPP to SRVP and RNFL thickness. Higher VPPs correlate with less SRVP amplitude (VPP=-3.5SRVP+45.9, r₂=0.25) and thinner RNFL (VPP=-0.28RNFL+53, r₂=0.3). The latter is expected as loss of SRVP at the disc should be associated with less pulsation in adjacent retinal veins. Both

observations support a relationship between reduced venous pulsation and glaucoma.

Conclusions: SRVP is present in all individuals; however the amplitude of pulsation is altered in glaucoma. Lower SRVP amplitude and higher VPP correlate with glaucoma severity. These dynamic parameters may be useful as novel biomarkers for glaucoma risk assessment.

Commercial Relationships: Mojtaba Golzan, None; William Morgan, None; Stuart Graham, None

Support: NHMRC 1020367

542 Genetics II

Thursday, May 09, 2013 10:30 AM-12:15 PM

Exhibit Hall Poster Session

Program #/Board # Range: 6216-6249/C0101-C0134

Organizing Section: Glaucoma

Program Number: 6216 **Poster Board Number:** C0101

Presentation Time: 10:30 AM - 12:15 PM

The association of single nucleotide polymorphisms in the connective tissue growth factor gene with pseudoexfoliation syndrome/glaucoma

Wool Suh¹, Changwon Kee². ¹Ophthalmology, Hallym University Sacred Heart Hosp, Anyang, Kyeonggi-do, Republic of Korea; ²Ophthalmology, Samsung Medical Center, Sungkyunkwan University School of Medicine, Seoul, Republic of Korea.

Purpose: To evaluate the association between single nucleotide polymorphisms of the connective tissue growth factor (CTGF) gene with pseudoexfoliation (PEX) syndrome/glaucoma in the South Korean population.

Methods: Patients with PEX syndrome were recruited and twelve single nucleotide polymorphisms (SNPs; rs6917644, rs9399005, rs2151532, rs928501, rs7768619, rs9388949, rs12192108, rs1475723, rs928505, rs233925, rs170881 and rs9388956) of CTGF were genotyped in genomic DNA extracted by the standard method from leucocytes isolated from the peripheral blood samples of study subjects. The Fisher's exact test was conducted for genotype frequency.

Results: A total of one hundred and seven PEX syndrome patients, including forty one pseudoexfoliative glaucoma patients, were enrolled in the study. In twelve SNPs, rs2151532 and rs928501 were correlated with PEX syndrome. In particular, rs2151532 was significantly correlated with pseudoexfoliative glaucoma. Other SNPs were not significantly associated with PEX syndrome ($P > 0.05$).

Conclusions: The rs2151532 and rs928501 SNPs in the CTGF gene were significantly associated with PEX syndrome, and in particular, rs2151532 SNP showed a significant correlation with pseudoexfoliative glaucoma.

Commercial Relationships: Wool Suh, None; Changwon Kee, None

Support: Samsung Biomedical Research Institute grant, GL1-B2-061-1, and by Basic Science Research Program through the National Research Foundation of Korea (NRF) funded by the Ministry of Education, Science and Technology (S-2012-0401-000).

Program Number: 6217 **Poster Board Number:** C0102

Presentation Time: 10:30 AM - 12:15 PM

CYP1B1 mutations, a major contributor to juvenile-onset open angle glaucoma

Khaled K. Abu-Amero^{1,3}, Jose Morales², Layla Ali Aljasim², Deepak P. Edward². ¹Ophthalmology, College of Med, King Saud Univ,

Riyadh, Saudi Arabia; ²King Khalied Eye Specilaist Hospital, Riyadh, Saudi Arabia; ³Ophthalmology, College of Medicine, Jacksonville, FL.

Purpose: To describe the genotype and phenotype in 14 unrelated Saudis with juvenile open angle glaucoma (JOAG).

Methods: Saudi patients with JOAG were recruited over a three month period. Detailed clinical history, course and genetic history were obtained. Genotyping was performed using PCR and direct Sanger sequencing for cytochrome P450, family 1, subfamily B (CYP1B1), Myocilin (MYOC) and latent-transforming growth factor beta-binding protein 2 (LTBP2) genes in JOAG patients. Additionally, 200 glaucoma-free ethnicity-matched controls were screened for mutations in the CYP1B1 gene.

Results: The mean age of JOAG subject's was 24 years and 13/14 had bilateral disease. Most patients had high intraocular pressures with moderately severe glaucomatous damage in at least one eye in 9/14 patients. Eleven (78.6%) patients had apparent sporadic inheritance and 3 (21.4%) presented with a family history of glaucoma. Overall, 12 patients (85.7%) had either a pathologic or potentially pathologic CYP1B1 mutation. Nine patients (64.3%) had CYP1B1 mutations in a homozygous status. Eight of these had a non-synonymous (g.3987 G>A; p.G61E) mutation in a homozygous status and one had a silent synonymous mutation (g.8184 C>T). Two patients (14.3%) had the g.3987 G>A mutation in a compound heterozygous status with another CYP1B1 mutation (g.8131 C>G; p.L432V). Two patients (14.3%) had CYP1B1 mutation (g.3987 G>A) in a heterozygous status with no other mutation, while one patient (7.1%) had no mutation(s) after sequencing the full coding region of the CYP1B1 gene. In the controls screened for mutations in the CYP1B1 gene, 14 (7%) had the p.G61E mutation in a heterozygous status with a minor allele frequency (MAF) of 0.035. The p.L432V mutation was detected in 30 (15%) controls in a heterozygous status and 2 (1%) controls in a homozygous status, raising doubts about its pathogenic status. None of the 14 patients had a pathologic-mutation in the MYOC or LTBP2 genes.

Conclusions: CYP1B1 mutant JOAG occurs at a high rate in the Saudi population with JOAG. Myocilin or LTBP2 gene-mutations do not appear to play a role in Juvenile-onset open angle glaucoma in this population. The glaucoma phenotype seen in this group of patients resembles that described previously in JOAG caused by MYOC mutations. A specific genotype-phenotype relationship was not demonstrated.

Commercial Relationships: Khaled K. Abu-Amero, None; Jose Morales, None; Layla Ali Aljasim, None; Deepak P. Edward, None

Program Number: 6218 **Poster Board Number:** C0103

Presentation Time: 10:30 AM - 12:15 PM

Last results of the Spanish Multicenter Genetic Glaucoma Group

Elena Milla^{1,5}, Susana Duch², Miguel Carballo³, Maria Jose Gamundi⁴. ¹Institut Comtal d'Oftalmologia and Hospital Clinic, Barcelona, Spain; ²Glaucoma, Institut Comtal d'Oftalmologia, Barcelona, Spain; ³Hospital de Terrassa, Barcelona, Spain; ⁴Hospital de Terrassa, Barcelona, Spain; ⁵Spanish Multicenter Genetic Glaucoma Group, 18 Spanish Eye Centers, Spain, Spain.

Purpose: clinical and genetic characterization of unrelated Spanish patients affected by glaucoma coming from different parts of Spain.

Methods: all individuals underwent complete ophthalmologic examination. Screening for mutations in MYOC and CYP1B1 by direct genomic sequencing was performed in 302 families affected with different forms of glaucoma.

Results: We identified one novel MYOC mutation in a primary open angle glaucoma family, and five previously reported MYOC

mutations in seven families affected by different subtypes of glaucoma. Three novel CYP1B1 mutations were described and thirteen known mutations found in patients mainly with primary congenital glaucoma.

Conclusions: We think that the high rate of CYP1B1 mutations found in (33.3%) our congenital glaucoma patients makes its genetic testing mandatory. The rate of MYOC mutations was similar to the one reported in the literature. The genetic diagnostic of our glaucoma patients was regarded as a useful tool in order to modulate their treatment.

Commercial Relationships: Elena Milla, None; Susana Duch, None; Miguel Carballo, None; Maria Jose Gamundi, None
Support: FIS 07/1210

Program Number: 6219 **Poster Board Number:** C0104

Presentation Time: 10:30 AM - 12:15 PM

Identification of S1 RNA Binding Domain-1 SRBD1 as a Major Gene Determining Glaucoma in Dogs

Nobuyuki Kanemaki¹, Kissaou T. Tchadre², Masaki Imayasu², Akira Meguro³, Nobuhisa Mizuki³. ¹Veterinary Teaching Hospital, Azabu University, Sagamihara, Japan; ²Central R&D Laboratory, Menicon Co., Ltd., Kasugai, Japan; ³Department of Ophthalmology, Yokohama City University School of Medicine, Yokohama, Japan.

Purpose: To investigate the association between glaucoma pathology in Shiba-Inu dog and the polymorphisms of glaucoma candidate genes, SRBD1, ELOVL5 and ADAMTS10.

Methods: Peripheral blood samples were collected from 47 glaucoma with high intraocular pressure (IOP, more than 25 mmHg) and 34 normal Shiba-Inu dogs with normal IOP (less than 25 mmHg). After purification of genomic DNA, SRBD1 gene polymorphisms (rs22018514 and rs22018513), ELOVL5 gene polymorphisms (rs22202438 and rs8643563), and ADAMTS10 gene polymorphisms (the 56097365 G>A variant) were analyzed by the direct DNA sequencing method. Twenty-two (22) glaucoma and 28 control Shih-Tzu dogs were also tested.

Results: The most statistically significant association was observed for rs22018513 (P=0.0019), with a 2.92-fold (95% confidence interval, 1.47-5.81) increased risk of glaucoma in Shiba-Inu dogs as well as Shih-Tzu dogs (P=0.037, odds ratio=7.17 (0.86-59.66)). For rs22018514, significant association was observed in Shiba-Inu dogs (P=0.0030, odds ratio=3.03 (1.43-6.40)) unlike no significant association in Shih-Tzu dogs (P=0.918, odds ratio=1.07 (0.30-3.76)). There were no significant associations between cases and controls for rs22202438, rs8643563 and ADAMTS10 gene polymorphisms (the 56097365 G>A variant) in Shiba-Inu and Shih-Tzu dogs.

Conclusions: The results showed that 2 SNPs of SRBD1 play an important role in the pathology of glaucoma in dog and therefore, SRBD1 is a susceptible gene for glaucoma in Shiba-Inu dog. We anticipated that the single nucleotide sequencing data from this study can be used as a genetic testing to determine for the first time with precision whether a dog has glaucoma and to predict whether a dog will develop glaucoma.

Commercial Relationships: Nobuyuki Kanemaki, None; Kissaou T. Tchadre, Menicon, Co. Ltd (E); Masaki Imayasu, Menicon Co., Ltd. (E); Akira Meguro, None; Nobuhisa Mizuki, None

Program Number: 6220 **Poster Board Number:** C0105

Presentation Time: 10:30 AM - 12:15 PM

MYOC Variants In POAG In Black South Africans

Susan E. Williams¹, Tasha Wainstein², Trevor R. Carmichael¹, Michele Ramsay². ¹Ophthalmology, University of the Witwatersrand, Johannesburg, South Africa; ²Human Genetics, University of the Witwatersrand, Johannesburg, South Africa.

Purpose: Mutations in the MYOC gene are important as causal factors in some forms of POAG. Sequencing of the MYOC gene in black South Africans previously identified 3 potentially pathogenic mutations. The aim of this study was to examine the role of these mutations in the etiology of POAG in this population.

Methods: The mutations are listed in Table 1. They were genotyped in 215 black South African POAG patients and 214 controls using the Illumina BeadXpress genotyping platform. Family members of participants identified with the mutations were counseled and screened for glaucoma with a clinical examination. Sanger sequencing was used for mutation detection.

Results: The results of the BeadXpress genotyping and the mutation screening are listed in Table 1. None of the relatives screened for Gly374Val had the mutation or POAG. A sibling of a similar age to the Lys500Arg index case carried the mutation but had no evidence of POAG whereas the index case's daughter was a POAG suspect but did not carry the mutation. Of the 4 relatives that were carriers of the Tyr453del mutation, 1 was diagnosed with POAG and 1 was a POAG suspect. The 19 year old daughter of a POAG patient and the 38 year old son of an unaffected control did not have POAG but carried the mutation. In this small sample, the penetrance of this mutation was 25% at 50 years and 75% at 70 years. POAG patients with the mutation have adult-onset POAG with high intraocular pressures and advanced cupping (Table 2).

Conclusions: Black South Africans with POAG may have a MYOC mutation that either causes or contributes to their risk for developing POAG in approximately 3.3%. The commonest mutation is a frameshift mutation (Tyr453del) that is incompletely penetrant. It is likely that the mutation causes gain-of-function due to a truncated protein. That the mutation is necessary but insufficient introduces a counseling dilemma. Mutation screening can, however, identify high-risk individuals who can be monitored to detect early signs of the disease. The Gly374Val mutation is predicted to be damaging to MYOC. It is an uncommon cause of POAG in this population. The Lys500Arg mutation is predicted to be benign and tolerated. In the family with the mutation, it did not segregate with the disease suggesting that it is a neutral polymorphism. This study has important implications for the management and counseling of black South African patients with POAG and their families.

Table 1. Potential MYOC mutations identified in black South Africans and their family members

Amino acid change	Gly374Val	Tyr453del	Lys500Arg
Nucleotide Sequence Change *	c.1121G>T	c.1357delT	c.1499A>G
Controls (214)	0	2	0
POAG (215)	2	5	2
Family members screened	4	15	6
Family members with the mutation	0	4	1

*Nucleotides numbered as in Ensembl accession number ENSG00000034971 (transcript ENST00000037502)

Table 2. Characteristics of POAG participants with the Tyr453del mutation compared with all the POAG participants

	Tyr453del+ (n=6)	POAG (n=247)	P
Gender	66.7% Female	50.2% Female	
Age at diagnosis (years)	62.2 ± 9.1	55.0 ± 13.6	0.119
IOP (mmHg)	33.6 ± 2.0	34.9 ± 9.1	0.184
CCT (µm)	490.7 ± 29.5	505.1 ± 37.9	0.294
VCDR	0.96 ± 0.06	0.89 ± 0.13	0.043
MD (dB)	-9.9 ± 5.1	-10.4 ± 5.4	0.860
GDx NFI	59.3 ± 17.5	68.2 ± 22.9	0.394
GDx TSNIT	38.4 ± 5.8	36.9 ± 8.7	0.651
Cataracts	50.0%	49.0%	
IOP control	60.0%	68.0%	
Severe visual impairment	50.0%	53.0%	
Glaucoma Surgery	40.0%	54.0%	

Commercial Relationships: Susan E. Williams, None; Tasha Wainstein, None; Trevor R. Carmichael, None; Michele Ramsay, None

Support: Trevor Carmichael has a South African MRC (Medical Research Council) Self-Initiated Research. Susan Williams holds a Carnegie Clinical Scientist PhD Fellowship.

Program Number: 6221 **Poster Board Number:** C0106

Presentation Time: 10:30 AM - 12:15 PM

Genetic Susceptibility Variations and Visual Field Progression in Chinese Patients with Primary Angle Closure Glaucoma

Xin Wei^{1,2}, Chia Chuen Khor^{3,4}, John Mark S. de Leon², Eranga N. Vithana^{2,4}, Monisha E. Nongpiur^{2,4}, Shamira Perera², Tin Aung^{2,4}.

¹Duke-National University of Singapore Graduate Medical School, Singapore, Singapore; ²Singapore Eye Research Institute, Singapore National Eye Center, Singapore, Singapore; ³Human Genetics, Genome Institute of Singapore, Singapore, Singapore; ⁴Department of Ophthalmology, National University Health System & National University of Singapore, Singapore, Singapore.

Purpose: Recently three susceptibility loci (rs3753841 in *COL11A1*, rs1015213, and rs11024102 in *PLEKHA7*) were found to be associated with primary angle closure glaucoma (PACG) through a genome-wide association study (Vithana EN et al, Nat Genetics 2012). We now investigate the contribution of these three loci on visual field (VF) progression in PACG patients with longitudinal VF data.

Methods: This was a retrospective case-only analysis in which PACG patients of Singaporean Chinese descent who had at least 5 years of follow-up and at least 5 VF tests (SITA 24-2, Carl Zeiss Meditec, Dublin, CA) were included. These patients had been previously genotyped for the 3 genetic variants. VF analysis was performed using pointwise linear regression (PROGRESSOR, Medisoft, Ltd, Leeds, England). Outcome measures were VF progression defined as 2 or more adjacent progressing points (slope p<0.01) in the same hemifield; and mean slope of sensitivity loss.

Results: A total of 355 eyes from 222 subjects were studied. The mean (SD) number of VF tests performed was 9.37 (4.15) and the mean (SD) duration of follow-up was 10.47 (3.13) years. For *COL11A1* rs3753841, 164 eyes were from wildtype subjects while

139 and 52 eyes were from heterozygous and homozygous variants, respectively. The rate of VF progression of eyes that were wild-type, heterozygous and homozygous for *COL11A1* was 14.02%, 9.35% and 3.85%, respectively (per allele odds ratio=0.56, P=0.03), although this observation was non-significant when corrected for multiple testing. The mean slope of sensitivity loss in the entire VF of eyes that were wild-type, heterozygous and homozygous for *COL11A1* did not show significant difference (P = 0.77) and neither did the mean slope of sensitivity loss among the progressing points (P = 0.89). No significant difference was found in the rate of progression, mean slope of sensitivity loss in the entire VF or among the progressing points for the other two loci.

Conclusions: We did not observe evidence of association between the three PACG susceptibility loci and progression of VF loss in this cohort of PACG patients drawn from the original GWAS study. We acknowledge that our current sample collection may be under-powered to detect such effect sizes with regards to VF progression. **Commercial Relationships:** Xin Wei, None; Chia Chuen Khor, None; John Mark S. de Leon, None; Eranga N. Vithana, None; Monisha E. Nongpiur, None; Shamira Perera, Carl Zeiss Meditec (R), Allergan (R), Pfizer (R); Tin Aung, Alcon (R), Alcon (C), Alcon (F), Allergan (R), Allergan (C), Carl Zeiss Meditec (F), Carl Zeiss Meditec (R), Ellex (F), Ellex (R), Santen (R)

Program Number: 6222 **Poster Board Number:** C0107

Presentation Time: 10:30 AM - 12:15 PM

The Association Between Ocular Biometric Parameters and the Three Novel Primary Angle Closure Glaucoma (PACG) Susceptibility Loci

Monisha E. Nongpiur^{1,2}, Chia Chuen Khor^{3,4}, Liang Xu⁵, Jost B.

Jonas⁶, Jin Da Wang⁵, Tien Y. Wong^{1,7}, Eranga N. Vithana¹, Tin

Aung^{1,7}. ¹Glaucoma, Singapore Eye Research Inst, Singapore,

Singapore; ²DUKE-NUS Graduate Medical School, Singapore,

Singapore; ³Genome Institute Of Singapore, Singapore, Singapore;

⁴Centre for Molecular Epidemiology, Singapore, Singapore; ⁵Beijing

Institute of Ophthalmology, Beijing, China; ⁶Ophthalmology,

Medical Faculty Mannheim-Heidelberg, Mannheim, Germany;

⁷Ophthalmology, Yong Loo Lin School of Medicine, Singapore,

Singapore.

Purpose: Three novel susceptibility loci for primary angle closure glaucoma (PACG) were recently identified (Vithana E et al, Nature Genetics 2012); *PLEKHA7* rs11024102, *COL11A1* rs3753841, and rs1015213 located in the intergenic region between *PCMTD1* and *ST18* genes on Chromosome 8q. The purpose of this study was to investigate the associations of these loci with the ocular biometric parameters, anterior chamber depth (ACD) and axial length (AL).

Methods: Genotype data on the three SNPs and ocular biometric data were available for 4 population-based studies including 3 from Singapore (Singapore Chinese Eye Study, Singapore Malay Eye Study, and Singapore Indian Eye Study) and one from China (Beijing Eye study). ACD and AL were measured using the IOLMaster (Carl Zeiss Meditec, Dublin, CA). Five readings were obtained and the average computed. The biometric measurements were excluded from any eye which was pseudophakic or aphakic.

Results: Genotype and ocular biometric data were available for 6413 population-based individuals of Chinese, Indian, and Malay ethnicity from Singapore, and 877 population-based Chinese subjects from Beijing, China. Significant association was found between ACD and rs1015213 (*PCMTD1*-*ST18*; p=0.02, beta = -0.032). There was no association between ACD and rs11024102 (*PLEKHA7*; p=0.11) or rs3753841 (*COL11A1*; p=0.24). We did not observe significant associations between AL and any of the three SNPs.

Conclusions: The association between ACD and the *PCMTD1*-*ST18*

locus suggests that the susceptibility to PACG may be mediated by shallower anterior chamber, but not overall eyeball length. The association of these SNPs with other angle closure related biometric parameters such as anterior chamber width is also worthy of being investigated.

Commercial Relationships: Monisha E. Nongpiur, None; Chiea Chuen Khor, None; Liang Xu, None; Jost B. Jonas, Allergan (C), MSD (C), Alimera (C), CellMed AG (P); Jin Da Wang, None; Tien Y. Wong, Allergan (C), Bayer (C), Novartis (C), Pfizer (C), GSK (F), Roche (F); Eranga N. Vithana, None; Tin Aung, Alcon (R), Alcon (C), Alcon (F), Allergan (R), Allergan (C), Carl Zeiss Meditec (F), Carl Zeiss Meditec (R), Ellex (F), Ellex (R), Santen (R)
Support: National Medical Research Council, Singapore and Biomedical Research Council, Singapore

Program Number: 6223 **Poster Board Number:** C0108

Presentation Time: 10:30 AM - 12:15 PM

Protein tyrosine phosphatase Meg2 deficient mice - A powerful model to study glaucoma disease?

Jacqueline Reinhard¹, Susanne Wiemann¹, Stephanie C. Joachim², Heiko Schmid², Bernd Denecke³, Yingchun Wang⁴, Gregory P. Downey^{5,6}, Andreas Faissner¹. ¹Cell Morphology & Molecular Neurobiology, Ruhr-University Bochum, Bochum, Germany; ²Experimental Eye Research Institute, Ruhr-University Bochum, Bochum, Germany; ³Interdisciplinary Center for Clinical Research, RWTH Aachen University, Aachen, Germany; ⁴Department of Medicine, University of Toronto, Toronto, ON, Canada; ⁵Department of Medicine, National Jewish Health, Denver, CO; ⁶Departments of Medicine and Integrated Department of Immunology, University of Colorado, Aurora, CO.

Purpose: Dephosphorylation of proteins on tyrosine residues via members of the protein tyrosine phosphatase (PTP) superfamily is a critical factor for the outcome of numerous diseases, including cancer or diabetes. Moreover, PTP members represent crucial signaling molecules in the regulation of the immune response.

In a previous study we described the dramatic retinal/eye phenotype of embryonic and early postnatal (P0) PTP-Meg2 knockout (KO) mice (Wang et al., 2005; ARVO 2012; in progress). In order to investigate the consequence of PTP-Meg2 loss in more detail, we performed retinal microarray analyses in P0 PTP-Meg2 KO mutants and wildtype (WT) control littermates. Surprisingly, based on this approach, we verified a dysregulation of several candidate genes highly associated with intraocular pressure (IOP) elevation, a hallmark of glaucoma disease. In the present consecutive study we investigated the potential “glaucoma phenotype” of adolescent PTP-Meg2 heterozygous (HET) mice.

Methods: Tonometry analysis was used to evaluate IOP in PTP-Meg2 HET and WT animals. Immunohistochemistry, electron microscopy, protein biochemical analyses as well as photopic electroretinogram (ERG) recordings were used to characterize adult PTP-Meg2 deficient mice.

Results: As verified by tonometry analysis, PTP-Meg2 HET mice develop a progressive IOP elevation during late adolescence. At one year of age, PTP-Meg2 HET animals exhibit a visible “glaucoma phenotype” accompanied by a dramatic loss of retinal ganglion cells and optic nerve degeneration. Finally, ERG recordings revealed that PTP-Meg2 HET mice exhibit reduced a- and b-wave amplitudes and implicit time prolongation, suggesting a progressive retinal damage.

Conclusions: In conclusion, PTP-Meg2 deficient mice may serve as a new powerful animal model to study the pathomechanisms involved in onset and progression of glaucoma disease. To our knowledge, this is the first report of a “glaucoma phenotype” in a PTP deficient animal.

Commercial Relationships: Jacqueline Reinhard, None; Susanne Wiemann, None; Stephanie C. Joachim, None; Heiko Schmid, None; Bernd Denecke, None; Yingchun Wang, None; Gregory P. Downey, None; Andreas Faissner, None

Support: German Research Council (DFG, SFB 509: neuronal mechanisms of vision); Research School of the Ruhr-University Bochum (DFG GSC 98/1); “Regulation of retinal stem cells by neural extracellular matrix and tyrosine phosphatases” (DFG, FA 159/14-1)

Program Number: 6224 **Poster Board Number:** C0109

Presentation Time: 10:30 AM - 12:15 PM

Association of Glutathione S Transferases Polymorphisms with Glaucoma: A Meta-analysis

Yibo Yu, Ke Yao. Eye Center, Second Affiliated Hospital, College of Medicine, Zhejiang University, Hangzhou, China.

Purpose: Glutathione S transferase (GST) polymorphisms have been considered risk factors for the development of glaucoma, including primary open angle glaucoma (POAG) and other types of glaucoma. However, the results remain controversial. In this study, we have conducted a meta-analysis to assess the association between polymorphisms of GSTM1, GSTT1 and GSTP1 and glaucoma risk.

Methods: Published literature from PubMed and other databases were retrieved. All studies evaluating the association between GSTM1, GSTT1 and GSTP1 polymorphisms and glaucoma risk were included. Pooled odds ratio (OR) and 95% confidence interval (CI) were calculated using random- or fixed-effects model.

Results: Twelve studies on GSTM1 (1109 cases and 844 controls), ten studies on GSTT1 (709 cases and 664 controls) and four studies on GSTP1 (543 cases and 511 controls) were included. By pooling all the studies, either GSTM1 or GSTT1 null polymorphism was not associated with a POAG risk, and this negative association maintained in Caucasian. The GSTP1 Ile 105 Val polymorphism was significantly correlated with increased POAG risk among Caucasian in a recessive model (Val/Val vs. Ile/Ile+Ile/Val: OR, 1.62, 95%CI: 1.00-2.61). Interestingly, increased glaucoma risk was associated with the combined GSTM1 and GSTT1 null genotypes (OR, 2.20; 95% CI, 1.47-3.31), and with the combined GSTM1 null and GSTP1 Val genotypes (OR, 1.86; 95% CI, 1.15-3.01).

Conclusions: This meta-analysis suggests that combinations of GST polymorphisms are associated with glaucoma risk. Given the limited sample size, the associations between single GST polymorphism and glaucoma risk await further investigation.

Commercial Relationships: Yibo Yu, None; Ke Yao, None

Support: Zhejiang Key Innovative Research Team Project of China (2009R50039)

Program Number: 6225 **Poster Board Number:** C0110

Presentation Time: 10:30 AM - 12:15 PM

Predicting Gene Networks and Transcription Factors in TNF α Treatment of Trabecular Meshwork Cells

Dongseok Choi¹, Lauren Hayashi², Kathryn Carr¹, Mary J. Kelley², Ted S. Acott². ¹Biostatistics, Public Hlth & Preventive Med, Oregon Health & Science Univ, Portland, OR; ²Casey Eye Institute, Oregon Health & Science Univ, Portland, OR.

Purpose: Tumor necrosis factor alpha (TNF α) is a crucial mediator of the therapeutic effects of laser trabeculoplasty on glaucoma. TNF α treatment increases matrix metalloproteinases (MMPs), enzymes that initiate turnover in the extracellular matrix (ECM), of trabecular meshwork (TM) cells. To further study ECM remodeling and its effects on aqueous humor outflow resistance, we conducted analyses to identify gene networks and their putative transcription factor binding sites by gene expression in response to TNF α treatment in TM cells.

Methods: Primary porcine TM cells were treated with recombinant human TNF α (10 ng/ml). At 12, 24, and 48 hours after treatment, total RNA was collected for gene expression profiling. The Significance Analysis of Microarrays was performed to identify differentially expressed genes with a q-value < 5%. TightCluster analysis produced small groups of significant genes by similar temporal patterns. Tight clusters up-regulated at 24 and 48 hr were analyzed for gene networks by Metacore. DNA promoter sequences for those genes were extracted using Ensembl Genome Browser. Masked sequences were collected in order to remove regions of interspersed repeats or areas of low complexity for 5K bp upstream with 2K bp downstream. The sequences were analyzed by CisModule to identify putative cis-regulatory motifs. The consensus sequences of binding sites predicted by CisModule were identified by TRANSFAC Professional database against known cis-regulatory motifs.

Results: The Metacore analysis produced several potential gene networks. At 24 hr, cluster 45 mapped to a network around CD44 and JNK1. At 48hr, cluster 14 mapped to a network surrounding BMP7 and cluster 16 at around SP1, STAT1 and SMAD. The CisModule and TRANSFAC analyses predicted potential transcription factors for each cluster. LRF, TFII-I, and unknown were predicted for cluster 45; MSX-1, CDXA, and RFX for cluster 14; and MAX, KID3, and WT1 for cluster 16.

Conclusions: We identified potential key networks of genes and their putative transcription factors in response to TNF α treatment of TM cells by combining biostatistics and bioinformatics tools. Transcription factors play a key role in regulating gene expression patterns. Further validation studies will be required to confirm the functionality of these networks and transcription factors.

Commercial Relationships: Dongseok Choi, None; Lauren Hayashi, None; Kathryn Carr, None; Mary J. Kelley, None; Ted S. Acott, None

Support: NIH/NEI EY19935, EY010572, EY003279, EY008247 and Research to Prevent Blindness

Program Number: 6226 **Poster Board Number:** C0111

Presentation Time: 10:30 AM - 12:15 PM

Mouse Genomic Loci Modulating Ganglion Cell Loss in Glaucoma

Eldon E. Geisert¹, Steven G. Hart¹, XiangDi Wang¹, Janey L. Wiggs².

¹Ophthalmology, Univ of Tennessee Health Sci Ctr, Memphis, TN;

²Ophthalmology, Harvard Medical School, Boston, MA.

Purpose: There is considerable evidence for differential susceptibility of retinal ganglion cells (RGCs) to injury. In human populations RGCs in some individuals are resistant to death even with extremely high intraocular pressures (IOPs), while in other individuals with relatively normal IOPs, the RGCs die. The current study examines the genetic basis of RGC susceptibility to acute elevated IOP in the BXD RI strain set, a mouse genetic reference panel.

Methods: To induce an acute elevation in IOP, we used a previously developed method (Samsel et al, IOVS; 52:1671-1675). The animals were deeply anesthetized and a 20 μ l injection of 5 μ m magnetic microspheres was made into the anterior chamber of the right eye. A hand held 0.5 Tesla magnet was used to pull the microspheres into the trabecular meshwork and impede drainage in the eye. Left eyes served as non-injected controls. The IOP was then measured over the next 21 days. For an animal to be included in the study the bead injected eye had to have an IOP above 25 mm Hg for two consecutive days. We quantified RGC loss by counting axons within the optic nerves of the injected eye and control eye for 24 BXD strains of mice (total of 49 mice).

Results: The injections resulted in an average increase in IOP of 11.8

mm Hg in the injected eye as compared to the contralateral control eye (average IOP of 12 mmHg). The eye with elevated IOP had an average loss of 17.4% of the axons relative to the non-injected control eye. We used this strain-specific quantitative data to map loci modulating axonal loss and identified a significant QTL on Chr 18. Potential candidate genes in the Chr 18 peak were defined by determining genes with cisQTLs in the peak using the ONC Retina Database and bioinformatic tools on GeneNetwork.org. For the locus on Chr 18, 7 candidates were identified (*Adnp2*, *C16orf25*, *Pias2*, *Katnal2*, *Hdhd2*, *Skorz* and *Smad2*) and were analyzed for association with human glaucoma using the results of the NEIGHBOR/GLAUGEN meta-analysis. Of these 7, one gene, *SMAD2*, had a significant P value ($p = 0.013$ when Bonferroni corrected for 7 candidates) associated with normal tension glaucoma patients but not with POAG populations.

Conclusions: This novel approach has identified a potential risk factor for normal tension glaucoma (*SMAD2*). *SMAD2* is part of the signaling pathway for TGF β , which is known to have a prominent association with glaucoma.

Commercial Relationships: Eldon E. Geisert, None; Steven G. Hart, None; XiangDi Wang, None; Janey L. Wiggs, None

Support: NEI Grant RO1EY178841, Unrestricted Grant from RPB NIH R01EY015872-05S1 and R01EY019126-02S1

Program Number: 6227 **Poster Board Number:** C0112

Presentation Time: 10:30 AM - 12:15 PM

Association between primary open-angle glaucoma and genetic variants associated with normal tension glaucoma

Fumihiko Mabuchi¹, Yoichi Sakurada¹, Kenji Kashiwagi¹, Zentaro Yamagata², Hiroyuki Iijima¹. ¹Ophthalmology, University of Yamanashi, Chuo, Japan; ²Health Sciences, University of Yamanashi, Chuo, Japan.

Purpose: To assess the association between primary open-angle glaucoma (POAG), including normal tension glaucoma (NTG) and high tension glaucoma (HTG), and the genetic variants associated with NTG.

Methods: One hundred and ninety three Japanese patients with NTG, 190 patients with HTG, and 184 control subjects without glaucoma were analyzed for 6 genetic variants associated with NTG; rs3213787 (near gene: *SRBD1*), rs735860 (*ELOVL5*), rs1063192 (*CDKN2B/CDKN2B-AS1*), rs10483727 (*SIX1/SIX6*), rs1900004 (*ATOH7*), and rs10451941 (*OPAI*). The risk (odds ratio) of NTG for each genetic variant was calculated using logistic regression model. The number of genetic variants with risk allele and products of the odds ratios of analyzed genetic variants for each patient were compared between the patients with NTG or HTG and the control subjects.

Results: The number of genetic variants with risk allele in patients with NTG (4.0 ± 1.1 , mean \pm standard deviation) and HTG (3.8 ± 1.1) were significantly higher ($P < 0.0001$ and $P = 0.0058$ respectively, Student's t-test) than that (3.5 ± 1.1) in the control subjects. Similarly, products of the odds ratios in patients with NTG (8.7 ± 4.9) and HTG (7.9 ± 4.7) were significantly higher ($P < 0.0001$ and $P = 0.0039$ respectively, Student's t-test) than that (6.6 ± 4.4) in the control subjects.

Conclusions: These data support that POAG is a complex disorder by multiple genetic factors, and suggest that not only genetic variants associated with intraocular pressure (IOP) elevation (IOP-related genetic factors), but also genetic variants associated with NTG (non-IOP-related genetic factors) contribute to the pathogenesis of HTG.

Commercial Relationships: Fumihiko Mabuchi, None; Yoichi Sakurada, None; Kenji Kashiwagi, None; Zentaro Yamagata, None; Hiroyuki Iijima, None

Support: Grant-in-Aid (No. 21592221) from the Ministry of Education, Science, Sports, and Culture, Japan

Program Number: 6228 **Poster Board Number:** C0113

Presentation Time: 10:30 AM - 12:15 PM

Analysis of Ophthalmic Clinical Data Association for CDKN2B-AS1 Genotype in Normal Subjects

Yoko Ikeda¹, Kazuhiko Mori¹, Morio Ueno¹, Masakazu Nakano², Yuichi Tokuda², Natsue Omi², Ryuichi Sato², Kengo Yoshii³, Kei Tashiro², Shigeru Kinoshita¹. ¹Ophthalmology, Kyoto Prefectural Univ of Med, Kamigyo-ku, Japan; ²Genomic Medical Sciences, Kyoto Prefectural University of Medicine, Kyoto, Japan; ³Judo Therapy, Takarazuka University of Medical and Health Care, Takarazuka, Japan.

Purpose: Several single nucleotide polymorphisms (SNPs) located in the CDKN2B-AS1 gene have been detected as marker SNPs for primary open-angle glaucoma, and especially for normal tension glaucoma. However, even in normal subjects, the risk allele for CDKN2B-AS1 exists in approximately 80% of them. The purpose of this study was to evaluate the clinical ophthalmic data differences according to genotype data of CDKN-2BAS1 in normal subjects.

Methods: This study involved 974 normal subjects (357 males, 617 females; mean age: 56.5±14.0 years) diagnosed as normal by glaucoma specialists after several ophthalmic examinations including optic disc photograph and visual field testing, and who had no familial history of glaucoma as determined by Affymetrix® 500K or 1000K microarray (Affymetrix, Inc., Santa Clara, CA) analysis. Of the 5 detected SNPs of CDKN2B-AS1, rs7865618 was selected as the representative SNP for statistical analysis. For clinical data, patient height, age, intraocular pressure (IOP), refractive error (RE), corneal radius (CR), axial length, optic disc area (DA), optic rim area (RA), central cornea thickness (CCT), anterior chamber depth (ACD), anterior chamber volume (ACV), anterior chamber angle (ACA) were statistically analyzed in regard to the genotype of rs7865618 (AA/AG/GG). DA and RA were measured by retinal tomography (HRT-II; Heidelberg Engineering GmbH, Heidelberg, Germany) and data were selected RE -12D</>+12D, SD <50. RE, CR, ACD, ACV, ACA were selected for both phakic eyes. ACD/ACV/ACA was measured by Pentacam® (OCULUS Optikgeräte GmbH, Wetzlar, Germany). If data was available for both eyes, the subject's right-eye data was selected. Statistical analysis was performed by use of one-way analysis of variance (ANOVA).

Results: The number of subjects with the AA, AG, and GG genotypes were 669, 276, and 29, respectively. No significant difference in mean age was found among the genotype groups. Patient height, CCT, DA, IOP, and RE were smaller in the GG group subjects than in the AA and AG groups subjects, however, IOP was significantly smaller than in the other two groups of subjects.

Conclusions: In normal subjects, IOP was significantly smaller in the GG genotype subjects who did not have the risk allele for CDKN2B-AS1.

Commercial Relationships: *Yoko Ikeda*, None; *Kazuhiko Mori*, Ocular Instruments, Inc. (P), Santen Pharmaceutical Co., Ltd. (P); *Morio Ueno*, None; *Masakazu Nakano*, None; *Yuichi Tokuda*, None; *Natsue Omi*, None; *Ryuichi Sato*, None; *Kengo Yoshii*, None; *Kei Tashiro*, None; *Shigeru Kinoshita*, Senju Pharmaceutical Co (P), Santen Pharmaceutical Co (P), Otsuka Pharmaceutical Co (C), Alcon (R), AMO (R), HOYA (R)

Program Number: 6229 **Poster Board Number:** C0114

Presentation Time: 10:30 AM - 12:15 PM

The Role of Protein-Coding Variants in South Africans with Exfoliation Glaucoma

Yutao Liu^{1,2}, Xuejun Qin¹, Jason Gibson¹, Susan E. Williams³, Robyn M. Rautenbach⁴, Trevor R. Carmichael³, Allison E. Ashley-Koch¹, R Rand Allingham², Michael A. Hauser^{1,2}. ¹Medicine, Duke University Medical Center, Durham, NC; ²Ophthalmology, Duke University Medical Center, Durham, NC; ³Neurosciences, University of the Witwatersrand, Johannesburg, South Africa; ⁴Surgical Sciences, Stellenbosch University, Stellenbosch, South Africa.

Purpose: Exfoliation glaucoma (XFG), also called pseudoexfoliation glaucoma, is the most common identifiable form of open-angle glaucoma. Previous genome-wide association studies have identified several genetic risk factors including *LOXL1* and *CNTNAP2*. Our purpose is to examine the role of protein-coding variants in South Africans with XFG.

Methods: Black South African subjects with XFG and age matched unaffected controls were recruited from the St. John Eye Hospital in Soweto (Johannesburg, South Africa) and East London Hospital Complex (Eastern Cape, South Africa) using standard clinical examination techniques. We used the Illumina Infinium HumanExome BeadChip containing over 250,000 coding variants to genotype a total of 105 XFG cases and 129 controls. A principal component analysis was performed to address population stratification in these South African samples. We performed the Fisher's exact test for variants with frequency greater than 0. We also performed logistic regression for all variants with the justification of age and gender for dominant, recessive, and additive models using SAS software.

Results: After quality control and genotype calling, over 71,000 variants were included in the analysis. Principal component analysis indicates that there is no population stratification in these genotyped samples. Our analysis did not identify any association with genome-wide significance (p value < 5 X 10⁻⁸), most probably due to our limited power for detection. For the Fisher's exact test, the two variants most strongly associated with XFG are rs116243478 in the lysocardiolipin acyltransferase (*LCLAT1*) gene (p value = 5.4 X 10⁻⁵) and rs113838785 in the dystrotelin (*DYTN*) gene (p value = 1.1 X 10⁻⁴). Several more promising candidates were also identified using logistic regression analysis with an additive model, including variant rs8078660 in gem-associated protein 4 (*GEMIN4*) (p value = 2.5 X 10⁻⁴).

Conclusions: We have performed a genome-wide association analysis for exfoliation glaucoma with more than 71,000 variants in a total of 234 South Africans. We did not identify any variants with genome-wide significant association with XFG. Several candidate variants suggest the potential involvement of a number of different genes. It is necessary to replicate our findings in other datasets.

Commercial Relationships: *Yutao Liu*, None; *Xuejun Qin*, None; *Jason Gibson*, None; *Susan E. Williams*, None; *Robyn M. Rautenbach*, None; *Trevor R. Carmichael*, None; *Allison E. Ashley-Koch*, None; *R Rand Allingham*, New World Medical (C); *Michael A. Hauser*, None

Support: R01EY013315 (MAH), R01EY019126 (MAH), R03EY014939 (RRA), and R01EY015543 (RRA), Glaucoma Research Foundation (YL), National Glaucoma Research of American Health Assistance Foundation (YL), The Glaucoma Foundation (YL).

Program Number: 6230 **Poster Board Number:** C0115

Presentation Time: 10:30 AM - 12:15 PM

Mouse Genomic Loci Modulating Corneal Thickness

XiangDi Wang¹, Steven G. Hart¹, Janey L. Wiggs², Eldon E. Geisert¹. ¹Ophthalmology, University of Tennessee Health Science Center,

Memphis, TN; ²Ophthalmology-Harvard Medical School, Mass Eye & Ear Infirmary, Boston, MA.

Purpose: One of the risk factors for developing glaucoma is central corneal thickness (CCT). We have used a mouse genetic reference panel (the BXD RI strain set) to define mammalian genomic loci modulating CCT.

Methods: CCT was measured in 50 BXD RI strains between 60-90 days of age. The mice were deeply anesthetized and the eyes were positioned in front of the Mouse Bore of a Bioptigen ocular contrast tomography (OCT) system. The cornea was put into the appropriate focal plane and scanned. The corneal scans were then saved to a portable hard drive for subsequent analysis. The central corneal thickness was measured three times for each eye using the Mouse Retina Program, In Vivo Vue Clinic, in the Bioptigen Software. CCT data for each strain was averaged and used to identify quantitative trait loci (QTLs) modulating this phenotype using the bioinformatics tools on GeneNetwork (www.genenetwork.org).

Results: This analysis revealed one significant QTL on Chr 13 and several suggestive QTLs on Chr 1, Chr 7, Chr 11 and Chr 16. The significant locus on Chr 13 was examined further to define potential candidate genes modulating this eye phenotype. Using the eye microarray dataset (HEIMED) on GeneNetwork, we identified cis-QTLs that could be modulating CCT in the BXD RI strain set. There were 11 genes that are cis-QTLs in this region of Chr 13: *Lyst*, *Hecw1*, *Cdc215*, *Rala*, *Vps41*, *Stard3nl*, *Sfrp4*, *Trim27*, *Zkscan3*, *Hist1h4b* and *Hist1h4i*. Of these 11 genes only three appeared to be expressed in our cornea array dataset: *Lyst* (lysosomal trafficking regulator), *Rala* (v-ral simian leukemia viral oncogene homolog) and *Trim27* (tripartite motif-containing 27). These candidate genes were examined to determine if they are potential risk factors for human glaucoma. *LYST* was found to have a significant p value ($p = 0.0084$) in relationship to all human glaucoma cases in the results of the NEIGHBOR/GLAUGEN meta-analysis when Bonferroni corrected for the three tests.

Conclusions: This novel approach has identified a putative gene modulating CCT in the mouse and a potential risk factor for primary open angle glaucoma.

Commercial Relationships: XiangDi Wang, None; Steven G. Hart, None; Janey L. Wiggs, None; Eldon E. Geisert, None
Support: NEI Grant RO1EY178841, Unrestricted Grant from Research to Prevent Blindness, NIH R01EY015872-05S1 and R01EY019126-02S1

Program Number: 6231 **Poster Board Number:** C0116

Presentation Time: 10:30 AM - 12:15 PM

Identification and Characterization of Genetic Factors Responsible for Cavitory Optic Disc Anomalies

Ralph J. Hazlewood¹, Ben Roos¹, Robert A. Honkanen², Lee M. Jampol³, Wallace L. Alward¹, Young H. Kwon¹, Edwin M. Stone^{1,4}, John H. Fingert^{1,5}. ¹Ophthalmology and Visual Sciences, University of Iowa, Iowa City, IA; ²Ophthalmology, State University of New York at Stony Brook, Stony Brook, NY; ³Ophthalmology, Feinberg School of Medicine, Northwestern University, Chicago, IL; ⁴Howard Hughes Medical Institute, Iowa City, IA; ⁵Anatomy and Cell Biology, University of Iowa, Iowa City, IA.

Purpose: To identify and characterize the gene that causes autosomal dominant, congenital malformations of the optic nerve known as cavitory optic disc anomaly (CODA) in a multiplex family with 17 affected members. Features of the nerve disease in CODA closely resemble that of glaucoma (excavated optic nerve head appearance) that occurs in the absence of elevated IOP, suggesting that the gene that causes CODA may also contribute to the pathophysiology of glaucoma.

©2013, Copyright by the Association for Research in Vision and Ophthalmology, Inc., all rights reserved. Go to iovs.org to access the version of record. For permission to reproduce any abstract, contact the ARVO Office at arvo@arvo.org.

Methods: The gene that causes CODA was previously mapped to a 13.5Mb locus on chromosome 12q14. The proband of the CODA pedigree was tested for copy number variations (CNVs) in the chromosome 12q14 region with custom comparative genomic hybridization using the NimbleGen platform (Madison, WI). CNVs were confirmed with quantitative PCR in the proband and in the remaining 16 affected family members as well as in a panel of 78 controls. Confirmed CNVs were analyzed for their effect on downstream genes using a luciferase reporter gene construct (pGL3, Promega, Madison, WI) in HEK293T cells.

Results: CGH experiments identified a triplication of a 6kb segment of DNA upstream of matrix metalloproteinase 19 (*MMP19*) in the proband of the CODA pedigree. Quantitative PCR experiments confirmed that the *MMP19* promoter CNV is present in the proband as well as in the additional 16 affected family members. No control subjects carried this mutation. Furthermore there were no instances of this variant in the database of genomic variants (projects.tcag.ca/variation). The luciferase reporter gene assay showed that the 6kb sequenced spanned by the CNV in CODA patients increased luciferase activity and functioned as a transcription enhancer. Moreover, a similar analysis of overlapping subdivisions of the DNA sequence in the 6kb CNV showed that a 1kb segment had a strong positive influence (8-fold higher) on downstream gene expression.

Conclusions: We have identified a copy number variation mutation in the promoter sequence of the *MMP19* gene that co-segregates with CODA in our large 17 member pedigree. Moreover we have shown that the CNV spans DNA sequences that powerfully enhance downstream genes (i.e. *MMP19*). These functional data strongly suggest that the genetic defects in *MMP19* cause CODA and that over-activity of this gene has an important role in the pathogenesis of this optic nerve disease.

Commercial Relationships: Ralph J. Hazlewood, None; Ben Roos, None; Robert A. Honkanen, None; Lee M. Jampol, Pfizer (C), Baxter International (C), Stem Cell Organization/Quintiles (C); Wallace L. Alward, None; Young H. Kwon, None; Edwin M. Stone, None; John H. Fingert, None

Support: Research to Prevent Blindness Career Development Award, Lew R. Wasserman Award of Research to Prevent Blindness, University of Iowa Dean's Graduate Fellowship, Genetics NIH T32 Training Grant 2T32GM008629-16, and NIH 2R01EY010564-11A1

Program Number: 6232 **Poster Board Number:** C0117

Presentation Time: 10:30 AM - 12:15 PM

Association Study of Multiple Gene Polymorphisms with the Risk of Adult-Onset Primary Open-Angle Glaucoma in a Mexican Population

Jesus Cabral¹, Beatriz Buentello¹, Dalia C. Guadarrama¹, Juan C. Zenteno^{1,4}, Celia Elizondo², Antonio Miranda³. ¹RESEARCH UNIT GENETICS, INSTITUTION OF OPHTHALMOLOGY CONDE DE VALENCIANA, Mexico City, Mexico; ²GLAUCOMA DEPARTMENT, INSTITUTION OF OPHTHALMOLOGY CONDE DE VALENCIANA, Mexico City, Mexico; ³DEPARTMENT OF GENETICS, NATIONAL INSTITUTE OF REHABILITATION, Mexico City, Mexico; ⁴DEPARTMENT OF BIOCHEMISTRY, NATIONAL AUTONOMOUS UNIVERSITY OF MEXICO, Mexico City, Mexico.

Purpose: The purpose of this work was to investigate the association of multiple primary open-angle glaucoma (POAG) risk alleles in a Mexican population.

Methods: A total of 26 well-known associated alleles located in 11 different genes, including MYOC, CYP1B1, OPTN, IL-1A, TNF, OPA1, EDNRA, AGTR2, MTHFR, GSTM1, and GSTT1 were

genotyped. Frequencies of these variants were compared in a group of 218 individuals (118 with POAG and 100 healthy controls). DNA was extracted from blood leukocytes, and genotyping was performed using PCR as well as direct sequencing. Comparisons of continuous variables were tested by Student's t-test, and corrected chi-squared statistics were applied for categorical variables.

Results: Individual SNP analysis showed that no specific variants are related to an elevated risk for developing POAG. Nevertheless, CG genotype for rs5335 polymorphism in EDNRA provides an estimated odds ratio of 0.5 (95% CI, 0.3-0.9; $p=0.03$), displaying a protective effect against the development of POAG. Moreover, the association with a protective effect against POAG of one haplotype, consisting of rs1056827 and rs100012 in CYP1B1 gene, was statistically significant ($p=0.0045$; OR=0.3; 95% CI, 0.1-0.7).

Conclusions: This is the first case-control study of POAG-risk alleles for multiple genes in a Latino population. Our results show a protective effect conferred by EDNRA rs5335, and a CYP1B1 haplotype consisting of rs1056827 and rs100012. This investigation emphasizes the importance of genotyping distinct POAG ethnic groups.

Commercial Relationships: Jesus Cabral, None; Beatriz Buentello, None; Dalia C. Guadarrama, None; Juan C. Zenteno, None; Celia Elizondo, None; Antonio Miranda, None

Program Number: 6233 **Poster Board Number:** C0118

Presentation Time: 10:30 AM - 12:15 PM

A genetic variant in TMC01 is strongly associated with primary open angle, primary angle closure and pseudoexfoliation glaucoma

Shazia Micheal^{1,2}, Humaira Ayub^{2,1}, Muhammad I. Khan^{2,3}, Bjorn Bakker¹, Frederieke E. Schoenmaker-Koller¹, Mahmood Ali⁴, Farah Akhtar⁴, Raheel Qamar^{1,5}, Anneke I. Den Hollander^{1,3}.

¹Ophthalmology, UMC St Radboud, Nijmegen, Netherlands; ²Biosciences, COMSATS Institute of Information Technology, Islamabad, Pakistan; ³Human Genetics, Radboud University Nijmegen Medical Centre, Nijmegen, Netherlands; ⁴Glaucoma, Al-Shifa Trust Eye Hospital, Rawalpindi, Pakistan; ⁵Shifa College of Medicine, Shifa Tameer-e-Millat University, Islamabad, Pakistan.

Purpose: Despite the different etiology of primary open angle glaucoma (POAG), primary angle closure glaucoma (PACG) and pseudoexfoliative glaucoma (PEXG), several studies have suggested overlapping genetic risk factors for these forms of glaucoma. Therefore, the aim of this study was to evaluate the role of genetic variants recently associated with POAG in different types of glaucoma using POAG, PCAG and PEXG patient cohorts from Pakistan.

Methods: Six variants in *CDKN2B-ASI* (rs4977756), *CDKN2B* (rs1063192), *ATOH7* (rs1900004), *CAV1* (rs4236601), *TMC01* (rs4656461) and *SIX1* (rs10483727) were genotyped using Taqman assays. A total of 513 unrelated glaucoma patients (268 POAG, 125 PACG and 120 PEXG) and 233 healthy controls were included in the study. Genotypic and allelic associations were analyzed by Chi-squared tests.

Results: The frequency of the A allele of *TMC01* rs4656461 was significantly higher in POAG (90.5%; $p<0.001$; OR 2.90), PACG (90.0%; $p<0.001$; OR 2.75) and PEXG (91.7%; $p<0.001$; OR 3.36) patients compared to control individuals (76.6%). The T allele of *ATOH7* rs1900004 was observed less frequently in PACG patients (24.4%; $p=0.03$; OR 0.69) compared to control individuals (31.8%). The A allele of *CAV1* rs4236601 was found more frequently in POAG (26.3%; $p=0.008$; OR 1.49) compared to control individuals (19.3%)

Conclusions: The *TMC01* rs4656461 variant is strongly associated

with POAG, PACG and PEXG in the Pakistani population. Our study was unable to confirm previous associations reported for variants in *CDKN2B-ASI*, *CDKN2B* and *SIX1* with any type of glaucoma.

Commercial Relationships: Shazia Micheal, None; Humaira Ayub, None; Muhammad I. Khan, None; Bjorn Bakker, None; Frederieke E. Schoenmaker-Koller, None; Mahmood Ali, None; Farah Akhtar, None; Raheel Qamar, None; Anneke I. Den Hollander, None

Program Number: 6234 **Poster Board Number:** C0119

Presentation Time: 10:30 AM - 12:15 PM

The association between CAV1/2 region loci and their relation with primary open angle glaucoma

Stephanie Loomis^{1,2}, Louis R. Pasquale^{1,2}, Jae H. Kang², Michael A. Hauser^{4,5}, Brian Yaspan³, Jonathan L. Haines³, Janey L. Wiggs¹.

¹Department of Ophthalmology, Massachusetts Eye and Ear Infirmary, Boston, MA; ²Department of Medicine, Channing Division of Network Medicine, Boston, MA; ³Center for Human Genetics Research, Vanderbilt University, Nashville, TN; ⁴Department of Ophthalmology, Duke University, Durham, NC; ⁵Department of Medicine, Duke University Medical Center, Durham, NC.

Purpose: To assess the association between single nucleotide polymorphisms (SNPs) in the *CAV1/2* region in relation to primary open angle glaucoma (POAG) in two genome-wide association studies with imputed data.

Methods: We measured the association between 70 SNPs located within 50kb of the *CAV1/2* region in two large POAG datasets, the Glaucoma Genes and Environment (GLAUGEN) study (976 cases, 1140 controls) and the National Eye Institute Glaucoma Human Genetics Collaboration (NEIGHBOR) consortium (2032 cases, 2290 controls). Genotyping was performed on the Illumina Human 660WQuadv1C BeadChip array and imputed to 2.5 million markers with MACH using the HapMap 2.3 reference panel. We used logistic regression models of POAG in the overall population and in men and women separately, and we conducted secondary analyses of POAG subtypes defined by intraocular pressure (IOP) and visual field (VF) defect. Results from each dataset were meta-analyzed with the METAL software package. A Bonferroni corrected significance level of 7.14×10^{-4} was used to account for the 70 SNPs tested.

Results: We found significant associations between ten *CAV1/2* SNPs and POAG (top SNP rs4236601 pooled $p=1.7 \times 10^{-7}$). One significant association was observed among women (top SNP rs4236601 pooled $p=1.19 \times 10^{-5}$) but none in men (top SNP rs17588172 pooled $p=1.82 \times 10^{-3}$). When the outcome was stratified by type of VF loss, five *CAV1/2* SNPs were associated with POAG with paracentral VF loss only (top SNP rs17588172 pooled $p=1.14 \times 10^{-4}$) and none with POAG with peripheral VF loss only (top SNP rs4236601 pooled $p=8.59 \times 10^{-4}$). There were two SNPs associated with normal tension glaucoma (NTG) overall (top rs10270569 pooled $p=5.08 \times 10^{-4}$) and one SNP associated with NTG among men (rs10270569 pooled $p=6.93 \times 10^{-4}$) but not among women. There were no significant SNPs in relation to high tension POAG (HTG) overall or stratified by gender.

Conclusions: Within our dataset, *CAV1/2* SNPs were significantly associated with POAG overall, particularly among women. *CAV1/2* SNPs were also significantly associated with POAG cases with only paracentral visual field defects and with normal tension glaucoma. These data affirm the potential role of *CAV1/2* in POAG and indicate that *CAV1/2* may have differing effects on POAG pathogenesis by gender and by type of visual field defect.

Commercial Relationships: Stephanie Loomis, None; Louis R. Pasquale, None; Jae H. Kang, None; Michael A. Hauser, None;

Brian Yaspan, Genentech (E); **Jonathan L. Haines**, Arctic Dx (I), AMD genes (P); **Janey L. Wiggs**, None
Support: NEI RO1 EY 015473 HG004728 HG005259 EY 015872 - 05S1 EY 019126 - 02S1

Program Number: 6235 **Poster Board Number:** C0120

Presentation Time: 10:30 AM - 12:15 PM

Next Generation Sequencing Identifies Novel Variants of Mitochondrial DNA in Normal-Tension Glaucoma Patients

Dong Myung Kim¹, Jin Wook Jeoung¹, Moon-Woo Seong², Sung Sup Park². ¹Ophthalmology, Seoul National University Hospital, Seoul, Republic of Korea; ²Laboratory Medicine, Seoul National University Hospital, Seoul, Republic of Korea.

Purpose: Since up to 21% of normal-tension glaucoma (NTG) patients were reported to have a family history, it is suggested that these patients may be genetically predisposed to developing NTG. In this study, we performed a genetic analysis of the mitochondrial gene and revealed the genetic risk variants in the NTG patients.

Methods: DNA was extracted from peripheral blood of the NTG patients and normal control subjects. For the 20 NTG patients (discovery sample), the entire mitochondrial DNA (mtDNA) was sequenced using the next generation sequencing. From these results, we revealed new genetic risk variants for NTG patients. For the candidate genetic variants, we performed a disease-gene association study in the independent case (n=76) - control (n=82) populations (replication sample). For the replication sample, we used the Sanger's sequencing method.

Results: This study identified 156 different novel mtDNA sequence changes. Of these, 21 sequence variants were identified at the frequency of more than 15%, which were located in the ND2-ND6, RNR1, RNR2, COX1, COX3, ATP6, ATP8, and CYTB genes. For the 21 candidate genetic variants, a disease-gene association study was performed. The frequencies of 12372G>A (ND5 gene) and 14766C>T (CYTB gene) were significantly different between NTG patients and controls (18.9% vs 2.4%, P=0.002; 8.0% vs 0.0%, P=0.028). However, only the association with 12372G>A in ND5 gene resisted to Bonferroni correction for multiple tests.

Conclusions: This study reveals a spectrum of mtDNA variants in patients with NTG. These results suggest that mitochondrial dysfunction may be a risk factor for the development of NTG.

Commercial Relationships: **Dong Myung Kim**, None; **Jin Wook Jeoung**, None; **Moon-Woo Seong**, None; **Sung Sup Park**, None

Program Number: 6236 **Poster Board Number:** C0121

Presentation Time: 10:30 AM - 12:15 PM

Revisit the association of CAV1/CAV2 with primary open-angle glaucoma

Li Jia Chen, Pancy O.S. Tam, Chi Pui Pang. Ophthalmology & Visual Sciences, The Chinese University of Hong Kong, Hong Kong, China.

Purpose: A genome-wide association study identified SNP rs4236601 near the CAV1 and CAV2 genes to be strongly associated with primary open angle glaucoma (POAG). However, results from follow-up studies remained controversial. In this study, we investigated the associations of 6 tag SNPs at the CAV1/CAV2 locus with POAG.

Methods: We studied a total of 1572 unrelated Chinese Han individuals, including a cohort of 626 POAG and 546 controls from southern China, and 200 POAG and 200 controls from northern China. Six tag SNPs, including rs4236601, were genotyped by TaqMan technology.

Results: Three SNPs showed mild associations with POAG in the southern cohort. The SNP rs4236601[AG] showed a significantly

increased risk (OR=3.55), while another two SNPs showed reduced risks (OR=0.57 and 0.56). The haplotype block that contained rs4236601 and one protective SNP gave the strongest omnibus association. The haplotype G-C had a protective effect (OR=0.67), while A-T increased the risk of POAG (OR=3.52). When the southern and northern Chinese cohorts were combined, rs4236601[AG] remained significantly associated with POAG.

Conclusions: While our results confirmed the association of rs4236601 with POAG, we also identified a protective SNP at the CAV1/CAV2 POAG locus. Results of this study suggest that the CAV1/CAV2 locus may contribute different roles to the mechanism of POAG.

Commercial Relationships: **Li Jia Chen**, None; **Pancy O.S. Tam**, None; **Chi Pui Pang**, None

Program Number: 6237 **Poster Board Number:** C0122

Presentation Time: 10:30 AM - 12:15 PM

Clinical Profile Of A Large Family With Primary Open Angle Glaucoma (POAG) In South Indian Population

MOHIDEEN A. KADER¹, Rengappa Ramakrishnan¹, Subbiah Ramaswami Krishnadas², Prasanthi Namburi³, Periasamy Sundaresan³, Alan L. Robin⁴, Pradeep Y. Ramulu⁵, John H. Fingert⁶.

¹Glaucoma, Aravind Eye Hospital, Tirunelveli, India; ²Glaucoma, Aravind Eye Hospital, Madurai, India; ³Genetics, Aravind Medical Research Foundation, Madurai, India; ⁴John Hopkins University, Baltimore, MD; ⁵Wilmer Eye Institute, Baltimore, MD; ⁶Department of Ophthalmology and Visual Sciences, Carver College of Medicine, University of Iowa, Iowa City, IA.

Purpose: Family history of glaucoma is a significant risk factor for primary open angle glaucoma (POAG). Many of the known glaucoma-causing genes have been identified with studies of large pedigrees that have many members affected with glaucoma. Herein, we assessed the clinical features of POAG amongst members of a large South-Indian pedigree with a high prevalence of early-onset POAG.

Methods: Eighty four members of the large pedigree underwent a complete ocular examination, including applanation tonometry, pachymetry, gonioscopy and fundus examination at screening camp in their home town. The POAG and POAG suspect members underwent perimetry testing at base hospital to confirm the diagnosis.

Results: Fourteen (17%) of 84 participants were diagnosed with POAG. The mean age of those diagnosed with POAG was 58 years (range 34-86, SD 16) and was significantly greater than the age of the glaucoma suspects (mean age 52; range 36-68) or normal family members (mean age 31; range 5-75) (p<0.001). Eight patients (10%) were diagnosed as having suspect POAG and 62 patients (74%) had no evidence of either POAG or ocular hypertension. Mean intraocular pressure (IOP) was significantly higher (p<0.001) in patients with POAG (21.0 mm Hg ± 6.1) than in either glaucoma suspects (17.0 mm Hg ± 2.8) or normal family members (15.6 mm Hg ± 2.5). Similarly, central corneal thickness (CCT) was significantly thinner (p<0.01) in patients with POAG (533 microns ± 40) than in glaucoma suspects (554 microns ± 38) or normal family members (555 microns ± 33). Finally, cup-to-disc ratio was significantly larger (p<0.001) in glaucoma patients (0.74 ± 0.14) than in glaucoma suspects (0.56 ± 0.09) or normal family members (0.50 ± 0.04). The inheritance pattern of glaucoma in the pedigree most closely matches an autosomal dominant pattern.

Conclusions: Our large POAG pedigree has distinct clinical features. This pedigree has a highly heritable form of POAG, and the carefully collected clinical features of the disease, that are presented in this report, are likely to assist ongoing studies to identify new glaucoma causing genes that may be important in this Indian population.

Commercial Relationships: MOHIDEEN A. KADER, None; **Rengappa Ramakrishnan**, None; **Subbiah Ramaswami Krishnadas**, None; **Prasanthi Namburi**, None; **Periasamy Sundaresan**, None; **Alan L. Robin**, merck (C), merck (R), Aerie (C), Aerie (I), Sucampo (E), Glaukos (C), Glaukos (I), Allergan (R); **Pradeep Y. Ramulu**, Tissue Banks International (C); **John H. Fingert**, None

Program Number: 6238 **Poster Board Number:** C0123

Presentation Time: 10:30 AM - 12:15 PM

POAG blood and hyaluronic acid challenged monocytes upregulate CD44s and isoforms: A new biomarker?

Paulius Kuprys¹, Algis Grybauskas¹, Kevin Skuran¹, Paul A. Knepper^{1,2}. ¹Ophthalmology and Visual Sciences, University of Illinois at Chicago, Chicago, IL; ²Ophthalmology, Northwestern University Medical School, Chicago, IL.

Purpose: CD44 is an important cell surface receptor that has multiple functions, such as cell-cell interactions, innate immune system signaling, and hyaluronic acid (HA) binding. CD44 is present as a standard form (CD44s), and as variant isoforms due to alternatively spliced exons. These variant isoforms are associated with a number of diseases ranging from cancer to neurodegeneration. In patients with primary open-angle glaucoma (POAG) aqueous humor content of CD44 is increased, whereas HA is decreased. The purpose of this study is to determine if the CD44 message changes in POAG patients compared to normal patients.

Methods: Peripheral blood monocytes were negatively selected from POAG patients (n=4) and normals (n=4) using density gradient centrifugation with a rosetting antibody. Isolated monocytes were split into RNA isolation and culture groups. RNA was isolated and used as a template for RT-PCR. PCR was used to amplify cDNA with primers constructed around the CD44 variant exons. PCR products were visualized on a 1.5% agarose gel with ethidium bromide under UV light. Products were identified by size with a DNA ladder. PCR band intensities were quantified, and normalized using GAPDH. Cultured monocytes were incubated for 48 hours and treated with treatment medium containing low molecular weight HA (LMW-HA) or plain treatment medium. After treatment, RNA was isolated and subjected to downstream applications as described above.

Results: Normal and POAG isolated blood monocytes expressed CD44s and isoforms containing variant exons 8 (v8), 9 (v9), and 10 (v10). CD44s and variants containing v10 were increased in POAG monocytes in comparison to normal monocytes. The ratio of CD44v8-10 relative to CD44 isoforms containing v10 was significantly downregulated in POAG monocytes in comparison to normal monocytes (P<0.05). This ratio relative to CD44s is also downregulated in POAG monocytes in comparison to normal monocytes (P<0.05). LMW-HA treatment appeared to upregulate CD44 variant isoforms containing v10 in monocytes with a more pronounced effect in monocytes derived from POAG patients.

Conclusions: Upregulation of CD44s and v10 in POAG monocytes indicates a translational feature of the disease process and may contribute to an inflammatory signal in POAG. This is the first demonstration of a systemic change in the CD44 message in POAG patients and may serve as a biomarker of the disease.

Commercial Relationships: Paulius Kuprys, None; Algis Grybauskas, None; Kevin Skuran, None; Paul A. Knepper, None **Support:** American Health Assistance Foundation, Research to Prevent Blindness

Program Number: 6239 **Poster Board Number:** C0124

Presentation Time: 10:30 AM - 12:15 PM

Rare Genetic Variants in African Americans with Primary Open Angle Glaucoma

Allison E. Ashley-Koch¹, Xuejun Qin¹, Jason Gibson¹, Yutao Liu^{1,2}, Janey L. Wiggs³, Julia E. Richards⁴, Sayoko E. Moroi⁴, Christopher A. Girkin⁵, R Rand Allingham², Michael A. Hauser^{1,2}. ¹Center for Human Genetics, Duke University Medical Center, Durham, NC; ²Department of Ophthalmology, Duke University Medical Center, Durham, NC; ³Massachusetts Eye and Ear Infirmary, Harvard Medical School, Boston, MA; ⁴Department of Ophthalmology and Visual Sciences, University of Michigan Medical School, Ann Arbor, MI; ⁵Department of Ophthalmology, University of Alabama at Birmingham School of Medicine, Birmingham, AL.

Purpose: African Americans are 4 times more likely to develop primary open angle glaucoma (POAG) than Caucasians, but little is known about their genetic risk factors. In contrast, genome wide association studies (GWAS) have successfully identified several POAG risk genes in Caucasians including CAV1/2, CDKN2BAS, TMCO1, SIX1/SIX6, and an intergenic region on 8p22. We have reported that these common susceptibility alleles in Caucasians were not associated with POAG in African Americans (Allingham et al, ARVO, 2012). Here, we evaluate whether rare variants in these or other genes contribute to POAG risk in African Americans.

Methods: The Illumina Infinium HumanExome BeadChip containing over 250,000 variants was genotyped in 666 POAG cases and 668 controls. Principle component analysis of ancestry informative markers on the Beadchip was used to identify population stratification. Rare variant association tests which collapse variants by gene were performed using Plink-Seq.

Results: 130,402 SNPs were polymorphic and after excluding common (>5%) and non-coding variants, 94,240 SNPs remained available for analysis. Known Caucasian POAG loci had marginal coverage on the chip, preventing an analysis of rare variants in African Americans. Five genes with rare variants demonstrated marginal association with POAG in our data set. These were Ewing tumor-associated antigen 1 (ETAA1; p=5x10⁻⁶ variable threshold test; p=6x10⁻⁶ burden test), aminoglycoside phosphotransferase domain-containing protein 1 (AGPHD1; p=9x10⁻⁶ C-alpha test), transmembrane and coiled-coil domain 4 (TMCO4; p=9x10⁻⁶ alpha test), synuclein-alpha interacting protein (SNCAIP; p=0.0001 variable threshold test; p=3x10⁻⁵ burden test) and polyhomeotic-like 2 (PHC2; p=1x10⁻⁵ variable threshold test; p=2x10⁻⁵ burden test).

Conclusions: We have identified multiple biologic pathways associated with POAG pathogenesis in both African Americans and Caucasians. Although we could not evaluate TMCO1, we identified support for TMCO4 in African American POAG risk. Our results also implicate the ubiquitination pathway in POAG etiology. PHC2 is part of the polycomb group of genes and believed to be involved in histone ubiquitination. CDKN2BAS, identified in Caucasian POAG, is also part of the ubiquitination pathway. Future directions include performing rare variant imputation, sequencing of selected candidate genes, and performing a GWAS with common variants.

Commercial Relationships: Allison E. Ashley-Koch, None; Xuejun Qin, None; Jason Gibson, None; Yutao Liu, None; Janey L. Wiggs, None; Julia E. Richards, None; Sayoko E. Moroi, Merck (F), Wolters Kluwer (F); Christopher A. Girkin, SOLX (F), Heidelberg Engineering (F); R Rand Allingham, New World Medical (C); Michael A. Hauser, None **Support:** NIH grants EY13315, EY019126 and EY011671 and RPB

Program Number: 6240 **Poster Board Number:** C0125

Presentation Time: 10:30 AM - 12:15 PM

Secondary Glaucoma in transthyretin (TTR)-related Familial Amyloid Polyneuropathy

Antoine Rousseau¹, Emmanuel Barreau¹, Godefroy Kaswin¹, Mohamed Mgarrech¹, Marie Théaudin², Cécile Cauquil², David Adams², Marc Labetoulle¹. ¹Ophthalmology, Bicetre Hospital, South Paris University, Le Kremlin Bicêtre, France; ²Neurology, Bicetre Hospital, South Paris University, Le Kremlin Bicêtre, France.

Purpose: To describe the clinical features of secondary glaucoma associated with transthyretin (TTR)-related Familial Amyloid Polyneuropathy (FAP).

Methods: In this retrospective monocentric study, five patients with FAP associated secondary glaucoma were seen at the ophthalmologic consultation of the french national center for FAP between november 2011 and november 2012. The exact mutation of the amyloidogenic TTR variants was analysed for all patients. All patients had a comprehensive ophthalmic examination including Best corrected Visual acuity (BCVA), ocular pressure, slit lamp photographs, gonioscopy, fundus examination with optic disc photography, ultrasound pathymetry, automated perimetry, and OCT RNFL. Glaucomatous optic neuropathy was diagnosed based on the presence of visual field abnormalities, neuroretinal rim thinning, excavation or RNFL defects. Medical and surgical treatments were analysed for all patients.

Results: All cases had bilateral involvement except two monophthalmic patients (1 case of traumatism, and one case of Phtisis bulbi following multiple retinal detachment surgical procedures). All patients were of portuguese origin. Molecular biological examination showed Val30Met mutation in all patients. There were 4 women and one man with a mean age of 52±8 years. Mean BCVA was 0.83±0.9 LogMAR. Three eyes had a BCVA below 20/400. Mean ocular pressure was 27±3mmHg. Mean deviation was -17.6±11.2dB. Amyloid deposition at the pupillary border, fringed pupil and pigmented deposition in the irido-corneal angle were noted in all affected eyes. One patient had bilateral amyloid deposition on the lens anterior capsule. Three patients had concomitant vitreous involvement. Patients were treated with 2.4±2.1 ocular hypotensive drugs. Four eyes had been treated with at least one filtering surgery.

Conclusions: Although limited by the small size of the sample, our results are comparable to those available in previously published reports : FAP-associated secondary glaucoma is a very severe disease, associated with amyloid deposits in the anterior chamber and characteristic pupil deformation. Systematic and comprehensive eye examination should be performed in all patients affected with FAP in order to improve early detection of glaucoma.

Commercial Relationships: Antoine Rousseau, None; Emmanuel Barreau, None; Godefroy Kaswin, None; Mohamed Mgarrech, None; Marie Théaudin, Pfizer (R); Cécile Cauquil, None; David Adams, None; Marc Labetoulle, None

Program Number: 6241 **Poster Board Number:** C0126

Presentation Time: 10:30 AM - 12:15 PM

Identification and expression of candidate genes in pseudoexfoliation

Kamesh Dhamodaran¹, Reshma S. Shetty¹, Murali Subramani¹, Vinay Patil², Bhujang K. Shetty², Debashish Das¹. ¹Stem Cell Research Laboratory, Narayana Nethralaya Post Graduate Inst of Ophthalmology, Bangalore, India; ²Cataract and Refractive Lens Surgery, Narayana Nethralaya Post Graduate Inst of Ophthalmology, Bangalore, India.

Purpose: To identify the biomarker for early diagnosis of developing pseudoexfoliation with or without glaucoma.

Methods: After informed consent, fifteen samples of aqueous humor and lens was collected from patients who underwent surgery for PEX, PEX with glaucoma or glaucoma alone. The samples from cataract patients (Control) without any history of glaucoma and/or

PEX. Molecular analysis by mRNA expression was done by quantitative PCR for the following genes LOXL1, CLU, MYOC, OPTN and Elvovl5.

Results: Interestingly, qPCR analysis shows two fold increase of Clusterin expression was identified in aqueous humor and not in lens from PEX patients compared to pseudoexfoliation with glaucoma (XFG) and isolated glaucoma (POAG). Also well known susceptible LOXL1 gene was expressed in higher levels on both PEX and XFG patients aqueous humor consistent with previous reports. On the other hand, POAG or Normal tension glaucoma (NTG) marker ELOVL5 was observed in aqueous humor of PEX and XFG patients. As we expect MYOC shows predominant expression in aqueous humor from glaucoma patients.

Conclusions: In this study we showed that pseudoexfoliation candidate gene expression (LOXL1, CLU) pattern in patients with aqueous humor and lens. We are also confirming that higher expression of Myoclin in POAG patients. Finally we conclude that LOXL1, CLU, MYOC, OPTN and Elvovl5 as a marker for identifying predisposition of PEX and developing glaucoma.

Commercial Relationships: Kamesh Dhamodaran, None; Reshma S. Shetty, None; Murali Subramani, None; Vinay Patil, None; Bhujang K. Shetty, None; Debashish Das, None

Program Number: 6242 **Poster Board Number:** C0127

Presentation Time: 10:30 AM - 12:15 PM

Expanded Phenotype of Axenfeld Spectrum: Congenital Hypothyroidism and Glaucoma

Elena Bitrian¹, Elizabeth W. McPherson², Alana L. Grajewski^{1,3}.

¹Ophthalmology, University of Minnesota, Minneapolis, MN;

²Genetics, Marshfield Clinic, Marshfield, WI; ³Pediatric Glaucoma, Bascom Palmer Eye Institute, Miami, FL.

Purpose: To report a new familial variant of Axenfeld-Rieger syndrome with anterior chamber abnormalities, congenital glaucoma, congenital hypothyroidism, hearing loss, microcephaly, developmental delay and limb abnormalities.

Methods: Eight individuals in 3 generations from the same family with specific ocular and systemic characteristics were identified. The subjects underwent clinical examination, blood and genetic testing.

Results: Eight subjects from this family, belonging to three different generations, presented anterior segment anomalies characteristic of Axenfeld-Rieger's syndrome: thick anterior displaced Schwalbe's line, variable degrees of iris atrophy and congenital glaucoma. Five of the family members presented congenital hypothyroidism, all had microcephaly, four had developmental delay and all eight had minor limb abnormalities (hypoplastic toes and one with severe metatarsus adductus). Four patients had hearing loss. There were also some minor facial abnormalities like flat midface and thin upper lip.

All the children in the family had bilateral congenital glaucoma and required multiple glaucoma angle surgeries and glaucoma shunt implants. They presented congenital hypothyroidism, microcephaly and developmental delay. One of the patients underwent genetic testing and had normal karyotype (46, XY) and was negative for mutations in PITX2 and FOXC1. CGH microarray and extensive biomechanical testing including lactate, pyruvate, very long chain fatty acids, amino acids, organic acids, carnitine, acylcarnitine profile and carbohydrate deficient transferring had all negative results.

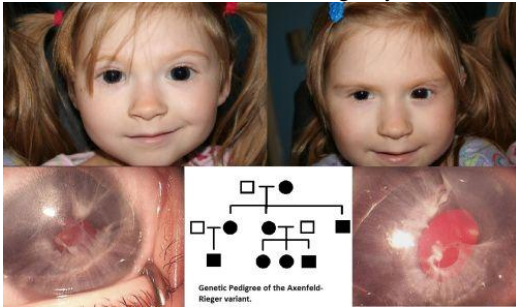
None of the patients had hypodontia or periumbilical abnormalities which are usually seen in individuals with Axenfeld-Rieger type 1 and have PITX2 mutation. None had hydrocephalus, dental or cardiac abnormalities seen in Axenfeld-Rieger type 2, or in Axenfeld-Rieger type 3 with mutations of FOXC1. They were also different than other syndromes with anterior chamber anomalies such as SHORT syndrome or Peter Plus. Table1 shows differences between ARS and

this new variant.

Conclusions: This is a new autosomal dominant variant of Axenfeld-Rieger syndrome, with congenital hypothyroidism, microcephaly, developmental delay, hearing loss and minor limb abnormalities.

	AXENFELD-RIEGER	NEW VARIANT
Posterior embryotoxon and iris abnormalities	Yes	Yes
Mild craniofacial dimorphism	Yes	Yes
Hearing loss	Yes	Yes
Maxillary and dental abnormalities	Yes	No
Redundant umbilical skin	Yes	No
Glaucoma	Late childhood or adults	Congenital
Hypothyroidism	No	Congenital
Microcephaly	No	Yes
Developmental delay	No	Yes
Limb abnormalities	No	Yes

Differences between Axenfeld-Rieger syndrome and the new variant.



Genetic pedigree of the family and clinical findings.

Commercial Relationships: Elena Bitrian, None; Elizabeth W. McPherson, None; Alana L. Grajewski, Alcon (R)

Program Number: 6243 **Poster Board Number:** C0128

Presentation Time: 10:30 AM - 12:15 PM

Candidate regulatory lysyl oxidase-like 1 (LOXL1) variants in pseudoexfoliation syndrome/glaucoma are associated with differential LOXL1 expression

Matthias Zenkel¹, Francesca Pasutto², Jasmine Onderka¹, Anita W. Krysta¹, Angelika Moessner¹, Friedrich E. Kruse¹, Ursula Schlotzer-Schrehardt¹. ¹Department of Ophthalmology, University Erlangen Nuernberg, Erlangen, Germany, ²Department of Human Genetics, University Erlangen Nuernberg, Erlangen, Germany.

Purpose: Candidate regulatory single nucleotide polymorphisms (SNPs) in the lysyl oxidase-like 1 (LOXL1) gene, the main genetic risk factor for pseudoexfoliation (PEX) syndrome/glaucoma, have been identified and suggested to influence expression and/or splicing of LOXL1 mRNA. To determine the role of these SNPs in PEX pathophysiology, we investigated the expression and size of LOXL1 mRNA in ocular tissues of PEX and control patients in correlation with the individual SNP genotypes.

Methods: Total RNA and genomic DNA were isolated simultaneously from iridal tissue specimens, obtained from donor eyes with PEX syndrome and age-matched normal donor eyes (n=20 for each group). The mRNA expression of LOXL1 was measured by quantitative real-time PCR assays. LOXL1 mRNA size was analyzed by reverse transcription (RT)-PCR using primers located in the 5'- and 3'- untranslated regions of the LOXL1 mRNA. SNPs located in the promoter region (rs12914489 and rs16958477) and the first intron (rs1992314 and rs2028387) of the LOXL1 gene were genotyped by direct sequencing and correlated to LOXL1 expression.

Results: The frequencies of the risk G-allele of rs12914489 and the risk C-allele of rs16958477 were 49% and 31% in PEX cases, and

42% and 24% in control cases, respectively. The frequencies of the risk C-allele of rs1992314 and the risk A-allele of rs2028387 were 43% and 42% in PEX cases, and 30% and 32% in control cases. The risk alleles of rs12914489 and rs16958477 were not significantly associated with alterations in LOXL1 expression levels. In contrast, the expression of LOXL1 displayed a significant increase by 40% (p<0.02) with two copies of the risk alleles of rs1992314 (CC) and rs2028387 (AA), as compared to the heterozygous alleles as well as to the homozygous non-risk alleles of rs1992314 (GG) and 2028387 (CC). This increase was strongly correlated (r=0.99, p<0.0001) with the presence of a risk-conferring haplotype C-A. RT-PCR analysis resulted in a single LOXL1 transcript in PEX and control cases arguing against alternative splicing events of LOXL1 mRNA in ocular tissues.

Conclusions: These data suggest, that the two intronic variants rs1992314 and rs2028387, which are associated with PEX syndrome in both Caucasian and black South African populations, are potentially functional variants for the disease by affecting LOXL1 gene expression in ocular tissues.

Commercial Relationships: Matthias Zenkel, None; Francesca Pasutto, None; Jasmine Onderka, None; Anita W. Krysta, None; Angelika Moessner, None; Friedrich E. Kruse, None; Ursula Schlotzer-Schrehardt, None

Program Number: 6244 **Poster Board Number:** C0129

Presentation Time: 10:30 AM - 12:15 PM

Spatial Distribution of Mutations in ASB10 and MYOC

Colin Marrs¹, Sarah J. Garnai¹, Namita Natalie Lopes¹, David M. Reed¹, Kari E. Branham¹, Mohammad I. Othman¹, Sayoko E. Moroi¹, John R. Heckenlively¹, Hemant S. Pawar¹, Julia E. Richards^{1,2}.

¹Ophthalmology and Visual Sciences, University of Michigan, Ann Arbor, MI; ²Epidemiology, University of Michigan, Ann Arbor, MI.

Purpose: To evaluate distribution of specific mutation types in ASB10 and MYOC, two genes that have been implicated in open-angle glaucoma (OAG).

Methods: All subjects provided informed consent under a protocol approved by the University of Michigan Institutional Review Board. The inclusion criteria met standards used in the NEIGHBOR genome-wide association study. Features of OAG cases included age at onset ≥ 35 years, either high or normal intraocular pressures (IOP), glaucomatous optic disc cupping, glaucomatous visual field loss, and absence of other causes for the visual field loss. The inclusion criteria for the controls were IOP <21 mm Hg and cup-to-disc ratio ≤ 0.5 . ASB10 exons were sequenced from both case and control DNA.

Results: We sequenced the ASB10 gene in DNA from 228 cases and 319 controls, and used MYOC data that we have previously reported; additional data on these two genes came from the literature. The spatial distribution of causative mutations along MYOC is clearly asymmetric; the majority of causative changes are located in the third exon encoding the olfactomedin-related domain. Further examination of myocilin shows a cluster of causative charge changes in the olfactomedin-related domain that raises questions about whether that region of the protein might be especially sensitive to charge changes. While sequence variants in ASB10 are not confined to one region of the protein, asymmetry of the mutation distribution for the first exon of isoforms 1 and 2 and the alternative first exon of isoform 3 raises questions about the functional roles of different isoforms.

Conclusions: Sequence variants are expected to show similar spatial distribution along genes in cases and controls if the variants have no functional impact. The skewed distribution along the gene between cases and controls is consistent with the known causative role of MYOC in glaucoma. Differences in geographic localization of some ASB10 mutations raise questions about whether disease involvement

might be specific to some isoforms. The distribution of sequence variants along these two genes between case and control populations will be presented and aspects of asymmetry will be discussed relative to the functional domains of the proteins.

Commercial Relationships: Colin Marrs, None; Sarah J. Garnai, None; Namita Natalie Lopes, None; David M. Reed, None; Kari E. Branham, Arctic DX (P); Mohammad I. Othman, None; Sayoko E. Moroi, Merck (F), Wolters Kluwer (F); John R. Heckenlively, None; Hemant S. Pawar, None; Julia E. Richards, None
Support: NEI Grant EY011671, NEI Grant EY007003, RPB

Program Number: 6245 **Poster Board Number:** C0130

Presentation Time: 10:30 AM - 12:15 PM

Conserved anatomic features in sibling pairs concordant for angle closure

PALANISWAMY KRISHNAMURTHY¹, Rengaraj Venkatesh¹, Pradeep Y. Ramulu², Srinivasan Kavitha¹, David S. Friedman², Harry Quigley², Robert Wojciechowski³, Fiona Seager². ¹Aravind Eye Hospital, PONDICHERRY, India; ²Wilmer Eye Institute, BALTIMORE, MD; ³Johns Hopkins Bloomberg School of Public Health, BALTIMORE, MD.

Purpose: To compare the inter-sibling differences in ocular parameters for sibling pairs who are concordant or discordant for angle closure.

Methods: Two hundred and one patients with angle closure (PACS, PAC, or PACG) were recruited from the Aravind Eye Hospital in Pondicherry. All patients and one similarly-aged sibling underwent the following testing: (1) subjective refraction to determine spherical error, (2) pachymetry to determine central corneal thickness (CCT), (3) A-scan to determine anterior chamber depth (ACD), lens thickness and axial length, and (4) anterior segment OCT to determine anterior chamber width, anterior chamber volume, and lens vault. The presence/absence of angle closure was characterized in siblings through a gonioscopic exam conducted by a masked physician, and used to characterize sibling pairs as concordant or discordant with regards to angle closure. Differences in proband/sibling ocular parameters in concordant and discordant sibling pairs were assessed through correlation analyses and through comparison of absolute proband-sib differences in the measured parameters.

Results: 133 sibling pairs (66%) were concordant for angle closure, while 68 (34%) were discordant. Greater inter-sibling correlation was observed for concordant sib pairs as compared to discordant sib pairs with regards to axial length ($r=0.47$ vs. 0.33), anterior chamber depth ($r=0.20$ vs. -0.16), CCT ($r=0.55$ vs. 0.37), and lens vault ($r=0.25$ vs. 0.20). All other parameters showed similar correlations for concordant and discordant sib pairs (r values within 0.05 of each other). Larger proband-sibling differences were noted in discordant sibling pairs as compared to concordant sibling pairs for axial length ($\Delta=0.66$ vs. 0.16 mm, $p<0.001$), anterior chamber depth ($\Delta=0.51$ vs. 0.07 mm, $p<0.001$), anterior chamber volume ($\Delta=30$ vs. 12 mm³, $p<0.001$), lens vault ($\Delta=0.33$ vs. 0.11 mm, $p<0.001$), and anterior chamber width ($\Delta=0.25$ vs. 0.08 mm, $p=0.02$), but not for central corneal thickness, lens thickness, or spherical error.

Conclusions: Axial length, anterior chamber depth and volume, and lens vault are more highly preserved in sibling pairs concordant for angle closure as compared to sibling pairs discordant for angle closure. This finding suggests that preservation of these features across family members plays an important role in the heritability of angle closure.

Commercial Relationships: PALANISWAMY KRISHNAMURTHY, None; Rengaraj Venkatesh, None; Pradeep Y. Ramulu, None; Srinivasan Kavitha, None; David S. Friedman,

Alcon (C), Bausch & Lomb (C), Merck (C), QLT, Inc (C), Allergan (C), Nidek (C); Harry Quigley, Sensimed (C), Genetech (C), Merck (C), Sucampo (C); Robert Wojciechowski, None; Fiona Seager, None

Support: Wilmer Internal Grants and Research to Prevent Blindness

Program Number: 6246 **Poster Board Number:** C0131

Presentation Time: 10:30 AM - 12:15 PM

Exome chip analysis identifies rare variants associated with primary open angle glaucoma

William K. Scott¹, Monique D. Courtenay¹, Donald L. Budenz³, Richard K. Lee², Jonathan L. Haines⁴, Margaret A. Pericak-Vance¹. ¹Hussman Institute of Human Genomics, University of Miami, Miami, FL; ²Bascom Palmer Eye Institute, University of Miami, Miami, FL; ³Ophthalmology, University of North Carolina, Chapel Hill, NC; ⁴Center for Human Genetics Research, Vanderbilt University, Nashville, TN.

Purpose: Primary open angle glaucoma (POAG) is a complex disorder with heterogeneous etiology comprising genetic and environmental factors. Family-based linkage studies have identified a few genes with rare mutations underlying POAG, and large case-control studies (and meta-analysis) of common variants have recently reproducibly implicated variants in the *CDKN2BAS* and *SIX1/SIX6* genes. The purpose of this study was to examine rare variants (RV) captured on the human ExomeChip to identify additional POAG genes or RV in existing genes associated with POAG.

Methods: White POAG cases ($n=314$, mean age 73, 75% normotensive POAG) and controls ($n=797$, mean age 74.5) were genotyped using the Illumina HumanExome-12v1 Array. This array includes coding region variants across the genome, with a majority of variants (88%) being rare (minor allele frequency $<5\%$). POAG cases were evaluated and classified using procedures developed by the NEIGHBOR consortium. After quality control, 243,101 variants were tested for association with POAG using logistic regression models, controlling for population stratification using 5 principal components obtained from EIGENSTRAT.

Results: No variant met Bonferroni criteria (2×10^{-7}) for significant association, but 28 coding variants, all in novel genes for POAG, were suggestively associated at $p<0.0001$. All but one of these variants were more common in controls than cases. The other variant, rs36117280 (M313V), in *CACNA1H*, was 1.8 times as likely in cases than controls. Additionally, intronic variants in *CDKN2BAS* were nominally associated with POAG ($p<0.001$), as was an intergenic variant in the *SIX1/SIX6* region ($p<0.05$).

Conclusions: Initial analysis of rare coding sequence variants in a POAG sample suggests that such variants may contribute to the complex etiology of POAG. The increase in the *CACNA1H* (Cav3.2) M313V variant in cases is interesting, given the prior association of POAG with the Cav1/2 region, and further implicates variation in calcium channel genes in POAG.

Commercial Relationships: William K. Scott, Duke University/ArcticDx (P); Monique D. Courtenay, None; Donald L. Budenz, None; Richard K. Lee, National Eye Institute (F); Jonathan L. Haines, Arctic Dx (I), AMD genes (P); Margaret A. Pericak-Vance, None

Program Number: 6247 **Poster Board Number:** C0132

Presentation Time: 10:30 AM - 12:15 PM

Association between IL1A, IL1B and TNFA polymorphisms and glaucoma in a Brazilian population

Mariana Oliveira^{1,2}, Jose Paulo C. Vasconcellos^{2,1}, Vital P. Costa², Galina Ananina¹, Monica B. Melo¹. ¹Center of Molecular Biology and Genetic Engineering, University of Campinas, UNICAMP,

Campinas, Brazil; ²Department of Ophthalmology, Faculty of Medical Sciences, University of Campinas, UNICAMP, Campinas, Brazil.

Purpose: Glaucoma is a progressive atrophy of the optic disc characterized by loss of retinal ganglion cells, which leads to a corresponding visual field defect. It's the major cause of irreversible blindness worldwide. Linkage analysis, association studies and candidate genes approaches have been performed in order to identify disease-causing genes and variants of susceptibility associated with POAG. Among them there are genes that codify for cytokines (IL1A, IL1B and TNFA), which have been associated in previous studies with higher risk for the development of POAG in some populations. The aim of this study was to evaluate the association of seven polymorphisms in the TNFA, IL1A and IL1B genes, in Brazilian POAG patients.

Methods: A case control study including 172 unrelated POAG patients and 138 healthy matched individuals was conducted to evaluate the frequency distribution of polymorphisms in the IL1A, IL1B and TNFA genes as well as genotype/phenotype correlation. Comprehensive ophthalmic evaluation was performed and genomic DNA was obtained from case and control groups. Seven single nucleotide polymorphisms (SNPs): IL1A (-889C/T; rs1800587), IL1A (+4845G/T; rs17561), IL1B (-31C/T; rs1143627), IL1B (-511C/T; rs16944), IL1B (3953C/T; rs1143634), TNFA (-238G/A; rs361525) and TNFA (-308G/A; rs1800629) were genotyped through direct sequencing. The association of individual SNPs was tested by chi-square test and logistic regression. The p-value was corrected for multiple tests.

Results: There was an association of the -31 C/T polymorphism in the IL1B gene with POAG (p=0,00909). No significant differences were observed for the other SNPs between POAG patients and controls. Among patients with POAG, an analysis comparing genotypes and clinical data as intraocular pressure, vertical cup to disc ratio and number of surgical procedures necessary to IOP control was performed and no statistical differences among these groups were observed.

Conclusions: Results suggest that in this Brazilian population sample the -31C/T polymorphism in the IL1B gene may be considered a risk allele for the development of POAG. A similar study with additional and larger cohorts of patients using also other population groups is necessary to further substantiate the observation.

Commercial Relationships: Mariana Oliveira, None; Jose Paulo C. Vasconcellos, None; Vital P. Costa, None; Galina Ananina, None; Monica B. Melo, None

Support: FAPESP

Program Number: 6248 **Poster Board Number:** C0133

Presentation Time: 10:30 AM - 12:15 PM

Functional Analysis of LOXL1 Missense Variants in the Pathophysiology of Pseudoexfoliation Syndrome/Glaucoma

Ursula Schlotzer-Schrehardt¹, Takako Sasaki², Matthias Zenkel¹, Friedrich E. Kruse¹, Anita W. Krysta¹. ¹Department of Ophthalmology, University of Erlangen-Nürnberg, Erlangen, Germany; ²Department of Experimental Medicine I, University of Erlangen-Nürnberg, Erlangen, Germany.

Purpose: To evaluate a potential functional role of the two non-synonymous coding polymorphisms rs1048661 (R141L) and rs3825942 (G153D) of LOXL1 (lysyl oxidase-like 1) in the pathophysiology of pseudoexfoliation (PEX) syndrome/glaucoma, a complex disorder of the elastic fiber system.

Methods: Haplotypes (G-G, T-G, G-A, T-A) of the LOXL1 variants rs1048661 and rs3825942 were generated by site-directed mutagenesis of full-length human LOXL1 cDNA. HEK-EBNA cells

and primary Tenon's capsule fibroblasts (hTCF) obtained from normal and PEX patients were stably transfected with the LOXL1 constructs. Cell lysates, supernatants, and purified LOXL1 proteins were comparatively analyzed by Western blotting, proteolytic processing, activity assays, and protein binding assays. Their effect on extracellular matrix synthesis and assembly in vitro was analyzed by real-time PCR and immunocytochemistry with and without stimulation by TGF-β1.

Results: Stable clones produced a high steady-state level of LOXL1, which was 50-fold increased compared to non-transfected cells. Quantitative analysis of LOXL1 mRNA and protein expression/secretion, which was significantly increased by TGF-β1, did not show any significant differences between the four haplotypes. Proteolytic cleavage by endoproteases BMP-1 and furin as well as amine oxidase activities were also not different between LOXL1 variants. In the hTCF expression system, TGF-β1 stimulated co-expression of LOXL1 and elastic proteins (tropoelastin, fibrillin-1, fibulin-4 and -5) up to 30-fold and promoted incorporation of elastin into a microfibrillar scaffold 14-18 days post-confluence. The risk G-G variant displayed earlier and significantly higher expression levels of tropoelastin and fibulin-5 compared to the non-risk variant G-A. In contrast to LOXL1 (G-A), LOXL1 (G-G) also showed distinct colocalization with fibulin-5 on elastic microfibrils. Binding assays using purified LOXL1 proteins confirmed significantly increased binding of the risk variant G-G to fibulin-4 and -5, by tendency also to tropoelastin, but not to fibrillin-1, compared to the non-risk variant G-A.

Conclusions: Subtle functional differences regarding induction of elastogenesis and elastic matrix binding properties of LOXL1 risk variants may, in cooperation with TGF-β1, contribute to the formation and aggregation of elastotic PEX material and thus to the development of PEX syndrome/glaucoma.

Commercial Relationships: Ursula Schlotzer-Schrehardt, None; Takako Sasaki, None; Matthias Zenkel, None; Friedrich E. Kruse, None; Anita W. Krysta, None
Support: DFG grant SCHL 366/8-1

Program Number: 6249 **Poster Board Number:** C0134

Presentation Time: 10:30 AM - 12:15 PM

Mapping of two modifier loci for glaucoma severity on chromosome 20

Vincent Raymond^{1,2}, Pascal Belleau¹, Stéphane Dubois¹, Rose Arseneault¹, Éric Shink^{1,2}, Jean-Louis Anctil³, Gilles Côté³, Michael A. Walter⁴, Marcel Amyot⁵. ¹Neurosciences, CHU de Québec/CHUL (Université Laval Hospital) Research Centre, Québec City, QC, Canada; ²Molecular Medicine, Université Laval, Québec City, QC, Canada; ³Ophthalmology, Université Laval, Québec City, QC, Canada; ⁴Medical Genetics, University of Alberta, Edmonton, AB, Canada; ⁵Ophthalmology, Université de Montréal, Montréal, QC, Canada.

Purpose: Primary open-angle glaucoma (POAG) is a polygenic disease caused by genetic and environmental risk factors. To understand how gene-gene interactions lead to POAG, it is essential to identify the modifiers that alter glaucoma endophenotypes. The goal of our study was to map such modifiers using families that showed variable expressivity of the disorder while segregating a primary disease-causing gene.

Methods: For the past 50 years, we have been investigating the French-Canadian autosomal dominant glaucoma CA pedigree (749 people) in which the MYOC^{K423E} mutation expresses a very wide phenotypic variability. To assess heritability of the endophenotypes, all eye examination records of myocilin mutant carriers were revised to extract 6 quantitative trait values for glaucoma. Genome-wide

ARVO 2013 Annual Meeting Abstracts by Scientific Section/Group – Glaucoma

linkage analysis were initiated by genotyping 408 microsatellite markers in 184 members. Linkage values were calculated using a Bayesian MCMC method implemented in LOKI. This procedure calculates L-score values by estimating the posterior probability of linkage divided by the prior probability. Interactions between modifier effects and MYOC were evaluated using *MEON (Modifier Effects On Neighborhoods)*, a procedure developed to assess the strength of gene-gene interactions.

Results: 133 of the CA members were heterozygous for the MYOC^{K423E} mutation with 114 of them affected. The other 17 heterozygotes were asymptomatic even if 9 of them were ≥ 35 years of age at their last exam. Only 2 of the traits selected for heritability analysis displayed a significant genetic component. Both were relative to intraocular pressures (IOP), 1. age-at-onset defined as age at which IOP raised ≥ 22 mm Hg and 2. maximal IOP. Our linkage analysis then revealed that two distinct 5 cM regions on chromosome 20 were linked to variable age-at-onset. The first locus, mapped at $\sim 20q13$, displayed an L-score value ≥ 10 . The second locus, located between D20S189 and D20S898 at 20p12, showed an L-score value of ~ 8 . Interestingly, these 2 markers mapped within the *GLCIK* locus that encodes a gene for early-onset OAG. Common modifier alleles identified the patients who contributed to the linked endophenotype.

Conclusions: We mapped two novel modifier loci for glaucoma severity. These 2 elements constitute a specific type of modifiers that might function by altering the age at which the first episode of intraocular hypertension occurs in mutant myocilin heterozygotes.

Commercial Relationships: Vincent Raymond, None; Pascal Belleau, None; Stéphane Dubois, None; Rose Arseneault, None; Éric Shink, None; Jean-Louis Anctil, None; Gilles Côté, None; Michael A. Walter, None; Marcel Amyot, None

Support: CIHR/IRSC, FRQS Vision Research Network, The Glaucoma Foundation (USA), Fondation des Maladies de l'Oeil